NEW INSIGHTS INTO RENAL FIBROSIS AND THERAPEUTIC EFFECTS OF NATURAL PRODUCTS

EDITED BY: Dan-Qian Chen and Zhiyong Guo
PUBLISHED IN: Frontiers in Pharmacology

frontiers Research Topics

ISSN 1664-8714
ISBN 978-2-88976-272-9
DOI 10.3389/978-2-88976-272-9

About Frontiers

Frontiers is more than just an open-access publisher of scholarly articles: it is a pioneering approach to the world of academia, radically improving the way scholarly research is managed. The grand vision of Frontiers is a world where all people have an equal opportunity to seek, share and generate knowledge. Frontiers provides immediate and permanent online open access to all its publications, but this alone is not enough to realize our grand goals.

Frontiers Journal Series

The Frontiers Journal Series is a multi-tier and interdisciplinary set of open-access, online journals, promising a paradigm shift from the current review, selection and dissemination processes in academic publishing. All Frontiers journals are driven by researchers for researchers; therefore, they constitute a service to the scholarly community. At the same time, the Frontiers Journal Series operates on a revolutionary invention, the tiered publishing system, initially addressing specific communities of scholars, and gradually climbing up to broader public understanding, thus serving the interests of the lay society, too.

Dedication to Quality

Each Frontiers article is a landmark of the highest quality, thanks to genuinely collaborative interactions between authors and review editors, who include some of the world's best academicians. Research must be certified by peers before entering a stream of knowledge that may eventually reach the public - and shape society; therefore, Frontiers only applies the most rigorous and unbiased reviews.
Frontiers revolutionizes research publishing by freely delivering the most outstanding research, evaluated with no bias from both the academic and social point of view. By applying the most advanced information technologies, Frontiers is catapulting scholarly publishing into a new generation.

What are Frontiers Research Topics?

Frontiers Research Topics are very popular trademarks of the Frontiers Journals Series: they are collections of at least ten articles, all centered on a particular subject. With their unique mix of varied contributions from Original Research to Review Articles, Frontiers Research Topics unify the most influential researchers, the latest key findings and historical advances in a hot research area! Find out more on how to host your own Frontiers Research Topic or contribute to one as an author by contacting the Frontiers Editorial Office: frontiersin.org/about/contact

NEW INSIGHTS INTO RENAL FIBROSIS AND THERAPEUTIC EFFECTS OF NATURAL PRODUCTS

Topic Editors:
Dan-Qian Chen, Northwest University, China
Zhiyong Guo, Second Military Medical University, China

Citation: Chen, D.-Q., Guo, Z., eds. (2022). New Insights Into Renal Fibrosis and Therapeutic Effects of Natural Products. Lausanne: Frontiers Media SA.
doi: 10.3389/978-2-88976-272-9

Table of Contents

frontiers | Frontiers in Pharmacology

EDITORIAL
published: 16 May 2022
doi: 10.3389/fphar.2022.923773

Editorial: New Insights Into Renal Fibrosis and Therapeutic Effects of Natural Products

Ying Xu[1], *Danqian Chen*[2] *and Zhiyong Guo*[1]*

[1]Department of Nephrology, Changhai Hospital, Naval Medical University, Shanghai, China, [2]Faculty of Life Science & Medicine, Northwest University, Xi'an, China

Keywords: editorial, renal fibrosis (RF), natural producct, therapeutic effect, new insight

Editorial on the Research Topic

New Insights Into Renal Fibrosis and Therapeutic Effects of Natural Products

Renal fibrosis is the progressive and complicated process manifested by histological aberrance and functional decline in the kidney. The pathogenesis involves multiple molecular pathways and cellular targets leading to myofibroblast activation and accumulation of extracellular matrix, which is in response to excessive epithelial injury and inflammation. Formation and exacerbation of fibrosis during the development of chronic kidney disease (CKD) is the common pathway to end-stage renal failure. However, few interventions are available that specifically target the pathogenesis of renal fibrosis. Emerging evidences prove that natural product therapy directly targets the pathogenesis of renal fibrosis, and exhibits beneficial effects in clinical. Further research (such as multi-omics studies and network pharmacology) is urgently needed to investigate the puzzle from the active compounds to underlying mechanisms and therapeutic targets of natural product against renal fibrosis.

The Research Topic intends to highlight the latest advances from the active compounds to underlying mechanisms and therapeutic targets molecular mechanism of natural product against renal fibrosis. The issue includes 25 articles that is contributed by more than 200 authors in the fields of renal pharmacology. We have generated a collaborative discussion that facilitated the development of new mechanisms, new therapeutic targets, and candidate drugs from natural product against renal fibrosis.

New mechanisms of renal fibrosis and the protective effects of natural product have been investigated and uncovered. Fibrosis-related signaling pathways are the common therapeutic targets, especially TGF-β pathway. Zheng et al. illustrate that astragalus polysaccharide extract plays a beneficial role in reducing renal inflammation and fibrosis and in improving renal function by regulating the TGF-β/ILK pathway in hypertensive mice. Ren et al. confirm that natural flavonoid pectolinarigenin alleviates renal fibrosis to delay hyperuricemic nephropathy via suppressing TGFβ/SMAD3 and JAK2/STAT3 signaling pathways. By targeting non-TGF-β pathway, Yu et al. report the medical leech saliva extract, hirudin, protects the kidney from fibrotic injury by ameliorating renal autophagy impairment via PI3K/Akt pathway. Liu et al. demonstrate that quercetin alleviates podocytes apoptosis *in vitro* and *in vivo* by regulating the EGFR pathway, providing a novel approach to reveal the therapeutic mechanisms of quercetin against DN. Gong et al. identify proanthocyanidins (OPC) as active compounds of grape seeds. OPC exhibits beneficial protection against cadmium-induced DN in multidimensional aspects by the regulation of oxidative-antioxidative status, metal-binding ability, mediation of the levels of essential elements, and activation of the p38 MAPK and Keap1/Nrf2 signaling pathways.

Additionally, metabolic regulation and kidney-gut axis function as a promising therapeutic target against renal fibrosis. Ma et al. prove that farrerol reverses oxidative stress, inflammation, and fibrosis

Edited and reviewed by:
Giuseppe Remuzzi, Mario Negri Pharmacological Research Institute (IRCCS), Italy

***Correspondence:**
Zhiyong Guo
drguozhiyong@163.com

Specialty section:
This article was submitted to Renal Pharmacology, a section of the journal Frontiers in Pharmacology

Received: *19 April 2022*
Accepted: *26 April 2022*
Published: *16 May 2022*

Citation:
Xu Y, Chen D and Guo Z (2022) Editorial: New Insights Into Renal Fibrosis and Therapeutic Effects of Natural Products. Front. Pharmacol. 13:923773. doi: 10.3389/fphar.2022.923773

in renal tubular epithelial cells by activating Nrf2 and subsequently increasing PINK/Parkin-mediated mitophagy and eliminating damaged mitochondria. Xiang et al. show that the restoration of PPARα activity delays diabetic nephropathy progression and attenuates lipid metabolism disorders by downregulating miR-21 expression to improve mitochondrial function. Li et al. report that maintaining the balance of mitochondrial dynamics exhibits renoprotection in kidney by inhibiting mitochondrial fission and promoting mitochondrial fusion via the downregulation of the primary mediator proteins of mitochondrial fission (Drp1 and Fis1) and the upregulation of fusion proteins (Opa1 and Mfn1). Zhang et al. carries out the serum metabonomics analysis of patients with diabetic kidney disease and shows the potential role of specific gut microbiota in the progression of renal fibrosis and diabetic kidney disease that involves the dysfunction of phenylalanine and tryptophan metabolisms. This study suggests the kidney-gut axis functions as a potential therapeutic target of renal fibrosis.

Since Chinese herbal medicine exhibits beneficial effects against renal fibrosis, the lack of randomized controlled trial and clear mechanism hinder natural product to pass modern assessments. Here, Shao et al. summarized five Chinese herbal medicines with sufficient clinical efficacy, high frequency of use, and well-studied mechanism, including *Abelmoschus manihot* and Huangkui capsule, *Salvia miltiorrhiza* and its components (tanshinone II A, salvianolic acid A and B); *Rhizoma coptidis* and its monomer berberine; *Tripterygium wilfordii* and its components (triptolide, tripterygium glycosides); *Kudzu* root *Pueraria* and its monomer Puerarin. The researches of these five Chinese herbal medicines set the study pattern for natural product against renal fibrosis, which are the promising candidate for widespread and standardized application.

Beyond to five Chinese herbal medicines, studies from the present issue provide the clinical evidences of natural products against renal fibrosis and explore underlying mechanisms. Mahuang Fuzi and Shenzhuo Decoction (MFSD), a Chinese herbal formula, is a promising candidate for renal fibrosis and CKD treatment in clinial. Dong et al. designed a multicenter, nonrandomized, single-arm clinical trial to explore the clinical effects of MFSD on idiopathic membranous nephropathy (MN), presenting an inspiring result that MFSD has significantly beneficial effects on idiopathic MN treatment, and has the same beneficial effects on patients with MN who are newly treated and who accepted with immunosuppressive therapy without remission. Further study from the same group by Gao et al. investigates the main active compounds of MFSD by high-performance liquid chromatography-mass spectrometry (HPLC-MS) and more than 30 active compounds are identified. These active compounds alleviate podocyte injury by modulating autophagy-related protein and Wnt/β-catenin pathway, indicating autophagy and Wnt/β-catenin pathway as potential targets of MFSD for MN treatment. Zhang et al. demonstrate the anti-fibrotic and anti-inflammatory effects of Bupi Yishen Formula *in vivo* and *in vitro* by suppressing TLR4-mediated NF-κB signaling.The study of Luo et al. reveals the anti-oxidant and anti-inflammatory ability of Shenkang injection (SKI) in kidney, and identifies chrysophanol, emodin, and rhein as active compounds against renal fibrosis via simultaneously targeting IκB/NF-κB and Keap1/Nrf2 signaling pathways. Jia et al. report TLYS decoction improves mitochondrial dynamics to attenuates renal fibrosis and renal function decline by suppressing oxidative stress and mitophagy. The comparative network pharmacology analysis is the alternative approach to explore the mechanisms of natural products with limited experiments. Chan et al. performed comparative network pharmacology to figure out the mechanism of Liu-wei-di-huang-wan. Liu-wei-di-huang-wan may ameliorate fibrosis, angiogenesis, inflammation, disease susceptibility, and oxidative stress via modulating TNF signaling pathway, which could be validated through clinical trials.

In conclusion, the collection of 25 articles in the Research Topic contributes to better understanding of natural products against renal fibrosis from the active compounds to underlying mechanisms and therapeutic targets. These studies provide promising and potential candidates against renal fibrosis by modulating novel pathways in clinical trial and animal experiment. Accompanying with the evolution of high throughput screening method and model, novel candidates and therapeutic targets will emerge to facilitate the drug discovery, which hold great potential for treatment with renal fibrosis.

AUTHOR CONTRIBUTIONS

YX wrote the manuscript of the editorial. D-QC and ZG amended and revised the final version. All authors contributed to the article and approved the submitted version.

Conflict of Interest: The authors declare that the research was conducted in the absence of any commercial or financial relationships that could be construed as a potential conflict of interest.

frontiers in Pharmacology

REVIEW
published: 16 August 2021
doi: 10.3389/fphar.2021.719880

Targeting the Wnt/β-Catenin Signaling Pathway as a Potential Therapeutic Strategy in Renal Tubulointerstitial Fibrosis

Shan-Shan Li[1,2], *Qian Sun*[1,2], *Meng-Ru Hua*[3], *Ping Suo*[3], *Jia-Rong Chen*[4], *Xiao-Yong Yu*[1]* *and Ying-Yong Zhao*[3]*

[1]Department of Nephrology, Shaanxi Traditional Chinese Medicine Hospital, Xi'an, China, [2]The First School of Clinical Medicine, Shaanxi University of Traditional Chinese Medicine, Xianyang, China, [3]Faculty of Life Science and Medicine, Northwest University, Xi'an, China, [4]Department of Clinical Pharmacy, Affiliated Hospital of Chengdu University, Chengdu, China

The Wnt/β-catenin signaling pathway plays important roles in embryonic development and tissue homeostasis. Wnt signaling is induced, and β-catenin is activated, associated with the development and progression of renal fibrosis. Wnt/β-catenin controls the expression of various downstream mediators such as snail1, twist, matrix metalloproteinase-7, plasminogen activator inhibitor-1, transient receptor potential canonical 6, and renin-angiotensin system components in epithelial cells, fibroblast, and macrophages. In addition, Wnt/β-catenin is usually intertwined with other signaling pathways to promote renal interstitial fibrosis. Actually, given the crucial of Wnt/β-catenin signaling in renal fibrogenesis, blocking this signaling may benefit renal interstitial fibrosis. There are several antagonists of Wnt signaling that negatively control Wnt activation, and these include soluble Fzd-related proteins, the family of Dickkopf 1 proteins, Klotho and Wnt inhibitory factor-1. Furthermore, numerous emerging small-molecule β-catenin inhibitors cannot be ignored to prevent and treat renal fibrosis. Moreover, we reviewed the knowledge focusing on anti-fibrotic effects of natural products commonly used in kidney disease by inhibiting the Wnt/β-catenin signaling pathway. Therefore, in this review, we summarize recent advances in the regulation, downstream targets, role, and mechanisms of Wnt/β-catenin signaling in renal fibrosis pathogenesis. We also discuss the therapeutic potential of targeting this pathway to treat renal fibrosis; this may shed new insights into effective treatment strategies to prevent and treat renal fibrosis.

Keywords: Wnt/β-catenin, chronic kidney disease, renal fibrosis, traditional Chinese medicine, natural product

OPEN ACCESS

Edited by:
Zhiyong Guo,
Second Military Medical University, China

Reviewed by:
Songyan Gao,
Shanghai University, China
Dong Wang,
Anhui University of Chinese Medicine, China

***Correspondence:**
Xiao-Yong Yu
gub70725@126.com
Ying-Yong Zhao
zyy@nwu.edu.cn

Specialty section:
This article was submitted to Renal Pharmacology, a section of the journal Frontiers in Pharmacology

Received: *03 June 2021*
Accepted: *03 August 2021*
Published: *16 August 2021*

Citation:
Li S-S, Sun Q, Hua M-R, Suo P, Chen J-R, Yu X-Y and Zhao Y-Y (2021) Targeting the Wnt/β-Catenin Signaling Pathway as a Potential Therapeutic Strategy in Renal Tubulointerstitial Fibrosis. Front. Pharmacol. 12:719880. doi: 10.3389/fphar.2021.719880

INTRODUCTION

Chronic kidney disease (CKD) is an increasingly serious public health problem due to its high prevalence and mortality and greatly increases the risk of end-stage renal disease (ESRD), and cardiovascular disease (Webster et al., 2017). Renal fibrosis is the final pathological, dynamic, progressive, and irreversible process common to any ongoing CKD or maladaptive repair (Djudjaj and Boor, 2019). Renal fibrosis is the accumulation of scars in the parenchyma that is a pathological expansion of the normal wound healing process, characterized by inflammation, myofibroblast activation, migration, and matrix deposition and remodeling, leading to the replacement of

functional parenchyma by fibrotic tissues (Humphreys, 2018; Distler et al., 2019). Renal interstitial fibrosis is mainly driven by various pro-fibrotic growth factors, forming a fibrotic microenvironment in the interstitial space (Chen et al., 2018c; Tang et al., 2019). In other words, the major pathological events of renal fibrosis include inflammatory cell infiltration, fibroblast activation and proliferation, and abnormal increase and excessive deposition of extracellular matrix (ECM) components, mainly composed of collagen, fibronectin, and proteoglycans (Liu et al., 2021). With the ECM continuous deposition, scar tissue replaces normal tissue, tubules, and peritubular capillaries are lost, resulting in disruption of tissue architecture and loss of renal function (Xing et al., 2021). Additionally, there is growing evidence that ECM-derived components could be used as danger-associated molecular patterns (DAMPs). As an important promoter of fibrogenesis, as long as the inflammatory stimulation persists, these DAMPs are generated and release signals during the phase cell activation and damage, ultimately promoting inflammation to fibrosis and kidney disease (Nastase et al., 2018).

The Wnt/β-catenin signaling pathway is an evolutionarily conserved developmental signaling pathway, playing an extremely important role in organogenesis, tissue homeostasis, and disease progression of multicellular organisms (Schunk et al., 2021). There are 19 identified encoding Wnt genes in the mammalian genome, all of which are cysteine-rich proteins (Langton et al., 2016). Wnt protein induces β-catenin-dependent signaling through Wnt receptor coiled Frizzled (FZD) and co-receptors low-density lipoprotein receptor-related protein-5/protein-6 (LRP5/6) (Janda et al., 2017). In addition, there are other receptors and co-receptors, including the tyrosine kinase receptors RYK, single transmembrane receptor tyrosine kinase, G-protein coupled receptor, etc., that trigger various downstream signaling pathways (Foulquier et al., 2018). Continuous accumulation of intracellular β-catenin signaling plays a crucial role in developing renal fibrosis, podocyte injury, proteinuria, persistent tissue damage during acute kidney injury, and cystic kidney diseases (Miao et al., 2019; Schunk et al., 2021). The latest research shows that given the crucial role of Wnt/β-catenin signaling in renal fibrogenesis, blocking this signaling may be beneficial to alleviate renal fibrosis (Xie et al., 2021; Yiu et al., 2021). Recent studies have shown that apigenin (API) could effectively relieve renal fibrosis via co-inhibiting uric acid (UA) reabsorption and the Wnt/β-catenin signaling pathway (Li et al., 2021). In addition, ischemia-reperfusion injury (IRI) could increase indoleamine-2,3-dioxygenase (IDO) expression to activate the Wnt/β-catenin pathway leading to renal fibrosis. Prostaglandin E2 (PGE2) could ameliorate kidney fibrosis via inhibiting IDO expression and reducing β-catenin resulting in lower expressions of α-smooth muscle actin (α-SMA), fibronectin (Pan et al., 2021). *In vivo* and *in vitro*, it has proved that the abnormally expressed cannabinoid receptor type 2 (CB2) is closely related to renal fibrosis via β-arrestin 1-induced β-catenin activation, and β-catenin could promote the activation and expression of CB2, and finally forms the vicious circle in the CB2/β-catenin pathway (Zhou et al., 2021). Therefore, it is of great significance to clarify the cellular and molecular mechanisms of the Wnt/β-catenin signaling pathway in tubulointerstitial fibrosis and provide a new treatment strategy for antifibrosis and delaying CKD progression. In this review, we summarize recent advances on the involvement of Wnt/β-catenin in the pathogenesis of tubulointerstitial fibrosis and the intervention effect of natural products targeting the Wnt/β-catenin signaling pathway.

WNT/β-CATENIN SIGNALING PATHWAYS

The mechanisms of Wnt signaling consist of two main branches: the canonical and non-canonical pathways (Schunk et al., 2021). The canonical pathway is also known as the Wnt/β-catenin pathway. Furthermore, two master non-canonical pathways are the Wnt/planar cell polarity pathway (Wnt/PCP pathway) and the Wnt/calcium pathway (Wnt/Ca^{2+} pathway) (Hu et al., 2020). According to downstream effects, all Wnt ligands are divided into two categories: one is canonical, Wnt ligands that induce β-catenin-dependent pathway, including Wnt1, 2, 3, 8a, 8b, 10a, and 10b, and the other is non-canonical, Wnt ligands that mediate β-catenin-independent pathway, including Wnt4, 5a, 5b, 6, 7a, 7b, and 11 (Acebron and Niehrs, 2016). In the canonical Wnt/β-catenin signaling pathway, Wnt molecules transmit the intracellular signal in the intracellular matrix through interacting with FZD receptors and the co-receptor LRP5/6 (**Figure 1**). FZD proteins have seven transmembrane receptors, with a cysteine-rich domain responsible for the binding of Wnt proteins (Schunk et al., 2021). Since the activation of LRP5/6 depends on the binding of the canonical Wnt ligands to the FZD receptors, they are considered to be the key co-receptors of the canonical Wnt signaling pathway (Huang et al., 2019). After that, the interaction triggers the intracellular signal cascade and promotes the accumulation of non-phosphorylated β-catenin, which translocates into the nucleus, and cooperates with the transcription factors T cell factor (TCF)/lymphatic enhancer-binding factor (LEF) to trigger the transcription of Wnt target genes (Tessa et al., 2020). β-Catenin is an important co-factor that binds multiple transcriptional molecules and mediates fibrogenic signaling pathways (Yang et al., 2021). In a steady-state, β-catenin is inactivated by a "destruction complex," which includes the proteins glycogen synthase kinase 3β (GSK3β), adenomatous polyposis coli (APC), casein kinase 1 (CK1), and axin (Wang et al., 2020a). The protein complex mediates the phosphorylation, ubiquitinylation, and degradation of β-catenin, and through continuous ubiquitination and degradation, the cytoplasmic levels are kept at a low level (Schunk et al., 2021). However, once Wnt ligands bind to co-receptors on cytomembrane, the combination of FZD and Dishevelled (DVL) could provide a recruitment platform for the β-catenin destruction (Gammons et al., 2016). DVL protein is recruited, and the 'destruction complex' is disrupted, protecting β-catenin from inactivation and degradation, thus leading to the stabilization, accumulation, and nuclear translocation of β-catenin (Nusse and Clevers, 2017). An increasing number of studies have demonstrated that fibroblast signaling pathways all merge on

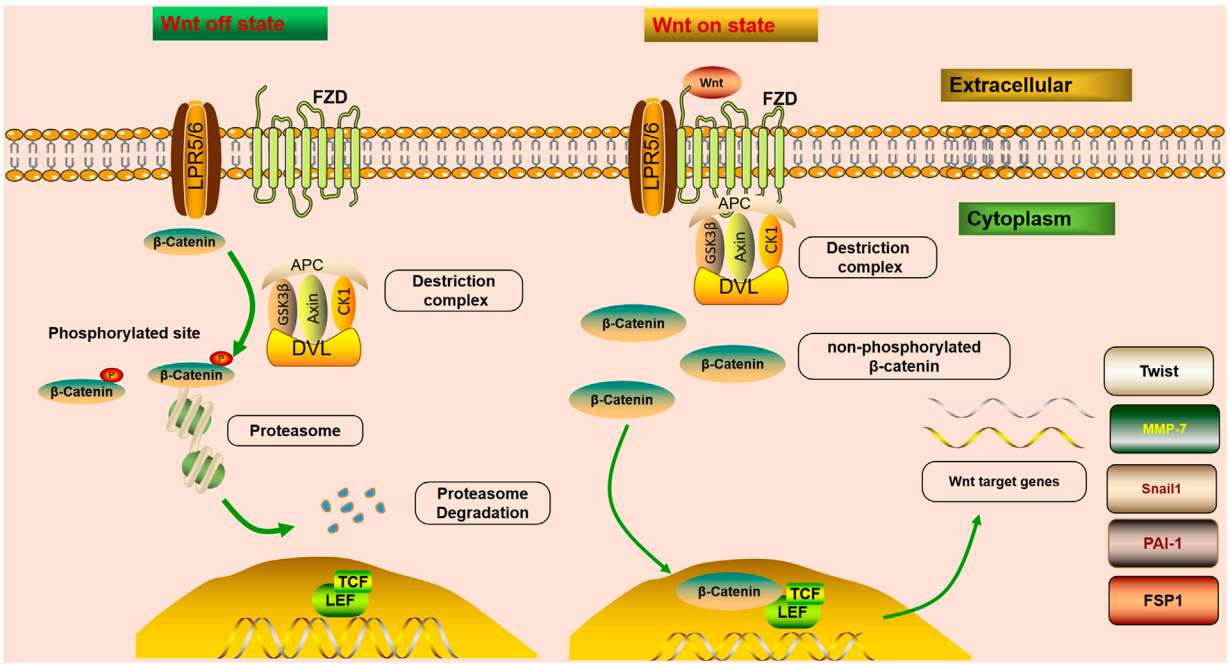

FIGURE 1 | Wnt/β-catenin signaling is off or on state. In steady-state, β-catenin is inactivated by a "destruction complex," and phosphorylation, ubiquitinylated, and degraded of β-catenin is mediated by the protein complex. Wnt on state; Wnt molecules transmit the intracellular signal in the intracellular matrix through interacting with FZD receptors and LRP5/6. After that, the interaction triggers the intracellular signal cascade and promotes the accumulation of non-phosphorylated β-catenin, which translocates into the nucleus, and cooperates with TCF/LEF to trigger the transcription of Wnt target genes. Once Wnt ligands bind to co-receptors on cytomembrane, the combination of FZD and DVL could provide a recruitment platform for the β-catenin destruction. Wnt/β-catenin controls the expression of various downstream mediators implicated in renal fibrosis, such as Snail1, MMP-7, PAI-1, Twist, and FSP1.

β-catenin to promote the β-catenin/TCF complex and mediate fibrogenesis (Yang et al., 2021). β-Catenin integrates the inputs of transforming growth factor β (TGF-β)/Smad, integrin/ILK, the Wnt/β-catenin pathway and renin-angiotensin system (RAS), which are activated in fibrotic primary and allograft kidney diseases (Huang et al., 2019).

WNT/β-CATENIN SIGNALING PATHWAY IN RENAL FIBROSIS

The Wnt/β-catenin pathway is one of the crucial signaling pathways resulting in kidney disease. An increasing number of studies have demonstrated that the activation of the Wnt/β-catenin signaling pathway serves a key role in promoting renal fibrosis by controlling the expression of various downstream mediators implicated in renal fibrosis (Chen et al., 2017b; Feng et al., 2019a; Schunk et al., 2021) (**Figure 1**). The transient activation of many signaling pathways has a beneficial effect on repairing damaged tissues. However, their sustained activation promotes fibrosis (Edeling et al., 2016). It has been confirmed that severe ischemia/reperfusion injury leads to sustained and excessive activation of Wnt/β-catenin, accompanied by interstitial myofibroblast activation and ECM deposition, characteristics of renal fibrotic lesions development (Xiao et al., 2016). Therefore, sustained and exaggerated Wnt/β-catenin activation mediates fibroblast activation. Although transient Wnt/β-catenin activation promotes tissue regeneration and repair after kidney injury, sustained or uncontrolled Wnt/β-catenin signaling stimulates podocyte injury and proteinuria, ultimately leading to irreversible renal fibrosis (Schunk et al., 2021).

Fibroblast

Fibroblasts are the main driving force for scar formation after kidney injury (Miao et al., 2021). The continuous activation of fibroblasts leads to the secretion of ECM components, such as collagen, proteoglycan, and fibronectin, leading to the development of renal fibrosis (Feng et al., 2019b). As an ECM glycoprotein, fibronectin serves a key role in wound healing and fibrosis by regulating the deposition of collagen and other ECM molecules. A study confirmed that upregulated Wnt/β-catenin signaling is related to the response of epithelial cells to wound, renal tubular cell damage, fibrous collagen, and immunoglobulin transcript expression (Venner et al., 2016). Thus, Wnt protein derived from renal tubules may play a critical role in fibroblast activation and renal fibrosis (Zhou et al., 2017). There is a complex regulatory network between renal tubular epithelial cells and fibroblasts, regulated by autocrine and paracrine Wnt/β-catenin signaling (Maarouf et al., 2016). The activated Wnt/β-catenin pathway can promote the fibroblast proliferation and differentiation of fibroblasts towards myofibroblasts; myofibroblasts are critical contributors to renal fibrosis. Their characteristics are secreting fibronectin and increasing the

expression of α-SMA (Zhou et al., 2017). In a high glucose environment, activating the Wnt/β-catenin pathway could promote renal mesangial cell proliferation and fibronectin production. Interestingly, fibronectin is an important target gene of Wnt/β-catenin (Zhang et al., 2014). Therefore, inhibiting the activity of Wnt/β-catenin signaling in fibroblasts may help alleviate the progression of renal fibrosis (Duan et al., 2020).

Macrophages

According to the activation mechanism and cell function, macrophages are divided into classically activated macrophages (M1) and alternatively activated macrophages (M2) (Wang et al., 2014a). M1, a pro-inflammatory phenotype, releases cytokines that inhibit the proliferation of surrounding cells and damage contiguous tissue, while M2, an anti-inflammatory phenotype, releases cytokines that promote the proliferation of contiguous cells and tissue repair (Wang et al., 2014a; Cosin-Roger et al., 2019). If macrophages fail to acquire a tissue-healing phenotype, dysregulated signals can be drivers of disease processes, such as sustained, exuberant inflammation and fibrosis (Smigiel and Parks, 2018). Thus, macrophages serve a key role in immune surveillance and in the maintenance of renal homeostasis. Macrophages recruited from the bone marrow can transition directly into myofibroblasts during renal injury. This process is defined as macrophage-to-myofibroblast transition, which may play a crucial role in the progression of chronic inflammation to pathogenic fibrosis (Tang et al., 2019). Sustained accumulation and activation of macrophages in kidney tissue could lead to the production of multiple pro-fibrotic cytokines and ultimately induce renal fibrosis. Additionally, as key inflammatory cells, macrophages could promote ECM synthesis and deposition, resulting in renal fibrosis by releasing inflammatory cytokines, TGF-β, and matrix-degrading enzyme inhibitors (Yang et al., 2019). Activation of Wnt/β-catenin signaling stimulates renal inflammation, comprising macrophages infiltration, pro-inflammatory cytokines release, and cell adhesion molecules expression in renal injury. Moreover, tubular cell-derived Wnt ligands mediate pro-inflammatory activation of renal macrophages during fibrosis (Wong et al., 2018). Previous studies have shown that the hyperactive of Wnt/β-catenin signaling could promote renal fibrosis by stimulating macrophage M2 polarization and promoting the proliferation and accumulation of macrophages. The continuous accumulation and activation of macrophages may lead to various fibrotic cytokines and ultimately lead to kidney fibrosis (Feng et al., 2018). Therefore, as an important source of Wnt protein in adult tissues, macrophages proliferate and accumulate in kidney tissues through the activation of the Wnt/β-catenin signal, considered a key factor in renal fibrosis (Cosin-Roger et al., 2019).

Snail1

Snail family zinc finger 1 (Snail1) is a transcription factor expressed during embryonic renal development and is widely expressed in various kidney injury models, including unilateral ureteral obstruction (UUO), 5/6 nephrectomy, and hypoxia. It is involved in regulating fatty acid metabolism, cell cycle arrest, and inflammatory response, major biological processes responsible for renal fibrogenesis (Simon-Tillaux and Hertig, 2017). Snail1 is a key transcription factor driving epithelial-mesenchymal transition (EMT); the stabilized β-catenin enters the cell nucleus, forms a complex with TCF, and activates the transcription of Snail1 to drive EMT. Moreover, the up-regulation of TGF-β1 promotes Snail1-mediated EMT of renal tubular epithelial cells during renal fibrosis. Not only that, but also Snail1 is a critical transcription target of β-catenin that upregulates β-catenin transcriptional activity; as such, both β-catenin and Snail1 may be activated simultaneously to produce an additive or synergistic effect in promoting EMT (García de Herreros and Baulida, 2012). Thus, the Snail1-induced EMT process is a key mechanism that initiates the reaction cascade leading to fibrosis (Bai et al., 2016). Additionally, it has been found in a modern study that the Snail1/β-catenin signaling pathway may be involved in promoting renal fibrosis related to diabetes (Kim et al., 2017). Furthermore, it has been demonstrated that Snail1s could interact with β-catenin functionally, thereby increasing the expression of Wnt-dependent target genes (Stemmer et al., 2008).

Matrix Metalloproteinase-7

MMP-7, also known as matrilysin, is a secreted zinc- and calcium-dependent endopeptidase, a transcriptional target of classic Wnt/β-catenin signaling, a pathological mediator, and therapeutic target of renal fibrosis (Wozniak et al., 2021). Under normal physiologic conditions, MMP-7 is almost not expressed in adult kidneys but upregulated in various renal diseases, including AKI and CKD (Wozniak et al., 2021). MMP-7 can degrade ECM components and cleave various substrates, such as E-cadherin, Fas ligand, and nephrin. Therefore, it plays a key role in regulating various biological processes, such as cell proliferation, apoptosis, EMT, and podocyte damage (Tan et al., 2019). Furthermore, MMP-7, via its proteolytic activity, mediates proteolytic degradation of E-cadherin, resulting in β-catenin liberation and activation, leading to renal fibrosis in a Wnt-independent fashion. It is worth noting that the release of β-catenin mediated by MMP-7 further induces the expression of MMP-7, eventually forming a vicious circle (Liu et al., 2020). In other words, on the one hand, activation of Wnt/β-catenin promotes the occurrence of fibrosis by upregulating pro-fibrotic mediators, including MMP-7, PAI-1. On the other hand, MMP-7, as the most powerful β-catenin downstream target, can activate the Wnt/β-catenin signaling pathway after renal injury (Tan et al., 2019). In summary, renal MMP-7 levels correlate with Wnt/β-catenin activity, and urinary MMP-7 may be a noninvasive biomarker of pro-fibrotic signaling in the kidney. However, in several AKI animal models (IRI, cisplatin administration, and folic-acid induced AKI), MMP7 exerts protective effects on the kidney as an adaptive response. Therefore, the role of MMP-7 as a therapeutic target for kidney disease needs further study.

Plasminogen Activator Inhibitor-1

PAI-1, as a member of the serine protease inhibitor family, interferes with ECM and fibrin degradation, mediated by urokinase-type plasminogen activator (uPA) and tissue-type plasminogen activator (tPA) to suppress fibrinolysis and contribute to interstitial fibrosis in the kidney injury (Flevaris and Vaughan, 2017). Increasing evidence shows the role of PAI1 in renal fibrosis (Zhou et al., 2015a). PAI-1 promotes fibrosis by participating in various cellular processes, such as inflammation, cell adhesion, and migration. Conversely, some specific factors that promote fibrosis, such as oxidative stress and hypoxia, could also affect the expression of the PAI-1 gene (Rabieian et al., 2018). And depleting PAI-1 can alleviate interstitial fibrosis by decreasing fibroblast activation and proliferation in the renal interstitium (Yao et al., 2019). Therefore, PAI-1, a key molecule in renal fibrosis progression, has increased expression in various kidney disease models (Hamasaki et al., 2013). In addition, a recent study indicated that PAI-1 could promote cell migration through LRP1-dependent β-catenin activation (Kozlova et al., 2015). Since the promoter region of PAI-1 contains a TCF/LEF binding site, PAI-1 is an important target gene of β-catenin signaling in renal injury (Malik et al., 2020).

Components of the Renin-Angiotensin System

The RAS serves a vital role in maintaining renal hemodynamics and the occurrence of hypertension and kidney disease (Navar, 2014). Unanimously, renal tissue RAS has various pathophysiological functions in regulating blood pressure, growth of kidney cells, and glomerular sclerosis, leading to renal fibrosis development (Urushihara et al., 2012). The (pro) renin receptor ((P)RR), consisting of 350 amino acids, has been considered as a single-transmembrane protein encoded by ATP6AP2, an X chromosome-located gene, and the transmembrane receptors enhance the tissue RAS by binding to their ligands renin and/or prorenin; therefore, it is initially considered to be an important part of the RAS and is ubiquitously expressed in the human body (Ramkumar and Kohan, 2016; Ichihara and Yatabe, 2019). The receptor plays crucial roles in various pathways, involved in extensive physiological and pathological processes, such as the cell cycle, autophagy, acid-base balance, energy metabolism, T cell homeostasis, blood pressure regulation, cardiac remodeling, and maintaining podocyte structure (Ichihara and Yatabe, 2019; Wang et al., 2020a). The Wnt-RAS signaling serves a vital role in the development and progression of CKD (Zhou et al., 2020). There are putative TCF/LEF binding sites in the RAS promoter region through bioinformatics analyses, and β-catenin could trigger LEF-1 to bind to these sites in renal tubular cells (Zhou et al., 2015b). In addition, (P)RR is necessary for signal transduction through FZD-LRP5/6 (Li et al., 2017). Moreover, accumulating evidence has demonstrated that (P)RR is a downstream target and a crucial element in Wnt signal transmission, promoting kidney damage and fibrosis through amplifying Wnt/β-catenin signaling transduction. In addition, Wnt/β-catenin, as the main upstream regulator, controls the expression of multiple RAS genes. In other words, the overactivity of β-catenin or different Wnt ligands leads to the expression of all RAS genes (Zhou and Liu, 2015; Zhao et al., 2018). Hence, targeting Wnt/β-catenin would concurrently inhibit all RAS genes, accordingly suppressing inflammation and alleviating renal fibrosis (Zhou and Liu, 2016). Studies have demonstrated that the fibrogenic action of Wnt/β-catenin is dependent on RAS activation, and Wnt/β-catenin regulates multiple RAS genes. At the same time, RAS can induce the expression of multiple Wnt genes *in vivo* and *in vitro*; as such, the Wnt/β-catenin-RAS axis can be known as a vicious circle in aggravating the renal injury (Xiao et al., 2019).

Transient Receptor Potential Canonical 6

TRPC6 has been implicated in the pathogenesis of kidney diseases, including focal segmental glomerulosclerosis (FSGS), diabetic nephropathy (DN), immune-mediated kidney disease, and renal fibrosis. As a result, TRPC6 has become a critical target of therapeutic agents to prevent and treat various kidney diseases (Hall et al., 2019). TRPC6 is another transcriptional target of the Wnt/β-catenin signaling cascade, and the Wnt/β-catenin signaling pathway may potentially be active in the pathogenesis of TRPC6-mediated diabetic podocyte injury (Zhang et al., 2013; Kim and Dryer, 2021). TRPC6 knockout shows protection on UUO-triggered kidney tubulointerstitial injury, interstitial fibrosis, and α-SMA expression (Gu et al., 2020). Mutations and over-activation in TRPC6 channel activity play an important role in podocyte damage in DN(Staruschenko et al., 2019; Wang et al., 2020c), However its role in renal fibrosis and the interaction with the Wnt signaling pathway in renal fibrosis still need further study.

In summary, the Wnt/β-catenin signaling pathway could activate renal fibrosis-related cytokines and up-regulate the expression of downstream target genes, eventually inhibit the main pathological process in the fibrosis process, and improve renal fibrosis. Therefore, we can further explore the downstream targets of the Wnt/β-catenin signaling pathway on this basis to further improve the mechanism of the Wnt/β-catenin signaling pathway in renal fibrosis.

THE CROSSTALK BETWEEN WNT/β-CATENIN AND OTHER SIGNALING PATHWAYS ON RENAL INTERSTITIAL FIBROSIS

Various pathways intersect and regulate each other to induce appropriate responses to a series of complex stimuli. Therefore, the synergy between other pathological signaling pathways and Wnt may play an important role in promoting renal fibrosis. RNA sequencing showed that deleting TGF-β receptors in proximal renal tubular cells regulated many growth factor pathways, but Wnt/β-catenin signaling is the most affected pathway due to the activity of β-catenin that is impaired *in vivo* and *in vitro* (Nlandu-Khodo et al., 2017). The participation of the Wnt signaling pathway enhances the pro-fibrotic effect of

the TGF-β signaling pathway (Yang et al., 2020). In hypoxic pathological damage of organs, overactivation hypoxia-inducible factor-1α (HIF-1α) activates the Wnt/β-catenin signaling pathway, thereby aggravating renal interstitial fibrosis development (Qi et al., 2017). Although the Hedgehog (HH) signaling pathway is considered upstream of the Wnt/β-catenin signaling pathway, there is overlap between the two phenotypic results, suggesting a synergistic effect. Wnt and Notch interact mostly synergistically in the stem cell and epithelial cell compartment to trigger fibrosis development via suppressing epithelial differentiation; Notch, as a negative regulator of the Wnt/β-catenin signaling pathway, promotes β-catenin degradation by establishing a complex with β-catenin (Edeling et al., 2016; Chatterjee and Sil, 2019). However, the mechanism of the interaction between the signaling pathways is still unclear, and the studies on the mechanism of their synergy with the Wnt/β-catenin signaling pathway should be further explored.

TARGETING WNT/β-CATENIN SIGNALING AS A THERAPEUTIC POTENTIAL FOR RENAL FIBROSIS

Accumulating evidence has demonstrated that inhibiting the Wnt signaling pathway could alleviate renal interstitial fibrosis by attenuating apoptosis and expression of fibrosis-associated markers in renal cells (Ren et al., 2019; Cai et al., 2020; Huang et al., 2020). Endogenous Wnt inhibitors can negatively regulate the Wnt signaling pathway by binding to Wnt ligands competitively with Wnt receptors or co-receptors, such as Dickkopf1 (DKK1), secreted frizzled protein 1 (Sfrp1), Wnt inhibitor 1 (Wif-1), Klotho (Kawazoe et al., 2021). In addition, exogenous Wnt signaling inhibitors accompanied by natural products cannot be ignored to prevent and treat renal fibrosis. Collectively, the Wnt/β-catenin signaling pathway may serve as a potential treatment strategy for renal fibrotic disorders.

Endogenous Wnt Inhibitors

Secreted Frizzled-Related Protein1

Humans have five secreted frizzled-related proteins (Sfrp1-5) with cysteine-rich domains (CRD), and these Sfrps have a strong homology with FZD receptors, therefore compete with FZD receptors for Wnt binding. In other words, Sfrps act as a Wnt inhibitor. The Sfrp family consists of secreted glycoproteins that can competitively bind to Wnt, inhibiting the canonical and non-canonical Wnt signaling pathways (Cruciat and Niehrs, 2013). Studies have confirmed that Sfrp1 regulates cell proliferation and differentiation by regulating Wnt/β-catenin signaling, showing low expression in various tumor tissues (Qiao et al., 2017). Thus, Sfrp1 is a Wnt antagonist that acts as a negative regulator of Wnt/β-catenin signaling and serves a key role in fibrotic diseases. In the mouse model of UUO, knockout of Sfrp1 significantly increases the expression of α-SMA and the protein level of vimentin; meanwhile, it decreases the protein level of E-cadherin, which enhances the epithelial to mesenchymal transition (Matsuyama et al., 2014). Additionally, down-regulation of Sfrp1 activates the Wnt/β-catenin signaling pathway, increased ECM deposition, eventually lead to renal fibrosis. Therefore, Sfrp1 acts as a negative regulator of the Wnt signaling pathway and suppresses renal fibrosis via inhibiting the Wnt/β-catenin signaling pathway.

Klotho

Klotho, an anti-aging protein, reduces renal fibrosis after AKI. Klotho serves a key role in regulating various cellular processes by interacting with multiple signaling molecules, including oxidative stress, fibrosis, inflammation, autophagy, and apoptosis (Hu et al., 2013). Therefore, Klotho is a critical gene, controlling aging and kidney homeostasis, and an ideal intervention target for various kidney diseases and even extrarenal complications (Xia and Cao, 2021). Furthermore, Klotho plays an important role in anti-fibrotic activities by inhibiting oxidative stress and excessive inflammation. Hence, Klotho deficiency enhances renal fibrosis (Lindberg et al., 2014). It has been shown that the extracellular domain of Klotho inhibits Wnt signaling via binding to multiple Wnt ligands (Muñoz-Castañeda et al., 2020). Thus, Klotho is a critical negative regulator of canonical Wnt signaling and suppresses renal fibrosis in the obstructed kidney model by simultaneously suppressing multiple growth factor signaling pathways such as fibroblast growth factor-2 (FGF-2), Wnt, and TGF-β1 (Guan et al., 2014). A study has found that Klotho represses the Wnt/β-catenin pathway in renal tubular epithelial cells (TECs) to exert a stronger anti-fibrotic effect (Zhang et al., 2018a). Wnt/β-catenin activation is considered to be the key factor resulting in Klotho downregulation (Muñoz-Castañeda et al., 2017). In addition, the upregulation of Klotho prevents Wnt activation, thereby inhibiting the deposition of ECM and reducing the transcription of cytokines, ultimately improving renal fibrosis (Zhou L. et al., 2013). Therefore, Klotho is termed an antagonist of endogenous Wnt/β-catenin activity, and increasing Klotho levels could be a strategy to reduce the morbidity and mortality of kidney-related diseases (Muñoz-Castañeda et al., 2020).

Dickkopf 1

DKK1 is an important member of the DKK family (DKK1, DKK2, DKK3, DKK4) and is widely expressed in many fields. It has been considered a secreted protein that can suppress the Wnt signaling transduction pathway (Huang et al., 2018). DKK1 may play a crucial role in the fibrotic process in several organs such as the liver, lungs, and kidneys (Klavdianou et al., 2017). Gene therapy using DKK1 significantly suppresses fibroblast-specific protein 1(fsp1), a marker for fibroblasts and myofibroblasts, type I collagen, and fibronectin mRNA in the model of obstructive nephropathy, thereby repressing the activation of myofibroblast and improving renal fibrosis (He et al., 2009). *In vivo*, DKK1 effectively inhibited inflammation and fibrosis associated with ureteral obstruction (Johnson et al., 2017). DKK1 can inhibit the canonical Wnt signaling pathway through binding to LRP5/6, as well as interrupting the formation of the LRP and Wnt protein complex. (Hou et al., 2021), Therefore, DKK1 is termed an inhibitor of canonical Wnt/β-catenin signaling (Lipphardt et al., 2019). As a Wnt

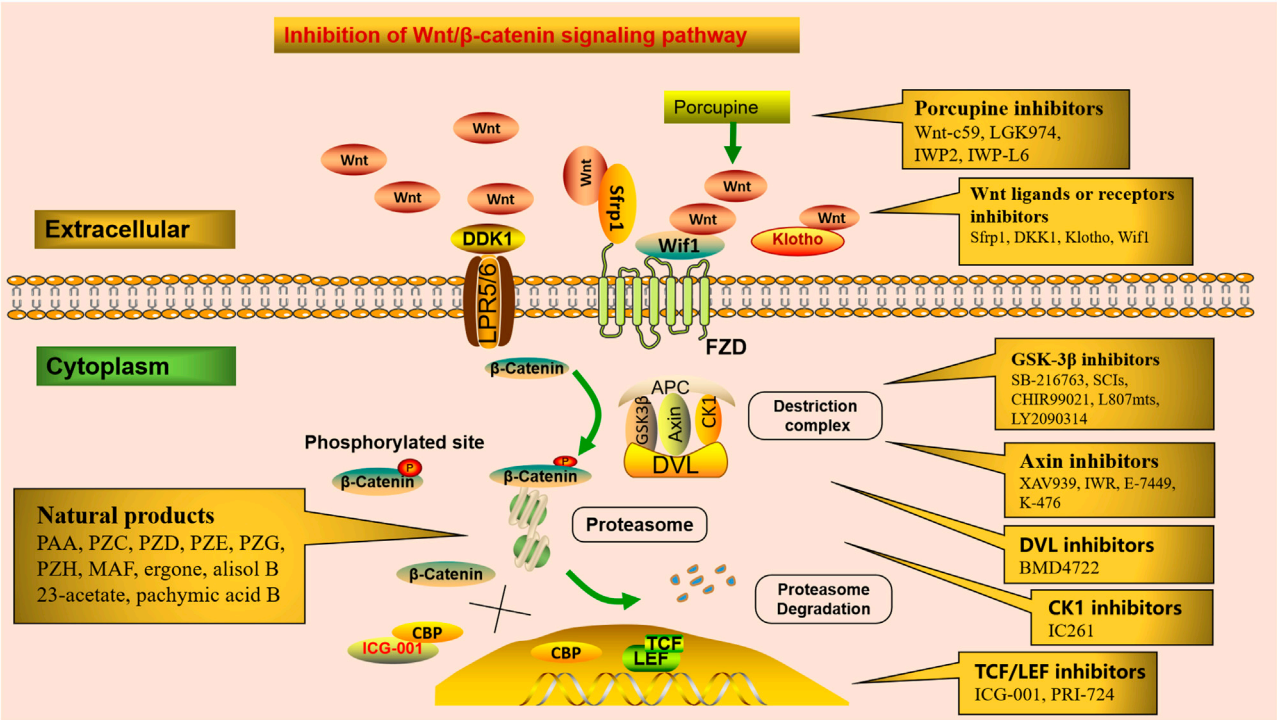

FIGURE 2 | Potential therapeutic targets in the Wnt/*β*-catenin signaling. Numerous small molecules inhibit Wnt/*β*-catenin signaling at different steps of the pathway. Porcupine inhibitors prevent Wnt ligands secretion. Receptor or co-receptor inhibitors prevent the receptor actions of Wnt ligands. Inhibitors of GSK3*β*, axin, DVL, and CK1 interfere with Wnt/*β*-catenin downstream signaling. Inhibitors of TCF/LEF suppress Wnt/*β*-catenin-dependent gene transcription. Several natural products alleviate renal fibrosis by regulating the Wnt/*β*-catenin signaling pathway.

antagonist, DKK1 blocks Wnt-mediated fibrosis and also down-regulates its expression under fibrotic conditions. Therefore, it is termed a comprehensive regulator of the Wnt signaling pathway and has been proven to participate in renal fibrosis, glucose metabolism, and inflammation (Huang et al., 2018). Overall, there is no doubt that the outlook for DKK1 target therapy is promising. DKK1, DKK2, and DKK4 act as Wnt antagonists by directly binding to LRP5/6, thereby inhibiting Wnt/*β*-catenin-dependent signaling (Joiner et al., 2013). However, in UUO rat models and adenine-induced nephropathy, DKK3 is a major driver of renal fibrosis (Federico et al., 2016), and the exact role of DKK3 on Wnt/*β*-catenin signaling remains poorly unclear.

Wnt Inhibitor Factor 1

Wif-1 is an antagonist of the Wnt signaling pathway, inhibiting the Wnt signaling pathway by binding to the Wnt ligand. Hypermethylation of the Wif-1 promoter leads to down-regulation of Wif-1 expression, which activates the Wnt signaling pathway, further promotes cell proliferation, and induces cell apoptosis (Lin et al., 2017). On the contrary, the recovered Wif-1 expression level inhibits the Wnt signaling pathway. In fibroblasts from Systemic sclerosis (SSc) patients, an autoimmune disease characterized by extensive visceral organ and skin fibrosis, expression of Wif-1 is decreased. And knockdown of Wif-1 in normal fibroblasts induces Wnt signaling and collagen production (Svegliati et al., 2014). In the prevention and treatment of various diseases, Wif-1 plays an important role in inhibiting cell proliferation and migration by inhibiting the Wnt/*β*-catenin signaling pathway, but its role in renal fibrosis needs further study.

Exogenous Wnt Inhibitors

The Wnt/*β*-catenin signaling pathway can be therapeutically targeted at several steps (**Figure 2**). Firstly, blocking the production of all active Wnts. Porcupine (PORCN) is a membrane-bound O-acyltransferase required for Wnt palmitoylation, secretion, and biologic activity, and PORCN inhibitors prevent the release of Wnt ligands, such as Wnt-c59, LGK974(Wnt-974), IWP2, and IWP-L6 (Moon et al., 2017). Secondly, inhibitors of GSK3*β*, axin, DVL, and CK1 interfere with Wnt/*β*-catenin downstream signaling. Numerous studies have shown that GSK-3*β* activation plays a wide spectrum of important roles in tissue fibrosis (Zhuang et al., 2018; Zeng et al., 2019). SB-216763, a GSK-3*β* inhibitor, protects against Aldo-induced renal injury by activating autophagy and might be a therapeutic option for renal fibrosis (Zhang et al., 2018b). Substrate competitive inhibitors (SCIs), a novel small molecule GSK-3 inhibitor, is considered to be highly selective and more suitable for clinical practice (Rippin et al., 2020). In addition, CHIR99021 (Ng-Blichfeldt et al., 2019), L807mts, (Licht-Murava et al., 2016) and LY2090314 (Tu et al., 2017) have been produced

as emerging small molecule inhibitors of GSK-3β. Tankyrase (Tnks) is a transferase that targets axin for proteasome degradation, and loss of Tnks activity leads to accelerated β-catenin destruction. XAV939 and inhibitors of Wnt response (IWR) act as Tankyrase inhibitors, which ultimately promote β-catenin degradation and inhibit Wnt/β-catenin signaling transcription (Kulak et al., 2015). In addition, E-7449 (Plummer et al., 2020) and K-476 (Kinosada et al., 2021), as new inhibitors of Tnks, have been widely used in anti-tumor therapy, and their anti-fibrotic mechanism needs to be further studied. BMD4722 specifically inhibits DVL by inhibiting the protein-protein interaction approach (Ma et al., 2018). IC261 is discovered as an ATP-competitive inhibitor of CK1 (Xian et al., 2021). Finally, inhibitors of TCF/LEF prevent Wnt/β-catenin-dependent gene transcription. CREB-binding protein (CBP) acts as a co-activator of multiple transcription factors for Wnt signal transduction formed with TCF. ICG-001, a small-molecule β-catenin inhibitor, inhibits the canonical Wnt/β-catenin signaling pathway by binding to CBP and blocking the interaction between β-catenin and CBP (Akcora et al., 2018). It inhibits renal tubular EMT by suppressing the transcription of a series of β-catenin-driven genes, such as Snail1, PAI-1, collagen I, fibronectin, and RAS, thereby ameliorates interstitial myofibroblast activation, represses matrix deposition, relieves proteinuria, ameliorates kidney inflammation, and alleviates fibrosis and exerts renal protection (Xiao et al., 2019). In a UUO murine model, ICG-001 could reduce the macrophage-to-myofibroblast transition of bone marrow-derived macrophages in renal fibrosis by inhibiting the β-catenin/TCF interaction (Yang et al., 2019). Therefore, ICG-001 not only prevents but reverses established fibrosis (Henderson et al., 2010). Moreover, PRI-724, as a selective inhibitor of CBP/β-catenin interaction, specifically destroys the interaction between β-catenin and CBP and has an encouraging effect in anti-liver fibrosis (Nishikawa et al., 2018).

Specific Inhibition of Wnt/β-Catenin Signaling by Natural Products

Modern clinical pharmacological studies have confirmed that Chinese herbal medicines (CHMs) have a wide range of biological activities and play a broad and important role in regulating immune function by exerting their anti-cancer, anti-inflammatory, and anti-fibrosis effects (Zhao, 2013; Chen et al., 2016; Chen et al., 2018a; Wu et al., 2021). Clinical trials and experimental studies have shown that CHMs have great advantages in reducing proteinuria and improving renal function, by focusing on the anti-inflammatory, anti-oxidative, anti-apoptotic and anti-fibrotic effects (Chen et al., 2019a; Miao et al., 2020; Wang et al., 2020b; Wang et al., 2021a; Wang et al., 2021b). In addition, CHMs play a vital role in alleviating renal fibrosis by regulating the Wnt/β-catenin signaling pathway (Liu et al., 2019; Dai et al., 2020).

"Concept of holism" and "treatment based on syndrome differentiation" are the basic principles of traditional Chinese medicine (TCM) throughout the treatment of diseases. A study confirmed that *Qishen Yiqi dripping pill (QYDP)* reduces the renal Wnt1, β-catenin, TGF-β1, and Smad2 gene expression and downregulates collagen I, α-SMA, and fibronectin expression significantly in diabetic rats. The study results showed that *QYDP* ameliorates kidney function and renal fibrosis in diabetic rats by repressing the Wnt/β-catenin and TGF-β/Smad2 signaling pathways (Zhang et al., 2020). *Qingshen Buyang Formula* significantly reduces the expression of collagen I and fibronectin, the main components of ECM. Furthermore, by inhibiting EMT and Wnt/β-catenin signaling pathway, it improves renal injury and relieves renal fibrosis (Zhang et al., 2019). *Zhen-Wu-tang* alleviates adenine-induced chronic renal failure (CRF) by regulating the canonical Wnt4/β-catenin signaling, associated with improvement of renal fibrosis because it suppresses the overexpression of collagen IV and fibronectin, two key components of fibrosis (La et al., 2018). *Huang Gan Formula* is a new prescription developed and simplified based on *uremia clearing granule* and the theoretical basis of TCM. *HGF* inhibits the Wnt/β-catenin signaling pathway, significantly reducing glomerulosclerosis and tubular interstitial fibrosis and improving residual renal function (Mo et al., 2015).

Several compounds isolated from natural products promote urination and eliminate edema, which greatly benefits renal disease and fibrosis (Zhao et al., 2009; Zhao et al., 2012a; Zhao L. et al., 2013; Zhao Y.-Y. et al., 2013; Tian et al., 2014; Zhao et al., 2014). As an edible mushroom, *Poria Cocos* is widely used for diuretic, anti-inflammatory, antioxidant, lipid-lowering, and anti-fibrotic effects (Zhao et al., 2012b; Feng et al., 2013; Wang et al., 2013b; Miao et al., 2016; Chen et al., 2019b; Feng et al., 2019c). Poricoic acid A (PAA), as the main triterpenoid compound of *Poria Cocos*, exhibits renoprotective effects, (Chen et al., 2019c; Feng et al., 2019a; Chen et al., 2020a) and PAA showed anti-fibrotic effects via regulating the Wnt/β-catenin pathway (Chen et al., 2019d). In the HK-2 cell and UUO model, *poricoic acid ZC (PZC)*, *poricoic acid ZD (PZD),* and *poricoic acid ZE (PZE)* could alleviate renal fibrosis by effectively blocking RAS by simultaneously targeting multiple RAS components, correlated with activation of Wnt/β-catenin pathways (Wang et al., 2018a). Additionally, *poricoic acid ZG (PZG)* and *poricoic acid ZH (PZH)* significantly suppress the activation of Wnt/β-catenin signaling and relieve renal fibrosis (Wang et al., 2018b). 25-O-methylalisol F is a new tetracyclic triterpenoid compound isolated from the *Alismatis rhizome* that exhibits renoprotective effects (Chen et al., 2014; Feng et al., 2014; Tian et al., 2014; Dou et al., 2018), and is a novel RAS inhibitor by simultaneously targeting multiple RAS components (Chen et al., 2018b). Ergone, alisol B 23-acetate, and pachymic acid B inhibit ECM accumulation, suppress oxidative stress and inflammation, and regulates the Wnt/β-catenin signaling pathway (Zhao et al., 2011; Chen et al., 2017a; Chen et al., 2019e; Chen et al., 2020b).

Curcumin alleviated ECM accumulation in diabetic nephropathy by down-regulating Wnt/β-catenin signaling and rescued diabetic renal injury (Ho et al., 2016). *Salvia miltiorrhiza* extracts relieve renal injury by suppressing the relative expression levels of wnt4, β-catenin, and TGF-β in renal tissue (Xiang et al., 2019). *Salidroside* protects against T1DM-induced kidney injury and renal fibrosis by ameliorating TGF-β1 and the Wnt1/3a/

TABLE 1 | Summary of small molecular inhibitors of Wnt/β-catenin signaling.

Inhibitors	Targets	Effect	Reference(s)
Sfrp1	FZD	Ameliorates renal fibrosis	Henderson et al. (2020)
Klotho	Wnt ligands	Ameliorates renal fibrosis	Zhang et al. (2018a)
DDK1	LRP5/6	Ameliorates renal fibrosis	Lipphardt et al. (2019)
Wif1	Wnt ligands	Ameliorates fibrosis	Lin et al. (2017)
Wnt-c59	PORCN	Prevents Wnt ligands secretion	Proffitt et al. (2013)
LGK974	PORCN	Prevents Wnt ligands secretion	Moon et al. (2017)
IWP2	PORCN	Prevents Wnt ligands secretion	Wang et al. (2013a)
IWP-L6	PORCN	Prevents Wnt ligands secretion	Wang et al. (2013a)
SB-216763	GSK-3β	Inhibits Wnt signaling	Zhang et al. (2018b)
SCIs	GSK-3β	Inhibits Wnt signaling	Rippin et al. (2020)
CHIR99021	GSK-3β	Inhibits Wnt signaling	Ng-Blichfeldt et al. (2019)
L807mts	GSK-3β	Inhibits Wnt signaling	Licht-Murava et al. (2016)
LY2090314	GSK-3β	Inhibits Wnt signaling	Tu et al. (2017)
XAV939	Tnks and axin	Inhibits Wnt signaling	Kulak et al. (2015)
IWR	Tnks and axin	Inhibits Wnt signaling	Kulak et al. (2015)
E-7449	Tnks and axin	Inhibits Wnt signaling	Plummer et al. (2020)
K-476	Tnks and axin	Inhibits Wnt signaling	Kinosada et al. (2021)
BMD4722	DVL	Inhibits Wnt signaling	Ma et al. (2018)
IC261	CK1	Inhibits Wnt signaling	Xian et al. (2021)
ICG-001	CBP	Inhibits Wnt signaling	Akcora et al. (2018)
PRI-724	CBP	Inhibits Wnt signaling	Nishikawa et al. (2018)
PAA	Wnt/β-catenin signaling	Ameliorates fibrosis	Chen et al. (2019a)
PZC	Wnt/β-catenin signaling	Ameliorates fibrosis	Wang et al. (2018a)
PZD	Wnt/β-catenin signaling	Ameliorates fibrosis	Wang et al. (2018b)
PZE	Wnt/β-catenin signaling	Ameliorates fibrosis	Wang et al. (2018a)
PZG	Wnt/β-catenin signaling	Ameliorates fibrosis	Wang et al. (2018a)
PZH	Wnt/β-catenin signaling	Ameliorates fibrosis	Wang et al. (2018b)
MAF	Wnt/β-catenin signaling	Inhibits RSA	Chen et al. (2018a)
Ergone	Wnt/β-catenin signaling	Repress ECM accumulation	Chen et al. (2017a)
Alisol B 23-acetate	Wnt/β-catenin signaling	Repress ECM accumulation	Chen et al. (2017b)
Pachymic acid B	Wnt/β-catenin signaling	Repress ECM accumulation	Chen et al. (2017a)
Curcumin	Wnt/β-catenin signaling	Repress ECM accumulation	Ho et al. (2016)
Salvia	Wnt/β-catenin signaling	Relieve renal injury	Xiang et al. (2019)
Salidroside	Wnt/β-catenin signaling	Ameliorates fibrosis	Shati and Alfaifi (2020)
TW	Wnt/β-catenin signaling	Relieve renal injury	Chang et al. (2018)
Triptonide	Wnt/β-catenin signaling	Relieve renal injury	Chinison et al. (2016)
AS-IV	Wnt/β-catenin signaling	Ameliorates fibrosis	Wang et al. (2014a)
Quercetin	Wnt/β-catenin signaling	Ameliorates fibrosis	Ren et al. (2016)

β-catenin signaling pathway (Shati and Alfaifi, 2020). It has been demonstrated that *Tripterygium wilfordii* treatment inhibits the upregulation of Wnt1 and β-catenin expression in hyperglycemia-induced kidney tissue and attenuates the renal injury in rats caused by diabetes (Chang et al., 2018). *Triptonide* can effectively inhibit canonical Wnt/β-catenin signaling by targeting the downstream C-terminal transcription domain of β-catenin or a nuclear component associated with β-catenin (Chinison et al., 2016). *Astragaloside IV* has been shown to have possible inhibitory effects on renal interstitial fibrosis by effectively inhibiting the upregulation of proteins in the Wnt/β-catenin signaling pathway in UUO model rats (Wang et al., 2014b). Quercetin inhibits β-catenin signaling transduction, thereby inhibiting the activation of fibroblasts and renal fibrosis (Ren et al., 2016).

In short, based on the findings described above, the Wnt/β-catenin signaling pathway can be therapeutically targeted at several steps. Lots of emerging small molecule inhibitors that target Wnt and/or β-catenin are under development (**Table 1**). Additionally, the natural products, active ingredients, crude extracts, and traditional Chinese medicine formulas play an important role in anti-kidney fibrosis by inhibiting the Wnt/β-catenin signaling pathway. However, the specific molecular mechanisms of numerous inhibitors still need in-depth study, and more inhibitors need to be further developed.

CONCLUDING REMARKS

In summary, Wnt/β-catenin signaling plays a role in the pathogenesis of renal interstitial fibrosis, and targeting this pathway to treat renal fibrosis could yield positive results. Accumulating evidence has demonstrated that the role of Wnt/β-catenin signaling in the process of kidney repair and regeneration after AKI cannot be ignored (Kuure et al., 2007; Lasagni et al., 2015; Zhou et al., 2016; Jiao et al., 2017), and activating Wnt/β-catenin signaling could alleviate AKI (Li et al., 2020). A moderate increase in Wnt/β-catenin signaling is beneficial, but excessive activation of this pathway could trigger renal fibrosis (Guo et al., 2019; Sun et al., 2020). In

addition, early intervention, but not late with β-catenin inhibitor significantly attenuates the apoptosis and inflammation induced by aristolochic acid (AA) (Kuang et al., 2021). Therefore, the dual role of Wnt/β-catenin signaling in CKD needs further study. And more researches are required to determine whether this pathway should be augmented in AKI to CKD. If so, the optimal treatment duration and the safe and effective dose also need to be determined.

At present, there are many studies on the Wnt/β-catenin signaling pathway. However, the mechanism of the non-canonical Wnt pathway in renal fibrosis still needs further investigation; Additionally, there are few clinical studies targeting Wnt/β-catenin signaling pathway to treat renal fibrosis, which is also the direction of our future efforts. since an FZD receptor can interact with different Wnt ligands to activate the Wnt pathway, coupled with the presence of several Wnt ligands. Therefore, understanding the selective binding of each Wnt protein to a specific FZD receptor and the resulting cascade reaction requires further research; Many signaling pathways play an important role in the process of renal fibrosis. However, the studies on the mechanism of their synergy with the Wnt/β-catenin signaling pathway should be further explored. In addition, a better understanding of the interactions between these pathways is needed to identify key molecules that regulate their interactions, which may serve as potential therapeutic targets; More small molecules that inhibit Wnt/β-catenin signaling are in development, which will explore more strategies to regulate this signaling pathway and provide more options for the effective therapies of renal fibrosis. The traditional Chinese medicine compound formula for the effective treatment of renal fibrosis is complex, and the active ingredients of Chinese medicine monomers or extracts are unknown. Therefore, the advantages of emerging natural products, CHMs, or new drugs in anti-renal fibrosis still need long-term research. Furthermore, to fully clarify the therapeutic effect of natural products in renal fibrosis, there is an urgent need to conduct studies that pay attention to identifying active ingredients, exploring action mechanisms, and rigorous pharmacological evaluation to ensure safety and accord the standards for clinical use. In conclusion, Wnt/β-catenin provides a broad prospect for treating renal interstitial fibrosis, but the understanding of Wnt/β-catenin remains a significant challenge.

AUTHOR CONTRIBUTIONS

Y-YZ, X-YY, and J-RC were responsible for the conception. S-SL wrote the manuscript. S-SL and QS prepared the figures and tables. M-RH and PS are responsible for revising. Y-YZ and X-YY checked the article. S-SL were responsible for the final approval of the version to be submitted. All authors read and approved the final manuscript.

FUNDING

This study was supported by the Shaanxi Key Science and Technology Plan Project (No. 2019ZDLSF04-04-02), National Natural Science Foundation of China (Nos. 82074002, 81673578, 81872985), and National Key Research and Development Project of China (No. 2019YFC1709405).

REFERENCES

Acebron, S. P., and Niehrs, C. (2016). β-Catenin-Independent Roles of Wnt/LRP6 Signaling. *Trends Cel Biol.* 26 (12), 956–967. doi:10.1016/j.tcb.2016.07.009

Akcora, B. Ö., Storm, G., and Bansal, R. (2018). Inhibition of Canonical WNT Signaling Pathway by β-catenin/CBP Inhibitor ICG-001 Ameliorates Liver Fibrosis *In Vivo* through Suppression of Stromal CXCL12. *Biochim. Biophys. Acta (Bba) - Mol. Basis Dis.* 1864 (3), 804–818. doi:10.1016/j.bbadis.2017.12.001

Bai, X., Geng, J., Zhou, Z., Tian, J., and Li, X. (2016). MicroRNA-130b Improves Renal Tubulointerstitial Fibrosis via Repression of Snail-Induced Epithelial-Mesenchymal Transition in Diabetic Nephropathy. *Sci. Rep.* 6, 20475. doi:10.1038/srep20475

Cai, J., Liu, Z., Huang, X., Shu, S., Hu, X., Zheng, M., et al. (2020). The Deacetylase Sirtuin 6 Protects against Kidney Fibrosis by Epigenetically Blocking β-catenin Target Gene Expression. *Kidney Int.* 97 (1), 106–118. doi:10.1016/j.kint.2019.08.028

Chang, B., Chen, W., Zhang, Y., Yang, P., and Liu, L. (2018). Tripterygium Wilfordii Mitigates Hyperglycemia-Induced Upregulated Wnt/β-Catenin Expression and Kidney Injury in Diabetic Rats. *Exp. Ther. Med.* 15 (4), 3874–3882. doi:10.3892/etm.2018.5901

Chatterjee, S., and Sil, P. C. (2019). Targeting the Crosstalks of Wnt Pathway with Hedgehog and Notch for Cancer Therapy. *Pharmacol. Res.* 142, 251–261. doi:10.1016/j.phrs.2019.02.027

Chen, D.-Q., Cao, G., Chen, H., Argyopoulos, C. P., Yu, H., Su, W., et al. (2019c). Identification of Serum Metabolites Associating with Chronic Kidney Disease Progression and Anti-fibrotic Effect of 5-methoxytryptophan. *Nat. Commun.* 10 (1), 1476. doi:10.1038/s41467-019-09329-0

Chen, D.-Q., Cao, G., Chen, H., Liu, D., Su, W., Yu, X.-Y., et al. (2017a). Gene and Protein Expressions and Metabolomics Exhibit Activated Redox Signaling and Wnt/β-Catenin Pathway Are Associated with Metabolite Dysfunction in Patients with Chronic Kidney Disease. *Redox Biol.* 12, 505–521. doi:10.1016/j.redox.2017.03.017

Chen, D.-Q., Cao, G., Zhao, H., Chen, L., Yang, T., Wang, M., et al. (2019b). Combined Melatonin and Poricoic Acid A Inhibits Renal Fibrosis through Modulating the Interaction of Smad3 and β-catenin Pathway in AKI-To-CKD Continuum. *Ther. Adv. Chronic Dis.* 10, 204062231986911. doi:10.1177/2040622319869116

Chen, D.-Q., Feng, Y.-L., Cao, G., and Zhao, Y.-Y. (2018a). Natural Products as a Source for Antifibrosis Therapy. *Trends Pharmacol. Sci.* 39 (11), 937–952. doi:10.1016/j.tips.2018.09.002

Chen, D.-Q., Feng, Y.-L., Chen, L., Liu, J.-R., Wang, M., Vaziri, N. D., et al. (2019a). Poricoic Acid A Enhances Melatonin Inhibition of AKI-To-CKD Transition by Regulating Gas6/Axl NF κB/Nrf2 axis. *Free Radic. Biol. Med.* 134, 484–497. doi:10.1016/j.freeradbiomed.2019.01.046

Chen, D.-Q., Feng, Y.-L., Tian, T., Chen, H., Yin, L., Zhao, Y.-Y., et al. (2014). Diuretic and Anti-diuretic Activities of Fractions of Alismatis Rhizoma. *J. Ethnopharmacology* 157, 114–118. doi:10.1016/j.jep.2014.09.022

Chen, D.-Q., Wang, Y.-N., Vaziri, N. D., Chen, L., Hu, H.-H., and Zhao, Y.-Y. (2020a). Poricoic Acid A Activates AMPK to Attenuate Fibroblast Activation and Abnormal Extracellular Matrix Remodelling in Renal Fibrosis. *Phytomedicine* 72, 153232. doi:10.1016/j.phymed.2020.153232

Chen, H., Tian, T., Miao, H., and Zhao, Y.-Y. (2016). Traditional Uses, Fermentation, Phytochemistry and Pharmacology of Phellinus Linteus: A Review. *Fitoterapia* 113, 6–26. doi:10.1016/j.fitote.2016.06.009

Chen, H., Wang, M.-C., Chen, Y.-Y., Chen, L., Wang, Y.-N., Vaziri, N. D., et al. (2020b). Alisol B 23-acetate Attenuates CKD Progression by Regulating the

Renin-Angiotensin System and Gut-Kidney axis. *Ther. Adv. Chronic Dis.* 11, 204062232092002. doi:10.1177/2040622320920025

Chen, H., Yang, T., Wang, M.-C., Chen, D.-Q., Yang, Y., and Zhao, Y.-Y. (2018b). Novel RAS Inhibitor 25-O-Methylalisol F Attenuates Epithelial-To-Mesenchymal Transition and Tubulo-Interstitial Fibrosis by Selectively Inhibiting TGF-β-Mediated Smad3 Phosphorylation. *Phytomedicine* 42, 207–218. doi:10.1016/j.phymed.2018.03.034

Chen, L., Cao, G., Wang, M., Feng, Y. L., Chen, D. Q., Vaziri, N. D., et al. (2019d). The Matrix Metalloproteinase-13 Inhibitor Poricoic Acid ZI Ameliorates Renal Fibrosis by Mitigating Epithelial-Mesenchymal Transition. *Mol. Nutr. Food Res.* 63 (13), e1900132. doi:10.1002/mnfr.201900132

Chen, L., Chen, D.-Q., Liu, J.-R., Zhang, J., Vaziri, N. D., Zhuang, S., et al. (2019e). Unilateral Ureteral Obstruction Causes Gut Microbial Dysbiosis and Metabolome Disorders Contributing to Tubulointerstitial Fibrosis. *Exp. Mol. Med.* 51 (3), 1–18. doi:10.1038/s12276-019-0234-2

Chen, L., Chen, D.-Q., Wang, M., Liu, D., Chen, H., Dou, F., et al. (2017b). Role of RAS/Wnt/β-catenin axis Activation in the Pathogenesis of Podocyte Injury and Tubulo-Interstitial Nephropathy. *Chem. Biol. Interact.* 273, 56–72. doi:10.1016/j.cbi.2017.05.025

Chen, L., Yang, T., Lu, D.-W., Zhao, H., Feng, Y.-L., Chen, H., et al. (2018c). Central Role of Dysregulation of TGF-β/Smad in CKD Progression and Potential Targets of its Treatment. *Biomed. Pharmacother.* 101, 670–681. doi:10.1016/j.biopha.2018.02.090

Chinison, J., Aguilar, J. S., Avalos, A., Huang, Y., Wang, Z., Cameron, D. J., et al. (2016). Triptonide Effectively Inhibits Wnt/β-Catenin Signaling via C-Terminal Transactivation Domain of β-catenin. *Sci. Rep.* 6, 32779. doi:10.1038/srep32779

Cosin-Roger, J., Ortiz-Masià, M. D., and Barrachina, M. D. (2019). Macrophages as an Emerging Source of Wnt Ligands: Relevance in Mucosal Integrity. *Front. Immunol.* 10, 2297. doi:10.3389/fimmu.2019.02297

Cruciat, C.-M., and Niehrs, C. (2013). Secreted and Transmembrane Wnt Inhibitors and Activators. *Cold Spring Harbor Perspect. Biol.* 5 (3), a015081. doi:10.1101/cshperspect.a015081

Dai, H., Liu, F., Qiu, X., Liu, W., Dong, Z., Jia, Y., et al. (2020). Alleviation by Mahuang Fuzi and Shenzhuo Decoction in High Glucose-Induced Podocyte Injury by Inhibiting the Activation of Wnt/β-Catenin Signaling Pathway, Resulting in Activation of Podocyte Autophagy. *Evid. Based Complement. Alternat. Med.* 2020, 1–11. doi:10.1155/2020/7809427

Distler, J. H. W., Györfi, A.-H., Ramanujam, M., Whitfield, M. L., Königshoff, M., and Lafyatis, R. (2019). Shared and Distinct Mechanisms of Fibrosis. *Nat. Rev. Rheumatol.* 15 (12), 705–730. doi:10.1038/s41584-019-0322-7

Djudjaj, S., and Boor, P. (2019). Cellular and Molecular Mechanisms of Kidney Fibrosis. *Mol. Aspects Med.* 65, 16–36. doi:10.1016/j.mam.2018.06.002

Dou, F., Miao, H., Wang, J. W., Chen, L., Wang, M., Chen, H., et al. (2018). An Integrated Lipidomics and Phenotype Study Reveals Protective Effect and Biochemical Mechanism of Traditionally Used Alisma Orientale Juzepzuk in Chronic Renal Disease. *Front. Pharmacol.* 9, 53. doi:10.3389/fphar.2018.00053

Duan, Y., Qiu, Y., Huang, X., Dai, C., Yang, J., and He, W. (2020). Deletion of FHL2 in Fibroblasts Attenuates Fibroblasts Activation and Kidney Fibrosis via Restraining TGF-B1-Induced Wnt/β-Catenin Signaling. *J. Mol. Med.* 98 (2), 291–307. doi:10.1007/s00109-019-01870-1

Edeling, M., Ragi, G., Huang, S., Pavenstädt, H., and Susztak, K. (2016). Developmental Signalling Pathways in Renal Fibrosis: the Roles of Notch, Wnt and Hedgehog. *Nat. Rev. Nephrol.* 12 (7), 426–439. doi:10.1038/nrneph.2016.54

Federico, G., Meister, M., Mathow, D., Heine, G. H., Moldenhauer, G., Popovic, Z. V., et al. (2016). Tubular Dickkopf-3 Promotes the Development of Renal Atrophy and Fibrosis. *JCI Insight* 1 (1), e84916. doi:10.1172/jci.insight.84916

Feng, Y.-L., Cao, G., Chen, D.-Q., Vaziri, N. D., Chen, L., Zhang, J., et al. (2019b). Microbiome-metabolomics Reveals Gut Microbiota Associated with Glycine-Conjugated Metabolites and Polyamine Metabolism in Chronic Kidney Disease. *Cell. Mol. Life Sci.* 76 (24), 4961–4978. doi:10.1007/s00018-019-03155-9

Feng, Y.-L., Chen, H., Chen, D.-Q., Vaziri, N. D., Su, W., Ma, S.-X., et al. (2019c). Activated NF-κB/Nrf2 and Wnt/β-Catenin Pathways Are Associated with Lipid Metabolism in CKD Patients with Microalbuminuria and Macroalbuminuria. *Biochim. Biophys. Acta (Bba) - Mol. Basis Dis.* 1865 (9), 2317–2332. doi:10.1016/j.bbadis.2019.05.010

Feng, Y.-L., Chen, H., Tian, T., Chen, D.-Q., Zhao, Y.-Y., and Lin, R.-C. (2014). Diuretic and Anti-diuretic Activities of the Ethanol and Aqueous Extracts of Alismatis Rhizoma. *J. Ethnopharmacol.* 154 (2), 386–390. doi:10.1016/j.jep.2014.04.017

Feng, Y.-L., Lei, P., Tian, T., Yin, L., Chen, D.-Q., Chen, H., et al. (2013). Diuretic Activity of Some Fractions of the Epidermis of Poria Cocos. *J. Ethnopharmacol.* 150 (3), 1114–1118. doi:10.1016/j.jep.2013.10.043

Feng, Y. L., Chen, D. Q., Vaziri, N. D., Guo, Y., and Zhao, Y. Y. (2019a). Small Molecule Inhibitors of Epithelial-Mesenchymal Transition for the Treatment of Cancer and Fibrosis. *Med. Res. Rev.* 40, 54–78. doi:10.1002/med.21596

Feng, Y., Ren, J., Gui, Y., Wei, W., Shu, B., Lu, Q., et al. (2018). Wnt/β-Catenin-Promoted Macrophage Alternative Activation Contributes to Kidney Fibrosis. *J. Am. Soc. Nephrol.* 29 (1), 182–193. doi:10.1681/asn.2017040391

Flevaris, P., and Vaughan, D. (2017). The Role of Plasminogen Activator Inhibitor Type-1 in Fibrosis. *Semin. Thromb. Hemost.* 43 (2), 169–177. doi:10.1055/s-0036-1586228

Foulquier, S., Daskalopoulos, E. P., Lluri, G., Hermans, K. C. M., Deb, A., and Blankesteijn, W. M. (2018). WNT Signaling in Cardiac and Vascular Disease. *Pharmacol. Rev.* 70 (1), 68–141. doi:10.1124/pr.117.013896

Gammons, M. V., Rutherford, T. J., Steinhart, Z., Angers, S., and Bienz, M. (2016). Essential Role of the Dishevelled DEP Domain in a Wnt-dependent Human-Cell-Based Complementation Assay. *J. Cell Sci.* 129 (20), 3892–3902. doi:10.1242/jcs.195685

García de Herreros, A., and Baulida, J. (2012). Cooperation, Amplification, and Feed-Back in Epithelial-Mesenchymal Transition. *Biochim. Biophys. Acta (Bba) - Rev. Cancer* 1825 (2), 223–228. doi:10.1016/j.bbcan.2012.01.003

Gu, L.-f., Ge, H.-t., Zhao, L., Wang, Y.-j., Zhang, F., Tang, H.-t., et al. (2020). Huangkui Capsule Ameliorates Renal Fibrosis in a Unilateral Ureteral Obstruction Mouse Model through TRPC6 Dependent Signaling Pathways. *Front. Pharmacol.* 11, 996. doi:10.3389/fphar.2020.00996

Guan, X., Nie, L., He, T., Yang, K., Xiao, T., Wang, S., et al. (2014). Klotho Suppresses Renal Tubulo-Interstitial Fibrosis by Controlling Basic Fibroblast Growth Factor-2 Signalling. *J. Pathol.* 234 (4), 560–572. doi:10.1002/path.4420

Guo, Q., Zhong, W., Duan, A., Sun, G., Cui, W., Zhuang, X., et al. (2019). Protective or Deleterious Role of Wnt/beta-Catenin Signaling in Diabetic Nephropathy: An Unresolved Issue. *Pharmacol. Res.* 144, 151–157. doi:10.1016/j.phrs.2019.03.022

Hall, G., Wang, L., and Spurney, R. F. (2019). TRPC Channels in Proteinuric Kidney Diseases. *Cells* 9 (1), 44. doi:10.3390/cells9010044

Hamasaki, Y., Doi, K., Maeda-Mamiya, R., Ogasawara, E., Katagiri, D., Tanaka, T., et al. (2013). A 5-hydroxytryptamine Receptor Antagonist, Sarpogrelate, Reduces Renal Tubulointerstitial Fibrosis by Suppressing PAI-1. *Am. J. Physiol. Renal Physiol.* 305 (12), F1796–F1803. doi:10.1152/ajprenal.00151.2013

He, W., Dai, C., Li, Y., Zeng, G., Monga, S. P., and Liu, Y. (2009). Wnt/β-Catenin Signaling Promotes Renal Interstitial Fibrosis. *J. Am. Soc. Nephrol.* 20 (4), 765–776. doi:10.1681/asn.2008060566

Henderson, J., Wilkinson, S., Przyborski, S., Stratton, R., and O'Reilly, S. (2020). microRNA27a-3p Mediates Reduction of the Wnt Antagonist sFRP-1 in Systemic Sclerosis. *Epigenetics* 16, 808–817. doi:10.1080/15592294.2020.1827715

Henderson, W. R., Jr., Chi, E. Y., Ye, X., Nguyen, C., Tien, Y.-t., Zhou, B., et al. (2010). Inhibition of Wnt/ -catenin/CREB Binding Protein (CBP) Signaling Reverses Pulmonary Fibrosis. *Proc. Natl. Acad. Sci.* 107 (32), 14309–14314. doi:10.1073/pnas.1001520107

Ho, C., Hsu, Y.-C., Lei, C.-C., Mau, S.-C., Shih, Y.-H., and Lin, C.-L. (2016). Curcumin Rescues Diabetic Renal Fibrosis by Targeting Superoxide-Mediated Wnt Signaling Pathways. *Am. J. Med. Sci.* 351 (3), 286–295. doi:10.1016/j.amjms.2015.12.017

Hou, N.-N., Kan, C.-X., Huang, N., Liu, Y.-P., Mao, E.-W., Ma, Y.-T., et al. (2021). Relationship between Serum Dickkopf-1 and Albuminuria in Patients with Type 2 Diabetes. *World J. Diabetes* 12 (1), 47–55. doi:10.4239/wjd.v12.i1.47

Hu, H.-H., Cao, G., Wu, X.-Q., Vaziri, N. D., and Zhao, Y.-Y. (2020). Wnt Signaling Pathway in Aging-Related Tissue Fibrosis and Therapies. *Ageing Res. Rev.* 60, 101063. doi:10.1016/j.arr.2020.101063

Hu, M. C., Kuro-o, M., and Moe, O. W. (2013). Klotho and Chronic Kidney Disease. *Contrib. Nephrol.* 180, 47–63. doi:10.1159/000346778

Huang, H., Huang, X., Luo, S., Zhang, H., Hu, F., Chen, R., et al. (2020). The MicroRNA MiR-29c Alleviates Renal Fibrosis via TPM1-Mediated Suppression of the Wnt/β-Catenin Pathway. *Front. Physiol.* 11, 331. doi:10.3389/fphys.2020.00331

Huang, P., Yan, R., Zhang, X., Wang, L., Ke, X., and Qu, Y. (2019). Activating Wnt/β-Catenin Signaling Pathway for Disease Therapy: Challenges and Opportunities. *Pharmacol. Ther.* 196, 79–90. doi:10.1016/j.pharmthera.2018.11.008

Huang, Y., Liu, L., and Liu, A. (2018). Dickkopf-1: Current Knowledge and Related Diseases. *Life Sci.* 209, 249–254. doi:10.1016/j.lfs.2018.08.019

Humphreys, B. D. (2018). Mechanisms of Renal Fibrosis. *Annu. Rev. Physiol.* 80, 309–326. doi:10.1146/annurev-physiol-022516-034227

Ichihara, A., and Yatabe, M. S. (2019). The (Pro)renin Receptor in Health and Disease. *Nat. Rev. Nephrol.* 15 (11), 693–712. doi:10.1038/s41581-019-0160-5

Janda, C. Y., Dang, L. T., You, C., Chang, J., de Lau, W., Zhong, Z. A., et al. (2017). Surrogate Wnt Agonists that Phenocopy Canonical Wnt and β-catenin Signalling. *Nature* 545 (7653), 234–237. doi:10.1038/nature22306

Jiao, X., Cai, J., Yu, X., and Ding, X. (2017). Paracrine Activation of the Wnt/β-Catenin Pathway by Bone Marrow Stem Cell Attenuates Cisplatin-Induced Kidney Injury. *Cell Physiol. Biochem.* 44 (5), 1980–1994. doi:10.1159/000485904

Johnson, B. G., Ren, S., Karaca, G., Gomez, I. G., Fligny, C., Smith, B., et al. (2017). Connective Tissue Growth Factor Domain 4 Amplifies Fibrotic Kidney Disease through Activation of LDL Receptor-Related Protein 6. *J. Am. Soc. Nephrol.* 28 (6), 1769–1782. doi:10.1681/asn.2016080826

Joiner, D. M., Ke, J., Zhong, Z., Xu, H. E., and Williams, B. O. (2013). LRP5 and LRP6 in Development and Disease. *Trends Endocrinol. Metab.* 24 (1), 31–39. doi:10.1016/j.tem.2012.10.003

Kawazoe, M., Kaneko, K., and Nanki, T. (2021). Glucocorticoid Therapy Suppresses Wnt Signaling by Reducing the Ratio of Serum Wnt3a to Wnt Inhibitors, sFRP-1 and Wif-1. *Clin. Rheumatol.* 40, 2947–2954. doi:10.1007/s10067-020-05554-x

Kim, D. Y., Kang, M.-K., Park, S.-H., Lee, E.-J., Kim, Y.-H., Oh, H., et al. (2017). Eucalyptol Ameliorates Snail1/β-catenin-dependent Diabetic Disjunction of Renal Tubular Epithelial Cells and Tubulointerstitial Fibrosis. *Oncotarget* 8 (63), 106190–106205. doi:10.18632/oncotarget.22311

Kim, E. Y., and Dryer, S. E. (2021). Effects of TRPC6 Inactivation on Glomerulosclerosis and Renal Fibrosis in Aging Rats. *Cells* 10 (4), 856. doi:10.3390/cells10040856

Kinosada, H., Okada-Iwasaki, R., Kunieda, K., Suzuki-Imaizumi, M., Takahashi, Y., Miyagi, H., et al. (2021). The Dual Pocket Binding Novel Tankyrase Inhibitor K-476 Enhances the Efficacy of Immune Checkpoint Inhibitor by Attracting CD8+ T Cells to Tumors. *Am. J. Cancer Res.* 11 (1), 264–276.

Klavdianou, K., Liossis, S.-N., and Daoussis, D. (2017). Dkk1: A Key Molecule in Joint Remodelling and Fibrosis. *Mediterr. J. Rheumatol.* 28 (4), 174–182. doi:10.31138/mjr.28.4.174

Kozlova, N., Jensen, J. K., Franklin Chi, T., Samoylenko, A., and Kietzmann, T. (2015). PAI-1 Modulates Cell Migration in a LRP1-dependent Manner via β-catenin and ERK1/2. *Thromb. Haemost.* 113 (5), 988–998. doi:10.1160/th14-08-0678

Kuang, Q., Wu, S., Xue, N., Wang, X., Ding, X., and Fang, Y. (2021). Selective Wnt/β-Catenin Pathway Activation Concomitant with Sustained Overexpression of miR-21 Is Responsible for Aristolochic Acid-Induced AKI-To-CKD Transition. *Front. Pharmacol.* 12, 667282. doi:10.3389/fphar.2021.667282

Kulak, O., Chen, H., Holohan, B., Wu, X., He, H., Borek, D., et al. (2015). Disruption of Wnt/β-Catenin Signaling and Telomeric Shortening Are Inextricable Consequences of Tankyrase Inhibition in Human Cells. *Mol. Cel. Biol.* 35 (14), 2425–2435. doi:10.1128/mcb.00392-15

Kuure, S., Popsueva, A., Jakobson, M., Sainio, K., and Sariola, H. (2007). Glycogen Synthase Kinase-3 Inactivation and Stabilization of β-Catenin Induce Nephron Differentiation in Isolated Mouse and Rat Kidney Mesenchymes. *J. Am. Soc. Nephrol.* 18 (4), 1130–1139. doi:10.1681/asn.2006111206

La, L., Wang, L., Qin, F., Jiang, J., He, S., Wang, C., et al. (2018). Zhen-wu-tang Ameliorates Adenine-Induced Chronic Renal Failure in Rats: Regulation of the Canonical Wnt4/beta-Catenin Signaling in the Kidneys. *J. Ethnopharmacology* 219, 81–90. doi:10.1016/j.jep.2017.12.013

Langton, P. F., Kakugawa, S., and Vincent, J.-P. (2016). Making, Exporting, and Modulating Wnts. *Trends Cel Biol.* 26 (10), 756–765. doi:10.1016/j.tcb.2016.05.011

Lasagni, L., Angelotti, M. L., Ronconi, E., Lombardi, D., Nardi, S., Peired, A., et al. (2015). Podocyte Regeneration Driven by Renal Progenitors Determines Glomerular Disease Remission and Can Be Pharmacologically Enhanced. *Stem Cell Rep.* 5 (2), 248–263. doi:10.1016/j.stemcr.2015.07.003

Li, X., Zheng, P., Ji, T., Tang, B., Wang, Y., and Bai, S. (2020). LINC00052 Ameliorates Acute Kidney Injury by Sponging miR-532-3p and Activating the Wnt Signaling Pathway. *Aging* 13 (1), 340–350. doi:10.18632/aging.104152

Li, Y., Zhao, Z., Luo, J., Jiang, Y., Li, L., Chen, Y., et al. (2021). Apigenin Ameliorates Hyperuricemic Nephropathy by Inhibiting URAT1 and GLUT9 and Relieving Renal Fibrosis via the Wnt/β-Catenin Pathway. *Phytomedicine* 87, 153585. doi:10.1016/j.phymed.2021.153585

Li, Z., Zhou, L., Wang, Y., Miao, J., Hong, X., Hou, F. F., et al. (2017). (Pro)renin Receptor is an Amplifier of Wnt/β-Catenin Signaling in Kidney Injury and Fibrosis. *J. Am. Soc. Nephrol.* 28 (8), 2393–2408. doi:10.1681/asn.2016070811

Licht-Murava, A., Paz, R., Vaks, L., Avrahami, L., Plotkin, B., Eisenstein, M., et al. (2016). A Unique Type of GSK-3 Inhibitor Brings New Opportunities to the Clinic. *Sci. Signal.* 9 (454), ra110. doi:10.1126/scisignal.aah7102

Lin, B., Hong, H., Jiang, X., Li, C., Zhu, S., Tang, N., et al. (2017). WNT Inhibitory Factor 1 Promoter Hypermethylation Is an Early Event during Gallbladder Cancer Tumorigenesis that Predicts Poor Survival. *Gene* 622, 42–49. doi:10.1016/j.gene.2017.04.034

Lindberg, K., Amin, R., Moe, O. W., Hu, M.-C., Erben, R. G., Östman Wernerson, A., et al. (2014). The Kidney Is the Principal Organ Mediating Klotho Effects. *J. Am. Soc. Nephrol.* 25 (10), 2169–2175. doi:10.1681/asn.2013111209

Lipphardt, M., Dihazi, H., Jeon, N. L., Dadafarin, S., Ratliff, B. B., Rowe, D. W., et al. (2019). Dickkopf-3 in Aberrant Endothelial Secretome Triggers Renal Fibroblast Activation and Endothelial-Mesenchymal Transition. *Nephrol. Dial. Transpl.* 34 (1), 49–62. doi:10.1093/ndt/gfy100

Liu, D., Chen, L., Zhao, H., Vaziri, N. D., Ma, S.-C., and Zhao, Y.-Y. (2019). Small Molecules from Natural Products Targeting the Wnt/β-Catenin Pathway as a Therapeutic Strategy. *Biomed. Pharmacother.* 117, 108990. doi:10.1016/j.biopha.2019.108990

Liu, Y., Su, Y.-Y., Yang, Q., and Zhou, T. (2021). Stem Cells in the Treatment of Renal Fibrosis: A Review of Preclinical and Clinical Studies of Renal Fibrosis Pathogenesis. *Stem Cell Res. Ther.* 12 (1), 333. doi:10.1186/s13287-021-02391-w

Liu, Z., Tan, R. J., and Liu, Y. (2020). The Many Faces of Matrix Metalloproteinase-7 in Kidney Diseases. *Biomolecules* 10 (6), 960. doi:10.3390/biom10060960

Ma, S., Choi, J., Jin, X., Kim, H.-Y., Yun, J.-H., Lee, W., et al. (2018). Discovery of a Small-Molecule Inhibitor of Dvl-CXXC5 Interaction by Computational Approaches. *J. Comput. Aided Mol. Des.* 32 (5), 643–655. doi:10.1007/s10822-018-0118-x

Maarouf, O. H., Aravamudhan, A., Rangarajan, D., Kusaba, T., Zhang, V., Welborn, J., et al. (2016). Paracrine Wnt1 Drives Interstitial Fibrosis Without Inflammation by Tubulointerstitial Cross-Talk. *J. Am. Soc. Nephrol.* 27 (3), 781–790. doi:10.1681/asn.2014121188

Malik, S. A., Modarage, K., and Goggolidou, P. (2020). The Role of Wnt Signalling in Chronic Kidney Disease (CKD). *Genes* 11 (5), 496. doi:10.3390/genes11050496

Matsuyama, M., Nomori, A., Nakakuni, K., Shimono, A., and Fukushima, M. (2014). Secreted Frizzled-Related Protein 1 (Sfrp1) Regulates the Progression of Renal Fibrosis in a Mouse Model of Obstructive Nephropathy. *J. Biol. Chem.* 289 (45), 31526–31533. doi:10.1074/jbc.M114.584565

Miao, H., Cao, G., Wu, X. Q., Chen, Y. Y., Chen, D. Q., Chen, L., et al. (2020). Identification of Endogenous 1-aminopyrene as a Novel Mediator of Progressive Chronic Kidney Disease via Aryl Hydrocarbon Receptor Activation. *Br. J. Pharmacol.* 177 (15), 3415–3435. doi:10.1111/bph.15062

Miao, H., Wu, X.-Q., Zhang, D.-D., Wang, Y.-N., Guo, Y., Li, P., et al. (2021). Deciphering the Cellular Mechanisms Underlying Fibrosis-Associated Diseases and Therapeutic Avenues. *Pharmacol. Res.* 163, 105316. doi:10.1016/j.phrs.2020.105316

Miao, H., Zhao, Y.-H., Vaziri, N. D., Tang, D.-D., Chen, H., Chen, H., et al. (2016). Lipidomics Biomarkers of Diet-Induced Hyperlipidemia and its Treatment with Poria Cocos. *J. Agric. Food Chem.* 64 (4), 969–979. doi:10.1021/acs.jafc.5b05350

Miao, J., Liu, J., Niu, J., Zhang, Y., Shen, W., Luo, C., et al. (2019). Wnt/β-catenin/RAS Signaling Mediates Age-related Renal Fibrosis and Is Associated with Mitochondrial Dysfunction. *Aging Cell* 18 (5), e13004. doi:10.1111/acel.13004

Mo, L., Xiao, X., Song, S., Miao, H., Liu, S., Guo, D., et al. (2015). Protective Effect of Huang Gan Formula in 5/6 Nephrectomized Rats by Depressing the Wnt/β-Catenin Signaling Pathway. *Drug Des. Devel. Ther.* 9, 2867–2881. doi:10.2147/dddt.S81157

Moon, J., Zhou, H., Zhang, L.-s., Tan, W., Liu, Y., Zhang, S., et al. (2017). Blockade to Pathological Remodeling of Infarcted Heart Tissue Using a porcupine Antagonist. *Proc. Natl. Acad. Sci. USA* 114 (7), 1649–1654. doi:10.1073/pnas.1621346114

Muñoz-Castañeda, J. R., Herencia, C., Pendón-Ruiz de Mier, M. V., Rodriguez-Ortiz, M. E., Diaz-Tocados, J. M., Vergara, N., et al. (2017). Differential Regulation of Renal Klotho and FGFR1 in normal and Uremic Rats. *Faseb j* 31 (9), 3858–3867. doi:10.1096/fj.201700006R

Muñoz-Castañeda, J. R., Rodelo-Haad, C., Pendon-Ruiz de Mier, M. V., Martin-Malo, A., Santamaria, R., and Rodriguez, M. (2020). Klotho/FGF23 and Wnt Signaling as Important Players in the Comorbidities Associated With Chronic Kidney Disease. *Toxins* 12 (3), 185. doi:10.3390/toxins12030185

Nastase, M. V., Zeng-Brouwers, J., Wygrecka, M., and Schaefer, L. (2018). Targeting Renal Fibrosis: Mechanisms and Drug Delivery Systems. *Adv. Drug Deliv. Rev.* 129, 295–307. doi:10.1016/j.addr.2017.12.019

Navar, L. G. (2014). Intrarenal Renin-Angiotensin System in Regulation of Glomerular Function. *Curr. Opin. Nephrol. Hypertens.* 23 (1), 38–45. doi:10.1097/01.mnh.0000436544.86508.f1

Ng-Blichfeldt, J.-P., de Jong, T., Kortekaas, R. K., Wu, X., Lindner, M., Guryev, V., et al. (2019). TGF-β Activation Impairs Fibroblast Ability to Support Adult Lung Epithelial Progenitor Cell Organoid Formation. *Am. J. Physiol. Lung Cell Mol. Physiol.* 317 (1), L14–l28. doi:10.1152/ajplung.00400.2018

Nishikawa, K., Osawa, Y., and Kimura, K. (2018). Wnt/β-Catenin Signaling as a Potential Target for the Treatment of Liver Cirrhosis Using Antifibrotic Drugs. *Int. J. Mol. Sci.* 19 (10), 3103. doi:10.3390/ijms19103103

Nlandu-Khodo, S., Neelisetty, S., Phillips, M., Manolopoulou, M., Bhave, G., May, L., et al. (2017). Blocking TGF-β and β-Catenin Epithelial Crosstalk Exacerbates CKD. *J. Am. Soc. Nephrol.* 28 (12), 3490–3503. doi:10.1681/asn.2016121351

Nusse, R., and Clevers, H. (2017). Wnt/β-Catenin Signaling, Disease, and Emerging Therapeutic Modalities. *Cell* 169 (6), 985–999. doi:10.1016/j.cell.2017.05.016

Pan, B., Zhang, H., Hong, Y., Ma, M., Wan, X., and Cao, C. (2021). Indoleamine-2,3-Dioxygenase Activates Wnt/β-Catenin Inducing Kidney Fibrosis after Acute Kidney Injury. *Gerontology*, 1–9. doi:10.1159/00051504

Plummer, R., Dua, D., Cresti, N., Drew, Y., Stephens, P., Foegh, M., et al. (2020). First-in-Human Study of the PARP/Tankyrase Inhibitor E7449 in Patients with Advanced Solid Tumours and Evaluation of a Novel Drug-Response Predictor. *Br. J. Cancer* 123 (4), 525–533. doi:10.1038/s41416-020-0916-5

Proffitt, K. D., Madan, B., Ke, Z., Pendharkar, V., Ding, L., Lee, M. A., et al. (2013). Pharmacological Inhibition of the Wnt Acyltransferase PORCN Prevents Growth of WNT-Driven Mammary Cancer. *Cancer Res.* 73 (2), 502–507. doi:10.1158/0008-5472.Can-12-2258

Qi, C., Zhang, J., Chen, X., Wan, J., Wang, J., Zhang, P., et al. (2017). Hypoxia Stimulates Neural Stem Cell Proliferation by Increasing HIF-1α E-xpression and A-ctivating Wnt/β-C-atenin S-ignaling. *Cell Mol. Biol.* 63 (7), 12–19. doi:10.14715/cmb/2017.63.7.2

Qiao, B., He, B.-X., Cai, J.-H., Tao, Q., and King-Yin Lam, A. (2017). MicroRNA-27a-3p Modulates the Wnt/β-Catenin Signaling Pathway to Promote Epithelial-Mesenchymal Transition in Oral Squamous Carcinoma Stem Cells by Targeting SFRP1. *Sci. Rep.* 7, 44688. doi:10.1038/srep44688

Rabieian, R., Boshtam, M., Zareei, M., Kouhpayeh, S., Masoudifar, A., and Mirzaei, H. (2018). Plasminogen Activator Inhibitor Type-1 as a Regulator of Fibrosis. *J. Cell Biochem.* 119 (1), 17–27. doi:10.1002/jcb.26146

Ramkumar, N., and Kohan, D. E. (2016). The Nephron (Pro)renin Receptor: Function and Significance. *Am. J. Physiol. Renal Physiol.* 311 (6), F1145–f1148. doi:10.1152/ajprenal.00476.2016

Ren, J., Li, J., Liu, X., Feng, Y., Gui, Y., Yang, J., et al. (2016). Quercetin Inhibits Fibroblast Activation and Kidney Fibrosis Involving the Suppression of Mammalian Target of Rapamycin and β-catenin Signaling. *Sci. Rep.* 6, 23968. doi:10.1038/srep23968

Ren, X., Zhu, R., Liu, G., Xue, F., Wang, Y., Xu, J., et al. (2019). Effect of Sitagliptin on Tubulointerstitial Wnt/β-Catenin Signalling in Diabetic Nephropathy. *Nephrology* 24 (11), 1189–1197. doi:10.1111/nep.13641

Rippin, I., Khazanov, N., Ben Joseph, S., Kudinov, T., Berent, E., Arciniegas Ruiz, S. M., et al. (2020). Discovery and Design of Novel Small Molecule GSK-3 Inhibitors Targeting the Substrate Binding Site. *Int. J. Mol. Sci.* 21 (22), 8709. doi:10.3390/ijms21228709

Schunk, S. J., Floege, J., Fliser, D., and Speer, T. (2021). WNT-β-catenin Signalling - A Versatile Player in Kidney Injury and Repair. *Nat. Rev. Nephrol.* 17 (3), 172–184. doi:10.1038/s41581-020-00343-w

Shati, A. A., and Alfaifi, M. Y. (2020). Salidroside Protects against Diabetes Mellitus-Induced Kidney Injury and Renal Fibrosis by Attenuating TGF-β1 and Wnt1/3a/β-Catenin Signalling. *Clin. Exp. Pharmacol. Physiol.* 47 (10), 1692–1704. doi:10.1111/1440-1681.13355

Simon-Tillaux, N., and Hertig, A. (2017). Snail and Kidney Fibrosis. *Nephrol. Dial. Transpl.* 32 (2), 224–233. doi:10.1093/ndt/gfw333

Smigiel, K. S., and Parks, W. C. (2018). Macrophages, Wound Healing, and Fibrosis: Recent Insights. *Curr. Rheumatol. Rep.* 20 (4), 17. doi:10.1007/s11926-018-0725-5

Staruschenko, A., Spires, D., and Palygin, O. (2019). Role of TRPC6 in Progression of Diabetic Kidney Disease. *Curr. Hypertens. Rep.* 21 (7), 48. doi:10.1007/s11906-019-0960-9

Stemmer, V., de Craene, B., Berx, G., and Behrens, J. (2008). Snail Promotes Wnt Target Gene Expression and Interacts with β-catenin. *Oncogene* 27 (37), 5075–5080. doi:10.1038/onc.2008.140

Sun, Z., Xu, S., Cai, Q., Zhou, W., Jiao, X., Bao, M., et al. (2020). Wnt/β-Catenin Agonist BIO Alleviates Cisplatin-Induced Nephrotoxicity without Compromising its Efficacy of Anti-proliferation in Ovarian Cancer. *Life Sci.* 263, 118672. doi:10.1016/j.lfs.2020.118672

Svegliati, S., Marrone, G., Pezone, A., Spadoni, T., Grieco, A., Moroncini, G., et al. (2014). Oxidative DNA Damage Induces the ATM-Mediated Transcriptional Suppression of the Wnt Inhibitor WIF-1 in Systemic Sclerosis and Fibrosis. *Sci. Signal.* 7 (341), ra84. doi:10.1126/scisignal.2004592

Tan, R. J., Li, Y., Rush, B. M., Cerqueira, D. M., Zhou, D., Fu, H., et al. (2019). Tubular Injury Triggers Podocyte Dysfunction by β-Catenin-Driven Release of MMP-7. *JCI Insight* 4 (24). doi:10.1172/jci.insight.122399

Tang, P. M.-K., Nikolic-Paterson, D. J., and Lan, H.-Y. (2019). Macrophages: Versatile Players in Renal Inflammation and Fibrosis. *Nat. Rev. Nephrol.* 15 (3), 144–158. doi:10.1038/s41581-019-0110-2

Tessa, H., David, M. W., and S, G. L. (2020). Wnt/β-Catenin in Acute Kidney Injury and Progression to Chronic Kidney Disease. *Semin. Nephrol.* 40 (2), 126–137. doi:10.1016/j.semnephrol.2020.01.004

Tian, T., Chen, H., and Zhao, Y.-Y. (2014). Traditional Uses, Phytochemistry, Pharmacology, Toxicology and Quality Control of Alisma Orientale (Sam.) Juzep: A Review. *J. Ethnopharmacol.* 158, 373–387. doi:10.1016/j.jep.2014.10.061

Tu, C., Xu, R., Koleti, M., and Zoldan, J. (2017). Glycogen Synthase Kinase-3 Inhibition Sensitizes Human Induced Pluripotent Stem Cells to Thiol-Containing Antioxidants Induced Apoptosis. *Stem Cell Res.* 23, 182–187. doi:10.1016/j.scr.2017.07.019

Urushihara, M., Kinoshita, Y., Kondo, S., and Kagami, S. (2012). Involvement of the Intrarenal Renin-Angiotensin System in Experimental Models of Glomerulonephritis. *J. Biomed. Biotechnol.* 2012, 1–6. doi:10.1155/2012/601786

Venner, J. M., Famulski, K. S., Reeve, J., Chang, J., and Halloran, P. F. (2016). Relationships Among Injury, Fibrosis, and Time in Human Kidney Transplants. *JCI Insight* 1 (1), e85323. doi:10.1172/jci.insight.85323

Wang, J., Nishiyama, A., Matsuyama, M., Wang, Z., and Yuan, Y. (2020a). The (Pro)renin Receptor: a Novel Biomarker and Potential Therapeutic Target for Various Cancers. *Cell Commun. Signal* 18 (1), 39. doi:10.1186/s12964-020-0531-3

Wang, L., Chi, Y.-F., Yuan, Z.-T., Zhou, W.-C., Yin, P.-H., Zhang, X.-M., et al. (2014a). Astragaloside IV Inhibits the Up-Regulation of Wnt/β-Catenin Signaling in Rats with Unilateral Ureteral Obstruction. *Cell Physiol. Biochem.* 33 (5), 1316–1328. doi:10.1159/000358699

Wang, M., Chen, D.-Q., Chen, L., Cao, G., Zhao, H., Liu, D., et al. (2018a). Novel Inhibitors of the Cellular Renin-Angiotensin System Components, Poricoic Acids, Target Smad3 Phosphorylation and Wnt/β-Catenin Pathway against Renal Fibrosis. *Br. J. Pharmacol.* 175 (13), 2689–2708. doi:10.1111/bph.14333

Wang, M., Chen, D.-Q., Chen, L., Liu, D., Zhao, H., Zhang, Z.-H., et al. (2018b). Novel RAS Inhibitors Poricoic Acid ZG and Poricoic Acid ZH Attenuate Renal Fibrosis via a Wnt/β-Catenin Pathway and Targeted Phosphorylation of Smad3 Signaling. *J. Agric. Food Chem.* 66 (8), 1828–1842. doi:10.1021/acs.jafc.8b00099

Wang, M., Hu, H.-H., Chen, Y.-Y., Chen, L., Wu, X.-Q., and Zhao, Y.-Y. (2020b). Novel Poricoic Acids Attenuate Renal Fibrosis through Regulating Redox Signalling and Aryl Hydrocarbon Receptor Activation. *Phytomedicine* 79, 153323. doi:10.1016/j.phymed.2020.153323

Wang, N., Liang, H., and Zen, K. (2014b). Molecular Mechanisms that Influence the Macrophage m1-m2 Polarization Balance. *Front. Immunol.* 5, 614. doi:10.3389/fimmu.2014.00614

Wang, Q., Tian, X., Wang, Y., Wang, Y., Li, J., Zhao, T., et al. (2020c). Role of Transient Receptor Potential Canonical Channel 6 (TRPC6) in Diabetic Kidney Disease by Regulating Podocyte Actin Cytoskeleton Rearrangement. *J. Diabetes Res.* 2020, 1–11. doi:10.1155/2020/6897390

Wang, X., Moon, J., Dodge, M. E., Pan, X., Zhang, L., Hanson, J. M., et al. (2013a). The Development of Highly Potent Inhibitors for Porcupine. *J. Med. Chem.* 56 (6), 2700–2704. doi:10.1021/jm400159c

Wang, Y.-N., Hu, H.-H., Zhang, D.-D., Wu, X.-Q., Liu, J.-L., Guo, Y., et al. (2021a). The Dysregulation of Eicosanoids and Bile Acids Correlates with Impaired Kidney Function and Renal Fibrosis in Chronic Renal Failure. *Metabolites* 11 (2), 127. doi:10.3390/metabo11020127

Wang, Y.-N., Wu, X.-Q., Zhang, D.-D., Hu, H.-H., Liu, J.-L., Vaziri, N. D., et al. (2021b). Polyporus Umbellatus Protects Against Renal Fibrosis by Regulating Intrarenal Fatty Acyl Metabolites. *Front. Pharmacol.* 12, 633566. doi:10.3389/fphar.2021.633566

Wang, Y.-Z., Zhang, J., Zhao, Y.-L., Li, T., Shen, T., Li, J.-Q., et al. (2013b). Mycology, Cultivation, Traditional Uses, Phytochemistry and Pharmacology of Wolfiporia cocos (Schwein.) Ryvarden et Gilb.: A review. *J. Ethnopharmacol.* 147 (2), 265–276. doi:10.1016/j.jep.2013.03.027

Webster, A. C., Nagler, E. V., Morton, R. L., and Masson, P. (2017). Chronic Kidney Disease. *Lancet* 389 (10075), 1238–1252. doi:10.1016/s0140-6736(16)32064-5

Wong, D. W. L., Yiu, W. H., Chan, K. W., Li, Y., Li, B., Lok, S. W. Y., et al. (2018). Activated Renal Tubular Wnt/β-Catenin Signaling Triggers Renal Inflammation during Overload Proteinuria. *Kidney Int.* 93 (6), 1367–1383. doi:10.1016/j.kint.2017.12.017

Wozniak, J., Floege, J., Ostendorf, T., and Ludwig, A. (2021). Key Metalloproteinase-Mediated Pathways in the Kidney. *Nat. Rev. Nephrol.* 17, 513–527. doi:10.1038/s41581-021-00415-5

Wu, X.-Q., Zhang, D.-D., Wang, Y.-N., Tan, Y.-Q., Yu, X.-Y., and Zhao, Y.-Y. (2021). AGE/RAGE in Diabetic Kidney Disease and Ageing Kidney. *Free Radic. Biol. Med.* 171, 260–271. doi:10.1016/j.freeradbiomed.2021.05.025

Xia, J., and Cao, W. (2021). Epigenetic Modifications of Klotho Expression in Kidney Diseases. *J. Mol. Med.* 99 (5), 581–592. doi:10.1007/s00109-021-02044-8

Xian, J., Bu, F., Wang, Y., Long, F., Zhang, Z., Wu, C., et al. (2021). A Rationale for Drug Design provided by Co-Crystal Structure of IC261 in Complex with Tubulin. *Molecules* 26 (4), 946. doi:10.3390/molecules26040946

Xiang, X., Cai, H.-D., Su, S.-l., Dai, X.-x., Zhu, Y., Guo, J.-m., et al. (2019). Salvia Miltiorrhiza Protects against Diabetic Nephropathy through Metabolome Regulation and Wnt/β-Catenin and TGF-β Signaling Inhibition. *Pharmacol. Res.* 139, 26–40. doi:10.1016/j.phrs.2018.10.030

Xiao, L., Xu, B., Zhou, L., Tan, R. J., Zhou, D., Fu, H., et al. (2019). Wnt/β-catenin Regulates Blood Pressure and Kidney Injury in Rats. *Biochim. Biophys. Acta (Bba) - Mol. Basis Dis.* 1865 (6), 1313–1322. doi:10.1016/j.bbadis.2019.01.027

Xiao, L., Zhou, D., Tan, R. J., Fu, H., Zhou, L., Hou, F. F., et al. (2016). Sustained Activation of Wnt/β-Catenin Signaling Drives AKI to CKD Progression. *J. Am. Soc. Nephrol.* 27 (6), 1727–1740. doi:10.1681/asn.2015040449

Xie, H., Miao, N., Xu, D., Zhou, Z., Ni, J., Yin, F., et al. (2021). FoxM1 Promotes Wnt/β-Catenin Pathway Activation and Renal Fibrosis via Transcriptionally Regulating Multi-Wnts Expressions. *J. Cell Mol. Med.* 25 (4), 1958–1971. doi:10.1111/jcmm.15948

Xing, L., Chang, X., Shen, L., Zhang, C., Fan, Y., Cho, C., et al. (2021). Progress in Drug Delivery System for Fibrosis Therapy. *Asian J. Pharm. Sci.* 16 (1), 47–61. doi:10.1016/j.ajps.2020.06.005

Yang, X., Wang, H., Tu, Y., Li, Y., Zou, Y., Li, G., et al. (2020). WNT1-Inducible Signaling Protein-1 Mediates TGF-β1-Induced Renal Fibrosis in Tubular Epithelial Cells and Unilateral Ureteral Obstruction Mouse Models via Autophagy. *J. Cell Physiol.* 235 (3), 2009–2022. doi:10.1002/jcp.29187

Yang, Y., Feng, X., Liu, X., Wang, Y., Hu, M., Cao, Q., et al. (2019). Fate Alteration of Bone Marrow-Derived Macrophages Ameliorates Kidney Fibrosis in Murine Model of Unilateral Ureteral Obstruction. *Nephrol. Dial. Transpl.* 34 (10), 1657–1668. doi:10.1093/ndt/gfy381

Yang, Y., Nankivell, B. J., Hua, W., Rao, P., Ren, X., Yu, H., et al. (2021). Renal Tubular Cell Binding of β-Catenin to TCF1 versus FoxO1 is Associated with Chronic Interstitial Fibrosis in Transplanted Kidneys. *Am. J. Transpl.* 21 (2), 727–739. doi:10.1111/ajt.16287

Yao, L., Wright, M. F., Farmer, B. C., Peterson, L. S., Khan, A. M., Zhong, J., et al. (2019). Fibroblast-Specific Plasminogen Activator Inhibitor-1 Depletion Ameliorates Renal Interstitial Fibrosis after Unilateral Ureteral Obstruction. *Nephrol. Dial. Transpl.* 34 (12), 2042–2050. doi:10.1093/ndt/gfz050

Yiu, W. H., Li, Y., Lok, S. W. Y., Chan, K. W., Chan, L. Y. Y., Leung, J. C. K., et al. (2021). Protective Role of Kallistatin in Renal Fibrosis via Modulation of Wnt/β-Catenin Signaling. *Clin. Sci.* 135 (3), 429–446. doi:10.1042/cs20201161

Zeng, Z., Wang, Q., Yang, X., Ren, Y., Jiao, S., Zhu, Q., et al. (2019). Qishen Granule Attenuates Cardiac Fibrosis by Regulating TGF-β /Smad3 and GSK-3β Pathway. *Phytomedicine* 62, 152949. doi:10.1016/j.phymed.2019.152949

Zhang, F., Wan, X., Cao, Y.-Z., Sun, D., and Cao, C.-C. (2018a). Klotho Gene-Modified BMSCs Showed Elevated Antifibrotic Effects by Inhibiting the Wnt/β-Catenin Pathway in Kidneys After Acute Injury. *Cell Biol. Int.* 42 (12), 1670–1679. doi:10.1002/cbin.11068

Zhang, Q., Xiao, X., Zheng, J., Li, M., Yu, M., Ping, F., et al. (2020). Qishen Yiqi Dripping Pill Protects against Diabetic Nephropathy by Inhibiting the Wnt/β-Catenin and Transforming Growth Factor-β/Smad Signaling Pathways in Rats. *Front. Physiol.* 11, 613324. doi:10.3389/fphys.2020.613324

Zhang, X., Fang, J., Chen, Z., Zhao, B., Wu, S., and Pan, Y. (2019). Qingshen Buyang Formula Attenuates Renal Fibrosis in 5/6 Nephrectomized Rats via Inhibiting EMT and Wnt/β-Catenin Pathway. *Evid. Based Complement. Alternat. Med.* 2019, 5370847. doi:10.1155/2019/5370847

Zhang, Y. D., Ding, X. J., Dai, H. Y., Peng, W. S., Guo, N. F., Zhang, Y., et al. (2018b). SB-216763, A GSK-3β Inhibitor, Protects against Aldosterone-Induced Cardiac, and Renal Injury by Activating Autophagy. *J. Cell Biochem.* 119 (7), 5934–5943. doi:10.1002/jcb.26788

Zhang, Z.-H., Zhao, Y.-Y., Cheng, X.-l., Dai, Z., Zhou, C., Bai, X., et al. (2013). General Toxicity of Pinellia Ternata (Thunb.) Berit. In Rat: a Metabonomic Method for Profiling of Serum Metabolic Changes. *J. Ethnopharmacol.* 149 (1), 303–310. doi:10.1016/j.jep.2013.06.039

Zhang, Z.-Y., Mai, Y., Yang, H., Dong, P.-Y., Zheng, X.-L., and Yang, G.-S. (2014). CTSB Promotes Porcine Preadipocytes Differentiation by Degrading Fibronectin and Attenuating the Wnt/β-Catenin Signaling Pathway. *Mol. Cell Biochem.* 395 (1-2), 53–64. doi:10.1007/s11010-014-2111-6

Zhao, Y.-Y., Cheng, X.-L., Cui, J.-H., Yan, X.-R., Wei, F., Bai, X., et al. (2012a). Effect of Ergosta-4,6,8(14),22-Tetraen-3-One (Ergone) on Adenine-Induced Chronic Renal Failure Rat: A Serum Metabonomic Study Based on Ultra Performance Liquid Chromatography/High-Sensitivity Mass Spectrometry Coupled with MassLynx I-FIT Algorithm. *Clin. Chim. Acta* 413 (19–20), 1438–1445. doi:10.1016/j.cca.2012.06.005

Zhao, Y.-Y., Feng, Y.-L., Du, X., Xi, Z.-H., Cheng, X.-L., and Wei, F. (2012b). Diuretic Activity of the Ethanol and Aqueous Extracts of the Surface Layer of Poria Cocos in Rat. *J. Ethnopharmacol.* 144 (3), 775–778. doi:10.1016/j.jep.2012.09.033

Zhao, Y.-Y., Li, H.-T., Feng, Y.-L., Bai, X., and Lin, R.-C. (2013). Urinary Metabonomic Study of the Surface Layer of Poria Cocos as an Effective Treatment for Chronic Renal Injury in Rats. *J. Ethnopharmacol.* 148 (2), 403–410. doi:10.1016/j.jep.2013.04.018

Zhao, Y.-Y. (2013). Traditional Uses, Phytochemistry, Pharmacology, Pharmacokinetics and Quality Control of Polyporus Umbellatus (Pers.) Fries: A Review. *J. Ethnopharmacol.* 149 (1), 35–48. doi:10.1016/j.jep.2013.06.031

Zhao, Y.-y., Xie, R.-m., Chao, X., Zhang, Y., Lin, R.-c., and Sun, W.-j. (2009). Bioactivity-Directed Isolation, Identification of Diuretic Compounds from *Polyporus umbellatus*. *J. Ethnopharmacol.* 126 (1), 184–187. doi:10.1016/j.jep.2009.07.033

Zhao, Y.-Y., Zhang, L., Mao, J.-R., Cheng, X.-H., Lin, R.-C., Zhang, Y., et al. (2011). Ergosta-4,6,8(14),22-Tetraen-3-One Isolated from Polyporus Umbellatus Prevents Early Renal Injury in Aristolochic Acid-Induced Nephropathy

Rats. *J. Pharm. Pharmacol.* 63 (12), 1581–1586. doi:10.1111/j.2042-7158.2011.01361.x

Zhao, Y., Wang, C., Wang, C., Hong, X., Miao, J., Liao, Y., et al. (2018). An Essential Role for Wnt/β-Catenin Signaling in Mediating Hypertensive Heart Disease. *Sci. Rep.* 8 (1), 8996. doi:10.1038/s41598-018-27064-2

Zhao, Y. Y., Chen, H., Tian, T., Chen, D. Q., Bai, X., and Wei, F. (2014). A Pharmaco-Metabonomic Study on Chronic Kidney Disease and Therapeutic Effect of Ergone by UPLC-QTOF/HDMS. *PLoS One* 9 (9), e115467. doi:10.1371/journal.pone.0115467

Zhou, D., Fu, H., Zhang, L., Zhang, K., Min, Y., Xiao, L., et al. (2017). Tubule-Derived Wnts are Required for Fibroblast Activation and Kidney Fibrosis. *J. Am. Soc. Nephrol.* 28 (8), 2322–2336. doi:10.1681/asn.2016080902

Zhou, D., Tan, R. J., Fu, H., and Liu, Y. (2016). Wnt/β-Catenin Signaling in Kidney Injury and Repair: A Double-Edged Sword. *Lab. Invest.* 96 (2), 156–167. doi:10.1038/labinvest.2015.153

Zhou, G., Li, J., Zeng, T., Yang, P., and Li, A. (2020). The Regulation Effect of WNT-RAS Signaling in Hypothalamic Paraventricular Nucleus on Renal Fibrosis. *J. Nephrol.* 33 (2), 289–297. doi:10.1007/s40620-019-00637-8

Zhou, L., Li, Y., Hao, S., Zhou, D., Tan, R. J., Nie, J., et al. (2015b). Multiple Genes of the Renin-Angiotensin System Are Novel Targets of Wnt/β-Catenin Signaling. *J. Am. Soc. Nephrol.* 26 (1), 107–120. doi:10.1681/asn.2014010085

Zhou, L., Li, Y., Zhou, D., Tan, R. J., and Liu, Y. (2013). Loss of Klotho Contributes to Kidney Injury by Derepression of Wnt/β-Catenin Signaling. *J. Am. Soc. Nephrol.* 24 (5), 771–785. doi:10.1681/asn.2012080865

Zhou, L., and Liu, Y. (2016). Wnt/β-Catenin Signaling and Renin-Angiotensin System in Chronic Kidney Disease. *Curr. Opin. Nephrol. Hypertens.* 25 (2), 100–106. doi:10.1097/mnh.0000000000000205

Zhou, L., and Liu, Y. (2015). Wnt/β-Catenin Signalling and Podocyte Dysfunction in Proteinuric Kidney Disease. *Nat. Rev. Nephrol.* 11 (9), 535–545. doi:10.1038/nrneph.2015.88

Zhou, L., Mo, H., Miao, J., Zhou, D., Tan, R. J., Hou, F. F., et al. (2015a). Klotho Ameliorates Kidney Injury and Fibrosis and Normalizes Blood Pressure by Targeting the Renin-Angiotensin System. *Am. J. Pathol.* 185 (12), 3211–3223. doi:10.1016/j.ajpath.2015.08.004

Zhou, S., Wu, Q., Lin, X., Ling, X., Miao, J., Liu, X., et al. (2021). Cannabinoid Receptor Type 2 Promotes Kidney Fibrosis Through Orchestrating β-catenin Signaling. *Kidney Int.* 99 (2), 364–381. doi:10.1016/j.kint.2020.09.025

Zhuang, S., Hua, X., He, K., Zhou, T., Zhang, J., Wu, H., et al. (2018). Inhibition of GSK-3β Induces AP-1-mediated Osteopontin Expression to Promote Cholestatic Liver Fibrosis. *FASEB J.* 32 (8), 4494–4503. doi:10.1096/fj.201701137R

Conflict of Interest: The authors declare that the research was conducted in the absence of any commercial or financial relationships that could be construed as a potential conflict of interest.

Publisher's Note: All claims expressed in this article are solely those of the authors and do not necessarily represent those of their affiliated organizations, or those of the publisher, the editors and the reviewers. Any product that may be evaluated in this article, or claim that may be made by its manufacturer, is not guaranteed or endorsed by the publisher.

GLOSSARY

α-SMA α-smooth muscle actin
AA aristolochic acid
AKI acute kidney injury
APC adenomatous polyposis coli
API apigenin
CB2 cannabinoid receptor type 2
CBP CREB-binding protein
CHMs Chinese herbal medicines
CK1 casein kinase 1
CKD Chronic kidney disease
CRD cysteine-rich domains
CRF chronic renal failure
DAMPs danger-associated molecular patterns
DKK1 Dickkopf1
DN diabetic nephropathy
DVL Dishevelled
ECM extracellular matrix
EMT epithelial-mesenchymal transition
ESRD end-stage renal disease
fsp1 fibroblast-specific protein 1
FGF-2 fibroblast growth factor-2
FSGS glomerulosclerosis
FZD Frizzled
GSK3β glycogen synthase kinase 3β
HH Hedgehog
HIF-1α hypoxia inducible factor-1α
IDO indoleamine-2,3-dioxygenase
IRI ischemia-reperfusion injury
IWR inhibitors of Wnt response
LEF lymphatic enhancer-binding factor
LRP5/6 low-density lipoprotein receptor-related protein-5/protein-6
MMP-7 matrix metalloproteinase-7
PAA Poricoic acid A
PAI-1 plasminogen activator inhibitor-1
PGE2 prostaglandin E2
PORCN Porcupine
(P)RR (pro)renin receptor
PZC poricoic acid ZC
PZD poricoic acid ZD
PZE poricoic acid ZE
PZG poricoic acid ZG
PZH poricoic acid ZH
RAS renin-angiotensin system
SCIs Substrate competitive inhibitors
Sfrp1 secreted frizzled protein 1
Snail1 Snail family zinc finger 1
SSc Systemic sclerosis
tPA tissue-type plasminogen activator
TCF transcription factors T cell factor
TCM traditional Chinese medicine
TECs tubular epithelial cells
TGF-β transforming growth factor β
Tnks Tankyrase
TRPC6 transient receptor potential canonical 6
UA uric acid
Upa urokinase-type plasminogen activator
UUO unilateral ureteral obstruction
Wif-1 Wnt inhibitor 1
Wnt/Ca^{2+} pathway Wnt/calcium pathway
Wnt/PCP pathway Wnt/planar cell polarity pathway

frontiers in Pharmacology

ORIGINAL RESEARCH
published: 13 September 2021
doi: 10.3389/fphar.2021.708575

Renoprotective Effects of Maslinic Acid on Experimental Renal Fibrosis in Unilateral Ureteral Obstruction Model via Targeting MyD88

*Wenjuan Sun, Chang Hyun Byon, Dong Hyun Kim, Hoon In Choi, Jung Sun Park, Soo Yeon Joo, In Jin Kim, Inae Jung, Eun Hui Bae, Seong Kwon Ma and Soo Wan Kim**

Department of Internal Medicine, Chonnam National University Medical School, Gwangju, South Korea

Maslinic acid (MA), also named crategolic acid, is a pentacyclic triterpene extracted from fruits and vegetables. Although various beneficial pharmacological effects of MA have been revealed, its effect on renal fibrosis remains unclear. This study was designed to clarify whether MA could attenuate renal fibrosis and determine the putative underlying molecular mechanisms. We demonstrated that MA-treated mice with unilateral ureteral obstruction (UUO) developed a histological injury of low severity and exhibited downregulated expression of fibrotic markers, including α-smooth muscle actin (α-SMA), vimentin, and fibronectin by 38, 44 and 40%, and upregulated expression of E-cadherin by 70% as compared with untreated UUO mice. Moreover, MA treatment restored the expression levels of α-SMA, connective tissue growth factor, and vimentin to 10, 7.8 and 38% of those induced by transforming growth factor (TGF)-β in NRK49F cells. MA decreased expression of Smad2/3 phosphorylation and Smad4 in UUO kidneys and TGF-β treated NRK49F cells ($p < 0.05$, respectively). Notably, MA specifically interferes with MyD88, an adaptor protein, thereby mitigating Smad4 nuclear expression ($p < 0.01$ compared to TGF-β treated group) and ameliorating renal fibrotic changes ($p < 0.01$ for each fibrotic markers compared to TGF-β induced cells). In addition, in the UUO model and lipopolysaccharide-induced NRK49F cells, MA treatment decreased the expression of IL-1β, TGF-α and MCP-1, ICAM-1, associated with the suppression of NF-κB signaling. These findings suggest that MA is a potential agent that can reduce renal interstitial fibrosis, to some extent, via targeting TGF-β/Smad and MyD88 signaling.

Keywords: maslinic acid, renal interstitial fibrosis, MyD88, Smad4 nuclear expression, unilateral ureteral obstruction, NF-κB

OPEN ACCESS

Edited by:
Zhiyong Guo,
Second Military Medical University, China

Reviewed by:
George Shehatou,
Delta University, Egypt
Adrian M Ramos,
Health Research Institute Foundation Jimenez Diaz (IIS-FJD), Spain

****Correspondence:***
Soo Wan Kim
skimw@chonnam.ac.kr

Specialty section:
This article was submitted to Renal Pharmacology, a section of the journal Frontiers in Pharmacology

Received: *12 May 2021*
Accepted: *30 August 2021*
Published: *13 September 2021*

Citation:
Sun W, Byon CH, Kim DH, Choi HI, Park JS, Joo SY, Kim IJ, Jung I, Bae EH, Ma SK and Kim SW (2021) Renoprotective Effects of Maslinic Acid on Experimental Renal Fibrosis in Unilateral Ureteral Obstruction Model via Targeting MyD88. Front. Pharmacol. 12:708575. doi: 10.3389/fphar.2021.708575

INTRODUCTION

Chronic kidney disease (CKD) is a significant health problem. In recent years, the increasing prevalence of CKD is evident among about 5% of younger adults (aged 20–39 years) as well as nearly half of older adults (aged 70 years and above) (Chou and Chen, 2021). A key step involved in CKD is renal fibrosis, which includes glomerular fibrosis and tubulointerstitial fibrosis. Renal interstitial fibrosis is characterized by the excessive production and deposition of extracellular matrix (ECM) proteins and is strongly correlated with tubulointerstitial inflammation (Liu, 2011; Urban et al., 2015; Humphreys, 2018). This process has been confirmed to involve the following key events: loss of

epithelial adhesions, reorganization of the cytoskeleton, *de novo* synthesis of α-smooth muscle actin (α-SMA), destruction of the tubular basement membrane, and enhanced cell migration and interstitial invasion (Geiger and Yamada, 2011; Bülow and Boor, 2019). These events involve changes in the expression of many proteins, such as the early downregulation of E-cadherin expression, which leads to decreased intercellular adhesion, upregulated mesenchymal vimentin expression, and increased protein synthesis such as fibronectin and collagen (I and III) synthesis (Bonnans et al., 2014; Škovierová et al., 2018; Theocharis et al., 2019). In the kidneys, connective tissue growth factor (CTGF) is mainly expressed in parietal epithelial cells, some interstitial cells, and visceral epithelial cells. Transforming growth factor (TGF)-β induces CTGF release, thus enhancing the production of fibronectin, collagen I, and vascular endothelial growth factor (Gupta et al., 2000; Gore-Hyer et al., 2002). Ultimately, all these processes of interstitial fibrosis lead to kidney failure, regardless of the underlying disease.

Unilateral ureteral obstruction (UUO) is a classic and widely used model of experimental renal interstitial fibrosis. This model is established via ligation of one side of the ureter, leading to urinary tract obstruction. The obstruction injury of the kidney is accompanied by tubular atrophy and irreversible interstitial fibrosis, and its hallmark event is the excessive production and deposition of ECM in the interstitium (Popper et al., 2019). ECM proteins are produced and secreted by myofibroblasts, and it has been demonstrated that epithelial-mesenchymal transition (EMT) and interstitial fibroblast activation are two important events for transdifferentiation of myofibroblast cells (Savagner, 2001).

TGF-β is a key mediator driving the fibrotic reaction of most organs (Pohlers et al., 2009). It is synthesized and secreted by inflammatory cells and various effector cells. TGF-β activation leads to the formation and deposition of ECM components; thus, it may become a potential and effective anti-fibrotic target (Chen et al., 2018; Hao et al., 2019). Two signaling pathways are associated with renal fibrosis: Smad as well as non-Smad signaling pathways mediated by TGF-β. In the Smad signaling pathway, binding of TGF-β to its ligand induces the recruitment and phosphorylation of serine-threonine kinases at type I receptors, which in turn phosphorylate Smads (p-Smad2/3). Subsequently, a signaling complex with Smad4 is formed and translocated into the nucleus, thereby upregulating the expression of α-SMA, vimentin, fibronectin, and other ECM proteins or downregulating that of E-cadherin (Wendt et al., 2009; Pardali et al., 2017).

MyD88 is a moderately sized adaptor protein involved in the Toll-like receptor (TLR) and interleukin (IL)-1β receptor signaling pathways involved in mammalian host defense (Brightbill and Modlin, 2000). Most TLR signaling mechanisms mediated by TLR2, TLR5, and TLR9 critically require MyD88 for the initiation of the signaling cascade by assembling a so called "myddosome" high-scaffold signaling complex, which ultimately results in the activation of nuclear factor (NF)-κB (Kawasaki and Kawai, 2014; Chen et al., 2020). Additionally, evidence has indicated that IL-1β can enhance TGF-β signaling and eventually lead to EMT (Artlett, 2012; Zhang et al., 2016). Previous reports suggest that EMT develops as a result of IL-1β binding to its receptors and downstream activation of MyD88 and the c-JUN transcription factor, which could aggravate TGF-β/Smad-mediated fibrosis via increased TGF-β expression (Lee et al., 2006; Jia et al., 2014; Liu X. et al., 2020). Since few studies have focused on the direct association between MyD88 and TGF-β mediated renal fibrosis, further studies are needed to define the functional implications of MyD88 in the TGF-β/Smad signaling pathway. Inflammation has an important role in the development of chronic renal ailments. UUO causes kidney damage primarily through an interstitial inflammatory response, apoptosis, and gradual interstitial fibrosis (Nogueira et al., 2017). Among them, inflammatory reactions are distinguished by an overabundance of cytokines, like pro-inflammasome interleukin (IL)-1β, tumor necrosis factor-α (TNF-α), monocyte chemoattractant protein-1 (MCP-1), and intercellular adhesion molecule-1 (ICAM-1) (Imig and Ryan, 2013; Black et al., 2019).

The NF-κB signaling system is the primary regulator of immunological and inflammatory responses. Also, the activation of NF-κB could result in renal inflammation, tubular EMT, and ECM buildup. (Zavadil and Böttinger, 2005; Tamada et al., 2006). The NF-κB complex is usually inactive and located in the cytoplasm while bound to IκB inhibitor proteins; however, after activation of pro-inflammasome, NF-κB is activated and translocates to the nucleus, where it forms the p65/p50 complex to control target gene transcription (Mussbacher et al., 2019). Lipopolysaccharide (LPS), is well known for its toxicity in the pathogenesis of sepsis in various organs (Kiemer et al., 2002; Hamesch et al., 2015; Liu Z. et al., 2020). Some evidence suggests that renal tubular epithelial cells undergo apoptotic and necrotic processes when LPS-induced inflammation is activated (Bascands et al., 2009). Accordingly, LPS-induced kidney injury may be useful for inflammation associated mechanism study in kidney disease.

MA is a pentacyclic triterpene that occurs naturally in the protective wax-like coating of the leaves and fruit of *Olea europaea L* (Hashmi et al., 2015). Extensive studies have focused on the protective effect of MA against cancer (Reyes-Zurita et al., 2009; Wei et al., 2019; Liu Y. et al., 2020). Furthermore, MA has been confirmed to affect various organs, such as the brain, heart, liver and bones (Qian et al., 2015; Liou et al., 2019; Chen et al., 2021; Shaik et al., 2021). Mechanistic studies have revealed that MA functions in many biological processes, including metabolism, apoptosis, inflammation, and cell proliferation via the NF-κB, PI3K-AKT, and other signaling pathways (Fukumitsu et al., 2016; Liu et al., 2018; Bae et al., 2020; Lee et al., 2020). Especially, Liu et al. found that MA treatment inhibits cardiac hypertrophy and cardiac fibrosis in mice via reduced phosphorylation of ERK and AKT signaling molecules (Liu et al., 2018). Also, researchers demonstrated that MA improves oxidative stress and renal function in streptozotocin-induced diabetic rats (Mkhwanazi et al., 2014). However, to date, there has been no report on the antifibrotic potential of MA in the kidneys.

The aim of our current study was to explore whether MA could exert anti-fibrotic effects on renal interstitial fibrosis. In

addition, the role of MA in the TGF-β/Smad pathway mediated by MyD88 was also investigated.

MATERIALS AND METHODS

Reagents and Antibodies

MA (M6699) was purchased from Sigma-Aldrich (St. Louis, MO, United States). The following primary antibodies were used for immunoblotting: anti-α-SMA (A2547; Sigma); anti-E-cadherin (#610182; BD Transduction Laboratories, San Jose, CA, United States); anti-fibronectin (SC-71114), anti-β-actin (SC-47778), anti-CTGF (SC-14939), anti-Smad6 (SC-25321), and Smad7 (SC-11392), anti-p-(NF)-κB-P65 (SC-33020), anti-(NF)-κB-P65 (SC-372) and MyD88 siRNA (SC-106986) from Santa Cruz Biotechnology (Santa Cruz, CA, United States); anti-GAPDH (AM4300; Ambion, Austin, TX, United States); anti-Lamin B antibody (ab16048, Abcam, Cambridge, United Kingdom); and anti-TGF-β (#3711S), anti-T-Smad2/3 (#3102S), anti-p-Smad2/3 (#8828S), anti-Smad4 (#38454S), anti-MyD88 (#4283S), and anti-vimentin (#5741S) from Cell Signaling Technology (Danvers, MA, United States); anti-F4/80 (MCA497GA, Bio-Rad, Hercules, CA).

Animal Experiments

Five-week-old male C57BL/6 mice (15–20 g) were purchased from Samtako (Osan, South Korea). Mice were randomized into three groups: sham-operated, UUO, and MA-treated UUO (UUO + MA) groups (n = 6 each). UUO was generated by ligation of the left ureter. The abdominal cavity was exposed through a midventral incision, and a 40 silk ligature was placed at the left proximal ureter under isoflurane anesthesia (792632; Sigma). The sham group received the same surgical procedures without ureter ligation. After 24 h of ligation, the UUO + MA group was intraperitoneally injected with MA at 20 mg/kg/day for 6 days (dissolved in 20 μl DMSO), based on a previous report (Ampofo et al., 2019). Sham-operated group was treated with DMSO. All mice were euthanized and the kidneys were harvested on day 7. All animal experiments were approved by the Animal Care Regulations Committee of Chonnam National University Medical School (CNUHIACUC-20033), and our protocols conformed to the institutional guidelines for experimental animal care and use.

Cell Culture and Treatment

Rat kidney interstitial fibroblast (NRK49F) cells and rat proximal tubular epithelial (NRK-52E) cells (American Type Culture Collection, Manassas, VA, United States) were cultured in high-glucose Dulbecco's modified Eagle's medium (DMEM; Welgene, Daegu, South Korea) containing 5% fetal bovine serum (FBS) and 1% streptomycin/penicillin at 37°C under a 5% CO_2 atmosphere. After starvation with 0.5% FBS medium for 24 h, cells were pretreated with MA or vehicle-alone (DMSO) for 2 h and then incubated with TGF-β (10 ng/ml) for 30 min and harvested or displace to 5% FBS medium for 24 h. The starvation of NRK49F cell and NRK52E cell was incubated with LPS (25 ng/ml or 200 ng/ml) for 2 h. Recombinant TGF-β was purchased from Pepro Tech (Rocky Hill, NJ, United States). LPS was purchased from Sigma Chemical (Escherichia Coli 0111:B4, St. Louis, MO). MA was dissolved in dimethyl sulfoxide to obtain a 20 mM stock solution and stored at −20°C.

Histology

Tissue sections were fixed with 4% paraformaldehyde and then embedded in paraffin sections. After dewaxing, the slides were processed for hematoxylin and eosin (H&E) staining. The kidney slides were stained with Gill's hematoxylin for 5 min, washed with tap water, differentiated with 0.3% acid alcohol, and incubated in eosin and phloxine for 2 min. Finally, the sections were dehydrated and mounted.

Periodic acid-Schiff (PAS) staining was performed according to the manufacturer's instructions. The tubular damage was evaluated as reversible or irreversible, previously described by Cohen A et al. (Cohen, 2007). The reversible damaged tubular was identified as the brush border absence. The irreversible damage was recognized by the presence of mild dilatation; flattened epithelial cells and loss of brush border; denudation of basement membranes, tubular necrosis, and cell apoptosis. The damaged tubules per histological field were averaged, obtaining 10 values per animal for each variable.

For Masson's trichrome staining, the sections were deparaffinized and rehydrated through a series of 100, 95, and 70% alcohol and then re-fixed in Bouin's solution for 1 h at 56°C to improve staining quality. After rinsing with running tap water for 5–10 min to remove the yellow color, the sections were incubated in Weigert's iron hematoxylin solution and kept in Biebrich scarlet/acid fuchsin solution for 10–15 min.

The sections were differentiated in phosphotungstic-phosphomolybdic acid solution for 10 min, transferred directly to aniline blue solution for 10 min, subsequently incubated with acetic acid for 2 min, and rapidly dehydrated with ethanol and xylene. Collagen deposition, nuclei, and muscle fibers were stained blue, black, and red, respectively.

Real-Time PCR

RNA from the kidney tissue was extracted with TRIzol RNA reagent (Invitrogen, Carlsbad, CA), and the concentration was quantified with NanoDrop™(Ultraspec 2000; Pharmacia Biotech, Cambridge, United Kingdom). cDNA was synthesized using Smart Cycler II System (Cepheid, Sunnyvale, CA). SYBR green was used for real-time PCR as dye to detect DNA. Relative levels of mRNA were determined by real-time PCR, using a Rotor-GeneTM 3000 Detector System (Corbette research, Mortlake, New South Wales, Australia). Sequences of primers are listed in **Supplementary Table S1**. The amount of the reagents was based on the instructions on the kit (GoTaq Master Mix, Cat. No. M7122). PCR conditions were as follows: 1) 95°C for 5 min; 2) 95°C for 20 s; 3) 58–60°C for 20 s (optimized for each primer pair); 4) 72°C for 30 s to detect SYBR Green. The Corbett Research Software was used to collect and evaluate data. The gene expression was calculated using the comparative critical threshold (Ct) values from quadruplicate measurements, with normalization to GAPDH as an internal control.

Immunohistochemical Staining

Immunohistochemical staining was performed with primary α-SMA antibody (A2547; Sigma) and horseradish peroxidase-conjugated anti-mouse IgG secondary antibody (Dako, Glostrup, Denmark). Sirius red staining was performed with a Picro Sirius Red Stain Kit (ab150681; Connective Tissue Stain; Abcam, Cambridge, United Kingdom). Visual fields were selected randomly in digital images of each section under ×20 magnification. The stained sections were imaged with a Nikon microscope (Tokyo, Japan). Quantitative analysis of the stained sections was performed using ImageJ software.

Cytotoxicity Assay

NRK49F cells were seeded into 96-well plates at a density of 1×10^4 cells/mL in a volume of 100 µl/well and allowed to attach for 24 h. The cells were starved with 0.5% FBS medium for 24 h and then treated with the indicated amounts of MA at 10, 20, 40, 80, and 100 µM or vehicle-alone (DMSO) for an additional 24 h. Cell viability was determined by an EZ-Cytox1000 kit (Dogen, Daejeon, South Korea) following the manufacturer's instructions. Absorbance was measured at 450 nm using a microplate reader (Bio-Tek Instruments, Winooski, VT, United States).

siRNA Knockdown

RNA interference of MyD88 was performed using rat siRNA from Santa Cruz Biotechnology (SC-106986). Cells were transfected with either scrambled siRNA (siScr) or siRNA against MyD88 (siMyD88) at 20 nM using DharmaFECT 1 transfection reagent according to the manufacturer's protocol (Park et al., 2019).

Western Blotting

Total proteins from kidneys or cells frozen in liquid nitrogen were lysed in ice-cold RIPA buffer (Thermo Scientific, Waltham, MA, United States). After brief centrifugation at 13000 ×g, tissue/cell debris was removed, and the supernatant was collected. The protein concentration was determined using a BCA Protein Assay kit (Thermo Scientific) according to the manufacturer's instructions. Equal amounts of lysates were electrophoresed using sodium dodecyl sulfate-polyacrylamide gel electrophoresis (Invitrogen, Carlsbad, CA, United States). Separated proteins were transferred to polyvinylidene fluoride membranes and blotted with specific antibodies (Kim et al., 2019). The densitometric analysis was conducted using ImageJ software.

Nuclear Extract Preparation

To prepare nuclear extracts, cells were lysed using NE-PER nuclear extraction reagent (NER; Pierce Biotechnology, Rockford, IL, United States) according to the manufacturer's protocol. Briefly, NRK49F cells were harvested by scraping in cold PBS and then centrifuged at 13000 ×g for 2 min. After removing the supernatant, 100 µl of ice-cold cytoplasmic extraction reagent (CER) was added to the dried cell pellets. After incubation in ice for 10 min, ice-cold CER II (5.5 µl) was added to the tube, which was centrifuged at 16000 ×g for 5 min, and the pellet fraction was suspended in 50 µl of ice-cold NER. After the tube was centrifuged at 16000 ×g for 10 min, the supernatant (nuclear extract) fraction was transferred to a new tube, and protein concentrations were measured by BCA assay.

Statistical Analysis

The differences between groups were determined using one-way analysis of variance (ANOVA) and followed by Tukey's post-hoc test for parametric data and Kruskal-Wallis test with Dunn's multiple comparison post-hoc tests for nonparametric data of tubular damage. Parametric variables were expressed as mean ± SD, and nonparametric variables were expressed as medians with interquartile (25th and 75th percentiles) ranges for continuous variables. p-Values < 0.05 were considered statistically significant. All statistical analyses were performed using GraphPad Prism 9 (GraphPad Software, San Diego, CA).

RESULTS

MA Ameliorates Histopathological Damages and Renal Fibrosis in UUO Model

We examined the effects of MA on renal interstitial fibrosis in the UUO mouse model (**Figure 1** A-E. H&E staining exhibited inflammatory cell infiltration in the obstructed kidney of the UUO group, whereas a normal renal cortex was observed in the Sham group. Compared with that in the UUO group, the renal injury in the UUO + MA group was reduced. PAS staining showed tubular brush border fracture, tubular atrophy and dilatation in the UUO group. However, the UUO + MA group presented less damage in a similar area. Consistently, based on Masson's trichrome staining, remarkable ECM deposition was evident in kidneys in the UUO group, whereas those in the UUO + MA group displayed less collagen deposition with less scope and extent of ECM deposition.

To evaluate ECM protein expression among the groups, α-SMA expression was analyzed via immunohistochemistry and collagen I/III deposition was examined using Sirius red staining. UUO kidneys showed increased immunolabeling of collagen I/III and α-SMA, which was attenuated in the UUO + MA group.

MA Inhibits Renal Tubular ECM Deposition and EMT in UUO Model

Immunoblotting analysis revealed that MA treatment downregulated protein expression of α-SMA, vimentin, and fibronectin in kidneys by 38, 44 and 40% respectively, as compared with untreated UUO group. In contrast, E-cadherin expression was markedly downregulated in UUO kidneys, which was recovered in the UUO + MA group, by approximately 70%. (**Figures 2A–E**).

MA Attenuates TGF-β-Stimulated Fibrotic Changes in NRK49F Cells

We further investigated the cytotoxic effects of MA on TGF-β-stimulated NRK49F cells (**Figure 3A**). Cytotoxicity assay

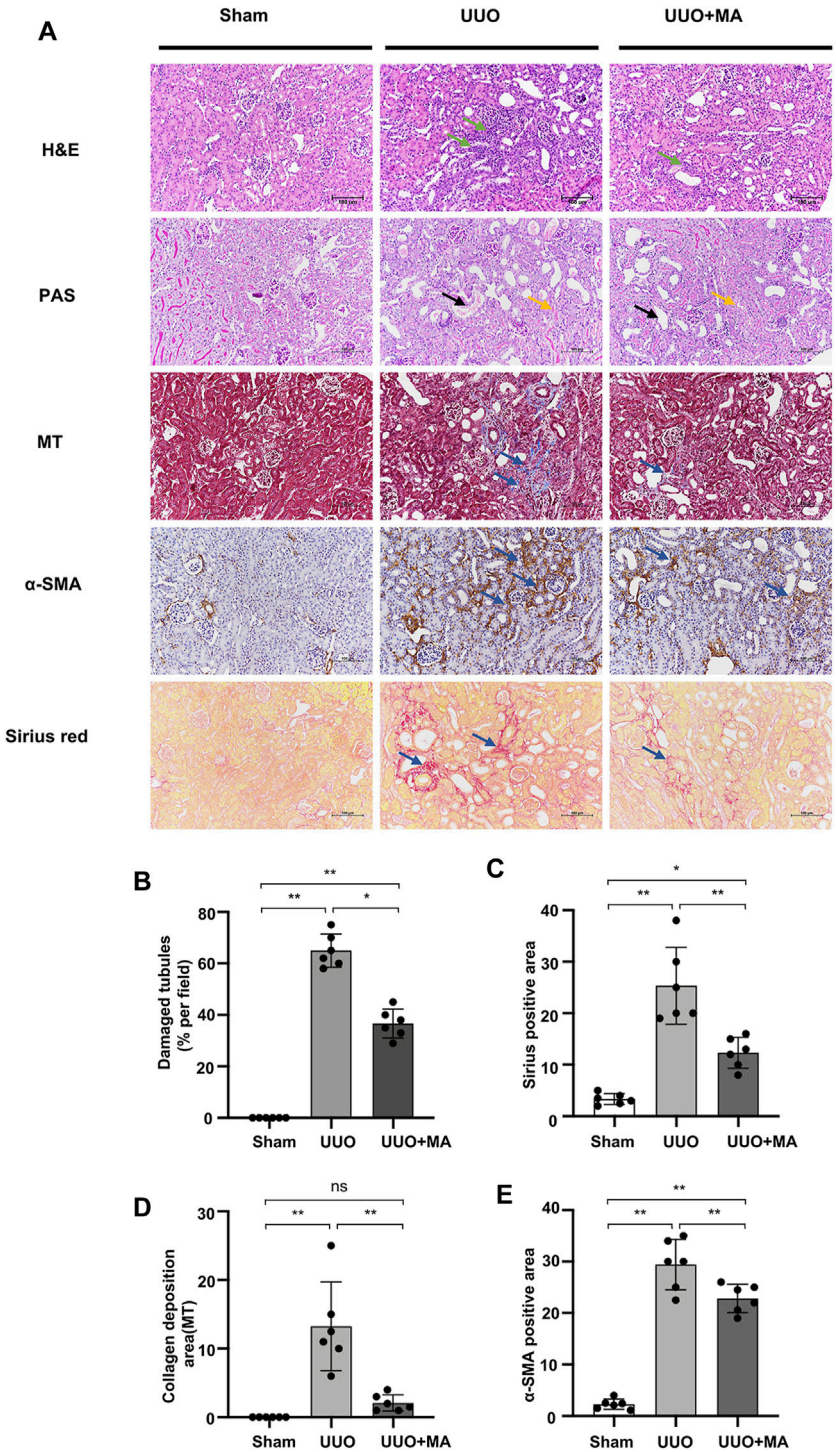

FIGURE 1 | MA ameliorates histopathological damages and renal fibrosis in UUO model. **(A)** Histological changes were assessed by H&E and PAS staining. Typical interstitial tubular positive changes were indicated as follows; inflammatory cell infiltration (green arrow) in H&E stain; tubular brush border fracture (yellow arrow), and tubular atrophy and dilatation (black arrow) in PAS stain. Interstitial fibrosis (blue arrow) was assessed by MT, immunohistochemistry of α-SMA and Sirius red staining. Original magnification = ×20. Bar = 100 μm. **(B)** Kruskal-Wallis test for tubular damage, n = 6. *$p < 0.05$, **$p < 0.01$, ns: no significance. **(C–E)** Statistical significance was presented as the mean ± SD, $n = 6$. *$p < 0.05$, **$p < 0.01$, ns: no significance. HE, hematoxylin and eosin; PAS, Periodic Acid-Schiff stain; MT, Masson's trichrome stain; MA, maslinic acid; UUO, unilateral ureteral obstruction.

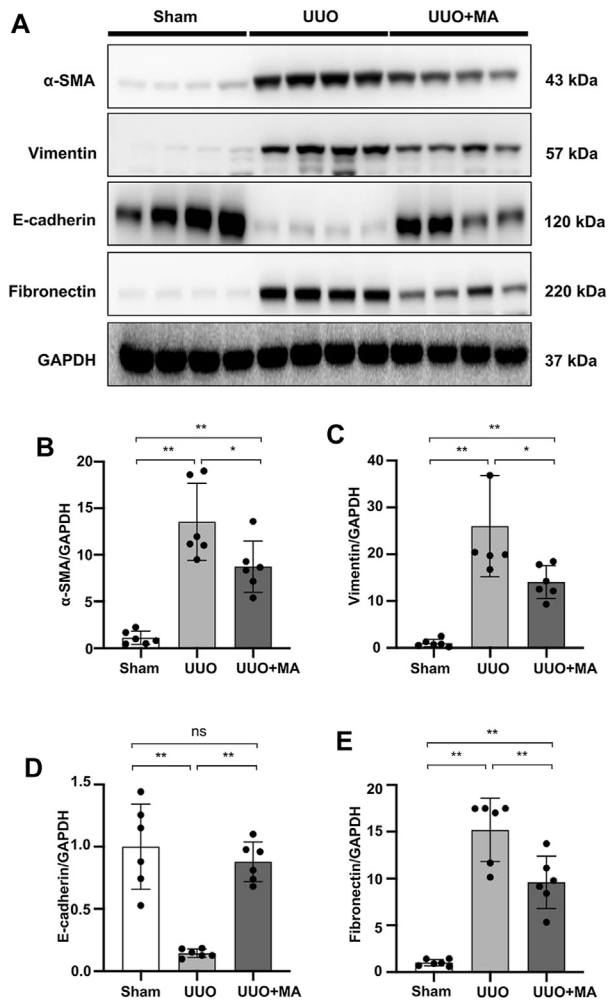

FIGURE 2 | MA inhibits renal tubular ECM deposition and EMT in the UUO model. **(A)** Expression of α-SMA, vimentin, E-cadherin, and fibronectin in kidney tissues was detected by western blot and quantified by densitometry. **(B–E)** Statistical significance was presented as the mean ± SD, $n = 6$. $^{*}p < 0.05$, $^{**}p < 0.01$, ns: no significance. MA, maslinic acid; UUO, unilateral ureteral obstruction.

showed no statistically significant changes in cell viability following treatment with 10–40 μM of MA, suggesting that the MA concentration in this range had no cytotoxic effect on NRK49F cells. TGF-β induced expression level of α-SMA, CTGF, and vimentin by TGF-β treatment was gradually reduced in a dose-dependent manner with the pretreatment of MA (40 μM MA treatment decreased to 10, 7.8 and 38% of TGF-β induced cell levels) (**Figures 3B–E**).

MA Suppresses the TGF-β/Smad Signaling Pathway and Downregulates MyD88 Expression in UUO Model and NRK49F Cells

As mentioned above, the TGF-β/Smad signaling pathway plays a key role in the pathogenesis of kidney fibrosis. UUO kidneys exhibited upregulated expression of TGF-β, p-Smad2/3, and Smad4. However, MA treatment significantly suppressed the expression of these fibrotic makers in UUO kidneys (**Figures 4A–E**). We further demonstrated that TGF-β-induced Smad2/3 phosphorylation and Smad4 expression were attenuated by pretreating NRK49F cells with MA (**Figures 4G–I**).

Also, the expression of MyD88 in the UUO model was significantly upregulated compared with that in the sham group, whereas its expression was remarkably downregulated following MA treatment (**Figures 4A,F**). Moreover, MyD88 expression induced after TGF-β stimulation was downregulated by MA pretreatment (**Figures 4G,J**). MyD88 mRNA levels were increased in UUO kidneys and TGF-β treated NRK49F cells. These increases were also reversed by MA treatment (**Supplementary Figures S1A,B**).

MA Reduces the TGF-β-Induced Nuclear Localization of Smad2/3 and Smad4 in TGF-β-Stimulated NRK49F Cells

The effect of MA on Smad signaling in response to TGF-β was further examined by Smad nuclear translocation. Pre-incubating NRK49F cells with MA significantly reduced the TGF-β–induced Smad2/3 and Smad4 nuclear translocation, but did not affect the nuclear expression of Smad6 and Smad7 (**Figures 5A–F**).

MyD88 Silencing Inhibits Fibrosis in TGF-β-Stimulated NRK49F Cells

To evaluate the close relationship between MyD88 and fibrotic changes in NRK49F cells, cells were transfected with siRNA against MyD88 and then subjected to TGF-β insult for 30 min. After 24 h in fresh media, TGF-β-induced increased expression level of α-SMA, CTGF, and vimentin was significantly reduced by MyD88 knockdown (**Figures 6A–E**).

MyD88 Silencing Hinders Nuclear Expression of Smad4 in TGF-β-Stimulated NRK49F Cells

In a previous study, MyD88 was shown to be directly upstream of the Smad4 signaling cascade (Samba-Mondonga et al., 2018). To evaluate the effect of MyD88 on the TGF-β/Smad signaling pathway, we examined the effect of MyD88 knockdown on Smad4 expression in NRK49F cells. Nuclear expression of Smad4 was induced by TGF-β within 30 min, which was significantly downregulated in the nucleus after transfection of siRNA targeting MyD88 (**Figures 7A–E**).

MA Ameliorates Renal Macrophage Infiltration and Inflammation in UUO Mice Model Associated With the Suppression of NF-κB Signaling

As the F4/80 molecule was established as a unique marker of murine macrophages, we assessed the effects of MA on the production of macrophages marker F4/80. Immunohistochemistry showed that there was clearly positive F4/80 antigen expression in UUO

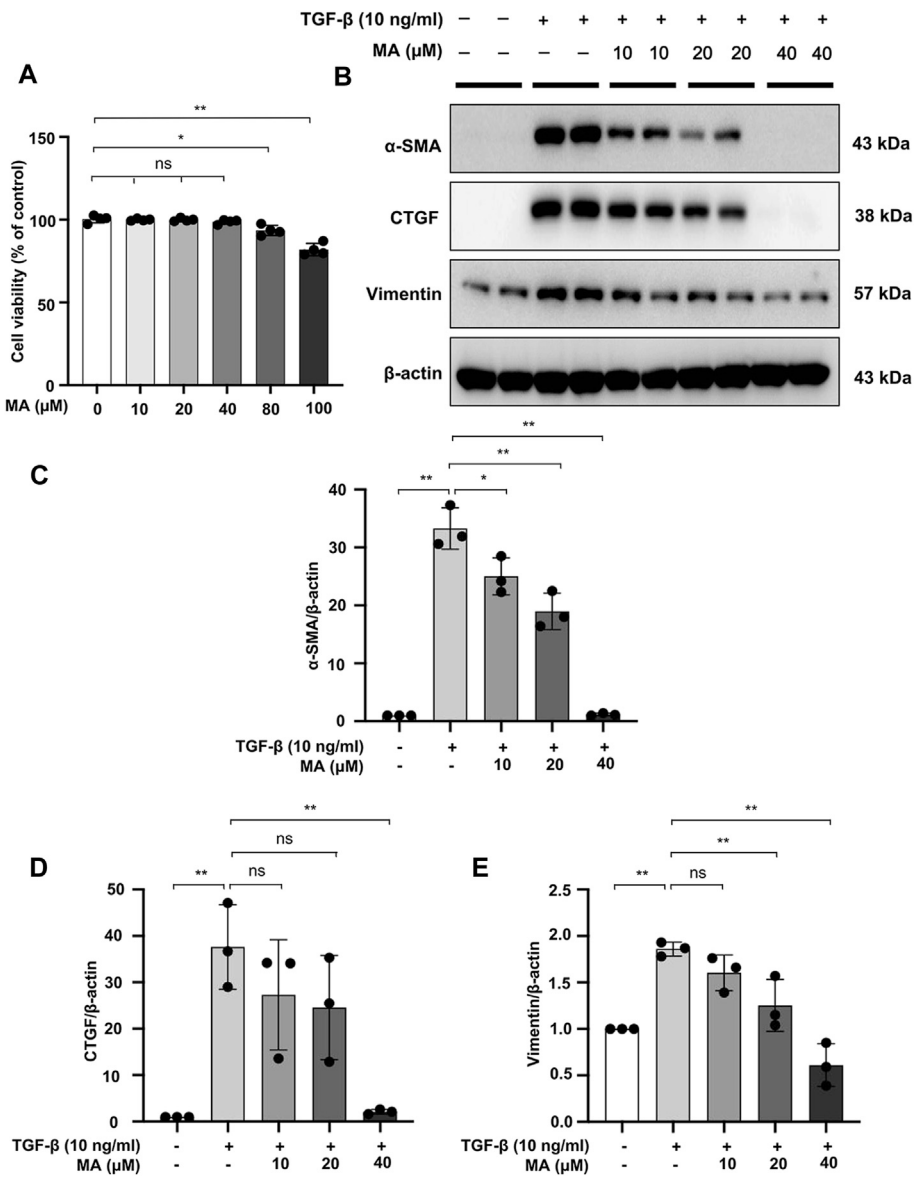

FIGURE 3 | MA attenuates TGF-β-stimulated fibrotic changes in NRK49F cells. **(A)** Cells were treated with MA for 24 h, and cytotoxicity assays were conducted. **(B)** Expression of α-SMA, CTGF, and vimentin in TGF-β-stimulated NRK49F cells was detected by western blot and quantified by densitometry. Cells were pretreated with MA for 2 h after starvation with 0.5% FBS medium, treated with TGF-β (10 ng/ml) for 30 min, and incubated in 5% FBS medium for 24 h. **(C–E)** The Statistical significance was presented as the mean ± SD, $n = 3$. $^{*}p < 0.05$, $^{**}p < 0.01$, ns: no significance. MA, maslinic acid.

kidneys, while it was significantly reduced by MA treatment (**Figures 8A,B**).

We evaluated the mRNA levels of pro-inflammatory cytokines and cell adhesion molecules. Real-time PCR revealed that the mRNA levels of IL-1β, TNF-α, MCP-1, and ICAM-1 were increased in UUO kidneys, which was reversed by MA pretreatment (**Figures 8C–F**). We further investigated the underlying signaling mechanisms by which MA protects against inflammation. To elucidate NF-κB signaling in UUO kidneys, we detected the protein level of p-P65 and P65. Compared with sham group, the protein levels of total p-P65 and P65 were significantly increased in UUO kidneys, while the MA treatment reversed these changes (**Figures 8G–I**).

MA Attenuates LPS-Induced Inflammation in NRK49F Cells and Suppresses NF-κB Signaling

mRNA levels of IL-1β, TNF-α, MCP-1, and ICAM-1 were increased in NRK49F cells by LPS treatment, the changes of which were ameliorated by MA co-administration (**Figures 9A–D**). These results supported the notion that MA exerted anti-inflammatory effect against the UUO injury and LPS. The

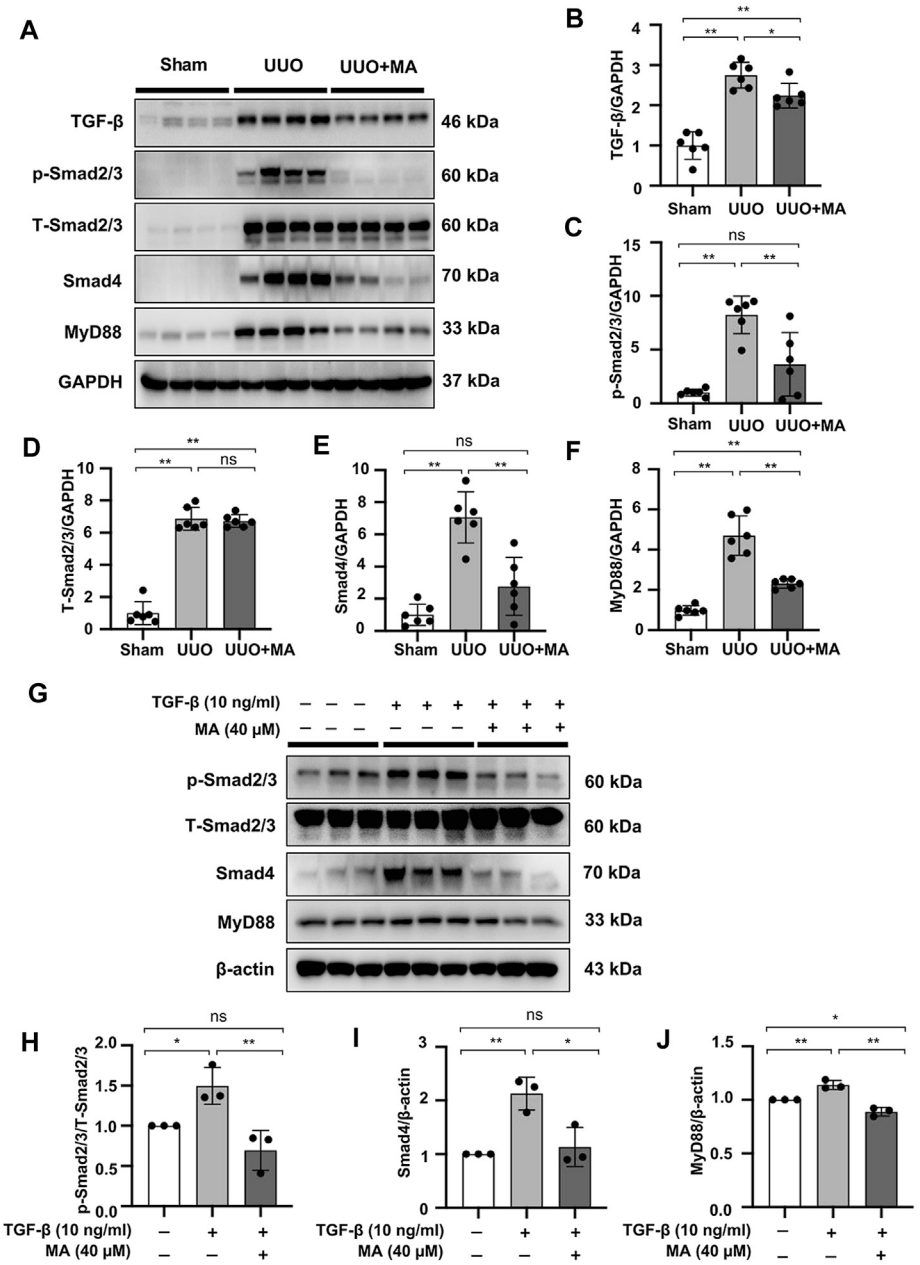

FIGURE 4 | MA suppresses the TGF-β/Smad signaling pathway and downregulates MyD88 expression in UUO model and NRK49F cells. **(A)** Expression of TGF-β, p-Smad2/3, T-Smad2/3, Smad4, and MyD88 in the kidney model was detected by western blot and quantified by densitometry. **(B–F)** Statistical significance was presented as the mean ± SD, $n = 6$. $^{*}p < 0.05$, $^{**}p < 0.01$, ns: no significance. **(G)** Expression of p-Smad2/3, T-Smad2/3, Smad4, and MyD88 in TGF-β-treated NRK49F cells was detected by western blot and quantified by densitometry. Cells were pretreated with MA for 2 h after starvation with 0.5% FBS medium and then treated with TGF-β (10 ng/ml) for 30 min **(H–J)** Statistical significance was presented as the mean ± SD, $n = 3$. $^{*}p < 0.05$, $^{**}p < 0.01$, ns: no significance. MA, maslinic acid; UUO, unilateral ureteral obstruction; RT-PCR, Real-Time PCR.

protein expressions of MyD88 and p-P65 in LPS treated NRK49F cells were higher than those in control group and MA only group, which were reduced by MA treatment (**Figures 9E–G**). Taken together, these results indicated that MA prevented the MyD88 and NF-κB signaling thereby suppressing the inflammatory response in the UUO model and LPS induced NRK49F cell lines.

MA Attenuates LPS-Induced Inflammation in NRK52E Cells and Suppresses NF-κB Signaling

mRNA levels of IL-1β, TNF-α, MCP-1, and ICAM-1 checked were increased by LPS treatment in NRK52E cells, MA decreased the mRNA expressions of IL-1β and TNF-α, but not MCP-1 and

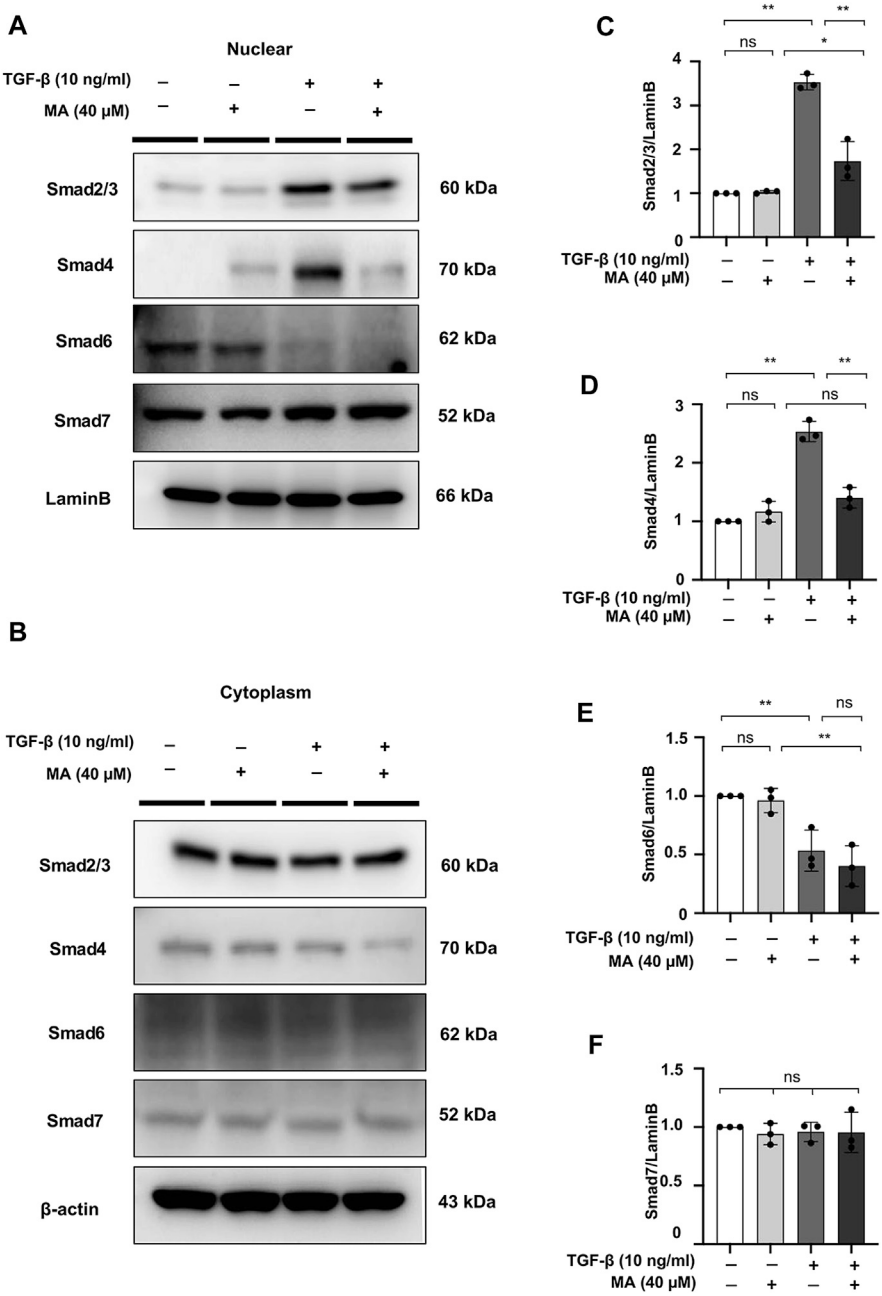

FIGURE 5 | MA reduces the TGF-β-induced nuclear localization of Smad2/3 and Smad4 in TGF-β-stimulated NRK49F cells. **(A,B)** Western blotting revealed that Smad2/3 and Smad4 nuclear translocation was blocked by MA, MA does not affect Smad6 or Smad7 nuclear expression in TGF-β-stimulated NRK49F cells. NRK49F cells were pre-treated with MA for 2 h and then treated with TGF-β (10 ng/ml) for 30 min for Smad2/3, Smad4 and Smad7 or 24 h for Smad6. Cytoplasmic and nuclear proteins were separated using CER/NER buffer. β-actin and Lamin B indicate the cytoplasmic and nuclear fractions, respectively. **(C–F)** Statistical significance was presented as the mean ± SD, $n = 3$. *$p < 0.05$, **$p < 0.01$, ns: no significance.

ICAM-1 (**Figures 10A–D**). MyD88 and p-P65 protein levels were increased by LPS treatment in NRK52E cells, which were reduced in MA treatment (**Figures 10E–G**). We further determined whether MA also inhibits the NF-κB signaling by TGF-β stimulation. No activation of p-P65 was observed by TGF-β in NRK49F and NRK52E cells (**Supplementary Figures S2A–E**).

DISCUSSION

In this study, we found that MA plays a beneficial role to attenuate renal interstitial fibrosis by negatively regulating the TGF-β/Smad and NF-κB pathway *via* targeting MyD88. Renal interstitial fibrosis has a prominent role in the development and progression of kidney injury. It is characterized by a large accumulation of ECM, which is

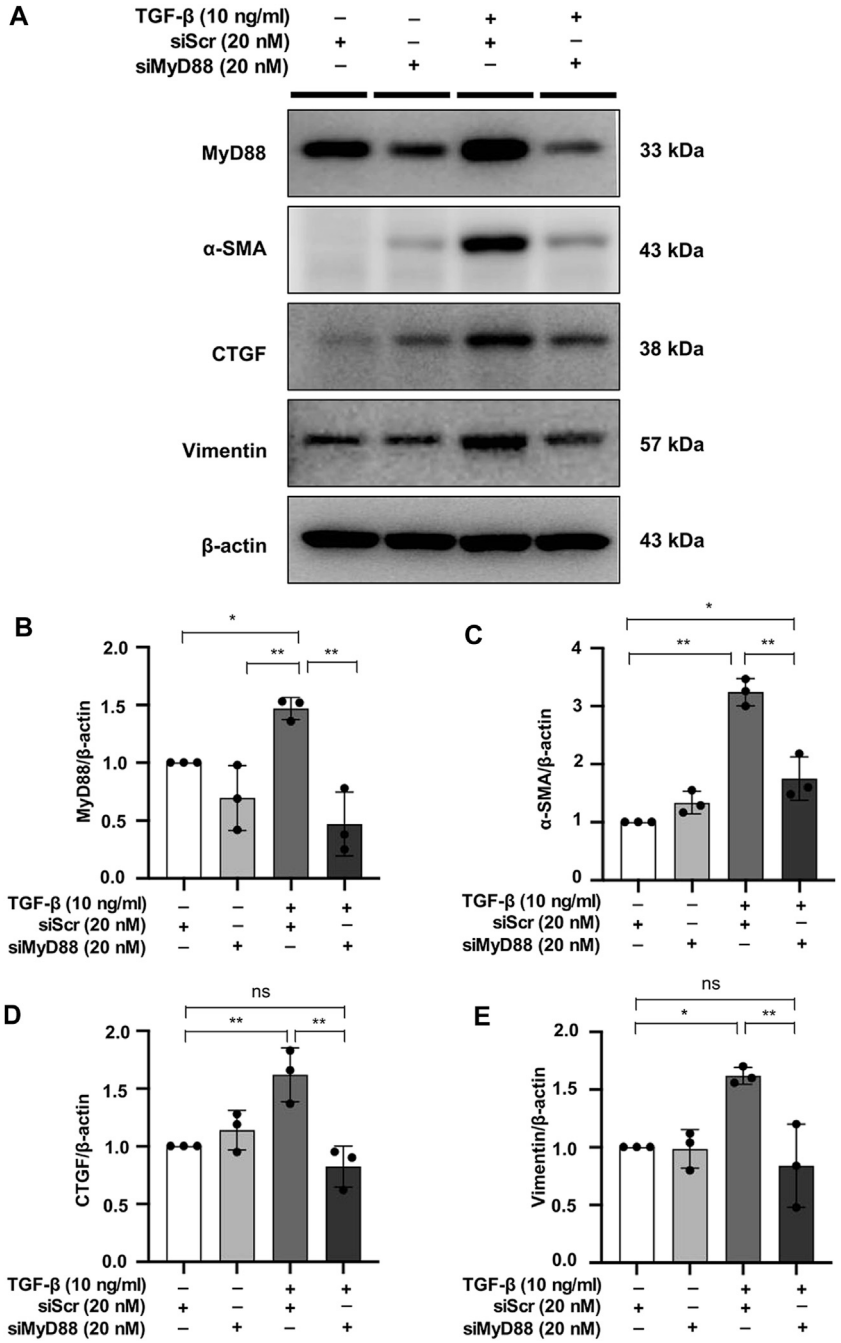

FIGURE 6 | MyD88 silencing inhibits fibrosis in TGF-β-stimulated NRK49F cells. **(A)** Western blotting demonstrated that MyD88 silencing facilitated the effect on the protein expression of α-SMA, CTGF, and vimentin in TGF-β-stimulated NRK49F cells. NRK49F cells were transfected with siMyD88 or siScr for 24 h in high-glucose DMEM without FBS, starved with 0.5% FBS medium, treated with TGF-β (10 ng/ml) for 30 min, and then incubated in 5% FBS medium for 24 h. Western blotting demonstrated that MyD88 expression was significantly reduced by the specific siRNA. Results were normalized to β-actin expression. **(B–E)** Statistical significance was presented as the mean ± SD, $n = 3$. $^{*}p < 0.05$, $^{**}p < 0.01$, ns: no significance. MA, maslinic acid; siRNA, small interfering RNA.

a complex network of collagen, elastin, several glycoproteins (e.g., fibronectin), and proteoglycans (Frantz et al., 2010; Mutsaers et al., 2015). Here, we demonstrated that MA treatment effectively downregulated ECM protein expression, suggesting that MA is effective in the treatment of renal fibrosis.

Fibroblast-to-myofibroblast transition, a representative process among several routes of exaggerated ECM accumulation in renal fibrosis, is characterized by the expression of mesenchymal cell products such as α-SMA, vimentin (intermediate filament), and collagen I (Klingberg

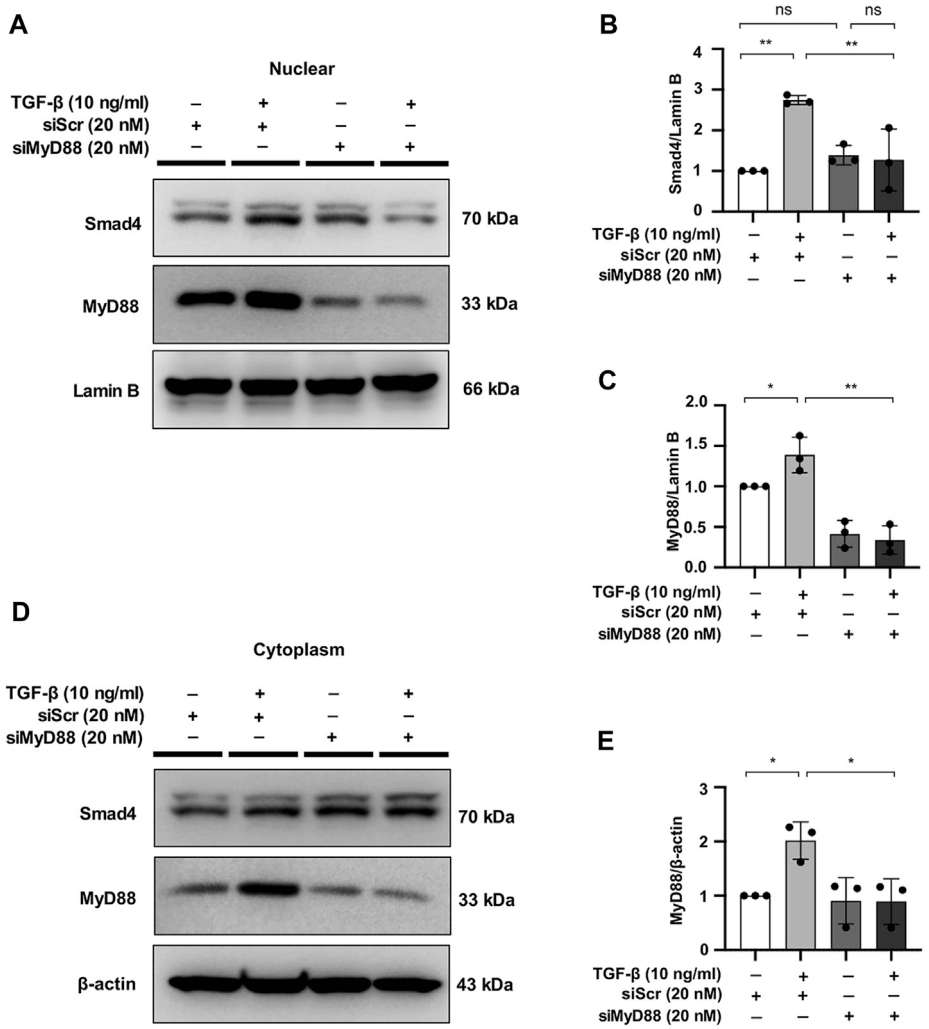

FIGURE 7 | MyD88 silencing hinders nuclear expression of Smad4 in TGF-β-stimulated NRK49F cells. **(A,D)** Western blotting revealed that Smad4 nuclear translocation was blocked by siMyD88 transfection in TGF-β-stimulated NRK49F cells. NRK49F cells were transfected with siMyD88 or siScr for 24 h in high-glucose DMEM without FBS, starved with 0.5% FBS medium, and then treated with TGF-β (10 ng/ml) for 30 min. Western blotting demonstrated that MyD88 expression was significantly reduced by the specific siRNA. Cytoplasmic and nuclear proteins were separated using CER/NER buffer. β-actin and Lamin B indicate the cytoplasmic and nuclear fractions, respectively. **(B,C,E)** Statistical significance was presented as the mean ± SD, $n = 3$. *$p < 0.05$, **$p < 0.01$, ns: no significance. MA, maslinic acid; siRNA, small interfering RNA.

et al., 2013; Desai et al., 2014). Additionally, downregulation of the expression and function of E-cadherin, an epithelial cell adhesion receptor essential in the maintenance of tubular epithelial integrity and cell-cell adhesion, is a phenotypic hallmark during EMT of tubular epithelial cells (Liu, 2004; Nieto et al., 2016). To investigate the effect of MA on ECM protein expression and EMT in renal fibrosis, we employed the UUO model and finally demonstrated that MA had an ameliorative effect on renal tubular injury and fibrosis. At the molecular level, we demonstrated that MA could reverse the expression of ECM, such as α-SMA, vimentin, and fibronectin. Moreover, a drastic decrease in E-cadherin in the kidney of UUO group was restored to a certain extent by MA treatment, further indicating that MA could delay EMT progression in UUO model. Collectively, the results demonstrated that MA is a beneficial effector of anti-fibrosis in the kidney of UUO model, leading to decreased ECM accumulation and EMT levels.

The increases in molecular markers, such as α-SMA, vimentin, and CTGF, represent the induction of TGF-β-stimulated fibrosis in NRK49F cells. Previous studies demonstrated that at least some pro-fibrotic effects of TGF-β were mediated through the upregulation of its downstream effector, CTGF (Biernacka et al., 2011). The downregulated expression of these fibrosis-related proteins clearly demonstrates the dose-dependent effects of MA pretreatment in NRK49F cells, which was consistent with the observation *in vivo*.

Our study also demonstrated that MA treatment attenuated the TGF-β/Smad pathway. In renal fibrosis, TGF-β is considered the master regulator of EMT and ECM accumulation (Xu et al., 2009; Bon et al., 2019). It is generally accepted that TGF-β

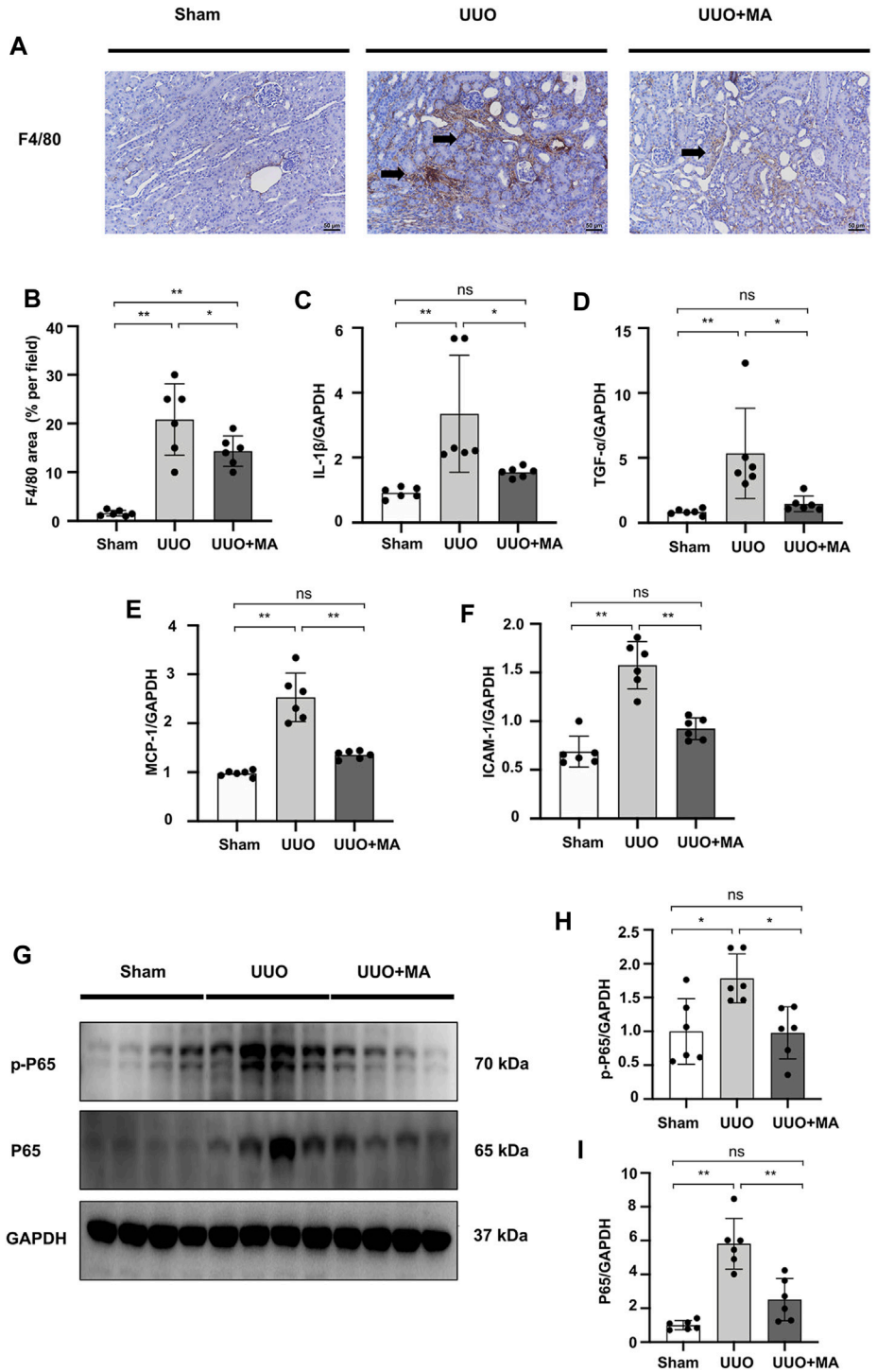

FIGURE 8 | MA ameliorates renal macrophage infiltration and inflammation in UUO mice model associated with the suppression of NF-κB signaling. **(A)** Expression of F4/80 in kidneys was detected by immunohistochemistry with positive areas indicated by black arrows. Original magnification = ×20. Bar = 50 μm. **(C–F)** mRNA expression levels of IL-1β, TNF-α, MCP-1 and ICAM-1 were evaluated in UUO mice detected by RT-PCR. Results were normalized to GAPDH expression. Statistical significance was presented as the mean ± SD, $n = 6$. $^{*}p < 0.05$, $^{**}p < 0.01$, ns: no significance. **(G)** The protein levels of p-P65, P65 were detected by western blot and quantified by densitometry. (B,H,I) Statistical significance was presented as the mean ± SD, $n = 6$. $^{*}p < 0.05$, $^{**}p < 0.01$, ns: no significance. MA, maslinic acid; UUO, unilateral ureteral obstruction; RT-PCR, Real-Time PCR.

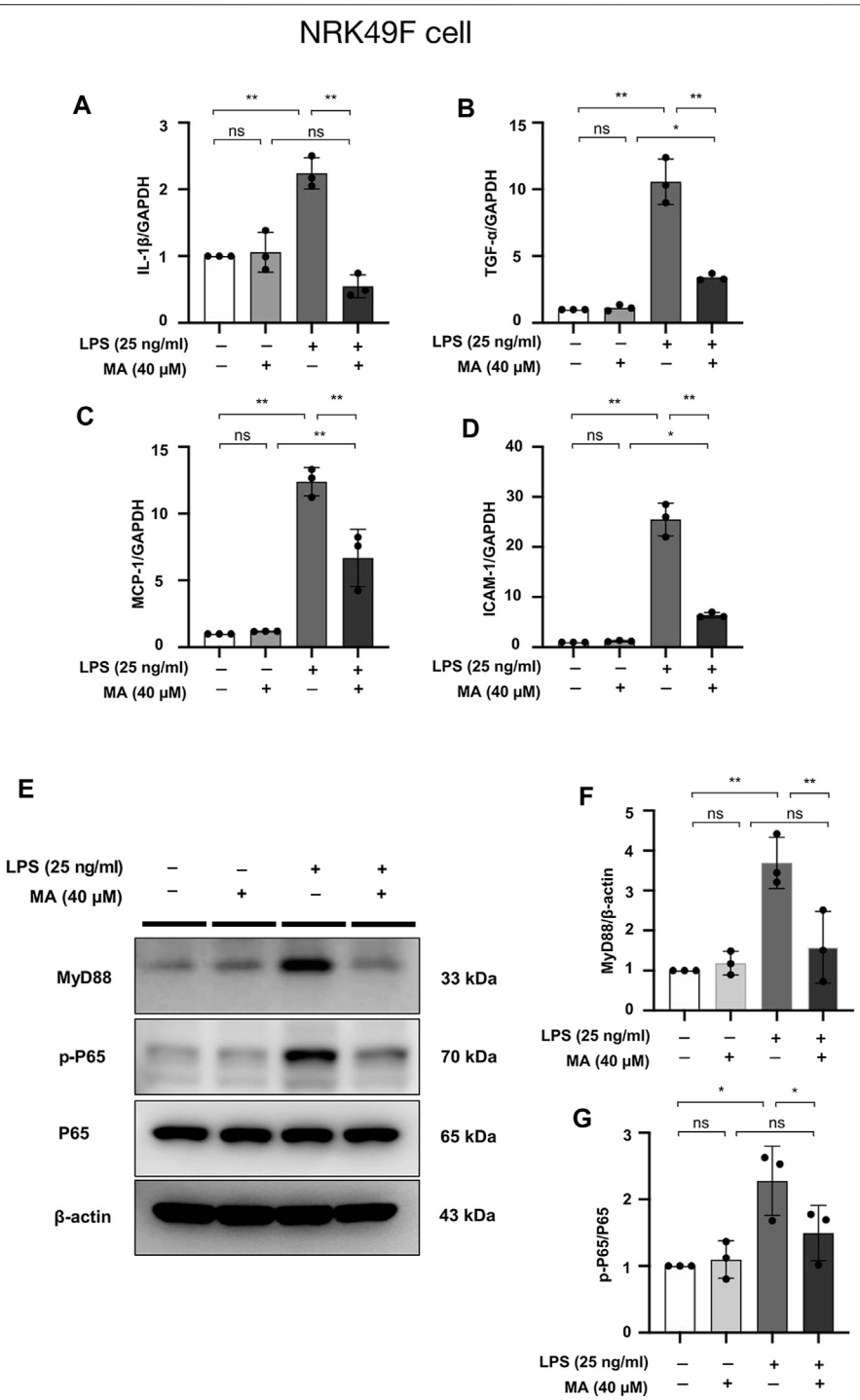

FIGURE 9 | MA attenuates LPS-induced inflammation in NRK49F cells and suppresses NF-κB Signaling. **(A–D)** mRNA expression levels of IL-1β, TNF-α, MCP-1 and ICAM-1 were evaluated in LPS-treated NRK49F cells and determined by RT-PCR. Cells were pretreated with MA for 2 h after starvation with 0.5% FBS medium, then treated with LPS (25 ng/ml) for 2 h. Results were normalized to GAPDH expression. The data are presented as the mean ± SD, $n = 3$. $^{*}p < 0.05$, $^{**}p < 0.01$, ns: no significance. MA, maslinic acid; LPS, Lipopolysaccharide; RT-PCR, Real-Time PCR. **(E)** Expression of p-P65, P65 and MyD88 in LPS-treated NRK49F cells was detected by western blot and quantified by densitometry. Cells were pretreated with MA for 2 h after starvation with 0.5% FBS medium and then treated with LPS (25 ng/ml) for 2 h. **(F,G)** Statistical significance was presented as the mean ± SD, $n = 3$. $^{*}p < 0.05$, $^{**}p < 0.01$, ns: no significance. MA, maslinic acid; LPS, Lipopolysaccharide.

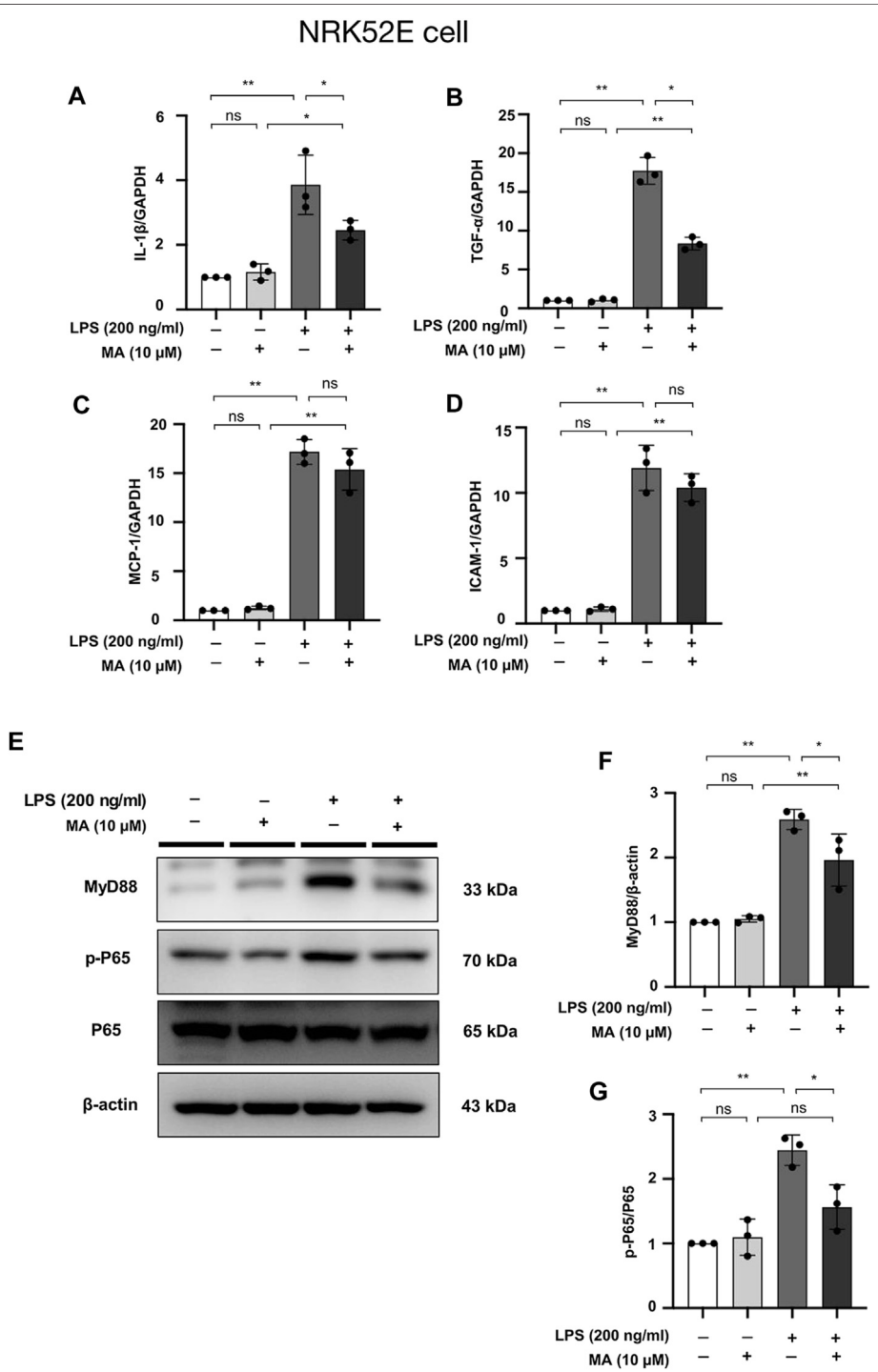

FIGURE 10 | MA attenuates LPS-induced inflammation in NRK52E cells and suppresses NF-κB Signaling. **(A–D)** mRNA expression levels of IL-1β, TNF-α, MCP-1 and ICAM-1 were evaluated in LPS-treated NRK52E cells and determined by RT-PCR. Cells were pretreated with MA for 2 h after starvation with 0.5% FBS medium, then treated with LPS (200 ng/ml) for 2 h. Results were normalized to GAPDH expression. The data are presented as the mean ± SD, $n = 3$. $^{*}p < 0.05$, $^{**}p < 0.01$, ns: no significance. MA, maslinic acid; LPS, Lipopolysaccharide; RT-PCR, Real-Time PCR. **(E)** Expression of p-P65, P65 and MyD88 in LPS-treated NRK52E cells was detected by western blot and quantified by densitometry. Cells were pretreated with MA for 2 h after starvation with 0.5% FBS medium and then treated with LPS (200 ng/ml) for 2 h. **(F,G)** Statistical significance was presented as the mean ± SD, $n = 3$. $^{*}p < 0.05$, $^{**}p < 0.01$, ns: no significance. MA, maslinic acid; LPS, Lipopolysaccharide.

interacts with TGF-β receptors to phosphorylate Smad2/3, subsequently activating p-Smad oligomerization with Smad4 and translocating them to the nucleus, where they jointly transactivate downstream fibrogenesis genes (Schnaper et al., 2003; Choi et al., 2012). Based on the notion that the inhibition of Smad2/3 phosphorylation will reduce fibrosis

levels, we successfully identified the ability of MA to suppress Smad2/3 phosphorylation *in vivo* as well as *in vitro*, suggesting that negative regulation of MA in renal fibrosis occurs through the downregulation of p-Smad2/3, at least in part. Of interest, MA also blocked Smad2/3 and Smad4 nuclear translocation, suggesting that the inhibitory effect of MA appears to be Smad2/3 and Smad4 specific upon TGF-β stimulation. Additionally, we extend regulatory studies of MA to other Smad family members, Smad6 and Smad7 have been reported as an intracellular negative regulator of TGF-β signaling, particularly in R-Smad activation, these two factors could inhibit the phosphorylation of Smad2/3, thereby blocking TGF-β signaling (Kretzschmar and Massagué, 1998; Zimmerman and Padgett, 2000). MA treatment did not affect the nuclear expression of Smad6 and Smad7 suggesting that MA selectively downregulates nuclear activation of Smad2/3 and Smad4, and subsequently inhibits fibrosis in NRK49F cells.

The role of Myd88 in kidney fibrosis remains controversial (Skuginna et al., 2011; Anders and Lech, 2013). Recent studies suggested the abnormal activation of TLR4/Myd88 might play a role in the pathogenesis of kidney inflammation and fibrosis (González-Guerrero et al., 2017; Ma et al., 2021). In addition, Myd88 knockout mice had less UUO induced interstitial fibrosis associated with improved renal function (Braga et al., 2012). Also, inhibited activation of MyD88 could ameliorate kidney injury in UUO (Lu et al., 2018). Myd88 deficiency was protective against renal interstitial fibrosis and chronic allograft injury (Wu et al., 2012). These findings suggest that MyD88 is a potential therapeutic target for renal fibrosis. In the present study, we have demonstrated that MA treatment decreased tubulointerstitial fibrosis associated with downregulation of Myd88 and TGF-β/Smad signaling pathways. TGF-β-induced activation of α-SMA, CTGF and vimentin was reduced by Myd88 knockdown in NRK49F cells. Moreover, TGF-β induced nuclear activation of Smad4 in NRK49F cells was significantly downregulated by transfection of siRNA targeting MyD88. These findings are consistent with recent study demonstrating that MyD88 expression levels affect Smad4 protein levels in Hub7 hepatoma cells through the Toll/IL-1 receptor domain of the MyD88 protein (Samba-Mondonga et al., 2018). Taken together with the present study, MA exerts its anti-fibrotic effects on the TGF-β/Smad pathway via targeting MyD88.

The kidney damage that occurs in CKD is at least partly promoted by the immune system (Kurts et al., 2013). Different types of kidney injury and repair involve tissue remodeling mediated by the immune infiltration of renal tubular interstitial macrophages. In particular, some pan-markers like F4/80 antigen is a mature cell surface glycoprotein expressed at high levels on various macrophages (Tian et al., 2015). In this study, we detected the level of labeled F4/80 antigen. The results revealed a less infiltration of F4/80 IHC staining positive area in MA treat kidneys compared to those in UUO kidneys, which proved that MA reduces the macrophage accumulation and infiltration in UUO mice model.

Inflammation is another pathologic process engaged in renal fibrosis (Meng et al., 2014). We further examined to address the impact of MA on inflammatory state. Our results indicated that the administration of MA inhibits the expression of pro-inflammatory cytokines and cell adhesion molecules such as IL-1β, TNF-α, MCP-1, and ICAM-1, suggesting that MA may ameliorate renal fibrosis by the inhibition of inflammatory response. It has been suggested that NF-κB is a recognized downstream pro-inflammatory signaling pathway of MyD88 (Kawai and Akira, 2007), and LPS-induced NF-κB nuclear translocation is primarily dependent on MyD88 (Sakai et al., 2017). The present study also demonstrated that increased expression of p-P65 in UUO kidneys and LPS-treated cells (NRK49F cells and NRK52E cells) was counteracted by MA treatment. These changes were associated with MA induced MyD88 downregulation, and suggested that MyD88 inhibition by MA may be associated with inhibition of NF-κB signaling followed by anti-inflammatory and anti-fibrotic effects.

It should be mention that our current research has some notable limitations. Firstly, research lacks preventive design used. In addition, it remains to be elucidated whether the beneficial effect of MA is unique to the UUO kidneys or may be a more general characteristic beyond UUO in other experimental animal models involving different injury mechanisms (Yang et al., 2010). Thus, a comprehensive study on the other experimental models should be conducted over the following studies.

In conclusion, our present study suggested that MA is not only a potential agent for reducing renal fibrosis by directly targeting TGF-β/Smad signaling, but also an effective inhibitor of MyD88 that may be involved in Smad4 nuclear expression or localization and NF-κB signaling. We believe that MA may be an attractive therapeutic candidate for progressive kidney disease. Furthermore, we clarified novel cross-regulation between MyD88 and the TGF-β/Smad pathway, thus identifying MyD88 as a potential therapeutic target in renal fibrosis. These findings may contribute to the identification of novel signaling pathways involved in renal fibrosis and help to unveil the pathogenesis of CKD in the near future.

DATA AVAILABILITY STATEMENT

The original contributions presented in the study are included in the article/**Supplementary Material**, further inquiries can be directed to the corresponding author.

ETHICS STATEMENT

The animal study was reviewed and approved by the Chonnam National University Medical School.

AUTHOR CONTRIBUTIONS

WS and CB conceived and designed the research; DK, HC, and JP interpreted results of experiments; WS and SK drafted the manuscript; CB, DK, HC, JP, SJ, IK, IJ, EB, SM, and SK edited and revised the manuscript; and all authors approved the final version of manuscript.

FUNDING

This research was supported by the National Research Foundation of Korea (NRF) funded by the Korean government (MSIT) (NRF-2019R1A2C2086276).

SUPPLEMENTARY MATERIAL

The Supplementary Material for this article can be found online at: https://www.frontiersin.org/articles/10.3389/fphar.2021.708575/full#supplementary-material

REFERENCES

Ampofo, E., Berg, J. J., Menger, M. D., and Laschke, M. W. (2019). Maslinic Acid Alleviates Ischemia/reperfusion-Induced Inflammation by Downregulation of NFκB-Mediated Adhesion Molecule Expression. *Sci. Rep.* 9 (1), 6119. doi:10.1038/s41598-019-42465-7

Anders, H. J., and Lech, M. (2013). NOD-like and Toll-like Receptors or Inflammasomes Contribute to Kidney Disease in a Canonical and a Non-canonical Manner. *Kidney Int.* 84 (2), 225–228. doi:10.1038/ki.2013.122

Artlett, C. M. (2012). The Role of the NLRP3 Inflammasome in Fibrosis. *Open Rheumatol. J.* 6, 80–86. doi:10.2174/1874312901206010080

Bae, H. J., Kim, J., Kim, J., Goo, N., Cai, M., Cho, K., et al. (2020). The Effect of Maslinic Acid on Cognitive Dysfunction Induced by Cholinergic Blockade in Mice. *Br. J. Pharmacol.* 177 (14), 3197–3209. doi:10.1111/bph.15042

Bascands, J. L., Bachvarova, M., Neau, E., Schanstra, J. P., and Bachvarov, D. (2009). Molecular Determinants of LPS-Induced Acute Renal Inflammation: Implication of the Kinin B1 Receptor. *Biochem. Biophys. Res. Commun.* 386 (2), 407–412. doi:10.1016/j.bbrc.2009.06.063

Biernacka, A., Dobaczewski, M., and Frangogiannis, N. G. (2011). TGF-β Signaling in Fibrosis. *Growth Factors* 29 (5), 196–202. doi:10.3109/08977194.2011.595714

Black, L. M., Lever, J. M., and Agarwal, A. (2019). Renal Inflammation and Fibrosis: A Double-Edged Sword. *J. Histochem. Cytochem.* 67 (9), 663–681. doi:10.1369/0022155419852932

Bon, H., Hales, P., Lumb, S., Holdsworth, G., Johnson, T., Qureshi, O., et al. (2019). Spontaneous Extracellular Matrix Accumulation in a Human *In Vitro* Model of Renal Fibrosis Is Mediated by αV Integrins. *Nephron* 142 (4), 328–350. doi:10.1159/000499506

Bonnans, C., Chou, J., and Werb, Z. (2014). Remodelling the Extracellular Matrix in Development and Disease. *Nat. Rev. Mol. Cel Biol* 15 (12), 786–801. doi:10.1038/nrm3904

Braga, T. T., Correa-Costa, M., Guise, Y. F., Castoldi, A., de Oliveira, C. D., Hyane, M. I., et al. (2012). MyD88 Signaling Pathway Is Involved in Renal Fibrosis by Favoring a TH2 Immune Response and Activating Alternative M2 Macrophages. *Mol. Med.* 18, 1231–1239. doi:10.2119/molmed.2012.00131

Brightbill, H. D., and Modlin, R. L. (2000). Toll-like Receptors: Molecular Mechanisms of the Mammalian Immune Response. *Immunology* 101 (1), 1–10. doi:10.1046/j.1365-2567.2000.00093.x

Bülow, R. D., and Boor, P. (2019). Extracellular Matrix in Kidney Fibrosis: More Than Just a Scaffold. *J. Histochem. Cytochem.* 67 (9), 643–661. doi:10.1369/0022155419849388

Chen, L., Yang, T., Lu, D. W., Zhao, H., Feng, Y. L., Chen, H., et al. (2018). Central Role of Dysregulation of TGF-β/Smad in CKD Progression and Potential Targets of its Treatment. *Biomed. Pharmacother.* 101, 670–681. doi:10.1016/j.biopha.2018.02.090

Chen, L., Zheng, L., Chen, P., and Liang, G. (2020). Myeloid Differentiation Primary Response Protein 88 (MyD88): The Central Hub of TLR/IL-1R Signaling. *J. Med. Chem.* 63 (22), 13316–13329. doi:10.1021/acs.jmedchem.0c00884

Chen, Y. L., Yan, D. Y., Wu, C. Y., Xuan, J. W., Jin, C. Q., Hu, X. L., et al. (2021). Maslinic Acid Prevents IL-1β-induced Inflammatory Response in Osteoarthritis via PI3K/AKT/NF-κB Pathways. *J. Cel Physiol* 236 (3), 1939–1949. doi:10.1002/jcp.29977

Choi, M. E., Ding, Y., and Kim, S. I. (2012). TGF-β Signaling via TAK1 Pathway: Role in Kidney Fibrosis. *Semin. Nephrol.* 32 (3), 244–252. doi:10.1016/j.semnephrol.2012.04.003

Chou, Y. H., and Chen, Y. M. (2021). Aging and Renal Disease: Old Questions for New Challenges. *Aging Dis.* 12 (2), 515–528. doi:10.14336/ad.2020.0703

Cohen, A. H. (2007). "Renal Anatomy and Basic Concepts and Methods in Renal Pathology," in *Fundamentals of Renal Pathology*. Editors A. B. Fogo, A. H. Cohen, J. C. Jennette, J. A. Bruijn, and R. B. Colvin (New York, NY: Springer), 3–17.

Desai, V. D., Hsia, H. C., and Schwarzbauer, J. E. (2014). Reversible Modulation of Myofibroblast Differentiation in Adipose-Derived Mesenchymal Stem Cells. *PLOS ONE* 9 (1), e86865. doi:10.1371/journal.pone.0086865

Frantz, C., Stewart, K. M., and Weaver, V. M. (2010). The Extracellular Matrix at a Glance. *J. Cel Sci* 123 (Pt 24), 4195–4200. doi:10.1242/jcs.023820

Fukumitsu, S., Villareal, M. O., Fujitsuka, T., Aida, K., and Isoda, H. (2016). Anti-inflammatory and Anti-arthritic Effects of Pentacyclic Triterpenoids Maslinic Acid through NF-Kb Inactivation. *Mol. Nutr. Food Res.* 60 (2), 399–409. doi:10.1002/mnfr.201500465

Geiger, B., and Yamada, K. M. (2011). Molecular Architecture and Function of Matrix Adhesions. *Cold Spring Harb Perspect. Biol.* 3 (5), a005033. doi:10.1101/cshperspect.a005033

González-Guerrero, C., Cannata-Ortiz, P., Guerri, C., Egido, J., Ortiz, A., and Ramos, A. M. (2017). TLR4-mediated Inflammation Is a Key Pathogenic Event Leading to Kidney Damage and Fibrosis in Cyclosporine Nephrotoxicity. *Arch. Toxicol.* 91 (4), 1925–1939. doi:10.1007/s00204-016-1830-8

Gore-Hyer, E., Shegogue, D., Markiewicz, M., Lo, S., Hazen-Martin, D., Greene, E. L., et al. (2002). TGF-beta and CTGF Have Overlapping and Distinct Fibrogenic Effects on Human Renal Cells. *Am. J. Physiol. Ren. Physiol* 283 (4), F707–F716. doi:10.1152/ajprenal.00007.2002

Gupta, S., Clarkson, M. R., Duggan, J., and Brady, H. R. (2000). Connective Tissue Growth Factor: Potential Role in Glomerulosclerosis and Tubulointerstitial Fibrosis. *Kidney Int.* 58 (4), 1389–1399. doi:10.1046/j.1523-1755.2000.00301.x

Hamesch, K., Borkham-Kamphorst, E., Strnad, P., and Weiskirchen, R. (2015). Lipopolysaccharide-induced Inflammatory Liver Injury in Mice. *Lab. Anim.* 49 (1 Suppl. l), 37–46. doi:10.1177/0023677215570087

Hao, Y., Baker, D., and Ten Dijke, P. (2019). TGF-β-Mediated Epithelial-Mesenchymal Transition and Cancer Metastasis. *Int. J. Mol. Sci.* 20 (11), 2767. doi:10.3390/ijms20112767

Hashmi, M. A., Khan, A., Hanif, M., Farooq, U., and Perveen, S. (2015). Traditional Uses, Phytochemistry, and Pharmacology of *Olea Europaea* (Olive). *Evid. Based Complement. Alternat Med.* 2015, 541591. doi:10.1155/2015/541591

Humphreys, B. D. (2018). Mechanisms of Renal Fibrosis. *Annu. Rev. Physiol.* 80 (1), 309–326. doi:10.1146/annurev-physiol-022516-034227

Imig, J. D., and Ryan, M. J. (2013). Immune and Inflammatory Role in Renal Disease. *Compr. Physiol.* 3 (2), 957–976. doi:10.1002/cphy.c120028

Jia, R. J., Cao, L., Zhang, L., Jing, W., Chen, R., Zhu, M. H., et al. (2014). Enhanced Myeloid Differentiation Factor 88 Promotes Tumor Metastasis via Induction of Epithelial-Mesenchymal Transition in Human Hepatocellular Carcinoma. *Cell Death Dis* 5, e1103. doi:10.1038/cddis.2014.71

Kawai, T., and Akira, S. (2007). Signaling to NF-kappaB by Toll-like Receptors. *Trends Mol. Med.* 13 (11), 460–469. doi:10.1016/j.molmed.2007.09.002

Kawasaki, T., and Kawai, T. (2014). Toll-Like Receptor Signaling Pathways. *Front. Immunol.* 5, 461. doi:10.3389/fimmu.2014.00461

Kiemer, A. K., Müller, C., and Vollmar, A. M. (2002). Inhibition of LPS-Induced Nitric Oxide and TNF-Alpha Production by Alpha-Lipoic Acid in Rat Kupffer Cells and in RAW 264.7 Murine Macrophages. *Immunol. Cel Biol* 80 (6), 550–557. doi:10.1046/j.1440-1711.2002.01124.x

Kim, D. H., Choi, H. I., Park, J. S., Kim, C. S., Bae, E. H., Ma, S. K., et al. (2019). Src-mediated Crosstalk between FXR and YAP Protects against Renal Fibrosis. *FASEB J.* 33 (10), 11109–11122. doi:10.1096/fj.201900325R

Klingberg, F., Hinz, B., and White, E. S. (2013). The Myofibroblast Matrix: Implications for Tissue Repair and Fibrosis. *J. Pathol.* 229 (2), 298–309. doi:10.1002/path.4104

Kretzschmar, M., and Massagué, J. (1998). SMADs: Mediators and Regulators of TGF-Beta Signaling. *Curr. Opin. Genet. Dev.* 8 (1), 103–111. doi:10.1016/s0959-437x(98)80069-5

Kurts, C., Panzer, U., Anders, H. J., and Rees, A. J. (2013). The Immune System and Kidney Disease: Basic Concepts and Clinical Implications. *Nat. Rev. Immunol.* 13 (10), 738–753. doi:10.1038/nri3523

Lee, K.-Y., Ito, K., Hayashi, R., Jazrawi, E. P. I., Barnes, P. J., and Adcock, I. M. (2006). NF-κB and Activator Protein 1 Response Elements and the Role of Histone Modifications in IL-1β-Induced TGF-B1 Gene Transcription. *J. Immunol.* 176 (1), 603–615. doi:10.4049/jimmunol.176.1.603

Lee, W., Kim, J., Park, E. K., and Bae, J. S. (2020). Maslinic Acid Ameliorates Inflammation via the Downregulation of NF-Kb and STAT-1. *Antioxidants (Basel)* 9 (2), 106. doi:10.3390/antiox9020106

Liou, C. J., Dai, Y. W., Wang, C. L., Fang, L. W., and Huang, W. C. (2019). Maslinic Acid Protects against Obesity-Induced Nonalcoholic Fatty Liver Disease in Mice through Regulation of the Sirt1/AMPK Signaling Pathway. *FASEB J.* 33 (11), 11791–11803. doi:10.1096/fj.201900413RRR

Liu, X., Chen, J. G., Munshi, M., Hunter, Z. R., Xu, L., Kofides, A., et al. (2020a). Expression of the Prosurvival Kinase HCK Requires PAX5 and Mutated MYD88 Signaling in MYD88-Driven B-Cell Lymphomas. *Blood Adv.* 4, 141–153. doi:10.1182/bloodadvances.2019000947

Liu, Y. (2011). Cellular and Molecular Mechanisms of Renal Fibrosis. *Nat. Rev. Nephrol.* 7 (12), 684–696. doi:10.1038/nrneph.2011.149

Liu, Y. (2004). Epithelial to Mesenchymal Transition in Renal Fibrogenesis: Pathologic Significance, Molecular Mechanism, and Therapeutic Intervention. *J. Am. Soc. Nephrol.* 15 (1), 1–12. doi:10.1097/01.Asn.0000106015.29070.E7

Liu, Y., Lu, H., Dong, Q., Hao, X., and Qiao, L. (2020b). Maslinic Acid Induces Anticancer Effects in Human Neuroblastoma Cells Mediated via Apoptosis Induction and Caspase Activation, Inhibition of Cell Migration and Invasion and Targeting MAPK/ERK Signaling Pathway. *AMB Express* 10 (1), 104. doi:10.1186/s13568-020-01035-1

Liu, Y. L., Kong, C. Y., Song, P., Zhou, H., Zhao, X. S., and Tang, Q. Z. (2018). Maslinic Acid Protects against Pressure Overload-Induced Cardiac Hypertrophy in Mice. *J. Pharmacol. Sci.* 138 (2), 116–122. doi:10.1016/j.jphs.2018.08.014

Liu, Z., Ji, J., Zheng, D., Su, L., Peng, T., and Tang, J. (2020c). Protective Role of Endothelial Calpain Knockout in Lipopolysaccharide-Induced Acute Kidney Injury via Attenuation of the P38-iNOS Pathway and NO/ROS Production. *Exp. Mol. Med.* 52 (4), 702–712. doi:10.1038/s12276-020-0426-9

Lu, H., Wu, L., Liu, L., Ruan, Q., Zhang, X., Hong, W., et al. (2018). Quercetin Ameliorates Kidney Injury and Fibrosis by Modulating M1/M2 Macrophage Polarization. *Biochem. Pharmacol.* 154, 203–212. doi:10.1016/j.bcp.2018.05.007

Ma, J. Q., Zhang, Y. J., Tian, Z. K., and Liu, C. M. (2021). Bixin Attenuates Carbon Tetrachloride Induced Oxidative Stress, Inflammation and Fibrosis in Kidney by Regulating the Nrf2/TLR4/MyD88 and PPAR-Γ/tgf-β1/Smad3 Pathway. *Int. Immunopharmacol* 90, 107117. doi:10.1016/j.intimp.2020.107117

Meng, X. M., Nikolic-Paterson, D. J., and Lan, H. Y. (2014). Inflammatory Processes in Renal Fibrosis. *Nat. Rev. Nephrol.* 10 (9), 493–503. doi:10.1038/nrneph.2014.114

Mkhwanazi, B. N., Serumula, M. R., Myburg, R. B., Van Heerden, F. R., and Musabayane, C. T. (2014). Antioxidant Effects of Maslinic Acid in Livers, Hearts and Kidneys of Streptozotocin-Induced Diabetic Rats: Effects on Kidney Function. *Ren. Fail.* 36 (3), 419–431. doi:10.3109/0886022X.2013.867799

Mussbacher, M., Salzmann, M., Brostjan, C., Hoesel, B., Schoergenhofer, C., Datler, H., et al. (2019). Cell Type-specific Roles of NF-Kb Linking Inflammation and Thrombosis. *Front. Immunol.* 10 (85). doi:10.3389/fimmu.2019.0008585

Mutsaers, H. A., Stribos, E. G., Glorieux, G., Vanholder, R., and Olinga, P. (2015). Chronic Kidney Disease and Fibrosis: The Role of Uremic Retention Solutes. *Front. Med. (Lausanne)* 2, 60. doi:10.3389/fmed.2015.00060

Nieto, M. A., Huang, R. Y., Jackson, R. A., and Thiery, J. P. (2016). EMT: 2016. *Cell* 166 (1), 21–45. doi:10.1016/j.cell.2016.06.028

Nogueira, A., Pires, M. J., and Oliveira, P. A. (2017). Pathophysiological Mechanisms of Renal Fibrosis: A Review of Animal Models and Therapeutic Strategies. *In Vivo* 31 (1), 1–22. doi:10.21873/invivo.11019

Pardali, E., Sanchez-Duffhues, G., Gomez-Puerto, M. C., and Ten Dijke, P. (2017). TGF-β-Induced Endothelial-Mesenchymal Transition in Fibrotic Diseases. *Int. J. Mol. Sci.* 18 (10). doi:10.3390/ijms18102157

Park, J. S., Choi, H. I., Kim, D. H., Kim, C. S., Bae, E. H., Ma, S. K., et al. (2019). RON Receptor Tyrosine Kinase Regulates Epithelial Mesenchymal Transition and the Expression of Pro-fibrotic Markers via Src/Smad Signaling in HK-2 and NRK49F Cells. *Int. J. Mol. Sci.* 20 (21), 5489. doi:10.3390/ijms20215489

Pohlers, D., Brenmoehl, J., Löffler, I., Müller, C. K., Leipner, C., Schultze-Mosgau, S., et al. (2009). TGF-beta and Fibrosis in Different Organs - Molecular Pathway Imprints. *Biochim. Biophys. Acta* 1792 (8), 746–756. doi:10.1016/j.bbadis.2009.06.004

Popper, B., Rammer, M. T., Gasparitsch, M., Singer, T., Keller, U., Döring, Y., et al. (2019). Neonatal Obstructive Nephropathy Induces Necroptosis and Necroinflammation. *Sci. Rep.* 9 (1), 18600. doi:10.1038/s41598-019-55079-w

Qian, Y., Huang, M., Guan, T., Chen, L., Cao, L., Han, X. J., et al. (2015). Maslinic Acid Promotes Synaptogenesis and Axon Growth via Akt/GSK-3β Activation in Cerebral Ischemia Model. *Eur. J. Pharmacol.* 764, 298–305. doi:10.1016/j.ejphar.2015.07.028

Reyes-Zurita, F. J., Rufino-Palomares, E. E., Lupiáñez, J. A., and Cascante, M. (2009). Maslinic Acid, a Natural Triterpene from Olea Europaea L., Induces Apoptosis in HT29 Human colon-cancer Cells via the Mitochondrial Apoptotic Pathway. *Cancer Lett.* 273 (1), 44–54. doi:10.1016/j.canlet.2008.07.033

Sakai, J., Cammarota, E., Wright, J. A., Cicuta, P., Gottschalk, R. A., Li, N., et al. (2017). Lipopolysaccharide-induced NF-Kb Nuclear Translocation Is Primarily Dependent on MyD88, but TNFα Expression Requires TRIF and MyD88. *Sci. Rep.* 7 (1), 1428–1429. doi:10.1038/s41598-017-01600-y

Samba-Mondonga, M., Calvé, A., Mallette, F. A., and Santos, M. M. (2018). MyD88 Regulates the Expression of SMAD4 and the Iron Regulatory Hormone Hepcidin. *Front Cel Dev Biol* 6 (105), 105. doi:10.3389/fcell.2018.00105

Savagner, P. (2001). Leaving the Neighborhood: Molecular Mechanisms Involved during Epithelial-Mesenchymal Transition. *BioEssays* 23 (10), 912–923. doi:10.1002/bies.1132

Schnaper, H. W., Hayashida, T., Hubchak, S. C., and Poncelet, A. C. (2003). TGF-beta Signal Transduction and Mesangial Cell Fibrogenesis. *Am. J. Physiol. Ren. Physiol* 284 (2), F243–F252. doi:10.1152/ajprenal.00300.2002

Shaik, A. H., Shaik, S. R., Shaik, A. S., Daoud, A., Salim, M., and Kodidhela, L. D. (2021). Analysis of Maslinic Acid and Gallic Acid Compounds as Xanthine Oxidase Inhibitors in Isoprenaline Administered Myocardial Necrotic Rats. *Saudi J. Biol. Sci.* 28 (4), 2575–2580. doi:10.1016/j.sjbs.2021.01.062

Škovierová, H., Okajčeková, T., Strnádel, J., Vidomanová, E., and Halašová, E. (2018). Molecular Regulation of Epithelial-To-Mesenchymal Transition in Tumorigenesis (Review). *Int. J. Mol. Med.* 41 (3), 1187–1200. doi:10.3892/ijmm.2017.3320

Skuginna, V., Lech, M., Allam, R., Ryu, M., Clauss, S., Susanti, H. E., et al. (2011). Toll-Like Receptor Signaling and SIGIRR in Renal Fibrosis upon Unilateral Ureteral Obstruction. *PLOS ONE* 6 (4), e19204. doi:10.1371/journal.pone.0019204

Tamada, S., Asai, T., Kuwabara, N., Iwai, T., Uchida, J., Teramoto, K., et al. (2006). Molecular Mechanisms and Therapeutic Strategies of Chronic Renal Injury: the Role of Nuclear Factor kappaB Activation in the Development of Renal Fibrosis. *J. Pharmacol. Sci.* 100 (1), 17–21. doi:10.1254/jphs.fmj05003x4

Theocharis, A. D., Manou, D., and Karamanos, N. K. (2019). The Extracellular Matrix as a Multitasking Player in Disease. *Febs j* 286 (15), 2830–2869. doi:10.1111/febs.14818

Tian, S., Zhang, L., Tang, J., Guo, X., Dong, K., and Chen, S. Y. (2015). HMGB1 Exacerbates Renal Tubulointerstitial Fibrosis through Facilitating M1 Macrophage Phenotype at the Early Stage of Obstructive Injury. *Am. J. Physiol. Ren. Physiol* 308 (1), F69–F75. doi:10.1152/ajprenal.00484.2014

Urban, M. L., Manenti, L., and Vaglio, A. (2015). Fibrosis-A Common Pathway to Organ Injury and Failure. *N. Engl. J. Med.* 373 (1), 95–96. doi:10.1056/NEJMc1504848

Wei, Q., Zhang, B., Li, P., Wen, X., and Yang, J. (2019). Maslinic Acid Inhibits Colon Tumorigenesis by the AMPK-mTOR Signaling Pathway. *J. Agric. Food Chem.* 67 (15), 4259–4272. doi:10.1021/acs.jafc.9b00170

Wendt, M. K., Allington, T. M., and Schiemann, W. P. (2009). Mechanisms of the Epithelial-Mesenchymal Transition by TGF-Beta. *Future Oncol.* 5 (8), 1145–1168. doi:10.2217/fon.09.90

Wu, H., Noordmans, G. A., O'Brien, M. R., Ma, J., Zhao, C. Y., Zhang, G. Y., et al. (2012). Absence of MyD88 Signaling Induces Donor-specific Kidney Allograft

Tolerance. *J. Am. Soc. Nephrol.* 23 (10), 1701–1716. doi:10.1681/ASN.2012010052

Xu, J., Lamouille, S., and Derynck, R. (2009). TGF-beta-induced Epithelial to Mesenchymal Transition. *Cell Res* 19 (2), 156–172. doi:10.1038/cr.2009.5

Yang, L., Besschetnova, T. Y., Brooks, C. R., Shah, J. V., and Bonventre, J. V. (2010). Epithelial Cell Cycle Arrest in G2/M Mediates Kidney Fibrosis after Injury. *Nat. Med.* 16 (5), 535–543. 531p following 143. doi:10.1038/nm.2144

Zavadil, J., and Böttinger, E. P. (2005). TGF-beta and Epithelial-To-Mesenchymal Transitions. *Oncogene* 24 (37), 5764–5774. doi:10.1038/sj.onc.1208927

Zhang, L. L., Huang, S., Ma, X. X., Zhang, W. Y., Wang, D., Jin, S. Y., et al. (2016). Corrigendum to "Angiotensin(1-7) Attenuated Angiotensin II-Induced Hepatocyte EMT by Inhibiting NOX-Derived H2O2-Activated NLRP3 inflammasome/IL-1β/Smad Circuit". *Free Radic. Biol. Med.* 99, 531–543. doi:10.1016/j.freeradbiomed.2016.09.001

Zimmerman, C. M., and Padgett, R. W. (2000). Transforming Growth Factor Beta Signaling Mediators and Modulators. *Gene* 249 (1-2), 17–30. doi:10.1016/s0378-1119(00)00162-1

Conflict of Interest: The authors declare that the research was conducted in the absence of any commercial or financial relationships that could be construed as a potential conflict of interest.

Publisher's Note: All claims expressed in this article are solely those of the authors and do not necessarily represent those of their affiliated organizations, or those of the publisher, the editors and the reviewers. Any product that may be evaluated in this article, or claim that may be made by its manufacturer, is not guaranteed or endorsed by the publisher.

frontiers in Pharmacology

ORIGINAL RESEARCH
published: 21 September 2021
doi: 10.3389/fphar.2021.741801

Transcriptome-Based Network Analysis Reveals Hirudin Potentiates Anti-Renal Fibrosis Efficacy in UUO Rats

Hang-Xing Yu[1,2], Wei Lin[1,2], Kang Yang[3], Li-Juan Wei[1,2], Jun-Li Chen[1,2], Xin-Yue Liu[1,2], Ke Zhong[1,2], Xin Chen[1,2], Ming Pei[1,2]* and Hong-Tao Yang[1,2]**

[1]Department of Nephrology, First Teaching Hospital of Tianjin University of Traditional Chinese Medicine, Tianjin, China, [2]National Clinical Research Center for Chinese Medicine Acupuncture and Moxibustion, Tianjin, China, [3]Kidney Disease Treatment Center, The First Affiliated Hospital of Henan University of CM, Zhengzhou, China

OPEN ACCESS

Edited by:
Zhiyong Guo,
Second Military Medical University, China

Reviewed by:
Xin Dong,
Shanghai University, China
Wing Wang,
Southern Medical University, China

***Correspondence:**
Xin Chen
heerkeli@126.com
Ming Pei
mingpei@163.com
Hong-Tao Yang
tjtcmht@126.com

Specialty section:
This article was submitted to Renal Pharmacology, a section of the journal Frontiers in Pharmacology

Received: 15 July 2021
Accepted: 07 September 2021
Published: 21 September 2021

Citation:
Yu H-X, Lin W, Yang K, Wei L-J, Chen J-L, Liu X-Y, Zhong K, Chen X, Pei M and Yang H-T (2021) Transcriptome-Based Network Analysis Reveals Hirudin Potentiates Anti-Renal Fibrosis Efficacy in UUO Rats. Front. Pharmacol. 12:741801. doi: 10.3389/fphar.2021.741801

Background: Hirudin has been widely used in the treatment of antifibrosis. Previous studies have shown that hirudin can effectively improve the clinical remission rate of chronic kidney disease. However, the mechanism of its renal protection has not been systematically investigated.

Methods: In this study, the reliability of UUO-induced renal interstitial fibrosis was evaluated by histopathological verification. High-throughput transcriptome sequencing was used to elucidate the molecular mechanism of hirudin, differentially expressed mRNAs were identified, and their functions were analyzed by GO analysis and GSEA. In addition, the RNA-seq results were validated by *in vitro* and vivo experiments.

Results: We found 322 identical differential expressed genes (IDEs) in the UUO hirudin-treated group compared with the sham group. Functional enrichment analysis indicated that cellular amino acid metabolic processes were the most obvious enrichment pathways in biological processes. In terms of molecular functional enrichment analysis, IDEs were mainly enriched in coenzyme binding, pyridoxal phosphate binding and other pathways. In addition, microbody is the most obvious pathway for cellular components. A total of 115 signaling pathways were enriched, and AMPK, JAK-STAT, and PI3K-Akt signaling pathways were the important signaling pathways enriched. We found that PI3K, p-Akt, and mTOR expression were significantly reduced by hirudin treatment. In particular, our

Abbreviations: α-SMA, α smooth muscle actin; ACEI, angiotensin converting enzyme inhibitors; Akt, protein kinase B; AMPK, Adenosine 5-monophosphate (AMP)-activated protein kinase; ANOVA , analysis of variance; ARB, Angiotensin Receptor Blocker; CKD, Chronic kidney disease; Col1, Recombinant Collagen Type I; DAB, diaminobenzidine; DEG, differentially expressed gene; E-Cad, E-Cadherin; ECL, enhanced chemiluminescence system; ECM, extracellular matrix; ESRD, end-stage renal disease; FBS, fetal bovine serum; FN, Fibronectin; FPKM, Fragments Per kilobase of an exon model per Million mapped fragments; GADPH,glyceraldehyde-3-phosphate dehydrogenase; GO, gene ontology; GSEA, Gene Set Enrichment Analysis; HE, hematoxylin and eosin ; HIF-1,Hypoxia-inducible factor 1; IgA, Immunoglobulin A; IDEs, identical differential expressed genes; IHC, immunohistochemistry; JAK-STAT, Janus kinase-signal transducer and activator of transcription; LC3, light chain 3; MMP, Mitochondrial membrane potential; mTOR, mammalian target of rapamycin; NLRP3, Nlrfamily pyrin domain-containing 3; NRK-52E, Normal rat kidney epithelial cell line; PI3K, phosphatidylinositol kinase-3; RIF, Renal interstitial fibrosis; SDS-PAGE, sodium dodecyl sulfate-polyacrylamide gel electrophoresis; SD rats, Sprague-Dawley rats; TGF-β1, transforming growth factor-β1; UUO, unilateral ureteral obstruction.

results showed that hirudin could induce a decrease in the expression of autophagy-related proteins such as P62, LC3, Beclin-1 in TGF-β1-induced NRK-52E cells.

Conclusion: Our results suggest that hirudin may protect the kidney by ameliorating renal autophagy impairment through modulating the PI3K/Akt pathway.

Keywords: renal fibrosis (RF), natural products, hirudin (PubChem CID: 72941487), transcriptome (RNA-seq), UUO (unilateral ureteral obstruction)

INTRODUCTION

Chronic kidney disease (CKD) is one of the major diseases that seriously endanger human health and is characterized by high incidence, low awareness, elevated medical costs and high risk of combined cardiovascular events (Yang C. et al., 2020; Luyckx et al., 2020). About 10.8% of adults in China have CKD, and the prevalence is as high as 18.3% in Central and Southwest China (Zhang et al., 2012; Huang et al., 2019). CKD affects 8–16% of the world's population (Coresh, Josef et al., 2007; Jha, Vivekanand et al., 2013). In developed countries, CKD is most often attributed to diabetes and hypertension. However, less than 5% of people with early CKD report being aware of their disease (Chen et al., 2019). CKD usually has no obvious symptoms in the early stage, but when it progresses to the middle and late stage, as the kidney function declines, the body accumulates too many toxins leading to a series of uremic symptoms, requiring dialysis or even kidney transplantation, which seriously affects the quality of life of patients and brings a huge economic burden (Drawz and Rahman, 2015).

Renal interstitial fibrosis (RIF), a common pathway and the main pathological basis for the development of various CKD to end-stage renal disease (ESRD), mainly manifested as glomerulosclerosis and RIF, which is triggered by the inability of the kidney to be completely repaired due to abnormal tissue repair/regeneration after chronic and continuous injury, resulting in the replacement of normal tissue by fibrous tissue and loss of function, eventually causing renal failure, and the degree of RIF is closely related to the decline in renal function, often suggesting a poor prognosis for patients (Tang et al., 2019), is a common pathological feature of most CKD (Drawz and Rahman, 2015).

Therefore, to inhibit RIF is significant for the treatment of CKD. Many drugs used in clinical practice have anti-retrofibrotic effects, such as ACEI, ARB, aldosterone inhibitors, statins, endothelin receptors, beta-blockers, acetylsalicylic acid, metformin, and MMP inhibitors (Brewster and Perazella, 2004; Kanbay et al., 2009; Manns et al., 2012; Böhm et al., 2017; Rangarajan et al., 2018; Zhang et al., 2020), Among them, ACEI and ARB are the first-line drugs for the clinical treatment of CKD (KDOQI, 2012; Chen et al., 2018). The antifibrotic effect of ACEI/ARB may also arise from the preventive effect on glomerular injury induced by aldosterone or high intra-glomerular pressure (Obata et al., 1997; Wang et al., 2013). Although these drugs have shown some improvement in fibrosis, their therapeutic targets do not focus on fibrosis. Currently, the lack of exclusive drug targets for RIF and drugs targeting RIF severely hampers the treatment of CKD, so new drug targets and their targeting drugs are yet to be developed.

Hirudin is a bioactive protein extracted from the saliva of medical leeches, consisting of 65–66 amino acids, with a relative molecular weight of 7 kD, and is the main substance for leeches to exert their anticoagulant effect (Markwardt, 1991). Hirudin is excreted in urine principally in the form of prototype and metabolites through renal metabolism (Zhang and Lan, 2018). Studies have shown that hirudin is mostly distributed in the kidney and plasma, its pharmacokinetics is dose-dependent, and its metabolism *in vivo* depends on renal function (Robson et al., 2002)which provides a theoretical basis for the application of hirudin to blood concentrations in CKD.

Recently, hirudin has been used to treat diabetic nephropathy, IgA nephropathy and other chronic kidney diseases (Deng et al., 2019; Han et al., 2020), however, its specific mechanism of action in patients with CKD is not unclear. In this study, the regulatory mechanism of hirudin against CKD was investigated by RNA sequencing, differentially expressed gene (DEG) identification and annotation, gene ontology (GO) function and Gene Set Enrichment Analysis (GSEA) enrichment.

MATERIALS AND METHODS

Animal Experiments

Eighteen healthy male SD rats with body weight (200 ± 20 g), purchased from Beijing Viton Lever Laboratory Animal Co. The animal production license number is SCXK (Jing) 2016–0006, and the animal quality certificate is No.110011200110536318. After 1 week of adaptive feeding, rats were randomly divided into sham group, unilateral ureteral obstruction (UUO) group, and UUO hirudin treatment group, with six rats in each group. Except for the sham group, the rats in all groups underwent left unilateral ureteral obstruction according to Martínez's method (Martínez-Klimova et al., 2019). The rats were fasted the night before surgery and the left unilateral ureteral obstruction was performed under aseptic conditions. We first injected 10% chloral hydrate (3 ml/kg) intraperitoneally, and after the rats were anesthetized, they were fixed in prone position, and a longitudinal incision of about 1.5 cm in length was made on the left side of the spine, about 0.5 cm below the lumbar point of the ribs, and the left ureter were isolated, ligated and disconnected layer by layer. The rats in the sham group were treated as the UUO group except that they were not ligated and the ureter was not disconnected. The corresponding drug was given to each group of rats on the same day after the operation. The dose of the

drug administered was determined according to the animal/human surface area method of conversion and combined with the results of the previous experiments (Yang K. et al., 2020). UUO hirudin treatment group with a dose of 40 IU/kg/d by tail vein injection, and the UUO group as well as Sham group with stroke-physiological saline solution (SPSS) by tail vein injection too. This study was approved by the Animal Protection and Utilization Committee of the first teaching hospital of Tianjin university of traditional Chinese medicine (Tianjin, China), in accordance with our institutional regulations.

Sample Collection

Rats were anesthetized by intraperitoneal injection of 10% chloral hydrate (3 ml/kg) after 14 days of continuous tail vein administration. Subsequently, the rats were executed by cervical dislocation and the left kidney was removed. we divided the left kidney of each rat in each group into two parts along the coronal plane of the longitudinal axis of the kidney. A fresh half of the left kidney from all six rats in each group was fixed in 4% paraformaldehyde at room temperature for 24 h, while the other half of the left kidney from each group was rapidly frozen in liquid nitrogen and stored at −80°C until use.

Morphology Analysis

After the rats were executed, the left side of the obstructed kidney tissue was left, and the kidney was incised along the sagittal plane and fixed in 10% neutral formalin solution for 24 h, followed by gradient dehydration, hyalinization, paraffin immersion, paraffin bedding, hematoxylin and eosin (HE) staining. Histological sections of the kidney were dewaxed and dehydrated, after that stained with an acidic complex of hematoxylin and Ponceau red liquid dye, followed by direct staining of the histological sections. Then soaked in 1% phosphomolybdic acid solution and stained directly with aniline blue solution and 1% acetic acid. The observed collagen is represented as a blue area for the degree of fibrosis, and the interstitial collagen deposition in Masson staining sections was observed under optical microscope.

Cell Culture

Normal rat kidney epithelial cell line (NRK-52E) was purchased from Pronosai Life Sciences Co. (Wuhan, China). Cells were cultured in 90% high glucose DMEM (Thermo Fisher Science, Inc., United States) and 10% fetal bovine serum (FBS) at 37°C and 5% CO^2 concentration. Then, NRK-52E cells were treated with 5 ng/ml TGF-β1 for 48 h to establish an *in vitro* fibrosis model.

Cell Viability Assay

NRK-52E cells in excellent growth condition were prepared in cell suspension, and the cell density was adjusted to 8×10^4 cells/mL at 100 μL per well and inoculated in 96-well plates. The cells were divided into control group and experimental group, and the experimental group was added with different concentrations (2.5, 5,7.5,10,12.5.15,17.5, and 20 IU/ml) of hirudin (patent no. ZL03113566.8,100 IU/vial, Canton Xike Kang Biotechnology Co. Ltd.,Guangxi, China), while the control group was added with fresh medium, and three replicate wells were set up for each group. After incubation for 24 and 48 h, 10 μL of CCK-8 reagent (Bioworld, BD0079-1) was added to each well and incubated for another 4 h. The 96-well plates were placed under an enzyme marker to determine the OD value at 450 nm, and the cell viability was calculated based on the OD value to determine the appropriate concentration of hirudin to continue the experiment. All samples were assayed at least three times.

Detection of Fibrosis-Associated Protein Expression in Kidney Tissues by Western Blot

Total protein was extracted from obstructed kidney tissues or cells using 2×SDS lysate, and the protein concentration was determined by BCA protein assay kit (Solarbio life sciences Co., Beijing, China); 10% sodium dodecyl sulfate-polyacrylamide gel electrophoresis (SDS-PAGE) gel was used for electrophoretic separation, and the separation was transferred to PVDF membrane (Pierce Corporation, United States). The PVDF membrane was immersed in QuickBlock™ Western blocking solution (Beyotime Biotechnology, P0252) for 30 min at room temperature then incubated overnight at 4°C with anti-FN(1:2000, Proteintech, 15613-1-AP), anti-Col1 (1:1,000,Abcam, ab184993), anti-Col3 (1:1,000,Abcam, ab7778), anti- E-Cad (1: 5,000, Proteintech, 20874-1-AP) , anti- PI3K (1:1,000, CST, 4,249), anti- Akt (1:1,000, CST, 4,691), anti-p-Akt (1:2000, CST, 4,060), anti-mTOR (1:1,000, CST, 1983), anti-Beclin1 (1: 2000, Bioworld, AP0768),anti-P62 (1:500, Wanleibio,WL02385) and anti-GADPH (1:10,000, Proteintech, 10494-1-AP) respectively. After washing the membrane 3 times with TBST, the membrane was incubated with HRP-conjugated AffiniPure goat anti-mouse IgG (1:10,000, Proteintech, SA00001-1) or anti-rabbit IgG (1:10,000, Proteintech, SA00001-2) for 1 h at room temperature and washed 3 times again with TBST. Lastly, the membranes were added with enhanced chemiluminescence system (ECL) detection kit (Boster, China), ImageJ software was used for grayscale analysis of the image bands, and GAPDH was used as an internal reference for semi-quantitative analysis of the target proteins.

Real-Time PCR

Total real-time polymerase chain reaction RNA was extracted using Trizol reagent (Invitgen, Carlsad, CA, United States), and the concentration of RNA for each sample was measured using an ND5000 ultra-micro UV spectrophotometer and reverse transcribed using the All-in-One™ First-Strand cDNA Synthesis Kit (GeneCopoeia Cat. No. AORT-0050) for reverse transcription. Target genes were analyzed by RT-qPCR according to the manufacturer's instructions (Applied Biosystems Inc., Foster City, CA, United States). GAPDH forward primer is 5′-TCCTGCACCACCAACTGCTTAG-3'; reverse primer is 5′-AGTGGCAGTGATGGCATGGACT-3'; FN primer forward is 5 ′-ATGAGAAGCCTGGATCCCCT-3′ and the reverse is 5′-GGAAGGGTAACCAGTTGGGG-3'; COL1 is forward:5′- GGGCAACAGCAGATTCACCTACAC-3′ and reverse:5′-CAAGGAATGGCAGGCGAGATGG-3'; for COL3, forward:5′- AGTGGCCATAATGGGGAACG-3′ and reverse:

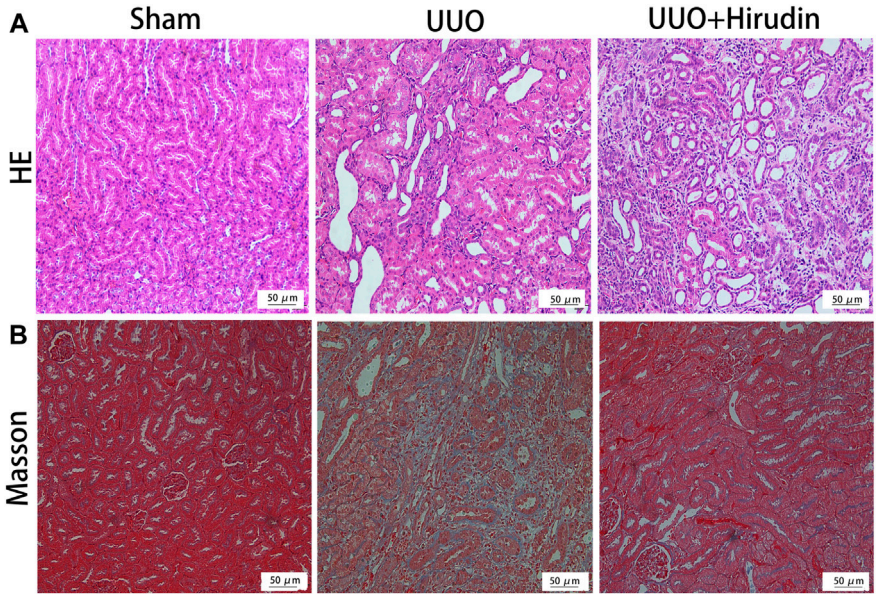

FIGURE 1 | Effect of hirudin on renal histopathological alterations in unilateral ureteral obstruction (UUO)-induced renal interstitial fibrosis (RIF) rats. **(A)** HE staining showed that hirudin significantly reduced tubular dilatation or atrophy, interstitial fibrosis and inflammatory cell infiltration in the UUO rats (magnification×200). **(B)** Masson trichrome staining showed that hirudin significantly reduced renal tubulointerstitial damage and total collagen deposition in UUO rats. (magnification×400).

5′-CACCTTTGTCACCTCGTGGA-3'. GAPDH was used as an internal control. Expression differences were assessed by the $2^{-\Delta\Delta CT}$ method.

Immunohistochemical Staining

Similar to HE staining, kidney tissues were fixed in paraffin and next cut into paraffin-embedded kidney sections using a microtome. The tissue sections were then dewaxed, rehydrated and subjected to antigen retrieval in 0.01 M citrate buffer (pH 6.0). After washing twice with PBS (0.01 M, pH 7.4), sections were prepared for blocking with primary antibodies against α-SMA (1:1,500, Proteintech, 14395-1-AP) and PI3K (1:300, Proteintech, 20584-1-AP) and incubated overnight, followed by biotin labeled secondary antibodies. Bound antibodies were visualized with diaminobenzidine (DAB) staining and imaged (magnification, × 200) using a light microscope (TE 2000, Nikon, Japan). Brown granule staining in the cytoplasm and/or nucleus represents positive expression of α-SMA and PI3K.

Cellular Immunofluorescence Staining

NRK-52E cells were crawled, then treated with TGF-β1 and hirudin for 24 h, fixed with 4% paraformaldehyde, followed by the addition of 0.1% Triton X-100 to break the membrane for 10 min, and blocked with 10% FBS to eliminate non-characteristic fluorescent color development. After treatment with rabbit anti-rat LC3 (1:300, Proteintech, 14600-1-AP) and Beclin-1 (1:100, Bioworld, AP0768), and DyLight 488/594-labeled secondary antibody, the nuclei were stained with DAPI and sealed with anti-quenching blocker, and finally placed under a fluorescent microscope and photographed. The nuclei were stained with DAPI and blocked with anti-quenching blocker. The expression levels of the corresponding proteins were expressed as the integrated absorbance values.

Transcriptional and Bioinformatics Analysis

High quality RNA was used for library construction and high-throughput sequencing. The RNA sequencing libraries were performed using the NEBNext Ultra RNA Library Prep Kit according to the manufacturer's protocol. The library was subsequently sequenced by CaptalBio technology Co. Ltd. (Beijing, China) on a Novaseq6000 platform (Illumina, Chicago, IL, United States). Transcriptome analysis was performed using the rat reference genome-based read mapping. Gene expression levels were estimated using Fragments Per kilobase of an exon model per Million mapped fragments (FPKM) values.

Statistical Analysis

All experiments were performed at least three times. SPSS 26.0 and GraphPad prism8 software were used for statistical analysis of the data, and all data were expressed as mean ± standard deviation. One-way analysis of variance (ANOVA) was used for comparison between groups. Tukey's test was used to compare multiple methods. $p < 0.05$ was considered significant.

RESULTS

Hirudin Mitigated Renal Interstitial Fibrosis

We initially investigated the effects of resveratrol on interstitial fibrosis in the kidneys of UUO models, which is a typical model of

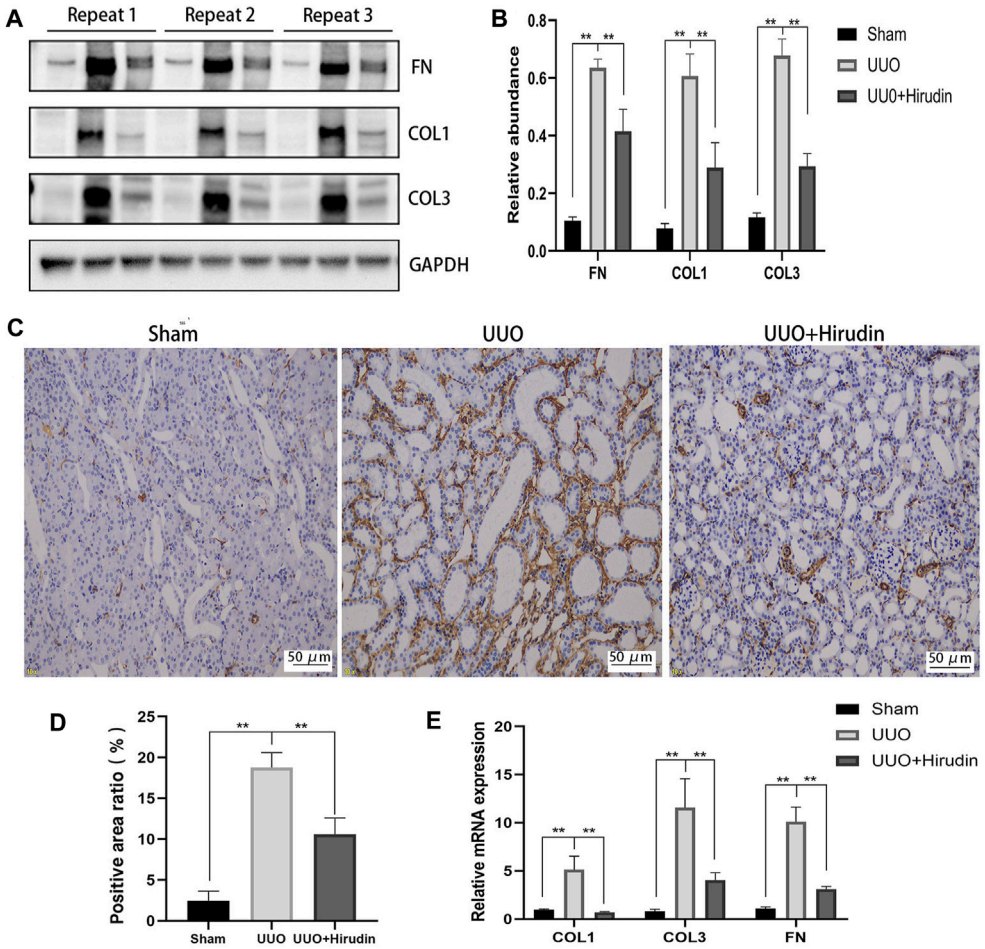

FIGURE 2 | Effect of hirudin on inhibition of FN, COL1, COL3 and α-SMA induced by unilateral ureteral obstruction (UUO). **(A)** Effect of hirudin on FN, COL1 and COL3 in UUO kidney tissues, as determined by Western blot. **(B)** Effect of hirudin on FN, COL1 and COL3 in UUO kidney tissues, according to the results of Western blot. **(C)** Effect of hirudin on α-SMA in UUO kidney tissues, as determined by Immunohistochemical staining (magnification ×200). **(D)** Effect of hirudin on α-SMA in UUO kidney tissues, according to the results of Immunohistochemical staining. **(E)** Effect of hirudin on FN, COL1 and COL3 in UUO kidney tissues, according to the results of RT-qPCR. Data are expressed as mean ± SD for six rats per group. ** indicates $p < 0.01$and * indicates $p < 0.05$.

RIF (Song et al., 2014). There were no rats died during the experiment. The extent of kidney injury in the 14 days rats was evaluated by HE staining (**Figure 1A**). Briefly, the kidney tissue structure of the control group was normal. On the 14 days, the renal tubular structure of the UUO group rats was severely damaged, with massive necrosis of epithelial cells, atrophy and collapse of interstitium, thickening or disappearance of basement membrane, and obvious proliferation of renal interstitial fibrous tissue with a large number of monocytes and macrophages infiltration. The above pathological damage was significantly reduced after hirudin treatment compared with the UUO group. Masson trichrome staining was performed at 14 days to assess the extent of fibrosis in the rat kidney tissue (**Figure 1B**). No significant fibrosis was seen in the kidney tissues of the control rats. The model kidney disturbed cell arrangement, disrupted tubular structure and obvious proliferation of fibrous connective tissue; compared with the UUO group, the kidney fibrosis was reduced in the hirudin-treated group.

Expressions of Fibrosis-Associated Genes in Rat Kidney Tissues

Next, we examined the protein levels of fibrosis markers in the kidney tissues of each group. The expression of proteins COL1, COL3, and FN, which are closely related to fibrosis formation, was upregulated in the UUO group compared with the Sham group, and the expression was reversed after hirudin treatment (**Figures 2A,B**). Based on the biological importance of α-SMA in mediating RIF, we next assessed the protein levels of α-SMA in rat kidney tissues by immunohistochemistry (IHC). Compared with the Sham group, α-SMA positive expression was increased in the UUO group rats and was downregulated by hirudin treatment

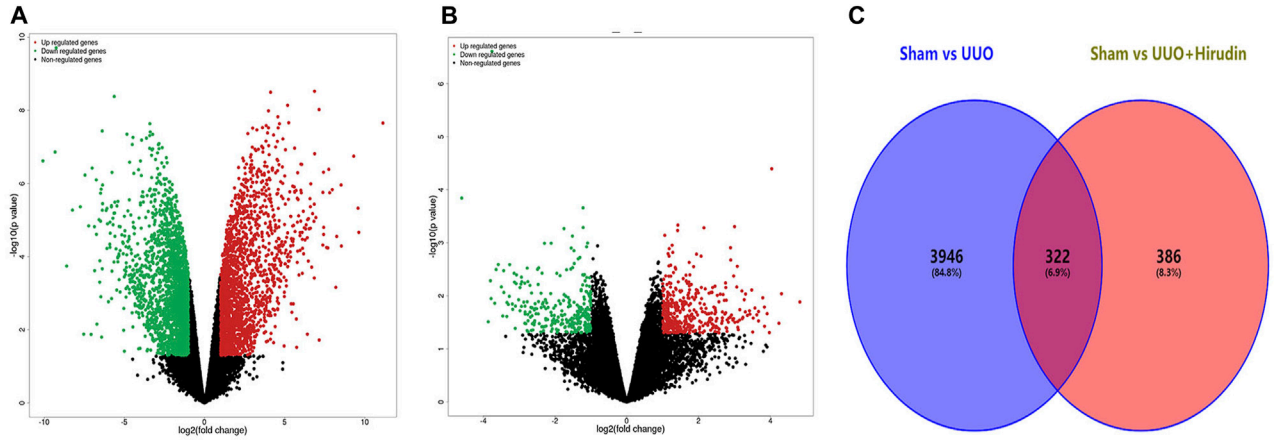

FIGURE 3 | Transcriptomic assay and bioinformatics analysis. **(A)** Compared Sham group with UUO group, filtering of DEGs was presented by volcano. **(B)** Compared UUO hirudin-treated group with UUO group, filtering of DEGs was presented by volcano. **(C)** Venn diagram of overlapping genes derived from transcriptome analysis in a pairwise comparison. Red color represents upregulated genes, while green color shows downregulated genes.

(**Figures 2C,D**). The expression trends of COL1, COL3, and FN mRNA were further confirmed by RT-qPCR to be consistent with protein expression (**Figure 2E**), and thus the transcript levels were statistically significant between the groups.

Transcriptomic Analysis of Hirudin in the Treatment of Renal Interstitial Fibrosis

We performed a comparative analysis of transcriptome analysis and gene expression between the Sham group, the UUO group and the UUO hirudin-treated group. In total, the RNA-Seq results included 30,408 differential expressed genes (DEGs, | log2FoldChange | ≥1). Among them, the Sham and UUO groups had 15,112 DEGs, while there were 15,296 DEGs between Sham and UUO hirudin-treated group. In which, 2013 genes were up-regulated and 2,255 genes were down-regulated in the UUO group compared to the Sham group (**Figure 3A**). 708 genes were changed, of which 419 genes were up-regulated and 289 genes were down-regulated in the UUO hirudin-treated group compared with the UUO group (**Figure 3B**). We then mapped the differentially expressed genes from the above two results to obtain 322 identical differential expressed genes (IDEs), which were the potential target genes for hirudin against kidney fibrosis (**Figure 3C**). Of these genes, 169 common genes were consistently upregulated and 153 common genes were consistently downregulated.

PI3K/Akt Signaling Serves as a Candidate Pathway in Hirudin Against CKD

To further discover the potential functional pathways of hirudin for CKD treatment, we performed GSEA analysis on IDEs. A total of 115 signaling pathways were enriched, as shown in **Figure 4A**, AMPK, JAK-STAT and PI3K-Akt signaling pathways were the important signaling pathways enriched. PI3K/Akt signaling pathway ranking five was priorly chosen to be verified in the following experiments. To explore the biological functions of IDEs, we performed Gene Ontology (GO) pathway annotation, and the results showed that cellular amino acid metabolic process was the most significantly enriched pathway in biological processes (**Figure 4B**). For molecular functional enrichment analysis, IDEs were mainly enriched in coenzyme binding, pyridoxal phosphate binding and other pathways (**Figure 4C**). In addition, microbody is the most obvious pathway for cellular components (**Figure 4D**).

PI3K and Akt Play an Important Role in the Treatment of Chronic Kidney Disease With Hirudin

Based on the above results, PI3K, Akt, mTOR were selected as potential targets and their expressions were further examined by RT-qPCR. **Figure 5E** shows the mRNA expression trends of PI3K, p-Akt, and mTOR, and thus the transcript levels were statistically significant between the groups. In addition, using the same remaining samples for Western blot analysis, the expression of PI3K, p-Akt, and mTOR was significantly elevated in the UUO group of rats, whereas it was significantly suppressed in the UUO hirudin-treated group (**Figures 5A–D**). These results suggest that hirudin can inhibit the PI3K/Akt signaling pathway, which is involved in the construction of the UUO rats and hirudin treatment of RIF.

Effect of Hirudin on NRK-52E Cell Viability After TGF-β1treatment

To avoid the potential toxic effects of hirudin on NRK-52E cells and to explore the effective and safe dose of hirudin, we treated NRK-52E cells at 0,2.5,5,7.5,10,12.5,15, 17.5 and 20 IU/ml concentrations of hirudin for 24 and 48 h, respectively. Hirudin was found to significantly reduce the increase in cell viability induced by 10 ng/ml TGF-β1, and this inhibition showed a dose-dependent effect. In addition, cell viability was significantly inhibited at hirudin concentrations >10 IU/ml for 24 h and at hirudin concentrations >5 IU/ml for 48 h

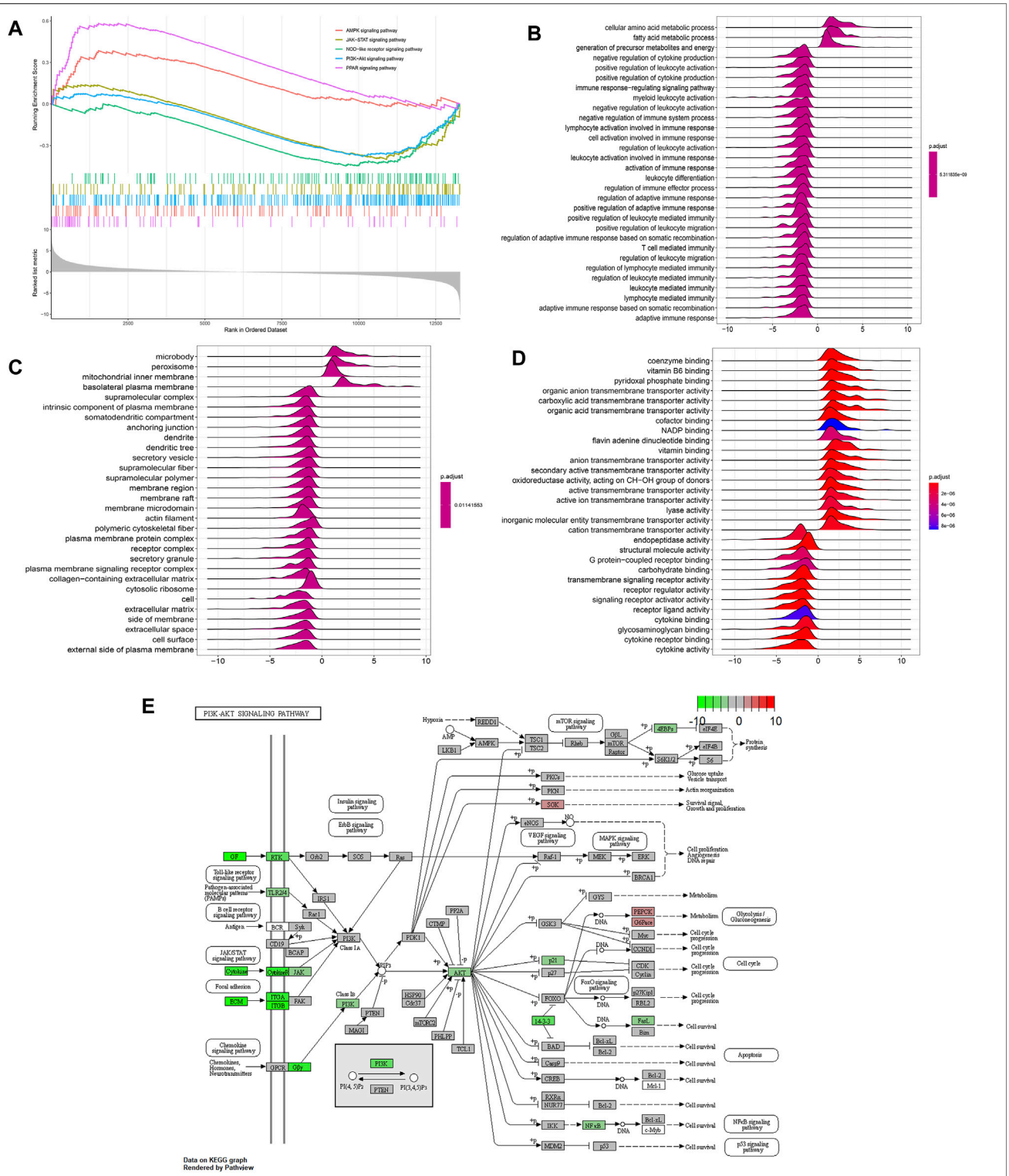

FIGURE 4 | Functional analysis of the kidney transcriptome by hirudin treatment. **(A)** Gene Set Enrichment Analysis (GSEA) of hirudin treatment-related key pathways. **(B)** biological processes (BP) of GO analysis of hirudin treatment-related functional annotations. **(C)** molecular function (MF) of GO analysis of hirudin treatment-related functional annotations. **(D)** cellular component (CC) of GO analysis of hirudin treatment-related functional annotations. **(E)** Schematic diagram of hirudin against RIF through PI3K/Akt pathway.

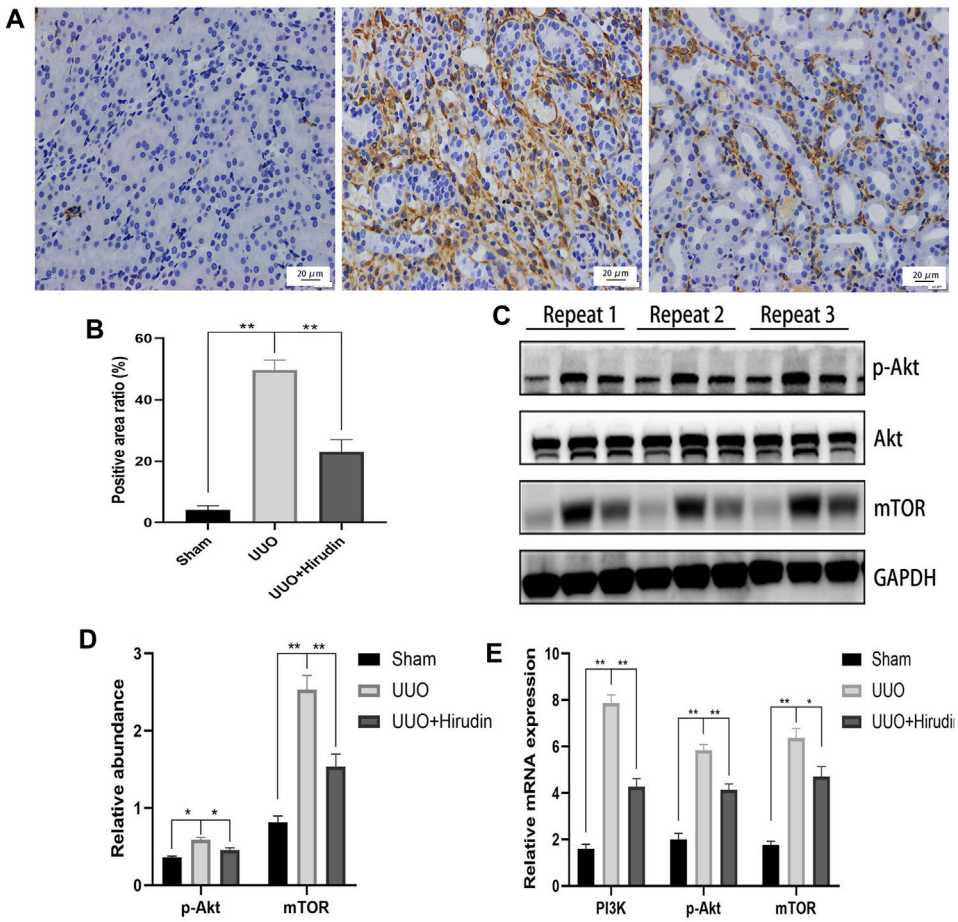

FIGURE 5 | Hirudin inhibited the PI3K/Akt signaling pathway in UUO kidneys. **(A)** Effect of hirudin on PI3K in UUO kidney tissues, as determined by immunohistochemical staining. (magnification ×400) **(B)** Hirudin reduced the PI3K positive expression area in UUO kidneys, according to the results of immunohistochemical staining. **(C)** Effect of hirudin on p-Akt and mTOR in UUO kidney tissues, as determined by Western blot. **(D)** Effect of hirudin on p-Akt and mTOR in UUO kidney tissues, according to the results of Western blot. **(E)** Effect of hirudin on PI3K, p-Akt and mTOR in UUO kidney tissues, according to the results of RT-qPCR. Data are expressed as mean ± SD for six rats per group. ** indicates $p < 0.01$and * indicates $p < 0.05$.

(**Figure 6A**). Therefore, we concluded that intervention with hirudin had no significant inhibitory effect on the cell viability of NRK-52E cells at a concentration of 10 IU/ml for 24 h. Thereby, we used 10 IU/ml of hirudin in the following experiments. To assess whether hirudin has antifibrotic properties *in vitro*, we analyzed the expression of fibrosis-associated proteins, which are reliable markers of TGF-β1-induced fibrosis after activation. Treatment with TGF-β1 significantly induced the expression of COL1, FN but decreased E-Cad expression.

We observed that treatment of NRK-52E with 10 IU/ml of hirudin for 24 h had an inhibitory effect on COL1 and FN expression in TGF-β1-induced NRK-52E cells, while promoting E-Cad expression (**Figures 6B,C**). This result was consistent with the expression of COL1, FN, and E-Cad at the mRNA level (**Figure 6D**).

Hirudin Inhibits PI3K/Akt Signaling Pathway

We further examined the effect of hirudin on regulating the PI3K/Akt pathway in NRK-52E. The expression of PI3K, p-Akt and mTOR was significantly upregulated after TGF-β1 treatment compared to the control group. However, hirudin treatment inhibited their increased expression (**Figures 7A,B**). Furthermore, we treated NRK-52E cells in the TGF-β1 group using the PI3K inhibitor wortmannin to investigate whether attenuating renal fibrosis in the TGF-β1 group was caused by inhibition of the PI3K/Akt pathway. As shown in **Figures 7C,D**, wortmannin treatment partially reversed the TGF-β1-induced increase in PI3K compared to cells in the TGF-β1 group. In addition, p-Akt and mTOR were correspondingly reduced by wortmannin treatment ($p < 0.01$). These data confirm that renal fibrosis is inhibited and restored by blocking the PI3K/Akt pathway.

Hirudin Ameliorated Autophagy Disorders

Changes in autophagy are important for the physiological function of the kidney and the course of disease development (Kaushal et al., 2020; Tang et al., 2020). And PI3K/Akt signaling pathway is the classical pathway of autophagy (Reedquist et al.,

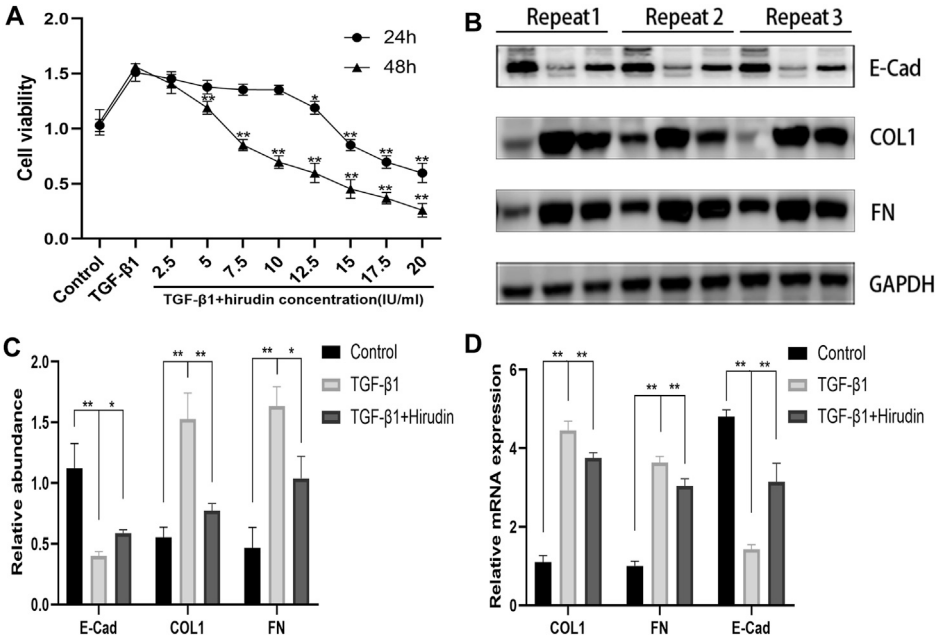

FIGURE 6 | Hirudin attenuates renal interstitial fibrosis in TGF-β1 induced NRK-52E cells. **(A)** CCK-8 assay showed that the ability of cell viability was decreased in NRK-52E cells by treatment with hirudin. **(B)** Effect of hirudin on COL1, FN and E-Cad in NRK-52E cells, as determined by Western blot. **(C)** Effect of hirudin on COL1, FN and E-Cad in NRK-52E cells, according to the results of Western blot. **(D)** Effect of hirudin on COL1, FN and E-Cad in NRK-52E cells, according to the results of RT-qPCR. Data are expressed as mean ± SD (n = 3 for each group). ** indicates $p < 0.01$ and * indicates $p < 0.05$.

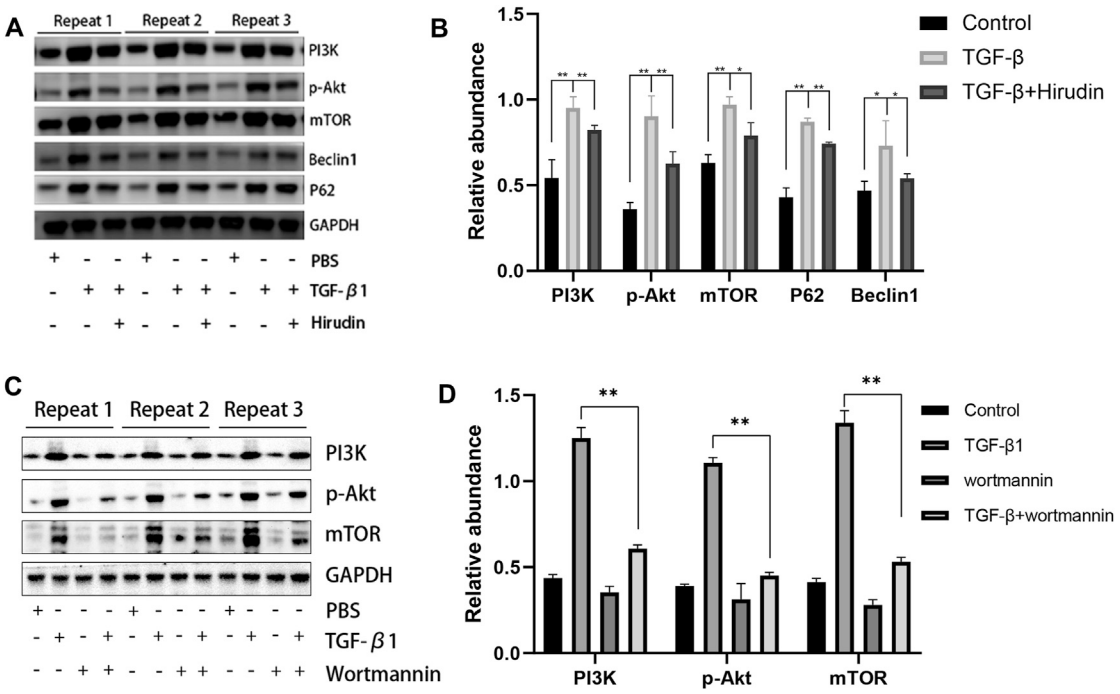

FIGURE 7 | Hirudin inhibits the PI3K/Akt signaling pathway in TGF-β1-treated NRK-52E cells. **(A)** Effect of hirudin on PI3K, p-Akt, mTOR, Beclin1 and P62 in TGF-β1-treated NRK-52E cells, as determined by Western blot. **(B)** Effect of hirudin on PI3K, p-Akt, mTOR, Beclin1 and P62 in TGF-β1-treated NRK-52E cells, according to the results of Western blot. **(C)** Effect of wortmannin on PI3K, p-Akt, mTOR in TGF-β1-treated NRK-52E cells, as determined by Western blot.**(D)** Effect of wortmannin on PI3K, p-Akt, mTOR in TGF-β1-treated NRK-52E cells, according to the results of Western blot. Data are expressed as mean ± SD (n = 3 for each group). ** indicates $p < 0.01$ and * indicates $p < 0.05$.

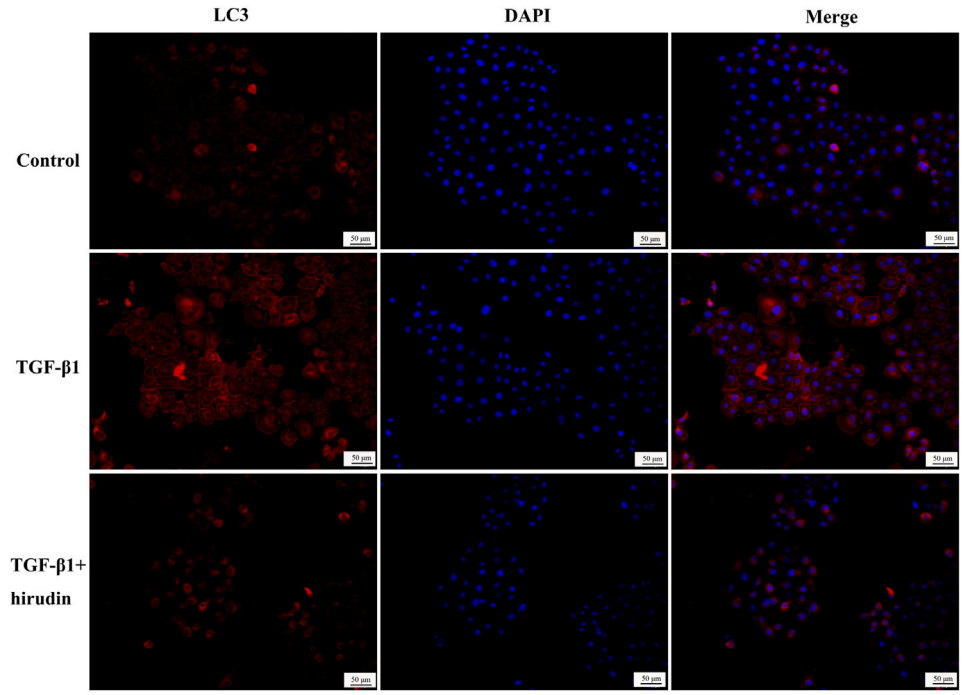

FIGURE 8 | Cellular immunofluorescence detection of LC3 protein expression.

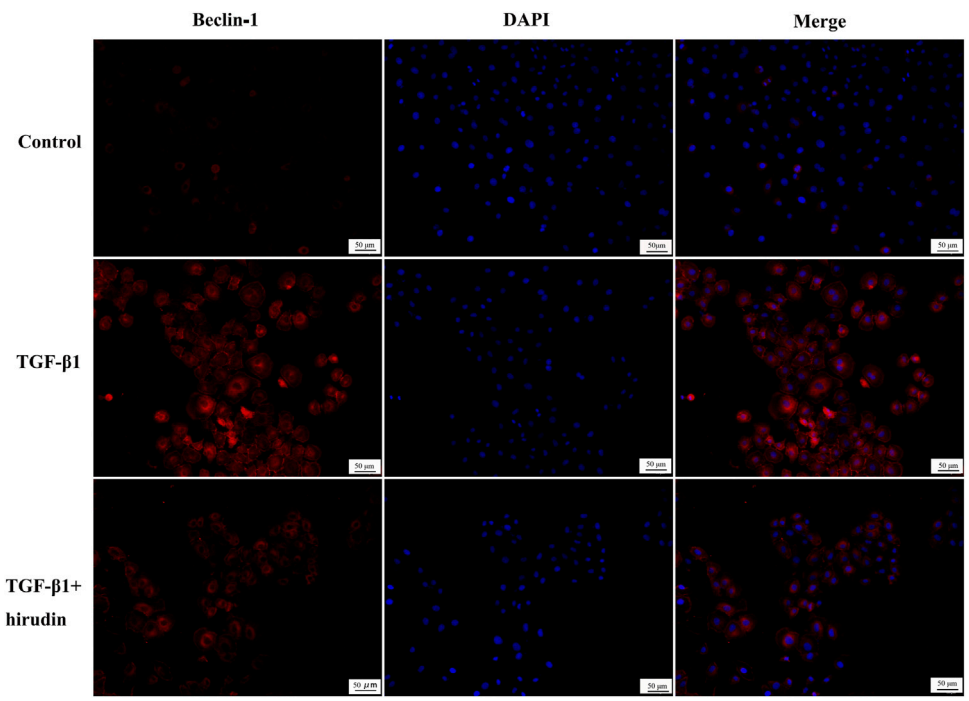

FIGURE 9 | Cellular immunofluorescence detection of Beclin-1 protein expression.

2006; Jung et al., 2010). Therefore we then tested the effect of TGF-β1 on the autophagic capacity of NRK-52E cells. Western blotting results showed that the expression of P62 and Beclin-1 was increased in the TGF-β1 group compared with the Control group; the expression of P62 and Beclin-1 was significantly decreased in the TGF-β1+Hirudin group compared with the

TGF-β1 group (**Figures 7A,B**). Immunofluorescence assay results showed that intracellular autophagy marker proteins LC3 and Beclin-1 were significantly increased in the TGF-β1 group compared with the Control group; intracellular LC3 and Beclin-1 were significantly decreased in the TGF-β1+Hirudin group compared with the TGF-β1 group (**Figures 8**, **9**). In conclusion, hirudin could attenuate TGF-β1-induced autophagy impairment in NRK-52E cells.

DISCUSSIONS

Leeches are the dried bodies of the annelids W. pigra Whitman, H. nipponica Whitman, or W. acranulata Whitman, and modern pharmacological studies indicate that leeches mainly have anticoagulant and antithrombotic effects (Eldor et al., 1996). The hirudin in leeches is the strongest specific inhibitor of thrombin found so far (Markwardt, 1994). Therefore, the presence of hirudin in leeches and its content has become an important criterion for measuring the efficacy of medicinal leeches (Zhang et al., 2013). In addition to its anticoagulant effect, hirudin also has some anti-inflammatory and anti-fibrotic effects (Li et al., 2019; Shen et al., 2019). However, there are few reports on the anti-nephrogenic fibrotic effects of hirudin. UUO is a common way to elucidate the pathological mechanisms associated with RIF, such as glomerulosclerosis, inflammatory cell infiltration, interstitial ECM aggregation, and collagen deposition (Nishida et al., 2007; Islam et al., 2016). In this study, we evaluated the effect of hirudin in improving renal function by detecting renal fibrosis indexes. The experimental results illustrated that hirudin significantly improved the renal fibrosis-related protein levels in UUO rats, suggesting its protective effect on renal function in UUO rats. To further investigate the molecular mechanism of the renal protective effect of hirudin, we identified 322 mRNAs (including 169 up-regulated mRNAs and 153 down-regulated mRNAs) that were differentially expressed in the hirudin-treated group compared with the UUO group.

Functional enrichment analysis showed that these genes were significantly enriched in relation to Go-BP, such as negative regulation of cytokine production, positive regulation of cytokine production, adaptive immune response, activation of immune response and cell activation involved in immune response, were significantly enriched. response, activation of immune response and cell activation involved in immune response, etc. It was shown that cytokines TGF-β, HIF-1, and NLRP3 promote the development of chronic kidney disease and influence the immune status of CKD. Corresponding to the GO results, pathway enrichment analysis enriched 115 terms, including AMPK signaling pathway, JAK-STAT signaling pathway and PI3K-Akt signaling pathway.

The adenylate-activated protein kinase (AMPK) pathway is involved in the development of CKD (Guo et al., 2014; Ha et al., 2014). Activation of the AMPK signaling pathway reduces oxidative stress in chronic kidney disease (Kidokoro et al., 2013), decreases the expression of inflammatory factors in plasma and renal tissues of CKD patients (Xie et al., 2017), and inhibits the development of renal tubular fibrosis (Ishibashi et al., 2012).

The JAK/STAT signaling pathway is an important class of cytokine signaling pathway that is widely involved in cell proliferation, differentiation, apoptosis and inflammatory response, and has a regulatory role in various renal diseases (Chuang and He, 2010; Wiezel et al., 2014; Pace et al., 2019). This pathway can be involved in the development of obstructive nephropathy, diabetic nephropathy and acute kidney injury by regulating the expression of JAK and STAT family factors, and inhibition of this signaling pathway can help to slow down the progression of CKD (Liu et al., 2020; Zhao et al., 2020).

The phosphatidylinositol kinase-3 (PI3K)/protein kinase B (Akt) signaling pathway is also an important signaling pathway in chronic kidney disease, and overactivation of this signaling pathway can trigger the onset and development of CKD (Lu et al., 2019). We randomly selected the PI3K-Akt signaling pathway for validation. Our study suggests that PIK3/Akt signaling pathway activation is involved in the development of CKD. After hirudin treatment, PI3K protein was reduced in renal tissues of UUO rats as well as in TGF-β-induced NRK-52E cells. The same trend was observed for Akt phosphorylation levels. We conclude that hirudin is able to alleviate renal tissue injury by inhibiting the activation of the PIK3/Akt signaling pathway. The PI3K/Akt signaling pathway is the most classical signaling pathway in the regulation of cellular autophagy, and it plays an important role (Chen and Debnath, 2013; Yu et al., 2015). In recent years, an increasing number of studies have found that PI3K/Akt pathway-regulated cellular autophagy is closely associated with the development and pathological progression of chronic kidney diseases such as diabetic nephropathy and RIF (Kimura et al., 2017; Liu et al., 2017; Lin et al., 2019).

There is also extensive research evidence further suggesting the presence of autophagy-deficient kidneys in CKD patients (Kume et al., 2012; Lin et al., 2019; Choi, 2020). Based on these findings, the hypothesis that defective autophagy in the kidney may increase the susceptibility of renal cells to the associated injury, leading to treatment-emergent resistant proteinuria and progressive decline in renal function, was then proposed (Leventhal et al., 2014). Therefore, restoring autophagy as a treatment for CKD may become a new therapeutic option. LC3 is widely used as a marker of autophagy, and the transition from LC3I to LC3II suggests the formation of autophagosomes. In addition, ubiquitin-binding protein P62 is another marker protein reflecting autophagic activity, and its accumulation in the cytoplasm suggests diminished autophagic activity. Beclin1 also positively regulates autophagic activity by binding to PI3K3C, forming a core complex that initiates autophagy (Yang and Klionsky, 2010). Our results showed that the expression levels of P62, Beclin-1 and LC3 were significantly increased after TGF-β intervention in NRK-52E cells, suggesting an intracellular impairment of autophagy, which was reversed by hirudin. Therefore, we suggest that hirudin has a nephroprotective effect and ameliorates autophagy impairment in renal injury, and this effect is associated with the PIK3/Akt signaling cascade.

In this study, we investigated the mechanism of action of hirudin against RIF from the perspective of transcriptomic analysis and *in vivo* and *in vitro* experimental validation, and there are some areas for improvement in the follow-up study.

First, clinical data and samples need to be studied to support our findings. Second, RIF is a complex pathological process involving various mechanisms such as autophagy, oxidative stress, impaired energy metabolism, and apoptosis, and further elucidation is still needed for the specific mechanism of hirudin against RIF.

The anti-renal fibrotic effect of hirudin has been studied, but its mechanism of action has not been fully elucidated. In the present study, we investigated the molecular mechanism of the anti-renal fibrosis effect of hirudin from the whole transcriptome and *ex vivo* experiments. The results showed that hirudin ameliorated renal fibrosis in rats by a mechanism involving the regulation of the PIK3/Akt signaling pathway and thus the activation of autophagy.

DATA AVAILABILITY STATEMENT

The data presented in the study are deposited in the GEO repository, accession number GSE181380.

ETHICS STATEMENT

The animal study was reviewed and approved by Animal Protection and Utilization Committee of the first teaching hospital of Tianjin university of traditional Chinese medicine.

AUTHOR CONTRIBUTIONS

H-XY, WL conceived the original screening and research plans; H-TY, CX supervised the experiments; L-JW, KY performed most of the in vitro experiments; MP and J-LC performed the in vivo experiments. XL provided technical assistance. H-XY, WL conceived the project and wrote the article with contributions of all the authors.

FUNDING

This work was supported by the National Natural Science Foundation of China (grant numbers 81873263).

REFERENCES

Böhm, M., Schumacher, H., Teo, K. K., Lonn, E. M., Mahfoud, F., Mann, J. F. E., et al. (2017). Achieved Blood Pressure and Cardiovascular Outcomes in High-Risk Patients: Results from ONTARGET and TRANSCEND Trials. *Lancet* 389, 2226–2237. doi:10.1016/S0140-6736(17)30754-7

Brewster, U. C., and Perazella, M. A. (2004). The Renin-Angiotensin-Aldosterone System and the Kidney: Effects on Kidney Disease. *Am. J. Med.* 116, 263–272. doi:10.1016/j.amjmed.2003.09.034

Chen, D. Q., Feng, Y. L., Cao, G., and Zhao, Y. Y. (2018). Natural Products as a Source for Antifibrosis Therapy. *Trends Pharmacol. Sci.* 39, 937–952. doi:10.1016/j.tips.2018.09.002

Chen, N., and Debnath, J. (2013). IκB Kinase Complex (IKK) Triggers Detachment-Induced Autophagy in Mammary Epithelial Cells Independently of the PI3K-AKT-MTORC1 Pathway. *Autophagy* 9, 1214–1227. doi:10.4161/auto.24870

Chen, T. K., Knicely, D. H., and Grams, M. E. (2019). Chronic Kidney Disease Diagnosis and Management: A Review. *Jama* 322, 1294–1304. doi:10.1001/jama.2019.14745

Choi, M. E. (2020). Autophagy in Kidney Disease. *Annu. Rev. Physiol.* 82, 297–322. doi:10.1146/annurev-physiol-021119-034658

Chuang, P. Y., and He, J. C. (2010). JAK/STAT Signaling in Renal Diseases. *Kidney Int.* 78, 231–234. doi:10.1038/ki.2010.158

Coresh, J., Selvin, E., Stevens, L. A., Manzi, J., Kusek, J. W., Eggers, P., et al. (2007). Prevalence of Chronic Kidney Disease in the United States. *JAMA* 298, 2038–2047. doi:10.1001/jama.298.17.2038

Deng, F., Zhang, J., Li, Y., Wang, W., Hong, D., Li, G., et al. (2019). Hirudin Ameliorates Immunoglobulin A Nephropathy by Inhibition of Fibrosis and Inflammatory Response. *Ren. Fail.* 41, 104–112. doi:10.1080/0886022X.2019.1583113

Drawz, P., and Rahman, M. (2015). Chronic Kidney Disease. *Ann. Intern. Med.* 162, Itc1–16. doi:10.7326/AITC201506020

Eldor, A., Orevi, M., and Rigbi, M. (1996). The Role of the Leech in Medical Therapeutics. *Blood Rev.* 10, 201–209. doi:10.1016/s0268-960x(96)90000-4

Guo, Y. N., Wang, J. C., Cai, G. Y., Hu, X., Cui, S. Y., Lv, Y., et al. (2014). AMPK-mediated Downregulation of Connexin43 and Premature Senescence of Mesangial Cells under High-Glucose Conditions. *Exp. Gerontol.* 51, 71–81. doi:10.1016/j.exger.2013.12.016

Ha, T. S., Park, H. Y., Nam, J. A., and Han, G. D. (2014). Diabetic Conditions Modulate the Adenosine Monophosphate-Activated Protein Kinase of Podocytes. *Kidney Res. Clin. Pract.* 33, 26–32. doi:10.1016/j.krcp.2014.02.001

Han, J., Pang, X., Zhang, Y., Peng, Z., Shi, X., and Xing, Y. (2020). Hirudin Protects against Kidney Damage in Streptozotocin-Induced Diabetic Nephropathy Rats by Inhibiting Inflammation via P38 MAPK/NF-κB Pathway. *Drug Des. Devel Ther.* 14, 3223–3234. doi:10.2147/DDDT.S257613

Huang, Y. M., Xu, D., Long, J., Shi, Y., Zhang, L., Wang, H., et al. (2019). Spectrum of Chronic Kidney Disease in China: A National Study Based on Hospitalized Patients from 2010 to 2015. *Nephrology (Carlton)* 24, 725–736. doi:10.1111/nep.13489

Ishibashi, Y., Matsui, T., Takeuchi, M., and Yamagishi, S. (2012). Metformin Inhibits Advanced Glycation End Products (AGEs)-Induced Renal Tubular Cell Injury by Suppressing Reactive Oxygen Species Generation via Reducing Receptor for AGEs (RAGE) Expression. *Horm. Metab. Res.* 44, 891–895. doi:10.1055/s-0032-1321878

Islam, M. A., Kim, S., Firdous, J., Lee, A. Y., Hong, S. H., Seo, M. K., et al. (2016). A High Affinity Kidney Targeting by Chitobionic Acid-Conjugated Polysorbitol Gene Transporter Alleviates Unilateral Ureteral Obstruction in Rats. *Biomaterials* 102, 43–57. doi:10.1016/j.biomaterials.2016.06.013

Jha, V., Garcia-Garcia, G., Iseki, K., Li, Z., Naicker, S., Plattner, B., et al. (2013). Chronic Kidney Disease: Global Dimension and Perspectives. *Lancet* 382 (9888), 260–272. doi:10.1016/S0140-6736(13)60687-X

Jung, C. H., Ro, S. H., Cao, J., Otto, N. M., and Kim, D. H. (2010). mTOR Regulation of Autophagy. *FEBS Lett.* 584, 1287–1295. doi:10.1016/j.febslet.2010.01.017

Kanbay, M., Turgut, F., Covic, A., and Goldsmith, D. (2009). Statin Treatment for Dyslipidemia in Chronic Kidney Disease and Renal Transplantation: a Review of the Evidence. *J. Nephrol.* 22, 598–609.

Kaushal, G. P., Chandrashekar, K., Juncos, L. A., and Shah, S. V. (2020). Autophagy Function and Regulation in Kidney Disease. *Biomolecules* 10, 100. doi:10.3390/biom10010100

KDOQI (2012). KDOQI Clinical Practice Guideline for Diabetes and CKD: 2012 Update. *Am. J. Kidney Dis.* 60, 850–886. doi:10.1053/j.ajkd.2012.07.005

Kidokoro, K., Satoh, M., Channon, K. M., Yada, T., Sasaki, T., and Kashihara, N. (2013). Maintenance of Endothelial Guanosine Triphosphate Cyclohydrolase I Ameliorates Diabetic Nephropathy. *J. Am. Soc. Nephrol.* 24, 1139–1150. doi:10.1681/ASN.2012080783

Kimura, T., Isaka, Y., and Yoshimori, T. (2017). Autophagy and Kidney Inflammation. *Autophagy* 13, 997–1003. doi:10.1080/15548627.2017.1309485

Kume, S., Thomas, M. C., and Koya, D. (2012). Nutrient Sensing, Autophagy, and Diabetic Nephropathy. *Diabetes* 61, 23–29. doi:10.2337/db11-0555

Leventhal, J. S., He, J. C., and Ross, M. J. (2014). Autophagy and Immune Response in Kidneys. *Semin. Nephrol.* 34, 53–61. doi:10.1016/j.semnephrol.2013.11.008

Li, X., Zhu, Z., Gao, S., Zhang, L., Cheng, X., Li, S., et al. (2019). Inhibition of Fibrin Formation Reduces Neuroinflammation and Improves Long-Term Outcome

after Intracerebral Hemorrhage. *Int. Immunopharmacol* 72, 473–478. doi:10.1016/j.intimp.2019.04.029

Lin, T. A., Wu, V. C., and Wang, C. Y. (2019). Autophagy in Chronic Kidney Diseases. *Cells* 8, 61. doi:10.3390/cells8010061

Liu, N., Xu, L., Shi, Y., and Zhuang, S. (2017). Podocyte Autophagy: A Potential Therapeutic Target to Prevent the Progression of Diabetic Nephropathy. *J. Diabetes Res.* 2017, 3560238. doi:10.1155/2017/3560238

Liu, Y., Feng, Q., Miao, J., Wu, Q., Zhou, S., Shen, W., et al. (2020). C-X-C Motif Chemokine Receptor 4 Aggravates Renal Fibrosis through Activating JAK/STAT/GSK3β/β-catenin Pathway. *J. Cel Mol Med* 24, 3837–3855. doi:10.1111/jcmm.14973

Lu, Q., Wang, W. W., Zhang, M. Z., Ma, Z. X., Qiu, X. R., Shen, M., et al. (2019). ROS Induces Epithelial-Mesenchymal Transition via the TGF-β1/PI3K/Akt/mTOR Pathway in Diabetic Nephropathy. *Exp. Ther. Med.* 17, 835–846. doi:10.3892/etm.2018.7014

Luyckx, V. A., Cherney, D. Z. I., and Bello, A. K. (2020). Preventing CKD in Developed Countries. *Kidney Int. Rep.* 5, 263–277. doi:10.1016/j.ekir.2019.12.003

Manns, B., Tonelli, M., Culleton, B., Faris, P., McLaughlin, K., Chin, R., et al. (2012). A Cluster Randomized Trial of an Enhanced eGFR Prompt in Chronic Kidney Disease. *Clin. J. Am. Soc. Nephrol.* 7, 565–572. doi:10.2215/CJN.12391211

Markwardt, F. (1991). Past, Present and Future of Hirudin. *Haemostasis* 21 (Suppl. 1), 11–26. doi:10.1159/000216258

Markwardt, F. (1994). The Development of Hirudin as an Antithrombotic Drug. *Thromb. Res.* 74, 1–23. doi:10.1016/0049-3848(94)90032-9

Martínez-Klimova, E., Aparicio-Trejo, O. E., Tapia, E., and Pedraza-Chaverri, J. (2019). Unilateral Ureteral Obstruction as a Model to Investigate Fibrosis-Attenuating Treatments. *Biomolecules* 9, 4–141. doi:10.3390/biom9040141

Nishida, M., Okumura, Y., Ozawa, S., Shiraishi, I., Itoi, T., and Hamaoka, K. (2007). MMP-2 Inhibition Reduces Renal Macrophage Infiltration with Increased Fibrosis in UUO. *Biochem. Biophys. Res. Commun.* 354, 133–139. doi:10.1016/j.bbrc.2006.12.165

Obata, J., Nakamura, T., Kuroyanagi, R., Yoshida, Y., Guo, D. F., and Inagami, T. (1997). Candesartan Prevents the Progression of Glomerulosclerosis in Genetic Hypertensive Rats. *Kidney Int. Suppl.* 63, S229–S231.

Pace, J., Paladugu, P., Das, B., He, J. C., and Mallipattu, S. K. (2019). Targeting STAT3 Signaling in Kidney Disease. *Am. J. Physiol. Ren. Physiol* 316, F1151–f1161. doi:10.1152/ajprenal.00034.2019

Rangarajan, S., Bone, N. B., Zmijewska, A. A., Jiang, S., Park, D. W., Bernard, K., et al. (2018). Metformin Reverses Established Lung Fibrosis in a Bleomycin Model. *Nat. Med.* 24, 1121–1127. doi:10.1038/s41591-018-0087-6

Reedquist, K. A., Ludikhuize, J., and Tak, P. P. (2006). Phosphoinositide 3-kinase Signalling and FoxO Transcription Factors in Rheumatoid Arthritis. *Biochem. Soc. Trans.* 34, 727–730. doi:10.1042/BST0340727

Robson, R., White, H., Aylward, P., and Frampton, C. (2002). Bivalirudin Pharmacokinetics and Pharmacodynamics: Effect of Renal Function, Dose, and Gender. *Clin. Pharmacol. Ther.* 71, 433–439. doi:10.1067/mcp.2002.124522

Shen, L., Lei, S., Huang, L., Li, S., Yi, S., Breitzig, M., et al. (2019). Therapeutic Effects of the rhSOD2-Hirudin Fusion Protein on Bleomycin-Induced Pulmonary Fibrosis in Mice. *Eur. J. Pharmacol.* 852, 77–89. doi:10.1016/j.ejphar.2019.03.001

Song, K., Wang, F., Li, Q., Shi, Y. B., Zheng, H. F., Peng, H., et al. (2014). Hydrogen Sulfide Inhibits the Renal Fibrosis of Obstructive Nephropathy. *Kidney Int.* 85, 1318–1329. doi:10.1038/ki.2013.449

Tang, C., Livingston, M. J., Liu, Z., and Dong, Z. (2020). Autophagy in Kidney Homeostasis and Disease. *Nat. Rev. Nephrol.* 16, 489–508. doi:10.1038/s41581-020-0309-2

Tang, P. M., Nikolic-Paterson, D. J., and Lan, H. Y. (2019). Macrophages: Versatile Players in Renal Inflammation and Fibrosis. *Nat. Rev. Nephrol.* 15, 144–158. doi:10.1038/s41581-019-0110-2

Wang, H., Fu, W., Jin, Z., Wang, Y., Yao, W., Yin, P., et al. (2013). Advanced IgA Nephropathy with Impaired Renal Function Benefits from Losartan Treatment in Rats. *Ren. Fail.* 35 (6), 812–818. doi:10.3109/0886022X.2013.794686

Wiezel, D., Assadi, M. H., Landau, D., Troib, A., Kachko, L., Rabkin, R., et al. (2014). Impaired Renal Growth Hormone JAK/STAT5 Signaling in Chronic Kidney Disease. *Nephrol. Dial. Transpl.* 29, 791–799. doi:10.1093/ndt/gfu003

Xie, R., Zhang, H., Wang, X. Z., Yang, X. Z., Wu, S. N., Wang, H. G., et al. (2017). The Protective Effect of Betulinic Acid (BA) Diabetic Nephropathy on Streptozotocin (STZ)-induced Diabetic Rats. *Food Funct.* 8, 299–306. doi:10.1039/c6fo01601d

Yang, C., Wang, H., Zhao, X., Matsushita, K., Coresh, J., Zhang, L., et al. (2020a). CKD in China: Evolving Spectrum and Public Health Implications. *Am. J. Kidney Dis.* 76, 258–264. doi:10.1053/j.ajkd.2019.05.032

Yang, K., Fan, B., Zhao, Q., Ji, Y., Liu, P., Gao, S., et al. (2020b). Hirudin Ameliorates Renal Interstitial Fibrosis via Regulating TGF-β1/Smad and NF-Kb Signaling in UUO Rat Model. *Evid. Based Complement. Alternat Med.* 2020, 7291075. doi:10.1155/2020/7291075

Yang, Z., and Klionsky, D. J. (2010). Mammalian Autophagy: Core Molecular Machinery and Signaling Regulation. *Curr. Opin. Cel Biol* 22, 124–131. doi:10.1016/j.ceb.2009.11.014

Yu, X., Long, Y. C., and Shen, H. M. (2015). Differential Regulatory Functions of Three Classes of Phosphatidylinositol and Phosphoinositide 3-kinases in Autophagy. *Autophagy* 11, 1711–1728. doi:10.1080/15548627.2015.1043076

Zhang, J., and Lan, N. (2018). Hirudin Variants Production by Genetic Engineered Microbial Factory. *Biotechnol. Genet. Eng. Rev.* 34, 261–280. doi:10.1080/02648725.2018.1506898

Zhang, L., Wang, F., Wang, L., Wang, W., Liu, B., Liu, J., et al. (2012). Prevalence of Chronic Kidney Disease in China: a Cross-Sectional Survey. *Lancet* 379, 815–822. doi:10.1016/S0140-6736(12)60033-6

Zhang, W., Zhang, R. X., Li, J., Liang, F., and Qian, Z. Z. (2013). [Species Study on Chinese Medicine Leech and Discussion on its Resource Sustainable Utilization]. *Zhongguo Zhong Yao Za Zhi* 38, 914–918.

Zhang, Y., He, D., Zhang, W., Xing, Y., Guo, Y., Wang, F., et al. (2020). ACE Inhibitor Benefit to Kidney and Cardiovascular Outcomes for Patients with Non-dialysis Chronic Kidney Disease Stages 3-5: A Network Meta-Analysis of Randomised Clinical Trials. *Drugs* 80, 797–811. doi:10.1007/s40265-020-01290-3

Zhao, X., Zhang, E., Ren, X., Bai, X., Wang, D., Bai, L., et al. (2020). Edaravone Alleviates Cell Apoptosis and Mitochondrial Injury in Ischemia-Reperfusion-Induced Kidney Injury via the JAK/STAT Pathway. *Biol. Res.* 53, 28. doi:10.1186/s40659-020-00297-0

Conflict of Interest: The authors declare that the research was conducted in the absence of any commercial or financial relationships that could be construed as a potential conflict of interest.

Publisher's Note: All claims expressed in this article are solely those of the authors and do not necessarily represent those of their affiliated organizations, or those of the publisher, the editors and the reviewers. Any product that may be evaluated in this article, or claim that may be made by its manufacturer, is not guaranteed or endorsed by the publisher.

frontiers in Pharmacology

ORIGINAL RESEARCH
published: 06 October 2021
doi: 10.3389/fphar.2021.706617

Astragalus Polysaccharide Reduces Blood Pressure, Renal Damage, and Dysfunction Through the TGF-β1-ILK Pathway

Wei Zheng[1†], *Tao Huang*[1†], *Qi-Zhen Tang*[1†], *Shi Li*[2], *Jie Qin*[1*] and *Feng Chen*[1*]

[1]Department of Urology, First Affiliated Hospital of Dalian Medical University, Dalian, China, [2]Department of Urology, Dalian Central Hospital, Dalian, China

OPEN ACCESS

Edited by:
Dan-Qian Chen,
Northwest University, China

Reviewed by:
Anping Xu,
Sun Yat-sen Memorial Hospital, China
Mingjun Zhu,
First Affiliated Hospital of Henan University of Traditional Chinese Medicine, China
Nirupama Ramkumar,
The University of Utah, United States

***Correspondence:**
Jie Qin
qinjieac@163.com
Feng Chen
dmuchenfeng@163.com

[†]These authors have contributed equally to this work

Specialty section:
This article was submitted to Renal Pharmacology, a section of the journal Frontiers in Pharmacology

Received: 07 May 2021
Accepted: 19 August 2021
Published: 06 October 2021

Citation:
Zheng W, Huang T, Tang Q-Z Li S, Qin J and Chen F (2021) Astragalus *Polysaccharide Reduces Blood Pressure, Renal Damage, and Dysfunction Through the TGF-*β*1-ILK Pathway.* Front. Pharmacol. 12:706617. doi: 10.3389/fphar.2021.706617

Background: *Astragalus* polysaccharide extract (APS) has been shown to exhibit antioxidant and anti-inflammatory potential in the treatment of several diseases. However, whether APS could protect against renal damage in hypertensive mice is unknown.

Methods: Hematoxylin and eosin staining, immunohistochemistry, real-time polymerase chain reaction, and Western blotting were used to investigate the effect of APS on the renal damage in deoxycorticosterone acetate- (DOCA) salt- and angiotensin II- (Ang II-) induced hypertensive mice and to elucidate the underlying mechanisms.

Results: Our data demonstrated that APS significantly reduced blood pressure in DOCA-salt- and Ang II-treated mice. Furthermore, APS reduced the inflammatory response and renal fibrosis, thereby improving renal function. Furthermore, the levels of serum creatinine, urea nitrogen, and uric acid increased in DOCA-salt-treated mice, alleviated by APS administration. At the molecular level, DOCA-salt and Ang II increased the mRNA levels of IL-1β, IL-6, α-SMA, collagen I, and collagen III, while APS significantly inhibited these effects. APS inhibited the TGF-β1/ILK signaling pathway, which was activated in hypertensive mice due to the administration of DOCA-salt.

Conclusion: Our results suggest that APS plays a beneficial role in improving renal dysfunction in hypertensive mice.

Keywords: *Astragalus* polysaccharides, hypertension, transforming growth factor-β, integrin linked kinase, renal damage

INTRODUCTION

Hypertension is a major risk factor for cardiovascular diseases (Doyle 1991; Elliott 2007) and is considered a chronic and low-grade inflammatory disease causing inflammatory reaction in the kidneys (Mennuni et al., 2014). In the human body, the kidney is a physiologically, structurally, and metabolically (Krishnan et al., 2016) complicated organ. Inflammation is a key pathology in hypertensive and inflammation-injured kidneys. In turn, injury to the tubules induces inflammatory responses and results in renal fibrosis (Ying and Wu., 2017).

The transforming growth factor-β (TGF-β) family consists of different growth factors and has many functions involved in development and fibrosis (Nüchel et al., 2018). For example, TGF-β

could promote the growth and production of fibroblasts and could also inhibit the proliferation of epithelial, endothelial, and immune cells (Massagué., 2012). TGF-β1 is the best-characterized isoform of the TGF-β superfamily and is a potent fibrogenic cytokine. Furthermore, TGF-β1 promotes the formation of myofibroblasts, which induce organ fibrosis (Border and Noble, 1994; Frangogiannis, 2020). These are the most important effector cells that produce and stiffen excessive amounts of extracellular matrix, resulting in fibrotic changes in tissues (Tomasek et al., 2002). Recent studies have shown that it is a key intercellular mediator that controls TGF-β1-induced epithelial–mesenchymal transition in renal tubular epithelial cells (Higgins et al., 2018). Integrin-linked kinase (ILK) is an important protein located in focal adhesions. ILK transduces integrin signaling to the interior of the cell and mediates diverse cellular processes by interacting with the cytoplasmic domain of β-integrins. ILK has many functions that regulate cell survival, proliferation, adhesion, differentiation, and migration (Alasseiri et al., 2018; Huang et al., 2019). Several studies have found that ILK is induced simultaneously by TGF-β1 in a Smad-dependent manner (Janji et al., 1999; Zhang and Huag., 2018).

Astragalus polysaccharides are the main bioactive components extracted from *Astragalus membranaceus*. *Astragalus* polysaccharide extract (APS) is famous for its various pharmacological activities (Yang et al., 2019; Sun et al., 2021). APS is a critical active ingredient responsible for various bioactivities of *Astragalus membranaceus*. APS is well known to have various properties, including antioxidant, immunomodulatory, anti-inflammatory, antidiabetic, antiatherosclerosis, hematopoiesis, hepatoprotective, and neuroprotective properties (Huang et al., 2017; Tian et al., 2017). A recent study found that APS could inhibit the activity of TGF-β1 and reduce the formation of extracellular matrix in diabetic rats (Meng et al., 2020). In our study, we used APS as a protective agent to investigate its healing effect in hypertensive kidneys.

MATERIALS AND METHODS

Chemicals and Antibodies

APS (batch number: HQ090312, purity >98% by HPLC) was purchased from Sciphar (Xi'an, Shanxi Province, China). Primary antibodies, such as anti-TGF-β1 (3711s), anti-Smad2/3 (8685s), anti-phospho-Smad2/3 (8828s), anti-phospho-P65 (3033s), anti-P65 (4764s), and anti-GAPDH (5174s), were purchased from Cell Signaling Technology. Anti-ILK (ab236455) was purchased from Abcam. Secondary antibodies, namely, goat anti-rabbit IgG polyclonal antibody and anti-mouse IgG, were purchased from Proteintech, China.

Animals and Treatment

In our study, we used 8-week-old male C57BL/6J mice (average weight, 23–25 g) for all wild-type (WT) experiments. All animals were maintained under a 12 h light-dark cycle with free access to food and water. All *in vivo* experiments were performed according to the Protection of Animals Act and the National Institutes of Health Guide (NIH Publication No. 85-23) for the Care and Use of Laboratory Animals (Krishnan et al., 2016). The study was approved by the Institutional Animal Care and Use Committee of the University of Dalian Medical University (SCXK 2015-2003). For the *in vivo* study, we examined the protective effect of APS in two different hypertensive models, in which the mice were randomly divided into four groups: control, APS, hypertensive, and hypertensive + APS groups. We used APS as a protective agent, which was intravenously injected into mice 2 days before surgery (angiotensin II (Ang II) infusion model or one kidney/deoxycorticosterone acetate/salt model), and 200 mg/kg of APS was administered every 2 days after the surgery (Yang et al., 2019).

One Kidney/Deoxycorticosterone Acetate/Salt Model of Hypertension

The first hypertensive model in our study was a kidney/deoxycorticosterone acetate/salt model. In this study, all surgeries were performed under anesthesia induced by the inhalation of 2% isoflurane. Under anesthesia, we removed the left kidney of the WT mice and implanted a deoxycorticosterone acetate pellet (DOCA, 2.4 mg/day; Innovative Research of America, Sarasota, FL, United States) and replaced their drinking water with 0.9% saline (1K/DOCA/salt) to induce a hypertensive model (Wang et al., 2016). Mice in the control group in this model were also uninephrectomized but received a placebo pellet (Innovative Research of America) and normal drinking water (1 K/placebo).

Angiotensin II-Infusion Model of Hypertension

Another hypertensive model in our study was the angiotensin II infusion model. WT mice were infused with saline or angiotensin II (Ang II) at a dose of 0.7 mg/kg/day (Model 1004, Alzet, Cupertino, CA, United States) for 28 days. The control group mice received the vehicle for Ang II (i.e., 0.9% saline) with osmotic minipumps as previously described (Krishnan et al., 2016).

Blood Pressure Measurements

Blood pressure (BP) was measured using the tail-cuff method (SoftronBP-98A; Softron, Tokyo, Japan). Before treatment, we first recorded the BP of each mouse before the surgery as their basic BP value and regarded them as −1 and 0 days. After surgery, we measured the BP on days 3, 6, 9, 12, 15, 18, and 21 for the DOCA model, whereas for the Ang II-infused model, BP was measured on days 3, 7, 10, 14, 21, and 28 (Krishnan et al., 2019).

Renal Function, Histopathology, and Immunohistochemical Staining

After the study period, mice were fasted for 12 h. We collected serum from each group of mice and processed it for the analysis of serum creatinine, urea nitrogen, and uric acid concentrations

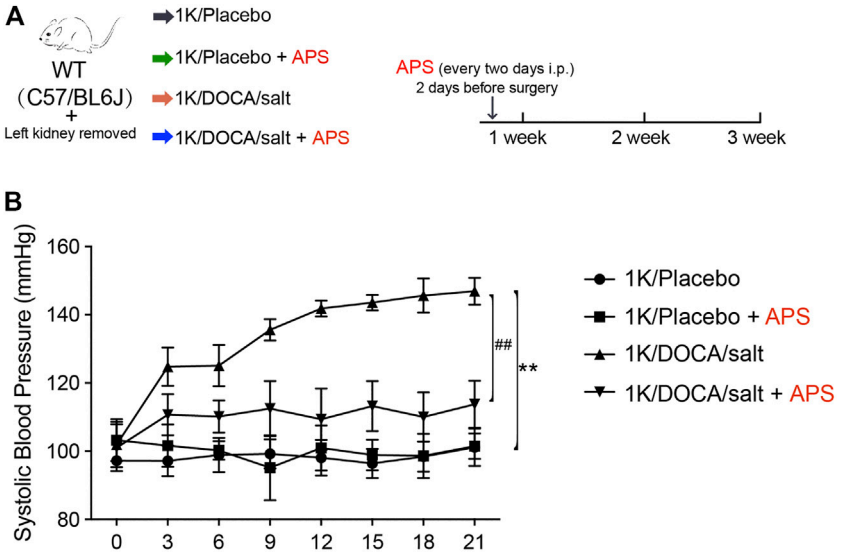

FIGURE 1 | Treatment with APS prevents DOCA-induced hypertension. **(A)** Diagrammatic representation of treatment of different groups of mice: 1K/placebo, 1K/placebo + APS, 1K/DOCA/salt, and 1K/DOCA/salt + APS. **(B)** Average systolic blood pressure of each group before and after DOCA treatment obtained by telemetry (n = 6 per group). $^{**}P < 0.01$ versus control mice. $^{\#\#}P < 0.01$ versus DOCA + APS mice.

using an enzyme-linked immunosorbent assay (ELISA) according to the manufacturer's instructions (R&D System, Minneapolis, MN). Approximately 60 μl of serum was used for each measurement.

After the study period, all the mice were sacrificed under anesthesia. We fixed the kidney tissues with 4% paraformaldehyde (PFA) for more than 24 h, followed by embedding in paraffin. All sections (4 μm) were subjected to hematoxylin and eosin (H&E), periodic acid-Schiff (PAS), and Masson's trichromatic staining. Immunochemistry was performed with the primary antibody anti-α-smooth muscle actin (α-SMA), which was purchased from Sigma-Aldrich. The degree of injury was graded semiquantitatively and blindly by two independent researchers from 10 randomly chosen fields of each kidney section, according to the extent of injury involved in each field as follows: 0, normal; 1, <10%; 2, 11–25%; 3, 26–75%; and 4, >75% of the observed tubules (Huang, et al., 2019).

Cells and Treatment

Human renal proximal tubular cells (HK-2 cells) and bone marrow-derived macrophages (iBMDMs) were obtained from Dalian Medical University. HK-2 cells and iBMDMs were cultivated in DMEM (Gibco) basic medium supplemented with 5% fetal bovine serum and 100 U/ml penicillin–100 μg/ml streptomycin antibiotics at 37°C under a 5% CO_2-humidified environment. For the *in vitro* study, HK-2 cells were pretreated with APS (100 μg/ml) or an inhibitor of TGF-β (disitertide, P144, 100 μg/ml) for 3 h and then treated with saline or Ang II (100 nM) for 24 h (Sun et al., 2021; Jun et al., 2019).

Real-Time PCR Analysis

According to the manufacturer's instructions, we used TRIzol regent (Invitrogen, New York) to purify the total RNA from the fresh kidneys and cells. The first-strand cDNA (1–2 μg) was synthesized with Superscript II (TAKARA, Japan). All the primer sequences were synthesized by Sangon Biotech Company (Shanghai, China). The primer sequences were listed as follows: IL-1β: forward 5′-TGC CAC CTT TTG ACA GTG ATG-3′ and reverse 5′-TTC TTG TGA CCC TGA GCG AC-3′; IL-6: forward 5′-TTC CAT CCA GTT GCC TTC TTG-3′ and reverse 5′-TTG GGA GTG GTA TCC TCT TGT GA-3′; collagen I: forward 5′-TGA CTG GAA GAG CGG AGA GTA C-3′ and reverse 5′-TTC GGG CTG ATG TAC CAG TTC-3′; collagen III: forward 5′-AAA TTC TGC CAC CCC GAA CT-3′ and reverse 5′-CCA GTG CTT ACG TGG GAC AGT-3′; and GAPDH: forward 5′-GGT TGT CTC CTG CGA CTT CA-3′ and reverse 5′-GGT GGT CCA GGG TTT CTT ACT C-3′. We used GAPDH as the internal control and normalized the resulting transcript levels to those of GAPDH gene. The results were analyzed using the ΔΔCt technique.

Immunoblot Analysis

Total proteins were purified from snap frozen kidney tissue and cells using RIPA buffer (PSMF: RIPA = 1:100; Solar-Bioscience Technology, Beijing, CA). The protein lysates were separated by electrophoresis on 10% SDS–PAGE gels and transferred onto polyvinylidene difluoride membranes. The blots were incubated with primary antibodies at 4°C overnight. On the following day, the blots were treated with goat anti-rabbit or anti-mouse secondary antibodies. We used ImageJ software for the densitometric analysis, and GAPDH was used as an internal control.

Cell Migration Assays

For the cell migration assay, HK-2 cells were pretreated with saline or Ang II (100 nM) for 24 h and then blocked with PBS, P144, or APS

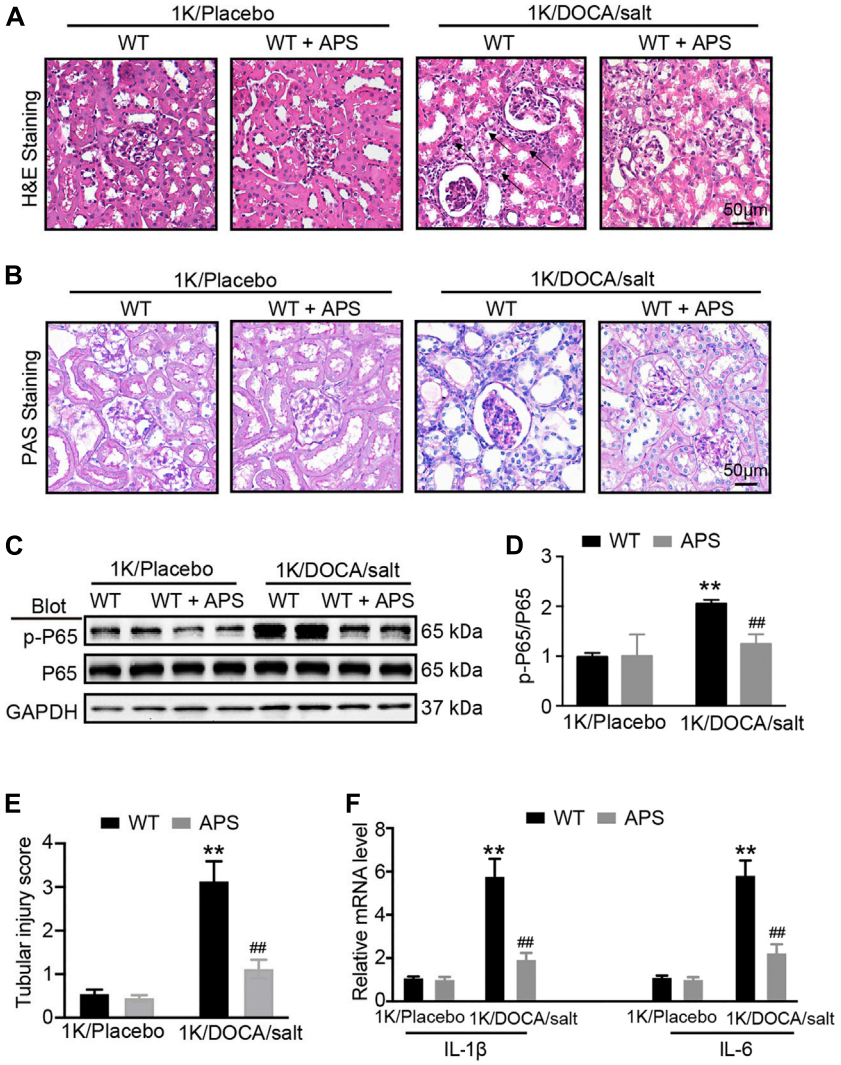

FIGURE 2 | APS reduces inflammation reaction in DOCA-treated mice. **(A)** H&E staining of each group were analyzed (scale bar 50 μm, n = 6 per group). **(B)** PAS staining of each group were analyzed (scale bar 50 μm, n = 6 per group). **(C)** Immunoblotting analysis of phospho-p65 and p65 protein in each group (n = 4 per group). **(D)** Quantification of protein bands (n = 4). **(E)** Tubular injury score was computed from the percentage of damaged tubulars. Based on the different degree of tubular injury, the score was divided into 0, normal; 1, <10%; 2, 11–25%; 3, 26–75%; 4, >75% of the observed tubules. **(F)** qPCR analysis of IL-1β and IL-6 mRNA expression levels in the kidney (n = 6). $^{**}P < 0.01$ versus control mice. $^{\#\#}P < 0.01$ versus DOCA + APS mice.

(100 μg/ml) for an additional 3 h. The isolated iBMDMs (5×10^4) were added to the upper chambers of the transwell inserts in a 24-well cell culture plate (8 μm pore, Corning, New York, United States). Conditioned medium obtained from Ang II-pretreated HK-2 cells was added to the lower wells. After 24 h of exposure, cells that had migrated to the lower surface were fixed with 4% formalin, stained with 4',6-diamidino-2-phenylindole (DAPI), and counted in six randomly chosen fields using an inverted microscope (Olympus, IX73, Japan) (Liao, et al., 2012).

Statistics

All data in our study are expressed as mean ± SD and tested with SPSS19.0. Systolic BP pressure data were analyzed using two-way repeated measures ANOVA followed by the Bonferroni post hoc two-tailed analysis. Other data were analyzed using either Student's unpaired t-test or one-way ANOVA followed by the Bonferroni post hoc two-tailed analysis. Statistical significance was set at $p < 0.05$. Data were graphed using GraphPad Prism 9.0.

RESULTS

Treatment with APS Alleviates the Increase in Systolic BP in 1K/DOCA/Salt-Induced Mice

We established a 1K/DOCA mouse model to investigate the protective effects of APS (**Figure 1A**). In this study, we found

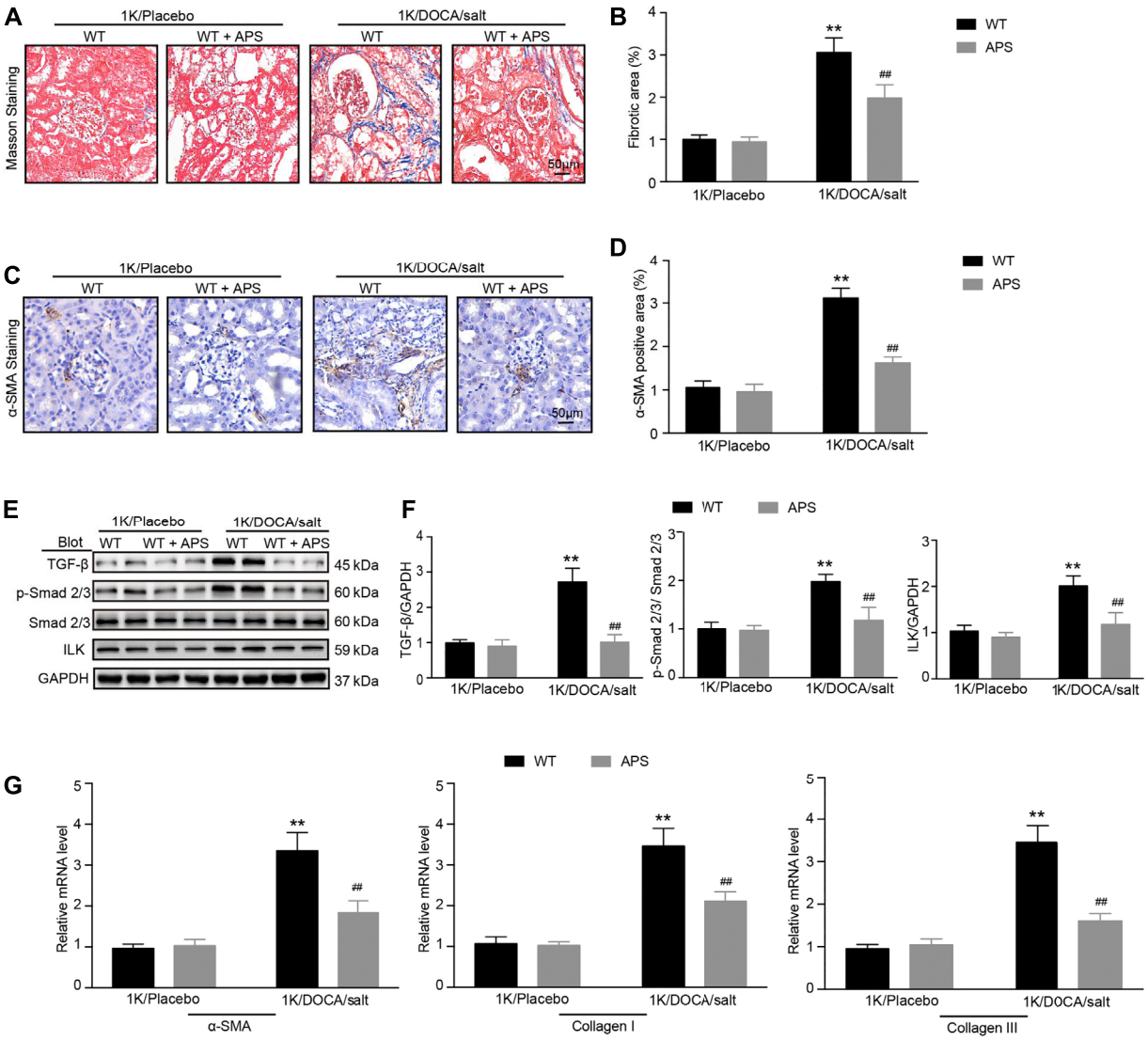

FIGURE 3 | APS prevents collagen deposition in DOCA-treated mice. **(A)** Masson staining of each group was analyzed (scale bar 50 μm). **(B)** Percentage of the fibrotic area was analyzed (n = 6 per group). **(C)** Immunochemistry staining of the kidney sections with α-SMA (scale bar 50 μm). **(D)** Quantification of α-SMA-positive area (n = 6). **(E)** Immunoblotting analysis of TGF-β1, phospho-Smad2/3, Smad2/3, and ILK protein in each group (n = 4 per group). **(F)** Quantification of protein bands (n = 4). **(G)** qPCR analysis of α-SMA, collagen I, and collagen III mRNA expression levels in the kidney (n = 6). $^{**}P < 0.01$ versus control mice. $^{\#\#}P < 0.01$ versus DOCA + APS mice.

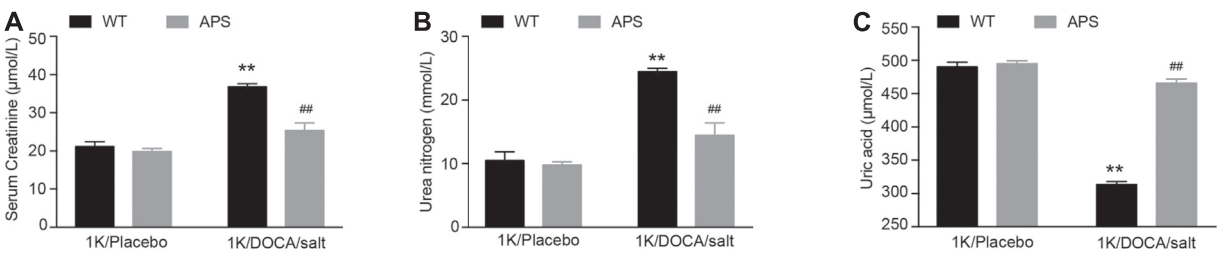

FIGURE 4 | APS improves the kidney function in DOCA-treated mice. **(A)** The level of serum creatinine in each group (n = 6 per group). **(B)** The level of urea nitrogen in each group (n = 6 per group). **(C)** The level of uric acid in each group (n = 6 per group). $^{**}P < 0.01$ versus control mice. $^{\#\#}P < 0.01$ versus DOCA + APS mice.

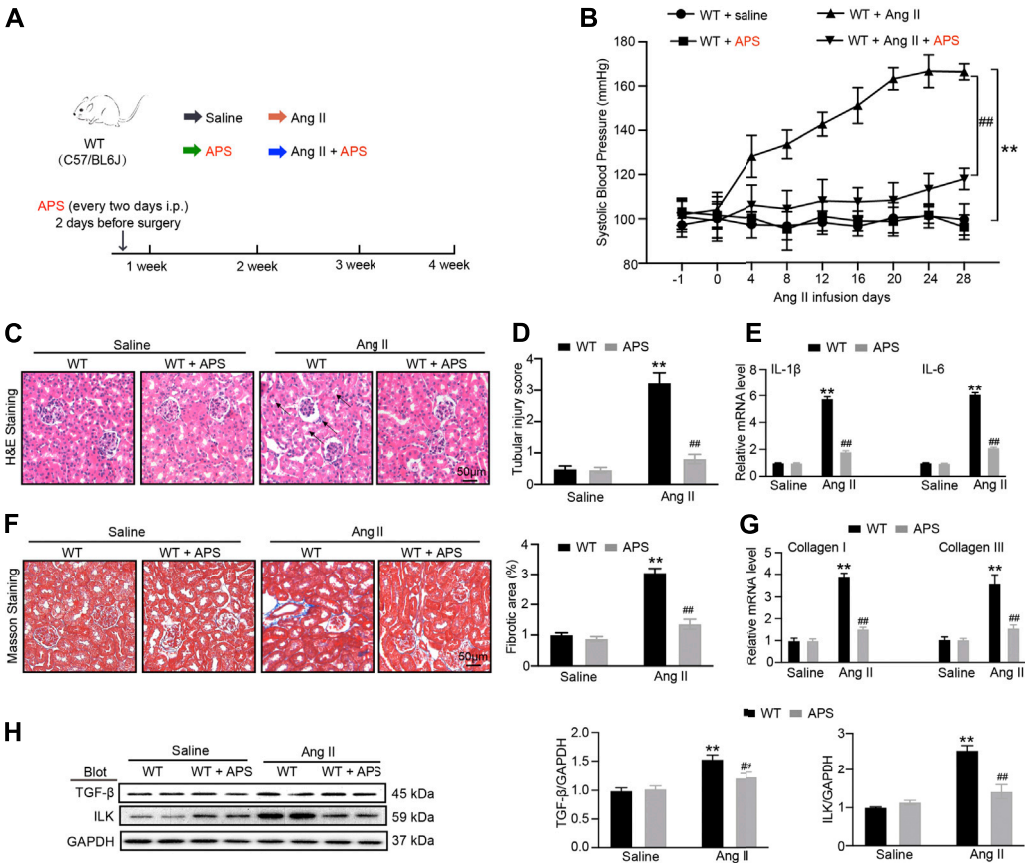

FIGURE 5 | Treatment with APS prevents Ang II-induced hypertension. **(A)** Diagrammatic representation of treatment of different groups of mice: saline, APS, Ang II, and Ang II + APS. **(B)** Average systolic blood pressure of each group before and after Ang II treatment obtained by telemetry ($n = 6$ per group). **(C)** H&E staining of each group were analyzed (scale bar 50 μm, $n = 6$ per group). **(D)** Tubular injury score was computed from the percentage of damaged tubulars. Based on the different degrees of tubular injury, the score was divided into 0, normal; 1, <10%; 2, 11–25%; 3, 26–75%; 4, >75% of the observed tubules. **(E)** qPCR analysis of IL-1β and IL-6 mRNA expression levels in the kidney ($n = 6$). **(F)** Masson staining of each group was analyzed (right, scale bar 50 μm). Percentage of the fibrotic area was analyzed (left, $n = 6$ per group). **(G)** qPCR analysis of collagen I and collagen III mRNA expression levels in the kidney ($n = 6$). **(H)** Immunoblotting analysis of TGF-β1 and ILK protein in each group ($n = 4$ per group). $^{**}P < 0.01$ versus control mice. $^{\#\#}P < 0.01$ versus Ang II + APS mice.

that after treatment with 1K/DOCA/salt, the systolic BP of WT mice was increased by 40–50 mmHg. However, after treatment with APS, the increase in BP was reduced (**Figure 1B**).

APS Reduces the Inflammation Reaction in the Kidneys of 1K/DOCA/Salt-Treated Mice

We used H&E staining and PAS staining to examine the renal damage in the 1K/DOCA/salt group and the effect of APS. The staining results revealed increased tubular dilation and tubular cell atrophy in 1K/DOCA/salt kidneys; however, following APS treatment, the tubular injury score decreased (**Figures 2A,B,E**).

In addition, we evaluated the expression of phosphorylated p65 and inflammation-related genes in the kidneys of 1K/DOCA/salt-induced hypertensive mice. We found that the phosphorylation of p65 and the expression of inflammation-related genes, including those encoding IL-1β and IL-6, were increased compared with the observations in the saline group (**Figures 2C,D**); however, after treatment with APS, both decreased (**Figure 2F**). The results confirmed that APS regulated the inflammatory response in 1K/DOCA/salt mice, leading to the attenuation of the renal injury in the mice.

APS Reduces the Expression of the Fibrosis Makers in the Kidneys of 1K/DOCA/Salt-Treated Mice

Kidney sections from 1K/DOCA/salt-treated mice displayed distinct collagen deposition in the renal interstitium compared with the control mice (**Figures 3A,B**), and collagen deposition was reduced in the 1K/DOCA/salt-treated mice (**Figures 3A,B**). The number of α-SMA-positive myofibroblasts was lower in the APS-treated mice than in the 1K/DOCA/salt-treated mice (**Figures 3C,D**). In addition, when compared with the control group, treatment with DOCA induced the activation of TGF-β and Smad2/3 signaling in 1K/DOCA/salt-treated mice, which was also blocked in APS-treated mice (**Figures 3E,F**). Furthermore, ILK expression was detected. Following

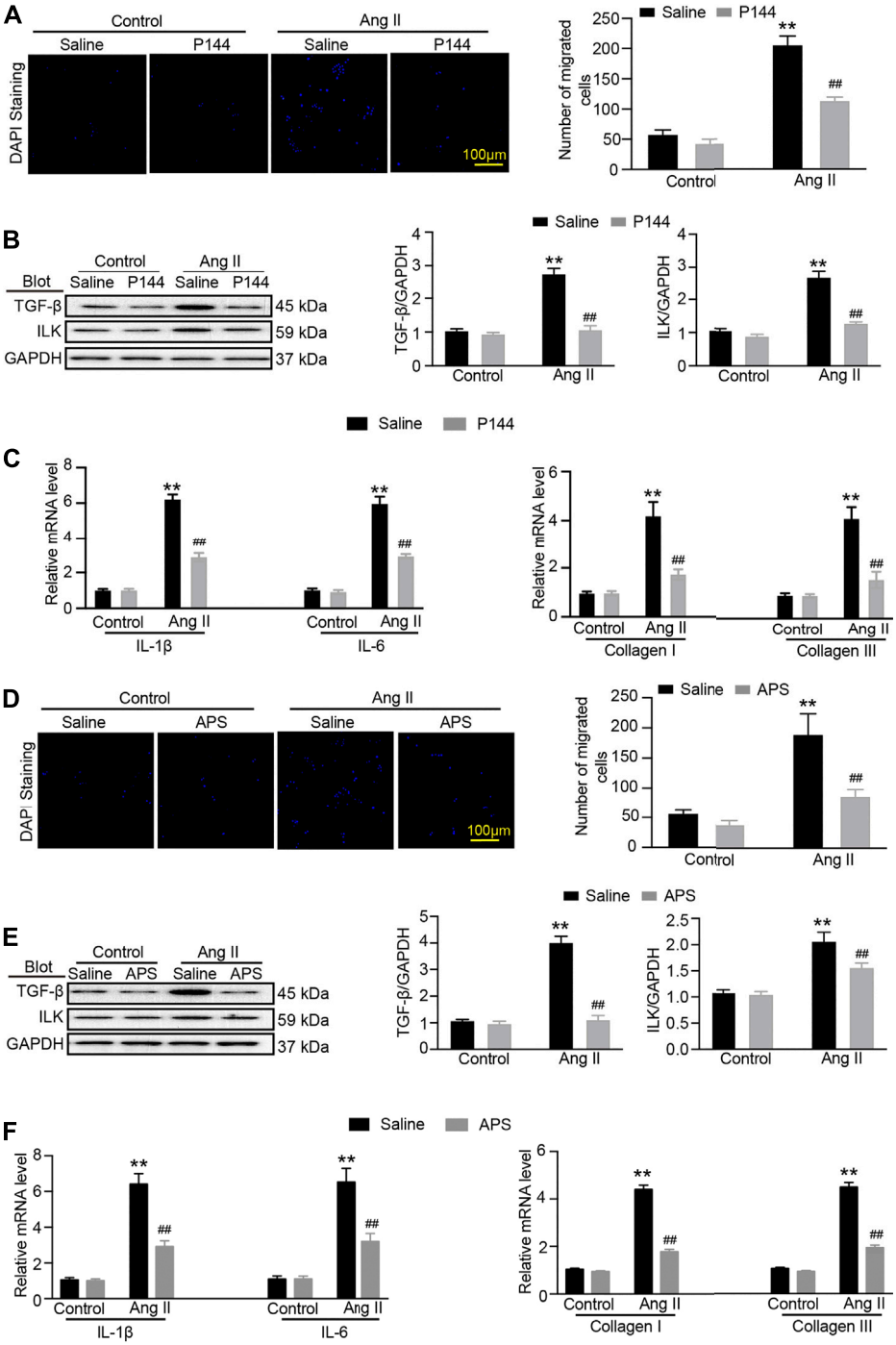

FIGURE 6 | APS decreases the expression of ILK through regulating the TGF-β pathway in Ang-II-treated HK-2 cells. **(A)** Migration ability of iBMDM was assessed using a transwell assay. iBMDM was added to the upper chambers, and conditioned media obtained from Ang II and P144-pretreated HK-2 cells were added to the lower wells. The migrated iBMDM was stained with DAPI to visualize nuclei (left), and the migrated cells were quantified (right, scale bar 100 μm). **(B)** Immunoblotting analysis of TGF-β1 and ILK protein in each group ($n = 3$ per group). **(C)** qPCR analysis of IL-1β, IL-6, collagen I, and collagen III mRNA expression levels in the kidney ($n = 6$). **(D)** Migration ability of iBMDM to Ang II and APS-pretreated HK-2 cells was added as described above. The migrated iBMDM was stained with DAPI to visualize nuclei (left), and the migrated cells were quantified (right, scale bar 100 μm). **(E)** Immunoblotting analysis of TGF-β1 and ILK protein in each group ($n = 3$ per group). **(F)** qPCR analysis of IL-1β, IL-6, collagen I, and collagen III mRNA expression levels in the kidney ($n = 6$). $^{**}P < 0.01$ versus control group. $^{\#\#}P < 0.01$ versus Ang II + P144 group or Ang II + APS group.

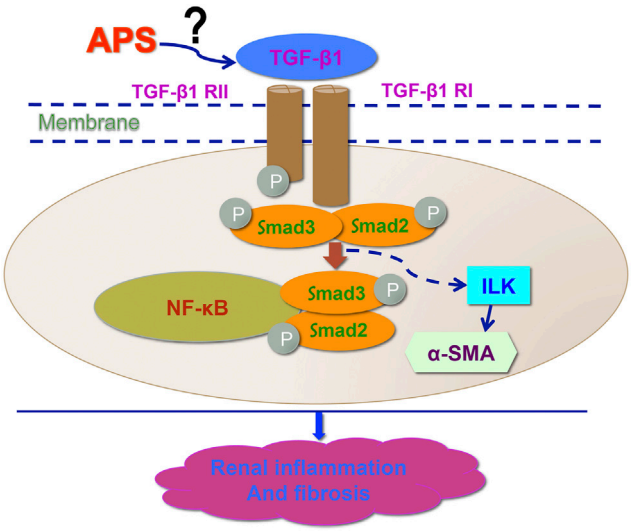

FIGURE 7 | Working model for APS in the regulation of DOCA-induced hypertensive kidney modeling. After treatment with APS reduces the expression of ILK and downregulates the TGF-β/Smad signaling pathway to improve the kidney function and reduce the injury in hypertensive kidney.

treatment with APS, ILK expression was lower than that observed in 1K/DOCA/salt-treated mice (**Figures 3E,F**). Along with the increase in fibrosis signaling, the gene expression of α-SMA, collagen I, and collagen III also increased following IK/DOCA/salt treatment (**Figure 3G**). Treatment with APS reduced the mRNA expression of collagen I and collagen III (**Figure 3G**).

APS Improves Kidney Function in 1K/DOCA/Salt-Treated Mice

Inflammation and fibrosis of the kidneys are associated with impaired function and a shift in the pressure-natriuresis relationship (Wang et al., 2020). We examined the levels of serum creatinine, urea nitrogen, and uric acid in 1K/DOCA/salt-treated mice (Huang et al., 2019). After treatment with 1K/DOCA/salt, the levels of serum creatinine and urea nitrogen increased compared with those in the control, but after treatment with APS, the levels of both decreased (**Figures 4A,B**). The level of uric acid increased after treatment with APS compared with that in 1K/DOCA/salt mice (**Figure 4C**). The results confirmed that APS could rescue kidney function injury in 1K/DOCA/salt mice.

APS Attenuates the Renal Injury in Ang II Infusion Mice

To further detect the effect of APS, we established a 1K/DOCA mouse model (**Figure 5A**). After Ang II infusion for 28 days, systolic BP was lower in the APS-treated mice than in WT mice (**Figure 5B**). We used H&E staining to examine the renal injury in Ang II-treated mice. We also used H&E and Masson staining to observe the renal injury of Ang II infusion mice treated with APS and evaluated the protective effect of APS. The staining results revealed increased tubular dilation, tubular cell atrophy, and collagen deposition in Ang II-infused mice (**Figures 5C,D,F**), but after treatment with APS, the tubular injury score and collagen deposition decreased in Ang II-infused mice (**Figures 5C,D,F**). In addition, we examined the gene expression of IL-1β, IL-6, collagen I, and collagen III and observed it to be increased after Ang II infusion. APS treatment alleviated the increase in the gene expression (**Figures 5E,G**). Furthermore, we detected the expression of TGF-β and ILK proteins, and the results showed that after treatment with APS, the expression of both proteins was decreased in Ang II-infused mice (**Figure 5H**).

APS Pretreatment Reduces the Damage in Ang II-Induced HK-2 Cells

To confirm that APS could alleviate renal damage through the TGF-β/ILK pathway in hypertensive mice, we used the inhibitor of TGF-β, P144. The migration assay results showed that after treatment with P144, the migration of iBMDMs decreased. In addition, the expression of TGF-β and ILK decreased after pretreatment with P144 in Ang II-treated HK-2 cells. We next detected the expression of inflammatory and fibrosis makers and found that the levels of IL-1β, IL-6, collagen I, and collagen III were reduced following pretreatment with P144 in Ang II-induced cells (**Figures 6A–C**). Similar results were observed in Ang II-induced cells that were pretreated with APS (**Figures 6D–F**).

DISCUSSION

Hypertension contributes to more than 10% of the deaths worldwide (Caillon et al., 2019). Renal damage is a frequent event in hypertension. A benign to malignant form of nephropathy depends on several factors, such as individual susceptibility, degree of hypertension, type of etiology, and underlying kidney disease (Wenzel et al., 2017). Prior analyses have revealed that several pathological changes are always observed in renal damage, including kidney enlargement and thickening, widening of the glomerular capillary basement membrane, glomerular sclerosis, tubular atrophy, and renal interstitial fibrosis (Eddy, 2004; Shankland, 2006; Romagnani and Remuzzi., 2013). However, the mechanism of renal damage remains unclear. To our knowledge, the present study demonstrates that APS could ameliorate the increase in BP and renal injury in both Ang II infusion and one kidney/deoxycorticosterone acetate/salt mouse models. Hypertension is a chronic inflammatory disease. It is well known that hypertension is associated with increased expression of inflammatory cytokines and the accumulation of macrophages in the kidneys (Gu et al., 2006). These inflammatory reactions contribute to renal fibrosis and injury. Moreover, renal fibrosis and injury disrupt pressure natriuresis and reset BP at a chronically elevated level (Blasi et al., 2003). APS could reduce the increase in BP and renal damage, and the treatment mechanism may be related to its anti-inflammatory and antifibrotic effects. We have a limitation in the present study.

The noninvasive tail cuff method provides a useful tool in detecting BP, but it is incapable in continually measuring the blood pressure and imposes substantial amounts of thermal and restraint stress to affect BP and heart rate. Thus, the effect of APS on hypertension needs to further confirm by radiotelemetry in the future.

TGF-β has tropic functions of promoting fibrosis in many systems and diseases. ILK is one of the downstream targets of TGF-β based on several studies that have found that the expression of ILK is regulated by TGF-β in different disease models (Jan et al., 1999). In our *in vivo* study, APS was used as a protective agent. We found that APS could reduce renal inflammation and fibrosis and improve renal function in both 1K/DOCA/salt-treated and Ang II-infused mice. Furthermore, we also found that APS could decrease the expression of TGF-β and ILK, which are involved in the growth and production of fibroblasts and cell migration (Border ad Noble, 1994; Alasseiri et al., 2018; Huang et al., 2019; Frangogiannis., 2020). To elucidate the mechanism underlying the protective effects of APS, we used an inhibitor of TGF-β (P144) in an *in vitro* study and found that following pretreatment with P144, the migration of iBMDMs and the expression of the ILK protein were both decreased. These results confirmed that ILK activity was regulated by TGF-β inhibition. In addition, we pretreated Ang II-treated HK-2 cells with APS and obtained similar results. These results illustrate that APS can inhibit the activity of ILK by inhibiting the expression of TGF-β. Furthermore, the levels of inflammation and fibrosis gene markers also showed that pretreatment with APS could alleviate the renal injury in an *in vitro* hypertensive model by regulating the TGF-β/ILK pathway. This study highlights APS as a new medicine for therapies aimed at reducing BP and end organ damage associated with hypertension (**Figure 7**).

APS is regarded as the most active component of *Astragalus* roots. Previous studies have demonstrated that APS has diverse potential effects, including anti-inflammatory, antioxidative, and antitumor effects (Auyeung et al., 2016; Liu et al., 2017). TGF-β is one of the most important regulatory molecules in the development of renal fibrosis, and TGF-β also plays an important role in the synthesis of the extracellular matrix in the kidney (Annes et al., 2004; Buscemi et al., 2011). Hypertension can upregulate the expression of TGF-β and collagen synthesis in the kidney. The increase in collagen synthesis leads to a decrease in the degradation of the extracellular matrix, with a subsequent promotion of thickening of the glomerular and tubular basement membrane, extracellular matrix deposition, and renal interstitial fibrosis (Lu and Crowley, 2018). In our study, we found that APS could reduce the expression of TGF-β, which is involved in fibrosis in 1K/DOCA/salt-treated mice. This result suggests that APS could attenuate the presence of TGF-β to regulate the development of fibrosis in hypertension. In addition, we detected TGF-β signaling as a downstream mechanism of ILK expression and the phosphorylation of p65. The results showed that APS could also reduce the expression of ILK, the phosphorylation of the p65 protein, and the deposition of collagen in 1K/DOCA/salt-treated mice. These observations suggest that APS exhibits an anti-inflammatory potential, with the ability to inhibit the adhesion and migration of some inflammatory cells.

In China, traditional Chinese medicine has been used for many years for the treatment of hypertension. Several clinical cases have shown remarkable results, and traditional Chinese medicine has become more popular worldwide (Cao, et al., 2019). In our study, we examined the effect of APS on both 1K/DOCA/salt-treated and Ang II-infused mouse models of hypertension. The results of our analyses could form the basis for the development of novel strategies for the amelioration of renal dysfunction and BP in hypertension.

CONCLUSION

APS is effective in reducing renal inflammation and fibrosis and in improving renal function by regulating the TGF-β/ILK pathway.

DATA AVAILABILITY STATEMENT

The raw data supporting the conclusions of this article will be made available by the authors, without undue reservation.

ETHICS STATEMENT

The animal study was reviewed and approved by The National Institutes of Health Guide for the Care and Use of Laboratory Animals.

AUTHOR CONTRIBUTIONS

WZ, TH and QZT contributed equally to this work. FC and JQ designed the experiment. WZ, TH and QZT performed in vitro and vivo experiments and analyzed the results. All authors contributed to the article and approved the submitted version.

FUNDING

This work was supported by grants from the Education Office of Liaoning Province (WZ, Grant Number LZ2020062).

REFERENCES

Alasseiri, M., Ahmed, A. U., and Williams, B. R. G. (2018). Mechanisms and Consequences of Constitutive Activation of Integrin-Linked Kinase in Acute Myeloid Leukemia. *Cytokine Growth Factor. Rev.* 43, 1–7. doi:10.1016/j.cytogfr.2018.06.001

Annes, J. P., Chen, Y., Munger, J. S., and Rifkin, D. B. (2004). Integrin alphaVbeta6-Mediated Activation of Latent TGF-Beta Requires the Latent TGF-Beta Binding Protein-1. *J. Cel Biol* 165 (5), 723–734. doi:10.1083/jcb.200312172

Auyeung, K. K., Han, Q. B., and Ko, J. K. (2016). Astragalus Membranaceus: A Review of its Protection against Inflammation and Gastrointestinal Cancers. *Am. J. Chin. Med.* 44 (1), 1–22. doi:10.1142/S0192415X16500014

Blasi, E. R., Rocha, R., Rudolph, A. E., Blomme, E. A., Polly, M. L., and McMahon, E. G. (2003). Aldosterone/salt Induces Renal Inflammation and Fibrosis in Hypertensive Rats. *Kidney Int.* 63 (5), 1791–1800. doi:10.1046/j.1523-1755.2003.0092910.1046/j.1523-1755.2003.00929.x

Border, W. A., and Noble, N. A. (1994). Transforming Growth Factor Beta in Tissue Fibrosis. *N. Engl. J. Med.* 331 (19), 1286–1292. doi:10.1056/NEJM199411103311907

Buscemi, L., Ramonet, D., Klingberg, F., Formey, A., Smith-Clerc, J., Meister, J. J., et al. (2011). The Single-Molecule Mechanics of the Latent TGF-B1 Complex. *Curr. Biol.* 21 (24), 2046–2054. doi:10.1016/j.cub.2011.11.037

Caillon, A., Paradis, P., and Schiffrin, E. L. (2019). Role of Immune Cells in Hypertension. *Br. J. Pharmacol.* 176 (12), 1818–1828. doi:10.1111/bph.14427

Cao, X., Wei, R., Zhou, J., Zhang, X., Gong, W., Jin, T., et al. (2019). Wenshen Jianpi Recipe, a Blended Traditional Chinese Medicine, Ameliorates Proteinuria and Renal Injury in a Rat Model of Diabetic Nephropathy. *BMC Complement. Altern. Med.* 19 (1), 193. doi:10.1186/s12906-019-2598-1

Doyle, A. E. (1991). Hypertension and Vascular Disease. *Am. J. Hypertens.* 4 (2 Pt 2), 103S–106S. doi:10.1093/ajh/4.2.103s

Eddy, A. A. (2004). Proteinuria and Interstitial Injury. *Nephrol. Dial. Transpl.* 19 (2), 277–281. doi:10.1093/ndt/gfg533

Elliott, W. J. (2007). Systemic Hypertension. *Curr. Probl. Cardiol.* 32 (4), 201–259. doi:10.1016/j.cpcardiol.2007.01.002

Frangogiannis, N. (2020). Transforming Growth Factor-β in Tissue Fibrosis. *J. Exp. Med.* 217 (3), e20190103. doi:10.1084/jem.20190103

Gu, J. W., Tian, N., Shparago, M., Tan, W., Bailey, A. P., and Manning, R. D., Jr (2006). Renal NF-kappaB Activation and TNF-Alpha Upregulation Correlate with Salt-Sensitive Hypertension in Dahl Salt-Sensitive Rats. *Am. J. Physiol. Regul. Integr. Comp. Physiol.* 291 (6), R1817–R1824. doi:10.1152/ajpregu.00153.2006

Higgins, S. P., Tang, Y., Higgins, C. E., Mian, B., Zhang, W., Czekay, R. P., et al. (2018). TGF-β1/p53 Signaling in Renal Fibrogenesis. *Cell Signal* 43, 1–10. doi:10.1016/j.cellsig.2017.11.005

Huang, M., Zhu, S., Huang, H., He, J., Tsuji, K., Jin, W. W., et al. (2019). Integrin-Linked Kinase Deficiency in Collecting Duct Principal Cell Promotes Necroptosis of Principal Cell and Contributes to Kidney Inflammation and Fibrosis. *J. Am. Soc. Nephrol.* 30 (11), 2073–2090. doi:10.1681/ASN.2018111162

Huang, Y. C., Tsay, H. J., Lu, M. K., Lin, C. H., Yeh, C. W., Liu, H. K., et al. (2017). Astragalus Membranaceus-Polysaccharides Ameliorates Obesity, Hepatic Steatosis, Neuroinflammation and Cognition Impairment without Affecting Amyloid Deposition in Metabolically Stressed APPswe/PS1dE9 Mice. *Int. J. Mol. Sci.* 18 (12), 2746. doi:10.3390/ijms18122746

Janji, B., Melchior, C., Gouon, V., Vallar, L., and Kieffer, N. (1999). Autocrine TGF-Beta-Regulated Expression of Adhesion Receptors and Integrin-Linked Kinase in HT-144 Melanoma Cells Correlates with Their Metastatic Phenotype. *Int. J. Cancer* 83 (2), 255–262. doi:10.1002/(sici)1097-0215(19991008)83:2<255::aid-ijc18>3.0.co;2-x

Krishnan, S. M., Dowling, J. K., Ling, Y. H., Diep, H., Chan, C. T., Ferens, D., et al. (2016). Inflammasome Activity Is Essential for One Kidney/deoxycorticosterone Acetate/salt-Induced Hypertension in Mice. *Br. J. Pharmacol.* 173 (4), 752–765. doi:10.1111/bph.13230

Krishnan, S. M., Ling, Y. H., Huuskes, B. M., Ferens, D. M., Saini, N., Chan, C. T., et al. (2019). Pharmacological Inhibition of the NLRP3 Inflammasome Reduces Blood Pressure, Renal Damage, and Dysfunction in Salt-Sensitive Hypertension. *Cardiovasc. Res.* 115 (4), 776–787. doi:10.1093/cvr/cvy252

Liao, Y. H., Xia, N., Zhou, S. F., Tang, T. T., Yan, X. X., Lv, B. J., et al. (2012). Interleukin-17A Contributes to Myocardial Ischemia/reperfusion Injury by Regulating Cardiomyocyte Apoptosis and Neutrophil Infiltration. *J. Am. Coll. Cardiol.* 59 (4), 420–429. doi:10.1016/j.jacc.2011.10.863

Liu, L., Chen, S., Xu, X., Hou, B., and Mo, F. (2017). *Astragalus* Polysaccharides Combined with Ibuprofen Exhibit a Therapeutic Effect on Septic Rats via an Anti-inflammatory Cholinergic Pathway. *Exp. Ther. Med.* 14 (4), 3127–3130. doi:10.3892/etm.2017.4865

Lu, X., and Crowley, S. D. (2018). Inflammation in Salt-Sensitive Hypertension and Renal Damage. *Curr. Hypertens. Rep.* 20 (12), 103. doi:10.1007/s11906-018-0903-x

Massagué, J. (2012). TGFβ Signalling in Context. *Nat. Rev. Mol. Cel Biol* 13 (10), 616–630. doi:10.1038/nrm3434

Meng, X., Wei, M., Wang, D., Qu, X., Zhang, K., Zhang, N., et al. (2020). Astragalus Polysaccharides Protect Renal Function and Affect the TGF-β/Smad Signaling Pathway in Streptozotocin-Induced Diabetic Rats. *J. Int. Med. Res.* 48 (5), 300060520903612. doi:10.1177/0300060520903612

Mennuni, S., Rubattu, S., Pierelli, G., Tocci, G., Fofi, C., and Volpe, M. (2014). Hypertension and Kidneys: Unraveling Complex Molecular Mechanisms Underlying Hypertensive Renal Damage. *J. Hum. Hypertens.* 28 (2), 74–79. doi:10.1038/jhh.2013.55

Nüchel, J., Ghatak, S., Zuk, A. V., Illerhaus, A., Mörgelin, M., Schönborn, K., et al. (2018). TGFB1 Is Secreted through an Unconventional Pathway Dependent on the Autophagic Machinery and Cytoskeletal Regulators. *Autophagy* 14 (3), 465–486. doi:10.1080/15548627.2017.1422850

Romagnani, P., and Remuzzi, G. (2013). Renal Progenitors in Non-diabetic and Diabetic Nephropathies. *Trends Endocrinol. Metab.* 24 (1), 13–20. doi:10.1016/j.tem.2012.09.002

Shankland, S. J. (2006). The Podocyte's Response to Injury: Role in Proteinuria and Glomerulosclerosis. *Kidney Int.* 69 (12), 2131–2147. doi:10.1038/sj.ki.5000410

Sun, J., Wei, S., Zhang, Y., and Li, J. (2021). Protective Effects of Astragalus Polysaccharide on Sepsis-Induced Acute Kidney Injury. *Anal. Cel Pathol (Amst)* 2021, 7178253. doi:10.1155/2021/7178253

Tian, Z., Liu, Y., Yang, B., Zhang, J., He, H., Ge, H., et al. (2017). Astagalus Polysaccharide Attenuates Murine Colitis through Inhibiton of the NLRP3 Inflammasome. *Planta Med.* 83 (1-02), 70–77. doi:10.1055/s-0042-108589

Tomasek, J. J., Gabbiani, G., Hinz, B., Chaponnier, C., and Brown, R. A. (2002). Myofibroblasts and Mechano-Regulation of Connective Tissue Remodelling. *Nat. Rev. Mol. Cel Biol* 3 (5), 349–363. doi:10.1038/nrm809

Wang, J., Tian, J., Sun, J., Gao, M., and Dong, Y. (2020). Two Identified Subsets of CD8 T Cells in Obstructed Kidneys Play Different Roles in Inflammation and Fibrosis. *Aging (Albany NY)* 12 (17), 17528–17540. doi:10.18632/aging.103764

Wang, L., Zhao, X. C., Cui, W., Ma, Y. Q., Ren, H. L., Zhou, X., et al. (2016). Genetic and Pharmacologic Inhibition of the Chemokine Receptor CXCR2 Prevents Experimental Hypertension and Vascular Dysfunction. *Circulation* 134 (18), 1353–1368. doi:10.1161/CIRCULATIONAHA.115.020754

Wenzel, U. O., Bode, M., Köhl, J., and Ehmke, H. (2017). A Pathogenic Role of Complement in Arterial Hypertension and Hypertensive End Organ Damage. *Am. J. Physiol. Heart Circ. Physiol.* 312 (3), H349–H354. doi:10.1152/ajpheart.00759.2016

Yang, J., Zhuang, Y., and Liu, J. (2019). Upregulation of microRNA-590 in R-heumatoid A-rthritis P-romotes A-poptosis of B-one C-ells through T-ransforming G-rowth F-actor-β1/phosphoinositide 3-kinase/Akt S-ignaling. *Int. J. Mol. Med.* 43 (5), 2212–2220. doi:10.3892/ijmm.2019.4116

Ying, Q., and Wu, G. (2017). Molecular Mechanisms Involved in Podocyte EMT and Concomitant Diabetic Kidney Diseases: an Update. *Ren. Fail.* 39 (1), 474–483. doi:10.1080/0886022X.2017.1313164

Zhang, Y., and Huang, W. (2018). Transforming Growth Factor β1 (TGF-B1)-Stimulated Integrin-Linked Kinase (ILK) Regulates Migration and Epithelial-Mesenchymal Transition (EMT) of Human Lens Epithelial Cells via Nuclear Factor κB (NF-Kb). *Med. Sci. Monit.* 24, 7424–7430. doi:10.12659/MSM.910601

Conflict of Interest: The authors declare that the research was conducted in the absence of any commercial or financial relationships that could be construed as a potential conflict of interest.

Publisher's Note: All claims expressed in this article are solely those of the authors and do not necessarily represent those of their affiliated organizations or those of the publisher, the editors, and the reviewers. Any product that may be evaluated in this article, or claim that may be made by its manufacturer, is not guaranteed or endorsed by the publisher.

frontiers in Pharmacology

ORIGINAL RESEARCH
published: 12 October 2021
doi: 10.3389/fphar.2021.762756

Tongluo Yishen Decoction Ameliorates Renal Fibrosis *via* Regulating Mitochondrial Dysfunction Induced by Oxidative Stress in Unilateral Ureteral Obstruction Rats

Qi Jia[1†], Lin Han[2†], Xiaoyu Zhang[1], Wenning Yang[3], Yushan Gao[2], Yifan Shen[4], Bing Li[5], Shuyan Wang[2], Mingzhen Qin[6], Scott Lowe[7], Jianguo Qin[1] and Gaimei Hao[8]**

[1]Department of Nephropathy, Dongfang Hospital, Beijing University of Chinese Medicine, Beijing, China, [2]School of Basic Medicine, Beijing University of Chinese Medicine, Beijing, China, [3]School of Chinese Materia Medica, Beijing University of Chinese Medicine, Beijing, China, [4]Emergency Department, Shanghai Municipal Hospital of Traditional Chinese Medicine, Shanghai University of Traditional Chinese Medicine, Shang Hai, China, [5]Beijing First Hospital of Integrated Chinese and Western Medicine, Beijing, China, [6]Dongzhimen Hospital, Beijing University of Chinese Medicine, Beijing, China, [7]Kansas City University of Medicine and Biosciences, College of Osteopathic Medicine, Kansas City, MO, United States, [8]Institute of Basic Theory for Chinese Medicine, China Academy of Chinese Medical Sciences, Beijing, China

OPEN ACCESS

Edited by:
Zhiyong Guo, Second Military Medical University, China

Reviewed by:
Ryan Williams, City College of New York (CUNY), United States
Ana Karina Aranda, National Autonomous University of Mexico, Mexico

***Correspondence:**
Gaimei Hao
haogaimei@163.com
Jianguo Qin
qindoctor@163.com

[†]These authors have contributed equally to this work and share first authorship

Specialty section:
This article was submitted to Renal Pharmacology, a section of the journal Frontiers in Pharmacology

Received: *22 August 2021*
Accepted: *27 September 2021*
Published: *12 October 2021*

Citation:
Jia Q, Han L, Zhang X, Yang W, Gao Y, Shen Y, Li B, Wang S, Qin M, Lowe S, Qin J and Hao G (2021) Tongluo Yishen Decoction Ameliorates Renal Fibrosis via Regulating Mitochondrial Dysfunction Induced by Oxidative Stress in Unilateral Ureteral Obstruction Rats. Front. Pharmacol. 12:762756. doi: 10.3389/fphar.2021.762756

Tongluo Yishen (TLYS) decoction is an herb that is extensively applied for the treatment of chronic kidney disease (CKD) in traditional Chinese medicine. In this study, 37 different dominant chemical constituents of TLYS were identified. Rats with unilateral ureteral obstruction (UUO) were used as animal models, and TLYS decoction was administered orally for 14 days. TLYS decoction reduced the levels of renal function indicators, serum creatinine levels and blood urea nitrogen levels and alleviated renal pathological changes. Gene Ontology (GO) and KEGG pathway analyses of RNA sequencing data showed that TLYS decoction had significant effects on biological processes, cellular components and molecular functions in UUO rats and that the phagosome (a membrane source in the early stages of autophagy), lysosome (an important component of autolysosome), and oxidation pathways (which contribute to mitochondrial function) might be related to the antifibrotic effects of TLYS decoction. Moreover, we found significant mitochondrial function impairment, including a decreased mitochondrial membrane potential (MMP) and an imbalance in mitochondrial dynamics, excessive oxidative stress, and activation of Pink1/Parkin-mediated mitophagy in UUO rats. Treatment with TLYS decoction significantly increased the MMP, normalized mitochondrial dynamics and ameliorated renal injury. Moreover, TLYS alleviated the mitophagy clearance deficiency. In conclusion, our study showed that TLYS decoction can ameliorate mitochondrial dynamics by reducing oxidative stress and regulating mitophagy, thereby relieving renal injury, protecting renal function, and reducing renal fibrosis. This study provides support for the application of and further research on TLYS decoction.

Keywords: tongluo yishen decoction, obstruction-induced renal fibrosis, mitochondria, oxidative stress, mitophagy, Chinese medicine

INTRODUCTION

Chronic kidney disease (CKD) is a leading global public health issue associated with substantial comorbidities and reduced life expectancy (Mills et al., 2015). Currently, this disease affects approximately 10% of the world's adult population, but effective treatments for its prevention and progression are lacking (Levin et al., 2017). Most patients with renal failure who progress to end-stage renal disease (ESRD) in low- and middle-income countries have little access to dialysis and kidney transplantation (Jha et al., 2013; Liyanage et al., 2015). The pathologic changes of renal fibrosis include renal interstitial fibrosis (RIF) and glomerular sclerosis, which involve epithelial injury, the inflammatory response and multiple signal transduction pathways. Studies have shown that compared with glomerulosclerosis, RIF is considered to be a crucial determinant leading to ESRD (Zeisberg and Neilson 2010). The current treatments for RIF include immunosuppressants, angiotensin-converting enzyme inhibitors, angiotensin II receptor antagonists, vitamin D and erythropoietin. Nevertheless, these treatments are still limited, and alternative therapeutic strategies are urgently needed.

Extensive studies have shown that oxidative stress is an important pathogenic mechanism of RIF, and the main cause of oxidative stress is the production of excessive reactive oxygen species (ROS) by the mitochondria (Sharma 2014; Nakanishi et al., 2019; Kitada et al., 2020). As the most important energy storage and supply sites, mitochondria are indispensable organelles in cells, but defective and aging mitochondria produce toxic ROS (Tang et al., 2021). Furthermore, ROS accumulation induces changes in mitochondrial membrane permeability and leads to the loss of mitochondrial membrane potential (MMP). Thus, clearance of damaged mitochondria is critical for cell survival to reduce the concentration of ROS. Mitophagy, a highly selective type of autophagy that eliminates damaged and aging mitochondria, is considered an important way to maintain mitochondrial quality and the stability of the intracellular environment (Li et al., 2020). In recent years, mitophagy via the PTEN-induced putative kinase 1 (Pink1)/Parkin pathways has been emphasized (Zhuet al., 2013). In normal mitochondria, Pink1 is continuously transferred to the mitochondrial intima, where it is cleaved by proteasomal degradation. However, the pathway by which Pink1 enters the mitochondrial inner membrane is blocked after loss of MMP, and Pink1 aggregates in the outer membrane of mitochondria, where it recruits and phosphorylates Parkin. Then, mitochondria are targeted for selective removal (Koyano et al., 2014; Li et al., 2020). Therefore, the clearance of damaged mitochondria by mitophagy has therapeutic potential for the treatment of RIF.

As a supplementary treatment, Chinese herbal medicine based on traditional Chinese medicine (TCM) has been widely used clinically in China for up to 2000 years. According to TCM theories, blood stasis is considered to be a key pathological factor in the pathogenesis of RIF (Guo, Li, and Rao 2019). Tongluo Yishen (TLYS) decoction has been clinically used for CKD treatment for decades and can reduce blood stasis and promote blood circulation, according to the theory of TCM. TLYS is composed of *Salvia miltiorrhiza bunge* (Danshen), *Carthamus tinctorius L.* (Honghua), *Achyranthes bidentata Bl.* (Niuxi), and *Spatholobus suberectus Dunn* (Jixueteng). These herbs or extracts are considered potential candidates for treating kidney diseases. Their bioactive properties include antioxidation (Cai et al., 2018; Do et al., 2018; Wang et al., 2020), inhibition of mitophagy (Liu et al., 2020), inhibition of epithelial to mesenchymal transition (EMT) (Li et al., 2017) and antifibrotic effects (Wang et al., 2010). However, the mechanisms of TLYS in the treatment of RIF need further study.

Hence, in this study, we focused on the effects of TLYS on renal function and mitochondrial quality. We found that TLYS ameliorated mitochondrial dysfunction, reduced oxidative stress and regulated Pink1/Parkin-mediated mitophagy in rats with unilateral ureteral obstruction (UUO). Our findings provide better insight into the molecular mechanism of TLYS as a treatment for RIF.

MATERIALS AND METHODS

Preparation of Tongluoyishen Decoction

A total of 60 g of raw herbal pieces, including *Salvia sinica* Migo (25 g), *Achyranthes bidentata* Blume (10 g), *Salvia coccinea* Linn (15 g) and *Caulis Spatholobi* (10 g), was used. The herbal ingredients are shown in **Table 1**. Each herb was purchased from Dongfang Hospital affiliated with Beijing University of Traditional Chinese Medicine. The above herbs were boiled in a 10-fold volume of water at 100°C for 1.0 h. After filtration, the first extraction was boiled in an 8-fold volume of water for 0.5 h. Finally, both filtrates were mixed and concentrated to a volume of 60 ml containing 1 g/ml raw herbs. Valsartan capsules (Beijing Novartis Pharmaceutical Co., Ltd., batch number X2,375) were provided by Novartis (Bale, Switzerland).

UHPLC-MS Analysis

TLYS decoction extract was combined with methanol and double distilled water (1:1, v/v) at 1:20, sonicated for 30 min and filtered through a 0.22 microns filtration membrane. Quality control of TLYS was performed using a UHPLC System (Dionex Ultimate 3,000, Thermo Corporation, United States) coupled with a mass spectrometer (LTQ-Oribitrap XL, Thermo Scientific). The chromatographic column was an Acquity UPLC C18 column (2.1 mm × 100 mm, 1.7 μm). The chromatographic conditions were as follows: 0.1% formic acid water (A) and methanol (B) were used as the mobile phase. The gradient elution conditions were as follows: 0–3 min, 5%–5% B; 3–45 min, 5%–75% B; 45–45.1 min, 75%–5% B; 45.1–50 min, 5% B. The column temperature was 30°C. The flow rate was 0.3 ml· min-1' and the injection volume was 2 μL. A mass spectrometer equipped with an electrospray ionization source was used for both positive and negative ion mode with the mass range of 120–1800 m/z. The ionization voltages were 3500 V (positive mode) and 3000 V (negative mode), the capillary temperature was 320°C, the sheath gas flow rate was 35 arb and the auxiliary gas flow rate was 10 arb. XCMS software was used to import mass spectra. Peak integration, peak extraction, peak alignment, peak identification and retention time correction were carried out.

TABLE 1 | The herbal composition and proportion of TLYS decoction.

Scientific name	Pinyin name	Plant part used	Batch number	Herb dose (g)	Composition (%)
Salvia miltiorrhiza bunge	Danshen	Root	20200509	25	41.67
Carthamus tinctorius L.	Honghua	Flower	20111610	10	16.67
Achyranthes bidentata Bl.	Niuxi	Root	xf8311	15	25
Spatholobus suberectus Dunn	Jixueteng	Stem	20042303	10	16.67

Material identification of peaks was conducted with information collected from the databases and literature.

Animal Model and Experimental Design

Male Sprague-Dawley (SD) rats (n = 15 per group, 180–200 g, 7–8 weeks of age) were provided by Beijing Vital River Laboratory Animal Technology Co., Ltd. (certificate number: SCXK (Beijing) 2016–0,006). The animal operation in this study was carried out according to the "Guiding Principles in the Use and Care of Animals" published by the US National Institutes of Health (NIH Publishing, No. 85–23, revised in 1996). This procedure was completed under the supervision of the Laboratory Animal Ethics Committee of Dongfang Hospital affiliated with Beijing University of Chinese Medicine (permit no. 202004). All animals were kept in a clean room at 22 ± 2°C and had free access to water and food.

As previously described, the UUO model was established in SD rats by ligation of the left ureter and sacrifice 14 days later (Masaki et al., 2003). In short, the rats were anesthetized by intraperitoneal injection of pentobarbital (50 mg/kg body weight); the left ureter was exposed via a midline incision and was ligated at two points with 4–0 silk sutures. The sham group underwent identical surgical procedures except for ligation of the ureter. The rats were randomly divided into four groups as follows: sham group, UUO group, TLYS group, and valsartan group. In the sham group and the UUO group, an equal volume of physiological saline was administered. The adult daily dosage for TLYS was 60 g. The daily dosage of TLYS in rats was calculated to be 7.8 g/kg by a correction factor equal to the human-rat body surface area ratio (6.3) (Xuan et al., 2021). The valsartan group was given 30 mg/kg/d of valsartan intragastrically.

Measurement of Serum Creatinine (Scr) and Blood Urea Nitrogen (BUN)

The Scr and BUN levels were measured with a creatinine assay kit (C011-1, Nanjing Jiancheng Bioengineering Institute, Nanjing, China) and BUN assay kit according to the manufacturer's instructions (C013-1, Nanjing Jiancheng Bioengineering Institute, Nanjing, China).

Histological Examination

Six kidneys from each group were immediately fixed with 10% formalin, dehydrated, embedded in paraffin, and sectioned to a thickness of 5 μm. These sections were then stained with hematoxylin and eosin (H&E) and Masson's trichrome. The kidney injury score was determined based on tubular atrophy and degeneration, renal papillary necrosis, interstitial inflammation, and fibrous hyperplasia as previously reported (Debelle et al., 2002).

Immunohistochemistry (IHC) Staining

Five-micron thick paraffin-embedded kidney sections were deparaffinized, followed by antigen retrieval in ethylenediaminetetraacetic acid (1 mM). The samples were blocked with 0.3% H_2O_2 in methanol and 5% BSA. Kidney sections were incubated with α-SMA (1:200, 14395-1-AP, Proteintech, United States) and TGF-β1 (1:200, ab92486, Abcam, United States) primary antibodies overnight at 4°C, followed by horseradish peroxidase (HRP)-conjugated secondary antibodies (PV9001, Beijing Zhongshan Jinqiao Biotechnology Co., Ltd., Beijing). The reaction was visualized with DAB staining using a Leica Aperio Versa 8 system (Leica, Wetzlar, Germany). The cumulative optical density of the area of interest analysis was calculated using ImageJ software.

RNA Sequencing (RNA-Seq) Analysis

Total RNA of rat kidney cortical tissue (three samples per group) was extracted using TRIzol (Invitrogen, Carlsbad, CA, United States). After total RNA extraction, eukaryotic mRNA was enriched with oligo (dT) beads, and rRNA-enriched prokaryotic mRNA was removed with a Ribo-Zerotm magnetic kit (Epicentre). Then, fragmentation buffer was used to fragment the enriched mRNA fragments into short fragments, which were reverse-transcribed into cDNA with random primers. The second strand of cDNA was synthesized by DNA polymerase I, RNase H, dNTP and buffer. The cDNA fragment was then purified with a QIAquick PCR extraction kit, the ends were repaired, poly (A) was added and the fragments were attached to the Illumina sequencing adapter. The ligation products were detected by agarose gel electrophoresis, PCR amplification and Illumina HiSeqTM 2,500 sequencing.

First, the raw data were filtered, and the clean data obtained after filtering were compared to the reference genome of the species. Second, the expression level of each gene was calculated according to the comparison results. On this basis, differential expression analysis, enrichment analysis and clustering analysis of the samples were further performed. Finally, we used DESeq for gene expression analysis and screening of differentially expressed genes as follows: multiple expression differences | log2FoldChange |>1, significance p-value<0.05. The Pearson correlation coefficient between all samples was calculated using the function cor, and hierarchical clustering was performed using

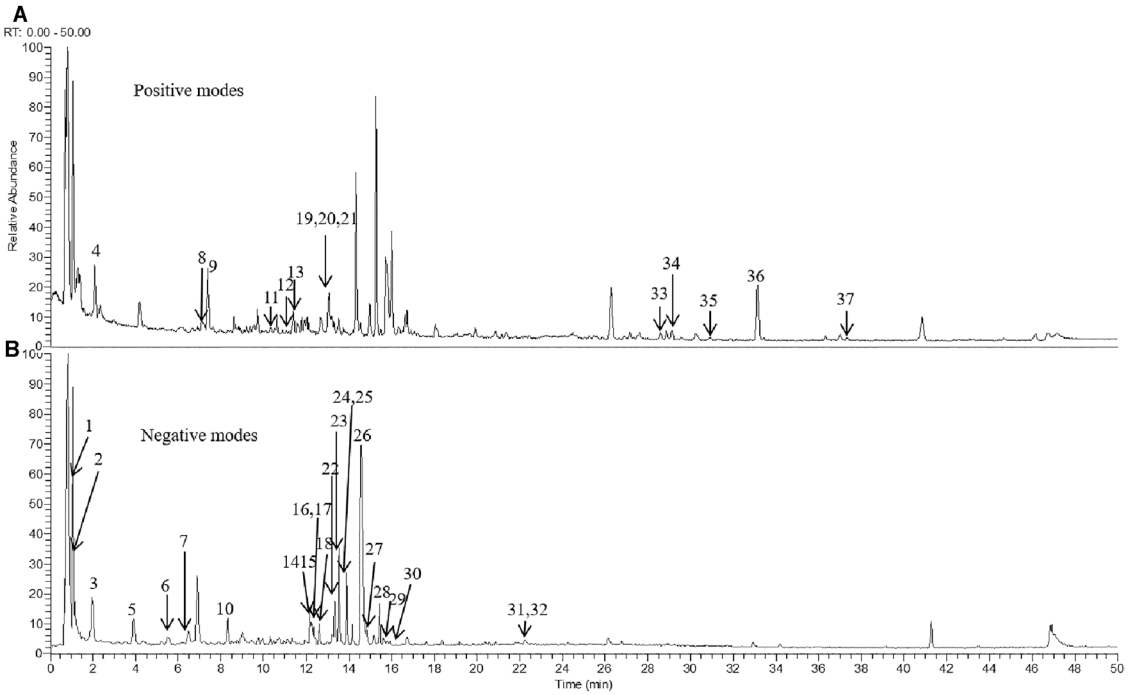

FIGURE 1 | TLYS samples were examined by UHPLC–MS. Total ion chromatography in positive **(A)** and negative **(B)** ion modes for TLYS samples are shown.

the hclust function in the stats package in R software. Then, GO function and KEGG pathway enrichment analyses were performed on the differentially expressed genes (DEGs).

Determination of the Mitochondrial Membrane Potential

Mitochondria were extracted from renal tissue using a mitochondrial extraction kit (C3606, Beyotime, China). Briefly, fresh kidneys were harvested, cut into small pieces, and washed thrice with precooled PBS. After digestion with trypsin, the renal tissues were homogenized in mitochondrial isolation reagent using a Dounce tissue grinder on ice. The homogenate was then centrifuged at 600 *g* for 10 min, and the supernatant was centrifuged at 1,500 *g* for 15 min to isolate the mitochondria. The change in MMP was measured by the JC-1 fluorescent probe, and the JC-1 red/green fluorescence intensity ratio was used to represent MMP. Fresh isolated mitochondria were incubated with 10 μg/ml JC-1 (at 37°C for 20 min), and the fluorescence intensity was measured by a Synergy H1 fluorometer microplate reader (BioTek, United States).

Renal Biochemical Marker Analysis

Renal tissues were homogenized followed by ultrasonic disruption to obtain renal tissue homogenates and then centrifuged at 3,000 rpm for 15 min at 4°C. Dihydroethidium (DHE) fluorescence was used to detect the level of ROS in rat renal tissues. Detection of the malondialdehyde (MDA) level as well as the superoxide dismutase (SOD) and glutathione peroxidase (GSH-Px) activities was performed according to the instructions provided by Shanghai Biyuntian Biotechnology Co., Ltd. (Shanghai, China).

Immunofluorescence Staining

Frozen sections were used to assess colocalization of Pink1 and TOM20. Kidney sections were blocked with 5% bovine serum albumin for 30 min at room temperature, followed by incubation overnight at 4°C with primary antibodies against Pink1 (1:200, SC517353, Santa Cruz, United States) and TOM20 (1:200, 11802-1-AP, Proteintech, United States). After the samples were washed with PBS, an Alexa Fluor 488-conjugated goat anti-mouse secondary antibody (1:300) and Alexa Fluor 594-conjugated goat anti-rabbit secondary antibody (1:300) were added for 1 h at room temperature. Finally, the slides were stained with DAPI solution for 10 min and captured by a laser scanning confocal fluorescence microscope (Olympus FV 1000, Japan). Ten nonoverlapping high-power fields (40X) were randomly captured in each specimen and analyzed by ImageJ software.

Western Blot Analysis

For western blot assays, renal tissues were lysed and homogenized in RIPA buffer supplemented with protease inhibitor cocktail l (C0001-1, Targetmol, China) and quantified with a BCA kit (P0013C, Beyotime, China). Protein sample extracts (30 mg/lane) were separated by SDS-PAGE and transferred onto a polyvinylidene difluoride membrane (PVDF). After the membranes were blocked with 5% BSA, they were incubated with the primary antibodies at 4°C overnight, followed by HRP-conjugated secondary antibody. Then, the membranes were incubated with HRP-conjugated secondary antibody (Boster

TABLE 2 | Components identified in TLYS decoction.

Peak NO.	*t*R/ min	Moleculear formulla	Dection pattern	m/z	Secondary debris (MS/MS)	Source	Identification	CAS
1	0.83	$C_6H_8O_7$	–	191.01950	111, 87, 85	Unknown	Citric acid or isocitric acid	77-92-9 or 320-77-4
2	1.05	$C_6H_8O_7$	–	191.01950	111, 87, 85	Unknown	Citric acid or isocitric acid	77-92-9 or 320-77-4
3	1.96	$C_9H_{10}O_5$	–	197.04533	179, 135, 123	*Salvia miltiorrhiza* Bge	Danshensu	76822-21-4
4	2.08	$C_9H_{11}NO_2$	+	166.08610	120	Unknown	L-Phenylalanine	63-91-2
5	3.90	$C_7H_6O_3$	–	137.02415	93	Unknown	4-Hydroxybenzoic acid	99-96-7
6	5.53	$C_{15}H_{14}O_6$	–	289.07170	245, 203, 125	*Spatholobus suberectus* Dunn	Catechin	7295-85-4
7	6.47	$C_9H_8O_4$	–	179.03477	135	*Salvia miltiorrhiza* Bge	Caffeic acid	331-39-5
8	7.13	$C_{33}H_{38}O_{23}$	+	803.18799	303, 479	*Carthamus tinctorius* L	2-(3,4-dihydroxyphenyl-3-{[2-O-(β-D-erythro-hexopyranosyl)-β-D-glycero-hexopyranosyl] oxy}-5-hydroxy-4-oxo-4H-chromen-7-yl-β-D-threo-hexopyranosi-duronic acid	—
9	7.38	$C_{27}H_{32}O_{16}$	+	613.17627	355, 313, 211	*Carthamus tinctorius* L	Safflomin A	78281-02-4
10	8.31	$C_{15}H_{14}O_6$	–	289.07156	245, 203, 109, 125	*Spatholobus suberectus* Dunn	L-Epicatechin	490-46-0
11	10.31	$C_{33}H_{40}O_{21}$	+	773.21393	303	*Carthamus tinctorius* L	Cyanidin 3-O-β-(2″-ecaf-feoyl-glucopyranosyl)-(1→2)-O-β-galactopyranoside	—
12	11.19	$C_{27}H_{30}O_{16}$	+	611.16095	287	*Carthamus tinctorius* L	Rutin	153-18-4
13	11.33	$C_{21}H_{20}O_{12}$	+	465.10281	303	*Carthamus tinctorius* L	6-Hydroxykaempferol-3-O-glucoside	—
14	12.17	$C_{27}H_{44}O_7$	–	525.30650 [M + COOH]$^-$	159, 319, 301, 83	*Achyranthes bidentata* Bl	β-Ecdysone	5289-74-7
15	12.26	$C_{27}H_{30}O_{15}$	–	593.15110	285, 255, 227	*Carthamus tinctorius* L	Kaempferol-3-O-rutinoside	17650-84-9
16	12.33	$C_{27}H_{22}O_{12}$	–	537.1037	109, 185, 295	*Salvia miltiorrhiza* Bge	Lithospermic acid	28831-65-4
17	12.42	$C_{27}H_{44}O_7$	–	525.30650 [M + COOH]$^-$	159, 319, 479	*Achyranthes bidentata* Bl	β-Ecdysone isomer	—
18	12.60	$C_{27}H_{44}O_7$	–	525.30650 [M + COOH]$^-$	159, 319, 479	*Achyranthes bidentata* Bl	β-Ecdysone isomer	—
19	13.03	$C_{27}H_{44}O_7$	+	481.31573	171	*Achyranthes bidentata* Bl	Inokosterone	15130-85-5
20	13.09	$C_{27}H_{30}O_{15}$	+	617.14709	–	*Carthamus tinctorius* L	Safflor Yellow A	85532-77-0
21	13.14	$C_{27}H_{30}O_{15}$	+	595.16571	287	*Carthamus tinctorius* L	Kaempferol 3-rutinoside	17650-84-9
22	13.33	$C_{36}H_{30}O_{16}$	–	717.14703	339, 321	*Salvia miltiorrhiza* Bge	Salvianolic acid E	142998-46-7
23	13.54	$C_{18}H_{16}O_8$	–	359.07700	161	*Salvia miltiorrhiza* Bge	Rosmarinic acid	20283-92-5
24	13.87	$C_{26}H_{22}O_{10}$	–	493.11349	295,185	*Salvia miltiorrhiza* Bge	Salvianolic acid A	96574-01-5
25	13.87	$C_{26}H_{20}O_{10}$	–	537.10360 [M + COOH]$^-$	293, 197, 135, 105	*Salvia miltiorrhiza* Bge	Salvianolic acid C	15841-09-3
26	14.59	$C_{36}H_{30}O_{16}$	–	717.14612	339, 321	*Salvia miltiorrhiza* Bge	Salvianolic acid B	121521-90-2
27	14.82	$C_{26}H_{22}O_{10}$	–	493.11380	109, 185, 295	*Salvia miltiorrhiza* Bge	Salvianolic acid A isomer	—
28	15.43	$C_{36}H_{30}O_{16}$	–	717.14673	321, 339, 519	*Salvia miltiorrhiza* Bge	Salvianolic acid Y	1638738-76-7
29	15.61	$C_{26}H_{22}O_{10}$	–	493.11400	109, 185, 295	*Salvia miltiorrhiza* Bge	Salvianolic acid A isomer	—
30	15.75	$C_{19}H_{18}O_8$	–	373.09310	135, 179	*Salvia miltiorrhiza* Bge	Methyl rosmarinate	99353-00-1
31	22.28	$C_{42}H_{66}O_{14}$	–	793.43870	631, 569, 455, 113	*Achyranthes bidentata* Bl	Chikusetsu saponin IVa	51415-02-2

(Continued on following page)

TABLE 2 | (*Continued*) Components identified in TLYS decoction.

Peak NO.	tR/ min	Moleculear formulla	Dection pattern	m/z	Secondary debris (MS/MS)	Source	Identification	CAS
32	22.28	$C_{47}H_{72}O_{20}$	–	955.45600	835, 793, 631, 455, 161	*Achyranthes bidentata* Bl	Achyranthoside G	—
33	28.59	$C_{19}H_{20}O_3$	+	297.14822	253, 238, 211	*Salvia miltiorrhiza* Bge	Cryptotanshinone isomer	—
34	29.12	$C_{18}H_{14}O_3$	+	279.10147	261,233	*Salvia miltiorrhiza* Bge	Dihydrotanshinone I	87205-99-0
35	31.27	$C_{19}H_{18}O_3$	+	295.13306	90, 277, 249, 225	*Salvia miltiorrhiza* Bge	Tanshinone IIA isomer	—
36	33.14	$C_{19}H_{20}O_3$	+	297.14822	251, 254, 279, 282	*Salvia miltiorrhiza* Bge	Cryptotanshinone	35825-57-1
37	37.32	$C_{19}H_{18}O_3$	+	295.13306	277, 249, 235, 90	*Salvia miltiorrhiza* Bge	Tanshinone IIA	568-72-9

Biological Technology Co., Ltd., China) at room temperature for 1 h. Films were scanned by a ChemiScope 6,000 system (Qinxiang, Shanghai, China). ImageJ software was used to measure the protein bands based on that of GAPDH.

Immunofluorescence Staining

Frozen sections were used to assess colocalization of Pink1 and TOM20. Kidney sections were blocked with 5% bovine serum albumin for 30 min at room temperature, followed by incubation overnight at 4°C with primary antibodies against Pink1 (1:200, SC517353, Santa Cruz, United States) and TOM20 (1:200, 11802-1-AP Proteintech, United States). After the samples were washed with PBS, an Alexa Fluor 488-conjugated goat anti-mouse secondary antibody (1:300) and Alexa Fluor 594-conjugated goat anti-rabbit secondary antibody (1:300) were added for 1 h at room temperature. Finally, the slides were stained with DAPI solution for 10 min and captured by a laser scanning confocal fluorescence microscope (Olympus FV 1000, Japan). Ten nonoverlapping high-power fields (40X) were randomly captured in each specimen and analyzed by ImageJ software.

Statistical Analysis

GraphPad Prism software was used for statistical analysis. Quantitative data are expressed as the mean ± standard error of the mean (SEM). One-way ANOVA was used for all experimental data followed by Dunnett's test. A p value <0.05 was considered significant.

RESULTS

Identification of the Chemical Components in Tongluo Yishen Decoction

To evaluate the major chemical components, we analyzed TLYS decoction using UHPLC-MS in positive and negative ion mode (**Figure 1**). Thirty-seven compounds (6 organic acids, 5 diterpene quinones, 4 sterones, 6 flavonoids, 10 phenolic acids and 6 other compounds) were detected at relatively high levels. The detailed information is shown in **Table 2**.

The Effect of Tongluo Yishen Decoction on Renal Function and Histological Injury

To study the effects of TLYS decoction on renal fibrosis, we adopted a rat model of UUO with 14-days TLYS treatment. We found that in the UUO group, the level of Scr was significantly higher than that in the sham group (66.79 ± 1.93 μmol/L vs 40.14 ± 1.83 μmol/L), and TLYS treatment partly decreased the levels to 57.25 ± 1.20 μmol/L (**Figure 2A**). Similarly, the rats with UUO showed significantly higher levels (4.36 ± 0.23 mmol/L) of BUN than the control rats (3.04 ± 0.11 mmol/L), while TLYS treatment significantly reduced the BUN levels to 3.52 ± 0.12 mmol/L (**Figure 2B**). As a positive control group, losartan (30 mg/kg) decreased serum concentration of BUN ($p < 0.05$) but not Scr. H&E staining and Masson's trichrome staining were used to evaluate renal pathological injury (**Figure 2C**). H&E staining showed that the UUO group exhibited notable tubule atrophy and lumen dilation with diffuse interstitial inflammation. TLYS treatment attenuated kidney tubulointerstitial injury following UUO whereas the positive control, losartan, decreased the tubulointerstitial injury (**Figure 2D**). Masson's staining showed substantial interstitial fibrosis in the UUO group; this fibrosis was significantly attenuated in the TLYS-treated rats (**Figure 2E**). These data suggested that treatment with TLYS could significantly mitigate renal injury.

The Effect of Tongluo Yishen Decoction on Renal Fibrosis

Given the protective effect of TLYS on renal fibrosis, we investigated the expression of α-SMA and TGF-β1 by immunohistochemistry. As shown in **Figures 3A,B**, the expression of α-SMA in the tubular interstitium was much higher in the UUO group than in the sham group. However, in the TLYS group, this increase was significantly suppressed. In addition, compared with the sham group, the UUO group showed a dramatic increase in TGF-β1 levels, while TLYS treatment significantly inhibited this abnormal increase in TGF-β1 (**Figures 3A,C**). Similarly, valsartan treatment

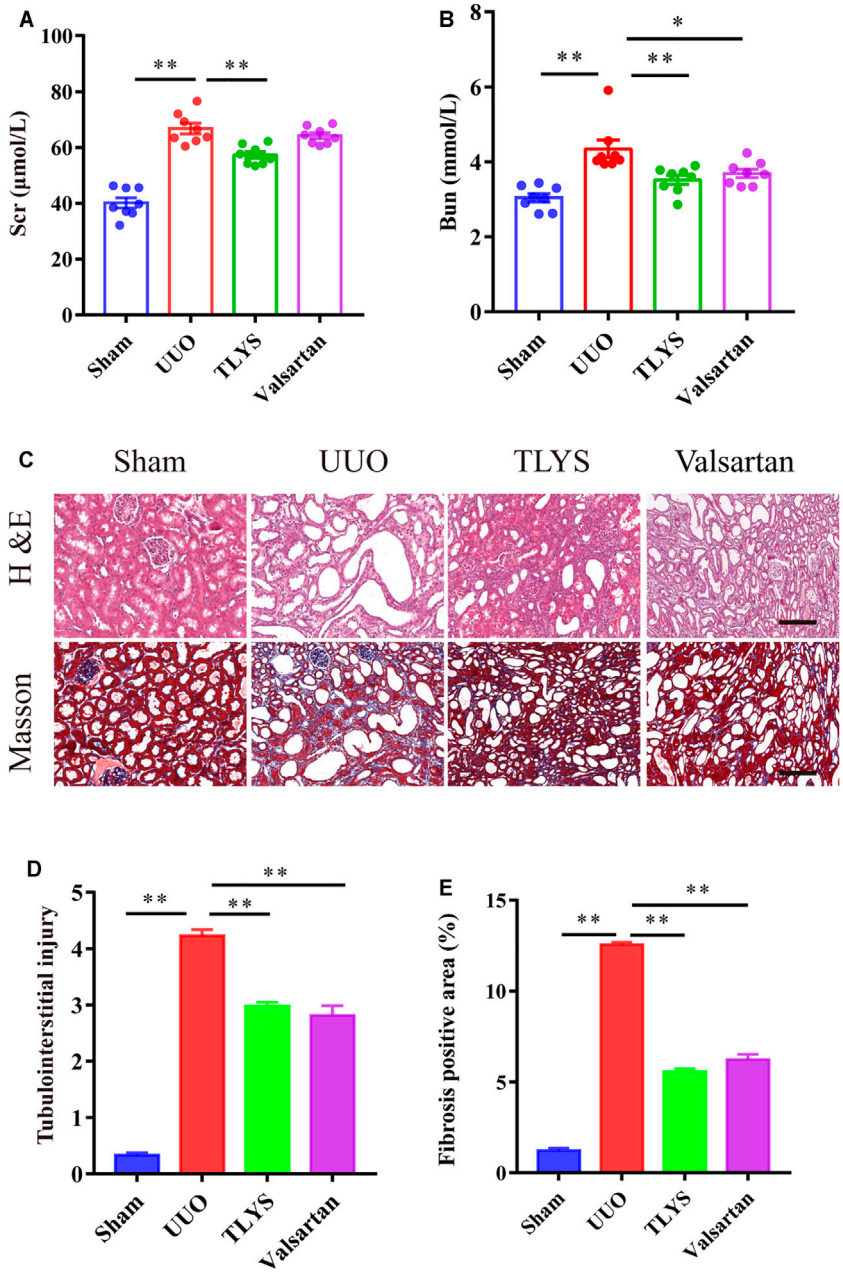

FIGURE 2 | TLYS decoction alleviates renal function and pathological kidney injuries in UUO rats. **(A,B)** serum creatinine and BUN were detected (n = 8). **(C)** H&E and Masson's trichrome were performed to evaluate kidney injury (n = 6). **(D)** Tubular damage scores based on H&E staining. **(E)** quantification of collagen areas according to Masson's trichrome staining. The magnification of the images is ×200, scale bar = 50 μm. Data were presented as means ± SEM. *p < 0.05, **p < 0.01.

significantly reduced the level of α-SMA and TGF-β1 (**Figures 3A–C**).

Tongluo Yishen Decoction Showed Comprehensive Regulatory Effects in the Rats With UUO

To explore the mechanisms of TLYS decoction, we performed RNA-Seq analysis. There were 1,541 DEGs with upregulated expression and 877 DEGs with downregulated expression in the UUO group relative to the sham group. Ninety-five DEGs had upregulated expression and 200 DEGs had downregulated expression in the TLYS group relative to the UUO group. Additionally, the differences were significant (|log2 (fold-change)| > 1 and p < 0.05, **Figures 4A,B**). Next, these overlapping DEGs were analyzed by GO analysis of biological processes, cellular components, and molecular functions. The number of DEGs with upregulated

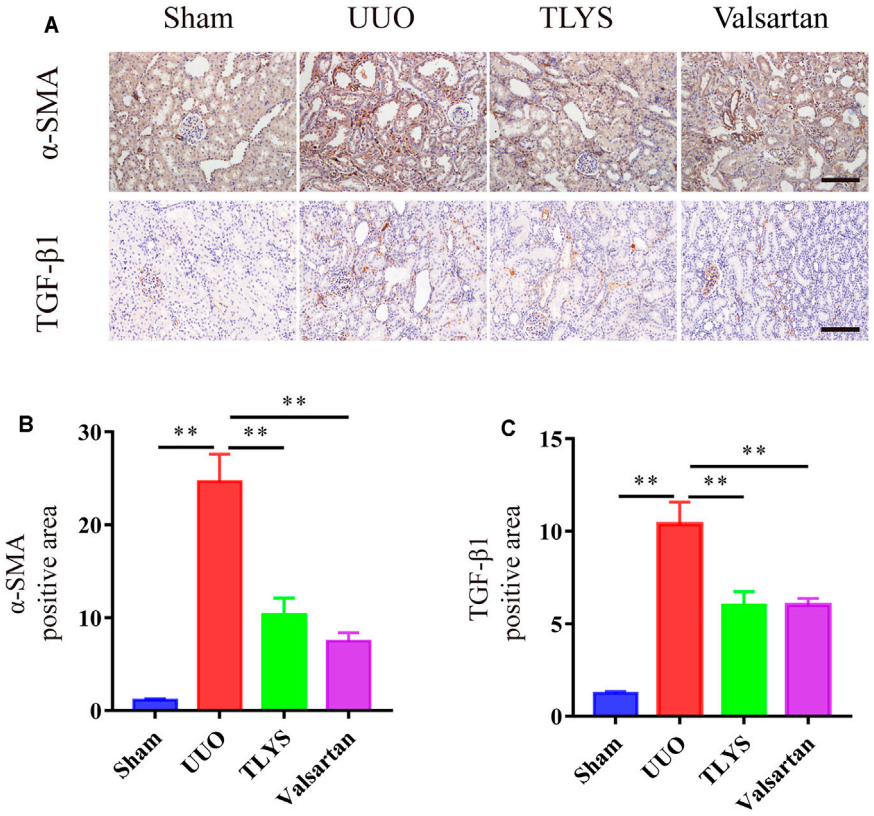

FIGURE 3 | TLYS decoction suppresses a-SMA expression and TGF-β1 expression in UUO rats. **(A–D)** Expression levels of a-SMA and TGF-β1 in the kidney were detected by immunohistochemistry and analyzed the optical intensity of the abovementioned proteins was measured (n = 6). The magnification of the images is ×200, scale bar = 50 μm. Data were presented as means ± SEM (n = 6). *p < 0.05, **p < 0.01.

expression was significantly higher, whereas the number of DEGs with downregulated expression was lower in the UUO group than in the sham group (**Figure 4C**). After TLYS treatment, the number of DEGs with downregulated expression significantly increased and was greater than that of DEGs with upregulated expression (**Figure 4D**). These results further showed that TLYS has a comprehensive regulatory effect in the rats with UUO.

To screen out the most representative DEG group affected by TLYS, we performed a trend analysis of all selected DEGs. DEGs were divided into 8 categories (**Figure 5A**), of which profiles 2, 6 and 7 were significant (**Figure 5B**). We calculated the proportion of each DEG trend in the corresponding pathways, and signal transduction was commonly affected by the above three DEG trends (**Figure 5C**). Then, by KEGG enrichment analysis, three significant pathways were identified for TLYS treatment; the pathways were phagosomes (a membrane source in the earlier stages of autophagy), lysosome (an important component of autolysosome), and oxidative phosphorylation, which may participate in mitochondrial function (**Figure 5D**). Therefore, TLYS treatment might be associated with mitochondrial dysfunction and mitophagy in the rats with UUO.

Tongluo Yishen Decoction Ameliorated Mitochondrial Function and Mitochondrial Dynamics

A reduction in MMP suggests damage to mitochondrial function, which is indicated by a lower ratio of red-to-green fluorescence. The MMP was lower in the UUO group than in the sham group, but TLYS increased the MMP level (**Figure 6A**). Mitochondrial division and fusion are crucial for maintaining morphology and function. The expression of proteins related to mitochondrial fusion (Mfn1 and Mfn2) showed a significant reduction in the UUO group (p < 0.01), and this trend was reversed after TLYS treatment (p < 0.01) (**Figures 6B–D**). As shown in **Figures 6B,E,F**, the expression of the proteins related to mitochondrial fission (Drp1 and Mff) was upregulated in the UUO group compared with the sham group, and TLYS treatment significantly prevented this trend.

Tongluo Yishen Decoction Ameliorated Oxidative Stress in the Rats With UUO

Oxidative stress induced by the accumulation of ROS causes serious damage to mitochondria; therefore, we investigated the effects of TLYS on oxidative stress. Our results demonstrated that the activities of SOD and GSH-PX were significantly lower and that the content of

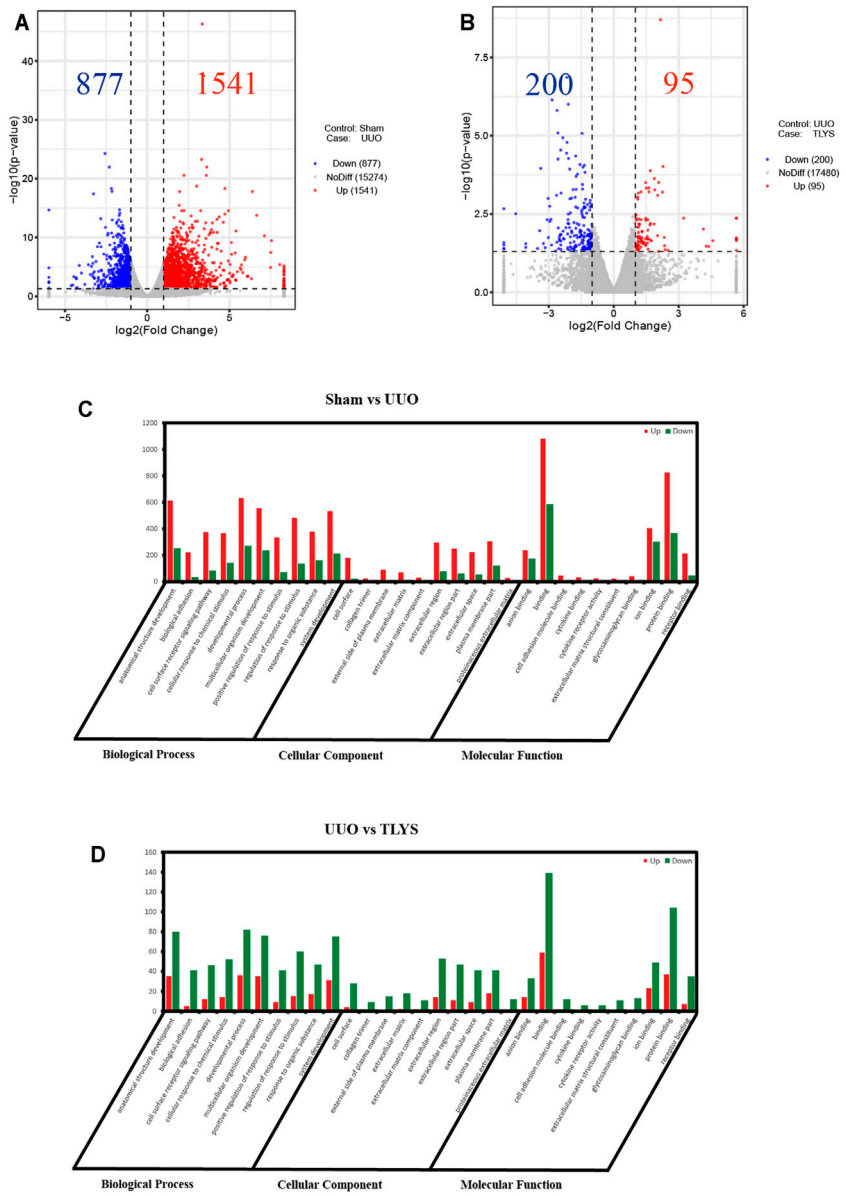

FIGURE 4 | TLYS decoction played comprehensive regulatory roles in UUO rats. **(A,B)** Volcano plot of genes with significant differences, FDR <0.05, |log FC|> 1. **(C,D)** Gene Ontology (GO) function analysis of genes with significant differences in three experimental groups. Three independent samples were tested in each experimental group.

ROS and MDA was higher in the UUO group than in the sham group. Interestingly, TLYS treatment significantly enhanced the levels of SOD and GSH-PX and inhibited the increase in ROS and MDA (**Figures 7A–D**). The results indicated that TLYS could ameliorate oxidative stress in the rats with UUO.

Tongluo Yishen Decoction Alleviated Pink1/Parkin-Mediated Mitophagy in the Rats With UUO

Damaged mitochondria can be degraded by mitophagy, which is driven by Pink1/Parkin signaling. In our study, we assessed the protein expression of this pathway. Compared with the sham group, the UUO group showed significantly increased protein levels of Pink1 and Parkin in the kidney. However, TLYS treatment significantly decreased the expression of Pink1 and Parkin. Moreover, immunofluorescence confirmed and further revealed that Pink1 in the renal tubular epithelial cell was diminished in the rats with UUO compared with the sham rats (**Figures 8A–C**). The colocalization of mitochondria (marked by TOM20) and Pink1 was markedly decreased in the TLYS group compared with the UUO group (**Figure 8D**). These results suggested that the translocation of Pink1 from the cytoplasm to mitochondria machinery is inhibited, resulting in

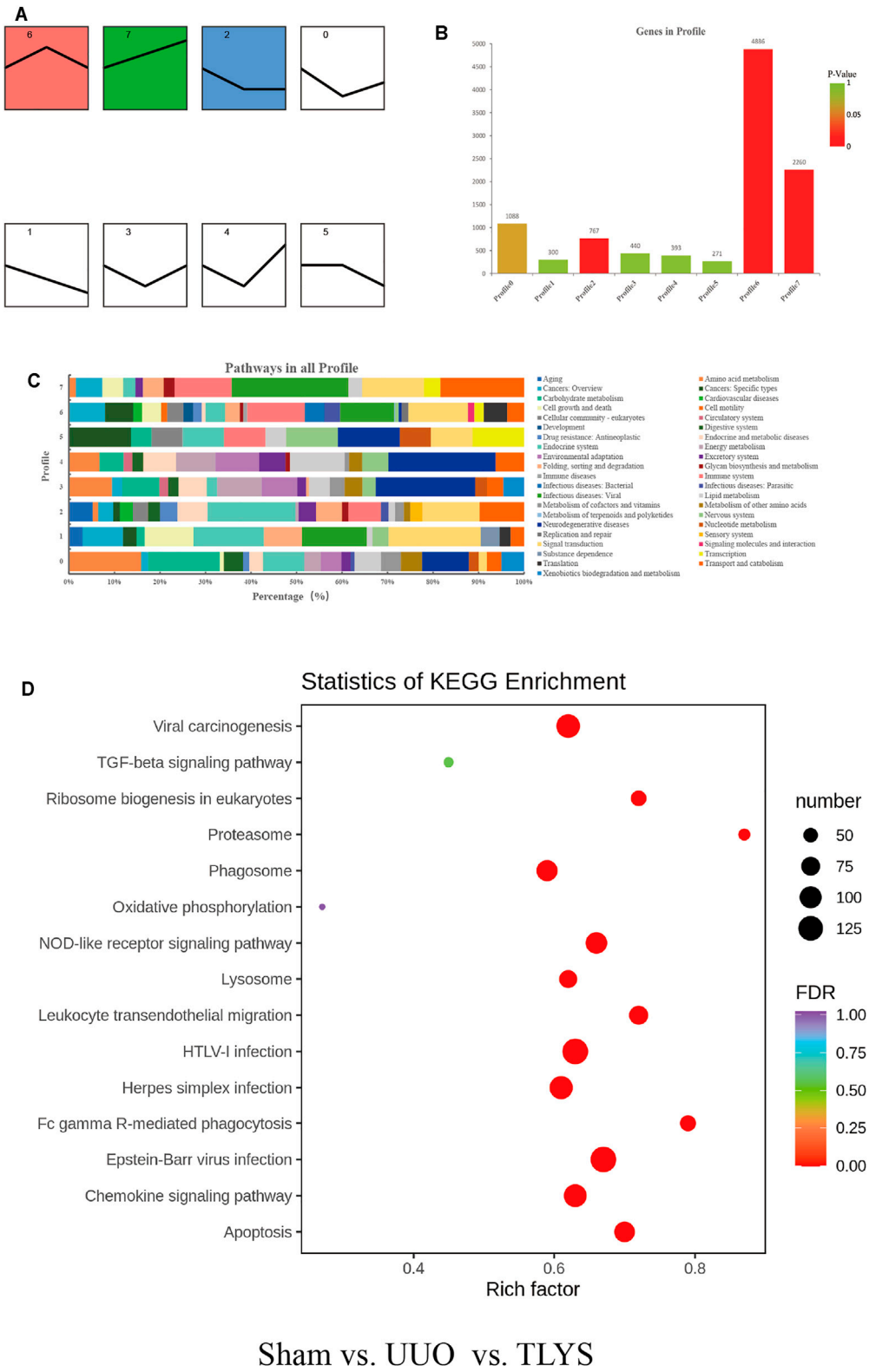

FIGURE 5 | TLYS decoction may be related to mitochondria and mitophagy in UUO rats. **(A)** All trends (profile 0–7) of genes with significant differences. **(B)** Histogram of the four trends (red) with significant differences, $p < 0.05$. **(C)** Pathway-related gene distribution (%) in all profiles. **(D)** Bubble diagram of Kyoto Encyclopedia of Genes and Genomes (KEGG) pathway enrichment. Three independent samples were tested in each experimental group.

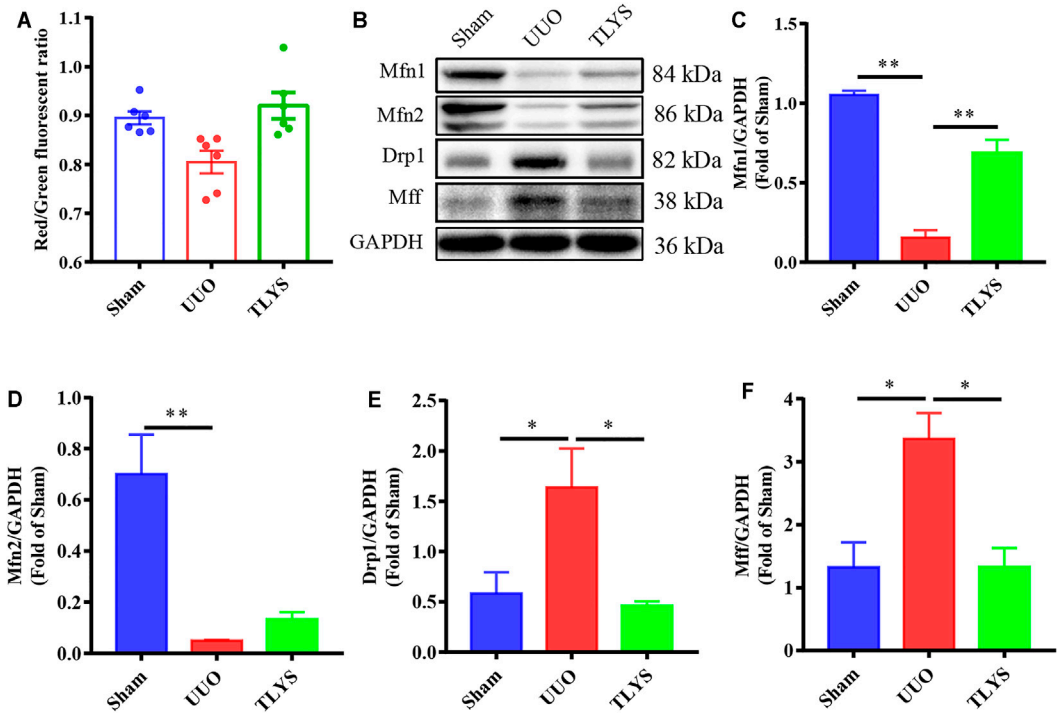

FIGURE 6 | TLYS decoction attenuated mitochondrial function and dynamics in UUO rats. **(A)** Mitochondrial membrane potential (MMP) assessed using a JC-1 fluorescence probe ($n = 6$). **(B–F)** The protein levels of Mfn1, Mfn2, Drp1, and Mff were assayed by Western blot and analyzed semi-quantitatively. Data were presented as means ± SEM. $^{*}p < 0.05$, $^{**}p < 0.01$.

the accumulation of Pink1 at the outer mitochondrial membrane in the UUO group, and TLYS could reverse this change. These data indicated that TLYS inhibited Pink1/Parkin-mediated mitophagy in the rats with UUO.

DISCUSSION

Although the definite pathological mechanism of CKD remains unclear, RIF is regarded as the final common pathway of CKD leading to end-stage renal failure, without regard to etiology (Boor and Floege 2011). RIF is closely associated with a deterioration in renal function in patients with CKD (Nangaku 2006). Because the pathogenesis of RIF has not yet been fully clarified, effective and specific therapeutic methods for the treatment of RIF are lacking, and the development of strategies to prevent and intervene in RIF would be beneficial for patients with CKD. TLYS decoction is composed of four herbs, and 38 different compounds were identified by UHPLC-MS analysis. Studies have also shown that quercetin and salvianolic acid B can effectively improve RIF. Furthermore, in a model of acute pancreatitis, tanshinone IIA decreased ROS release and protected the mitochondrial structure (Chen et al., 2020). In addition, achyranthes was reported to have a protective effect on the kidney by reducing the accumulation of ROS and apoptosis in the renal tissues of mice with acute kidney injury (Wang et al., 2020). These protective effects and mechanisms are consistent with our observations in this study. These ingredients may be involved in the protective effect of TLYS in RIF. In this study, we investigated the renal protective effects of TLYS in rats with UUO and its underlying molecular mechanisms. Renal function is assessed by Scr and BUN, which reflect glomerular filtration barrier impairment and renal filtration function. In this study, we found that TLYS reduced the levels of Scr and BUN in the rats with UUO. This finding suggested that TLYS plays a crucial role in improving renal function in these rats. RIF is a dynamic and converging process characterized by activated tubulointerstitial myofibroblasts and ECM, and activated myofibroblasts are thought to be a major contributor to the pathogenesis of RIF (Nangaku 2006). α-SMA is a marker protein of myofibroblasts, and TGF-β1 is a key mediator in progressive renal fibrosis. TGF-β1 can enhance fibroblast growth and collagen production and promote the differentiation of fibroblasts into myofibroblasts, which secrete ECM components (Meng, Nikolic-Paterson, and Lan 2016). In this study, α-SMA and TGF-β1 levels were significantly lower in the TLYS group than in the UUO group, indicating that TLYS might alleviate RIF through its antifibrotic effect.

Next-generation high-throughput RNA-Seq is an unbiased technology that can objectively reveal gene expression changes in disease and reveal unknown transcripts that are not annotated in current databases (Trapnell et al., 2010). In this study, we found that three significant pathways (phagosomes, lysosome, and oxidative phosphorylation pathways) were affected in UUO by TLYS treatment. Then, we observed the abnormal mitochondrial function during UUO and found that it was improved by TLYS

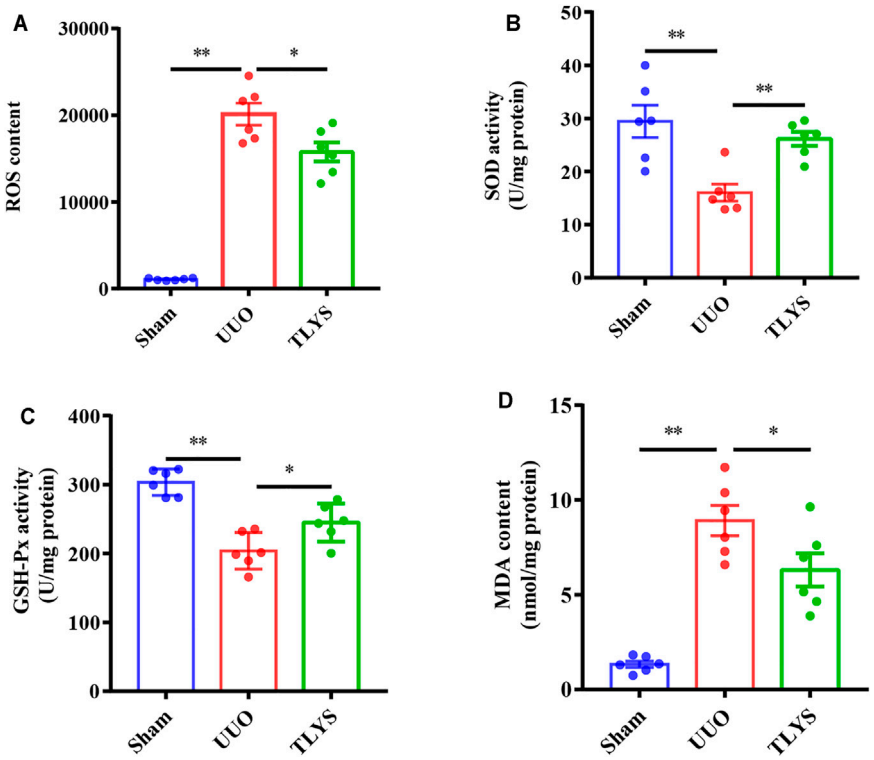

FIGURE 7 | TLYS decoction ameliorated oxidative stress in UUO rats. The renal tissues were taken to evaluate the contents of ROS **(A)**, superoxide dismutase (SOD) **(B)**, glutathione peroxidase (GSH-Px) **(C)**, and malondialdehyde (MDA) (n = 6). Data were presented as means ± SEM. $^{*}p < 0.05$, $^{**}p < 0.01$.

treatment, which might rescue mitochondrial function by inhibiting oxidative stress.

The increase in ROS in the cytoplasm triggers the opening of mitochondrial permeability transition pores and leads to dissipation of the MMP, inhibition of ATP production, and induction of mitochondrial swelling (Yang et al., 2017). Mitochondrial outer membrane fusion is mediated by Mfn1 and Mfn2, and the recruitment of Drp1 from the cytosol to the outer mitochondrial membrane is mediated by its receptor proteins (Mff), which are involved in mitochondrial division. Although in several CKD models, there is a shift of mitochondrial dynamics toward fission (Hallan and Sharma 2016; Xiao et al., 2017; Aparicio-Trejo et al., 2018), the involvement of this change in UUO is still under discussion. Our results indicated that there was mitochondrial damage (decreased MMP) and a dynamic imbalance of mitochondria (upregulated Drp1 and Mff expression, downregulated Mfn1 and Mfn2 expression) in the rats with UUO. Interestingly, TLYS treatment could preserve the stability of mitochondrial structures.

For mitochondrial damage, excessive oxidative stress causes the most serious damage to mitochondrial membrane permeability, especially lipid peroxidation of the inner membrane. Oxidative stress includes increasing levels of ROS and the loss of antioxidant enzymes, such as SOD and GSH-PX, which play crucial roles in protecting kidneys against oxidative stress. Previous studies demonstrated that MDA was significantly increased in rats with ureteral obstruction compared with sham-treated rats (Shi et al., 2020). ROS production and RIF are enhanced by deficiencies in these antioxidant enzymes (Aranda-Rivera et al., 2021). In our study, UUO led to a decrease in the activities of SOD and GSH-PX compared to those of the sham group. In contrast, the MDA level was markedly increased compared with that in the sham group. TLYS treatment mitigated the oxidative stress induced by UUO. Briefly, the above results indicated that TLYS may reduce mitochondrial damage through antioxidative stress in the rats with UUO. However, the abnormal mitochondria clearance and the regulatory effects of TLYS on mitophagy need further study.

Mitophagy, mediated by the Pink1/Parkin pathway, is a major mechanism to remove damaged mitochondria (Zhu et al., 2013). Autophagic flow is a dynamic process, and an increase in Pink1/Parkin levels does not indicate normal mitophagic flow, as illustrated by the increase in the number of damaged mitochondria and autophagic bodies in these models (Aparicio-Trejo et al., 2019; Avila-Rojas et al., 2019; Aparicio-Trejo et al., 2020), which could indicate disruption downstream of mitophagic flux. Therefore, it is not clear whether mitophagic flow is carried out properly in tubular epithelial cells in the rats with UUO due to the accumulation of damaged mitochondrial bodies observed by electron microscopy. In this context, Sang et al. (Sang et al., 2020)showed that the upregulation of renal calcineurin 1 induced translocation of Drp1 to the mitochondria, increasd mitochondrial fission, and regulated mitochondrial dynamics.

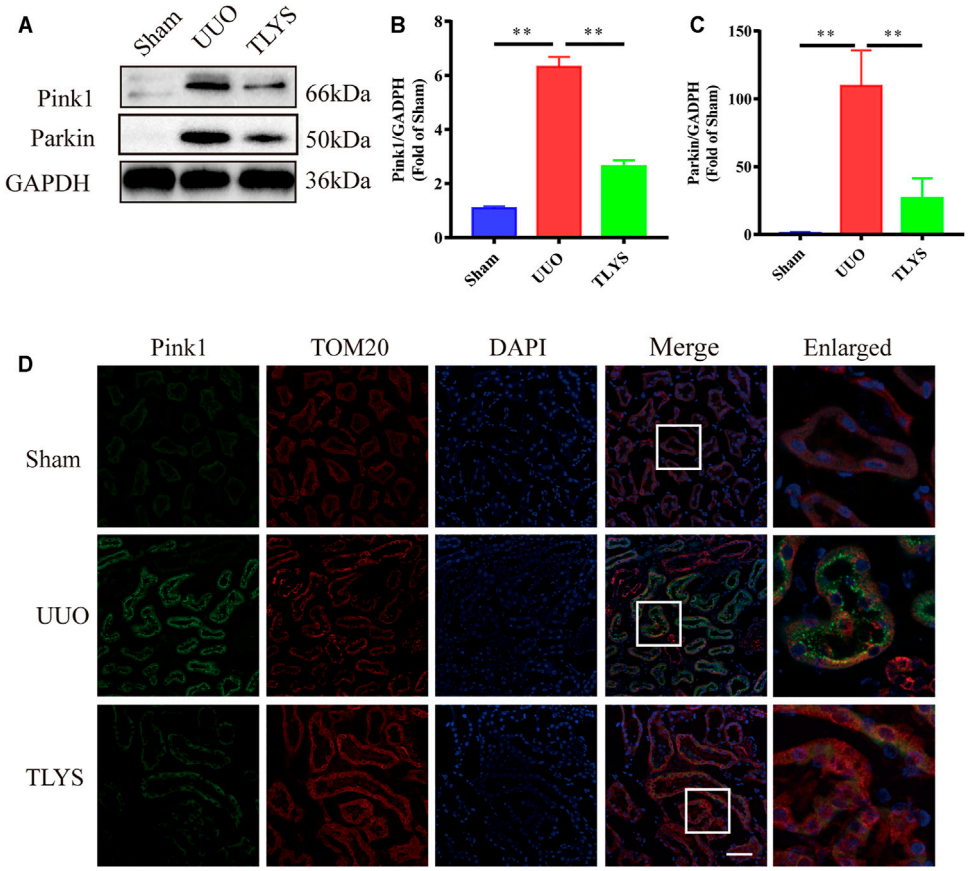

FIGURE 8 | TLYS decoction alleviated Pink1/Parkin-mediated mitophagy in the rats with UUO. **(A-C)** The expression of Drp1, Pink1, Parkin and Mfn2 by Western blot (n = 6) and analyzed semi-quantitatively. **(D)** Images of tissues co-stained for the mitochondrial markers Pink1 (green), TOMM20 (red) and nuclear (blue), scale bar = 50 μm, (n = 6). Data were presented as means ± SEM. $^{*}p < 0.05$, $^{**}p < 0.01$.

However, the increase in mitochondrial fission, PINK1 and Parkin may also indicate mitophagic dysfunction. Similarly, our results indicated that there is an activation in Pink1/Parkin-mediated mitophagy, including increased Pink1 and Parkin levels. TLYS could decrease Pink1 and Parkin levels and alleviate the translocation of Pink1 from the cytoplasm to mitochondria. Overall, the above results show that overactivation in Pink1/Parkin-mediated mitophagy occurs in UUO rats, and TLYS can improve damaged mitochondria function via Pink1/Parkin-mediated mitophagy to protect against RTC (renal tubular cell) injury. However, autophagic activation has different effects in kidneys with different statuses or under different stress factors. Therefore, more studies of each of the steps of mitophagic flow are still needed to elucidate its role in kidney obstructive damage.

In conclusion, our study showed that TLYS decoction can ameliorate renal pathological damage and improve renal function in UUO rats. This renoprotective effect may be related to a reduction in oxidative stress; thus, TLYS can improve mitochondrial function and dynamics to protect against RTC injury.

DATA AVAILABILITY STATEMENT

The data presented in the study are deposited in the NCBI repository, accession number PRJNA767261.

ETHICS STATEMENT

The animal study was reviewed and approved by the Laboratory Animal Ethics Committee of Dongfang Hospital affiliated with Beijing University of Chinese Medicine. Written informed consent was obtained from the owners for the participation of their animals in this study.

AUTHOR CONTRIBUTIONS

JQ, GH, and QJ designed the experiments. LH, XZ, WY, and YS performed the animal experiments. QJ, LH, and BL conducted the molecular biology experiments. SW, MQ, and SL analyzed and interpreted the data. QJ and LH wrote the manuscript.

FUNDING

The National Natural Science Foundation of China (Grant No. 81173407) and the independent project of China Academy of Chinese Medical Sciences (yz202013) supported this study.

SUPPLEMENTARY MATERIAL

The Supplementary Material for this article can be found online at: https://www.frontiersin.org/articles/10.3389/fphar.2021.762756/full#supplementary-material

REFERENCES

Aparicio-Trejo, O. E., Avila-Rojas, S. H., Tapia, E., Rojas-Morales, P., León-Contreras, J. C., Martínez-Klimova, E., et al. (2020). Chronic Impairment of Mitochondrial Bioenergetics and β-oxidation Promotes Experimental AKI-To-CKD Transition Induced by Folic Acid. *Free Radic. Biol. Med.* 154, 18–32. doi:10.1016/j.freeradbiomed.2020.04.016

Aparicio-Trejo, O. E., Reyes-Fermín, L. M., Briones-Herrera, A., Tapia, E., León-Contreras, J. C., Hernández-Pando, R., et al. (2019). Protective Effects of N-Acetyl-Cysteine in Mitochondria Bioenergetics, Oxidative Stress, Dynamics and S-Glutathionylation Alterations in Acute Kidney Damage Induced by Folic Acid. *Free Radic. Biol. Med.* 130, 379–396. doi:10.1016/j.freeradbiomed.2018.11.005

Aparicio-Trejo, O. E., Tapia, E., Sánchez-Lozada, L. G., and Pedraza-Chaverri, J. (2018). Mitochondrial Bioenergetics, Redox State, Dynamics and Turnover Alterations in Renal Mass Reduction Models of Chronic Kidney Diseases and Their Possible Implications in the Progression of This Illness. *Pharmacol. Res.* 135, 1–11. doi:10.1016/j.phrs.2018.07.015

Aranda-Rivera, A. K., Cruz-Gregorio, A., Aparicio-Trejo, O. E., Ortega-Lozano, A. J., and Pedraza-Chaverri, J. (2021). Redox Signaling Pathways in Unilateral Ureteral Obstruction (UUO)-induced Renal Fibrosis. *Free Radic. Biol. Med.* 172, 65–81. doi:10.1016/j.freeradbiomed.2021.05.034

Avila-Rojas, S. H., Lira-León, A., Aparicio-Trejo, O. E., Reyes-Fermín, L. M., and Pedraza-Chaverri, J. (2019). Role of Autophagy on Heavy Metal-Induced Renal Damage and the Protective Effects of Curcumin in Autophagy and Kidney Preservation. *Medicina (Kaunas)* 55 (7), 360. doi:10.3390/medicina55070360

Boor, P., and Floege, J. (2011). Chronic Kidney Disease Growth Factors in Renal Fibrosis. *Clin. Exp. Pharmacol. Physiol.* 38 (7), 441–450. doi:10.1111/j.1440-1681.2011.05487.x

Cai, H., Su, S., Li, Y., Zeng, H., Zhu, Z., Guo, J., et al. (2018). Protective Effects of Salvia Miltiorrhiza on Adenine-Induced Chronic Renal Failure by Regulating the Metabolic Profiling and Modulating the NADPH oxidase/ROS/ERK and TGF-β/Smad Signaling Pathways. *J. Ethnopharmacol* 212, 153–165. doi:10.1016/j.jep.2017.09.021

Chen, W., Yuan, C., Lu, Y., Zhu, Q., Ma, X., Xiao, W., et al. (2020). Tanshinone IIA Protects against Acute Pancreatitis in Mice by Inhibiting Oxidative Stress via the Nrf2/ROS Pathway. *Oxid Med. Cel Longev* 2020, 5390482. doi:10.1155/2020/5390482

Debelle, F. D., Nortier, J. L., De Prez, E. G., Garbar, C. H., Vienne, A. R., Salmon, I. J., et al. (2002). Aristolochic Acids Induce Chronic Renal Failure with Interstitial Fibrosis in Salt-Depleted Rats. *J. Am. Soc. Nephrol.* 13 (2), 431–436. doi:10.1681/asn.v132431

Do, M. H., Hur, J., Choi, J., Kim, Y., Park, H. Y., and Ha, S. K. (2018). Spatholobus Suberectus Ameliorates Diabetes-Induced Renal Damage by Suppressing Advanced Glycation End Products in Db/db Mice. *Int. J. Mol. Sci.* 19 (9). doi:10.3390/ijms19092774

Guo, C., Li, S., and Rao, X. R. (2019). New Goals and Strategies of Chinese Medicine in Prevention and Treatment of Chronic Kidney Disease. *Chin. J. Integr. Med.* 25 (3), 163–167. doi:10.1007/s11655-019-3065-z

Hallan, S., and Sharma, K. (2016). The Role of Mitochondria in Diabetic Kidney Disease. *Curr. Diab Rep.* 16 (7), 61. doi:10.1007/s11892-016-0748-0

Jha, V., Garcia-Garcia, G., Iseki, K., Li, Z., Naicker, S., Plattner, B., et al. (2013). Chronic Kidney Disease: Global Dimension and Perspectives. *Lancet* 382 (9888), 260–272. doi:10.1016/s0140-6736(13)60687-x

Kitada, M., Xu, J., Ogura, Y., Monno, I., and Koya, D. (2020). Manganese Superoxide Dismutase Dysfunction and the Pathogenesis of Kidney Disease. *Front. Physiol.* 11, 755. doi:10.3389/fphys.2020.00755

Koyano, F., Okatsu, K., Kosako, H., Tamura, Y., Go, E., Kimura, M., et al. (2014). Ubiquitin Is Phosphorylated by PINK1 to Activate Parkin. *Nature* 510 (7503), 162–166. doi:10.1038/nature13392

Levin, A., Tonelli, M., Bonventre, J., Coresh, J., Donner, J. A., Fogo, A. B., et al. (2017). Global Kidney Health 2017 and beyond: a Roadmap for Closing Gaps in Care, Research, and Policy. *Lancet* 390 (10105), 1888–1917. doi:10.1016/s0140-6736(17)30788-2

Li, J., Zhang, C., He, W., Qiao, H., Chen, J., Wang, K., et al. (2017). Coordination-driven Assembly of Catechol-Modified Chitosan for the Kidney-specific Delivery of Salvianolic Acid B to Treat Renal Fibrosis. *Biomater. Sci.* 6 (1), 179–188. doi:10.1039/c7bm00811b

Li, W., Cheng, H., Li, G., and Zhang, L. (2020). Mitochondrial Damage and the Road to Exhaustion. *Cell Metab* 32 (6), 905–907. doi:10.1016/j.cmet.2020.11.004

Liu, X., Lu, J., Liu, S., Huang, D., Chen, M., Xiong, G., et al. (2020). Huangqi-Danshen Decoction Alleviates Diabetic Nephropathy in Db/db Mice by Inhibiting PINK1/Parkin-Mediated Mitophagy. *Am. J. Transl Res.* 12 (3), 989–998.

Liyanage, T., Ninomiya, T., Jha, V., Neal, B., Patrice, H. M., Okpechi, I., et al. (2015). Worldwide Access to Treatment for End-Stage Kidney Disease: a Systematic Review. *Lancet* 385 (9981), 1975–1982. doi:10.1016/s0140-6736(14)61601-9

Masaki, T., Foti, R., Hill, P. A., Ikezumi, Y., Atkins, R. C., and Nikolic-Paterson, D. J. (2003). Activation of the ERK Pathway Precedes Tubular Proliferation in the Obstructed Rat Kidney. *Kidney Int.* 63 (4), 1256–1264. doi:10.1046/j.1523-1755.2003.00874.x

Meng, X. M., Nikolic-Paterson, D. J., and Lan, H. Y. (2016). TGF-β: the Master Regulator of Fibrosis. *Nat. Rev. Nephrol.* 12 (6), 325–338. doi:10.1038/nrneph.2016.48

Mills, K. T., Xu, Y., Zhang, W., Bundy, J. D., Chen, C. S., Kelly, T. N., et al. (2015). A Systematic Analysis of Worldwide Population-Based Data on the Global burden of Chronic Kidney Disease in 2010. *Kidney Int.* 88 (5), 950–957. doi:10.1038/ki.2015.230

Nakanishi, T., Kuragano, T., Nanami, M., Nagasawa, Y., and Hasuike, Y. (2019). Misdistribution of Iron and Oxidative Stress in Chronic Kidney Disease. *Free Radic. Biol. Med.* 133, 248–253. doi:10.1016/j.freeradbiomed.2018.06.025

Nangaku, M. (2006). Chronic Hypoxia and Tubulointerstitial Injury: a Final Common Pathway to End-Stage Renal Failure. *J. Am. Soc. Nephrol.* 17 (1), 17–25. doi:10.1681/asn.2005070757

Sang, X. Y., Xiao, J. J., Liu, Q., Zhu, R., Dai, J. J., Zhang, C., et al. (2020). Regulators of Calcineurin 1 Deficiency Attenuates Tubulointerstitial Fibrosis through Improving Mitochondrial Fitness. *FASEB J.* 34 (11). doi:10.1096/fj.202000781RRR

Sharma, K. (2014). Obesity, Oxidative Stress, and Fibrosis in Chronic Kidney Disease. *Kidney Int. Supplements.* 4 (1), 113–117. doi:10.1038/kisup.2014.21

Shi, Z., Wang, Q., Zhang, Y., and Jiang, D. (2020). Extracellular Vesicles Produced by Bone Marrow Mesenchymal Stem Cells Attenuate Renal Fibrosis, in Part by Inhibiting the RhoA/ROCK Pathway, in a UUO Rat Model. *Stem Cel Res Ther.* 11 (1), 253. doi:10.1186/s13287-020-01767-8

Tang, C., Cai, J., Yin, X. M., Weinberg, J. M., Venkatachalam, M. A., and Dong, Z. (2021). Mitochondrial Quality Control in Kidney Injury and Repair. *Nat. Rev. Nephrol.* 17 (5), 299–318. doi:10.1038/s41581-020-00369-0

Trapnell, C., Williams, B. A., Pertea, G., Mortazavi, A., Kwan, G., van Baren, M. J., et al. (2010). Transcript Assembly and Quantification by RNA-Seq Reveals Unannotated Transcripts and Isoform Switching during Cell Differentiation. *Nat. Biotechnol.* 28 (5), 511–515. doi:10.1038/nbt.1621

Wang, Q. L., Tao, Y. Y., Yuan, J. L., Shen, L., and Liu, C. H. (2010). Salvianolic Acid B Prevents Epithelial-To-Mesenchymal Transition through the TGF-Beta1

Signal Transduction Pathway *In Vivo* and *In Vitro*. *BMC Cel Biol* 11, 31. doi:10.1186/1471-2121-11-31

Wang, S., Zeng, M., Li, B., Kan, Y., Zhang, B., Zheng, X., et al. (2020). Raw and Salt-Processed Achyranthes Bidentata Attenuate LPS-Induced Acute Kidney Injury by Inhibiting ROS and Apoptosis via an Estrogen-like Pathway. *Biomed. Pharmacother.* 129, 110403. doi:10.1016/j.biopha.2020.110403

Xiao, L., Xu, X., Zhang, F., Wang, M., Xu, Y., Tang, D., et al. (2017). The Mitochondria-Targeted Antioxidant MitoQ Ameliorated Tubular Injury Mediated by Mitophagy in Diabetic Kidney Disease via Nrf2/PINK1. *Redox Biol.* 11, 297–311. doi:10.1016/j.redox.2016.12.022

Xuan, C., Xi, Y.-M., Zhang, Y.-D., Tao, C.-H., Zhang, L.-Y., and Cao, W.-F. (2021). Yiqi Jiedu Huayu Decoction Alleviates Renal Injury in Rats with Diabetic Nephropathy by Promoting Autophagy. *Front. Pharmacol.* 12. doi:10.3389/fphar.2021.624404

Yang, S., Han, Y., Liu, J., Song, P., Xu, X., Zhao, L., et al. (2017). Mitochondria: A Novel Therapeutic Target in Diabetic Nephropathy. *Curr. Med. Chem.* 24 (29), 3185–3202. doi:10.2174/0929867324666170509121003

Zeisberg, M., and Neilson, E. G. (2010). Mechanisms of Tubulointerstitial Fibrosis. *J. Am. Soc. Nephrol.* 21 (11), 1819–1834. doi:10.1681/asn.2010080793

Zhu, J., Wang, K. Z., and Chu, C. T. (2013). After the Banquet: Mitochondrial Biogenesis, Mitophagy, and Cell Survival. *Autophagy* 9 (11), 1663–1676. doi:10.4161/auto.24135

Conflict of Interest: The authors declare that the research was conducted in the absence of any commercial or financial relationships that could be construed as a potential conflict of interest.

Publisher's Note: All claims expressed in this article are solely those of the authors and do not necessarily represent those of their affiliated organizations, or those of the publisher, the editors and the reviewers. Any product that may be evaluated in this article, or claim that may be made by its manufacturer, is not guaranteed or endorsed by the publisher.

frontiers in Pharmacology

ORIGINAL RESEARCH
published: 18 October 2021
doi: 10.3389/fphar.2021.724744

Effect of Mahuang Fuzi and Shenzhuo Decoction on Idiopathic Membranous Nephropathy: A Multicenter, Nonrandomized, Single-Arm Clinical Trial

*Zhaocheng Dong[1†], Haoran Dai[2†], Yu Gao[1,3†], Hanxue Jiang[1], Meiqi Liu[1,4], Fei Liu[1,4], Wenbin Liu[4], Zhendong Feng[5], Xiaoyan Zhang[6], Aijie Ren[7], Xiaolan Li[8], Hongliang Rui[1], Xuefei Tian[9], Guiming Li[10] and Baoli Liu[1,2]**

[1]Beijing Hospital of Traditional Chinese Medicine Affiliated to Capital Medical University, Beijing, China, [2]Shunyi Branch, Beijing Traditional Chinese Medicine Hospital, Beijing, China, [3]Capital Medical University, Beijing, China, [4]Beijing University of Chinese Medicine, Beijing, China, [5]Beijing Chinese Medicine Hospital Pinggu Hospital, Beijing, China, [6]Yanqing Hospital of Beijing Chinese Medicine Hospital, Beijing, China, [7]Tangshan Fengrun Hospital of Traditional Chinese Medicine, Tangshan, China, [8]Zhangjiakou Hospital of Traditional Chinese Medicine, Zhangjiakou, China, [9]Department of Internal Medicine, Yale University School of Medicine, New Haven, CT, United States, [10]Department of Nephrology, Feicheng Mining Center Hospital, Tai'an, China

OPEN ACCESS

Edited by:
Dan-Qian Chen,
Northwest University, China

Reviewed by:
Zou Chuan,
Guangdong Provincial Hospital of Chinese Medicine, China
Bin Zhu,
Hangzhou Hospital of Traditional Chinese Medicine, China

***Correspondence:**
Baoli Liu
liubaoli@bjzhongyi.com

[†]These authors share first authorship

Specialty section:
This article was submitted to Renal Pharmacology, a section of the journal Frontiers in Pharmacology

Received: 14 June 2021
Accepted: 09 August 2021
Published: 18 October 2021

Citation:
Dong Z, Dai H, Gao Y, Jiang H, Liu M, Liu F, Liu W, Feng Z, Zhang X, Ren A, Li X, Rui H, Tian X, Li G and Liu B (2021) Effect of Mahuang Fuzi and Shenzhuo Decoction on Idiopathic Membranous Nephropathy: A Multicenter, Nonrandomized, Single-Arm Clinical Trial. Front. Pharmacol. 12:724744. doi: 10.3389/fphar.2021.724744

Objective: To explore the clinical effect of Mahuang Fuzi and Shenzhuo Decoction on idiopathic membranous nephropathy.

Methods: This study is a multicenter, nonrandomized, single-arm clinical trial carried out as per the objective performance criteria, with the target being set at 35.0%. 184 cases of patients suffering from idiopathic membranous nephropathy with Shaoyin Taiyin syndrome were collected. These patients were treated with Mahuang Fuzi and Shenzhuo Decoction with a follow-up period of 3 years. The 24-hour urine protein and blood albumin were observed, and the remission rates of the patients were compared with the target.

Results: The mean follow-up time was 18 (12.5, 30) months, and the remission rate was 61.4%, which is a statistically significant difference from the target group of 35%. The remission rates for patients who had and had not used immunosuppressive therapy were 59.6 and 65.5%, respectively, but the difference was not statistically significant ($p = 0.254$). However, the albumin before the treatment and the course of treatment of the patients was significantly correlated with the disease remission ($p < 0.05$). However, the albumin before the treatment and the course of treatment of the patients was significantly correlated with the disease remission ($p < 0.05$). There were no significant changes in renal function before and after treatment, and no severe adverse events occurred during treatment.

Conclusion: Mahuang Fuzi and Shenzhuo Decoction have significant effects on idiopathic membranous nephropathy, and has the same effect on patients with membranous nephropathy who are newly treated as well as those who have been treated with immunosuppressive therapy without remission. In addition, the efficacy of this regimen is related to the albumin and the duration of the therapy, but not to 24-hour urine protein or other factors.

Keywords: idiopathic membranous nephropathy, Mahuang Fuzi and Shenzhuo Decoction, objective performance criteria, single-arm clinical trial, herbal medicine

INTRODUCTION

Idiopathic membranous nephropathy (IMN) is one of the pathological types of primary nephrotic syndrome (NS), with approximately 5–10 patients per million population (Ruggenenti et al., 2017). The prevalence of this disease in China is increasing year by year, second only to IgA nephropathy in primary NS (Xu et al., 2016). IMN is an immune-mediated disease caused by the deposition of IgG and complement components in the underlying epithelium of the glomerular capillary wall. About one-third of patients with this disease will develop the end-stage renal disease (ESRD) (Keri et al., 2019). In contrast, the remaining third of patients will experience clinical remission with immunosuppressive therapy (IST), while the remainder will experience spontaneous remission with continued stable renal function (Couser, 2017). Although IST is effective, it also has significant toxic side effects, such as those of cyclophosphamide, including hyperglycemia, myelosuppression, infection, infertility, and cancer (van den Brand, 2017). In addition, these drugs also have a recurrence rate after discontinuation (Fervenza et al., 2017). This presents opportunities and challenges for traditional Chinese medicine in the treatment of this disease. Mahuang Fuzi and Shenzhuo Decoction (MFSD) is a common prescription used by Baoli Liu to treat the Shaoyin Taiyin syndrome of IMN. This study is a multicenter, nonrandomized, single-arm, clinical trial, using the objective performance criteria method to explore the effect of MFSD on idiopathic membranous nephropathy.

METHODS

Inclusion Criteria

1) Patients meeting the diagnostic criteria of IMN in modern medicine, diagnosed by pathology and light or electron microscopy (Couser, 2017).
2) Patients meeting the diagnostic criteria of Shaoyin Taiyin syndrome in traditional Chinese medicine (formulated based on the standard of *Interpreting Zhang Zhongjing Medicine* compiled by Feng Shilun). Primary symptoms include the following: aversion to cold, chills in the hands and feet, back pain, swelling, abdominal distension, loose or dry stools, soft tongue, thin greasy or slippery coated with water, and sunken pulse. Secondary symptoms include the following: fatigue and weakness, shortness of breath, laziness in words, sweating, scanty urination, and nighttime frequency. Patients with the above three primary symptoms and two secondary symptoms can be determined to have Shaoyin Taiyin syndrome (Feng and Zhang, 2011).
3) Patients who have complete case information and have been receiving traditional Chinese medicine treatment in our department for more than 8 months.
4) Patients aged between 16 and 80 years.
5) Patients with CKD1-3 (GFR>30 ml/min).

Exclusion Criteria

1) Patients with CKD stage 3 or above.
2) Patients with other types of glomerular diseases.
3) Patients with confirmed secondary hepatitis B, systemic lupus erythematosus, tumors, and other factors.
4) Patients with acute central nervous system disease, severe gastrointestinal disease, history of HIV infection, history of mental illness, history of malignant tumor, and prohibition of immunosuppressive agents.
5) Patients with serious diseases, other organs dysfunctions, and life-threatening complications such as severe infection.
6) Pregnant or lactating women undergoing other clinical trials. Patients with any of the above conditions must be excluded from the study.

Experimental Design and Sample Size Calculation

This study is a single-arm clinical trial with the objective performance criteria, and the efficacy of traditional Chinese medicine in the treatment of IMN was evaluated by setting a target value in advance. According to the literature, about one-third of patients with IMN are in spontaneous remission, clinical remission after IST, and no remission in ESRD (Couser, 2017). Because our team previously counted 108 outpatients with IMN, 50.0% of them did not respond after routine use of immunosuppressant (unpublished). In addition, during the progression of IMN, about one-third of the patients have spontaneous responses to effective immunosuppressive therapy and ineffective immunosuppressive therapy, meaning that, for newly treated IMN patients, the response rate to modern medical therapy is about 66.7%. Therefore, for the remaining 50.0% of the newly treated patients with IMN who came to our TCM outpatient department, only 66.7% of them could achieve remission if they continued to be treated with modern medical regimens. These remission patients accounted for 33.3% of our TCM clinics. Therefore, the target value of treatment was 35.0% (higher than the calculated value: $50\% \times 1/3 \times 2 = 33.3\%$), with an expected target value of 45.0% to determine the efficacy. According to the requirement of single-arm clinical study with the objective performance criteria, the sample size was calculated and the shedding rate was designed to be 10%. The target value $P_0 = 0.35$ and the target value $P_1 = 0.45$ were set according to the formula used to calculate the sample size of the single-group target value test (US. FDA, 2013). The calculated results were 183, the designed shedding rate of this study was 10%, and the calculated test sample size was 202 cases in total.

Case Shedding and Treatment

All subjects who complete the informed consent form and are screened for admission to the trial are referred to as shedding

cases whenever or for any reason they withdraw, as long as the observation period specified in the protocol is not completed. The case records of exfoliation shall be kept, stating the cause of exfoliation, and converted to the final result based on the final test result.

Treatment Options

The treatment group was treated on the basis of the KDIGO clinical practice guidelines issued in 2012 (Rojas-Rivera et al., 2019): 1) high-quality low protein and low phosphorus; 2) angiotensin-converting enzyme inhibitors (ACEIs) or angiotensin receptor blockers (ARBs) control blood pressure between 120-135/75-85 mmHg; 3) symptomatic diuretic, correct water, electrolyte, and acid–base balance; 4) anti-infection treatment for infected persons; and 5) conventional low molecular weight heparin anticoagulation for serum albumin below 25 g/L. The base prescription is MFSD, which contains Ma Huang (*Ephedra sinica* Stapf.) 15 g, Hei Fu Zi (*Aconitum carmichaeli* Debx.) 15 g (boiled first), Zhi Gan Cao (*Glycyrrhiza uralensis* Fisch.) 6 g, Gan Jiang (*Zingiber officinale* Rosc.) 20 g, Fu Ling (*Poria cocos* (Schw.) Wolf) 30 g, and Chao Bai Zhu (*Atractylodes macrocephala* Koldz.) 20 g. The main ingredients of these medicines in Chinese prescriptions are detailed in **Supplementary Table S1**. The dosage is as follows: 1 dose daily, boiled with 400 ml water, and taken in the morning and evening for 6–36 months. The distribution of herbs and collection of patient-related information will be conducted during the outpatient hours. Patients who are not seen in time will be followed up by telephone or online, and the initiative will be taken to mail the herbs to these patients if necessary.

Observation Indicators and Methods

Main Curative Effect Index and Curative Effect Standard

The patient's blood albumin and 24-hour urine protein quantification were monitored regularly to determine the remission (Kanigicherla et al., 2013). 1) Complete remission (CR): 24-h urine protein quantification <0.3 g, normal renal function and blood albumin, and disappearance of clinical symptoms. 2) Partial remission (PR): 24-h urine protein quantitative <3.5 h and a decrease of more than 50% from the base value, blood albumin increased before treatment, and normal renal function. 3) Non-remission (NR): the quantitative decrease of 24-h urine protein was less than 50% from the base value or deteriorated renal function, and the blood albumin was less than 30 g/L, without improvement in clinical symptoms.

Safety Standard

To observe whether hepatic and renal injury and other adverse reactions occurred in the treatment group during treatment.

Statistical Analysis

The statistical analysis plan was developed according to the acquired data, and SPSS Statistics 20.0 software was adopted for analysis. The measurement data conforming to the normal distribution are expressed as the mean ± standard deviation, and the enumeration data and measurement data not conforming to the normal distribution are expressed as the median (interquaternary interval). In single-group analysis and comparison between two groups, the paired design quantitative data *t* test was used for measurement data conforming to the normal distribution, and the paired design sign rank-sum test or $\chi 2$ test was used for counting data and measurement data not conforming to normal distribution. Kaplan–Meier survival analysis was used to perform the log-rank test to compare the remission status of different groups, and survival curves were drawn. If the survival curves of two groups were intersected, the Breslow test would be used. Data relating to remission were selected to build the model, and remission or non-remission was taken as the dependent variable. The goodness-fit of the model was tested by the Hosmer–Lemeshow test. Based on this, a binary logistics regression analysis was conducted, and the ROC curve was plotted to calculate the cutoff value.

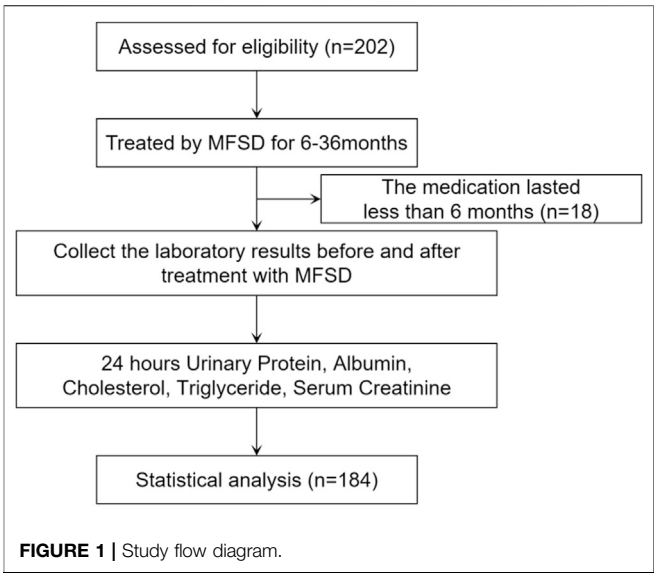

FIGURE 1 | Study flow diagram.

RESULTS

Baseline Results

A total of 202 IMN patients admitted to the Beijing Hospital of Traditional Chinese Medicine, Shunyi Branch of Beijing Hospital of Traditional Chinese Medicine, Yanqing Hospital of Beijing Hospital of Traditional Chinese Medicine, Tangshan Fengrun Hospital of Traditional Chinese Medicine, and Zhangjiakou Hospital of Traditional Chinese Medicine from September 2016 to January 2019 were selected as the research subjects. 18 patients who had been treated for less than 6 months were not included in the analysis based on clinical experience. Therefore, a total of 184 IMNs were included in the study (**Figure 1**), including 114 males and 70 females. The patients were aged 17–80 years, with a mean age of 50 (38, 60) years. The mean follow-up period was 18 (12.5, 30) months. 40 patients (21.7% of the total) were at low risk, 59 patients (32.1% of the total) were at moderate risk, and 85

TABLE 1 | Baseline characteristics of the subjects (grouped according to whether they had used immunosuppressive therapy in the past).

	Treated (*N* = 126)	Untreated (*N* = 58)	*p*-value
Gender			0.052
Male	84 (66.7%)	30 (51.7%)	
Female	42 (33.3%)	28 (48.3%)	
Age	51 (40, 63)	47 (35, 59)	0.041
Nephrotic syndrome	81 (64.3%)	39 (67.2%)	0.696
Albumin (g/L)	25.61 ± 7.74	25.38 ± 7.35	0.849
24-h urine protein (g/24 h)	6.99 (4.00, 11.53)	6.25 (4.53, 9.47)	0.507
Cholesterol (mmol/L)	6.53 (5.25, 8.38)	6.12 (5.55, 7.44)	0.570
Triglyceride (mmol/L)	2.20 (1.50, 3.23)	2.20 (1.48, 3.51)	0.602
Risk ranking			0.487
Low	30 (23.8%)	10 (17.2%)	
Medium	33 (26.2%)	26 (44.8%)	
High	63 (50.0%)	22 (37.9%)	
Renal function			
Serum creatinine (μmol/L)	72.00 (61.05, 93.75)	64.40 (57.00, 77.60)	0.008
eGFR (ml/min)	99.21 ± 35.84	112.82 ± 25.14	0.019
Treatment course (month)	18 (13, 30)	18.5 (12, 30)	0.773
Medical history			
Hypertension	44	25	0.287
Diabetes	21	5	0.145

patients (46.2% of the total) were at high risk. Among the patients studied, 126 patients had not been relieved by regular immunosuppressive therapy, and 58 patients had not been treated with immunosuppressive therapy. Of the patients who had previously received immunosuppressive therapy, 48 had received cyclophosphamide, 48 had received cyclosporine, 15 had received tacrolimus, 3 had received mycophenolate mofetil, 28 had received tripterygium glycosides, and 18 had received other regimens such as prednisone alone, leflunomide, and hydroxychloroquine. No patients had received the rituximab regimen. In addition, 106 patients had received only one treatment regimen, 11 patients had received two treatment regimens, and 9 patients had received three or more treatment regimens without remission (**Supplementary Table S2**).

Patients were grouped according to whether or not they had previously used immunosuppressants, and baseline levels were compared between the two groups. We identified 84 males and 42 females (mean 51 (40, 63) years old) with previous immunosuppressive therapy. Eighty-one patients, or 64.3% of the total, had nephrotic syndrome. 23.8% of patients were at low risk, 26.2% at medium risk, and 50.0% at high risk. The mean serum albumin was 25.61 ± 7.74 g/L, the mean 24-hour urine protein was 6.99 (4.00, 11.53) g/24 h, the mean cholesterol was 6.53 (5.25, 8.38) mmol/L, triglyceride was 2.20 (1.50, 3.23) mmol/L, serum creatinine was 72.00 (61.05, 93.75) μmmol/L, and the estimated glomerular filtration rate was 99.21 ± 35.84 ml/min. The mean follow-up period was 18 (13, 30) months. 44 patients had hypertension in the past, and 21 patients had diabetes. 30 males and 28 females (mean 47 (35, 59) years old) were not treated with immunosuppressive agents. 39 patients have nephrotic syndrome, accounting for 67.2% of the total. 17.2% of the patients were at low risk, 44.8% at medium risk, and 37.9% at high risk. The mean serum albumin was 25.38 ± 7.35 g/L, the mean 24-hour urine protein was 6.25 (4.53, 9.47) g/24 h, the mean cholesterol was 6.12 (5.55, 7.44) mmol/L, triglyceride was 2.20 (1.48, 3.51) mmol/L, serum creatinine was 64.40 (57.00, 77.60) μmmol/L, and the estimated glomerular filtration rate was 112.82 ± 25.14 ml/min. The mean follow-up period was 18.5 (12, 30) months. There were 25 patients with hypertension and 5 patients with diabetes. When comparing the two groups at baseline, we found that there was no statistical significance in the composition of gender between the two groups ($p = 0.052$). Patients who had received immunosuppressive therapy were older than those who had not, and the difference was statistically significant ($p < 0.05$). There were no significant differences in serum albumin, 24-hour urinary protein, total cholesterol, and triglyceride between the two groups ($p > 0.05$). The serum creatinine of patients who had received previous immunosuppressive therapy was significantly higher than that of patients who had not, and their glomerular filtration rate was significantly lower ($p < 0.05$). There was no significant difference in the risk ranking, treatment course, and medical history between the two groups ($p > 0.05$) (**Table 1**).

Efficacy Results

All the 184 included patients with IMN were followed up until December 2019, of which 113 met the criteria for remission and 71 did not, so the remission rate is 61.4% [95% C.I. 54.4–68.4%]. The target remission rate set by this regimen was 35.0%, the target remission rate was 45%, and the lower limit of the 95% confidence interval was greater than the target value and target value, proving that this regimen has significant efficacy (**Supplementary Table S3**). Of all patients included, the remission rate was 59.6%, the complete remission rate was 16.7%, the partial remission rate was 42.9% for those who had received previous immunosuppressive therapy, while for those who had not, these rates were 65.5, 10.4, and 55.1%, respectively. There was no significant difference in the remission rate between the two groups ($p = 0.254$).

For patients who had been treated for 6–12 months, these rates were 39.1, 6.5, and 32.6%, respectively. Among these patients, those who had received previous immunosuppressive therapy had a remission rate of 32.3%, the complete remission rate of 6.5%, and

TABLE 2 | Composition of remission rates (grouped by previous use of immunosuppressive therapy).

	All	Treated	Untreated	*p*-value
All				0.254
CR	27/184 (14.7%)	21/126 (16.7%)	6/58 (10.4%)	
PR	86/184 (46.7%)	54/126 (42.9%)	32/58 (55.1%)	
Both	113/184 (61.4%)	75/126 (59.6%)	38/58 (65.5%)	
6–12 Months				0.359
CR	3/46 (6.5%)	2/31 (6.5%)	1/15 (6.7%)	
PR	15/46 (32.6%)	8/31 (25.8%)	7/15 (46.7%)	
Both	18/46 (39.1%)	10/31 (32.3%)	8/15 (53.3%)	
13–24 Months				0.122
CR	11/72 (15.3%)	10/48 (20.8%)	1/24 (4.2%)	
PR	36/72 (50.0%)	23/48 (47.9%)	13/24 (54.2%)	
Both	47/72 (65.3%)	33/48 (68.7%)	14/24 (58.3%)	
25–36 Months				0.375
CR	13/66 (19.7%)	9/47 (19.1%)	4/19 (21.1%)	
PR	35/66 (53.0%)	23/47 (48.9%)	12/19 (63.2%)	
Both	48/66 (72.7%)	32/47 (68.1%)	16/19 (82.2%)	

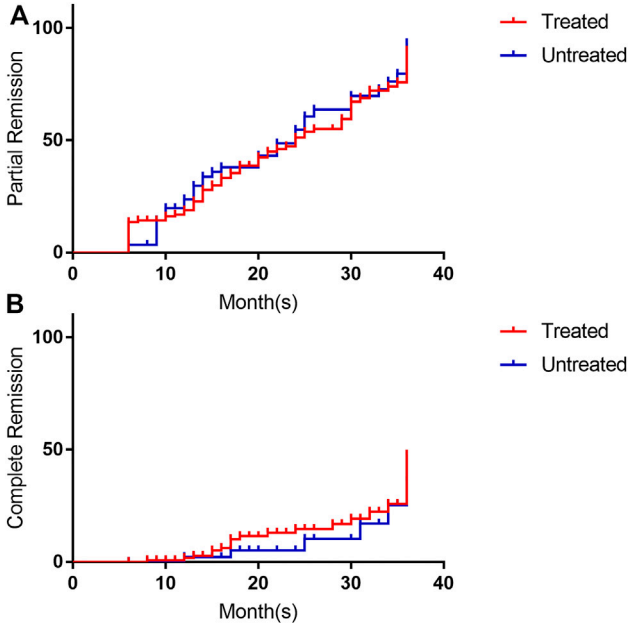

FIGURE 2 | Survival analysis of remission rates (grouped by previous use of immunosuppressive therapy). **(A)** is the survival analysis of partial response rate, and **(B)** is the survival analysis of complete response rate. The red line is treated with immunosuppressive, the blue line is un-treated with immunosuppressive. Its annotation is consistent with the grouping words in **Table 1**.

the partial remission rate of 25.8%, while these rates for those who had not received immunosuppressive therapy were 53.3, 6.7, and 46.7%, respectively. There was no significant difference in the remission rate between the two groups (p = 0.359).

For patients who took the drug for 13–24 months, the remission rate was 65.3%, complete remission rate 15.3%, and partial remission rate 50.0%. Among them, these rates for patients who had been regularly treated with immunosuppressive therapy were 68.7, 20.8, and 47.9%, respectively, while for those who had not, these rates were 58.3, 4.2, and 54.2%, respectively. There was no significant difference in the remission rate between the two groups (p = 0.122).

For patients who took the drug for 25–36 months, these rates were 72.7, 19.7, and 53.0%. Among them, patients who had been regularly treated with immunosuppressive therapy had rates of 68.1, 19.1, and 48.9%, respectively, while those who had not been treated with immunosuppressive therapy had rates of 82.2, 21.1, and 63.2%. There was no significant difference in the remission rate between the two groups (p = 0.375; **Table 2**). The Kaplan–Meier survival analysis was performed based on the time to remission between the two groups, and the results showed that there was no statistically significant difference in the partial remission rate (p = 0.641) or complete remission rate (p = 0.346) between the two groups (**Figure 2**).

After treatment with MFSD, the serum albumin increased to an average of 37.35 (30.75, 41.70) g/L, the 24-hour urinary protein quantified to an average of 2.23 (0.70, 4.10) g/24h, while the average values for the total cholesterol and the triglyceride decreased to 5.33 (4.49, 6.55) mmol/L and 1.69 (1.03, 2.45) mmol/L, respectively. These results were significantly different from those of the baseline before treatment, and were statistically significant (p < 0.001). In addition, the average serum creatinine was 69.20 (55.00, 83.03) μmol/L (p = 0.239), and the average estimated glomerular filtration rate was 107.36 ± 36.46 ml/min (p = 0.127). There was no significant difference between before and after treatment.

Patients were grouped according to whether they had used immunosuppressants in the past, and the results of various laboratory tests after treatment were compared between the two groups. For patients who had received immunosuppressive therapy, after treatment with MFSD, the average serum albumin increased to 37.85 (30.33, 41.73) g/L, the average 24-hour urinary protein level was 2.18 (0.71, 4.47) g/24 h, the average total cholesterol decreased to 5.38 (4.52, 6.75) mmol/L, and the average triglyceride was 1.69 (1.02, 2.66) mmol/L. These results were significantly different from those of the

TABLE 3 | Test results before and after treatment (grouped according to the previous application of immunosuppressive therapy).

	Prior treatment	Post-treatment	*p*-value
Albumin (g/L)	24.95 (20.00, 31.00)	37.35 (30.75, 41.70)	< 0.001
24-hour urine protein (g/24 h)	6.57 (4.29, 10.21)	2.23 (0.70, 4.10)	< 0.001
Cholesterol (mmol/L)	6.36 (5.39, 8.17)	5.33 (4.49, 6.55)	< 0.001
Triglyceride (mmol/L)	2.20 (1.48, 3.30)	1.69 (1.03, 2.45)	< 0.001
Serum creatinine (μmol/L)	71.00 (59.20, 85.10)	69.20 (55.00, 83.03)	0.239
eGFR (ml/min)	103.23 ± 33.54	107.36 ± 36.46	0.127
Treated	**Prior treatment**	**Post-treatment**	***p*-value**
Albumin (g/L)	25.00 (19.70, 31.85)	37.85 (30.33, 41.73)	< 0.001
24-h urine protein (g/24 h)	6.99 (4.00, 11.53)	2.18 (0.71, 4.47)	< 0.001
Cholesterol (mmol/L)	6.53 (5.25, 8.38)	5.38 (4.52, 6.75)	< 0.001
Triglyceride (mmol/L)	2.20 (1.50, 3.23)	1.69 (1.02, 2.66)	< 0.001
Serum creatinine (μmol/L)	72.00 (61.05, 93.75)	70.90 (55.00, 87.80)	0.074
eGFR (ml/min)	99.21 ± 35.84	104.73 ± 38.29	0.066
Untreated	**Prior treatment**	**Post-treatment**	***p*-value**
Albumin (g/L)	25.38 ± 7.35	35.45 ± 7.81	< 0.001
24-h urine protein (g/24 h)	6.25 (4.53, 9.47)	2.30 (0.56, 3.72)	< 0.001
Cholesterol (mmol/L)	6.12 (5.55, 7.44)	5.04 (4.30, 6.43)	0.002
Triglyceride (mmol/L)	2.20 (1.48, 3.51)	1.68 (1.08, 2.38)	0.001
Serum creatinine (μmol/L)	66.26 ± 14.34	67.90 ± 18.26	0.385
eGFR (ml/min)	112.82 ± 25.14	113.74 ± 31.08	0.901

baseline before treatment, and were statistically significant ($p < 0.001$). After treatment, the serum creatinine decreased to an average of 70.90 (55.00, 87.80) μmol/L ($p = 0.074$), and the estimated glomerular filtration rate increased to an average of 104.73 ± 38.29 ml/min ($p = 0.066$). There was no statistical significance between the above combination and the difference before treatment.

For patients who had not received immunosuppressive therapy, after treatment with MFSD, the serum albumin increased to an average of 35.45 ± 7.81 g/L, the 24-hour urinary protein quantitative mean was 2.30 (0.56, 3.72) g/24 h, the total cholesterol decreased to an average of 5.04 (4.30, 6.43) mmol/L, and the triglyceride was 1.68 (1.08, 2.38) mmol/L. There were significant differences between the above results and the baseline before treatment, and were statistically significant ($p < 0.05$). The average serum creatinine after treatment was 67.90 ± 18.26 μmol/L ($p = 0.385$), and the average estimated glomerular filtration rate was 113.74 ± 31.08 ($p = 0.901$). There was no significant difference between the above combination and before treatment (**Table 3**).

Prognostic Correlation Analysis

Patients were grouped according to whether they relieve or not. The following factors are compared between the two groups: gender, age, pathological type, nephrotic syndrome history, serum albumin before treatment, 24-h urinary protein before treatment, cholesterol before treatment, triglycerides before treatment, serum creatinine before treatment, the estimated glomerular filtration rate before treatment, immunosuppressive therapy history, and medical history. Factors with statistical differences were screened out. There were no significant differences in gender composition and mean age between the two groups ($p > 0.1$) when comparing the baseline levels of the two groups. The proportion of patients with nephrotic syndrome was significantly lower in the remission group than that in the non-remission group, and there was a significant difference between the risk ranking of the two groups ($p < 0.001$). Patients who had remission had significantly higher serum albumin levels and lower 24-hour urinary protein levels than those who did not ($p < 0.001$). The total cholesterol of patients with remission was significantly lower than that of patients without remission ($p = 0.029$). Patients who achieved remission had slightly lower triglycerides than those who did not, but the difference was not statistically significant ($p = 0.183$). In terms of renal function, there were no significant differences in serum creatinine and the estimated glomerular filtration rate between the two groups ($p > 0.1$). The mean treatment course for patients who achieved remission was significantly longer than that for those who did not ($p = 0.001$). Patients who had a previous history of hypertension achieved remission at a significantly lower rate than those who had not ($p = 0.047$). However, previous use of tacrolimus was associated with remission ($p = 0.020$) (**Supplementary Table S4**).

Previous histories of hypertension, tacrolimus, nephrotic syndrome, risk ranking, and treatment course were selected as Model A. The histories of hypertension, tacrolimus, serum albumin before treatment, 24-hour urinary protein before treatment, cholesterol before treatment, and course of treatment were used as Model B. Age, gender, history of hypertension, tacrolimus, serum albumin before treatment, 24-hour urinary protein before treatment, cholesterol before treatment, triglyceride before treatment, and the course of treatment were taken as Model C. According to the above, binary logistics regression is carried out. Based on Model A, we found that only previous use of tacrolimus, nephrotic syndrome, risk ranking, and treatment course were associated with remission from MFSD ($p < 0.05$). Using Model B, we found that only pretreatment serum albumin and duration of treatment were associated with remission from MFSD ($p < 0.05$), and tacrolimus medication history was no longer associated with remission ($p = 0.224$). Based on Model C, we found that serum albumin before treatment and the duration of treatment were still related with the remission of MFSD ($p < 0.05$; **Table 4**; **Supplementary Table S5**).

In order to further reflect the effects of serum albumin and 24-hour urinary protein quantification before treatment and treatment course on remission, we found through the ROC curve that the cutoff value of serum albumin before treatment was 22.95 g/L and the cutoff value of treatment course was 12.50 months, so 24-hour urinary protein quantification was difficult to be predicted whether patients were in remission or not (**Figure 3**).

TABLE 4 | Correlation between baseline predictors and mitigation outcomes in binary logistics regression analysis.

	Model A		Model B		Model C	
	Or (95%C.I.)	*p*-value	Or (95%C.I.)	*p*-value	Or (95%C.I.)	*p*-value
Gender					1.199 (0.517–2.782)	0.673
Age					1.000 (0.971–1.031)	0.975
Hypertension	0.609 (0.303–1.224)	0.163	0.801 (0.363–1.768)	0.583	0.783 (0.340–1.801)	0.565
Tacrolimus	0.269 (0.077–0.944)	0.040	0.435 (0.114–1.666)	0.224	0.409 (0.102–1.647)	0.209
Nephrotic Syndrome	0.346 (0.130–0.924)	0.034				
Risk Ranking	0.510 (0.284–0.915)	0.024				
Albumin (g/L)			1.096 (1.024–1.174)	0.008	1.093 (1.020–1.171)	0.012
24-h Urine Protein (g/24 h)			0.904 (0.815–1.002)	0.055	0.893 (0.802–0.994)	0.038
Cholesterol (mmol/L)			0.963 (0.810–1.144)	0.666	0.917 (0.750–1.120)	0.397
Triglyceride (mmol/L)					1.103 (0.898–1.354)	0.351
Treatment Course (Month)	1.074 (1.034–1.116)	<0.001	1.079 (1.032–1.128)	0.001	1.076 (1.028–1.127)	0.002

Safety Results

During the treatment period, no kidney damage (**Table 3**) and other adverse reactions, such as headache, nausea, and sweating, were observed in the treatment.

DISCUSSION

Although the treatment of IMN has been mature, the toxic side effects and recurrence rate are still important problems to be solved urgently (Liu et al., 2019). Moreover, for newly treated IMN patients, the most classic Italian protocol clinically used for the treatment of IMN had an overall remission rate of 58% at year 1, 54% at year 2, and 66% at year 3 (Ponticelli, 1992). The overall response rate of IMN after 1 year of cyclosporine treatment was 52% and that after 2 years of cyclosporine treatment was 20% (Fervenza, 2019). The overall response rates of IMN treated with rituximab were 60% at both year 1 and year 2 (Fervenza, 2019). The overall response rates of MFSD treatment were 53.3, 58.3, and 82.2% for year 1, year 2, and year 3, respectively. In short, the efficacy of herbal medicine for newly treated IMN patients is comparable to the current commonly used the immunosuppressive therapy regimen, and its total remission rate in the third year is much higher than that of the Italian regimen. In addition, there was no statistically significant difference between the efficacy of unremitted patients treated with immunosuppression and those who underwent initial MFSD treatment. These illustrate the advantages of the traditional Chinese medicine.

Although spontaneous remission has been reported in IMN patients with impaired renal function (Polanco et al., 2012), we classified them according to the risk level specified in the KDIGO guidelines and analyzed the number and use of previous immunosuppressive regimens. We found that 46.2% of 184 patients were at high risk, while 16.5% of these patients had unremission with two or more immunosuppressive regimens. However, we found no statistically significant correlation between previous use of immunosuppressants and whether remission was achieved with MFSD. These might prove that herbal medicine is effective in treating IMN, especially refractory IMN. On the other hand, 126 patients were treated with immunosuppressive therapy regularly, accounting for 68.5% of the total, which was higher than the 50% previously observed. This indicates that the target value of this study is accurately specified and the efficacy results have certain credibility.

In traditional Chinese medicine (TCM), there is no such disease named as “idiopathic membranous nephropathy,” as most patients have edema as the first symptom, so the disease can be classified as “edema disease” in TCM (Chen et al., 2013). Edema is due to fluid retention in the skin and subcutaneous tissue. This is a manifestation of the disturbance of the Qi-transformation function of the whole body (Wang et al., 2018). The location of this disease is on the surface. When we discuss its TCM pathogenesis, we must use modern medicine’s description of the clinical symptoms of IMN. IMN usually occurs in the elderly, with edema as the first symptom and thromboembolism (Alfaadhel and Cattran, 2015). “*Shang Han Lun*” records that “aversion to cold with fever belongs to the Yang syndrome, aversion to cold without fever belongs to the Yin syndrome.” The insidious onset of this disease, unlike other sudden onset of edema, coincides with the fact that IMN “belongs to Yin syndrome.” This is further supported by the

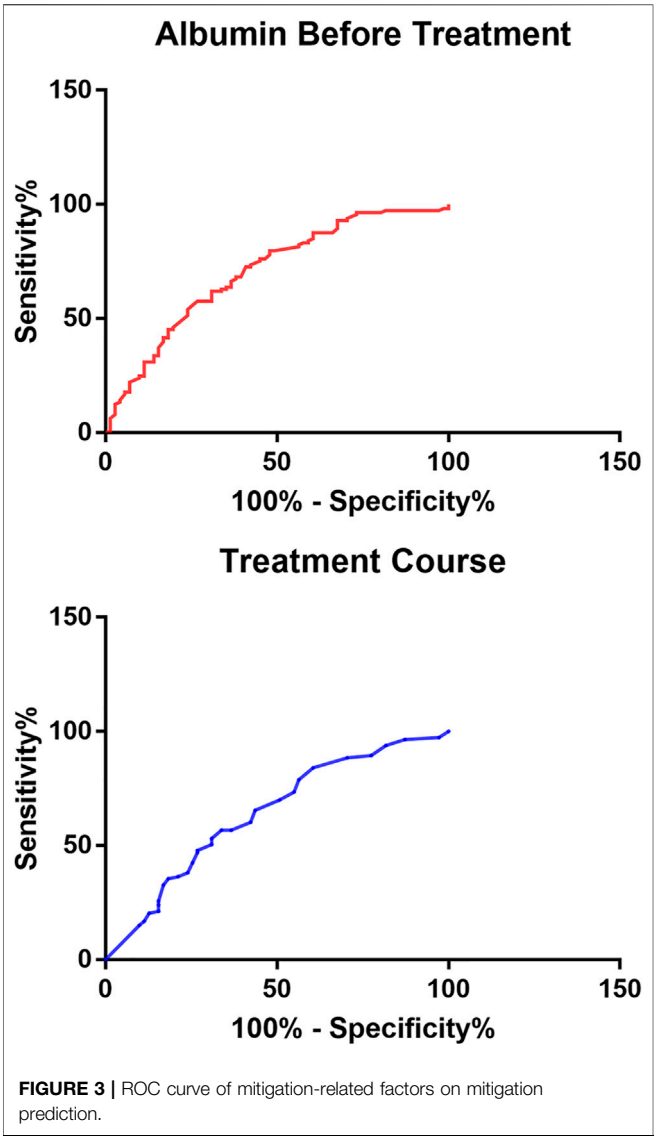

FIGURE 3 | ROC curve of mitigation-related factors on mitigation prediction.

fact that the disease is more commonly seen in the elderly (Kim et al., 2019). Thromboembolism indicates the presence of "blood stasis" in pathological products (Wang et al., 2017). Given it is Yin syndrome, the IMN patients have deficiency of Yang and excess of Yin, as the explanation in the "*Huang Di Nei Jing Su Wen*": "the excess of Yin causes internal cold, warm qi is left while cold qi stays alone, thus causing blood coagulation." To sum up, the pathogenesis of IMN is the deficiency of Yang and excess of Yin, and its pathological products are mainly water and blood stasis. According to Mr. Hu xishu's syndrome differentiation system of *the six syndromes and the eight guiding principles*, or *Liu Jing Ba Gang* in Chinese, this disease belongs to the combination of exterior Yin syndrome and interior Yin syndrome, and is distinguished as Shaoyin Taiyin syndrome (Feng and Zhang, 2011). However, MFSD is used to treat the edema of Shaoyin Taiyin syndrome in "*Jin Gui Yao Lüe*," namely, NS in modern medicine. Therefore, we compared the data in terms of whether or not there was NS.

The results of this study showed that MFSD could effectively treat IMN, and had no significant correlation with whether the presence of kidney syndrome, ineffectiveness of immunosuppressive treatment, gender, age, or previous medical history, *etc*. The following conclusions can be drawn from this study. First, this prescription can treat IMN that cannot be solved by current immunosuppressive regimens, indicating that the target of MFSD is different from or significantly exceeds that of traditional immunosuppressive regimens, which is a prototype for future ideas for new drug development. But the exact prescribing mechanism needs further study. Second, this course of treatment is the key to efficacy, which is stable after 12 months of administration. However, for each patient, the disease changes at each stage still need to be observed and analyzed to comprehensively evaluate whether there is any relapse of IMN treated by this prescription. Third, the efficacy of this prescription is related to the initial blood albumin, indicating the importance of albumin in evaluating the prognosis of patients. However, the disease remission still depends on whether the urine protein is reduced (Rojas-Rivera et al., 2019). We believe that with the development of IMN studies, the understanding of the blood albumin level will be deepened and be used as the evaluation criterion for efficacy. Finally, this subject is a single-arm clinical trial with objective performance criteria, not a randomized controlled trial, so there is a degree of bias in the data results. In the future, we will conduct a randomized controlled trial to comprehensively evaluate the difference in efficacy and safety between MFSD and IST, so as to demonstrate the advantages of TCM treatment more comprehensively.

DATA AVAILABILITY STATEMENT

The raw data supporting the conclusion of this article will be made available by the authors, without undue reservation.

ETHICS STATEMENT

The studies involving human participants were reviewed and approved by the Medical Ethics Committee of Beijing Hospital of Traditional Chinese Medicine. The patients/participants provided their written informed consent to participate in this study.

AUTHOR CONTRIBUTIONS

BL and HD were responsible for conception of the study. YG, ML, FL, XZ, ZF, AR, and XL are responsible for data analysis and interpretation. ZD was involved in drafting the manuscript. BL, XT, HJ, HR, and GL are responsible for key modifications of important content. BL and HD were responsible for approving the final version to be published and agree to be responsible for all aspects of the work and to ensure that issues relating to the accuracy or completeness of any part of the work are properly investigated and resolved. The authenticity of the original data in

this paper has been confirmed by BL and HD, and they are responsible for this.

FUNDING

This work was supported by the National Key Research and Development Project (No. 2019YFC1709402 to BL), Capital's Funds for Health Improvement and Research (No. 2020-2-2234 to BL), Research and Cultivation Program of Beijing Municipal Hospital Management Center (No. PZ2019016 to HD), and Capital clinical characteristics application research and promotion (No. Z161100000516024 to BL).

SUPPLEMENTARY MATERIAL

The Supplementary Material for this article can be found online at: https://www.frontiersin.org/articles/10.3389/fphar.2021.724744/full#supplementary-material

REFERENCES

Alfaadhel, T., and Cattran, D. (2015). Management of Membranous Nephropathy in Western Countries. *Kidney Dis. (Basel)* 1, 126–137. doi:10.1159/000437287

Chen, Y., Deng, Y., Ni, Z., Chen, N., Chen, X., Shi, W., et al. (2013). Efficacy and Safety of Traditional Chinese Medicine (Shenqi Particle) for Patients with Idiopathic Membranous Nephropathy: a Multicenter Randomized Controlled Clinical Trial. *Am. J. Kidney Dis.* 62, 1068–1076. doi:10.1053/j.ajkd.2013.05.005

Couser, W. G. (2017). Primary Membranous Nephropathy. *Clin. J. Am. Soc. Nephrol.* 12, 983–997. doi:10.2215/CJN.11761116

Feng, S. L., and Zhang, C. E. (2011). *Interpretation of Zhang Zhongjing Medical Science - Prescription of Liu Jing*. Beijing: People's Military Medical Press.

Fervenza, F. C., Appel, G. B., Barbour, S. J., Rovin, B. H., Lafayette, R. A., Aslam, N., et al. (2017). Rituximab or Cyclosporine in the Treatment of Membranous Nephropathy. *N. Engl. J. Med.* 381 (1), 36–46. doi:10.1056/NEJMoa1814427

Kanigicherla, D., Gummadova, J., McKenzie, E. A., Roberts, S. A., Harris, S., Nikam, M., et al. (2013). Anti-PLA2R Antibodies Measured by ELISA Predict Long-Term Outcome in a Prevalent Population of Patients with Idiopathic Membranous Nephropathy. *Kidney Int.* 83, 940–948. doi:10.1038/ki.2012.486

Keri, K. C., Blumenthal, S., Kulkarni, V., Beck, L., and Chongkrairatanakul, T. (2019). Primary Membranous Nephropathy: Comprehensive Review and Historical Perspective. *Postgrad. Med. J.* 95, 23–31. doi:10.1136/postgradmedj-2018-135729

Kim, Y., Yoon, H. E., Chung, B. H., Choi, B. S., Park, C. W., Yang, C. W., et al. (2019). Clinical Outcomes and Effects of Treatment in Older Patients with Idiopathic Membranous Nephropathy. *Korean J. Intern. Med.* 34, 1091–1099. doi:10.3904/kjim.2018.139

Liu, D., Yang, Y., Qing, F. S., Hu, B., and Yu, X. (2019). Risk of Infection with Different Immunosuppressive Drugs Combined with Glucocorticoids for the Treatment of Idiopathic Membranous Nephropathy: A Pairwise and Network Meta-Analysis. *Int. Immunopharmacol.* 70, 354–361. doi:10.1016/j.intimp.2019.03.002

Polanco, N., Gutiérrez, E., Rivera, F., Castellanos, I., Baltar, J., Lorenzo, D., et al. (2012). Spontaneous Remission of Nephrotic Syndrome in Membranous Nephropathy with Chronic Renal Impairment. *Nephrol. Dial. Transpl.* 27, 231–234. doi:10.1093/ndt/gfr285

Ponticelli, C., Zucchelli, P., Passerini, P., and Cesana, B. (1992). Methylprednisolone Plus Chlorambucil as Compared with Methylprednisolone Alone for the Treatment of Idiopathic Membranous Nephropathy. The Italian Idiopathic Membranous Nephropathy Treatment Study Group. *N. Engl. J. Med.* 327, 599–603. doi:10.1056/NEJM199208273270904

Rojas-Rivera, Jorge. Enrique., Carriazo, Sol., and Ortiz, Alberto. (2019). Treatment of Idiopathic Membranous Nephropathy in adults:KDIGO 2012, Cyclophosphamide and Cyclosporine A Are Out, Rituximab Is the New normal. *Clin. Kidney J.* 12, 629–638.

Ruggenenti, P., Fervenza, F. C., and Remuzzi, G. (2017). Treatment of Membranous Nephropathy: Time for a Paradigm Shift. *Nat. Rev. Nephrol.* 13, 563–579. doi:10.1038/nrneph.2017.92

U. S. Food and Drug Administration (2009). Summary of Safety and Effectiveness Data (SSED). [2013-02-21] Availableat: http://www.fda.gov/downloads/AdvisoryCommittees/CommitteesMeetingMaterials/MedicalDevices/MedicalDevicesAdvisoryCommittee/CirculatorySystemDevicesPanel/UCM152225.pdf.

Van den Brand, Jan. A. J. G., Ruggenenti, P., Chianca, A., Hofstra, J. M., Perna, A., Ruggiero, B., et al. (2017). Safety of Rituximab Compared with Steroids and Cyclophosphamide for Idiopathic Membranous Nephropathy. *J. Am. Soc. Nephrol.* 28 (9), 2729–2737. doi:10.1681/ASN.2016091022

Wang, X. Q., Wang, L., Tu, Y. C., and Zhang, Y. C. (2018). Traditional Chinese Medicine for Refractory Nephrotic Syndrome: Strategies and Promising Treatments. *Evid. Based Complement. Alternat Med.* 2018, 8746349. doi:10.1155/2018/8746349

Wang, Z., Tang, Z., Zhu, W., Ge, L., and Ge, J. (2017). Efficacy and Safety of Traditional Chinese Medicine on Thromboembolic Events in Patients with Atrial Fibrillation: A Systematic Review and Meta-Analysis. *Complement. Ther. Med.* 32, 1–10. doi:10.1016/j.ctim.2017.03.006

Xu, X., Wang, G., Chen, N., Lu, T., Nie, S., Xu, G., et al. (2016). Long-Term Exposure to Air Pollution and Increased Risk of Membranous Nephropathy in China. *J. Am. Soc. Nephrol.* 27, 3739–3746. doi:10.1681/ASN.2016010093

Conflict of Interest: The authors declare that the research was conducted in the absence of any commercial or financial relationships that could be construed as a potential conflict of interest.

Publisher's Note: All claims expressed in this article are solely those of the authors and do not necessarily represent those of their affiliated organizations, or those of the publisher, the editors, and the reviewers. Any product that may be evaluated in this article, or claim that may be made by its manufacturer, is not guaranteed or endorsed by the publisher.

frontiers in Pharmacology

REVIEW
published: 04 November 2021
doi: 10.3389/fphar.2021.774414

New Insights Into the Effects of Individual Chinese Herbal Medicines on Chronic Kidney Disease

Minghai Shao[1], *Chaoyang Ye*[1], *George Bayliss*[2] *and Shougang Zhuang*[2,3]*

[1]Department of Nephrology, Shuguang Hospital, Shanghai University of Traditional Chinese Medicine, Shanghai, China, [2]Department of Medicine, Rhode Island Hospital and Alpert Medical School, Brown University, Providence, RI, United States, [3]Department of Nephrology, Shanghai East Hospital, Tongji University School of Medicine, Shanghai, China

The clinical and experimental study into the effects of Chinese herbal medicines on chronic kidney disease has evolved over the past 40 years with new insight into their mechanism and evidence of their clinical effects. Among the many traditional Chinese herbs examined in chronic renal disease, five were found to have evidence of sufficient clinical efficacy, high frequency of use, and well-studied mechanism. They are: *Abelmoschus manihot* and *Huangkui capsule*, *Salvia miltiorrhiza* and its components (tanshinone II A, salvianolic acid A and B); *Rhizoma coptidis* and its monomer *berberine*; *Tripterygium wilfordii* and its components (triptolide, tripterygium glycosides); Kudzu root *Pueraria* and its monomer *Puerarin*. These Chinese herbal medications have pharmaceutical effects against fibrosis, inflammation and oxidative stress and also promote renal repair and regeneration. This article reviews their clinical efficacy, anti-fibrotic effects in animal models, and molecular mechanism of action.

Keywords: renal fibrosis, Chinese herbs, monomers, chronic kidney disease, *Abelmoschus manihot*, *Salvia miltiorrhiza*, therapeutic molecular mechanism

OPEN ACCESS

Edited by:
Dan-Qian Chen,
Northwest University, China

Reviewed by:
Yifei Zhong,
Longhua Hospital, China
Yue Tu,
Nanjing University of Chinese Medicine, China

***Correspondence:**
Shougang Zhuang
szhuang@lifespan.org

Specialty section:
This article was submitted to Renal Pharmacology, a section of the journal Frontiers in Pharmacology

Received: *11 September 2021*
Accepted: *20 October 2021*
Published: *04 November 2021*

Citation:
Shao M, Ye C, Bayliss G and Zhuang S (2021) New Insights Into the Effects of Individual Chinese Herbal Medicines on Chronic Kidney Disease. Front. Pharmacol. 12:774414. doi: 10.3389/fphar.2021.774414

INTRODUCTION

Chronic kidney disease (CKD) is a global public health issue, affecting more than 10% of the world's population (Glassock et al., 2017; Ruiz-Ortega et al., 2020). The burden of CKD is not only restricted to the requirement of renal replacement therapy for end stage of renal disease (ESRD), but also associated with cardiovascular events and mortality (Glassock et al., 2017). Although the etiology of CKD and pathological course are diverse, renal interstitial fibrosis and gradual loss of nephron mass are the common pathological changes. Renal fibrosis is characterized by activation of renal interstitial fibroblasts and deposition of extracellular matrix components that are driven by multiple signaling pathways, transcriptional factors, inflammatory factors, oxidative stress and vasoactive substances, including angiotensin (Liu 2011; Meng, et al., 2016; Ruiz-Ortega, et al., 2020). Current treatment of patients with CKD most still relies mostly on an angiotensin-converting enzyme inhibitor (ACEI) and an angiotensin receptor blocker (ARB), however, these drugs only ameliorate, but not halt the progression of CKD to ESRD (Ruiz-Ortega et al., 2020). The limitations of Western medicine in curing or slowing progression of CKD may drive some patients to seek alternative treatments such as Chinese herbal medicines.

Chinese herbal medicines have been extensively used to treat CKD and other chronic diseases in China and some Asian countries. However, high-quality clinical evidence is lacking to support use of Chinese herbal medicines for CKD treatment worldwide. In 2015, Lin et al., published the first population-based retrospective cohort study on the use of Chinese herbal medicine in CKD patients

(Lin et al., 2015). By searching for the Taiwan National Health Insurance Research Database from 2000 to 2005, they found that among the 24,971 study patients, 11,351 received prescribed Chinese herbal medicine after CKD diagnosis. After adjusting confounding variable, the group using Chinese herbal medicine exhibited a significantly reduced ESRD risk (60%) compared with the nonuse group. This provides solid evidence of the association between the use of Chinese herbal medicines with reduced ESRD risk in patients with CKD. Further analysis of Chinese herbal medicines used in this population of CKD patients revealed that the formulas classified as "blood-regulating," "dampness-dispelling," or "harmonizing" were strongly associated with the protection effect against CKD (Lin et al., 2015), suggesting that these classes of Chinese herbal formulas contain therapeutic components that prevent CKD progression.

A Chinese herbal medicine formula usually contains several medicinal herbs. Identifying the role of individual herbs is essential for understanding the role and mechanism of a Chinese herbal medicine formula in treating various diseases including CKD. In the past 40 years, many such studies have been conducted to search for medicinal herbs that are effective for treating CKD. Five were found to have evidence of sufficient clinical efficacy, high frequency of use, and well-studied mechanism. These herbs include *Abelmoschus Manihot*, *Salvia miltiorrhiza, Rhizoma coptidis*, *Tripterygium wilfordii*, and *Kudzu root Pueraria.* Interestingly, these five Chinese medicinal herbs are also major components in either blood-regulating, dampness-dispelling, heat-clearing, or harmonizing formula associated with beneficial effect to CKD patients as mentioned above (Lin et al., 2015). Moreover, the extract and/or monomer of these five medicinal herbs have been made and tested in animal models of CKD and/or patents with CKD (see below). A prospective, open-label, multicenter, randomized controlled trial demonstrated that Huangkui capsule, a single-plant drug extracted from the dry corolla of Flos A. Manihot, was more effective than the angiotensin-receptor blocker losartan in reducing proteinuria in patients with primary glomerular disease after 24 weeks of treatment (Zhang, et al., 2014), which resulted in its approval by the China Food and Drug Administration to treat CKD stages 1–2 with primary glomerular disease.

In this article, we review the therapeutic effect of these five medicinal herbs in animal models of CKD (**Table 1**) and their clinical efficacy in CKD patients (**Table 2**) as well as molecular mechanism of their actions. We also discuss the challenge and directions of medicinal herb research associated with CKD.

ABELMOSCHUS MANIHOT AND HUANGKUI CAPSULE

Abelmoschus manihot, also called as "*Huangkui*" in Chinese, is an annual flowering herb plant in the family of Malvaceae. As a traditional Chinese medicine (TCM), the ethanol extract of the flower in *Abelmoschus manihot* is made as *Huangkui* capsule and has been used for medication of the patients with kidney diseases. Studies have confirmed that the major pharmacologically bioactive constituents in the flower of Abelmoschus Manihot are seven flavonoids, including Rutin, Hyperoside, Hibifolin, Isoquercetin, Myricetin, Quercetin, and Quercetin-3-O-robinobioside (Guo, et al., 2015a).

Animal Studies

The biological effects of *Abelmoschus manihot* have been studied in several animal models of CKD, including 5/6 nephrectomy (Gu, et al., 2020), adriamycin-induced nephropathy (Li, et al., 2019), and streptozotocin-induced diabetic nephropathy (DN) (Liao, et al., 2019). The overall results show that treatment with *Abelmoschus Manihot* can improve kidney function, attenuate kidney damage and tubulointerstitial fibrosis, and reduce proteinuria (Cai, et al., 2017). These beneficial effects are related to inhibition of inflammation (Li, et al., 2019), anti-oxidative stress (Liao, et al., 2019), inhibiting renal epithelial-mesenchymal transition (EMT) (Gu, et al., 2020; Peng, et al., 2016), remodeling the intestinal microbiota and inhibiting micro-inflammation (Tu, et al., 2020). Mechanistically, Abelmoschus Manihot is able to suppress ROS-ERK1/2-mediated NLRP3 (NLR Family Pyrin Domain Containing 3) inflammasome activation (Li, et al., 2019), reduce tumor necrosis factor-α (TNF-α) and transforming growth factor-β1 (TGF-β1) protein expression (Tu, et al., 2013), inhibiting p38MAPK signaling pathway (Tu, et al., 2013) and autophagy-mediated macrophage polarization (Tu, et al., 2020). *Abelmoschus manihot* can also prevent glomerular podocyte apoptosis (Zhou, et al., 2012) by a mechanism associated with activating peroxisome proliferator-activated receptor (PPAR)-alpha/gamma (Ge, et al., 2016), inhibiting iRhom2/TACE signaling pathway (Liu, et al., 2017), attenuating endoplasmic reticulum stress (ERS) (Ge, et al., 2016; Liu, et al., 2017), and regulating autophagy and mitochondrial dynamics (Kim, et al., 2018). Moreover, *Abelmoschus manihot* has an ability to reduce oxidative stress and inflammation via modulation of AMPK (AMP-activated protein kinase)-Sirt1-PGC-1α (peroxisome proliferator-activated receptor-gamma coactivator-α) signaling axis (Liao, et al., 2019) and NADPH oxidase/ROS/ERK pathway (Cai, et al., 2017).

Clinical Studies

Abelmoschus manihot is one of the important drugs for the treatment of CKD. It has been reported that treatment with *Abelmoschus manihot* can reduce proteinuria and improve renal function in patients with diabetic kidney disease (DKD) (Shi, et al., 2019), IgA nephropathy (Li, et al., 2020a), and CKD stages 1–2 (Zhang, et al., 2014). In a meta-analysis identified 72 clinical investigations involving 5,895 participants. Compared to a RAS blocker alone, combined treatment of Abelmoschus Manihot with a RAS blocker was more effective in reducing 24 h urinary protein (24 h UP), urinary albumin excretion rate (UAER), and serum creatinine (SCr) levels. *Abelmoschus manihot* did not increase adverse events (Shi, et al., 2019). Recently, a multicenter randomized controlled clinical trial for determining the efficacy of Abelmoschus Manihot were conducted in a total of 417 patients with biopsy-proven primary glomerular disease (Zhang, et al., 2014) (CKD stage

TABLE 1 | Recent animal studies on Chinese herbal medicines with anti-renal fibrosis function.

Herbal/extract	Animal model	Outcome	Mechanism	Reference
Abelmoschus	5/6 nephrectomy	↓EMT	↓PI3K-Akt-eNOS, ERK1/2	Gu, et al. (2020); Peng, et al. (2016)
Manihot	ADRN	↓OX, inflammation	↓ROS-ERK1/2-NLRP3 ↓NADPH oxidase/ROS/ERK	Li, et al. (2019); Cai, et al. (2017)
	UNE-ADR	↓inflammation, glomerulosclerosis	↓TNF-α,TGF-β1, p38MAPK	Tu, et al. (2013)
	STZ-DN mice	↓OX	↑AMPK-Sirt1-PGC-1	Liao, et al. (2019)
	UNE-STZ-DN	↓podocyte apoptosis	↑PPAR-α/γ ↓ iRhom2/TACE,ERS	Ge, et al. (2016); Liu, et al. (2017)
	UNE-STZ-HFD-DN	↓podocyte loss, FN	Regulating autophagy, mitochondrial dynamics	Kim, et al. (2018)
	UPPR rat	↑intestinal microbiota ↓micro-inflammation	autophagy-mediated macrophage polarization	Tu, et al. (2020)
Salvianolic Acid A, Tanshinone IIA	5/6 nephrectomy	↓OX, inflammation	↑Akt/GSK-3β/Nrf2, BMP-7, Smad6 ↓NF-kB, p38 MAPK, TGF-β/Smads	Zhang, et al. (2019b); Zhang, et al. (2019a); Zhang, et al. (2018); Wang, et al. (2015b)
Salvianolic acid A	ADR-MCD rats	↓proteinuria, podocyte injury	↑PPAR-γ/Angptl4, Nrf2/HO-1	Wang, et al. (2019b)
Tanshinone IIA	STZ-DN	↓ERS, albuminuria	↓PERK	(Xu, et al., 2020a)
		↓pathological damage	↓OX, inflammation	Chen, et al. (2017)
Salvianolic Acid A	STZ-HFD-DN	↓OX, inflammation, endothelial permeability; ↑autophagy	↓AGE-RAGE-RhoA/ROCK, AGE-RAGE-Nox4 axis	Hou, et al. (2017)
Salvianolic Acid B	UUO rat	↓pathological damage	↓heparanase/syndecan 1	Hu, et al. (2020)
Salvianolic Acid A, C	UUO rat	↑renal function, tubular function ↓pathological damage	↓CCL5 and CXCL10	Li, et al. (2015)
Tanshinone IIA	AD-PO-UAN	↓OX	↓ NOX4, MAPK	Zhang et al. (2020c)
Salvianolic Acid B	RIRI rats	↓OX, inflammation; caspase-1-mediated pyroptosis	↑ PI3K/Akt; ↓ Nrf2 pathway	Ma et al., (2017b) Pang, et al. (2020)
Tanshinone IIA	ioversol-CIN	↓tubular necrosis, apoptosis, OX	↑ Nrf2/ARE activation	Liang, et al. (2018)
Tanshinone I	AAI-KI	↓kidney injury	↑cytochrome P450 1A	Feng, et al. (2013)
Salvianolic Acid B	FA-RTI mice	↓tubular injury	↓ ERS	Mai, et al. (2020)
Berberine	UUO rats	↓ECM, inflammation, OX	↓TGF-b1/Smad3	Wang, et al. (2014)
	DKD Murine	improve metabolism; ↓podocyte damage, glomerulosclerosis, mitochondrial dysfunction	↓mitochondrial ROS ↑PGC-1α	Qin, et al. (2020)
	STZ-DN	↓proteinuria, TIF, podocytes injury	↑AMPK phosphorylation ↓NF-k-light-chain-enhancer, TGFb1/Smad3	Sun et al. (2015); Zhang et al. (2020b) Li and Zhang, (2017)
			↑Drp1	Qin, et al. (2019)
	STZ-DN	↓inflammation	↓TLR4/NF-kB	Sun et al. (2015) Zhu et al. (2018)
	STZ-DN	↓ECM	↓Nrf2; regulating MMPs/TIMPs	Ni, et al. (2015)
	STZ-DN	↑renal pathology	↑GRKs	Wang, et al. (2013)
	SHR	↓hypertension, renal damage	↓RAS, IL-6, IL-17, IL-23	Guo, et al. (2015b)
	2K1C-RV-HTN rats	↓hypertension, sympathoexcitation	ROS/Erk1/2/iNOS	Tian, et al. (2019)
tripterygium glycosides	NUE-STZ-DN	↓glomerulosclerosis, TIF, microinflammation	↓macrophage infiltration, TNF-a, IL-1b, TGF-b1, p38 MAPK, NF-kB	Wu, et al. (2017)
Triptolide	STZ-HFD-DN	↓MA, inflammation, pathological damage	regulating Th cell balance ↓macrophage infiltration	Guo et al. (2016)
	STZ-HFD-DN	↓renal EMT	MiR-188-5p-PI3K/AKT	Xue et al. (2018)
	STZ-DN	↓renal ECM	↓microRNA-137/Notch1	Han, et al. (2018)
	STZ-DN	restoring autophagy	↓miR-141-3p/PTEN/Akt/mTOR	Li, et al. (2017b)
	UUO rats	↓inflammatory, ECM; immune activity	↓TGF-β1, CTGF, MCP1, osteopontin	Yuan, et al. (2011)
	PKD adult rats	↓disease progression; ↑renal function	↓JAK2-STAT3	Jing, et al. (2018)
	DOCA-salt hypertension	↓pathological damage	↓inflammatory	Zhang, et al. (2020a)
	FSGS rats	↓kidney injury, podocyte apoptosis	↓ IL4	Li, et al. (2020c)
Puerarin	UUO murine	↓ECM, TIF, epithelial cell apoptosis	↓NOX4; ↓phosphorylation of p38, ERK, JNK, MAPK	Zhou, et al. (2017)
	STZ-DM eNOS(−/−) mice	↓OX, albuminuria, kidney injury	↓NOX4↑; deacetylation of SIRT1-NF-κB	Li et al. (2017a); Xu, et al. (2020c)
	STZ-DN	↓pathological damage, apoptosis	↑miRNA-145-5p ↓TLR4/MyD88/NF-κB (p65)	Li et al. (2017a); Xu, et al. (2020c)
	STZ- DN mice	↓UACR, kidney injury	↑HMOX1, Sirt1-mediated podocyte autophagy	Li, et al. (2020b)
	STZ- DN rats	↓kidney hypertrophy, OX, podocyte injury	↑nephrin, podocin ↓MMP9	Zhong, et al. (2014)

(Continued on following page)

TABLE 1 | (*Continued*) Recent animal studies on Chinese herbal medicines with anti-renal fibrosis function.

Herbal/extract	Animal model	Outcome	Mechanism	Reference
	STZ-DN mice	↑autophagy, nephrin, podocin, podocalyxin	↑ PERK/eIF2α/ATF4 ↓HIF-1alpha, VEGF	Xu et al. (2020b) Shukla, et al. (2017)
	STZ-DN rats	↓renal AGEs contents	↓AGEs, RAGE	Shen, et al. (2009)

↑: increase or activation or improve; ↓: decrease or inhibition; AAI: aristolochic acid I; ADR: Adriamycin; ADRN: adriamycin nephropathy; AD-PO-UAN: adenine and potassium oxonate-induced uric acid nephropathy mice; AMPK: AMP-activated protein kinase; BMP-7: bone morphogenetic protein 7; CTGF: connective tissue growth factor; CIN: Contrast-Induced Nephropathy; DN: diabetic nephropathy; DM: diabetes mellitus; DKD: diabetic kidney disease; Drp1: dynamin-related protein 1; ECM: extracellular matrix; EMT: epithelial-mesenchymal transition; EMTD: epithelial-myofibroblast trans-*differentiation; ERS: endoplasmic reticulum stress; eNOS(−/−): endothelial nitric oxide synthase-null mice; FA-RTI: fatty acids-induced renal tubular injury; FSGS: focal segmental glomerular sclerosis; GRKs: G protein-coupled receptor kinases; HFD: high-fat diet; KI: kidney injury; MMPs: matrix metalloproteinases; MCD: minimal change disease; NF: nuclear factor; NLRP3: NLR Family Pyrin Domain Containing 3; OX: oxidative stress; PGC-1: peroxisome proliferator-activated receptor-gamma coactivator-1; PKD: polycystic kidney disease; PO: potassium oxonate; PPAR: peroxisome proliferator-activated receptor; RIRI: renal ischemia-reperfusion injury; SHR: spontaneously hypertensive rats; STZ: Streptozotocin; STZ-DN: streptozotocin induced diabetic nephropathy; STZ-HFD-DN: streptozotocin induced and high-fat diet diabetic nephropathy; UACR: urinary albumin creatinine ratio; MA: urine micro-albumin; UNE: unilateral nephrectomy; UPPR: rat models were induced by uninephrectomy, potassium oxonate, and proinflammatory diet; UUO: unilateral ureteral obstruction; TIF: tubulointerstitial fibrosis; TIMPs: tissue inhibitor of metalloproteinases; TNF-a: tumor necrosis factor-a; TGF-b1: transforming growth factor-b1; 2K1C-RV-HTN:Two-kidney, one-clip renovascular hypertensive rats.*

TABLE 2 | Clinical studies on the efficacy of CHM in the CKD.

Chinese herbal name	Disease	N	Therapeutic arms	Primary outcome	Study period	References
Abelmoschus Manihot (Huangkui capsule)	IgAN (24hUTP 0.5–3.0 g/d, eGFR≥ 45 ml/min/1.73 m^2)	1,470	Huangkui capsule/placebo vs. losartan placebo	24 h UTP (mg/d)	48 weeks	Li, et al. (2020a)
	DN	5,895	Huangkui capsule + RAS blocker vs. RAS blocker	24 hUTP (g/d); UAER (mug/min); SCr(umol/L)	Meta-Analysis	Shi, et al. (2019)
	CKD1-2, primary glomerular disease (biopsy), moderate proteinuria	417	Huangkui capsule vs. losartan vs. Huangkui capsule + losartan	24 hUTP (mg/d)	24 weeks	Zhang, et al. (2014)
Tanshinone	CKD	1,857	Tanshinone vs. control	24 hUTP (g/d); eGFR	Meta-Analysis	Zhou, et al. (2020)
Tanshinone IIA	hypertensive nephropathy	1,696	Tanshinone IIA/ARBs vs. ARBs	eGFR	Meta-Analysis	Xu, et al. (2019)
Berberine	hypertensive patients with type 2 diabetes mellitus	69	control vs. berberine add-on	UACR (μg/mg)	2 years	Dai, et al. (2015)
Tripterygium Glycosides	DN	1,810	tripterygium glycosides + ARBs vs. ARBs	24 hUTP (g/d); UAER (mg/min); SCr	Meta-Analysis	Wu, et al. (2020a)
Tripterygium Wilfordii	DKD (stage IV)	1,414	Tripterygium Wilfordii +(ARB/ACEI) vs. (ARB/ACEI)	24 hUTP (g/d); Alb(g/l); TER	Meta-Analysis	Ren, et al. (2019)
Tripterygium Preparations	CKD	4,386	Tripterygium preparations vs. placebo, standard care, or other immunosuppressive treatment	UPE; SCr(mg/dL); CR; PR; relapse	Meta-Analysis	Zhu, et al. (2013)
Tripterygium glycosides	DN	70	Tripterygium glycosides + ARBs vs. ARBs	24 h UTP	48 weeks	Lengnan, et al. (2020)
Puerarin	DN(Stage III)	669	Puerarin + ACEI vs. ACEI	UACR (mug/min)	Meta-Analysis	Wang, et al. (2015a)

24 h UTP: 24 h urinary total protein; Alb: serum albumin; ACEI: angiotensin-converting enzyme inhibitors; ARB: angiotensin receptor blockers; CKD: chronic kidney disease; CR: complete remission; DN: diabetic nephropathy; DKD: diabetic kidney disease; eGFR: estimated glomerularfiltrationrate; IgAN: IgA nephropathy; PR partial remission; RAS: renin angiotensin system; SCr: serum creatinine; TER: total effective rate; UACR: Urinary Albumin Creatinine Ratio; UAER: urinary albumin excretion rate; Tripterygium Preparations: Tripterygium glycoside tablets, Tripterygium hypoglaucum Hutch tablets, and Tripterygium granules or extracts.

1–2, with moderate proteinuria) from 26 hospitals in China. The results show that *Abelmoschus manihot* can effectively reduce urine protein, and no obvious adverse events were identified. In another multicenter randomized clinical trial, 1470 biopsy-proven IgAN patients (proteinuria between 0.5 and 3.0 g/d and eGFR of >/ = 45 ml/min/1.73 m^2 were treated with either *Abelmoschus manihot* or losartan at 1:1, observed for 48 weeks. The results indicated that the effectiveness of *Abelmoschus manihot* was similar to losartan in reducing urinary proteins (Li, et al., 2020a). The eGFR was stable and did not show a significant decline in both treatment groups during the 48-weeks follow-up. The rates of adverse events did not differ between the two treatment groups (Li, et al., 2020a). Thus, *Abelmoschus manihot* can be used to treat patients who may not tolerate ACEI/ARB due to hypotension or other disease. As such, *Abelmoschus manihot* appears effective and safe in improving proteinuria and preserve renal function in patients with CKD. The long-term benefits of *Abelmoschus manihot* in reducing the risk of progressive renal dysfunction remain unclear and need further study.

SALVIA MILTIORRHIZA AND ITS COMPONENTS: TANSHINONE AND SALVIANOLIC ACID

Salvia miltiorrhiza, also called "*Danshen*" in Chinese, is a popular Chinese herb from dried roots of *S. miltiorrhiza* Bunge, has been used for over 2,000 years for the treatment of cardiovascular diseases without obvious side effects (Yan, et al., 2018). The active ingredient of *Danshen* is tanshinone, which contains more than 50 compounds such as tanshinone I, tanshinone IIA, and tanshinone IIB as well as the water-soluble compounds salvianolic acid A (SAA), salvianolic acid B, and tanshinol (Xue, et al., 2019). Injection of Sodium tanshinone IIA sulfonate (STS), the extract of *Danshen*, has been widely used in current clinical practice in China to treat CKD in recent years.

Animal Studies

Several models of CKD were used to study the efficacy and action of mechanisms of *Salvia miltiorrhiza*. In the five-sixth nephrectomy model (Zhang, et al., 2019b) (Zhang, et al., 2019a) (Zhang, et al., 2018) (Wang, et al., 2015b), administration of Salvianolic acid A (SAA) and Tanshinone IIA were shown to attenuate oxidative stress and inflammation by activating the Akt/GSK-3beta/Nrf2 signaling pathway and up-regulation of bone morphogenetic protein 7 (BMP-7) and Smad6 as well as inhibiting NF-κB and p38 MAPK and TGF-β/Smad signaling pathways. In adriamycin (ADR)-induced minimal change disease (MCD) rat model, SAA exhibited a significant anti-proteinuria effect (Wang, et al., 2019b). In a rat model of STZ-induced diabetes, Tanshinone IIA and SAA attenuates renal damage via inhibiting oxidative stress and inflammation (Chen, et al., 2017) (Hou, et al., 2017). SAA restored glomerular endothelial permeability *via* AGE-RAGE-RhoA/ROCK and disturbed autophagy *via* AGE-RAGE-Nox4 axis (Hou, et al., 2017). Tanshinone IIA also reduced endoplasmic reticulum stress via attenuated PERK signaling activities (Xu, et al., 2020a). In UUO rats, Salvianolic acid B attenuates renal interstitial fibrosis by regulating the heparanase/syndecan-1 axis (Hu, et al., 2020), Salvianolic acid A and C reduced the secretion of renal inflammatory cytokines CCL5 and CXCL10 to protect renal function, improve tubular function and renal pathology (Li, et al., 2015). In adenine and potassium oxonate-induced uric acid nephropathy mice or renal ischemia-reperfusion injury rats, Tanshinone IIA suppressed oxidative stress-activated MAPK pathways (Zhang, et al., 2020c), and salvianolic Acid B modulates caspase-1-mediated pyroptosis *via* blocking Nrf2 Pathway (Pang, et al., 2020), suppressing oxidative stress and inflammation through activation of PI3K/Akt signaling pathway (Ma, et al., 2017b). Furthermore, tanshinone IIA attenuates contrast-induced nephropathy *via* enhancing Nrf2/ARE activation rats (Liang, et al., 2018). Tanshinone I protects mice from aristolochic acid I-induced kidney injury by induction of cytochrome P450 1A (Feng, et al., 2013). Salvianolic Acid B protects against fatty acid-induced renal tubular injury *via* inhibition of endoplasmic reticulum stress, play an important role in obesity-related kidney injury (Mai, et al., 2020). Overall, Salvia miltiorrhiza can protect against kidney disease through diverse mechanisms involved in inhibiting multiple profibrotic pathways.

Clinical Studies

Many small-clinical trials have been performed to evaluate the efficacy of *Salvia miltiorrhiza* in patients with CKD. A recent meta-analysis has summarized the results of *Salvia miltiorrhiza* (tanshinone) for CKD treatment (Zhou, et al., 2020). Twenty-one studies were reviewed in this meta-analysis, which involved 1857 patients including 954 cases from the *salvia miltiorrhiza* treatment group and 903 cases from the control group. It was found that *Salvia miltiorrhiza* could reduce urine protein levels, improve kidney function, and attenuate CKD without significant side effects. Among 21 studies included in this meta-analysis, only 2 evaluated the safety of tanshinone, tanshinone administration did not significantly the side effects.

Recently, another meta-analysis assessed the efficacy and safety of Sodium tanshinone IIA sulfonate in treatment of hypertensive nephropathy. Sixteen clinical trials involving 1,696 patients were included in this meta-analysis. It was interestingly found that a combination of Tanshinone IIA (TIIA) and angiotensin receptor blockers (ARBs) was more effective than ARB monotherapy in modulating hypertensive nephropathy (Xu, et al., 2019). This was indicated by improved eGFR and reduced urinary protein, serum creatinine, cystatin-C, and better control in systolic blood pressure (SBP) and diastolic blood pressure (DBP) in group combined with STS plus ARBs than in ARBs alone group. Thus, it appears that STS can be used as an adjuvant agent in the management of hypertensive nephropathy. Nevertheless, all included trials in this meta-analysis report were published in Chinese, sample size for individual trials were small and the treatment course was short (2–4 weeks). To achieve more conclusive results, other large-scale, multicenter, long-term and rigorously designed RCTs should be conducted in the future.

RHIZOMA COPTIDIS AND ITS COMPONENTS BERBERINE

Rhizoma coptidis is known as "*Huanglian*" in Chinese. Modern pharmacological studies have demonstrated that *Rhizoma coptidis* and its component berberine have various pharmacological activities, including anti-inflammatory, hypoglycemic, antihypertensive, antibacterial, and other effects.

Animal Studies

The potential effects of berberine on renal interstitial fibrosis has been examined in animal models of UUO, DKD and hypertensive nephropathy. In a rat model of UUO, it was found that administration of berberine (200 mg/kg per day) attenuated deposition of extracellular matrix, inhibited inflammation, reduced oxidative stress and suppressed TGFβ1/Smad3 signaling pathways (Wang, et al., 2014). In a murine model of DKD, berberine treatment was observed to reverse the disordered metabolism, podocyte damage, glomerulosclerosis, lipid accumulation, excessive generation of mitochondrial ROS,

mitochondrial dysfunction, and deficient fatty acid oxidation through a mechanism associates with inactivation of the PGC-1alpha signaling pathway (Qin, et al., 2020). Berberine could also significantly inhibited urine protein excretion, ameliorated tubulointerstitial fibrosis, protect glomerular podocytes in this model (Sun, et al., 2015, Zhang, et al., 2020b, Li and Zhang 2017, Qin, et al., 2019). The renoprotective effect of berberine is related to activating autophagy *via* AMPK phosphorylation (Zhang, et al., 2020b), inhibiting inflammation *via* suppressing TLR4/NF-κB pathway (Sun, et al., 2015) (Zhu, et al., 2018), inhibiting the Nrf2 pathway, and regulating the proteins expression of the matrix metalloproteinases (MMPs)/tissue inhibitors of metalloproteinases (TIMPs) (Ni, et al., 2015) and G protein-coupled receptor kinases (GRKs) (Wang, et al., 2013). In addition, berberine could delay the onset and attenuate the severity of hypertension, ameliorate hypertension-induced renal damage in spontaneously hypertensive rats. This action of berberine is associated with inhibition RAS activities and expression of some pre-inflammatory cytokines IL-6, IL-17, and IL-23 (Guo, et al., 2015b). The anti-hypertension and anti-inflammatory effects were also observed in two-kidney, one-clip (2K1C) renovascular hypertensive rats, associated with inhibition of the ROS/Erk1/2/iNOS pathway (Tian, et al., 2019).

Clinical Studies

Clinical studies have shown that berberine treatment is beneficial for hypertensive patients with T2DM (Dai, et al., 2015). In a 2-years random clinical trial on 69 hypertensive patients with T2DM, whose blood pressure and fasting plasma glucose were adequately controlled prior to the study, were enrolled and randomly assigned into add-on (36 cases) and control (33 cases) groups. Berberine was orally administrated to the patients in the add-on group concomitantly with standard hypotensive and hypoglycemic treatment. Adequately control of blood pressure and glucose was observed in those two groups. In the berberine add-on group of patients, a significant reduction in UACR, urinary osteopontin and KIM-1 was further observed in addition to improved renal hemodynamics, reduced renal inflammation, and oxidative stress. Therefore, berberine might be used as an alternative therapeutic strategy for the management of kidney injury. Other clinical trials are needed to investigate the efficacy of berberine in CKD induced by other etiologies.

TRIPTERYGIUM WILFORDII AND ITS COMPONENTS: TRIPTOLIDE, TRIPTERYGIUM GLYCOSIDES

Triptolide and tripterygium glycosides are the main bioactive constituents isolated from the Chinese herb *Tripterygium wilfordii*, also called as "Leigongteng." Pharmacological studies have shown that Triptolide exhibits multiple effects, including renal protective, antitumor, anti-inflammatory, immunosuppressive, cardioprotective, antiangiogenesis activities, and multiorgan toxicity effects. Triptolides have been extensively used to treat some primary and secondary kidney disease such as nephritis, minimal change disease and membranous nephropathy in humans. Its anti-fibrotic effects have been also reported in some of animal models as indicated below.

Animal Studies

In a rat model of diabetic nephropathy, tripterygium glycosides was shown to attenuate glomerulosclerosis and interstitial fibrosis and exert anti-microinflammatory effects (Wu, et al., 2017). The effect of Triptolide-elicited renoprotection in diabetic nephropathy is associated with regulating T cell balance and reducing macrophage infiltration to the kidney (Guo, et al., 2016), attenuates renal tubular EMT (Xue, et al., 2018), prevents extracellular matrix accumulation by targeting microRNA-137/Notch1 (Han, et al., 2018) and miR-141-3p/PTEN/Akt/mTOR pathway (Li, et al., 2017b). In a rat UUO model, treatment with Triptolide also decreased interstitial collagen deposition, inhibited renal interstitial fibroblast activation and suppressed production of proinflammtory and profibrogenetic factors, including TGF-β1, connective tissue growth factor (CTGF), MCP1 and osteopontin (Yuan, et al., 2011). Additionally, triptolide administration significantly delayed disease progression and improved renal function in an adult rat model of polycystic kidney disease through inhibiting the JAK2-STAT3 pathway (Jing, et al., 2018), attenuates renal damage by limiting inflammatory responses in DOCA-salt hypertension (Zhang, et al., 2020a), and inhibits podocyte apoptosis by targeting IL4 to alleviate kidney injury in FSGS rats (Li, et al., 2020c).

Clinical Studies

Two meta-analyses (Ren, et al., 2019; Wu, et al., 2020a) evaluated the clinical efficacy and safety of Tripterygium wilfordii/tripterygium glycosides combined with ARB/ACEI in the treatment of stage IV DKD. In the controlled trial (RCT), 1414 participants (Ren, et al., 2019) were evaluated in detail, and another meta-analysis included 23 studies, including a total of 1810 DN patients (Wu, et al., 2020a). Tripterygium wilfordii/tripterygium glycosides combined with ARB/ACEI significantly improved 24-h urinary total protein (24 h-UTP), urinary UAER, SCr, and albumin more than did ARB/ARB alone. Some minor side effects such as abnormal liver function tests were observed in the combined treatment group, with the risk of adverse reactions increased by 8%. Moreover, a prospective, randomized controlled trial for assessing the efficacy of tripterygium wilfordii in Stage IV-DN is still in progress (Lengnan, et al., 2020).

A systematic review and meta-analysis of Tripterygium wilfordii polyglycosides in the treatment of CKD indicate that among 75 trials that included 4,386 participants, treatment with tripterygium polyglycoside preparation reduces proteinuria, lowers serum creatinine, improves the complete remission rate by 56%, improves the complete or partial remission rate by 24%, and reduces the relapse rate by 58% (Zhu, et al., 2013). Tripterygium polyglycoside preparation group also increased liver function abnormalities and menstrual changes (Zhu, et al., 2013).

KUDZU ROOT PUERARIA AND ITS COMPONENT PUERARIN

Puerarin is natural flavonoid extracted from the Chinese medical herb Radix puerariae, also called as "*Gegen*". Many studies have demonstrated that puerarin has a renoprotective effect in animal model of AKI induced by various nephrotoxicants such as cisplatin (Wu, et al., 2020b) (Ma, et al., 2017a), methotrexate (Liu, et al., 2018), lead (Liu, et al., 2012) and carbon tetrachloride. Recently, the effect of puerarin on CKD and mechanism involved have also been examined in animal models of UUO and DA.

Animal Studies

Puerarin treatment attenuates renal tubulointerstitial fibrosis in a murine model of UUO, as evidenced by decreased the accumulation of ECM and reduced renal tubule damage. Mechanistically, puerarin inhibited renal epithelial cell apoptosis, reduced expression of NOX4 and inhibited phosphorylation of phosphorylation of p38, ERK, and JNK, three MAPK pathways associated with renal fibrosis (Zhou, et al., 2017). In a murine model of diabetic nephropathy, puerarin also exhibits a potent renoprotective and anti-fibrotic effect through a mechanism associated with suppression of NOX4 and miRNA-140-5p expression (Li, et al., 2017a; Xu, et al., 2020c), promotion of podocyte autophagy (Li, et al., 2020b), down-regulation of MMP9 (Zhong, et al., 2014), and activation of the PERK/eIF2α/ATF4 signaling pathway (Xu, et al., 2020b). In addition, puerarin also reduces the contents and expression of advanced glycation end products in the diabetic kidney (Shen, et al., 2009) and restores the expression of nephrin by inhibiting the expression of HIF-1alpha and VEGF (Shukla, et al., 2017).

Clinical Studies

A meta-analysis has assessed the beneficial and harmful effects of puerarin plus ACEI compared with ACEI alone for the treatment of individuals with stage III DN. Ten RCTs involving 669 participants were included in this meta-analysis. All trials were conducted in China and published in Chinese. Treatment of DN with puerarin plus ACEI significantly decreased the urinary albumin excretion rate (UAER) but had no effect on 24-hUTP. One trial reported abdominal discomfort and nausea (2 cases) in the treatment group. Although these studies suggest that puerarin can reduce proteinuria of individuals with stage III DN (Wang, et al., 2015a). Further clinical trials with more samples and multiple centers should be conducted to verify the beneficial results for DN.

COMMON MECHANISMS OF CHINESE HERBAL MEDICINES IN TREATING KIDNEY DISEASE

Combining the content of this article and previous literature review (Zhao, et al., 2020; Zhong, et al., 2013), we identify that eight Chinese herbal medicine have anti-inflammatory, anti-oxidant, anti-apoptotic effects, reducing extracellular matrix deposition, and anti-fibrosis. Among them, *Salvia miltiorrhiza, Rhizoma coptidis, Abelmoschus manihot* can interrupt almost all the processes leading to renal fibrogenesis. A summary of the common mechanisms of these Chinese herbal medicines in the treatment of kidney diseases is shown in **Figure 1**.

CONCLUSION AND PERSPECTIVE

Although preclinical animal studies often indicate therapeutic benefits of Chinese herbal medicine in models of CKD, convincing evidence for or against Chinese herbal medicine for patients with CKD is limited. Here we summerized recent advances on the therapeutic effect of five Chinese herbal compounds, either single-herbal or monomer, on CKD. Their anti-fibrotic effects are involved in the regulation of immunity, alteration of hemodynamic changes, anti-oxidative stress and fibrosis. Clearly, more research is needed to identify the active ingredients of herbal medicines effective for the treatment of CKD and the mechanism of action involved. Determination of a monomer with definite curative effect and mechanism of action, and optimization of the formulation of TCM through modern scientific research will further improve and confirm the clinical curative effect. Below are several issues that should be considered.

First, clinical efficacy research should be strengthened. Although some single Chinese medicines or monomers have conducted RCT studies and meta-analysis, such as "Huangkui" capsules, most others have only small samples of clinical controlled observations, such as berberine. Therefore, a large-sample, long-period RCT studies should be initiated on the basis of physicians' personal clinical experience and small-sample clinical observations to confirm the clinical efficacy of TCM against renal fibrosis.

Second, mechanism study should be focused on the most critical action of mechanism in a given drug. For example, tanshinone IIA, berberine, and triptolide all have anti-inflammatory and anti-oxidant actions, but it remain unclear which herb is stronger in those actions. Puerarin has anti-inflammatory and antioxidant effects, regulating podocyte autophagy, tubular epithelial cell autophagy and apoptosis. It is unknown which is the most critical action of puerarin against renal fibrosis. A recent study (Zhong, et al., 2019) showing that arctigenin attenuates diabetic kidney disease through the activation of PP2A in podocytes gives us a good example and enlightenment to pursue in depth understanding of modern pharmacology of Chinese herbal medicine.

Third, the role and action of mechanism of monomer compounds need to be explored in depth**.** The research on the combination of Chinese medicine monomers is worth of exploration in the future. *Salvia miltiorrhiza* and *Rhizoma coptidis* often appear in one prescription of Chinese herbal medicine to treat CKD such as Shenshuaining Capsule (Cui, et al., 2016), Yishen Zhishuai Granules and Shenshuai II Recipe (Wang, et al., 2019a). According to the classic theory of Chinese traditional Medicine, *Rhizoma coptidis* is capable of clearing heat and dampness, purging fire and detoxification, as well as inducing Qi, whereas *Salvia miltiorrhiza* has an ability to activate blood and remove stasis as well as cool blood and detoxify. The combination of these two herbs can act in concert to eliminate

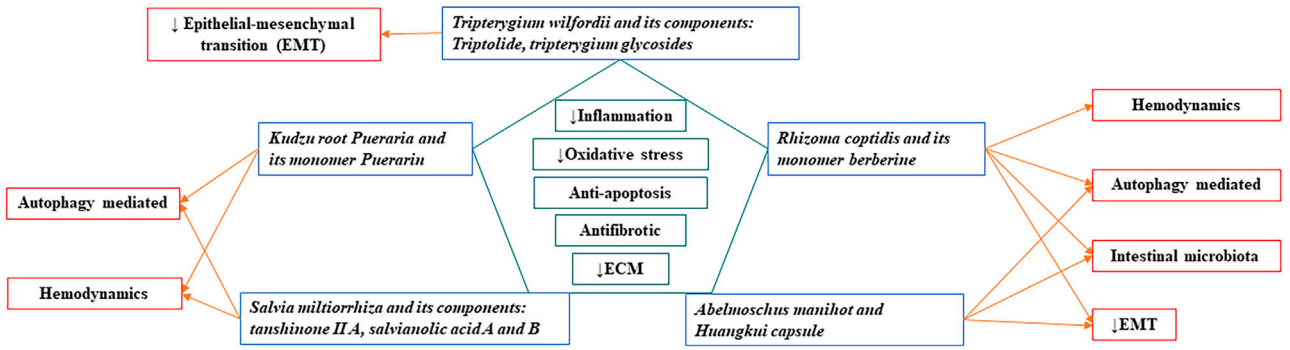

FIGURE 1 | Common mechanisms of Chinese herbal medicines in treating kidney disease.

the most common pathogenic syndromes of CKD, such as dampness, heat, blood stasis, and toxicity. Future research is necessary to explore the synergistic effect and mechanism of berberine and salvianolic acid on renal fibrosis in order to further elucidate the clinical significance and mechanism of action of *Salvia miltiorrhiza* and *Rhizoma coptidis*.

Fourth, the systems approach is necessary for exploring the synergistic effects of TCM in kidney disease. The systems approach in TCM is a methodology that combines computational and experimental tools to discover novel therapeutic agents, identify their candidate targets, and understand their therapeutic mechanisms. Traditional medicine often is a mixed formula composing of several types of herbs, and a formula with mixed herbs usually works better than single ones. However, the mechanism of action of individual herbs and their synergistic effects in a formula are frequently unknown, thus, the systems approach should be utilized to analyze the interactions among compounds in order to determine the synergistic effects of TCM in a given formula. To achieve this goal, we need to 1) identify the active ingredients from traditional medicine mixtures using modern technologies such as gas chromatography-mass spectrometr, 2) identify targets of active ingredients by developing predictive network models and analyzing the complex interactions among herbs, compounds, herb-target, and compound-target networks. 3) determine the biological activity and toxicity profile of individual active compounds and multiple ingredients in diverse combinations using both *in vitro* techniques and animal models of kidney disease, 4) elucidate the action of mechanism of each active compounds and their synergistic effects by using advanced systems approaches such as mass spectrometry and affymetrix microarrays for gene expression analysis, and 5) conduct clinical trial to assess the therapeutic effect of single active compounds and multiple ingredients with different combinations.

AUTHOR CONTRIBUTIONS

MS and CY drafted the manuscript, SZ and GB edited it. All the authors approved it for publication.

FUNDING

This project is supported by the National Natural Science Foundation of China (2020-81973807 to MS; 81670623 and 81830021 to SZ); State Outstanding Talents of Traditional Chinese Medicine Project of National Administration of Traditional Chinese Medicine (NATCM:2017-124 to MS); National key R&D Program of China (2018YFA0108802 to SZ), and US National Institutes of Health (2R01DK08506505A1 to SZ).

REFERENCES

Cai, H. D., Su, S. L., Qian, D. W., Guo, S., Tao, W. W., Cong, X. D., et al. (2017). Renal Protective Effect and Action Mechanism of Huangkui Capsule and its Main Five Flavonoids. *J. Ethnopharmacol* 206, 152–159. doi:10.1016/j.jep.2017.02.046

Chen, X., Wu, R., Kong, Y., Yang, Y., Gao, Y., Sun, D., et al. (2017). Tanshinone IIA Attenuates Renal Damage in STZ-Induced Diabetic Rats via Inhibiting Oxidative Stress and Inflammation. *Oncotarget* 8, 31915–31922. doi:10.18632/oncotarget.16651

Cui, R. Z., Xie, Y. M., Liao, X., and Wang, J. D. (2016). Shenshuaining Capsules as Adjuvant Treatment for Chronic Renal Failure: Systematic Review and Meta-Analysis of Randomized Controlled Trials]: Systematic Review and Meta-Analysis of Randomized Controlled Trials. *Zhongguo Zhong Yao Za Zhi* 41, 2149–2161. doi:10.4268/cjcmm20161128

Dai, P., Wang, J., Lin, L., Zhang, Y., and Wang, Z. (2015). Renoprotective Effects of Berberine as Adjuvant Therapy for Hypertensive Patients with Type 2 Diabetes Mellitus: Evaluation via Biochemical Markers and Color Doppler Ultrasonography. *Exp. Ther. Med.* 10, 869–876. doi:10.3892/etm.2015.2585

Feng, C., Xie, X., Wu, M., Li, C., Gao, M., Liu, M., et al. (2013). Tanshinone I Protects Mice from Aristolochic Acid I-Induced Kidney Injury by Induction of CYP1A. *Environ. Toxicol. Pharmacol.* 36, 850–857. doi:10.1016/j.etap.2013.07.017

Ge, J., Miao, J. J., Sun, X. Y., and Yu, J. Y. (2016). Huangkui Capsule, an Extract from Abelmoschus Manihot (L.) Medic, Improves Diabetic Nephropathy via Activating Peroxisome Proliferator-Activated Receptor (PPAR)-α/γ and Attenuating Endoplasmic Reticulum Stress in Rats. *J. Ethnopharmacol* 189, 238–249. doi:10.1016/j.jep.2016.05.033

Glassock, R. J., Warnock, D. G., and Delanaye, P. (2017). The Global burden of Chronic Kidney Disease: Estimates, Variability and Pitfalls. *Nat. Rev. Nephrol.* 13, 104–114. doi:10.1038/nrneph.2016.163

Gu, L., Hong, F., Fan, K., Zhao, L., Zhang, C., Yu, B., et al. (2020). Integrated Network Pharmacology Analysis and Pharmacological Evaluation to Explore the Active Components and Mechanism of Abelmoschus Manihot (L.) Medik. On Renal Fibrosis. *Drug Des. Devel Ther.* 14, 4053–4067. doi:10.2147/DDDT.S264898

Guo, H., Pan, C., Chang, B., Wu, X., Guo, J., Zhou, Y., et al. (2016). Triptolide Improves Diabetic Nephropathy by Regulating Th Cell Balance and Macrophage Infiltration in Rat Models of Diabetic Nephropathy. *Exp. Clin. Endocrinol. Diabetes* 124, 389–398. doi:10.1055/s-0042-106083

Guo, J. M., Lu, Y. W., Shang, E. X., Li, T., Liu, Y., Duan, J. A., et al. (2015a). Metabolite Identification Strategy of Non-targeted Metabolomics and its Application for the Identification of Components in Chinese Multicomponent Medicine Abelmoschus Manihot L. *Phytomedicine* 22, 579–587. doi:10.1016/j.phymed.2015.02.002

Guo, Z., Sun, H., Zhang, H., and Zhang, Y. (2015b). Anti-hypertensive and Renoprotective Effects of Berberine in Spontaneously Hypertensive Rats. *Clin. Exp. Hypertens.* 37, 332–339. doi:10.3109/10641963.2014.972560

Han, F., Wang, S., Chang, Y., Li, C., Yang, J., Han, Z., et al. (2018). Triptolide Prevents Extracellular Matrix Accumulation in Experimental Diabetic Kidney Disease by Targeting microRNA-137/Notch1 Pathway. *J. Cel Physiol* 233, 2225–2237. doi:10.1002/jcp.26092

Hou, B., Qiang, G., Zhao, Y., Yang, X., Chen, X., Yan, Y., et al. (2017). Salvianolic Acid A Protects against Diabetic Nephropathy through Ameliorating Glomerular Endothelial Dysfunction via Inhibiting AGE-RAGE Signaling. *Cell Physiol Biochem* 44, 2378–2394. doi:10.1159/000486154

Hu, Y., Wang, M., Pan, Y., Li, Q., and Xu, L. (2020). Salvianolic Acid B Attenuates Renal Interstitial Fibrosis by Regulating the HPSE/SDC1 axis. *Mol. Med. Rep.* 22, 1325–1334. doi:10.3892/mmr.2020.11229

Jing, Y., Wu, M., Zhang, D., Chen, D., Yang, M., Mei, S., et al. (2018). Triptolide Delays Disease Progression in an Adult Rat Model of Polycystic Kidney Disease through the JAK2-STAT3 Pathway. *Am. J. Physiol. Ren. Physiol* 315, F479–F486. doi:10.1152/ajprenal.00329.2017

Kim, H., Dusabimana, T., Kim, S. R., Je, J., Jeong, K., Kang, M. C., et al. (2018). Supplementation of Abelmoschus Manihot Ameliorates Diabetic Nephropathy and Hepatic Steatosis by Activating Autophagy in Mice. *Nutrients* 10. doi:10.3390/nu10111703

Lengnan, X., Ban, Z., Haitao, W., Lili, L., Aiqun, C., Huan, W., et al. (2020). Tripterygium Wilfordii Hook F Treatment for Stage IV Diabetic Nephropathy: Protocol for a Prospective, Randomized Controlled Trial. *Biomed. Res. Int.* 2020, 9181037. doi:10.1155/2020/9181037

Li, J., Gu, T., Fu, X., and Zhao, R. (2015). Effect of Salvianolic Acid A and C Compatibility on Inflammatory Cytokines in Rats with Unilateral Ureteral Obstruction. *J. Tradit Chin. Med.* 35, 564–570. doi:10.1016/s0254-6272(15)30140-0

Li, P., Lin, H., Ni, Z., Zhan, Y., He, Y., Yang, H., et al. (2020a). Efficacy and Safety of Abelmoschus Manihot for IgA Nephropathy: A Multicenter Randomized Clinical Trial. *Phytomedicine* 76, 153231. doi:10.1016/j.phymed.2020.153231

Li, W., He, W., Xia, P., Sun, W., Shi, M., Zhou, Y., et al. (2019). Total Extracts of Abelmoschus Manihot L. Attenuates Adriamycin-Induced Renal Tubule Injury via Suppression of ROS-Erk1/2-Mediated NLRP3 Inflammasome Activation. *Front. Pharmacol.* 10, 567. doi:10.3389/fphar.2019.00567

Li, X., Cai, W., Lee, K., Liu, B., Deng, Y., Chen, Y., et al. (2017a). Puerarin Attenuates Diabetic Kidney Injury through the Suppression of NOX4 Expression in Podocytes. *Sci. Rep.* 7, 14603. doi:10.1038/s41598-017-14906-8

Li, X., Zhu, Q., Zheng, R., Yan, J., Wei, M., Fan, Y., et al. (2020b). Puerarin Attenuates Diabetic Nephropathy by Promoting Autophagy in Podocytes. *Front. Physiol.* 11, 73. doi:10.3389/fphys.2020.00073

Li, X. Y., Wang, S. S., Han, Z., Han, F., Chang, Y. P., Yang, Y., et al. (2017b). Triptolide Restores Autophagy to Alleviate Diabetic Renal Fibrosis through the miR-141-3p/PTEN/Akt/mTOR Pathway. *Mol. Ther. Nucleic Acids* 9, 48–56. doi:10.1016/j.omtn.2017.08.011

Li, Y., Jiang, X., Song, L., Yang, M., and Pan, J. (2020c). Anti-apoptosis Mechanism of Triptolide Based on Network Pharmacology in Focal Segmental Glomerulosclerosis Rats. *Biosci. Rep.* 40. doi:10.1042/BSR20192920

Li, Z., and Zhang, W. (2017). Protective Effect of Berberine on Renal Fibrosis Caused by Diabetic Nephropathy. *Mol. Med. Rep.* 16, 1055–1062. doi:10.3892/mmr.2017.6707

Liang, R., Zhao, Q., Jian, G., Cheng, D., Wang, N., Zhang, G., et al. (2018). Tanshinone IIA Attenuates Contrast-Induced Nephropathy via Nrf2 Activation in Rats. *Cel Physiol Biochem* 46, 2616–2623. doi:10.1159/000489688

Liao, Z., Zhang, J., Wang, J., Yan, T., Xu, F., Wu, B., et al. (2019). The Anti-nephritic Activity of a Polysaccharide from Okra (Abelmoschus Esculentus (L.) Moench) via Modulation of AMPK-Sirt1-PGC-1α Signaling axis Mediated Anti-oxidative in Type 2 Diabetes Model Mice. *Int. J. Biol. Macromol* 140, 568–576. doi:10.1016/j.ijbiomac.2019.08.149

Lin, M. Y., Chiu, Y. W., Chang, J. S., Lin, H. L., Lee, C. T., Chiu, G. F., et al. (2015). Association of Prescribed Chinese Herbal Medicine Use with Risk of End-Stage Renal Disease in Patients with Chronic Kidney Disease. *Kidney Int.* 88, 1365–1373. doi:10.1038/ki.2015.226

Liu, C. M., Ma, J. Q., and Sun, Y. Z. (2012). Puerarin Protects Rat Kidney from lead-induced Apoptosis by Modulating the PI3K/Akt/eNOS Pathway. *Toxicol. Appl. Pharmacol.* 258, 330–342. doi:10.1016/j.taap.2011.11.015

Liu, Q., Liu, Z., Huo, X., Wang, C., Meng, Q., Sun, H., et al. (2018). Puerarin Improves Methotrexate-Induced Renal Damage by Up-Regulating Renal Expression of Oat1 and Oat3 *In Vivo* and *In Vitro*. *Biomed. Pharmacother.* 103, 915–922. doi:10.1016/j.biopha.2018.04.122

Liu, S., Ye, L., Tao, J., Ge, C., Huang, L., and Yu, J. (2017). Total Flavones of Abelmoschus Manihot Improve Diabetic Nephropathy by Inhibiting the iRhom2/TACE Signalling Pathway Activity in Rats. *Pharm. Biol.* 56, 1–11. doi:10.1080/13880209.2017.1412467

Liu, Y. (2011). Cellular and Molecular Mechanisms of Renal Fibrosis. *Nat. Rev. Nephrol.* 7, 684–696. doi:10.1038/nrneph.2011.149

Ma, X., Yan, L., Zhu, Q., and Shao, F. (2017a). Puerarin Attenuates Cisplatin-Induced Rat Nephrotoxicity: The Involvement of TLR4/NF-Kb Signaling Pathway. *PLoS One* 12, e0171612. doi:10.1371/journal.pone.0171612

Ma, Z. G., Xia, H. Q., Cui, S. L., and Yu, J. (2017b). Attenuation of Renal Ischemic Reperfusion Injury by Salvianolic Acid B via Suppressing Oxidative Stress and Inflammation through PI3K/Akt Signaling Pathway. *Braz. J. Med. Biol. Res.* 50, e5954. doi:10.1590/1414-431X20175954

Mai, X., Yin, X., Chen, P., and Zhang, M. (2020). Salvianolic Acid B Protects against Fatty Acid-Induced Renal Tubular Injury via Inhibition of Endoplasmic Reticulum Stress. *Front. Pharmacol.* 11, 574229. doi:10.3389/fphar.2020.574229

Meng, X. M., Nikolic-Paterson, D. J., and Lan, H. Y. (2016). TGF-β: the Master Regulator of Fibrosis. *Nat. Rev. Nephrol.* 12, 325–338. doi:10.1038/nrneph.2016.48

Ni, W. J., Ding, H. H., Zhou, H., Qiu, Y. Y., and Tang, L. Q. (2015). Renoprotective Effects of Berberine through Regulation of the MMPs/TIMPs System in Streptozocin-Induced Diabetic Nephropathy in Rats. *Eur. J. Pharmacol.* 764, 448–456. doi:10.1016/j.ejphar.2015.07.040

Pang, Y., Zhang, P. C., Lu, R. R., Li, H. L., Li, J. C., Fu, H. X., et al. (2020). Andrade-Oliveira Salvianolic Acid B Modulates Caspase-1-Mediated Pyroptosis in Renal Ischemia-Reperfusion Injury via Nrf2 Pathway. *Front. Pharmacol.* 11, 541426. doi:10.3389/fphar.2020.541426

Peng, C. H., Chyau, C. C., Wang, C. J., Lin, H. T., Huang, C. N., and Ker, Y. B. (2016). Abelmoschus Esculentus Fractions Potently Inhibited the Pathogenic Targets Associated with Diabetic Renal Epithelial to Mesenchymal Transition. *Food Funct.* 7, 728–740. doi:10.1039/c5fo01214g

Qin, X., Jiang, M., Zhao, Y., Gong, J., Su, H., Yuan, F., et al. (2020). Berberine Protects against Diabetic Kidney Disease via Promoting PGC-1α-Regulated Mitochondrial Energy Homeostasis. *Br. J. Pharmacol.* 177, 3646–3661. doi:10.1111/bph.14935

Qin, X., Zhao, Y., Gong, J., Huang, W., Su, H., Yuan, F., et al. (2019). Berberine Protects Glomerular Podocytes via Inhibiting Drp1-Mediated Mitochondrial Fission and Dysfunction. *Theranostics* 9, 1698–1713. doi:10.7150/thno.30640

Ren, D., Zuo, C., and Xu, G. (2019). Clinical Efficacy and Safety of Tripterygium Wilfordii Hook in the Treatment of Diabetic Kidney Disease Stage IV: A Meta-Analysis of Randomized Controlled Trials. *Medicine (Baltimore)* 98, e14604. doi:10.1097/MD.0000000000014604

Ruiz-Ortega, M., Rayego-Mateos, S., Lamas, S., Ortiz, A., and Rodrigues-Diez, R. R. (2020). Targeting the Progression of Chronic Kidney Disease. *Nat. Rev. Nephrol.* 16, 269–288. doi:10.1038/s41581-019-0248-y

Shen, J. G., Yao, M. F., Chen, X. C., Feng, Y. F., Ye, Y. H., and Tong, Z. H. (2009). Effects of Puerarin on Receptor for Advanced Glycation End Products in Nephridial Tissue of Streptozotocin-Induced Diabetic Rats. *Mol. Biol. Rep.* 36, 2229–2233. doi:10.1007/s11033-008-9438-6

Shi, L., Feng, L., Zhang, M., Li, X., Yang, Y., Zhang, Y., et al. (2019). Abelmoschus Manihot for Diabetic Nephropathy: A Systematic Review and Meta-Analysis. *Evid. Based Complement. Alternat Med.* 2019, 9679234. doi:10.1155/2019/9679234

Shukla, R., Pandey, N., Banerjee, S., and Tripathi, Y. B. (2017). Effect of Extract of Pueraria Tuberosa on Expression of Hypoxia Inducible Factor-1α and Vascular Endothelial Growth Factor in Kidney of Diabetic Rats. *Biomed. Pharmacother.* 93, 276–285. doi:10.1016/j.biopha.2017.06.045

Sun, S. F., Zhao, T. T., Zhang, H. J., Huang, X. R., Zhang, W. K., Zhang, L., et al. (2015). Renoprotective Effect of Berberine on Type 2 Diabetic Nephropathy in Rats. *Clin. Exp. Pharmacol. Physiol.* 42, 662–670. doi:10.1111/1440-1681.12402

Tian, H., Kang, Y. M., Gao, H. L., Shi, X. L., Fu, L. Y., Li, Y., et al. (2019). Chronic Infusion of Berberine into the Hypothalamic Paraventricular Nucleus Attenuates Hypertension and Sympathoexcitation via the ROS/Erk1/2/iNOS Pathway. *Phytomedicine* 52, 216–224. doi:10.1016/j.phymed.2018.09.206

Tu, Y., Fang, Q. J., Sun, W., Liu, B. H., Liu, Y. L., Wu, W., et al. (2020). Total Flavones of Abelmoschus Manihot Remodels Gut Microbiota and Inhibits Microinflammation in Chronic Renal Failure Progression by Targeting Autophagy-Mediated Macrophage Polarization. *Front. Pharmacol.* 11, 566611. doi:10.3389/fphar.2020.566611

Tu, Y., Sun, W., Wan, Y. G., Che, X. Y., Pu, H. P., Yin, X. J., et al. (2013). Huangkui Capsule, an Extract from Abelmoschus Manihot (L.) Medic, Ameliorates Adriamycin-Induced Renal Inflammation and Glomerular Injury via Inhibiting p38MAPK Signaling Pathway Activity in Rats. *J. Ethnopharmacol* 147, 311–320. doi:10.1016/j.jep.2013.03.006

Wang, B., Chen, S., Yan, X., Li, M., Li, D., Lv, P., et al. (2015a). The Therapeutic Effect and Possible Harm of Puerarin for Treatment of Stage III Diabetic Nephropathy: a Meta-Analysis. *Altern. Ther. Health Med.* 21, 36–44.

Wang, D. T., Huang, R. H., Cheng, X., Zhang, Z. H., Yang, Y. J., and Lin, X. (2015b). Tanshinone IIA Attenuates Renal Fibrosis and Inflammation via Altering Expression of TGF-β/Smad and NF-Kb Signaling Pathway in 5/6 Nephrectomized Rats. *Int. Immunopharmacol* 26, 4–12. doi:10.1016/j.intimp.2015.02.027

Wang, F. L., Tang, L. Q., Yang, F., Zhu, L. N., Cai, M., and Wei, W. (2013). Renoprotective Effects of Berberine and its Possible Molecular Mechanisms in Combination of High-Fat Diet and Low-Dose Streptozotocin-Induced Diabetic Rats. *Mol. Biol. Rep.* 40, 2405–2418. doi:10.1007/s11033-012-2321-5

Wang, F. M., Yang, Y. J., Ma, L. L., Tian, X. J., and He, Y. Q. (2014). Berberine Ameliorates Renal Interstitial Fibrosis Induced by Unilateral Ureteral Obstruction in Rats. *Nephrology (Carlton)* 19, 542–551. doi:10.1111/nep.12271

Wang, M., Yang, L., Yang, J., and Wang, C. (2019a). Shen Shuai IIRecipe Attenuates Renal Injury and Fibrosis in Chronic Kidney Disease by Regulating NLRP3 Inflammasome and Sirt1/Smad3 Deacetylation Pathway. *BMC Complement. Altern. Med.* 19, 107. doi:10.1186/s12906-019-2524-6

Wang, X., Qi, D., Fu, F., Li, X., Liu, Y., Ji, K., et al. (2019b). Therapeutic and Antiproteinuric Effects of Salvianolic Acid A in Combined with Low-Dose Prednisone in Minimal Change Disease Rats: Involvement of PPARγ/Angptl4 and Nrf2/HO-1 Pathways. *Eur. J. Pharmacol.* 858, 172342. doi:10.1016/j.ejphar.2019.04.023

Wu, W., Yang, J. J., Yang, H. M., Huang, M. M., Fang, Q. J., Shi, G., et al. (2017). Multi-glycoside of Tripterygium Wilfordii Hook. F. Attenuates Glomerulosclerosis in a Rat Model of Diabetic Nephropathy by Exerting Anti-microinflammatory Effects without Affecting Hyperglycemia. *Int. J. Mol. Med.* 40, 721–730. doi:10.3892/ijmm.2017.3068

Wu, X., Huang, Y., Zhang, Y., He, C., Zhao, Y., Wang, L., et al. (2020a). Efficacy of Tripterygium Glycosides Combined with ARB on Diabetic Nephropathy: a Meta-Analysis. *Biosci. Rep.* 40. doi:10.1042/BSR20202391

Wu, Z., Li, C., Li, Q., Li, J., and Lu, X. (2020b). Puerarin Alleviates Cisplatin-Induced Acute Renal Damage and Upregulates microRNA-31-Related Signaling. *Exp. Ther. Med.* 20, 3122–3129. doi:10.3892/etm.2020.9081

Xu, J., Zhang, C., Shi, X., Li, J., Liu, M., Jiang, W., et al. (2019). Efficacy and Safety of Sodium Tanshinone IIA Sulfonate Injection on Hypertensive Nephropathy: A Systematic Review and Meta-Analysis. *Front. Pharmacol.* 10, 1542. doi:10.3389/fphar.2019.01542

Xu, S., He, L., Ding, K., Zhang, L., Xu, X., Wang, S., et al. (2020a). Tanshinone IIA Ameliorates Streptozotocin-Induced Diabetic Nephropathy, Partly by Attenuating PERK Pathway-Induced Fibrosis. *Drug Des. Devel Ther.* 14, 5773–5782. doi:10.2147/DDDT.S257734

Xu, X., Chen, B., Huang, Q., Wu, Y., and Liang, T. (2020b). The Effects of Puerarin on Autophagy through Regulating of the PERK/eIF2α/ATF4 Signaling Pathway Influences Renal Function in Diabetic Nephropathy. *Diabetes Metab. Syndr. Obes.* 13, 2583–2592. doi:10.2147/DMSO.S256457

Xu, Y., Xiong, Y., Xu, C., and Xu, C. (2020c). Standard Puerarin Prevents Diabetic Renal Damage by Inhibiting miRNA-140-5p Expression. *Diabetes Metab. Syndr. Obes.* 13, 3947–3958. doi:10.2147/dmso.S273952

Xue, J., Jin, X., Wan, X., Yin, X., Fang, M., Liu, T., et al. (2019). Effects and Mechanism of Tanshinone II A in Proliferation, Apoptosis, and Migration of Human Colon Cancer Cells. *Med. Sci. Monit.* 25, 4793–4800. doi:10.12659/msm.914446

Xue, M., Cheng, Y., Han, F., Chang, Y., Yang, Y., Li, X., et al. (2018). Triptolide Attenuates Renal Tubular Epithelial-Mesenchymal Transition via the MiR-188-5p-Mediated PI3K/AKT Pathway in Diabetic Kidney Disease. *Int. J. Biol. Sci.* 14, 1545–1557. doi:10.7150/ijbs.24032

Yan, S. H., Zhao, N. W., Geng, Z. R., Shen, J. Y., Liu, F. M., Yan, D., et al. (2018). Modulations of Keap1-Nrf2 Signaling axis by TIIA Ameliorated the Oxidative Stress-Induced Myocardial Apoptosis. *Free Radic. Biol. Med.* 115, 191–201. doi:10.1016/j.freeradbiomed.2017.12.001

Yuan, X. P., He, X. S., Wang, C. X., Liu, L. S., and Fu, Q. (2011). Triptolide Attenuates Renal Interstitial Fibrosis in Rats with Unilateral Ureteral Obstruction. *Nephrology (Carlton)* 16, 200–210. doi:10.1111/j.1440-1797.2010.01359.x

Zhang, G., Cui, G., Tong, S., and Cao, Q. (2019a). Salvianolic Acid A Alleviates the Renal Damage in Rats with Chronic Renal Failure1. *Acta Cir Bras* 34, e201900204. doi:10.1590/s0102-8650201900204

Zhang, H. F., Wang, J. H., Wang, Y. L., Gao, C., Gu, Y. T., Huang, J., et al. (2019b). Salvianolic Acid A Protects the Kidney against Oxidative Stress by Activating the Akt/GSK-3β/Nrf2 Signaling Pathway and Inhibiting the NF-Kb Signaling Pathway in 5/6 Nephrectomized Rats. *Oxid Med. Cel Longev* 2019, 2853534. doi:10.1155/2019/2853534

Zhang, H. F., Wang, Y. L., Gao, C., Gu, Y. T., Huang, J., Wang, J. H., et al. (2018). Salvianolic Acid A Attenuates Kidney Injury and Inflammation by Inhibiting NF-Kb and P38 MAPK Signaling Pathways in 5/6 Nephrectomized Rats. *Acta Pharmacol. Sin* 39, 1855–1864. doi:10.1038/s41401-018-0026-6

Zhang, J., Zhu, M., Zhang, S., Xie, S., Gao, Y., and Wang, Y. (2020a). Triptolide Attenuates Renal Damage by Limiting Inflammatory Responses in DOCA-Salt Hypertension. *Int. Immunopharmacol* 89, 107035. doi:10.1016/j.intimp.2020.107035

Zhang, L., Li, P., Xing, C. Y., Zhao, J. Y., He, Y. N., Wang, J. Q., et al. (2014). Efficacy and Safety of Abelmoschus Manihot for Primary Glomerular Disease: a Prospective, Multicenter Randomized Controlled Clinical Trial. *Am. J. Kidney Dis.* 64, 57–65. doi:10.1053/j.ajkd.2014.01.431

Zhang, M., Zhang, Y., Xiao, D., Zhang, J., Wang, X., Guan, F., et al. (2020b). Highly Bioavailable Berberine Formulation Ameliorates Diabetic Nephropathy through the Inhibition of Glomerular Mesangial Matrix Expansion and the Activation of Autophagy. *Eur. J. Pharmacol.* 873, 172955. doi:10.1016/j.ejphar.2020.172955

Zhang, X. W., Zhou, M., An, L., Zhang, P., Li, P., and Chen, J. (2020c). Lipophilic Extract and Tanshinone IIA Derived from Salvia Miltiorrhiza Attenuate Uric Acid Nephropathy through Suppressing Oxidative Stress-Activated MAPK Pathways. *Am. J. Chin. Med.* 48, 1455–1473. doi:10.1142/S0192415X20500718

Zhao, M., Yu, Y., Wang, R., Chang, M., Ma, S., Qu, H., et al. (2020). Mechanisms and Efficacy of Chinese Herbal Medicines in Chronic Kidney Disease. *Front. Pharmacol.* 11, 619201. doi:10.3389/fphar.2020.619201

Zhong, Y., Deng, Y., Chen, Y., Chuang, P. Y., and Cijiang He, J. (2013). Therapeutic Use of Traditional Chinese Herbal Medications for Chronic Kidney Diseases. *Kidney Int.* 84, 1108–1118. doi:10.1038/ki.2013.276

Zhong, Y., Lee, K., Deng, Y., Ma, Y., Chen, Y., Li, X., et al. (2019). Arctigenin Attenuates Diabetic Kidney Disease through the Activation of PP2A in Podocytes. *Nat. Commun.* 10, 4523. doi:10.1038/s41467-019-12433-w

Zhong, Y., Zhang, X., Cai, X., Wang, K., Chen, Y., and Deng, Y. (2014). Puerarin Attenuated Early Diabetic Kidney Injury through Down-Regulation of Matrix Metalloproteinase 9 in Streptozotocin-Induced Diabetic Rats. *PLoS One* 9, e85690. doi:10.1371/journal.pone.0085690

Zhou, L., An, X. F., Teng, S. C., Liu, J. S., Shang, W. B., Zhang, A. H., et al. (2012). Pretreatment with the Total Flavone Glycosides of Flos Abelmoschus Manihot and Hyperoside Prevents Glomerular Podocyte Apoptosis in Streptozotocin-Induced Diabetic Nephropathy. *J. Med. Food* 15, 461–468. doi:10.1089/jmf.2011.1921

Zhou, X., Bai, C., Sun, X., Gong, X., Yang, Y., Chen, C., et al. (2017). Puerarin Attenuates Renal Fibrosis by Reducing Oxidative Stress Induced-Epithelial Cell Apoptosis via MAPK Signal Pathways *In Vivo* and *In Vitro*. *Ren. Fail.* 39, 423–431. doi:10.1080/0886022x.2017.1305409

Zhou, Y., Jiang, S. M., Li, L., Wang, Y., Ding, L., Liu, C. X., et al. (2020). Efficacy and Safety of Tanshinone for Chronic Kidney Disease: A Meta-Analysis. *Evid. Based Complement. Alternat Med.* 2020, 3091814. doi:10.1155/2020/3091814

Zhu, B., Wang, Y., Jardine, M., Jun, M., Lv, J. C., Cass, A., et al. (2013). Tripterygium Preparations for the Treatment of CKD: a Systematic Review and Meta-Analysis. *Am. J. Kidney Dis.* 62, 515–530. doi:10.1053/j.ajkd.2013.02.374

Zhu, L., Han, J., Yuan, R., Xue, L., and Pang, W. (2018). Berberine Ameliorates Diabetic Nephropathy by Inhibiting TLR4/NF-Kb Pathway. *Biol. Res.* 51, 9. doi:10.1186/s40659-018-0157-8

Conflict of Interest: The authors declare that the research was conducted in the absence of any commercial or financial relationships that could be construed as a potential conflict of interest.

Publisher's Note: All claims expressed in this article are solely those of the authors and do not necessarily represent those of their affiliated organizations, or those of the publisher, the editors and the reviewers. Any product that may be evaluated in this article, or claim that may be made by its manufacturer, is not guaranteed or endorsed by the publisher.

frontiers in Pharmacology

ORIGINAL RESEARCH
published: 11 November 2021
doi: 10.3389/fphar.2021.768700

Farrerol Ameliorated Cisplatin-Induced Chronic Kidney Disease Through Mitophagy Induction *via* Nrf2/PINK1 Pathway

Ning Ma[1,2†], *Zhentong wei*[2†], *Jianqiang Hu*[1], *Wenjing Gu*[3] *and Xinxin Ci*[1,2*]

[1]Institute of Translational Medicine, The First Hospital of Jilin University, Changchun, China, [2]Department of Obstetrics and Gynecology, The First Hospital of Jilin University, Changchun, China, [3]Department of Otolaryngology Head and Neck Surgery, The First Hospital of Jilin University, Changchun, China

Previously, Our study has showed that farrerol can activate Nrf2 and ameliorate cisplatin-induced acute kidney injury (AKI). Mitophagy reportedly can prevent diabetic nephropathy, cisplatin-induced AKI and other related nephropathy. In this study, we evaluated the correlation between mitophagy and the protective effect of the Nrf2 activator farrerol on cisplatin-induced CKD by using C57BL/6 wild-type and Nrf2 knockout mice. We confirmed that Nrf2 and PINK1/Parkin-mediated mitophagy was significantly increased on the 3rd day of cisplatin stimulation but was reduced on the 38th day of cisplatin stimulation. Similar to previous results, farrerol activated Nrf2 on the 38th day of cisplatin administration, subsequently stimulating the Nrf2-targeted antioxidant enzymes HO-1 and NQO1. In addition, farrerol triggered PINK1/Parkin-mediated mitophagy by recruiting the receptor proteins LC3 and p62/SQSTM1, thereby eliminating damaged mitochondria. Furthermore, genetic deletion of Nrf2 reduced PINK1/Parkin-mediated mitophagy activation and led to increased renal tubular necrosis and renal fibrosis. We also found that farrerol alleviated inflammation and renal fibrosis by inhibiting p-NF-κB/NLRP3 and TGF-β/Smad signaling. These data indicated that farrerol effectively inhibited cisplatin-induced inflammation and renal fibrosis by activating Nrf2 and PINK1/Parkin-mediated mitophagy, which provides a potential novel therapeutic target for CKD.

Keywords: chronic kidney disease, mitophagy, Nrf2, PINK1, acute kidney injury

OPEN ACCESS

Edited by:
Zhiyong Guo,
Second Military Medical University, China

Reviewed by:
Kyung Pyo Kang,
Jeonbuk National University, South Korea
Yunwen Yang,
Nanjing Children's Hospital, China

***Correspondence:**
Xinxin Ci
cixinxin@jlu.edu.cn

†*These authors have contributed equally to this work*

Specialty section:
This article was submitted to Renal Pharmacology, a section of the journal Frontiers in Pharmacology

Received: *01 September 2021*
Accepted: *28 October 2021*
Published: *11 November 2021*

Citation:
Ma N, wei Z, Hu J, Gu W and Ci X (2021) Farrerol Ameliorated Cisplatin-Induced Chronic Kidney Disease Through Mitophagy Induction via Nrf2/PINK1 Pathway. Front. Pharmacol. 12:768700. doi: 10.3389/fphar.2021.768700

INTRODUCTION

Cisplatin (CDDP), a platinum drug, has been universally utilized to treat bladder cancer, ovarian cancer and other solid tumors (Dasari and Tchounwou, 2014). However, the dominant factor restricting the clinical use of cisplatin is its nephrotoxicity (Zhu et al., 2015). Although hydration is extensively used to eliminate cisplatin-induced nephrotoxicity in clinical practice, patients receiving cisplatin chemotherapy remain at a higher hazard of acute kidney injury (AKI) (Pabla and Dong,

Abbreviations: α-SMA, alpha smooth muscle actin; AKI, acute kidney injury; ARE, antioxidant response elements; CDDP, Cisplatin; CDDP-AKI, cisplatin-induced AKI; CDDP-CKD, cisplatin-induced CKD; CKD, chronic kidney disease; GSH, glutathione; H&E, hematoxylin and eosin; HO-1, heme oxygenase-1; MDA, malondialdehyde; MPO, myeloperoxidase; NQO1, NAD(P)H quinone oxidoreductase 1; Nrf2, nuclear factor erythrocyte 2-related factor 2; ROS, reactive oxygen species; sMaf, small Maf; SOD, superoxide dismutase; TEM, tumor growth factor β; TGF-β, tumor growth factor β; TIM23, translocase of mitochondrial inner membrane 23; TOM20, translocase homolog of mitochondrial outer membrane 20.

2008). Moreover, patients with severe and recurrent AKI are more likely to develop chronic kidney disease (CKD), which is accompanied by persistent renal dysfunction, development of fibrosis, and inflammation (Chawla et al., 2011; Thakar et al., 2011; Basile et al., 2016). What's more, the death rate of CKD has continued to increase at a rate of 1% annually, and this life-threatening disease has become a global burden in the past few years (Eckardt et al., 2013). Owing to the lack of knowledge about the pathological mechanisms involved in the development of CKD, there are currently few clinical strategies or treatments that substantially improve kidney function or prevent disease progression (Bin et al., 2017; Forbes and Thorburn, 2018). Therefore, there is an urgent need to study and understand the mechanism of CKD occurrence and development.

Cell necrosis and inflammation in the proximal tubules are hallmarks of cisplatin-induced AKI (CDDP-AKI), and maladaptive or incomplete repair of kidney tubules following serious or recurrent AKI causes kidney fibrosis and ultimately exacerbates CKD (Himmelfarb et al., 2002; Vaziri, 2004). When a large amount of cisplatin accumulates in epithelial tubule cells, it can induce cells to produce excessive reactive oxygen species (ROS) due to mitochondrial dysfunction, leading to cisplatin-induced renal dysfunction (Szeto, 2006; Oh et al., 2016; Wei et al., 2020). Excessive production of ROS in cells disrupts the redox balance in CKD, causing further oxidative stress, kidney tissue damage and dysfunction (Ma et al., 2019).

Moreover, damaged renal tubular epithelial cells can induce inflammation by triggering a variety of proinflammatory cytokines, during which NF-κB, an important regulator of the renal inflammatory response mechanism, activates the expression of NLRP3 (Lorenz et al., 2014; Guo et al., 2015). Subsequently, the NLRP3 inflammasome triggers cleaved caspase-1 and IL-1β activation, which in turn triggers the release of proinflammatory mediators (Oberg et al., 2004; Tucker et al., 2015; Xu et al., 2015). In addition, persistent kidney damage or chronic unresolved inflammation can cause tissue repair failure and promote the production of tumor growth factor β (TGF-β) (Meng et al., 2015; Qin et al., 2016). A growing number of studies have illustrated that under pathological stimulation, overexpression of TGF-β in mouse kidneys can directly stimulate the expression of excessive collagen I and alpha smooth muscle actin (α-SMA) proteins, by activating regulatory Smad transcription factors (Liu, 2006; Meng et al., 2015). In addition, TGF-β increases the level of ROS in the kidney, and the generated ROS stimulate TGF-β-related fibroblast activation and myofibroblast differentiation, which further promotes the development of renal fibrosis (Kopp et al., 1996; Clouthier et al., 1997).

Nuclear factor erythrocyte 2-related factor 2 (Nrf2) is stimulated by ROS-mediated tissue damage, liberated from Keap1 and transferred to the nucleus. Subsequently, Nrf2 combines with small Maf (sMaf) proteins to form heterodimers that induce the expression of downstream antioxidants and detoxification enzymes, including heme oxygenase-1 (HO-1), NAD(P)H quinone oxidoreductase 1 (NQO1), superoxide dismutase (SOD) and glutathione (GSH) (Qin et al., 2016; Wei et al., 2020). To a certain extent, Nrf2 balances the effect of hydrogen peroxide and lipid peroxidation, thus ameliorating TGF-β-mediated profibrotic signals (Oh et al., 2012a; Oh et al., 2012b). Moreover, one study pointed out that Nrf2-mediated PINK1 transcriptional regulation restores mitophagy and abnormal mitochondrial dynamics in renal tubular cells (Xiao et al., 2017). More experiments have shown that autophagy alleviates protein aggregates in the endoplasmic reticulum and mitochondria as well as other specific cargoes with high selectivity (Mizumura et al., 2014; Guimaraes et al., 2015; Yoshii and Mizushima, 2015). Among these processes, mitophagy specifically eliminates excessive and/or damaged mitochondria (Khaminets et al., 2015). Due to the abundant mitochondria and higher rate of oxygen consumption, mitophagy is particularly necessary to maintaining the homeostasis of mitochondria in the kidneys (Ralto et al., 2020). PINK1/Parkin-mediated mitophagy is the most important mechanism for identifying and labeling mitochondria under cellular stress. Ubiquitinated PINK1/Parkin recruits the receptor protein p62/SQSTM1, which causes autophagosome formation and elimination of damaged mitochondria by connecting ubiquitin-labeled mitochondria with LC3 in the autophagosome membrane (Bueno et al., 2015; Zimmermann and Reichert, 2017). Previous studies have found that knocking down PINK1/Parkin enhances cisplatin-induced mitochondrial dysfunction and increases human renal proximal tubular cell damage by inhibiting mitophagy (Zhao et al., 2017). In addition, diabetic mouse kidney tubular damage is partially reversed and mitochondrial fragmentation and apoptosis are improved by regulating the Nrf2/PINK1-mediated mitophagy of renal tubular cells (Xiao et al., 2017). Moreover, new strategies for Nrf2/PINK1-mediated mitophagy have been used to treat kidney disease in CKD animal models. Many natural products that activate Nrf2 can counteract oxidative damage by controlling the Nrf2/ARE signaling pathway.

Our previous experiments have proven that farrerol is a novel Nrf2 activator that can improve cisplatin-induced nephrotoxicity by activating Nrf2, thereby regulating the related oxidation, inflammation and apoptosis signaling pathways (Ma et al., 2019). The protective effect of farrerol against cisplatin-induced CKD (CDDP-CKD) has not been previously reported. Here, the function and underlying mechanism of farrerol in CDDP-CKD were measured and evaluated using related experimental models.

MATERIALS AND METHODS

Reagents and Chemicals

Farrerol and cisplatin (15663-27-1) were obtained from Chengdu Pufei De Biotech Co., Ltd. (Chengdu, China) and MedChemExpress (New Jersey, United States), respectively. Primary antibodies against Nrf2(ab31163), Keap1 (ab139729), HO-1 (ab68477), NQO1 (ab80588), PINK1 (p0076), NOX4 (A11274) and β-actin (km9001) were obtained from Sigma-Aldrich (St. Louis, MO, United States), Sungene Biotech Co., Ltd (Tianjin, China) and Abcam (Cambridge, MA, United States). Antibodies specific to KIM-1 (AF 1817), NGAL (AF 1857), TGF-β (E-AB-33090), E-cadherin (E-AB-

70249), Smad (E-AB-21040), collagen I (E-AB-34264), α-SMA (E-AB-21040), NLRP3 (MAB7578) and p-NF-Kb (13346) were purchased from R&D Systems (Minnesota, MN, United States), Elabscience Biotechnology (Wuhan, China) and Cell Signaling Technology (Boston, MA, United States).

Experimental Design and Animal Procedures

C57BL/6 wildtype and Nrf2-knockout mice were purchased from Vital River (Beijing, China) and Jackson Laboratory (Bar Harbor, ME, United States), respectively. C57BL/6 wild-type and Nrf2 knockout mice were randomly assigned to experimental groups receiving the following treatments: control (saline), CDDP (10 mg/kg) only, farrerol (10 mg/kg) only, or CDDP (10 mg/kg) + farrerol (10 mg/kg). The mice were administered farrerol at 10 mg/kg body weight by intraperitoneal injection beginning 1 day before the first CDDP injection and daily until the day of harvest in the CDDP-AKI mouse group or 5 days after the second cisplatin injection in the CDDP-CKD mouse group. The mice were euthanized on day 3 (CDDP-AKI) or day 38 (CDDP-CKD) after the first administration of cisplatin. C57BL/6 wild-type and Nrf2 knockout mice were maintained on a normal diet and provided free access to drinking water during this experiment. All mice were kept in a specific pathogen-free facility, and this experiment was approved by the Animal Health and Research Ethics Committee of Jilin University.

Biochemical Index Assays

Kidney function was analyzed according to the BUN and SCr levels. Serum samples of BUN and SCr were collected and measured using the relevant kits purchased from Nanjing Jiancheng Bioengineering Institute (Nanjing, China), and then the content of BUN (640 nm) and SCr (546 nm) in the serum sample is obtained by measuring the OD value and data processing. In addition, kidneys were homogenized and dissolved in extraction buffer, and the levels of MPO, MDA, SOD, and GSH were analyzed using kits (Keygen Biotech. Co., Ltd., Nanjing, China) according to the manufacturer's instructions.

Histological Analyses

Fresh kidney tissue was dissected and immediately fixed with 4% paraformaldehyde. Then, a microscope was used to analyze sections from the paraffin-embedded mouse kidneys stained with hematoxylin and eosin (H&E) or Masson reagents. The damaged tubule scores were divided into the following levels: grade 0, no damage; grade 1, <25%; grade 2, 25–49%; grade 3, 50–74%; and grade 4, ≥75%. Additionally, Masson's staining was used to evaluate the renal tissue fibrosis area.

Western Blotting

The kidney tissue protein was separated by 10 or 12.5% sodium lauryl sulfate polyacrylamide gel electrophoresis and transferred to a polyvinylidene fluoride membrane. The membrane was blocked and shaken in 5% skim milk and then incubated with the corresponding primary and secondary antibodies for protein detection. Then, we used ECL to observe the bands and utilized ImageJ gel analysis software to quantitatively analyze the band intensities.

Immunohistochemistry

Paraffin-embedded kidney sections were deparaffinized and rehydrated. Then, we processed and microwaved the slices in citrate buffer and subsequently blocked them with 5% BSA for 20 min. The slides were incubated with primary antibodies against α-SMA and then incubated with secondary antibodies. Then, an optical microscope was used to observe the changes in kidney morphology and the area of positive staining.

Transmission Electron Microscopy (TEM)

Fresh kidneys were harvested and prefixed with glutaraldehyde and then fixed with osmium tetroxide. Afterwards, the samples were dehydrated in ethanol containing 3% uranyl acetate and embedded in epoxy resin and propylene oxide. After polymerization, the samples were cut into 70 nm-thick sections, stained, and then inspected with TEM. The quantification of mitochondrial contour measurements (feret minimum and maximum, area, perimeter, aspect ratio, shape factor, and roundness) in the kidney tissue sample were calculated using ImageJ software. Feret minimum and maximum represent the longest and shorted diameter in mitochondrial. Area, perimeter, aspect ratio, and roundness describe the degree of flatness of a contour. The shape factor corresponds to the outline of a contours. Contour measures are related as follows:

$$Aspect\ Ratio = \frac{MaxDiameter}{MinDiameter}$$

$$Shape\ factor = \frac{Perimeter}{\sqrt{Area}}$$

$$Roundness = \frac{4 \cdot Area}{\pi \cdot MaxDiameter^2}$$

Cell Experiment

Human renal tubular epithelial cells line (HK-2) obtained from Chinese Cell Bank (Beijing, China) were maintained in DMEF containing 10% fetal bovine serum, 100U/ml penicillin-streptomycin, in a 37°C, 5% CO2 incubator. After 72 h of transfection of HK-2 cells with the control siRNA or Nrf2 siRNA, HK-2 cells were seeded in a 6-well plate (5 × 105 cells/well), treated with or without farrerol (20 μM) for 24 h, and then collected cells for western blotting.

Statistical Analysis

The data are presented as the mean ± SEM and were analyzed using SPSS 19.0 (IBM). The experimental data were compared by one-way analysis of variance (ANOVA). Statistical significance was defined as $p < 0.05$.

RESULTS

Effects of Farrerol on Cisplatin-Induced Chronic Kidney Damage

Firstly, we compared the changes in body weight, kidney index, BUN, and SCr of farrerol pretreatment before cisplatin injection

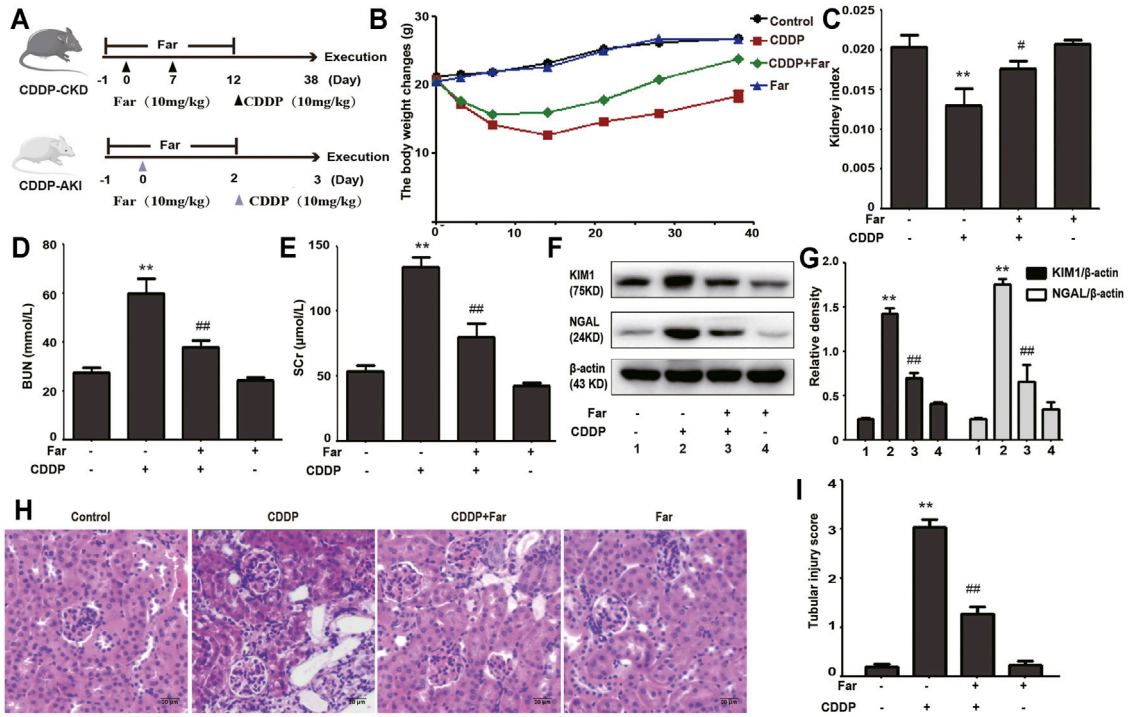

FIGURE 1 | Cisplatin-induced CKD is inhibited by farrerol. **(A)** The mouse models of CDDP-induced CKD and AKI combined with farrerol were established as follows. CDDP-CKD mouse model: Mice were treated daily with farrerol (10 mg/kg/d) or vehicle beginning 1 day before the first intraperitoneal cisplatin injection until 5 days after the second cisplatin injection. Subsequently, on the 31st day following the second CDDP administration, all mice were euthanized. CDDP-AKI mouse model: On day 0, mice were given cisplatin (10 mg/kg) or vehicle, and farrerol was given daily from day -1 to day 2. Subsequently, the mice were sacrificed 1 day after the last farrerol treatment. **(B)** The body weight changes were measured by measuring the mouse weights at 0, 3, 7, 14, 21, 28, and 38 days. **(C)** The kidney index refers to the kidney weight divided by the weight on day 38. BUN **(D)** and SCr **(E)** levels were evaluated in whole blood on the 38th day of CDDP treatment. The above data are presented as the mean ± SEM (n = 6 in each group). **(F,G)** KIM1 and NGAL immunoblotting and densitometry normalized to β-actin protein were applied to assess the degree of renal tubular damage. **(H,I)** H&E-stained micrographs of kidney sections were used to quantify renal tubular damage. All experiments were performed three times. $^{*}p < 0.05$ and $^{**}p < 0.01$ compared with the control group; $^{\#}p < 0.05$ and $^{\#\#}p < 0.01$ compared with the CDDP group.

and farrerol (not pretreatment) after cisplatin injection in mice to establish a reasonable mice model. As shown in **Supplementary Figure S1**, we found that farrerol pretreatment before cisplatin injection exert more pronounced protective effect on the kidneys than farrerol (not pretreatment) after cisplatin injection. Therefore, we chose to use farrerol pretreatment to evaluate the protective effect of farrerol against recurrent cisplatin treatment. On the day before the first intraperitoneal injection of cisplatin, the mice were pretreated with intraperitoneal farrerol (10 mg/kg) or vehicle, and farrerol administration was continued daily until 5 days after the second intraperitoneal injection of cisplatin (day -1 to day 12, 10 mg/kg). The mice were sacrificed on the 3rd and 38th days after the first injection of cisplatin to establish AKI and CKD models, respectively (**Figure 1A**). As shown in **Figure 1B**, the weight of mice treated with cisplatin decreased significantly, and farrerol significantly reversed this trend. Moreover, analysis of the kidney index also indicated that farrerol significantly improved the CKD caused by cisplatin (**Figure 1C**). In addition, farrerol improved CDDP-CKD, and this protective effect was demonstrated by renal index analysis (**Figure 1C**). In addition, farrerol pretreatment substantially alleviated the levels of BUN, SCr and the proximal tubular damage marker proteins NGAL and KIM1 (**Figures 1D–G**). We further elucidated the protective effect of farrerol on the mouse model by scoring H&E-stained sections and found that farrerol markedly reduced CDDP-induced histological lesions, such as tubular dilation and brush-border loss (**Figures 1H,I**).

Farrerol Relieves Cisplatin-Associated Inflammation and Kidney Fibrosis *in Vivo*

Notably, damaged tubular epithelial cells can cause the release of a variety of proinflammatory cytokines to induce kidney inflammation (Lorenz et al., 2014). To determine whether cisplatin induces inflammation in renal tubular epithelial cells, immunoblotting was performed to detect the levels of inflammation-mediated proteins. As shown in **Figures 2A,B**, cisplatin stimulation significantly increased the expression of p-NF-κB and NLRP3 and upregulated downstream cleaved caspase-1 and IL-1β. Furthermore, farrerol significantly

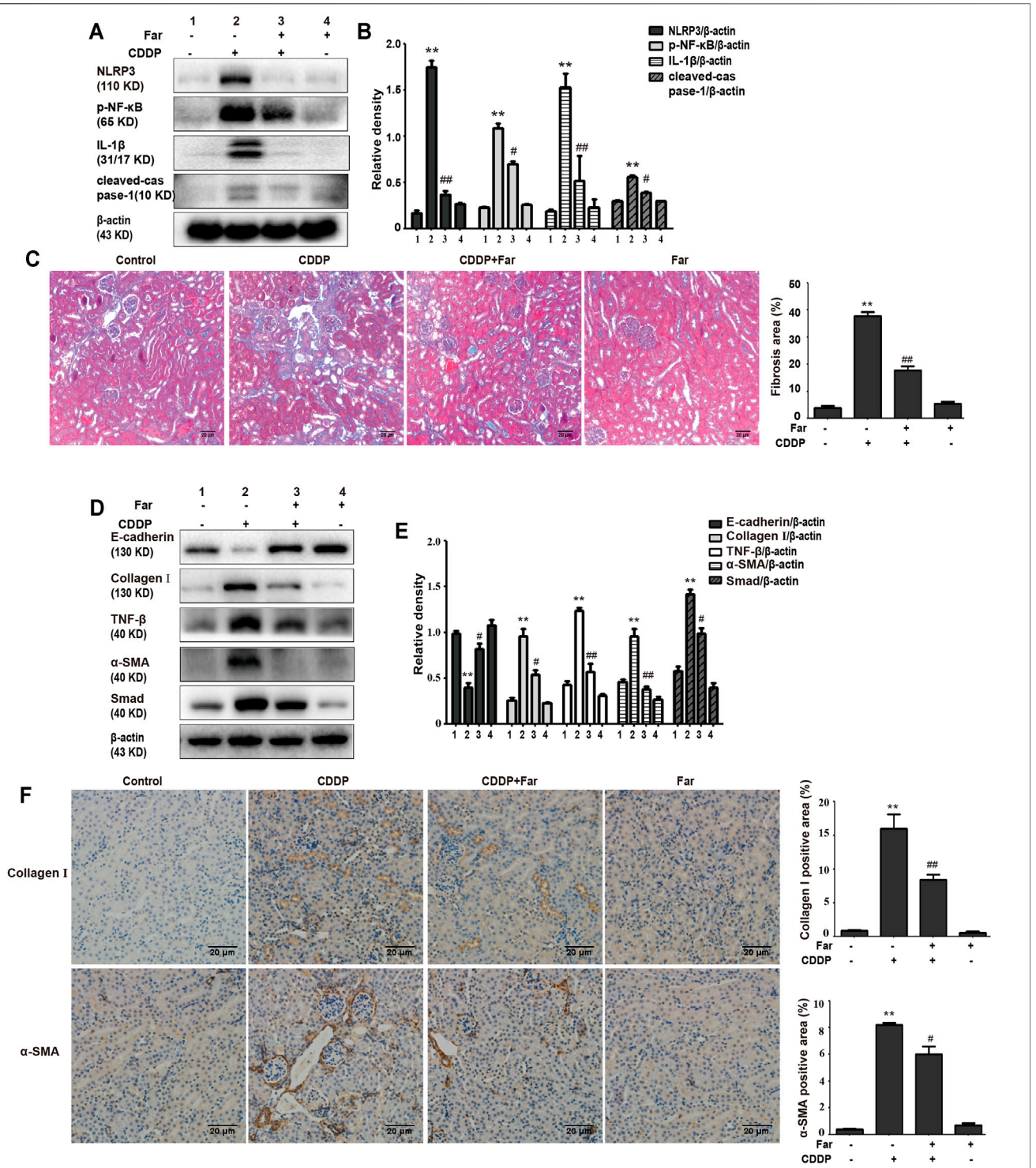

FIGURE 2 | Farrerol ameliorates cisplatin-induced inflammation and kidney fibrosis in mice. The protein levels of p-NF-κB, NLRP3, cleaved caspase-1 and IL-1β in C57BL/6 mice were investigated by western blotting **(A)** and analyzed by densitometry analysis **(B)**. **(C)** Masson staining of renal sections and quantitative analysis of fibrosis area in the kidney tissue. Western blotting images of TGF-β, E-cadherin and the fibrosis-related proteins Smad, collagen I and α-SMA in the kidney are shown **(D)** and evaluated **(E)**. **(F)** Immunohistochemical analysis of collagen I and α-SMA (control $n = 6$, farrerol $n = 6$, cisplatin $n = 6$, and CDDP + farrerol = 6). A quantitative analysis of collagen I and α-SMA positive area in the kidney tissue. Data are shown as mean ± SEM. All experiments were performed three times. $^{*}p < 0.05$ and $^{**}p < 0.01$ vs. the control group; $^{\#}p < 0.05$ and $^{\#\#}p < 0.01$ vs. the CDDP group. β-actin was used as an internal control.

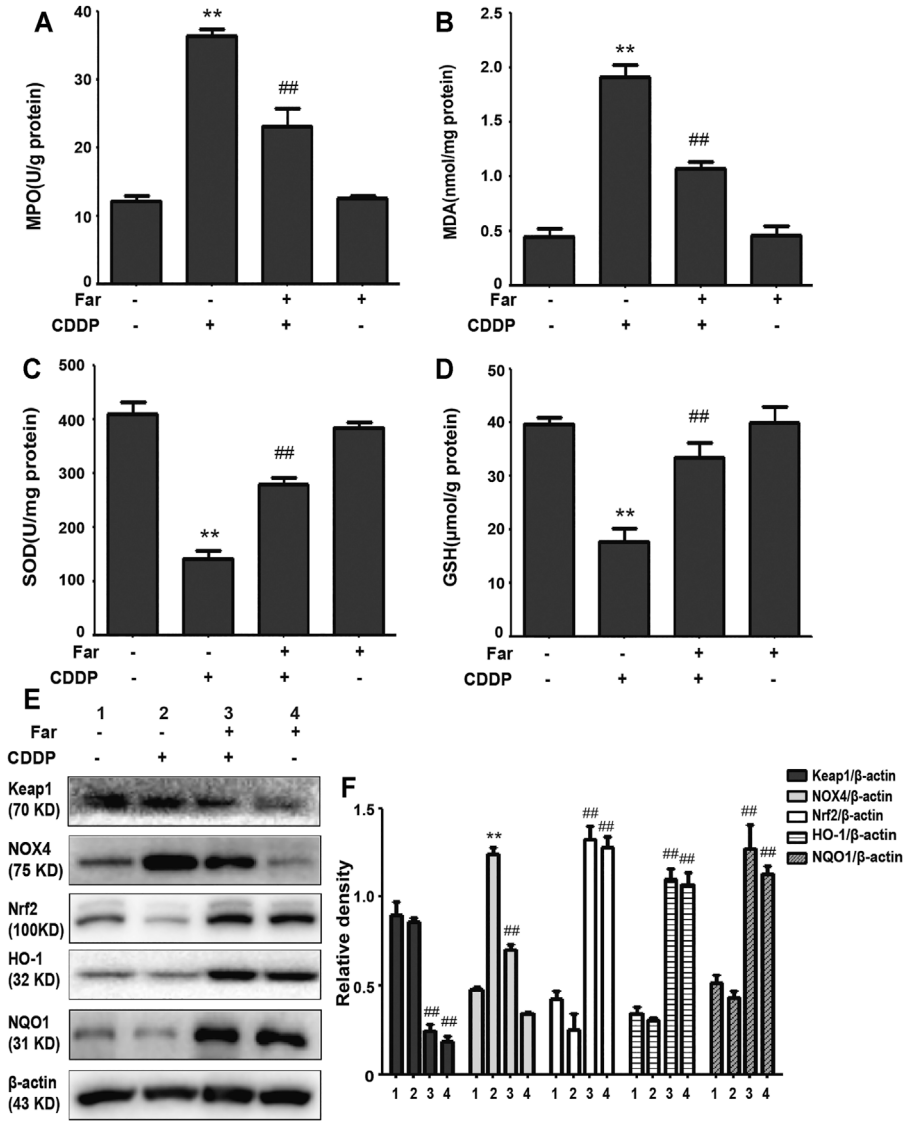

FIGURE 3 | Farrerol alleviates cisplatin-induced oxidative stress *in vivo*. **(A–D)** Mice were sacrificed on the 38th day after the first cisplatin administration, and renal tissues were collected. The contents of MPO, MDA, SOD, and GSH in kidney tissue were measured. Data are expressed as the mean ± SEM (n = 6 per group). **(E,F)** Kidney tissue lysates were analyzed by immunoblotting with specific antibodies against Keap1, NOX4, Nrf2, HO-1, and NQO1. The expression levels of the abovementioned oxidation pathway-related proteins were quantified by densitometry and standardized to β-actin. Data are expressed as the mean ± SEM. $^{*}p < 0.05$ and $^{**}p < 0.01$ compared with the control group; $^{\#}p < 0.05$ and $^{\#\#}p < 0.01$ compared with the CDDP group.

reduced the inflammatory response by inhibiting p-NF-κB and its downstream targets. In addition, persistent kidney damage and unresolved inflammation may lead to failure of tissue repair, thereby promoting the development of fibrosis (Qin et al., 2016). Mice treated with cisplatin showed a significant increase in fibrosis area that was reduced with farrerol pretreatment (**Figure 2C**). Moreover, cisplatin-induced fibrosis led to a substantial increase in TGF-β, stimulated the expression of fibrosis-related proteins (such as Smad, collagen I and α-SMA) and decreased the level of the antifibrotic protein E-cadherin (**Figures 2D,E**). To further illustrate that farrerol has a therapeutic effect on cisplatin-induced fibrosis, we conducted immunostaining of collagen I and α-SMA and confirmed that farrerol improves renal fibrosis (**Figure 2F**).

Farrerol Alleviates Cisplatin-Induced Oxidative Stress *in Vivo*

Repeated stimulation with cisplatin induces the production and accumulation of excess ROS in the proximal tubules of the kidney, causing an imbalance in the body's redox system. After pretreatment with farrerol, the contents of MDA and MPO,

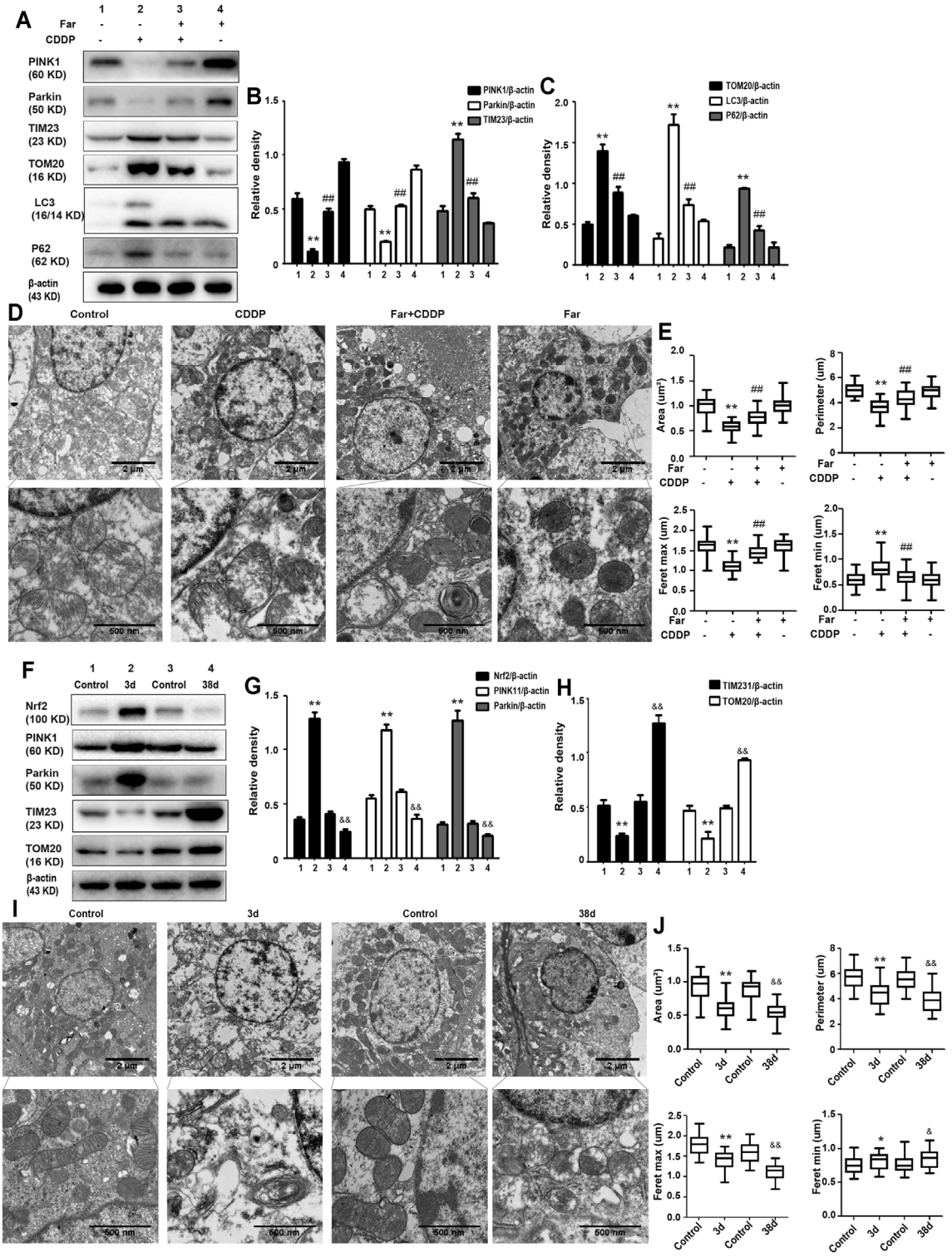

FIGURE 4 | The effect of CDDP on the Nrf2- and PINK1/Parkin-related mitophagy pathways in AKI and CKD. **(A–C)** Immunoblot analysis of PINK1, Parkin, TIM23, TOM20, LC3, and P62. **(D,E)** Representative TEM images of mitochondrial morphology in renal tubular epithelial cells. Data were shown as quantification of mitochondrial contour measurements from $n = 6$ mice per group. **(F–H)** Western blotting and densitometry analysis of Nrf2, PINK1, Parkin, TIM23, and TOM20. **(I,J)** Representative TEM images of autophagosomes/mitochondria in kidney tubular epithelial cells on day 3 and day 38 after the first injection of cisplatin. All experiments were performed three times. Data were shown as quantification of mitochondrial contour measurements from $n = 6$ mice per group. Data are expressed as the mean ± SEM. $^{\&}p < 0.05$ and $^{\&\&}p < 0.01$ $^{*}p < 0.05$ and $^{**}p < 0.01$ vs. the control group (CDDP-AKI mice); $^{*}p < 0.05$ and $^{**}p < 0.01$ vs. the control group (CDDP-CKD mice); $^{\#}p < 0.05$ and $^{\#\#}p < 0.01$ vs. the CDDP group.

TABLE 1 | Contour measurements of mitochondria.

Parameters	Control		Far	
	Control	CDDP	Control	CDDP
Roundness	0.467 ± 0.051	0.591 ± 0.073	0.514 ± 0.082	0.478 ± 0.065
Aspect ratio	2.503 ± 0.069	1.649 ± 0.089	2.316 ± 0.029	2.606 ± 0.059
Shape factor	5.209 ± 0.313	4.202 ± 0.305	4.91 ± 0.346	5.122 ± 0.262

which are key to the ROS-induced imbalance of the CKD redox system, were greatly reduced, and the contents of the antioxidant enzymes GSH and SOD were increased (**Figures 3A–D**). Previous experiments have shown that the antioxidant capacity of farrerol involves the activation of Nrf2. Therefore, we examined whether the antioxidant effect of farrerol on CDDP-CKD is related to the upregulation of Nrf2-mediated signaling pathways. The results showed that farrerol can effectively activate Nrf2 and its downstream target proteins HO-1 and NQO1 while reducing the levels of Keap1 and NOX4 (**Figures 3E,F**).

Farrerol Activates PINK1/Parkin-Mediated Mitophagy and Protects Against the Exacerbation of Kidney Damage in Cisplatin-induced CKD Mice

Mitophagy eliminates damaged mitochondria in renal tubular cells during the process of kidney damage and repair (Lin Q. et al., 2019). Moreover, Nrf2 also restores the mitochondrial dynamics of renal tubular cells by regulating PINK1-mediated mitophagy (Xiao et al., 2017). Thus, the possible involvement of the Nrf2/PINK1-mediated mitophagy pathway was tested in our experimental model. Similar to previous results, farrerol, as a Nrf2 activator, triggered PINK1/Parkin-mediated mitophagy on the 38th day of cisplatin administration, increased the accumulation of LC3 and decreased the protein expression of translocase of mitochondrial inner membrane 23 (TIM23), translocase homolog of mitochondrial outer membrane 20 (TOM20) and P62 (**Figures 4A–C**). Then, we also evaluated the effect of cisplatin on mitochondria through TEM and found that farrerol can reduce mitochondrial damage and activated mitophagy in the kidney (**Figures 4D,E**; **Table 1**). To better understand the role of mitophagy in cisplatin-induced kidney injury, we compared acute and chronic cisplatin-related mouse models. In our study, we found that Nrf2, PINK1, and Parkin were significantly increased on the third day of cisplatin stimulation. Moreover, we also found accumulation of LC3II, which suggested that autophagy was activated, and reduced levels of TIM23 and TOM20, indicating mitochondrial clearance by mitophagy. Most importantly, we also found that the changes in these proteins were significantly reversed on day 38 of cisplatin stimulation (**Figures 4F–H**). In addition, we also observed clear autophagosomes/mitophagosomes on the 3rd day of cisplatin stimulation, but on the 38th day, we observed a large number of damaged mitochondria and almost no autophagosomes/mitophagosomes unobserved on the 38th day, accompanied by a large number of damaged mitochondria (**Figures 4I,J**; **Table 2**).

Nrf2 Knockout Aggravates Cisplatin-Induced Kidney Damage and Renal Fibrosis

Next, we assessed whether Nrf2 knockdown exacerbates kidney damage in mice. Changes in body weight, renal function index (BUN, SCr, KIM1, NGAL) and histological characteristics (H&E staining) were measured to assess kidney function in the mouse model. Compared with that of wild-type mice, the kidney function of Nrf2 knockout mice deteriorated significantly after treatment with cisplatin (**Figures 5A–H**). Most importantly, these results indicated that farrerol had little protective effect on Nrf2-deficient mice. In addition, compared with the wild-type mice, the Nrf2 knockout mice pretreated with farrerol did not exhibit a decrease in the area of fibrosis. In contrast, more fibrotic areas, a decrease in the antifibrotic protein E-cadherin, and an increase in the fibrosis-related protein collagen I were observed (**Figures 6A–E**).

Nrf2 Deficiency Exacerbates Oxidative Stress in Cisplatin-induced CKD Mice

To test whether the effect of farrerol on chronic oxidative stress induced by repeated CDDP stimulation is Nrf2 dependent, we measured and compared various oxidative stress markers in Nrf2 knockout and wild-type mice. As shown in **Figures 7A,B**, we observed no significant changes in Nrf2 or its downstream targets HO-1 and NQO1 in wild-type mice. In addition, in Nrf2 knockout mice, the increase in MPO and MDA and the decrease in SOD and GSH content induced by cisplatin were more pronounced, and this phenomenon was not reversed by farrerol pretreatment (**Figures 7C–F**).

Knockdown of Nrf2 Partially Abolishes PINK1/Parkin-Mediated Mitophagy Activated by Farrerol Pretreatment in Mice

Nrf2 null mice and wild-type mice were utilized to further explore the relationship between Nrf2 and PINK1. After analyzing the Western blot in **Figures 8A–E**, we found that farrerol did not upregulate the expression of the mitophagy-

TABLE 2 | Contour measurements of mitochondria.

Parameters	3d		38d	
	Control	CDDP	Control	CDDP
Roundness	0.347 ± 0.075	0.411 ± 0.208	0.337 ± 0.069	0.526 ± 0.344
Aspect ratio	2.468 ± 0.063	1.659 ± 0.064	2.066 ± 0.062	1.361 ± 1.121
Shape factor	5.837 ± 0.746	5.235 ± 1.886	5.611 ± 0.733	4.743 ± 2.256

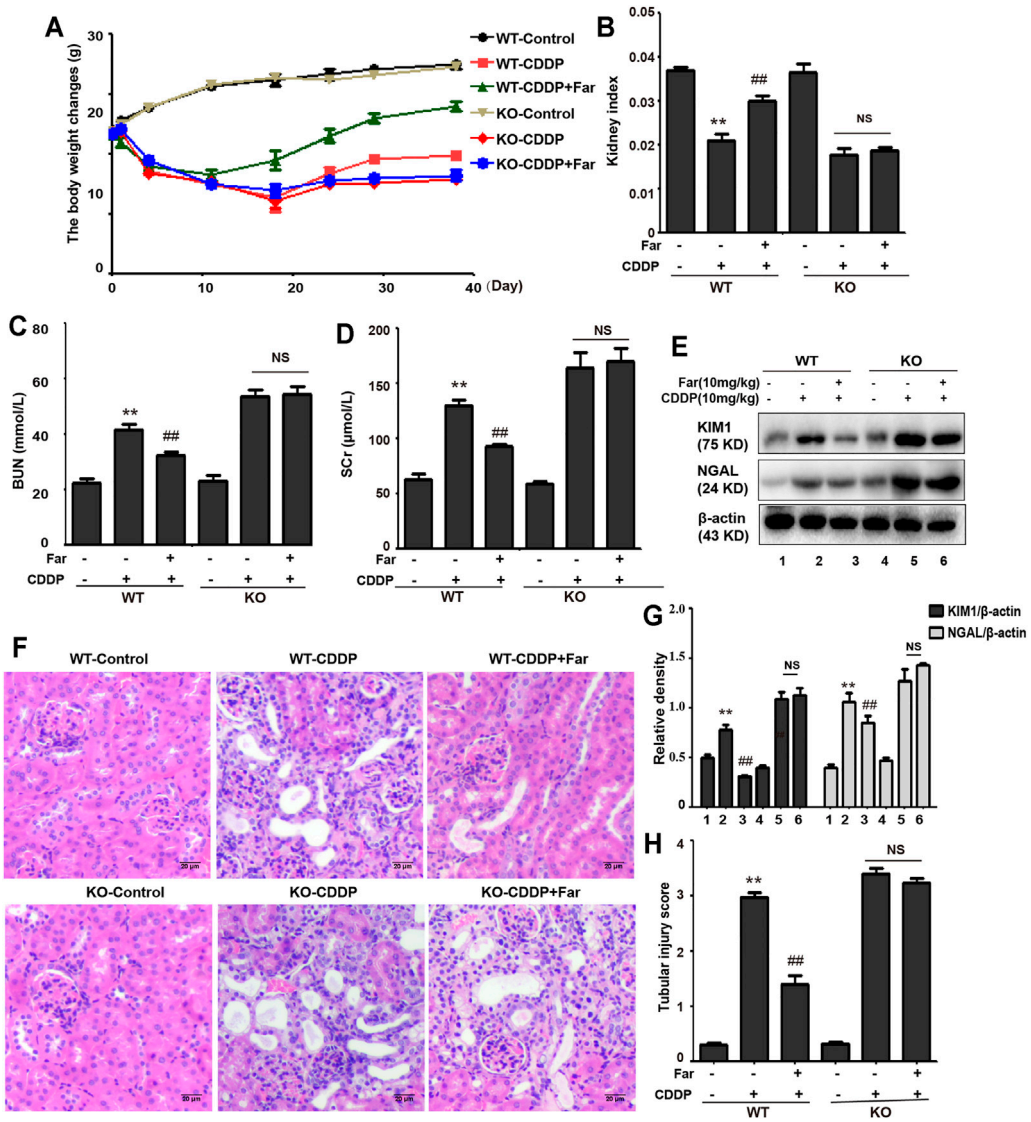

FIGURE 5 | Nrf2 knockout exacerbates CDDP-induced kidney damage. C57BL/6 wild-type mice and Nrf2 knockout C57BL/6 mice were treated with cisplatin intraperitoneally on day 0 and day 7 (10 mg/kg per dose). Then, the mice were sacrificed on the 31st day after the second administration of CDDP, and kidneys and whole blood were collected. Changes in weight **(A)** and kidney index **(B)** of wild-type and Nrf2 knockout mice were evaluated. The collected whole blood was used to measure BUN **(C)** and SCr **(D)**. **(E,F)** Kidney tissue lysates were analyzed by immunoblotting with specific antibodies against KIM1 and NGAL. **(G,H)** Typical photomicrographs of kidney sections were used to quantify kidney damage. The data are shown as the mean ± SEM (n = 6 in each group). All experiments were performed three times. $^{*}p < 0.05$ and $^{**}p < 0.01$ compared with the control group; $^{\#}p < 0.05$ and $^{\#\#}p < 0.01$ compared with the CDDP group. NS, no specificity; WT, wild-type C57BL/6 mice; KO, Nrf2 knockout C57BL/6 mice.

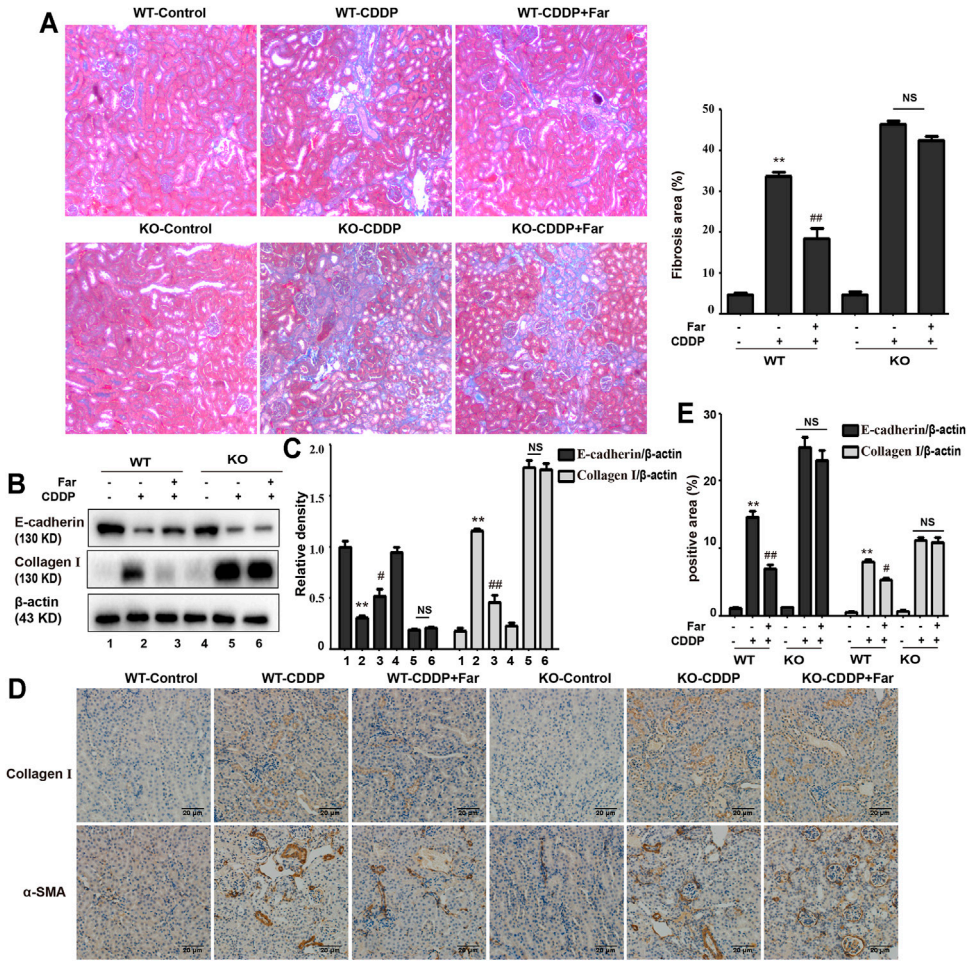

FIGURE 6 | Nrf2 knockout exacerbates CDDP-induced renal fibrosis. **(A)** Masson staining was utilized to show the fibrotic areas in the kidneys of different CDDP-CKD mice. A quantitative analysis of fibrosis area in the kidney tissue. **(B,C)** Western blotting images and quantification of E-cadherin and collagen I in mouse kidney tissue lysates normalized to *β*-actin. **(D)** Representative images of collagen I and *α*-SMA immunohistochemical analysis of mouse kidneys. **(E)** A quantitative analysis of collagen I and *α*-SMA positive area in the kidney tissue. Data are shown as mean ± SEM. All experiments were conducted three times. $^{*}p < 0.05$ and $^{**}p < 0.01$ compared with the control group; $^{\#}p < 0.05$ and $^{\#\#}p < 0.01$ compared with the CDDP group. NS, no specificity; WT, wild-type C57BL/6 mice; KO, Nrf2 knockout C57BL/6 mice.

related proteins PINK1 and Parkin in Nrf2 knockout mice but resulted in an increase in TIM23 and TOM20 protein expression, which indicated that the knockout of the Nrf2 gene partially eliminated PINK1/Parkin-mediated mitophagy. Furthermore, TEM analysis showed that mitochondria were more damaged in Nrf2 knockout mice, and autophagosomes/mitophagosomes were hardly observed (**Figures 8F,G**; **Table 3**). These data indicated that the protective effect of farrerol against CDDP-CKD is mediated *via* activation of Nrf2 and PINK1/Parkin-mediated mitophagy. In order to directly observe the relationship between Nrf2 expression regulation and PINK1 transcription, based on the previous experiment (Ma et al., 2019), we treated the HK-2 cells with farrerol for 24 h. The results showed that farrerol could hardly activate the protein expression of PINK1. This result further proveed the above conclusion that Nrf2 can play a role mainly by regulating the expression of PINK1(**Figures 8H,I**).

DISCUSSION

The development of CKD is defined as a progressive decline in the glomerular filtration rate accompanied by the loss of kidney function and the accumulation of fibrous tissue. As a multifactorial disorder, the origin of CKD mainly involves diabetes, glomerulonephritis, kidney stones, drugs, and nephrotoxin (Levey and Coresh, 2012; Hill et al., 2016). Deterioration of renal function can be triggered by the nephrotoxicity of many therapeutic drugs, among which cisplatin is an important drug that causes acute and chronic kidney injury related to nephrotoxicity (Lin T. et al., 2019). Although cisplatin is a clinically effective chemotherapeutic drug, due to its nephrotoxicity, multicycle administration of cisplatin can cause permanent loss of kidney function. Even after successful cisplatin treatment, severe and life-limiting CKD may occur (Pabla and Dong, 2008). The transcription factor Nrf2, a regulator of

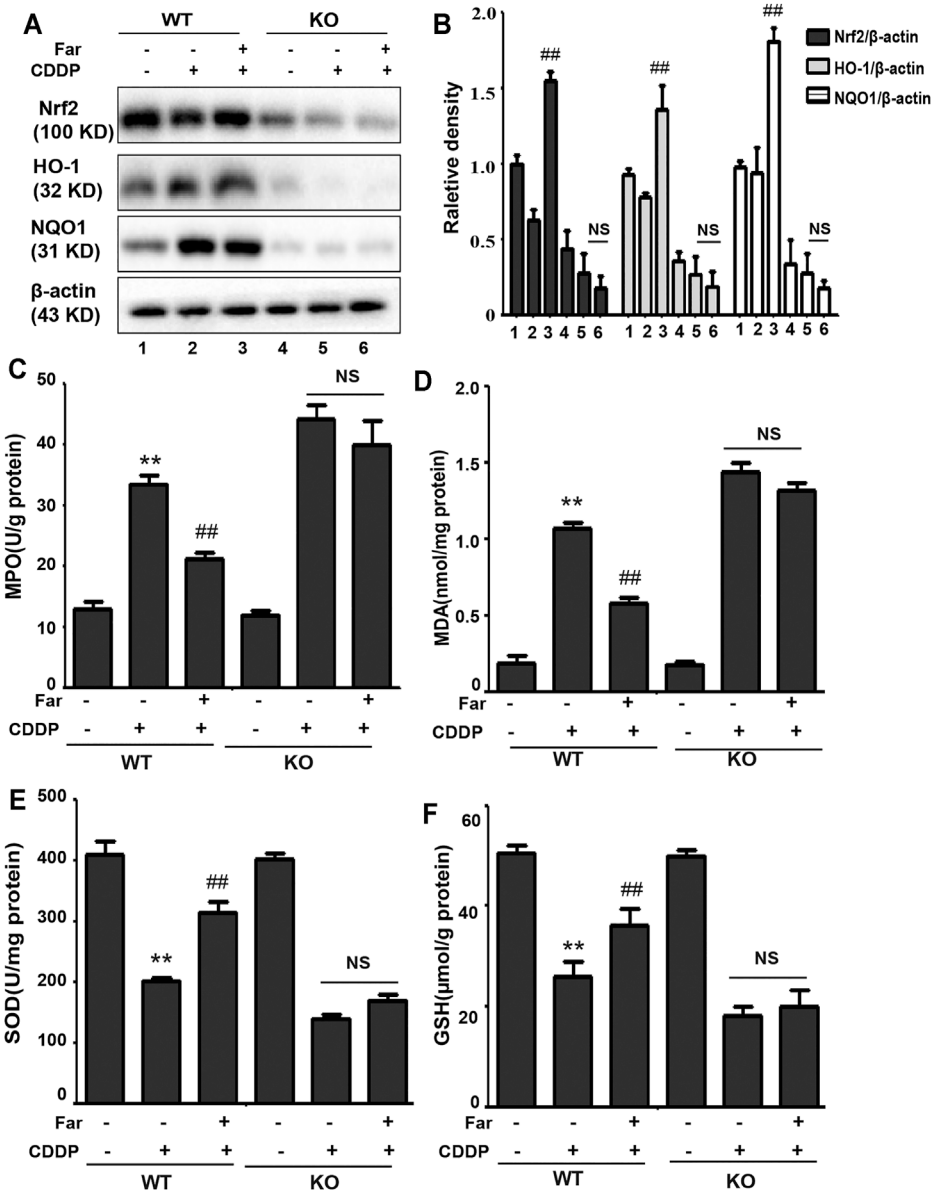

FIGURE 7 | Nrf2 deficiency exacerbates oxidative stress in CDDP-CKD mouse models. **(A,B)** Western blot analysis of Nrf2, HO-1, and NQO1 in wild-type and Nrf2 knockout mouse kidneys. **(C–F)** The indicators MPO, MDA, SOD and GSH were assessed in kidney tissues. Data are expressed as the mean ± SEM ($n = 6$ per group). All of the data displayed represent the mean of three independent experiments. $^{*}p < 0.05$ and $^{**}p < 0.01$ vs. the control group; $^{\#}p < 0.05$ and $^{\#\#}p < 0.01$ vs. the CDDP group. NS, no specificity. β-actin was used as an internal control.

cytoprotective proteins driven by ARE, is an essential factor in adjusting cell redox homeostasis. It has been reported that compared with wild-type mice, Nrf2-deficient mice have markedly deteriorated kidney function, as indicated by enhancements in BUN and SCr, more serious histological injury, and a higher tubular damage score (Liu et al., 2009). In our experiments, we also compared the changes in kidney function of Nrf2-null mice and wild-type mice after multiple injections of cisplatin and found an identical trend (**Figures 5A–D,G,H**). In addition, we tested proximal tubule damage markers and found that the levels of KIM1 and NGAL in Nrf2 knockout mice were significantly increased (**Figures 5E,F**). This result also supported that Nrf2 knockout mice are more sensitive to cisplatin and are more likely to suffer severe kidney damage. Farrerol, a new type of 2,3-dihydroflavonoid isolated from rhododendron, has been shown in our previous experiments to improve cisplatin-mediated AKI by upregulating Nrf2. Moreover, pretreatment with farrerol ameliorated cisplatin toxicity in Nrf2 wild-type mice but exerted little protective effect on Nrf2 knockout mice (Ma et al., 2019).

When a large amount of cisplatin accumulates in epithelial tubule cells, it can induce excessive ROS production, which causes oxidation reactions and renal damage. Malondialdehyde (MDA) and

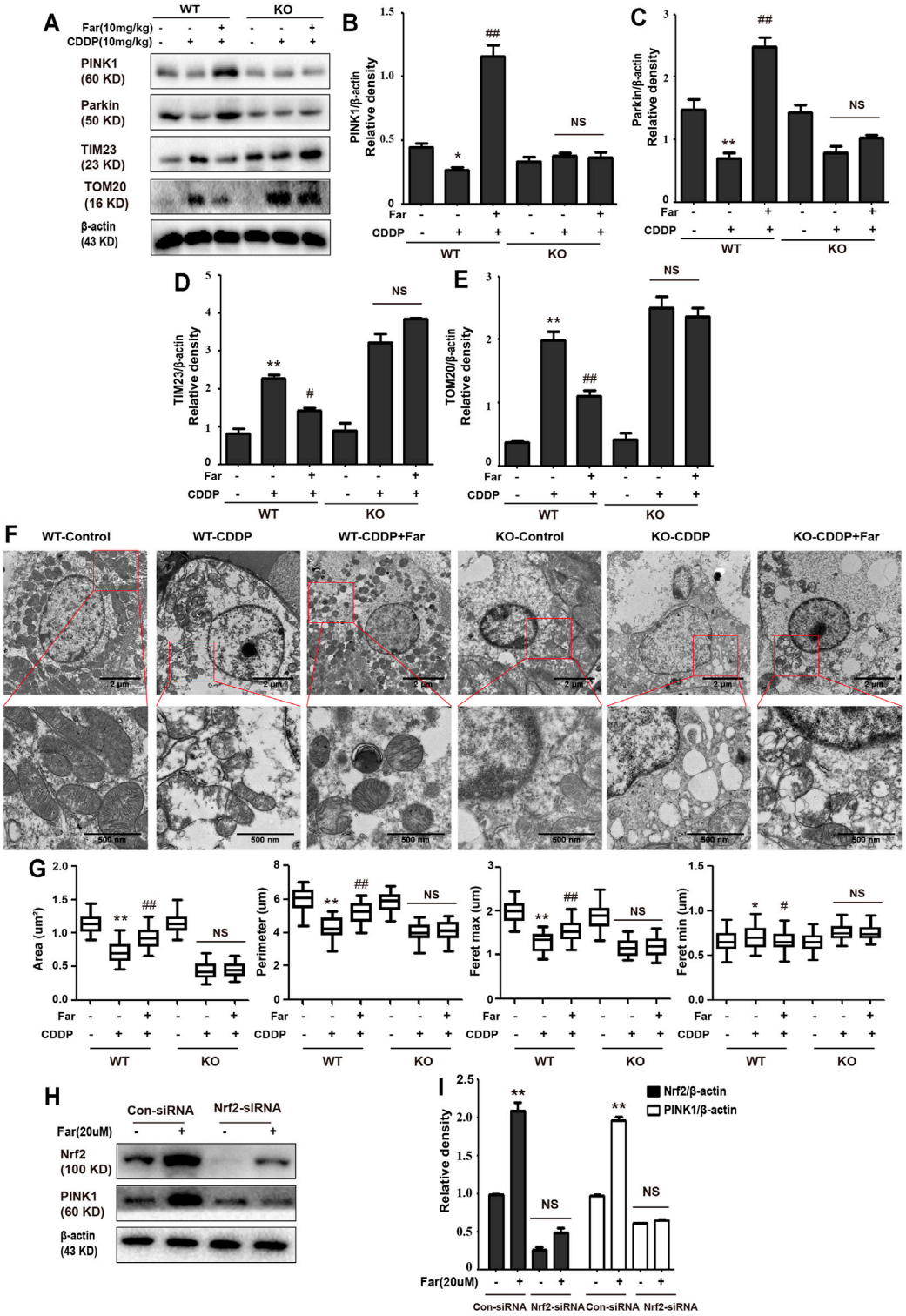

FIGURE 8 | Knockdown of Nrf2 partially abolishes PINK1/Parkin-mediated mitophagy activated by farrerol pretreatment in mice. The expression levels of the mitophagy-mediating proteins PINK1, Parkin, TIM23 and TOM20 in wild-type and Nrf2 knockout mice were investigated by Western blotting **(A)** and analyzed by densitometry analysis **(B–E)**. **(F)** Representative TEM images of mitochondrial morphology in kidney tubular epithelial cells of wild-type and Nrf2 knockout mice. **(G)** Data were shown as quantification of mitochondrial contour measurements from $n = 6$ mice per group. Data are expressed as the mean ± SEM. (H, I) HK-2 cells were transfected with a Nrf2 siRNA or Nrf2-negative control siRNA for 72 h and exposed to farrerol (20 μM)for 24 h, and the protein levels were subsequently detected with western blotting. The levels of Nrf2 and PINK1 were determined. $^{*}p < 0.05$ and $^{**}p < 0.01$ compared with the control group; $^{\#}p < 0.05$ and $^{\#\#}p < 0.01$ compared with the CDDP group. NS, no specificity. β-actin was used as an internal control.

TABLE 3 | Contour measurements of mitochondria.

Parameters	Nrf2-WT			Nrf2-KO		
	Control	CDDP	CDDP + Far	Control	CDDP	CDDP + Far
Roundness	0.395 ± 0.115	0.583 ± 0.242	0.501 ± 0.140	0.427 ± 0.267	0.604 ± 0.298	0.596 ± 0.337
Aspect ratio	3.11 ± 0.628	1.855 ± 0.268	2.461 ± 0.717	2.994 ± 0.713	1.568 ± 0.481	1.581 ± 0.311
Shape factor	5.588 ± 0.852	4.101 ± 1.118	4.723 ± 1.047	5.466 ± 0.609	3.952 ± 1.452	4.086 ± 1.316

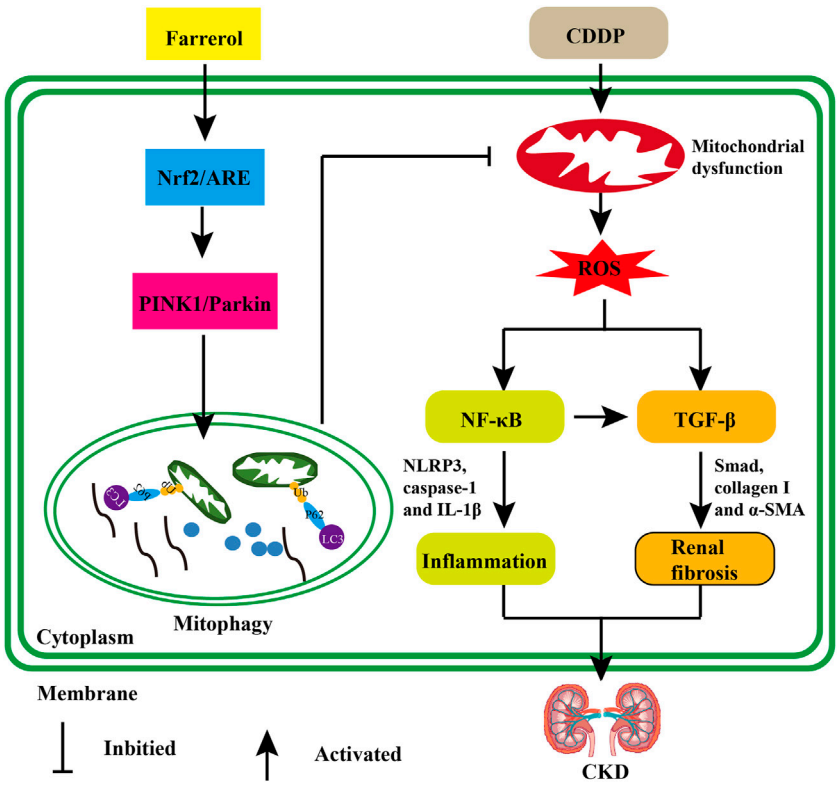

FIGURE 9 | The protective effect of farrerol against CDDP-related CKD and its potential mechanism. Cisplatin can accumulate in epithelial tubule cells, causing mitochondrial dysfunction and excessive ROS. Damaged cells can induce inflammation by triggering the activation of p-NF-κB/NLRP3. In addition, the generated ROS or chronic unresolved inflammation can also stimulate the production of renal fibrosis and the development of CKD *via* TGF-*β*/Smad signaling. Farrerol can activate Nrf2/ARE, then increase PINK1/Parkin-mediated mitophagy and eliminate damaged mitochondria.

myeloperoxidase (MPO) levels are crucial to the imbalance between the accentuated pro-oxidant and deficient antioxidant capacity that occurs in CKD (Ma et al., 2019). Our experiments indicated that farrerol lowered the levels of MDA and MPO and enhanced the levels of GSH and SOD (**Figures 3A–D**). Additionally, damaged renal tubular epithelial cells can trigger a variety of proinflammatory factors to induce kidney inflammation. NF-κB is a heterodimer composed of p50 and p65 that can activate the NLRP3 inflammasome and mediate inflammation. In this study, farrerol significantly inhibited the release of proinflammatory mediators and protected kidney function. Our experiments further showed that this protective effect was achieved by inhibiting p-NF-κB and NLRP3 and reducing cleaved caspase-1 and IL-1*β* (**Figures 2A,B**). Moreover, successive kidney damage or chronic unresolved inflammation may cause tissue repair failure and promote the formation of renal fibrosis. In cisplatin-induced fibrosis, the activation of the TGF-*β* pathway released regulatory factors that further promoted the excessive expression of Smad, collagen I and *α*-SMA (**Figures 2D–F**). In addition, we found that farrerol effectively inhibited the fibrosis process and improve CDDP-CKD (**Figure 2C**). Related research has emphasized that mitochondrial pathology is crucial in AKI development and kidney repair after AKI. Therefore, timely elimination of injured mitochondria in renal tubular cells represents an important quality control mechanism for cell homeostasis and survival during kidney damage and repair (Ralto et al., 2020). Mitophagy, a selective form of autophagy,

specifically eliminates excessive or damaged mitochondria. Previous studies have shown that inhibiting mitophagy induces a decline in mitochondrial function and enhances CDDP-AKI, while activating mitophagy protects cells from mitochondrial dysfunction and cisplatin-induced cell damage (Jiang et al., 2012; Zhao et al., 2017). In our mouse model, the possible involvement of the PINK1/Parkin-mediated mitophagy pathway was tested. As shown in **Figures 4F–J** and **Table 2**, immunoblotting showed that the levels of PINK1 and Parkin were significantly increased and the expression of the mitochondrial membrane proteins TIM23 and TOM20 was reduced on the third day of cisplatin stimulation. Most importantly, we also found that the levels of these proteins were significantly reduced on day 38. Similar to previous results, farrerol, a Nrf2 activator, triggered the PINK1/Parkin-mediated mitophagy pathway on the 38th day of cisplatin administration (**Figures 4A–E**; **Table 1**). Moreover, Nrf2-mediated PINK1 transcriptional regulation restores impaired mitophagy and abnormal mitochondrial dynamics in renal tubular cells (Xiao et al., 2017). Therefore, to further explore the relationship between Nrf2 and PINK1, we used Nrf2 null mice and wild-type mice and found that farrerol did not significantly activate mitophagy-related indicators in Nrf2 knockout mice (**Figures 8A–G**; **Supplementary Figure S1**; **Table 3**). These data indicated that the protective effect of farrerol against CDDP-CKD is mediated *via* activation of Nrf2 and PINK1/Parkin-mediated mitophagy.

CONCLUSION

In summary, our research showed that farrerol reversed oxidative stress, inflammation and fibrosis in renal tubular epithelial cells, thereby improving cisplatin-mediated renal insufficiency. This protective mechanism of the kidney can be achieved by activating Nrf2 and subsequently increasing PINK/Parkin-mediated mitophagy and eliminating damaged mitochondria (**Figure 9**). These experiments demonstrated that farrerol provides a potential novel treatment for CDDP-CKD.

DATA AVAILABILITY STATEMENT

The original contributions presented in the study are included in the article/**Supplementary Material**, further inquiries can be directed to the corresponding author.

ETHICS STATEMENT

The animal study was reviewed and approved by the Animal Health and Research Ethics Committee of Jilin University.

AUTHOR CONTRIBUTIONS

NM and XC designed the experiments; NM and ZW writed, reviewed and Edited the main text; NM and ZW Investigated the experiments; JH and WG conducted formal analysis and validation; ZW and XC supervised this experiment. All data were generated in-house, and no paper mill was used. All authors agree to be accountable for all aspects of work ensuring integrity and accuracy.

FUNDING

This work was supported by the National Natural Science Foundation of China (Grant No. 81970576) and the Natural Science Foundation of Jilin (Nos 20200201378JC and JLSCZD 2019-065).

SUPPLEMENTARY MATERIAL

The Supplementary Material for this article can be found online at: https://www.frontiersin.org/articles/10.3389/fphar.2021.768700/full#supplementary-material

REFERENCES

Basile, D. P., Bonventre, J. V., Mehta, R., Nangaku, M., Unwin, R., Rosner, M. H., et al. (2016). Progression after AKI: Understanding Maladaptive Repair Processes to Predict and Identify Therapeutic Treatments. *J. Am. Soc. Nephrol.* 27, 687–697. doi:10.1681/ASN.2015030309

Bin Feng, F., Meng, R., Bin Huang, H., Bi, Y., Shen, S., and Zhu, D. (2017). Silymarin Protects against Renal Injury through Normalization of Lipid Metabolism and Mitochondrial Biogenesis in High Fat-Fed Mice. *Free Radic. Biol. Med.* 110, 240–249. doi:10.1016/j.freeradbiomed.2017.06.009

Bueno, M., Lai, Y. C., Romero, Y., Brands, J., St Croix, C. M., Kamga, C., et al. (2015). PINK1 Deficiency Impairs Mitochondrial Homeostasis and Promotes Lung Fibrosis. *J. Clin. Invest.* 125, 521–538. doi:10.1172/JCI74942

Chawla, L. S., Amdur, R. L., Amodeo, S., Kimmel, P. L., and Palant, C. E. (2011). The Severity of Acute Kidney Injury Predicts Progression to Chronic Kidney Disease. *Kidney Int.* 79, 1361–1369. doi:10.1038/ki.2011.42

Clouthier, D. E., Comerford, S. A., and Hammer, R. E. (1997). Hepatic Fibrosis, Glomerulosclerosis, and a Lipodystrophy-like Syndrome in PEPCK-TGF-Beta1 Transgenic Mice. *J. Clin. Invest.* 100, 2697–2713. doi:10.1172/JCI119815

Dasari, S., and Tchounwou, P. B. (2014). Cisplatin in Cancer Therapy: Molecular Mechanisms of Action. *Eur. J. Pharmacol.* 740, 364–378. doi:10.1016/j.ejphar.2014.07.025

Eckardt, K. U., Coresh, J., Devuyst, O., Johnson, R. J., Köttgen, A., Levey, A. S., et al. (2013). Evolving Importance of Kidney Disease: from Subspecialty to Global Health burden. *Lancet* 382, 158–169. doi:10.1016/S0140-6736(13)60439-0

Forbes, J. M., and Thorburn, D. R. (2018). Mitochondrial Dysfunction in Diabetic Kidney Disease. *Nat. Rev. Nephrol.* 14, 291–312. doi:10.1038/nrneph.2018.9

Guimaraes, R. S., Delorme-Axford, E., Klionsky, D. J., and Reggiori, F. (2015). Assays for the Biochemical and Ultrastructural Measurement of Selective and Nonselective Types of Autophagy in the Yeast *Saccharomyces cerevisiae*. *Methods* 75, 141–150. doi:10.1016/j.ymeth.2014.11.023

Guo, H., Callaway, J. B., and Ting, J. P. (2015). Inflammasomes: Mechanism of Action, Role in Disease, and Therapeutics. *Nat. Med.* 21, 677–687. doi:10.1038/nm.3893

Hill, N. R., Fatoba, S. T., Oke, J. L., Hirst, J. A., O'Callaghan, C. A., Lasserson, D. S., et al. (2016). Global Prevalence of Chronic Kidney Disease - A Systematic Review and Meta-Analysis. *PLoS One* 11, e0158765. doi:10.1371/journal.pone.0158765

Himmelfarb, J., Stenvinkel, P., Ikizler, T. A., and Hakim, R. M. (2002). The Elephant in Uremia: Oxidant Stress as a Unifying Concept of

Cardiovascular Disease in Uremia. *Kidney Int.* 62, 1524–1538. doi:10.1046/j.1523-1755.2002.00600.x

Jiang, M., Wei, Q., Dong, G., Komatsu, M., Su, Y., and Dong, Z. (2012). Autophagy in Proximal Tubules Protects against Acute Kidney Injury. *Kidney Int.* 82, 1271–1283. doi:10.1038/ki.2012.261

Khaminets, A., Heinrich, T., Mari, M., Grumati, P., Huebner, A. K., Akutsu, M., et al. (2015). Regulation of Endoplasmic Reticulum Turnover by Selective Autophagy. *Nature* 522, 354–358. doi:10.1038/nature14498

Kopp, J. B., Factor, V. M., Mozes, M., Nagy, P., Sanderson, N., Böttinger, E. P., et al. (1996). Transgenic Mice with Increased Plasma Levels of TGF-Beta 1 Develop Progressive Renal Disease. *Lab. Invest.* 74, 991–1003.

Levey, A. S., and Coresh, J. (2012). Chronic Kidney Disease. *Lancet* 379, 165–180. doi:10.1016/S0140-6736(11)60178-5

Lin, Q., Li, S., Jiang, N., Shao, X., Zhang, M., Jin, H., et al. (2019a). PINK1-parkin Pathway of Mitophagy Protects against Contrast-Induced Acute Kidney Injury via Decreasing Mitochondrial ROS and NLRP3 Inflammasome Activation. *Redox Biol.* 26, 101254. doi:10.1016/j.redox.2019.101254

Lin, T. A., Wu, V. C., and Wang, C. Y. (2019b). Autophagy in Chronic Kidney Diseases. *Cells* 8, 61. doi:10.3390/cells8010061

Liu, M., Grigoryev, D. N., Crow, M. T., Haas, M., Yamamoto, M., Reddy, S. P., et al. (2009). Transcription Factor Nrf2 Is Protective during Ischemic and Nephrotoxic Acute Kidney Injury in Mice. *Kidney Int.* 76, 277–285. doi:10.1038/ki.2009.157

Liu, Y. (2006). Renal Fibrosis: New Insights into the Pathogenesis and Therapeutics. *Kidney Int.* 69, 213–217. doi:10.1038/sj.ki.5000054

Lorenz, G., Darisipudi, M. N., and Anders, H. J. (2014). Canonical and Non-canonical Effects of the NLRP3 Inflammasome in Kidney Inflammation and Fibrosis. *Nephrol. Dial. Transpl.* 29, 41–48. doi:10.1093/ndt/gft332

Ma, N., Wei, W., Fan, X., and Ci, X. (2019). Farrerol Attenuates Cisplatin-Induced Nephrotoxicity by Inhibiting the Reactive Oxygen Species-Mediated Oxidation, Inflammation, and Apoptotic Signaling Pathways. *Front. Physiol.* 10, 1419. doi:10.3389/fphys.2019.01419

Meng, X. M., Tang, P. M., Li, J., and Lan, H. Y. (2015). TGF-β/Smad Signaling in Renal Fibrosis. *Front. Physiol.* 6, 82. doi:10.3389/fphys.2015.00082

Mizumura, K., Choi, A. M., and Ryter, S. W. (2014). Emerging Role of Selective Autophagy in Human Diseases. *Front. Pharmacol.* 5, 244. doi:10.3389/fphar.2014.00244

Oberg, B. P., McMenamin, E., Lucas, F. L., McMonagle, E., Morrow, J., Ikizler, T. A., et al. (2004). Increased Prevalence of Oxidant Stress and Inflammation in Patients with Moderate to Severe Chronic Kidney Disease. *Kidney Int.* 65, 1009–1016. doi:10.1111/j.1523-1755.2004.00465.x

Oh, C. J., Kim, J. Y., Choi, Y. K., Kim, H. J., Jeong, J. Y., Bae, K. H., et al. (2012a). Dimethylfumarate Attenuates Renal Fibrosis via NF-E2-Related Factor 2-mediated Inhibition of Transforming Growth Factor-β/Smad Signaling. *PLoS One* 7, e45870. doi:10.1371/journal.pone.0045870

Oh, C. J., Kim, J. Y., Min, A. K., Park, K. G., Harris, R. A., Kim, H. J., et al. (2012b). Sulforaphane Attenuates Hepatic Fibrosis via NF-E2-Related Factor 2-mediated Inhibition of Transforming Growth Factor-β/Smad Signaling. *Free Radic. Biol. Med.* 52, 671–682. doi:10.1016/j.freeradbiomed.2011.11.012

Oh, G. S., Kim, H. J., Shen, A., Lee, S. B., Yang, S. H., Shim, H., et al. (2016). New Therapeutic Concept of NAD Redox Balance for Cisplatin Nephrotoxicity. *Biomed. Res. Int.* 2016, 4048390. doi:10.1155/2016/4048390

Pabla, N., and Dong, Z. (2008). Cisplatin Nephrotoxicity: Mechanisms and Renoprotective Strategies. *Kidney Int.* 73, 994–1007. doi:10.1038/sj.ki.5002786

Qin, T., Yin, S., Yang, J., Zhang, Q., Liu, Y., Huang, F., et al. (2016). Sinomenine Attenuates Renal Fibrosis through Nrf2-Mediated Inhibition of Oxidative Stress and TGFβ Signaling. *Toxicol. Appl. Pharmacol.* 304, 1–8. doi:10.1016/j.taap.2016.05.009

Ralto, K. M., Rhee, E. P., and Parikh, S. M. (2020). NAD+ Homeostasis in Renal Health and Disease. *Nat. Rev. Nephrol.* 16, 99–111. doi:10.1038/s41581-019-0216-6

Szeto, H. H. (2006). Mitochondria-targeted Peptide Antioxidants: Novel Neuroprotective Agents. *AAPS J.* 8, E521–E531. doi:10.1208/aapsj080362

Thakar, C. V., Christianson, A., Himmelfarb, J., and Leonard, A. C. (2011). Acute Kidney Injury Episodes and Chronic Kidney Disease Risk in Diabetes Mellitus. *Clin. J. Am. Soc. Nephrol.* 6, 2567–2572. doi:10.2215/CJN.01120211

Tucker, P. S., Scanlan, A. T., and Dalbo, V. J. (2015). Chronic Kidney Disease Influences Multiple Systems: Describing the Relationship between Oxidative Stress, Inflammation, Kidney Damage, and Concomitant Disease. *Oxid Med. Cel Longev* 2015, 806358. doi:10.1155/2015/806358

Vaziri, N. D. (2004). Oxidative Stress in Uremia: Nature, Mechanisms, and Potential Consequences. *Semin. Nephrol.* 24, 469–473. doi:10.1016/j.semnephrol.2004.06.026

Wei, W., Ma, N., Fan, X., Yu, Q., and Ci, X. (2020). The Role of Nrf2 in Acute Kidney Injury: Novel Molecular Mechanisms and Therapeutic Approaches. *Free Radic. Biol. Med.* 158, 1–12. doi:10.1016/j.freeradbiomed.2020.06.025

Xiao, L., Xu, X., Zhang, F., Wang, M., Xu, Y., Tang, D., et al. (2017). The Mitochondria-Targeted Antioxidant MitoQ Ameliorated Tubular Injury Mediated by Mitophagy in Diabetic Kidney Disease via Nrf2/PINK1. *Redox Biol.* 11, 297–311. doi:10.1016/j.redox.2016.12.022

Xu, G., Luo, K., Liu, H., Huang, T., Fang, X., and Tu, W. (2015). The Progress of Inflammation and Oxidative Stress in Patients with Chronic Kidney Disease. *Ren. Fail.* 37, 45–49. doi:10.3109/0886022X.2014.964141

Yoshii, S. R., and Mizushima, N. (2015). Autophagy Machinery in the Context of Mammalian Mitophagy. *Biochim. Biophys. Acta* 1853, 2797–2801. doi:10.1016/j.bbamcr.2015.01.013

Zhao, C., Chen, Z., Xu, X., An, X., Duan, S., Huang, Z., et al. (2017). Pink1/Parkin-mediated Mitophagy Play a Protective Role in Cisplatin Induced Renal Tubular Epithelial Cells Injury. *Exp. Cel Res* 350, 390–397. doi:10.1016/j.yexcr.2016.12.015

Zhu, S., Pabla, N., Tang, C., He, L., and Dong, Z. (2015). DNA Damage Response in Cisplatin-Induced Nephrotoxicity. *Arch. Toxicol.* 89, 2197–2205. doi:10.1007/s00204-015-1633-3

Zimmermann, M., and Reichert, A. S. (2017). How to Get Rid of Mitochondria: Crosstalk and Regulation of Multiple Mitophagy Pathways. *Biol. Chem.* 399, 29–45. doi:10.1515/hsz-2017-0206

Conflict of Interest: The authors declare that the research was conducted in the absence of any commercial or financial relationships that could be construed as a potential conflict of interest.

Publisher's Note: All claims expressed in this article are solely those of the authors and do not necessarily represent those of their affiliated organizations, or those of the publisher, the editors and the reviewers. Any product that may be evaluated in this article, or claim that may be made by its manufacturer, is not guaranteed or endorsed by the publisher.

frontiers in Pharmacology

ORIGINAL RESEARCH
published: 15 November 2021
doi: 10.3389/fphar.2021.761572

Uncovering Bupi Yishen Formula Pharmacological Mechanisms Against Chronic Kidney Disease by Network Pharmacology and Experimental Validation

Difei Zhang[1,2†], *Bingran Liu*[1†], *Xina Jie*[1,2], *Jiankun Deng*[1], *Zhaoyu Lu*[1,2], *Fuhua Lu*[1,2*] and *Xusheng Liu*[1,2*]

[1]The Second Clinical College of Guangzhou University of Chinese Medicine, Guangzhou, China, [2]Department of Nephrology, Guangdong Provincial Hospital of Chinese Medicine, Guangzhou, China

OPEN ACCESS

Edited by:
Dan-Qian Chen,
Northwest University, China

Reviewed by:
Yonggui Wu,
First Affiliated Hospital of Anhui Medical University, China
Yange Tian,
Henan University of Traditional Chinese Medicine, China

***Correspondence:**
Fuhua Lu
lufuhua@gzucm.edu.cn
Xusheng Liu
liuxusheng@gzucm.edu.cn

†These authors have contributed equally to this work

Specialty section:
This article was submitted to Renal Pharmacology, a section of the journal Frontiers in Pharmacology

Received: 20 August 2021
Accepted: 26 October 2021
Published: 15 November 2021

Citation:
Zhang D, Liu B, Jie X, Deng J, Lu Z, Lu F and Liu X (2021) Uncovering Bupi Yishen Formula Pharmacological Mechanisms Against Chronic Kidney Disease by Network Pharmacology and Experimental Validation. Front. Pharmacol. 12:761572. doi: 10.3389/fphar.2021.761572

Chronic kidney disease (CKD) is a leading public health problem with high morbidity and mortality, but the therapies remain limited. Bupi Yishen Formula (BYF) - a patent traditional Chinese medicine (TCM) formula - has been proved to be effective for CKD treatment in a high-quality clinical trial. However, BYF's underlying mechanism is unclear. Thus, we aimed to reveal BYF pharmacological mechanism against CKD by network pharmacology and experimental studies. Network pharmacology-based analysis of the drug-compound-target interaction was used to predict the potential pharmacological mechanism and biological basis of BYF. We performed a comprehensive study by detecting the expression levels of fibrotic and inflammatory markers and main molecules of candidate signal pathway in adenine-induced CKD rats and TGF-β1-induced HK-2 cells with the treatment of BYF by western blotting and RT-qPCR analyses. Using small interfering RNA, we assessed the effect of BYF on the TLR4-mediated NF-κB mechanism for CKD renal fibrosis and inflammation. Network pharmacology analysis results identified 369 common targets from BYF and CKD. Based on these common targets, the BYF intervention pathway was analyzed by Gene Ontology (GO) and Kyoto Encyclopedia of Genes and Genomes (KEGG) enrichment analysis. We found that Toll-like receptor (TLR) and NF-κB signaling pathways were enriched. Then, we demonstrated that BYF significantly improved the adenine-induced CKD rat model condition by kidney dysfunction improvement and reversing renal fibrosis and inflammation. Subsequently, we investigated BYF's effect on the TLR4/NF-κB signaling pathway. We found that TLR4 and phospho-NF-κB (p-p65 and p-IKβα) expression was significantly upregulated in adenine-induced CKD rats, then partially downregulated by BYF. Furthermore, BYF inhibited fibrotic and inflammatory responses, as well as TLR4, p-p65, and p-IKβα in TGF-β1-induced HK-2 cells. Additionally, the BYF inhibitory effect on fibrosis and inflammation, and NF-κB pathway activation were significantly reduced in TGF-β1-induced HK-2 cells transfected with TLR4 siRNA. Altogether, these findings demonstrated that the suppression of TLR4-mediated NF-κB signaling was an

important anti-fibrotic and anti-inflammatory mechanism for BYF against CKD. It also provided a molecular basis for new CKD treatment drug candidates.

Keywords: traditional Chinese medicine, bupi yishen formula, chronic kidney disease, network pharmacology, experimental study

INTRODUCTION

Chronic kidney disease (CKD) is a worldwide public health problem with an estimated global prevalence of 8–16% (Jha, et al., 2013). CKD affects approximately 8–10% of the Western countries population (Lameire, et al., 2005), and >15% of U.S. adults may have CKD. In China, the total CKD prevalence is around 10.8% and affects more than 120 million individuals (Zhang, et al., 2012). Also, CKD is associated with adverse cardiovascular events and high mortality risk (Bello, et al., 2011). However, there are limited treatment options available for CKD patients. The main approach to delay CKD progression is renin-angiotensin system (RAS) blockade, as well as blood pressure and glycemic control (Palmer, et al., 2015; Breyer and Susztak, 2016). These therapeutic strategies are insufficient to impair CKD progression to end-stage renal disease (ESRD). Therefore, it is urgent to develop effective medications to prevent CKD progression.

Traditional Chinese medicine (TCM) is commonly used in conjunction with Western medications for CKD treatment in China and other Asian countries (Li and Wang, 2005; Wojcikowski, et al., 2006; Zhong, et al., 2013). However, the use of TCM in CKD treatment remains controversial, especially because of renal toxicities present in some TCM (Feng, et al., 2018; Yang B et al., 2018; Omer Mohamed, et al., 2020). There is also emerging solid evidence of the beneficial effects of TCM prescribed for CKD patients in mainland China (Zhang, et al., 2014; Li, et al., 2020; Wu, et al., 2021) and Taiwan (Lin, et al., 2015), supporting that TCM can be promising for the development of new therapeutic drugs for CKD treatment.

The Bupi Yishen Formula (BYF), a patent TCM, is composed of eight herbs, which are modified from one traditional Si-Jun-Zi Decoction (SJZD). SJZD was recorded in Tai Ping Hui Min He Ji Ju Fang (A.D.1078-1,110) and is used to replenish "Qi" and reinforce "Spleen". Based on TCM theory, BYF can "reinforce the Spleen and invigorate the Kidney" and "dispel dampness and resolve turbidity", suggesting that it could be used for CKD treatment. Over the past decade, BYF has been clinically applied as a basic treatment for CKD patients. Our recently published multicenter randomized controlled trial demonstrated that BYF significantly improved kidney function in non-diabetic CKD4 patients, as evidenced by a slower decline slope of the estimated glomerular filtration rate (eGFR) and a lower composite outcome risk (Mao, et al., 2020). However, BYF's underlying reno-protective mechanism remains unknown and requires investigation.

In this study, we first identified the BYF and CKD common targets. Then, we analyzed the intervention pathways based on these common targets using network pharmacology. Second, we examined BYF's therapeutic effect on CKD *in vivo*. We used an adenine-induced CKD rat model and found that BYF reduced renal fibrosis and inflammation, and simultaneously inhibited the TLR4/NF-κb pathway. Finally, the BYF regulatory mechanism on renal fibrosis and inflammation was validated *in vitro* with TGF-β1-induced HK2 cells and TLR4 siRNA. Altogether, our study demonstrated that BYF reduced renal fibrosis and inflammation by TLR4-mediated NF-κb signaling pathway suppression, which may be a key mechanism of its therapeutic effect on CKD.

MATERIALS AND METHODS

Active Compounds and Corresponding Drug Targets Collection

The BYF chemical compounds were screened using TCMSP (http://tcmspw.com/tcmsp.php) (Ru, et al., 2014), TCMID (http://www.megabionet.org/tcmia/), and BATMAN-TCM (http://bionet.ncpsb.org/batman-tcm/index.php.Home/Index/index). Compounds that showed DL ≥ 0.18 and OB ≥ 30% were retrieved as active by ADME analysis (Wang, et al., 2015). We collected active compounds targets with the TCMSP and SYMMAP (http://www.symmap.org) databases (Wu, et al., 2019), then retrieved the target's gene name and ID using the Uniprot (https://www.uniprot.org/) database.

Disease and Drug-Disease Common Targets Collection

The genes of targets related to "Chronic kidney disease" were screened *via* GeneCards (https://www.genecards.org/) (Stelzer, et al., 2011), OMIM (https://www.omim.org/) (Amberger, et al., 2015), TTD (http://db.idrblab.net/ttd/), MALACARDS (https://www.malacards.org/) (Rappaport, et al., 2017), and DisGeNET database (http://disgenet.org/) (Piñero, et al., 2017). After removing duplicated genes, the common targets associated with BYF and CKD were collected as the candidates.

Drug-Compound-Target Interaction Network Construction

To analyze the relationship between drugs, active compounds, and candidate targets, a drug-compound-target interaction network was constructed using Cytoscape 3.6.1 software. In the network, different targets, active compounds, and drugs were represented as different colors and shapes nodes.

Protein-Protein Interaction Network Construction

The String database contains a large number of PPI relationships (von Mering, et al., 2005). The candidate targets were unloaded

onto the String database (https://string-db.org/) to obtain related information about protein interactions. Then, a PPI network was Constructed using Cytoscape 3.6.1 software. Besides, the median of three topological indexes was calculated (BC, CC, and DC), and the core PPI network targets were screened.

Enrichment Analysis

Gene Ontology (GO) functional and Kyoto Encyclopedia of Genes and Genomes (KEGG) pathway enrichment analysis were performed based on the candidate targets using DAVID 6.8. The downloaded results were sorted using *p* and count values. The workflow used for this study was shown in **Supplementary Figure S1**.

BYF Water Extract Preparation

BYF contains eight Chinese herbs. The related BYF herbal information and chemical composition analysis were performed as previously described (Zhang, et al., 2018; Mao, et al., 2020). Raw herbs were purchased from Jiangyin Tianjiang Pharmaceutical Co., Ltd. (Jiangsu, China). The eight BYF components, including Astragali radix (30 g), Codonopsitis radix (15 g), Atractylodis macrocephalae rhizome (12 g), Poria (15 g), Diosscoreae rhizome (15 g), Coicis semen (20 g), Cuscutae semen (12 g), and Salviae miltiorrhizae radix et rhizome (15 g), were boiled twice (1 h each) in ddH2O (w/v). The extract was condensed and stored at −20 °C. Before treatment, the BYF extract was dissolved in distilled water.

Animals and Experimental Treatment

This animal experiment was performed according to protocols approved by the Institutional Ethics Review Boards of the Second Clinical College of Guangzhou University of Chinese Medicine, Guangzhou, China (approval No. 2020021). Twenty-four male Spraque-Dawley (SD) rats (~200 g of weight) were purchased from the Guangdong Experimental Animal Center (Guangzhou, China). They were housed in the SPF animal breeding room with a 12-h light/12-h dark cycle and the temperature was maintained at 22–25°C. Rats were randomly divided into four groups (n = 6 for each group): 1) control (CTL); 2) untreated CKD (CKD); 3) CKD treated with BYF-Low dose (BYF-L); and 4) CKD treated with BYF-High dose (BYF-H). The CKD in rats was induced by intra-gastric gavage with adenine (Sigma-Aldrich, St Louis, MO, USA) at 200 mg/kg for 4 weeks (Chen, et al., 2017; Thakur, et al., 2018). Rats in the CKD treatment groups received BYF extract doses of 15 g/kg/d (BYF-L) and 30 g/kg/d (BYF-H) for 4 weeks with simultaneous adenine administering. Rats in CTL received normal adenine-free saline solution for 4 weeks.

Biochemical Analysis of Serum and Urine Samples

Serum creatinine and urea, 24 h urinary protein, urinary albumin to creatinine ratio, aspartate transaminase (AST), and alanine transaminase (ALT) were measured using a Roche automatic biochemistry analyzer (Hitachi, 7180, Tokyo, Japan) following the manufacturer's instructions. Analyses were performed in the Laboratory Department of the University City Hospital of Guangdong Hospital of Traditional Chinese Medicine.

Histological Examination

Rat kidney samples were fixed with 4% buffered paraformaldehyde (pH 7.4) at 4°C overnight, dehydrated in graded alcohols, and embedded in paraffin. The paraffin-embedded kidneys were cut into 2 μm sections and stained with hematoxylin and eosin (HE), periodic acid-Schiff (PAS), and Masson's trichrome for pathological changes evaluation. The tubular atrophy score was performed in PAS staining. The interstitial fibrosis was assessed by collagen deposition area in Trichrome staining using the ImageJ software (NIH, Bethesda, MD, United States).

Immunohistochemical Analysis

For immunohistochemistry staining, 2 μm paraffin-embedded sections were deparaffinized and rehydrated. The antigens were repaired with 1% (w/v) Tris-EDTA solution by high temperature and pressure for 10 min. Sections were blocked with BSA, then incubated with primary antibodies. The following antibodies were used: TGF-β1 (3711; Cell Signaling Technology), α-SMA (19,245; Cell Signaling Technology), fibronectin (NBP1-91258, Novus), and TLR4 (sc-293072, Santa Cruz). The secondary antibody was horseradish-peroxidase (HRP) goat anti-rabbit IgG (J31126; Transgen Biotech).

Cell Culture and Treatment

The HK-2 cells were cultured in DMEM/F12 supplemented with 10% FBS, 25 mM glucose, and 1% penicillin and streptomycin. They were incubated in a 37°C humidified incubator supplied with 5% CO_2. The HK-2 cells were passaged using 0.25% Trypsin at a 1:6–8 ratio every 3–4 days. At 80% confluence, the cells were starved in 0.5% FBS overnight. Then, cells were divided into negative control (CTL), TGF-β1, and BYF groups. The TGF-β1 group was treated with 10 ng/ml TGF-β1 for 48 h. The BYF group was treated with 10 ng/ml TGF-β1 for 24 h, then treated with 32 mg/ml BYF for 24 h.

Cell Viability

The CCK-8 assay was applied to assess the BYF effect on cell viability, following the manufacturer's instructions. First, serum-starved HK-2 cells were treated with different BYF concentrations (0, 32, 64, 128, 188, 256, 375, 512, 750, 1,500 mg/ml) with or without TGF-β1 for 48 h. Second, 10 μl of CCK-8 reagent reacted with HK-2 cells at 37°C for 2 h. Finally, the supernatant was removed, and the optical density was measured at 490 nm using a microplate reader (TECAN, Mannedorf, Switzerland).

TRL4 Downregulation by Small Interfering RNA

Transfection of siRNA was used to downregulate TRL4 in the HK-2 cells. The HK-2 cells were transfected with 10 μM siRNA targeting TRL4 (si-TRL4) or control siRNA (si-CTL) using Lipofectamine 2000 reagent (Invitrogen, Carlsbad, CA, United States), according to the manufacturer's protocols. After siRNA transfection, cells were incubated with or without BYF for 48 h, with or without TGF-β1.

RNA Extraction and qPCR Analysis

Total RNA was extracted from the kidney cortex and HK2 cells using TRIzol Reagent (Invitrogen, Carlsbad, CA). About 500 ng of extracted RNA was reversely transcribed to cDNA with the QuantiTect Reverse Transcription Kit. Then, cDNA samples were used to conducted real-time PCR analysis with an SYBR Green I Kit. Gene expression quantification was normalized to Glyceraldehyde-3-Phosphate dehydrogenase (GAPDH). The expression level fold change relative to the control group was calculated using the $2^{-\triangle\triangle Ct}$ method. The primers used for this study are described in **Supplementary Table S1**.

Western Blotting Analysis

The kidney cortex and cultured cells were lysed in radioimmunoprecipitation assay (RIPA) buffer containing a protease inhibitor cocktail (Roche) and phosphatase inhibitor. Protein concentration was measured by a BCA detection kit (Thermo Fisher Scientific). The same protein amount (50 μg) was electrophoresed using 10% SDS-PAGE gels, then transferred to polyvinylidene difluoride membranes (Millipore, Billerica, MA, United States). The membranes were blocked with 5% nonfat milk for 1 h, then incubated with primary antibodies overnight at 4°C. Membranes were incubated with horseradish peroxidase (HRP)-conjugated anti-mouse IgG (Boster, BA1050) or HRP-conjugated anti-rabbit IgG (Boster, BA1054) for 1 h at room temperature. Their HRP activity was visualized using an enhanced chemiluminescence reagent (Bio-RAD, Bio-Rad universal Hood II, California, United States) and Image Lab System (Bio-RAD 5.2.1) was used for densitometric analysis. The primary antibodies used for this study included TGF-β1 (3711; Cell Signaling Technology); α-SMA (19,245; Cell Signaling Technology); fibronectin (NBP1-91258, Novus); Collagen I (NB600-408, Novus); Collagen III (NBP1-05119, Novus); Smad3 (9523S; Cell Signaling Technology); p-Smad3 (9520S; Cell Signaling Technology); TLR4 (sc-293072, Santa Cruz); NF-κb (p65, ab16502, Abcam); p-NF-κb (p-p65, 3033S, Cell Signaling Technology); IKβα (4814S, Cell Signaling Technology); p-IKβα (2859s, Cell Signaling Technology); and MyD88 (ab219413, Abcam).

Statistical Analyses

Each analysis is representative of at least three independent repeats of experiment. GraphPad Prism five software (GraphPad Software Inc, La Jolla, CA) was used for statistical analysis. The data are represented as mean ± standard deviations (SD). Differences between two groups were analyzed using a 2-tailed Student's t-test and two-way analysis of variance (ANOVA) was used for comparison between three or more groups. A p-value < 0.05 was considered statistically significant.

RESULTS

BYF Active Compounds and Candidate Targets in CKD

Using TCMSP, TCMID, and Batman-TCM databases, 603 chemical compounds were screened in BYF's eight components. Based on the DL ≥ 0.18 and OB ≥ 30%, 294 active compounds were selected acting on 2134 potential targets (**Supplementary Tables S2, S3**). According to OMIM, TTD, MALACARDS, and DisGeNET databases, 1,157 predicted CKD-associated targets were obtained (**Supplementary Table S4**). After merging active compounds and CKD targets, 369 common targets were recognized as candidates, which could be the biological basis of BYF's effect on CKD (**Figure 1A** and **Supplementary Table S5**). Through network analysis, a drug-compound-target interaction network was established to generate the BYF active compounds for 369 candidate targets based on the 294 active compounds identified in the eight herbs (**Figure 1B**). From this network, we found that different compounds act on multiple targets, and vice versa. Additionally, a PPI network was established based on the 369 candidate targets by importing the candidate targets gene IDs to the STRING database (**Figure 1C**). The PPI network showed that there is a close interaction between those targets. The 30 core targets obtained from this PPI network showed that PI3K, AKT, IL6, TNF, NF-κb, and TLR4 were the most relevant (**Supplementary Table S6**).

Functional Enrichment Analysis of BYF Candidate Targets in CKD

GO functional enrichment analysis was annotated from three aspects: biological process, molecular function, and cellular component. To discover the BYF pharmacological mechanisms in CKD treatment, 369 candidate targets were inputted to the DAVID 6.8 database for GO enrichment analysis (**Figures 2A–C**). The results indicated that the following mechanisms were related to BYF against CKD: inflammatory response, NF-κB transcription factor activation, apoptotic process, plasma membranes, and protein binding. To further explore the relationship between these candidate targets and their corresponding pathways, KEGG pathway enrichment analysis was performed *via* the DAVID 6.8 database (**Figure 2D**). The results indicated the Toll-like receptor (TLR) signaling, TNF signaling, PI3K-AKT signaling, apoptosis, and HIF-1 signaling pathways are related to BYF mechanisms against CKD.

BYF Improved Renal Function in an Adenine-Induced CKD Rat Model

Treatment with BYF significantly increased the body weight and decreased the urine volume in adenine-induced CKD rats (**Figures 1A,B**). Compared with CTL, the levels of 24 h urinary protein excretion and urine albumin-to-creatinine ratio in CKD were increased, and in BYF groups they were reduced (**Figures 1C,D**). The CKD group showed higher serum creatinine and urea compared to CTL, which could be restored by BYF treatment (**Figures 1E,F**). Moreover, the ALT and AST serum levels were not significantly different between the four groups (**Figures 1G–I**). This indicates that the two BYF treatment dosages that we utilized are safe. In HE staining, CKD rats showed obvious renal tubular dilation and massive inflammatory cells infiltration, and BYF treatment inhibited these changes. In PAS staining, CKD rats indicated severe loss of tubular epithelial cells, chronic tubular atrophy, and

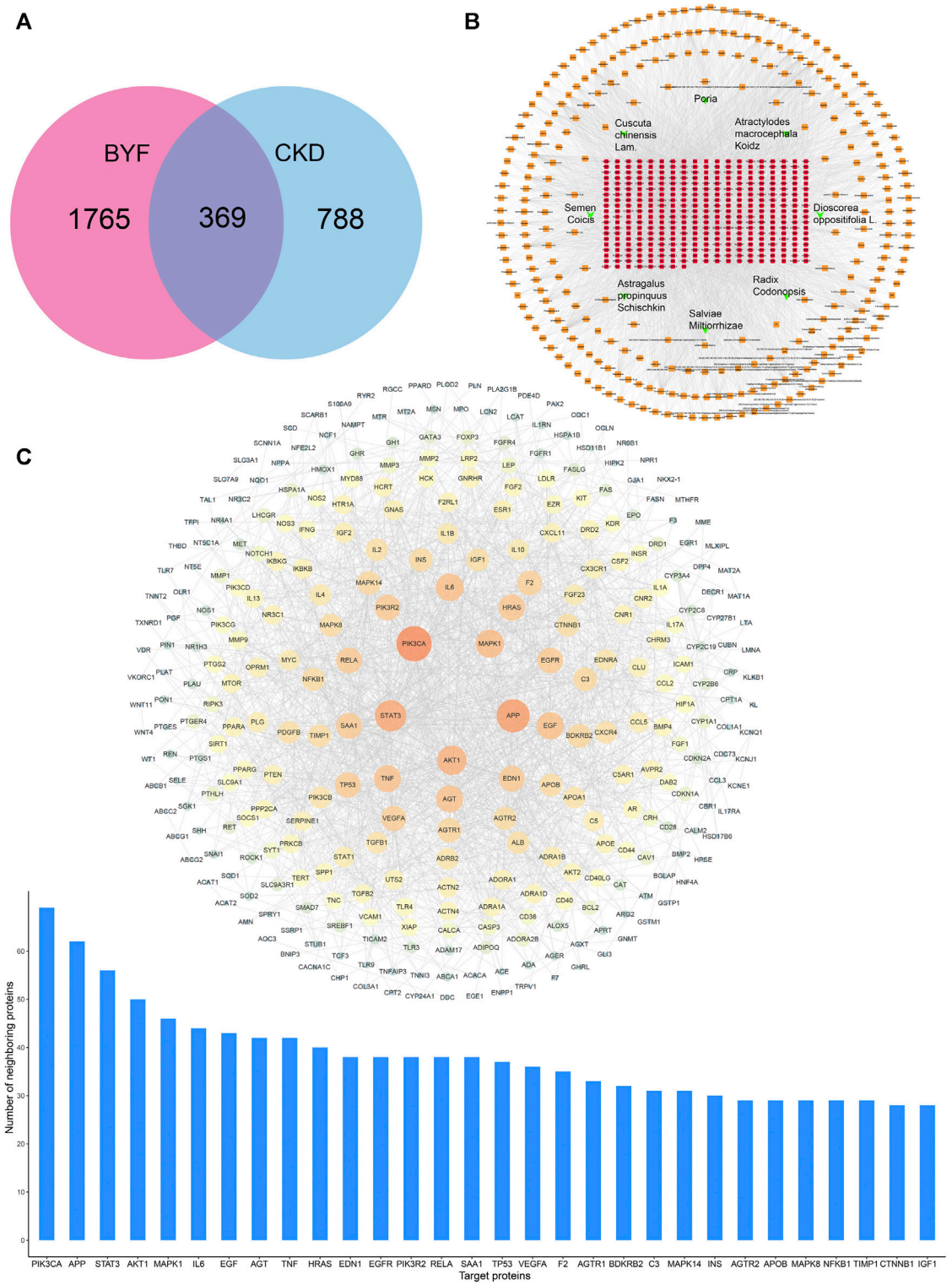

FIGURE 1 | BYF network pharmacology analysis against CKD. **(A)** Venn diagram revealing BYF and CKD common target genes; **(B)** Drug-compound–target interaction network diagram; **(C)** PPI network and the proteins with the top 30˚ among common BYF and CKD targets.

glomerulosclerosis, recovered by BYF (**Figures 3J,K**). Masson staining showed interstitial fibrosis in the CKD, and that BYF treatment significantly decreased collagen deposition (**Figures 3J–L**). Altogether, these results suggested that the CKD model was successfully established and that BYF improved kidney function and reduced structural damage in CKD rats.

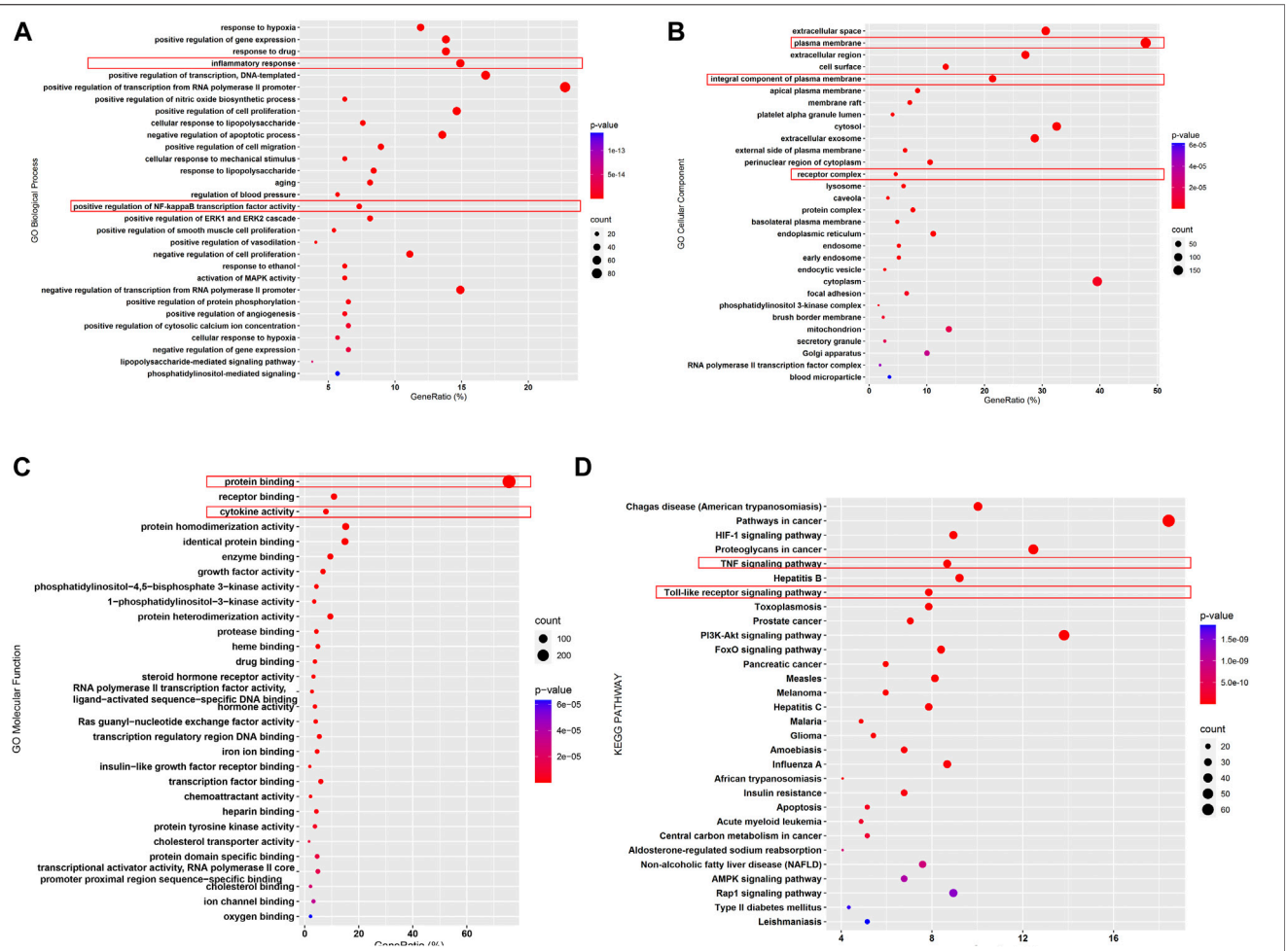

FIGURE 2 | Enrichment analysis of BYF candidate targets against CKD. GO enrichment analysis revealed the related biological process **(A)**, molecular function **(B)**, and cellular component **(C)**; KEGG pathway analysis revealed the related pathways **(D)**.

BYF Attenuated Renal Fibrosis and Inflammation in Adenine-Induced CKD Rats

Renal fibrosis has been long considered as the common and final manifestation of nearly all CKD progressive forms. Thus, we further examined the BYF effect on renal fibrosis by fibrotic markers. Immunohistochemical staining showed that the α-SMA, TGF-β1, and Fibronectin protein levels increased in CKD, which was decreased by BYF treatment (**Figures 4A,B**). Western blotting (WB) indicated that the expression levels of TGF-β1, Fibronectin, α-SMA, Collagen I and III, and p-Smad3 also increased in CKD. In contrast, BYF administration significantly reduced these proteins level (**Figures 4C,D**). Similarly, fibrotic markers mRNA expression increased in CKD and was reversed by BYF treatment (**Figure 4E**). Interestingly, BYF treatment also remarkedly downregulated proinflammatory factors mRNA level, including interleukin-1β (IL-1β), IL-6, MCP-1, and tumor necrosis factor-alpha (TNF-α) in the kidneys of CKD rats (**Figure 4F**). Altogether, these results suggested that BYF could inhibit the increase in TGF-β1/Smad3-mediated fibrotic markers production and reduced inflammatory cytokines release. This provided further evidence of the BYF's beneficial effect on CKD.

BYF Inhibited TLR4/NF-KB Signaling Pathway in The Kidneys of Adenine-Induced CKD Rats

Recent studies revealed that the TLR4/NF-κB signaling pathways are closely associated with kidney fibrosis and CKD progression (Wang, et al., 2008; Liu, et al., 2015; Pérez-Ferro, et al., 2016) by augmenting TGF-β/Smads responses (Bhattacharyya, et al., 2013) and activating inflammatory cytokines (Chen, et al., 2018). Since BYF could target TLR and NF-κB pathways based on the network pharmacology analysis, the anti-fibrotic and anti-inflammatory effects of BYF on CKD were explored. The TLR4 mRNA expression and protein expression by immunohistochemical staining were significantly upregulated in CKD and downregulated by BYF (**Figures 5A,B**). Western blot analysis showed that the protein levels of TLR4, p-NF-κB (p-p65 and p-IKβα), and

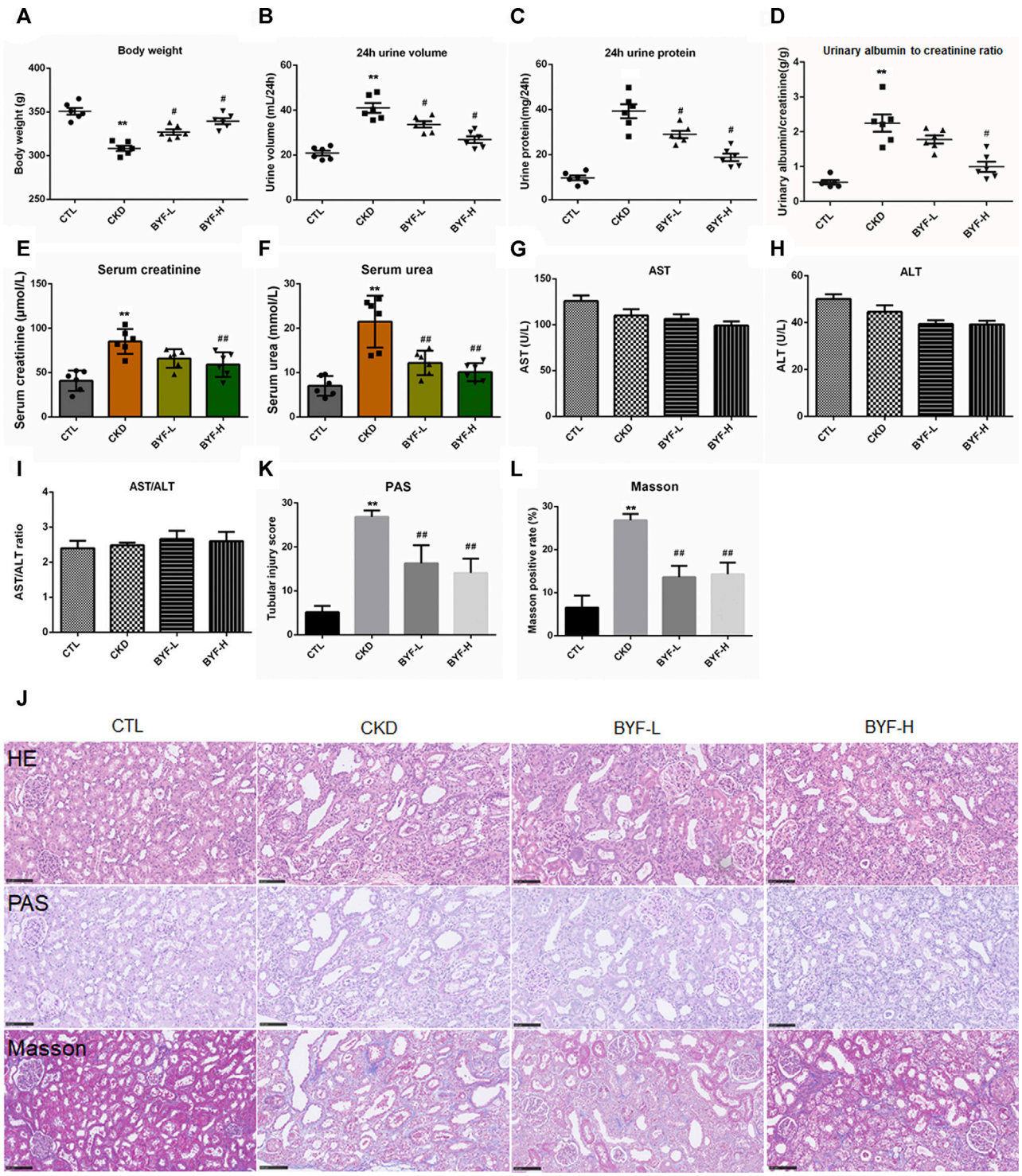

FIGURE 3 | BYF improves kidney function and reduces renal pathological injury in adenine-induced CKD rats. BYF administration effectively increased body weight **(A)** and reduced urine volume **(B)**. In CKD rats, BYF reduced 24 h urinary protein excretion **(C)**, urinary albumin-to-creatinine ratio **(D)**, serum creatinine **(E)** and urea **(F)**. **(G)** Serum ALT, **(H)** AST, **(I)** and ALT/AST levels. **(J)** HE, PAS, and Masson's trichrome staining representative micrographs in indicated groups (scale bar = 100 μm). **(K)** Chronic tubular atrophy score. **(L)** Quantitative analysis of Masson trichromatic positive rate. All values were presented as means ± SD. n = 6 rats per group. $^{*}p < 0.05$ and $^{**}p < 0.01$ vs. the CTL group; $^{\#}p < 0.05$ and $^{\#\#}p < 0.01$ vs. the CKD group.

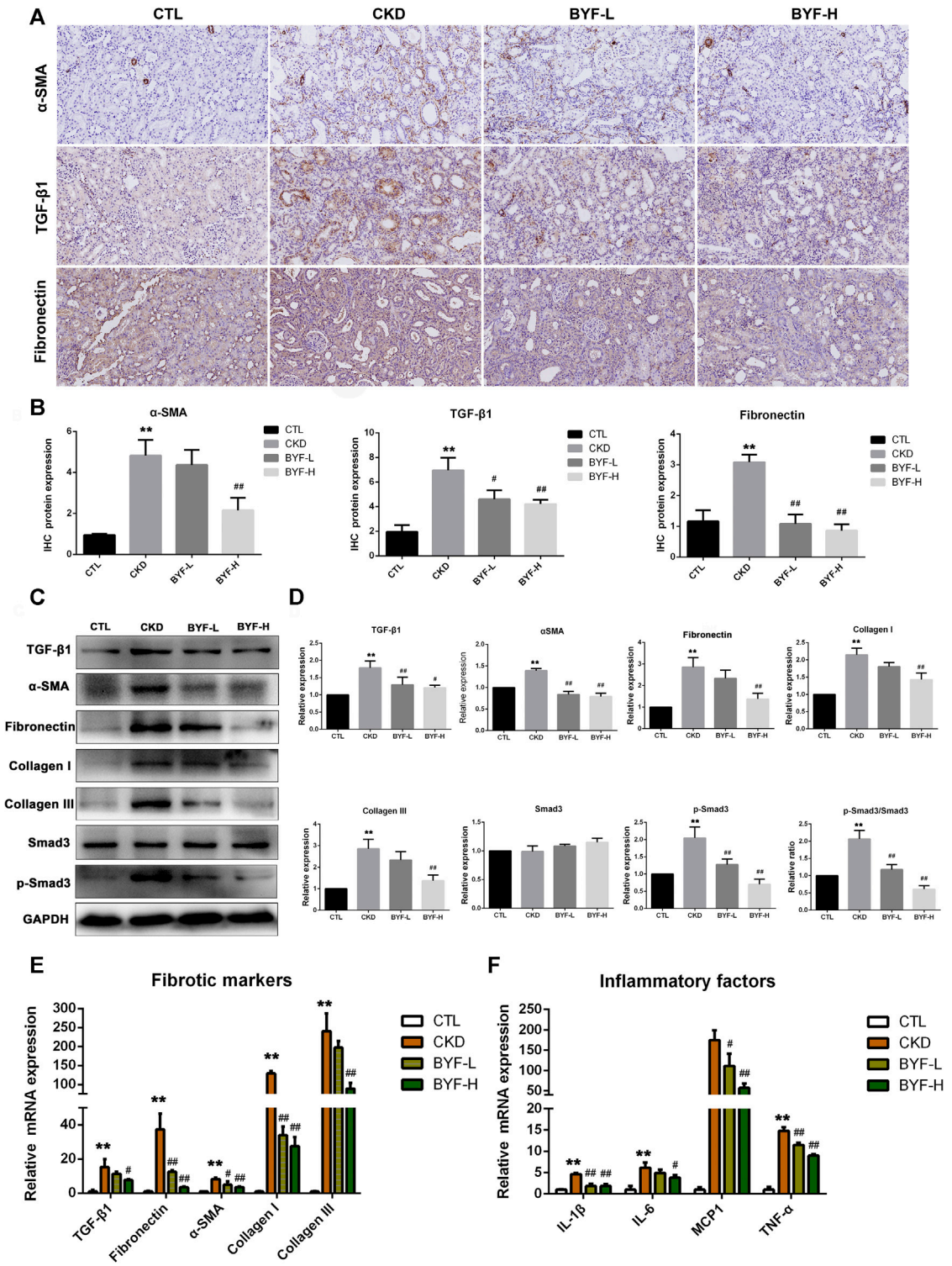

FIGURE 4 | BYF reduces fibrotic and inflammatory markers expression levels in the kidney of adenine-induced CKD rats. α-SMA, TGF-β1, and Fibronectin immunohistochemical staining representative micrographs **(A)** and quantitative analysis **(B)**. TGF-β1, Fibronectin, α-SMA, Collagen I and III, and p-Smad3 WB vaαlidation **(C)** and quantitative analysis **(D)**. qPCR validation of fibrotic markers **(E)** and proinflammatory factors **(F)** in indicated groups. Scale bar = 100 μm. All values are presented as means ± SD. n = 3 rats per group. $^{*}p < 0.05$ and $^{**}p < 0.01$ vs. the CTL group; $^{\#}p < 0.05$ and $^{\#\#}p < 0.01$ vs. the CKD group.

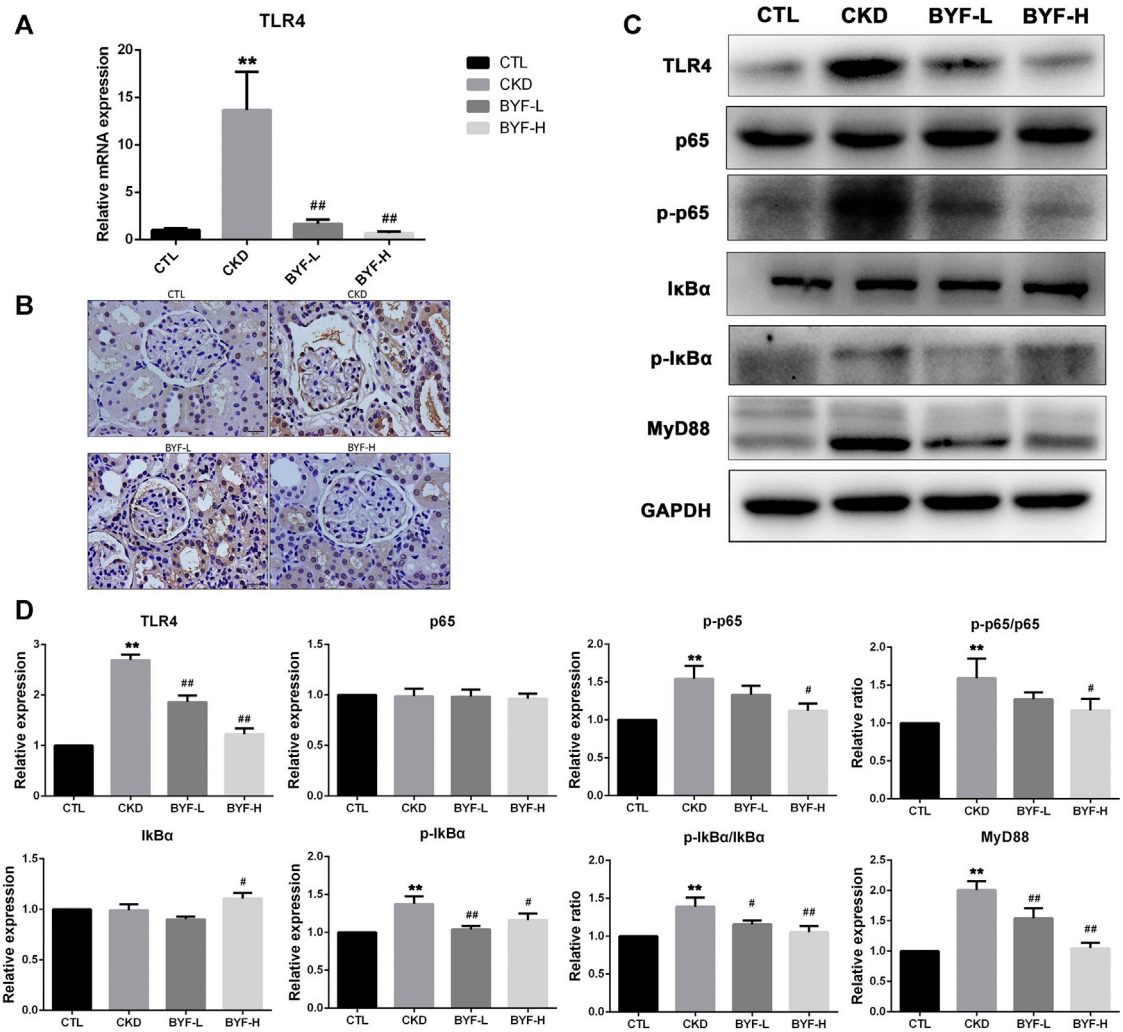

FIGURE 5 | BYF suppresses TLR4/NF-κB signaling pathway in adenine-induced CKD rats. qPCR validation of TLR4 **(A)** and immunohistochemical staining of TLR4 **(B)** in indicated groups. TLR4, p65, p-p65, IKβα, p-IKβα, and MyD88 WB validation **(C)** and quantitative analysis **(D)** in indicated groups. All values are presented as means ± SD. n = 3 rats per group. $^{*}p < 0.05$ and $^{**}p < 0.01$ vs. the CTL group; $^{\#}p < 0.05$ and $^{\#\#}p < 0.01$ vs. the CKD group.

MyD88 in kidney tissues were significantly increased in CKD compared to CTL, while BYF treatment restored these proteins with the high doses effect being generally more evident (**Figures 5C,D**). These results indicated that BYF treatment might attenuate CKD by improving renal fibrosis and inflammation *via* TLR4/NF-κB mechanism**.**

BYF Improved Fibrogenesis and Inflammation by Inhibiting TLR4-Mediated NFκB Signaling Pathway in TGF-β1-Induced HK2 Cells

Renal proximal tubular cells are the major sites of kidney injury and are critical in fibrosis development (Liu, et al., 2018). Based on the inhibitory effect on renal fibrosis and inflammation in adenine-induced CKD rats, TGF-β1-induced HK-2 cells were used to study the BYF protection *in vitro*. To explore an optimal BYF concentration, different concentrations (0, 32, 64, 128, 188, 256, 375, 512, 750, 1,500 mg/ml) were added to HK-2 cells for 24 h. CCK-8 assay showed that the cell viability at 32 mg/ml was optimum (**Supplementary Figure S2**). Based on these results, 32 mg/ml of BYF was used in the subsequent experiments.

To evaluate the anti-fibrotic and anti-inflammatory effects of BYF *in vitro*, the fibrotic and inflammatory markers expression level was detected in TGF-β1-induced HK-2 cells. Results showed that BYF markedly reduced the elevated α-SMA, Fibronectin, and TGF-β1, as well as TNF-α, IL-1β, and IL-6 mRNA levels in TGF-β1-induced HK-2 cells (**Figure 6A,B**). Likewise, TGF-β1, α-SMA, Fibronectin, Collagen III, and p-Smad3 protein expression levels reduced after BYF treatment (**Figures 6C,D**). Next, we

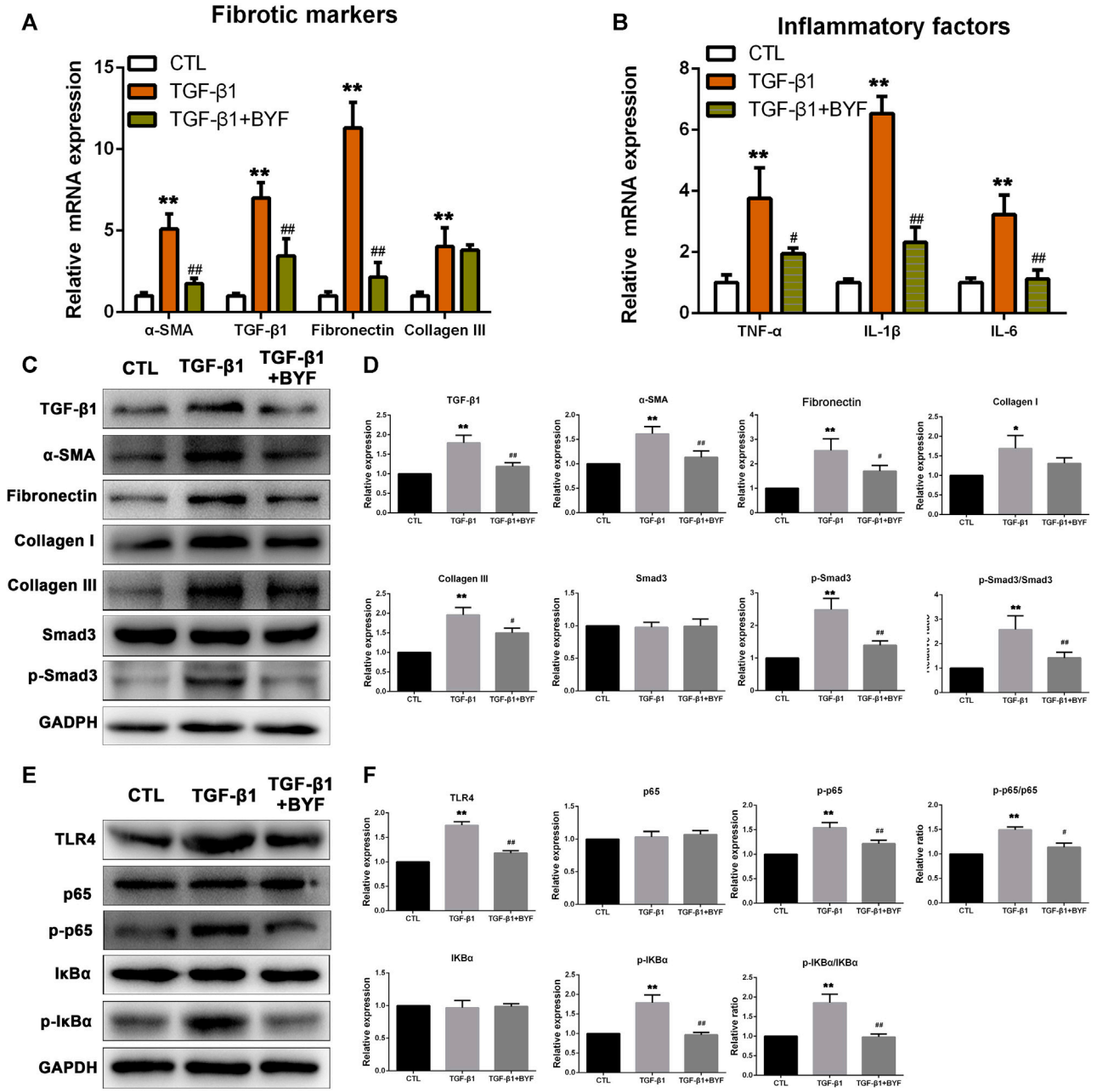

FIGURE 6 | BYF treatment decreases fibrotic and inflammatory markers expression levels and inhibits TLR4/NF-κB signaling pathway in the TGF-β1-induced HK2 cells. qPCR validation of fibrotic markers **(A)** and inflammatory factors **(B)** between groups. Fibrotic markers WB validation **(C)** and quantitative analysis **(D)** in indicated groups. TLR4/NF-KB signaling main proteins WB validation **(E)** and quantitative analysis **(F)** in indicated groups. All values are presented as means ± SD. n = 3 independent experiments for each indicator. $^{*}p < 0.05$ and $^{**}p < 0.01$ vs. the CTL group; $^{\#}p < 0.05$ and $^{\#\#}p < 0.01$ vs. the CKD group.

investigated the mechanisms whereby BYF inhibits renal fibrosis and inflammation in TGF-β1-induced HK-2 cells. Cells treated with TGF-β1 increased the TLR4, p-p65, and p-IKβα protein levels, while BYF treatment reduced it (**Figures 6E,F**). These results suggested that BYF likely inhibited fibrogenesis and inflammation *in vitro* by TLR4/NF-KB pathway suppression.

To better understand TRL4/NF-κb signaling functional role in TRL4-mediated renal fibrosis and inflammation, we knocked down TRL4 in HK2 cells by siRNA. TLR4 mRNA expression was significantly downregulated (**Figure 7A**). The expression levels of fibrotic and inflammatory markers showed that BYF treatment could not markedly decrease the fibronectin, TGF-β1, and α-SMA mRNA levels, as well as TNF-α, IL-1β, and IL-6 in

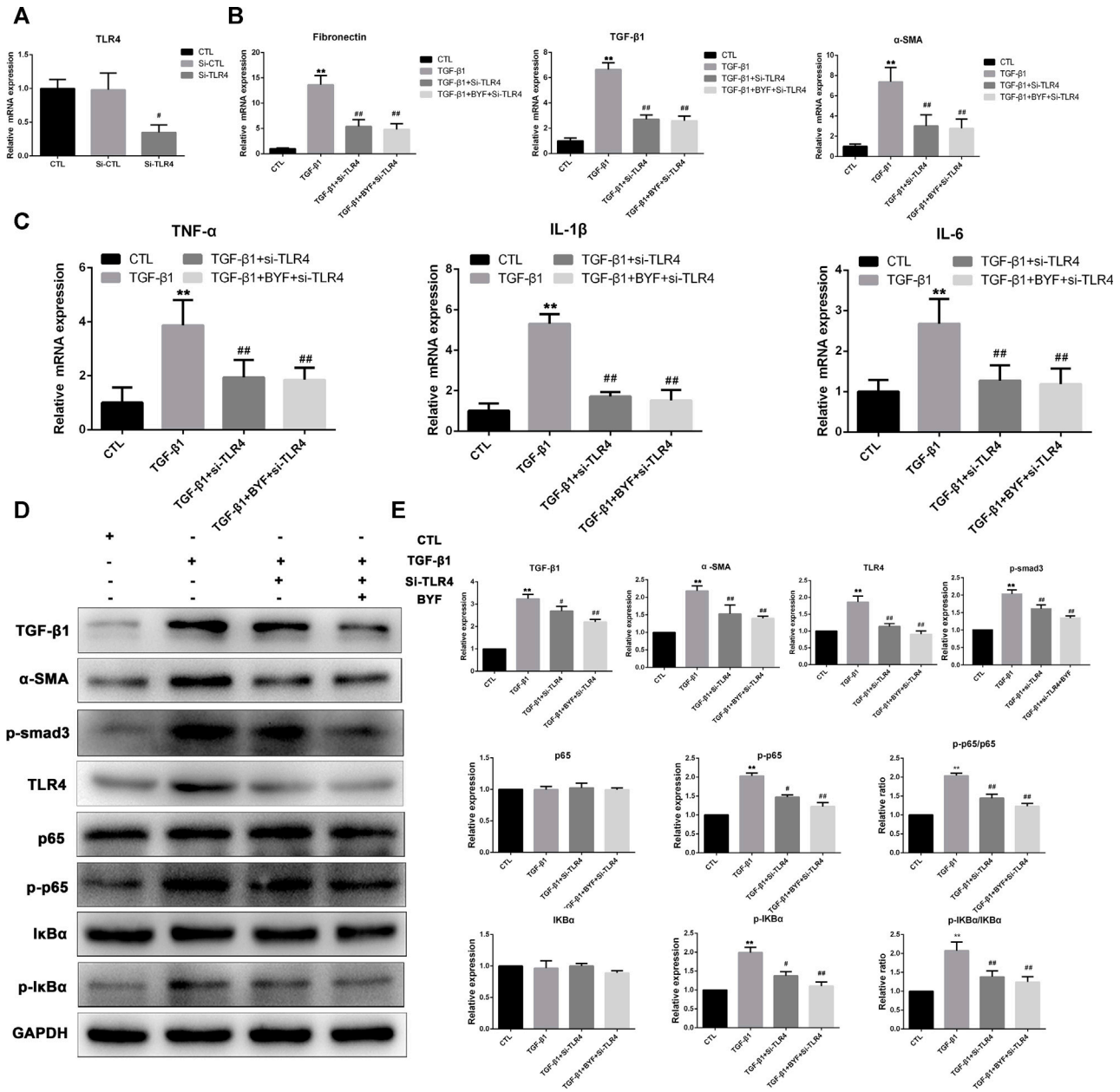

FIGURE 7 | Silencing TLR4 significantly suppresses BYF inhibitory effect on TGF-β1-induced fibrogenesis and inflammation and NF-κB pathway activation in HK2 cells. **(A)** TLR4 qPCR validation in HK-2 cells transfected with TLR4 siRNA. **(B)** Fibrotic markers qPCR validation between groups. **(C)** Inflammatory factors qPCR validation between groups. TLR4/NF-κB signaling rescue assay WB validation **(D)** and quantitative analysis **(E)** in indicated groups. All values are presented as means ± SD. n = 3 independent experiments for each indicator. $^{*}p < 0.05$ and $^{**}p < 0.01$ vs. the CTL group; $^{\#}p < 0.05$ and $^{\#\#}p < 0.01$ vs. the CKD group.

TGF-β1-induced HK-2 cells silenced with TLR4 siRNA (**Figures 7B,C**). Next, WB showed that silencing TRL4 markedly suppressed the TGF-β1 activation effect on the NF-κb pathway in HK2 cells with reduced p-p65, and p-IKβα expression levels, compared with the TGF-β1 group. Furthermore, BYF did not significantly reduce the levels when TLR4 was silenced (**Figures 7D,E**). Altogether, these results demonstrated that the BYF might have a protective effect *via* the TLR4-mediated NF-κB mechanism to reduce CKD renal fibrosis and inflammation.

DISCUSSION

Although our previous clinical study revealed that BYF have protective effects on delaying kidney function progression among

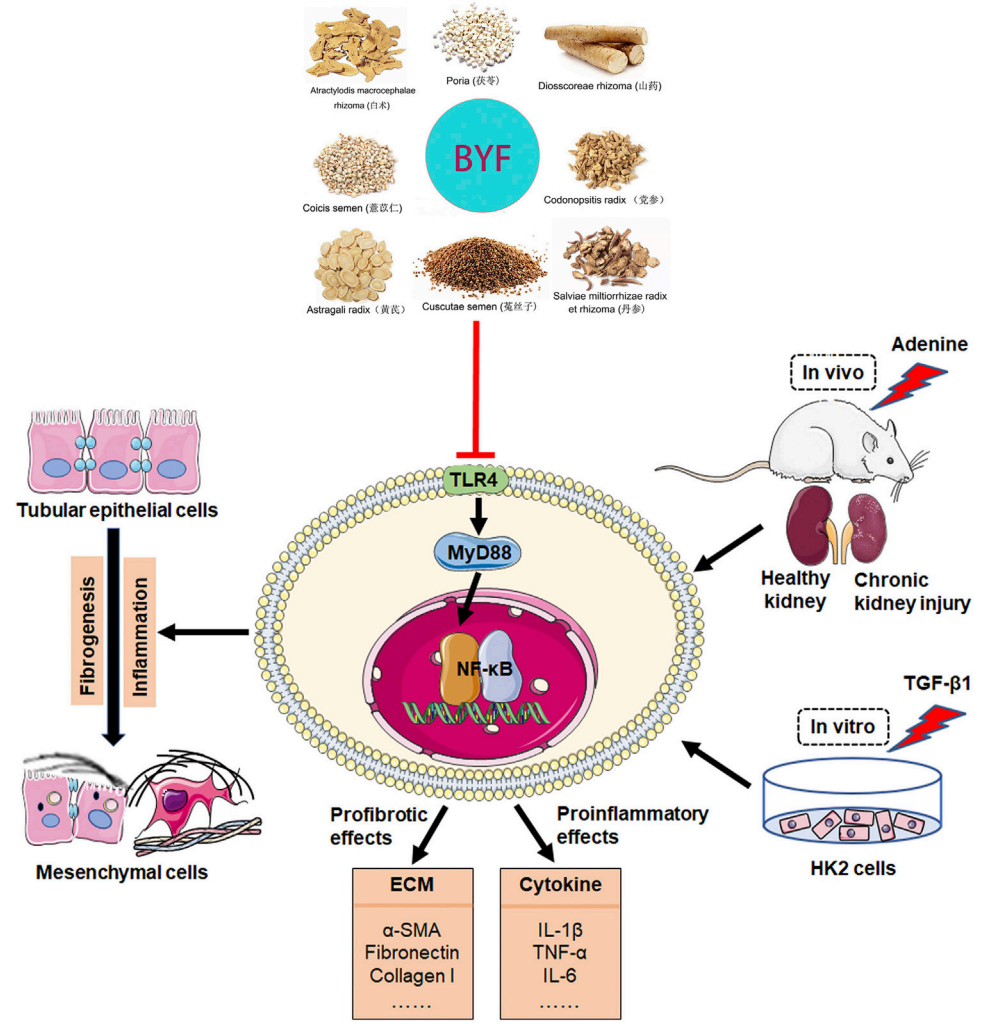

FIGURE 8 | BYF regulation on the TLR4/NF-κb signaling pathway in CKD.

advanced CKD patients (Mao, et al., 2020), its pharmacological mechanisms remain ambiguous. In this study, we investigated the BYF effect on CKD *in vivo* and *in vitro*. We explored its potential mechanisms combining network pharmacology, histopathology, and molecular biology. Network pharmacology-based analysis predicted that BYF protected against CKD through the TLR/NF-κB signaling pathway and the inflammatory and fibrotic response triggered by this pathway. Experimental validation indicated that BYF effectively inhibited the fibrosis and inflammatory response in adenine-induced CKD rats and TGF-β1-induced HK-2 cells. Also, these results showed that BYF alleviated renal fibrosis and inflammation *via* TLR4/NF-κB signaling pathway modulation. The putative anti-fibrotic and anti-inflammatory BYF mechanism in CKD is shown in **Figure 8**.

BYF is composed of eight Chinese herbs and has complex bioactive compounds. Therefore, it is difficult to clearfy its molecular mechanism through traditional pharmacological techniques. Network pharmacology-based analysis integrates a series of disciplines and techniques, including genomics, proteomics, and systems biology (Kim, et al., 2019). Thus, network pharmacology provides an effective method to clarify the multifaceted biological phenomenon mechanism of such complex compounds in Chinese herbal formulations. To explore the BYF molecular mechanism, we selected 369 common BYF and CKD targets, constructed a drug-compound-target network, and executed GO and KEGG enrichment analysis. Results suggested that TLR and NF-κB signaling pathway plays an important role in BYF pharmacological mechanism during CKD treatment. Compounds associated with BYF may directly act on TLR4/NF-κB signaling pathway and interfere with the downstream TGF-β1/Smad3 signaling pathway and inflammatory response, resulting in the inhibition of profibrotic factors (α-SMA, Fibronectin, Collagen I and III) as well as the release of proinflammation cytokines (TNF-α, IL-1β, IL-8). Interestingly, the network pharmacology results showed that BYF may also interfere with the downstream targets, like PI3K, AKT, and TNF (except for the main molecules in the TLR4/NF-

κB pathway), with or without TLR2/3 interference. These findings indicated that BYF may interfere with CKD by multiple pathways through multiple compounds from different Chinese herbs.

Many animal models have been developed to study CKD pathogenesis and treatment in humans. However, most models do not mimic CKD complexity in humans, and the adenine diet or gavage model in rodents is an exception (Yokozawa, et al., 1986; Diwan, et al., 2018). Intra-gastric gavage of 200 mg/kg adenine in rats for 4 weeks has been well-accepted as a model to study kidney damage since this intervention mimick most of the functional and structural changes observed in human CKD (Chen, et al., 2017; Yang H, et al., 2018). We observed high levels of proteinuria, serum creatinine and urea, as well as tubular atrophy, inflammatory cells infiltration, and collagen synthesis during the 4 weeks in the adenine-induced CKD rats. Furthermore, BYF treatment partially recovered the kidney dysfunction and histopathological injury compared to the adenine-induced CKD group. These results suggested that a successful CKD rat model induced by adenine gavage was established.

Inflammation and fibrosis are two CKD pathological features. It has been proven that TGF-β1, α-SMA, and extracellular matrix (ECM) proteins such as fibronectin, and collagen I and III are master markers in kidney fibrosis development (Zeisberg and Neilson, 2010; Liu, 2011). Our results indicated that BYF markedly inhibited these fibrotic markers expression levels in adenine-induced CKD rat and TGF-β1-induced HK-2 cells, suggesting its anti-fibrotic effect in the kidney. Also, we found that BYF significantly decreased the proinflammatory factors mRNA levels, including IL-1β, IL-6, MCP-1, and TNF-α, *in vivo* and *in vitro*, indicating its anti-inflammatory effect in the kidney. Besides, TGF-β/Smads signaling prominent activation was observed (with increased TGF-β1 and p-Smad3 levels), which was reversed by BYF treatment. These results demonstrated that BYF protected against CKD through anti-fibrotic and anti-inflammatory effects.

It is well known that the TLR signaling pathway is one of the most crucial pathways in the host immune response in an infected environment, responding to different microorganisms and endogenous ligands (Mollen, et al., 2006). TLR4, an important member of the Toll-like family, is located in the cell membrane and cytoplasm and is crucial in the kidney fibrosis process (Bhattacharyya, et al., 2013; Pérez-Ferro, et al., 2016). NF-κB, an important transcription activator, modulates and regulates inflammatory mediators, and induces cytokines production (Mitchell, et al., 2016). It was reported that TLR4 enhances the downstream activation of the NF-κB pathway, which ultimately results in the inflammation reaction (Ciesielska, et al., 2021). In this study, we found that the TLR4, p-p65, p-IKβα, and MyD88 proteins levels were significantly increased in adenine-induced CKD rats, which markedly decreased after BYF treatment. These results suggested that BYF treatment may partially heal CKD by renal inflammation and fibrosis reduction *via* TLR4/NF-κB suppression mechanism.

Many kidney cell types (e.g., tubular, myofibroblasts, endothelial, and inflammatory) are involved in the development and progression of renal fibrogenesis and inflammation under pathological conditions (Liu, 2011). However, emerging evidence indicated that proximal tubular epithelial cells are the major injury sites and are critical in injury repair and fibrosis development (Yang, et al., 2010; Kang, et al., 2015; Liu, et al., 2018). TGF-β1 is one of the most powerful profibrotic cytokines and is vital in renal inflammation and fibrosis by downstream Smad3 signaling activation (Sutariya, et al., 2016; Gu, et al., 2020). It was also demonstrated that TGF-β signaling could be activated by TLR4 in a hepatic fibrogenesis mice model (Seki, et al., 2007). Therefore, we examined the BYF protective effects and TLR4/NF-κ b mechanism on TGF-β1-induced HK2 cells. We found that BYF markedly decreased fibrotic and inflammatory markers expression, and inhibited the protein expression of main molecules in the TLR4/NF-KB signaling pathway in TGF-β1-induced HK-2 cells. These results were consistent with previous research results obtained from adenine-induced CKD rat models. Then, we showed that the BYF anti-fibrotic and anti-inflammatory inhibition effects on the NF-κB pathway were diminished when TLR4 was silenced with siRNA in TGF-β1-induced HK-2 cells. Collectively, these findings demonstrated that the TLR4/NF-κB signaling suppression was an important anti-fibrotic and anti-inflammatory mechanism by which BYF partially healed CKD.

CONCLUSION

Our results indicated that BYF could significantly reduce renal fibrosis and inflammation by TLR4/NF-κB signaling pathway inhibition. Although these preliminary findings could not fully explain the underlying mechanism of the BYF protective effect, they provided further support for clinical trials aiming to assess the BYF effects against CKD progression. However, whether BYF has a beneficial role in any non-adenine-induced CKD rat model needs to be further elucidated. Moreover, due to the TCM complex composition, new technologies are required to investigate the material basis and underlying mechanisms of BYF on CKD.

DATA AVAILABILITY STATEMENT

The original contributions presented in the study are included in the article/**Supplementary Material**, further inquiries can be directed to the corresponding authors.

ETHICS STATEMENT

The animal study was reviewed and approved by The Institutional Ethics Review Boards of the Second Clinical College of Guangzhou University of Chinese Medicine, Guangzhou, China (approval No. 2020021).

AUTHOR CONTRIBUTIONS

All authors contributed to the study design, experiments, data analysis, and interpretation. XL and FL conceived of and designed the study. DZ and BL carried out the experiments. XJ and JD performed network pharmacology and experimental data analysis. ZL contributed to methodology. DZ edited and revised the manuscript. All authors have reviewed and approved the final manuscript.

FUNDING

This work was supported by the National Natural Science Foundation of China (No. 81904099, No.81873261) and China Postdoctoral Science Foundation (No. 2020M672559).

ACKNOWLEDGMENTS

We are grateful for technical support from research team of the Department of Nephrology, Guangdong Provincial Hospital of Traditional Chinese Medicine.

SUPPLEMENTARY MATERIAL

The Supplementary Material for this article can be found online at: https://www.frontiersin.org/articles/10.3389/fphar.2021.761572/full#supplementary-material

Supplementary Figure S1 | Graphical Abstract Study design: workflow used for the study.

Supplementary Figure S2 | BYF dose-dependent effect on cell viability by the CCK8 assay after 24 h.

REFERENCES

Amberger, J. S., Bocchini, C. A., Schiettecatte, F., Scott, A. F., and Hamosh, A. (2015). OMIM.org: Online Mendelian Inheritance in Man (OMIM®), an Online Catalog of Human Genes and Genetic Disorders. *Nucleic Acids Res.* 43, D789–D798. doi:10.1093/nar/gku1205

Bello, A. K., Hemmelgarn, B., Lloyd, A., James, M. T., Manns, B. J., Klarenbach, S., et al. (2011). Associations Among Estimated Glomerular Filtration Rate, Proteinuria, and Adverse Cardiovascular Outcomes. *Clin. J. Am. Soc. Nephrol.* 6, 1418–1426. doi:10.2215/CJN.09741110

Bhattacharyya, S., Kelley, K., Melichian, D. S., Tamaki, Z., Fang, F., Su, Y., et al. (2013). Toll-like Receptor 4 Signaling Augments Transforming Growth Factor-β Responses: a Novel Mechanism for Maintaining and Amplifying Fibrosis in Scleroderma. *Am. J. Pathol.* 182, 192–205. doi:10.1016/j.ajpath.2012.09.007

Breyer, M. D., and Susztak, K. (2016). Developing Treatments for Chronic Kidney Disease in the 21st Century. *Semin. Nephrol.* 36, 436–447. doi:10.1016/j.semnephrol.2016.08.001

Chen, C. Y., Kao, C. L., and Liu, C. M. (2018). The Cancer Prevention, Anti-inflammatory and Anti-oxidation of Bioactive Phytochemicals Targeting the TLR4 Signaling Pathway. *Int. J. Mol. Sci.* 19, 2729. doi:10.3390/ijms19092729

Chen, D. Q., Chen, H., Chen, L., Vaziri, N. D., Wang, M., Li, X. R., et al. (2017). The Link between Phenotype and Fatty Acid Metabolism in Advanced Chronic Kidney Disease. *Nephrol. Dial. Transpl.* 32, 1154–1166. official publication of the European Dialysis and Transplant Association - European Renal Association. doi:10.1093/ndt/gfw415

Ciesielska, A., Matyjek, M., and Kwiatkowska, K. (2021). TLR4 and CD14 Trafficking and its Influence on LPS-Induced Pro-inflammatory Signaling. *Cell Mol Life Sci* 78, 1233–1261. doi:10.1007/s00018-020-03656-y

Diwan, V., Brown, L., and Gobe, G. C. (2018). Adenine-induced Chronic Kidney Disease in Rats. *Nephrology (Carlton)* 23, 5–11. doi:10.1111/nep.13180

Feng, X., Fang, S. N., Gao, Y. X., Liu, J. P., and Chen, W. (2018). Current Research Situation of Nephrotoxicity of Chinese Herbal Medicine. *Zhongguo Zhong Yao Za Zhi* 43, 417–424. doi:10.19540/j.cnki.cjcmm.2018.0009

Gu, Y. Y., Liu, X. S., Huang, X. R., Yu, X. Q., and Lan, H. Y. (2020). Diverse Role of TGF-β in Kidney Disease. *Front Cel Dev Biol* 8, 123. doi:10.3389/fcell.2020.00123

Jha, V., Garcia-Garcia, G., Iseki, K., Li, Z., Naicker, S., Plattner, B., et al. (2013). Chronic Kidney Disease: Global Dimension and Perspectives. *Lancet* 382, 260–272. doi:10.1016/S0140-6736(13)60687-X

Kang, H. M., Ahn, S. H., Choi, P., Ko, Y. A., Han, S. H., Chinga, F., et al. (2015). Defective Fatty Acid Oxidation in Renal Tubular Epithelial Cells Has a Key Role in Kidney Fibrosis Development. *Nat. Med.* 21, 37–46. doi:10.1038/nm.3762

Kim, S. K., Lee, S., Lee, M. K., and Lee, S. (2019). A Systems Pharmacology Approach to Investigate the Mechanism of Oryeong-San Formula for the Treatment of Hypertension. *J. Ethnopharmacol* 244, 112129. doi:10.1016/j.jep.2019.112129

Lameire, N., Jager, K., Van Biesen, W. I. M., de Bacquer, D., and Vanholder, R. (2005). Chronic Kidney Disease: A European Perspective. *Kidney Int.* 68 (Suppl. ment), S30–S38. doi:10.1111/j.1523-1755.2005.09907.x

Li, P., Lin, H., Ni, Z., Zhan, Y., He, Y., Yang, H., et al. (2020). Efficacy and Safety of Abelmoschus Manihot for IgA Nephropathy: A Multicenter Randomized Clinical Trial. *Phytomedicine* 76, 153231. doi:10.1016/j.phymed.2020.153231

Li, X., and Wang, H. (2005). Chinese Herbal Medicine in the Treatment of Chronic Kidney Disease. *Adv. Chronic Kidney Dis.* 12, 276–281. doi:10.1016/j.ackd.2005.03.007

Lin, M. Y., Chiu, Y. W., Chang, J. S., Lin, H. L., Lee, C. T., Chiu, G. F., et al. (2015). Association of Prescribed Chinese Herbal Medicine Use with Risk of End-Stage Renal Disease in Patients with Chronic Kidney Disease. *Kidney Int.* 88, 1365–1373. doi:10.1038/ki.2015.226

Liu, B. C., Tang, T. T., Lv, L. L., and Lan, H. Y. (2018). Renal Tubule Injury: a Driving Force toward Chronic Kidney Disease. *Kidney Int.* 93, 568–579. doi:10.1016/j.kint.2017.09.033

Liu, Y. (2011). Cellular and Molecular Mechanisms of Renal Fibrosis. *Nat. Rev. Nephrolnephrology* 7, 684–696. doi:10.1038/nrneph.2011.149

Liu, Z., Kan, Y. H., Wei, Y. D., Li, X. J., Yang, F., Hou, Y., et al. (2015). Decreased Number of CD14+TLR4+ Monocytes and Their Impaired Cytokine Responses to Lipopolysaccharide in Patients with Chronic Kidney Disease. *J. Huazhong Univ. Sci. Technolog Med. Sci.* 35, 206–211. Medical sciences = Hua zhong ke ji da xue xue bao. Yi xue Ying De wen ban = Huazhong keji daxue xuebao. Yixue Yingdewen ban. doi:10.1007/s11596-015-1412-7

Mao, W., Yang, N., Zhang, L., Li, C., Wu, Y., Ouyang, W., et al. (2020). Bupi Yishen Formula versus Losartan for Non-diabetic Stage 4 Chronic Kidney Disease: A Randomized Controlled Trial. *Front. Pharmacol.* 11, 627185. doi:10.3389/fphar.2020.627185

Mitchell, S., Vargas, J., and Hoffmann, A. (2016). Signaling via the NFκB System. *Wiley Interdiscip. Rev. Syst. Biol. Med.* 8, 227–241. doi:10.1002/wsbm.1331

Mollen, K. P., Anand, R. J., Tsung, A., Prince, J. M., Levy, R. M., and Billiar, T. R. (2006). Emerging Paradigm: Toll-like Receptor 4-sentinel for the Detection of Tissue Damage. *Shock* 26, 430–437. doi:10.1097/01.shk.0000228797.41044.08

Omer Mohamed, H. A., Osman, O. M., Ali, H. H., Asiri, M. N., Hassan, A. A., Almangah, I. M., et al. (2020). A Complicated Chinese Herbal Medicine Nephrotoxicity. *Saudi J. Kidney Dis. Transplsaudi Arabia* 31, 533–536. an official publication of the Saudi Center for Organ Transplantation. doi:10.4103/1319-2442.284032

Palmer, S. C., Mavridis, D., Navarese, E., Craig, J. C., Tonelli, M., Salanti, G., et al. (2015). Comparative Efficacy and Safety of Blood Pressure-Lowering Agents in Adults with Diabetes and Kidney Disease: a Network Meta-Analysis. *Lancet* 385, 2047–2056. doi:10.1016/S0140-6736(14)62459-4

Pérez-Ferro, M., Serrano Del Castillo, C., and Sánchez-Pernaute, O. (2016). Cell Membrane-Bound TLR2 and TLR4: Potential Predictors of Active Systemic Lupus Erythematosus and Lupus Nephritis. *J. Rheumatol.* 43, 1444–1445. doi:10.3899/jrheum.151386

Piñero, J., Bravo, À., Queralt-Rosinach, N., Gutiérrez-Sacristán, A., Deu-Pons, J., Centeno, E., et al. (2017). DisGeNET: a Comprehensive Platform Integrating Information on Human Disease-Associated Genes and Variants. *Nucleic Acids Res.* 45, D833–833D839. doi:10.1093/nar/gkw943

Rappaport, N., Twik, M., Plaschkes, I., Nudel, R., Iny Stein, T., Levitt, J., et al. (2017). MalaCards: an Amalgamated Human Disease Compendium with Diverse Clinical and Genetic Annotation and Structured Search. *Nucleic Acids Res.* 45, D877–877D887. doi:10.1093/nar/gkw1012

Ru, J., Li, P., Wang, J., Zhou, W., Li, B., Huang, C., et al. (2014). TCMSP: a Database of Systems Pharmacology for Drug Discovery from Herbal Medicines. *J. Cheminform* 6, 13. doi:10.1186/1758-2946-6-13

Seki, E., De Minicis, S., Osterreicher, C. H., Kluwe, J., Osawa, Y., Brenner, D. A., et al. (2007). TLR4 Enhances TGF-Beta Signaling and Hepatic Fibrosis. *Nat. Med.* 13, 1324–1332. doi:10.1038/nm1663

Stelzer, G., Dalah, I., Stein, T. I., Satanower, Y., Rosen, N., Nativ, N., et al. (2011). In-silico Human Genomics with GeneCards. *Hum. Genomics* 5, 709–717. doi:10.1186/1479-7364-5-6-709

Sutariya, B., Jhonsa, D., and Saraf, M. N. (2016). TGF-β: the Connecting Link between Nephropathy and Fibrosis. *Immunopharmacol Immunotoxicol* 38, 39–49. doi:10.3109/08923973.2015.1127382

Thakur, R., Sharma, A., Lingaraju, M. C., Begum, J., Kumar, D., Mathesh, K., et al. (2018). Ameliorative Effect of Ursolic Acid on Renal Fibrosis in Adenine-Induced Chronic Kidney Disease in Rats. *Biomed. Pharmacother.* 101, 972–980. doi:10.1016/j.biopha.2018.02.143

von Mering, C., Jensen, L. J., Snel, B., Hooper, S. D., Krupp, M., Foglierini, M., et al. (2005). STRING: Known and Predicted Protein-Protein Associations, Integrated and Transferred across Organisms. *Nucleic Acids Res.* 33, D433–D437. doi:10.1093/nar/gki005

Wang, H., Jiang, X. M., Xu, J. H., Xu, J., Tong, J. X., and Wang, Y. W. (2008). The Profile of Gene Expression and Role of Nuclear Factor Kappa B on Glomerular Injury in Rats with Thy-1 Nephritis. *Clin. Exp. Immunol.* 152, 559–567. doi:10.1111/j.1365-2249.2008.03654.x

Wang, Y., Zheng, C., Huang, C., Li, Y., Chen, X., Wu, Z., et al. (2015). Systems Pharmacology Dissecting Holistic Medicine for Treatment of Complex Diseases: An Example Using Cardiocerebrovascular Diseases Treated by TCM. *Evidence-Based Complementary and Alternative Medicine. eCAM* 2015, 980190. doi:10.1155/2015/980190

Wojcikowski, K., Johnson, D. W., and Gobe, G. (2006). Herbs or Natural Substances as Complementary Therapies for Chronic Kidney Disease: Ideas for Future Studies. *J. Lab. Clin. Med.* 147, 160–166. doi:10.1016/j.lab.2005.11.011

Wu, Y., Li, C., Zhang, L., Zou, C., Xu, P., Wen, Z., et al. (2021). Effectiveness of Chinese Herbal Medicine Combined with Western Medicine on Deferring Dialysis Initiation for Nondialysis Chronic Kidney Disease Stage 5 Patients: a Multicenter Prospective Nonrandomized Controlled Study. *Ann. Transl Med.* 9, 490. doi:10.21037/atm-21-871

Wu, Y., Zhang, F., Yang, K., Fang, S., Bu, D., Li, H., et al. (2019). SymMap: an Integrative Database of Traditional Chinese Medicine Enhanced by Symptom Mapping. *Nucleic Acids Res.* 47, D1110–1110D1117. doi:10.1093/nar/gky1021

Yang, B., Xie, Y., Guo, M., Rosner, M. H., Yang, H., and Ronco, C. (2018). Nephrotoxicity and Chinese Herbal Medicine. *Clin. J. Am. Soc. Nephrol.* 13, 1605–1611. doi:10.2215/CJN.11571017

Yang, H., Song, Y., Liang, Y. N., and Li, R. (2018). Quercetin Treatment Improves Renal Function and Protects the Kidney in a Rat Model of Adenine-Induced Chronic Kidney Disease. *Med. Sci. Monit.* 24, 4760–4766. doi:10.12659/MSM.909259

Yang, L., Besschetnova, T. Y., Brooks, C. R., Shah, J. V., and Bonventre, J. V. (2010). Epithelial Cell Cycle Arrest in G2/M Mediates Kidney Fibrosis after Injury. *Nat. Med.* 16, 535–143. 1p following 143. doi:10.1038/nm.2144

Yokozawa, T., Zheng, P. D., Oura, H., and Koizumi, F. (1986). Animal Model of Adenine-Induced Chronic Renal Failure in Rats. *Nephron* 44, 230–234. doi:10.1159/000183992

Zeisberg, M., and Neilson, E. G. (2010). Mechanisms of Tubulointerstitial Fibrosis. *J. Am. Soc. Nephrol.* 21, 1819–1834. doi:10.1681/ASN.2010080793

Zhang, J., Xu, W., Wang, P., Huang, J., Bai, J. Q., Huang, Z. H., et al. (2018). Chemical Analysis and Multi-Component Determination in Chinese Medicine Preparation Bupi Yishen Formula Using Ultra-high Performance Liquid Chromatography with Linear Ion Trap-Orbitrap Mass Spectrometry and Triple-Quadrupole Tandem Mass Spectrometry. *Front. Pharmacol.* 9, 568. doi:10.3389/fphar.2018.00568

Zhang, L., Li, P., Xing, C. Y., Zhao, J. Y., He, Y. N., Wang, J. Q., et al. (2014). Efficacy and Safety of Abelmoschus Manihot for Primary Glomerular Disease: a Prospective, Multicenter Randomized Controlled Clinical Trial. *Am. J. Kidney Dis.* 64, 57–65. doi:10.1053/j.ajkd.2014.01.431

Zhang, L., Wang, F., Wang, L., Wang, W., Liu, B., Liu, J., et al. (2012). Prevalence of Chronic Kidney Disease in China: a Cross-Sectional Survey. *Lancet* 379, 815–822. doi:10.1016/S0140-6736(12)60033-6

Zhong, Y., Deng, Y., Chen, Y., Chuang, P. Y., and Cijiang He, J. (2013). Therapeutic Use of Traditional Chinese Herbal Medications for Chronic Kidney Diseases. *Kidney Int.* 84, 1108–1118. doi:10.1038/ki.2013.276

Conflict of Interest: The authors declare that the research was conducted in the absence of any commercial or financial relationships that could be construed as a potential conflict of interest.

Publisher's Note: All claims expressed in this article are solely those of the authors and do not necessarily represent those of their affiliated organizations, or those of the publisher, the editors and the reviewers. Any product that may be evaluated in this article, or claim that may be made by its manufacturer, is not guaranteed or endorsed by the publisher.

frontiers in Pharmacology

ORIGINAL RESEARCH
published: 24 November 2021
doi: 10.3389/fphar.2021.757508

The Role of Gut Microbiota and Microbiota-Related Serum Metabolites in the Progression of Diabetic Kidney Disease

Qing Zhang[1,2], Yanmei Zhang[1,2], Lu Zeng[1,2], Guowei Chen[2], La Zhang[2], Meifang Liu[1,2], Hongqin Sheng[1,2], Xiaoxuan Hu[2], Jingxu Su[2], Duo Zhang[1,2], Fuhua Lu[1,2], Xusheng Liu[1,2]* and Lei Zhang[1,2]**

[1]The Second Clinical Medical College, Guangzhou University of Chinese Medicine, Guangzhou, China, [2]State Key Laboratory of Dampness Syndrome of Chinese Medicine, Guangdong Provincial Key Laboratory of Clinical Research on Traditional Chinese Medicine Syndrome, The Second Affiliated Hospital of Guangzhou University of Chinese Medicine, Guangzhou, China

OPEN ACCESS

Edited by:
Dan-Qian Chen,
Northwest University, China

Reviewed by:
Xiaoli Nie,
Southern Medical University, China
Dong Zhou,
University of Connecticut,
United States

***Correspondence:**
Fuhua Lu
lufuhua@gzucm.edu.cn
Xusheng Liu
liuxusheng@gzucm.edu.cn
Lei Zhang
zhanglei@gzucm.edu.cn

Specialty section:
This article was submitted to Renal Pharmacology, a section of the journal Frontiers in Pharmacology

Received: 12 August 2021
Accepted: 15 October 2021
Published: 24 November 2021

Citation:
Zhang Q, Zhang Y, Zeng L, Chen G, Zhang L, Liu M, Sheng H, Hu X, Su J, Zhang D, Lu F, Liu X and Zhang L (2021) The Role of Gut Microbiota and Microbiota-Related Serum Metabolites in the Progression of Diabetic Kidney Disease. Front. Pharmacol. 12:757508. doi: 10.3389/fphar.2021.757508

Objective: Diabetic kidney disease (DKD) has become the major cause of end-stage renal disease (ESRD) associated with the progression of renal fibrosis. As gut microbiota dysbiosis is closely related to renal damage and fibrosis, we investigated the role of gut microbiota and microbiota-related serum metabolites in DKD progression in this study.

Methods: Fecal and serum samples obtained from predialysis DKD patients from January 2017 to December 2019 were detected using 16S rRNA gene sequencing and liquid chromatography-mass spectrometry, respectively. Forty-one predialysis patients were divided into two groups according to their estimated glomerular filtration rate (eGFR): the DKD non-ESRD group (eGFR ≥ 15 ml/min/1.73 m^2) (n = 22), and the DKD ESRD group (eGFR < 15 ml/min/1.73 m^2) (n = 19). The metabolic pathways related to differential serum metabolites were obtained by the KEGG pathway analysis. Differences between the two groups relative to gut microbiota profiles and serum metabolites were investigated, and associations between gut microbiota and metabolite concentrations were assessed. Correlations between clinical indicators and both microbiota-related metabolites and gut microbiota were calculated by Spearman rank correlation coefficient and visualized by heatmap.

Results: Eleven different intestinal floras and 239 different serum metabolites were identified between the two groups. Of 239 serum metabolites, 192 related to the 11 different intestinal flora were mainly enriched in six metabolic pathways, among which, phenylalanine and tryptophan metabolic pathways were most associated with DKD progression. Four microbiota-related metabolites in the phenylalanine metabolic pathway [hippuric acid (HA), L-(–)-3-phenylactic acid, *trans*-3-hydroxy-cinnamate, and dihydro-3-coumaric acid] and indole-3 acetic acid (IAA) in the tryptophan metabolic pathway positively correlated with DKD progression, whereas L-tryptophan in the tryptophan metabolic pathway had a negative correlation. Intestinal flora *g_Abiotrophia* and *g_norank_f_Peptococcaceae* were positively correlated with the increase in renal function indicators and serum metabolite HA. *G_Lachnospiraceae_NC2004_Group* was

negatively correlated with the increase in renal function indicators and serum metabolites [L-(–)-3-phenyllactic acid and IAA].

Conclusions: This study highlights the interaction among gut microbiota, serum metabolites, and clinical indicators in predialysis DKD patients, and provides new insights into the role of gut microbiota and microbiota-related serum metabolites that were enriched in the phenylalanine and tryptophan metabolic pathways, which correlated with the progression of DKD.

Keywords: diabetic kidney disease, gut microbiota, serum metabolites, phenylalanine metabolic pathway, tryptophan metabolic pathway, G_Abiotrophia, G_norank_f_Peptococcaceae, G_Lachnospiraceae_NC2004_Group running title

INTRODUCTION

Diabetic kidney disease (DKD) reflects one of the most common microvascular complications of diabetes, typically characterized by albuminuria or reduced estimated glomerular filtration rate (eGFR) (de Boer et al., 2011; Afkarian et al., 2016). Although advances have occurred in the clinical treatment of DKD, consisting of strict control of blood glucose and blood pressure, and the widely prescribed angiotensin-converting enzyme inhibitors (ACEI) and angiotensin II receptor antagonists (ARB), renal damage can progress (Umanath and Lewis, 2018) with interstitial fibrosis and glomerulosclerosis, and DKD remains the major cause of end-stage renal disease (ESRD) (Ma et al., 2019). Therefore, it is necessary and urgent to elucidate the mechanism of renal fibrosis in DKD and find new biomarkers or targets associated with the progressive renal function decline in DKD patients.

According to the "gut–kidney axis" hypothesis, dysregulation of intestinal microbiota irritates renal tissue through uremic toxins, causing systemic micro-inflammation, renal injury, and fibrosis (Ramezani and Raj, 2014). Recent studies reported that intestinal microbiota has emerged as a pivotal regulator of DKD occurrence in patient with diabetes (Andrade-Oliveira et al., 2015) (Tao et al., 2019). In diabetic patients, the intestinal flora dysbiosis causes intestinal mucosal barrier damage, allowing gut-derived uremic toxins to enter the systemic circulation, which in turn incites an inflammatory response and oxidative stress, and results in insulin resistance, β-cell dysfunction, and kidney injury (Koppe et al., 2018). Age- and gender-matched DKD patients had lower intestinal Prevotella_9 than diabetic patients without kidney disease (Tao et al., 2019), which can produce short-chain fatty acids and reduce the inflammatory reaction of kidney injury. The abundance of Firmicutes in DKD is lower, whereas the abundance of Proteobacteria is higher than that of healthy people and diabetics without renal disease. As inflammation, oxidative stress, and insulin resistance are involved in the renal fibrosis in DKD, then contribute to the development and progression of DKD (Parwani and Mandal, 2020; Rayego-Mateos et al., 2020), therefore, we hypothesized that alteration in intestinal flora may play a crucial role in the progression of DKD to ESRD.

Metabolomics is a powerful tool to screen for changes in metabolic profiles and to characterize mechanisms of pathological changes (Dumas, 2012; Kwan et al., 2020). It can identify and analyze small-molecule metabolites (<1,500 Da) in serum, urine, and feces. In DKD patients, metabolomics plays a great role in screening metabolic biomarkers and detecting abnormal changes in their living organisms (Eid et al., 2019; Kwan et al., 2020). Some urinary metabolites such as indoxyl sulfate, creatinine, and the methoxylated form of phenylacetic acid have been associated with low eGFR in nonproteinuric type 2 diabetes mellitus (Ng et al., 2012). Serum metabolites, such as creatinine, aspartic acid, γ-butyrobetaine, citrulline, symmetric dimethylarginine, kynurenine, azelaic acid, and galactaric acid, can distinguish between DKD with macroalbuminuria and diabetic patients without albuminuria (Hirayama et al., 2012).

The large and complex microbial community in the human intestinal tract has a profound impact on human metabolic phenotype. As the mediator of the interaction between intestinal flora and diseases, the metabolites can more directly show the relationship between intestinal flora and diseases. Ma et al. combined 16S rRNA and metabolomics technology and determined that flora-metabolites combined with the flora-bacteria might represent a new detection method for breast cancer (Ma et al., 2020). Evidence has confirmed that it is possible to characterize the relationship between intestinal microecology and disease by associating intestinal microflora with metabolites via multiomics-integrated methods. Gut microbiota and related metabolites, such as tryptophan metabolism and polyamine metabolism, have been reported to mediate renal fibrosis in the rat model of CKD (Feng et al., 2019; Hu et al., 2020b; Liu JR. et al., 2021). However, very few studies have explored the role of gut microbiota and microbiota-related metabolites in the DKD progression.

In the present study, we aimed to investigate gut microbiota profiles and serum metabolic characteristics in predialysis DKD patients that were associated with DKD progression and to explore the correlation between intestinal flora and metabolic disorders using multiomics technology of 16S rRNA gene sequencing and metabolomics.

MATERIALS AND METHODS

Study Design

This study detected fecal and serum samples of 41 predialysis DKD patients from January 2017 to December 2019 in Guangdong Provincial Hospital of Chinese Medicine. The

patients were divided into two groups according to their renal function (eGFR): the DKD non-ESRD group (GFR ≥ 15 ml/min/1.73 m^2), and the DKD ESRD group (eGFR < 15 ml/min/1.73 m^2). The study protocol was approved by the Institutional Ethics Committee of Guangdong Provincial Hospital of Chinese Medicine (No. ZE2020-193-01), and informed consent was obtained before sample collection.

Patients

Serum and fecal samples of predialysis DKD patients were obtained from the biological resource bank of Guangdong Province Hospital of Chinese Medicine. Estimated glomerular filtration rate (eGFR) was calculated using the chronic kidney disease epidemiology collaboration (CKD-EPI) equation (National Kidney Foundation, 2002).

Inclusion and Exclusion Criteria

The inclusion criteria were age from 18 to 85 years, diagnosis of DKD, and nonrenal replacement therapy. Note: renal replacement therapy refers to hemodialysis, peritoneal dialysis, and renal transplantation.

The exclusion criteria were incomplete clinical data, concomitant active malignant tumor, pulmonary infection, acute coronary heart disease, and other acute complications, antibiotics or probiotics having been taken 3 months prior to sample collection, and corticosteroid or immunosuppressive therapy prior to sample collection.

Sample Collection

At least 1 g of fresh feces was collected by sterilized cotton swabs in a special fecal collection tube. Blood samples were collected by venipuncture in EDTA tubes; serum was separated by centrifugation. Feces and serum were stored immediately at −80 °C until further processing.

16s rRNA Sequencing and Data Processing

DNA Extraction and PCR Amplification

Microbial community genomic DNA was extracted from feces samples using the E. Z.N.A.® soil DNA Kit (Omega Bio-tek, Norcross, GA, United States). The DNA extract was checked on 1% agarose gel, and DNA concentration and purity were determined with NanoDrop 2000 UV-vis spectrophotometer (Thermo Scientific, Wilmington, DE, United States). The hypervariable region V3–V4 of the bacterial 16S rRNA gene were amplified with primer pairs 338F (5′-ACTCCTACGGGAGGCAGCAG-3′) and 806R (5′-GGACTACHVGGGTWTCTAAT-3′) by an ABI GeneAmp® 9700 PCR thermocycler (ABI, CA, United States). The PCR product was extracted from 2% agarose gel and purified using the AxyPrep DNA Gel Extraction Kit (Axygen Biosciences, Union City, CA, United States) and quantified using Quantus™ Fluorometer (Promega, United States).

Illumina MiSeq Sequencing

Purified amplicons were pooled in equimolar and paired-end sequenced on an Illumina MiSeq PE300 platform/NovaSeq PE250 platform (Illumina, San Diego, CA, United States) according to the standard protocols by Majorbio Bio-Pharm Technology Co. Ltd. (Shanghai, China).

Processing of Sequencing Data

The raw 16S rRNA gene sequencing reads were demultiplexed, quality-filtered by fast version 0.20.0 (Chen et al., 2018) and merged by FLASH version 1.2.7 (Magoc and Salzberg, 2011). Operational taxonomic units (OTUs) with 97% similarity cutoff were clustered using UPARSE version 7.1 (Edgar, 2013), and chimeric sequences were identified and removed. The taxonomy of each OTU representative sequence was analyzed by RDP Classifier version 2.2 (Wang et al., 2007) against the 16S rRNA database (e.g., Silva v132) using confidence threshold of 0.7.

Liquid Chromatography-Mass Spectrometry Detection

Metabolite Extraction

The metabolites were extracted from 100 μl of liquid sample and treated by high-throughput tissue crusher Wonbio-96c (Shanghai Wanbo Biotechnology Co., Ltd.), then followed by ultrasound for 30 min. After centrifugation, the supernatant was carefully transferred to sample vials for LC-MS/MS analysis.

UPLC-MS/MS Analysis

Chromatographic separation of the metabolites was performed on an ExionLC™ AD system (AB Sciex, United States) equipped with an ACQUITY UPLC HSS T3 column (Waters, Milford, CT, United States). The UPLC system was coupled to a quadrupole-time-of-flight mass spectrometer (Triple TOF™5600+, AB Sciex, United States) equipped with an electrospray ionization (ESI) source operating in positive mode and negative mode. Data acquisition was performed with the data-dependent acquisition (DDA) mode.

Data Preprocessing and Annotation

The raw data were imported into the Progenesis QI 2.3 (Nonlinear Dynamics, Waters, United States) for peak detection and alignment. Mass spectra of these metabolic features were identified by using the accurate mass, MS/MS fragments spectra, and isotope ratio difference with search in reliable biochemical databases, such as the Human Metabolome Database (http://www.hmdb.ca/) and Metlin database (https://metlin.scripps.edu/).

Statistical Analysis

Results were expressed as frequencies and percentages for categorical variables, mean ± SD for continuous normally distributed variables, and median (interquartile range, IQRs) for continuous variables that were not normally distributed. Categorical variables for the patient characteristics were compared using the chi-square test or Fisher's exact test, and the continuous variables were tested with *t*-test or nonparametric Wilcoxon rank sum test. All analyses were performed using the SPSS version 19.0 (SPSS Inc., Chicago, IL, United States) and "ropls" (Version 1.6.2, http://bioconductor.org/packages/release/

bioc/html/ropls.html) R package from Bioconductor on the Majorbio Cloud Platform (www.majorbio.com) with a two-sided p-value less than 0.05 considered significant.

Gut Microbiota Analysis

We used rarefaction curves and species accumulation curves to ensure that the sample size or sequencing depth reached saturation in our study. Gut microbiota alpha diversity index (Shannon index, Chao index) was analyzed on mothur software (version 1.30.1, http://www.mothur.org/), tested by nonparametric Wilcoxon rank sum test, and $p < 0.05$ was considered statistically significant. Beta diversity measured the difference in OTU composition between different samples and was assessed using partial least squares discriminant analysis (PLS-DA), which is a supervised analysis suitable for high-dimensional data. The corresponding statistical significance of the beta diversity was measured separately by ANOSIM.

Compositional differences between the two groups from the phylum to genus level were tested with nonparametric Wilcoxon rank-sum test. Variation at the taxonomic level was determined by linear discriminant analysis (LDA) effect size (LDA score >1, $p < 0.05$) calculated by the LEfSe software (http://huttenhower.sph.harvard.edu/). The correlation between biochemical indicators and various microbes was calculated by Spearman rank correlation coefficient and visualized by heatmap in R using the "heatmap" package.

Metabolomic Analysis

Orthogonal partial least squares discriminate analysis (OPLS-DA) was used for statistical analysis to determine global metabolic changes between comparable groups. All metabolite variables were scaled to Pareto scaling prior to conducting the OPLS-DA. The model validity was evaluated from model parameters R^2 and Q^2, which provided information for the interpretability and predictability, respectively, of the model and avoided the risk of overfitting. Variable importance in the projection (VIP) was calculated in the OPLS-DA model. Values of p were estimated with paired Student's t-test on single-dimensional statistical analysis. Metabolites with VIP >1 and $p < 0.05$ were considered statistically significant. We used the area under the receiver operating characteristic (ROC) curve to assess the accuracy of the metabolites in predicting DKD progression.

Differential metabolites between the two groups were summarized and mapped into their biochemical pathways through metabolic enrichment and pathway analysis based on database search (KEGG, http://www.genome.jp/kegg/). These metabolites could be classified according to the pathways they involved or the functions they performed. Enrichment analysis was used to analyze a group of metabolites in a function node whether it appears or not. Scipy. stats (Python packages) (https://docs.scipy.org/doc/scipy/) was exploited to identify statistically significantly enriched pathways using Fisher's exact test.

The correlation between differential metabolites and various microbes was calculated by Spearman rank correlation coefficient and visualized by heatmap in R software using the "heatmap" package.

RESULTS

Clinical and Biochemical Characteristics

Samples from 41 predialysis patients were divided into the DKD non-ESRD group (eGFR ≥ 15 ml/min/1.73 m^2 group) (n = 22) or the DKD ESRD group (eGFR < 15 ml/min/1.73 m^2 group) (n = 19), with mean ages of 69.63 ± 13.01 and 61.89 ± 9.85 in the two groups, respectively. Compared with the DKD non-ESRD group, the levels of serum creatinine and blood urea nitrogen were higher in the DKD ESRD group ($p < 0.001$). There were no significant differences in other baseline indicators between the two groups (**Table 1**).

Gut Microbiota Analysis

Alpha Diversity and Beta Diversity

The rarefaction curve indicated that the sequencing depth of each sample approached the expected level (**Supplementary Figure S1**). Alpha diversity analysis revealed no significant difference in gut microbiota diversity between each group based on Chao and Shannon indices ($p > 0.05$) (**Supplementary Figure S2**). The result of beta diversity based on PLS-DA showed that the microbial composition between groups was significantly different (**Figure 1A**).

Relative Abundance of Species

The relative abundance percentage of gut microbiota at the phylum and genus level was analyzed to identify taxa that could display significant differences in the two groups. At the phylum level, Firmicutes and Bacteroidota were the most abundant, and their mean relative abundance were similar in the DKD ESRD and DKD non-ESRD groups, accounting for 44.02 ± 14.30% and 39.05 ± 16.09% in the DKD ESRD group, and 47.78 ± 19.61% and 39.58 ± 18.90% in the DKD non-ESRD group, respectively (**Figure 1B**). At the genus level, *Bacteroides* represented the highest abundance of OTU in the two groups. The mean relative abundance for *Bacteroides* was similar in the two groups, accounting for 28.74 ± 17.60% in the DKD ESRD group and 30.33 ± 22.34% in the DKD non-ESRD group. The mean relative abundance for *Faecalibacterium* was also similar in the two groups, accounting for 3.99 ± 2.91% in the DKD ESRD group and 5.84 ± 7.04% in the DKD non-ESRD group. Likewise, other gut microbiota, such as *Blautia*, *Escherichia–Shigella*, *Fusobacterium*, etc., did not demonstrate a significant difference in their relative abundance in either DKD ESRD or DKD non-ESRD group (**Figure 1C**).

Different Species Analysis

Based on the LDA selection, 10 differential intestinal flora at the genus level and one differential intestinal flora at the family level were identified in the fecal samples between the two groups (LDA > 1, $p < 0.05$). Compared with the DKD non-ESRD group, the levels of *g_Tyzzerella*, *g_Ruminococcaceae*, *g_Catenibacillus*, *g_Abiotrophia*, *g_norank_f_Peptococcaceae*, *g_norank_f_norank_o_Oscillospirales*, and f_Aerococcaceae were significantly higher, and the levels of *g_Olsenella*, *g_Faecalicoccus*, *g_Lachnospiraceae_NC2004_group*, and *g_Staphylococcus* were significantly lower in the DKD ESRD group (**Figure 1D**).

TABLE 1 | Patient clinical and biochemical characteristics.

Characteristics	Total (n = 41)	DKD non-ESRD group (n = 22)	DKD ESRD group (n = 19)
Male, n. (%)	27 (65.85%)	16 (72.73%)	11 (57.89%)
Age (years)	65.39 ± 11.38	69.63 ± 13.01	61.89 ± 9.85
Blood pressures (mmHg)			
Systolic	158.49 ± 22.36	160.90 ± 21.98	156.00 ± 23.48
Diastolic	82.63 ± 11.91	84.22 ± 13.1	79.47 ± 10.16
SCr (μmol/L)	372.90 ± 232.59	189.70 ± 74.64*	577.02 ± 164.35
eGFR (ml/min/1.73 m^2)	22.91 ± 18.81	36.01 ± 16.77*	7.78 ± 2.37
24hU-pro (g/24 h) (IQR)	3.82 (1.38, 5.16)	3.00 (0.95, 5.7)	3.83 (1.94, 5.01)
HbA1c (%)	6.40 (5.56, 7.45)	6.90 (5.70, 7.60)	5.85 (5.38, 7.10)
UA (μmol/L) (IQR)	476.50 (370.00, 574.00)	451.00 (357.50, 574.00)	508.00 (434.00, 587.00)
BUN (mmol/L) (IQR)	17.70 (11.01, 24.47)	11.23 (8.36, 13.52)*	23.47 (20.48, 29.98)
Triglycerides (mmol/L) (IQR)	1.75 (1.16, 2.37)	1.63 (0.88, 2.03)	2.11 (1.42, 2.62)
Cholesterol (mmol/L)	5.18 ± 1.77	5.34 ± 1.82	4.97 ± 1.86
HDL (mmol/L)	1.13 ± 0.35	1.33 ± 0.59	1.03 ± 0.35
LDL (mmol/L)	3.42 ± 1.60	3.66 ± 1.71	3.13 ± 1.50
Serum albumin (g/L)	35.23 ± 5.65	34.44 ± 6.72	36.10 ± 3.84
AST (U/L) (IQR)	16.00 (13.00, 20.00)	17.00 (13.00, 21.00)	16.00 (11.00, 20.50)
ALT (U/L) (IQR)	12.00 (9.00, 21.00)	14.00 (10.75, 21.25)	9.00 (7.00, 16.00)

Note. Abbreviations: SCr, serum creatinine; eGFR, estimated glomerular filtration rate; 24hU-pro, 24-h urinary protein quantity; UA, uric acid; BUN, blood urea nitrogen; LDL, low-density lipoprotein; HDL, high-density lipoprotein; AST, glutamic oxaloacetic transaminase; ALT, alanine aminotransferase; IQR, interquartile range; DKD, diabetic kidney disease; ESRD, end-stage renal disease.

p < 0.05 vs. DKD ESRD group.

Correlation Analysis Between the Intestinal Flora and Clinical Indicators

Correlation analysis of the 10 differential intestinal floras at the genus level and the clinical indicators of the patient showed that *g_Abiotrophia* had a positive correlation with serum creatinine and 24-h urinary protein, and negative correlation with eGFR ($p < 0.05$). *G_norank_f_Peptococcaceae* had a positive correlation with serum creatinine and a negative correlation with eGFR ($p < 0.05$). In contrast, g_*Lachnospiraceae_NC2004_group* had a strong negative correlation with serum creatinine and a positive correlation with eGFR ($p < 0.05$). *G_norank_f_norank_o_Oscillospirales* and *g_unclassified_f_Ruminococcaceae* had a strong negative correlation with glycosylated hemoglobin (HbA1c) ($p < 0.05$) (**Figure 1E**).

Serum Metabolomics Analysis

Different Serum Metabolites Between Groups

The profile of metabolites showed definite separation between the two groups in OPLS-DA score plots (**Figure 2A**). Different serum metabolites (239) were obtained (VIP > 1, $p < 0.05$) based on the OPLS-DA model (**Supplementary Table S1**) and were included in further analysis. Nineteen metabolites, with VIP >3 and $p < 0.05$, had a higher concentration in the DKD ESRD group and are shown in **Table 2**.

Pathway Enrichment of Different Metabolites Analysis

Enrichment pathway analysis of 239 different metabolites showed that phenylalanine metabolism, caffeine metabolism, pantothenate and CoA biosynthesis, and steroid hormone biosynthesis were involved in the DKD progression (**Figure 2B**). Correlation networks were drawn to show the four metabolic pathways as well as the changes in their relevant different metabolites between groups (**Figure 2C**).

Compared with the DKD non-ESRD group, the concentration of hippuric acid (HA), L-(−)-3-phenyllactic acid, dihydro-3-coumaric acid, and *trans*-3-hydroxycinnamate enriched in the phenylalanine metabolism pathway, 7-methylxanthine and 1-methyluric acid enriched in the caffeine metabolism pathway, R-pantothenate enriched in the pantothenate and CoA biosynthesis pathway, and *trans*-dehydroandrosterone, cortisol, tetrahydrocortisone, and etiocholanolone enriched in the steroid hormone biosynthesis pathway was higher in the DKD ESRD group. In contrast, L-valine enriched in the pantothenate and CoA biosynthesis pathway had a lower concentration in the DKD ESRD group.

Integrating Multiomics Analysis

Microbiota-Related Metabolites Analysis

Interomics correlation analyses were used to further explore the correlation between the gut microbiota and metabolome composition. Based on the intestinal flora participating in the metabolism of the host, the correlation of 11 between-group different intestinal floras and 239 between-group different metabolites was calculated and illustrated in the form of a correlation coefficient matrix heat map (**Supplementary Figure S3**). Microbiota-related metabolites (192) were screened out based on $p < 0.05$ according to previous studies (Walker et al., 2016; Nunez Lopez et al., 2019; Wei et al., 2020; Wu et al., 2021) (**Supplementary Table S2**).

Pathway Enrichment Analysis of Microbiota-Related Metabolites

There were 192 microbiota-related metabolites submitted to the KEGG website for metabolic pathway enrichment analysis. Six enriched pathways with significant differences between groups were identified (**Figure 3A**), among which, the phenylalanine and

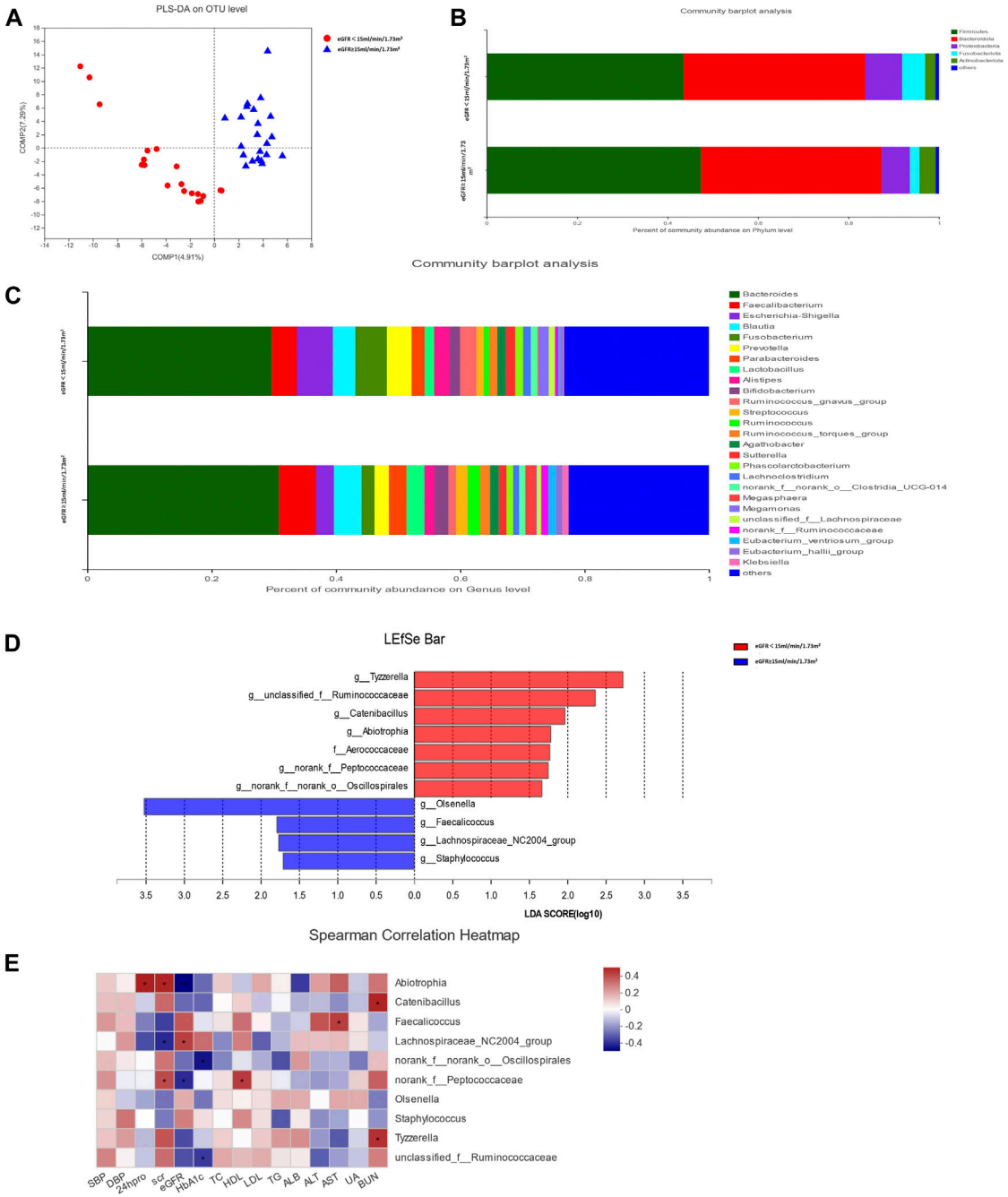

FIGURE 1 | Gut microbiota analysis between groups in diabetic kidney disease (DKD) patients. **(A)** Analysis of beta diversity using partial least squares discriminant analysis (PLS-DA) revealed that the microbial composition between groups was significantly different. One dot in the figure represents one sample. **(B)** The composition and relative abundance of intestinal microbiota at the phylum level. **(C)** The composition and relative abundance of intestinal microbiota at the genus level. **(D)** Linear discriminant analysis (LDA) effect size (LEfSe) bar plot. The LEfSe was used to identify the species that significantly differed between groups. **(E)** Correlation heatmap analysis between the intestinal flora and clinical indicators. Red represents a positive correlation, and blue represents a negative correlation.

tryptophan metabolic pathways were selected as the pathways most associated with DKD progression, according to the impact value and *p*-value in the KEGG analysis. Correlation networks between the intestinal flora and microbiota-related metabolites enriched on the two pathways were constructed (**Figures 3B,C**).

Four microbiota-related metabolites enriched on the phenylalanine metabolic pathway [HA, L-(−)-3-phenylactic acid, *trans*-3-hydroxy-cinnamate and dihydro-3-coumaric acid] had higher concentrations in the DKD ESRD group, compared with the other group. Among 11 differential

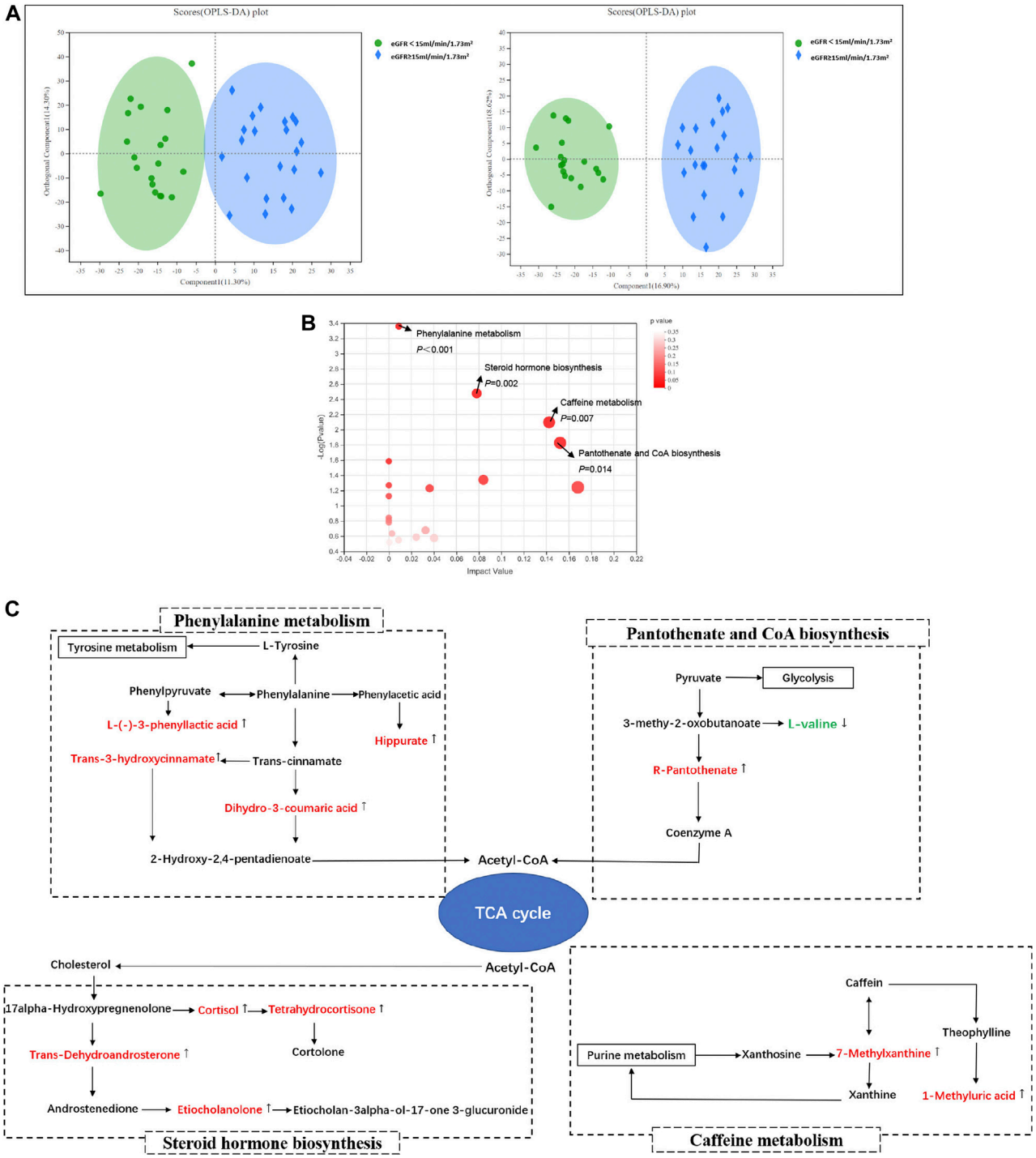

FIGURE 2 | Serum metabolomics analysis between groups in DKD patients. **(A)** Orthogonal partial least squares discriminate analysis (OPLS-DA) score plots of serum metabolic profiling in positive mode (left) and negative mode (right); positive mode: $R^2X = 0.256$, $R^2Y = 0.857$, $Q^2 = 0.702$; negative mode: $R^2X = 0.255$, $R^2Y = 0.930$, $Q^2 = 0.694$; **(B)** The bubble plot of KEGG analysis. Each bubble in the figure represents a KEGG pathway. The horizontal axis indicates the relative importance of metabolites in the pathway, and the vertical axis indicates the statistical significance of metabolites in the pathway; **(C)** Schematic diagram of phenylalanine metabolism, caffein metabolism, pantothenic acid and coenzyme A biosynthesis, steroid hormone biosynthesis, and their relevant differential metabolite alterations during DKD progression. The upregulated metabolites in the DKD ESRD group were labeled with red and downregulated metabolites in the DKD ESRD group with green.

TABLE 2 | Differential serum metabolites between groups in DKD patients (VIP > 3 and $p < 0.05$).

Metabolite	Compound ID	M/Z	Metabolite changes	VIP_	FC	AUC	95% CI
5a-Androst-3-en-17-one	HMDB0006046	273.220	↑	4.305	4.846	0.931	[0.86, 1]
Trans-Dehydroandrosterone	C01227	289.215	↑	4.284	2.238	0.938	[0.869, 1]
Tryptophyl-cysteine	HMDB0029080	330.085	↑	4.212	2.471	0.997	[0.991,1]
5-Androstene-3b,16b,17a-triol	HMDB0000523	307.226	↑	3.992	3.513	0.931	[0.859, 1]
Oxindole	C12312	134.059	↑	3.931	2.467	0.913	[0.828, 0.999]
3,4,5-Trihydroxy-6-[(3-methy lbut-enoyl)oxy]oxane-2-carboxylic acid	HMDB0128920	318.117	↑	3.823	3.118	0.877	[0.766, 0.988]
6-Dehydrotestosterone	—	287.200	↑	3.779	2.545	0.845	[0.719, 0.971]
(2E,4E)-2,7-Dimethyl-2,4-octadienedioic acid	HMDB0034099	181.085	↑	3.528	1.761	0.931	[0.852, 1]
O-Adipoylcarnitine	HMDB0061677	290.159	↑	3.523	1.380	0.965	[0.921, 1]
Mono-(2-ethyl-5-carboxypentyl) phthalate	HMDB0094647	331.114	↑	3.508	2.567	0.881	[0.781, 0.982]
Atrolactic acid	C05584	167.069	↑	3.457	1.616	0.925	[0.848, 1]
Benzenebutanoic acid	HMDB0000543	165.091	↑	3.411	2.310	0.915	[0.830, 1]
3,5-Cyclo-5alpha,17alpha-pregn-20-yne-6beta,17-diol	C15468	315.231	↑	3.396	2.162	0.929	[0.850, 1]
Indoleacetyl glutamine	HMDB0013240	304.128	↑	3.202	1.618	0.813	[0.669, 0.958]
{[3-(2,5-Dihydroxyphenyl) prop-2-en-1-yl]oxy}sulfonic acid	HMDB0134083	291.018	↑	3.191	4.360	0.975	[0.940, 1]
N-Acetylproline	HMDB0094701	199.107	↑	3.183	1.514	0.922	[0.828, 1]
1-Methyluric acid	C16359/ HMDB0003099	183.050	↑	3.182	2.714	0.85	[0.732, 0.968]
3,4,5-Trimethoxyphenyl acetate	HMDB0031722	209.080	↑	3.056	1.473	0.872	[0.756, 0.988]
3-Indole carboxylic acid glucuronide	HMDB0013189	336.071	↑	3.011	2.243	0.959	[0.902, 1]

Note. Abbreviations: M/Z, mass-to-charge ratio; VIP, the variable importance in projection; FC, fold change; AUC, area under curve. Metabolite changes in the DKD ESRD group are shown as (↑) for increase or (↓) for decrease. Compound ID starting with C is from the KEGG database. Compound ID starting with HMDB is from the Human Metabolome Database.

intestinal floras, *g_unclassified_f_Ruminococcaceae*, f_Aerococcaceae, *g_norank_f_Peptococcaceae*, *g_Catenibacillus*, *g_Abiotrophia*, and *g_norank_f_norank_o_Oscillospirales* were positively correlated with HA. *G_Lachnospiraceae_NC2004_Group* was negatively correlated with L-(−)-3-phenylactic acid. *F_Aerococcaceae and g_ Abiotrophia* were positively correlated with *trans*-3-hydroxy-cinnamate. *G_ Tyzzerella* was positively correlated with dihydro-3-coumaric acid (**Figure 3B**).

As microbiota-related metabolites enriched on the tryptophan metabolic pathway, indole-3 acetic acid (IAA) was highly expressed, and L-tryptophan had low expression in the DKD ESRD group compared with the DKD non-ESRD group. Among 11 differential intestinal floras, *g_Olsenella*, *g_Faecalicoccus*, and *g_Lachnospiraceae_NC2004_Group* were negatively correlated with indole-3 acetic acid. *G_Tyzzerella* was negatively correlated with L-tryptophan (**Figure 3C**).

Correlation Analysis Between Microbiota-Related Metabolites and Clinical Biomarkers

To further verify the role of microbiota-related metabolites enriched on the phenylalanine and tryptophan metabolic pathways in DKD progression, a correlation analysis between the above six microbiota-related metabolites and clinical indicators was undertaken. Consistent with the results of comparison between groups, HA, L-(−)-3-phenyllactic acid, and dihydro-3-coumaric acid in the phenylalanine metabolic pathway and IAA in the tryptophan metabolic pathway were positively correlated with serum creatinine and negatively correlated with eGFR, whereas L-tryptophan in the tryptophan metabolic pathway was opposite (**Figure 3D**).

DISCUSSION

In this study, 11 significantly different intestinal flora and 239 significantly different metabolites were identified between the DKD non-ESRD group and the DKD ESRD group. The phenylalanine and tryptophan metabolic pathways were most associated with DKD progression. Four microbiota-related metabolites in the phenylalanine metabolic pathway [HA, L-(−)- 3-phenylactic acid, *trans*-3-hydroxy-cinnamate, dihydro-3-coumaric acid], and IAA in the tryptophan metabolic pathway positively correlated with DKD progression, whereas L-tryptophan in the tryptophan metabolic pathway had a negative correlation. Intestinal flora *g_Abiotrophia* and *g_norank_f_Peptococcaceae*, both of which positively correlated with DKD progression, had a positive correlation with a high level of HA. *G_Lachnospiraceae_NC2004_Group*, which negatively correlated with DKD progression, also had a negative correlation with a high level of IAA and L-(−)-3-phenyllactic acid, simultaneously. In addition, g_*Tyzzerella* was positively correlated with dihydro-3-coumaric acid and negatively correlated with L-tryptophan. *G_unclassified_f_Ruminococcaceae* was positively correlated with HA, but negatively with HbA1c. These results indicated the potential role of specific gut microbiota in the DKD progression associated with the phenylalanine and tryptophan metabolism.

This study identified the phenylalanine metabolic pathway as the one most associated with DKD progression. Three microbiota-related serum metabolites [HA, L-(−)-3-phenylactic acid, and dihydro-3-coumaric acid] in the phenylalanine metabolic pathway were positively correlated with deterioration of renal function in DKD patients. Abnormal

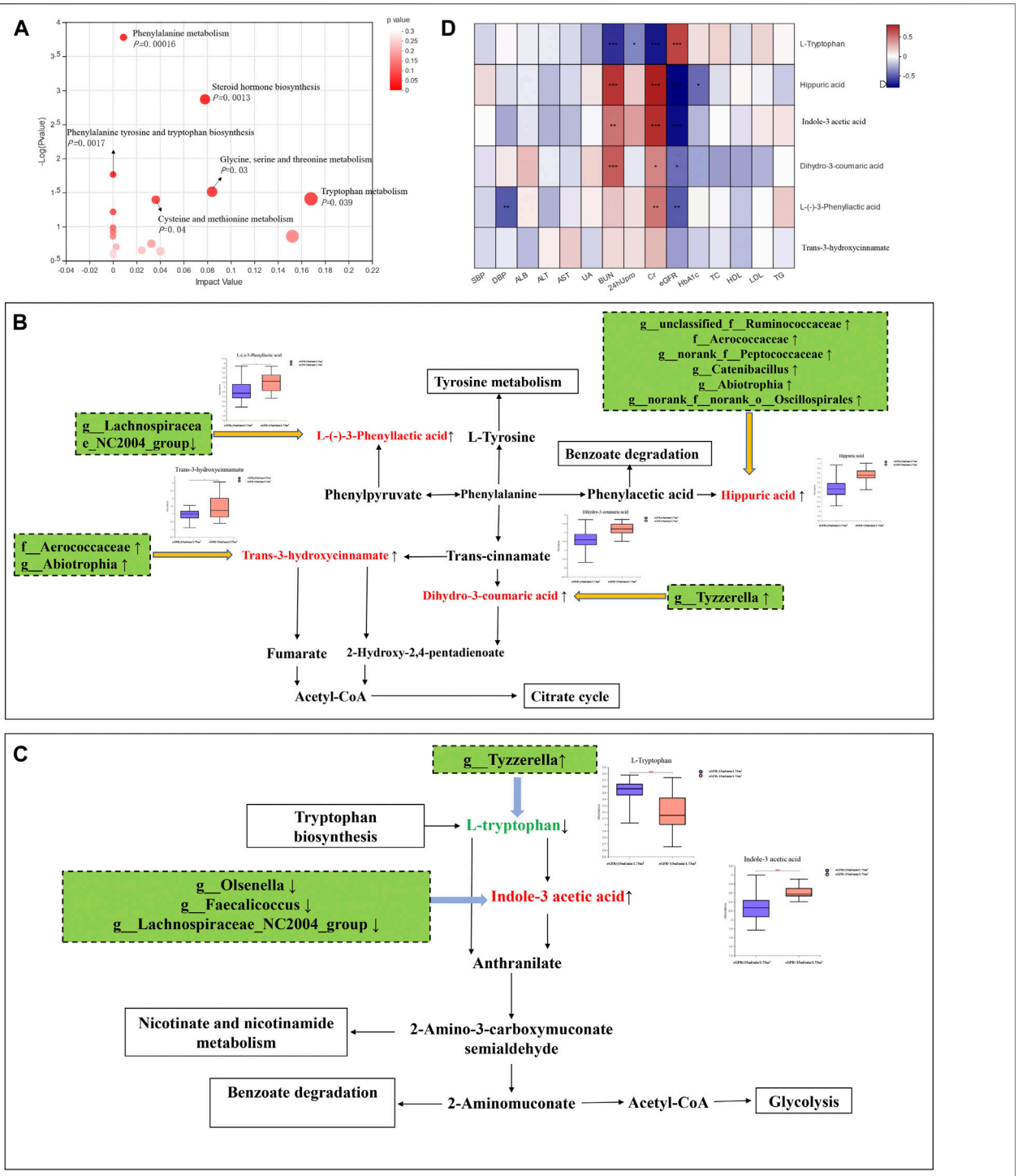

FIGURE 3 | Integrating multiomics analysis. **(A)** The bubble plot of KEGG analysis. Each bubble in the figure represents a KEGG pathway. The horizontal axis indicates the relative importance of metabolites in the pathway, and the vertical axis indicates the statistical significance of metabolites in the pathway. **(B)** Metabolic pathway map of phenylalanine metabolism. The metabolites shown in red are the differential metabolites that are highly expressed in the DKD ESRD group. Other related metabolic pathways were expressed in solid wire frame. **(C)** Metabolic pathway map of tryptophan metabolism. The metabolites expressed in red and green were statistically different between the two groups. Red metabolites express upregulated in the DKD ESRD group; green metabolites express downregulated in the DKD ESRD group. Other related metabolic pathways were expressed in solid wire frame. **(D)** Correlation analysis between different metabolites in enrichment pathway and clinical indicators.

phenylalanine metabolism has previously been demonstrated in patients with diabetes (Liu Y. et al., 2019) and type 2 diabetic animal models (Pan et al., 2020). However, its role in the DKD progression remains unclear.

As intermediates of phenylalanine metabolism, HA, which is a common protein-bound uremic toxin (PBUT) in patients with ESRD, is related to the progress of renal fibrosis due to its oxidative stress-associated toxicity (Sun et al., 2020). It is generated from the metabolism of many dietary components including phenylalanine and polyphenolic compounds, such as catechins and cinnamic acid from vegetables, fruit, tea, and coffee (Lees et al., 2013). These compounds are converted into benzoic acid, then further converted into HA, which is excreted in the urine. There has been no study that has investigated the impact of the serum metabolites L-(−)-3-phenylactic acid and dihydro-3-coumaric acid on DKD progression. Previous studies have indicated that they might be involved in the synthesis of HA. L-(−)-3-phenyllactic acid is an organic compound belonging to the class of phenylpropanoic acids, which could be derived from catechins by the colonic microbiota (Olthof et al., 2001). Dihydro-3-coumaric acid, also named 3-hydroxyphenylpropionic acid, belongs to hydroxycinnamic acid derivatives of cinnamic acid. These two metabolites may undergo further metabolism to benzoic acid and finally metabolized to HA (Phipps et al., 1998).

The gut microbiota makes up the largest microecosystem in the human body and is closely related to metabolic disorders in kidney disease. Several studies have reported the relationship between gut microbiota and phenylalanine metabolism in CKD patients (Hu et al., 2020a; Ren et al., 2020; Wu et al., 2020), but the evidence is mainly based on the functional analysis of gut microbiome. Very few studies explored the relationship between gut microbiota and phenylalanine metabolism in DKD patients (Fang et al., 2021). The present research mainly focused on the potential role of gut microbial and protein-bound uremic toxins, such as HA, which originate from the gut microbial metabolism of phenylalanine (Koppe et al., 2018; Fernandes et al., 2019).

Studies have demonstrated the significance of the gut microbiota in contributing to the synthesis of HA in phenylalanine metabolism (Phipps et al., 1998; Olthof et al., 2001; Olthof et al., 2003). For example, perturbation of hippurate levels has often been attributed to gut microbial activity. The phenolic dietary components are metabolized to phenylpropionic acids by the colonic microbiota, and are then absorbed and metabolized in the liver via β-oxidation to produce benzoic acid, before glycine conjugation and excreted as hippurate. It was proposed that type II diabetes is often related to obesity. The change in hippurate levels is due, at least in part, to potential differences in the microbiota as a result of the "obese microbiome," relative proportion alteration of Firmicutes and Bacteroidetes (Lees et al., 2013).

This study indicated the potential role of intestinal bacteria *g_Abiotrophia* and *g_norank_f_Peptococcaceae* in DKD progression, and their positive correlation with serum HA concentration in DKD, which has not been previously reported. However, an increasing amount of evidence has suggested their involvement in abnormal glucose and lipid metabolism and insulin resistance (Liu D. et al., 2019; Liu YK. et al., 2021; Yuan et al., 2021), supporting our findings and the hypothesis of their role in DKD progression. Furthermore, *g_Abiotrophia* was positively correlated with dihydro-3-coumaric acid, indicating its important role in the synthesis of HA and phenylalanine metabolism.

Consistent with prior studies, *f_Ruminococcaceae* was positively correlated with serum HA concentration in this study. Ruminococcaceae has been considered as a principal short-chain fatty acid-producing bacteria, significantly increased in fecal samples of patients with insulin resistance, and T2D patients compared with healthy subjects (Zhao et al., 2019). Suppressing the growth of Ruminococcaceae has exerted hypoglycemic effects in diabetic animal models (Hu et al., 2019; Zhang et al., 2020). However, no significant correlation between Ruminococcaceae and serum renal function indicators of DKD patients was observed in our study, consistent with prior reports (Lecamwasam et al., 2020). Interestingly, although Ruminococcaceae represented the highest abundance in the fecal sample of DKD patients, the relative abundance of this gut microbe does not change across the stages (1–5) of diabetic CKD.

In concert with previous studies (Debnath et al., 2017; Hasegawa and Inagi, 2021), our study reported the association of the tryptophan metabolic pathway with DKD progression, in which IAA was positively correlated with renal function deterioration, whereas L-tryptophan was just the opposite. Known as a gut-derived protein-bound uremic toxin, IAA is produced by dietary tryptophan metabolism, which stimulates glomerular sclerosis and interstitial fibrosis in the kidneys (Rysz et al., 2021) due to its prooxidant and proinflammatory effect (Gondouin et al., 2013; Dou et al., 2015; Lin et al., 2019). Tryptophan is digested by intestinal bacteria (*E. coli*, *Proteus vulgaris*, *Paracolobactrum coliforme*, *Achromobacter liquefaciens*, and *Bacteroides* spp) to indole (Keszthelyi et al., 2009; Fang et al., 2021), which could evolve into IAA by adding carboxymethyl to the indole ring. Studies have seldom reported the positive effects of pre-, pro-, and synbiotics on the change in serum IAA in CKD patients (Rysz et al., 2021). Therefore, it is meaningful to explore the role of gut microbiota in IAA synthesis to find a new therapeutic strategy. In this study, we observed an inverse correlation between intestinal flora (*g_Lachnospiraceae_NC2004_Group*, *g_Olsenella*, *and g_Faecalicoccus*) and serum IAA, among which, *g_Lachnospiraceae_NC2004_Group* was negatively correlated with L-(−)-3-phenyllactic acid and serum creatinine level, indicating its potential role in the DKD progression via both the phenylalanine and tryptophan metabolic pathways. *G_Lachnospiraceae_NC2004_Group* is a Firmicutes member belonging to *f_Lachnospiraceae*, which was mainly involved in the generation of IAA (Gryp et al., 2020). It is a predominant anaerobic bacteria in the microbial community of healthy populations, producing short-chain fatty acids (Egerton et al.,

2020), converting primary bile acids to secondary bile acids and resisting colonization by pathogens (Sorbara et al., 2020). There has been no study that reported an association between *g_Olsenella*, *g_Faecalicoccus*, and IAA synthesis, and their role in DKD progression.

G_Tyzzerella was negatively correlated with L-tryptophan and positively correlated with dihydro-3-coumaric acid, indicating its association with the phenylalanine and tryptophan metabolic disorders. As previously reported, *g_Tyzzerella* expression was increased in people at high cardiovascular risk (Kelly et al., 2016), and correlated with circulating inflammatory IL-1β (Grant et al., 2021), which may be closely associated with inflammatory injury of DKD. However, there was no relation between g_*Tyzzerella* and DKD renal function indicators in this study. The role of g_*Tyzzerella* in DKD progression needs further investigation.

This study reported the relationship between intestinal microecology and DKD progression by associating intestinal microflora with metabolites via multiomics-integrated methods. The results identified the potential role of *g_Abiotrophia*, *g_norank_f_Peptococcaceae*, and *g_Lachnospiraceae_NC2004_Group* in DKD progression, and their involvement in phenylalanine and tryptophan metabolism. These findings offer real promise in finding a new therapeutic strategy that targets protein-bound uremic toxin HA and IAA in DKD. However, our study has some limitations. First, because this was a retrospective study, we lack records of patient drug and dietary intake, so it was not possible to account for the influence that drugs and dietary habits might have had on intestinal flora and the metabolic profile. Second, the sample size was small and would need to be expanded in future studies. Nevertheless, all participants were residents of Guangdong Province, with characteristics and living habits that were relatively concentrated and consistent. Third, the result of gut microbiota is based on 16S rRNA gene sequencing. Further analysis based on gut metagenome, which could provide more bacterial information, is needed.

In conclusion, this study highlights the complex, interactive network of gut microbiota, serum metabolites, and clinical indicators of predialysis DKD patients and provides new insights into the role of gut microbiota and microbiota-related serum metabolites enriched in phenylalanine and tryptophan metabolic pathways in the progression of DKD.

DATA AVAILABILITY STATEMENT

The original data of 16s rRNA sequencing have been deposited into NCBI databases under the BioProject accession code PRJNA771477 and the BioSample accession number is SAMN22310870.

ETHICS STATEMENT

The studies involving human participants were reviewed and approved by the study protocol was approved by the Institutional Ethics Committee of Guangdong Provincial Hospital of Chinese Medicine (No. ZE2020-193-01). The patients/participants provided their written informed consent to participate in this study.

AUTHOR CONTRIBUTIONS

LeZ and XL received the funding. They participated in the design and coordination, data analysis, interpretation of the results, helped to draft the manuscript, and read and approved the final manuscript. FL participated in the design and coordination, data interpretation, collected the serum and fecal samples of the participants, and read and approved the final manuscript. QZ performed the statistical analyses, participated in the interpretation of the results, drafting of the manuscript, and read and approved the final manuscript. All other authors participated in the study design, helped to collect the serum and fecal samples of the participants, read and commented on interim drafts, and approved the final manuscript.

FUNDING

This study was supported by the project from the State Key Laboratory of Dampness Syndrome of Chinese Medicine (SZ2020ZZ22, SZ2021ZZ43, SZ2021ZZ16), Guangdong Provincial Key Laboratory of Clinical Research on Traditional Chinese Medicine (ZH2020KF02).

ACKNOWLEDGMENTS

The authors would like to express their gratitude to EditSprings (https://www.editsprings.com/) for the expert linguistic services provided.

SUPPLEMENTARY MATERIAL

The Supplementary Material for this article can be found online at: https://www.frontiersin.org/articles/10.3389/fphar.2021.757508/full#supplementary-material

REFERENCES

Afkarian, M., Zelnick, L. R., Hall, Y. N., Heagerty, P. J., Tuttle, K., Weiss, N. S., et al. (2016). Clinical Manifestations of Kidney Disease Among US Adults with Diabetes, 1988-2014. *JAMA* 316 (6), 602–610. doi:10.1001/jama.2016.10924

Andrade-Oliveira, V., Amano, M. T., Correa-Costa, M., Castoldi, A., Felizardo, R. J., de Almeida, D. C., et al. (2015). Gut Bacteria Products Prevent AKI Induced by Ischemia-Reperfusion. *J. Am. Soc. Nephrol.* 26 (8), 1877–1888. doi:10.1681/ASN.2014030288

Chen, S., Zhou, Y., Chen, Y., and Gu, J. (2018). Fastp: an Ultra-fast All-In-One FASTQ Preprocessor. *Bioinformatics* 34 (17), i884–i890. doi:10.1093/bioinformatics/bty560

de Boer, I. H., Rue, T. C., Hall, Y. N., Heagerty, P. J., Weiss, N. S., and Himmelfarb, J. (2011). Temporal Trends in the Prevalence of Diabetic Kidney Disease in the United States. *JAMA* 305 (24), 2532–2539. doi:10.1001/jama.2011.861

Debnath, S., Velagapudi, C., Redus, L., Thameem, F., Kasinath, B., Hura, C. E., et al. (2017). Tryptophan Metabolism in Patients with Chronic Kidney Disease Secondary to Type 2 Diabetes: Relationship to Inflammatory Markers. *Int. J. Tryptophan Res.* 10, 1178646917694600. doi:10.1177/1178646917694600

Dou, L., Sallée, M., Cerini, C., Poitevin, S., Gondouin, B., Jourde-Chiche, N., et al. (2015). The Cardiovascular Effect of the Uremic Solute Indole-3 Acetic Acid. *J. Am. Soc. Nephrol.* 26 (4), 876–887. doi:10.1681/ASN.2013121283

Dumas, M. E. (2012). Metabolome 2.0: Quantitative Genetics and Network Biology of Metabolic Phenotypes. *Mol. Biosyst.* 8 (10), 2494–2502. doi:10.1039/c2mb25167a

Edgar, R. C. (2013). UPARSE: Highly Accurate OTU Sequences from Microbial Amplicon Reads. *Nat. Methods* 10 (10), 996–998. doi:10.1038/nmeth.2604

Egerton, S., Donoso, F., Fitzgerald, P., Gite, S., Fouhy, F., Whooley, J., et al. (2020). Investigating the Potential of Fish Oil as a Nutraceutical in an Animal Model of Early Life Stress. *Nutr. Neurosci.* 31, 1–23. doi:10.1080/1028415X.2020.1753322

Eid, S., Sas, K. M., Abcouwer, S. F., Feldman, E. L., Gardner, T. W., Pennathur, S., et al. (2019). New Insights into the Mechanisms of Diabetic Complications: Role of Lipids and Lipid Metabolism. *Diabetologia* 62 (9), 1539–1549. doi:10.1007/s00125-019-4959-1

Fang, Q., Liu, N., Zheng, B., Guo, F., Zeng, X., Huang, X., et al. (2021). Roles of Gut Microbial Metabolites in Diabetic Kidney Disease. *Front. Endocrinol. (Lausanne)* 12, 636175. doi:10.3389/fendo.2021.636175

Feng, Y. L., Cao, G., Chen, D. Q., Vaziri, N. D., Chen, L., Zhang, J., et al. (2019). Microbiome-metabolomics Reveals Gut Microbiota Associated with Glycine-Conjugated Metabolites and Polyamine Metabolism in Chronic Kidney Disease. *Cell Mol. Life Sci.* 76 (24), 4961–4978. doi:10.1007/s00018-019-03155-9

Fernandes, R., Viana, S. D., Nunes, S., and Reis, F. (2019). Diabetic Gut Microbiota Dysbiosis as an Inflammaging and Immunosenescence Condition that Fosters Progression of Retinopathy and Nephropathy. *Biochim. Biophys. Acta Mol. Basis Dis.* 1865 (7), 1876–1897. doi:10.1016/j.bbadis.2018.09.032

Gondouin, B., Cerini, C., Dou, L., Sallée, M., Duval-Sabatier, A., Pletinck, A., et al. (2013). Indolic Uremic Solutes Increase Tissue Factor Production in Endothelial Cells by the Aryl Hydrocarbon Receptor Pathway. *Kidney Int.* 84 (4), 733–744. doi:10.1038/ki.2013.133

Grant, C. V., Loman, B. R., Bailey, M. T., and Pyter, L. M. (2021). Manipulations of the Gut Microbiome Alter Chemotherapy-Induced Inflammation and Behavioral Side Effects in Female Mice. *Brain Behav. Immun.* 95, 401–412. doi:10.1016/j.bbi.2021.04.014

Gryp, T., Huys, G. R. B., Joossens, M., Van Biesen, W., Glorieux, G., and Vaneechoutte, M. (2020). Isolation and Quantification of Uremic Toxin Precursor-Generating Gut Bacteria in Chronic Kidney Disease Patients. *Int. J. Mol. Sci.* 21 (6), 1986. doi:10.3390/ijms21061986

Hasegawa, S., and Inagi, R. (2021). Harnessing Metabolomics to Describe the Pathophysiology Underlying Progression in Diabetic Kidney Disease. *Curr. Diab. Rep.* 21 (7), 21. doi:10.1007/s11892-021-01390-8

Hirayama, A., Nakashima, E., Sugimoto, M., Akiyama, S., Sato, W., Maruyama, S., et al. (2012). Metabolic Profiling Reveals New Serum Biomarkers for Differentiating Diabetic Nephropathy. *Anal. Bioanal. Chem.* 404 (10), 3101–3109. doi:10.1007/s00216-012-6412-x

Hu, T. G., Wen, P., Shen, W. Z., Liu, F., Li, Q., Li, E. N., et al. (2019). Effect of 1-Deoxynojirimycin Isolated from Mulberry Leaves on Glucose Metabolism and Gut Microbiota in a Streptozotocin-Induced Diabetic Mouse Model. *J. Nat. Prod.* 82 (8), 2189–2200. doi:10.1021/acs.jnatprod.9b00205

Hu, X., Ouyang, S., Xie, Y., Gong, Z., and Du, J. (2020a). Characterizing the Gut Microbiota in Patients with Chronic Kidney Disease. *Postgrad. Med.* 132 (6), 495–505. doi:10.1080/00325481.2020.1744335

Hu, X., Xie, Y., Xiao, Y., Zeng, W., Gong, Z., and Du, J. (2020b). Longitudinal Analysis of Fecal Microbiome and Metabolome during Renal Fibrotic Progression in a Unilateral Ureteral Obstruction Animal Model. *Eur. J. Pharmacol.* 886, 173555. doi:10.1016/j.ejphar.2020.173555

Kelly, T. N., Bazzano, L. A., Ajami, N. J., He, H., Zhao, J., Petrosino, J. F., et al. (2016). Gut Microbiome Associates with Lifetime Cardiovascular Disease Risk Profile Among Bogalusa Heart Study Participants. *Circ. Res.* 119 (8), 956–964. doi:10.1161/CIRCRESAHA.116.309219

Keszthelyi, D., Troost, F. J., and Masclee, A. A. (2009). Understanding the Role of Tryptophan and Serotonin Metabolism in Gastrointestinal Function. *Neurogastroenterol. Motil.* 21 (12), 1239–1249. doi:10.1111/j.1365-2982.2009.01370.x

Koppe, L., Fouque, D., and Soulage, C. O. (2018). Metabolic Abnormalities in Diabetes and Kidney Disease: Role of Uremic Toxins. *Curr. Diab. Rep.* 18 (10), 97. doi:10.1007/s11892-018-1064-7

Kwan, B., Fuhrer, T., Zhang, J., Darshi, M., Van Espen, B., Montemayor, D., et al. (2020). Metabolomic Markers of Kidney Function Decline in Patients with Diabetes: Evidence from the Chronic Renal Insufficiency Cohort (CRIC) Study. *Am. J. Kidney Dis.* 76 (4), 511–520. doi:10.1053/j.ajkd.2020.01.019

Lecamwasam, A., Nelson, T. M., Rivera, L., Ekinci, E. I., Saffery, R., and Dwyer, K. M. (2020). Gut Microbiome Composition Remains Stable in Individuals with Diabetes-Related Early to Late Stage Chronic Kidney Disease. *Biomedicines* 9 (1), 19. doi:10.3390/biomedicines9010019

Lees, H. J., Swann, J. R., Wilson, I. D., Nicholson, J. K., and Holmes, E. (2013). Hippurate: the Natural History of a Mammalian-Microbial Cometabolite. *J. Proteome Res.* 12 (4), 1527–1546. doi:10.1021/pr300900b

Lin, Y. T., Wu, P. H., Lee, H. H., Mubanga, M., Chen, C. S., Kuo, M. C., et al. (2019). Indole-3 Acetic Acid Increased Risk of Impaired Cognitive Function in Patients Receiving Hemodialysis. *Neurotoxicology* 73, 85–91. doi:10.1016/j.neuro.2019.02.019

Liu, D., Huang, J., Luo, Y., Wen, B., Wu, W., Zeng, H., et al. (2019a). Fuzhuan Brick Tea Attenuates High-Fat Diet-Induced Obesity and Associated Metabolic Disorders by Shaping Gut Microbiota. *J. Agric. Food Chem.* 67 (49), 13589–13604. doi:10.1021/acs.jafc.9b05833

Liu, Y., Chen, X., Liu, Y., Chen, T., Zhang, Q., Zhang, H., et al. (2019b). Metabolomic Study of the Protective Effect of Gandi Capsule for Diabetic Nephropathy. *Chem. Biol. Interact* 314, 108815. doi:10.1016/j.cbi.2019.108815

Liu, J. R., Miao, H., Deng, D. Q., Vaziri, N. D., Li, P., and Zhao, Y. Y. (2021a). Gut Microbiota-Derived Tryptophan Metabolism Mediates Renal Fibrosis by Aryl Hydrocarbon Receptor Signaling Activation. *Cel Mol. Life Sci.* 78 (3), 909–922. doi:10.1007/s00018-020-03645-1

Liu, Y. K., Chen, V., He, J. Z., Zheng, X., Xu, X., and Zhou, X. D. (2021b). A Salivary Microbiome-Based Auxiliary Diagnostic Model for Type 2 Diabetes Mellitus. *Arch. Oral Biol.* 126, 105118. doi:10.1016/j.archoralbio.2021.105118

Ma, L., Jiang, Y., Kong, X., Liu, Q., Zhao, H., Zhao, T., et al. (2019). Interaction of MTHFR C677T Polymorphism with Smoking in Susceptibility to Diabetic Nephropathy in Chinese Men with Type 2 Diabetes. *J. Hum. Genet.* 64 (1), 23–28. doi:10.1038/s10038-018-0531-y

Ma, J., Sun, L., Liu, Y., Ren, H., Shen, Y., Bi, F., et al. (2020). Alter between Gut Bacteria and Blood Metabolites and the Anti-tumor Effects of Faecalibacterium Prausnitzii in Breast Cancer. *BMC Microbiol.* 20 (1), 82. doi:10.1186/s12866-020-01739-1

Magoc, T., and Salzberg, S. L. (2011). FLASH: Fast Length Adjustment of Short Reads to Improve Genome Assemblies. *Bioinformatics* 27 (21), 2957–2963. doi:10.1093/bioinformatics/btr507

National Kidney Foundation (2002). K/DOQI Clinical Practice Guidelines for Chronic Kidney Disease: Evaluation, Classification, and Stratification. *Am. J. Kidney Dis.* 39 (2 Suppl. 1), S1–S266.

Ng, D. P., Salim, A., Liu, Y., Zou, L., Xu, F. G., Huang, S., et al. (2012). A Metabolomic Study of Low Estimated GFR in Non-proteinuric Type 2 Diabetes Mellitus. *Diabetologia* 55 (2), 499–508. doi:10.1007/s00125-011-2339-6

Nunez Lopez, Y. O., Retnakaran, R., Zinman, B., Pratley, R. E., and Seyhan, A. A. (2019). Predicting and Understanding the Response to Short-Term Intensive Insulin Therapy in People with Early Type 2 Diabetes. *Mol. Metab.* 20, 63–78. doi:10.1016/j.molmet.2018.11.003

Olthof, M. R., Hollman, P. C., and Katan, M. B. (2001). Chlorogenic Acid and Caffeic Acid Are Absorbed in Humans. *J. Nutr.* 131 (1), 66–71. doi:10.1093/jn/131.1.66

Olthof, M. R., Hollman, P. C., Buijsman, M. N., van Amelsvoort, J. M., and Katan, M. B. (2003). Chlorogenic Acid, Quercetin-3-Rutinoside and Black tea Phenols Are Extensively Metabolized in Humans. *J. Nutr.* 133 (6), 1806–1814. doi:10.1093/jn/133.6.1806

Pan, L., Li, Z., Wang, Y., Zhang, B., Liu, G., and Liu, J. (2020). Network Pharmacology and Metabolomics Study on the Intervention of Traditional Chinese Medicine Huanglian Decoction in Rats with Type 2 Diabetes Mellitus. *J. Ethnopharmacol.* 258, 112842. doi:10.1016/j.jep.2020.112842

Parwani, K., and Mandal, P. (2020). Role of Advanced Glycation End Products and Insulin Resistance in Diabetic Nephropathy. *Arch. Physiol. Biochem.* 30, 1–13. doi:10.1080/13813455.2020.1797106

Phipps, A. N., Stewart, J., Wright, B., and Wilson, I. D. (1998). Effect of Diet on the Urinary Excretion of Hippuric Acid and Other Dietary-Derived Aromatics in Rat. A Complex Interaction between Diet, Gut Microflora and Substrate Specificity. *Xenobiotica* 28 (5), 527–537. doi:10.1080/004982598239443

Ramezani, A., and Raj, D. S. (2014). The Gut Microbiome, Kidney Disease, and Targeted Interventions. *J. Am. Soc. Nephrol.* 25 (4), 657–670. doi:10.1681/ASN.2013080905

Rayego-Mateos, S., Morgado-Pascual, J. L., Opazo-Ríos, L., Guerrero-Hue, M., García-Caballero, C., Vázquez-Carballo, C., et al. (2020). Pathogenic Pathways and Therapeutic Approaches Targeting Inflammation in Diabetic Nephropathy. *Int. J. Mol. Sci.* 21 (11), 3798. doi:10.3390/ijms21113798

Ren, Z., Fan, Y., Li, A., Shen, Q., Wu, J., Ren, L., et al. (2020). Alterations of the Human Gut Microbiome in Chronic Kidney Disease. *Adv. Sci. (Weinh)* 7 (20), 2001936. doi:10.1002/advs.202001936

Rysz, J., Franczyk, B., Ławiński, J., Olszewski, R., Ciałkowska-Rysz, A., and Gluba-Brzózka, A. (2021). The Impact of CKD on Uremic Toxins and Gut Microbiota. *Toxins (Basel)* 13 (4), 252. doi:10.3390/toxins13040252

Sorbara, M. T., Littmann, E. R., Fontana, E., Moody, T. U., Kohout, C. E., Gjonbalaj, M., et al. (2020). Functional and Genomic Variation between Human-Derived Isolates of Lachnospiraceae Reveals Inter- and Intra-Species Diversity. *Cell Host Microbe* 28 (1), 134. doi:10.1016/j.chom.2020.05.005

Sun, B., Wang, X., Liu, X., Wang, L., Ren, F., Wang, X., et al. (2020). Hippuric Acid Promotes Renal Fibrosis by Disrupting Redox Homeostasis via Facilitation of NRF2-KEAP1-CUL3 Interactions in Chronic Kidney Disease. *Antioxidants (Basel)* 9 (9), 783. doi:10.3390/antiox9090783

Tao, S., Li, L., Li, L., Liu, Y., Ren, Q., Shi, M., et al. (2019). Understanding the Gut-Kidney axis Among Biopsy-Proven Diabetic Nephropathy, Type 2 Diabetes Mellitus and Healthy Controls: an Analysis of the Gut Microbiota Composition. *Acta Diabetol.* 56 (5), 581–592. doi:10.1007/s00592-019-01316-7

Umanath, K., and Lewis, J. B. (2018). Update on Diabetic Nephropathy: Core Curriculum 2018. *Am. J. Kidney Dis.* 71 (6), 884–895. doi:10.1053/j.ajkd.2017.10.026

Walker, D. I., Uppal, K., Zhang, L., Vermeulen, R., Smith, M., Hu, W., et al. (2016). High-resolution Metabolomics of Occupational Exposure to Trichloroethylene. *Int. J. Epidemiol.* 45 (5), 1517–1527. doi:10.1093/ije/dyw218

Wang, Q., Garrity, G. M., Tiedje, J. M., and Cole, J. R. (2007). Naive Bayesian Classifier for Rapid Assignment of rRNA Sequences into the New Bacterial Taxonomy. *Appl. Environ. Microbiol.* 73 (16), 5261–5267. doi:10.1128/AEM.00062-07

Wei, B., Zhong, Q. W., Ke, S. Z., Zhou, T. S., Xu, Q. L., Wang, S. J., et al. (2020). Sargassum Fusiforme Polysaccharides Prevent High-Fat Diet-Induced Early Fasting Hypoglycemia and Regulate the Gut Microbiota Composition. *Mar. Drugs* 18 (9), 444. doi:10.3390/md18090444

Wu, I. W., Lin, C. Y., Chang, L. C., Lee, C. C., Chiu, C. Y., Hsu, H. J., et al. (2020). Gut Microbiota as Diagnostic Tools for Mirroring Disease Progression and Circulating Nephrotoxin Levels in Chronic Kidney Disease: Discovery and Validation Study. *Int. J. Biol. Sci.* 16 (3), 420–434. doi:10.7150/ijbs.37421

Wu, X., Li, J., Yan, T., Ke, X., Li, X., Zhu, Y., et al. (2021). HOXB7 Acts as an Oncogenic Biomarker in Head and Neck Squamous Cell Carcinoma. *Cancer Cel Int.* 21 (1), 393. doi:10.1186/s12935-021-02093-6

Yuan, X., Chen, R., Zhang, Y., Lin, X., Yang, X., and McCormick, K. L. (2021). Gut Microbiota of Chinese Obese Children and Adolescents with and without Insulin Resistance. *Front. Endocrinol. (Lausanne)* 12, 636272. doi:10.3389/fendo.2021.636272

Zhang, H. H., Liu, J., Lv, Y. J., Jiang, Y. L., Pan, J. X., Zhu, Y. J., et al. (2020). Changes in Intestinal Microbiota of Type 2 Diabetes in Mice in Response to Dietary Supplementation with Instant Tea or Matcha. *Can. J. Diabetes* 44 (1), 44–52. doi:10.1016/j.jcjd.2019.04.021

Zhao, L., Lou, H., Peng, Y., Chen, S., Zhang, Y., and Li, X. (2019). Comprehensive Relationships between Gut Microbiome and Faecal Metabolome in Individuals with Type 2 Diabetes and its Complications. *Endocrine* 66 (3), 526–537. doi:10.1007/s12020-019-02103-8

Conflict of Interest: The authors declare that the research was conducted in the absence of any commercial or financial relationships that could be construed as a potential conflict of interest.

Publisher's Note: All claims expressed in this article are solely those of the authors and do not necessarily represent those of their affiliated organizations, or those of the publisher, the editors and the reviewers. Any product that may be evaluated in this article, or claim that may be made by its manufacturer, is not guaranteed or endorsed by the publisher.

frontiers in Pharmacology

REVIEW
published: 10 December 2021
doi: 10.3389/fphar.2021.768100

Caveolin-1 Regulates Cellular Metabolism: A Potential Therapeutic Target in Kidney Disease

Shilu Luo[1,2], *Ming Yang*[1,2], *Hao Zhao*[1,2], *Yachun Han*[1,2], *Na Jiang*[1,2], *Jinfei Yang*[1,2], *Wei Chen*[1,2], *Chenrui Li*[1,2], *Yan Liu*[1,2], *Chanyue Zhao*[1,2] *and Lin Sun*[1,2]*

[1]*Department of Nephrology, The Second Xiangya Hospital, Central South University, Changsha, China,* [2]*Hunan Key Laboratory of Kidney Disease and Blood Purification, Changsha, China*

The kidney is an energy-consuming organ, and cellular metabolism plays an indispensable role in kidney-related diseases. Caveolin-1 (Cav-1), a multifunctional membrane protein, is the main component of caveolae on the plasma membrane. Caveolae are represented by tiny invaginations that are abundant on the plasma membrane and that serve as a platform to regulate cellular endocytosis, stress responses, and signal transduction. However, caveolae have received increasing attention as a metabolic platform that mediates the endocytosis of albumin, cholesterol, and glucose, participates in cellular metabolic reprogramming and is involved in the progression of kidney disease. It is worth noting that caveolae mainly depend on Cav-1 to perform the abovementioned cellular functions. Furthermore, the mechanism by which Cav-1 regulates cellular metabolism and participates in the pathophysiology of kidney diseases has not been completely elucidated. In this review, we introduce the structure and function of Cav-1 and its functions in regulating cellular metabolism, autophagy, and oxidative stress, focusing on the relationship between Cav-1 in cellular metabolism and kidney disease; in addition, Cav-1 that serves as a potential therapeutic target for treatment of kidney disease is also described.

Keywords: caveolin-1 (Cav-1), cellular metabolism, kidney disease, oxidative stress, autophagy

OPEN ACCESS

Edited by:
Dan-Qian Chen,
Northwest University, China

Reviewed by:
Yaming Jiu,
Institut Pasteur of Shanghai (CAS), China
Joan Krepinsky,
McMaster University, Canada
Cecilia Jacques G. de Almeida,
Oswaldo Cruz Foundation, Brazil

***Correspondence:**
Lin Sun
sunlin@csu.edu.cn

Specialty section:
This article was submitted to Renal Pharmacology, a section of the journal Frontiers in Pharmacology

Received: *31 August 2021*
Accepted: *08 November 2021*
Published: *10 December 2021*

Citation:
Luo S, Yang M, Zhao H, Han Y, Jiang N, Yang J, Chen W, Li C, Liu Y, Zhao C and Sun L (2021) Caveolin-1 Regulates Cellular Metabolism: A Potential Therapeutic Target in Kidney Disease. Front. Pharmacol. 12:768100. doi: 10.3389/fphar.2021.768100

1 INTRODUCTION

Kidney disease is currently a challenging public health problem worldwide and is receiving increasing attention. The kidney is a highly metabolically active organ, and cellular energy metabolism is very important for maintaining kidney homeostasis (Gewin, 2021). In addition to inflammation, metabolic disorders are another form of diseased kidney dysfunction and play a key role in renal fibrosis (Kang et al., 2015). The scaffold protein caveolin-1 (Cav-1) on the cell membrane is a key protein to maintain energy homeostasis by regulating energy metabolism and mediating the signal transduction of glucose and lipid metabolism (Baudrand et al., 2016), which is closely associated with metabolic-related diseases such as diabetes (Bonds et al., 2019; Haddad et al., 2020), obesity (Chang et al., 2017), cardiovascular disease (Mayurasakorn et al., 2018), and cancer (Sotgia et al., 2012; Zhang Z. et al., 2020). With increased research on Cav-1, it has been demonstrated that Cav-1 plays an important role in the process of renal fibrosis (Shihata et al., 2017). However, the mechanism by which Cav-1 regulates cellular metabolism and kidney disease is not clearly understood. This review comprehensively describes the structure, expression, and regulation as well as the associated signaling pathway of Cav-1, which may be a potential drug

target for metabolic-related kidney disease. Specifically, we describe the role of Cav-1 in regulating cellular glucose and lipid metabolism, cellular oxidative stress, and autophagy.

2 CAVEOLIN FAMILY

The caveolin family consists of three members, namely, caveolin-1 (Cav-1), caveolin-2 (Cav-2), and caveolin-3 (Cav-3). Cav-1 was identified in 1989 by Glenney et al. as the first family member of caveolin proteins (Glenney, 1989). They isolated a 22 kDa cytoskeleton protein from *Rous sarcoma virus*–transformed chicken fibroblasts, which was a substrate for tyrosine phosphorylation (Glenney, 1989). Subsequently, Rothberg et al. found that the 22 kDa membrane protein was part of the plasma membrane of the cell and named it caveolin (Rothberg et al., 1992). In addition, it has been demonstrated that the VIP21 protein (21 kDa) from canine renal epithelial cells (MDCK) has only eight–amino acid (aa) sequences that differ from human Cav-1. VIP21 is equivalent to caveolin in canines; thus, Cav-1 is also known as VIP21 (Glenney, 1992; Kurzchalia et al., 1992). Furthermore, caveolin was officially renamed Cav-1 in 1996 by Scherer et al. (Scherer et al., 1996). After they identified a vesicular protein–related protein, Cav-2, of about 20 kDa by microsequencing the vesicular protein–enriched membrane of adipocytes (Scherer et al., 1996). Subsequently, Tang et al. (Tang et al., 1996) found the same DNA sequence as *CAV1* in rat hearts using a gene probe, namely, *CAV3* (about 17 KDa), which was 65% identical and 85% similar to *CAV1*, whereas *CAV1* and *CAV2* had 38% identical and 58% similar DNA sequences.

CAV1 and *CAV2* are both located on human chromosome 7q31.1, whereas *CAV3* is located on 3p25 (Engelman et al., 1998; Williams and Lisanti, 2004). Cav-1 exists in two isoforms (α and β), and each monomer has a hairpin conformation capable of dimerization (Fujimoto et al., 2000; Kogo and Fujimoto, 2000; Williams and Lisanti, 2004). Cav-1α contains 1–178 (24 kDa) residues, whereas Cav-1β contains 32–178 (21 kDa) residues (Scherer et al., 1995). In addition, the protein translation start site of Cav-1α starts from the first aa, whereas Cav-1β starts from the 32nd aa residue; thus, their N-terminal sequences are different (Scherer et al., 1995). Previous studies have suggested that these two monomers are encoded by different mRNAs (Kogo and Fujimoto, 2000). Furthermore, it is worth noting that only Cav-1α has tyrosine-14 phosphorylation sites but is not seen in Cav-1β due to the absence of a specific sequence at the N-terminus (Scherer et al., 1995; Vainonen et al., 2004). Cav-1 and Cav-2 are coexpressed in a variety of mammalian cells [such as endothelial cells (ECs), vascular smooth muscle cells, type I pneumocytes, and liver and kidney cells], whereas Cav-3 is mainly expressed not only in muscle cell but also in other cell types, such as astrocytes (Ikezu et al., 1998; Williams and Lisanti, 2004). Interestingly, it has been reported that Cav-1 is mainly in the glomeruli of the kidney (Breton et al., 1998; Sörensson et al., 2002; Moriyama et al., 2011). Furthermore, the subcellular localization of caveolins has been shown to be located in Golgi apparatus, endoplasmic reticulum (ER), mitochondria, nucleus, peroxisomes, lipid droplets (LDs) (Fridolfsson et al., 2014), and mitochondria-associated membranes (MAMs) (Sala-Vila et al., 2016). The Cav-1 protein sequence consists of four domains: an N-terminal domain (1–81 aa), an oligomerization domain (61–101 aa) including the scaffolding domain (82–101 aa), an intramembrane domain (102–134 aa), and a C-terminal domain (135–178 aa) (Filippini and D'Alessio, 2020; Root et al., 2015; Wong et al., 2020). Both the N-terminus and C-terminus of Cav-1 are exposed to the cytoplasm, and the C-terminal domain contains ubiquitination sites, whereas its N-terminal domain contains two phosphorylation sites: tyrosine-14 (Li et al., 1996b) and serine-80 (Schlegel et al., 2001). Tyrosine-14 (Y14) can be phosphorylated by the Src tyrosine kinase family (such as Src, Abl, and Fyn) (Wong et al., 2020) to regulate signaling proteins, whereas serine-80 (S80) phosphorylated Cav-1 is mainly targeted to the ER and participates in the secretion of Cav-1 (Schlegel et al., 2001). The C-terminal domain contains three palmitoylation sites (Cys133/143/156), and the palmitoylation site and the intramembrane domain (in the form of a U-shaped conformation) are embedded in the cell lipid bilayer (Hoop et al., 2012; Root et al., 2015; Park et al., 2019). In addition, the scaffold domain of Cav-1 carrying a cholesterol recognition aa consensus can bind cholesterol (Yang et al., 2014; Krishna and Sengupta, 2019) and other subtypes of caveolin, which is necessary for the formation of caveolin homo or hetero oligomers (Epand et al., 2005; Hoop et al., 2012).

Emerging evidence has shown that the scaffold domain of Cav-1 (CSD) plays a key role in tumor progression and cellular metabolic reprogramming (Bernatchez, 2020; Gopu et al., 2020). The CSD is a highly hydrophobic region composed of a 20-aa stretch of caveolin residues (Li et al., 1996a; Wong et al., 2021). It can bind proteins (such as src family kinases and G protein subunits) that contain a caveolin binding motif (CBM) consensus (Li et al., 1996a; Collins et al., 2012). The CBM includes three motifs: ΩXΩXXXXΩXXΩ, ΩXXXΩXXΩ, and the combination sequence ΩXΩXXXXΩXΩ (Ω is a Phe, Tyr, or Trp residue, X can be any aa) (Collins et al., 2012). Couet et al. found that the epidermal growth factor receptor (EGFR) kinase interacts directly with the caveolin scaffolding domain *via* its conserved caveolin binding motif, which may mediate caveolae signaling (Couet et al., 1997). However, it remains controversial whether CSD/CBM binding effectively mediates caveolae-related signaling. For instance, Collins et al. (Collins et al., 2012) stated that the CBM in most signal proteins is buried and difficult to access, and CBM sequences in caveolae-associated proteins are not abundant; thus, the interaction of CBM/CSD-mediated caveolae signaling needs to be reassessed (Collins et al., 2012). Nevertheless, Zakrzewicz et al. determined that the glycolytic enzyme enolase 1 with a CBM corecognition sequence can be transported to the cell membrane and combined with the CSD of Cav-1, which may affect cell migration and cell invasion (Zakrzewicz et al., 2014). It is worth noting that the consensus CBM of enolase 1 is not buried in the protein core but exposed on the surface of the protein, which makes it accessible for interactions with the CSD (Zakrzewicz et al., 2014). Furthermore, Okada et al. confirmed that the CSD domain of Cav-1 plays a key role in the cell cycle, migration, and proliferation of cancer cells and may provide a

platform for specific signal transduction (Okada et al., 2019). In summary, caveolin may regulate other protein activities through CSD binding to the CBM, and its activity depends on binding to the CBM of other proteins.

3 REGULATION OF CAVEOLIN-1 EXPRESSION

The expression of Cav-1 is regulated by three ways: genomic epigenetic modification, transcription, and posttranscriptional regulation mechanisms. The genomic epigenetic modification of *CAV1* can be divided into DNA methylation modification and histone modification (such as methylation, acetylation, phosphorylation, and ubiquitination) (Yan et al., 2020). Zschocke et al. (Zschocke et al., 2002) found that ectopic expression of estrogen receptor caused DNA methylation or histone deacetylation changes of *CAV1* in nerve cells, thereby regulating its mRNA expression. Subsequently, Sanders et al. (Sanders et al., 2017) found that after treatment of normal fibroblasts with transforming growth factor–β1 (TGF-β1), the mRNA expression of *CAV1* was downregulated through histone modification (H3 lysine 4 trimethylation) instead of DNA methylation, which may be associated with idiopathic pulmonary fibrosis. In addition, Yan et al. reviewed the possible mechanism of *CAV1* DNA methylation in chronic lung disease and regarded it as a possible target for early diagnosis and treatment of the chronic lung disease (Yan et al., 2020). However, whether its application as a biomarker requires further research.

The promoter sequence of *CAV1* includes three G+C-rich potential sterol regulatory elements (SREs), a CAAT sequence, a Sp1 consensus sequence (Bist et al., 1997; Dasari et al., 2006; Chen et al., 2011), and a functional peroxisome proliferator response element (Llaverias et al., 2004). Therefore, the increase in intracellular free cholesterol can regulate the mRNA expression of *CAV1* by stimulating the binding of SRE-binding protein 1 (SPEBP-1) to the cholesterol regulatory element in the *CAV1* promoter (Bist et al., 1997). Other transcription factors, including P53 (Bist et al., 2000), c-myc (Xie et al., 2003), GAT-binding factor 6 (GAT-6) (Boopathi et al., 2011), NF-κB (Thangavel et al., 2019), forkhead box O (FoxO) (van den Heuvel et al., 2005), and FoxM1 (Huang et al., 2012), can also bind to the related E-BOX of the promoter of the *CAV1* and regulate its transcription. These findings suggest that the Cav-1 may have a potential regulatory role in cellular metabolism, inflammation, and fibrosis.

Many factors contribute to the posttranscriptional regulation of *CAV1*, such as microRNA (miRNA), long noncoding RNAs (lncRNA), and circular RNA (circRNA), as well as other proteins. Among them, miRNAs, including miR-199a-5p (Zhong et al., 2020), miR-96 (Chen et al., 2020), miR-124 (Torrejón et al., 2017), miR-103/107 (Zhang et al., 2015), miR-204 (Huang et al., 2019), miR-130a (Wang et al., 2016), and miR-103-3p (Wang et al., 2021), have been demonstrated that to recognize homologous *CAV1* mRNA and cause the degradation of *CAV1* mRNA or inhibit its translation. In addition, lncRNAs, including lncRNA ANRIL (Zhong et al., 2020), lnc-BMP1-1 (Ling et al., 2020), and lncRNA IMFLNC1 (Wang J. et al., 2020), can regulate the protein expression and function of Cav-1. A recent study has shown that circRNA though some miRNAs, playing key role in posttranscriptional regulation of *CAV1* (Luo Z. et al., 2020; Zhu et al., 2020). Zhao et al. (Li et al., 2020) found that the circRNA TADA2A, contains rich binding sites of miR526b, which plays a competitive inhibitory effect, thereby releasing the inhibitory effect of miRNA526b o*n CAV1* and then increasing the expression level of Cav-1. Furthermore, some proteins, such as Cavin-1 (Hansen and Nichols, 2010; Liu et al., 2014), flotillin-1 (Vassilieva et al., 2009), and RNA-binding protein HuR (Cao et al., 2021) can also affect the protein expression and stability of Cav-1. E3 ubiquitin ligase ZNRF1 and catalase induce Cav-1 ubiquitinated (Rungtabnapa et al., 2011; Burana et al., 2016; Lee et al., 2017). In addition, the Src kinase can bind to the Tyr14 site of Cav-1 and then induces its phosphorylation, leading to instability and degradation of Cav-1 (Yoon et al., 2019). Furthermore, it has been reported that Cav-1 can be degraded by palmitic acid–induced autophagy to promote astrocyte apoptosis and inflammation (Chen et al., 2018), which indicates that the expression of Cav-1 is not only regulated by noncoding RNA but that its stability and activity are also regulated by other proteins and enzymes as well as autophagy, which, in turn, affects the function of the Cav-1 protein.

4 CAVEOLIN-1 AND CELLULAR METABOLISM

4.1 The Role of Caveolin-1 in the Formation of Caveolae on the Cell Membrane

An important physiological function of Cav-1 is to act as the core component of caveolae and participate in its biogenesis (**Figure 1**). Caveolae consist of a special membrane invagination on lipid rafts and are abundant in the plasma membrane of many mammalian cells (Parton et al., 2018). They are mainly composed of integral membrane proteins (caveolin proteins), peripheral membrane proteins (cavin proteins), and lipids (including cholesterol, sphingolipids, phosphatidylserine, glycosphingolipids, and sphingomyelin) assembled on the plasma membrane (Hirama et al., 2017), shaped like a bulb or flask, with a diameter about 50–100 nm (Cheng and Nichols, 2016). The caveolin family is the main scaffold protein involved in the formation of caveolae, which mainly refers to Cav-1; whereas in the muscle cells, it mainly refers to Cav-3 (Rothberg et al., 1992). The cavin family (including cavin-1, cavin-2, cavin-3, and cavin-4) assists in the formation of caveolae (Hill et al., 2008; Kovtun et al., 2015). Cavin-1, also known as polymerase I and transcript release factor, can bind to caveolin in a lipid-dependent manner, thereby stabilizing the curvature of caveolae (Hill et al., 2008). Cavin-2 (serum deprivation protein response) can directly bind to cavin-1 and target cavin-1 to participate in the biogenesis of caveolae by regulating the size of caveolae and inducing the expansion of caveolae-derived membrane-like tubules (Hansen et al., 2009). Cavin-3 (sdr-related gene product that binds to c-kinase) mainly

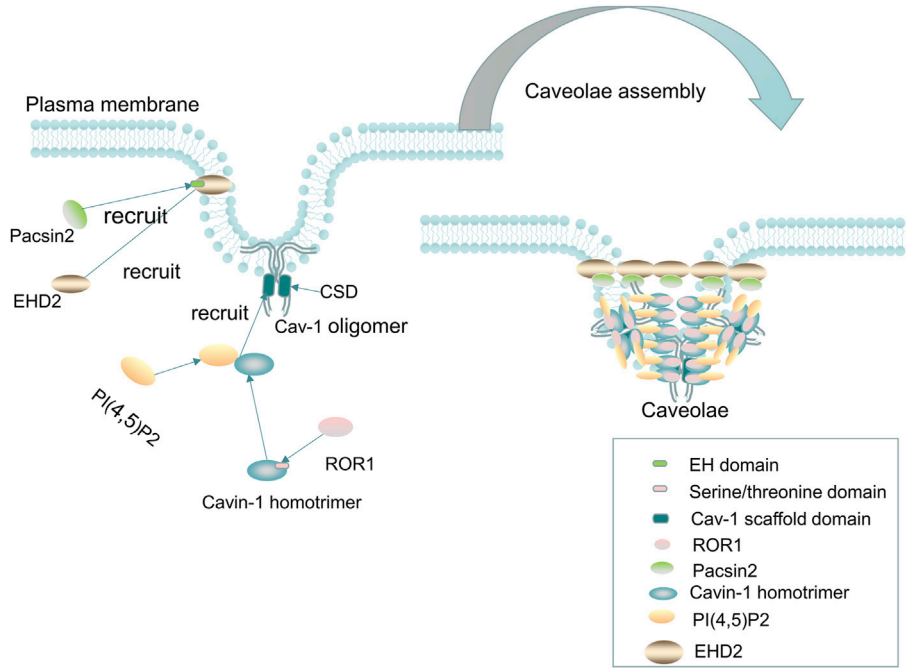

FIGURE 1 | Cav-1 and caveolae. Cav-1 is essential for the formation of caveolae. The cholesterol-containing scaffold protein domain (CSD) of Cav-1 binds to cholesterol on the plasma membrane, and then, the Cavin-1 complex, EHD2, PACSIN2, and ROR1 are recruited to form mature caveolae. The recruited cavin-1 first binds to lipids [such as phosphatidylserine, and PI(4,5)P2] and then binds to the cholesterol-containing scaffold protein domain of Cav-1 to stabilize the curvature of the membrane. Two-thirds of the kinase domain of ROR1, as the scaffold protein of cavin-1 and Cav-1, binds to cavin-1, thereby promoting the binding of Cav-1 and preventing autophagy degradation of Cav-1. In addition, EHD2 is recruited to the neck of caveolae to form a loop through oligomerization, and then, Pacsin2 binds to the EH domain of EHD2 to maintain the stability of Caveolae and the distribution of Cav-1 on the plasma membrane. Without EHD2, the stability of caveolae and the distribution of Cav-1 on the plasma membrane will be difficult to maintain, resulting in dissociation of the caveolae from the plasma membrane.

regulates the membrane targeting function of caveolae (McMahon et al., 2009; Parton et al., 2018). Cavin-4, also known as muscle-restricted coiled-coil protein (MURC), is mainly restricted to expression in muscle cells and may not be important for the formation of caveolae (Parton et al., 2018). In addition, other components, such as Eps-15 homologous domain composition 2 (EHD2), PACSIN2/Syndapin II (PACSIN2), and receptor tyrosine kinase-like orphan receptor 1 (ROR1) (Yamaguchi et al., 2016) can also play an important role in modulating the function of caveolae (Parton, 2018).

The formation of caveolae mainly involves the following steps: first, caveolins, as integral membrane proteins, are synthesized in the ER, and then, Cav-1 and Cav-2 monomers are cotranslationally inserted into the membrane of the ER and form oligomerized 8S-Cav oligomers, which contain 7–14 caveolins (Han et al., 2020). The complex of oligomerized 8S-Cav oligomers is transported to the Golgi complex in the form of coat protein II (COPII) vesicle-dependent transport machinery, where Cav-1 assembles into a cholesterol-rich complex (a 70s-Cav complex composed of 18–25 8S-Cav subunits), and the 70s-Cav complex is subsequently transported and partially inserted into the plasma membrane and binds to cholesterol on the plasma membrane through its CSD domain, recruiting the cavin-1 complex, EHD2, PACSIN2, and ROR1 to form mature caveolae (Parton and del Pozo, 2013; Busija et al., 2017; Parton et al., 2018; Parton et al., 2020b).

The recruited peripheral protein cavin-1 first binds to lipids [such as phosphatidylserine and PI(4,5)P2] and then binds to the cholesterol-containing scaffold protein domain of Cav-1 to stabilize the curvature of the membrane and produce classic spherical caveolae (Hill et al., 2008). Plasma membrane insertion of EHD2 requires the binding of ATP and is oligomerized to form a ring in the neck of caveolae (Morén et al., 2012; Hoernke et al., 2017), and then, Pacsin2 binds to the EH domain of EHD2 to maintain the stability of caveolae and the distribution of Cav-1 on the plasma membrane (Hubert et al., 2020a). In addition, excessive lipid accumulation in the caveolae can cause caveolae to scission from the plasma membrane, especially in the absence of EHD2 restriction (Hubert et al., 2020b). Furthermore, EHD2 was found to regulate lipid metabolism, and loss of EHD2 caused caveolae to dissociate from the plasma membrane, while increasing fatty acid intake and promoting lipid deposition and the size of LDs (Matthaeus et al., 2020). ROR1, as a scaffold protein of cavin-1 and Cav-1, can interact with cavin-1 through its richest C-terminal serine/threonine domain, and two-thirds of the kinase domain binds to cavin-1, thus promoting the binding of Cav-1 and cavin-1 on the plasma membrane and maintaining Cav-1 expression by inhibiting lysosomal-dependent degradation and corresponding vesicle formation (Yamaguchi et al., 2016). When caveolae lack the abovementioned caveolae-related proteins to maintain their stability or subjected to mechanical

stimuli (such as membrane tension or stress stimuli), Cav-1 and cavin can be released into the cytoplasm, and non-caveolae Cav-1 and cavin can recovered and reorganized into caveolae on the plasma membrane or be degraded by lysosomes (Parton et al., 2020b). In addition, non-caveola Cav-1 may also have an important physiological role independent of being a constituent of caveolae.

4.2 Caveolin-1 Mediates Protein Membrane Targeting, Endocytosis, and Signal Transduction

Cav-1 regulates various enzyme activities or receptor expression and targets them to the cell membrane. It has been found that the increased expression of Cav-1 can recruit glycolytic enzymes [phosphofructokinase (Vallejo and Hardin, 2005), aldolase (Raikar et al., 2006), and fatty acid translocase (CD36) (Ring et al., 2006)] and nervous system–related receptors [such as neurotrophin receptor, P2Y2 nucleotide receptor (Martinez et al., 2016), and heme oxygenase-1 (HO-1)] displaces to the cell membrane, where they directly binds the CSD of Cav-1 and then mediates downstream signal molecule transduction or fatty acid uptake (Abumrad et al., 2021), eventually affecting cellular metabolism.

Cav-1 not only affects membrane targeting of corresponding proteins but also mediates the endocytosis of some viruses, enzymes, macromolecular substances, and receptors. For example, Cav-1 participates in the endocytosis of BK virus (Moriyama et al., 2007), simian virus 40 (Damm et al., 2005), hepatitis B virus (Macovei et al., 2010), and human immunodeficiency virus (Huang et al., 2007; Mergia, 2017). However, unlike the abovementioned viruses, the SARS coronavirus entry into host cells through a novel clathrin-independent and caveolae-independent endocytic pathway (Filippini and D'Alessio, 2020; Wang et al., 2008). In addition, Cav-1 might mediate the endocytosis of receptor activin-like kinase 1 (ALK-1), which involves the bone formation protein-9 (BMP-9)/Cav-1/ALK-1 signaling pathway (Tao et al., 2020). The low expression of BMP-9 in lung ECs of mice with a knockout the *CAV1* blocks the endocytosis of ALK-1, thereby reducing the endocytosis of ALK-1–mediated low-density lipoprotein (LDL) (Tao et al., 2020). Furthermore, previous studies have found that Cav-1 can mediate the endocytosis of macromolecular protein substances, such as insulin-like growth factor (IGF)–binding protein 5 (Yamaguchi et al., 2011), albumin (Chatterjee et al., 2017), glucose transporter 4 (Glut-4) (Yuan et al., 2007), LDL, gap junction protein connexin 36 (Cx36) (Kotova et al., 2020), receptors including GM-CSF receptor β (Zsiros et al., 2019), TGF-β1 receptor (Siegert et al., 2018), and glucagon receptors (Krilov et al., 2011). Interestingly, Han et al. (Han et al., 2019) found that, in hepatocytes, Cav-1 can regulate the expression of metabolic genes induced by TGF-β. In addition, the above proteins were coexpressed with Cav-1 and could be transendocytosed, which is essential for inflammation, fibrosis, and insulin-related signal transduction, eventually affecting the cellular metabolism (Campos et al., 2019), growth, and senescence (Volonte and Galbiati, 2020). Moreover, Cav-1 also regulates T cell antigen receptor (TCR) and B cell antigen receptor (BCR) signal transduction and regulates the innate inflammatory immune response (Fiala and Minguet, 2018).

Cav-1 is also involved in the regulation of various signal transduction pathways by recruiting multiple receptors, such as receptor tyrosine kinase, G protein–coupled receptors, G proteins, protein kinases, and phosphatases (Boscher and Nabi, 2012), binds to the sequence of the CSD of Cav-1, and then positively or negatively regulates downstream signal transduction. For example, Eph receptor tyrosine kinases (EphB1 and EphA2 receptor) are positively regulated by Cav-1 and activate downstream signaling molecules, such as extracellular regulatory protein kinase (ERK) and protein kinase B (PKB or AKT) signal transduction (Vihanto et al., 2006). In addition, the insulin receptor (IR) (Chen et al., 2008) can be activated by phosphorylated Cav-1 and binds to LDL receptor–related protein 6, thereby mediating the Akt-mTORC1 signaling pathway and regulating aerobic glycolysis in cancer cells (Tahir et al., 2013).

Cav-1 negatively regulates the membrane receptors of the tyrosine kinase family [such as EGFR (Janković et al., 2017; Yang et al., 2018) and TGF-β (Lee et al., 2007; Oliveira et al., 2017)] and then modulates cell proliferation and metastasis. Similarly, G protein–coupled receptors [such as G protein–coupled receptor kinase 2 (GRK2) (Liu et al., 2017), angiotensin receptor (Ang-II) (Ishizaka et al., 1998), and P2Y2 receptor (Martínez et al., 2019)] are also regulated by Cav-1. Liu et al. (Liu et al., 2017) established a rat model of liver injury and found that the expression of phosphorylated Cav-1 increased and that Cav-1 interacted with GRK2, thereby inhibiting eNOS activity. In addition, Cav-1 promotes Ang-II–mediated Akt and EGFR signaling to cause glomerular mesangial cell hypertrophy (Umesalma et al., 2016), whereas Ang-II–mediated calcium influx is reduced (Adebiyi et al., 2014). In addition, Cav-1 can also regulates the P2Y2 receptor to increase the activity of pERK1/2 and Akt, promoting the survival of astrocytoma cells and interfering with the process of brain injury (Martínez et al., 2019). Recently, the TCR and BCR signaling pathways were found to be regulated by the abovementioned Cav-1 (Tomassian et al., 2011; Fiala and Minguet, 2018), which not only positively regulates Toll-like receptor-9 (TLR-9) to promote MyD88-mediated TRAF3 and IRF3 signal transduction (Yang et al., 2019) but also negatively regulates TLR-9 and TLR-4 to intensify the downstream inflammation cascade and promote the progression of diabetes (Zhu et al., 2017). These data indicate that Cav-1 has a huge signal transduction network, which plays an important role in cellular biological activities, including cell metabolism and growth.

4.3 Caveolin-1 and Lipid Metabolism

4.3.1 Caveolin-1 and Biogenesis of Lipid Droplets

LDs are organelles with special structures that are ubiquitous in most eukaryotic cells and are involved in regulating energy metabolism and maintaining cellular homeostasis (Walther and Farese, 2012; Olzmann and Carvalho, 2019; Henne et al., 2020). The hydrophobic core of LDs is composed of triacylglycerols (TGs) and sterol esters (SEs) as neutral lipids and is surrounded by an ER-derived phospholipid monolayer,

which is decorated with integral and peripheral proteins (Bersuker and Olzmann, 2017; Gao et al., 2019). The synthesis of neutral lipids is the first step in the formation of LDs. In mammalian cells, it is mainly catalyzed by ER diacylglycerol acyltransferase (DGAT) enzyme (DGAT1/2) and cholesterol acyltransferase (ACAT) enzyme (ACAT1/2) synthesis; among them, DGAT catalyzes the synthesis of TGs, whereas ACAT catalyzes the synthesis of SEs (Walther and Farese, 2012; Walther et al., 2017). The newly synthesized neutral lipid forms a lens-like structure between the leaflets of the ER bilayer and then can gradually fuse into larger and more stable lenses and buds from the ER to form nascent LDs (Renne et al., 2020). During this process, a continuous supply of phospholipids from the ER is needed to assist in the further expansion of LDs (Renne et al., 2020). In addition, some specific proteins are transported to the surface of LDs to promote their growth and expansion, such as glycerol-3-phosphate acyltransferase 4, DGAT2, adipose triglyceride lipase (ATGL), and other proteins, reaching the surface of LDs through ER-LD membrane bridges (Wilfling et al., 2014; Walther et al., 2017). Cytoplasmic proteins such as Perilipin family proteins and CCT1 are targeted to LDs through their hydrophobic domains (Walther et al., 2017). The perilipin family proteins PLINs1-5 are the main LD-related proteins and mainly refer to PLIN1 (perilipin A), PLIN2 (adipophilin), PLIN3 (TIP47), PLIN4 (S3-12), and PLIN5 (MLDP) (Itabe et al., 2017), which may regulate intracellular lipolysis. PLIN1 is highly expressed in mature adipocytes and forms a complex with α/β-hydrolase D5 (ABHD5) (CGI-58) on the surface of LDs under basic conditions (Sztalryd and Brasaemle, 2017). When PLIN1 is phosphorylated by cAMP, phosphorylated CGI-58 dissociates from it and binds to phosphorylated ATGL to activate triglyceride hydrolysis (Sztalryd and Brasaemle, 2017). In addition, cytoplasmic hormone-sensitive lipase (HSL) is phosphorylated by PKA and can be transported to the surface of LDs to participate in lipolysis (Frühbeck et al., 2014; Itabe et al., 2017). Furthermore, herein, we describe an important integral membrane protein, Cav-1, related to LD biogenesis and metabolism.

Cav-1 is one of the resident proteins of LDs and is involved in LD biogenesis (Pezeshkian et al., 2018). Roy et al. proposed that caveolin plays a cholesterol-trafficking role, and dominant-negative caveolin (CavDGV) can inhibit the signal transduced by H-Ras and change the distribution of cholesterol (Roy et al., 1999). Pol et al. showed that mutant caveolin protein (Cav-3DGV) accumulates in the ER and is targeted to the limiting membrane of LDs (Pol et al., 2001). However, Blouin et al. found that the expression level of Cav-1 affects the size of LDs, and in adipocytes lacking *CAV1*, the species of phospholipids on the LD surface are reduced, and only small LDs can be formed (Blouin et al., 2010). The accumulation of Cav-1 in the ER is targeted to LDs, which is related to its hydrophobic domain, especially its COOH-terminal domain sequence (Ostermeyer et al., 2004). Robenek et al. proposed a LD biogenesis model and hypothesized that the process of LD formation involves the synthesize lipid on the ER membrane, accumulation in the center of the bilayer to form a disc, and separation of Cav-1 from the ER membrane into LDs (Robenek et al., 2004). Furthermore, they stated that Cav-1 is not limited to the outer membrane monolayer around the LD but also present in the core of LDs (Robenek et al., 2004). Conversely, Cav-1 tends to be distributed in the lipid bilayer at the edge of the triolein lens and does not affect the curvature of the lipid lens but affects the distribution of surface neutral lipids and phospholipids on the LD surface (Pezeshkian et al., 2018). Moreover, *CAV1* null adipocytes/fat pads increase protein kinase A (PKA) activity, which leads to phosphorylation of HSL and perilipin followed by the activation of lipolysis (Cohen et al., 2004). In addition, *CAV1* gene knockout in the ECs increase the autocrine activity of prostaglandin I2 (PGI2), which acts as a stimulus to activate the cAMP/PKA pathway to promote the phosphorylation of HSL to increase lipolysis and reduce the formation of LDs, but it does not reduced triglyceride synthesis or fatty acid uptake (Kuo et al., 2018), suggesting that Cav-1 may play an important role in LD accumulation (**Figure 2**). Interestingly, previous studies have shown that exogenous addition of fatty acids may act as a signal to promote caveolin targeting LDs in nonadipocyte types (Liu et al., 2004; Pol et al., 2004). Similarly, Le Lay et al. found that, in adipocytes, an increase in exogenous cholesterol promotes the activation of Src, which triggers dynamin-dependent caveolae budding and trafficking of Cav-1 from the plasma membrane to LDs (Le Lay et al., 2006). Recently, the role of LD organelles (such as the ER, mitochondria, peroxisomes, lysosomes, and nucleus) in regulating lipid metabolism has attracted more attention (Barbosa et al., 2015; Barbosa and Siniossoglou, 2017; Suzuki, 2017; Geltinger et al., 2020). Yokomori et al. proposed that the transport of Cav-1 from the ER to LDs may be related to liver cirrhosis, and the connection between the ER and LDs may be a potential mechanism (Yokomori et al., 2019). Because Cav-1 is an important component of the membrane of each suborganelle, the role of Cav-1 in the communication of organelles and lipid metabolism may need to be addressed in the future.

4.3.2 Caveolin-1 Regulates Cholesterol Homeostasis

Cav-1 has a high affinity for cholesterol and participates in the regulation of cellular cholesterol homeostasis, including cholesterol transport, cholesterol signal transduction, and cholesterol metabolism (Fielding and Fielding, 1995; Smart et al., 1996; Ikonen and Parton, 2000). Cholesterol metabolism includes endogenous synthesis, exogenous uptake, esterification, and efflux (Chang et al., 2006). The endogenous synthesis of cholesterol is regulated by SREBPs, which have three subtypes, namely, SREBP1a, SREBP1c, and SREBP2 (DeBose-Boyd and Ye, 2018). Among them, SREBP2 is mainly involved in cholesterol metabolism, SREBP1c participates in fatty acid synthesis, and SREBP1a regulates both cholesterol and fatty acid synthesis (Luo J. et al., 2020). SREBP2 is considered to be a key mediator of cholesterol biosynthesis, is synthesized in the ER, and then interacts with insulin-induced gene-1 protein (INSG-1) and SREBP cleavage activation protein (SCAP). When cholesterol in the ER is exhausted, INSG-1 can be degraded by lysosomes, and the SREBP2 and SCAP complexes are sorted into COPII-coated vesicles and escorted to the Golgi apparatus, where

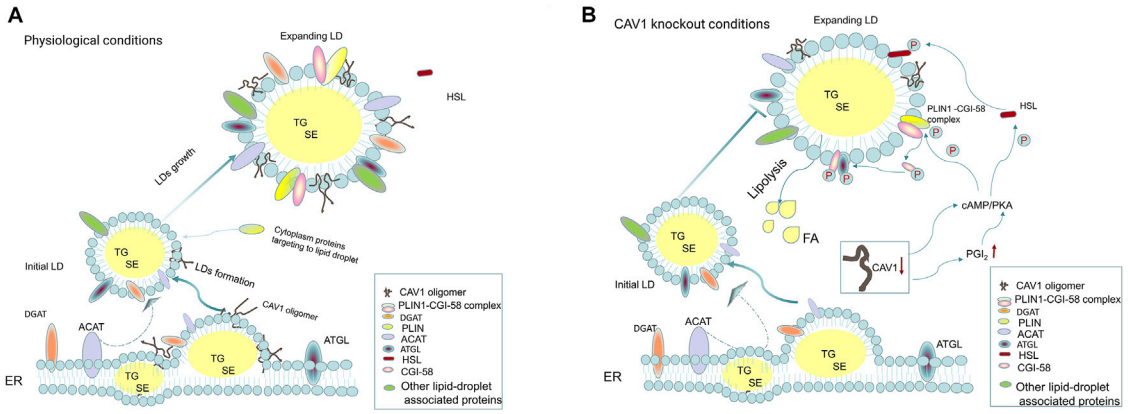

FIGURE 2 | Cav-1 and lipid droplet biogenesis. **(A)** Under physiological conditions, the initial step of lipid droplets (LDs) formation is the synthesis of neutral lipids (TGs and SEs) by DGAT and ACAT on the ER, which serve as the core of LDs. As the LDs gradually expand, LD-associated proteins and ER-derived monolayer phospholipids are distributed around neutral lipids, promoting the initial lipid droplets to become enlarged lipid droplets. Cytoplasmic proteins, such as PLIN family proteins, are involved in regulating lipid droplet metabolism and can target the lipid droplet surface, among which PLIN1 binds to CGI-58 protein to form the PLIN1-CGI-58 complex. The newly synthesized caveolin-1 is inserted into the bilayer of the ER and fused and transferred to the LDs. Caveolin-1 is involved in LD biosynthesis; on the one hand, it may affect the distribution of phospholipids on the surface of LDs, and on the other hand, it is essential for the expansion of LDs. **(B)** When *CAV1* is knocked out in cells (such as adipocytes and endothelial cells), the following processes may be affected: 1. growth and expansion of new lipid droplets are hindered; 2. the reduction in caveolin-1 expression can increase the phosphorylation of HSL and PLIN1 in a cAMP-dependent manner to enhance lipolysis. The latter is regulated by the PGI2/cAMP/PKA pathway, leading to phosphorylation of PLIN1 and CGI-58. Phosphorylated CGI-58 dissociates from PLIN1 and activates ATGL to co-activate lipolysis.

SREBP2 is processed by site 1 protease (S1P) and site 2 protease (S2P) cleavage, exposing the active N-terminal domain, and enters the nucleus to combine with the promoter regulatory element (SRE), thereby activating the transcription of cholesterol synthesis genes (Afonso et al., 2018; Brown et al., 2018; Yan et al., 2021). Interestingly, a previous study has shown that Cav-1 plays an important role in the transport of intracellular cholesterol, transporting newly synthesized cholesterol from the ER to caveolae and participating in the composition of the cell membrane (Smart et al., 1996). In skin fibroblasts, the expression of Cav-1 is also affected by cellular cholesterol levels, SREBP1 can inhibit the transcription of *CAV1*, and low levels of Cav-1 can further affect cholesterol homeostasis (Bist et al., 1997). As described in the review by Bosch et al., the loss of *CAV1* in cells (such as fibroblasts) leads to the accumulation of cholesterol on the ER, which may be transported to mitochondria *via* MAMs, and the accumulation of cholesterol on mitochondria leads to mitochondrial dysfunction and increased reactive oxygen species (ROS) production, eventually affecting cellular metabolism (Bosch et al., 2011). Pol et al. found that, in hamster kidney (BHK) cells transfected with mutant *CAV3* (Cav-3DGV), a dominant negative mutant, intracellular cholesterol transport to the cell membrane was blocked, resulting in the redistribution of cholesterol, which was characterized by reduced plasma membrane cholesterol, accumulation of free cholesterol in the lysosomes, and reduced cholesterol efflux and synthesis (Pol et al., 2001). Furthermore, Frank et al. demonstrated that the loss of *CAV1* in mouse embryonic fibroblasts (MEFs) and mouse peritoneal macrophages leads to an increased accumulation of cholesterol in the ER, and the accumulation of cholesterol can increase the activity of acyl-CoA-cholesterol acyltransferase (ACAT) and reduce the synthesis of free cholesterol (Frank et al., 2006). ACAT (including ACAT1/2) is an enzyme that is involved in the esterification of cholesterol, and its role is to esterify free cholesterol and prevent free cholesterol from accumulating freely in cells and then causing lipotoxicity (Luo J. et al., 2020). Recently, Xu et al. reported that overexpression of ACAT1/2 in 3T3-L1 adipocytes promoted the colocalization of Cav-1 and free cholesterol on the surface of LDs, impairing the function of adipocytes and cholesterol homeostasis (Xu et al., 2019). This information indicated that Cav-1 is closely related to cholesterol homeostasis and that Cav-1 may play a key intermediate mediator role in cellular cholesterol metabolism.

To maintain cholesterol homeostasis, cells not only esterify free cholesterol but also need to remove excess cholesterol through efflux. Current knowledge indicates that the scavenger receptor-B1 (SR-BI) and ATP-binding cassette (ABC) transporter family proteins ABCA1 and ABCG1 can escort cholesterol in macrophages to various extracellular receptors (such as apoA-I, HDL, and LDL) and then transport them to the peripheral blood, thereby reducing the burden of cholesterol in the cell (Sharma and Agnihotri, 2019; Plummer et al., 2021). Furthermore, it has been found that Cav-1 and SR-BI are simultaneously upregulated in differentiated THP-1 macrophages, and their coexpression promotes the efflux of cholesteryl esters to HDL (Matveev et al., 1999). However, another study found that SR-BI–mediated selective cholesteryl ester uptake in human embryonic kidney 293 or Fischer rat thyroid (FRT) cells was not affected by Cav-1 expression (Wang et al., 2003). In addition, deficiency *CAV1* gene in macrophages had a slight effect on ABCA1-mediated cellular cholesterol efflux to apoA-I but did not affect SR-BI and ABCG1-mediated cholesterol efflux to the HDL receptor (Frank et al., 2006), which indicates

that the Cav-1 can regulate intracellular cholesterol efflux in different cell lines.

4.4 Caveolin-1 and Glucose Metabolism

It is currently known that Cav-1 is involved in regulating glucose metabolism (Nwosu et al., 2016; Gopu et al., 2020). The loss of *CAV1* causes impairs glucose homeostasis and dyslipidemia, which is reversed by downstream aldosterone (MR) inhibition (Baudrand et al., 2016). Significantly increased *CAV1* mRNA in the peripheral blood of patients with metabolic syndrome has been observed (de Souza et al., 2020). In contrast, Luo et al. found that mRNA expression of *CAV1* is decreased in patients with type 2 diabetes, which may occur through direct binding of miR-103 to *CAV1* (Luo M. et al., 2020). Furthermore, Fachim et al. demonstrated that changes in lifestyle (such as exercise or diet) can cause DNA methylation in the *CAV1* transcript region and affect its expression in adipose tissue and peripheral blood cells in patients with type 2 diabetes (Fachim et al., 2020). They observed that decreased expression of Cav-1 in adipose tissue but increased expression in peripheral blood (Fachim et al., 2020). However, whether the changes of Cav-1 in other organs of patients with type 2 diabetes will affect other signaling proteins to regulate the progression of diabetes is worthy of further investigation. Furthermore, current evidence from various studies has shown that Cav-1 affects glucose metabolism by regulating a variety of glucose uptake transporters (Yuan et al., 2007; Elvira et al., 2013; Varela-Guruceaga et al., 2018). Lee et al. found that the expression of Cav-1 affects SGLT1 receptor–mediated glucose uptake on renal tubular epithelial cells by affecting the cAMP/Epac/PKA signaling pathway (Lee et al., 2012). In addition, the enhanced expression of ERK, p38MAPK, and NF-κB can increase the activity of SGLT1 and promote its binding to Cav-1 in renal tubular epithelial cells to increase glucose uptake (Lee et al., 2012). In addition, Cav-1 can upregulate the expression of SGLT1 (Elvira et al., 2013), indicating that Cav-1 may play a key role in glucose uptake by renal tubules, but the role of blood glucose in diabetes may need to be studied in the future.

Moreover, Cav-1 can regulate GLUT4 to mediate glucose uptake, which is related to insulin-related signaling pathways (Yuan et al., 2007). Long-term high glucose stimulates adipocytes and reduces the sensitivity of Cav-1 to insulin and inhibits IR and PKB (AKT-2) phosphorylation, which affect the GLUT4 in the intracellular glucose storage vesicles to transport to the plasma membrane caveolae and bind to Cav-1 and subsequently mediate glucose uptake (Palacios-Ortega et al., 2016). In contrast, in a high-glucose environment, the caveolae-related coiled-coil protein (NECC2) is highly expressed on adipocytes, which is closely linked to insulin-related glucose uptake by triggering insulin induction of NECC2 transport to the cell surface and binding to Cav-1 (Trávez et al., 2018). At this point, the IR binds to the scaffold domain of Cav-1 and then activates the PI3K/Akt signaling pathway (Trávez et al., 2018). However, Cav-1 regulates glucose metabolism in tumor cells mainly by regulating glucose transporter 3 (GLUT3/SLC2A3) uptake of glucose, which leads to increased aerobic glycolysis and increases intracellular ATP production, thus maintaining the growth and survival of tumor cells (Ali et al., 2019). Further investigations have shown that the abnormally increased expression of Cav-1 in tumor cells is related to the methylation of CpG sites, and the upregulation of Cav-1 expression then increases the activity of HMGA1 and promotes the translocation of HMGA1 into the nucleus, where HMGA1 binds to the promoter of GLUT3 and promotes its transcription (Ha et al., 2012). In addition, Cav-1 also affects mitochondrial function, increasing ATP production and inhibiting phosphorylation of AMPK at the Thr172 residue and modulating autophagy by the AMPK-TP53/p53 pathway in cancer cells (Ha and Chi, 2012). Further research demonstrated that the hypoxia response elements (HREs) of hypoxia inducible factor-1α (HIF-1α) bind to the promoter of *CAV1* under hypoxic conditions and inhibit the transcript level of *CAV1*, reducing the translocation of GLUT4 to the plasma membrane and resulting in decreased glucose uptake (Varela-Guruceaga et al., 2018). In addition, glucose uptake mediated by GLUT4 membrane translocation is related to AMP-activated protein kinase (AMPK), which is a key sensor of glucose metabolism (Hu et al., 2017). Therefore, it is worth noting that Cav-1 plays an indispensable role in regulating cellular metabolism and may be a novel or important target in metabolic-related diseases.

4.5 Caveolin-1 and Autophagy

Autophagy plays an important role in cellular metabolism, and a recent study reported that autophagy are closely related to cellular metabolism and cell survival (Tan and Miyamoto, 2015). Participation in the regulation of autophagy is one of the functions of Cav-1. Cav-1 can bind to the autophagy-related protein 5 (ATG-5), ATG12, and ATG5-ATG12 complex in lung epithelial cells and inhibit the formation and function of autophagosomes (Chen et al., 2014). When the cells are under stress (such as starvation), knockout of *CAV1* gene in MEFs can promote the formation of late autophagy lysosomes, enhance autophagic flux and promote cell survival, and it is involved in tumor progression (Shi et al., 2015). Deficiency of *CAV1* gene in human aortic ECs causes connexin-43 and ATG5 from the plasma membrane to combine with several ATGs (such as ATG12, ATG16, and IP3R), which are involved in the initial steps of autophagosome formation to promote the formation of autophagosomes, thus inhibiting vascular inflammation and arterial wall macrophage infiltration (Zhang X. et al., 2020). However, in cisplatin-treated lung cancer cells, silencing *CAV1* with siRNA inhibits the activation of Rho-related coiled-coil kinase 1 (ROCK1), thereby affecting Parkin-related mitochondrial autophagy and protecting against mitochondrial apoptosis and functional damage (Liu et al., 2020). In addition, under oxidative stress, Cav-1 phosphorylates at tyrosine-14, binds to beclin-1, and promotes its translocation to mitochondria, promoting mitochondrial autophagy (Nah et al., 2017). Recent studies have shown that the HIF-1α–Cav-1 signaling axis mediates autophagy to regulate cellular metabolism and promote the survival and metastasis of breast cancer cells (Wang N. et al., 2020). In addition, the close relationship between Cav-1 and autophagy plays an important role in regulating lipid metabolism. Bai et al. found that, in human umbilical vein ECs treated with high glucose, autophagy

degradation of Cav-1 mediated by the AMPK/mTOR/PIK3C3 pathway is inhibited, thereby increasing the expression of Cav-1 and cavin, and then, LC3 is recruited and bound, subsequently inhibiting Cav-1-CAVIN1-LC3B-mediated autophagy degradation of Cav-1. This process eventually manifests as the increased expression of Cav-1 to promote the formation of caveolae and mediates the increase in LDL endocytosis (Bai et al., 2020). Interestingly, Xue et al. found that overexpression of *CAV1* in L02 cells treated with alcohol and oleic acid can inhibit the Akt/mTOR pathway, thereby activating autophagy and alleviating cellular lipid deposition (Xue et al., 2020). The above information indicates that Cav-1 has different roles in the regulation of autophagy and cellular metabolism in different cell lines.

4.6 Caveolin-1 and Oxidative Stress

Oxidative stress is the key factor in cellular metabolism (Liu et al., 2019). It has been demonstrated that Cav-1 regulates oxidative stress and participates in the process of cellular life. Under oxidative stress, the expression of Cav-1 is increased in nucleus pulposus cells and related to premature senescence, whereas silencing the expression of *CAV1* can reduce the protein expression of p53 and p21 to protect cells from senescence (Ding et al., 2017). In contrast, under oxidative stress, Cav-1 is abundantly expressed in chondrocytes and transferred from the plasma membrane to the nucleus to participate in the repair of DNA damage (Goutas et al., 2020). In addition, overexpression of *CAV1* in rhabdomyosarcoma cells, the cell cycle is blocked in the G2/M phase, which is accompanied by the reduced expression of p21, p16, and cleaved caspase-3, whereas the production of catalase is increased; therefore, Cav-1 enhances DNA repair and protects against cellular senescence and apoptosis from oxidative stress (Codenotti et al., 2021). However, interestingly, Goutas et al. did not observe a displacement of Cav-1 and the DNA damage repair in patients with osteoarthritis (Goutas et al., 2020). Thus, the role of Cav-1 in DNA repair in cells requires further confirmation.

There is a closed relationship between oxidative stress and inflammation. Studies have shown that the Cav-1 regulates oxidative stress and affects inflammation. Wang et al. found that high-fat diet-fed $ApoE^{-/-}$ mice with atherosclerosis show increased activity of JNK-related signals, oxidative stress, and inflammation, whereas these changes were rescued in mice with a double knockout of ApoE and *CAV1* (Wang et al., 2018). In contrast, in mice with liver injury induced by carbon tetrachloride (CCl_4), *CAV1* gene knockout can aggravate oxidative stress and activate the TGF-β signaling pathway and the production of proinflammatory factors, such as IL-1β and IL-6, leading to liver fibrosis (Ji et al., 2018). Furthermore, in E11 murine kidney podocytes, Cav-1 promotes the production of antioxidant enzymes and inhibits the oxidative stress response induced by H_2O_2, alleviating the inflammatory damage of podocytes (Chen et al., 2017). Conversely, Cav-1 also affects the energy conversion of cells (Fernández-Rojo et al., 2012). Recently, Shao et al. found that knockdown of *CAV1* with shRNA in pancreatic stellate cells promotes the production of ROS, and the production of ROS further reduces the expression of Cav-1 (Shao et al., 2020). This Cav-1-ROS positive feedback induces the conversion of cell energy metabolism to glycolysis, and the products of glycolysis promote cell energy production through mitochondrial oxidative phosphorylation, which further promotes the proliferation of pancreatic cancer cells (Shao et al., 2020). This information indicates that Cav-1 plays an important role in regulating oxidative stress and inflammation by affecting cellular metabolism.

4.7 Other Functions of Caveolin-1: Mechanical Sensing and Vesicle Transport

Cav-1, as the main component protein of caveolae, is involved not only in regulating metabolism but also in mechanical transduction and vesicle transport. Cav-1 phosphorylation is essential for caveolae to perform signal transduction, endocytosis (Nabi and Le, 2003) and lipid transport (Pilch and Liu, 2011); enzymes (Coelho-Santos et al., 2016), viruses (Xing et al., 2020), and LDL (Gerbod-Giannone et al., 2019) enter the cell through caveolae-dependent endocytosis, which is related to phosphorylation of Cav-1. Caveolae act as a cell membrane sensor (Parton and del Pozo, 2013) and mechanical sensor (Sinha et al., 2011), which can quickly adapt to sudden and acute mechanical stress stimulation (Sinha et al., 2011). When the cell responds to a variety of stimuli, such as osmotic/stretch, shear, ultraviolet, and oxidative stimuli, the tension of the cell membrane increases, which promotes caveolae disassembly (Parton et al., 2020a). The above stimuli cause caveolae flattening and may eventually induce cavin dissociation, changes in lipid distribution on the cell membrane, and Cav-1 tyrosine phosphorylation (Parton et al., 2020a). Phosphorylated Cav-1 can regulate actin to detach caveolae from the plasma membrane and enter the cytoplasm (Zimnicka et al., 2016) and then traffic to LDs, which may be involved in cell lipid metabolism (Matthaeus and Taraska, 2020). It is particularly noteworthy that the relationship between Cav-1 and lipid metabolism has aroused widespread research interest. Recent studies have found that Cav-1 regulates lipid metabolism and participates in kidney-related diseases (Chen et al., 2016; Mitrofanova et al., 2019). Therefore, we focused on the relationship between Cav-1 regulation of cellular metabolism and the kidney.

5 CAVEOLIN-1 AND KIDNEY DISEASE

5.1 Acute Kidney Disease

Cav-1 is involved in the pathophysiology of acute kidney injury (AKI). Zager et al. found that the expression of Cav-1 was increased in ischemia ± reperfusion–induced AKI mice and verified that the destruction of the caveolae in the damage of renal tubular epithelial cells, which causes cholesterol and Cav-1 are separated from the plasma membrane, leading to free cholesterol deposits in the lumen of the renal tubules and an increased level of urine Cav-1 (Zager et al., 2002). Accordingly, Cav-1 was considered a possible biomarker of AKI (Zager et al., 2002). In addition, proximal renal tubular injury leads to

increased destruction of caveolae, and Cav-1 translocates into the cytoplasm; activates the expression of PDGFR-β, EGFR, and Rho guanosine triphosphatase (GTPase) signaling proteins; and participates in the process of renal tubular cell regeneration (Mahmoudi et al., 2003; Fujigaki et al., 2007). Likely, in ischemic reperfusion AKI mice treated with EPO, a significant increase in the expression of Cav-1 in blood and kidney tissue is observed (Kongkham et al., 2016). In addition, Cav-1 has also been found to be highly expressed in apoptotic tubular cells, although it remains controversial whether Cav-1 plays a role in promoting repair or apoptosis in AKI (Mahmoudi et al., 2003). Notably, Moore et al. reported that Cav-1 is a tissue fibrosis inhibitor, and its genetic polymorphisms are associated with renal transplantation fibrosis and allogeneic transplantation failure (Moore et al., 2010). Furthermore, another recent study has demonstrated increased expression of Cav-1 in the serum of patients with kidney transplant, which associated with a decreased incidence of tubulointerstitial rejection (Emmerich et al., 2021). From the above information, it can be seen that Cav-1 has different roles in AKI, and its detailed mechanism still lacks experimental verification.

5.2 Glomerulus Nephritis

Although glomerulonephritis is an immune-mediated disease, recent studies have shown that consistent changes in the kidney transcriptome are consistent with the metabolic reprogramming of different forms of glomerulonephritis (Grayson et al., 2018), which may indicate that abnormal cellular metabolism also plays an important role in this disease. Tamai et al. showed, for the first time, that caveolae are present in mesangial cells and the Cav-1 is located on caveolae, as detection by electron microscope (Tamai et al., 2001). Furthermore, they demonstrated that Cav-1 can bind to PDGF receptors to mediate the PDGF pathway and modulate mesangial proliferative glomerulonephritis (Tamai et al., 2001). In addition, Ostalska-Nowicka et al. verified that the expression of Cav-1 in parietal epithelial cells is significantly lower in children diagnosed with focal segmental glomerulosclerosis and lupus glomerulonephritis than in those with minimal change disease, Schönlein-Henoch glomerulopathy, or in controls (Ostalska-Nowicka et al., 2007). Furthermore, the high expression level of Cav-1 in glomerular ECs is positively correlated with proteinuria, and it is suggested that Cav-1 mediates EC endocytosis of albumin and participates in the progression of glomerular-related diseases (Moriyama et al., 2011; Moriyama et al., 2017). Although current studies suggest that Cav-1 may regulate the progression of glomerular associated diseases by endocytosing of macromolecules (cholesterol or albumin), the mechanism by which Cav-1 modulates the development of glomerular diseases requires further study.

5.3 Diabetic Kidney Disease

Previous studies have shown that Cav-1 has antifibrotic properties by regulating cell proliferation, migration and adhesion, as well as inhibiting the TGF-β signaling pathway in diabetic kidney disease (DKD) (Gvaramia et al., 2013; Shihata et al., 2017; Van Krieken and Krepinsky, 2017). In addition, Cav-1 might also regulate glucose uptake and mediate the endocytosis of urinary albumin; therefore, it is considered a potential therapeutic target for DKD (Van Krieken and Krepinsky, 2017). Arya et al. found that, in rats with diabetic nephropathy, the highly expressed Cav-1 can bind to nitric oxide synthase (eNOS) and inhibit its signal transduction, thereby reducing the production of NO and eventually leading to increased level of serum urea nitrogen, blood creatinine and urine protein, whereas the above changes can be reversed by Cav-1 inhibitors (Arya et al., 2011). Conversely, in renal mesangial cells treated with high glucose, Cav-1 phosphorylated by Src kinase can activate RhoA, which may be related to the development of glomerular matrix accumulation in DKD (Wu et al., 2014). Xie et al. showed that, in mesangial cells treated with high glucose, RhoA/Rock promotes the translocation of NF-kB into the nucleus to increase the transcription level of inflammatory factors such as ICAM-1, TGF-β1, and FN and ultimately leads to the production of mesangial cell matrix (Xie et al., 2013). Furthermore, high glucose has been shown to induce an increase in the production of mitochondrial ROS (mtROS) and vascular endothelial growth factor (VEGF), and mtROS in glomerular ECs, which activates Src kinase to phosphorylate Cav-1, leading to increased albumin endocytosis and massive proteinuria (Xie et al., 2013). Furthermore, under high-glucose conditions, phosphorylation of Cav-1 upregulates the expression of TLR-4 and promotes the secretion of pro-inflammatory factors, such as TNF-α, IL-6, IL-1β, and MCP-1 in podocytes and accelerates the process of DKD (Sun et al., 2014b). More importantly, diabetic mice with deficiency of *CAV1* gene in mesangial cells showed a significant inhibitory effect on the PKCβ1/ROS/RhoA/Rho-kinase signaling pathway; the expression of TGFβ1, FN, and collagen I is reduced, whereas the expression of AMPK is upregulated (Zhang et al., 2012; Guan et al., 2013). However, how Cav-1 regulates AMPK expression affects the development of DKD is unknown. Another study found that *CAV1* knockout in mesangial cells of diabetic mice upregulates the protein expression of follistatin, which neutralizes and inhibits activin, ultimately decreasing proteinuria, glomerular sclerosis, and extracellular matrix accumulation (Zhang et al., 2019). SMPDL3b is an enzyme related to lipid metabolism, which can downregulate the expression of ceramide-1-phosphate and affect the phosphorylation of AKT, leading to podocyte damage (Mitrofanova et al., 2019). In mice carrying a specific knockout of the SMPDL3b in podocytes, the Cav-1 combines with IRB to transduce insulin signals and phosphorylate Akt, which reduces podocyte damage and delays the progression of DKD (Mitrofanova et al., 2019). These data suggest that Cav-1, a cell metabolism related molecule, plays a critical role in kidney injury in DKD.

5.4 Clear Cell Renal Cell Carcinoma

Metabolic reprogramming in clear cell renal cell carcinoma (RCC) has been recognized (Wettersten et al., 2017). It has been reported that Cav-1 inhibits breast cancer stem cells through metabolic reprogramming (Wang S. et al., 2020). Recent evidence has shown that Cav-1 is considered one of the possible prognostic biomarkers of clear cell RCC (Waalkes et al., 2011). Cav-1, which is increased significantly in RCC kidney tissue, can regulate the growth and metastasis of cancer cells (Joo et al., 2004; Steffens et al., 2011). In addition, the

TABLE 1 | Potential therapeutic target of Cav-1 in kidney disease.

Category	Compound/ Effector	Mechanism	Major findings in kidney disease	References
Chemical compounds	Methyl-beta-cyclodextrin	Destroy caveolae	1. Mesangial cells: the production of collagen I and fibronectin is reduced, which reduces mesangial expansion and mesangial cell hypertrophy. 2. Endothelial cells: protect the filtration function of the kidneys and reduce proteinuria.	Moriyama et al. (2017), Peng et al. (2007), Zhang et al. (2007)
	Filipin	Destroy caveolae	Mesangial cells: mainly reduce the internal pressure of the glomerulus and relieve glomerular sclerosis.	Peng et al. (2007), Zhang et al. (2007)
	Daidzein	Inhibit the expression of Cav-1	1. Inhibit the Cav-1-eNOS pathway, increase kidney NO production, and reduce blood urea nitrogen, serum creatinine, urine protein, and collagen content in diabetic rats 2. Renal tubular cells: anti-inflammatory, antioxidant, reduction of urine protein, creatinine, and urea nitrogen.	Arya et al. (2011), Meng et al. (2017), Tomar et al. (2020)
Extract from Traditional Chinese Medicines	Curcumin	Inhibition of Cav-1 Y14 phosphorylation	Podocytes: reduce the damage caused by pro-inflammatory factors to podocytes and alleviate oxidative stress and apoptosis of podocytes.	Sun et al. (2014a)
	Salidroside	Inhibit Cav-1 Y14 phosphorylation	Endothelial cells: protect the filtration function of the kidneys and reduce proteinuria.	Wu et al. (2016)
	Catalpol	Inhibit Cav-1 Y14 phosphorylation	Reduce kidney damage and inhibiting mesangial cell proliferation by improving lipid metabolism, IGF-1 signaling.	Bai et al. (2019), Zhou et al. (2014)
Rock inhibitor	Fasudil	Inhibit Cav-1/RhoA and VEGF/Cav-1 pathways	1. Mesangial cells: reduce the production of ICAM-1, TGF-β1, and FN and alleviate renal fibrosis. 2.Podocytes: reduce the inflammatory damage of IL-6 and MCP-1 to podocytes.	Huang et al. (2021), Jin et al. (2015), Xie et al. (2013)
Noncoding RNA	miR-204	Inhibit Cav-1/TRPM3-mediated autophagy	miR-204 indirectly inhibits TRPM3-mediated downstream LC3B-related autophagy through Cav-1, thereby inhibiting the progression of clear cell renal cell carcinoma.	Hall et al. (2014)
	CircAKT1	Sponge miR-338-3p and upregulate Cav-1 expression	Promote the proliferation, migration, invasion, and epithelial-mesenchymal transition (EMT) of clear cell renal cell carcinoma cells.	Zhu et al. (2020)

expression of Cav-1 and phosphorylated ERK-1/2 in local RCC tissues is also considered to be a predictor of metastasis of RCC (Campbell et al., 2013). The Cav-1/AKT/mTOR axis has been shown to promote the proliferation of cancer cells and vascular metastasis (Campbell et al., 2008). Recently, Zhang et al. found that Cav-1 binds to oxidized low-density apolipoprotein receptor 1 (LOX-1) to induce lipid deposition and promote tumor cell proliferation, but this effect can be reversed by celastrol (Zhang et al., 2021). Although Cav-1 participates in the metabolism of cancer cells and regulates the survival of cancer cells, the relationship between Cav-1 and RCC merits in-depth study.

6 THERAPEUTIC PROMISING

Because Cav-1 plays an important role in cellular metabolism and activities related to cellular life, especially the development of various kidney diseases, recent studies targeting Cav-1 for the treatment of various diseases, especially kidney diseases, have become a research hotspot (**Table 1**). Here, we focus on some chemical compounds, drugs, and various extracts from traditional Chinese medicine, which target Cav-1 or its associated signaling pathway and summarize their application in kidney diseases.

6.1 Caveolin-1 Inhibitor

6.1.1 Chemical Compound

Methyl-β-cyclodextrin (MβCD), filipin, and daidzein are the more common inhibitors of Cav-1 (Woodman et al., 2004; Peng et al., 2007; Gao et al., 2014). Recent studies have shown that the effects of these drugs on the functions of Cav-1 may be secondary to the disruption of caveolae. MβCD and filipin can destroy the structure of caveolae and reduce Cav-1 phosphorylation and downstream signaling pathways, such as the Cav-1/RhoA and Scr/Cav-1/EGFR/Akt signaling pathways, resulting in the prevention of fibronectin and collagen I production and alleviation of glomerulosclerosis (Peng et al., 2007; Zhang et al., 2007). In addition, MβCD can affect the signal transduction of ANG-II receptors and reduce glomerular mesangial hyperplasia (Adebiyi et al., 2014). Previous studies have shown that Cav-1 located on caveolae of glomerular ECs (HRGECs) mediates albumin entry into glomerular ECs and transcytosis, leading to proteinuria in glomerular diseases, whereas MβCD can reverse the abovementioned changes (Moriyama et al., 2015; Moriyama et al., 2017). In addition, Daidzein, another inhibitor of Cav-1 (Sharma et al., 2012; Gao et al., 2014), has been found to have anti-inflammatory, antioxidative stress, and renoprotective effects in the mice with AKI induced by cisplatin (Meng et al., 2017; Tomar et al., 2020).

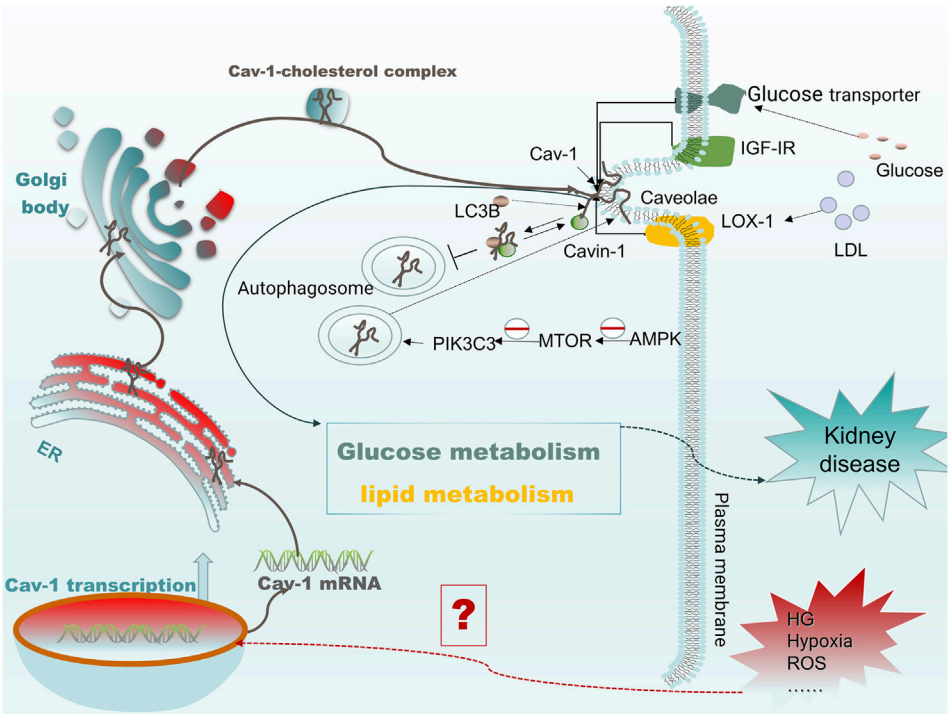

FIGURE 3 | Cav-1 mediates protein membrane targeting and regulates cellular metabolism. When cells are subjected to harmful external stimuli (such as high glucose and oxidative stress), the transcription levels of *CAV1* increase, which promotes the formation of caveolae on the cell membrane. The expressed Cav-1 can then recruit receptors such as IGF-IR, glucose transporter, and LOX-1 to caveolae and bind there to Cav-1 and subsequently regulate glucose or lipid metabolism by mediating specific receptor signals. In addition, under high glucose conditions, blocking autophagy induced by the AMPK-MTOR-PIK3C3 pathway reduces the degradation of Cav-1 by autophagy, resulting in increased expression of cavin and Cav-1. The high expression of Cav-1 recruits LC3B and binds together to inhibit the formation of autophagosomes, further inhibiting autophagic degradation of Cav-1 and leading to an increase in the formation of caveolae, which eventually mediates increased endocytosis of low-density apolipoprotein.

Furthermore, Daidzein can also reverse the pathological changes in diabetic rats and reduces urine protein, blood creatinine, and urea nitrogen by inhibiting the Cav-1/eNOS/NO pathway (Arya et al., 2011). In addition, Daidzein has a potential effect on diabetes, and its complications are mediate by regulating cellular metabolism, including glucose and lipid metabolism, as well as oxidative stress (Das et al., 2018). Daidzein improves hyperglycemia, insulin resistance, dyslipidemia, obesity, and inflammation (Das et al., 2018). These data suggest that Cav-1 inhibitors can affect the progression of kidney disease by regulating cellular metabolism, but the precise mechanism is still unclear.

6.1.2 Traditional Chinese Medicine Extracts

Curcumin, as an extract from traditional herbal medicine, has multiple functions, such as antioxidation, anti-inflammatory, and antifibrosis activities (Santos-Parker et al., 2017; Tsuda, 2018; Kong et al., 2020). It can regulate the fibrosis process of kidney disease through Cav-1–related signaling pathways (Sun et al., 2017). Under high-glucose conditions, the Cav-1/TLR-4 signaling pathway mediates pro-inflammatory factors, such as TNF-α, IL-6, IL-1β, and MCP-1, to induce the reversal of podocyte damage in response to curcumin (Sun et al., 2014b). In addition, Curcumin can also inhibit the phosphorylation of Cav-1 under high-glucose conditions and alleviate the oxidative stress and apoptosis of podocytes, as well as the epithelial-mesenchymal transition (EMT) and proteinuria of podocytes, eventually delaying the progression of diabetic mice (Sun et al., 2014a; Sun et al., 2016).

Salidroside (SAL) is an active ingredient isolated from the traditional Chinese medicine rhodiola that has a protective effect on kidney diseases. Wu et al. found that SAL upregulates AMPK and downregulates Src kinase under high-glucose conditions, thereby inhibiting Cav-1 phosphorylation, inhibiting glomerular ECs (GECs) albumin endocytosis, and reducing albuminuria in diabetic mice (Wu et al., 2016). Xue et al. found that SAL can activate the Sirt1/PGC-1α axis to promote mitochondrial biogenesis and alleviate pathological changes in diabetic mice, as shown by decrease in urine albumin, blood urea nitrogen and serum creatinine (Xue et al., 2019). Furthermore, SAL inhibits the TLR4/NF-κB and MAPK pathways to prevent inflammation and fibrosis, protecting kidney function (Li et al., 2019). Previous studies have shown that Cav-1 regulates the TLR4 signaling pathway and participates in the inflammatory response of podocytes (Sun et al., 2014b). Whether SAL regulates the Cav-1/TLR4 pathway to reduce renal inflammatory damage requires follow-up research.

Catalpol was previously found to have neuroprotective effects in diabetic mice by increasing the expression of Cav-1 and PKC

(Zhou et al., 2014). The review by Bai et al. summarized that the ability of catalpol to reduce kidney damage by improving lipid metabolism and IGF-1 signal transduction (Bai et al., 2019). On the basis of the function of Cav-1 in regulating lipid metabolism, catalpol may play a key role in kidney disease by regulating the expression of Cav-1.

6.1.3 Rock Inhibitor: Fasudil

It has been reported that Cav-1 plays a key role in regulating the RhoA/Rock pathway, which is involved in inflammation and apoptosis in kidney disease (Peng et al., 2007; Wu et al., 2014; Nozaki et al., 2015; Zhao et al., 2015). Fasudil, a Rock inhibitor, blocks the VEGF/Src/Cav-1/signaling pathway to alleviate renal inflammation, glomerulosclerosis, and proteinuria in diabetic mice (Xie et al., 2013; Jin et al., 2015). In addition, Rock inhibitor also plays an important role in cellular metabolism. In high-fat–fed mice, fasudil can activate AMPK, thereby promoting lipid metabolism (Noda et al., 2014; Noda et al., 2015). Furthermore, in diabetic mice, the RhoA/ROCK/NF-κB signaling pathway is inhibited when pancreatic islets are transplanted into mice, and the production of podocyte inflammatory factors such as IL-6 and MCP-1, is reduced, reversing podocyte damage (Huang et al., 2021). Recently, the role of Rho family GTPases in regulating cell glucose metabolism and maintaining glucose homeostasis has also received increasing attention (Møller et al., 2019; Machin et al., 2021). Therefore, whether Rock inhibitors indirectly affect Cav-1–related signaling pathways to regulate kidney energy metabolism still needs to be addressed.

6.1.4 Noncoding RNA

Many studies have shown that noncoding RNAs regulate the expression of Cav-1 and affect its downstream events. It has been found that miR-204 (Hall et al., 2014) and circAKT1 (Zhu et al., 2020) affect the progression of kidney disease by regulating Cav-1. Hall et al. found that, in VHL (−) RCC cells, miR-204 indirectly affects the transient receptor potential melastatin 3 (TRPM3)–induced autophagy by inhibiting the expression of Cav-1, which, in turn, affects the development of RCC (Hall et al., 2014). In addition, Zhu et al. found that circAKT1, which is highly expressed in clear cell RCC, promotes the proliferation and progression of renal cancer cells by upregulating the expression of Cav-1 by sponging miR-338-3p (Zhu et al., 2020). However, Mehta et al. recently found that *CAV1* deficiency in glomerular mesangial cells can inhibit miR299a-5p, which may posttranscriptionally regulate the expression of follostatin, thereby exerting an anti-renal fibrosis effect (Mehta et al., 2021). The above studies may indicate that noncoding RNAs are involved in the progression of Cav-1–mediated kidney disease.

7 CONCLUSION AND PERSPECTIVES

Cav-1 is a metabolism-related membrane protein in a variety of cell types, which is involved in the pathophysiology of a variety of diseases by a large signaling network system. Despite recent studies showing robust evidence for the critical role of Cav-1 in metabolic disorders, oxidative stress, and autophagy, most of the studies indicated that Cav-1 is a potential therapeutic target in cancer and cardiovascular diseases, whereas few studies have been conducted in kidney disease. Because cellular metabolic homeostasis is critical in kidney disease, here, we propose that Cav-1 is closely linked to kidney disease through the regulation of cellular metabolism. When cells are subjected to stress and other stimuli, the expression of Cav-1 is increased, and it is then translocated to the cell membrane. At the membrane, it recruits specific receptors and molecules such as IGF-IR, glucose transporters, and LOX-1 into the caveolae, mediating downstream signal transduction and affecting cellular metabolism including glucose and lipid metabolism. Conversely, in vascular ECs treated with high glucose, autophagy induced by the AMPK-MTOR-PIK3C3 pathway is blocked to reduce the degradation of Cav-1 by autophagy, whereas the increased expression of Cav-1 inhibits the formation of downstream autophagosomes by recruiting and binding to LC3B, thus further inhibiting the autophagic degradation of Cav-1 and leading to an increase in caveolae formation. This process mediates the increase in endocytosis of low-density apolipoprotein and affects cellular metabolism (Bai et al., 2020). As mentioned above, Cav-1 may have a potential role in kidney disease by regulating cellular metabolism (**Figure 3**). In addition, we also describe Cav-1 and its related signaling molecules as potential therapeutic targets based on the use of related inhibitors and extract from traditional medicines in various kidney diseases. This review may open up new horizons for future investigations of the role of Cav-1 in kidney and other disease.

AUTHOR CONTRIBUTIONS

All authors listed have made a substantial, direct, and intellectual contribution to the work and approved it for publication.

FUNDING

This work was supported by the National Natural Science Foundation of China (81730018) and the National Key R&D Program of China (2018YFC1314002).

REFERENCES

Abumrad, N. A., Cabodevilla, A. G., Samovski, D., Pietka, T., Basu, D., and Goldberg, I. J. (2021). Endothelial Cell Receptors in Tissue Lipid Uptake and Metabolism. *Circ. Res.* 128 (3), 433–450. doi:10.1161/circresaha.120.318003

Adebiyi, A., Soni, H., John, T. A., and Yang, F. (2014). Lipid Rafts Are Required for Signal Transduction by Angiotensin II Receptor Type 1 in Neonatal Glomerular Mesangial Cells. *Exp. Cel Res* 324 (1), 92–104. doi:10.1016/j.yexcr.2014.03.011

Afonso, M. S., Machado, R. M., Lavrador, M. S., Quintao, E. C. R., Moore, K. J., and Lottenberg, A. M. (2018). Molecular Pathways Underlying Cholesterol Homeostasis. *Nutrients* 10 (6), 760. doi:10.3390/nu10060760

Ali, A., Levantini, E., Fhu, C. W., Teo, J. T., Clohessy, J. G., Goggi, J. L., et al. (2019). CAV1 - GLUT3 Signaling Is Important for Cellular Energy and Can Be Targeted by Atorvastatin in Non-small Cell Lung Cancer. *Theranostics* 9 (21), 6157–6174. doi:10.7150/thno.35805

Arya, A., Yadav, H. N., and Sharma, P. L. (2011). Involvement of Vascular Endothelial Nitric Oxide Synthase in Development of Experimental Diabetic Nephropathy in Rats. *Mol. Cel Biochem* 354 (1-2), 57–66. doi:10.1007/s11010-011-0805-6

Bai, X., Yang, X., Jia, X., Rong, Y., Chen, L., Zeng, T., et al. (2020). CAV1-CAVIN1-LC3B-mediated Autophagy Regulates High Glucose-Stimulated LDL Transcytosis. *Autophagy* 16 (6), 1111–1129. doi:10.1080/15548627.2019.1659613

Bai, Y., Zhu, R., Tian, Y., Li, R., Chen, B., Zhang, H., et al. (2019). Catalpol in Diabetes and its Complications: A Review of Pharmacology, Pharmacokinetics, and Safety. *Molecules* 24 (18), 3302. doi:10.3390/molecules24183302

Barbosa, A. D., Savage, D. B., and Siniossoglou, S. (2015). Lipid Droplet-Organelle Interactions: Emerging Roles in Lipid Metabolism. *Curr. Opin. Cel Biol* 35, 91–97. doi:10.1016/j.ceb.2015.04.017

Barbosa, A. D., and Siniossoglou, S. (2017). Function of Lipid Droplet-Organelle Interactions in Lipid Homeostasis. *Biochim. Biophys. Acta Mol. Cel Res* 1864 (9), 1459–1468. doi:10.1016/j.bbamcr.2017.04.001

Baudrand, R., Gupta, N., Garza, A. E., Vaidya, A., Leopold, J. A., Hopkins, P. N., et al. (2016). Caveolin 1 Modulates Aldosterone-Mediated Pathways of Glucose and Lipid Homeostasis. *J. Am. Heart Assoc.* 5 (10), e003845. doi:10.1161/jaha.116.003845

Bernatchez, P. (2020). Endothelial Caveolin and its Scaffolding Domain in Cancer. *Cancer Metastasis Rev.* 39 (2), 471–483. doi:10.1007/s10555-020-09895-6

Bersuker, K., and Olzmann, J. A. (2017). Establishing the Lipid Droplet Proteome: Mechanisms of Lipid Droplet Protein Targeting and Degradation. *Biochim. Biophys. Acta Mol. Cel Biol Lipids* 1862 (10 Pt B), 1166–1177. doi:10.1016/j.bbalip.2017.06.006

Bist, A., Fielding, C. J., and Fielding, P. E. (2000). p53 Regulates Caveolin Gene Transcription, Cell Cholesterol, and Growth by a Novel Mechanism. *Biochemistry* 39 (8), 1966–1972. doi:10.1021/bi991721h

Bist, A., Fielding, P. E., and Fielding, C. J. (1997). Two Sterol Regulatory Element-like Sequences Mediate Up-Regulation of Caveolin Gene Transcription in Response to Low Density Lipoprotein Free Cholesterol. *Proc. Natl. Acad. Sci. U S A.* 94 (20), 10693–10698. doi:10.1073/pnas.94.20.10693

Blouin, C. M., Le Lay, S., Eberl, A., Köfeler, H. C., Guerrera, I. C., Klein, C., et al. (2010). Lipid Droplet Analysis in Caveolin-Deficient Adipocytes: Alterations in Surface Phospholipid Composition and Maturation Defects. *J. Lipid Res.* 51 (5), 945–956. doi:10.1194/jlr.M001016

Bonds, J. A., Shetti, A., Bheri, A., Chen, Z., Disouky, A., Tai, L., et al. (2019). Depletion of Caveolin-1 in Type 2 Diabetes Model Induces Alzheimer's Disease Pathology Precursors. *J. Neurosci.* 39 (43), 8576–8583. doi:10.1523/jneurosci.0730-19.2019

Boopathi, E., Gomes, C. M., Goldfarb, R., John, M., Srinivasan, V. G., Alanzi, J., et al. (2011). Transcriptional Repression of Caveolin-1 (CAV1) Gene Expression by GATA-6 in Bladder Smooth Muscle Hypertrophy in Mice and Human Beings. *Am. J. Pathol.* 178 (5), 2236–2251. doi:10.1016/j.ajpath.2011.01.038

Bosch, M., Marí, M., Gross, S. P., Fernández-Checa, J. C., and Pol, A. (2011). Mitochondrial Cholesterol: a Connection between Caveolin, Metabolism, and Disease. *Traffic* 12 (11), 1483–1489. doi:10.1111/j.1600-0854.2011.01259.x

Boscher, C., and Nabi, I. R. (2012). Caveolin-1: Role in Cell Signaling. *Adv. Exp. Med. Biol.* 729, 29–50. doi:10.1007/978-1-4614-1222-9_3

Breton, S., Lisanti, M. P., Tyszkowski, R., McLaughlin, M., and Brown, D. (1998). Basolateral Distribution of Caveolin-1 in the Kidney. Absence from H+-atpase-coated Endocytic Vesicles in Intercalated Cells. *J. Histochem. Cytochem.* 46 (2), 205–214. doi:10.1177/002215549804600209

Brown, M. S., Radhakrishnan, A., and Goldstein, J. L. (2018). Retrospective on Cholesterol Homeostasis: The Central Role of Scap. *Annu. Rev. Biochem.* 87, 783–807. doi:10.1146/annurev-biochem-062917-011852

Burana, D., Yoshihara, H., Tanno, H., Yamamoto, A., Saeki, Y., Tanaka, K., et al. (2016). The Ankrd13 Family of Ubiquitin-Interacting Motif-Bearing Proteins Regulates Valosin-Containing Protein/p97 Protein-Mediated Lysosomal Trafficking of Caveolin 1. *J. Biol. Chem.* 291 (12), 6218–6231. doi:10.1074/jbc.M115.710707

Busija, A. R., Patel, H. H., and Insel, P. A. (2017). Caveolins and Cavins in the Trafficking, Maturation, and Degradation of Caveolae: Implications for Cell Physiology. *Am. J. Physiol. Cel Physiol* 312 (4), C459–c477. doi:10.1152/ajpcell.00355.2016

Campbell, L., Al-Jayyoussi, G., Gutteridge, R., Gumbleton, N., Griffiths, R., Gumbleton, S., et al. (2013). Caveolin-1 in Renal Cell Carcinoma Promotes Tumour Cell Invasion, and in Co-operation with pERK Predicts Metastases in Patients with Clinically Confined Disease. *J. Transl Med.* 11, 255. doi:10.1186/1479-5876-11-255

Campbell, L., Jasani, B., Edwards, K., Gumbleton, M., and Griffiths, D. F. (2008). Combined Expression of Caveolin-1 and an Activated AKT/mTOR Pathway Predicts Reduced Disease-free Survival in Clinically Confined Renal Cell Carcinoma. *Br. J. Cancer* 98 (5), 931–940. doi:10.1038/sj.bjc.6604243

Campos, A., Burgos-Ravanal, R., González, M. F., Huilcaman, R., Lobos González, L., and Quest, A. F. G. (2019). Cell Intrinsic and Extrinsic Mechanisms of Caveolin-1-Enhanced Metastasis. *Biomolecules* 9 (8), 314. doi:10.3390/biom9080314

Cao, S., Xiao, L., Wang, J., Chen, G., and Liu, Y. (2021). The RNA-Binding Protein HuR Regulates Intestinal Epithelial Restitution by Modulating Caveolin-1 Gene Expression. *Biochem. J.* 478 (1), 247–260. doi:10.1042/bcj20200372

Chang, C. C., Chen, C. Y., Wen, H. C., Huang, C. Y., Hung, M. S., Lu, H. C., et al. (2017). Caveolin-1 Secreted from Adipose Tissues and Adipocytes Functions as an Adipogenesis Enhancer. *Obesity (Silver Spring)* 25 (11), 1932–1940. doi:10.1002/oby.21970

Chang, T. Y., Chang, C. C., Ohgami, N., and Yamauchi, Y. (2006). Cholesterol Sensing, Trafficking, and Esterification. *Annu. Rev. Cel Dev Biol* 22, 129–157. doi:10.1146/annurev.cellbio.22.010305.104656

Chatterjee, M., Ben-Josef, E., Robb, R., Vedaie, M., Seum, S., Thirumoorthy, K., et al. (2017). Caveolae-Mediated Endocytosis Is Critical for Albumin Cellular Uptake and Response to Albumin-Bound Chemotherapy. *Cancer Res.* 77 (21), 5925–5937. doi:10.1158/0008-5472.Can-17-0604

Chen, J., Capozza, F., Wu, A., Deangelis, T., Sun, H., Lisanti, M., et al. (2008). Regulation of Insulin Receptor Substrate-1 Expression Levels by Caveolin-1. *J. Cel Physiol* 217 (1), 281–289. doi:10.1002/jcp.21498

Chen, W., Chen, Y., Qin, L., Li, A., Zhao, X., Wang, X., et al. (2011). Transcription Factor Sp1 Is Essential for the Regulation of the Porcine Caveolin-1 Gene. *DNA Cel Biol* 30 (7), 491–497. doi:10.1089/dna.2010.1202

Chen, Y., Liu, C., Xie, B., Chen, S., Zhuang, Y., and Zhang, S. (2020). miR-96 Exerts an Oncogenic Role in the Progression of Cervical Cancer by Targeting CAV-1. *Mol. Med. Rep.* 22 (1), 543–550. doi:10.3892/mmr.2020.11101

Chen, Y. H., Lin, W. W., Liu, C. S., Hsu, L. S., Lin, Y. M., and Su, S. L. (2016). Caveolin-1 Expression Ameliorates Nephrotic Damage in a Rabbit Model of Cholesterol-Induced Hypercholesterolemia. *PLoS One* 11 (4), e0154210. doi:10.1371/journal.pone.0154210

Chen, Y. H., Lin, W. W., Liu, C. S., and Su, S. L. (2017). H2O2 Induces Caveolin-1 D-egradation and I-mpaired M-itochondrial F-unction in E11 P-odocytes. *Mol. Med. Rep.* 16 (5), 7841–7847. doi:10.3892/mmr.2017.7497

Chen, Z., Nie, S. D., Qu, M. L., Zhou, D., Wu, L. Y., Shi, X. J., et al. (2018). The Autophagic Degradation of Cav-1 Contributes to PA-induced Apoptosis and Inflammation of Astrocytes. *Cell Death Dis* 9 (7), 771. doi:10.1038/s41419-018-0795-3

Chen, Z. H., Cao, J. F., Zhou, J. S., Liu, H., Che, L. Q., Mizumura, K., et al. (2014). Interaction of Caveolin-1 with ATG12-ATG5 System Suppresses Autophagy in Lung Epithelial Cells. *Am. J. Physiol. Lung Cel Mol Physiol* 306 (11), L1016–L1025. doi:10.1152/ajplung.00268.2013

Cheng, J. P. X., and Nichols, B. J. (2016). Caveolae: One Function or Many. *Trends Cel Biol* 26 (3), 177–189. doi:10.1016/j.tcb.2015.10.010

Codenotti, S., Marampon, F., Triggiani, L., Bonù, M. L., Magrini, S. M., Ceccaroli, P., et al. (2021). Caveolin-1 Promotes Radioresistance in Rhabdomyosarcoma through Increased Oxidative Stress protection and DNA Repair. *Cancer Lett.* 505, 1–12. doi:10.1016/j.canlet.2021.02.005

Coelho-Santos, V., Socodato, R., Portugal, C., Leitão, R. A., Rito, M., Barbosa, M., et al. (2016). Methylphenidate-triggered ROS Generation Promotes Caveolae-Mediated Transcytosis via Rac1 Signaling and C-src-dependent Caveolin-1 Phosphorylation in Human Brain Endothelial Cells. *Cell Mol Life Sci* 73 (24), 4701–4716. doi:10.1007/s00018-016-2301-3

Cohen, A. W., Razani, B., Schubert, W., Williams, T. M., Wang, X. B., Iyengar, P., et al. (2004). Role of Caveolin-1 in the Modulation of Lipolysis and Lipid Droplet Formation. *Diabetes* 53 (5), 1261–1270. doi:10.2337/diabetes.53.5.1261

Collins, B. M., Davis, M. J., Hancock, J. F., and Parton, R. G. (2012). Structure-based Reassessment of the Caveolin Signaling Model: Do Caveolae Regulate Signaling through Caveolin-Protein Interactions. *Dev. Cel* 23 (1), 11–20. doi:10.1016/j.devcel.2012.06.012

Couet, J., Sargiacomo, M., and Lisanti, M. P. (1997). Interaction of a Receptor Tyrosine Kinase, EGF-R, with Caveolins. Caveolin Binding Negatively Regulates Tyrosine and Serine/threonine Kinase Activities. *J. Biol. Chem.* 272 (48), 30429–30438. doi:10.1074/jbc.272.48.30429

Damm, E. M., Pelkmans, L., Kartenbeck, J., Mezzacasa, A., Kurzchalia, T., and Helenius, A. (2005). Clathrin- and Caveolin-1-independent Endocytosis: Entry of Simian Virus 40 into Cells Devoid of Caveolae. *J. Cel Biol* 168 (3), 477–488. doi:10.1083/jcb.200407113

Das, D., Sarkar, S., Bordoloi, J., Wann, S. B., Kalita, J., and Manna, P. (2018). Daidzein, its Effects on Impaired Glucose and Lipid Metabolism and Vascular Inflammation Associated with Type 2 Diabetes. *Biofactors* 44 (5), 407–417. doi:10.1002/biof.1439

Dasari, A., Bartholomew, J. N., Volonte, D., and Galbiati, F. (2006). Oxidative Stress Induces Premature Senescence by Stimulating Caveolin-1 Gene Transcription through P38 Mitogen-Activated Protein kinase/Sp1-Mediated Activation of Two GC-Rich Promoter Elements. *Cancer Res.* 66 (22), 10805–10814. doi:10.1158/0008-5472.Can-06-1236

de Souza, G. M., de Albuquerque Borborema, M. E., de Lucena, T. M. C., da Silva Santos, A. F., de Lima, B. R., de Oliveira, D. C., et al. (2020). Caveolin-1 (CAV-1) up Regulation in Metabolic Syndrome: All Roads Leading to the Same End. *Mol. Biol. Rep.* 47 (11), 9245–9250. doi:10.1007/s11033-020-05945-y

DeBose-Boyd, R. A., and Ye, J. (2018). SREBPs in Lipid Metabolism, Insulin Signaling, and beyond. *Trends Biochem. Sci.* 43 (5), 358–368. doi:10.1016/j.tibs.2018.01.005

Ding, L., Zeng, Q., Wu, J., Li, D., Wang, H., Lu, W., et al. (2017). Caveolin-1 R-egulates O-xidative S-tress-induced S-enescence in N-ucleus P-ulposus C-ells P-rimarily via the P-53/p21 S-ignaling P-athway I-n vitro. *Mol. Med. Rep.* 16 (6), 9521–9527. doi:10.3892/mmr.2017.7789

Elvira, B., Honisch, S., Almilaji, A., Pakladok, T., Liu, G., Shumilina, E., et al. (2013). Up-regulation of Na(+)-Coupled Glucose Transporter SGLT1 by Caveolin-1. *Biochim. Biophys. Acta* 1828 (11), 2394–2398. doi:10.1016/j.bbamem.2013.06.007

Emmerich, F., Zschiedrich, S., Reichenbach-Braun, C., Süsal, C., Minguet, S., Pauly, M. C., et al. (2021). Low Pre-transplant Caveolin-1 Serum Concentrations Are Associated with Acute Cellular Tubulointerstitial Rejection in Kidney Transplantation. *Molecules* 26 (9), 2648. doi:10.3390/molecules26092648

Engelman, J. A., Zhang, X. L., Galbiati, F., and Lisanti, M. P. (1998). Chromosomal Localization, Genomic Organization, and Developmental Expression of the Murine Caveolin Gene Family (Cav-1, -2, and -3). Cav-1 and Cav-2 Genes Map to a Known Tumor Suppressor Locus (6-A2/7q31). *FEBS Lett.* 429 (3), 330–336. doi:10.1016/s0014-5793(98)00619-x

Epand, R. M., Sayer, B. G., and Epand, R. F. (2005). Caveolin Scaffolding Region and Cholesterol-Rich Domains in Membranes. *J. Mol. Biol.* 345 (2), 339–350. doi:10.1016/j.jmb.2004.10.064

Fachim, H. A., Siddals, K., Malipatil, N., Donn, R. P., Moreno, G. Y., Dalton, C. F., et al. (2020). Lifestyle Intervention in Individuals with Impaired Glucose Regulation Affects Caveolin-1 Expression and DNA Methylation. *Adipocyte* 9 (1), 96–107. doi:10.1080/21623945.2020.1732513

Fernández-Rojo, M. A., Restall, C., Ferguson, C., Martel, N., Martin, S., Bosch, M., et al. (2012). Caveolin-1 Orchestrates the Balance between Glucose and Lipid-dependent Energy Metabolism: Implications for Liver Regeneration. *Hepatology* 55 (5), 1574–1584. doi:10.1002/hep.24810

Fiala, G. J., and Minguet, S. (2018). Caveolin-1: The Unnoticed Player in TCR and BCR Signaling. *Adv. Immunol.* 137, 83–133. doi:10.1016/bs.ai.2017.12.002

Fielding, P. E., and Fielding, C. J. (1995). Plasma Membrane Caveolae Mediate the Efflux of Cellular Free Cholesterol. *Biochemistry* 34 (44), 14288–14292. doi:10.1021/bi00044a004

Filippini, A., and D'Alessio, A. (2020). Caveolae and Lipid Rafts in Endothelium: Valuable Organelles for Multiple Functions. *Biomolecules* 10 (9), 1218. doi:10.3390/biom10091218

Frank, P. G., Cheung, M. W., Pavlides, S., Llaverias, G., Park, D. S., and Lisanti, M. P. (2006). Caveolin-1 and Regulation of Cellular Cholesterol Homeostasis. *Am. J. Physiol. Heart Circ. Physiol.* 291 (2), H677–H686. doi:10.1152/ajpheart.01092.2005

Fridolfsson, H. N., Roth, D. M., Insel, P. A., and Patel, H. H. (2014). Regulation of Intracellular Signaling and Function by Caveolin. *Faseb j* 28 (9), 3823–3831. doi:10.1096/fj.14-252320

Frühbeck, G., Méndez-Giménez, L., Fernández-Formoso, J.-A., Fernández, S., and Rodríguez, A. (2014). Regulation of Adipocyte Lipolysis. *Nutr. Res. Rev.* 27 (1), 63–93. doi:10.1017/s095442241400002x

Fujigaki, Y., Sakakima, M., Sun, Y., Goto, T., Ohashi, N., Fukasawa, H., et al. (2007). Immunohistochemical Study on Caveolin-1alpha in Regenerating Process of Tubular Cells in Gentamicin-Induced Acute Tubular Injury in Rats. *Virchows Arch.* 450 (6), 671–681. doi:10.1007/s00428-007-0417-4

Fujimoto, T., Kogo, H., Nomura, R., and Une, T. (2000). Isoforms of Caveolin-1 and Caveolar Structure. *J. Cel Sci* 113 Pt 19, 3509–3517. doi:10.1242/jcs.113.19.3509

Gao, M., Huang, X., Song, B. L., and Yang, H. (2019). The Biogenesis of Lipid Droplets: Lipids Take center Stage. *Prog. Lipid Res.* 75, 100989. doi:10.1016/j.plipres.2019.100989

Gao, Y., Zhao, Y., Pan, J., Yang, L., Huang, T., Feng, X., et al. (2014). Treadmill Exercise Promotes Angiogenesis in the Ischemic Penumbra of Rat Brains through Caveolin-1/VEGF Signaling Pathways. *Brain Res.* 1585, 83–90. doi:10.1016/j.brainres.2014.08.032

Geltinger, F., Schartel, L., Wiederstein, M., Tevini, J., Aigner, E., Felder, T. K., et al. (2020). Friend or Foe: Lipid Droplets as Organelles for Protein and Lipid Storage in Cellular Stress Response, Aging and Disease. *Molecules* 25 (21), 5053. doi:10.3390/molecules25215053

Gerbod-Giannone, M. C., Dallet, L., Naudin, G., Sahin, A., Decossas, M., Poussard, S., et al. (2019). Involvement of Caveolin-1 and CD36 in Native LDL Endocytosis by Endothelial Cells. *Biochim. Biophys. Acta Gen. Subj* 1863 (5), 830–838. doi:10.1016/j.bbagen.2019.01.005

Gewin, L. S. (2021). Sugar or Fat? Renal Tubular Metabolism Reviewed in Health and Disease. *Nutrients* 13 (5), 1580. doi:10.3390/nu13051580

Glenney, J. R., Jr. (1992). The Sequence of Human Caveolin Reveals Identity with VIP21, a Component of Transport Vesicles. *FEBS Lett.* 314 (1), 45–48. doi:10.1016/0014-5793(92)81458-x

Glenney, J. R., Jr. (1989). Tyrosine Phosphorylation of a 22-kDa Protein Is Correlated with Transformation by Rous Sarcoma Virus. *J. Biol. Chem.* 264 (34), 20163–20166. doi:10.1016/s0021-9258(19)47038-5

Gopu, V., Fan, L., Shetty, R. S., Nagaraja, M. R., and Shetty, S. (2020). Caveolin-1 Scaffolding Domain Peptide Regulates Glucose Metabolism in Lung Fibrosis. *JCI Insight* 5 (19), e137969. doi:10.1172/jci.insight.137969

Goutas, A., Papathanasiou, I., Mourmoura, E., Tsesmelis, K., Tsezou, A., and Trachana, V. (2020). Oxidative Stress Response Is Mediated by Overexpression and Spatiotemporal Regulation of Caveolin-1. *Antioxidants (Basel)* 9 (8), 766. doi:10.3390/antiox9080766

Grayson, P. C., Eddy, S., Taroni, J. N., Lightfoot, Y. L., Mariani, L., Parikh, H., et al. (2018). Metabolic Pathways and Immunometabolism in Rare Kidney Diseases. *Ann. Rheum. Dis.* 77 (8), 1226–1233. doi:10.1136/annrheumdis-2017-212935

Guan, T. H., Chen, G., Gao, B., Janssen, M. R., Uttarwar, L., Ingram, A. J., et al. (2013). Caveolin-1 Deficiency Protects against Mesangial Matrix Expansion in a Mouse Model of Type 1 Diabetic Nephropathy. *Diabetologia* 56 (9), 2068–2077. doi:10.1007/s00125-013-2968-z

Gvaramia, D., Blaauboer, M. E., Hanemaaijer, R., and Everts, V. (2013). Role of Caveolin-1 in Fibrotic Diseases. *Matrix Biol.* 32 (6), 307–315. doi:10.1016/j.matbio.2013.03.005

Ha, T. K., and Chi, S. G. (2012). CAV1/caveolin 1 Enhances Aerobic Glycolysis in colon Cancer Cells via Activation of SLC2A3/GLUT3 Transcription. *Autophagy* 8 (11), 1684–1685. doi:10.4161/auto.21487

Ha, T. K., Her, N. G., Lee, M. G., Ryu, B. K., Lee, J. H., Han, J., et al. (2012). Caveolin-1 Increases Aerobic Glycolysis in Colorectal Cancers by Stimulating HMGA1-Mediated GLUT3 Transcription. *Cancer Res.* 72 (16), 4097–4109. doi:10.1158/0008-5472.Can-12-0448

Haddad, D., Al Madhoun, A., Nizam, R., and Al-Mulla, F. (2020). Role of Caveolin-1 in Diabetes and its Complications. *Oxid Med. Cel Longev* 2020, 9761539. doi:10.1155/2020/9761539

Hall, D. P., Cost, N. G., Hegde, S., Kellner, E., Mikhaylova, O., Stratton, Y., et al. (2014). TRPM3 and miR-204 Establish a Regulatory Circuit that Controls Oncogenic Autophagy in clear Cell Renal Cell Carcinoma. *Cancer Cell* 26 (5), 738–753. doi:10.1016/j.ccell.2014.09.015

Han, B., Porta, J. C., Hanks, J. L., Peskova, Y., Binshtein, E., Dryden, K., et al. (2020). Structure and Assembly of CAV1 8S Complexes Revealed by Single Particle Electron Microscopy. *Sci. Adv.* 6 (49), eabc6185. doi:10.1126/sciadv.abc6185

Han, M., Nwosu, Z. C., Piorońska, W., Ebert, M. P., Dooley, S., and Meyer, C. (2019). Caveolin-1 Impacts on TGF-β Regulation of Metabolic Gene Signatures in Hepatocytes. *Front. Physiol.* 10, 1606. doi:10.3389/fphys.2019.01606

Hansen, C. G., Bright, N. A., Howard, G., and Nichols, B. J. (2009). SDPR Induces Membrane Curvature and Functions in the Formation of Caveolae. *Nat. Cel Biol* 11 (7), 807–814. doi:10.1038/ncb1887

Hansen, C. G., and Nichols, B. J. (2010). Exploring the Caves: Cavins, Caveolins and Caveolae. *Trends Cel Biol* 20 (4), 177–186. doi:10.1016/j.tcb.2010.01.005

Henne, M., Goodman, J. M., and Hariri, H. (2020). Spatial Compartmentalization of Lipid Droplet Biogenesis. *Biochim. Biophys. Acta Mol. Cel Biol Lipids* 1865 (1), 158499. doi:10.1016/j.bbalip.2019.07.008

Hill, M. M., Bastiani, M., Luetterforst, R., Kirkham, M., Kirkham, A., Nixon, S. J., et al. (2008). PTRF-cavin, a Conserved Cytoplasmic Protein Required for Caveola Formation and Function. *Cell* 132 (1), 113–124. doi:10.1016/j.cell.2007.11.042

Hirama, T., Das, R., Yang, Y., Ferguson, C., Won, A., Yip, C. M., et al. (2017). Phosphatidylserine Dictates the Assembly and Dynamics of Caveolae in the Plasma Membrane. *J. Biol. Chem.* 292 (34), 14292–14307. doi:10.1074/jbc.M117.791400

Hoernke, M., Mohan, J., Larsson, E., Blomberg, J., Kahra, D., Westenhoff, S., et al. (2017). EHD2 Restrains Dynamics of Caveolae by an ATP-dependent, Membrane-Bound, Open Conformation. *Proc. Natl. Acad. Sci. U S A.* 114 (22), E4360–e4369. doi:10.1073/pnas.1614066114

Hoop, C. L., Sivanandam, V. N., Kodali, R., Srnec, M. N., and van der Wel, P. C. (2012). Structural Characterization of the Caveolin Scaffolding Domain in Association with Cholesterol-Rich Membranes. *Biochemistry* 51 (1), 90–99. doi:10.1021/bi201356v

Hu, R., Yan, H., Fei, X., Liu, H., and Wu, J. (2017). Modulation of Glucose Metabolism by a Natural Compound from Chloranthus Japonicus via Activation of AMP-Activated Protein Kinase. *Sci. Rep.* 7 (1), 778. doi:10.1038/s41598-017-00925-y

Huang, C., Qiu, Z., Wang, L., Peng, Z., Jia, Z., Logsdon, C. D., et al. (2012). A Novel FoxM1-Caveolin Signaling Pathway Promotes Pancreatic Cancer Invasion and Metastasis. *Cancer Res.* 72 (3), 655–665. doi:10.1158/0008-5472.Can-11-3102

Huang, C., Zhou, Y., Huang, H., Zheng, Y., Kong, L., Zhang, H., et al. (2021). Islet Transplantation Reverses Podocyte Injury in Diabetic Nephropathy or Induced by High Glucose via Inhibiting RhoA/ROCK/NF-κB Signaling Pathway. *J. Diabetes Res.* 2021, 9570405. doi:10.1155/2021/9570405

Huang, G., Lou, T., Pan, J., Ye, Z., Yin, Z., Li, L., et al. (2019). MiR-204 Reduces Cisplatin Resistance in Non-small Cell Lung Cancer through Suppression of the caveolin-1/AKT/Bad Pathway. *Aging (Albany NY)* 11 (7), 2138–2150. doi:10.18632/aging.101907

Huang, J. H., Lu, L., Lu, H., Chen, X., Jiang, S., and Chen, Y. H. (2007). Identification of the HIV-1 Gp41 Core-Binding Motif in the Scaffolding Domain of Caveolin-1. *J. Biol. Chem.* 282 (9), 6143–6152. doi:10.1074/jbc.M607701200

Hubert, M., Larsson, E., and Lundmark, R. (2020a). Keeping in Touch with the Membrane; Protein- and Lipid-Mediated Confinement of Caveolae to the Cell Surface. *Biochem. Soc. Trans.* 48 (1), 155–163. doi:10.1042/bst20190386

Hubert, M., Larsson, E., Vegesna, N. V. G., Ahnlund, M., Johansson, A. I., Moodie, L. W., et al. (2020b). Lipid Accumulation Controls the Balance between Surface Connection and Scission of Caveolae. *Elife* 9, e55038. doi:10.7554/eLife.55038

Ikezu, T., Ueda, H., Trapp, B. D., Nishiyama, K., Sha, J. F., Volonte, D., et al. (1998). Affinity-purification and Characterization of Caveolins from the Brain: Differential Expression of Caveolin-1, -2, and -3 in Brain Endothelial and Astroglial Cell Types. *Brain Res.* 804 (2), 177–192. doi:10.1016/s0006-8993(98)00498-3

Ikonen, E., and Parton, R. G. (2000). Caveolins and Cellular Cholesterol Balance. *Traffic* 1 (3), 212–217. doi:10.1034/j.1600-0854.2000.010303.x

Ishizaka, N., Griendling, K. K., Lassègue, B., and Alexander, R. W. (1998). Angiotensin II Type 1 Receptor: Relationship with Caveolae and Caveolin after Initial Agonist Stimulation. *Hypertension* 32 (3), 459–466. doi:10.1161/01.hyp.32.3.459

Itabe, H., Yamaguchi, T., Nimura, S., and Sasabe, N. (2017). Perilipins: a Diversity of Intracellular Lipid Droplet Proteins. *Lipids Health Dis.* 16 (1), 83. doi:10.1186/s12944-017-0473-y

Janković, J., Tatić, S., Božić, V., Živaljević, V., Cvejić, D., and Paskaš, S. (2017). Inverse Expression of Caveolin-1 and EGFR in Thyroid Cancer Patients. *Hum. Pathol.* 61, 164–172. doi:10.1016/j.humpath.2016.10.020

Ji, D. G., Zhang, Y., Yao, S. M., Zhai, X. J., Zhang, L. R., Zhang, Y. Z., et al. (2018). Cav-1 Deficiency Promotes Liver Fibrosis in Carbon Tetrachloride (CCl4)-Induced Mice by Regulation of Oxidative Stress and Inflammation Responses. *Biomed. Pharmacother.* 102, 26–33. doi:10.1016/j.biopha.2018.03.016

Jin, J., Peng, C., Wu, S. Z., Chen, H. M., and Zhang, B. F. (2015). Blocking VEGF/Caveolin-1 Signaling Contributes to Renal protection of Fasudil in Streptozotocin-Induced Diabetic Rats. *Acta Pharmacol. Sin* 36 (7), 831–840. doi:10.1038/aps.2015.23

Joo, H. J., Oh, D. K., Kim, Y. S., Lee, K. B., and Kim, S. J. (2004). Increased Expression of Caveolin-1 and Microvessel Density Correlates with Metastasis and Poor Prognosis in clear Cell Renal Cell Carcinoma. *BJU Int.* 93 (3), 291–296. doi:10.1111/j.1464-410x.2004.04604.x

Kang, H. M., Ahn, S. H., Choi, P., Ko, Y. A., Han, S. H., Chinga, F., et al. (2015). Defective Fatty Acid Oxidation in Renal Tubular Epithelial Cells Has a Key Role in Kidney Fibrosis Development. *Nat. Med.* 21 (1), 37–46. doi:10.1038/nm.3762

Kogo, H., and Fujimoto, T. (2000). Caveolin-1 Isoforms Are Encoded by Distinct mRNAs. Identification of Mouse Caveolin-1 mRNA Variants Caused by Alternative Transcription Initiation and Splicing. *FEBS Lett.* 465 (2-3), 119–123. doi:10.1016/s0014-5793(99)01730-5

Kong, D., Zhang, Z., Chen, L., Huang, W., Zhang, F., Wang, L., et al. (2020). Curcumin Blunts Epithelial-Mesenchymal Transition of Hepatocytes to Alleviate Hepatic Fibrosis through Regulating Oxidative Stress and Autophagy. *Redox Biol.* 36, 101600. doi:10.1016/j.redox.2020.101600

Kongkham, S., Sriwong, S., and Tasanarong, A. (2016). Erythropoietin Administration Promotes Expression of VEGF in Renal Ischemic–Reperfusion Injury in Rat Model. *J. Med. Assoc. Thai* 99 (Suppl. 4), S246–S255.

Kotova, A., Timonina, K., and Zoidl, G. R. (2020). Endocytosis of Connexin 36 Is Mediated by Interaction with Caveolin-1. *Int. J. Mol. Sci.* 21 (15). doi:10.3390/ijms21155401

Kovtun, O., Tillu, V. A., Ariotti, N., Parton, R. G., and Collins, B. M. (2015). Cavin Family Proteins and the Assembly of Caveolae. *J. Cel Sci* 128 (7), 1269–1278. doi:10.1242/jcs.167866

Krilov, L., Nguyen, A., Miyazaki, T., Unson, C. G., Williams, R., Lee, N. H., et al. (2011). Dual Mode of Glucagon Receptor Internalization: Role of PKCα, GRKs and β-arrestins. *Exp. Cel Res* 317 (20), 2981–2994. doi:10.1016/j.yexcr.2011.10.001

Krishna, A., and Sengupta, D. (2019). Interplay between Membrane Curvature and Cholesterol: Role of Palmitoylated Caveolin-1. *Biophys. J.* 116 (1), 69–78. doi:10.1016/j.bpj.2018.11.3127

Kuo, A., Lee, M. Y., Yang, K., Gross, R. W., and Sessa, W. C. (2018). Caveolin-1 Regulates Lipid Droplet Metabolism in Endothelial Cells via Autocrine Prostacyclin-Stimulated, cAMP-Mediated Lipolysis. *J. Biol. Chem.* 293 (3), 973–983. doi:10.1074/jbc.RA117.000980

Kurzchalia, T. V., Dupree, P., Parton, R. G., Kellner, R., Virta, H., Lehnert, M., et al. (1992). VIP21, a 21-kD Membrane Protein Is an Integral Component of Trans-golgi-network-derived Transport Vesicles. *J. Cel Biol* 118 (5), 1003–1014. doi:10.1083/jcb.118.5.1003

Le Lay, S., Hajduch, E., Lindsay, M. R., Le Lièpvre, X., Thiele, C., Ferré, P., et al. (2006). Cholesterol-induced Caveolin Targeting to Lipid Droplets in Adipocytes: a Role for Caveolar Endocytosis. *Traffic* 7 (5), 549–561. doi:10.1111/j.1600-0854.2006.00406.x

Lee, C. Y., Lai, T. Y., Tsai, M. K., Chang, Y. C., Ho, Y. H., Yu, I. S., et al. (2017). The Ubiquitin Ligase ZNRF1 Promotes Caveolin-1 Ubiquitination and Degradation to Modulate Inflammation. *Nat. Commun.* 8, 15502. doi:10.1038/ncomms15502

Lee, E. K., Lee, Y. S., Han, I. O., and Park, S. H. (2007). Expression of Caveolin-1 Reduces Cellular Responses to TGF-Beta1 through Down-Regulating the Expression of TGF-Beta Type II Receptor Gene in NIH3T3 Fibroblast Cells. *Biochem. Biophys. Res. Commun.* 359 (2), 385–390. doi:10.1016/j.bbrc.2007.05.121

Lee, Y. J., Kim, M. O., Ryu, J. M., and Han, H. J. (2012). Regulation of SGLT Expression and Localization through Epac/PKA-dependent Caveolin-1 and F-Actin Activation in Renal Proximal Tubule Cells. *Biochim. Biophys. Acta* 1823 (4), 971–982. doi:10.1016/j.bbamcr.2011.12.011

Li, J., Li, P., Zhang, G., Qin, P., Zhang, D., and Zhao, W. (2020). CircRNA TADA2A Relieves Idiopathic Pulmonary Fibrosis by Inhibiting Proliferation and Activation of Fibroblasts. *Cel Death Dis* 11 (7), 553. doi:10.1038/s41419-020-02747-9

Li, R., Guo, Y., Zhang, Y., Zhang, X., Zhu, L., and Yan, T. (2019). Salidroside Ameliorates Renal Interstitial Fibrosis by Inhibiting the TLR4/NF-Kb and MAPK Signaling Pathways. *Int. J. Mol. Sci.* 20 (5), 1103. doi:10.3390/ijms20051103

Li, S., Couet, J., and Lisanti, M. P. (1996a). Src Tyrosine Kinases, Galpha Subunits, and H-Ras Share a Common Membrane-Anchored Scaffolding Protein, Caveolin. Caveolin Binding Negatively Regulates the Auto-Activation of Src Tyrosine Kinases. *J. Biol. Chem.* 271 (46), 29182–29190. doi:10.1074/jbc.271.46.29182

Li, S., Seitz, R., and Lisanti, M. P. (1996b). Phosphorylation of Caveolin by Src Tyrosine Kinases. The Alpha-Isoform of Caveolin Is Selectively Phosphorylated by V-Src *In Vivo*. *J. Biol. Chem.* 271 (7), 3863–3868. doi:10.1074/jbc.271.7.3863

Ling, X., Li, Y., Qiu, F., Lu, X., Yang, L., Chen, J., et al. (2020). Down Expression of Lnc-BMP1-1 Decreases that of Caveolin-1 Is Associated with the Lung Cancer Susceptibility and Cigarette Smoking History. *Aging (Albany NY)* 12 (1), 462–480. doi:10.18632/aging.102633

Liu, A., Wu, Q., Guo, J., Ares, I., Rodríguez, J. L., Martínez-Larrañaga, M. R., et al. (2019). Statins: Adverse Reactions, Oxidative Stress and Metabolic Interactions. *Pharmacol. Ther.* 195, 54–84. doi:10.1016/j.pharmthera.2018.10.004

Liu, L., Xu, H. X., Wang, W. Q., Wu, C. T., Chen, T., Qin, Y., et al. (2014). Cavin-1 Is Essential for the Tumor-Promoting Effect of Caveolin-1 and Enhances its Prognostic Potency in Pancreatic Cancer. *Oncogene* 33 (21), 2728–2736. doi:10.1038/onc.2013.223

Liu, P., Ying, Y., Zhao, Y., Mundy, D. I., Zhu, M., and Anderson, R. G. (2004). Chinese Hamster Ovary K2 Cell Lipid Droplets Appear to Be Metabolic Organelles Involved in Membrane Traffic. *J. Biol. Chem.* 279 (5), 3787–3792. doi:10.1074/jbc.M311945200

Liu, S., Premont, R. T., Singh, S., and Rockey, D. C. (2017). Caveolin 1 and G-Protein-Coupled Receptor Kinase-2 Coregulate Endothelial Nitric Oxide Synthase Activity in Sinusoidal Endothelial Cells. *Am. J. Pathol.* 187 (4), 896–907. doi:10.1016/j.ajpath.2016.11.017

Liu, Y., Fu, Y., Hu, X., Chen, S., Miao, J., Wang, Y., et al. (2020). Caveolin-1 Knockdown Increases the Therapeutic Sensitivity of Lung Cancer to Cisplatin-Induced Apoptosis by Repressing Parkin-Related Mitophagy and Activating the ROCK1 Pathway. *J. Cel Physiol* 235 (2), 1197–1208. doi:10.1002/jcp.29033

Llaverias, G., Vázquez-Carrera, M., Sánchez, R. M., Noé, V., Ciudad, C. J., Laguna, J. C., et al. (2004). Rosiglitazone Upregulates Caveolin-1 Expression in THP-1 Cells through a PPAR-dependent Mechanism. *J. Lipid Res.* 45 (11), 2015–2024. doi:10.1194/jlr.M400049-JLR200

Luo, J., Yang, H., and Song, B. L. (2020a). Mechanisms and Regulation of Cholesterol Homeostasis. *Nat. Rev. Mol. Cel Biol* 21 (4), 225–245. doi:10.1038/s41580-019-0190-7

Luo, M., Xu, C., Luo, Y., Wang, G., Wu, J., and Wan, Q. (2020b). Circulating miR-103 Family as Potential Biomarkers for Type 2 Diabetes through Targeting CAV-1 and SFRP4. *Acta Diabetol.* 57 (3), 309–322. doi:10.1007/s00592-019-01430-6

Luo, Z., Rong, Z., Zhang, J., Zhu, Z., Yu, Z., Li, T., et al. (2020c). Circular RNA circCCDC9 Acts as a miR-6792-3p Sponge to Suppress the Progression of Gastric Cancer through Regulating CAV1 Expression. *Mol. Cancer* 19 (1), 86. doi:10.1186/s12943-020-01203-8

Machin, P. A., Tsonou, E., Hornigold, D. C., and Welch, H. C. E. (2021). Rho Family GTPases and Rho GEFs in Glucose Homeostasis. *Cells* 10 (4), 915. doi:10.3390/cells10040915

Macovei, A., Radulescu, C., Lazar, C., Petrescu, S., Durantel, D., Dwek, R. A., et al. (2010). Hepatitis B Virus Requires Intact Caveolin-1 Function for Productive Infection in HepaRG Cells. *J. Virol.* 84 (1), 243–253. doi:10.1128/jvi.01207-09

Mahmoudi, M., Willgoss, D., Cuttle, L., Yang, T., Pat, B., Winterford, C., et al. (2003). *In Vivo* and *In Vitro* Models Demonstrate a Role for Caveolin-1 in the Pathogenesis of Ischaemic Acute Renal Failure. *J. Pathol.* 200 (3), 396–405. doi:10.1002/path.1368

Martínez, M., Martínez, N. A., Miranda, J. D., Maldonado, H. M., and Silva Ortiz, W. I. (2019). Caveolin-1 Regulates P2Y2 Receptor Signaling during Mechanical Injury in Human 1321N1 Astrocytoma. *Biomolecules* 9 (10), 622. doi:10.3390/biom9100622

Martinez, N. A., Ayala, A. M., Martinez, M., Martinez-Rivera, F. J., Miranda, J. D., and Silva, W. I. (2016). Caveolin-1 Regulates the P2Y2 Receptor Signaling in Human 1321N1 Astrocytoma Cells. *J. Biol. Chem.* 291 (23), 12208–12222. doi:10.1074/jbc.M116.730226

Matthaeus, C., Lahmann, I., Kunz, S., Jonas, W., Melo, A. A., Lehmann, M., et al. (2020). EHD2-mediated Restriction of Caveolar Dynamics Regulates Cellular Fatty Acid Uptake. *Proc. Natl. Acad. Sci. U S A.* 117 (13), 7471–7481. doi:10.1073/pnas.1918415117

Matthaeus, C., and Taraska, J. W. (2020). Energy and Dynamics of Caveolae Trafficking. *Front Cel Dev Biol* 8, 614472. doi:10.3389/fcell.2020.614472

Matveev, S., van der Westhuyzen, D. R., and Smart, E. J. (1999). Co-expression of Scavenger Receptor-BI and Caveolin-1 Is Associated with Enhanced Selective Cholesteryl Ester Uptake in THP-1 Macrophages. *J. Lipid Res.* 40 (9), 1647–1654. doi:10.1016/s0022-2275(20)33410-6

Mayurasakorn, K., Hasanah, N., Homma, T., Homma, M., Rangel, I. K., Garza, A. E., et al. (2018). Caloric Restriction Improves Glucose Homeostasis, yet Increases Cardiometabolic Risk in Caveolin-1-Deficient Mice. *Metabolism* 83, 92–101. doi:10.1016/j.metabol.2018.01.012

McMahon, K. A., Zajicek, H., Li, W. P., Peyton, M. J., Minna, J. D., Hernandez, V. J., et al. (2009). SRBC/cavin-3 Is a Caveolin Adapter Protein that Regulates Caveolae Function. *Embo j* 28 (8), 1001–1015. doi:10.1038/emboj.2009.46

Mehta, N., Li, R., Zhang, D., Soomro, A., He, J., Zhang, I., et al. (2021). miR299a-5p Promotes Renal Fibrosis by Suppressing the Antifibrotic Actions of Follistatin. *Sci. Rep.* 11 (1), 88. doi:10.1038/s41598-020-80199-z

Meng, H., Fu, G., Shen, J., Shen, K., Xu, Z., Wang, Y., et al. (2017). Ameliorative Effect of Daidzein on Cisplatin-Induced Nephrotoxicity in Mice via Modulation of Inflammation, Oxidative Stress, and Cell Death. *Oxid Med. Cel Longev* 2017, 3140680. doi:10.1155/2017/3140680

Mergia, A. (2017). The Role of Caveolin 1 in HIV Infection and Pathogenesis. *Viruses* 9 (6), 129. doi:10.3390/v9060129

Mitrofanova, A., Mallela, S. K., Ducasa, G. M., Yoo, T. H., Rosenfeld-Gur, E., Zelnik, I. D., et al. (2019). SMPDL3b Modulates Insulin Receptor Signaling in Diabetic Kidney Disease. *Nat. Commun.* 10 (1), 2692. doi:10.1038/s41467-019-10584-4

Møller, L. L. V., Klip, A., and Sylow, L. (2019). Rho GTPases-Emerging Regulators of Glucose Homeostasis and Metabolic Health. *Cells* 8 (5), 434. doi:10.3390/cells8050434

Moore, J., McKnight, A. J., Simmonds, M. J., Courtney, A. E., Hanvesakul, R., Brand, O. J., et al. (2010). Association of Caveolin-1 Gene Polymorphism with Kidney Transplant Fibrosis and Allograft Failure. *Jama* 303 (13), 1282–1287. doi:10.1001/jama.2010.356

Morén, B., Shah, C., Howes, M. T., Schieber, N. L., McMahon, H. T., Parton, R. G., et al. (2012). EHD2 Regulates Caveolar Dynamics via ATP-Driven Targeting and Oligomerization. *Mol. Biol. Cel* 23 (7), 1316–1329. doi:10.1091/mbc.E11-09-0787

Moriyama, T., Marquez, J. P., Wakatsuki, T., and Sorokin, A. (2007). Caveolar Endocytosis Is Critical for BK Virus Infection of Human Renal Proximal Tubular Epithelial Cells. *J. Virol.* 81 (16), 8552–8562. doi:10.1128/jvi.00924-07

Moriyama, T., Sasaki, K., Karasawa, K., Uchida, K., and Nitta, K. (2017). Intracellular Transcytosis of Albumin in Glomerular Endothelial Cells after Endocytosis through Caveolae. *J. Cel Physiol* 232 (12), 3565–3573. doi:10.1002/jcp.25817

Moriyama, T., Takei, T., Itabashi, M., Uchida, K., Tsuchiya, K., and Nitta, K. (2015). Caveolae May Enable Albumin to Enter Human Renal Glomerular Endothelial Cells. *J. Cel Biochem* 116 (6), 1060–1069. doi:10.1002/jcb.25061

Moriyama, T., Tsuruta, Y., Shimizu, A., Itabashi, M., Takei, T., Horita, S., et al. (2011). The Significance of Caveolae in the Glomeruli in Glomerular Disease. *J. Clin. Pathol.* 64 (6), 504–509. doi:10.1136/jcp.2010.087023

Nabi, I. R., and Le, P. U. (2003). Caveolae/raft-dependent Endocytosis. *J. Cel Biol* 161 (4), 673–677. doi:10.1083/jcb.200302028

Nah, J., Yoo, S. M., Jung, S., Jeong, E. I., Park, M., Kaang, B. K., et al. (2017). Phosphorylated CAV1 Activates Autophagy through an Interaction with BECN1 under Oxidative Stress. *Cel Death Dis* 8 (5), e2822. doi:10.1038/cddis.2017.71

Noda, K., Godo, S., Saito, H., Tsutsui, M., and Shimokawa, H. (2015). Opposing Roles of Nitric Oxide and Rho-Kinase in Lipid Metabolism in Mice. *Tohoku J. Exp. Med.* 235 (3), 171–183. doi:10.1620/tjem.235.171

Noda, K., Nakajima, S., Godo, S., Saito, H., Ikeda, S., Shimizu, T., et al. (2014). Rho-kinase Inhibition Ameliorates Metabolic Disorders through Activation of

AMPK Pathway in Mice. *PLoS One* 9 (11), e110446. doi:10.1371/journal.pone.0110446

Nozaki, Y., Kinoshita, K., Hino, S., Yano, T., Niki, K., Hirooka, Y., et al. (2015). Signaling Rho-Kinase Mediates Inflammation and Apoptosis in T Cells and Renal Tubules in Cisplatin Nephrotoxicity. *Am. J. Physiol. Ren. Physiol* 308 (8), F899–F909. doi:10.1152/ajprenal.00362.2014

Nwosu, Z. C., Ebert, M. P., Dooley, S., and Meyer, C. (2016). Caveolin-1 in the Regulation of Cell Metabolism: a Cancer Perspective. *Mol. Cancer* 15 (1), 71. doi:10.1186/s12943-016-0558-7

Okada, S., Raja, S. A., Okerblom, J., Boddu, A., Horikawa, Y., Ray, S., et al. (2019). Deletion of Caveolin Scaffolding Domain Alters Cancer Cell Migration. *Cell Cycle* 18 (11), 1268–1280. doi:10.1080/15384101.2019.1618118

Oliveira, S. D. S., Castellon, M., Chen, J., Bonini, M. G., Gu, X., Elliott, M. H., et al. (2017). Inflammation-induced Caveolin-1 and BMPRII Depletion Promotes Endothelial Dysfunction and TGF-β-Driven Pulmonary Vascular Remodeling. *Am. J. Physiol. Lung Cel Mol Physiol* 312 (5), L760–l771. doi:10.1152/ajplung.00484.2016

Olzmann, J. A., and Carvalho, P. (2019). Dynamics and Functions of Lipid Droplets. *Nat. Rev. Mol. Cel Biol* 20 (3), 137–155. doi:10.1038/s41580-018-0085-z

Ostalska-Nowicka, D., Nowicki, M., Zachwieja, J., Kasper, M., and Witt, M. (2007). The Significance of Caveolin-1 Expression in Parietal Epithelial Cells of Bowman's Capsule. *Histopathology* 51 (5), 611–621. doi:10.1111/j.1365-2559.2007.02844.x

Ostermeyer, A. G., Ramcharan, L. T., Zeng, Y., Lublin, D. M., and Brown, D. A. (2004). Role of the Hydrophobic Domain in Targeting Caveolin-1 to Lipid Droplets. *J. Cel Biol* 164 (1), 69–78. doi:10.1083/jcb.200303037

Palacios-Ortega, S., Varela-Guruceaga, M., Martínez, J. A., de Miguel, C., and Milagro, F. I. (2016). Effects of High Glucose on Caveolin-1 and Insulin Signaling in 3T3-L1 Adipocytes. *Adipocyte* 5 (1), 65–80. doi:10.1080/21623945.2015.1122856

Park, S., Glover, K. J., and Im, W. (2019). U-shaped Caveolin-1 Conformations Are Tightly Regulated by Hydrogen Bonds with Lipids. *J. Comput. Chem.* 40 (16), 1570–1577. doi:10.1002/jcc.25807

Parton, R. G. (2018). Caveolae: Structure, Function, and Relationship to Disease. *Annu. Rev. Cel Dev Biol* 34, 111–136. doi:10.1146/annurev-cellbio-100617-062737

Parton, R. G., and del Pozo, M. A. (2013). Caveolae as Plasma Membrane Sensors, Protectors and Organizers. *Nat. Rev. Mol. Cel Biol* 14 (2), 98–112. doi:10.1038/nrm3512

Parton, R. G., Kozlov, M. M., and Ariotti, N. (2020a). Caveolae and Lipid Sorting: Shaping the Cellular Response to Stress. *J. Cel Biol* 219 (4), e201905071. doi:10.1083/jcb.201905071

Parton, R. G., McMahon, K. A., and Wu, Y. (2020b). Caveolae: Formation, Dynamics, and Function. *Curr. Opin. Cel Biol* 65, 8–16. doi:10.1016/j.ceb.2020.02.001

Parton, R. G., Tillu, V. A., and Collins, B. M. (2018). Caveolae. *Curr. Biol.* 28 (8), R402–r405. doi:10.1016/j.cub.2017.11.075

Peng, F., Wu, D., Ingram, A. J., Zhang, B., Gao, B., and Krepinsky, J. C. (2007). RhoA Activation in Mesangial Cells by Mechanical Strain Depends on Caveolae and Caveolin-1 Interaction. *J. Am. Soc. Nephrol.* 18 (1), 189–198. doi:10.1681/asn.2006050498

Pezeshkian, W., Chevrot, G., and Khandelia, H. (2018). The Role of Caveolin-1 in Lipid Droplets and Their Biogenesis. *Chem. Phys. Lipids* 211, 93–99. doi:10.1016/j.chemphyslip.2017.11.010

Pilch, P. F., and Liu, L. (2011). Fat Caves: Caveolae, Lipid Trafficking and Lipid Metabolism in Adipocytes. *Trends Endocrinol. Metab.* 22 (8), 318–324. doi:10.1016/j.tem.2011.04.001

Plummer, A. M., Culbertson, A. T., and Liao, M. (2021). The ABCs of Sterol Transport. *Annu. Rev. Physiol.* 83, 153–181. doi:10.1146/annurev-physiol-031620-094944

Pol, A., Luetterforst, R., Lindsay, M., Heino, S., Ikonen, E., and Parton, R. G. (2001). A Caveolin Dominant Negative Mutant Associates with Lipid Bodies and Induces Intracellular Cholesterol Imbalance. *J. Cel Biol* 152 (5), 1057–1070. doi:10.1083/jcb.152.5.1057

Pol, A., Martin, S., Fernandez, M. A., Ferguson, C., Carozzi, A., Luetterforst, R., et al. (2004). Dynamic and Regulated Association of Caveolin with Lipid Bodies: Modulation of Lipid Body Motility and Function by a Dominant Negative Mutant. *Mol. Biol. Cel* 15 (1), 99–110. doi:10.1091/mbc.e03-06-0368

Raikar, L. S., Vallejo, J., Lloyd, P. G., and Hardin, C. D. (2006). Overexpression of Caveolin-1 Results in Increased Plasma Membrane Targeting of Glycolytic Enzymes: the Structural Basis for a Membrane Associated Metabolic Compartment. *J. Cel Biochem* 98 (4), 861–871. doi:10.1002/jcb.20732

Renne, M. F., Klug, Y. A., and Carvalho, P. (2020). Lipid Droplet Biogenesis: A Mystery "unmixing". *Semin. Cel Dev Biol* 108, 14–23. doi:10.1016/j.semcdb.2020.03.001

Ring, A., Le Lay, S., Pohl, J., Verkade, P., and Stremmel, W. (2006). Caveolin-1 Is Required for Fatty Acid Translocase (FAT/CD36) Localization and Function at the Plasma Membrane of Mouse Embryonic Fibroblasts. *Biochim. Biophys. Acta* 1761 (4), 416–423. doi:10.1016/j.bbalip.2006.03.016

Robenek, M. J., Severs, N. J., Schlattmann, K., Plenz, G., Zimmer, K. P., Troyer, D., et al. (2004). Lipids Partition Caveolin-1 from ER Membranes into Lipid Droplets: Updating the Model of Lipid Droplet Biogenesis. *Faseb j* 18 (7), 866–868. doi:10.1096/fj.03-0782fje

Root, K. T., Plucinsky, S. M., and Glover, K. J. (2015). Recent Progress in the Topology, Structure, and Oligomerization of Caveolin: a Building Block of Caveolae. *Curr. Top. Membr.* 75, 305–336. doi:10.1016/bs.ctm.2015.03.007

Rothberg, K. G., Heuser, J. E., Donzell, W. C., Ying, Y. S., Glenney, J. R., and Anderson, R. G. (1992). Caveolin, a Protein Component of Caveolae Membrane coats. *Cell* 68 (4), 673–682. doi:10.1016/0092-8674(92)90143-z

Roy, S., Luetterforst, R., Harding, A., Apolloni, A., Etheridge, M., Stang, E., et al. (1999). Dominant-negative Caveolin Inhibits H-Ras Function by Disrupting Cholesterol-Rich Plasma Membrane Domains. *Nat. Cel Biol* 1 (2), 98–105. doi:10.1038/10067

Rungtabnapa, P., Nimmannit, U., Halim, H., Rojanasakul, Y., and Chanvorachote, P. (2011). Hydrogen Peroxide Inhibits Non-small Cell Lung Cancer Cell Anoikis through the Inhibition of Caveolin-1 Degradation. *Am. J. Physiol. Cel Physiol* 300 (2), C235–C245. doi:10.1152/ajpcell.00249.2010

Sala-Vila, A., Navarro-Lérida, I., Sánchez-Alvarez, M., Bosch, M., Calvo, C., López, J. A., et al. (2016). Interplay between Hepatic Mitochondria-Associated Membranes, Lipid Metabolism and Caveolin-1 in Mice. *Sci. Rep.* 6, 27351. doi:10.1038/srep27351

Sanders, Y. Y., Liu, H., Scruggs, A. M., Duncan, S. R., Huang, S. K., and Thannickal, V. J. (2017). Epigenetic Regulation of Caveolin-1 Gene Expression in Lung Fibroblasts. *Am. J. Respir. Cel Mol Biol* 56 (1), 50–61. doi:10.1165/rcmb.2016-0034OC

Santos-Parker, J. R., Strahler, T. R., Bassett, C. J., Bispham, N. Z., Chonchol, M. B., and Seals, D. R. (2017). Curcumin Supplementation Improves Vascular Endothelial Function in Healthy Middle-Aged and Older Adults by Increasing Nitric Oxide Bioavailability and Reducing Oxidative Stress. *Aging (Albany NY)* 9 (1), 187–208. doi:10.18632/aging.101149

Scherer, P. E., Okamoto, T., Chun, M., Nishimoto, I., Lodish, H. F., and Lisanti, M. P. (1996). Identification, Sequence, and Expression of Caveolin-2 Defines a Caveolin Gene Family. *Proc. Natl. Acad. Sci. U S A.* 93 (1), 131–135. doi:10.1073/pnas.93.1.131

Scherer, P. E., Tang, Z., Chun, M., Sargiacomo, M., Lodish, H. F., and Lisanti, M. P. (1995). Caveolin Isoforms Differ in Their N-Terminal Protein Sequence and Subcellular Distribution. Identification and Epitope Mapping of an Isoform-specific Monoclonal Antibody Probe. *J. Biol. Chem.* 270 (27), 16395–16401. doi:10.1074/jbc.270.27.16395

Schlegel, A., Arvan, P., and Lisanti, M. P. (2001). Caveolin-1 Binding to Endoplasmic Reticulum Membranes and Entry into the Regulated Secretory Pathway Are Regulated by Serine Phosphorylation. Protein Sorting at the Level of the Endoplasmic Reticulum. *J. Biol. Chem.* 276 (6), 4398–4408. doi:10.1074/jbc.M005448200

Shao, S., Qin, T., Qian, W., Yue, Y., Xiao, Y., Li, X., et al. (2020). Positive Feedback in Cav-1-ROS Signalling in PSCs Mediates Metabolic Coupling between PSCs and Tumour Cells. *J. Cel Mol Med* 24 (16), 9397–9408. doi:10.1111/jcmm.15596

Sharma, B., and Agnihotri, N. (2019). Role of Cholesterol Homeostasis and its Efflux Pathways in Cancer Progression. *J. Steroid Biochem. Mol. Biol.* 191, 105377. doi:10.1016/j.jsbmb.2019.105377

Sharma, S., Singh, M., and Sharma, P. L. (2012). Ameliorative Effect of Daidzein: a Caveolin-1 Inhibitor in Vascular Endothelium Dysfunction Induced by Ovariectomy. *Indian J. Exp. Biol.* 50 (1), 28–34.

Shi, Y., Tan, S. H., Ng, S., Zhou, J., Yang, N. D., Koo, G. B., et al. (2015). Critical Role of CAV1/caveolin-1 in Cell Stress Responses in Human Breast Cancer Cells via Modulation of Lysosomal Function and Autophagy. *Autophagy* 11 (5), 769–784. doi:10.1080/15548627.2015.1034411

Shihata, W. A., Putra, M. R. A., and Chin-Dusting, J. P. F. (2017). Is There a Potential Therapeutic Role for Caveolin-1 in Fibrosis. *Front. Pharmacol.* 8, 567. doi:10.3389/fphar.2017.00567

Siegert, A. M., Serra-Peinado, C., Gutiérrez-Martínez, E., Rodríguez-Pascual, F., Fabregat, I., and Egea, G. (2018). Altered TGF-β Endocytic Trafficking Contributes to the Increased Signaling in Marfan Syndrome. *Biochim. Biophys. Acta Mol. Basis Dis.* 1864 (2), 554–562. doi:10.1016/j.bbadis.2017.11.015

Sinha, B., Köster, D., Ruez, R., Gonnord, P., Bastiani, M., Abankwa, D., et al. (2011). Cells Respond to Mechanical Stress by Rapid Disassembly of Caveolae. *Cell* 144 (3), 402–413. doi:10.1016/j.cell.2010.12.031

Smart, E. J., Ying, Ys., Donzell, W. C., and Anderson, R. G. (1996). A Role for Caveolin in Transport of Cholesterol from Endoplasmic Reticulum to Plasma Membrane. *J. Biol. Chem.* 271 (46), 29427–29435. doi:10.1074/jbc.271.46.29427

Sörensson, J., Fierlbeck, W., Heider, T., Schwarz, K., Park, D. S., Mundel, P., et al. (2002). Glomerular Endothelial Fenestrae *In Vivo* Are Not Formed from Caveolae. *J. Am. Soc. Nephrol.* 13 (11), 2639–2647. doi:10.1097/01.asn.0000033277.32822.23

Sotgia, F., Martinez-Outschoorn, U. E., Howell, A., Pestell, R. G., Pavlides, S., and Lisanti, M. P. (2012). Caveolin-1 and Cancer Metabolism in the Tumor Microenvironment: Markers, Models, and Mechanisms. *Annu. Rev. Pathol.* 7, 423–467. doi:10.1146/annurev-pathol-011811-120856

Steffens, S., Schrader, A. J., Blasig, H., Vetter, G., Eggers, H., Tränkenschuh, W., et al. (2011). Caveolin 1 Protein Expression in Renal Cell Carcinoma Predicts Survival. *BMC Urol.* 11, 25. doi:10.1186/1471-2490-11-25

Sun, L. N., Chen, Z. X., Liu, X. C., Liu, H. Y., Guan, G. J., and Liu, G. (2014a). Curcumin Ameliorates Epithelial-To-Mesenchymal Transition of Podocytes *In Vivo* and *In Vitro* via Regulating Caveolin-1. *Biomed. Pharmacother.* 68 (8), 1079–1088. doi:10.1016/j.biopha.2014.10.005

Sun, L. N., Liu, X. C., Chen, X. J., Guan, G. J., and Liu, G. (2016). Curcumin Attenuates High Glucose-Induced Podocyte Apoptosis by Regulating Functional Connections between Caveolin-1 Phosphorylation and ROS. *Acta Pharmacol. Sin* 37 (5), 645–655. doi:10.1038/aps.2015.159

Sun, L. N., Yang, Z. Y., Lv, S. S., Liu, X. C., Guan, G. J., and Liu, G. (2014b). Curcumin Prevents Diabetic Nephropathy against Inflammatory Response via Reversing Caveolin-1 Tyr14 Phosphorylation Influenced TLR4 Activation. *Int. Immunopharmacol* 23 (1), 236–246. doi:10.1016/j.intimp.2014.08.023

Sun, X., Liu, Y., Li, C., Wang, X., Zhu, R., Liu, C., et al. (2017). Recent Advances of Curcumin in the Prevention and Treatment of Renal Fibrosis. *Biomed. Res. Int.* 2017, 2418671. doi:10.1155/2017/2418671

Suzuki, M. (2017). Regulation of Lipid Metabolism via a Connection between the Endoplasmic Reticulum and Lipid Droplets. *Anat. Sci. Int.* 92 (1), 50–54. doi:10.1007/s12565-016-0378-2

Sztalryd, C., and Brasaemle, D. L. (2017). The Perilipin Family of Lipid Droplet Proteins: Gatekeepers of Intracellular Lipolysis. *Biochim. Biophys. Acta Mol. Cel Biol Lipids* 1862 (10 Pt B), 1221–1232. doi:10.1016/j.bbalip.2017.07.009

Tahir, S. A., Yang, G., Goltsov, A., Song, K. D., Ren, C., Wang, J., et al. (2013). Caveolin-1-LRP6 Signaling Module Stimulates Aerobic Glycolysis in Prostate Cancer. *Cancer Res.* 73 (6), 1900–1911. doi:10.1158/0008-5472.Can-12-3040

Tamai, O., Oka, N., Kikuchi, T., Koda, Y., Soejima, M., Wada, Y., et al. (2001). Caveolae in Mesangial Cells and Caveolin Expression in Mesangial Proliferative Glomerulonephritis. *Kidney Int.* 59 (2), 471–480. doi:10.1046/j.1523-1755.2001.059002471.x

Tan, V. P., and Miyamoto, S. (2015). HK2/hexokinase-II Integrates Glycolysis and Autophagy to Confer Cellular protection. *Autophagy* 11 (6), 963–964. doi:10.1080/15548627.2015.1042195

Tang, Z., Scherer, P. E., Okamoto, T., Song, K., Chu, C., Kohtz, D. S., et al. (1996). Molecular Cloning of Caveolin-3, a Novel Member of the Caveolin Gene Family Expressed Predominantly in Muscle. *J. Biol. Chem.* 271 (4), 2255–2261. doi:10.1074/jbc.271.4.2255

Tao, B., Kraehling, J. R., Ghaffari, S., Ramirez, C. M., Lee, S., Fowler, J. W., et al. (2020). BMP-9 and LDL Crosstalk Regulates ALK-1 Endocytosis and LDL Transcytosis in Endothelial Cells. *J. Biol. Chem.* 295 (52), 18179–18188. doi:10.1074/jbc.RA120.015680

Thangavel, C., Gomes, C. M., Zderic, S. A., Javed, E., Addya, S., Singh, J., et al. (2019). NF-κB and GATA-Binding Factor 6 Repress Transcription of Caveolins in Bladder Smooth Muscle Hypertrophy. *Am. J. Pathol.* 189 (4), 847–867. doi:10.1016/j.ajpath.2018.12.013

Tomar, A., Kaushik, S., Khan, S. I., Bisht, K., Nag, T. C., Arya, D. S., et al. (2020). The Dietary Isoflavone Daidzein Mitigates Oxidative Stress, Apoptosis, and Inflammation in CDDP-Induced Kidney Injury in Rats: Impact of the MAPK Signaling Pathway. *J. Biochem. Mol. Toxicol.* 34 (2), e22431. doi:10.1002/jbt.22431

Tomassian, T., Humphries, L. A., Liu, S. D., Silva, O., Brooks, D. G., and Miceli, M. C. (2011). Caveolin-1 Orchestrates TCR Synaptic Polarity, Signal Specificity, and Function in CD8 T Cells. *J. Immunol.* 187 (6), 2993–3002. doi:10.4049/jimmunol.1101447

Torrejón, B., Cristóbal, I., Rojo, F., and García-Foncillas, J. (2017). Caveolin-1 Is Markedly Downregulated in Patients with Early-Stage Colorectal Cancer. *World J. Surg.* 41 (10), 2625–2630. doi:10.1007/s00268-017-4065-9

Trávez, A., Rabanal-Ruiz, Y., López-Alcalá, J., Molero-Murillo, L., Díaz-Ruiz, A., Guzmán-Ruiz, R., et al. (2018). The Caveolae-Associated Coiled-Coil Protein, NECC2, Regulates Insulin Signalling in Adipocytes. *J. Cel Mol Med* 22 (11), 5648–5661. doi:10.1111/jcmm.13840

Tsuda, T. (2018). Curcumin as a Functional Food-Derived Factor: Degradation Products, Metabolites, Bioactivity, and Future Perspectives. *Food Funct.* 9 (2), 705–714. doi:10.1039/c7fo01242j

Umesalma, S., Houwen, F. K., Baumbach, G. L., and Chan, S. L. (2016). Roles of Caveolin-1 in Angiotensin II-Induced Hypertrophy and Inward Remodeling of Cerebral Pial Arterioles. *Hypertension* 67 (3), 623–629. doi:10.1161/hypertensionaha.115.06565

Vainonen, J. P., Aboulaich, N., Turkina, M. V., Strålfors, P., and Vener, A. V. (2004). N-terminal Processing and Modifications of Caveolin-1 in Caveolae from Human Adipocytes. *Biochem. Biophys. Res. Commun.* 320 (2), 480–486. doi:10.1016/j.bbrc.2004.05.196

Vallejo, J., and Hardin, C. D. (2005). Expression of Caveolin-1 in Lymphocytes Induces Caveolae Formation and Recruitment of Phosphofructokinase to the Plasma Membrane. *Faseb j* 19 (6), 586–587. doi:10.1096/fj.04-2380fje

van den Heuvel, A. P., Schulze, A., and Burgering, B. M. (2005). Direct Control of Caveolin-1 Expression by FOXO Transcription Factors. *Biochem. J.* 385 (Pt 3), 795–802. doi:10.1042/bj20041449

Van Krieken, R., and Krepinsky, J. C. (2017). Caveolin-1 in the Pathogenesis of Diabetic Nephropathy: Potential Therapeutic Target. *Curr. Diab Rep.* 17 (3), 19. doi:10.1007/s11892-017-0844-9

Varela-Guruceaga, M., Milagro, F. I., Martínez, J. A., and de Miguel, C. (2018). Effect of Hypoxia on Caveolae-Related Protein Expression and Insulin Signaling in Adipocytes. *Mol. Cel Endocrinol* 473, 257–267. doi:10.1016/j.mce.2018.01.026

Vassilieva, E. V., Ivanov, A. I., and Nusrat, A. (2009). Flotillin-1 Stabilizes Caveolin-1 in Intestinal Epithelial Cells. *Biochem. Biophys. Res. Commun.* 379 (2), 460–465. doi:10.1016/j.bbrc.2008.12.118

Vihanto, M. M., Vindis, C., Djonov, V., Cerretti, D. P., and Huynh-Do, U. (2006). Caveolin-1 Is Required for Signaling and Membrane Targeting of EphB1 Receptor Tyrosine Kinase. *J. Cel Sci* 119 (Pt 11), 2299–2309. doi:10.1242/jcs.02946

Volonte, D., and Galbiati, F. (2020). Caveolin-1, a Master Regulator of Cellular Senescence. *Cancer Metastasis Rev.* 39 (2), 397–414. doi:10.1007/s10555-020-09875-w

Waalkes, S., Eggers, H., Blasig, H., Atschekzei, F., Kramer, M. W., Hennenlotter, J., et al. (2011). Caveolin 1 mRNA Is Overexpressed in Malignant Renal Tissue and Might Serve as a Novel Diagnostic Marker for Renal Cancer. *Biomark Med.* 5 (2), 219–225. doi:10.2217/bmm.11.12

Walther, T. C., Chung, J., and Farese, R. V., Jr. (2017). Lipid Droplet Biogenesis. *Annu. Rev. Cel Dev Biol* 33, 491–510. doi:10.1146/annurev-cellbio-100616-060608

Walther, T. C., and Farese, R. V., Jr. (2012). Lipid Droplets and Cellular Lipid Metabolism. *Annu. Rev. Biochem.* 81, 687–714. doi:10.1146/annurev-biochem-061009-102430

Wang, D. X., Pan, Y. Q., Liu, B., and Dai, L. (2018). Cav-1 Promotes Atherosclerosis by Activating JNK-Associated Signaling. *Biochem. Biophys. Res. Commun.* 503 (2), 513–520. doi:10.1016/j.bbrc.2018.05.036

Wang, H., Yang, P., Liu, K., Guo, F., Zhang, Y., Zhang, G., et al. (2008). SARS Coronavirus Entry into Host Cells through a Novel Clathrin- and Caveolae-independent Endocytic Pathway. *Cell Res* 18 (2), 290–301. doi:10.1038/cr.2008.15

Wang, J., Chen, M. Y., Chen, J. F., Ren, Q. L., Zhang, J. Q., Cao, H., et al. (2020a). LncRNA IMFlnc1 Promotes Porcine Intramuscular Adipocyte Adipogenesis by Sponging miR-199a-5p to Up-Regulate CAV-1. *BMC Mol. Cel Biol* 21 (1), 77. doi:10.1186/s12860-020-00324-8

Wang, L., Connelly, M. A., Ostermeyer, A. G., Chen, H. H., Williams, D. L., and Brown, D. A. (2003). Caveolin-1 Does Not Affect SR-BI-Mediated Cholesterol Efflux or Selective Uptake of Cholesteryl Ester in Two Cell Lines. *J. Lipid Res.* 44 (4), 807–815. doi:10.1194/jlr.M200449-JLR200

Wang, L., Zhao, Y., Gang, S., Geng, T., Li, M., Xu, L., et al. (2021). Inhibition of miR-103-3p Preserves Neurovascular Integrity through Caveolin-1 in Experimental Subarachnoid Hemorrhage. *Neuroscience* 461, 91–101. doi:10.1016/j.neuroscience.2021.03.007

Wang, M. D., Wang, Y., Xia, Y. P., Dai, J. W., Gao, L., Wang, S. Q., et al. (2016). High Serum MiR-130a Levels Are Associated with Severe Perihematomal Edema and Predict Adverse Outcome in Acute ICH. *Mol. Neurobiol.* 53 (2), 1310–1321. doi:10.1007/s12035-015-9099-0

Wang, N., Muhetaer, G., Zhang, X., Yang, B., Wang, C., Zhang, Y., et al. (2020b). Sanguisorba Officinalis L. Suppresses Triple-Negative Breast Cancer Metastasis by Inhibiting Late-phase Autophagy via Hif-1α/Caveolin-1 Signaling. *Front. Pharmacol.* 11, 591400. doi:10.3389/fphar.2020.591400

Wang, S., Wang, N., Zheng, Y., Yang, B., Liu, P., Zhang, F., et al. (2020c). Caveolin-1 Inhibits Breast Cancer Stem Cells via C-Myc-Mediated Metabolic Reprogramming. *Cel Death Dis* 11 (6), 450. doi:10.1038/s41419-020-2667-x

Wettersten, H. I., Aboud, O. A., Lara, P. N., Jr., and Weiss, R. H. (2017). Metabolic Reprogramming in clear Cell Renal Cell Carcinoma. *Nat. Rev. Nephrol.* 13 (7), 410–419. doi:10.1038/nrneph.2017.59

Wilfling, F., Haas, J. T., Walther, T. C., and Farese, R. V., Jr. (2014). Lipid Droplet Biogenesis. *Curr. Opin. Cel Biol* 29, 39–45. doi:10.1016/j.ceb.2014.03.008

Williams, T. M., and Lisanti, M. P. (2004). The Caveolin Proteins. *Genome Biol.* 5 (3), 214. doi:10.1186/gb-2004-5-3-214

Wong, T. H., Dickson, F. H., Timmins, L. R., and Nabi, I. R. (2020). Tyrosine Phosphorylation of Tumor Cell Caveolin-1: Impact on Cancer Progression. *Cancer Metastasis Rev.* 39 (2), 455–469. doi:10.1007/s10555-020-09892-9

Wong, T. H., Khater, I. M., Joshi, B., Shahsavari, M., Hamarneh, G., and Nabi, I. R. (2021). Single Molecule Network Analysis Identifies Structural Changes to Caveolae and Scaffolds Due to Mutation of the Caveolin-1 Scaffolding Domain. *Sci. Rep.* 11 (1), 7810. doi:10.1038/s41598-021-86770-6

Woodman, O. L., Missen, M. A., and Boujaoude, M. (2004). Daidzein and 17 Beta-Estradiol Enhance Nitric Oxide Synthase Activity Associated with an Increase in Calmodulin and a Decrease in Caveolin-1. *J. Cardiovasc. Pharmacol.* 44 (2), 155–163. doi:10.1097/00005344-200408000-00003

Wu, D., Yang, X., Zheng, T., Xing, S., Wang, J., Chi, J., et al. (2016). A Novel Mechanism of Action for Salidroside to Alleviate Diabetic Albuminuria: Effects on Albumin Transcytosis across Glomerular Endothelial Cells. *Am. J. Physiol. Endocrinol. Metab.* 310 (3), E225–E237. doi:10.1152/ajpendo.00391.2015

Wu, S. Z., Peng, F. F., Li, J. L., Ye, F., Lei, S. Q., and Zhang, B. F. (2014). Akt and RhoA Activation in Response to High Glucose Require Caveolin-1 Phosphorylation in Mesangial Cells. *Am. J. Physiol. Ren. Physiol* 306 (11), F1308–F1317. doi:10.1152/ajprenal.00447.2013

Xie, X., Peng, J., Chang, X., Huang, K., Huang, J., Wang, S., et al. (2013). Activation of RhoA/ROCK Regulates NF-Kb Signaling Pathway in Experimental Diabetic Nephropathy. *Mol. Cel Endocrinol* 369 (1-2), 86–97. doi:10.1016/j.mce.2013.01.007

Xie, Z., Zeng, X., Waldman, T., and Glazer, R. I. (2003). Transformation of Mammary Epithelial Cells by 3-phosphoinositide- Dependent Protein Kinase-1 Activates Beta-Catenin and C-Myc, and Down-Regulates Caveolin-1. *Cancer Res.* 63 (17), 5370–5375. Available at: https://cancerres.aacrjournals.org/content/canres/63/17/5370.full.pdf.

Xing, Y., Wen, Z., Gao, W., Lin, Z., Zhong, J., and Jiu, Y. (2020). Multifaceted Functions of Host Cell Caveolae/Caveolin-1 in Virus Infections. *Viruses* 12 (5), 487. doi:10.3390/v12050487

Xu, Y., Du, X., Turner, N., Brown, A. J., and Yang, H. (2019). Enhanced Acyl-CoA: cholesterol Acyltransferase Activity Increases Cholesterol Levels on the Lipid Droplet Surface and Impairs Adipocyte Function. *J. Biol. Chem.* 294 (50), 19306–19321. doi:10.1074/jbc.RA119.011160

Xue, H., Li, P., Luo, Y., Wu, C., Liu, Y., Qin, X., et al. (2019). Salidroside Stimulates the Sirt1/PGC-1α axis and Ameliorates Diabetic Nephropathy in Mice. *Phytomedicine* 54, 240–247. doi:10.1016/j.phymed.2018.10.031

Xue, W., Wang, J., Jiang, W., Shi, C., Wang, X., Huang, Y., et al. (2020). Caveolin-1 Alleviates Lipid Accumulation in NAFLD Associated with Promoting Autophagy by Inhibiting the Akt/mTOR Pathway. *Eur. J. Pharmacol.* 871, 172910. doi:10.1016/j.ejphar.2020.172910

Yamaguchi, T., Lu, C., Ida, L., Yanagisawa, K., Usukura, J., Cheng, J., et al. (2016). ROR1 Sustains Caveolae and Survival Signalling as a Scaffold of Cavin-1 and Caveolin-1. *Nat. Commun.* 7, 10060. doi:10.1038/ncomms10060

Yamaguchi, Y., Yasuoka, H., Stolz, D. B., and Feghali-Bostwick, C. A. (2011). Decreased Caveolin-1 Levels Contribute to Fibrosis and Deposition of Extracellular IGFBP-5. *J. Cel Mol Med* 15 (4), 957–969. doi:10.1111/j.1582-4934.2010.01063.x

Yan, F., Su, L., Chen, X., Wang, X., Gao, H., and Zeng, Y. (2020). Molecular Regulation and Clinical Significance of Caveolin-1 Methylation in Chronic Lung Diseases. *Clin. Transl Med.* 10 (1), 151–160. doi:10.1002/ctm2.2

Yan, R., Cao, P., Song, W., Qian, H., Du, X., Coates, H. W., et al. (2021). A Structure of Human Scap Bound to Insig-2 Suggests How Their Interaction Is Regulated by Sterols. *Science* 371 (6533), eabb2224. doi:10.1126/science.abb2224

Yang, G., Xu, H., Li, Z., and Li, F. (2014). Interactions of Caveolin-1 Scaffolding and Intramembrane Regions Containing a CRAC Motif with Cholesterol in Lipid Bilayers. *Biochim. Biophys. Acta* 1838 (10), 2588–2599. doi:10.1016/j.bbamem.2014.06.018

Yang, J., Zhu, T., Zhao, R., Gao, D., Cui, Y., Wang, K., et al. (2018). Caveolin-1 Inhibits Proliferation, Migration, and Invasion of Human Colorectal Cancer Cells by Suppressing Phosphorylation of Epidermal Growth Factor Receptor. *Med. Sci. Monit.* 24, 332–341. doi:10.12659/msm.907782

Yang, Z., Wang, L., Yu, H., Wang, R., Gou, Y., Zhang, M., et al. (2019). Membrane TLR9 Positive Neutrophil Mediated MPLA Protects against Fatal Bacterial Sepsis. *Theranostics* 9 (21), 6269–6283. doi:10.7150/thno.37139

Yokomori, H., Ando, W., and Oda, M. (2019). Caveolin-1 Is Related to Lipid Droplet Formation in Hepatic Stellate Cells in Human Liver. *Acta Histochem.* 121 (2), 113–118. doi:10.1016/j.acthis.2018.10.008

Yoon, H. J., Kim, D. H., Kim, S. J., Jang, J. H., and Surh, Y. J. (2019). Src-mediated Phosphorylation, Ubiquitination and Degradation of Caveolin-1 Promotes Breast Cancer Cell Stemness. *Cancer Lett.* 449, 8–19. doi:10.1016/j.canlet.2019.01.021

Yuan, T., Hong, S., Yao, Y., and Liao, K. (2007). Glut-4 Is Translocated to Both Caveolae and Non-caveolar Lipid Rafts, but Is Partially Internalized through Caveolae in Insulin-Stimulated Adipocytes. *Cel Res* 17 (9), 772–782. doi:10.1038/cr.2007.73

Zager, R. A., Johnson, A., Hanson, S., and dela Rosa, V. (2002). Altered Cholesterol Localization and Caveolin Expression during the Evolution of Acute Renal Failure. *Kidney Int.* 61 (5), 1674–1683. doi:10.1046/j.1523-1755.2002.00316.x

Zakrzewicz, D., Didiasova, M., Zakrzewicz, A., Hocke, A. C., Uhle, F., Markart, P., et al. (2014). The Interaction of Enolase-1 with Caveolae-Associated Proteins Regulates its Subcellular Localization. *Biochem. J.* 460 (2), 295–307. doi:10.1042/bj20130945

Zhang, B., Peng, F., Wu, D., Ingram, A. J., Gao, B., and Krepinsky, J. C. (2007). Caveolin-1 Phosphorylation Is Required for Stretch-Induced EGFR and Akt Activation in Mesangial Cells. *Cell Signal* 19 (8), 1690–1700. doi:10.1016/j.cellsig.2007.03.005

Zhang, C. J., Zhu, N., Wang, Y. X., Liu, L. P., Zhao, T. J., Wu, H. T., et al. (2021). Celastrol Attenuates Lipid Accumulation and Stemness of Clear Cell Renal Cell Carcinoma via CAV-1/LOX-1 Pathway. *Front. Pharmacol.* 12, 658092. doi:10.3389/fphar.2021.658092

Zhang, D., Gava, A. L., Van Krieken, R., Mehta, N., Li, R., Gao, B., et al. (2019). The Caveolin-1 Regulated Protein Follistatin Protects against Diabetic Kidney Disease. *Kidney Int.* 96 (5), 1134–1149. doi:10.1016/j.kint.2019.05.032

Zhang, X., Ramírez, C. M., Aryal, B., Madrigal-Matute, J., Liu, X., Diaz, A., et al. (2020a). Cav-1 (Caveolin-1) Deficiency Increases Autophagy in the Endothelium and Attenuates Vascular Inflammation and Atherosclerosis. *Arterioscler Thromb. Vasc. Biol.* 40 (6), 1510–1522. doi:10.1161/atvbaha.120.314291

Zhang, Y., Peng, F., Gao, B., Ingram, A. J., and Krepinsky, J. C. (2012). High Glucose-Induced RhoA Activation Requires Caveolae and PKCβ1-Mediated ROS Generation. *Am. J. Physiol. Ren. Physiol* 302 (1), F159–F172. doi:10.1152/ajprenal.00749.2010

Zhang, Y., Qu, X., Li, C., Fan, Y., Che, X., Wang, X., et al. (2015). miR-103/107 Modulates Multidrug Resistance in Human Gastric Carcinoma by Downregulating Cav-1. *Tumour Biolcell Mol. Life Sci.* 36 (4), 2277–2285. doi:10.1007/s13277-014-2835-7

Zhang, Z., Gao, Z., Rajthala, S., Sapkota, D., Dongre, H., Parajuli, H., et al. (2020b). Metabolic Reprogramming of normal Oral Fibroblasts Correlated with

Increased Glycolytic Metabolism of Oral Squamous Cell Carcinoma and Precedes Their Activation into Carcinoma Associated Fibroblasts. 77 (46), 1115–1133. doi:10.1007/s00018-019-03209-y

Zhao, R., Liu, K., Huang, Z., Wang, J., Pan, Y., Huang, Y., et al. (2015). Genetic Variants in Caveolin-1 and RhoA/ROCK1 Are Associated with Clear Cell Renal Cell Carcinoma Risk in a Chinese Population. *PLoS One* 10 (6), e0128771. doi:10.1371/journal.pone.0128771

Zhong, W., Li, Y. C., Huang, Q. Y., and Tang, X. Q. (2020). lncRNA ANRIL Ameliorates Oxygen and Glucose Deprivation (OGD) Induced Injury in Neuron Cells via miR-199a-5p/CAV-1 Axis. *Neurochem. Res.* 45 (4), 772–782. doi:10.1007/s11064-019-02951-w

Zhou, H., Liu, J., Ren, L., Liu, W., Xing, Q., Men, L., et al. (2014). Relationship between [corrected] Spatial Memory in Diabetic Rats and Protein Kinase Cγ, Caveolin-1 in the hippocampus and Neuroprotective Effect of Catalpol. *Chin. Med. J. (Engl)* 127 (5), 916–923. doi:10.3760/cma.j.issn.0366-6999.20132137

Zhu, Q., Zhan, D., Zhu, P., Chong, Y., and Yang, Y. (2020). CircAKT1 Acts as a Sponge of miR-338-3p to Facilitate clear Cell Renal Cell Carcinoma Progression by Up-Regulating CAV1. *Biochem. Biophys. Res. Commun.* 532 (4), 584–590. doi:10.1016/j.bbrc.2020.08.081

Zhu, T., Meng, Q., Ji, J., Zhang, L., and Lou, X. (2017). TLR4 and Caveolin-1 in Monocytes Are Associated with Inflammatory Conditions in Diabetic Neuropathy. *Clin. Transl Sci.* 10 (3), 178–184. doi:10.1111/cts.12434

Zimnicka, A. M., Husain, Y. S., Shajahan, A. N., Sverdlov, M., Chaga, O., Chen, Z., et al. (2016). Src-dependent Phosphorylation of Caveolin-1 Tyr-14 Promotes Swelling and Release of Caveolae. *Mol. Biol. Cel* 27 (13), 2090–2106. doi:10.1091/mbc.E15-11-0756

Zschocke, J., Manthey, D., Bayatti, N., van der Burg, B., Goodenough, S., and Behl, C. (2002). Estrogen Receptor Alpha-Mediated Silencing of Caveolin Gene Expression in Neuronal Cells. *J. Biol. Chem.* 277 (41), 38772–38780. doi:10.1074/jbc.M205664200

Zsiros, V., Katz, S., Doczi, N., and Kiss, A. L. (2019). Endocytosis of GM-CSF Receptor β Is Essential for Signal Transduction Regulating Mesothelial-Macrophage Transition. *Biochim. Biophys. Acta Mol. Cel Res* 1866 (9), 1450–1462. doi:10.1016/j.bbamcr.2019.06.005

Conflict of Interest: The authors declare that the research was conducted in the absence of any commercial or financial relationships that could be construed as a potential conflict of interest.

Publisher's Note: All claims expressed in this article are solely those of the authors and do not necessarily represent those of their affiliated organizations, or those of the publisher, the editors and the reviewers. Any product that may be evaluated in this article, or claim that may be made by its manufacturer, is not guaranteed or endorsed by the publisher.

frontiers in Pharmacology

REVIEW
published: 22 December 2021
doi: 10.3389/fphar.2021.807119

Insulin-Like Growth Factor Binding Proteins in Kidney Disease

Shuqiang Wang[1,2], *Kun Chi*[1], *Di Wu*[1] *and Quan Hong*[1]*

[1]*Department of Nephrology, Chinese PLA General Hospital, Chinese PLA Institute of Nephrology, State Key Laboratory of Kidney Diseases, National Clinical Research Center for Kidney Diseases, Beijing Key Laboratory of Kidney Diseases, Beijing, China,* [2]*Department of Nephrology, Peking University Shenzhen Hospital, Shenzhen, China*

The seven members of the insulin-like growth factor (IGF) binding protein family (IGFBPs) were initially considered to be the regulatory proteins of IGFs in the blood circulation, mainly as the subsequent reserve for bidirectional regulation of IGF function during environmental changes. However, in recent years, IGFBPs has been found to have many functions independent of IGFs. The role of IGFBPs in regulating transcription, inducing cell migration and apoptosis is closely related to the occurrence and development of kidney disease. IGFBP-1, IGFBP-3, IGFBP-4 are closely associated with diabetes and diabetic nephropathy. IGFBP-3, IGFBP-4, IGFBP-5, IGFBP-6 are involved in different kidney disease such as diabetes, FSGS and CKD physiological process as apoptosis proteins, IGFBP-7 has been used in clinical practice as a biomarker for early diagnosis and prognosis of AKI. This review focuses on the differential expression and pathogenesis of IGFBPs in kidney disease.

Keywords: IGFBPs, kidney disease, function, mechanism, biomarker

OPEN ACCESS

Edited by:
Zhiyong Guo,
Second Military Medical University, China

Reviewed by:
Prasanna K. Santhekadur,
JSS Academy of Higher Education and Research, India
Jianlou Niu,
Wenzhou Medical University, China

***Correspondence:**
Quan Hong
hongquan@301hospital.com.cn

Specialty section:
This article was submitted to Renal Pharmacology, a section of the journal Frontiers in Pharmacology

Received: *01 November 2021*
Accepted: *08 December 2021*
Published: *22 December 2021*

Citation:
Wang S, Chi K, Wu D and Hong Q (2021) Insulin-Like Growth Factor Binding Proteins in Kidney Disease. Front. Pharmacol. 12:807119. doi: 10.3389/fphar.2021.807119

INTRODUCTION

Insulin-like growth factors (IGFs), including IGF-I and IGF-II, are members of the insulin superfamily of growth promoting peptides, and are one of the most abundant and common growth factor polypeptides. IGFs have seven exclusive high-affinity IGF binding proteins (IGFBPs) *in vivo*. IGFBPs exists in blood circulation, extracellular tissue fluid and intracellular tissues, and they can regulate the half-life of IGF in blood circulation, the distribution of IGF in tissues and its binding to cell receptors (Baxter, 2014). It is precisely because of the presence of these seven IGFBPs that complicates the biological utilization and signal transduction of IGF.

IGFBPs is a class of secreted proteins that is able to interact with many ligands other than IGFs, and most of these interactions are believed to be independent of the IGF-IGFR signaling pathway, so these functions of IGFBPs are independent of IGFs/IGFR (Holbourn et al., 2008). At present, IGFBPs research is mainly focused on the tumor field. Multitudes of preclinical studies have shown that IGFBPs can inhibit the growth of tumors, but some studies believe that IGFBPs also exist as an oncogene. In addition, there is evidence that some IGFBPs may be potential biomarkers that can be used to evaluate tumor prognosis or therapeutic resistance.

In recent years, the role of IGFBPs in kidney disease has been taking serious gradually. Studies showed that the growth binding protein family are associated with the development of kidney, primary renal diseases such as mesangial proliferation of IgA nephropathy (IgAN), secondary kidney disease such as diabetic nephropathy (DN), and chronic kidney disease (CKD). Similar to tumors, researchers are also keen to find early diagnosis and prognostic biomarkers for these various kidney diseases. Currently, IGFBP-7 has been used as an early diagnosis and prognostic marker for acute renal insufficiency (AKI). Other IGFBPs are also identified as biomarkers in different kidney diseases

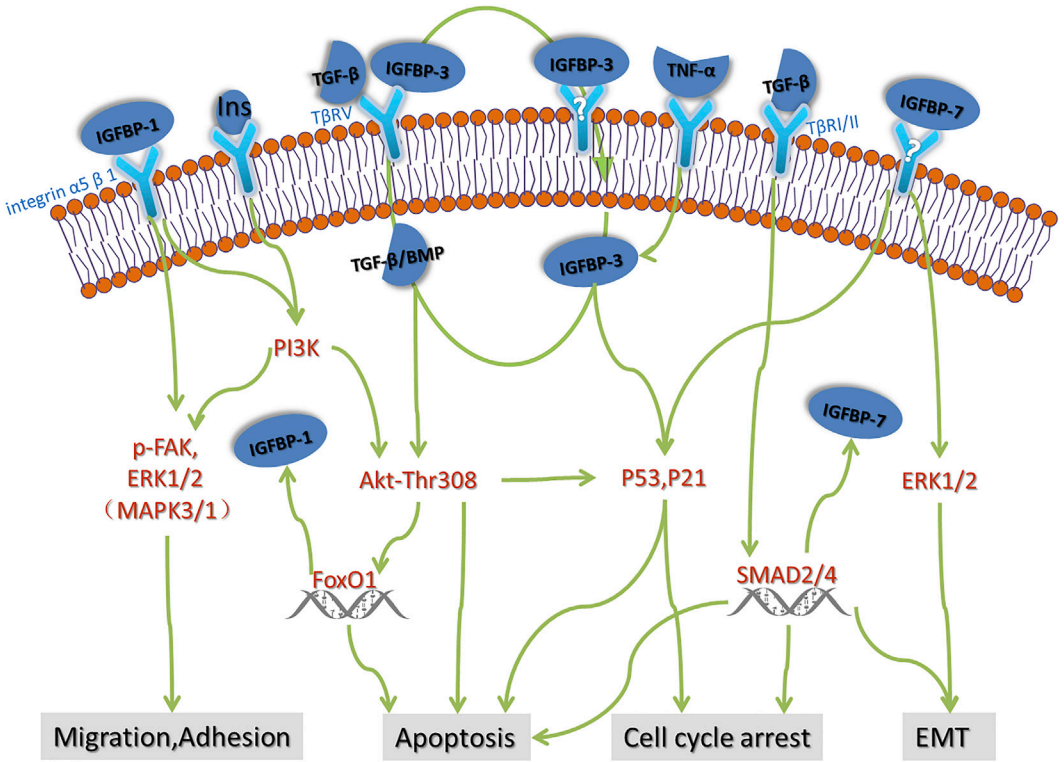

FIGURE 1 | Possible pathogenesis of IGFBPs in renal disease. There are few studies on the mechanism of action of IGFBPs in renal disease. Based on the advances in oncology and rheumatology, we speculate that some of the possible mechanisms of action of IGFBPs in renal disease including cell migration, adhesion, apoptosis, cell cycle arrest and EMT, which need to be further verified by strict basic experiments.

(**Table 1**). This review will review the basic research of the application of IGFBP family in kidney disease, and summarize the research status of IGFBPs in kidney disease, so as to provide some reference for new research.

THE BASIC MOLECULAR BIOLOGY OF THE IGFBP FAMILY

According to evolution tracking, the homology of IGFBP family genes expanded in the two basal vertebrate tetraploidization (2R) and recombined in the genome of early prochordate animals (Daza et al., 2011). Based on the strict definition of structure and function, there are six recognized IGFBP family proteins named IGFBP-1~IGFBP-6. Although there is still debate about whether IGFBP-7 should be classified as IGFBPs or defined as IGFBP-related protein (IGFBP-rPs) due to its weaker affinity for IGF-I and IGF-II compared with IGFBP-1~IGFBP-6, the name "IGFBP-7" is still widely used in the research.

The precursory IGFBP sequence generally has 240–328 amino acid residues before the cleavage of the signal peptide (Daza et al., 2011). Common post-translational modifications of IGFBP family proteins include n-terminal glycosylation, phosphorylation of serine/threonine, and partial proteolysis. The main domains of IGFBPs mainly include IGF binding domains at the amino terminal, heparin binding domains, insulin binding domains and the acid-labile subunit (ALS) in the central region, as well as RGD integrin-binding domains at the carboxyl terminal and nuclear localization domains (Firth and Baxter, 2002). Therefore, IGFBP family has a wide range of molecular functions. In addition to binding to IGF, IGFBP can also bind to cell membrane receptors, integrin family, and play a role directly in the nucleus. IGFBP-3, IGFBP-5 and IGFBP-6 enter the nucleus by binding to the nuclear transporter importin-β through NLS, the same nuclear localization domain at the c-terminal (Schedlich et al., 2000). There is no c-terminal NLS subunit in IGFBP-2, but a structure domain similar to NLS is in the center of IGFBP-2, which is suspected to mediate the nucleation of IGFBP-2 after the combination of importin-β (Azar et al., 2013). However, there is no research showing that the remaining IGFBP are able to import to the nucleus.

IGFBP-1

IGFBP-1 is the first IGF-binding protein with the molecular weight of 27.9 KDa. IGFBP-1 is high expressed in the female reproductive system and liver, but is low expressed in the kidney. In kidney, IGFBP-1 is mainly expressed in the glomerulus. IGFBP-1 is associated with body and kidney development. All of the whole weight, kidney weight and nephron of IGFBP-1 transgenic mice reduce slightly (Rajkumar et al., 1995). IGFBP-1

TABLE 1 | IGFBPs expression of kidney disease in serum and urine. More and more studies have been conducted on the expression of IGFBPs in renal diseases, mainly focusing on CKD and AKI. All IGFBPs expressions were elevated in the serum of CKD patients, and IGFBP-7 has been a representative marker of AKI, but studies of IGFBPs on primary renal disease still rare.

Disease	Sample	IGFBPs	References
MCD	Urine	IGFBP-1↑	Worthmann et al. (2010)
IgAN	Serum	IGFBP-1↑	Tokunaga et al. (2010)
FSGS	Urine	IGFBP-1↑,IGFBP-3↑	Worthmann et al. (2010)
DKD	Serum	IGFBP-1↑(T1D and DN)	(Gokulakrishnan et al., 2012; Gu et al., 2014; Al Shawaf et al., 2019)
	—	IGFBP-1↓(T2D)	—
	—	IGFBP-2↑,IGFBP-4↑	—
LN	Serum	IGFBP-2↑,IGFBP-4↑	(Wu et al., 2016b; Ding et al., 2016)
AKI	Serum	IGFBP-2↑,IGFBP-7↑	(Bai et al., 2018; Li et al., 2018)
	Urine	IGFBP-7↑	(Kashani et al., 2013; Bihorac et al., 2014)
CKD	Serum	IGFBP-1↑,IGFBP-2↑,IGFBP-3↑, IGFBP-5↑,IGFBP-4↑,IGFBP-6↑	(Fukuda et al., 1998; Ulinski et al., 2000; Dittmann et al., 2012; Sayanthooran et al., 2017; Mirna et al., 2020; Ravassa et al., 2020)

plays an important role in diabetes and diabetic nephropathy. IGFBP-1 is associated closely with obesity and insulin resistance (Maddux et al., 2006; Rajwani et al., 2012; Bernardo et al., 2015; Zaghlool et al., 2021). The diagnosis, treatment and prognosis of type 1 and type 2 diabetes mellitus are very different, and the mechanisms of diabetic kidney disease (DKD) are still unclear, the treatment of DKD is a difficulty in clinic. Type 1 diabetes (T1D) and DN had increased circulating IGFBP-1 level and decreased DNA methylation levels of the IGFBP-1 gene. Whereas, low serum IGFBP-1 levels and increased DNA methylation levels in the IGFBP-1 gene were associated with the risk of type 2 diabetes (T2D) (Gu et al., 2014), implies that IGFBP-1 is involved in different types of diabetes by different mechanisms. Glomerulus IGFBP-1 is reduced in early type 2 DKD and controlled by PI3K–FoxO1 activity in podocytes (Lay et al., 2021), thereby to play a role in DKD. In this way, IGFBP-1 may be a promising candidate for diagnoses and therapeutic development in the field of DM and DKD.

In addition, researchers explored the role of IGFBP-1 in other kidney disease. IGFBP-1 expression is elevated in IgA nephropathy, FSGS, acute kidney injury (AKI) and CKD. And it is correlated with estimated glomerular filtration rate (eGFR), cell proliferation (Gleeson et al., 2001), glomerular sclerosis (Doublier et al., 2000; Worthmann et al., 2010), erythropoietin induced stress state (Yamashita et al., 2016) and interstitial fibrosis (Tokunaga et al., 2010). But these mechanism needs to be tested further.

IGFBP-2

IGFBP-2 mRNA was high expressed in the liver and pancreas, less expressed in the kidney. In kidney, IGFBP-2 is mainly expressed in the mesangial cells. The molecular weight of IGFBP-2 is about 34.8 KDa. Studies of IGFBP-2 focused in secondary nephritis caused by autoimmune disease. Clinical studies found that serum IGFBP-2 is increased in lupus nephritis (LN), but there is controversy in whether IGFBP-2 is related to renal function. In some studies, serum IGFBP-2 level is correlated positively with serum creatinine and can be used as a marker of to reflect the activity and chronic degree of nephritis (Wu et al., 2016a; Ding et al., 2016). But in another study detected by cytokine antibody array, IGFBP-2 is highly related to the activity of SLE and LN, but no significant association with reduced renal function (Yan et al., 2020). This difference in results may due to different race, sample size and detection methods, thus we need more studies to get verification. In basic studies, the increased expression of IGFBP-2 in the outer cortical glomerulus may be associated with glomerular sclerosis and renal loss in lupus nephritis (Mohammed et al., 2003), and it may inhibit the mesangial proliferation induced by IGF-1 and enhance the extracellular matrix deposition (Wolf et al., 2000).

Except LN, IGFBP-2 in the blood can be used as an early diagnostic marker for AKI, and its sensitivity is higher than creatinine, urea nitrogen and cystatin C (Li et al., 2018), and this might be induced by hypoxia (Minchenko et al., 2015). In studies related to chronic kidney disease, circulating IGFBP-2 increased in CKD patients with different conditions, including experimental uremia, CKD caused by heart failure, and children with CKD (Powell et al., 1996; Tönshoff et al., 1997; Mahesh and Kaskel, 2008; Narayanan et al., 2012; Mirna et al., 2020; Ravassa et al., 2020). What's more, clinical studies have also tracked the renal function level and plasma IGFBP-2 concentration of more than 400 patients with diabetic nephropathy over an 8-year period, suggesting that IGFBP-2 is a biomarker to predict longitudinal deterioration of renal function in patients with type 2 diabetes (Narayanan et al., 2012).

IGFBP-3

IGFBP-3 is highly expressed in female reproductive system and less expressed in kidney. The molecular weight of IGFBP-3 is 31.6 KDa. IGFBP-3 is the most important IGFBPs in the blood, combining 75–90% IGF-I in circulation (Oh, 2012). Compared with other IGFBPs, IGFBP-3 is involved in a wider range of kidney diseases.

In primary nephropathy, IGFBP-3 is involved in the development of IgA nephropathy and podocytosis. IgA nephropathy is an important type of mesangial proliferative nephropathy. IGFBP-3 was found to be up-regulated in the kidney of experimental IgA nephropathy (Tokunaga et al.,

2010). Further research found that in mesangial cells, the expression and release of IGFBP-3 were regulated by IGF and TGF-β. IGFBP-3, TGF-β and IGF form feedback regulation in the glomerulus locally (Grellier et al., 1996). Micropathological nephropathy (MCD) and focal segmentsclerosing nephritis (FSGS) are podocyte diseases. There are few positive podocyte marker (PDX) cells in MCD and more positive cells in FSGS (Worthmann et al., 2010), suggesting that the glomerular podocyte shedding of FSGS is serious, and apoptosis is the important cause of podocyte shedding. Consistent with the excretion rate of PDX cells, the urine excretion rate and the expression in plasma of IGFBP-3 in active FSGS model mice and FSGS patients were significantly up-regulated (Srivastava et al., 2019), IGFBP-3 can be used as a noninvasive biomarker for diagnosis and prognosis of FSGS. In podocytosis, rodent studies have shown that IGFBP-3 regulate the TGF-β/BMP-7 signaling pathway of podocytes and induce apoptosis of podocytes (Peters et al., 2006), what's more, TGF-β induce up-regulation of IGFBP-3 mRNA expression in human podocytes (Worthmann et al., 2010). In addition, some tumor studies have confirmed that IGFBP-3 promote cell apoptosis through the P53 pathway induced by TGF-β or TNF-α (Besset et al., 1996; Williams et al., 2000). These studies remind us that there might be a positive feedback pathway between TGF-β and IGFBP-3, suggesting a role for IGFBP-3 as a general mediator of programmed death.

The pro-apoptotic effect of IGFBP-3 is also reflected in diabetic nephropathy. IGFBP-3 play an in-depth role in diabetes via apoptosis. Clinical studies showed that IGFBP-3 is down-regulated in Type 2 Diabetes patients with renal disfunction, and predict future renal decline in people with type 2 diabetes combined with apoA4 and CD5L (Peters et al., 2017; Peters et al., 2019). In terms of mechanism, IGFBP-3 mediates high glucose-induced apoptosis by blocking Akt phosphorylation at threonine 308 (pThr308) in mesangial cell and increasing oxidative stress in proximal tubular epithelial Cells (Vasylyeva et al., 2005; Yoo et al., 2011).

Except these, a study including a large population based of 4,028 men and women aged 20–81 years with adjusting for age, waist circumference and type 2 diabetes mellitus showed that IGFBP-3 increases in the blood circulation of in CKD and is negatively correlated with eGFR (Dittmann et al., 2012), However, whether IGFBP-3 is involved in the pathogenesis of CKD or merely serves as a biomarker to indicate the presence of CKD remains to be further studied.

IGFBP-4

IGFBP-4 is highly expressed in the female reproductive system and the liver, and a little less in kidney. IGFBP-4 has the molecular weight of 27.9 KDa. Like other IGFBPs, IGFBP-4 plays an important role in diabetes mellitus and diabetic nephropathy. People with DN have a significant increase in their plasma IGFBP-1 and IGFBP-4 (Al Shawaf et al., 2019), more importantly, IGFBP-4 fragments (including N- and C-terminal fragments (NT-IGFBP-4 and CT-IGFBP-4)) are related to cardiovascular mortality in type 1 diabetes patients no matter with or without nephropathy (Hjortebjerg et al., 2015). Cardiovascular events are endpoint of death in the vast majority of patients with DN, in this way, IGFBP-4 is potential to serve as a predictive marker for DN patients without affected by their own kidney disease.

Among other kidney diseases, IGFBP-4 was found high expressed in the serum of CKD patients, and this is correlated with the kidney failure degree, the reduced osteogenesis during osteodystrophia (Van Doorn et al., 2001), and growth retardation in children with CKD (Ulinski et al., 2000). Other studies have found that the serum concentration of IGFBP-4 is closely associated with the chronic index of lupus nephritis and the estimated glomerular filtration rate (eGFR), and can be used as a marker for lupus nephritis (Wu et al., 2016b).

IGFBP-5

IGFBP-5 is highly expressed in the female reproductive system, and the expression of the kidney is medium. The molecular weight of IGFBP-5 is 30.6 KDa. Previous studies showed that IGFBP-5 is highest expressed in mesangial cells (Matsell et al., 1994), thus most of the early studies are concentrated on mesangial cells. The heparin domain of IGFBP-5 mediate the migration of the mesangial cells by combining cdc42 in the high glucose environment (Abrass et al., 1997; Berfield et al., 2000), and IGFBP-5 increases in the glomerular hypertrophy of early diabetes (Schaeffer et al., 2010). But recent studies of single-cell sequencing and our exploration showed that IGFBP-5 is highly expressed in the renal interstitial, which is the highest in kidney vascular endothelial cell and closely related to CKD (Karaiskos et al., 2018; Park et al., 2018). Studies of IGFBP-5 in renal diseases are rare and non-systematic, however, its role in tumor migration, proliferation (Dong et al., 2020) and tissue fibrosis (Nguyen et al., 2018) suggests that IGFBP-5 might be a potential maker which can not be ignored in kidney disease.

IGFBP-6

IGFBP-6 is the smallest IGFBP with the molecular weight of 25.3 KDa mRNA and protein expression level of IGFBP-6 is high in the kidney. Interestingly, IGFBP-6 can be generated by cleavage of IGFBP-2 by protease in canine renal tubular epithelial cells (MDCK) (Shalamanova et al., 2001). IGFBP-6 was infrequently studied in the kidney, while mostly in proteomic studies of CKD. The abundance of IGFBP-6 in plasma of adults and children with CKD or ERSD were all significantly up-regulated (Jarkovská et al., 2005; Christensson et al., 2018), Consistent with these, the monitoring of plasma IGFBP-6 before and after kidney transplantation and at the time of rejection showed that IGFBP-6 indicate the status of renal function in patients with chronic renal insufficiency (Fukuda et al., 1998), level of IGFBP-6 increases significantly by 8–25 times with the decrease of renal function (Jehle et al., 2000). Meanwhile, the urine abundance of IGFBP-6 gradually increased with kidney

developments (CharltonNorwood et al., 2012; Wang and Li, 2015), and is associated with developmental retardation in children with CKD (Powell et al., 1997), suggesting that it was related to the kidney development process. However, these studies did not refer to the mechanism of IGFBP-6 involvement. But IGFBP-6 has been widely studied in tumor and nervous system as a pro-apoptotic protein (Wang et al., 2017; Qiu et al., 2018). Since cell senescence and apoptosis are also important in development and chronic kidney disease, we speculated that IGFBP-6 might be involved in development and fibrosis by regulating apoptosis of renal cells, but more basic research evidence is needed.

IGFBP-7

IGFBP-7 is high expressed in liver, kidney, bone and muscle, and the expression level is higher in renal tubules. The molecular weight of IGFBP-7 is 29.1 kda. Whether IGFBP-7 should be classified into the IGFBP family is still controversial currently. Because of the weak binding forces between IGFBP-7 and IGF, some studies suggest that they should be classified as IGFBP related proteins (IGFBP-rps). But IGFBP-7 plays a quite important role in kidney, and the main use of IGFBP-7 is the early predictive and prognostic marker for AKI(Bai et al., 2018; Cho et al., 2019). The diagnostic performance of TIMP-2 and IGFBP-7 as biomarkers of AKI was first described in Sapphire study (Kashani et al., 2013). This observational study including 744 patients across 20 North American and 15 European centers led to subsequent clinical study boom on IGFBP-7 and AKI induced by various causes. A year later, the Topaz study prospectively validated the urinary [TIMP-2]•[IGFBP-7] test's ability (at the 0.3 cutoff level) to identify critically ill patients at high risk for developing moderate to severe AKI within 12 h with the high sensitivity of 92% [95% confidence interval (CI), 85–98%] (Bihorac et al., 2014). Based on Sapphire and Topaz study, the urine compound of TIMP-2 and IGFBP-7 became the first US Food and Drug Administration (FDA)-approved biomarker for risk assessment of AKI in ICU patients in 2014 (Us Food and Drug Administ, 2014). In terms of pathogenic mechanism, TIMP-2 and IGFBP-7 have been confirmed to participate in cell apoptosis by p53, p21, p27 and ERK1/2 signaling as G1 cell-cycle arrest maker during the early phases of cell injury (Kashani et al., 2013; Wang et al., 2018).

SUMMARY AND OUTLOOK

The mRNA expression of IGFBP family is generally low in the kidney, and so far there is less research about IGFBPs in kidney disease, thus the location of most IGFBP in the kidney is not clear. The IGFBP family has a variety of functions, including control the development of the kidney by interacting with IGF, and regulating the biological process of cell proliferation, apoptosis and differentiation independent of IGF, thus participating in the development of IgA nephropathy, podocyte disease, lupus nephritis and diabetic nephropathy. IGFBP-1, IGFBP-3, IGFBP-4 are closely associated with diabetes and diabetic nephropathy. IGFBP-3, IGFBP-4, IGFBP-5, IGFBP-6 are involved in different kidney disease such as diabetes, FSGS and CKD physiological process as apoptosis proteins, IGFBP-7 has been used in clinical practice as a biomarker for early diagnosis and prognosis of AKI. Although the current studies on the mechanism of IGFBPs in kidney disease are still few and unsystematic. We describe the possible pathogenesis of IGFBPs in renal disease in **Figure 1** based on current studies. The existing studies suggest that the role of IGFBPs in kidney disease should not be ignored. We believe that future studies will reveal more important functions of IGFBP family.

AUTHOR CONTRIBUTIONS

SW and KC: Literature retrieval, sorting and article writing. DW and QH: topic design and guidance.

FUNDING

This work was supported by the Fostering Fund of National Key Research and Development Project (2018YFE0126600), Chinese PLA General Hospital for the National Distinguished Young Scholar Science Fund (2019- JQPY-002), the National Natural Science Foundation of China (Nos. 81870491 and 82070741).

REFERENCES

Abrass, C. K., Berfield, A. K., and Andress, D. L. (1997). Heparin Binding Domain of Insulin-like Growth Factor Binding Protein-5 Stimulates Mesangial Cell Migration. *Am. J. Physiol.* 273 (6), F899–F906. doi:10.1152/ajprenal.1997.273.6.F899

Al Shawaf, E., Abu-Farha, M., Devarajan, S., Alsairafi, Z., Al-Khairi, I., Cherian, P., et al. (2019). ANGPTL4: A Predictive Marker for Diabetic Nephropathy. *J. Diabetes Res.* 2019, 4943191. doi:10.1155/2019/4943191

Azar, W. J., Zivkovic, S., Werther, G. A., and Russo, V. C. (2013). IGFBP-2 Nuclear Translocation Is Mediated by a Functional NLS Sequence and is Essential for its Pro-Tumorigenic Actions in Cancer Cells. *Oncogene* 33 (5), 578–588. doi:10.1038/onc.2012.630

Bai, Z., Fang, F., Xu, Z., Lu, C., Wang, X., Chen, J., et al. (2018). Serum and Urine FGF23 and IGFBP-7 for the Prediction of Acute Kidney Injury in Critically Ill Children. *BMC Pediatr.* 18 (1), 192. doi:10.1186/s12887-018-1175-y

Baxter, R. C. (2014). IGF Binding Proteins in Cancer: Mechanistic and Clinical Insights. *Nat. Rev. Cancer* 14 (5), 329–341. doi:10.1038/nrc3720

Berfield, A. K., Andress, D. L., and Abrass, C. K. (2000). IGFBP-5(201-218) Stimulates Cdc42GAP Aggregation and Filopodia Formationin Migrating Mesangial Cells. *Kidney Int.* 57 (5), 1991–2003. doi:10.1046/j.1523-1755.2000.00049.x

Bernardo, A. P., Oliveira, J. C., Santos, O., Carvalho, M. J., Cabrita, A., and Rodrigues, A. (2015). Insulin Resistance in Nondiabetic Peritoneal Dialysis Patients: Associations with Body Composition, Peritoneal Transport, and Peritoneal Glucose Absorption. *Clin. J. Am. Soc. Nephrol.* 10 (12), 2205–2212. doi:10.2215/CJN.03170315

Besset, V., Le Magueresse-Battistoni, B., Collette, J., and Benahmed, M. (1996). Tumor Necrosis Factor Alpha Stimulates Insulin-like Growth Factor Binding Protein 3 Expression in Cultured Porcine Sertoli Cells. *Endocrinology* 137 (1), 296–303. doi:10.1210/endo.137.1.8536626

Bihorac, A., Chawla, L. S., Shaw, A. D., Al-Khafaji, A., Davison, D. L., Demuth, G. E., et al. (2014). Validation of Cell-Cycle Arrest Biomarkers for Acute Kidney Injury Using Clinical Adjudication. *Am. J. Respir. Crit. Care Med.* 189 (8), 932–939. doi:10.1164/rccm.201401-0077OC

Charlton, J. R., Norwood, V. F., Kiley, S. C., Gurka, M. J., and Chevalier, R. L. (2012). Evolution of the Urinary Proteome During Human Renal Development and Maturation: Variations with Gestational and Postnatal Age. *Pediatr. Res.* 72 (2), 179–185. doi:10.1038/pr.2012.63

Cho, W. Y., Lim, S. Y., Yang, J. H., Oh, S. W., Kim, M.-G., and Jo, S.-K. (2019). Urinary Tissue Inhibitor of Metalloproteinase-2 and Insulin-like Growth Factor-Binding Protein 7 as Biomarkers of Patients with Established Acute Kidney Injury. *Korean J. Intern. Med.* 35 (3), 662-671. doi:10.3904/kjim.2018.266

Christensson, A., Ash, J. A., Delisle, R. K., Gaspar, F. W., Ostroff, R., Grubb, A., et al. (2018). The Impact of the Glomerular Filtration Rate on the Human Plasma Proteome. *Proteomics Clin. Appl.* 12 (3), e1700067. doi:10.1002/prca.201700067

Daza, D. O., Sundström, G., Bergqvist, C. A., Duan, C., and Larhammar, D. (2011). Evolution of the Insulin-like Growth Factor Binding Protein (IGFBP) Family. *Endocrinology* 152 (6), 2278–2289. doi:10.1210/en.2011-0047

Ding, H., Kharboutli, M., Saxena, R., and Wu, T. (2016). Insulin-like Growth Factor Binding Protein-2 as a Novel Biomarker for Disease Activity and Renal Pathology Changes in Lupus Nephritis. *Clin. Exp. Immunol.* 184 (1), 11–18. doi:10.1111/cei.12743

Dittmann, K., Wallaschofski, H., Rettig, R., Stracke, S., Endlich, K., Völzke, H., et al. (2012). Association Between Serum Insulin-like Growth Factor I or IGF-Binding Protein 3 and Estimated Glomerular Filtration Rate: Results of a Population-Based Sample. *BMC Nephrol.* 13, 169. doi:10.1186/1471-2369-13-169

Dong, C., Zhang, J., Fang, S., and Liu, F. (2020). IGFBP5 Increases Cell Invasion and Inhibits Cell Proliferation by EMT and Akt Signaling Pathway in Glioblastoma Multiforme Cells. *Cell Div* 15, 4. doi:10.1186/s13008-020-00061-6

Doublier, S., Seurin, D., Fouqueray, B., Verpont, M. C., Callard, P., Striker, L. J., et al. (2000). Glomerulosclerosis in Mice Transgenic for Human Insulin-like Growth Factor-Binding Protein-1. *Kidney Int.* 57 (6), 2299–2307. doi:10.1046/j.1523-1755.2000.00090.x

Firth, S. M., and Baxter, R. C. (2002). Cellular Actions of the Insulin-like Growth Factor Binding Proteins. *Endocr. Rev.* 23 (6), 824–854. doi:10.1210/er.2001-0033

Fukuda, I., Hizuka, N., Okubo, Y., Takano, K., Asakawa-Yasumoto, K., Shizume, K., et al. (1998). Changes in Serum Insulin-like Growth Factor Binding Protein-2, -3, and -6 Levels in Patients with Chronic Renal Failure Following Renal Transplantation. *Growth Horm. IGF Res.* 8 (6), 481–486. doi:10.1016/s1096-6374(98)80301-8

Gleeson, L. M., Chakraborty, C., Mckinnon, T., and Lala, P. K. (2001). Insulin-like Growth Factor-Binding Protein 1 Stimulates Human Trophoblast Migration by Signaling through Alpha 5 Beta 1 Integrin via Mitogen-Activated Protein Kinase Pathway. *J. Clin. Endocrinol. Metab.* 86 (6), 2484–2493. doi:10.1210/jcem.86.6.7532

Gokulakrishnan, K., Velmurugan, K., Ganesan, S., and Mohan, V. (2012). Circulating Levels of Insulin-like Growth Factor Binding Protein-1 in Relation to Insulin Resistance, Type 2 Diabetes Mellitus, and Metabolic Syndrome (Chennai Urban Rural Epidemiology Study 118). *Metabolism* 61 (1), 43–46. doi:10.1016/j.metabol.2011.05.014

Grellier, P., Sabbah, M., Fouqueray, B., Woodruff, K., Yee, D., Abboud, H. E., et al. (1996). Characterization of Insulin-like Growth Factor Binding Proteins and Regulation of IGFBP3 in Human Mesangial Cells. *Kidney Int.* 49 (4), 1071–1078. doi:10.1038/ki.1996.156

Gu, T., Falhammar, H., Gu, H. F., and Brismar, K. (2014). Epigenetic Analyses of the Insulin-like Growth Factor Binding Protein 1 Gene in Type 1 Diabetes and Diabetic Nephropathy. *Clin. Epigenetics* 6 (1), 10. doi:10.1186/1868-7083-6-10

Hjortebjerg, R., Tarnow, L., Jorsal, A., Parving, H. H., Rossing, P., Bjerre, M., et al. (2015). IGFBP-4 Fragments as Markers of Cardiovascular Mortality in Type 1 Diabetes Patients with and without Nephropathy. *J. Clin. Endocrinol. Metab.* 100 (8), 3032–3040. doi:10.1210/jc.2015-2196

Holbourn, K. P., Acharya, K. R., and Perbal, B. (2008). The CCN Family of Proteins: Structure-Function Relationships. *Trends Biochem. Sci.* 33 (10), 461–473. doi:10.1016/j.tibs.2008.07.006

Jarkovská, Z., Rosická, M., Krsek, M., Sulková, S., Haluzík, M., Justová, V., et al. (2005). Plasma Ghrelin Levels in Patients with End-Stage Renal Disease. *Physiol. Res.* 54 (4), 403–408.

Jehle, P. M., Ostertag, A., Schulten, K., Schulz, W., Jehle, D. R., Stracke, S., et al. (2000). Insulin-like Growth Factor System Components in Hyperparathyroidism and Renal Osteodystrophy. *Kidney Int.* 57 (2), 423–436. doi:10.1046/j.1523-1755.2000.00862.x

Karaiskos, N., Rahmatollahi, M., Boltengagen, A., Liu, H., Hoehne, M., Rinschen, M., et al. (2018). A Single-Cell Transcriptome Atlas of the Mouse Glomerulus. *J. Am. Soc. Nephrol.* 29 (8), 2060–2068. doi:10.1681/ASN.2018030238

Kashani, K., Al-Khafaji, A., Ardiles, T., Artigas, A., Bagshaw, S. M., Bell, M., et al. (2013). Discovery and Validation of Cell Cycle Arrest Biomarkers in Human Acute Kidney Injury. *Crit. Care* 17 (1), R25. doi:10.1186/cc12503

Lay, A. C., Hale, L. J., Stowell-Connolly, H., Pope, R. J. P., Nair, V., Ju, W., et al. (2021). IGFBP-1 Expression Is Reduced in Human Type 2 Diabetic Glomeruli and Modulates β1-integrin/FAK Signalling in Human Podocytes. *Diabetologia* 64 (7), 1690–1702. doi:10.1007/s00125-021-05427-1

Li, H. L., Yan, Z., Ke, Z. P., Tian, X. F., Zhong, L. L., Lin, Y. T., et al. (2018). IGFBP2 Is a Potential Biomarker in Acute Kidney Injury (AKI) and Resveratrol-Loaded Nanoparticles Prevent AKI. *Oncotarget* 9 (93), 36551–36560. doi:10.18632/oncotarget.25663

Maddux, B. A., Chan, A., De Filippis, E. A., Mandarino, L. J., and Goldfine, I. D. (2006). IGF-binding Protein-1 Levels are Related to Insulin-Mediated Glucose Disposal and are a Potential Serum Marker of Insulin Resistance. *Diabetes Care* 29 (7), 1535–1537. doi:10.2337/dc05-1367

Mahesh, S., and Kaskel, F. (2008). Growth Hormone Axis in Chronic Kidney Disease. *Pediatr. Nephrol.* 23 (1), 41–48. doi:10.1007/s00467-007-0527-x

Matsell, D. G., Delhanty, P. J., Stepaniuk, O., Goodyear, C., and Han, V. K. (1994). Expression of Insulin-like Growth Factor and Binding Protein Genes during Nephrogenesis. *Kidney Int.* 46 (4), 1031–1042. doi:10.1038/ki.1994.364

Minchenko, D. O., Kharkova, Ap., Karbovskyi, Ll., and Minchenko, O. H. (2015). Expression of Insulin-like Growth Factor Binding Protein Genes and its Hypoxic Regulation in U87 Glioma Cells Depends on ERN1 Mediated Signaling Pathway of Endoplasmic Reticulum Stress. *Endocr. Regul.* 49 (2), 73–83. doi:10.4149/endo_2015_02_73

Mirna, M., Topf, A., Wernly, B., Rezar, R., Paar, V., Jung, C., et al. (2020). Novel Biomarkers in Patients with Chronic Kidney Disease: An Analysis of Patients Enrolled in the GCKD-Study. *J. Clin. Med.* 9 (3), 886. doi:10.3390/jcm9030886

Mohammed, J. A., Mok, A. Y., Parbtani, A., and Matsell, D. G. (2003). Increased Expression of Insulin-like Growth Factors in Progressive Glomerulonephritis of the MRL/lpr Mouse. *Lupus* 12 (8), 584–590. doi:10.1191/0961203303lu422oa

Narayanan, R. P., Fu, B., Heald, A. H., Siddals, K. W., Oliver, R. L., Hudson, J. E., et al. (2012). IGFBP2 is a Biomarker for Predicting Longitudinal Deterioration in Renal Function in Type 2 Diabetes. *Endocr. Connect* 1 (2), 95–102. doi:10.1530/EC-12-0053

Nguyen, X. X., Muhammad, L., Nietert, P. J., and Feghali-Bostwick, C. (2018). IGFBP-5 Promotes Fibrosis via Increasing Its Own Expression and that of Other Pro-fibrotic Mediators. *Front Endocrinol. (Lausanne)* 9, 601. doi:10.3389/fendo.2018.00601

Oh, Y. (2012). The Insulin-like Growth Factor System in Chronic Kidney Disease: Pathophysiology and Therapeutic Opportunities. *Kidney Res. Clin. Pract.* 31 (1), 26–37. doi:10.1016/j.krcp.2011.12.005

Park, J., Shrestha, R., Qiu, C., Kondo, A., Huang, S., Werth, M., et al. (2018). Single-cell Transcriptomics of the Mouse Kidney Reveals Potential Cellular Targets of Kidney Disease. *Science* 360 (6390), 758–763. doi:10.1126/science.aar2131

Peters, I., Tossidou, I., Achenbach, J., Woroniecki, R., Mengel, M., Park, J. K., et al. (2006). IGF-binding Protein-3 Modulates TGF-beta/BMP-Signaling in Glomerular Podocytes. *J. Am. Soc. Nephrol.* 17 (6), 1644–1656. doi:10.1681/ASN.2005111209

Peters, K. E., Davis, W. A., Ito, J., Bringans, S. D., Lipscombe, R. J., and Davis, T. M. E. (2019). Validation of a Protein Biomarker Test for Predicting Renal Decline in Type 2 Diabetes: The Fremantle Diabetes Study Phase II. *J. Diabetes Complications* 33 (12), 107406. doi:10.1016/j.jdiacomp.2019.07.003

Peters, K. E., Davis, W. A., Ito, J., Winfield, K., Stoll, T., Bringans, S. D., et al. (2017). Identification of Novel Circulating Biomarkers Predicting Rapid Decline in Renal Function in Type 2 Diabetes: The Fremantle Diabetes Study Phase II. *Diabetes Care* 40 (11), 1548–1555. doi:10.2337/dc17-0911

Powell, D. R., Liu, F., Baker, B. K., Hintz, R. L., Durham, S. K., Brewer, E. D., et al. (1997). Insulin-like Growth Factor-Binding Protein-6 Levels Are Elevated in Serum of Children with Chronic Renal Failure: a Report of the Southwest Pediatric Nephrology Study Group. *J. Clin. Endocrinol. Metab.* 82 (9), 2978–2984. doi:10.1210/jcem.82.9.4215

Powell, D. R., Liu, F., Baker, B. K., Lee, P. D., and Hintz, R. L. (1996). Insulin-like Growth Factor Binding Proteins as Growth Inhibitors in Children with Chronic Renal Failure. *Pediatr. Nephrol.* 10 (3), 343–347. doi:10.1007/BF00866778

Qiu, F., Gao, W., and Wang, B. (2018). Correlation of IGFBP-6 Expression with Apoptosis and Migration of Colorectal Carcinoma Cells. *Cancer Biomark* 21 (4), 893–898. doi:10.3233/CBM-170947

Rajkumar, K., Barron, D., Lewitt, M. S., and Murphy, L. J. (1995). Growth Retardation and Hyperglycemia in Insulin-like Growth Factor Binding Protein-1 Transgenic Mice. *Endocrinology* 136 (9), 4029–4034. doi:10.1210/endo.136.9.7544274

Rajwani, A., Ezzat, V., Smith, J., Yuldasheva, N. Y., Duncan, E. R., Gage, M., et al. (2012). Increasing Circulating IGFBP1 Levels Improves Insulin Sensitivity, Promotes Nitric Oxide Production, Lowers Blood Pressure, and Protects against Atherosclerosis. *Diabetes* 61 (4), 915–924. doi:10.2337/db11-0963

Ravassa, S., Beaumont, J., Cediel, G., Lupón, J., López, B., Querejeta, R., et al. (2020). Cardiorenal Interaction and Heart Failure Outcomes. A Role for Insulin-like Growth Factor Binding Protein 2 ? *Revista Española de Cardiología(English Edition)* 73 (10), 835–843. doi:10.1016/j.rec.2019.10.012

Sayanthooran, S., Magana-Arachchi, D. N., Gunerathne, L., and Abeysekera, T. (2017). Potential Diagnostic Biomarkers for Chronic Kidney Disease of Unknown Etiology (CKDu) in Sri Lanka: a Pilot Study. *BMC Nephrol.* 18 (1), 31. doi:10.1186/s12882-017-0440-x

Schaeffer, V., Hansen, K. M., Morris, D. R., and Abrass, C. K. (2010). Reductions in Laminin Beta2 mRNA Translation Are Responsible for Impaired IGFBP-5-Mediated Mesangial Cell Migration in the Presence of High Glucose. *Am. J. Physiol. Ren. Physiol* 298 (2), F314–F322. doi:10.1152/ajprenal.00483.2009

Schedlich, L. J., Le Page, S. L., Firth, S. M., Briggs, L. J., Jans, D. A., and Baxter, R. C. (2000). Nuclear Import of Insulin-like Growth Factor-Binding Protein-3 and -5 Is Mediated by the Importin Beta Subunit. *J. Biol. Chem.* 275 (31), 23462–23470. doi:10.1074/jbc.M002208200

Shalamanova, L., Kübler, B., Scharf, J. G., and Braulke, T. (2001). MDCK Cells Secrete Neutral Proteases Cleaving Insulin-like Growth Factor-Binding Protein-2 to -6. *Am. J. Physiol. Endocrinol. Metab.* 281 (6), E1221–E1229. doi:10.1152/ajpendo.2001.281.6.E1221

Srivastava, P., Solanki, A. K., Arif, E., Wolf, B. J., Janech, M. G., Budisavljevic, M. N., et al. (2019). Development of a Novel Cell-Based Assay to Diagnose Recurrent Focal Segmental Glomerulosclerosis Patients. *Kidney Int.* 95 (3), 708–716. doi:10.1016/j.kint.2018.10.030

Tokunaga, K., Uto, H., Takami, Y., Mera, K., Nishida, C., Yoshimine, Y., et al. (2010). Insulin-like Growth Factor Binding Protein-1 Levels Are Increased in Patients with IgA Nephropathy. *Biochem. Biophys. Res. Commun.* 399 (2), 144–149. doi:10.1016/j.bbrc.2010.07.032

Tönshoff, B., Powell, D. R., Zhao, D., Durham, S. K., Coleman, M. E., Domené, H. M., et al. (1997). Decreased hepatic insulin-like growth factor (IGF)-I and increased IGF binding protein-1 and -2 gene expression in experimental uremia. *Endocrinology* 138 (3), 938–946.

Ulinski, T., Mohan, S., Kiepe, D., Blum, W. F., Wingen, A. M., Mehls, O., et al. (2000). Serum Insulin-like Growth Factor Binding Protein (IGFBP)-4 and IGFBP-5 in Children with Chronic Renal Failure: Relationship to Growth and Glomerular Filtration Rate. The European Study Group for Nutritional Treatment of Chronic Renal Failure in Childhood. German Study Group for Growth Hormone Treatment in Chronic Renal Failure. *Pediatr. Nephrol.* 14 (7), 589–597. doi:10.1007/s004670000361

Us Food and Drug Administration. Letter to Astute Medical. Updated on Sep2014. Available at: http://www.accessdata.fda.gov/cdrh_docs/pdf13/den130031.pdf.

Van Doorn, J., Cornelissen, Aj., and Van Buul-Offers, S. C. (2001). Plasma Levels of Insulin-like Growth Factor Binding Protein-4 (IGFBP-4) under normal and Pathological Conditions. *Clin. Endocrinol. (Oxf)* 54 (5), 655–664. doi:10.1046/j.1365-2265.2001.01248.x

Vasylyeva, Tl., Chen, X., and Ferry, Rj. (2005). Insulin-like Growth Factor Binding Protein-3 Mediates Cytokine-Induced Mesangial Cell Apoptosis. *Growth Horm. IGF Res.* 15 (3), 207–214. doi:10.1016/j.ghir.2005.02.008

Wang, S., Liu, Y., Wu, C., Zhao, W., Zhang, J., Bao, G., et al. (2017). The Expression of IGFBP6 after Spinal Cord Injury: Implications for Neuronal Apoptosis. *Neurochem. Res.* 42 (2), 455–467. doi:10.1007/s11064-016-2092-9

Wang, X., Ma, T., Wan, X., Meng, Y., Zhao, Z., Bian, J., et al. (2018). IGFBP7 Regulates Sepsis-Induced Acute Kidney Injury through ERK1/2 Signaling. *J. Cell Biochem.*. doi:10.1002/jcb.28035

Wang, Z., and Li, M. (2015). Evolution of the Urinary Proteome during Human Renal Development and Maturation. *Adv. Exp. Med. Biol.* 845, 95–101. doi:10.1007/978-94-017-9523-4_10

Williams, A. C., Collard, T. J., Perks, C. M., Newcomb, P., Moorghen, M., Holly, J. M., et al. (2000). Increased P53-dependent Apoptosis by the Insulin-like Growth Factor Binding Protein IGFBP-3 in Human Colonic Adenoma-Derived Cells. *Cancer Res.* 60 (1), 22–27.

Wolf, E., Lahm, H., Wu, M., Wanke, R., and Hoeflich, A. (2000). Effects of IGFBP-2 Overexpression *in vitro* and *in vivo*. *Pediatr. Nephrol.* 14 (7), 572–578. doi:10.1007/s004670000362

Worthmann, K., Peters, I., Kümpers, P., Saleem, M., Becker, J. U., Agustian, P. A., et al. (2010). Urinary Excretion of IGFBP-1 and -3 Correlates with Disease Activity and Differentiates Focal Segmental Glomerulosclerosis and Minimal Change Disease. *Growth Factors* 28 (2), 129–138. doi:10.3109/08977190903512594

Wu, T., Ding, H., Han, J., Arriens, C., Wei, C., Han, W., et al. (2016). Antibody-Array-Based Proteomic Screening of Serum Markers in Systemic Lupus Erythematosus: A Discovery Study. *J. Proteome Res.* 15 (7), 2102–2114. doi:10.1021/acs.jproteome.5b00905

Wu, T., Xie, C., Han, J., Ye, Y., Singh, S., Zhou, J., et al. (2016). Insulin-Like Growth Factor Binding Protein-4 as a Marker of Chronic Lupus Nephritis. *PLoS One* 11 (3), e0151491. doi:10.1371/journal.pone.0151491

Yamashita, T., Noiri, E., Hamasaki, Y., Matsubara, T., Ishii, T., Yahagi, N., et al. (2016). Erythropoietin Concentration in Acute Kidney Injury Is Associated with Insulin-like Growth Factor-Binding Protein-1. *Nephrology (Carlton)* 21 (8), 693–699. doi:10.1111/nep.12656

Yan, C., Yu, L., Zhang, X. L., Shang, J. J., Ren, J., Fan, J., et al. (2020). Cytokine Profiling in Chinese SLE Patients: Correlations with Renal Dysfunction. *J. Immunol. Res.* 2020, 8146502. doi:10.1155/2020/8146502

Yoo, E -G., Lee, W. J., Kim, J. H., Chae, H -W., Hyun, S. E., Kim, D. H., et al. (2011). Insulin-Like Growth Factor-Binding Protein-3 Mediates High Glucose-Induced Apoptosis by Increasing Oxidative Stress in Proximal Tubular Epithelial Cells. *Endocrinology* 152 (8), 3135–3142. doi:10.1210/en.2010-1122

Zaghlool, S. B., Sharma, S., Molnar, M., Matías-García, P. R., Elhadad, M. A., Waldenberger, M., et al. (2021). Revealing the Role of the Human Blood Plasma Proteome in Obesity Using Genetic Drivers. *Nat. Commun.* 12 (1), 1279. doi:10.1038/s41467-021-21542-4

Conflict of Interest: The authors declare that the research was conducted in the absence of any commercial or financial relationships that could be construed as a potential conflict of interest.

Publisher's Note: All claims expressed in this article are solely those of the authors and do not necessarily represent those of their affiliated organizations, or those of the publisher, the editors and the reviewers. Any product that may be evaluated in this article, or claim that may be made by its manufacturer, is not guaranteed or endorsed by the publisher.

frontiers in Pharmacology

ORIGINAL RESEARCH
published: 22 December 2021
doi: 10.3389/fphar.2021.800522

Shenkang Injection and Its Three Anthraquinones Ameliorates Renal Fibrosis by Simultaneous Targeting IκB/NF-κB and Keap1/Nrf2 Signaling Pathways

Liang-Pu Luo[1,2], *Ping Suo*[1], *Li-Li Ren*[1], *Hong-Jiao Liu*[1], *Yamei Zhang*[3] *and Ying-Yong Zhao*[1]*

[1]*Faculty of Life Science and Medicine, Northwest University, Xi'an, China,* [2]*School of Traditional Chinese Medicine, Southern Medical University, Guangzhou, China,* [3]*Clinical Genetics Laboratory, Affiliated Hospital and Clinical Medical College of Chengdu University, Chengdu, China*

OPEN ACCESS

Edited by:
Zhiyong Guo,
Second Military Medical University, China

Reviewed by:
Liang Ma,
Sichuan University, China
Kun Gao,
Affiliated Hospital of Nanjing University of Chinese Medicine, China

***Correspondence:**
Ying-Yong Zhao
zyy@nwu.edu.cn

Specialty section:
This article was submitted to Renal Pharmacology, a section of the journal Frontiers in Pharmacology

Received: *23 October 2021*
Accepted: *17 November 2021*
Published: *22 December 2021*

Citation:
Luo L-P, Suo P, Ren L-L, Liu H-J, Zhang Y and Zhao Y-Y (2021) Shenkang Injection and Its Three Anthraquinones Ameliorates Renal Fibrosis by Simultaneous Targeting IκB/NF-κB and Keap1/Nrf2 Signaling Pathways. Front. Pharmacol. 12:800522. doi: 10.3389/fphar.2021.800522

Oxidative stress and inflammation are important and critical mediators in the development and progression of chronic kidney disease (CKD) and its complications. Shenkang injection (SKI) has been widely used to treat patients with CKD. Although the anti-oxidative and anti-inflammatory activity was involved in SKI against CKD, its bioactive components and underlying mechanism remain enigmatic. A rat model of adenine-induced chronic renal failure (CRF) is associated with, and largely driven by, oxidative stress and inflammation. Hence, we identified the anti-oxidative and anti-inflammatory components of SKI and further revealed their underlying mechanism in the adenine-induced CRF rats. Compared with control rats, the levels of creatinine, urea, uric acid, total cholesterol, triglyceride, and low-density lipoprotein cholesterol in serum were significantly increased in the adenine-induced CRF rats. However, treatment with SKI and its three anthraquinones including chrysophanol, emodin, and rhein could reverse these aberrant changes. They could significantly inhibit pro-fibrotic protein expressions including collagen I, α-SMA, fibronectin, and vimentin in the kidney tissues of the adenine-induced CRF rats. Of note, SKI and rhein showed the stronger inhibitory effect on these pro-fibrotic protein expressions than chrysophanol and emodin. Furthermore, they could improve dysregulation of IκB/NF-κB and Keap1/Nrf2 signaling pathways. Chrysophanol and emodin showed the stronger inhibitory effect on the NF-κB p65 protein expression than SKI and rhein. Rhein showed the strongest inhibitory effect on p65 downstream target gene products including NAD(P)H oxidase subunits ($p47^{phox}$, $p67^{phox}$, and $gp91^{phox}$) and COX-2, MCP-1, iNOS, and 12-LO in the kidney tissues. However, SKI and rhein showed the stronger inhibitory effect on the significantly downregulated anti-inflammatory and anti-oxidative protein expression nuclear Nrf2 and its target gene products including HO-1, catalase, GCLC, and NQO1 in the Keap1/Nrf2 signaling pathway than chrysophanol and emodin. This study first demonstrated that SKI and its major components protected against renal fibrosis by inhibiting oxidative stress and inflammation via simultaneous targeting IκB/NF-κB and Keap1/Nrf2 signaling

pathways, which illuminated the potential molecular mechanism of anti-oxidative and anti-inflammatory effects of SKI.

Keywords: chronic kidney disease, shenkang injection, chrysophanol (PubChem CID: 10208), emodin, rhein (PubChem CID: 10168), oxidative stress and inflammation, IkB/NF-kB signaling pathway, Keap1/Nrf2 signaling pathway

INTRODUCTION

Organ fibrosis is a pathological extension of the normal wound healing process characterized by oxidative stress and inflammation; myofibroblast activation and migration; and excessive synthesis, deposition, and remodeling of extracellular matrix (ECM) components, mainly including collagen, fibronectin, and α-smooth muscle actin (α-SMA) (Miao et al., 2021a). A variety of pathophysiological principles is shared by many fibrotic-associated diseases, such as cirrhosis, kidney fibrosis, myocardial fibrosis, and idiopathic pulmonary fibrosis (Miao et al., 2021a). Fibrotic diseases are estimated to account for up to 50% of deaths in the developed world (Mantovani and Zusi, 2020).

Renal fibrosis, characterized by tubulointerstitial fibrosis and glomerulosclerosis, is a chronic and progressive process influencing renal functions during aging and in chronic kidney disease (CKD), regardless of the cause (Bhargava et al., 2021; Li et al., 2021; Medina Rangel et al., 2021). CKD and renal fibrosis influence approximately 26–30 million adults, and 47% of 30-year-olds will develop CKD during their lifetime in America (Humphreys, 2018). About 11% of patients with stage 3 CKD will inevitably progress to end-stage renal disease (ESRD), requiring renal replacement therapies such as dialysis and transplantation (Chauveau, 2018; Jain et al., 2019; Carta et al., 2020; Sawhney and Gill, 2020). Additionally, CKD is also one of the strongest risk factors for cardiovascular disease (Yanai et al., 2021). The costs to care for patients with CKD are two times compared with as large as ESRD costs.

In the last two decades, angiotensin-converting enzyme inhibitors (ACEIs) or angiotensin receptor blockers (ARBs) have been widely recommended clinically as a standard therapy in patients with hypertension, cardiovascular disease, and CKD (Chen et al., 2019a). These drugs could effectively reduce proteinuria levels and slow down CKD progression and prevent its complications. However, chronic administration of ACEI or ARB led to the elevated levels of angiotensin II and aldosterone, which is known as angiotensin II and aldosterone escape (Wang et al., 2018). Despite these therapies, outcomes in patients with CKD remain poor.

Natural products have been widely used for prevention and treatment of renal fibrosis (Chen et al., 2018a; Chen et al., 2018b; Yang and Wu, 2021). Shenkang injection (SKI), approved by the State Food and Drug Administration of China (CFDA) in 1999, was used to treat CKD. SKI is composed of *Rhei Radix et Rhizoma* (Dahuang), *Salviae Miltiorrhizae Radix et Rhizoma* (Danshen), *Astragali Radix* (Huangqi), and *Carthami Flos* (Honghua) (Zou et al., 2020). Dahuang possessed anti-inflammatory, anti-bacterial, anti-cancer, and anti-fibrotic effects (Wang et al., 2012). Danshen exhibited anti-inflammatory, anti-oxidative, anti-tumor, cardioprotective, neuroprotective, and anti-fibrotic effects (Wang et al., 2021a). Huangqi showed anti-inflammatory, anti-oxidative, anti-infective, anti-diabesity, anti-tumor, anti-aging, and immune-enhancing properties (Salehi et al., 2021). The extracts and isolated compounds from Honghua presented various pharmacological properties, such as anti-inflammatory, anti-thrombotic, anti-tumor, anti-diabetic, and anti-myocardial ischemic effects (Tu et al., 2015). These published literatures indicated that anti-inflammatory and anti-oxidative effects were their common pharmacological activity. Therefore, it could be speculated that their anti-inflammatory and anti-oxidative effects were associated with CKD treatment of SKI. Recently, clinical studies have demonstrated that SKI could improve renal function in CKD, peritoneal dialysis patients with chronic renal failure (CRF), and diabetic nephropathy (Zhang et al., 2017; Song et al., 2019; Wang et al., 2020a; Qin et al., 2020; Zou et al., 2020; Ma, 2021). A seminal publication has highlighted that SKI treatment protected against CRF and symptoms related to CKD following treatment with traditional Chinese medicine was 73.05 and 98.00%, respectively, in a clinical trial of 2200 patients (Qin et al., 2021). The experimental studies revealed that SKI could improve renal function and inhibit tubulointerstitial fibrosis by anti-oxidative, anti-inflammatory, and anti-apoptotic effects in unilateral ureteral obstruction mice and rats, streptozotocin-induced mice, and renal ischemia–reperfusion injury (IRI) rats (Liu, 2018; Liu et al., 2019; Zhang et al., 2020; Qin et al., 2021) as well as renal tubular cells or mesangial cells treated by transforming growth factor-β1 (TGF-β1) or high glucose (Wu et al., 2015; Xu et al., 2016; Fu et al., 2019). Mechanistically, several preliminary studies have revealed that SKI alleviated CKD and renal fibrosis by inhibiting pro-inflammatory cytokines such as interleukin-6, interleukin-1β, and tumor necrosis factor-α (TNF-α) expression (Zhang et al., 2020) and modulating TGF-β1/Smad3 and JAK2/STAT3 signaling pathways (Wu et al., 2015; Qin et al., 2021). Although SKI has been demonstrated to have anti-oxidative and anti-inflammatory effects in the treatment of CKD, little is known about its underlying oxidative stress and inflammation-associated mechanisms.

Oxidative stress and inflammation played a central role in the pathogenesis and progression of CKD (Chen et al., 2018c). Oxidative stress and inflammation are inseparably linked as they form a vicious cycle in which oxidative stress provokes inflammation by several mechanisms including activation of the nuclear factor kappa B (NF-ĸB) which leads to the activation and recruitment of immune cells, meanwhile, activation of the nuclear factor-erythroid-2–related factor 2 (Nrf2) which regulates the basal activity and coordinated induction of numerous genes that encode various anti-oxidant and phase 2 detoxifying enzymes and

related proteins. In this research, a CRF rat model was induced by adenine orally, which was then administered with SKI and its bioactive components including chrysophanol, emodin, and rhein orally to determine whether they could improve CKD and slow down renal fibrosis by regulating the inhibitor of kappa B (IκB)/NF-κB and Keap1/Nrf2 signaling pathways. Furthermore, we used the TGF-β1–induced human proximal epithelial cells to explore the therapeutic mechanism of SKI and its bioactive components on renal injury.

MATERIALS AND METHODS

Chemicals and Reagents

SKI was purchased from Shijishenkang Pharmaceutical Company Ltd. (Xi'an, China). The primary antibodies including collagen I (ab34710, Abcam, United States), α-SMA (ab7817, Abcam, United States), fibronectin (ab2413, Abcam, United States), vimentin (ab92547, Abcam, United States), p-NF-κB p65 (13346, Cell Signaling Technology, United States), phosphorylated IκBα (p-IκBα, 2859, Cell Signaling Technology, United States), gene cyclooxygenase 2 (COX-2, ab62331, Abcam, United States), monocyte chemotactic protein-1 (MCP-1, ab7202, Abcam, United States), inducible nitric oxide synthase (iNOS, ab178945, Abcam, United States), 12-lipoxygenase (12-LO, ab167372, Abcam, United States), $p47^{phox}$ (ab795, Abcam, United States), $p67^{phox}$ (ab109366, Abcam, United States), and $gp91^{phox}$ (ab80508, Abcam, United States), Keap1 (ab196346, Abcam, United States), Nrf2 (ab31163, Abcam, United States), heme oxygenase 1 (HO-1, ab68477, Abcam, United States), catalase (ab16731, Abcam, United States), glutamate–cysteine ligase catalytic subunit (GCLC, ab190685, Abcam, United States), and NAD(P)H dehydrogenase quinone 1 (NQO1, ab28947, Abcam, United States) were purchased from Abcam Company (Cambridge, MA, United States) and Cell Signaling Technology (Danvers, MA, United States). Glyceraldehyde-3-phosphate dehydrogenase (GAPDH, 10494-1-AP) and histone H3 (17168-1-AP) were purchased from Proteintech Company (Wuhan, China).

Extraction and Isolation of Chrysophanol, Emodin, and Rhein

SKI (10 L) was concentrated using a rotatory evaporator in vacuum to yield 2.1 kg of dry brown extract. The concentrated extract was extracted with petroleum ether (3 × 7.5 L), ethyl acetate (3 × 7.5 L), and n-butanol (3 × 7.5 L), successively. The ethyl acetate extract was chromatographed on a MCI column. Elution was performed using a solvent mixture of MeOH/H_2O with an escalating amount of MeOH and similar fractions, identified by thin-layer chromatography, which were combined to yield five major fractions. The compounds were further isolated by the Sephadex LH-20 column, reversed-phase C-18 silica column, and semi-preparative high-performance liquid chromatography method. Finally, the compounds including chrysophanol, emodin, and rhein were identified by nuclear magnetic resonance spectrometry and reference substances.

CRF Model and Drug Administration

Male Sprague–Dawley rats (6–8 weeks old and weighing 180–210 g) were purchased from the Central Animal Breeding House of Xi'an Jiaotong University (Xi'an, Shaanxi, China). An adenine-induced CRF model was reproduced as described in detail previously (Wang et al., 2021b; Wang et al., 2021c). In brief, the rats were divided into six groups (n = 8/group) including control, adenine-induced CRF, SKI-treated group with CRF (CRF + SKI), chrysophanol-treated group with CRF (CRF + CHR), emodin-treated group with CRF (CRF + EMO), and rhein-treated group with CRF (CRF + RHE). Except for the control group, other groups with CRF were orally administered adenine (200 mg/kg/d) for 3 weeks. Treatment groups were administered SKI (20 ml/kg/d), chrysophanol (30 mg/kg/d), emodin (100 mg/kg/d), and rhein (150 mg/kg/d) for 3 weeks. The body weight of each rat was measured daily. After 3 weeks, individual rats were placed in metabolic cages (1 per cage) to obtain 24-h urine collections. The rats were anesthetized with 10% urethane and then blood samples and kidney tissues were collected for clinical biochemistry and histopathological analysis. All animal care and experimental procedures were approved by the Ethics Committee for Animal Experiments of Northwest University.

Renal Function Evaluation

The levels of creatinine, urea, uric acid, total cholesterol, triglyceride, and low-density lipoprotein cholesterol (LDL-C) in serum as well as creatinine in urine were determined using an Olympus AU6402 automatic analyzer.

Light Microscopic Study

Light microscopy was conducted using 10% formalin-fixed, paraffin-embedded biopsies stained with hematoxylin-eosin (H&E) and Masson's Trichrome stains, as previously described (Miao et al., 2020).

Immunohistochemistry

The specific protein expressions were examined on paraffin sections of kidney tissues as previously described (Miao et al., 2020).

Western Blot Analysis

All solutions, tubes, and centrifuges were maintained at 0–4°C. Cytoplasmic and nuclear proteins from kidney tissues were extracted based on our previous publication (Choi et al., 2010). Protein levels were detected using Western blotting as previously described (Miao et al., 2020). The blots were obtained using the enhanced chemiluminescence reagent, and the protein levels were normalized to the level of GAPDH or histone H3. Specific bands were analyzed using ImageJ 1.48v software.

Statistical Analysis

The data are presented as mean ± SEM. Statistical analyses were performed using GraphPad Prism software v6.0. A two-tailed unpaired Student's t-test was used for comparisons between two groups. Statistically significant differences amongst more than

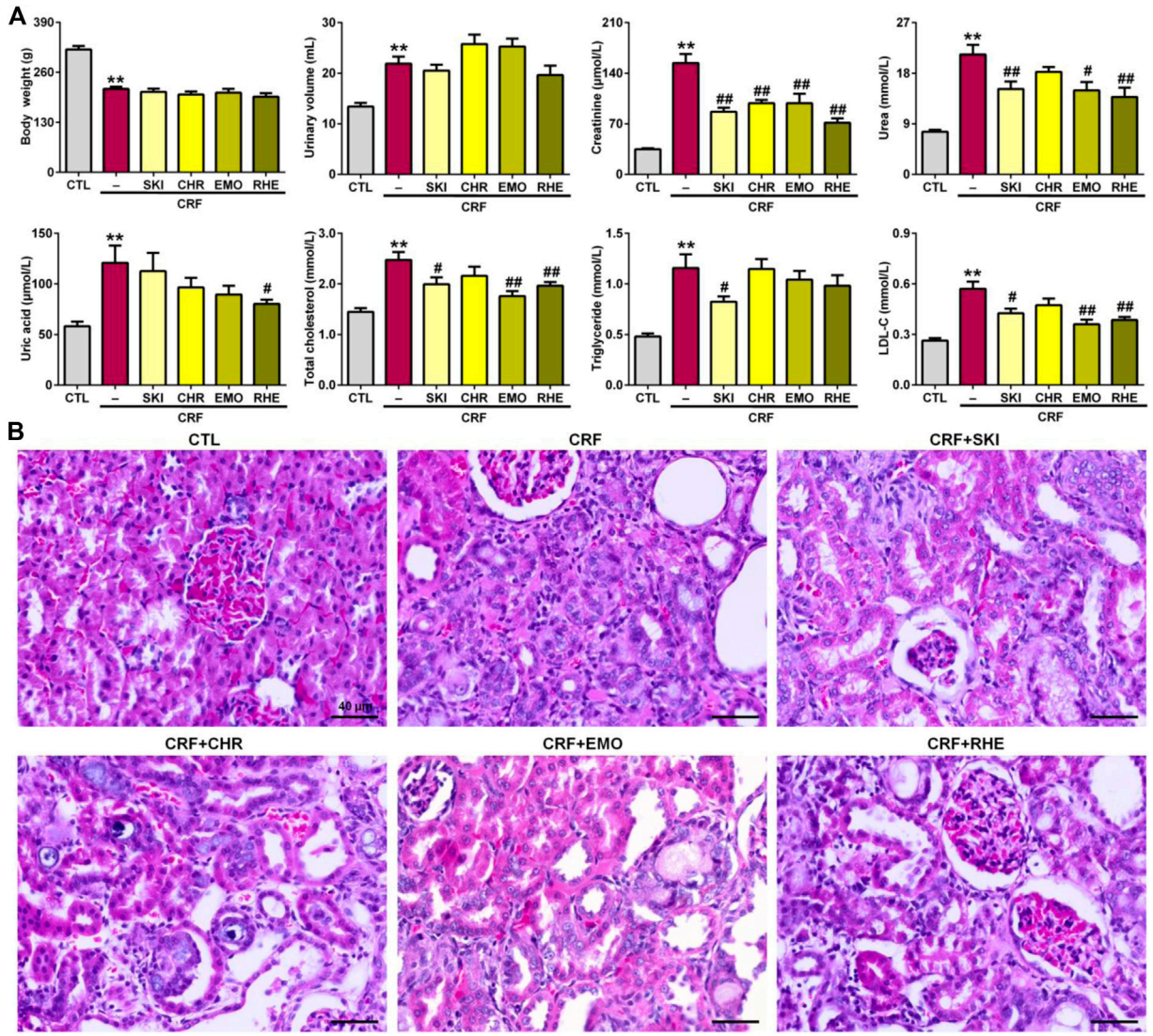

FIGURE 1 | SKI and three anthraquinones including chrysophanol, emodin, and rhein improved renal function and injury in the adenine-induced CRF rats. **(A)** Body weight and urinary volume as well as clinical serum biochemistry including creatinine, urea, uric acid, total cholesterol, triglyceride, and LDL-C in the different groups. $^{**}p <$ 0.01 compared with the CTL group; $^{\#}p < 0.05$, $^{\#\#}p < 0.01$ compared with the CRF group. **(B)** Images of H&E staining of the kidney tissues in the different groups. Scale bar, 40 μm.

two groups were analyzed by one-way analysis of variance followed by Dunnett's *post hoc* tests. $p < 0.05$ was considered significant differences.

RESULTS

SKI and Its Main Components Improved the Impaired Renal Function and Injury

The final metabolite of adenine is uric acid. After adenine given by the oral gavage, excessive adenine can be oxidized to 2,8-dihydroxyadenine via an 8-hydroxyadenine intermediate by xanthine dehydrogenase. Low solubility of 2,8-dihydroxyadenine can form precipitation in the renal tubules, which led to renal injury and fibrosis. As shown in **Figure 1A**, intragastric adenine led to significantly decreased body weight and increased urinary volume in CRF rats, while treatment with SKI and three anthraquinones including chrysophanol, emodin, and rhein did not produce the significant changes for body weight and urinary volume. The levels of creatinine, urea, uric acid, total cholesterol, triglyceride, and LDL-C in serum were significantly increased in the adenine-induced CRF group compared with the control group. Except for uric acid, all these increases were improved by treatment with SKI. Similarly, except for triglyceride, all these increases were improved by treatment with rhein. Treatment

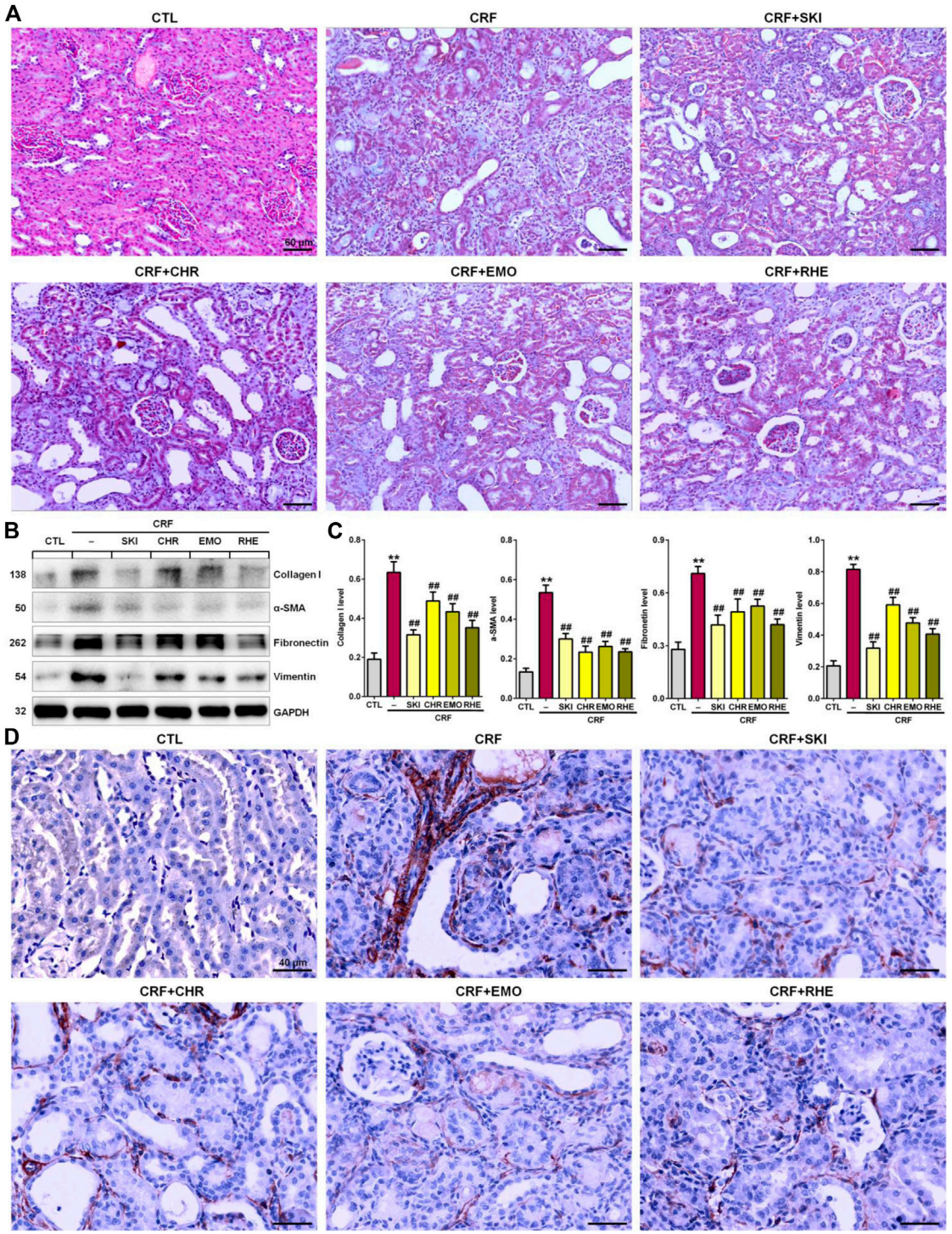

FIGURE 2 | SKI and three anthraquinones including chrysophanol, emodin, and rhein ameliorated renal fibrosis in the adenine-induced CRF rats. **(A)** Images of Masson's Trichrome staining of the kidney tissues in the different groups. Scale bar, 60 μm. **(B)** Expressions of profibrotic proteins including collagen I, α-SMA, fibronectin, and vimentin of the kidney tissues in the different groups. **(C)** Quantitative analysis of profibrotic protein expressions of the kidney tissues in the different groups. $^{**}p < 0.01$ compared with the CTL group; $^{\#\#}p < 0.01$ compared with the CRF group. **(D)** Immunohistochemical analysis with anti–α-SMA of the kidney tissues in the different groups. Scale bar, 40 μm.

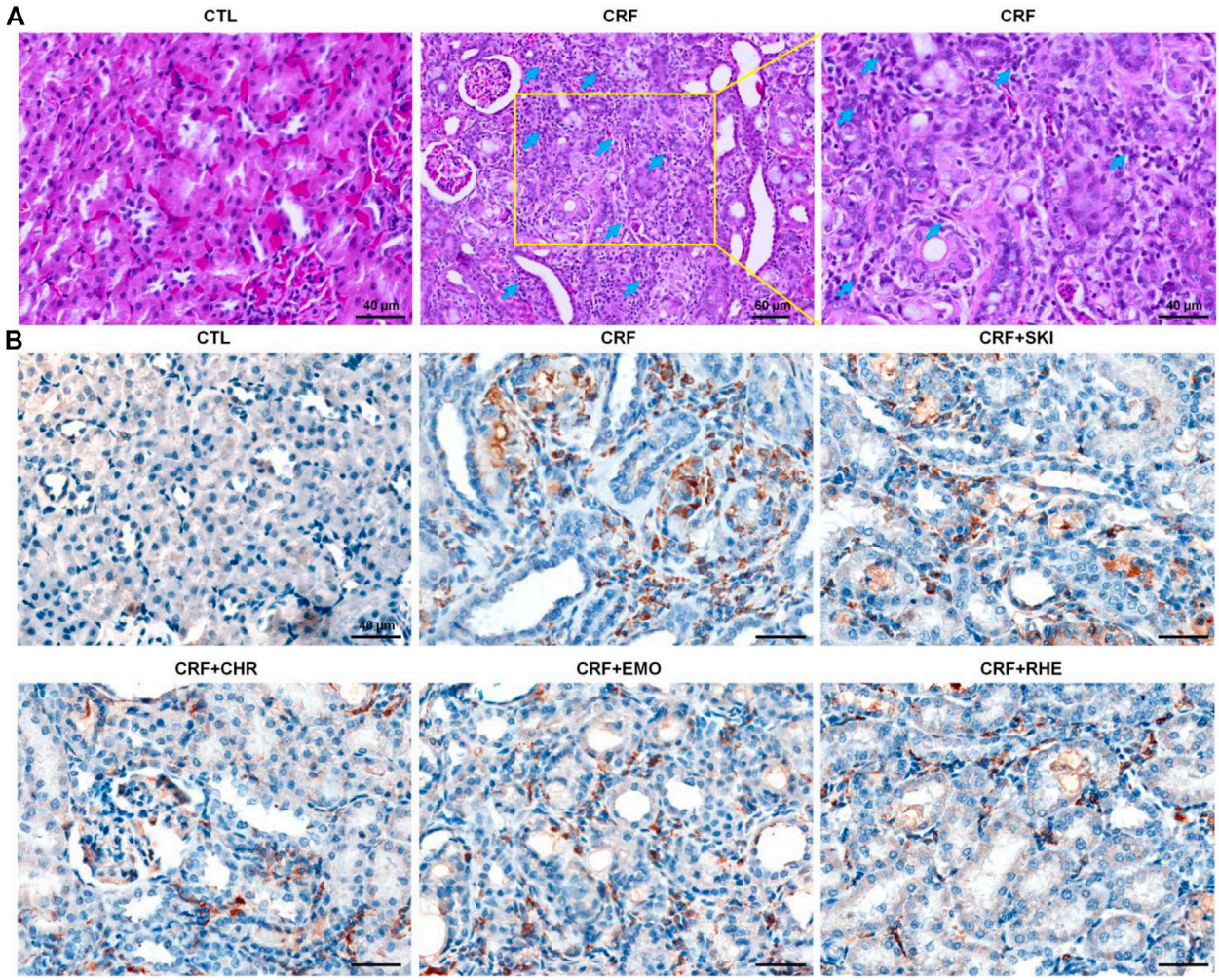

FIGURE 3 | SKI and three anthraquinones including chrysophanol, emodin, and rhein inhibited inflammation in the adenine-induced CRF rats. **(A)** Images of H&E staining of the kidney tissues in the different groups Scale bar, 40 and 60 μm. Numerous inflammatory cells were indicated by arrows. **(B)** Immunohistochemical analysis with anti-CD68 of the kidney tissues in the different groups. Scale bar, 40 μm.

with emodin significantly lowered the levels of creatinine, urea, TC, and LDL-C in the adenine-induced CRF group, while the levels of uric acid and triglyceride were decreased in the adenine-induced CRF group treated by emodin, but did not arrive at statistical significance. Treatment with chrysophanol only significantly lowered the creatinine levels in the adenine-induced CRF group. Compared with the control rats, H&E staining showed that the kidney tissues of the adenine-induced CRF rats showed severe inflammatory cell infiltration, tubular dilation, and interstitial fibrosis (**Figure 1B**). These injuries were improved by treatment with SKI and its main components including chrysophanol, emodin, and rhein. Collectively, these results demonstrated that SKI could improve the impaired renal function and ameliorate renal injury in the late stages of CKD. This effect was followed by rhein treatment. Similar results were observed in the adenine-induced CRF group treated by rhein. Furthermore, chrysophanol showed a certain renoprotective effect on adenine-induced renal function decline and damage.

SKI and Its Main Components Ameliorated Renal Fibrosis

Renal fibrosis is characterized by an excessive accumulation and deposition of ECM components. As shown in **Figure 2A**, Masson's Trichrome staining showed severe tubulointerstitial fibrosis in the kidney tissues of the adenine-induced CRF rats compared with the normal control rats. However, the fibrosis was improved by treatment with SKI and three anthraquinones including chrysophanol, emodin, and rhein. ECM components mainly included collagen I, collagen III, α-SMA, fibronectin, and vimentin. Therefore, we further determined the expression of pro-fibrotic proteins including collagen I, α-SMA, fibronectin, and vimentin. As shown in **Figures 2B,C**, the kidney tissues of

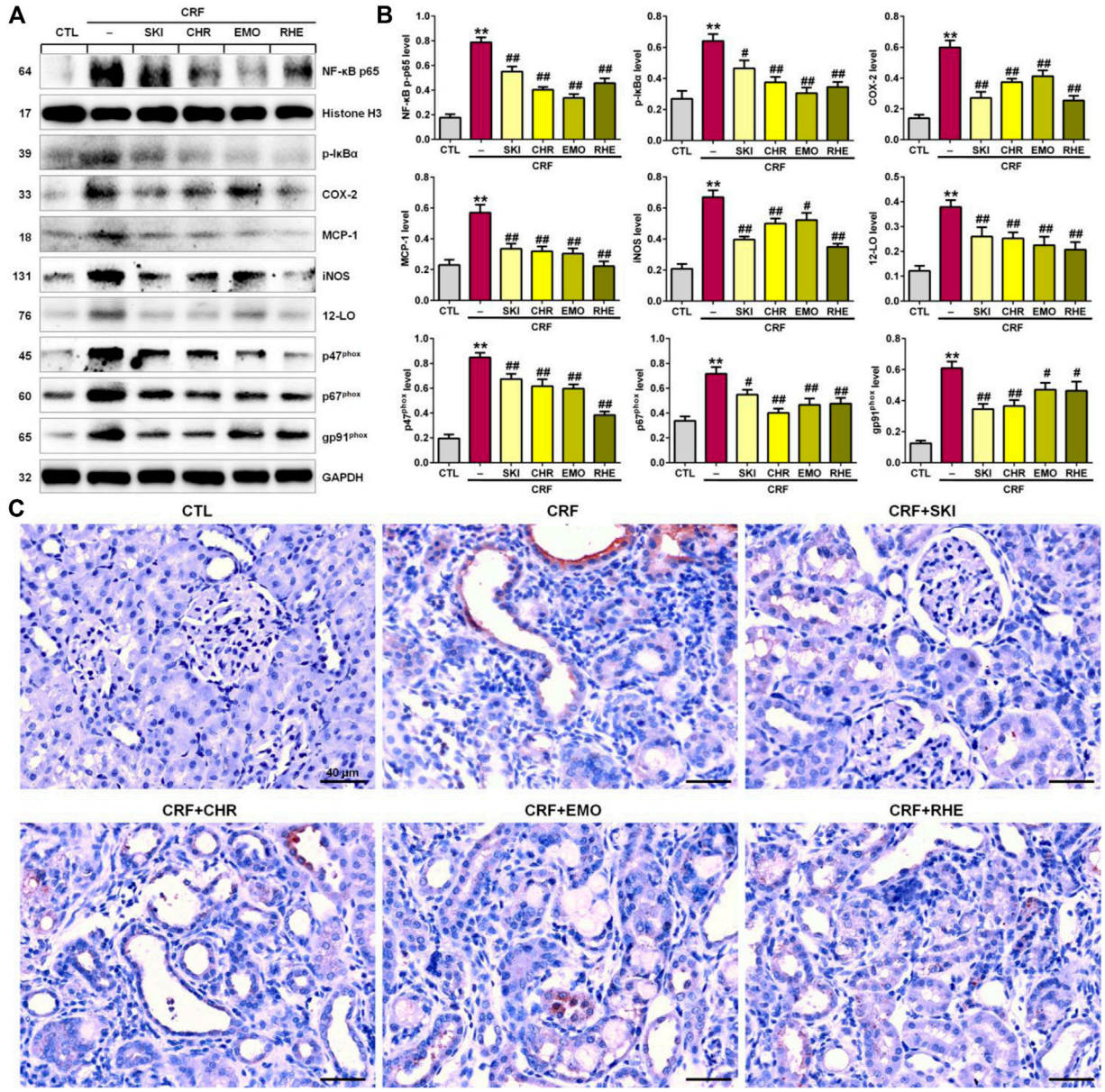

FIGURE 4 | SKI and three anthraquinones including chrysophanol, emodin, and rhein inhibited the pro-inflammatory IκB/NF-κB signaling pathway in the adenine-induced CRF rats. **(A)** Protein expressions of nuclear translocation of p65 and its downstream gene products including COX-2, MCP-1, iNOS, 12-LO, and NAD(P)H oxidase subunits ($p47^{phox}$, $p67^{phox}$, and $gp91^{phox}$) of the kidney tissues in the different groups. **(B)** Quantitative analysis of pro-inflammatory and pro-oxidative protein expressions of the kidney tissues in the different groups. $^{**}p < 0.01$ compared with the CTL group; $^{\#}p < 0.05$, $^{\#\#}p < 0.01$ compared with the CRF group. **(C)** Immunohistochemical analysis with anti–COX-2 of the kidney tissues in the different groups. Scale bar, 40 μm.

the adenine-induced CRF rats showed significant upregulation of protein expression of collagen I, α-SMA, fibronectin, and vimentin compared with the control rats. However, treatment with SKI and three anthraquinones showed significant inhibitory effect on these pro-fibrotic protein expressions in the kidney tissues of the adenine-induced CRF rats. Of note, SKI and rhein showed the stronger inhibitory effect on the pro-fibrotic protein expression than chrysophanol and emodin, which was consistent with the results of clinical biochemistry and histological analyses including H&E and Masson's Trichrome stainings. Additionally, immunohistochemistry analysis further demonstrated treatment with SKI and three anthraquinones could significantly inhibit the α-SMA expression in the kidney tissues of the adenine-induced CRF rats compared with those found in the CRF rats (**Figure 2D**). Of note, SKI and rhein showed the stronger inhibitory effect on the pro-fibrotic protein expression than chrysophanol and emodin. These results demonstrated that SKI and three anthraquinones protected against renal fibrosis in the adenine-induced CRF rats. Therefore, we concluded that anthraquinones might be one of the main renoprotective components of SKI.

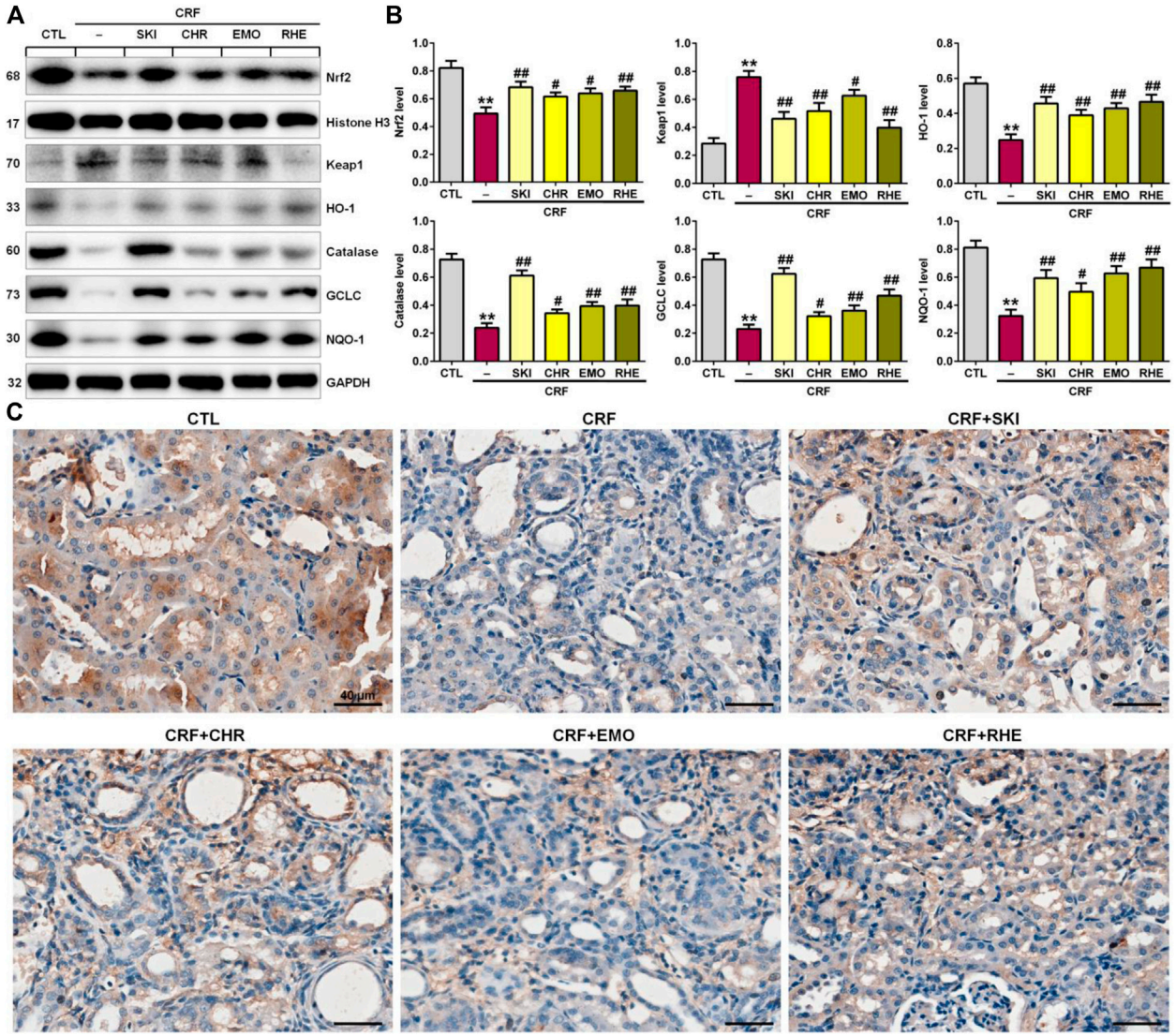

FIGURE 5 | SKI and three anthraquinones including chrysophanol, emodin, and rhein activated the anti-inflammatory and anti-oxidative Keap1/Nrf2 signaling pathway in the adenine-induced CRF rats. **(A)** Protein expressions of nuclear translocation of Nrf2 and its repressor, Keap1, and its downstream gene products including HO-1, catalase, GCLC, and NQO-1 of the kidney tissues in the different groups. **(B)** Quantitative analysis of anti-inflammatory and anti-oxidative protein expressions of the kidney tissues in the different groups. $^{**}p < 0.01$ compared with the CTL group; $^{\#}p < 0.05$, $^{\#\#}p < 0.01$ compared with the CRF group. **(C)** Immunohistochemical analysis with anti–HO-1 of the kidney tissues in the different groups. Scale bar, 40 μm.

SKI and Its Main Components Retarded Inflammation Response

Histopathological examination showed that severe inflammatory cell infiltration in the renal interstitium is one of the typical characteristics in rats induced by adenine (**Figure 3A**). CD68 is often used as a histochemical marker of inflammation response, which was involved in the monocytes/macrophages. Therefore, we determined the anti-CD68 expression in the kidney tissues of the adenine-induced CRF rats. As shown in **Figure 3B**, the renal interstitium of CRF rats showed significantly increased CD68 expression compared with that of the control rats. However, treatment with SKI and three anthraquinones showed significantly decreased CD68 expression in the renal interstitium of the adenine-induced CRF rats. Collectively, these results indicated administered adenine triggered oxidative stress and inflammation. Therefore, we speculated that the molecular mechanisms of SKI and three anthraquinones against tubulointerstitial fibrosis might be associated with the activation of oxidative stress and inflammation.

SKI and Its Main Components Ameliorated Renal Fibrosis by Inhibiting the IκB/NF-κB Signaling Pathway

The interplay between oxidative stress and inflammation form a vicious cycle in which oxidative stress triggers inflammation by various mechanisms such as the activation of the IκB/NF-κB

signaling pathway. As shown in **Figures 4A,B**, the kidney tissues of adenine-induced CRF rats showed significantly upregulated p-IκB and nuclear p65 levels compared with those of the control group, which indicated the activation of the IκB/NF-κB signaling pathway. This was accompanied by the significantly upregulated protein expressions of COX-2, MCP-1, iNOS, 12-LO, and NAD(P)H oxidase subunits ($p47^{phox}$, $p67^{phox}$, and $gp91^{phox}$) in the kidney tissues of the adenine-induced CRF rats compared with those of the control rats. However, these upregulated expressions were inhibited in the adenine-induced CRF rats treated by SKI and three anthraquinones. Additionally, immunohistochemistry analysis demonstrated that treatment with SKI and three anthraquinones could significantly inhibit the COX-2 expression in the kidney tissues of the adenine-induced CRF rats compared with that of the CRF rats (**Figure 4C**). Of note, chrysophanol and emodin showed the stronger inhibitory effect on the NF-κB p65 protein expression than SKI and rhein. Rhein showed the strongest inhibitory effect on p65 downstream target gene products. Taken together, these results indicated that the inhibition of the pro-inflammatory IκB/NF-κB signaling pathway was involved in SKI and three anthraquinones against renal fibrosis.

SKI and Its Main Components Ameliorated Renal Fibrosis by Activating the Keap1/Nrf2 Signaling Pathway

Increased oxidative stress activated the expression of the endogenous anti-oxidant proteins to reduce tissue damage, which was mediated by the activation of the Keap1/Nrf2 signaling pathway. As shown in **Figures 5A,B**, the adenine-induced CRF rats exhibited the significantly downregulated Nrf2 protein expression and upregulated Keap1 protein expression in the kidney tissues compared with the control rats. This was accompanied by significantly downregulated Nrf2 downstream target gene products including HO-1, catalase, GCLC, and NQO-1 in the kidney tissues of rats with adenine-induced CRF. These findings point to the impaired activation of the Nrf2 pathway in this model. However, these aberrant changes were reversed in the adenine-induced CRF rats treated by SKI and three anthraquinones. Additionally, immunohistochemistry analysis showed treatment with SKI and three anthraquinones could significantly enhance the COX-2 expression in the kidney tissues of the adenine-induced CRF rats compared with that of the CRF rats (**Figure 5C**). Furthermore, SKI and rhein showed the stronger inhibitory effect on the significantly downregulated anti-inflammatory and anti-oxidative protein expression in the Keap1/Nrf2 signaling pathway than chrysophanol and emodin, which was consistent with the results of their effects on the pro-fibrotic protein expression including collagen I, α-SMA, fibronectin, and vimentin. Taken together, these results indicated that the activation of the anti-inflammatory and anti-oxidative Keap1/Nrf2 signaling pathway was involved in SKI and three anthraquinones against renal fibrosis in the adenine-induced CRF rats.

DISCUSSION

The progression of CKD and renal fibrosis, one of the biggest issues in nephrology, indicated that patients inevitably progress ESRD and require dialysis or kidney transplantation (Webster et al., 2017; Aydin et al., 2019; Van Sandwijk et al., 2019). Numerous studies have demonstrated that renal fibrosis was associated with the dysbiosis or dysregulation of gut microbiota, non-coding RNAs, renin–angiotensin system, aryl hydrocarbon receptor, IκB/NF-κB, Keap1/Nrf2, TGF-β/Smad, and Wnt/β-catenin signaling pathways (Ma et al., 2018a; Chen et al., 2019b; Garg and Maurya, 2019; Zhao et al., 2019; Hu et al., 2020a; Miao et al., 2021b; Wang et al., 2021d; Wu et al., 2021; Zhou et al., 2021) as well as metabolite disorders including tryptophan metabolism and lipid metabolism (Zhao, 2013a; Zhao et al., 2015; Wang et al., 2019; Liu et al., 2021a). Further studies have demonstrated that activation of IκB/NF-κB and Keap1/Nrf2 signaling pathways could mediate or crosstalk these signaling pathways in both patients with CKD and experimental research studies (Chen et al., 2017a; Chen et al., 2017b; Chen et al., 2019c). Of note, IκB/NF-κB and Keap1/Nrf2 signaling pathways were the most important mediators in oxidative stress and inflammation that played a central role in the development and progression of CKD and its complications (Meng et al., 2014; Chen et al., 2016; Feng et al., 2019a). Oxidative stress was a status in which reactive oxygen species (ROS) generation surpassed the anti-oxidant defense system capacity. It led to the increased ROS production and damaged anti-oxidant capacity. Oxidative stress and inflammation were inseparably linked, as each begets and amplifies the other.

The activation of NF-κB and the impairment of Nrf2 were the most important pro-inflammatory and anti-inflammatory signals, respectively. The NF-κB activation mediated the expression of pro-inflammatory cytokines and chemokines, and oxidative stress evoked recruitment and activation of leukocytes and resident cells, thus triggering inflammation (Miao et al., 2021a). Although oxidative stress and inflammation had a central role in progression of CKD, ACEI and ARB have been used as first-line drugs for treatment of CKD and its complications. This led to the contradiction between the underlying pathomechanism elucidation and the treatment of CKD patients. Therefore, developing the agents to target oxidative stress and inflammation is necessary for the effective treatment of CKD patients.

The adenine diet led to severe CRF due to adenine-derived very low-soluble 2,8-dihydroxyadenine in the renal tubule, which induced tubulointerstitial nephritis, characterized by gross swelling, kidney discoloration and deformity, urinary concentrating ability loss (polyuria), azotemia (increased serum urea), anemia, hypertension, and minimal proteinuria (Zhao et al., 2014). The histopathological results showed tubulointerstitial damage including extensive inflammatory cell infiltration, tubular dilation, and fibrosis in the kidney tissues. Severe interstitial inflammatory cell infiltration was one of the most typical pathological features in the kidney tissues of adenine-induced CRF rats. Substantial evidence has demonstrated that many natural products, such as *Rhubarb*, *Astragalus*, and *Polyporus umbellatus*, showed the renoprotective activity by anti-oxidative and/or anti-inflammatory effects (Wang et al., 2012; Zhao, 2013b; Zhang et al., 2014; Shahzad et al., 2016; Liao et al., 2017). Although, the exact mechanisms for these natural products have not

been revealed, it has been suggested that they may possibly possess anti-oxidant and/or anti-inflammatory activity. Our current findings demonstrated rats with CRF showed the upregulating protein expression of p-IκBα and nuclear p65 indicating NF-κB activation in kidney tissues, meanwhile, this was accompanied by the upregulating protein expression of COX-2, MCP-1, iNOS, 12-LO, and NAD(P)H oxidase subunits ($p47^{phox}$, $p67^{phox}$, and $gp91^{phox}$) in the kidney tissues of the adenine-induced CRF rats. However, these upregulating expressions were inhibited by treatment of SKI. These results were in agreement with previous studies of natural products, such as *Poria cocos* and *Polyporus umbellatus* as well as their components including poricoic acid A, poricoic acid ZM, poricoic acid ZP, and ergone against renal fibrosis by targeting IκB/NF-κB and Keap1/Nrf2 signaling pathways (Feng et al., 2019b; Chen et al., 2019d; Chen et al., 2019e; Chen et al., 2019f; Wang et al., 2020b). Both clinical and experimental studies have demonstrated that SKI could improve renal function in CKD. Several previous publications have highlighted that SKI retarded renal fibrosis by inhibiting levels of interleukin-6, interleukin-1β, and TNF-α (Zhang et al., 2020) and modulating TGF-β1/Smad3 and JAK2/STAT3 signaling pathways (Wu et al., 2015; Qin et al., 2021). Another study has been demonstrated that treatment with SKI could inhibit the protein expression of NF-κB at both mRNA and protein levels in kidney tissues of renal ischemia–reperfusion injury mice with DN induced by high-fat diet and streptozocin (Liu, 2018). Little was known about its underlying anti-oxidative and anti-inflammatory mechanism. Our findings suggested that SKI retarded renal fibrosis by inhibiting the activation of the IκB/NF-κB signaling pathway. Therefore, our current works and that of others suggested that effective inhibition of activated oxidative stress and inflammation via the IκB/NF-κB signaling pathway retarded CRF progression.

In the bioactive fraction of ethyl acetate extract of SKI, we identified three anthraquinones including chrysophanol, emodin, and rhein that were major and bioactive components of *Rheum officinale*, which has been demonstrated to improve CKD and renal fibrosis (Wang et al., 2012; Zhang et al., 2018; Zeng et al., 2021). Compared with chrysophanol and emodin, rhein showed a strong inhibitory effect on renal fibrosis. Although rhein has been widely demonstrated to protect against renal fibrosis (Zeng et al., 2014; Hu et al., 2019; He et al., 2020; Wu et al., 2020; Yu et al., 2020), only two previous studies have reported that rhein protected against renal fibrosis by inhibiting the NF-κB p65 protein expression (Liu et al., 2021b) and lincRNA-COX2/miR-150-5p/STAT1 axis (Hu et al., 2020b). Similarly, a number of publications have demonstrated that emodin retarded renal fibrosis by modulating several pathways, such as TGF-β/Smad, TGF-β/BMP-7, PI3K/Akt/GSK-3β, and Bax/caspase-3 signaling pathways (Jing et al., 2017; Ma et al., 2018b; Yang et al., 2020; Liu et al., 2021c). Furthermore, several studies have demonstrated the inhibitory effect of emodin on renal fibrosis by suppressing the NF-κB p65 protein expression (Lu et al., 2020) or the levels of ROS, TNF-α, and interleukin-6 (Chen et al., 2017c; Jing et al., 2017). So far, no publication demonstrated the renoprotective effect of chrysophanol through modulating the IκB/NF-κB signaling pathway. Recently, two publications have demonstrated that chrysophanol protected against renal fibrosis by the TGF-β/Smad signaling pathway (Dou et al., 2020; Guo et al., 2020). Therefore, our study demonstrated that the inhibition of the activated IκB/NF-κB signaling pathway might be the underlying molecular mechanism of anti-oxidant and anti-inflammatory bioactivities of both SKI and three anthraquinones against renal fibrosis.

Compared with pro-inflammatory system, the natural anti-oxidant defense system contains many ROS scavenger molecules from exogenous dietary and endogenous components, anti-oxidant enzymes and substrates, and phase 2 detoxifying enzymes (Cuadrado et al., 2019). Each component contributes to their specific function and works in a collaborated way with the other components to exert their protective effects against tissue damage and dysfunction. Under physiological milieu, oxidative stress elicited increasing endogenous anti-oxidant and cytoprotective proteins and enzymes to restrain dysfunction and tissue damage (Cuadrado et al., 2019). This process was induced by the activation of the Nrf2 which plays a central role in the basal activity and coordinated regulation of about 250 genes such as HO-1, GCLC, NQO1, catalase, superoxide dismutase, thioredoxin, and glutamate–cysteine ligase (Chen et al., 2017a; Cuadrado et al., 2019). Our findings first demonstrated SKI treatment could upregulate nuclear Nrf2 protein expression and downregulate Keap1 protein expression in the kidney tissue of CRF rats, which was accompanied by upregulating Nrf2 downstream target gene products. To date, no publication demonstrated the renoprotective effect of SKI through activating the Keap1/Nrf2 signaling pathway. Our current findings first point to the beneficial effects of SKI on the impaired activation of the Keap1/Nrf2 pathway in the adenine-induced CRF rats.

Although increasing evidence has reported that chrysophanol, emodin, and rhein could improve many refractory diseases by the activation of the impaired Keap1/Nrf2 signaling pathway, and few studies demonstrated the renoprotective effect of chrysophanol, emodin, and rhein by regulating the Keap1/Nrf2 signaling pathway. Two previous *in vitro* studies have demonstrated that emodin could increase the activities of anti-oxidant enzymes such as catalase, glutathione peroxidase, superoxide dismutase, glutathione reductase, and glutathione S-transferase in the hypoxia/reoxygenation-induced HK-2 cells or cisplatin-induced human kidney HEK 293 cells (Waly et al., 2013; Chen et al., 2017c). Another *in vivo* experiment has demonstrated that emodin significantly inhibited the decreased renal cortical glutathione levels and superoxide dismutase activity in the cisplatin-induced nephrotoxicity rats (Ali et al., 2013). However, no publication demonstrated the renoprotective effect of chrysophanol and rhein through modulating the Keap1/Nrf2 signaling pathway. Therefore, our study revealed that activation of the impaired Keap1/Nrf2 signaling pathway might be also a potential molecular mechanism of anti-oxidant and anti-inflammatory bioactivities of both SKI and three anthraquinones against renal fibrosis.

Collectively, our current study first elucidated that SKI and its main components including chrysophanol, emodin, and rhein protected against renal fibrosis by inhibiting oxidative stress and inflammation via simultaneous targeting pro-inflammatory IκB/NF-κB and anti-inflammatory Keap1/Nrf2 signaling pathways, which revealed the underlying molecular mechanism of SKI and

its main components against renal fibrosis. These findings uncovered the potential effective material basis and molecular mechanism of the renoprotective effect of SKI, which will pave the way for discovery of lead compounds against renal fibrosis by inhibiting oxidative stress and inflammation via targeting the redox pathway.

CONCLUSION

This study first demonstrated that SKI and its components including chrysophanol, emodin, and rhein protected against renal fibrosis. Mechanistically, this study revealed the potential molecular mechanism of the anti-oxidative and anti-inflammatory effects of SKI by inhibiting oxidative stress and inflammation via simultaneous targeting IκB/NF-κB and Keap1/Nrf2 signaling pathways.

DATA AVAILABILITY STATEMENT

The raw data supporting the conclusion of this article will be made available by the authors, without undue reservation.

ETHICS STATEMENT

The animal study was reviewed and approved by Northwest University.

AUTHOR CONTRIBUTIONS

Y-YZ was responsible for the conception and design of the study; and L-PL, PS, L-LR, and H-JL for the data collection, analysis, and image processing. Y-YZ wrote the article; and Y-MZ revised the article. L-PL and Y-YZ were responsible for the final approval of the version to be submitted. All authors read and approved the final article.

FUNDING

This study was supported by the Shaanxi Key Science and Technology Plan Project (No. 2019ZDLSF04-04-02), National Key Research and Development Project (No. 2019YFC1709405), and National Natural Science Foundation of China (Nos. 82074002, 818729858).

REFERENCES

Ali, B. H., Al-Salam, S., Al Husseini, I. S., Al-Lawati, I., Waly, M., Yasin, J., et al. (2013). Abrogation of Cisplatin-Induced Nephrotoxicity by Emodin in Rats. *Fundam. Clin. Pharmacol.* 27 (2), 192–200. doi:10.1111/j.1472-8206.2011.01003.x

Aydin, Z., Karadag, S., Ozturk, S., Gursu, M., Uzun, S., Cebeci, E., et al. (2019). Evaluation of the Relationship between Advanced Oxidation End Products and Inflammatory Markers in Maintenance Hemodialysis Patients. *Jna* 1 (2), 24–30. doi:10.14302/issn.2574-4488.jna-19-3112

Bhargava, V., Singh, K., Meena, P., and Sanyal, R. (2021). Nephrogenic aystemic Fibrosis: A Frivolous Entity. *World J. Nephrol.* 10 (3), 29–36. doi:10.5527/wjn.v10.i3.29

Carta, P., Lorenzo, D., Luciano, M., Aida, L., Caroti, L., Cirami, L., et al. (2020). Malignancies after Renal Transplantation: A Single center Retrospective Study. *J. Nephrol. Hypertens.* 3 (1), 1009.

Chauveau, P. (2018). Nutrition in Chronic Kidney Disease: Nephrology Dialysis Transplantation Notable Advances in 2018. *Nephrol. Dial. Transpl.* 34 (6), 893–896. doi:10.1093/ndt/gfz077

Chen, D. Q., Cao, G., Chen, H., Argyopoulos, C. P., Yu, H., Su, W., et al. (2019). Identification of Serum Metabolites Associating with Chronic Kidney Disease Progression and Anti-fibrotic Effect of 5-methoxytryptophan. *Nat. Commun.* 10 (1), 1476. doi:10.1038/s41467-019-09329-0

Chen, D. Q., Cao, G., Chen, H., Liu, D., Su, W., Yu, X. Y., et al. (2017). Gene and Protein Expressions and Metabolomics Exhibit Activated Redox Signaling and Wnt/β-Catenin Pathway Are Associated with Metabolite Dysfunction in Patients with Chronic Kidney Disease. *Redox Biol.* 12, 505–521. doi:10.1016/j.redox.2017.03.017

Chen, D. Q., Feng, Y. L., Cao, G., and Zhao, Y. Y. (2018). Natural Products as a Source for Antifibrosis Therapy. *Trends Pharmacol. Sci.* 39 (11), 937–952. doi:10.1016/j.tips.2018.09.002

Chen, D. Q., Feng, Y. L., Chen, L., Liu, J. R., Wang, M., Vaziri, N. D., et al. (2019). Poricoic Acid A Enhances Melatonin Inhibition of AKI-To-CKD Transition by Regulating Gas6/AxlNFκB/Nrf2 axis. *Free Radic. Biol. Med.* 134, 484–497. doi:10.1016/j.freeradbiomed.2019.01.046

Chen, D. Q., Hu, H. H., Wang, Y. N., Feng, Y. L., Cao, G., and Zhao, Y. Y. (2018). Natural Products for the Prevention and Treatment of Kidney Disease. *Phytomedicine* 50, 50–60. doi:10.1016/j.phymed.2018.09.182

Chen, H., Cao, G., Chen, D. Q., Wang, M., Vaziri, N. D., Zhang, Z. H., et al. (2016). Metabolomics Insights into Activated Redox Signaling and Lipid Metabolism Dysfunction in Chronic Kidney Disease Progression. *Redox Biol.* 10, 168–178. doi:10.1016/j.redox.2016.09.014

Chen, H., Huang, R. S., Yu, X. X., Ye, Q., Pan, L. L., Shao, G. J., et al. (2017). Emodin Protects against Oxidative Stress and Apoptosis in HK-2 Renal Tubular Epithelial Cells after Hypoxia/reoxygenation. *Exp. Ther. Med.* 14 (1), 447–452. doi:10.3892/etm.2017.4473

Chen, L., Chen, D. Q., Liu, J. R., Zhang, J., Vaziri, N. D., Zhuang, S., et al. (2019). Unilateral Ureteral Obstruction Causes Gut Microbial Dysbiosis and Metabolome Disorders Contributing to Tubulointerstitial Fibrosis. *Exp. Mol. Med.* 51 (3), 1–18. doi:10.1038/s12276-019-0234-2

Chen, L., Chen, D. Q., Wang, M., Liu, D., Chen, H., Dou, F., et al. (2017). Role of RAS/Wnt/β-catenin axis Activation in the Pathogenesis of Podocyte Injury and Tubulo-Interstitial Nephropathy. *Chem. Biol. Interact* 273, 56–72. doi:10.1016/j.cbi.2017.05.025

Chen, L., Yang, T., Lu, D. W., Zhao, H., Feng, Y. L., Chen, H., et al. (2018). Central Role of Dysregulation of TGF-β/Smad in CKD Progression and Potential Targets of its Treatment. *Biomed. Pharmacother.* 101, 670–681. doi:10.1016/j.biopha.2018.02.090

Chen, T. K., Knicely, D. H., and Grams, M. E. (2019). Chronic Kidney Disease Diagnosis and Management: A Review. *JAMA* 322 (13), 1294–1304. doi:10.1001/jama.2019.14745

Chen, Y. Y., Chen, D. Q., Chen, L., Liu, J. R., Vaziri, N. D., Guo, Y., et al. (2019). Microbiome-metabolome Reveals the Contribution of Gut-Kidney axis on Kidney Disease. *J. Transl Med.* 17 (1), 5. doi:10.1186/s12967-018-1756-4

Chen, Y. Y., Yu, X. Y., Chen, L., Vaziri, N. D., Ma, S. C., and Zhao, Y. Y. (2019). Redox Signaling in Aging Kidney and Opportunity for Therapeutic Intervention through Natural Products. *Free Radic. Biol. Med.* 141, 141–149. doi:10.1016/j.freeradbiomed.2019.06.012

Choi, H. Y., Lim, J. E., and Hong, J. H. (2010). Curcumin Interrupts the Interaction between the Androgen Receptor and Wnt/β-Catenin Signaling Pathway in LNCaP Prostate Cancer Cells. *Prostate Cancer Prostatic Dis.* 13 (4), 343–349. doi:10.1038/pcan.2010.26

Cuadrado, A., Rojo, A. I., Wells, G., Hayes, J. D., Cousin, S. P., Rumsey, W. L., et al. (2019). Therapeutic Targeting of the NRF2 and KEAP1 Partnership in Chronic Diseases. *Nat. Rev. Drug Discov.* 18 (4), 295–317. doi:10.1038/s41573-018-0008-x

Dou, F., Ding, Y., Wang, C., Duan, J., Wang, W., Xu, H., et al. (2020). Chrysophanol Ameliorates Renal Interstitial Fibrosis by Inhibiting the TGF-β/Smad Signaling Pathway. *Biochem. Pharmacol.* 180, 114079. doi:10.1016/j.bcp.2020.114079

Feng, Y. L., Cao, G., Chen, D. Q., Vaziri, N. D., Chen, L., Zhang, J., et al. (2019). Microbiome-metabolomics Reveals Gut Microbiota Associated with Glycine-Conjugated Metabolites and Polyamine Metabolism in Chronic Kidney Disease. *Cell Mol Life Sci* 76 (24), 4961–4978. doi:10.1007/s00018-019-03155-9

Feng, Y. L., Chen, H., Chen, D. Q., Vaziri, N. D., Su, W., Ma, S. X., et al. (2019). Activated NF-κB/Nrf2 and Wnt/β-Catenin Pathways Are Associated with Lipid Metabolism in CKD Patients with Microalbuminuria and Macroalbuminuria. *Biochim. Biophys. Acta Mol. Basis Dis.* 1865 (9), 2317–2332. doi:10.1016/j.bbadis.2019.05.010

Fu, B., Yang, J., Chen, J., Lin, L., Chen, K., Zhang, W., et al. (2019). Preventive Effect of Shenkang Injection against High Glucose-Induced Senescence of Renal Tubular Cells. *Front. Med.* 13 (2), 267–276. doi:10.1007/s11684-017-0586-8

Garg, M., and Maurya, N. (2019). WNT/β-catenin Signaling in Urothelial Carcinoma of Bladder. *World J. Nephrol.* 8 (5), 83–94. doi:10.5527/wjn.v8.i5.83

Guo, C., Wang, Y., Piao, Y., Rao, X., and Yin, D. (2020). Chrysophanol Inhibits the Progression of Diabetic Nephropathy via Inactivation of TGF-β Pathway. *Drug Des. Devel Ther.* 14, 4951–4962. doi:10.2147/DDDT.S274191

He, X., Li, G., Chen, Y., Xiao, Q., Yu, X., Yu, X., et al. (2020). Pharmacokinetics and Pharmacodynamics of the Combination of Rhein and Curcumin in the Treatment of Chronic Kidney Disease in Rats. *Front. Pharmacol.* 11, 573118. doi:10.3389/fphar.2020.573118

Hu, H. C., Zheng, L. T., Yin, H. Y., Tao, Y., Luo, X. Q., Wei, K. S., et al. (2019). A Significant Association between Rhein and Diabetic Nephropathy in Animals: A Systematic Review and Meta-Analysis. *Front. Pharmacol.* 10, 1473. doi:10.3389/fphar.2019.01473

Hu, H. H., Cao, G., Wu, X. Q., Vaziri, N. D., and Zhao, Y. Y. (2020). Wnt Signaling Pathway in Aging-Related Tissue Fibrosis and Therapies. *Ageing Res. Rev.* 60, 101063. doi:10.1016/j.arr.2020.101063

Hu, J., Yang, Z., Wu, H., and Wang, D. (2020). Rhein Attenuates Renal Inflammatory Injury of Uric Acid Nephropathy via lincRNA-Cox2/miR-150-5p/STAT1 axis. *Int. Immunopharmacol* 85, 106620. doi:10.1016/j.intimp.2020.106620

Humphreys, B. D. (2018). Mechanisms of Renal Fibrosis. *Annu. Rev. Physiol.* 80, 309–326. doi:10.1146/annurev-physiol-022516-034227

Jain, D., Haddad, D. B., and Goel, N. (2019). Choice of Dialysis Modality Prior to Kidney Transplantation: Does it Matter? *World J. Nephrol.* 8 (1), 1–10. doi:10.5527/wjn.v8.i1.1

Jing, D., Bai, H., and Yin, S. (2017). Renoprotective Effects of Emodin against Diabetic Nephropathy in Rat Models Are Mediated via PI3K/Akt/GSK-3β and Bax/caspase-3 Signaling Pathways. *Exp. Ther. Med.* 14 (5), 5163–5169. doi:10.3892/etm.2017.5131

Li, S. S., Sun, Q., Hua, M. R., Suo, P., Chen, J. R., Yu, X. Y., et al. (2021). Targeting the Wnt/β-Catenin Signaling Pathway as a Potential Therapeutic Strategy in Renal Tubulointerstitial Fibrosis. *Front. Pharmacol.* 12, 719880. doi:10.3389/fphar.2021.719880

Liao, H., Hu, L., Cheng, X., Wang, X., Li, J., Banbury, L., et al. (2017). Are the Therapeutic Effects of Huangqi (Astragalus Membranaceus) on Diabetic Nephropathy Correlated with its Regulation of Macrophage iNOS Activity? *J. Immunol. Res.* 2017, 3780572. doi:10.1155/2017/3780572

Liu, J. R., Miao, H., Deng, D. Q., Vaziri, N. D., Li, P., and Zhao, Y. Y. (2021). Gut Microbiota-Derived Tryptophan Metabolism Mediates Renal Fibrosis by Aryl Hydrocarbon Receptor Signaling Activation. *Cel Mol Life Sci* 78 (3), 909–922. doi:10.1007/s00018-020-03645-1

Liu, M., Wang, L., Wu, X., Gao, K., Wang, F., Cui, J., et al. (2021). Rhein Protects 5/6 Nephrectomized Rat against Renal Injury by Reducing Inflammation via NF-Kb Signaling. *Int. Urol. Nephrol.* 53 (7), 1473–1482. doi:10.1007/s11255-020-02739-w

Liu, W., Gu, R., Lou, Y., He, C., Zhang, Q., and Li, D. (2021). Emodin-induced Autophagic Cell Death Hinders Epithelial-Mesenchymal Transition via Regulation of BMP-7/tgf-B1 in Renal Fibrosis. *J. Pharmacol. Sci.* 146 (4), 216–225. doi:10.1016/j.jphs.2021.03.009

Liu, Y., Shi, G., Yee, H., Wang, W., Han, W., Liu, B., et al. (2019). Shenkang Injection, a Modern Preparation of Chinese Patent Medicine, Diminishes Tubulointerstitial Fibrosis in Obstructive Nephropathy via Targeting Pericyte-Myofibroblast Transition. *Am. J. Transl Res.* 11 (4), 1980–1996.

Liu, Y., (2018). Protective Effect of Shenkang Injection against Renal Ischemia-Reperfusion Injury via Inflammation Inhibition in Type 2 Diabetic Rats. *Int. J. Clin. Exp. Med.* 11 (10), 10446–10457.

Lu, Z., Ji, C., Luo, X., Lan, Y., Han, L., Chen, Y., et al. (2020). Nanoparticle-mediated Delivery of Emodin via Colonic Irrigation Attenuates Renal Injury in 5/6 Nephrectomized Rats. *Front. Pharmacol.* 11, 606227. doi:10.3389/fphar.2020.606227

Ma, G., (2021). Effect of Shenkang Injection on TGF-B1 Level, Peritoneal Function and Microinflammatory Status in Peritoneal Dialysis Patients with Chronic Renal Failure. *Curr. Med. Sci.* 37 (3), 1359–1363.

Ma, L., Li, H., Zhang, S., Xiong, X., Chen, K., Jiang, P., et al. (2018). Emodin Ameliorates Renal Fibrosis in Rats via TGF-β1/Smad Signaling Pathway and Function Study of Smurf 2. *Int. Urol. Nephrol.* 50 (2), 373–382. doi:10.1007/s11255-017-1757-x

Ma, S.-X., Shang, Y.-Q., Zhang, H.-Q., and Su, W. (2018). Action Mechanisms and Therapeutic Targets of Renal Fibrosis. *Jna* 1 (2), 4–14. doi:10.14302/issn.2574-4488.jna-18-2443

Mantovani, A., and Zusi, C. (2020). PNPLA3 Gene and Kidney Disease. *Explor Med.* 1, 42–50. doi:10.37349/emed.2020.00004

Medina Rangel, P. X., Priyadarshini, A., and Tian, X. (2021). New Insights into the Immunity and Podocyte in Glomerular Health and Disease: From Pathogenesis to Therapy in Proteinuric Kidney Disease. *Integr. Med. Nephrol. Androl.* 8, 5.

Meng, X. M., Nikolic-Paterson, D. J., and Lan, H. Y. (2014). Inflammatory Processes in Renal Fibrosis. *Nat. Rev. Nephrol.* 10 (9), 493–503. doi:10.1038/nrneph.2014.114

Miao, H., Cao, G., Wu, X. Q., Chen, Y. Y., Chen, D. Q., Chen, L., et al. (2020). Identification of Endogenous 1-aminopyrene as a Novel Mediator of Progressive Chronic Kidney Disease via Aryl Hydrocarbon Receptor Activation. *Br. J. Pharmacol.* 177 (15), 3415–3435. doi:10.1111/bph.15062

Miao, H., Wu, X. Q., Zhang, D. D., Wang, Y. N., Guo, Y., and Li, P. (2021). Deciphering the Cellular Mechanisms Underlying Fibrosis-Associated Diseases and Therapeutic Avenues. *Pharmacol. Res.* 163, 105316. doi:10.1016/j.phrs.2020.105316

Miao, H., Wu, X., Wang, Y., Chen, D., Chen, L., Guo, Y., et al. (2021). 1-Hydroxypyrene Mediates Renal Fibrosis through Aryl Hydrocarbon Receptor Signalling Pathway. *Br. J. Pharmacol.* 10.1111/bph.15705.

Qin, T., Wu, L., Hua, Q., Song, Z., Pan, Y., and Liu, T. (2020). Prediction of the Mechanisms of Action of Shenkang in Chronic Kidney Disease: A Network Pharmacology Study and Experimental Validation. *J. Ethnopharmacol* 246, 112128. doi:10.1016/j.jep.2019.112128

Qin, T., Wu, Y., Liu, T., and Wu, L. (2021). Effect of Shenkang on Renal Fibrosis and Activation of Renal Interstitial Fibroblasts through the JAK2/STAT3 Pathway. *BMC Complement. Med. Ther.* 21 (1), 12. doi:10.1186/s12906-020-03180-3

Salehi, B., Carneiro, J. N. P., Rocha, J. E., Coutinho, H. D. M., Morais Braga, M. F. B., Sharifi-Rad, J., et al. (2021). Astragalus Species: Insights on its Chemical Composition toward Pharmacological Applications. *Phytotherapy Res.* 35 (5), 2445–2476. doi:10.1002/ptr.6974

Sawhney, H., and Gill, S. S. (2020). Renal Transplant Recipient Seizure Practical Management. *World J. Nephrol.* 9 (1), 1–8. doi:10.5527/wjn.v9.i1.1

Shahzad, M., Shabbir, A., Wojcikowski, K., Wohlmuth, H., and Gobe, G. C. (2016). The Antioxidant Effects of Radix Astragali (Astragalus Membranaceus and Related Species) in Protecting Tissues from Injury and Disease. *Curr. Drug Targets* 17 (12), 1331–1340. doi:10.2174/1389450116666150907104742

Song, Z., Qin, T., Pan, Y., Wu, L., Liu, T., and Hua, Q. (2019). Shenkang Injection Improves Coagulation in Patients with Chronic Kidney Disease: a Systematic Review and Meta-Analysis. *J. Tradit Chin. Med.* 39 (4), 451–458.

Tu, Y., Xue, Y., Guo, D., Sun, L., and Guo, M. (2015). Carthami Flos: a Review of its Ethnopharmacology, Pharmacology and Clinical Applications. *Revista Brasileira de Farmacognosia* 25 (5), 553–566. doi:10.1016/j.bjp.2015.06.001

Van Sandwijk, M. S., Klooster, A., Ten Berge, I. J., Diepstra, A., Florquin, S., Hoelbeek, J. J., et al. (2019). Complement Activation and Long-Term Graft Function in ABO-Incompatible Kidney Transplantation. *World J. Nephrol.* 8 (6), 95–108. doi:10.5527/wjn.v8.i6.95

Waly, M. I., Ali, B. H., Al-Lawati, I., and Nemmar, A. (2013). Protective Effects of Emodin against Cisplatin-Induced Oxidative Stress in Cultured Human Kidney (HEK 293) Cells. *J. Appl. Toxicol.* 33 (7), 626–630. doi:10.1002/jat.1788

Wang, H., Song, H., Yue, J., Li, J., Hou, Y. B., and Deng, J. L. (2012). Rheum Officinale (A Traditional Chinese Medicine) for Chronic Kidney Disease.

Cochrane Database Syst. Rev. (7), Cd008000. doi:10.1002/14651858.CD008000.pub2

Wang, M., Chen, D. Q., Chen, L., Cao, G., Zhao, H., Liu, D., et al. (2018). Novel Inhibitors of the Cellular Renin-Angiotensin System Components, Poricoic Acids, Target Smad3 Phosphorylation and Wnt/β-Catenin Pathway against Renal Fibrosis. *Br. J. Pharmacol.* 175 (13), 2689–2708. doi:10.1111/bph.14333

Wang, M., Hu, H. H., Chen, Y. Y., Chen, L., Wu, X. Q., and Zhao, Y. Y. (2020). Novel Poricoic Acids Attenuate Renal Fibrosis through Regulating Redox Signalling and Aryl Hydrocarbon Receptor Activation. *Phytomedicine* 79, 153323. doi:10.1016/j.phymed.2020.153323

Wang, R.-n., Zhao, H.-c., Huang, J.-y., Wang, H.-l., Li, J.-s., Lu, Y., et al. (2021). Challenges and strategies in progress of drug delivery system for traditional Chinese medicine Salviae Miltiorrhizae Radix et Rhizoma (Danshen). *Chin. Herbal Medicines* 13 (1), 78–89. doi:10.1016/j.chmed.2020.08.001

Wang, Y., Li, M., Li, C., Xu, S., Wu, J., Zhang, G., et al. (2020). Efficacy and Safety of Shenkang Injection as Adjuvant Therapy in Patients with Diabetic Nephropathy: A Protocol for Systematic Review and Meta-Analysis. *Medicine (Baltimore)* 99 (52), e23821. doi:10.1097/MD.0000000000023821

Wang, Y. N., Hu, H. H., Zhang, D. D., Wu, X. Q., Liu, J. L., Guo, Y., et al. (2021). The Dysregulation of Eicosanoids and Bile Acids Correlates with Impaired Kidney Function and Renal Fibrosis in Chronic Renal Failure. *Metabolites* 11 (2), 127. doi:10.3390/metabo11020127

Wang, Y. N., Ma, S. X., Chen, Y. Y., Chen, L., Liu, B. L., Liu, Q. Q., et al. (2019). Chronic Kidney Disease: Biomarker Diagnosis to Therapeutic Targets. *Clin. Chim. Acta* 499, 54–63. doi:10.1016/j.cca.2019.08.030

Wang, Y. N., Wu, X. Q., Zhang, D. D., Hu, H. H., Liu, J. L., Vaziri, N. D., et al. (2021). Polyporus Umbellatus Protects against Renal Fibrosis by Regulating Intrarenal Fatty Acyl Metabolites. *Front. Pharmacol.* 12, 633566. doi:10.3389/fphar.2021.633566

Wang, Y. N., Yang, C. E., Zhang, D. D., Chen, Y. Y., Yu, X. Y., Zhao, Y. Y., et al. (2021). Long Non-coding RNAs: A Double-Edged Sword in Aging Kidney and Renal Disease. *Chem. Biol. Interact* 337, 109396. doi:10.1016/j.cbi.2021.109396

Webster, A. C., Nagler, E. V., Morton, R. L., and Masson, P. (2017). Chronic Kidney Disease. *Lancet* 389 (10075), 1238–1252. doi:10.1016/S0140-6736(16)32064-5

Wu, X., Guan, Y., Yan, J., Liu, M., Yin, Y., Duan, J., et al. (2015). ShenKang Injection Suppresses Kidney Fibrosis and Oxidative Stress via Transforming Growth Factor-β/Smad3 Signalling Pathway *In Vivo* and *In Vitro*. *J. Pharm. Pharmacol.* 67 (8), 1054–1065. doi:10.1111/jphp.12412

Wu, X., Liu, M., Wei, G., Guan, Y., Duan, J., Xi, M., et al. (2020). Renal protection of Rhein against 5/6 Nephrectomied-Induced Chronic Kidney Disease: Role of SIRT3-Foxo3α Signalling Pathway. *J. Pharm. Pharmacol.* 72 (5), 699–708. doi:10.1111/jphp.13234

Wu, X. Q., Zhang, D. D., Wang, Y. N., Tan, Y. Q., Yu, X. Y., and Zhao, Y. Y. (2021). AGE/RAGE in Diabetic Kidney Disease and Ageing Kidney. *Free Radic. Biol. Med.* 171, 260–271. doi:10.1016/j.freeradbiomed.2021.05.025

Xu, S., Lv, Y., Zhao, J., Wang, J., Zhao, X., and Wang, S. (2016). Inhibitory Effects of Shenkang Injection and its Main Component Emodin on the Proliferation of High Glucose-induced R-enal M-esangial C-ells through C-ell C-ycle R-egulation and I-nduction of A-poptosis. *Mol. Med. Rep.* 14 (4), 3381–3388. doi:10.3892/mmr.2016.5631

Yanai, K., Ishibashi, K., and Morishita, Y. (2021). Systematic Review and Meta-Analysis of Renin-Angiotensin-Aldosterone System Blocker Effects on the Development of Cardiovascular Disease in Patients with Chronic Kidney Disease. *Front. Pharmacol.* 12, 662544. doi:10.3389/fphar.2021.662544

Yang, F., Deng, L., Li, J., Chen, M., Liu, Y., Hu, Y., et al. (2020). Emodin Retarded Renal Fibrosis through Regulating HGF and TGFβ-Smad Signaling Pathway. *Drug Des. Devel Ther.* 14, 3567–3575. doi:10.2147/DDDT.S245847

Yang, Y., and Wu, C. (2021). Traditional Chinese Medicine in Ameliorating Diabetic Kidney Disease via Modulating Gut Microbiota. *Integr. Med. Nephrol. Androl.* 8, 8.

Yu, W., Yang, W., Zhao, M. Y., and Meng, X. L. (2020). Functional Metabolomics Analysis Elucidating the Metabolic Biomarker and Key Pathway Change Associated with the Chronic Glomerulonephritis and Revealing Action Mechanism of Rhein. *Front. Pharmacol.* 11, 554783. doi:10.3389/fphar.2020.554783

Zeng, C. C., Liu, X., Chen, G. R., Wu, Q. J., Liu, W. W., Luo, H. Y., et al. (2014). The Molecular Mechanism of Rhein in Diabetic Nephropathy. *Evid. Based Complement. Alternat Med.* 2014, 487097. doi:10.1155/2014/487097

Zeng, J. Y., Wang, Y., Miao, M., and Bao, X. R. (2021). The Effects of Rhubarb for the Treatment of Diabetic Nephropathy in Animals: A Systematic Review and Meta-Analysis. *Front. Pharmacol.* 12, 602816. doi:10.3389/fphar.2021.602816

Zhang, B., Zhang, X.-l., Zhang, C.-y., Sun, G.-b., and Sun, X.-b. (2020). Shenkang Injection Protects against Diabetic Nephropathy in Streptozotocin (STZ)-induced Mice through Enhancement of Anti-oxidant and Anti-inflammatory Activities. *Chin. Herbal Medicines* 12 (3), 289–296. doi:10.1016/j.chmed.2020.05.004

Zhang, H. W., Lin, Z. X., Xu, C., Leung, C., and Chan, L. S. (2014). Astragalus (A Traditional Chinese Medicine) for Treating Chronic Kidney Disease. *Cochrane Database Syst. Rev.* (10), Cd008369. doi:10.1002/14651858.CD008369.pub2

Zhang, Y., Sun, J., Liu, H., and Zhai, X. (2017). Effects of Injection Shenkang and Alprostadil Combination on Contrast-Induced Nephropathy in Patient with Diabetes Complicated with Mild to Moderate Renal Insufficiency. *Bangladesh J. Pharmacol.* 12 (3), 308–312. doi:10.3329/bjp.v12i3.32070

Zhang, Z. H., Li, M. H., Liu, D., Chen, H., Chen, D. Q., Tan, N. H., et al. (2018). Rhubarb Protect against Tubulointerstitial Fibrosis by Inhibiting TGF-β/Smad Pathway and Improving Abnormal Metabolome in Chronic Kidney Disease. *Front. Pharmacol.* 9, 1029. doi:10.3389/fphar.2018.01029

Zhao, H., Chen, L., Yang, T., Feng, Y. L., Vaziri, N. D., Liu, B. L., et al. (2019). Aryl Hydrocarbon Receptor Activation Mediates Kidney Disease and Renal Cell Carcinoma. *J. Transl Med.* 17 (1), 302. doi:10.1186/s12967-019-2054-5

Zhao, Y. Y., Chen, H., Tian, T., Chen, D. Q., Bai, X., and Wei, F. (2014). A Pharmaco-Metabonomic Study on Chronic Kidney Disease and Therapeutic Effect of Ergone by UPLC-QTOF/HDMS. *PLoS One* 9 (9), e115467. doi:10.1371/journal.pone.0115467

Zhao, Y. Y. (2013). Metabolomics in Chronic Kidney Disease. *Clin. Chim. Acta* 422, 59–69. doi:10.1016/j.cca.2013.03.033

Zhao, Y. Y. (2013). Traditional Uses, Phytochemistry, Pharmacology, Pharmacokinetics and Quality Control of Polyporus Umbellatus (Pers.) Fries: a Review. *J. Ethnopharmacol* 149 (1), 35–48. doi:10.1016/j.jep.2013.06.031

Zhao, Y. Y., Vaziri, N. D., and Lin, R. C. (2015). Lipidomics: New Insight into Kidney Disease. *Adv. Clin. Chem.* 68, 153–175. doi:10.1016/bs.acc.2014.11.002

Zhou, X. F., Wang, Y., Luo, M. J., Zhao, T., and Li, P. (2021). Tangshen Formula Attenuates Renal Fibrosis by Downregulating Transforming Growth Factor β1/Smad3 and LncRNA-MEG3 in Rats with Diabetic Kidney Disease. *Integr. Med. Nephrol. Androl.* 8, 1. doi:10.4103/imna.imna_22_21

Zou, J. J., Zhou, X. T., Chen, Y. K., Liu, J. L., Wang, C., Ma, Y. R., et al. (2020). A Review on the Efficacy and Mechanism of Action of Shenkang Injection against Chronic Kidney Disease. *Biomed. Pharmacother.* 132, 110833. doi:10.1016/j.biopha.2020.110833

Conflict of Interest: The authors declare that the research was conducted in the absence of any commercial or financial relationships that could be construed as a potential conflict of interest.

Publisher's Note: All claims expressed in this article are solely those of the authors and do not necessarily represent those of their affiliated organizations, or those of the publisher, the editors, and the reviewers. Any product that may be evaluated in this article, or claim that may be made by its manufacturer, is not guaranteed or endorsed by the publisher.

frontiers in Pharmacology

ORIGINAL RESEARCH
published: 03 January 2022
doi: 10.3389/fphar.2021.801048

Proanthocyanidins Protect Against Cadmium-Induced Diabetic Nephropathy Through p38 MAPK and Keap1/Nrf2 Signaling Pathways

*Pin Gong[1], Peipei Wang[1], Sihui Pi[1], Yuxi Guo[1], Shuya Pei[1], Wenjuan Yang[1], Xiangna Chang[1], Lan Wang[1] and Fuxin Chen[2]**

[1]College of Food and Biotechnology, Shaanxi University of Science and Technology, Xi'an, China, [2]School of Chemistry and Chemical Engineering, Xi'an University of Science and Technology, Xi'an, China

Diabetic nephropathy (DN) is one of the most devastating complications of diabetes mellitus. Although cadmium (Cd) exposure might be involved in the pathogenesis of DN, the underlying mechanism is still unclear. In this study, we explored the protective effects and possible mechanism of proanthocyanidins (OPC) from grape seed using a mouse model of Cd-induced DN. The successful establishment of this model was verified by analyzing the physiological and biochemical indices of mice, including their body weight and tissue ratio; levels of blood glucose, creatinine, microalbumin, total cholesterol, triglycerides, high-density lipoprotein-cholesterol and low-density lipoprotein-cholesterol; and was based on histopathological examination. Oxidative-antioxidative status, elemental analysis, and key signaling pathway analysis were performed to explore the possible protective mechanism of OPC. The protective effects of OPC and its possible mechanism in preventing the progression of DN were investigated using a multidimensional approach, including its ability in regulating oxidative-antioxidative status (lipid peroxidation, protein carbonyl, superoxide dismutase, and glutathione GST, GSH-Px), metal-binding ability (Cd levels in the kidneys and urine and MT content) and mediation of essential elements (Zn, Ca, Cu, and Fe levels in the kidneys), and activation of the p38 MAPK and Keap1/Nrf2 signaling pathways. OPC exhibited a significant renoprotective effect, attributed to the metal-chelating ability, anti-oxidative effect, and mediation of oxidative stress-related signaling pathway. These results highlight the potential of OPC in preventing or treating DN in humans and suggest the dietary intake of grapes, which are rich in polyphenols, for the prevention of type 2 diabetes mellitus and its complications.

Keywords: cadmium, diabetic nephropathy, proanthocyanidins, Keap1/Nrf2 signaling pathway, p38 MAPK signaling pathway

OPEN ACCESS

Edited by:
Zhiyong Guo,
Second Military Medical University, China

Reviewed by:
Milton Prabu,
Annamalai University, India
Xiaoyong Yu,
Shaanxi Provincial Hospital of Traditional Chinese Medicine, China

****Correspondence:***
Fuxin Chen
chenfuxin1981@163.com

Specialty section:
This article was submitted to Renal Pharmacology, a section of the journal Frontiers in Pharmacology

Received: *24 October 2021*
Accepted: *03 December 2021*
Published: *03 January 2022*

Citation:
Gong P, Wang P, Pi S, Guo Y, Pei S, Yang W, Chang X, Wang L and Chen F (2022) Proanthocyanidins Protect Against Cadmium-Induced Diabetic Nephropathy Through p38 MAPK and Keap1/Nrf2 Signaling Pathways. Front. Pharmacol. 12:801048. doi: 10.3389/fphar.2021.801048

Abbreviations: ANOVA, one-way analysis of variance; BCA, bicinchoninic acid; Cd, cadmium; DN, diabetic nephropathy; ECL, chemiluminescence; GSH, glutathione; H&E, hematoxylin-eosin; HDL-C, high-density lipoprotein-cholesterol; HFSD, high fat and sugar diet; i.p.,intraperitoneally; LDL-C, low-density lipoprotein-cholesterol; mALB, microalbumin; MDA, malondialdehyde; NO, nitric oxide; OPC, proanthocyanidins; PAS, periodic acid-Schiff; PCO, protein carbonyl; PVDF, polyvinylidene difluoride; SOD, superoxide dismutase; TC, total cholesterol; TG, triglyceride.

INTRODUCTION

Diabetic nephropathy (DN) is the most devastating complication of diabetes mellitus that causes significant morbidity and mortality (Zoja et al., 2020). It is gradually becoming a leading cause of end-stage renal disease (Duran-Salgado and Rubio-Guerra, 2014; Hansrivijit et al., 2021). Epidemiological studies reveal that more than 25% of patients with diabetes suffer from DN (Reidy et al., 2014), which is characterized by a series of renal abnormalities including mesangial expansion, basement membrane thickening, tubulointerstitial fibrosis, and glomerulosclerosis (Reidy et al., 2014; Li et al., 2021; Medina Rangel et al., 2021). These changes result in a clinical presentation characterized by hypertension, proteinuria, and a progressive reduction in kidney function (Reidy et al., 2014).

Although several studies have shed light on the pathogenesis of DN, several aspects of its condition remain unclear; thus, further comprehensive investigations and evidence-based findings are needed to elucidate the mechanism underlying disease progression (Mantovani and Zusi, 2020; Miao et al., 2021a). Cadmium (Cd), a transition metal that is, toxic by nature and an environmental pollutant, is generated from industrial sources and found in air, water, food, and cigarette smoke. The primary target organs for Cd toxicity are the liver and kidneys. Epidemiological and experimental studies suggest that Cd may act as a risk factor in the pathogenesis of diabetes mellitus and renal disease (Edwards and Ackerman, 2016). A dose-response relationship has been reported between urinary Cd and albuminuria in Torres Strait subjects with type 2 diabetes. It has been suggested that Cd-mediated toxicity may intensify the effects of diabetes on the kidneys. Exposure to Cd could lead to hyperglycemia and accelerate the progression of diabetes mellitus (Tangvarasittichai et al., 2015). Cd accumulation in the kidneys results in generalized dysfunction accompanied by polyuria, glucosuria, and low-molecular-weight proteinuria (Madrigal et al., 2019). Previous studies suggest that Cd can accelerate the occurrence of DN in male Kunming mice treated with a high fat and sugar diet (HFSD) (Gong et al., 2017).

The molecular pathogenesis of DN is poorly understood and no new drugs have been approved for the therapy of DN in almost 20 years. Thus, there is an urgent need for the screening and identification of novel and efficacious drug candidates for the management of DN. Natural products has long been used to be an alternative therapy for the prevention and treatment of various renal diseases including DN (Chen et al., 2018a; Wang et al., 2018a; Chen et al., 2018b; Yang and Wu, 2021). Therefore, Natural products were considered as an important source of new drugs over past 4 decades (Izzo et al., 2020; Newman and Cragg, 2020; Miao et al., 2021b; Zhou et al., 2021). Proanthocyanidins (OPC) are condensed tannins that are derivatives of catechin and gallic acid that are composed of propelargonidins, procyanidins, and prodelphinidins. These compounds are widely distributed in grapes, green and black teas, grape seeds, and wine (Yokozawa et al., 2012). Of late, OPC have been receiving increased attention owing to their potential health benefits, such as their antioxidant properties with strong radical-scavenging, blood glucose lowering, anti-apoptotic, and anti-inflammatory properties among other biological activities (Yokozawa et al., 2012; Ruan et al., 2020). As OPC are known to reduce blood glucose levels, balance oxidative stress, and ameliorate inflammatory responses, we wanted to further explore if they could play a role in protecting against Cd-induced DN. To our knowledge, there lack studies that have elucidated the protective effects on Cd-induced DN in mice. Therefore, we hypothesized that if OPC could effectively protect against Cd-induced DN, a diet comprising this natural compound may serve as potential therapeutic agent and prevent Cd-induced renal damage.

One of the challenges in drug discovery, especially in the case of diabetes, is the lack of robust animal models that can mimic key features of human DN. In this study, we established a mouse model of DN using Cd exposure and HFSD treatment. The successful establishment of this model was verified based on physiological and histopathological investigations and determining the biochemical indices of mice. We investigated the protective effect and potential mechanism of OPC against Cd-induced DN. This study may provide useful clues for better understanding the etiology of DN and highlight novel insights regarding the use of OPC in a clinical setting.

METHODS

Materials and Reagents

OPC (purity > 99.50%) were purchased from Yifang S&T Co. Ltd. (Tianjin, China). Cadmium chloride and β-actin (sc-4778, Santa Cruz, CA) were purchased from Sigma-Aldrich Chemical Company (St. Louis, MO, United States) and stored at 4°C away from sunlight. Anti-MAPK (sc-393609, Santa Cruz, CA), anti-p38 (sc-81621, Santa Cruz, CA), anti-nuclear factor-erythroid-2-related factor 2 (Nrf2, sc-365949, Santa Cruz, CA), anti-Keap1 (sc-515432, Santa Cruz, CA), and horseradish peroxidase (HRP)-conjugated secondary antibodies (anti-rabbit) were obtained from Santa Cruz Biotechnology (CA, United States).

Animals Handing and Sample Preparation

Five-week-old male Kunming mice (weighing 20 ± 2 g) were supplied by Central Animal House, Xi'an JiaoTong University Health Science Center (Xi'an, China). The animals were housed in a specific pathogen free environment at a temperature of 22 ± 1°C and relative humidity of 50 ± 1%, and subjected to a 12/12 h light/dark cycle. All animals were provided free access to food and water and were allowed to acclimatize for 7 days prior to dosing. All animal studies complied with the regulations and guidelines of the Shaanxi University of Science and Technology Institutional Animal Care and were in accordance with the IACUC and AAALAC guidelines.

For experimental studies, the mice were randomly divided into the following four groups with 10 mice per group: control, DN, OPC, and HFSD. The mice in the control and HFSD groups were fed a standard pellet diet or HFSD and intraperitoneally (i.p.) administered physiological saline (0.9%) during the entire procedure. For the initial 12 weeks, mice in the DN and OPC

TABLE 1 | Detail protocols for model construction.

Group	Diet	Treatment	
		12 weeks	4 weeks
Control Group (Con)	standard pellet diet	0.9% saline i.p.	0.9% saline i.p.
DN group (DN)	High sugar and Fat diet	1 mg/kg $CdCl_2$ i.p.	0.9% saline i.p.
OPC treatment Group (DN + OPC)	High sugar and Fat diet	1 mg/kg $CdCl_2$ i.p.	5 mg/kg bw OPC
High Fat and sugar Group (HFSD)	High sugar and Fat diet	0.9% saline i.p.	0.9% saline i.p.

groups were fed HFSD and received a daily injection of 1 mg/kg $CdCl_2$ i.p. After treatment for 12 weeks, mice in the OPC group were administered OPC i.p. at a dose of 5 mg/kg body weight for consecutive 4 weeks. Mice in the DN group received 0.9% saline i.p. A detailed experimental protocol is listed in **Table 1** and was used in our study (Gong et al., 2017).

During the entire experimental period, the body weight and fasting blood glucose (FBG) levels of mice were recorded at regular intervals. Using metabolism cages, 24 h urine samples were collected for analysis. Mice were anesthetized by diethyl ether inhalation and sacrificed using cervical dislocation (Pavel et al., 2020). Blood samples were collected from the eyeballs of mice, centrifuged at 4°C to obtain serum, and frozen at −80°C. Kidneys were dissected and weighed immediately, washed clean, and either stored at −80°C or fixed in 10% formalin and stored until further use.

Renal tissues were accurately weighed, cut into pieces, and homogenized in a pre-cooled Teflon homogenizer with an appropriate amount of ice-cold Tris–HCl buffer (100 mM; pH 7.4) [sample weight (g):buffer volume (ml) = 1:9] to obtain the tissue homogenate. The supernatant was centrifuged at 12,000 rpm for 20 min at 4°C to obtain samples for subsequent assays.

Assessment of Blood and Urine Parameters

Fasting blood glucose (FBG) levels were determined using a glucometer and mice with FBG levels of more than 11.1 mmol/L were considered diabetic. Creatinine and microalbumin (mALB) levels in the urine were analyzed using the corresponding assay kits. Total cholesterol (TC), triglyceride (TG), high-density lipoprotein-cholesterol (HDL-C), and low-density lipoprotein-cholesterol (LDL-C) levels in the blood were determined based on enzymatic assays using commercial kits (Jiangchen Co., Nanjing, China) and following the manufacturer's instructions.

Renal Histopathology

For renal histopathological studies, the kidney sections from each mouse were fixed in 10% formalin immediately after dissection and washed using a gradient concentration of ethanol for dehydration, as previously described (Miao et al., 2020). The slides were transparentized with xylene, dipped in wax, and embedded in paraffin. The blocks were sectioned and stained with hematoxylin-eosin (H&E) to observe the normal cellular structure. Periodic acid-Schiff (PAS) staining was used to determine the glycogen content and Masson's trichrome staining was used to analyze collagen deposition. The stained sections were covered with a glass slide, dried, and observed using an optical microscope (Leica DM750).

Assessment of Antioxidative Status

Proteins in the kidney tissue homogenates were determined using a bicinchoninic acid (BCA) assay. The oxidative-antioxidative status in mouse kidneys was determined based on the malondialdehyde (MDA), protein carbonyl (PCO), superoxide dismutase (SOD), glutathione (GSH), glutathione S transferase (GST), and glutathione peroxidase (GSH-Px) levels using commercially procured kits. Renal nitric oxide (NO) levels were determined using a colorimetric method based on the Griess reaction.

Determination of Essential Elements and Metallothionein in Kidney

To quantify the content of essential elements, renal samples were accurately weighed and dry-ashed using a muffle furnace. The ash was solubilized in 3M HCl and appropriately diluted. The serum and urine samples were also pre-deposited, respectively. Tissue, serum, and urine samples were tested for Zn (213.9 nm), Fe (248.5 nm), Cu (324.8 nm), Ca (422.7 nm), and Cd (228.8 nm) using atomic absorption spectrometry (Hitachi Z-2000). The element levels are expressed as micrograms of the element per gram of wet tissue weight (μg/g w.t.w.) or micrograms of the element per milliliter sample (μg/ml) (Gong et al., 2008). MT content in mouse kidney was determined following the methods published by Gong et al. (2012).

Western Blotting Analysis

Western blotting analysis was performed following previously published studies (Chen et al., 2019a). RIPA buffer was used for the extraction of total protein. Renal tissues were first weighed, mixed with RIPA buffer supplemented with protease and phosphatase inhibitors (Roche Applied HEART), and homogenized at 4°C. The supernatant was centrifuged at 4°C and 13,000 × *g* for 30 min and transferred to a new enzyme-free tube. Proteins were quantified using a BCA kit.

Western blotting was performed using anti-MAPK (Santa Cruz, CA), anti-p38 (Santa Cruz, CA), anti-Nrf2 (Santa Cruz, CA), anti-Keap1 (Santa Cruz, CA), anti-actin (Santa Cruz, CA), and HRP-conjugated secondary antibodies (anti-rabbit) from Santa Cruz. Proteins were separated using electrophoresis on an SDS-polyacrylamide gel and the bands were electrophoretically transferred onto a polyvinylidene difluoride membrane. The membranes were blocked for 1 h at 37°C and

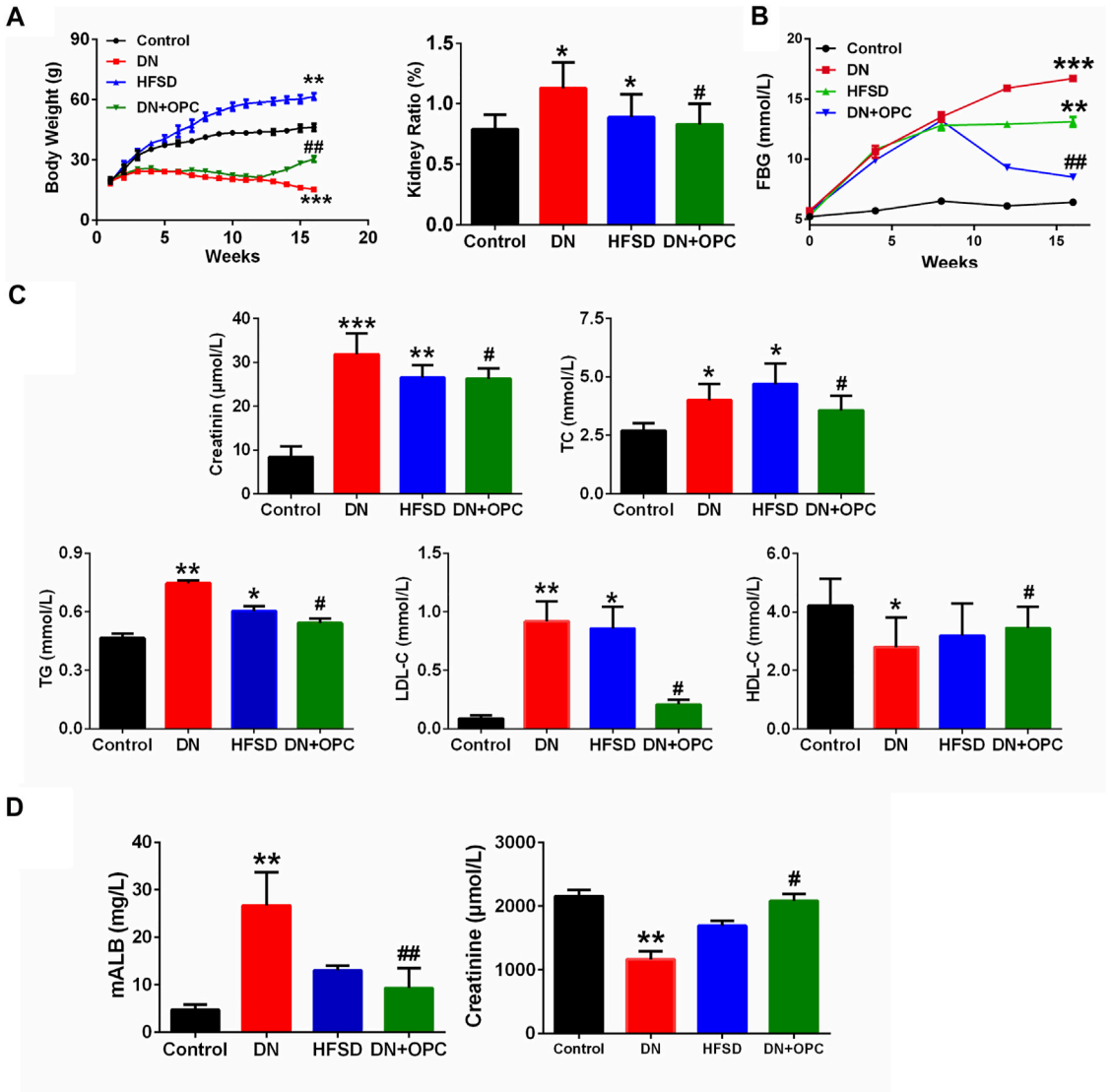

FIGURE 1 | Physiological and biochemical indexes **(A)** The body weight and kidney ratio in the different groups at week 16. kidney ratio equal to kidney weight/body weight. **(B)** FBG in the different groups. **(C)** Serum parameters in the different groups. Including serum creatine, TC contents, TG contents, LDL-C contents, and HDL-C contents in the different groups. **(D)** mALB contents and Urine creatinine in the different groups. $^{*}p < 0.05$, $^{**}p < 0.01$, $^{***}p < 0.001$ compared with control group; $^{\#}p < 0.05$, $^{\#\#}p < 0.01$, compared with DN group.

incubated with primary antibodies overnight at 4°C followed by hybridization with HRP-conjugated secondary antibodies for 1 h. Proteins were detected using the enhanced chemiluminescence (ECL) system and ECL Hyperfilm (Amersham Pharmacia Biotech, UK Ltd., Little Chalfont, Buckinghamshire, UK). The intensities of relative bands were quantified using densitometry.

Statistical Analysis

All values are expressed as mean ± standard deviation. All statistical tests were performed using SPSS version 20.0. Significant differences among the different groups were evaluated using one-way analysis of variance (ANOVA) followed by Dunnett's post hoc test. $p < 0.05$ was regarded significant differences.

RESULTS

Effects of OPC on Metabolic Dysfunction in Cd-Induced DN Mice

The body weight gain of DN mice was significantly decreased compared with the control mice. We found that the administration of OPC for 12–16 weeks could recover this decline ($p < 0.05$). When mice were treated only with HFSD, significant increases in body weight were observed (**Figure 1A**). Compared with the control group, the tissue ratio was significantly increased by 43.1% in the DN group and treatment with OPC could decrease this ratio. Moreover, the tissue ratio in the HFSD group also showed a significant

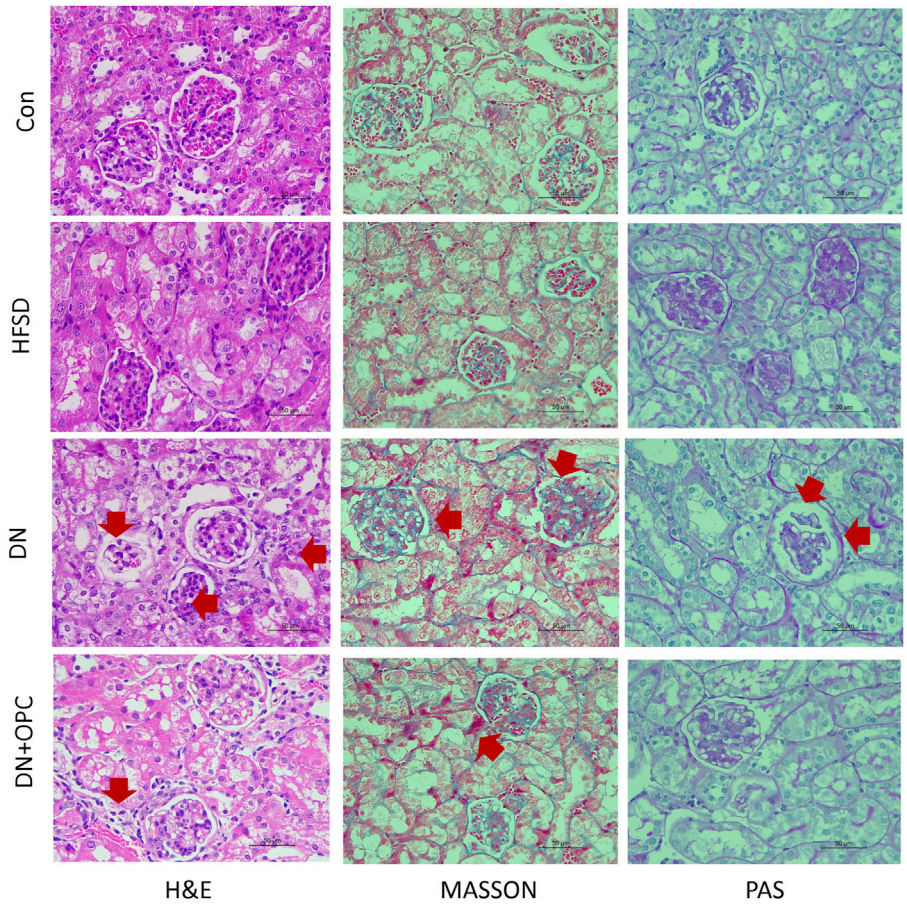

FIGURE 2 | Pathologic analysis of the kidneys. H&E staining in the different groups, including control, HFSD, DN, and DN + OPC groups, (*) represent glomerulus atrophy, (→) represent renal tubular necrosis. PAS staining in the different groups, including control, HFSD, DN, and DN + OPC groups, (→) represent mesangial expansion. MASSON staining in the different groups, including control, HFSD, DN, and DN + OPC groups. (→) represent inflammatory infiltrates, areas of tubulointerstitial fibrosis. Magnification times × 400 and scale bar in 50 μm.

increase of 12.7% compared with the control mice (**Figure 1A**).

Effects of OPC on Glucose and Lipid Metabolism in Cd-Induced DN Mice

FBG levels were also measured during the entire study. As shown in **Figure 1B**, in the initial 12 weeks, when treated with HFSD and/or Cd, the FBG levels of mice in the DN, OPC, and HFSD groups were all above 11.1 mmol/L, indicating that the animals were diabetic. The administration with OPC caused a significant decrease in FBG ($p < 0.01$), suggesting its possible role in lowering FBG. To determine the protective effects of OPC in mice with Cd-induced DN, the serum biochemical parameters, such as plasma TG, TC, HDL-C, and LDL-C, related to *in vivo* glucose and lipid metabolism were evaluated, and the results are presented in **Figure 1C**. The levels of TG, TC, and LDL-C of mice in the DN group were markedly increased, whereas HDL-C levels were significantly decreased compared with the control group. On the other hand, TG, TC, and LDL-C levels were found to be significantly decreased and HDL-C level was significantly increased in mice treated with OPC compared with those in the DN group. Additionally, the changes in TC, TG, HDL-C, and LDL-C levels of mice in the HFSD group were moderate, probably because Cd exposure accelerated the progression of DN.

Effects of OPC on the Renal Function in Cd-Induced DN Mice

Next, we determined renal function and evaluated the protective effects of OPC against Cd- and HFSD-induced DN. The combined effect of Cd and HFSD led to remarkable renal dysfunction as evidenced by serum/urine creatinine and urine mALB levels (**Figures 1C,D**). Plasma and urine creatinine levels were determined to assess the degree of renal injury. As shown in **Figure 1C**, plasma creatinine levels were remarkably elevated in mice in the DN group compared with the control mice. Creatinine levels of mice in the OPC group were 17.5% lower than those in the DN group. Of note, the change in urine creatinine levels showed an opposite trend; creatinine levels of mice in the DN group were remarkably decreased to 54% vs. those

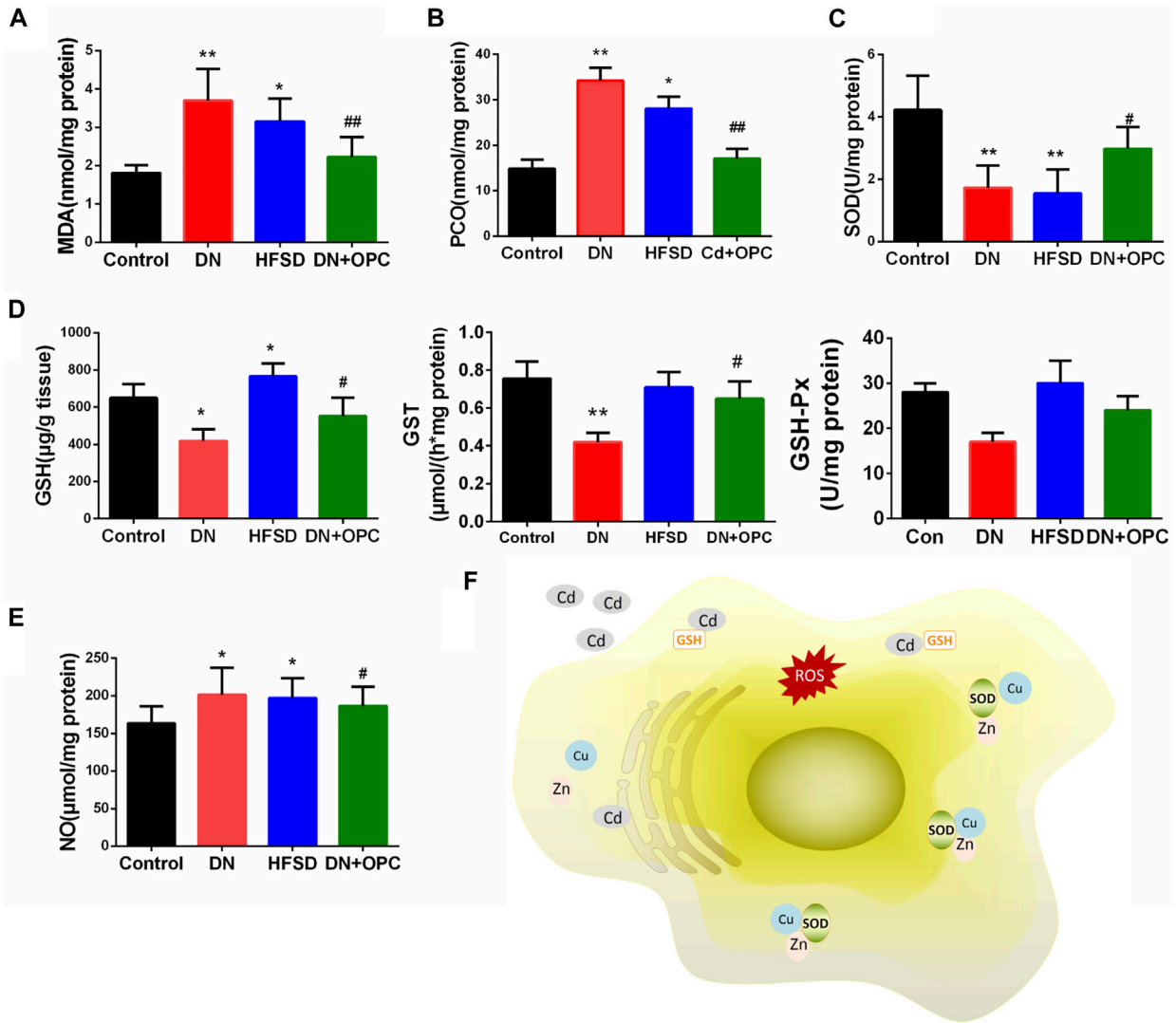

FIGURE 3 | Anti-oxidative parameters of the kidneys. **(A)** MDA levels. **(B)** PCO levels. **(C)** SOD activities. **(D)** GSH, GST, and GSH-Px content. **(E)** NO levels. **(F)** Possible mechanism of cadimium on oxidative stress. $^{*}p < 0.05$, $^{**}p < 0.01$, $^{***}p < 0.001$ compared with control group; and $^{\#}p < 0.05$, $^{\#\#}p < 0.01$, compared with DN group.

in the control group. However, OPC treatment effectively ameliorated this change and restored to near normal levels.

We also found that compared with the control group, urine mALB levels of mice in the DN group were significantly increased. OPC treatment greatly reduced mALB levels to 65.1% compared with those observed in the DN group (**Figure 1D**). These results indicated the protective effects of OPC against the development of DN.

Effects of OPC on the Renal Histology in Cd-Induced DN Mice

Kidney histology was studied using H&E staining, which revealed significant changes as glomerular thickening in the tissue samples of mice from the DN group (**Figure 2**). Interstitial and glomerular changes were noticeably ameliorated after OPC treatment (H&E staining, **Figure 2**). A diffuse expansion of the mesangial matrix and prominent thickening of the glomerular basement membrane to a mild extent was observed in samples from the DN group after PAS staining, which was greatly reduced after OPC treatment.

Moreover, renal histology was studied using Masson's staining (**Figure 2**), which demonstrated visible changes in the tissues from the DN groups, as evidenced by mild tubulointerstitial fibrosis, accumulation of extracellular matrix (ECM), tubular dilatation, and atrophy. OPC treatment was found to partly reduce the tubulointerstitial fibrosis index in the renal cortex and medulla. Collectively, these results indicated the protective role of OPC in Cd-induced DN by the amelioration of morphological changes.

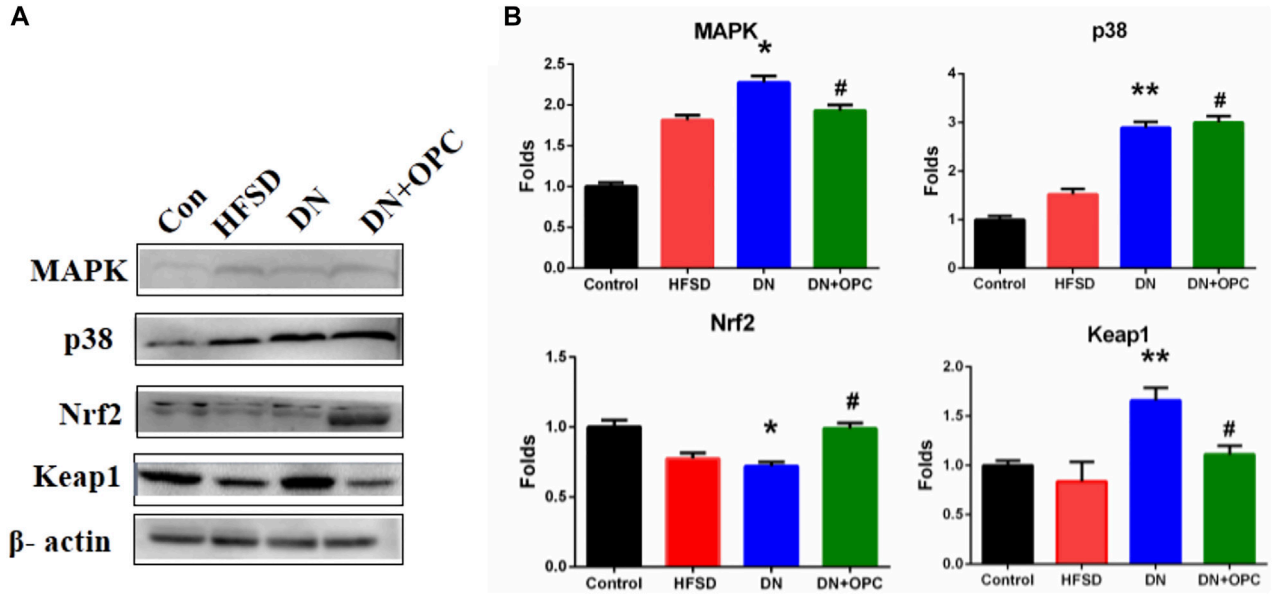

FIGURE 4 | Western blot analysis. **(A)** Protein Bands. **(B)** Quantitative analysis. Data were repeated three times. *$p < 0.05$, **$p < 0.01$, compared with control group and $^{\#}p < 0.05$ compared with DN group.

Effects of OPC on Renal Oxidative Stress Parameters and NO Levels in Cd-Induced DN Mice

As the pathology of DN is related to the overproduction of ROS and an imbalance in oxidative stress, we determined the oxidative stress parameters. As shown in **Figures 3A,B**, the MDA and PCO levels showed a 2.1-fold and 2.3-fold increase in the DN group, respectively, after exposure to Cd and HFSD. OPC treatment could attenuate oxidative stress by significantly decreasing MDA and PCO levels. As expected, the synergistic effect of Cd and HFSD resulted in a 59.1% decrease in SOD activities in mice with DN ($p < 0.01$), whereas OPC treatment could effectively reverse this decrease (**Figure 3C**).

We also found that compared to that in the control animals, the combined effect of Cd and HFSD could reduce GSH, GST and GSH-Px levels by 35.5, 44.4, and 39.2% in mice in the DN group, respectively, whereas OPC treatment significantly increased GSH, GST and GSH-Px levels (**Figure 3D**). Moreover, NO levels in the tissues of mice from the DN group were significantly increased co-treatment with Cd and HFSD (**Figure 3E**). However, NO levels were found to be reduced in tissues in the OPC group. Treatment with only HFSD led to significant changes in the oxidative and antioxidant parameters except for the NO levels.

Effects of OPC on p38 MAPK and Keap1/Nrf2 Pathway-Mediated Oxidative Stress

Western blotting was used to further confirm the role of oxidative stress in the progression of DN and to determine the protective mechanism of OPC in oxidative stress-related protein expression. Accordingly, we examined the protein expression of the p38 MAPK and Keap1/Nrf2 pathways. Our findings indicated that p38 and MAPK expression significantly increased in DN kidney samples; however, this increase was prevented after treatment with OPC (**Figure 4**).

There was a significant decrease in Nrf2 expression and an increased expression of Keap1 in the samples obtained from the DN group. However, treatment with OPC significantly increased Nrf2 and decreased Keap1 expression in diabetic conditions (**Figure 4**). These results suggested that OPC may exert protective effects in DN, which might be associated with p38 MAPK and Keap1/Nrf2 signaling pathways.

Effects of OPC on Elemental Levels in Cd-Induced DN Mice Kidneys

An imbalance in elemental levels is common in patients with DN. Thus, we investigated the changes in levels of the essential elements in DN and the effect of OPC on elemental levels. It can be seen in **Figure 5** that Cd was accumulated in the kidneys of mice in the DN and OPC-treated groups. A significant elevation of Cd levels was observed in samples obtained from the DN group (111.1-fold higher than that in the Control group; $p < 0.001$, compared to the Control group). This accumulation was reduced after OPC treatment and Cd levels in the kidneys were found to be reduced to 85.9% compared with those in the DN group. Cd was excreted in the urine in a small amount. OPC treatment led to a significant increase in Cd excretion (10.4 folds higher than that in the DN group; $p < 0.01$, compared with the DN group). There was no significant increase in Cd levels in the kidneys or urine of samples obtained from the HFSD group.

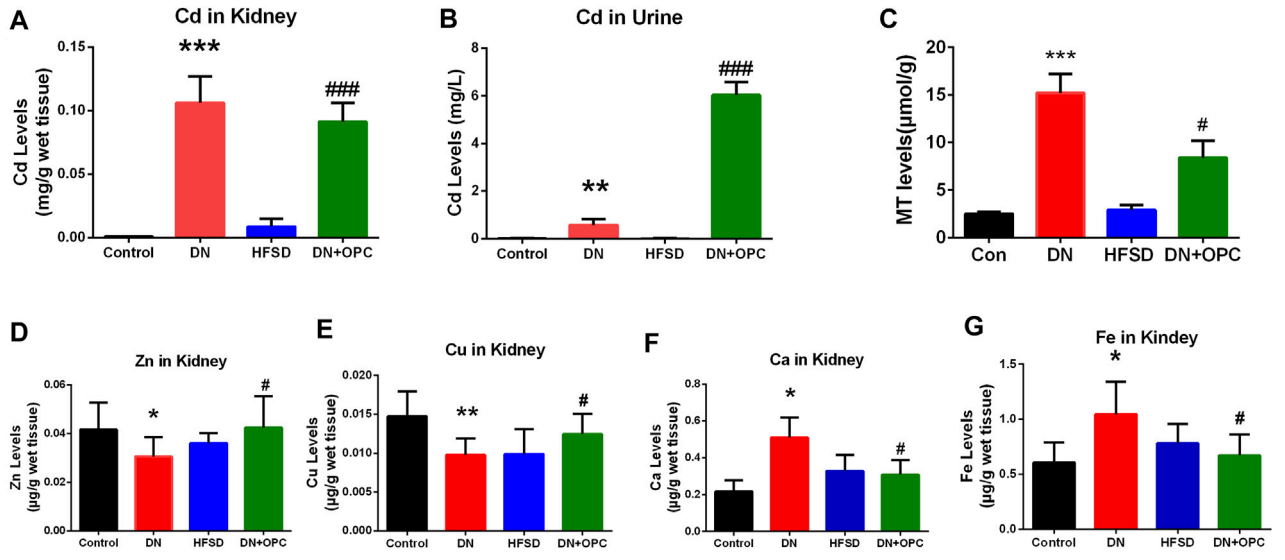

FIGURE 5 | Elemental analysis and MT content determination. **(A)** Cadmium content in kidney. **(B)** Cadmium content in urine. **(C)** MT content. **(D)** Zinc content in kidney. **(E)** Copper content in kidney. **(F)** Calcium content in kidney. **(G)** Iron content in kidney. $^{***}p < 0.001$, $^{**}p < 0.01$, $^{*}p < 0.05$ compared with control group and $^{\#}p < 0.05$, $^{\#\#}p < 0.01$, $^{\#\#\#}p < 0.001$, compared with DN group.

As seen in **Figure 5**, levels of the essential elements were significantly different among groups. Zn levels in the kidney tissues of mice from the DN group were significantly decreased to 73.3%, and OPC could restore these levels.

Cu levels showed a 1.34-fold increase in the tissue samples obtained from mice in the DN group compared with those from the control group. OPC could ameliorate this increase and return to normalcy. Ca and Fe levels in the tissue samples in the DN group showed a 2.35-fold and 1.72-fold increase, respectively, whereas OPC could effectively decrease this tendency and reduce Ca and Fe levels to 60.5 and 64.1%, respectively. Changes in the elemental levels in the HFSD group were not significant.

To further elucidate the mechanism of OPC chelating with cadmium, the content of MT in kidney were assessed. As shown in **Figure 5**, an increase of MT content in DN group was observed ($p < 0.001$), whereas the treatment of OPC could lower the content of MT, suggesting the binding ability of OPC with cadmium.

DISCUSSION

The progression of DN, one of the biggest problems in nephrology field, pointing to that patients progress end-stage renal disease and require dialysis (Aydin et al., 2019; Bacharaki et al., 2021) or kidney transplantation (Webster et al., 2017; Jain et al., 2019; Van Sandwijk et al., 2019). Recent epidemiological studies reveal a link between Cd exposure and the incidence of diabetes and its complications (Chen et al., 2006; Afridi et al., 2008; Akinloye et al., 2010; Satarug et al., 2010; Wallin et al., 2014). Several hypotheses have been proposed to explain the interplay between Cd exposure and incidence of diabetes and DN (Edwards and Prozialeck, 2009; Park et al., 2019). Gong *et al.* suggest that Cd might be a risk factor in DN pathology (Gong et al., 2017); however, the underlying mechanism of the role of Cd in the development and progression of DN is yet to be completely elucidated. In this study, we investigated the possible etiology of Cd-induced DN and studied OPC as novel and efficacious drug candidates in DN therapy.

A decrease in body weight in patients with diabetes may be due to the compensatory gluconeogenesis in cells to account for glucose deficit. Thus, weight reduction may be considered a marker of diabetes mellitus and its complications. The body weight reduction in DN mice is probably due to abnormal carbohydrate and lipid metabolism and increased protein catabolism (Ghosh et al., 1994). With the onset of DN, the kidney size and weight increased by an average of 15% and was accompanied by a progressive reduction in renal function. The increase in kidney weight was likely due to the development of renal hypertrophy. OPC are known to effectively alleviate kidney enlargement (Mansouri et al., 2011). Elevated FBG levels in mice with DN suggested the diabetogenic effect of Cd also revealed that the administration of OPC could effectively reduce the spike in blood glucose.

We also observed an increase of mALB levels in the DN group, which probably resulted from the damage to the renal glomeruli filtration barrier; however, the precise mechanism of this phenomenon is still unknown. A plausible explanation is that the severity of pro-oxidative stress in diabetes results in disturbed metabolism in the basement membrane (Ha and Kim, 1995). mALB is the predominant renal risk marker in patients with DN. The high mALB levels exacerbate renal damage. A decrease in mALB results in a proportional increase in renal function. Moreover, the creatinine in urine decreased as the concentration of creatinine in the blood was acutely increased 6–8 folds by creatinine infusion. This decrease was thought to be

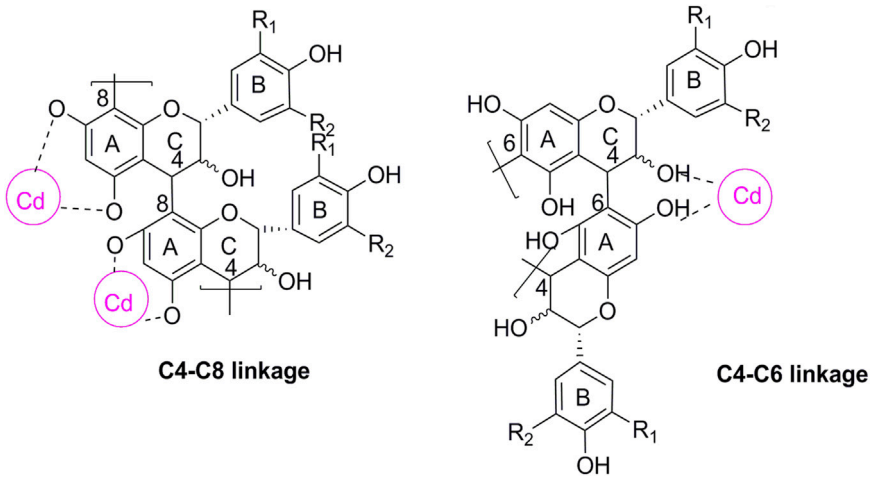

FIGURE 6 | Chemical structure of proanthocyanidin-cadmium polymers. R1, R2 = H, propelargonidins; R1 = OH, R2 = H, procyanidins; R1, R2 = OH, prodelphinidins. The cycle in purple represent the possible binding site for Cd.

due to the saturation of the tubular secretory mechanism (Perrone et al., 1992). The renal glomeruli from DN mice showed a characteristic morphology that correlated with mesangial cell proliferation and excessive accumulation of ECM (Ahn et al., 2004). We found that OPC exerted a protective effect, prevented the increase in mALB and creatinine levels, and retained renal morphology. Our findings were in agreement with the results of the study by Stefanovic *et al.* wherein grape seeds, which are rich in antioxidative bioflavonoids, were found to bring about a significant morphologic improvement and amelioration in kidney function (Stefanovic et al., 2000).

The unusually high levels of serum lipids are probably due to the increased mobilization of free fatty acids from the peripheral fat deposits, as insulin suppresses the production of hormone-sensitive lipase (Sugano et al., 2006; Vaziri, 2006). Therefore, elevated TG, TC, and LDL-C levels that were found in the DN group may also constitute risk markers during the development of DN. We found that OPC could abate the susceptibility of lipids to oxidation and stabilize the membrane lipids, thereby relieving oxidative stress by exerting hypocholesterolemic, hypotriglyceridemic, and hypophospholipidemic effects.

The significant increase in Cd levels in the tissue samples from the DN group suggested Cd accumulation, especially in the kidneys. The toxicity of Cd may be partly attributed to its long half-life and low excretion rate. The urine Cd levels were found to be remarkably elevated after OPC treatment, possibly suggesting the metal-chelating ability of OPC in reducing Cd levels *in vivo*. Grape seeds are a rich source of plant flavonoids and OPC oligomers. Proanthocyanidins from grape seed are polyphenolic compounds that are mainly concentrated in tree barks and outer skin of the seeds. OPC is of a diphenylpropane structure of C6 -C3 -C6. Most often found as a glycoside derivative, this compound class is composed of three monomer units of catechin, epicatechin, and epigallocatechin (Harborne and Mabry, 2013). OPC bind metals through complexation *via* their o-diphenol groups. Fine et al. found that OPC can chelate free iron molecules, and inhibit iron-induced lipid peroxidation (Fine, 2000). As seen in **Figure 6**, OPC can bind with Cd ions to form a covalent structure that can be excreted *via* urine.

Enteric neuropathy and microvascular disease affect the *in vivo* absorption of essential minerals in diabetic individuals (Eliasson et al., 1995). Cd competes with essential elements such as Ca, Zn, Fe, and Cu, thereby resulting in an imbalance. Low Zn levels may interfere with the ability of the pancreatic islet cells to produce insulin, especially in individuals with type 2 diabetes. Moreover, a decrease in Zn is linked to the overproduction of free radicals and increased lipid oxidation in patients with diabetes (DiSilvestro, 2000). Moreover, Zn deficiency may exacerbate the toxicity of other metals such as Fe and Cu. During hyperglycemia and inflammation, excess Fe results in the overproduction of ROS and may affect glucose control, leading to the development and progression of DN (Al-Hafidh Khattab and Al-Youzbaki, 2018). Intracellular calcium levels are increased in patients with diabetes. Ca^{2+} release in the cytosol accelerates Cd-induced mitochondrial injury, thus mediating cytochrome-c release and caspase-9 activation. Increased Cu levels have been correlated with the oxidation of LDL-C and alterations in arterial wall structure, eventually leading to infection, stress, and diabetes mellitus (Beshgetoor and Hambidge, 1998; Tan et al., 1999). Since MT is belived to play a privotal role in the detoxication of heavy metals, such as cadmium, and scavenging of free radicals, the metal ability of OPC were assessed by measuring the content of MT. It is obvious that OPC treatment could lower the content of MT, suggesting the protective of OPC against Cd-induced nephrotoxicity probably due to its ability to chelating metal ions (Gong et al., 2012).

When chronically exposuring to Cd, approximately 50% of the absorbed Cd is accumulated in the kidneys and causes damage to renal microtubules (Satarug et al., 2017). However, the mechanism for cadmium nephrotoxicity remains uncertain. Using a variety of cell culture systems or animal models, ROS

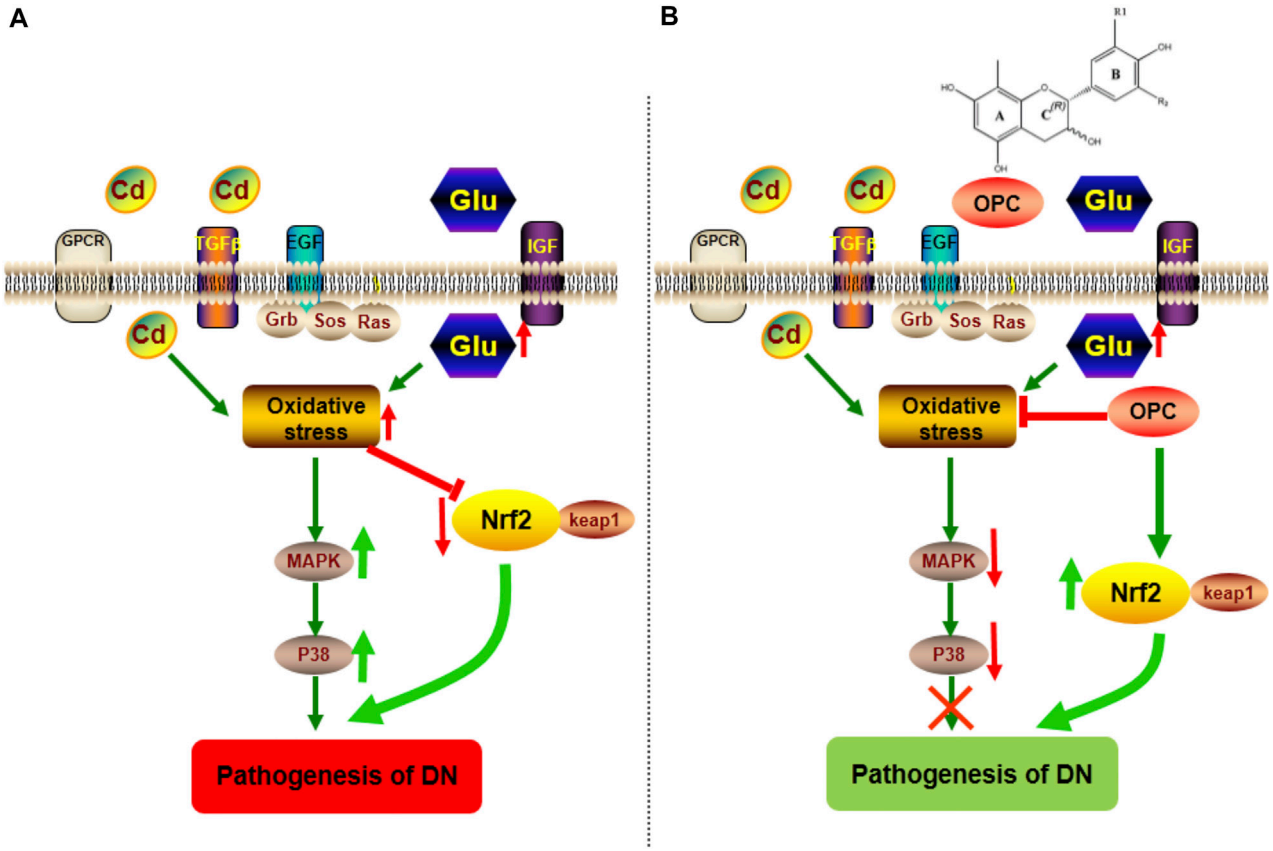

FIGURE 7 | Possible mechanism involved in the pathogenesis of DN and protective effect of OPC. **(A)** The combination of Cd and HFSD can induce the increase of oxidative stress, which activate the expression of p38 MAPK pathway, moreover, block the effect of Nrf2/Keap1 pathway. **(B)** The treatment of OPC can downregulate the expression of p38 MAPK pathway and activate Nrf2/Keap1pathway to exert its protective effect against the progressive of DN.

is thought to be associated with cadmium toxicity. Cadmium depletes glutathione and protein-bound sulfhydryl groups, leading to the production of reactive oxygen species, such as superoxide anions, hydrogen peroxide, and hydroxyl radicals. The depletion in renal GSH has been observed in response to oxidative stress by cadmium treatment, resulting in enhanced lipid peroxidation, and excessive lipid peroxidation caused increased GSH consumption. As GSH-dependent antioxidant enzymes, the decrease abilities of GST and GSH-Px probably due to reduced content of its substrate GSH. The detoxification effect of GST play a critical role for endogenous compounds such as peroxidised lipids, as well as the metabolism of xenobiotics. GSH-Px could eliminate hydrogen peroxide and lipid peroxides and thus interrupt the propagation of the lipid peroxidation reaction (Valavanidis et al., 2006). Moreover, the exposure to cadmium lead to the loss of Cu and Zn in the kidneys. Cu and Zn are antioxidant trace elements because they act as the cofactors of cytoplasmic superoxide dismutase (Pokusa and Kráľová Trančíková, 2017). The decreased SOD activity might be related to the loss of copper and zinc which are essential for the enzyme activity, resulting in the insufficient abilities to scavenge the superoxide anion produced during the normal metabolic process. Hamasaki *et al.* found that an imbalance between Zn and Cu is associated with renal dysfunction in humans, which is mediated by oxidative stress (Hamasaki et al., 2016). The increased production of different radical species accelerates the degradation of carbohydrates, lipids, and DNA, and further result in hyperglycemia and glucose auto-oxidation (Gong et al., 2017). As a result, oxidative stress induced by Cd may be an intervening factor in the toxic mechanism of Cd on renal tubules (**Figure 3F**).

Hyperglycemia-induced oxidative stress might also act as a common but key event in the development and progression of diabetes and its complications (Ceriello, 2000). Decreased SOD activity has been reported in diabetes (Mohora et al., 2006). Depletion of reduced GSH could significantly affect the overall redox potential of the cell. NO reacts with superoxide radicals and is converted to the harmful peroxynitrite, leading to increased levels of steady-state free radicals in the kidneys of diabetic individuals (Huie and Padmaja, 1993). Stadler *et al.* have demonstrated that NO production is increased in the kidneys of streptozocin-induced diabetic rats, which provides credible evidence for the involvement of ROS, NO, and peroxynitrite-derived species in the development and progression of early diabetic tissue damage (Stadler et al., 2003). OPC as free radical scavengers can increase free GSH levels to further

detoxify the products of lipid peroxidation (Bagchi et al., 2000), and then restoring the renal antioxidant defense system. OPC also promote insulin release by stimulating the surviving pancreatic cells and regulating insulin release, thereby facilitating serum glucose levels to normalcy. In the present study, combined treatment of cadmium and HFSD resulted in significant increase in TBARS and PCO as well as NO, significant decrease in antioxidant content in renal tissue, however, treatment with OPC could ameliorate these changes, indicating the protection offered by OPC against renal injury.

MAPK functions as a key point in several biochemical processes and participates in cellular processes such as proliferation, differentiation, and apoptosis. p38 MAPK is an important member of MAPK that plays a pathological role in diabetes and result in podocyte apoptosis (Susztak et al., 2006; Chuang et al., 2007). Hyperglycemia is known to activate p38 MAPK (Igarashi et al., 1999; Adhikary et al., 2004), which is associated with the apoptosis of pancreatic β-cells. The p38 pathway is also activated in the renal cortex following podocyte decrease, albuminuria, and glomerulosclerosis during early DN (Wang et al., 2018b). Nrf2 signaling pathway played a critical role in the pathogenesis of renal disease including DN (Chen et al., 2016; Chen et al., 2017; Chen et al., 2019a; Feng et al., 2019a; Wu et al., 2021). A decline in Nrf2 activity leads to the decreased transcription of several antioxidant enzymes and an increased accumulation of ROS. Nrf2 activation not only mediates glucose metabolism and glycogen formation but also plays a role in alleviating oxidative stress by neutralizing ROS and decreasing oxidative damage to the kidneys. Moreover, Nrf2 can negatively regulate TGF-β1 activity (Zheng et al., 2011). Increased evidence has indicated that a number of natural products improve renal injury by activating the impaired Keap1/Nrf2 signaling pathway (Chen et al., 2019b; Feng et al., 2019b; Chen et al., 2019c; Wang et al., 2020). OPC can activate Nrf2 expression associated with the MAPK pathway (Bak et al., 2012). We found that OPC could protect against Cd-induced toxicity by counteracting oxidative injury *via* regulation of the p38 MAPK pathway coupled with Keap1/Nrf2 pathway. The functional group at R2 moiety on OPC appeared important to the inhibitory action of MAPK-related signaling pathway, because prodelphinidin B2 3,3 di-O-gallate, having two galloyl moieties, showed strongest effect while prodelphinidin B2, having no galloyl moiety, failed to show such inhibitory effect (Hou et al., 2007). Our results indicated that targeting of the p38 MAPK and Keap1/Nrf2 signaling pathways might be involved in the pathogenesis of DN. Moreover, OPC triggered a complex crosstalk between p38 MAPK and Keap1/Nrf2 signaling pathway *via* modulating oxidative stress (**Figure 7**).

CONCLUSION

To summarize, we found that OPC from grape seeds exhibit morphological and functional protection in Cd-induced DN and its progression. The protective effects of OPC may be attributed to multidimensional aspects, including the regulation of oxidative-antioxidative status (LPO, PCO, SOD, and GSH), metal-binding ability (Cd in kidney and urine), mediation of the levels of essential elements (Zn, Ca, Cu, and Fe levels in the kidneys), and activation of the p38 MAPK and Keap1/Nrf2 signaling pathways. Based on our findings, it can be reasonably concluded that OPC from grapes can serve as functional foods in preventing the onset of type 2 diabetes mellitus and its complications. However, further studies on the mechanism of action and safe dose of grape OPC are required prior to its use in a clinical setting.

DATA AVAILABILITY STATEMENT

The raw data supporting the conclusion of this article will be made available by the authors, without undue reservation.

ETHICS STATEMENT

The animal study was reviewed and approved by the Shaanxi University of Science and Technology Institutional Animal Care.

AUTHOR CONTRIBUTIONS

PW, SiP, and ShP performed the treatment and assays with DN animals, carried out the statistical analysis, and assisted in writing the manuscript. XC and WY participated in the detection of metal levels and the protein expression analysis. LW and FC contributed to the research design and data analysis, and assisted in writing the manuscript. PG, YG, and FC conceived and participated in the project design and coordination and corrected the manuscript. All authors contributed to writing the final manuscript and approved it.

FUNDING

This study was funded by the grants from the Natural Science foundation of China (Nos. 21407104, 81803698, 31760016) which respond for the design and the study and collection, analysis. Moreover, Weiyang Project of Xi'an (Nos. 202036, 202131), Project from Xi'an City innovation plan- Agricultural Field (21NYYF0022), Project from Ningxia Zhong ning Goji Industry Innovation Research Institute (ZNGQCX-A-2020003) and General Plan of Shaanxi Province-Agricultural Field (No. 2021NY-161), Key industrial chain projects of Shaanxi Province-Agricultural Field (2021ZDLNY04-01) are responsible for the interpretation of data and in writing the manuscript.

ACKNOWLEDGMENTS

The authors would like to thank Shaanxi University of Science and Technology for providing lab and equipment to conduct this study.

REFERENCES

Adhikary, L., Chow, F., Nikolic-Paterson, D. J., Stambe, C., Dowling, J., Atkins, R. C., et al. (2004). Abnormal P38 Mitogen-Activated Protein Kinase Signalling in Human and Experimental Diabetic Nephropathy. *Diabetologia* 47, 1210–1222. %@ 0012-186X. doi:10.1007/s00125-004-1437-0

Afridi, H. I., Kazi, T. G., Kazi, N., Jamali, M. K., Arain, M. B., Jalbani, N., et al. (2008). Evaluation of Status of Toxic Metals in Biological Samples of Diabetes Mellitus Patients. *Diabetes Res. Clin. Pract.* 80, 280–288. %@ 0168-8227. doi:10.1016/j.diabres.2007.12.021

Ahn, J. D., Morishita, R., Kaneda, Y., Kim, H. J., Kim, Y. D., Lee, H. J., et al. (2004). Transcription Factor Decoy for AP-1 Reduces Mesangial Cell Proliferation and Extracellular Matrix Production *In Vitro* and *In Vivo*. *Gene Ther.* 11, 916–923. %@ 1476-5462. doi:10.1038/sj.gt.3302236

Akinloye, O., Ogunleye, K., and Oguntibeju, O. O. (2010). Cadmium, lead, Arsenic and Selenium Levels in Patients with Type 2 Diabetes Mellitus. *Afr. J. Biotechnol.* 9, 5189–5195. %@ 1684-5315.

Al-Hafidh Khattab, M. A., and Al-Youzbaki, W. B. (2018). THE RELATIONSHIP BETWEEN SERUM FERRITIN AND INSULIN RESISTANCE IN TYPE 2 DIABETIC PATIENTS TREATED BY METFORMIN. *Int. J. Pharm. Chem. Biol. Sci.* 8, 18–26.

Aydin, Z., Karadag, S., Ozturk, S., Gursu, M., Uzun, S., Cebeci, E., et al. (2019). Evaluation of the Relationship between Advanced Oxidation End Products and Inflammatory Markers in Maintenance Hemodialysis Patients. *Jna* 1, 24–30. doi:10.14302/issn.2574-4488.jna-19-3112

Bacharaki, D., Chrysanthopoulou, E., Grigoropoulou, S., Giannakopoulos, P., Simitsis, P., Frantzeskaki, F., et al. (2021). Siblings with Coronavirus Disease 2019 Infection and Opposite Outcome-The Hemodialysis's Better Outcome Paradox: Two Case Reports. *World J. Nephrol.* 10, 21–28. doi:10.5527/wjn.v10.i2.21

Bagchi, D., Bagchi, M., Stohs, S. J., Das, D. K., Ray, S. D., Kuszynski, C. A., et al. (2000). Free Radicals and Grape Seed Proanthocyanidin Extract: Importance in Human Health and Disease Prevention. *Toxicology* 148, 187–197. %@ 0300-483X. doi:10.1016/s0300-483x(00)00210-9

Bak, M.-J., Jun, M., and Jeong, W.-S. (2012). Procyanidins from Wild Grape (Vitis Amurensis) Seeds Regulate ARE-Mediated Enzyme Expression via Nrf2 Coupled with P38 and PI3K/Akt Pathway in HepG2 Cells. *Int. J. Mol. Sci.* 13, 801–818. doi:10.3390/ijms13010801

Beshgetoor, D., and Hambidge, M. (1998). Clinical Conditions Altering Copper Metabolism in Humans. *Am. J. Clin. Nutr.* 67, 1017S–1021S. %@ 0002-9165. doi:10.1093/ajcn/67.5.1017S

Ceriello, A. (2000). Oxidative Stress and Glycemic Regulation. *Metabolism* 49, 27–29. %@ 0026-0495. doi:10.1016/s0026-0495(00)80082-7

Chen, D. Q., Cao, G., Chen, H., Argyopoulos, C. P., Yu, H., Su, W., et al. (2019). Identification of Serum Metabolites Associating with Chronic Kidney Disease Progression and Anti-fibrotic Effect of 5-methoxytryptophan. *Nat. Commun.* 10, 1476. doi:10.1038/s41467-019-09329-0

Chen, D. Q., Feng, Y. L., Cao, G., and Zhao, Y. Y. (2018). Natural Products as a Source for Antifibrosis Therapy. *Trends Pharmacol. Sci.* 39, 937–952. doi:10.1016/j.tips.2018.09.002

Chen, D. Q., Hu, H. H., Wang, Y. N., Feng, Y. L., Cao, G., and Zhao, Y. Y. (2018). Natural Products for the Prevention and Treatment of Kidney Disease. *Phytomedicine* 50, 50–60. doi:10.1016/j.phymed.2018.09.182

Chen, D. Q., Cao, G., Chen, H., Liu, D., Su, W., Yu, X. Y., et al. (2017). Gene and Protein Expressions and Metabolomics Exhibit Activated Redox Signaling and Wnt/β-Catenin Pathway Are Associated with Metabolite Dysfunction in Patients with Chronic Kidney Disease. *Redox Biol.* 12, 505–521. doi:10.1016/j.redox.2017.03.017

Chen, D. Q., Feng, Y. L., Chen, L., Liu, J. R., Wang, M., Vaziri, N. D., et al. (2019). Poricoic Acid A Enhances Melatonin Inhibition of AKI-To-CKD Transition by Regulating Gas6/Axl-NF-κB/Nrf2 axis. *Free Radic. Biol. Med.* 134, 484–497. doi:10.1016/j.freeradbiomed.2019.01.046

Chen, H., Cao, G., Chen, D. Q., Wang, M., Vaziri, N. D., Zhang, Z. H., et al. (2016). Metabolomics Insights into Activated Redox Signaling and Lipid Metabolism Dysfunction in Chronic Kidney Disease Progression. *Redox Biol.* 10, 168–178. doi:10.1016/j.redox.2016.09.014

Chen, L., Lei, L., Jin, T., Nordberg, M., and Nordberg, G. F. (2006). Plasma Metallothionein Antibody, Urinary Cadmium, and Renal Dysfunction in a Chinese Type 2 Diabetic Population. *Diabetes care* 29, 2682–2687. %@ 0149-5992. doi:10.2337/dc06-1003

Chen, L., Chen, D. Q., Liu, J. R., Zhang, J., Vaziri, N. D., Zhuang, S., et al. (2019). Unilateral Ureteral Obstruction Causes Gut Microbial Dysbiosis and Metabolome Disorders Contributing to Tubulointerstitial Fibrosis. *Exp. Mol. Med.* 51, 38. doi:10.1038/s12276-019-0234-2

Chuang, P. Y., Yu, Q., Fang, W., Uribarri, J., and He, J. C. (2007). Advanced Glycation Endproducts Induce Podocyte Apoptosis by Activation of the FOXO4 Transcription Factor. *Kidney Int.* 72, 965–976. %@ 0085-2538. doi:10.1038/sj.ki.5002456

DiSilvestro, R. A. (2000). Zinc in Relation to Diabetes and Oxidative Disease. *J. Nutr.* 130, 1509S–1511S. %@ 0022-3166. doi:10.1093/jn/130.5.1509S

Duran-Salgado, M. B., and Rubio-Guerra, A. F. (2014). Diabetic Nephropathy and Inflammation. *World J. Diabetes* 5, 393–398. doi:10.4239/wjd.v5.i3.393

Edwards, J., and Ackerman, C. (2016). A Review of Diabetes Mellitus and Exposure to the Environmental Toxicant Cadmium with an Emphasis on Likely Mechanisms of Action. *Curr. Diabetes Rev.* 12, 252–258. %@ 1573-3998. doi:10.2174/1573399811666150812142922

Edwards, J. R., and Prozialeck, W. C. (2009). Cadmium, Diabetes and Chronic Kidney Disease. *Toxicol. Appl. Pharmacol.* 238, 289–293. %@ 0041-008X. doi:10.1016/j.taap.2009.03.007

Eliasson, B., Björnsson, E., Urbanavicius, V., Andersson, H., Fowelin, J., Attvall, S., et al. (1995). Hyperinsulinaemia Impairs Gastrointestinal Motility and Slows Carbohydrate Absorption. *Diabetologia* 38, 79–85. %@ 0012-186X. doi:10.1007/BF02369356

Feng, Y. L., Cao, G., Chen, D. Q., Vaziri, N. D., Chen, L., Zhang, J., et al. (2019). Microbiome-metabolomics Reveals Gut Microbiota Associated with Glycine-Conjugated Metabolites and Polyamine Metabolism in Chronic Kidney Disease. *Cell Mol. Life Sci. : CMLS* 76, 4961–4978. doi:10.1007/s00018-019-03155-9

Feng, Y. L., Chen, H., Chen, D. Q., Vaziri, N. D., Su, W., Ma, S. X., et al. (2019). Activated NF-κB/Nrf2 and Wnt/β-Catenin Pathways Are Associated with Lipid Metabolism in CKD Patients with Microalbuminuria and Macroalbuminuria. *Biochim. Biophys. Acta Mol. basis Dis.* 1865, 2317–2332. doi:10.1016/j.bbadis.2019.05.010

Fine, A. M. (2000). Oligomeric Proanthocyanidin Complexes: History, Structure, and Phytopharmaceutical Applications. *Altern. Med. Rev. a J. Clin. Ther.* 5 (2), 144–151.

Ghosh, R., Mukherjee, B., and Chatterjee, M. (1994). A Novel Effect of Selenium on Streptozotocin-Induced Diabetic Mice. *Diabetes Res. (Edinburgh, Scotland)* 25, 165–171. %@ 0265-5985.

Gong, P., Chang, X., Chen, X., Bai, X., Wen, H., Pi, S., et al. (2017). Metabolomics Study of Cadmium-Induced Diabetic Nephropathy and Protective Effect of Caffeic Acid Phenethyl Ester Using UPLC-Q-TOF-MS Combined with Pattern Recognition. *Environ. Toxicol. Pharmacol.* 54, 80–92. %@ 1382-6689. doi:10.1016/j.etap.2017.06.021

Gong, P., Chen, F., Liu, X., Gong, X., Wang, J., and Ma, Y. (2012). Protective Effect of Caffeic Acid Phenethyl Ester against Cadmium-Induced Renal Damage in Mice. *J. Toxicol. Sci.* 37, 415–425. doi:10.2131/jts.37.415

Gong, P., Chen, F. X., Ma, G. F., Feng, Y., Zhao, Q., and Wang, R. (2008). Endomorphin 1 Effectively Protects Cadmium Chloride-Induced Hepatic Damage in Mice. *Toxicology* 251, 35–44. %@ 0300-483X. doi:10.1016/j.tox.2008.07.051

Ha, H., and Kim, K. H. (1995). Role of Oxidative Stress in the Development of Diabetic Nephropathy. *Kidney Int.* Supplement 51, S18–S21.

Hamasaki, H., Kawashima, Y., and Yanai, H. (2016). Serum Zn/Cu Ratio Is Associated with Renal Function, Glycemic Control, and Metabolic Parameters in Japanese Patients with and without Type 2 Diabetes: a Cross-Sectional Study. *Front. Endocrinol.* 7, 147. doi:10.3389/fendo.2016.00147

Hansrivijit, P., Chen, Y.-J., Lnu, K., Trongtorsak, A., Puthenpura, M. M., Thongprayoon, C., et al. (2021). Prediction of Mortality Among Patients with Chronic Kidney Disease: A Systematic Review. *Wjn* 10, 59–75. doi:10.5527/wjn.v10.i4.59

Harborne, J. B., and Mabry, T. J. (2013). *The Flavonoids: Advances in Research*. Boston, MA: Springer. doi:10.1007/978-1-4899-2915-0

Hou, D.-X., Masuzaki, S., Hashimoto, F., Uto, T., Tanigawa, S., Fujii, M., et al. (2007). Green tea Proanthocyanidins Inhibit Cyclooxygenase-2 Expression in LPS-Activated Mouse Macrophages: Molecular Mechanisms and Structure–Activity Relationship. *Arch. Biochem. Biophys.* 460, 67–74. doi:10.1016/j.abb.2007.01.009

Huie, R. E., and Padmaja, S. (1993). The Reaction of NO with Superoxide. *Free Radic. Res. Commun.* 18, 195–199. %@ 8755-0199. doi:10.3109/10715769309145868

Igarashi, M., Wakasaki, H., Takahara, N., Ishii, H., Jiang, Z.-Y., Yamauchi, T., et al. (1999). Glucose or Diabetes Activates P38 Mitogen-Activated Protein Kinase via Different Pathways. *J. Clin. Invest.* 103, 185–195. %@ 0021-9738. doi:10.1172/JCI3326

Izzo, A. A., Teixeira, M., Alexander, S. P. H., Cirino, G., Docherty, J. R., George, C. H., et al. (2020). A Practical Guide for Transparent Reporting of Research on Natural Products in the British Journal of Pharmacology: Reproducibility of Natural Product Research. *Br. J. Pharmacol.* 177, 2169–2178. doi:10.1111/bph.15054

Jain, D., Haddad, D. B., and Goel, N. (2019). Choice of Dialysis Modality Prior to Kidney Transplantation: Does it Matter? *World J. Nephrol.* 8, 1–10. doi:10.5527/wjn.v8.i1.1

Li, S. S., Sun, Q., Hua, M. R., Suo, P., Chen, J. R., Yu, X. Y., et al. (2021). Targeting the Wnt/β-Catenin Signaling Pathway as a Potential Therapeutic Strategy in Renal Tubulointerstitial Fibrosis. *Front. Pharmacol.* 12, 719880. doi:10.3389/fphar.2021.719880

Madrigal, J. M., Ricardo, A. C., Persky, V., and Turyk, M. (2019). Associations between Blood Cadmium Concentration and Kidney Function in the U.S. Population: Impact of Sex, Diabetes and Hypertension. *Environ. Res.* 169, 180–188. %@ 0013-9351. doi:10.1016/j.envres.2018.11.009

Mansouri, E., Panahi, M., Ghaffari, M. A., and Ghorbani, A. (2011). Effects of Grape Seed Proanthocyanidin Extract on Oxidative Stress Induced by Diabetes in Rat Kidney. *Iranian Biomed. J.* 15, 100.

Mantovani, A., and Zusi, C. (2020). PNPLA3 Gene and Kidney Disease. *Explor Med.* 1, 42–50. doi:10.37349/emed.2020.00004

Medina Rangel, P. X., Priyadarshini, A., and Tian, X. (2021). New Insights into the Immunity and Podocyte in Glomerular Health and Disease: From Pathogenesis to Therapy in Proteinuric Kidney Disease. *Integr. Med. Nephrol. Androl.* 8, 5. doi:10.4103/imna.imna_26_21

Miao, H., Cao, G., Wu, X. Q., Chen, Y. Y., Chen, D. Q., Chen, L., et al. (2020). Identification of Endogenous 1-aminopyrene as a Novel Mediator of Progressive Chronic Kidney Disease via Aryl Hydrocarbon Receptor Activation. *Br. J. Pharmacol.* 177, 3415–3435. doi:10.1111/bph.15062

Miao, H., Wu, X. Q., Zhang, D. D., Wang, Y. N., Guo, Y., Li, P., et al. (2021). Deciphering the Cellular Mechanisms Underlying Fibrosis-Associated Diseases and Therapeutic Avenues. *Pharmacol. Res.* 163, 105316. doi:10.1016/j.phrs.2020.105316

Miao, H., Wu, X. Q., Wang, Y. N., Chen, D. Q., Chen, L., Vaziri, N. D., et al. (2021). 1-Hydroxypyrene Mediates Renal Fibrosis through Aryl Hydrocarbon Receptor Signalling Pathway. *Br. J. Pharmacol.* doi:10.1111/bph.15705

Mohora, M., Vîrgolici, B., Paveliu, F., Lixandru, D., Muscurel, C., and Greabu, M. (2006). Free Radical Activity in Obese Patients with Type 2 Diabetes Mellitus. *Rom. J. Intern. medicine= Revue roumaine de médecine interne* 44 (2), 69–78.

Newman, D. J., and Cragg, G. M. (2020). Natural Products as Sources of New Drugs over the Nearly Four Decades from 01/1981 to 09/2019. *J. Nat. Prod.* 83, 770–803. doi:10.1021/acs.jnatprod.9b01285

Park, C., Yook, J., Lim, H., and Hong, Y. (2019). Exposure to Cadmium Is Associated with Impaired Fasting Glucose. *Environ. Epidemiol.* 3, 303. doi:10.1097/01.EE9.0000609288.34911.56

Pavel, M. A., Petersen, E. N., Wang, H., Lerner, R. A., and Hansen, S. B. (2020). Studies on the Mechanism of General Anesthesia. *Proc. Natl. Acad. Sci.* 117 (24), 13757–13766. doi:10.1073/pnas.2004259117

Perrone, R. D., Madias, N. E., and Levey, A. S. (1992). Serum Creatinine as an index of Renal Function: New Insights into Old Concepts. *Clin. Chem.* 38, 1933–1953. %@ 0009-9147. doi:10.1093/clinchem/38.10.1933

Pokusa, M., and Kráľová Trančíková, A. (2017). The central Role of Biometals Maintains Oxidative Balance in the Context of Metabolic and Neurodegenerative Disorders. *Oxidative Med. Cell. longevity* 2017, 8210734. doi:10.1155/2017/8210734

Reidy, K., Kang, H. M., Hostetter, T., and Susztak, K. (2014). Molecular Mechanisms of Diabetic Kidney Disease. *J. Clin. Invest.* 124, 2333–2340. doi:10.1172/JCI72271

Ruan, Y., Jin, Q., Zeng, J., Ren, F., Xie, Z., Ji, K., et al. (2020). Grape Seed Proanthocyanidin Extract Ameliorates Cardiac Remodelling after Myocardial Infarction through PI3K/AKT Pathway in Mice. *Front. Pharmacol.* 11, 585984. doi:10.3389/fphar.2020.585984

Satarug, S., Garrett, S. H., Sens, M. A., and Sens, D. A. (2010). Cadmium, Environmental Exposure, and Health Outcomes. *Environ. Health Perspect.* 118, 182–190. %@ 0091-6765. doi:10.1289/ehp.0901234

Satarug, S., Vesey, D. A., and Gobe, G. C. (2017). Kidney Cadmium Toxicity, Diabetes and High Blood Pressure: the Perfect Storm. *Tohoku J. Exp. Med.* 241, 65–87. %@ 0040-8727. doi:10.1620/tjem.241.65

Stadler, K., Jenei, V., Von Bölcsházy, G., Somogyi, A., and Jakus, J. (2003). Increased Nitric Oxide Levels as an Early Sign of Premature Aging in Diabetes. *Free Radic. Biol. Med.* 35, 1240–1251. %@ 0891-5849. doi:10.1016/s0891-5849(03)00499-4

Sugano, M., Yamato, H., Hayashi, T., Ochiai, H., Kakuchi, J., Goto, S., et al. (2006). High-fat Diet in Low-Dose-Streptozotocin-Treated Heminephrectomized Rats Induces All Features of Human Type 2 Diabetic Nephropathy: a New Rat Model of Diabetic Nephropathy. *Nutr. Metab. Cardiovasc. Dis.* 16, 477–484. %@ 0939-4753. doi:10.1016/j.numecd.2005.08.007

Susztak, K., Raff, A. C., Schiffer, M., and Böttinger, E. P. (2006). Glucose-induced Reactive Oxygen Species Cause Apoptosis of Podocytes and Podocyte Depletion at the Onset of Diabetic Nephropathy. *Diabetes* 55, 225–233. %@ 0012-1797. doi:10.2337/diabetes.55.01.06.db05-0894

Tan, K. C. B., Ai, V. H. G., Chow, W. S., Chau, M. T., Leong, L., and Lam, K. S. L. (1999). Influence of Low Density Lipoprotein (LDL) Subfraction Profile and LDL Oxidation on Endothelium-dependent and Independent Vasodilation in Patients with Type 2 Diabetes. *J. Clin. Endocrinol. Metab.* 84, 3212–3216. %@ 0021-972X. doi:10.1210/jcem.84.9.5959

Tangvarasittichai, S., Niyomtam, S., Meemark, S., Pingmuangkaew, P., and Nunthawarasilp, P. (2015). Elevated Cadmium Exposure Associated with Hypertension, Diabetes and Chronic Kidney Disease, in the Population of Cadmium-Contaminated Area. *Int. J. Toxicol. Pharmacol. Res.* 7, 50–56.

Valavanidis, A., Vlahogianni, T., Dassenakis, M., and Scoullos, M. (2006). Molecular Biomarkers of Oxidative Stress in Aquatic Organisms in Relation to Toxic Environmental Pollutants. *Ecotoxicology Environ. Saf.* 64, 178–189. doi:10.1016/j.ecoenv.2005.03.013

Van Sandwijk, M. S., Klooster, A., Ten Berge, I. J., Diepstra, A., Florquin, S., Hoelbeek, J. J., et al. (2019). Complement Activation and Long-Term Graft Function in ABO-Incompatible Kidney Transplantation. *World J. Nephrol.* 8, 95–108. doi:10.5527/wjn.v8.i6.95

Vaziri, N. D. (2006). Dyslipidemia of Chronic Renal Failure: the Nature, Mechanisms, and Potential Consequences. *Am. J. Physiology-Renal Physiol.* 290, F262–F272. %@ 1931-857X. doi:10.1152/ajprenal.00099.2005

Stefanovic, V., Savic, V., Vlahovic, P., Cvetkovic, T., Najman, S., and Mitic-Zlatkovic, M. (2000). Reversal of Experimental Myoglobinuric Acute Renal Failure with Bioflavonoids from Seeds of Grape. *Ren. Fail.* 22, 255–266. %@ 0886-022X. doi:10.1081/jdi-100100870

Wallin, M., Sallsten, G., Lundh, T., and Barregard, L. (2014). Low-level Cadmium Exposure and Effects on Kidney Function. *Occup. Environ. Med.* 71, 848–854. %@ 1351-0711. doi:10.1136/oemed-2014-102279

Wang, M., Chen, D. Q., Chen, L., Cao, G., Zhao, H., Liu, D., et al. (2018). Novel Inhibitors of the Cellular Renin-Angiotensin System Components, Poricoic Acids, Target Smad3 Phosphorylation and Wnt/β-Catenin Pathway against Renal Fibrosis. *Br. J. Pharmacol.* 175, 2689–2708. doi:10.1111/bph.14333

Wang, M., Hu, H. H., Chen, Y. Y., Chen, L., Wu, X. Q., and Zhao, Y. Y. (2020). Novel Poricoic Acids Attenuate Renal Fibrosis through Regulating Redox Signalling and Aryl Hydrocarbon Receptor Activation. *Phytomedicine* 79, 153323. doi:10.1016/j.phymed.2020.153323

Wang, R.-M., Wang, Z.-B., Wang, Y., Liu, W.-Y., Li, Y., Tong, L.-C., et al. (2018). Swiprosin-1 Promotes Mitochondria-dependent Apoptosis of Glomerular Podocytes via P38 MAPK Pathway in Early-Stage Diabetic Nephropathy. *Cell Physiol. Biochem.* 45, 899–916. %@ 1015-8987. doi:10.1159/000487285

Webster, A. C., Nagler, E. V., Morton, R. L., and Masson, P. (2017). Chronic Kidney Disease. *Lancet* 389, 1238–1252. doi:10.1016/S0140-6736(16)32064-5

Wu, X. Q., Zhang, D. D., Wang, Y. N., Tan, Y. Q., Yu, X. Y., and Zhao, Y. Y. (2021). AGE/RAGE in Diabetic Kidney Disease and Ageing Kidney. *Free Radic. Biol. Med.* 171, 260–271. doi:10.1016/j.freeradbiomed.2021.05.025

Yang, Y., and Wu, C. (2021). Traditional Chinese Medicine in Ameliorating Diabetic Kidney Disease via Modulating Gut Microbiota. *Integr. Med. Nephrol. Androl.* 8, 8. doi:10.4103/imna.imna_28_21

Yokozawa, T., Cho, E. J., Park, C. H., and Kim, J. H. (2012). Protective Effect of Proanthocyanidin against Diabetic Oxidative Stress. *Evid Based. Complement. Altern. Med.* 2012, 623879. doi:10.1155/2012/623879

Zheng, H., Whitman, S. A., Wu, W., Wondrak, G. T., Wong, P. K., Fang, D., et al. (2011). Therapeutic Potential of Nrf2 Activators in Streptozotocin-Induced Diabetic Nephropathy. *Diabetes* 60, 3055–3066. %@ 0012-1797. doi:10.2337/db11-0807

Zhou, X. F., Wang, Y., Luo, M. J., Zhao, T. T., and Li, P. (2021). Tangshen Formula Attenuates Renal Fibrosis by Downregulating Transforming Growth Factor β1/Smad3 and LncRNA-MEG3 in Rats with Diabetic Kidney Disease. *Integr. Med. Nephrol. Androl.* 8, 2. doi:10.4103/imna.imna_22_21

Zoja, C., Xinaris, C., and Macconi, D. (2020). Diabetic Nephropathy: Novel Molecular Mechanisms and Therapeutic Targets. *Front. Pharmacol.* 11, 586892. doi:10.3389/fphar.2020.586892

Conflict of Interest: The authors declare that the research was conducted in the absence of any commercial or financial relationships that could be construed as a potential conflict of interest.

Publisher's Note: All claims expressed in this article are solely those of the authors and do not necessarily represent those of their affiliated organizations, or those of the publisher, the editors and the reviewers. Any product that may be evaluated in this article, or claim that may be made by its manufacturer, is not guaranteed or endorsed by the publisher.

frontiers in Pharmacology

ORIGINAL RESEARCH
published: 05 January 2022
doi: 10.3389/fphar.2021.792777

Quercetin Attenuates Podocyte Apoptosis of Diabetic Nephropathy Through Targeting EGFR Signaling

Yiqi Liu, Yuan Li, Liu Xu, Jiasen Shi, Xiujuan Yu, Xue Wang, Xizhi Li, Hong Jiang, Tingting Yang, Xiaoxing Yin, Lei Du and Qian Lu**

Jiangsu Key Laboratory of New Drug Research and Clinical Pharmacy, Xuzhou Medical University, Xuzhou, China

Podocytes injury is one of the leading causes of proteinuria in patients with diabetic nephropathy (DN), and is accompanied by podocytes apoptosis and the reduction of podocyte markers such as synaptopodin and nephrin. Therefore, attenuation of podocyte apoptosis is considered as an effective strategy to prevent the proteinuria in DN. In this study, we evaluated the anti-podocyte-apoptosis effect of quercetin which is a flavonol compound possessing an important role in prevention and treatment of DN and verified the effect by using *db/db* mice and high glucose (HG)-induced mouse podocytes (MPs). The results show that administration of quercetin attenuated the level of podocyte apoptosis by decreasing the expression of pro-apoptotic protein Bax, cleaved caspase 3 and increasing the expression of anti-apoptotic protein Bcl-2 in the *db/db* mice and HG-induced MPs. Furthermore, epidermal growth factor receptor (EGFR) was predicted to be the potential physiological target of quercetin by network pharmacology. *In vitro* and vivo experiments confirmed that quercetin inhibited activation of the EGFR signaling pathway by decreasing phosphorylation of EGFR and ERK1/2. Taken together, this study demonstrates that quercetin attenuated podocyte apoptosis through inhibiting EGFR signaling pathway, which provided a novel approach for further research of the mechanism of quercetin in the treatment of DN.

Keywords: quercetin, diabetic nephropathy, network pharmacology, podocyte apoptosis, EGFR

OPEN ACCESS

Edited by:
Zhiyong Guo,
Second Military Medical University, China

Reviewed by:
Yunwen Yang,
Nanjing Children's Hospital, China
Zhihao Liu,
Agricultural Research Service (USDA), United States

****Correspondence:***
Lei Du
dulei@xzhmu.edu.cn
Qian Lu
luqian@xzhmu.edu.cn

Specialty section:
This article was submitted to Renal Pharmacology, a section of the journal Frontiers in Pharmacology

Received: *11 October 2021*
Accepted: *13 December 2021*
Published: *05 January 2022*

Citation:
Liu Y, Li Y, Xu L, Shi J, Yu X, Wang X, Li X, Jiang H, Yang T, Yin X, Du L and Lu Q (2022) Quercetin Attenuates Podocyte Apoptosis of Diabetic Nephropathy Through Targeting EGFR Signaling. Front. Pharmacol. 12:792777. doi: 10.3389/fphar.2021.792777

INTRODUCTION

Diabetes is one of the fastest growing chronic diseases worldwide, which leads to devastating macrovascular and microvascular complications. Diabetic nephropathy (DN) is one of the most serious complications of diabetes (Gnudi et al., 2016). Glomerular hyperfiltration and proteinuria are the early clinical manifestations of DN. The pathological features of proteinuria formation are mesangial dilatation, endothelial cell degeneration and podocyte injury (Chen et al., 2015; Du et al., 2021). Podocyte injury undergoes the processes of podocyte hypertrophy, detachment, autophagy and apoptosis, accompanied by the reduction of podocyte marker proteins (nephrin and synaptopodin). The continuous consequences of podocyte injury destroy the renal glomerular filtration barrier, which leads to proteinuria (Nagata, 2016). Therefore, alleviation of podocyte injury is a key link to delay progression of DN.

Apoptosis is one of the mechanisms that induces podocyte injury during the progress from compensatory hypertrophy to cell detachment. Podocyte apoptosis mainly based on the emergence of apoptotic bodies along with the increased expression of pro-apoptotic protein Bax and cleaved

caspase-3. It has been reported that the apoptosis rate of podocytes is significantly increased in *db/db* mice, and *in vitro*, the high glucose is sufficient to induce apoptosis in podocytes (Liu et al., 2016). Pretreatment with *Abelmoschus manihot* (TFA), significantly decreased the number of apoptotic podocytes and the expression of pro-apoptosis related proteins caspase-3 and caspase-8 in DN rats, so as to reduce proteinuria and improve renal function (Zhou et al., 2012). Therefore, inhibition of podocyte apoptosis is an essential link for relieving podocyte injury and proteinuria.

Quercetin is a polyphenol belonging to the class of flavonoids existed in bupleuri, mulberry leaves and sophora japonica et al., which is reported to have an ameliorative effect on diabetic nephropathy induced by streptozocin (Feng et al., 2019). Modern pharmacological studies show that quercetin has multiple biological functions including anti-oxidation, anti-allergic, anti-infammatory, and anti-apoptotic effects (Gomes et al., 2014; Tang et al., 2020). In addition, it has been proven to have wide pharmacological effects on diabetic diseases. Our previous studies have demonstrated that quercetin prevents renal fibrosis in DN by restraining the proliferation of mesangial cells (MCs) and the epithelial-mesenchymal transition (EMT) of renal tubular epithelial cells induced by high glucose (Lu et al., 2015; Du et al., 2019). Quercetin has a protective effect on lupus nephritis via improving the permeability of the glomerular filtration barrier to reduce proteinuria (Dos Santos et al., 2018). It suggests that quercetin has an activity of supressing proteinuria. Take it further, rutin, a precursor of quercetin, attenuates renal tubular cell apoptosis by decreasing the caspase-3/7 activities (Qu et al., 2019). It shows that quercetin has an inhibitory effect on renal cell apoptosis. Quercetin may have potential activities in relieving podocyte injury and proteinuria through inhibition of podocyte apoptosis, however, it has not yet been fully understood.

Quercetin has potential activities on resisting diabetic nephropathy, but the mechanism of action is unclear. Network pharmacology is an emerging method based on the "disease-genes-drug" network, which can be used to predict the potential mechanism of active ingredients in diseases (Boezio et al., 2017). The method combines the ideas of system biology with multi-directional pharmacology, and integrates the biological network with drug action network to analyze the relationship between drugs and nodes or modules in the network. It has been proved to possess a certain credibility and feasibility through several previous experiments (Li and Zhang, 2013; Guo et al., 2020). In this research, the target databases of quercetin and diabetic nephropathy were constructed respectively, then took intersection of the two databases, and a total of 56 possible targets for quercetin in prevention of DN were obtained. Then, epidermal growth factor receptor (EGFR) was selected as our research object through a series of subsequent analysis including the protein-protein interaction (PPI) network analysis and kyoto encyclopedia of genes and genomes (KEGG) pathway enrichment analysis.

EGFR is the member of a family of receptor tyrosine kinase ErbB receptors (Chen et al., 2012; Li et al., 2021), which is widely expressed in glomeruli, proximal tubes and collecting ducts (Zhang et al., 2014). EGFR is composed of a single extracellular ligand binding domain, a transmembrane domain and a cytoplasmic domain containing a conserved protein tyrosine core (Chakraborty et al., 2014) and is activated by binding to its ligands, leading to phosphorylation of the intrinsic kinase domain then activation of the intracellular pathways (Chen et al., 2015). These pathways include the mitogen-activated protein kinase (MAPK), janus kinase (JAK) signal transducers and activators of Transcription (STAT), src kinase and phosphatidylinositol three kinase (PI3K) pathways. They are responsible for regulating cell proliferation, differentiation, and apoptosis. Previous experimental data revealed EGFR inhibition diminishs renal injury by reducing inflammation, oxidative stress, apoptosis and fibrosis both *in vivo* and *in vitro* (Skibba et al., 2016). Mice with podocyte-specific EGFR knockout showed less podocyte loss and lighter proteinuria in streptozotocin-induced Type 1 diabetes. In the cultured immortal mouse podocytes, EGFR was knocked down by transfection of specific mouse small interfering RNA sequences and found that downregulation of EGFR expression markedly attenuated the expression of cleaved caspase three and the phosphorylation of ERK in response to high-glucose exposure (Chen et al., 2015). It has been reported that quercetin potently suppresses the autophosphorylation of the EGFR in human colon carcinoma cell, and quercetin induces apoptosis via inhibition of EGFR in breast cancer cell lines (Balakrishnan et al., 2017). However, the role of quercetin in EGFR signaling pathway and podocyte apoptosis is not yet known.

The present study was designed to evaluate the effects of quercetin on the albuminuria and podocyte apoptosis in DN. Moreover, network pharmacology was applied to explore the underlying target of quercetin against DN. In addition, we determined whether quercetin attenuates podocyte apoptosis of DN through inhibiting EGFR signaling pathway.

MATERIALS AND METHODS

Cell Culture

Conditionally immortalized mouse podocytes (BLUEFBIO Biotechnology Company, Shanghai, China, ATCC number BFN60700330) were cultured in RPMI 1640 medium. Cells were grown in a 5% CO_2 humidified atmosphere at 33 °C and medium containing 100 U/ml IFNγ and 10% fetal bovine serum (FBS). Then podocytes were exposed to 37°C without IFNγ for 10 days to induce differentiation. The differentiated podocytes were grown in serum-free RPMI 1640 medium for 24 h prior to the experiment, which followed by treatment with 0.1% DMSO (solvent control DMSO) or glucose (HG, 40 mM, G7021, Sigma) or quercetin (5280343, Sigma, St. Louis, MO, United States) at a concentration of 10 μmol/L (Q10), 20 μmol/L (Q20), 40 μmol/L (Q40) or 1 μmol/L AG1478 (2934816, EMD Millipore, DE) for 24 h.

Animal Experiments

Eight-week-old genetically diabetic C57BL/KSJ *db/db* mice and their age-matched nondiabetic C57/KSJ *db/m* littermates (used as control animals) were obtained from the Model Animal Research

Center of Nanjing University, following the Guiding Principles for Care and Use of Laboratory Animals of Xuzhou Medical University. All mice used in experiments were male. The mice were housed in an animal facility conditioned with 12–12 h light-dark cycles and allowed free access to normal food and water. After acclimatization for 8 weeks, the mice were randomly divided into five groups with at least six mice in each group. The average initial body weight of each group was not significantly different ($p > 0.05$). These treatment groups were designated as *db/m* group (control group), *db/db* group (diabetes model group), QL group (low-dose quercetin-treated group, 50 mg kg^{-1}), QM group (medium-dose quercetin-treated group, 100 mg kg^{-1}), and QH group (high-dose quercetin-treated group, 150 mg kg^{-1}). Quercetin was dissolved in 0.5% carboxy methyl cellulose (CMC-Na) according to the expected dose of the treatment groups and was given to the mice via intragastric administration, whereas the mice of the *db/m* group and *db/db* group were given 0.5% CMC-Na through the same administration method for 8 weeks. After administration for 8 weeks, the mice were sacrificed and part of the kidney tissue was fixed in 4% paraformaldehyde, while the remaining tissue was stored at −80°C for biochemical analysis. Animal experiments were conducted in accordance to the principles provided by the National Institutes of Health's Guide for the Care and Use of Laboratory Animals. Experiments were conducted with approval of the Animal Ethics Committee of Xuzhou Medical University, which also conformed the Guidelines for Ethical Conduct in the Care and Use of Animals.

Network Pharmacology-Based Prediction of the Potential Actions of Quercetin on DN

Network pharmacology was carried out to identify the interactions between compounds and network target proteins. The putative quercetin targets were screened from ETCM (http://www.tcmip.cn/ETCM/), SymMap (http://www.symmap.org/), TCM-MESH (http://mesh.tcm.microbioinformatics.org/), TCMSP (https://old.tcmsp-e.com/tcmsp.php) four databases. Similarly, information on DN-associated target genes were gathered from the following databases: DrugBank (https://www.drugbank.ca/), OMIM (https://www.omim.org/), DisGeNet (http://www.disgenet.org/), Proteomics, then the possible targets of quercetin against DN were screened through the overlap analysis between putative targets of quercetin and known DN-associated targets. The potential target gene in quercetin was mapped to the disease target gene by using the ImageGP platform, and a Venn diagram was drawn to show results. In addition, the protein-protein interaction (PPI) network analysis was constructed to determine the potential targets and inherent pathways for investigating the actions of drugs by STRING (https://string-db.org/). Then, 12 topology analysis algorithms of Cytoscape 3.2.1 were used to screen out the key targets in PPI network. Screening of significant therapeutic targets was based on the high throughput reverse molecular docking (Gao et al., 2016; Sheng et al., 2017), hub results and the tissue distribution. The database for Annotation, Visualization and Integrated Discovery (DAVID) (https://david.ncifcrf.gov/) was used to analyze the Gene Ontology (GO) function and KEGG pathway enrichment of significant therapeutic targets. Finally, the relationships between these significantly enriched pathways and DN were further validated by literature reports.

TABLE 1 | Influence of quercetin on general parameters in experimental animals.

Groups	FBG (mmol/L)	BUN (mmol/L)	UACR (mg/g)
db/m	6.64 ± 0.65	5.85 ± 1.11	6.91 ± 0.13
db/db	40.74 ± 1.36$^{\#\#}$	10.56 ± 1.01$^{\#\#}$	45.98 ± 4.84$^{\#\#}$
db/db + QL	27.9 ± 1.74**	10.17 ± 1.42	39.56 ± 0.58**
db/db + QM	33.28 ± 3.29**	7.38 ± 0.58**	24.22 ± 3.39**
db/db + QH	32.1 ± 2.37**	5.05 ± 0.39**	20.44 ± 3.27**

Values represented mean ± SEM (n = 5/6 per group). db/m, *normal control;* db/db, *diabetic; QL, low dose quercetin (50 mg/kg/d); QM, medium dose quercetin (100 mg/kg/d); QH, high dose quercetin (150 mg/kg/d); FBG, fasting blood glucose; BUN, blood urea nitrogen; UACR, urinary albumin creatinine ratio.* $^{\#}p < 0.05$ *vs* db/m. $^{\#\#}p < 0.01$ *vs* db/m. $^{*}p < 0.05$ *vs* db/db. $^{**}p < 0.01$ *vs* db/db.

Measurement of Renal Function

Fasting blood glucose (FBG) was measured with a glucose assay Kit (Jiancheng Bioengineering Institute, Nanjing, China). Urinary albumin and the creatinine levels were detected by ELISA kits (Lanpai Biotechnology, Shanghai, China). The UACR (mg/g) was computed as urinary albumin/urinary creatinine. Blood urea nitrogen (BUN) was measured with ELISA kits. The ELISA kits were purchased from Lanpai Biotechnology (Shanghai, China). Results are expressed as the mean ± SEM. These biochemical indices were measured for estimating the progression of DN.

Renal Histology Analyses

Tissue sections of 4-μm thickness were prepared from paraffin-embedded kidney tissue. The sections were stained with periodic acid Schiff (PAS) (Liu et al., 2018), periodic acid-silver metheramine (PASM), Masson, and Sirius red after deparaffinization. Staining was conducted to assess kidney morphology, the glomerular basement membrane, glycogen deposition, and collagen accumulation. These kits were purchased from Solarbio, Beijing, China. Photographs were taken randomly and blindly under a microscope (OLYMPUS, Tokyo, Japan). Quantification of staining was performed using Image Pro Plus 6.0 and was expressed as the positive region. Representative views were shown.

Tunel Assay

Terminal deoxynucleotidyl transferase mediated dUTP nick-end labeling (TUNEL) assay (Roche, United States) is used to detect the nuclear DNA fragmentation of tissue cells in the early process of apoptosis. Sections were dewaxed and rehydrated according to standard protocols. After deparaffinization, sections were incubated with proteinase K working solution and prepared TUNEL reaction mixture for 15 min at 37°C. Sections were counterstained with DAPI (Beyotime Institute of Biotechnology, Nantong, China). The number of TUNEL

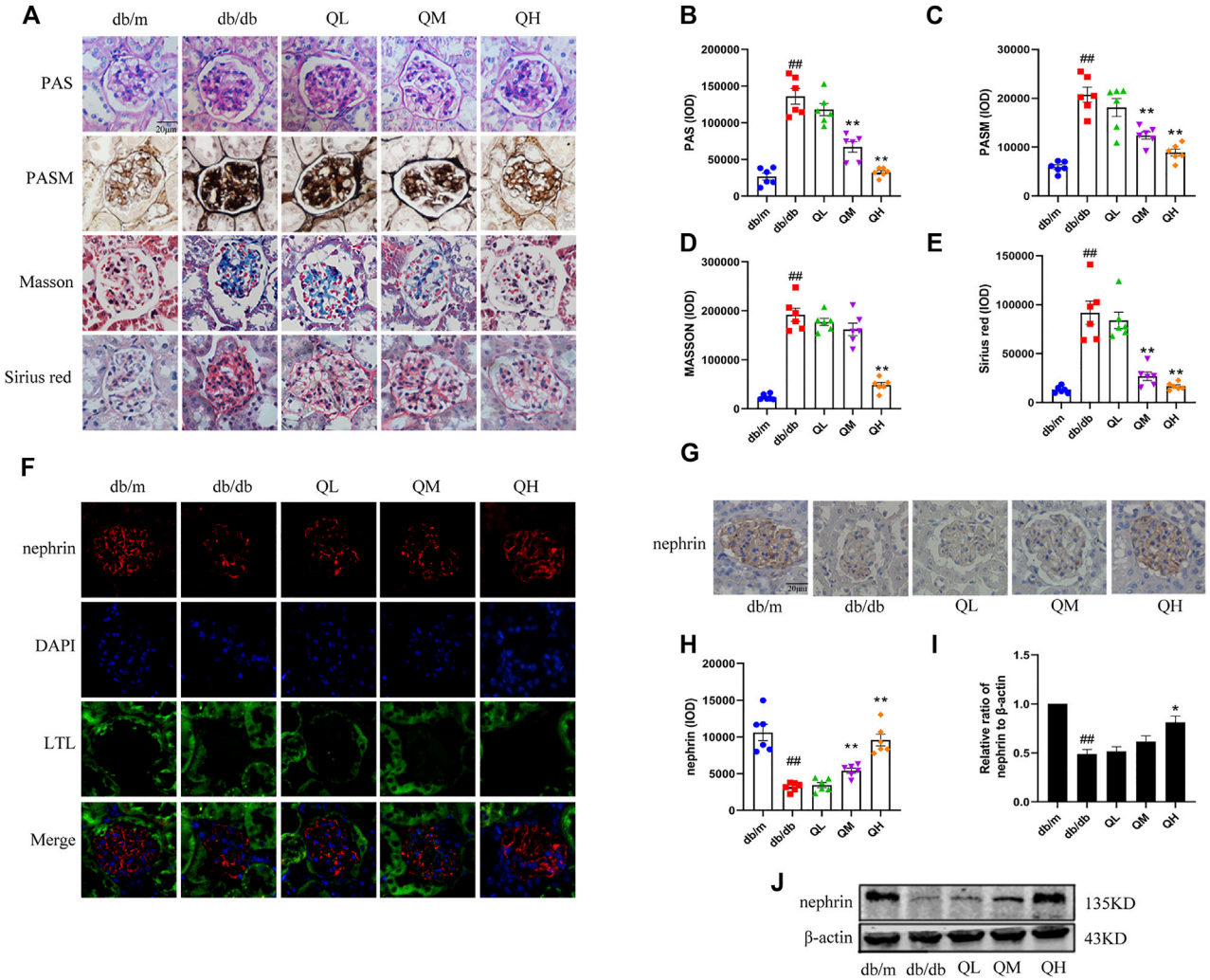

FIGURE 1 | Effects of quercetin on glomerular injury in diabetic mice. **(A)** PAS, PASM, Sirius red and Masson staining of renal cortex sections in diabetic mice. **(B–E)** Statistical analysis of PAS, PASM, Sirius red and Masson staining. **(F)** Distribution and expression of nephrin through immunofluorescence with specific antibodies against podocyte marker nephrin (red), renal tubular marker LTL (green) and DAPI (blue). **(G)** Immunohistochemical analysis of nephrin expression in the five groups. **(H,I)** Statistical analysis of nephrin expression. **(J)** Expression of nephrin through Western blotting. Data were expressed as mean ± SEM, n = 6. $^{\#}p < 0.05$ vs *db/m*. $^{\#\#}p < 0.01$ vs *db/m*. $^{*}p < 0.05$ vs *db/db*. $^{**}p < 0.01$ vs *db/db*.

positive cells per DAPI positive cells was used for quantitation of apoptotic cell.

Hoechst 33342 Staining and Annexin V-FITC/Propidium Iodide Assay

Hoechst 33342 is a blue fluorescent dye that can penetrate cell membranes and is less toxic to cells. It was often used to detect apoptosis and the staining was observed by fluorescence microscope. The Annexin-V-FITC Apoptosis Detection Kit (BD Biosciences, Franklin Lakes, NJ, United States, catalog no. 556547) was used to detect apoptosis by flow cytometry. Cells were exposed to various conditions of treatment for 24 h, and they were harvested and processed according to the manufacturer's instructions. Cells were considered viable if FITC Annexin V and PI staining were all negative; early apoptotic if FITC Annexin V staining was positive with negative PI staining; and late apoptotic or already dead if both FITC Annexin V and PI staining were positive (Li et al., 2017; Yao et al., 2020).

Immunohistochemistry

The fixed kidney section of a 4 μm thickness (Leica Company, Germany, RM2235) were deparaffinized in xylene 3333 rehydrated in a graded series of alcohols. Subsequently the sections were placed in 3% H_2O_2 for 10 min to eliminate endogenous peroxidase activity. After pepsin antigen retrieval for 30 min, the sections were washed with PBS 3 times for 3 min each time and then blocked with 2% BSA for 0.5 h at room temperature. The sections were incubated with mouse anti-synaptopodin antibody (1:200,

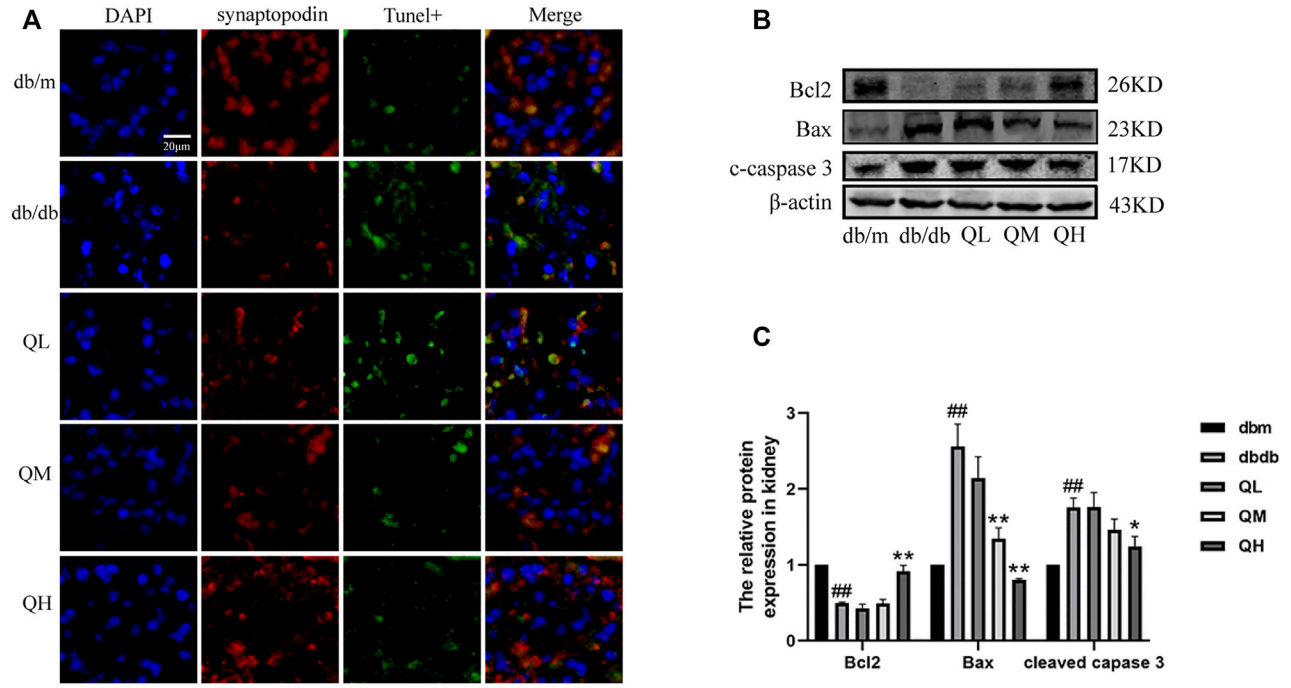

FIGURE 2 | Effects of quercetin on podocyte apoptosis in diabetic mice. **(A)** Apoptosis was assessed by TUNEL assay. **(B)** Expression of Bax, Bcl-2, cleaved caspase-3 through Western blotting. **(C)** Statistical analysis of Bax, Bcl-2, cleaved caspase-3 protein expression. Data were expressed as mean ± SEM, n = 6. $^{\#}p < 0.05$ vs *db/m*. $^{\#\#}p < 0.01$ vs *db/m*. $^{*}p < 0.05$ vs *db/db*. $^{**}p < 0.01$ vs *db/db*.

santa cruz biotechnology, sc-515842) at 37°C for 2 h or 4°C overnight. The sections were stained using a polymer HRP detection system (ZSGB-BIO, Beijing, China) and visualized with a DAB detection kit (Vector Laboratories Inc., Burlingame, CA, United States). After conventional dewatering and neutral balsam mounting, photographs were blindly taken at random felds under an Olympus BX43F fuorescence microscope (OLYMPUS, Japan) (Chen et al., 2019).

Immunofluorescence

Differentiated podocytes were fixed with cold methanol at −20°C for 20 min and permeabilized with 0.1% Triton X-100/PBS. After they were washed three times with cold PBS. The cells were blocked with 2% bovine serum albumin (BSA) for 1 h at room temperature and incubated with mouse anti-synaptopodin antibody (1:200, santa cruz biotechnology, sc-515842) or rabbit anti-cleaved caspase three antibody (1:400 Cell Signaling Technology, 9661) at 37°C for 2 h or 4°C overnight. Then, the cells were washed three times with PBS and incubated with a secondary antibody conjugated to DyLight 488 or DyLight 594 (Earthox, Millbrae, CA, United States) at 37°C for 1 h, respectively. Nuclei were counterstained with DAPI. The coverslips were mounted onto glass slides, and the images were viewed with an Olympus BX43F fluorescence microscope (OLYMPUS, Japan).

Western Blot

Protein analysis was performed on mouse renal cortex tissues (Ji et al., 2017) and cultured podocytes as described previously. EGFR, p-EGFR and cleaved caspase three antibodies were purchased from Cell Signaling (Beverly, MA, United States). ERK1/2, p-ERK1/2, Bcl2, Bax and synaptopodin antibodies were purchased from Abcam (Cambridge, United Kingdom). β-actin antibody was purchased from Santa Cruz Biotechnology (Santa Cruz, CA, United States).

Statistical Analysis

All data were presented as the means ± SEM. Statistical analysis was performed using SPSS software, version 16.0 (SPSS, Inc., Chicago, IL, United States). Statistical differences were determined using analysis of variance followed by Dunnett's test (Exp. versus Con.) using one trial analysis. A significant difference was defined as $p < 0.05$ compared with the control.

RESULTS

Quercetin Reversed the Alterations in Renal Functional Parameters in Diabetic Mice

The renal function levels of the experimental mice were examined after treatment with quercetin for 8 weeks. BUN and UACR levels are important indicators of renal function. The levels of BUN and UACR in diabetic mice treated with quercetin were significantly decreased, compared with those in the diabetic mice. In parallel, the FBG levels of the diabetic mice were obviously retrieved. During the period of the study, quercetin effectively prevented the progression of albuminuria as shown in **Table 1**. Collectively,

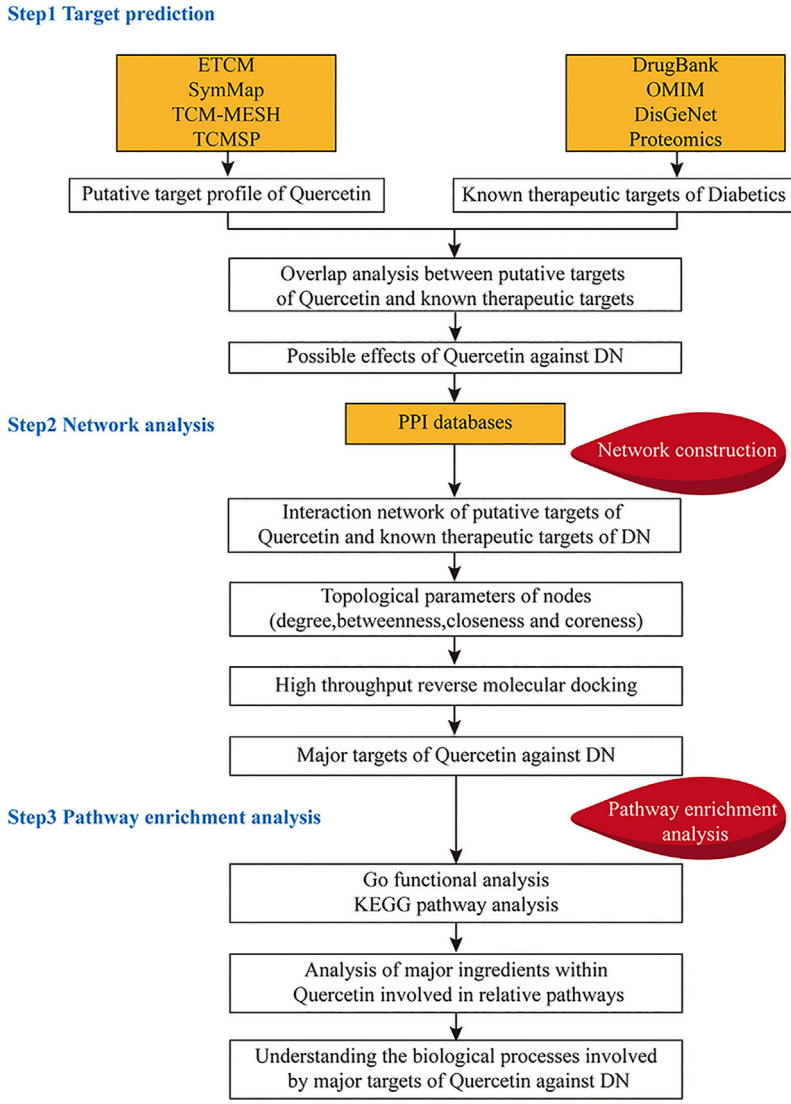

FIGURE 3 | The whole framework based on an integration strategy of network pharmacology.

these results indicated quercetin exerts protective effects on renal function.

Effects of Quercetin on Glomerular Injury in Diabetic Mice

To investigate the protection of quercetin toward DN, a series of staining methods was used in this study. PASM staining is an essential adjunct to the evaluation of change in the GBM. The GBM was markedly thickened in the diabetic group compared with the normal group when observed by PASM stain. Glycogen and collagen are components of the extracellular matrix. PAS, masson and sirius redstaining showed that glycogen and collagen deposition was enhanced in the diabetic mice renal cortex compared with control group, however, administration of quercetin in medium-dose and high-dose effectively reversed these levels (**Figures 1A–E**). We quantified expression levels of a podocyte marker protein, nephrin, indicated much less nephrin expression in diabetic mice by immunofluorescence (**Figure 1F**), immunohistochemistry (**Figures 1G,H**) and western blotting analysis (**Figure 1I,J**). However, treatment with quercetin significantly prevented reduction of nephrin. These results indicated that quercetin protects against glomerular injury in diabetic mice.

Quercetin Prevented Glomerular Podocyte Apoptosis in Diabetic Mice

TUNEL assay was used to detect apoptosis in glomeruli for observing the effect of quercetin on podocyte apoptosis under diabetic conditions. The number of apoptotic cells in glomeruli was noticeably increased from diabetic mice compared to the control group (**Figure 2A, B**. Further results showed that the pro-apoptotic

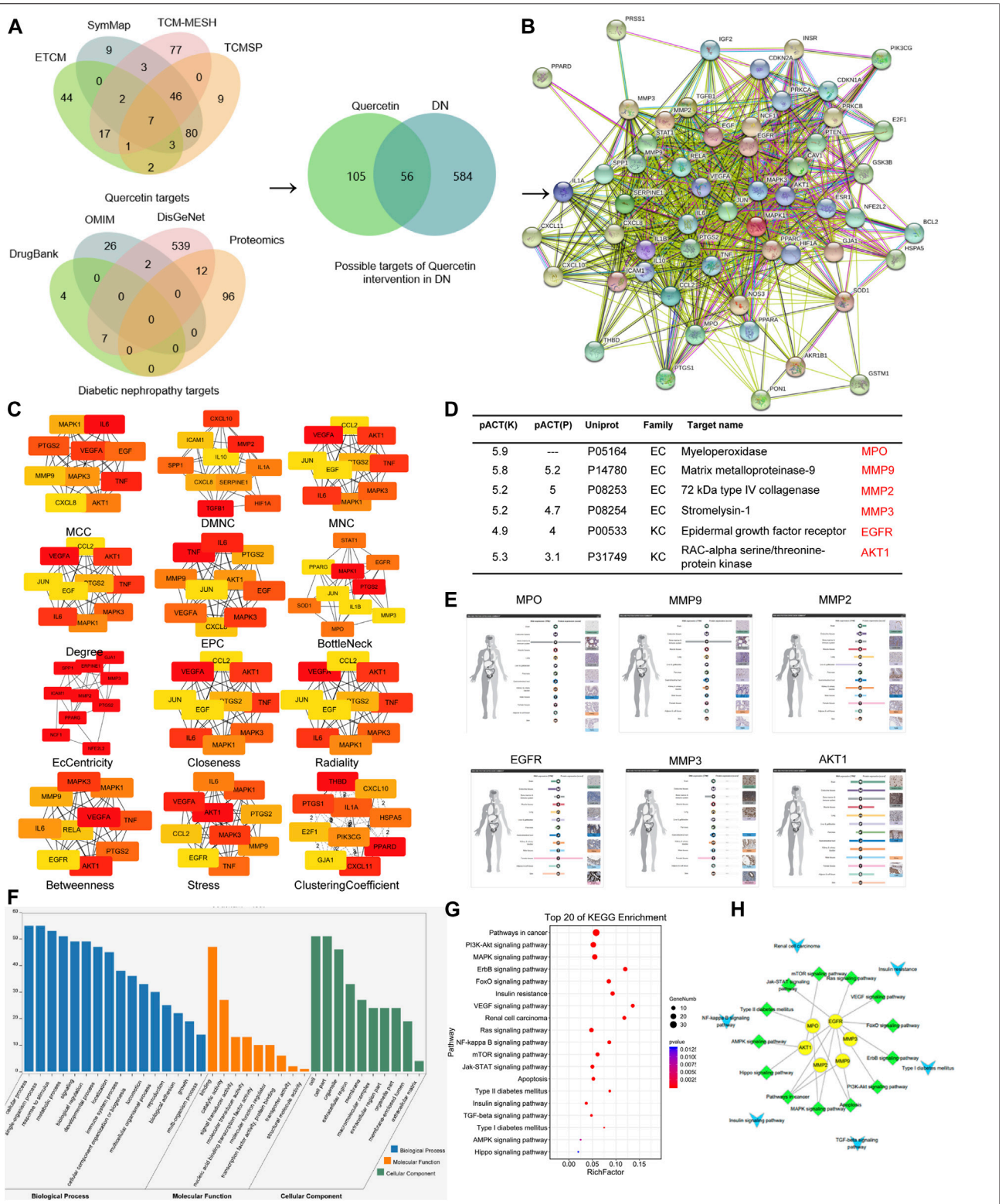

FIGURE 4 | EGFR was screened as the target of quercetin in DN through network pharmacology. **(A)** Matching of target genes between DN and quercetin. **(B)** Common target PPI network between DN and quercetin. **(C)** Hub genetic analysis. **(D)** Based on the high throughput reverse molecular docking and hub results. **(E)** The distribution of tissue. **(F)** Enriched GO terms for biological process (BP) of potential targets of quercetin. **(G,H)** KEGG pathway analysis of putative target genes of quercetin.

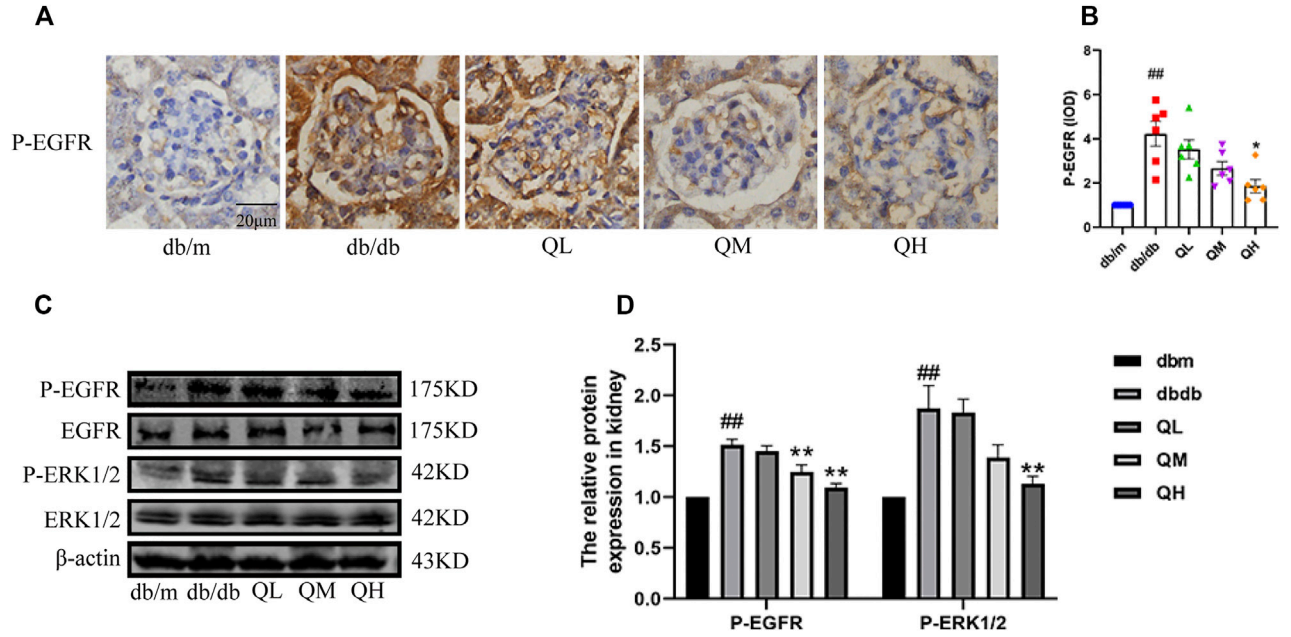

FIGURE 5 | Effects of quercetin on the EGFR pathway in diabetic mice. **(A)** Immunohistochemical analysis of P-EGFR (1068) expression in the five groups. **(B)** Statistical analysis of P-EGFR (1068) expression. **(C)** Phosphorylation of EGFR and ERK in renal cortex of diabetic mice through western blotting. **(D)** Statistical analysis of PEGFR/EGFR and PERK/ERK expression. Data were expressed as mean ± SEM, n = 6. $^{\#}p < 0.05$ vs *db/m*. $^{\#\#}p < 0.01$ vs *db/m*. $^{*}p < 0.05$ vs *db/db*. $^{**}p < 0.01$ vs *db/db*.

proteins Bax and cleaved Caspase-3 were significantly up-regulated and the anti-apoptotic protein Bcl-2 was markedly down-regulated in diabetic mice (**Figure 2C, D**). Above changes were reversed by the administration of quercetin, which demonstrated that quercetin inhibits apoptosis in diabetic mice.

Identification of EGFR Act as the Possible Target of Quercetin in the Prevention of Diabetic Nephropathy by Network Pharmacology Analysis

We obtained 161 drugs targets and 640 DN-related disease protein targets from respective databases. A total of 56 potential targets were gained based on the intersection of protein targets acting on quercetin and these are related to DN by using the ImageGP platform. The targets were exhibited in PPI and the key targets were used to screen out through 12 topology analysis algorithms of Cytoscape 3.2.1. The six key targets MPO, MMP9, MMP2, MMP3, EGFR, AKT1 were screened in this process, which suggested that these six targets probably served as significant therapeutic targets in DN. Then the tissue distribution of these targets indicating that EGFR, MMP2, and AKT1 were expressed in the kidney. GO analysis revealed that the functions of these potential targets are related to cell proliferation, differentiation and apoptosis. In the last step, we found that EGFR enriched the most pathways by KEGG pathway enrichment analysis. Therefore, EGFR was choosed as the target for quercetin intervention in DN, which synthesized all of the above analysis. All were shown in **Figures 3**, **4**. In addition, we evaluated the interaction between quercetin and EGFR by molecular docking scores (**Supplementary Figure S1**). The result showed that the docking score was -8.396, indicating a better combination of quercetin with EGFR.

Quercetin Inhibited the EGFR Pathway in Diabetic Mice

The expressions of total EGFR, phospho-EGFR and the downstream ERK in this pathway were examined to observe whether the EGFR signaling pathway can be activated in diabetic mice. Even though the raise in total EGFR and ERK expression did not reach statistical significance, the expression of phospho-EGFR and phospho-ERK markedly increased in diabetic mice compared with the normal group, and immunohistochemical results showed the same changes **Figure 5A, C**), suggesting EGFR was activated under diabetic conditions and quercetin could down-regulate the expressions of phospho-EGFR and phospho-ERK in diabetic mice (**Figure 5B, D**). Collectively, the data demonstrated that quercetin inhibited the EGFR pathway.

Effects of Quercetin and AG1478 on EGFR Pathway in HG-Induced Podocytes

In vitro, we evaluated the role of EGFR signaling through examining the expressions of phospho-EGFR and total EGFR and the downstream ERK in cultured podocytes, which were treated with HG, quercetin (40 μM) and AG1478 (EGFR inhibitor). DMSO was used as a control group for drug solvents and played no effect on their expression. CCK8 assay was used to investigate the cytotoxicity of the quercetin in podocyte. The data demonstrated that 40 μM of quercetin treatment for 24 h did not generate any conspicuous cytotoxic effects,

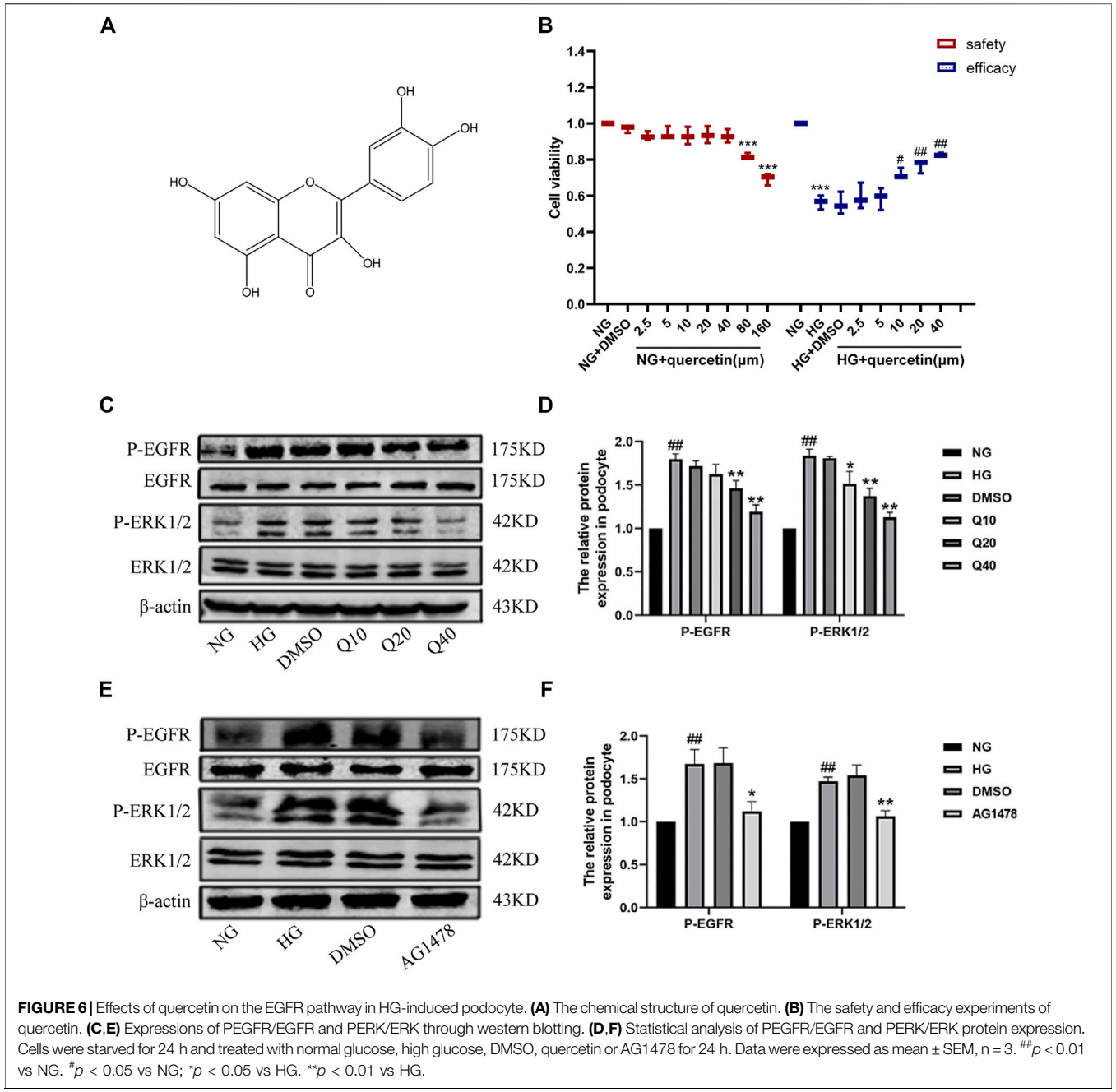

FIGURE 6 | Effects of quercetin on the EGFR pathway in HG-induced podocyte. **(A)** The chemical structure of quercetin. **(B)** The safety and efficacy experiments of quercetin. **(C,E)** Expressions of PEGFR/EGFR and PERK/ERK through western blotting. **(D,F)** Statistical analysis of PEGFR/EGFR and PERK/ERK protein expression. Cells were starved for 24 h and treated with normal glucose, high glucose, DMSO, quercetin or AG1478 for 24 h. Data were expressed as mean ± SEM, n = 3. $^{\#\#}p < 0.01$ vs NG. $^{\#}p < 0.05$ vs NG; $^{*}p < 0.05$ vs HG. $^{**}p < 0.01$ vs HG.

whereas 80 μM significantly declined cell viability (**Figure 6B**). Then we examined cell viability under different treatments to further evaluate whether quercetin protects podocyte against HG-induced apoptosis. High glucose inhibited cell viability, while treatment with quercetin raised cell viability dose dependently. Thus, doses of 10, 20 and 40 μM quercetin were used to examine its potential ability to prevent against DN in the following experiments. Western blotting results showed that the same changes in HG-induced podocyte as *in vivo* (**Figure 6C**), suggesting EGFR was activated under high glucose conditions, and quercetin could down-regulate the high expressions (**Figure 6D**). The differentiated podocytes were treated with HG for 24 h prominently increased EGFR phosphorylation, and pretreatment of the differentiated podocytes with the EGFR tyrosine kinase inhibitor (AG1478) and HG markedly prevented EGFR (**Figure 6E, F**, **Supplementary Figure S2**). So we used AG1478 to further explore the mechanism of quercetin on DN.

Quercetin Reversed Podocyte Apoptosis Through Inhibiting the EGFR Pathway

Podocyte apoptosis was detected by Annexin V-staining (**Figure 7C, E**), immunofluorescence and western blot analysis. We found that quercetin reversed HG-induced podocyte apoptosis through examining the expression of Bcl-2, Bax and cleaved caspase-3

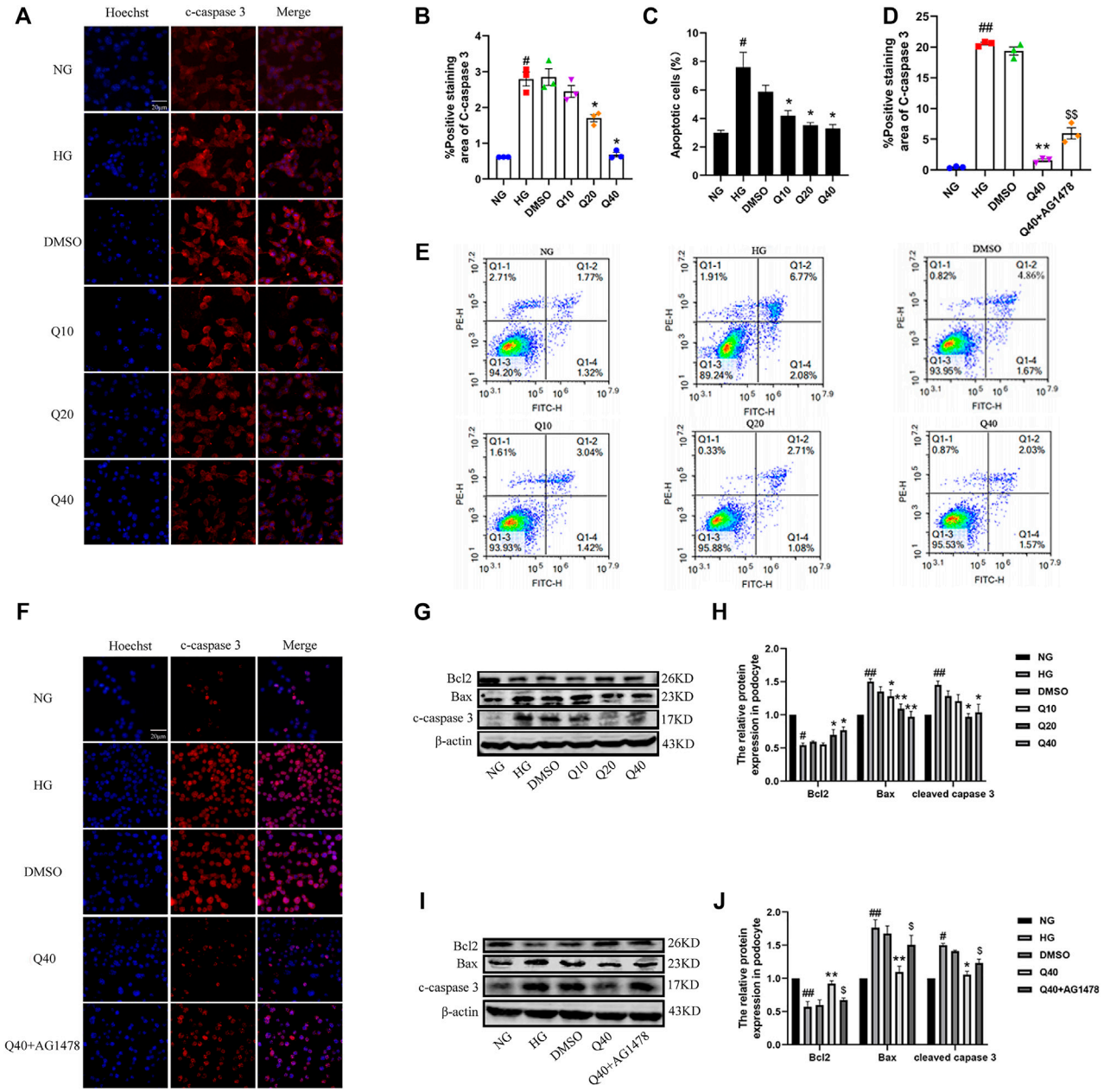

FIGURE 7 | Effects of quercetin on HG-induced podocyte apoptosis through the EGFR pathway. **(A,F)** Distribution and expression of cleaved caspase three in podocyte through immunofluorescence, the number of apoptotic cells was assessed by Hoechst 33342 staining. **(B,D)** Statistical analysis of cleaved caspase three expression. **(C)** Percentage of apoptotic podocytes. **(E)** Flow cytometry analysis of podocytes apoptosis with Annexin V-FITC/PI staining. **(G,I)** Expression of Bcl2, Bax and cleaved caspase three through western blotting. **(H,J)** Statistical analysis of Bcl2, Bax and cleaved caspase three protein expression. Data were expressed as mean ± SEM, n = 3. $^{\#\#}p < 0.01$ vs NG. $^{\#}p < 0.05$ vs NG; $^{*}p < 0.05$ vs HG. $^{**}p < 0.01$ vs HG. $^{\$}p < 0.05$vs Q40; $^{\$\$}p < 0.01$vs Q40.

(**Figure 7A, B, G, H**). To further investigate whether quercetin improved HG-induced podocyte apoptosis through the EGFR pathway, we used AG1478 to inhibit EGFR and then added quercetin to observe its effect on podocyte apoptosis. Compared to Q40 group, the improvement level of podocyte apoptosis was reduced in Q40 + AG1478 group (**Figure 7D, F, I, J**), indicating that quercetin supressed HG-induced podocyte apoptosis through the EGFR pathway.

Quercetin Inhibited HG-Induced Podocyte Injury Through the EGFR Pathway

We identified expression levels of synaptopodin and nephrin by immunofluorescence and western blotting analysis. As shown in **Figures 8A–F**, quercetin raised the low expression of synaptopodin and nephrin in HG-induced podocytes, but the upregulation effect was supressed in Q40 + AG1478 group (**Figure 8G–L**), verifying that

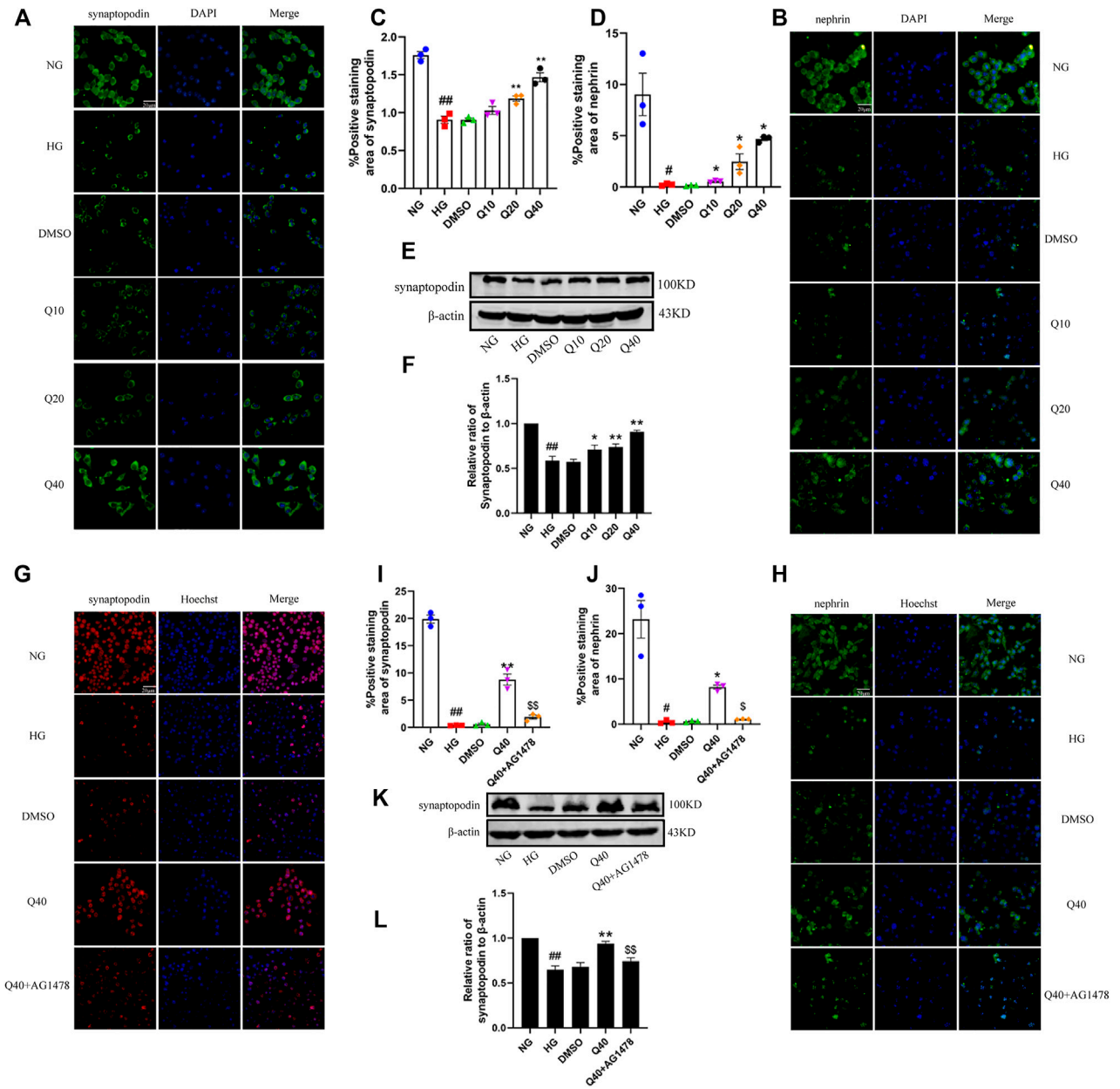

FIGURE 8 | Effects of quercetin on HG-induced podocyte injury through the EGFR pathway. **(A**,**B**,**G**,**H)** Distribution and expression of synaptopodin and nephrin in podocyte through immunofluorescence. **(C**,**D**,**I**,**J)** Statistical analysis of synaptopodin, nephrin expression. **(E**,**K)** Expression of synaptopodin through western blotting. **(F**,**L)** Statistical analysis of synaptopodin protein expression. Cells were starved for 24 h and treated with normal glucose, high glucose, DMSO, quercetin, AG1478 or Q40 + AG1478 for 24 h. Data were expressed as mean ± SEM, n = 3. $^{\#\#}p < 0.01$ vs NG. $^{\#}p < 0.05$ vs NG; $^{*}p < 0.05$ vs HG. $^{**}p < 0.01$ vs HG. $^{\$}p < 0.05$vs Q40; $^{\$\$}p < 0.01$vs Q40.

quercetin inhibited HG-induced podocyte injury through the EGFR pathway.

DISCUSSION

In spite of DN pathogenesis has made progress, its high incidence and poor prognosis have not been greatly improved. Therefore, excavating novel therapeutic targets for DN is significant. The appearance of proteinuria is regarded as the hallmark of DN at its early stage. Podocyte hypertrophy, detachment and apoptosis can all lead to the increase of proteinuria in patients with DN. A multitude of studies has demonstrated that therapies with lessening podocyte apoptosis have beneficial effects on kidney diseases (Liu et al., 2016; Jin et al., 2019). Therefore, lessening podocyte apoptosis is considered to be a potential novel therapeutic strategy for DN. The results presented here indicate that quercetin decreases the apoptosis rate of

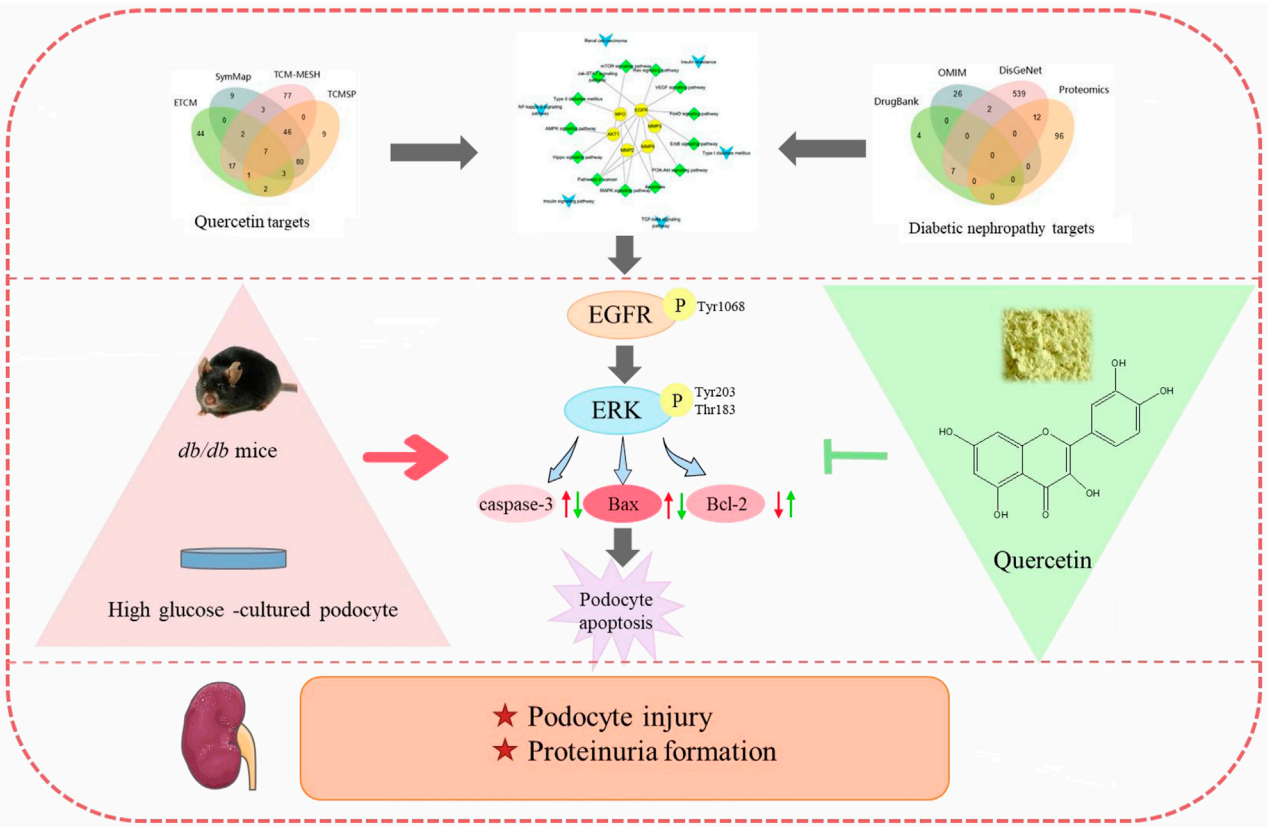

FIGURE 9 | Quercetin attenuates podocyte apoptosis of diabetic nephropathy through targeting EGFR signaling. EGFR was screened from quercetin targets and diabetic nephropathy targets by network pharmacology analysis. In diabetic nephropathy, the phosphorylation rate of EGFR and ERK were raised, leading to increased podocyte apoptosis, finally resulting in podocyte injury and proteinuria formation. By restraining the activation of EGFR signaling pathway, quercetin can relieve podocyte apoptosis and ameliorate podocyte injury, thus delaying the formation of proteinuria and the progression of diabetic nephropathy.

podocytes. Considering the protective effects of quercetin in podocytes, we hypothesize that quercetin has a protective role in diabetic nephropathy by reducing podocyte apoptosis.

Currently, hyperglycemia is regarded to be the dangerous triggering factor in the progression of diabetic nephropathy (Brownlee, 2005). Administrated quercetin in diabetic mice, a significant descent of the FBG levels was encouraging. The declining FBG level, which was statistically meaningful but absent clinically practical significance, indicating that quercetin may exert a protective effect on the kidney independent from the insulin receptor-dependent pathway. Notably, quercetin remarkably improved the signals of renal damage and dysfunction that were reflected by a reduction in BUN and UACR in diabetic mice. These results are supported by a previous study that similarly showed a remarkable effect of quercetin on ameliorating the renal function in diabetic nephropathic rats (Tang et al., 2020). Exposure to a high glucose milieu induces podocyte injury and leads to the impaired filtration barrier function of glomeruli, ultimately results in proteinuria (Xu et al., 2015; Qi et al., 2017). An abundance of evidence indicates that nephrin and synaptopodin is important in podocytes both for the slit membrane structure of interpodocytes and the integrity of the filtration barrier (Ettou et al., 2020). Our results demonstrated that the expression of nephrin was markedly decreased in diabetic mice and HG-induced podocytes, whereas quercetin treatment recovered the level of nephrin. Previous data suggested a protective effect of quercetin against podocyte injury through recovering podocytes foot processes with scarce focal fusion and increasing the expression of podocyte markers podocin in the lupus nephritis mice (Dos Santos et al., 2018), which is consistent with our results. These results indicated that quercetin improves renal function and protects against glomerular podocytes injury.

During the entire cell growth and development process, apoptosis serves a crucial role in maintaining cell stability, and dysregulation of apoptosis presents a dangerous factor in various diseases (Godse et al., 2017). Previous research showed that renal cellular apoptosis and the increased expression of apoptosis-related proteins Bax and caspase-3 lead to renal tubular atrophy and interstitial fibrosis, even aggravated renal damage in human lupus nephritis (Cui et al., 2012). Wang et al. found that the cleaved caspase-3 protein levels were significantly raised and the number of podocytes was significantly decreased in diabetic rats (Wang et al., 2019). At present study, the results showed markedly up-regulated levels of Bax, cleaved caspase-3, but a noticeably down-regulated level of Bcl-2 in HG-induced

podocytes and diabetic mice. However, treatment with quercetin reversed these changes, implying that quercetin can attenuate podocyte apoptosis under diabetic conditions. This result is in line with that of another experiment in which pretreatment with quercetin could have anti-apoptotic effect against lipopolysaccharide-induced osteoblast apoptosis (Guo et al., 2017).

Therefore, a better understanding of the molecular mechanisms underlying these effects is crucial. The approach of network pharmacology was regarded as the fastest and most effective screening method in the early study of drug effectiveness (Huang et al., 2020). We concluded that quercetin produces a multi-target effect in the treatment of DN by utilizing network pharmacology analysis. Here, we have only studied EGFR, the target with the largest number of enrichment pathways. Quercetin also acts on other signaling pathways possibly, including PI3K/AKT signaling pathway, MAPK signaling pathway and Hippo signaling pathway. We had previously found that quercetin inhibited EMT of renal tubular epithelial cells through PI3K/AKT signaling pathway, indicating that PI3K/AKT signaling pathway was activated in kidney. As a result, this discovery validates the value of our earlier work. In the current research, we hypothesized it was inhibition of EGFR that podocyte apoptosis was rescued by quercetin. Chen et al. reported that EGFR deletion in podocytes attenuates diabetic nephropathy (Chen et al., 2015). Another experiment revealed that inhibiting EGFR improved fibrosis and apoptosis in renal tissue by downregulating the expression of TGF-β, collagen IV and Bax, which is in accordance with ours (Skibba et al., 2016).

EGFR signaling cascade is a key regulator in cell proliferation, differentiation, division, survival, and disease development (Zhang et al., 2017). The EGFR small-molecule tyrosine kinase inhibitors (TKIs) emerge as a promising inhibitory approach targeting EGFR. AG1478 is one of the EGFR-TKIs (Zhang et al., 2008), which targets the adenosine triphosphate binding site on the intracellular kinase domain and prevents tyrosin kinase activation to inhibit EGFR (Pawara et al., 2021). In this experiment, AG1478 was used to examine the relationship between EGFR signaling pathways and quercetin-rescued podocyte apoptosis through detecting the expression of apoptosis-related proteins by co-cultured of AG1478 and quercetin. Expectedly, the observations indicated that quercetin abated the expression of Bax, cleaved caspase-3 through EGFR signaling pathway. This result is in line with that of another study in which EGFR inhibitor supressed podocyte hypertrophy, then led to the reduction of podocyte apoptosis and significantly decreased the albuminuria and glomerular enlargement (Lee et al., 2015). Consequently, quercetin, as a natural compound, is of noticeable help in the adjuvant therapy by inhibiting EGFR.

Taken together, this study provided a novel approach to reveal the therapeutic mechanisms of quercetin against DN, the experimental results demonstrated that quercetin inhibited podocytes apoptosis *in vitro* and *in vivo* by regulating the EGFR pathway. Quercetin shows great potential to be developed as a candidate drug for treating DN.

DATA AVAILABILITY STATEMENT

The raw data supporting the conclusions of this article will be made available by the authors, without undue reservation.

ETHICS STATEMENT

The animal study was reviewed and approved by The Animal Ethics Committee of Xuzhou Medical University.

AUTHOR CONTRIBUTIONS

Conceptualization, LD and QL; methodology, JSS and XJY; visualization and formal analysis, YQL and YL; writing-original draft preparation, YL; writing review and editing, YQL; software, LX and XZL; validation, HJ and XW; supervision, TTY and XXY; funding acquisition, LD, QL and XXY. All authors contributed to the article and approved the submitted version.

FUNDING

The work was supported by the National Natural Science Foundation of China (No.82073906, No.82003822, No.81973377, No.81903681), the Natural Science Foundation of the Jiangsu Higher Education Institutions of China (No. 20KJB310022, No. 19KJA460008) and the Postgraduate Innovative Project of Jiangsu Province (KYCX21_2732).

ACKNOWLEDGMENTS

We would like to show sincere appreciation to our colleagues for their valuable efforts and comments on this paper.

SUPPLEMENTARY MATERIAL

The Supplementary Material for this article can be found online at: https://www.frontiersin.org/articles/10.3389/fphar.2021.792777/full#supplementary-material

REFERENCES

Balakrishnan, S., Mukherjee, S., Das, S., Bhat, F. A., Raja Singh, P., Patra, C. R., et al. (2017). Gold Nanoparticles-Conjugated Quercetin Induces Apoptosis via Inhibition of EGFR/PI3K/Akt-mediated Pathway in Breast Cancer Cell Lines (MCF-7 and MDA-MB-231). *Cell Biochem Funct* 35 (4), 217–231. doi:10.1002/cbf.3266

Boezio, B., Audouze, K., Ducrot, P., and Taboureau, O. (2017). Network-based Approaches in Pharmacology. *Mol. Inform.* 36 (10). doi:10.1002/minf.201700048

Brownlee, M. (2005). The Pathobiology of Diabetic Complications: a Unifying Mechanism. *Diabetes* 54 (6), 1615–1625. doi:10.2337/diabetes.54.6.1615

Chakraborty, S., Li, L., Puliyappadamba, V. T., Guo, G., Hatanpaa, K. J., Mickey, B., et al. (2014). Constitutive and Ligand-Induced EGFR Signalling Triggers Distinct and Mutually Exclusive Downstream Signalling Networks. *Nat. Commun.* 5, 5811. doi:10.1038/ncomms6811

Chen, J., Chen, J. K., and Harris, R. C. (2015). EGF Receptor Deletion in Podocytes Attenuates Diabetic Nephropathy. *J. Am. Soc. Nephrol.* 26 (5), 1115–1125. doi:10.1681/ASN.2014020192

Chen, J., Chen, J. K., Nagai, K., Plieth, D., Tan, M., Lee, T. C., et al. (2012). EGFR Signaling Promotes TGFβ-dependent Renal Fibrosis. *J. Am. Soc. Nephrol.* 23 (2), 215–224. doi:10.1681/ASN.2011070645

Chen, Y. J., Kong, L., Tang, Z. Z., Zhang, Y. M., Liu, Y., Wang, T. Y., et al. (2019). Hesperetin Ameliorates Diabetic Nephropathy in Rats by Activating Nrf2/ARE/glyoxalase 1 Pathway. *Biomed. Pharmacother.* 111, 1166–1175. doi:10.1016/j.biopha.2019.01.030

Cui, J. H., Qiao, Q., Guo, Y., Zhang, Y. Q., Cheng, H., He, F. R., et al. (2012). Increased Apoptosis and Expression of FasL, Bax and Caspase-3 in Human Lupus Nephritis Class II and IV. *J. Nephrol.* 25 (2), 255–261. doi:10.5301/jn.2011.8451

Dos Santos, M., Poletti, P. T., Favero, G., Stacchiotti, A., Bonomini, F., Montanari, C. C., et al. (2018). Protective Effects of Quercetin Treatment in a Pristane-Induced Mouse Model of Lupus Nephritis. *Autoimmunity* 51 (2), 69–80. doi:10.1080/08916934.2018.1442828

Du, L., Qian, X., Li, Y., Li, X. Z., He, L. L., Xu, L., et al. (2021). Sirt1 Inhibits Renal Tubular Cell Epithelial-Mesenchymal Transition through YY1 Deacetylation in Diabetic Nephropathy. *Acta Pharmacol. Sin* 42 (2), 242–251. doi:10.1038/s41401-020-0450-2

Ettou, S., Jung, Y. L., Miyoshi, T., Jain, D., Hiratsuka, K., Schumacher, V., et al. (2020). Epigenetic Transcriptional Reprogramming by WT1 Mediates a Repair Response during Podocyte Injury. *Sci. Adv.* 6 (30), eabb5460. doi:10.1126/sciadv.abb5460

Feng, Y., Weng, H., Ling, L., Zeng, T., Zhang, Y., Chen, D., et al. (2019). Modulating the Gut Microbiota and Inflammation Is Involved in the Effect of Bupleurum Polysaccharides against Diabetic Nephropathy in Mice. *Int. J. Biol. Macromol* 132, 1001–1011. doi:10.1016/j.ijbiomac.2019.03.242

Gao, J., Wang, T., Qiu, S., Zhu, Y., Liang, L., and Zheng, Y. (2016). Structure-Based Drug Design of Small Molecule Peptide Deformylase Inhibitors to Treat Cancer. *Molecules* 21 (4), 396. doi:10.3390/molecules21040396

Gnudi, L., Coward, R. J. M., and Long, D. A. (2016). Diabetic Nephropathy: Perspective on Novel Molecular Mechanisms. *Trends Endocrinol. Metab.* 27 (11), 820–830. doi:10.1016/j.tem.2016.07.002

Godse, N. R., Khan, N., Yochum, Z. A., Gomez-Casal, R., Kemp, C., Shiwarski, D. J., et al. (2017). TMEM16A/ANO1 Inhibits Apoptosis via Downregulation of Bim Expression. *Clin. Cancer Res.* 23 (23), 7324–7332. doi:10.1158/1078-0432.Ccr-17-1561

omes, I. B., Porto, M. L., Santos, M. C., Campagnaro, B. P., Pereira, T. M., Meyrelles, S. S., et al. (2014). Renoprotective, Anti-oxidative and Anti-apoptotic Effects of Oral Low-Dose Quercetin in the C57BL/6J Model of Diabetic Nephropathy. *Lipids Health Dis.* 13, 184. doi:10.1186/1476-511x-13-184

Guo, C., Yang, R. J., Jang, K., Zhou, X. L., and Liu, Y. Z. (2017). Protective Effects of Pretreatment with Quercetin against Lipopolysaccharide-Induced Apoptosis and the Inhibition of Osteoblast Differentiation via the MAPK and Wnt/β-Catenin Pathways in MC3T3-E1 Cells. *Cell Physiol Biochem* 43 (4), 1547–1561. doi:10.1159/000481978

Guo, M. F., Dai, Y. J., Gao, J. R., and Chen, P. J. (2020). Uncovering the Mechanism of Astragalus Membranaceus in the Treatment of Diabetic Nephropathy Based on Network Pharmacology. *J. Diabetes Res.* 2020, 5947304. doi:10.1155/2020/5947304

Huang, Y., Lin, J., Yi, W., Liu, Q., Cao, L., Yan, Y., et al. (2020). Research on the Potential Mechanism of Gentiopicroside against Gastric Cancer Based on Network Pharmacology. *Drug Des. Devel Ther.* 14, 5109–5118. doi:10.2147/dddt.S270757

Ji, S., Tang, S., Li, K., Li, Z., Liang, W., Qiao, X., et al. (2017). Licoricidin Inhibits the Growth of SW480 Human Colorectal Adenocarcinoma Cells *In Vitro* and *In Vivo* by Inducing Cycle Arrest, Apoptosis and Autophagy. *Toxicol. Appl. Pharmacol.* 326, 25–33. doi:10.1016/j.taap.2017.04.015

Jin, J., Shi, Y., Gong, J., Zhao, L., Li, Y., He, Q., et al. (2019). Exosome Secreted from Adipose-Derived Stem Cells Attenuates Diabetic Nephropathy by Promoting Autophagy Flux and Inhibiting Apoptosis in Podocyte. *Stem Cel Res Ther* 10 (1), 95. doi:10.1186/s13287-019-1177-1

Lee, S. H., Moon, S. J., Paeng, J., Kang, H. Y., Nam, B. Y., Kim, S., et al. (2015). Podocyte Hypertrophy Precedes Apoptosis under Experimental Diabetic Conditions. *Apoptosis* 20 (8), 1056–1071. doi:10.1007/s10495-015-1134-0

Lei, D., Chengcheng, L., Xuan, Q., Yibing, C., Lei, W., Hao, Y., et al. (2019). Quercetin Inhibited Mesangial Cell Proliferation of Early Diabetic Nephropathy through the Hippo Pathway. *Pharmacol. Res.* 146, 104320. doi:10.1016/j.phrs.2019.104320

Li, D. H., Hu, P., Xu, S. T., Fang, C. Y., Tang, S., Wang, X. Y., et al. (2017). Lasiokaurin Derivatives: Synthesis, Antimicrobial and Antitumor Biological Evaluation, and Apoptosis-Inducing Effects. *Arch. Pharm. Res.* 40 (7), 796–806. doi:10.1007/s12272-016-0867-9

Li, S., and Zhang, B. (2013). Traditional Chinese Medicine Network Pharmacology: Theory, Methodology and Application. *Chin. J. Nat. Med.* 11 (2), 110–120. doi:10.1016/s1875-5364(13)60037-0

Li, Y., Pan, Y., Cao, S., Sasaki, K., Wang, Y., Niu, A., et al. (2021). Podocyte EGFR Inhibits Autophagy through Upregulation of Rubicon in Type 2 Diabetic Nephropathy. *Diabetes* 70 (2), 562–576. doi:10.2337/db20-0660

Liu, W. T., Peng, F. F., Li, H. Y., Chen, X. W., Gong, W. Q., Chen, W. J., et al. (2016). Metadherin Facilitates Podocyte Apoptosis in Diabetic Nephropathy. *Cell Death Dis* 7 (11), e2477. doi:10.1038/cddis.2016.335

Liu, Y. W., Hao, Y. C., Chen, Y. J., Yin, S. Y., Zhang, M. Y., Kong, L., et al. (2018). Protective Effects of Sarsasapogenin against Early Stage of Diabetic Nephropathy in Rats. *Phytother Res.* 32 (8), 1574–1582. doi:10.1002/ptr.6088

Lu, Q., Ji, X. J., Zhou, Y. X., Yao, X. Q., Liu, Y. Q., Zhang, F., et al. (2015). Quercetin Inhibits the mTORC1/p70S6K Signaling-Mediated Renal Tubular Epithelial-Mesenchymal Transition and Renal Fibrosis in Diabetic Nephropathy. *Pharmacol. Res.* 99, 237–247. doi:10.1016/j.phrs.2015.06.006

Nagata, M. (2016). Podocyte Injury and its Consequences. *Kidney Int.* 89 (6), 1221–1230. doi:10.1016/j.kint.2016.01.012

Pawara, R., Ahmad, I., Nayak, D., Wagh, S., Wadkar, A., Ansari, A., et al. (2021). Novel, Selective Acrylamide Linked Quinazolines for the Treatment of Double Mutant EGFR-L858r/t790m Non-small-cell Lung Cancer (NSCLC). *Bioorg. Chem.* 115, 105234. doi:10.1016/j.bioorg.2021.105234

Qi, W., Keenan, H. A., Li, Q., Ishikado, A., Kannt, A., Sadowski, T., et al. (2017). Pyruvate Kinase M2 Activation May Protect against the Progression of Diabetic Glomerular Pathology and Mitochondrial Dysfunction. *Nat. Med.* 23 (6), 753–762. doi:10.1038/nm.4328

Qu, S., Dai, C., Guo, H., Wang, C., Hao, Z., Tang, Q., et al. (2019). Rutin Attenuates Vancomycin-Induced Renal Tubular Cell Apoptosis via Suppression of Apoptosis, Mitochondrial Dysfunction, and Oxidative Stress. *Phytother Res.* 33 (8), 2056–2063. doi:10.1002/ptr.6391

Sheng, S., Huang, T., Wang, T., and Gao, J. (2017). Combined 3D-QSAR Modeling and Molecular Docking Study on spiro-derivatives as Inhibitors of Acetyl-CoA Carboxylase. *Med. Chem. Res. Int. J. Rapid Commun. Des. Mech. Action. biologically active Agents*. doi:10.1007/s00044-016-1743-3

Skibba, M., Qian, Y., Bao, Y., Lan, J., Peng, K., Zhao, Y., et al. (2016). New EGFR Inhibitor, 453, Prevents Renal Fibrosis in Angiotensin II-Stimulated Mice. *Eur. J. Pharmacol.* 789, 421–430. doi:10.1016/j.ejphar.2016.08.009

Tang, L., Li, K., Zhang, Y., Li, H., Li, A., Xu, Y., et al. (2020). Quercetin Liposomes Ameliorate Streptozotocin-Induced Diabetic Nephropathy in Diabetic Rats. *Sci. Rep.* 10 (1), 2440. doi:10.1038/s41598-020-59411-7

Wang, X., Tang, D., Zou, Y., Wu, X., Chen, Y., Li, H., et al. (2019). A Mitochondrial-Targeted Peptide Ameliorated Podocyte Apoptosis through a HOCl-Alb-Enhanced and Mitochondria-dependent Signalling Pathway in Diabetic Rats and *In Vitro*. *J. Enzyme Inhib. Med. Chem.* 34 (1), 394–404. doi:10.1080/14756366.2018.1488697

Xu, L., Fan, Q., Wang, X., Li, L., Lu, X., Yue, Y., et al. (2015). Ursolic Acid Improves Podocyte Injury Caused by High Glucose. *Nephrol. Dial. Transpl.* 32 (8), 1285–1293. doi:10.1093/ndt/gfv382

Yao, R., Xie, Y., Sun, X., Zhang, M., Zhou, J., Liu, L., et al. (2020). Identification of a Novel C-Myc Inhibitor 7594-0037 by Structure-Based Virtual Screening and Investigation of its Anti-cancer Effect on Multiple Myeloma. *Drug Des. Devel Ther.* 14, 3983–3993. doi:10.2147/DDDT.S264077

Zhang, M. Z., Wang, Y., Paueksakon, P., and Harris, R. C. (2014). Epidermal Growth Factor Receptor Inhibition Slows Progression of Diabetic Nephropathy

in Association with a Decrease in Endoplasmic Reticulum Stress and an Increase in Autophagy. *Diabetes* 63 (6), 2063–2072. doi:10.2337/db13-1279

Zhang, P., Zheng, Z., Ling, L., Yang, X., Zhang, N., Wang, X., et al. (2017). w09, a Novel Autophagy Enhancer, Induces Autophagy-dependent Cell Apoptosis via Activation of the EGFR-Mediated RAS-RAF1-Map2k-Mapk1/3 Pathway. *Autophagy* 13 (7), 1093–1112. doi:10.1080/15548627.2017.1319039

Zhang, Y. G., Qiang, D. U., Fang, W. G., Jin, M. L., and Tian, X. X. (2008). Tyrphostin AG1478 Suppresses Proliferation and Invasion of Human Breast Cancer Cells. *Int. J. Oncol* 33 (3), 595–602. doi:10.3892/ijo_00000045

Zhou, L., An, X. F., Teng, S. C., Liu, J. S., Shang, W. B., Zhang, A. H., et al. (2012). Pretreatment with the Total Flavone Glycosides of Flos Abelmoschus Manihot and Hyperoside Prevents Glomerular Podocyte Apoptosis in Streptozotocin-Induced Diabetic Nephropathy. *J. Med. Food* 15 (5), 461–468. doi:10.1089/jmf.2011.1921

Conflict of Interest: The authors declare that the research was conducted in the absence of any commercial or financial relationships that could be construed as a potential conflict of interest.

frontiers in Pharmacology

REVIEW
published: 25 January 2022
doi: 10.3389/fphar.2022.820071

Tetramethylpyrazine: An Active Ingredient of Chinese Herbal Medicine With Therapeutic Potential in Acute Kidney Injury and Renal Fibrosis

*Jun Li and Xuezhong Gong**

Department of Nephrology, Shanghai Municipal Hospital of Traditional Chinese Medicine, Shanghai University of Traditional Chinese Medicine, Shanghai, China

As an increasing public health concern worldwide, acute kidney injury (AKI) is characterized by rapid deterioration of kidney function. Although continuous renal replacement therapy (CRRT) could be used to treat severe AKI, effective drug treatment methods for AKI are largely lacking. Tetramethylpyrazine (TMP) is an active ingredient of Chinese herb *Ligusticum wallichii* (*Chuan Xiong*) with antioxidant and anti-inflammatory functions. In recent years, more and more clinical and experimental studies suggest that TMP might effectively prevent AKI. The present article reviews the potential mechanisms of TMP against AKI. Through search and review, a total of 23 studies were finally included. Our results indicate that the undergoing mechanisms of TMP preventing AKI are mainly related to reducing oxidative stress injury, inhibiting inflammation, preventing apoptosis of intrinsic renal cells, and regulating autophagy. Meanwhile, given that AKI and chronic kidney disease (CKD) are very tightly linked by each other, and AKI is also an important inducement of CKD, we thus summarized the potential of TMP impeding the progression of CKD through anti-renal fibrosis.

Keywords: tetramethylpyrazine, acute kidney injury, renal fibrosis, Chinese medicine, mechanism

OPEN ACCESS

Edited by:
Dan-Qian Chen,
Northwest University, China

Reviewed by:
Quan Hong,
Chinese PLA General Hospital, China
Ying Liu,
Central South University, China

****Correspondence:***
Xuezhong Gong
shnanshan@yeah.net

Specialty section:
This article was submitted to Renal Pharmacology, a section of the journal Frontiers in Pharmacology

Received: *22 November 2021*
Accepted: *10 January 2022*
Published: *25 January 2022*

Citation:
Li J and Gong X (2022) Tetramethylpyrazine: An Active Ingredient of Chinese Herbal Medicine With Therapeutic Potential in Acute Kidney Injury and Renal Fibrosis. Front. Pharmacol. 13:820071. doi: 10.3389/fphar.2022.820071

INTRODUCTION

Acute kidney injury (AKI) is characterized by an abrupt loss of renal function, mainly manifested by increased serum creatinine (sCr) levels and decreased urine output. The duration of AKI is generally less than 7 days, and the functional criteria are: increase in sCr by ≥50% within 7 days or increase in sCr by ≥ 0.3 mg/dl (26.5 μmol/L) within 2 days or oliguria for ≥6 h (Khwaja, 2012). A meta-analysis combined research data from 3,585,911 people from most areas north of the equator. The results reported that the combined morbidity and related mortality of AKI in adults were 21.6% and 23.9%, respectively, and 33.7% and 13.8% in children, respectively (Susantitaphong et al., 2013). Due to different medical resources, the cause and incidence of AKI vary greatly among different countries. In high-income countries, AKI is mostly hospital-acquired, mainly in elderly patients with multiple organ failure. In low- and middle-income countries, AKI mainly occurs as a complication of a single disease, and approximately 77% of AKI is community-acquired (Mehta et al., 2015; Hoste et al., 2018). The global burden of AKI-related mortality has exceeded the burden of breast cancer, heart failure or diabetes, and its medical burden is increasing (Lewington et al., 2013). In addition, AKI is associated with progressive chronic kidney disease (CKD) and the following end-stage renal

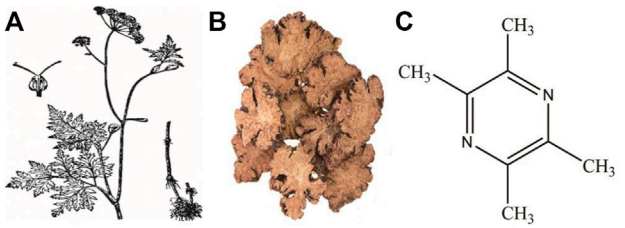

FIGURE 1 | Illustration of Ligusticum wallichii plant **(A)**, decoction pieces **(B)** and chemical structure of TMP **(C)**.

disease (ESRD), which further aggravates the harm of AKI. Many studies have reported some chemical and biological agents have beneficial effects on AKI but there is still a lack of accepted therapeutic drugs so far (Yang et al., 2016; Ronco et al., 2019). AKI patients not only have an increased risk of recent mortality and cardiovascular events, but also have a long-term risk of CKD (See et al., 2019). After the occurrence of AKI, if the kidney tissue is repaired excessively, repaired incompletely, or the damage persists, it might lead to renal dysfunction and renal fibrosis. The progression of AKI to CKD is a complex process involving the regulation of multiple cells and multiple signaling pathways, such as inflammatory damage, G2/M cell cycle arrest, oxidative stress and apoptosis, and these processes ultimately lead to or aggravate renal fibrosis (Vernon et al., 2010; He et al., 2017; Liu et al., 2017; Dong et al., 2018).

Tetramethylpyrazine (ligustrazine, TMP) is the active ingredient and characteristic alkaloid of the Chinese herbal medicine *Ligusticum wallichii* (*Chuan Xiong*) (**Figure 1**). TMP has the effects of inhibiting platelet aggregation, reducing blood viscosity, increasing coronary flow, scavenging free radicals, protecting cerebral vessels, and expanding renal vessels (Zou et al., 2018). The pyrazine ring on the TMP molecule is the key group for its pharmacological effect, but the methyl group in its side chain is easily excreted by oxidative metabolism, which leads to the short half-life of TMP and weakens its pharmacological effect (Wang et al., 2019). Pharmacokinetic studies have shown that after oral or intravenous injection, TMP is mainly distributed in tissues such as liver, brain, kidney, and small intestine, and is eventually excreted from urine through the kidney (Lou et al., 1986; Pan et al., 2021). In view of its anti-oxidative and anti-inflammatory effects, TMP is widely used in cardiovascular and cerebrovascular diseases (Zhao et al., 2016). To date, many studies have focused on the benefits of TMP in a variety of animal or cell models of AKI (Li et al., 2019). Through years of exploration, our team has also confirmed that TMP and Chinese herbal formulas containing *Chuan Xiong* have an intervention effect in AKI caused by contrast mediums (Gong, 2018; Norgren and Gong, 2018; Gong, 2020). TMP also could function as anti-renal fibrosis and be used in clinical to treat renal fibrosis and CKD. Although there are many reports on TMP effects in AKI, no systematic summary is available. Based on the evaluation of the evidence supporting this hypothesis, we mainly reviewed the therapeutic effects and mechanisms of TMP on AKI. Considering the close relationship between AKI and CKD, the present study also briefly summarized the effects of TMP on renal fibrosis and CKD.

CATEGORIES AND PATHOLOGY OF AKI

Although the cause of the disease is extremely complex, AKI is usually regarded as a single disease. Generally, it is divided into three categories based on anatomical location: pre-renal, intrinsic, and post-renal. In recent years, this simple classification method of AKI has been replaced by more specific etiological categories, since different etiologies often mean different pathological mechanisms (Bellomo et al., 2012). Related causes in the latter etiological categories include drugs, sepsis, toxins, cardiorenal, obstruction, hepatorenal, and renal hypoperfusion (**Figure 2**) (Privratsky et al., 2018; Huang et al., 2019; Jentzer et al., 2020; Simonetto et al., 2020; Molema et al., 2021). In terms of pathological manifestations, AKI is generally described as damage to renal tubular epithelial cells and vascular system (Linkermann et al., 2014; Sancho-Martínez et al., 2015). Due to pathological factors, a variety of stresses occur in AKI, including hypoxia, nutrient deprivation, energy consumption, oxidative damage, genotoxic stress, and endoplasmic reticulum stress. These stresses eventually affect renal tubular epithelial cells by causing oxidative stress damage, inflammation, necrosis, mitochondrial dysfunction, apoptosis, and autophagy (Sureshbabu et al., 2015; Cybulsky 2017; Kimura et al., 2017). Renal hypoperfusion is due to the lack of oxygen and nutrition in the nephrons, which activates the damage and death of epithelial cells through necrosis or apoptosis, ultimately leading to endothelial injury, inflammatory activation, and renal dysfunction (Makris and Spanou 2016). Nephrotoxic drugs and toxins have direct cytotoxic effects on renal tubular epithelial cells and endothelial cells. In addition, they impair hemodynamics and deposit metabolites (Yatim and Oberbarnscheidt, 2015; Wu and Huang, 2018). In sepsis, the reduction of effective circulating blood volume leads to a reduction in renal blood flow and oxygen delivery. Simultaneously, it is accompanied by immune inflammation and activation of the coagulation cascade (Peerapornratana et al., 2019). Although the mechanisms of renal hypoperfusion, nephrotoxic drugs, sepsis, and other causes of AKI are different, they all involve the pathophysiological links of hemodynamic changes, oxidative stress injury, and inflammation.

METHODS

This study required a systematic search of electronic databases to identify studies to determine the renal protective effect of TMP on AKI. The search was performed using PubMed and Embase. The following combination of terms were used as

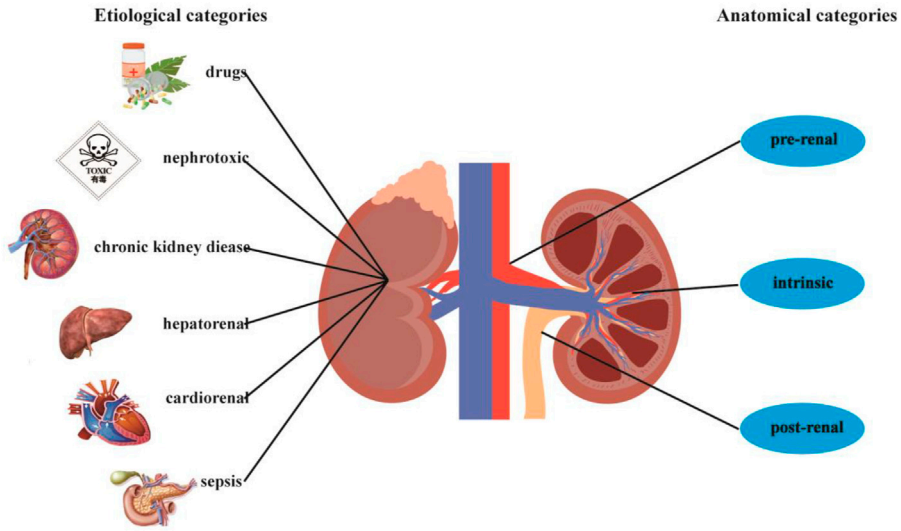

FIGURE 2 | Categories of the causes of AKI.

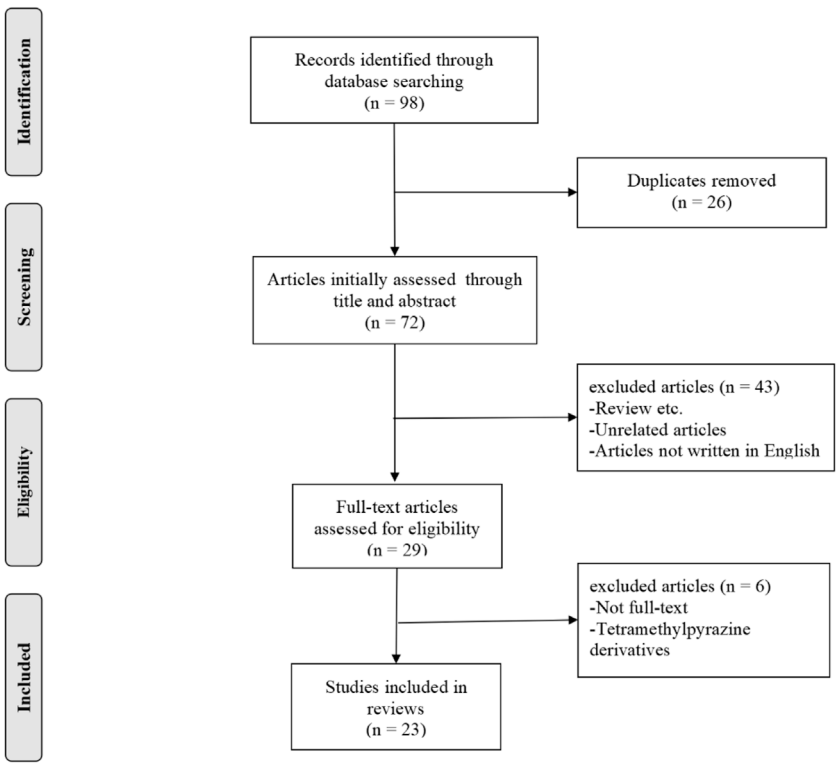

FIGURE 3 | Summary of the literature search process.

search keywords: "Tetramethylpyrazine" OR "Ligustrazine" AND "kidney injury" OR "Renal Injury" OR "Nephrotoxicity" OR "Renal ischemia." The specified exclusion criteria included: a) case reports, clinical studies, case series, editorials, and reviews; b) research on tetramethylpyrazine derivatives; and c) articles not written in English. A summary of the literature search process is presented in **Figure 3**.

TABLE 1 | *In vivo* and *in vitro* studies of TMP intervention AKI.

Type	Animal/ Cell	Model	Inducer	TMP	Histological score	Markers	References
In vivo	ICR mice	ethanol-induced AKI	absolute ethanol	10, 25, 50 mg/kg; p.o.	No scoring	SrCr↓, BUN↓, MDA↓, Cytc↓	Liu et al. (2002)
In vivo	Wistar rats	I/R injury	renal artery clipping + reperfusion	4 ml/kg; i.v.	proximal convoluted tubule: 0 = normal; 1 = mitoses and necrosis of individual cells; 2 = necrosis of all cells in adjacent tubules; 3 = necrosis confined to the distal third of, necrosis across the inner cortex; 4 = necrosis affecting all three segments of tubule	MDA↓, SOD↑, ET-1↓	Sun et al. (2002)
In vivo	Wistar rats	I/R injury	hepatic/renal I/R	not clear; i.v.	No scoring	SrCr↓, BUN↓, P-selectin↓	Chen et al. (2003)
In vivo	C57BL/6 mice	I/R injury	right nephrectomy + left renal ischemia	80 mg/kg; i.p.	number of necrotic and apoptotic cells, loss of tubular brush border, tubular dilatation, cast formation, and neutrophil infiltration: 0 = none; 1=< 10%; 2 = 11–25%; 3 = 26–45%; 4 = 46–75%; 5=> 76%	SrCr↓, BUN↓, MDA↓, SOD↑, Bcl-2↑, ICAM-1↓	Feng et al. (2004)
In vivo	SD rats	ANP-AKI	sodium taurocholate	6 g/L; i.v.	tubular epithelial cells: 0 = normal; 1 = notable cloudy swelling; 2 = swelling denaturation, interstitial congestion, edema and infiltration of inflammatory cells; 3 = diffuse coagulation necrosis	SrCr↓, BUN↓, TXA2/PGI2↓	Zhang et al. (2006)
In vitro and *In vivo*	SD rats/ NRK-52E cells	DI-AKI	gentamicin	80 mg/kg/ d; i.p.	No scoring	Bcl-xL↑, TNF-α↓, NF-κB↓, caspase-3↓, caspase-8↓, caspase-9↓	Juan et al. (2007)
In vivo	Wistar rats	DI-AKI	cisplatin	80 mg/kg/ d; p.o.	approximate extent of necrotic area in the cortical proximal tubules: 0 = no necrosis; 1 = a few focal necrotic spots; 2 = necrotic area about onehalf; 3 = necrotic spots about two-thirds; 4 = nearly all of the area necrotic	SrCr↓, BUN↓, GSH↑, NAG↓, SOD↑, TOX↑	Ali et al. (2008)
In vivo	SD rats	DI-AKI	Cisplatin	50, 100 mg/kg; i.p.	No scoring	SrCr↓, BUN↓, MDA↓, NAG↓, SOD↑, GSH↑, GST↑, NOS↓, NO↓	Liu et al. (2008)
In vivo	Wistar rats	DI-AKI	Gentamicin	100 mg/kg/ d; p.o.	No scoring	SrCr↓, BUN↓, UNAG↓	Ali et al. (2009)
In vivo and *In vitro*	C57B6 mice/ NRK-52E	DI-AKI	gentamicin	80 mg/kg/ d; i.p.	tubular necrosis: 0 = normal; 1 ≤ 10%; 2 = 10–25%; 3 = 26–75%; 4 ≥ 75% cells exhibiting necrosis	HO-1↑, Bcl-xL↑, Hax-1↑, NADPH↓, NF-κB↓, Cox-2↓, caspases-3↓, caspases-9↓	Sue et al. (2009)
In vivo	C57BL/6 mice	I/R injury	renal artery clipping + reperfusion	80 mg/kg; i.p.	positive tubular brush border, tubular dilatation, cast formation, neutrophil infiltration: 0 = none; 1 = 10%; 2 = 11–25%; 3 = 26–45%; 4 = 46–75%; 5 = 76%	MPO↓, MDA↓, SOD↑, TNF-α↓, ICAM-1↓	Feng et al. (2011)
In vivo	Lewis rats	severe burn	30% TBSA scald injury	40 mg/kg/ d; i.p.	expression of Bcl-2 and MICA: 0 = 0–5% stained; 1=> 5–25%; 2=> 25–50%; 3=> 50–75%; 4=> 75%	MDA↓, SOD↑, MICA↓, Bcl-2↓	Gao et al. (2012)
In vivo	SD rats	CIN		80 mg/kg/ d; i.p.	No scoring		Gong et al. (2013)

(Continued on following page)

TABLE 1 | (*Continued*) *In vivo* and *in vitro* studies of TMP intervention AKI.

Type	Animal/ Cell	Model	Inducer	TMP	Histological score	Markers	References
			L-NAME + indomethacin + iohexol			SrCr↓, BUN↓, phospho-p38 MAPK↓, FoxO1↓, Bcl-2↑, Bax↓, iNOS↓, CysC↓, UNAG↓, UGGT↓	
In vivo	SD rats	DI-AKI	Cadmium chloride (CdCl2)	50 mg/kg; i.p.	No scoring	BUN↓, kim-1↓, indoxyl sulfate↓, clusterin↓, MDA↓, SOD↓, GR↓, LDH↓, ALP↓	Lan et al. (2014)
In vitro	HK-2 cells	DI-AKI	sodium arsenite	—	No scoring	ROS↓, GSH↑, β-catenin↓, NF-κB↓, p38 MAPK↓, COX-2↓, TNF-α↓, Cytc oxidase↑, mitochondrial membrane potential↑	Gong et al. (2015)
In vitro	HK-2 cells	DI-AKI	sodium arsenite	—	No scoring	HO-1↓, ARS2↓ p38 MAPK↓, JNK↓, AP-1↓, Nrf2↓, NF-κB↓	Gong et al. (2016)
In vivo	SD rats	DI-AKI	Cadmium chloride (CdCl2)	50 mg/kg; i.p.	No scoring	SrCr↓, BUN↓, MDA↓, 4-HNE↓, GSH↑, GSH/GSSG↑, SAM↑, cystathionine↑, MATs↑, CBS↑	Kuang et al. (2017)
In vivo	SD rats	CIN	L-NAME + indomethacin + iohexol	80 mg/kg/ d; i.p.	No scoring	SrCr↓, BUN↓, Drp1↓, Mfn2↑, CCL2↓, CCR2↓, LC3B-II/I↓, Beclin-1↓, p62↑, procaspase 9↑, caspase 3↓, TNF-α↓, ROS↓, IL-6↓, CysC↓, UNAG↓, UGGT↓	Gong et al. (2019)
In vivo	SD rats	DI-AKI	Cisplatin	50, 100 mg/kg/ d; i.p.	No scoring	SrCr↓, BUN↓, HMGB1↓, TLR4↓, NF-κB↓, TNF-α↓, IL-1β↓, GSH↑, SOD↑, PPAR-γ↑, Nrf2↑, Bax↓, Bcl2↑, caspase-3↓, HO-1↑, NQO1↑, COX-2↓, iNOS↓, Kim-1↓	Michel and Menze, (2019)
In vivo	C57BL/6 mice	Sepsis-AKI	cecal ligation and puncture (CLP)	10, 30, 60 mg/kg; i.v.	pathological changes of renal cortex or outer zone of medulla: 0 = normal; 1 = less than 5%; 2 = 5–25%; 3 = 25–75%; 4= > 75%	Kim1↓, caspase- 3↓, NMDAR1↓	Ying et al. (2020)
In vivo	SD rats	I/R injury	renal artery clipping + reperfusion	40 mg/kg; i.p.	renal tubular injury: 1 = normal; 2 = 0–10%; 3 = 11–25%; 4 = 26–45%; 5 = 46–75%; 6= > 75%	TNF-α↓, IL-1β↓, IL-6↓, MDA↓, GSH↑, LC3B-II/I↑, Beclin-1↑	Chen et al. (2020)
In vivo and *In vitro*	SD rats/ NRK-52E cells	I/R injury	renal artery clipping + reperfusion/CoCl2/ OGD + reoxygenation	40 mg/kg; i.p.	injury in tubules of the outer medulla: 0 = none; 1 = 0–10%; 2 = 11–25%; 3 = 26–45%; 4 = 46–75%; 5=> 75%	SrCr↓, BUN↓, NOD2↓, TNF-α↓, IL-6↓, MCP-1↓, caspase-3/cleaved caspase-3↓, LC3A/B-II/I↑	Jiang et al. (2020)
In vivo and *In vitro*	SD rats/ NRK-52E cells	I/R injury	renal artery clipping + reperfusion/OGD + reoxygenation	200 mg/kg; p.o.	No scoring	SrCr↓, BUN↓, TNF-α↓, IL-6↓, NLRP3↓, HIF-1α↓, KIM-1↓	Sun et al. (2020)

RESULTS

Studies Characteristics and Mechanism

In total, 98 potentially relevant studies were screened. Ultimately, 23 experimental studies met the inclusion and exclusion criteria (**Table 1**). In **Table 1**, there are 17 *in vivo* studies, 2 *in vitro* studies, and four both. Of the 23 studies, 12 were on nephrotoxic drugs and toxins, seven on ischemia-reperfusion, two on contrast mediums, one on sepsis, and one on severe burns. These studies involve the use of TMP, including oral, intravenous, and intraperitoneal injections. Based on the results of these studies, TMP had a therapeutic effect on AKI caused by a variety of etiologies. In terms of mechanism, TMP could alleviate AKI by reducing oxidative stress, inflammation, mitochondrial and other organelle damage, or affecting cytoprotective mechanisms such as autophagy or apoptosis (**Figure 4**). The target highlighted by the red dashed line in the figure represents the key link for TMP to exert its effect. These mechanisms are described in detail below.

TMP Relieves Oxidative Stress Injury

Oxidative stress reflects a state of imbalance between the formation of reactive oxygen and nitrogen and antioxidant system. Oxidative stress occurs when the production of pro-oxidants or reactive oxygen species (ROS) exceeds the endogenous antioxidant capacity (Sies et al., 2017). ROS are several active molecules and free radicals derived from

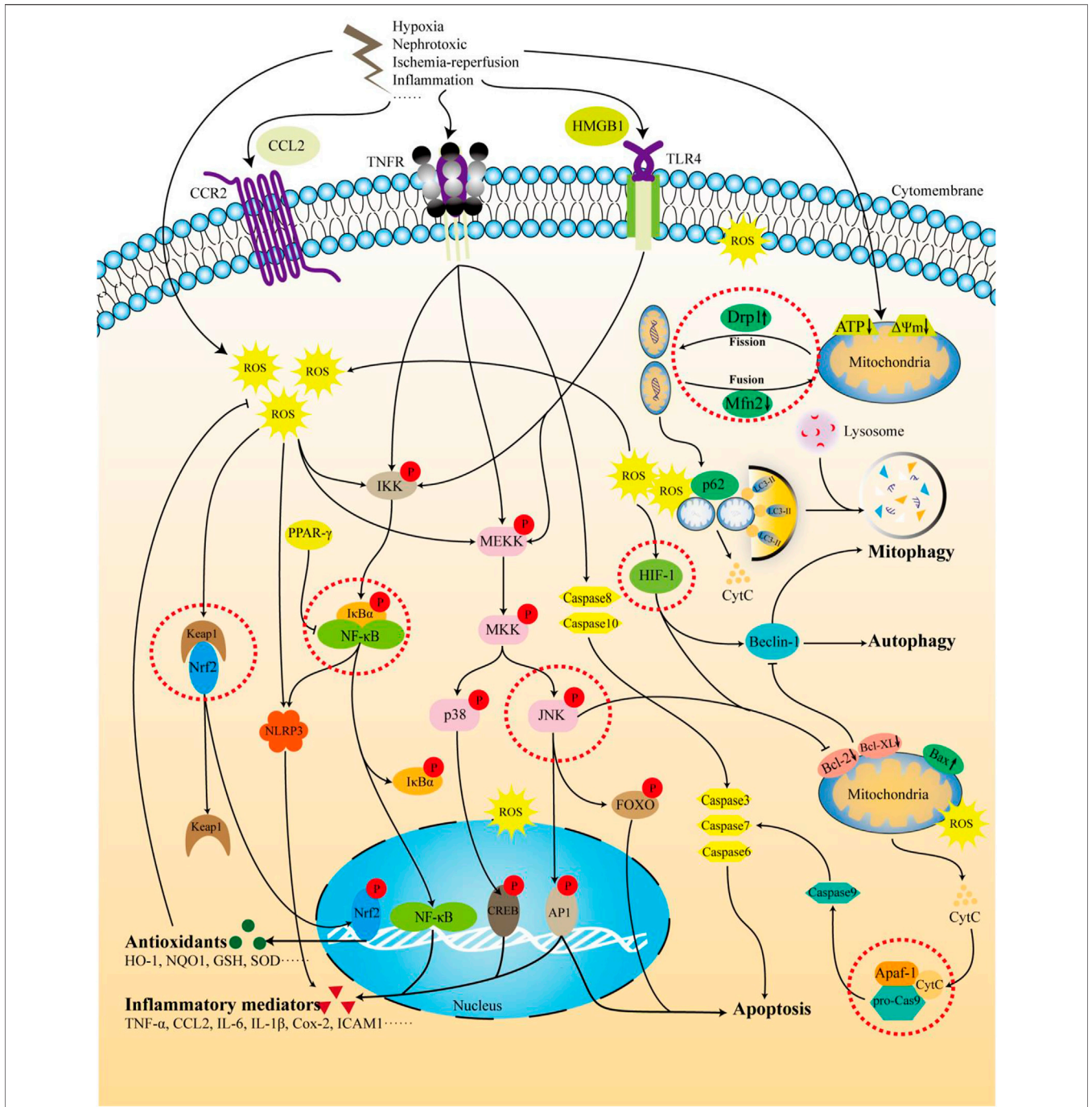

FIGURE 4 | The mechanism of TMP intervention in AKI. The figure summarizes the molecular pathways of TMP treatment of AKI involved in this review. Receptors such as TNR, TLR, and CCR2 are stimulated by nephrotoxic drugs, LPS, I/R, and inflammatory factors. In addition, hypoxia and I/R can also directly affect the mitochondrial quality control process and membrane potential, leading to the generation of ROS. The activation of the above receptors and the production of intracellular ROS can activate downstream pathways, further triggering inflammation, apoptosis, and autophagy, and ultimately leading to kidney damage. TMP can target Nfr2 and HIF-1 to activate the expression of antioxidant factors and enhance cell tolerance to oxidative stress. TMP can also inhibit TLR4 and TNFR or, by activating PPAR-γ, further inhibit the NF-κB pathway and reduce inflammation. In addition to the targeted inhibition of caspase-8/3/6/7 through the TNFR pathway, TMP can also affect mitochondrial-related apoptosis by inhibiting the ERK/JNK pathway. There is still controversy regarding the regulation of autophagy by TMP. It is generally believed that TMP activates the autophagy process and eliminates damaged mitochondria by targeting mitochondrial quality control, ultimately reducing cell damage.

molecular oxygen, including superoxide anions ($O2^-$) and hydroxyl radicals (OH). At high concentrations, ROS can be toxic to macromolecules, including lipids, proteins, and DNA, leading to the destruction of the integrity and capacity of the cell structure (Davies, 1987; Sies, 1997). Oxidative stress is an important pathological mechanism of AKI caused by various etiologies. In AKI induced by ischemia-reperfusion injury, sepsis, and contrast mediums, changes in renal hemodynamics can lead to increased ROS production. In the hypoxic state, electron transfer in the mitochondrial respiratory chain is obstructed, causing electron leakage. The leaked electrons combine with oxygen to generate a large amount of active oxygen (Granata et al., 2015; Kusirisin et al., 2020). Cisplatin and aminoglycoside drugs can induce mitochondrial dysfunction and increase the production of ROS and can also react with thiol-containing molecules, including glutathione (GSH). The consumption or inactivation of GSH and related antioxidants leads to the intracellular accumulation of endogenous ROS (Kruidering et al., 1997; Sureshbabu et al., 2015). Other studies have also shown that oxidative stress plays a key role in the development of AKI. For example, in a mouse model of renal I/R injury, heme oxygenase-1 knockout ($HO\text{-}1^{-/-}$) mice were found to be more sensitive to I/R injury, while increasing the incidence of renal injury and mortality rate (Tracz et al., 2007). Oxidative stress further leads to downstream effects such as inflammatory damage, necrosis, and apoptosis. During oxidative stress, TMP mainly inhibits ROS generation and activates the antioxidant system. Liu *et al.* studied the protective effect of TMP on cisplatin-induced nephrotoxicity in rats, using ligustrazine for 7 consecutive days of intraperitoneal injection, starting from 2 days before a single intravenous injection of cisplatin. The results showed that cisplatin increased the levels of MDA, NOS, and NO, while the levels of GSH, GST, and SOD decreased. These changes were reversed by TMP treatment (Liu et al., 2008). Nrf2 is an important regulator of the antioxidant system that can neutralize the activation of cellular oxidative stress. Under basic conditions, the Keap1/Nrf2 complex is easily degraded by ubiquitination. However, under oxidative stress conditions, Keap1 is oxidized, and Nrf2 is introduced into the nucleus and binds to the antioxidant response element in the gene promoter region to initiate the transcription of a series of antioxidant factors (Saito, 2013; Suzuki and Yamamoto, 2015). Michel *et al.* found that TMP pretreatment significantly activated the Nrf2 defense pathway in rats with nephrotoxicity induced by cisplatin indicated by the increase in levels of Nrf2 and downstream antioxidant enzymes such as HO-1 and NQO1 in the kidney. This also shows that TMP inhibits cisplatin-induced oxidative stress by activating the Nrf2 defense mechanism (Michel and Menze, 2019). However, the regulation of Nrf2 and HO-1 signals by TMP is obviously complex. For example, as a response biomarker for arsenic exposure in various types of cells, HO-1 was observed downregulated by TMP pretreatment in arsenic-induced nephrotoxicity cell model, so did Nrf2 (Gong et al., 2016). We speculated that the reasons for the above contradictory results are multifaceted and complicated. The protective effect of Nrf2 in the kidney is affected by its activation degree and duration, and there might be a delicate balance. Studies have shown that in mice with renal tubule-specific knockout of Keap1, moderate activation of Nrf2 might reduce the damage caused by ischemia or nephrotoxic substances, while excessive and continuous activation of Nrf2 loses this protective effect (Noel et al., 2016; Tan et al., 2016; Nezu et al., 2017). Moreover, the transcription of the HO-1 gene is complicated and might not only be regulated by Nrf2. For example, sodium arsenite has been shown to cause BACH1-specific HO-1 induction independent of Nrf2 (Reichard et al., 2016). Additionally, there is a functional κB element in the promoter of mouse HO-1 gene, which might be the mechanism of HO-1 upregulation *in vivo* mediated by NF-κB subunits p50 and p65 (Li et al., 2009). Our previously data indicated clearly that arsenic-induced HO-1 expression is mediated by multiple pathways, and the corresponding transcription factors includes Nrf2, NF-κB AP-1, p38 MAPK, and JNK (but not ERK) (Gong et al., 2016). As an organ rich in mitochondria, kidney is very susceptible to oxidative stress mediated damage, thus reducing mitochondrial-derived ROS might be another important way to protect kidney against oxidative stress injury (Gorin, 2016). Our previous study also found that TMP could improve abnormal mitochondrial dynamics and regulate mitochondrial damage in contrast-induced nephropathy (CIN) (Gong et al., 2019). In addition, oxidative stress also interacts with a variety of pathological processes in the AKI process, including inflammation and apoptosis, which are discussed below. Therefore, TMP has the therapeutic potential of antagonizing oxidative stress in AKI caused by various etiologies.

TMP Improves Inflammation

Inflammation is a physiological process that protects the body from acute damages such as ischemia, pathogens, or toxins. Inflammation is believed to play an important role in the pathogenesis of AKI. Basically, all immune cells, such as neutrophils, monocytes/macrophages, and NK cells are involved in the pathogenesis of AKI to varying degrees (Rabb et al., 2016). Activation of the inflammatory process in AKI is caused by multiple pathways. In models of ischemia, sepsis, and nephrotoxicity, the initial damage occurs in the tubular epithelium and vascular endothelial cells (Akcay et al., 2009). The above-mentioned damage induces the production of inflammatory mediators such as inflammatory factors, chemokines, and adhesion factors (TNF-α, TGF-β, IL-6, IL-1β, IL-18, CCL2, MCP-1, ICAM-1, and P-selectin), which help recruit leukocytes to the kidney. Neutrophils, macrophages, and lymphocytes infiltrate the injury site (McWilliam et al., 2021). In addition, oxidative stress can promote inflammation, and cell damage caused by inflammation further aggravates oxidative stress (Tucker et al., 2015). In the tetracycline-induced AKI rat model, the use of mitochondrial-targeted antioxidants significantly reduced the accumulation of dendritic cells and T cells in the kidney tissue, suggesting that mitochondrial-derived ROS are involved in antigen presentation and T-cell activation (Gentle et al., 2013). Under oxidative stress, NADPH oxidase (NOX) can interact with Toll-like receptor 4 (TLP4) to directly activate the nuclear transcription factor NF-κB

pathway, leading to an increase in the transcription of downstream inflammatory mediators and further increasing inflammation (El-Benna et al., 2016). Most of the studies in **Table 1** show an inhibitory effect on the level of inflammatory mediators, and the regulation of the NF-κB pathway is the key to TMP. NLRP3 is a member of the nucleotide-binding oligomerization domain-like receptor protein family (NLRPs) and is a common inflammasome. It promotes the maturation of the pro-inflammatory factors IL-1β and IL-18 by activating caspase-1 (Liston and Masters, 2017; Shi et al., 2017). The expression of signal sensing receptors such as TLRs and TNFRs and downstream gene expression proteins such as NF-κB and ROS is involved in the activation of NLRP3 (Xue et al., 2019). Many studies have shown that the NLRP3 inflammasome and its downstream apoptosis and inflammation play important roles in the occurrence and development of AKI (Bakker et al., 2014; Shen et al., 2016). Sun *et al.* explored the protective effect of TMP on renal ischemia-reperfusion injury in rats and its potential mechanism. The expression level of NLRP3 in NRK-52E cells increased after hypoxia and glucose deprivation, and decreased significantly after TMP treatment (Sun et al., 2020). As an important member of the CC subfamily of chemokines, CCL2 is also called monocyte chemotactic protein-1 (MCP-1). CCL2 is formed under pathological conditions such as pro-inflammatory stimuli (IL-8, TNF-α, and LPS stimulus). It usually binds to the extracellular specific ligand CCR2 to mediate the migration and activation of a variety of inflammatory cells (Kawaguchi-Niida et al., 2013). Our previous study found that the abundance of CCL2 and CCR2 in the renal tubules of rats with contrast-induced nephropathy (CIN) increased, accompanied by an increase in the concentration of IL-6 and TNF-α in the kidney and serum, and TMP could inhibit the CCL2/CCR2 pathway activation (Gong et al., 2019). The peroxisome proliferator-activated receptor (PPAR) is a member of the superfamily of nuclear transcription factors activated by ligands (Wu et al., 2018). PPAR-γ can inhibit the inflammatory response by competing with the inflammatory signaling pathway and the production of inflammatory mediators such as activator protein-1 (AP-1) and NF-κB (Ju et al., 2020). Studies have found that PPAR-γ expression is significantly reduced in cisplatin-induced acute kidney injury in rats, and TMP administration can significantly improve this change (Michel and Menze, 2019). In summary, TMP is a promising anti-inflammatory agent for treating AKI.

TMP Inhibits Apoptosis

Apoptosis refers to the biochemical process of cell breakdown by a set of specific proteins that interact with each other and program death-inducing signals. Unlike necrosis, apoptosis does not cause inflammation (Kønig et al., 2019). When a cell receives an apoptosis signal, it activates the initial caspases through different signaling pathways, reactivates the effector caspases, and degrades related substrates, eventually leading to cell apoptosis (Chota et al., 2021). Since there are many apoptotic signaling pathways, the upstream regulation of caspases is also different. Bcl-2 family molecules are involved in upstream regulatory pathways for the reception and transmission of apoptosis signals. They mainly regulate apoptosis *via* the mitochondrial pathway. When pro-apoptotic proteins receive apoptosis signals, they can release cytochrome C (Cytc) from the mitochondria to activate downstream caspases, then causing apoptosis (Singh et al., 2019). The permeability of the mitochondrial membrane is regulated by Bcl-2 family proteins. In renal epithelial cells, Bcl-2 members Bax and Bak cause an increase in membrane permeability, while Bcl-2 and Bcl-XL antagonize this "membrane attack" effect (Youle and Strasser, 2008). Intrarenal stress and ischemia both increase the ratio of Bax/Bcl2, which is the main determinant of cell death (Chien et al., 2005; Liu and Baliga, 2005). In most AKI models, the adjustment effect of TMP on the ratio of Bax/Bcl2 has been confirmed in many studies. Juan *et al.* showed that gentamicin significantly induced apoptosis in NRK-52E cells in a dose-dependent manner. TMP pretreatment can inactivate the activities of caspase-3, caspase-8, and caspase-9 stimulated by gentamicin, inhibit the release of Cytc, and increase the expression of Bcl-XL (Juan et al., 2007). Although renal tubular cell apoptosis is often reported in various AKI models, the upstream signaling pathways leading to apoptosis may be different (Havasi and Borkan, 2011; Linkermann et al., 2013). Although there are different initiation mechanisms, most apoptotic pathways cluster on the mitochondria. The endogenous mitochondrial apoptotic pathway begins with oxidative stress. ROS and other stress products enter the mitochondria with the Bax/Bcl-2 protein complex, promote the increase in mitochondrial permeability with other pro-apoptotic genes, and then release Cytc (Galluzzi et al., 2018). Therefore, the anti-oxidative stress ability of TMP can regulate the mitochondrial apoptosis pathway from the source. There is also a close relationship between apoptosis and mitochondrial dynamics. Previous studies have shown that in the early stage of apoptosis, Bax is transferred from the cytoplasm to the mitochondria before the caspases are activated, and, at the same time, dynein-related protein 1 (DRP1) is also transferred from the cytoplasm to the mitochondrial division site and then mediates mitochondrial division (Suen et al., 2008). Inhibiting the activity of Drp1 not only inhibits mitochondrial division but also inhibits the activation and apoptosis of caspases (Hoppins and Nunnari, 2012). In addition, high expression of mitochondrial outer membrane fusion proteins Mfn1 and Mfn2 can also inhibit apoptosis (Jian et al., 2018). Our previous found that TMP could improve abnormal mitochondrial dynamics by upregulating Mfn2 and downregulating Drp1 and alleviating the apoptosis of tubule epithelial cells caused by contrast agents (Gong et al., 2019). In addition, the external pathway of apoptosis mediated by TNFR may also be involved in renal tubular cell apoptosis in ischemic and septic AKI (Cunningham et al., 2002; Linkermann et al., 2014). TNFR knockout mice are resistant to cisplatin-induced AKI, supporting this pathogenesis (Ramesh and Reeves, 2004). TMP can simultaneously regulate the upstream ligand (TNF-α) and downstream signaling pathways (JNK and NF-κB) of the TNFR-mediated apoptosis pathway.

TMP Adjusts Autophagy

Autophagy is a process in which a double-membrane autophagosome encapsulates cytoplasm, organelles, and protein polymers and is transported to lysosomes for catabolism (Youle and Narendra, 2011). Under normal physiological conditions, low levels of basal autophagy maintain cell homeostasis by removing damaged proteins and organelles. The autophagy pathway is upregulated in stress states such as cell starvation, hypoxia, and endoplasmic reticulum stress (Feng et al., 2014). Autophagy is non-selective, but it can also selectively degrade damaged organelles such as mitophagy to clear damaged mitochondria. The formation of autophagosomes depends on the coordination of autophagy-related proteins, which mainly include the ULK1/2 complex, Beclin-1/class III PI3K complex, and autophagy-related genes (ATG). LC3-II is located in pre-autophagosomes and autophagosomes, and its level increases with the increase in autophagosome membranes. The Beclin-1/class III PI3K complex promotes the nucleation of autophagosomes on the phagocytic vesicle membrane. Both LC3-II and Beclin-1 are markers for autophagy detection (Dancourt and Melia, 2014). There are many reports on the link between AKI and autophagy, most of which indicate the protective effect of autophagy on AKI. Studies have found that the expression of LC3 in proximal tubule cells of ATG5-deficient mice after renal I/R injury is inhibited, suggesting that basic autophagy has a protective effect against renal injury caused by I/R injury (Kimura et al., 2011). In the CI-AKI rat and cell models established with iohexol, it was found that the expression of autophagy marker LC3-II in renal tubular epithelial cells increased, the mitochondrial damage of renal tubular cells increased after the use of autophagy inhibitors, and apoptosis increased (Ko et al., 2016). Although most studies have found that autophagy activated in renal tubular epithelial cells of various AKI plays a protective role, a few studies have suggested that autophagy aggravates cell damage in AKI. Chen *et al.* found that TMP could reduce renal I/R damage by enhancing autophagy, indicated by increased LC3-II/I ratio and Beclin-1 in kidney tissue (Chen et al., 2020). Another study found that TMP reduced inflammation in renal I/R injury and was related to the activation of autophagy (Jiang et al., 2020). Interestingly, in a study on CI-AKI, we found that the mechanism by which TMP protected the kidney from contrast agent damage was partly related to the inhibition of autophagy (Gong et al., 2019). The reason for this apparently contradictory result may be related to the different AKI models. Some studies have reported that autophagy induces cell metabolism imbalance and induces cell death in renal tubular epithelial cells induced by contrast agents, and this result can be attenuated by curcumin (Buyuklu et al., 2014). This shows that the role of autophagy in AKI is still controversial. As an upstream regulator of autophagy induction, ROS not only induces autophagy through the mitochondrial pathway but also induces mitophagy through the signaling pathway mediated by HIF-1 (Scherz-Shouval and Elazar, 2007; Zhang et al., 2008). The regulation of oxidative stress and HIF-1 by TMP is also one of the ways to regulate autophagy. In addition, there is an interaction between autophagy and apoptosis. In response to stress such as hypoxia, autophagy can prevent cells from triggering the apoptotic pathway by degrading misfolded proteins and damaged organelles. The inhibitory effect of Bcl-2 family proteins on autophagy in renal tubular cells has been confirmed in many experiments. In Bcl-2/GFP-LC3 transgenic mice, autophagy induced by ischemia-reperfusion was attenuated (Isaka et al., 2009). Studies have shown that enhancing the expression of Bcl-XL in the kidney is sufficient to inhibit autophagy induction and apoptosis (Chien et al., 2007). Regarding the mechanism by which Bcl-2 downregulates autophagy, it is generally believed that Bcl-2 family proteins bind Beclin-1 through the BH3 domain, blocking the necessary process of autophagosome formation. The details of the simultaneous regulation of autophagy and apoptosis by TMP are still unclear, and this may be a promising research direction. In short, the mechanism by which TMP interferes with autophagy in AKI is unclear, and there are still controversies.

THE POTENTIAL OF TMP PREVENTS CKD AND RENAL FIBROSIS

AKI and CKD are very tightly linked by each other. Many studies suggested that AKI is also an important inducement of chronic kidney disease (CKD) (Horne et al., 2017; See et al., 2019). There are many published data of TMP against CKD as well as renal fibrosis. In China, several TMP injections have been used to treat CKD in clinical, especially in diabetic nephropathy patients (Wang et al., 2012). Cao *et al.* reported that TMP had an inhibitory effect on the proliferation of human renal interstitial fibroblasts in a time- and concentration-dependent manner (Cao et al., 2006). Unilateral ureteral obstruction (UUO) model is a classic model for studying renal fibrosis, *Yuan et al.* reported that TMP treatment could reduce the score of interstitial collagen deposition, the density of macrophages, and the mRNA expressions of TGF-β1 and CTGF in this rat model (Yuan et al., 2012). The matrix accumulation caused by the reduction of the ratio of MMPS/TIMPS is the basic pathophysiological process of renal interstitial fibrosis (Kelly et al., 2010). Studies had found that TMP could inhibit the high expression of TIMP-1 and the imbalance of MMP-9/TIMP-1 ratio in UUO model rats, and thereby slow the progression of renal fibrosis (Li et al., 2017). TGF-β/Smad3 is the main pathway of renal fibrosis, and Smad7 could block the phosphorylation of Smad3, thereby limiting the effect of TGF-β (Meng et al., 2016; Chen et al., 2018). The results of Lu *et al.* showed that TMP could reduce the content of TGF-β1 in kidney tissue and restore the expression levels of Smad reverse regulators Smad7 and SnoN protein (Lu et al., 2009). In addition, aristolochic acid is very toxic to kidney, which would cause tubulointerstitial damage and renal fibrosis, and TMP has been reported to reduce the kidney damage caused by aristolochic acid in rats (Wang et al., 2006).

CONCLUSION AND PERSPECTIVE

Considering the importance of oxidative stress and inflammation in AKI, the application of TMP in AKI treatment deserves

attention. The present study mainly focuses on the experimental research of TMP in preventing AKI, and aims to synthesize the current knowledge in this field, concurrently, this study also briefly sums up the effects of TMP against renal fibrosis and CKD. Based on the collected data, TMP not only improves kidney function, reduces the level of kidney injury markers (including kim-1, CysC, UNAG, and UGGT), but also decreases the degree of pathological damage in kidney. Although the pathological mechanisms of AKI caused by various factors are different, the preventive effects of TMP against AKI are inseparable from the following four processes: oxidative stress, inflammatory mediators, apoptosis, and autophagy. These data support the potential application of TMP as a new therapeutic drug for AKI. It should be noted that these data mainly are preclinical studies, and the clinical application of TMP in AKI treatment still needs more rigorous clinical research data. As mentioned above, our group has been focusing on the basic experimental research of TMP against CI-AKI for more than 10 years (Gong et al., 2013, 2019; Gong, 2018; Norgren and Gong, 2018), and we hope these basic experimental research data should promote the followed clinical research progress of TMP treating CI-AKI and other types of AKI, not just for anti-renal fibrosis and the treatment of CKD.

AUTHOR CONTRIBUTIONS

XG and JL designed the work of review. JL and XG reviewed the literature available on this topic and wrote the paper. XG and JL revised the manuscript. All authors approved the paper for publication. As the leader of the project team, XG won the research fundings supporting this manuscript.

FUNDING

This project is supported by the National Natural Science Foundation of China (No.82074387 and No.81873280) and Shanghai Municipal Science and Technology Commission Project (No.20Y21902200).

ACKNOWLEDGMENTS

Meanwhile, the authors would like to thank Zongping Li and Zhiyong Song for advice and helpful discussion.

REFERENCES

Akcay, A., Nguyen, Q., and Edelstein, C. L. (2009). Mediators of Inflammation in Acute Kidney Injury. *Mediators Inflamm.* 2009, 137072. doi:10.1155/2009/137072

Ali, B. H., Al-Moundhri, M., Eldin, M. T., Nemmar, A., Al-Siyabi, S., and Annamalai, K. (2008). Amelioration of Cisplatin-Induced Nephrotoxicity in Rats by Tetramethylpyrazine, a Major Constituent of the Chinese Herb Ligusticum Wallichi. *Exp. Biol. Med. (Maywood)* 233 (7), 891–896. doi:10.3181/0711-RM-315

Ali, B. H., Al-Salam, S., Al-Husseini, I., and Nemmar, A. (2009). Comparative Protective Effect of N-Acetyl Cysteine and Tetramethylpyrazine in Rats with Gentamicin Nephrotoxicity. *J. Appl. Toxicol.* 29 (4), 302–307. doi:10.1002/jat.1409

Bakker, P. J., Butter, L. M., Claessen, N., Teske, G. J., Sutterwala, F. S., Florquin, S., et al. (2014). A Tissue-specific Role for Nlrp3 in Tubular Epithelial Repair after Renal Ischemia/reperfusion. *Am. J. Pathol.* 184 (7), 2013–2022. doi:10.1016/j.ajpath.2014.04.005

Bellomo, R., Kellum, J. A., and Ronco, C. (2012). Acute Kidney Injury. *Lancet* 380 (9843), 756–766. doi:10.1016/S0140-6736(11)61454-2

Buyuklu, M., Kandemir, F. M., Ozkaraca, M., Set, T., Bakirci, E. M., and Topal, E. (2014). Protective Effect of Curcumin against Contrast Induced Nephropathy in Rat Kidney: what Is Happening to Oxidative Stress, Inflammation, Autophagy and Apoptosis? *Eur. Rev. Med. Pharmacol. Sci.* 18 (4), 461–470. doi:10.1016/j.jep.2013.12.015

Cao, L., Sun, X., Yu, G., Guo, Q., Zhang, X., and Xu, K. (2006). "Effects of Ligustrazine on the Proliferation and Morphology of Human Renal Interstitial Fibroblasts. *Phytother Res.*26 1936–1937+1942. doi:10.1002/ptr.3630

Chen, J. L., Zhou, T., Chen, W. X., Zhu, J. S., Chen, N. W., Zhang, M. J., et al. (2003). Effect of Tetramethylpyrazine on P-Selectin and Hepatic/renal Ischemia and Reperfusion Injury in Rats. *World J. Gastroenterol.* 9 (7), 1563–1566. doi:10.3748/wjg.v9.i7.1563

Chen, L., Yang, T., Lu, D. W., Zhao, H., Feng, Y. L., Chen, H., et al. (2018). Central Role of Dysregulation of TGF-β/Smad in CKD Progression and Potential Targets of its Treatment. *Biomed. Pharmacother.* 101, 670–681. doi:10.1016/j.biopha.2018.02.090

Chen, P., Li, J., Liu, S., and Wei, R. (2020). Tetramethylpyrazine Attenuates Renal Ischemia-Reperfusion Injury in Rats through Inhibiting Inflammation and Oxidative Stress and Enhancing Autophagy. *Latin Am. J. Pharm.* 39 (6), 1094–1099.

Chien, C. T., Chiang-Ting, C., Chang, T. C., Tsai, C. C. Y., Ching-Yi, T., Shyue, S. K., et al. (2005). Adenovirus-mediated Bcl-2 Gene Transfer Inhibits Renal Ischemia/reperfusion Induced Tubular Oxidative Stress and Apoptosis. *Am. J. Transpl.* 5 (6), 1194–1203. doi:10.1111/j.1600-6143.2005.00826.x

Chien, C. T., Shyue, S. K., and Lai, M. K. (2007). Bcl-xL Augmentation Potentially Reduces Ischemia/reperfusion Induced Proximal and Distal Tubular Apoptosis and Autophagy. *Transplantation* 84 (9), 1183–1190. doi:10.1111/j.1600-6143.2005.00826.x10.1097/01.tp.0000287334.38933.e3

Chota, A., George, B. P., and Abrahamse, H. (2021). Interactions of Multidomain Pro-apoptotic and Anti-apoptotic Proteins in Cancer Cell Death. *Oncotarget* 12 (16), 1615–1626. doi:10.18632/oncotarget.28031

Cunningham, P. N., Dyanov, H. M., Park, P., Wang, J., Newell, K. A., and Quigg, R. J. (2002). Acute Renal Failure in Endotoxemia Is Caused by TNF Acting Directly on TNF Receptor-1 in Kidney. *J. Immunol.* 168 (11), 5817–5823. doi:10.4049/jimmunol.168.11.5817

Cybulsky, A. V. (2017). Endoplasmic Reticulum Stress, the Unfolded Protein Response and Autophagy in Kidney Diseases. *Nat. Rev. Nephrol.* 13 (11), 681–696. doi:10.1038/nrneph.2017.129

Dancourt, J., and Melia, T. J. (2014). Lipidation of the Autophagy Proteins LC3 and GABARAP Is a Membrane-Curvature Dependent Process. *Autophagy* 10 (8), 1470–1471. doi:10.4161/auto.29468

Davies, K. J. (1987). Protein Damage and Degradation by Oxygen Radicals. I. General Aspects. *J. Biol. Chem.* 262 (20), 9895–9901. doi:10.0000/PMID303687510.1016/s0021-9258(18)48018-0

Dong, W., Li, Z., Chen, Y., Zhang, L., Ye, Z., Liang, H., et al. (2018). Necrostatin-1 Attenuates Sepsis-Associated Acute Kidney Injury by Promoting Autophagosome Elimination in Renal Tubular Epithelial Cells. *Mol. Med. Rep.* 17 (2), 3194–3199. doi:10.3892/mmr.2017.8214

El-Benna, J., Hurtado-Nedelec, M., Marzaioli, V., Marie, J. C., Gougerot-Pocidalo, M. A., and Dang, P. M. (2016). Priming of the Neutrophil Respiratory Burst: Role in Host Defense and Inflammation. *Immunol. Rev.* 273 (1), 180–193. doi:10.1111/imr.12447

Feng, L., Ke, N., Cheng, F., Guo, Y., Li, S., Li, Q., et al. (2011). The Protective Mechanism of Ligustrazine against Renal Ischemia/reperfusion Injury. *J. Surg. Res.* 166 (2), 298–305. doi:10.1016/j.jss.2009.04.005

Feng, L., Xiong, Y., Cheng, F., Zhang, L., Li, S., and Li, Y. (2004). Effect of Ligustrazine on Ischemia-Reperfusion Injury in Murine Kidney. *Transpl. Proc* 36 (7), 1949–1951. doi:10.1016/j.transproceed.2004.07.050

Feng, Y., He, D., Yao, Z., and Klionsky, D. J. (2014). The Machinery of Macroautophagy. *Cell Res* 24 (1), 24–41. doi:10.1038/cr.2013.168

Galluzzi, L., Vitale, I., Aaronson, S. A., Abrams, J. M., Adam, D., Agostinis, P., et al. (2018). Molecular Mechanisms of Cell Death: Recommendations of the Nomenclature Committee on Cell Death 2018. *Cell Death Differ* 25 (3), 486–541. doi:10.1038/s41418-017-0012-4

Gao, C., Peng, H., Wang, S., and Zhang, X. (2012). Effects of Ligustrazine on Pancreatic and Renal Damage after Scald Injury. *Burns* 38 (1), 102–107. doi:10.1016/j.burns.2011.04.022

Gentle, M. E., Shi, S., Daehn, I., Zhang, T., Qi, H., Yu, L., et al. (2013). Epithelial Cell TGFβ Signaling Induces Acute Tubular Injury and Interstitial Inflammation. *J. Am. Soc. Nephrol.* 24 (5), 787–799. doi:10.1681/ASN.2012101024

Gong, X., Duan, Y., Zheng, J., Ye, Z., and Hei, T. K. (20192019). Tetramethylpyrazine Prevents Contrast-Induced Nephropathy via Modulating Tubular Cell Mitophagy and Suppressing Mitochondrial Fragmentation, CCL2/CCR2-Mediated Inflammation, and Intestinal Injury. *Oxid Med. Cel Longev* 2019, 7096912. doi:10.1155/2019/7096912

Gong, X., Ivanov, V. N., Davidson, M. M., and Hei, T. K. (2015). Tetramethylpyrazine (TMP) Protects against Sodium Arsenite-Induced Nephrotoxicity by Suppressing ROS Production, Mitochondrial Dysfunction, Pro-inflammatory Signaling Pathways and Programed Cell Death. *Arch. Toxicol.* 89 (7), 1057–1070. doi:10.1007/s00204-014-1302-y

Gong, X., Ivanov, V. N., and Hei, T. K. (2016). 2,3,5,6-Tetramethylpyrazine (TMP) Down-Regulated Arsenic-Induced Heme Oxygenase-1 and ARS2 Expression by Inhibiting Nrf2, NF-Kb, AP-1 and MAPK Pathways in Human Proximal Tubular Cells. *Arch. Toxicol.* 90 (9), 2187–2200. doi:10.1007/s00204-015-1600-z

Gong, X., Wang, Q., Tang, X., Wang, Y., Fu, D., Lu, H., et al. (2013). Tetramethylpyrazine Prevents Contrast-Induced Nephropathy by Inhibiting P38 MAPK and FoxO1 Signaling Pathways. *Am. J. Nephrol.* 37 (3), 199–207. doi:10.1159/000347033

Gong, X. Z. (2020). Chinese Medicine Might Be A Promising Way for A Solution to Arsenic Nephrotoxicity. *Chin. J. Integr. Med.* 26 (2), 83–87. doi:10.1007/s11655-019-3210-8

Gong, X. Z. (2018). Recent Advances in Chinese Medicine for Contrast-Induced Nephropathy. *Chin. J. Integr. Med.* 24 (1), 6–9. doi:10.1007/s11655-017-2906-x

Gorin, Y. (2016). The Kidney: An Organ in the Front Line of Oxidative Stress-Associated Pathologies. *Antioxid. Redox Signal.* 25 (12), 639–641. doi:10.1089/ars.2016.6804

Granata, S., Dalla Gassa, A., Tomei, P., Lupo, A., and Zaza, G. (2015). Mitochondria: a New Therapeutic Target in Chronic Kidney Disease. *Nutr. Metab. (Lond)* 12, 49. doi:10.1186/s12986-015-0044-z

Havasi, A., and Borkan, S. C. (2011). Apoptosis and Acute Kidney Injury. *Kidney Int.* 80 (1), 29–40. doi:10.1038/ki.2011.120

He, L., Wei, Q., Liu, J., Yi, M., Liu, Y., Liu, H., et al. (2017). AKI on CKD: Heightened Injury, Suppressed Repair, and the Underlying Mechanisms. *Kidney Int.* 92 (5), 1071–1083. doi:10.1016/j.kint.2017.06.030

Hoppins, S., and Nunnari, J. (2012). Cell Biology. Mitochondrial Dynamics and Apoptosis-Tthe ER Connection. *Science* 337 (6098), 1052–1054. doi:10.1126/science.1224709

Horne, K. L., Packington, R., Monaghan, J., Reilly, T., and Selby, N. M. (2017). Three-year Outcomes after Acute Kidney Injury: Results of a Prospective Parallel Group Cohort Study. *BMJ Open* 7 (3), e015316. doi:10.1136/bmjopen-2016-015316

Hoste, E. A. J., Kellum, J. A., Selby, N. M., Zarbock, A., Palevsky, P. M., Bagshaw, S. M., et al. (2018). Global Epidemiology and Outcomes of Acute Kidney Injury. *Nat. Rev. Nephrol.* 14 (10), 607–625. doi:10.1038/s41581-018-0052-0

Huang, J., Li, J., Lyu, Y., Miao, Q., and Pu, K. (2019). Molecular Optical Imaging Probes for Early Diagnosis of Drug-Induced Acute Kidney Injury. *Nat. Mater.* 18 (10), 1133–1143. doi:10.1038/s41563-019-0378-4

Isaka, Y., Suzuki, C., Abe, T., Okumi, M., Ichimaru, N., Imamura, R., et al. (2009). Bcl-2 Protects Tubular Epithelial Cells from Ischemia/reperfusion Injury by Dual Mechanisms. *Transpl. Proc* 41 (1), 52–54. doi:10.1016/j.transproceed.2008.10.026

Jentzer, J. C., Bihorac, A., Brusca, S. B., Del Rio-Pertuz, G., Kashani, K., Kazory, A., et al. (2020). Contemporary Management of Severe Acute Kidney Injury and Refractory Cardiorenal Syndrome: JACC Council Perspectives. *J. Am. Coll. Cardiol.* 76 (9), 1084–1101. doi:10.1016/j.jacc.2020.06.070

Jian, F., Chen, D., Chen, L., Yan, C., Lu, B., Zhu, Y., et al. (2018). Sam50 Regulates PINK1-Parkin-Mediated Mitophagy by Controlling PINK1 Stability and Mitochondrial Morphology. *Cell Rep* 23 (10), 2989–3005. doi:10.1016/j.celrep.2018.05.015

Jiang, G., Xin, R., Yuan, W., Zhang, L., Meng, X., Sun, W., et al. (2020). Ligustrazine Ameliorates Acute Kidney Injury through Downregulation of NOD2-mediated I-nflammation. *Int. J. Mol. Med.* 45 (3), 731–742. doi:10.3892/ijmm.2020.4464

Ju, Z., Su, M., Hong, J., Kim, E., and Jung, J. H. (2020). Anti-inflammatory Effects of an Optimized PPAR-γ Agonist via NF-Kb Pathway Inhibition. *Bioorg. Chem.* 96, 103611. doi:10.1016/j.bioorg.2020.103611

Juan, S. H., Chen, C. H., Hsu, Y. H., Hou, C. C., Chen, T. H., Lin, H., et al. (2007). Tetramethylpyrazine Protects Rat Renal Tubular Cell Apoptosis Induced by Gentamicin. *Nephrol. Dial. Transpl.* 22 (3), 732–739. doi:10.1093/ndt/gfl699

Kawaguchi-Niida, M., Yamamoto, T., Kato, Y., Inose, Y., and Shibata, N. (2013). MCP-1/CCR2 Signaling-Mediated Astrocytosis Is Accelerated in a Transgenic Mouse Model of SOD1-Mutated Familial ALS. *Acta Neuropathol. Commun.* 1, 21. doi:10.1186/2051-5960-1-21

Kelly, B. C., Markle, L. S., Vickers, J. L., Petitt, M. S., Raimer, S. S., and McNeese, C. (2010). The Imbalanced Expression of Matrix Metalloproteinases in Nephrogenic Systemic Fibrosis. *J. Am. Acad. Dermatol.* 63 (3), 483–489. doi:10.1016/j.jaad.2009.09.006

Khwaja, A. (2012). KDIGO Clinical Practice Guidelines for Acute Kidney Injury. *Nephron Clin. Pract.* 120 (4), c179–84. doi:10.1159/000339789

Kimura, T., Isaka, Y., and Yoshimori, T. (2017). Autophagy and Kidney Inflammation. *Autophagy* 13 (6), 997–1003. doi:10.1080/15548627.2017.1309485

Kimura, T., Takabatake, Y., Takahashi, A., Kaimori, J. Y., Matsui, I., Namba, T., et al. (2011). Autophagy Protects the Proximal Tubule from Degeneration and Acute Ischemic Injury. *J. Am. Soc. Nephrol.* 22 (5), 902–913. doi:10.1681/ASN.2010070705

Ko, G. J., Bae, S. Y., Hong, Y. A., Pyo, H. J., and Kwon, Y. J. (2016). Radiocontrast-induced Nephropathy Is Attenuated by Autophagy through Regulation of Apoptosis and Inflammation. *Hum. Exp. Toxicol.* 35 (7), 724–736. doi:10.1177/0960327115604198

Kønig, S. M., Rissler, V., Terkelsen, T., Lambrughi, M., and Papaleo, E. (2019). Alterations of the Interactome of Bcl-2 Proteins in Breast Cancer at the Transcriptional, Mutational and Structural Level. *Plos Comput. Biol.* 15 (12), e1007485. doi:10.1371/journal.pcbi.1007485

Kruidering, M., Van de Water, B., de Heer, E., Mulder, G. J., and Nagelkerke, J. F. (1997). Cisplatin-induced Nephrotoxicity in Porcine Proximal Tubular Cells: Mitochondrial Dysfunction by Inhibition of Complexes I to IV of the Respiratory Chain. *J. Pharmacol. Exp. Ther.* 280 (2), 638–649. doi:10.1016/j.bbi.2007.10.008

Kuang, W., Zhang, X., Zhu, W., and Lan, Z. (2017). Ligustrazine Modulates Renal Cysteine Biosynthesis in Rats Exposed to Cadmium. *Environ. Toxicol. Pharmacol.* 54, 125–132. doi:10.1016/j.etap.2017.07.003

Kusirisin, P., Chattipakorn, S. C., and Chattipakorn, N. (2020). Contrast-induced Nephropathy and Oxidative Stress: Mechanistic Insights for Better Interventional Approaches. *J. Transl Med.* 18 (1), 400. doi:10.1186/s12967-020-02574-8

Lan, Z., Bi, K. S., and Chen, X. H. (2014). Ligustrazine Attenuates Elevated Levels of Indoxyl Sulfate, Kidney Injury Molecule-1 and Clusterin in Rats Exposed to Cadmium. *Food Chem. Toxicol.* 63, 62–68. doi:10.1016/j.fct.2013.10.038

Lewington, A. J., Cerdá, J., and Mehta, R. L. (2013). Raising Awareness of Acute Kidney Injury: a Global Perspective of a Silent Killer. *Kidney Int.* 84 (3), 457–467. doi:10.1038/ki.2013.153

Li, H. D., Meng, X. M., Huang, C., Zhang, L., Lv, X. W., and Li, J. (2019). Application of Herbal Traditional Chinese Medicine in the Treatment of Acute Kidney Injury. *Front. Pharmacol.* 10, 376. doi:10.3389/fphar.2019.00376

Li, J., Yu, J., and Liu, Y. (2017). Effects of Ligustrazine on the Expression of MMP-9 and TIMP-1 in Renal Interstitial Fibrosis ratsCNKI:SUN:YXLL. *J. Med. Theor. Pract.* 25 (3), 3.

Li, Q., Guo, Y., Ou, Q., Cui, C., Wu, W. J., Tan, W., et al. (2009). Gene Transfer of Inducible Nitric Oxide Synthase Affords Cardioprotection by Upregulating Heme Oxygenase-1 via a Nuclear Factor-{kappa}B-dependent Pathway. *Circulation* 120 (13), 1222–1230. doi:10.1161/CIRCULATIONAHA.108.778688

Linkermann, A., Bräsen, J. H., Darding, M., Jin, M. K., Sanz, A. B., Heller, J. O., et al. (2013). Two Independent Pathways of Regulated Necrosis Mediate Ischemia-

Reperfusion Injury. *Proc. Natl. Acad. Sci. U S A.* 110 (29), 12024–12029. doi:10.1073/pnas.1305538110

Linkermann, A., Chen, G., Dong, G., Kunzendorf, U., Krautwald, S., and Dong, Z. (2014). Regulated Cell Death in AKI. *J. Am. Soc. Nephrol.* 25 (12), 2689–2701. doi:10.1681/ASN.2014030262

Liston, A., and Masters, S. L. (2017). Homeostasis-altering Molecular Processes as Mechanisms of Inflammasome Activation. *Nat. Rev. Immunol.* 17 (3), 208–214. doi:10.1038/nri.2016.151

Liu, C. F., Lin, M. H., Lin, C. C., Chang, H. W., and Lin, S. C. (2002). Protective Effect of Tetramethylpyrazine on Absolute Ethanol-Induced Renal Toxicity in Mice. *J. Biomed. Sci.* 9 (4), 299–302. doi:10.1007/BF02256584

Liu, H., and Baliga, R. (2005). Endoplasmic Reticulum Stress-Associated Caspase 12 Mediates Cisplatin-Induced LLC-PK1 Cell Apoptosis. *J. Am. Soc. Nephrol.* 16 (7), 1985–1992. doi:10.1681/ASN.2004090768

Liu, M., Ning, X., Li, R., Yang, Z., Yang, X., Sun, S., et al. (2017). Signalling Pathways Involved in Hypoxia-Induced Renal Fibrosis. *J. Cel Mol Med* 21 (7), 1248–1259. doi:10.1111/jcmm.13060

Liu, X. H., Li, J., Li, Q. X., Ai, Y. X., and Zhang, L. (2008). Protective Effects of Ligustrazine on Cisplatin-Induced Oxidative Stress, Apoptosis and Nephrotoxicity in Rats. *Environ. Toxicol. Pharmacol.* 26 (1), 49–55. doi:10.1016/j.etap.2008.01.006

Lou, Y., Zhang, H., Xia, C., and Chen, M. (1986). The Pharmacokinetics and *In Vivo* Fate of Ligustrazine Phosphate in Dogs and Rats. *Acta Pharmaceutica Sinica* (07), 481–487. doi:10.16438/j.0513-4870.1986.07.001

Lu, Min., Zhou, Juan., Wang, Fei., Liu, Yumin., and Zhang, Yue. (2009). Effects of Ligustrazine on the Expression of Smad7 and SnoN Protein in Renal Interstitial Fibrosis Model Rats. *China J. Chin. Materia Med.* 34 (01), 84–88. doi:10.3321/j.issn:1001-5302.2009.01.022

Makris, K., and Spanou, L. (2016). Acute Kidney Injury: Definition, Pathophysiology and Clinical Phenotypes. *Clin. Biochem. Rev.* 37 (2), 85–98.

McWilliam, S. J., Wright, R. D., Welsh, G. I., Tuffin, J., Budge, K. L., Swan, L., et al. (2021). The Complex Interplay between Kidney Injury and Inflammation. *Clin. Kidney J.* 14 (3), 780–788. doi:10.1093/ckj/sfaa164

Mehta, R. L., Cerdá, J., Burdmann, E. A., Tonelli, M., García-García, G., Jha, V., et al. (2015). International Society of Nephrology's 0by25 Initiative for Acute Kidney Injury (Zero Preventable Deaths by 2025): a Human Rights Case for Nephrology. *Lancet* 385 (9987), 2616–2643. doi:10.1016/S0140-6736(15)60126-X

Meng, X. M., Nikolic-Paterson, D. J., and Lan, H. Y. (2016). TGF-β: the Master Regulator of Fibrosis. *Nat. Rev. Nephrol.* 12 (6), 325–338. doi:10.1038/nrneph.2016.48

Michel, H. E., and Menze, E. T. (2019). Tetramethylpyrazine Guards against Cisplatin-Induced Nephrotoxicity in Rats through Inhibiting HMGB1/TLR4/NF-Kb and Activating Nrf2 and PPAR-γ Signaling Pathways. *Eur. J. Pharmacol.* 857, 172422. doi:10.1016/j.ejphar.2019.172422

Molema, G., Zijlstra, J. G., van Meurs, M., and Kamps, J. A. A. M. (2021). Renal Microvascular Endothelial Cell Responses in Sepsis-Induced Acute Kidney Injury. *Nat. Rev. Nephrol.* doi:10.1038/s41581-021-00489-1

Nezu, M., Souma, T., Yu, L., Suzuki, T., Saigusa, D., Ito, S., et al. (2017). Transcription Factor Nrf2 Hyperactivation in Early-phase Renal Ischemia-Reperfusion Injury Prevents Tubular Damage Progression. *Kidney Int.* 91 (2), 387–401. doi:10.1016/j.kint.2016.08.023

Nielsen, P. M., Laustsen, C., Bertelsen, L. B., Qi, H., Mikkelsen, E., Kristensen, M. L., et al. (2017). *In Situ* lactate Dehydrogenase Activity: a Novel Renal Cortical Imaging Biomarker of Tubular Injury? *Am. J. Physiol. Ren. Physiol* 312 (3), F465–F473. doi:10.1152/ajprenal.00561.2015

Noel, S., Arend, L. J., Bandapalle, S., Reddy, S. P., and Rabb, H. (2016). Kidney Epithelium Specific Deletion of Kelch-like ECH-Associated Protein 1 (Keap1) Causes Hydronephrosis in Mice. *BMC Nephrol.* 17 (1), 110. doi:10.1186/s12882-016-0310-y

Norgren, S., and Gong, X. Z. (2018). Contrast-induced Nephropathy-Time for Western Medicine and Chinese Medicine to Team up. *Chin. J. Integr. Med.* 24 (1), 3–5. doi:10.1007/s11655-017-2905-y

Pan, J., Zhang, L., Xiong, D., Li, B., and Qu, H. (2021). A HPLC-DAD-MS/MS Method for Simultaneous Determination of Six Active Ingredients of Salviae Miltiorrhizae and Ligustrazine Hydrochloride Injection in Rat Plasma and its Application to Pharmacokinetic Studies. *Curr. Drug Metab.* 22 (1), 60–69. doi:10.2174/1389200221999200819143230

Peerapornratana, S., Manrique-Caballero, C. L., Gómez, H., and Kellum, J. A. (2019). Acute Kidney Injury from Sepsis: Current Concepts, Epidemiology, Pathophysiology, Prevention and Treatment. *Kidney Int.* 96 (5), 1083–1099. doi:10.1016/j.kint.2019.05.026

Privratsky, J. R., Zhang, J., Lu, X., Rudemiller, N., Wei, Q., Yu, Y. R., et al. (2018). Interleukin 1 Receptor (IL-1R1) Activation Exacerbates Toxin-Induced Acute Kidney Injury. *Am. J. Physiol. Ren. Physiol* 315 (3), F682–F691. doi:10.1152/ajprenal.00104.2018

Rabb, H., Griffin, M. D., McKay, D. B., Swaminathan, S., Pickkers, P., Rosner, M. H., et al. (2016). Inflammation in AKI: Current Understanding, Key Questions, and Knowledge Gaps. *J. Am. Soc. Nephrol.* 27 (2), 371–379. doi:10.1681/ASN.2015030261

Ramesh, G., and Reeves, W. B. (2004). Inflammatory Cytokines in Acute Renal Failure. *Kidney Int. Suppl.* Suppl (91), S56–S61. doi:10.1111/j.1523-1755.2004.09109.x

Reichard, J. F., Sartor, M. A., and Puga, A. (2016). BACH1 Is a Specific Repressor of HMOX1 that Is Inactivated by Arsenite. *J. Biol. Chem.* 283 (33), 22363–22370. doi:10.1074/jbc.M801784200

Ronco, C., Bellomo, R., and Kellum, J. A. (2019). Acute Kidney Injury. *Lancet* 394 (10212), 1949–1964. doi:10.1016/S0140-6736(19)32563-2

Saito, H. (2013). Toxico-pharmacological Perspective of the Nrf2-Keap1 Defense System against Oxidative Stress in Kidney Diseases. *Biochem. Pharmacol.* 85 (7), 865–872. doi:10.1016/j.bcp.2013.01.006

Sancho-Martínez, S. M., López-Novoa, J. M., and López-Hernández, F. J. (2015). Pathophysiological Role of Different Tubular Epithelial Cell Death Modes in Acute Kidney Injury. *Clin. Kidney J.* 8 (5), 548–559. doi:10.1093/ckj/sfv069

Scherz-Shouval, R., and Elazar, Z. (2007). ROS, Mitochondria and the Regulation of Autophagy. *Trends Cel Biol* 17 (9), 422–427. doi:10.1016/j.tcb.2007.07.009

See, E. J., See, K., Glassford, N., Bailey, M., Johnson, D. W., Polkinghorne, K. R., et al. (2019). Long-term Risk of Adverse Outcomes after Acute Kidney Injury: a Systematic Review and Meta-Analysis of Cohort Studies Using Consensus Definitions of Exposure. *Kidney Int.* 95 (1), 160–172. doi:10.1016/j.kint.2018.08.036

Shen, J., Wang, L., Jiang, N., Mou, S., Zhang, M., Gu, L., et al. (2016). NLRP3 Inflammasome Mediates Contrast media-induced Acute Kidney Injury by Regulating Cell Apoptosis. *Sci. Rep.* 6, 34682. doi:10.1038/srep34682

Shi, J., Gao, W., and Shao, F. (2017). Pyroptosis: Gasdermin-Mediated Programmed Necrotic Cell Death. *Trends Biochem. Sci.* 42 (4), 245–254. doi:10.1016/j.tibs.2016.10.004

Sies, H., Berndt, C., and Jones, D. P. (2017). Oxidative Stress. *Annu. Rev. Biochem.* 86, 715–748. doi:10.1146/annurev-biochem-061516-045037

Sies, H. (1997). Oxidative Stress: Oxidants and Antioxidants. *Exp. Physiol.* 82 (2), 291–295. doi:10.1113/expphysiol.1997.sp004024

Simonetto, D. A., Gines, P., and Kamath, P. S. (2020). Hepatorenal Syndrome: Pathophysiology, Diagnosis, and Management. *BMJ* 370, m2687. doi:10.1136/bmj.m2687

Singh, R., Letai, A., and Sarosiek, K. (2019). Regulation of Apoptosis in Health and Disease: the Balancing Act of BCL-2 Family Proteins. *Nat. Rev. Mol. Cel Biol* 20 (3), 175–193. doi:10.1038/s41580-018-0089-8

Sue, Y. M., Cheng, C. F., Chang, C. C., Chou, Y., Chen, C. H., and Juan, S. H. (2009). Antioxidation and Anti-inflammation by Haem Oxygenase-1 Contribute to protection by Tetramethylpyrazine against Gentamicin-Induced Apoptosis in Murine Renal Tubular Cells. *Nephrol. Dial. Transpl.* 24 (3), 769–777. doi:10.1093/ndt/gfn545

Suen, D. F., Norris, K. L., and Youle, R. J. (2008). Mitochondrial Dynamics and Apoptosis. *Genes Dev.* 22 (12), 1577–1590. doi:10.1101/gad.1658508

Sun, L., Li, Y., Shi, J., Wang, X., and Wang, X. (2002). Protective Effects of Ligustrazine on Ischemia-Reperfusion Injury in Rat Kidneys. *Microsurgery* 22 (8), 343–346. doi:10.1002/micr.10058

Sun, W., Li, A., Wang, Z., Sun, X., Dong, M., Qi, F., et al. (2020). Tetramethylpyrazine Alleviates Acute Kidney Injury by Inhibiting NLRP3/HIF-1α and A-poptosis. *Mol. Med. Rep.* 22 (4), 2655–2664. doi:10.3892/mmr.2020.11378

Sureshbabu, A., Ryter, S. W., and Choi, M. E. (2015). Oxidative Stress and Autophagy: Crucial Modulators of Kidney Injury. *Redox Biol.* 4, 208–214. doi:10.1016/j.redox.2015.01.001

Susantitaphong, P., Cruz, D. N., Cerda, J., Abulfaraj, M., Alqahtani, F., Koulouridis, I., et al. (2013). World Incidence of AKI: a Meta-Analysis. *Clin. J. Am. Soc. Nephrol.* 8 (9), 1482–1493. doi:10.2215/cjn.00710113

Suzuki, T., and Yamamoto, M. (2015). Molecular Basis of the Keap1-Nrf2 System. *Free Radic. Biol. Med.* 88 (Pt B), 93–100. doi:10.1016/j.freeradbiomed.2015.06.006

Tan, R. J., Chartoumpekis, D. V., Rush, B. M., Zhou, D., Fu, H., Kensler, T. W., et al. (2016). Keap1 Hypomorphism Protects against Ischemic and Obstructive Kidney Disease. *Sci. Rep.* 6, 36185. doi:10.1038/srep36185

Tracz, M. J., Juncos, J. P., Croatt, A. J., Ackerman, A. W., Grande, J. P., Knutson, K. L., et al. (2007). Deficiency of Heme Oxygenase-1 Impairs Renal Hemodynamics and Exaggerates Systemic Inflammatory Responses to Renal Ischemia. *Kidney Int.* 72 (9), 1073–1080. doi:10.1038/sj.ki.5002471

Tucker, P. S., Scanlan, A. T., and Dalbo, V. J. (20152015). Chronic Kidney Disease Influences Multiple Systems: Describing the Relationship between Oxidative Stress, Inflammation, Kidney Damage, and Concomitant Disease. *Oxid Med. Cel Longev* 2015, 806358. doi:10.1155/2015/806358

Vernon, M. A., Mylonas, K. J., and Hughes, J. (2010). Macrophages and Renal Fibrosis. *Semin. Nephrol.* 30 (3), 302–317. doi:10.1016/j.semnephrol.2010.03.004

Wang, B., Ni, Q., Wang, X., and Lin, L. (2012). Meta-analysis of the Clinical Effect of Ligustrazine on Diabetic Nephropathy. *Am. J. Chin. Med.* 40 (1), 25–37. doi:10.1142/S0192415X12500036

Wang, H., Zhang, J., and Huang, J. (2006). The Effect of Aristolochic Acid on Rat Renal Function and Histopathology and the Intervention of Ligustrazine and Benazepril. *Chin. J. Integrated Traditional Chin. West. Med. Nephropathy* (06), 328–331+374. doi:10.3969/j.issn.1009-587X.2006.06.006

Wang, J., Hong, G., Li, G., Wang, W., and Liu, T. (2019). Novel Homo-Bivalent and Polyvalent Compounds Based on Ligustrazine and Heterocyclic Ring as Anticancer Agents. *Molecules* 24 (24), 4505. doi:10.3390/molecules24244505

Wu, H., and Huang, J. (2018). Drug-Induced Nephrotoxicity: Pathogenic Mechanisms, Biomarkers and Prevention Strategies. *Curr. Drug Metab.* 19 (7), 559–567. doi:10.2174/1389200218666171108154419

Wu, X. J., Sun, X. H., Wang, S. W., Chen, J. L., Bi, Y. H., and Jiang, D. X. (2018). Mifepristone Alleviates Cerebral Ischemia-Reperfusion Injury in Rats by Stimulating PPAR γ. *Eur. Rev. Med. Pharmacol. Sci.* 22 (17), 5688–5696. doi:10.26355/eurrev_201809_15836

Xue, Y., Enosi Tuipulotu, D., Tan, W. H., Kay, C., and Man, S. M. (2019). Emerging Activators and Regulators of Inflammasomes and Pyroptosis. *Trends Immunol.* 40 (11), 1035–1052. doi:10.1016/j.it.2019.09.005

Yang, Y., Song, M., Liu, Y., Liu, H., Sun, L., Peng, Y., et al. (2016). Renoprotective Approaches and Strategies in Acute Kidney Injury. *Pharmacol. Ther.* 163, 58–73. doi:10.1016/j.pharmthera.2016.03.015

Yatim, K. M., and Oberbarnscheidt, M. H. (2015). Endotoxin and AKI: Macrophages Protect after Preconditioning. *J. Am. Soc. Nephrol.* 26 (6), 1231–1232. doi:10.1681/ASN.2014101042

Ying, J., Wu, J., Zhang, Y., Han, Y., Qian, X., Yang, Q., et al. (2020). Ligustrazine Suppresses Renal NMDAR1 and Caspase-3 Expressions in a Mouse Model of Sepsis-Associated Acute Kidney Injury. *Mol. Cel Biochem* 464 (1-2), 73–81. doi:10.1007/s11010-019-03650-4

Youle, R. J., and Narendra, D. P. (2011). Mechanisms of Mitophagy. *Nat. Rev. Mol. Cel Biol* 12 (1), 9–14. doi:10.1038/nrm3028

Youle, R. J., and Strasser, A. (2008). The BCL-2 Protein Family: Opposing Activities that Mediate Cell Death. *Nat. Rev. Mol. Cel Biol* 9 (1), 47–59. doi:10.1038/nrm2308

Yuan, X. P., Liu, L. S., Fu, Q., and Wang, C. X. (2012). Effects of Ligustrazine on Ureteral Obstruction-Induced Renal Tubulointerstitial Fibrosis. *Phytother Res.* 26 (5), 697–703. doi:10.1002/ptr.3630

Zhang, H., Bosch-Marce, M., Shimoda, L. A., Tan, Y. S., Baek, J. H., Wesley, J. B., et al. (2008). Mitochondrial Autophagy Is an HIF-1-dependent Adaptive Metabolic Response to Hypoxia. *J. Biol. Chem.* 283 (16), 10892–10903. doi:10.1074/jbc.M800102200

Zhang, J. X., Dang, S. C., Qu, J. G., and Wang, X. Q. (2006). Ligustrazine Alleviates Acute Renal Injury in a Rat Model of Acute Necrotizing Pancreatitis. *World J. Gastroenterol.* 12 (47), 7705–7709. doi:10.3748/wjg.v12.i47.7705

Zhao, Y., Liu, Y., and Chen, K. (20162016). Mechanisms and Clinical Application of Tetramethylpyrazine (An Interesting Natural Compound Isolated from Ligusticum Wallichii): Current Status and Perspective. *Oxid Med. Cel Longev* 2016, 2124638. doi:10.1155/2016/2124638

Zou, J., Gao, P., Hao, X., Xu, H., Zhan, P., and Liu, X. (2018). Recent Progress in the Structural Modification and Pharmacological Activities of Ligustrazine Derivatives. *Eur. J. Med. Chem.* 147 (147), 150–162. doi:10.1016/j.ejmech.2018.01.097

Conflict of Interest: The authors declare that the research was conducted in the absence of any commercial or financial relationships that could be construed as a potential conflict of interest.

Publisher's Note: All claims expressed in this article are solely those of the authors and do not necessarily represent those of their affiliated organizations, or those of the publisher, the editors and the reviewers. Any product that may be evaluated in this article, or claim that may be made by its manufacturer, is not guaranteed or endorsed by the publisher.

GLOSSARY

ALP alkaline phosphatase
ANP acute necrotizing pancreatitis
ARS2 Arsenic response protein 2
BUN blood urea nitrogen
CBS cystathionine-beta-synthase
CIN contrast-induced nephropathy
COX-2 cyclooxygenase-2
ET-1 endothelin-1
FoxO1 Fork-head box O1 transcriptional factor
GR glutathione reductase
GSH glutathione
GSSG glutathione disulfide
GST Glutathione-S-transferase
HAX-1 HS-1-associated protein
HMGB1 high mobility group box 1
HIF-1 hypoxia inducible factor-1α
HO-1 Heme oxygenase-1
ICAM-1 intercellular cell adhesion molecule-1
IL interleukin
I/R Ischemia-reperfusion
kim-1 kidney injury molecule-1
LDH lactate dehydrogenase
LPO lipid peroxidation
MAPK Mitogen-activated protein kinase
MATs methionine adenosyltransferases
MCP-1 monocyte chemoattractant protein
MDA malondialdehyde
MICA major histocompatability complex class I chain-related antigen A
NAG N-acetyl-b-D-glucosaminidase
NF-κB Nuclear factor-κB
NLRP3 nucleotide-oligomerization domain-like receptor 3
NMDARs N-methyl-d-aspartate receptors
NO Nitric oxide
NOD2 Nucleotide-binding oligomerization domain-containing 2
NOS nitric oxide synthase
NQO1 NAD (P) H: quinone oxidoreductase 1
Nrf2 Nuclear factor erythroid derived-2
OGD oxygen-glucose deprivation
PGI2 prostaglandin I2
PPAR-γ peroxisome proliferator-activated receptor-gamma
ROS reactive oxygen species
SAM S-adenosylmethionine
SOD superoxide dismutase
SrCr serum creatinine
TBSA total body surface area
TLR4 toll-like receptor 4
TNF-α tumor necrosis factor
TOX total antioxidant activity
TXA2 thromboxane A2
4-HNE 4-hydroxynonenal

frontiers in Pharmacology

ORIGINAL RESEARCH
published: 27 January 2022
doi: 10.3389/fphar.2021.792139

Natural Flavonoid Pectolinarigenin Alleviated Hyperuricemic Nephropathy via Suppressing TGFβ/SMAD3 and JAK2/STAT3 Signaling Pathways

Qian Ren[1†], *Bo Wang*[1†], *Fan Guo*[1], *Rongshuang Huang*[1], *Zhouke Tan*[1,2*], *Liang Ma*[1*] and *Ping Fu*[1]

[1]Kidney Research Institute, National Clinical Research Center for Geriatrics and Division of Nephrology, West China Hospital of Sichuan University, Chengdu, China, [2]Division of Nephrology, ZunYi Medical University Affiliated Hospital, ZunYi, China

OPEN ACCESS

Edited by:
Zhiyong Guo,
Second Military Medical University, China

Reviewed by:
Haiyong Chen,
The University of Hong Kong, Hong Kong SAR, China
Zhangzhe Peng,
Central South University, China
Chongxiang Xiong,
Third Affiliated Hospital of Guangzhou Medical University, China

***Correspondence:**
Zhouke Tan
zhouke_tan@163.com
Liang Ma
liang_m@scu.edu.cn

[†]These authors have contributed equally to this work

Specialty section:
This article was submitted to Renal Pharmacology, a section of the journal Frontiers in Pharmacology

Received: 09 October 2021
Accepted: 30 November 2021
Published: 27 January 2022

Citation:
Ren Q, Wang B, Guo F, Huang R, Tan Z, Ma L and Fu P (2022) Natural Flavonoid Pectolinarigenin Alleviated Hyperuricemic Nephropathy via Suppressing TGFβ/SMAD3 and JAK2/STAT3 Signaling Pathways. Front. Pharmacol. 12:792139. doi: 10.3389/fphar.2021.792139

Natural flavonoid pectolinarigenin (PEC) was reported to alleviate tubulointerstitial fibrosis of unilateral ureteral obstruction (UUO) mice in our previous study. To further investigate nephroprotective effects of PEC in hyperuricemic nephropathy (HN), adenine and potassium oxonate induced HN mice and uric acid-treated mouse kidney epithelial (TCMK-1) cells were employed in the study. As a result, PEC significantly lowered serum uric acid level and restored hyperuricemia-related kidney injury in HN mice. Meanwhile, PEC alleviated inflammation, fibrosis, and reduced adipokine FABP4 content in the kidneys of HN mice and uric acid-treated TCMK-1 cells. Mechanistically, PEC inhibited the TGF-β1 expression as well as the phosphorylation of transcription factor SMAD3 and STAT3 to regulate the corresponding inflammatory and fibrotic gene expression in kidney tissues. In conclusion, our results suggested that PEC could inhibit the activation of SMAD3 and STAT3 signaling to suppress inflammation and fibrosis, and thereby alleviate HN in mice.

Keywords: hyperuricemic nephropathy, pectolinarigenin, renal fibrosis, inflammation, fatty acid-binding protein 4

INTRODUCTION

Hyperuricemia (HUA) is a metabolic disease characterized by elevated uric acid (UA) in blood, the prevalence of which has increased worldwide substantially in recent years (Dehlin et al., 2020; Dalbeth et al., 2021). Studies showed that HUA was highly associated with diabetes, hypertension, cardiovascular diseases, and chronic kidney diseases (CKD) (Pascart and Lioté, 2019). As serum UA is mainly secreted by the renal proximal tubules, HUA is a frequent finding in person with CKD due to decreased UA clearance (Johnson et al., 2013). In return, recent evidence suggested that HUA independently predicted the development and progression of CKD (Landa, 2018; Balakumar et al., 2020).

HUA-induced kidney injury, known as hyperuricemic nephropathy (HN), is featured by urate deposition, arteriolosclerosis, glomerular hypertension, and tubulointerstitial fibrosis and would eventually progress into end-stage renal diseases (ESRD) (Liu et al., 2015). The mechanism of HN is complex with many factors such as crystalline effect, oxidative stress, rennin-angiotensin system activation, and tubular epithelial cell transition having been postulated. Though controversial,

accumulating data suggested that the UA-lowering treatments could slower the progression of CKD (Liu et al., 2021; Yanai et al., 2021). Current first-line urate-lowering drugs are mainly xanthine oxidase (XO) inhibitors and uricosuric agents, both of which have limited application in clinics because of their low selectivity or toxic reaction (Balakumar et al., 2020). Hence, it is imperative to develop a new therapeutic agent for HN.

Flavonoid pectolinarigenin (PEC), a plant secondary metabolite that has various biological effects, is one of the major compounds in *Cirsium setidens* (Lee et al., 2017). Studies reported that pectolinarigenin conducted antimicrobial, antioxidant, anti-inflammatory, and antidiabetic activities (Cheriet et al., 2020). Meanwhile, PEC was found to suppress lipopolysaccharide-induced inflammation via NF-κB and MAPK pathways (Heimfarth et al., 2021). In addition, PEC derivatives exhibited selective activity against tumor cells, exhibiting anti-carcinogenic activity (Deng et al., 2020). In our previous study, PEC treatment exerted an anti-fibrotic effect in a mouse model of unilateral ureteral obstruction (UUO). However, the effect of PEC on HN remains unknown. The current study aimed to evaluate whether PEC could be a candidate for HN treatment and explore possible mechanisms.

MATERIALS AND METHODS

Chemicals and Materials

Pectolinarigenin (PEC) was obtained from Chengdu Chroma-Biotechnology Co., Ltd. (purity ≥99.0%). Antibodies against GAPDH, α-tubulin, fatty acid-binding protein (FABP4), IL-6, alpha-smooth muscle actin (α-SMA), janus kinase 2 (JAK2), p-JAK2, Smad3 and p-Smad3, and cleaved caspases 3 (C casp 3) were purchased from Hangzhou HuaAn Biotechnology Co., Ltd. (Hangzhou, China). Antibodies against Collagen-1(Col I), Fibronectin (FN), signal transducer and activator of transcription 3 (STAT3), p-STAT3, BAX, and Bcl2 were bought from Abcam (Cambridge, MA, United States). Anti-TNF-α antibody was bought from Affinity Bioscience (Cincinnati, OH, United States).

Animals

The HN model was established in male C57BL/6J mice (8–10 weeks old; 20–25 g) provided by the Animal Laboratory Center of Sichuan University (Chengdu, China). Forty mice were randomly assigned to five groups: Control (n = 8), HN (n = 8), Allopurinol (n = 8), PEC 25 mg/kg (n = 8), PEC 50 mg/kg (n = 8). The HN model was established by feeding mice with a mixture of adenine (0.16 g/kg) and potassium oxonate (2.4 g/kg) every other day for 4 weeks, as previously described (Ren et al., 2021). Allopurinol (10 mg/kg) and PEC (25 and 50 mg/kg) were orally given daily during the experiment along with HN establishment (for 4 weeks). The mice were sacrificed, and the kidneys were collected at the end of study. Ethical approval was granted by the Animal Ethics Committee of West China Hospital of Sichuan University (No. 2020061A).

Histologic Examination

Tissue sections were fixed with 10% phosphate buffered formalin and embedded in paraffin after dehydrating. Kidney slides of 4-μm thickness were subject to PAS staining for morphologic analysis and Masson staining for fibrotic analysis (Ren et al., 2021). Six pictures (×400) per kidney were randomly captured by light microscopy for semiquantitative analysis. The tubular injury score was evaluated on the base of histopathology of injured/damaged renal tubules and was graded from 0 to 4 (0: 0%; 1: <25%; 2: 26–50%; 3: 51–75%; 4: ≥76% of injured/damaged renal tubules) (Liu et al., 2015). The collagen positive area was measured by the ImageJ software.

Western Blotting Analysis

Total proteins were isolated from frozen kidney tissue or mouse kidney epithelial cells (TCMK-1, ATCC® CCL-139™, Beijing bnbio Co., Ltd., Beijing, China) using radio immune precipitation (RIPA) lysis buffer (P0013B, Beyotime Biotechnology, China) and quantified using a Pierce™ BCA Protein Assay Kit (23225, Thermo Scientific, Billerica, MA, United States). Equal amounts of protein lysate were separated on 10–12% SDS-PAGE as previously described (Ren et al., 2021). Immunoblots were visualized by the Immobilon Western Chemiluminescent HRP Substrate (WBKLS0500, Millipore Corporation, Billerica, MA, United States) with Bio-Rad Chemi Doc MP and densitometered by ImageJ 6.0 software (National Institutes of Health, Bethesda, MD, United States).

Immunohistochemistry Staining

Immunohistochemical staining was performed as previously described (Ren et al., 2021). The following primary antibodies were used: anti-α-SMA (1:100, Huabio), anti-STAT3 (1:200, Abcam), anti-p-STAT3 (1:100, Abcam), anti-FABP4 (1:100, Huabio). Images were examined and acquired with an AxioCamHRc digital camera (Carl Zeiss, Jena, Germany).

Quantitative Real-Time PCR Analysis

Total RNA in kidney tissues of mice or TCMK-1 cells was isolated with a total RNA extraction Kit (TP-01121, Foregene, Chengdu, China) according to the manufacturer's instructions. The concentration of mRNA was determined by a Scan Drop 100 (Analytik Jena, Thuringia, Germany) determiner. Quantitative real-time PCR assays were performed on a PCR system (CFX Connect; Bio-Rad, Hercules, CA, United States). The sequences of primers are shown in **Supplementary Table S1**. Statistical analysis was conducted using the comparative $2^{-\Delta\Delta CT}$ method with GAPDH or *β-actin* as the internal standard.

RNA-Seq Transcriptomic Assay

Total RNA was extracted from kidney tissues with Trizol reagent (Invitrogen, Carlsbad, CA, United States). Total RNA quality was assessed using the RNA 6000 Nano LabChip Kit (Agilent, CA, United States) of the Agilent Bioanalyzer 2100 system. The RNA-seq were performed by LC-BIO Bio-tech Ltd. (Hangzhou, China). Differentially expressed genes were defined as those with fold changes ≥1.5 and $p \leq 0.05$. Gene Ontology (GO) functions and Kyoto Encyclopedia of Genes and Genomes (KEGG) pathway enrichment analysis were performed using the OmicStudio tools at https://www.omicstudio.cn/tool.

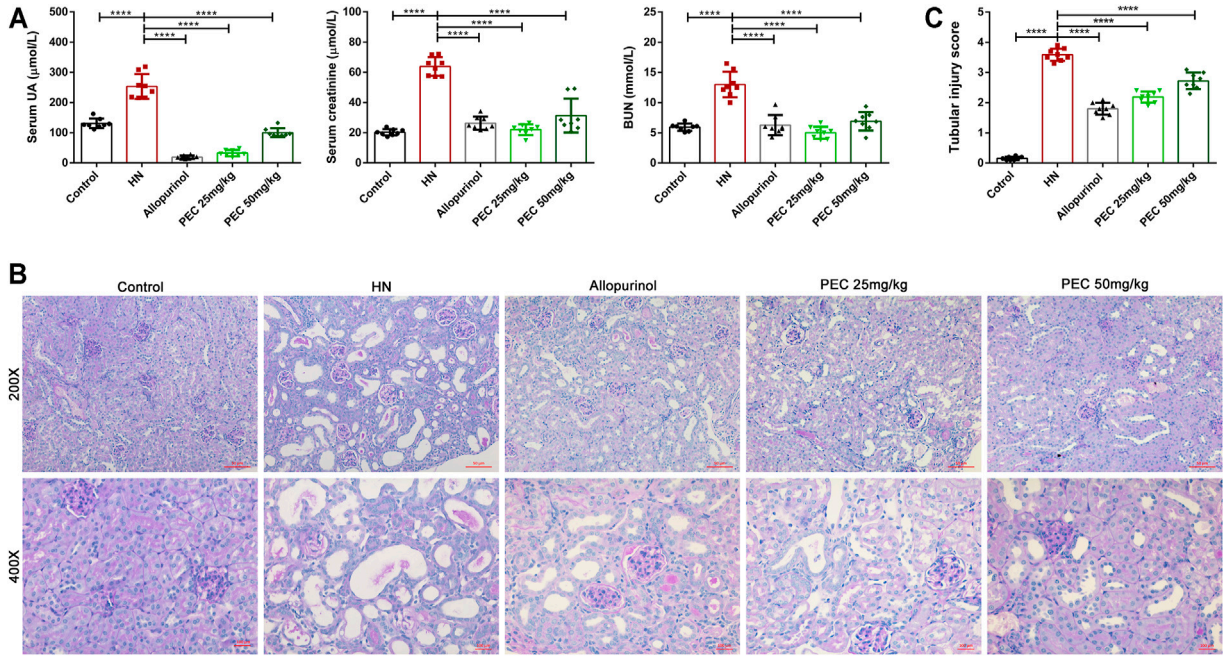

FIGURE 1 | Effects of PEC on serum UA and kidney function in HN mice. **(A)** Biochemical parameters (Serum UA, Serum creatinine, BUN) in mice. **(B)** PAS staining in the kidney. **(C)** Kidney injury score (n = 8). All data are represented as the mean ± SD. $^{**}p < 0.01$, $^{***}p < 0.001$, $^{****}p < 0.0001$.

Cell Culture and Treatment

TCMK-1 cells were cultured in DMEM (Sigma-Aldrich) supplemented with 5% FBS (SH30084.03, Hyclone, Australia) in a humidified atmosphere (5% CO_2, 37°C). After incubating with DMEM containing 0.5% FBS for 24 h, cells were exposed to UA (800 μM) and treated with PEC of various concentrations (25, 50, 100, 150, and 300 μM) for 24 h.

Cell Viability Assay

A Cell Counting Kit-8 assay (CCK-8, Meilunbio, Dalian, China) was employed to assess cytotoxicity. Briefly, TCMK-1 cells were seeded into a 96-well plate at a density of 5,000–10,000 cells/well and incubated with various concentrations of PEC (25, 50, 100, 150, and 300 μM) with or without UA. Cells cultured in DMEM containing the same amount of DMSO were used as control. Twenty-four hours after incubation, the cells were incubated with 10% CCK-8 reagent for 1 hour (37°C, dark). Finally, the absorbance was detected by a microplate reader (Synergy Mx, Biotek, Winooski, VT, United States) at a wavelength of 450 nm.

Statistical Analysis

Results are presented as the mean ± SD. Differences among multiple groups were compared using one-way analysis of variance (ANOVA) and a Tukey-Kramer *post hoc* test. Comparisons between two groups were performed using the two-tailed t test. All statistics were performed using Prism software (ver. 6.01; GraphPad, San Diego, CA, United States) and $p < 0.05$ was considered statistically significant.

RESULTS

Pectolinarigenin Lowered Serum Uric Acid Level, Improved Kidney Function, and Attenuated Renal Morphology in Hyperuricemic Nephropathy Mice

Administration of adenine and potassium oxonate successfully induced HN experimental mice as evidenced by increased serum UA level and aggravated kidney function. According to **Figure 1A**, the serum levels of UA (253.4 ± 14.49 μM vs. 131.0 ± 5.631 μM, $p < 0.05$), blood urea nitrogen (BUN) (13.00 ± 0.7513 mM vs. 5.939 ± 0.2137 mM, $p < 0.05$), and creatinine (63.86 ± 2.183 μM vs. 20.33 ± 0.7468 μM, $p < 0.05$) were significantly higher than those of control mice. After allopurinol and PEC treatment, the serum levels of UA, urea nitrogen, and creatinine were significantly decreased, and PEC at a dose of 25 mg/kg seems more superior in reducing above indexes than PEC with a higher dose (50 mg/kg). Observation of kidney changes in mice by PAS staining also showed that pathological changes in HN mice were alleviated by allopurinol and PEC treatment (**Figure 1B**). However, tubular injury scores of mice in the PEC 25 mg/kg group were similar to those of the PEC 50 mg/kg group, indicating no superiority of low dose PEC in attenuating renal histopathology (**Figure 1C**).

Analysis of Renal Transcriptome in Hyperuricemic Nephropathy Mice

To reveal the mechanism by which PEC improved kidney injury in HN mice, the RNA-seq analysis was applied. The

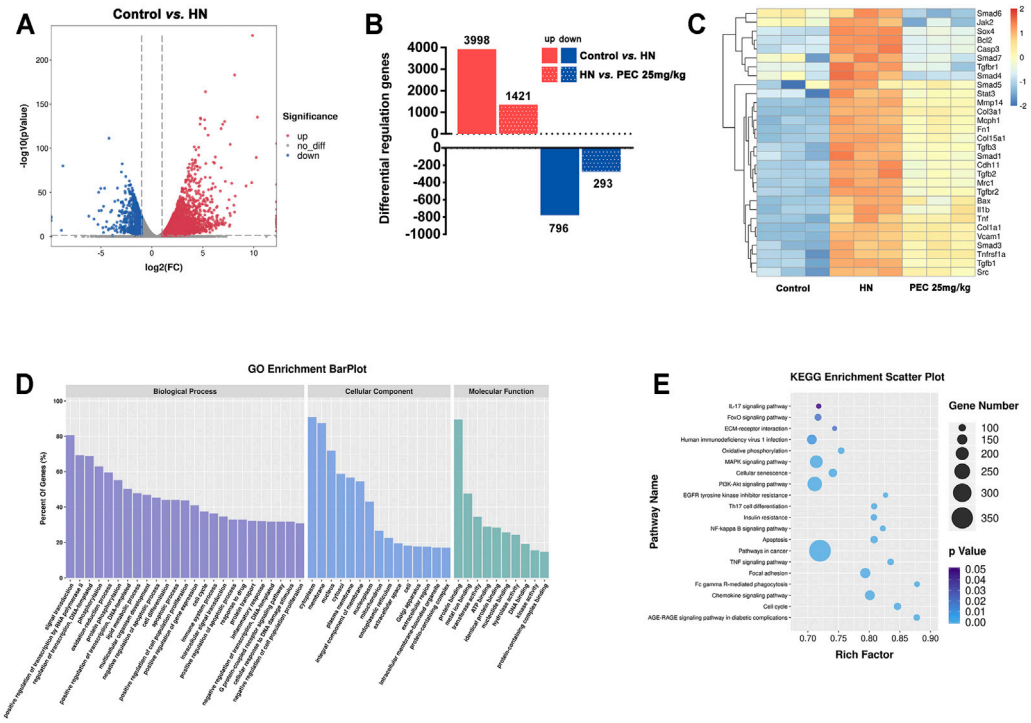

FIGURE 2 | Effects of PEC on gene expression in kidneys of HN mice. **(A)** Volcano plot of gene expression difference between Control and HN groups. **(B)** Differentially regulated genes difference between Control, HN, and PEC 25 mg/kg. **(C)** Heatmap of gene expression difference among Control, HN, and PEC 25 mg/kg. **(D)** GO analysis of differentially expressed genes. **(E)** KEGG analysis of differentially expressed genes.

results of volcano plot showed significantly different gene expression profile between control and HN mice (**Figure 2A**). Among these differentially expressed genes, 796 genes were up-regulated and 1,998 genes were down-regulated in kidneys of HN mice in comparison with control mice ($p < 0.05$). Remarkably, PEC 25 mg/kg significantly reversed the change of 1,421 down-regulated and 293 up-regulated genes ($p < 0.05$) (**Figure 2B**). The significant PEC-modulated genes were illustrated by heatmap in **Figure 2C**, and genes related to apoptosis (Bax), inflammation (il1b, Tnf), and fibrosis (Col-1a1, Fn1) were seen. Further GO and KEGG analysis also suggested that these differentially expressed genes were involved in processes of lipid metabolism, apoptosis, inflammatory response, and fibrogenesis (**Figures 2D,E**).

Pectolinarigenin Ameliorated Apoptosis, Reduced Expression of Proinflammatory Genes, and Improved Fibrosis in Kidneys of Hyperuricemic Nephropathy Mice

Consist with what transcriptome analysis found, the results from our western blot analysis showed that HN-induced kidney expression of apoptotic indicators was alleviated by PEC treatment (**Figures 3A,B**) ($p < 0.05$). In addition, the expression of proinflammatory cytokines (IL-6, TNF-α, MCP-1) was significantly increased in kidneys of HN mice and further decreased by PEC treatment (**Figure 3C**) ($p < 0.05$). Moreover, Masson's staining (blue) revealed a remarkable increase of renal interstitial fibrosis in HN mice, which was ameliorated by PEC (**Figure 4**) ($p < 0.05$). Accordingly, the elevated accumulation of fibrotic markers of α-SMA, Col I, and FN was observed in kidneys of HN mice, and PEC significantly reduced the accumulation of these corresponding genes (**Figure 5**) ($p < 0.05$). The above results illustrated that PEC alleviated renal apoptosis, inflammation, and fibrosis in HN mice.

Pectolinarigenin Downregulated the Expression of FABP4 in the Kidneys of Hyperuricemic Nephropathy Mice

Our early study indicated that the lipid-binding chaperone FABP4 was increased in kidneys of HN mice and played crucial role in HUA-induced renal inflammation and fibrosis (Shi et al., 2020a). In line with our previous findings, the expression of FABP4 in kidneys of HN mice was significantly increased ($p < 0.05$). PEC treatment largely inhibited the expression of FABP4 both in the mRNA and protein level, further demonstrating the role of PEC in HUA-induced inflammation and fibrosis (**Figure 6**) ($p < 0.05$).

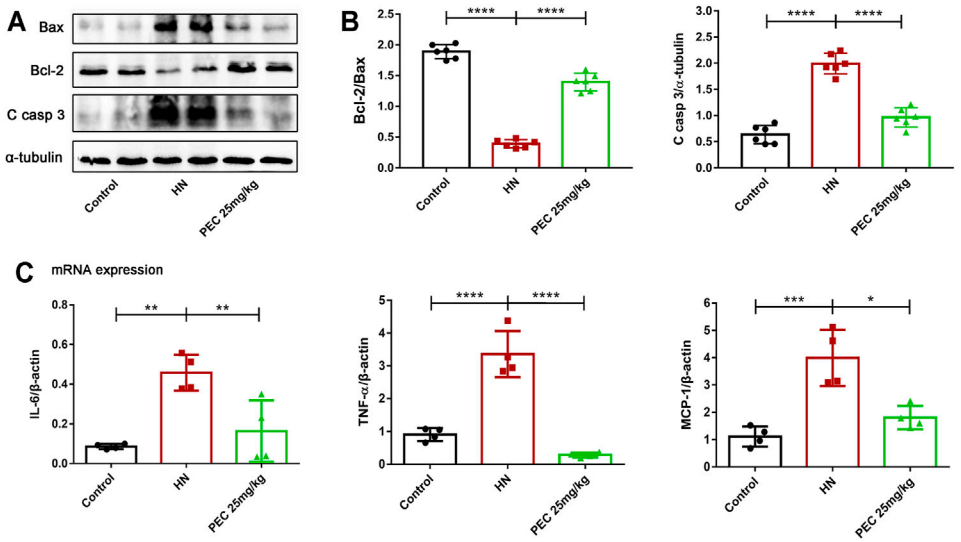

FIGURE 3 | Effects of PEC on kidney apoptosis and inflammation in HN mice. **(A,B)** The Bcl2/Bax, Cleaved caspase 3 (C casp 3) protein levels normalized by β-actin. **(C)** The mRNA expressions of IL-6, TNFα, and MCP-1 measured by real-time PCR analysis. All data are represented as the mean ± SD. $^{*}p < 0.05$, $^{**}p < 0.01$, $^{****}p < 0.0001$.

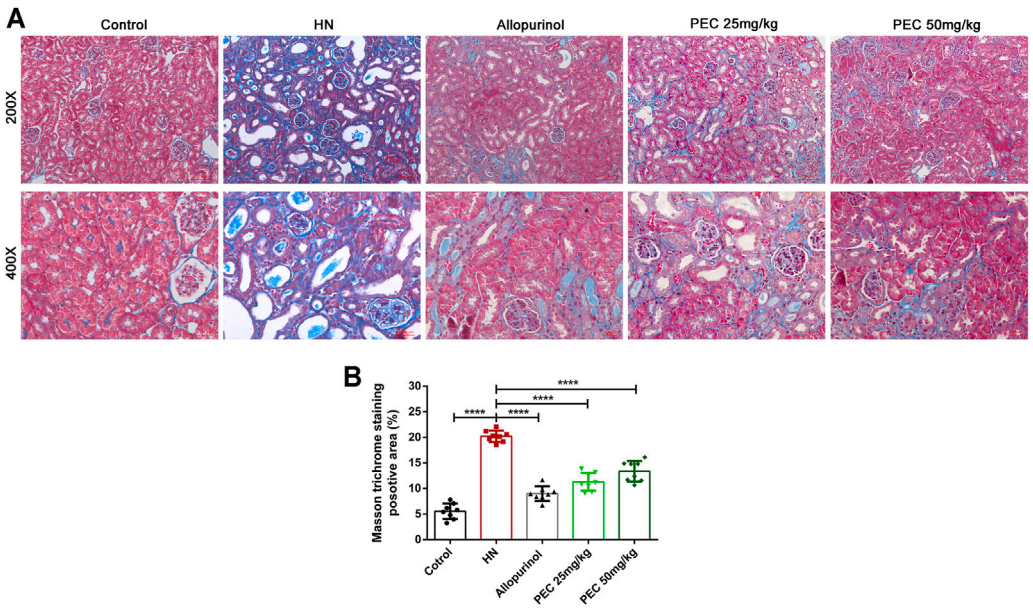

FIGURE 4 | Effects of PEC on kidney fibrosis in HN mice. **(A)** Masson's trichrome staining of mouse kidneys (×200 and ×400). **(B)** Quantitation of positive area in Masson's trichrome staining (n = 8). All data are represented as the mean ± SD. $^{****}p < 0.0001$.

Pectolinarigenin Suppressed the TGF-β/SMAD3 and JAK2/STAT3 Signaling Pathway in the Kidneys of Hyperuricemic Nephropathy Mice

As the most potent fibrogenic factor, TGF-β was considered to contribute to HUA-mediated renal fibrosis via the activation of Smad3 (Liu et al., 2015). To investigate the effect of PEC on the activation of TGF-β/Smad3 signaling in mice of HN, we measured the expression of TGF-β by western blot analysis. It was shown that TGF-β expression was significantly increased in kidneys of HN mice and decreased by PEC treatment (**Figure 7**) ($p < 0.05$). Meanwhile, kidney injury resulted in the phosphorylation of Smad3, which was remarkedly suppressed by PEC (**Figure 7**) ($p < 0.05$). Altogether, these results suggested that PEC could inhibit activation of TGF-β/Smad3 signaling pathway in the kidneys of HN mice.

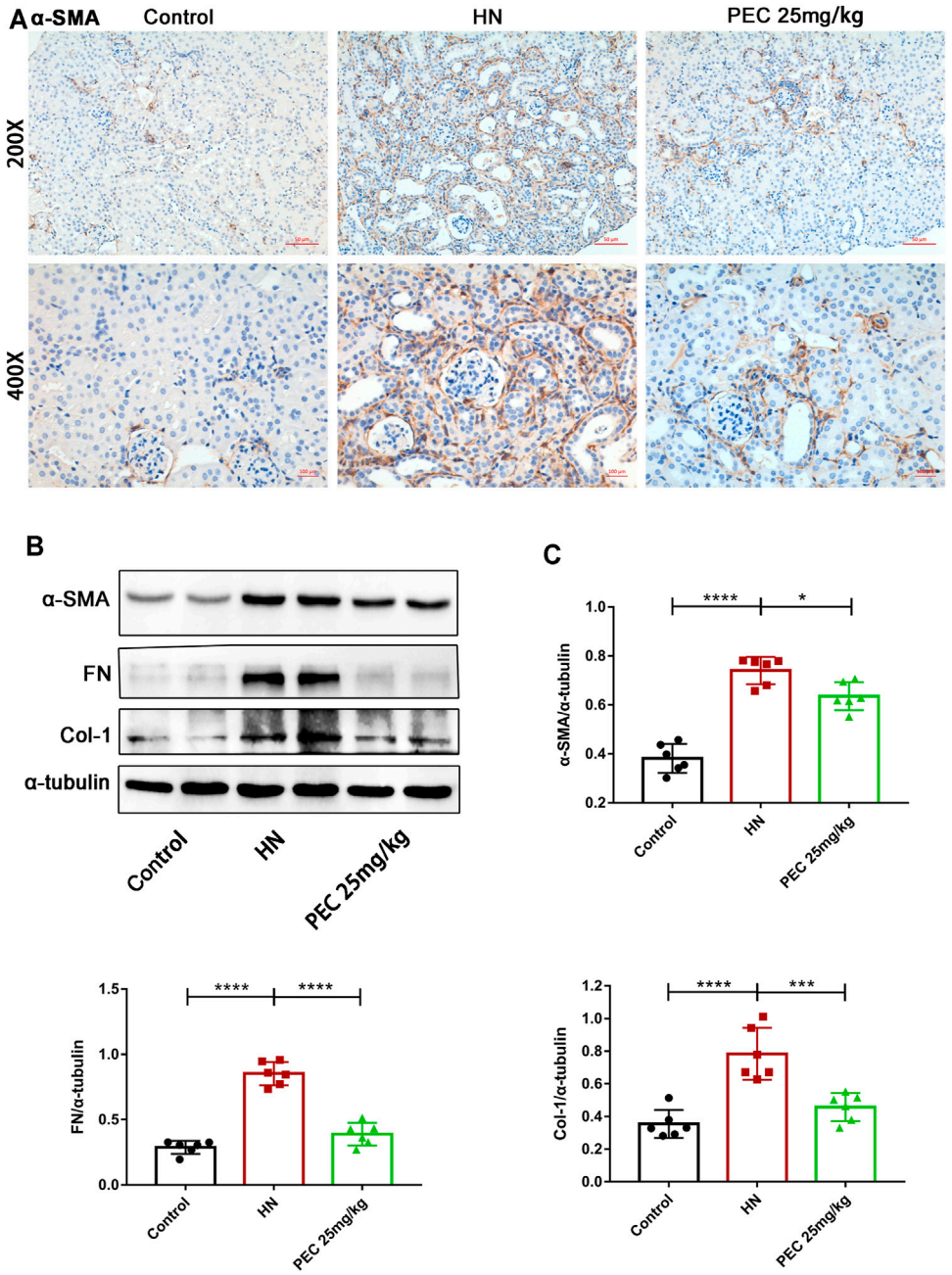

FIGURE 5 | Effects of PEC on kidney fibrotic expression in HN mice. **(A)** Photomicrographs of α-SMA immunostaining in kidneys of mice (×200 and ×400). **(B,C)** The α-SMA, FN, and Col I protein levels normalized by α-tubulin. All data are represented as the mean ± SD. *$p < 0.05$, ***$p < 0.001$, ****$p < 0.0001$.

STAT3 is a cytoplasmic transcription factor that could elicit diverse biological outcomes. Considerable studies have elucidated the role of STAT3 in mediating HUA-induced renal inflammation, apoptosis, and fibrosis (Shi et al., 2020b; Pan et al., 2021). To examine whether PEC could abrogate the activation of STAT3 in HN, the immunochemical staining and western blot analysis was employed to measure the expression of phosphorylated STAT3 (p-STAT3). As shown by **Figure 8**, the phosphorylation level of STAT3 was significantly increased in kidneys of HN mice, which was restored by PEC (**Figure 8**) ($p <$ 0.05). Additionally, immunochemical staining showed that HN-induced p-STAT3 was mainly located in renal tubules (**Figures 8A,B**).

Pectolinarigenin Inhibited Proinflammatory and Fibrotic Expression in Uric Acid-Stimulated TCMK-1 Cells

To further investigate the role of PEC in HN, TCMK-1 cells were treated with soluble UA (800 μM) for 24 h. As shown in

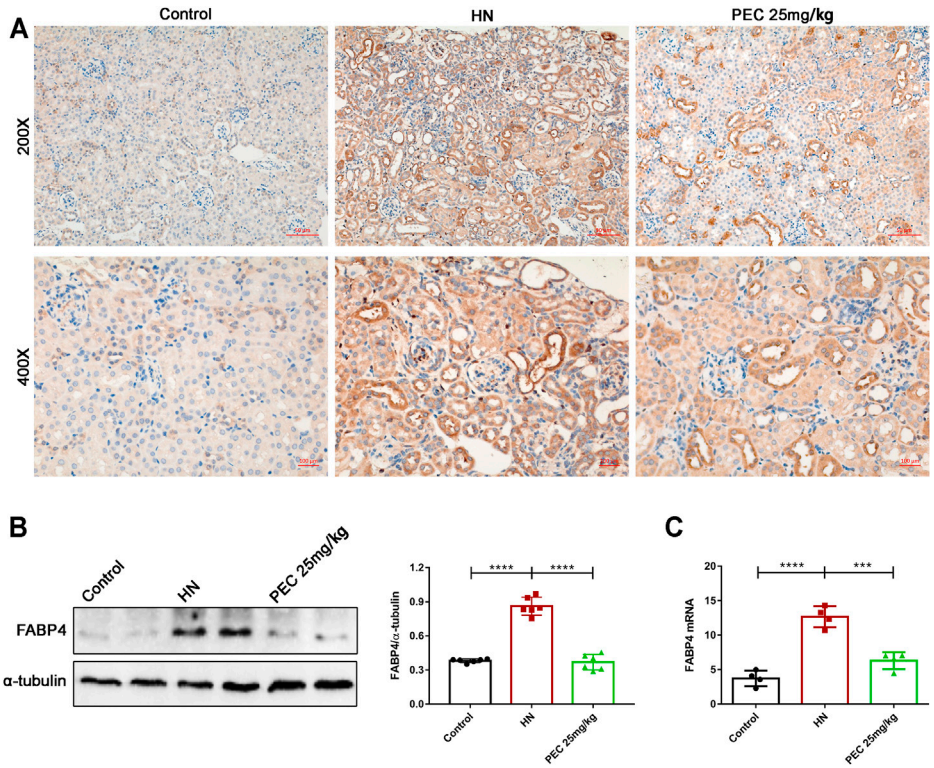

FIGURE 6 | Effects of PEC on FABP4 expression in kidneys of HN mice. **(A)** Photomicrographs of α-SMA immunostaining in kidneys of mice (×200 and ×400). **(B)** The FABP4 protein level normalized by α-tubulin. **(C)** The mRNA expressions of FABP4 measured by real-time PCR analysis. All data are represented as the mean ± SD (n = 3). ***p < 0.001, ****p < 0.0001.

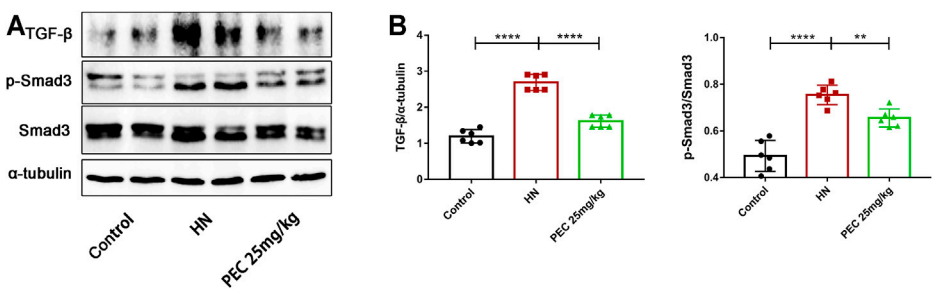

FIGURE 7 | Effects of PEC on the activation of TGF-β/SMAD3 signaling in kidneys of HN mice. **(A,B)** The TGF-β and p-Smad3/Smad3 protein levels normalized by α-tubulin. All data are represented as the mean ± SD (n = 3). **p < 0.01, ****p < 0.0001.

Figure 9A, PEC under 150 μM showed no cytotoxic effect for TCMK-cells and cells treated with PEC at 100 μM showed the highest cell viability. UA stimulation led to increased expression of IL-6, TNF-α, and FABP4 in TCMK-1 cells, and PEC (100 μM) significantly suppressed such expression (**Figures 9B–D**) (p < 0.05). Meanwhile, the fibrotic expression of α-SMA, FN, and Col I in UA-treated TCMK-1 cells was reduced by PEC (100 μM) (**Figures 9B–D**) (p < 0.05), thus confirming the anti-inflammatory and anti-fibrotic effects of PEC *in vitro*.

Pectolinarigenin Hindered TGF-β/SMAD3 and JAK2/STAT3 Activation in Uric Acid-Induced TCMK-1 Cells

After UA treatment, the expression of TGF-β and phosphorylated Smad3 were significantly increased in TCMK-1 cells, indicating that HUA could directly activate the TGF-β/Smad3 signaling pathway (**Figures 10A,B**) (p < 0.05). PEC (100 μM) successfully suppressed the expression of TGF-β and the phosphorylation of Smad3 indued by UA (**Figures 10A,B**) (p < 0.05). Similarly, UA stimulation resulted in the phosphorylation of JAK2 and STAT3,

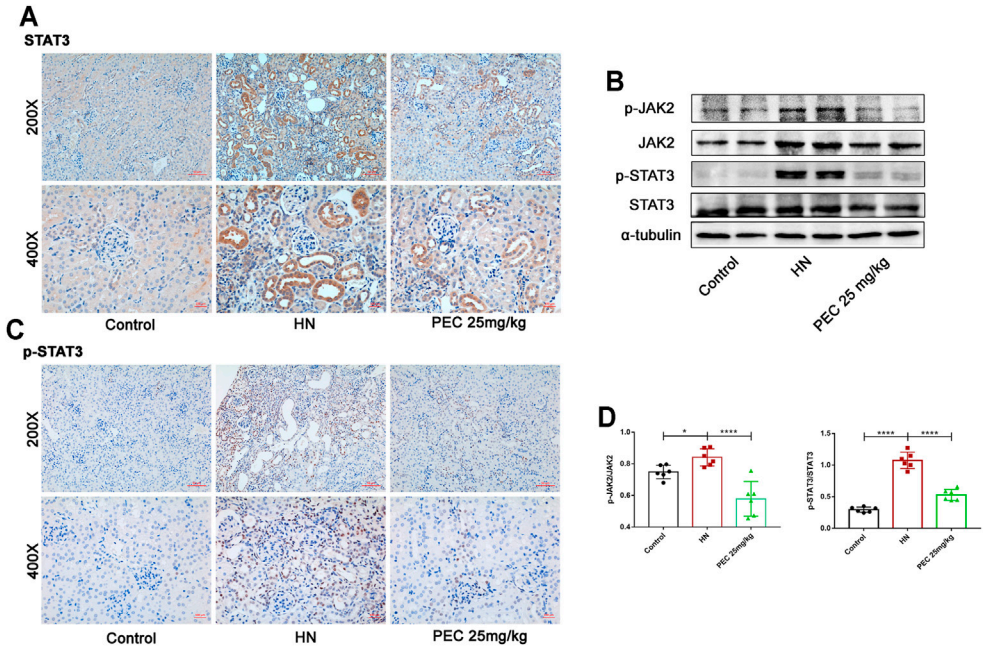

FIGURE 8 | Effects of PEC on the activation of JAK2/STAT3 signaling in kidneys of HN mice. **(A,B)** Photomicrographs of STAT3 and p-STAT3 immunostaining in kidneys of mice (×200 and ×400). **(C,D)** The p-JAK2/JAK2 and p-STAT3/STAT3 protein levels normalized by α-tubulin. All data are represented as the mean ± SD ($n = 3$). *$p < 0.05$, * ****$p < 0.0001$.

which was abrogated by PEC treatment (100 μM) (**Figures 10C,D**) ($p < 0.05$). Hence, consistent with our *in vivo* findings, PEC (100 μM) could inhibit the TGF-β/Smad3 and JAK2/STAT3 activation in UA-treated TCMK-1 cells.

DISCUSSION

Generally, UA is an antioxidant agent in a physiological medium (Dalbeth et al., 2021). Disturbance of the balance between UA production and excretion would lead to HUA that is considered as an independent risk factor for CKD progression (Johnson et al., 2013). Persistently high-serum UA levels was reported to trigger kidney inflammation and fibrosis that might contribute to HN (Lee et al., 2021). Current standard treatment for HUA is UA-lowering drugs represented by XO inhibitors and uricosuric agents, the nephroprotective effect of which remains controversy in CKD patients (Liu et al., 2021). Consequently, novel effective drugs for the prevention and treatment of HN need to be explored.

PEC is a natural flavonoid that showed therapeutic potential for inflammatory diseases, diabetes, and several types of cancers (Cheriet et al., 2020). Meanwhile, PEC could alleviate renal fibrosis in mice undergoing unilateral ureteral obstruction (UUO) (Li et al., 2021). However, the effects and underlying mechanism of PEC against HN remains unclear. In the present study, we noticed that PEC improved both HUA and renal damage in adenine and potassium oxonate-treated mice, as evidenced by reduced serum levels of UA, blood urea nitrogen (BUN), and creatinine and attenuated renal pathological changes. Remarkably, it was noticed that PEC at a dose of 25 mg/kg was more efficient in alleviating above biochemical parameters than PEC at a dose of 50 mg/kg. This might be explained by side effects of increased dosage as cytotoxicity effects of PEC have been reported by early studies (Lee et al., 2018). Moreover, PEC attenuated HUA-induced apoptosis characterized by the imbalance of Bcl-2/Bax and increased expression of cleaved caspase 3, suggesting the nephroprotective effects of PEC in HN.

Accumulation of UA increased the levels of inflammatory cytokines to mediate kidney injury (Li et al., 2016; Xu et al., 2021). In line with this, the elevated expression of IL-6, TNF-α, and MCP-1 were noticed in kidneys of HN mice and UA-stimulated TCMK-1cells, which was inhibited by PEC. The lipid transporter FABP4 is a potential mediator of inflammatory responses that has been suggested to play a crucial role in mediating renal inflammation and fibrosis in HN (Hotamisligil and Bernlohr, 2015; Shi et al., 2020a). Our results showed that PEC suppressed HUA-induced FABP4 expression, further illustrating its anti-inflammatory effects of PEC in HN.

Kidney fibrosis, the ultimate pathological outcome of HN, is characterized by the expression of mesenchymal cell products such as α-SMA, FN, and Col I (Lee et al., 2021). The TGF-β/Smad3 signaling pathway plays a critical role in mediating profibrotic response of renal epithelial cells and activating renal fibroblasts (Liu et al., 2015). TGF-β interacts with its receptors to phosphorylate Smad2/3 and subsequently regulates the transcription of profibrotic genes (Zhang et al., 2018). It was observed that HUA activated the TGF-β/Smad3 signaling pathway in HN mice (Balakumar et al., 2020; Shi et al., 2020b). In this study, we noticed that PEC successfully

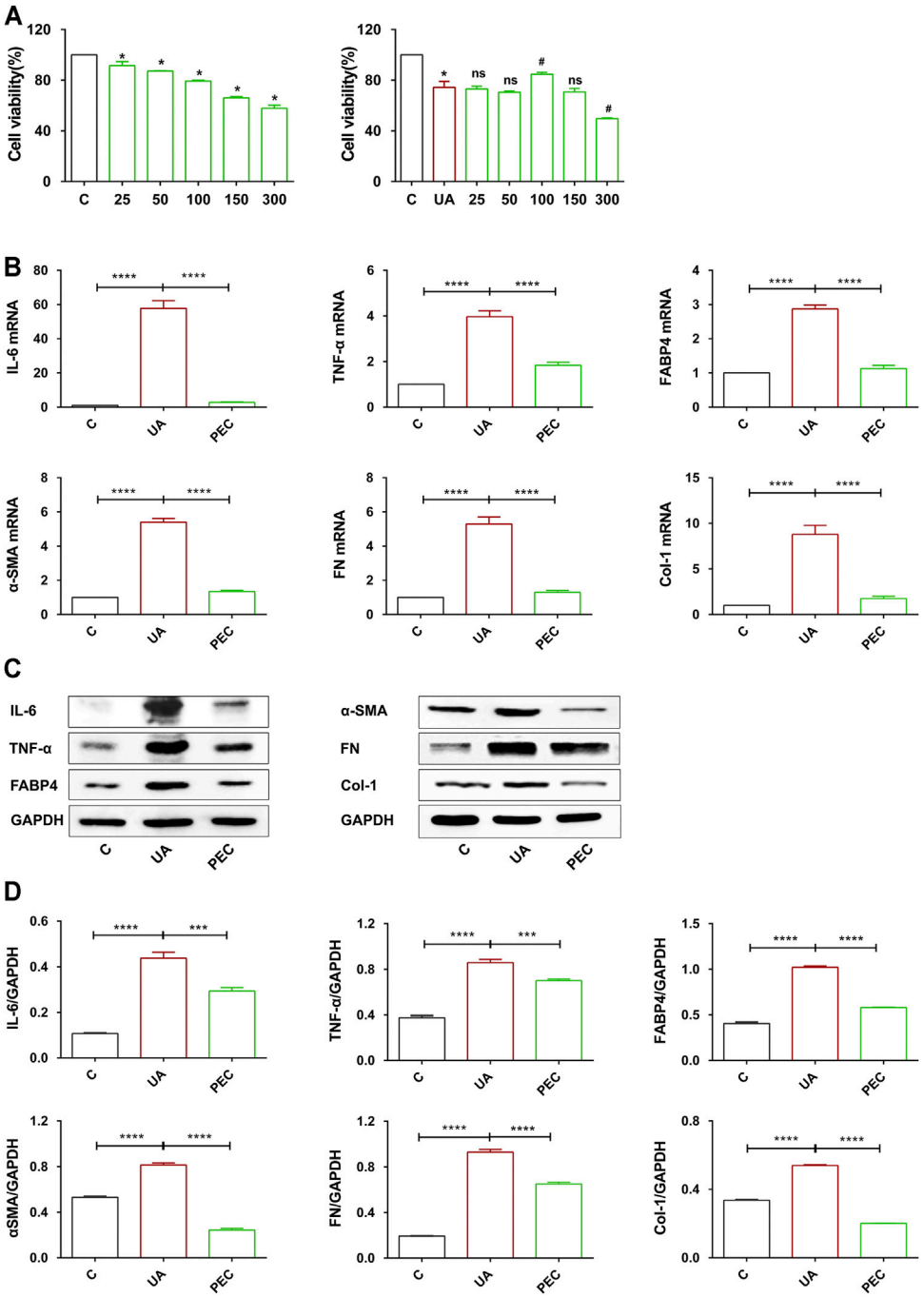

FIGURE 9 | Effects of PEC on the proinflammatory and fibrotic expression in UA-treated TCMK-1 cells. **(A)** Cytotoxicity of PEC-treated TCMK-1cells with or without UA. **(B)** The mRNA expressions of IL-6, TNFα, FABP4, α-SMA, FN, and Col I measured by real-time PCR analysis. **(C,D)** The IL-6, TNFα, FABP4, α-SMA, FN, and Col I protein levels normalized by GAPDH. All data are represented as the mean ± SD (n = 3). *p < 0.05, ***p < 0.001, ****p < 0.0001, #p < 0.05 compared with UA-treated cells, ns means no significance.

diminished HUA-induced TGF-β expression and Smad3 phosphorylation, which is in agreement with our previous finding that PEC blocked TGFβ1-induced SMAD3 phosphorylation in fibroblast (Li et al., 2021). Meanwhile, PEC significantly reduced the expression of α-SMA, FN, and Col I induced by HUA, suggesting that PEC suppressed the TGFβ1/Smad3 signaling pathway to alleviate kidney fibrosis in HN mice.

Considerable studies have implicated that activation of STAT3 via the IL-6/JAK2 cascade mediated inflammation and fibrosis in HN (Ren et al., 2021; Wu et al., 2021). Pharmacological inhibition

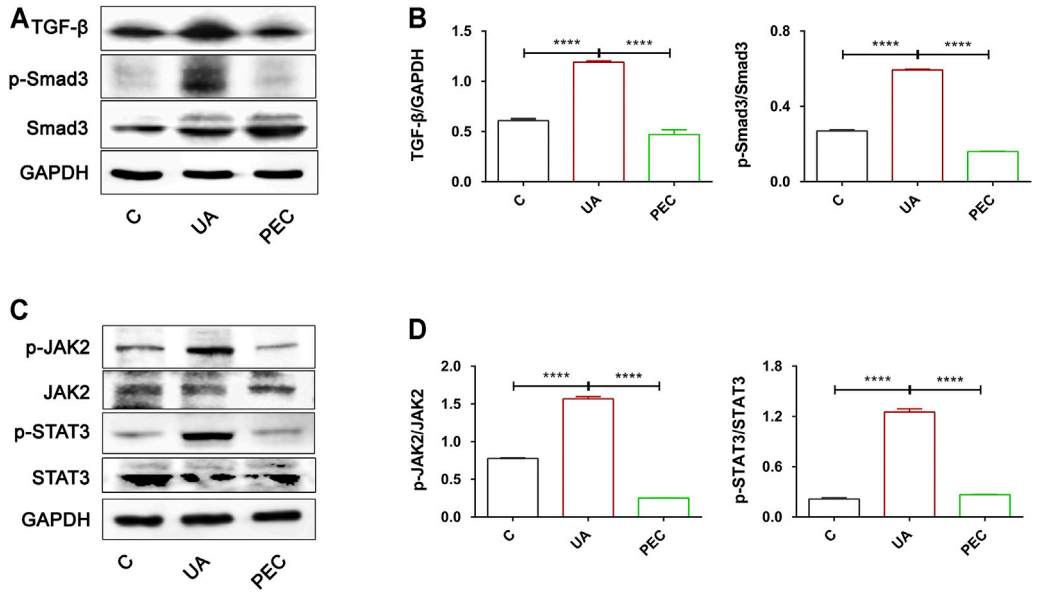

FIGURE 10 | Effects of PEC on the activation of TGF-β/SMAD3 and JAK2/STAT3 signaling pathways in UA-stimulated TCMK-1 cells. **(A,B)** The TGF-β and p-Smad3/Smad3 protein levels normalized by GAPDH. **(C,D)** The p-IAK2/JAK2 and p-STAT3/STAT3 protein levels normalized by α-tubulin. All data are represented as the mean ± SD (n = 3). ****p < 0.0001.

of STAT3 was reported to attenuate kidney injury, slow down fibrosis, and suppress multiple proinflammatory cytokine production in kidneys of HN mice (Pan et al., 2021). Studies have identified PEC as a STAT3 inhibitor to suppress tumor growth and metastasis (Zhang et al., 2016; Gan et al., 2019; Li et al., 2019). Our previous study also indicated that PEC inhibited the activation of STAT3 in kidneys of UUO mice (Li et al., 2021). In the current study, treatment with PEC suppressed the phosphorylation of STAT3 signaling in kidneys of HN mice and UA-induced TCMK-1 cells, which might be the mechanism by which PEC ameliorated kidney inflammation and fibrosis in HN.

In summary, anti-hyperuricemic and nephroprotective effects of PEC were firstly demonstrated in adenine and potassium oxonate-induced HN mice and UA-treated TCMK-1 cells. Our results suggested that PEC attenuated kidney inflammation and fibrosis induced by HUA. Mechanically, we found that the nephroprotective effects of PEC were associated with the inhibition of the Smad3 and STAT3 signaling pathways. Taken together, PEC may be a candidate drug for the treatment of hyperuricemic nephropathy.

DATA AVAILABILITY STATEMENT

The data presented in the study are accessible in the GEO repository, accession number GSE190205. The study can also be seen at: https://www.ncbi.nlm.nih.gov/geo/query/acc.cgi?acc=GSE190205

ETHICS STATEMENT

The animal study was reviewed and approved by the Animal Ethics Committee of West China Hospital of Sichuan University (No. 2020061A).

AUTHOR CONTRIBUTIONS

LM, ZT, and PF designed the study; BW, QR, FG, and RH carried out experiments and analyzed the data; QR and BW made the figures, drafted and revised the paper; all authors approved the final version of the manuscript.

FUNDING

This research was supported by grants from the National Natural Science Foundation of China (82060131), Key Research Program of Sichuan Province (2021YFQ0027), and the Science/Technology Project of Sichuan province (2020YFS0224).

SUPPLEMENTARY MATERIAL

The Supplementary Material for this article can be found online at: https://www.frontiersin.org/articles/10.3389/fphar.2021.792139/full#supplementary-material

REFERENCES

Balakumar, P., Alqahtani, A., Khan, N. A., Mahadevan, N., and Dhanaraj, S. A. (2020). Mechanistic Insights into Hyperuricemia-Associated Renal Abnormalities with Special Emphasis on Epithelial-To-Mesenchymal Transition: Pathologic Implications and Putative Pharmacologic Targets. *Pharmacol. Res.* 161, 105209. doi:10.1016/j.phrs.2020.105209

Cheriet, T., Ben-Bachir, B., Thamri, O., Seghiri, R., and Mancini, I. (2020). Isolation and Biological Properties of the Natural Flavonoids Pectolinarin and Pectolinarigenin-A Review. *Antibiotics* 9, 417. doi:10.3390/antibiotics9070417

Dalbeth, N., Gosling, A. L., Gaffo, A., and Abhishek, A. (2021). Gout. *Lancet* 397, 1843–1855. doi:10.1016/s0140-6736(21)00569-9

Dehlin, M., Jacobsson, L., and Roddy, E. (2020). Global Epidemiology of Gout: Prevalence, Incidence, Treatment Patterns and Risk Factors. *Nat. Rev. Rheumatol.* 16, 380–390. doi:10.1038/s41584-020-0441-1

Deng, Y., Zhang, Q., Li, Y., Wang, L., Yang, S., Chen, X., et al. (2020). Pectolinarigenin Inhibits Cell Viability, Migration and Invasion and Induces Apoptosis via a ROS-Mitochondrial Apoptotic Pathway in Melanoma Cells. *Oncol. Lett.* 20, 116. doi:10.3892/ol.2020.11977

Gan, C., Li, Y., Yu, Y., Yu, X., Liu, H., Zhang, Q., et al. (2019). Natural Product Pectolinarigenin Exhibits Potent Anti-metastatic Activity in Colorectal Carcinoma Cells *In Vitro* and *In Vivo*. *Bioorg. Med. Chem.* 27, 115089. doi:10.1016/j.bmc.2019.115089

Heimfarth, L., Nascimento, L. d. S., Amazonas Da Silva, M. d. J., Lucca Junior, W. d., Lima, E. S., Quintans-Junior, L. J., et al. (2021). Neuroprotective and Anti-inflammatory Effect of Pectolinarigenin, a Flavonoid from Amazonian *Aegiphila integrifolia* (Jacq.), against Lipopolysaccharide-Induced Inflammation in Astrocytes via NFκB and MAPK Pathways. *Food Chem. Toxicol.* 157, 112538. doi:10.1016/j.fct.2021.112538

Hotamisligil, G. S., and Bernlohr, D. A. (2015). Metabolic Functions of FABPs-Mmechanisms and Therapeutic Implications. *Nat. Rev. Endocrinol.* 11, 592–605. doi:10.1038/nrendo.2015.122

Johnson, R. J., Nakagawa, T., Jalal, D., Sánchez-Lozada, L. G., Kang, D. H., and Ritz, E. (2013). Uric Acid and Chronic Kidney Disease: Which is Chasing Which?. *Nephrol. Dial. Transpl.* 28, 2221–2228. doi:10.1093/ndt/gft029

Landa, C. E. M. (2018). Renal Effects of Hyperuricemia. *Contrib. Nephrol.* 192, 8–16. doi:10.1159/000484273

Lee, H. J., Venkatarame Gowda Saralamma, V., Kim, S. M., Ha, S. E., Vetrivel, P., Kim, E. H., et al. (2018). Comparative Proteomic Profiling of Tumor-Associated Proteins in Human Gastric Cancer Cells Treated with Pectolinarigenin. *Nutrients* 10, 1596. doi:10.3390/nu10111596

Lee, S., Lee, D. H., Kim, J. C., Um, B. H., Sung, S. H., Jeong, L. S., et al. (2017). Pectolinarigenin, an Aglycone of Pectolinarin, Has More Potent Inhibitory Activities on Melanogenesis Than Pectolinarin. *Biochem. Biophys. Res. Commun.* 493, 765–772. doi:10.1016/j.bbrc.2017.08.106

Lee, T. H., Chen, J. J., Wu, C. Y., Yang, C. W., and Yang, H. Y. (2021). Hyperuricemia and Progression of Chronic Kidney Disease: A Review from Physiology and Pathogenesis to the Role of Urate-Lowering Therapy. *Diagnostics* 11. doi:10.3390/diagnostics11091674

Li, Y., Gan, C., Zhang, Y., Yu, Y., Fan, C., Deng, Y., et al. (2019). Inhibition of Stat3 Signaling Pathway by Natural Product Pectolinarigenin Attenuates Breast Cancer Metastasis. *Front. Pharmacol.* 10, 1195. doi:10.3389/fphar.2019.01195

Li, Y., Guo, F., Huang, R., Ma, L., and Fu, P. (2021). Natural Flavonoid Pectolinarigenin Alleviated Kidney Fibrosis via Inhibiting the Activation of TGFβ/SMAD3 and JAK2/STAT3 Signaling. *Int. Immunopharmacol* 91, 107279. doi:10.1016/j.intimp.2020.107279

Li, Z., Sheng, Y., Liu, C., Li, K., Huang, X., Huang, J., et al. (2016). Nox4 Has a Crucial Role in Uric Acid-Induced Oxidative Stress and Apoptosis in Renal Tubular Cells. *Mol. Med. Rep.* 13, 4343–4348. doi:10.3892/mmr.2016.5083

Liu, N., Wang, L., Yang, T., Xiong, C., Xu, L., Shi, Y., et al. (2015). EGF Receptor Inhibition Alleviates Hyperuricemic Nephropathy. *J. Am. Soc. Nephrol.* 26, 2716–2729. doi:10.1681/ASN.2014080793

Liu, X., Qiu, Y., Li, D., Tan, J., Liang, X., and Qin, W. (2021). Effectiveness of Drug Treatments for Lowering Uric Acid on Renal Function in Patients With Chronic Kidney Disease and Hyperuricemia: A Network Meta-Analysis of Randomized Controlled Trials. *Front. Pharmacol.* 12, 690557. doi:10.3389/fphar.2021.690557

Pan, J., Shi, M., Guo, F., Ma, L., and Fu, P. (2021). Pharmacologic Inhibiting STAT3 Delays the Progression of Kidney Fibrosis in Hyperuricemia-Induced Chronic Kidney Disease. *Life Sci.* 285, 119946. doi:10.1016/j.lfs.2021.119946

Pascart, T., and Lioté, F. (2019). Gout: State of the Art After a Decade of Developments. *Rheumatology* 58, 27–44. doi:10.1093/rheumatology/key002

Ren, Q., Tao, S., Guo, F., Wang, B., Yang, L., Ma, L., et al. (2021). Natural Flavonol Fisetin Attenuated Hyperuricemic Nephropathy via Inhibiting IL-6/JAK2/STAT3 and TGF-β/SMAD3 Signaling. *Phytomedicine* 87, 153552. doi:10.1016/j.phymed.2021.153552

Shi, M., Guo, F., Liao, D., Huang, R., Feng, Y., Zeng, X., et al. (2020a). Pharmacological Inhibition of Fatty Acid-Binding Protein 4 Alleviated Kidney Inflammation and Fibrosis in Hyperuricemic Nephropathy. *Eur. J. Pharmacol.* 887, 173570. doi:10.1016/j.ejphar.2020.173570

Shi, Y., Tao, M., Ma, X., Hu, Y., Huang, G., Qiu, A., et al. (2020b). Delayed Treatment with an Autophagy Inhibitor 3-MA Alleviates the Progression of Hyperuricemic Nephropathy. *Cell Death Dis.* 11, 467. doi:10.1038/s41419-020-2673-z

Wu, Y.-L., Chen, J.-F., Jiang, L.-Y., Wu, X.-L., Liu, Y.-H., Gao, C.-J., et al. (2021). The Extract of Sonneratia Apetala Leaves and Branches Ameliorates Hyperuricemia in Mice by Regulating Renal Uric Acid Transporters and Suppressing the Activation of the JAK/STAT Signaling Pathway. *Front. Pharmacol.* 12, 698219. doi:10.3389/fphar.2021.698219

Xu, L., Lin, G., Yu, Q., Li, Q., Mai, L., Cheng, J., et al. (2021). Anti-Hyperuricemic and Nephroprotective Effects of Dihydroberberine in Potassium Oxonate- and Hypoxanthine-Induced Hyperuricemic Mice. *Front. Pharmacol.* 12, 645879. doi:10.3389/fphar.2021.645879

Yanai, H., Adachi, H., Hakoshima, M., and Katsuyama, H. (2021). Molecular Biological and Clinical Understanding of the Pathophysiology and Treatments of Hyperuricemia and its Association with Metabolic Syndrome, Cardiovascular Diseases and Chronic Kidney Disease. *Int. J. Mol. Sci.* 22. doi:10.3390/ijms22179221

Zhang, T., Li, S., Li, J., Yin, F., Hua, Y., Wang, Z., et al. (2016). Natural Product Pectolinarigenin Inhibits Osteosarcoma Growth and Metastasis via SHP-1-Mediated STAT3 Signaling Inhibition. *Cell Death Dis.* 7, e2421. doi:10.1038/cddis.2016.305

Zhang, Y., Meng, X. M., Huang, X. R., and Lan, H. Y. (2018). The Preventive and Therapeutic Implication for Renal Fibrosis by Targetting TGF-β/Smad3 Signaling. *Clin. Sci.* 132, 1403–1415. doi:10.1042/CS20180243

Conflict of Interest: The authors declare that the research was conducted in the absence of any commercial or financial relationships that could be construed as a potential conflict of interest.

frontiers in Pharmacology

ORIGINAL RESEARCH
published: 10 February 2022
doi: 10.3389/fphar.2021.801094

Cordyceps cicadae Ameliorates Renal Hypertensive Injury and Fibrosis Through the Regulation of SIRT1-Mediated Autophagy

Yuzi Cai[1,2†], Zhendong Feng[3†], Qi Jia[4†], Jing Guo[1,2], Pingna Zhang[1,2], Qihan Zhao[1,2], Yao Xian Wang[1,2], Yu Ning Liu[5] and Wei Jing Liu[2*]*

[1]Beijing University of Chinese Medicine, Beijing, China, [2]Key Laboratory of Chinese Internal Medicine of Ministry of Education, Beijing Dongzhimen Hospital Addiliated to Beijing University of Chinese Medicine, Beijing, China, [3]Department of Nephropathy, Beijing Traditional Chinese Medicine Hospital Pinggu Hospital, Beijing, China, [4]Department of Nephropathy, Dongfang Hospital, Beijing University of Chinese Medicine, Beijing, China, [5]Department of Endocrinology Nephropathy of Dongzhimen Hospital, Beijing University of Chinese Medicine, Beijing, China

OPEN ACCESS

Edited by:
Dan-Qian Chen,
Northwest University, China

Reviewed by:
Ming Wang,
Southern Medical University, China
Yuansheng Xie,
Chinese PLA General Hospital, China

****Correspondence:***
Yu Ning Liu
yunin1946@sina.com
Wei Jing Liu
liuweijing-1977@hotmail.com

[†]These authors have contributed equally to this work and share first authorship

Specialty section:
This article was submitted to Renal Pharmacology, a section of the journal Frontiers in Pharmacology

Received: *24 October 2021*
Accepted: *30 December 2021*
Published: *10 February 2022*

Citation:
Cai Y, Feng Z, Jia Q, Guo J, Zhang P, Zhao Q, Wang YX, Liu YN and Liu WJ (2022) Cordyceps cicadae Ameliorates Renal Hypertensive Injury and Fibrosis Through the Regulation of SIRT1-Mediated Autophagy. Front. Pharmacol. 12:801094. doi: 10.3389/fphar.2021.801094

Hypertensive renal injury is a complication of hypertension. *Cordyceps cicadae* (*C. cicadae*) is a traditional Chinese medicine used to treat chronic kidney diseases especially renal fibrosis. Autophagy is described as a cell self-renewal process that requires lysosomal degradation and is utilized for the maintenance of cellular energy homeostasis. The present study explores the mechanism underlying *C. cicadae*'s renoprotection on hypertensive nephropathy (HN). First, HN rat models were established on spontaneously hypertensive rats (SHRs). The expression of fibrosis-related protein and autophagy-associated protein was detected *in vivo*. NRK-52E cells exposed to AngII were chosen to observe the potential health benefits of *C. cicadae* on renal damage. The level of extracellular matrix accumulation was detected using capillary electrophoresis immunoquantification and immunohistochemistry. After treatment with lysosomal inhibitors (chloroquine) or an autophagy activator (rapamycin), the expression of Beclin-1, LC3II, and SQSTM1/p62 was further investigated. The study also investigated the change in sirtuin1 (SIRT1), fork head box O3a (FOXO3a), and peroxidation (superoxide dismutase (SOD) and malondialdehyde (MDA)) expression when intervened by resveratrol. The changes in SIRT1 and FOXO3a were measured in patients and the SHRs. Here, we observed that *C. cicadae* significantly decreased damage to renal tubular epithelial cells and TGFβ1, α-smooth muscle actin (α-SMA), collagen I (Col-1), and fibronectin expression. Meanwhile, autophagy defects were observed both *in vivo* and *in vitro*. *C. cicadae* intervention significantly downregulated Beclin-1 and LC3II and decreased SQSTM1/p62, showing an inhibition of autophagic vesicles and the alleviation of autophagy stress. These functions were suppressed by rapamycin, and the results were just as effective as the resveratrol treatment. HN patients and the SHRs exhibited decreased levels of SIRT1 and FOXO3a. We also observed a positive correlation between SIRT1/FOXO3a and antifibrotic effects. Similar to the resveratrol group, the expression of SIRT1/FOXO3a and oxidative stress were elevated by *C. cicadae in vivo*. Taken together, our findings show that *C. cicadae* ameliorates tubulointerstitial fibrosis and delays HN progression.

Renoprotection was likely attributable to the regulation of autophagic stress mediated by the SIRT1 pathway and achieved by regulating FOXO3a and oxidative stress.

Keywords: hypertensive renal injury, *Cordyceps cicadae*, autophagy, SIRT1, fibrosis

INTRODUCTION

Hypertensive renal injury is the primary underlying disease of renal failure (Aibara et al., 2020). Tubulointerstitial fibrosis is considered to be the primary pathogenesis for progressive hypertensive nephropathy (HN) (Liu et al., 2015; Bao et al., 2018; Tao et al., 2019). Renal function and arterial pressure are regulated by the renin–angiotensin–aldosterone system (RAAS) (Francois et al., 2004). Angiotensin II (AngII), the primary effector of RAAS, can accelerate renal interstitial fibrosis progression by affecting renal hemodynamics, regulating the growth of renal tubular epithelial cells (TEC), promoting the production of inflammatory and cellular cytokines, and promoting the accumulation and degradation of the extracellular matrix (ECM) containing TGFβ1, α-SMA, FN, and Col-1 (Lu et al., 2019; Yoon et al., 2020; Zhang J.-h. et al., 2021). Recent treatment schemes for HN have primarily focused on regulating blood pressure (BP) and protecting kidney function. RAAS inhibitors, such as angiotensin-converting enzyme (ACE) inhibitors and angiotensin receptor blockers (ARBs), are considered as first-line treatments for hypertensive individuals with kidney disease. To some extent, the existing treatment methods can delay the progression of hypertension but weakly participate in controlling hypertensive renal damage (Zhang et al., 2020). The potential health effects of traditional Chinese medicine (TCM) should be explored and developed.

Autophagy (macrophage) is described as a cell self-renewal process that relies on lysosomal degradation. Physiologically, active autophagy recognizes and degrades damaged proteins, invading pathogens, and aging organelles under dystrophic and stress stimuli and subsequently releases products that are degraded for reuse to maintain cell homeostasis (Mizushima and Komatsu, 2011; Rechter et al., 2016). Autophagy consists of four phases, namely, induction, nucleation, elongation, and diffusion, and these phases are tightly regulated by different signaling pathways, such as 5′ adenosine monophosphate-activated protein kinase (AMPK), lysosomal enzymes (Chen et al., 2016), and autophagy proteins (Atgs, including LC3II). SQSTM1/p62 is an indicator of autophagic flux and acts as an autophagy receptor involved in the targeting of cargo into autophagosomes. After the fusion of autophagosomes with lysosomes, the autophagosome content, including p62, is degraded (Lim et al., 2015). Pathologically, prolonged pathogenic factors enhance autophagy induction and disrupt lysosome function, exceeding the degradative capacity in cells and contributing toward autophagic stress and possibly stagnation of autophagy (Zheng et al., 2020). ECM remodeling is the hallmark of HN. Uncontrolled ECM accumulation due to an imbalance between formation and degeneration has been implicated in renovascular fibrosis (Chen et al., 2017). The central role of autophagy in altering ECM degradation has been investigated in previous studies (Cinque et al., 2015; Eckhart et al., 2019). The contribution of autophagy to HN remains unclear; however, defects in autophagy have been associated with intracellular aging and protein and organelle damage (Guo et al., 2020), as well as disorganization of ECM components and the occurrence of tubulointerstitial fibrosis (Li, et al., 2020). Autophagy is thus considered a potential therapeutic target for HN treatment.

Redox homeostasis disorder under pathological conditions results in excessive production of reactive oxygen species (ROS) (Ornatowski et al., 2020). Oxidative stress produced by pathologic and pharmacological factors plays an important role in controlling hypertension-related diseases under physiological conditions (Guzik and Touyz, 2017). Peroxidation dysfunction and inflammation, which are identified as significant functions underlying kidney diseases, modulate the autophagy inhibition or activation and lead to cellular recycling dysfunction (Lin et al., 2019; Li et al., 2021). Accumulating evidence demonstrates that autophagy is essential to support redox homeostasis. ROS activates autophagy, which maintains cellular adaptation and reduces oxidative damage by degrading and recycling damaged macromolecules and dysfunctional organelles in cells (Ornatowski et al., 2020). On the other hand, peroxidation levels, such those as of H_2O_2 and AngII, in abnormal conditions may induce apoptosis via silent information regulator 2 homolog 1 (SIRT1) and other signaling pathways (Lakhani et al., 2019; Park et al., 2020; Wu et al., 2020; Huang et al., 2021). Malondialdehyde (MDA) is a major byproduct in oxidative stress that affects kidney fibrogenesis related to hypertension (Chen et al., 2019). Superoxide dismutase (SOD) is an important antioxidant enzyme that plays an indispensable role in free-radical scavenging and blocking the progression of HN (da Silva Cristino Cordeiro et al., 2018). Both have been recognized as the primary factor related to the pathogenesis of chronic kidney disease (CKD) and a cause of renal fibrosis.

SIRT1 is ubiquitously expressed in the human body, including in kidney cells such as podocytes, glomerular mesangial cells, and tubular cells. Using deacetylating substrates, SIRT1 plays a role in regulating autophagy, oxidative stress, energetic homeostasis, and apoptosis (Zhang et al., 2017; Liu et al., 2018; Xu et al., 2020). Renal SIRT1 is cytoprotective and is correlated to BP regulation and sodium balance (Hao and Haase, 2010). Recent studies have focused on the role of SIRT1 in HN development and progression, primarily by protecting tubular cells from cellular stresses (Guclu et al., 2016; Huang X. et al., 2020; Martinez-Arroyo et al., 2020).

FOXO3a, a major downstream molecule of SIRT1, belongs to the fork head box O (FOXO) family of transcription factors. It has been suggested that the FOXO family serves as a SIRT1

deacetylate member that affects downstream pathways that control autophagy (Daitoku et al., 2011; Tang, 2016). However, SIRT1 largely influences FOXO3a-mediated transcription during oxidative stress and cell survival by controlling FOXO3a deacetylation (Kobayashi et al., 2005). Resveratrol (RES), a well-known SIRT1 activator and oxidative stress inhibitor, ameliorates renal tubular damage in DN by upregulating FOXO3a transcriptional activity and reinforces resistance to oxidative damage (Jiang et al., 2020). RES and its active component also regulate autophagy via the SIRT1/FOXO3a pathway in many diseases (Shi et al., 2012; Ni et al., 2013). Emerging evidence indicated that *C. cicadae* elevated the SIRT1 expression against kidney injury or renal interstitial fibrosis (Huang YS. et al., 2020). Additionally, RES treatment ameliorates renal function and glomerulosclerosis and increases SIRT1 deacetylase activity, subsequently decreasing the expression of acetylated FOXO3a and inhibiting the oxidative stress caused by hyperglycemia both *in vivo* and *in vitro* (Wang et al., 2017). Thus, this study aims to determine whether *C. cicadae* imparts a protective effect against NH via the SIRT1/FOXO3a/ROS pathway.

C. cicadae is a TCM that belongs to the family Cordycipitaceae, which is parasitic on *Cicada flammata* larvae. It has been utilized in the treatment of various diseases and to relieve exhaustion. Pharmacological studies have shown that the fungus contains biologically active chemical substances including nucleosides, cordycepic acid, cordycepin, beauvericin, and myriocin (Sun et al., 2017). *C. cicadae* has been historically utilized for liver and kidney protection, analgesia–antipyresis, blood fat reduction, and its antitumor activities (Qin et al., 2020). It is well known that the active ingredients extracted from *C. cicadae* are effective in ameliorating CKD induced by diabetes or hypertension. (Zheng et al., 2018; Huang X. et al., 2020; Liu et al., 2014). Evidence also suggests that *C. cicadae* relieved acute kidney injury through the inhibition of oxidative stress and inflammation (Deng et al., 2020). Based on our previous studies, we estimated that *C. cicadae* might protect renal functions against kidney fibrosis by alleviating renal autophagic stress through the regulation of the SIRT1/FOXO3a/ROS pathway. This hypothesis was assessed in spontaneously hypertensive rats (SHRs) and in AngII-cultured primary TECs.

MATERIALS AND METHODS

Human Renal Biopsy Samples

All clinical data derived from 25 patients (age range: 50–60 years) of the Affiliated Hospital of Guangdong Medical College (Zhanjiang, Guangdong, China) were de-identified. We searched for stored former kidney biopsy samples collected from December 2015 to December 2020. These kidney tissue specimens were obtained from patients diagnosed with biopsy-proven hypertensive renal injury ($n = 11$). The inclusion criteria of the control group were patients with mild urinary protein excretion or hematuria only and biopsy-proven minimal change ($n = 14$).

Animals

Thirty male SHRs (age: 8 weeks old; weight range: 170–210 g) and eight Wistar-Kyoto (WKY) rats (age: 8 weeks old; weight range: 170–210 g) were obtained from Beijing Vital River Co., Ltd. (Beijing, China) and housed under controlled laboratory conditions (25 ± 2°C temperature, 60 ± 1% humidity, and 07:00–19:00 light and 19:00–07:00 dark cycle) with *ad libitum* access to water. The experiments were conducted according to the *Guide for the Care and Use of Laboratory Animals* (eighth edition) (National Academies of Sciences, Engineering, and Medicine) and approved by the ethics committee of Beijing University of Chinese Medicine. Four groups were used: (1) the control WKY rats ($n = 8$), (2) SHRs ($n = 10$), (3) SHRs that received intraperitoneal injection of RES once a day (40 mg/kg/day, $n = 10$), and (4) SHRs treated with *C. cicadae* once a day (4 g/kg/day, $n = 10$). After overnight fasting on the 28th week, the animals were sacrificed, and renal tissue specimens were isolated for further analysis.

Detection of Urinary and Plasmatic Parameters

Blood plasma was collected via the abdominal aorta and then centrifuged at 3,500 rpm for 15 min (4°C). The blood samples were stored at −80°C until use. Twenty-four-hour urine samples were collected from the rats that were situated in a metabolic cage on the 14th and 28th weeks. Urinary creatinine levels were measured using an enzyme-linked immunosorbent assay (ELISA) kit (C011-2-1, Nanjing Jiancheng Bioengineering Institute, Nanjing, China); urinary albumin levels were measured using an ELISA kit (ab108789, Abcam, Cambridge, MA, United States); and levels of urinary β2-MG were measured using an ELISA kit (RKM100, R&D Systems, Minneapolis, MN, United States). The urinary kidney injury molecule-1 (KIM-1) concentration was measured using an ELISA kit (ab119597). All protocols were performed following the manufacturers' instructions.

Renal Histological Examination

The paraffin-embedded kidneys were sliced into 3-μm-thick sections and dewaxed in a xylene reagent tank, and this was followed by rehydration across an ethanol gradient. Hematoxylin and eosin (H&E) staining was conducted to assess the histological changes. Masson's trichrome staining (Masson) was used to evaluate fibrosis. The prepared sections were stained using a kit for Masson's trichrome staining (Nanjing Jiancheng Biological Reagent Co., Ltd., Nanjing, China). Images were captured using an Olympus BX60 microscope (Olympus, Tokyo, Japan) and a Zeiss optical microscope (Germany) equipped with a ZEN 2.3 (blue edition) image-capture software (Carl Zeiss Microscopy GmbH, Jena, Germany). Image-Pro Plus (IPP) 6.0 software (Media Cybernetics, United States) was utilized to estimate the degree of interstitial fibrosis. The above methods are described in detail in our previous study (Huang YS. et al., 2020).

Preparation of the Reagents and the *C. cicadae*-Containing Serum

C. cicadae was obtained from the Zhejiang BioAsia Pharmaceutical Co., Ltd. (Pinghu, Zhejiang, China). RES,

chloroquine (CQ), and rapamycin (RAP) were obtained from Sigma-Aldrich (St. Louis, MO, United States).

Sprague-Dawley rats weighing 250–300 g were randomly divided into negative control and treatment groups. The treatment group animals were treated with *C. cicadae* or distilled water (2 ml/day) as previously described. After a 1-week treatment, blood samples were collected from the abdominal aorta and centrifuged. Serum samples from all individual animals of each group were pooled and filtered through a 0.22 μm filter membrane. Medicated serum containing *C. cicadae* (CMS) was employed in the cell experiment.

Cell Culture and Treatment

NRK-52E cell lines were provided by the Institute of Nephrology of the General Hospital of the Chinese People's Liberation Army (Beijing, China). The cells were cultured at Dongzhimen Hospital of Beijing University of Chinese Medicine (Beijing, China) and supplemented with 10% fetal bovine serum (FBS, Gibco, United States) in a humidified 5% CO_2 atmosphere at a temperature of 37°C. The cells were subcultured every 2 to 3 days. In several experiments, the NRK-52E cells were incubated with AngII (10^{-7} mM), CMS (10%), and RES (25 μM). All cells were harvested for further analysis.

Cell Viability Assay

The viability of the NRK-52E cells treated with AngII (Sigma-Aldrich) was assessed using Cell Counting Kit-8 (CCK-8, Dojindo Laboratories, Kumamoto, Japan). The cells at a density of 5×10^3 cells per well were seeded into 96-well plates and then treated with AngII (10^{-4}, 10^{-5}, 10^{-6}, 10^{-7}, 10^{-8}, and 10^{-9} M) for various duration (24 and 72 h). Ten microliters of CCK-8 solution was added into each well and then cultured for another 1–4 h. Finally, the optical density (OD) value at a wavelength of 450 nm was measured to determine cell viability (Thermo Scientific, United States). The assay was repeated thrice. A CCK-8 assay was used to determine the safe and effective AngII concentration for the experiment. Different concentrations of CMS (10, 15, 20%) and RES (10, 25, 50, 100, 150 μM) were detected as above.

Detection of Cell Injury

There were four groups in the experiment: a control group, an AngII group, a CMS group, and a RES group. The cells were cultured as earlier described, and KIM-1 and neutrophil gelatinase-associated lipocalin (NGAL) abundance in the supernatant was determined by ELISA kits obtained from R&D Systems (DLCN20, Minneapolis, MN, United States) and Abcam (ab119597). All of the operational procedures were performed in accordance with the manufacturers' instruction.

MDA and SOD Detection

After treatment, the renal tissues or supernatant were collected, and MDA and SOD were quantified using an MDA assay kit (S0131, Beyotime Institute of Biotechnology, Jiangsu, China) and a SOD assay kit (S0101, Beyotime Institute of Biotechnology, Jiangsu, China) following the manufacturer's instruction.

Western Blot and Densitometric Analysis

Total protein from cells of rat kidney tissues was extracted by centrifugation at 12,000 rpm at 4°C for 20 min. The resulting supernatant was collected and used to determine total protein concentration using the BCA assay. Supernatants of various samples were heated for 10 min at 95°C in a sample loading buffer and later separated by SDS-PAGE and then transferred to nitrocellulose membranes. The membranes were blocked for 1 h with 5% nonfat milk in TBST buffer. To perform immunodetection, the blots were incubated at 4°C overnight with the following primary antibodies: anti-LC3II (ab51520), anti-SQSTM1/p62 (ab109012), beclin-1 (ab62557), anti-α-SMA (ab32575), anti-TGF-β1 (ab92486), anti-FN (ab2413), anti-Col-1 (ab34710), and anti-GAPDH antibody (10494-1-AP, ProteinTech, Rosemont, PA, United States). Except for the anti-GAPDH antibody, all primary antibodies were obtained from Abcam and employed at a 1:1,000 dilution. The peroxidase-linked secondary antibody (SA00001-2, ProteinTech, Rosemont, PA, United States) was diluted at 1: 5,000. Then, the membranes were visualized with an ECL advanced kit, and quantitation of protein bands was performed using the ImageJ software (NIH, Bethesda, MD, United States). The result of absorbance measurements and the grey values obtained from the densitometric analysis were expressed as means ± standard deviations (SDs) of the three determinations for each sample.

Capillary Electrophoresis Immunoquantification

Whole-cell protein was obtained for quantitative capillary isoelectric immunoassay. Protein levels were assessed using a capillary-based automated electrophoresis immunoquantification instrument (ProteinSimple, San Jose, CA, United States) following the manufacturer's standard instruction. Here, 3 μl of protein extract (final concentration: 1 μg/μl) was loaded with the following antibodies: anti-SIRT1 antibody (sc15404, Santa Cruz Biotechnology, Santa Cruz, CA, United States), anti-GAPDH antibody (10494-1-AP, ProteinTech), and anti-FOXO3a antibody (12829, Cell Signal Technology, Inc., United States). The run conditions were as recommended previously. Compass software (ProteinSimple ver. 3.1.8) was utilized to calculate and measure the immunoblots.

Immunostaining Analysis

Immunohistochemical and immunofluorescence analyses of samples were performed as described. Rabbit anti-SIRT1 (sc15404, Santa Cruz Biotechnology, Santa Cruz, CA, United States), rabbit anti-FOXO3a antibody (12829, Cell Signaling Technology, CA, United States), rabbit anti-α-SMA antibody (ab32575, Abcam, Cambridge, MA, United States), rabbit anti-LC3II antibody (ab51520, Abcam, Cambridge, MA, United States), rabbit anti-SQSTM1/p62 (ab109012), and fluorescein isothiocyanate-labeled goat anti-rabbit IgG (sc-2012, Santa Cruz Biotechnology, Santa Cruz, CA, United States) were used in the immunostaining assay for kidney tissues. Rabbit anti-FOXO3a antibody (12829, Cell

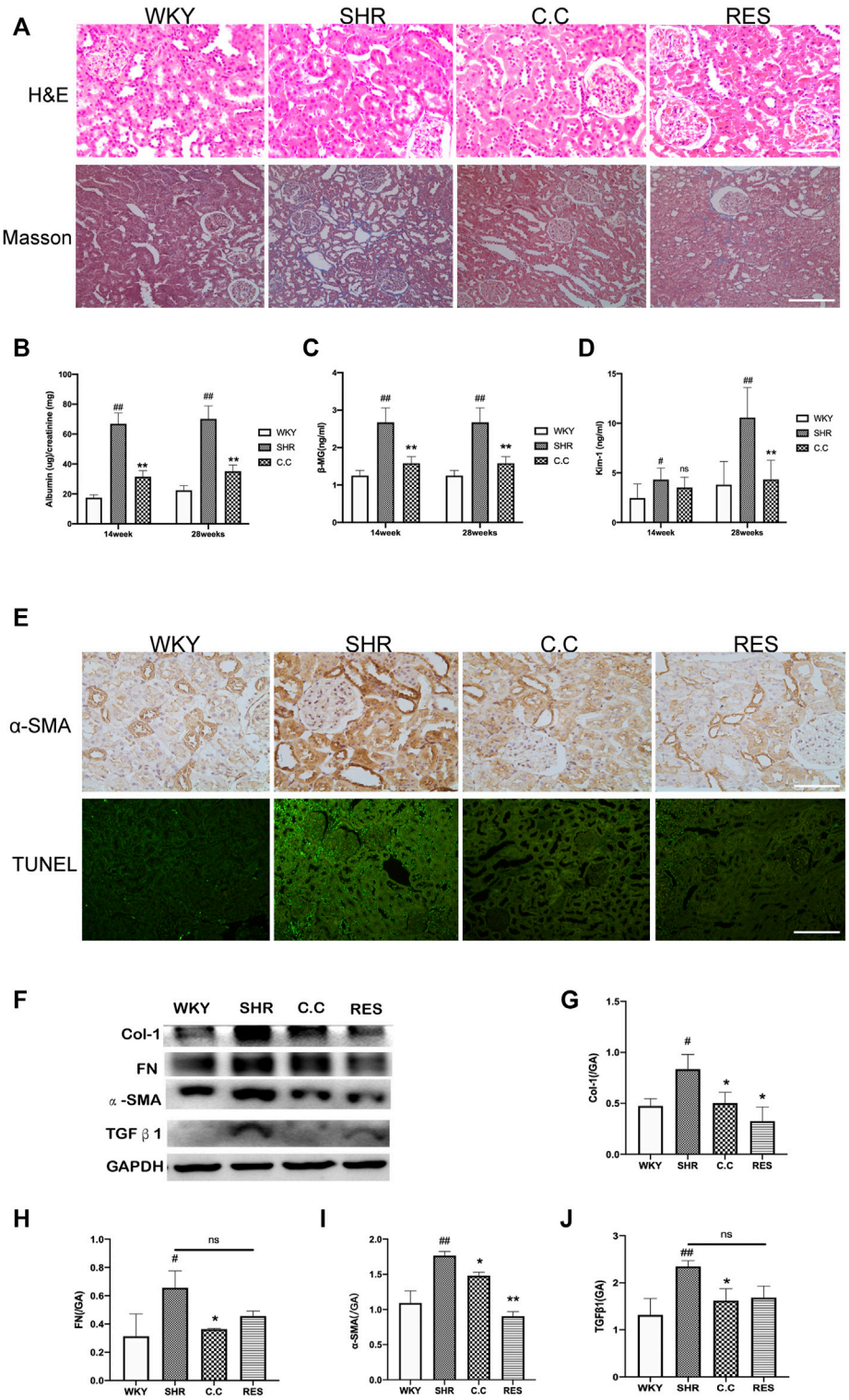

FIGURE 1 | *C. cicadae* alleviated SHR renal injury and fibrosis. **(A)** H&E staining (bar = 100 μm) and Masson's trichrome staining (bar = 40 μm). **(B)** *C. cicadae* treatment significantly decreases ACR levels after 14 and 28 weeks. **(C)** *C. cicadae* treatment significantly downregulates β2-MG expression after 14 and 28 weeks. **(D)** *C. cicadae* treatment significantly reduced β2-MG level at the 28th week. **(E)** The representative images and statistical graph of IHC staining for α-SMA (×200). Bar = 100 μm. Apoptosis in rat renal tubules of various groups was evaluated by TUNEL assay. Scale bar: 40 μm. **(F)** Effect of *C. cicadae* and RES on TGFβ1, α-SMA, FN, and Col-1 expression. **(G–J)** The relative intensities of fibrosis-related protein in kidneys were calculated after normalization against GAPDH. Data were presented as mean ± SD, $n = 10$ rats per group. For the WKY group vs the SHR group, #$p < 0.05$, ##$p < 0.01$. For the SHR group vs the *C. cicadae* group, *$p < 0.05$, **$p < 0.01$. N.S. No significance.

Signaling Technology, CA, United States), rabbit anti-SIRT1 (2977886, Millipore, Billerica, MA, United States), rabbit anti-LC3II antibody (ab51520, Abcam, Cambridge, MA, United States), rabbit anti-SQSTM1/p62 (ab109012), rabbit anti-α-SMA antibody (ab32575, Abcam, Cambridge, MA, United States), and Alexa Fluor 488 donkey anti-rabbit IgG (Invitrogen, Carlsbad, CA, United States) were used for immunostaining the cells. The nuclei of the cells were stained with DAPI. Immunopositive signals were detected using a confocal microscope (Leica Microsystems, Wetzlar, Germany) or an Olympus BX60 microscope (Olympus, Tokyo, Japan). The acquired images were analyzed using the IPP 6.0 software.

Statistical Analysis

Statistical analysis was conducted using the GraphPad Prism ver. 9.00 statistical software (SAS Institute, Abacus Concept, Inc., Berkeley, CA, United States). Results are shown as means ± SDs. Differences among groups were examined using one-way ANOVA, which was then followed by Bonferroni multiple-comparison test. Comparison among treatment groups was performed at a significance level of $p < 0.05$.

RESULTS

C. cicadae Alleviated Renal Injury and Fibrosis of the SHRs

We determined the impact of *C. cicadae* on renal damage and fibrosis after 28 weeks of induction *in vivo*. No significant histopathological differences among the four H&E-stained groups were detected. Masson's trichrome staining revealed that the SHR group developed fibrotic changes and severe renal interstitial fibrosis; in addition, *C. cicadae* significantly decreased collagen deposition (**Figure 1A**). A comparison of the WKY and SHR groups indicated significant differences in the albumin/creatinine ratio (ACR), as well as KIM-1 and β2-MG levels. Treatment with *C. cicadae* significantly downregulated ACR, KIM-1, and β2-MG levels by the 28th week, whereas no marked changes in KIM-1 level were detected on week 14 (**Figures 1B–D**). We also assessed the number of apoptotic kidney cells using the terminal transferase-mediated biotin dUTP nick-end labeling (TUNEL) assay, and immunohistochemical staining revealed that with prolonged AngII treatment, the SHR group showed a gradual increase in collagen fiber (α-SMA) expression and rate of renal intrinsic cell apoptosis, whereas ECM deposition and apoptotic TEC count significantly decreased with *C. cicadae* treatment after 28 weeks (**Figure 1E**). Similarly, the ECM accumulation was evaluated using western blot, and *C. cicadae* downregulated the TGFβ1, α-SMA, FN, and Col-1 expression and protected the hypertension-injured kidney tissue from progressive fibrosis (**Figures 1F–J**).

C. cicadae Attenuated AngII-Treated NRK-52E Cell Injury and Fibrosis

AngII was employed to simulate hypertensive renal injury. This study selected NRK-52E rat renal epithelial cells as the model of renal damage of hypertension. A dose-related change in cell activity and viability was observed in the NRK-52E cells exposed to various concentrations for 24 and 72 h. As shown in **Figure 2A**, the cell viability significantly decreased at an AngII concentration of 10^{-8} M ($p < 0.01$), and 10^{-7} M of AngII was chosen to be the optimal model concentration. We also detected the effect and safe concentration of *C. cicadae* by diluting the medicated serum. **Figure 2B** indicates that the NRK-52E cells remained in a steady growth environment at 10% *C. cicadae* serum. Eventually, we selected the 10% concentration in the following study. By the same method, the concentration of RES was confirmed to be 25 μM (**Figure 2C**).

Renal tubular epithelial cell damage was evaluated based on supernatant KIM-1 and NGAL levels, which were significantly upregulated in the AngII group relative to the control group (**Figures 2D,E**). However, *C. cicadae* treatment significantly downregulated KIM-1 and NGAL expression by 46% and 15%, respectively, relative to the model group. These findings coincided with the changes in kidney tissues obtained in the SHRs. The ECM accumulation was assessed using capillary electrophoresis immunoquantification (**Figure 2F**). α-SMA and Col-1 were significantly upregulated in the AngII group relative to the control group, which were reduced with *C. cicadae* treatment (**Figures 2G,H**).

C. cicadae Ameliorated Hypertensive Renal Fibrosis by Inhibiting Autophagic Stress

Autophagic stress means an increase in the autophagic flow. This process may be due to the generation of too many autophagic vesicles that cannot be degraded or a change in the autophagic flux due to problems with autophagic degradation. We next investigated whether *C. cicadae* could reduce fibrosis protein expression and suppress ECM accumulation by regulating autophagy. The autophagic markers LC3II and p62 and autophagosomal formation were employed to evaluate the condition of autophagy in the SHR kidney tissue using immunohistochemical staining. LC3II and p62 protein expression was upregulated in hypertensive renal damage, which was indicative of autophagic activation (**Figures 3A–C**). Similar observations were obtained using western blot (**Figure 3D**), whereas *C. cicadae* downregulated LC3II, beclin-1, and p62 expression (**Figures 3E–H**). In addition, we observed increased LC3II expression along with blocked p62 degradation for the 72-h-treated AngII NRK-52E cells, indicating enhanced autophagosome synthesis and the defect of LC3II-mediated protein degradation (**Figures 3I–L**). As shown in **Figures 3M,N**, the expression of LC3II and beclin-1 was suppressed after the *C. cicadae* treatment, indicating that *C. cicadae* inhibited autophagy.

To further investigate the impacts of autophagy on the renal fibrosis process, we treated the NRK-52E cells with lysosomal inhibitor CQ. As shown in **Figure 4A**, the CQ exacerbated autophagic activation caused by AngII. We also found that the autophagic inhibition effect of *C. cicadae* was blocked after being exposed to CQ for 72 h (**Figures 4B,C**). Then, the autophagy activator RAP was used. The immunofluorescence assay showed that the expression of α-SMA was reversed by the *C. cicadae*

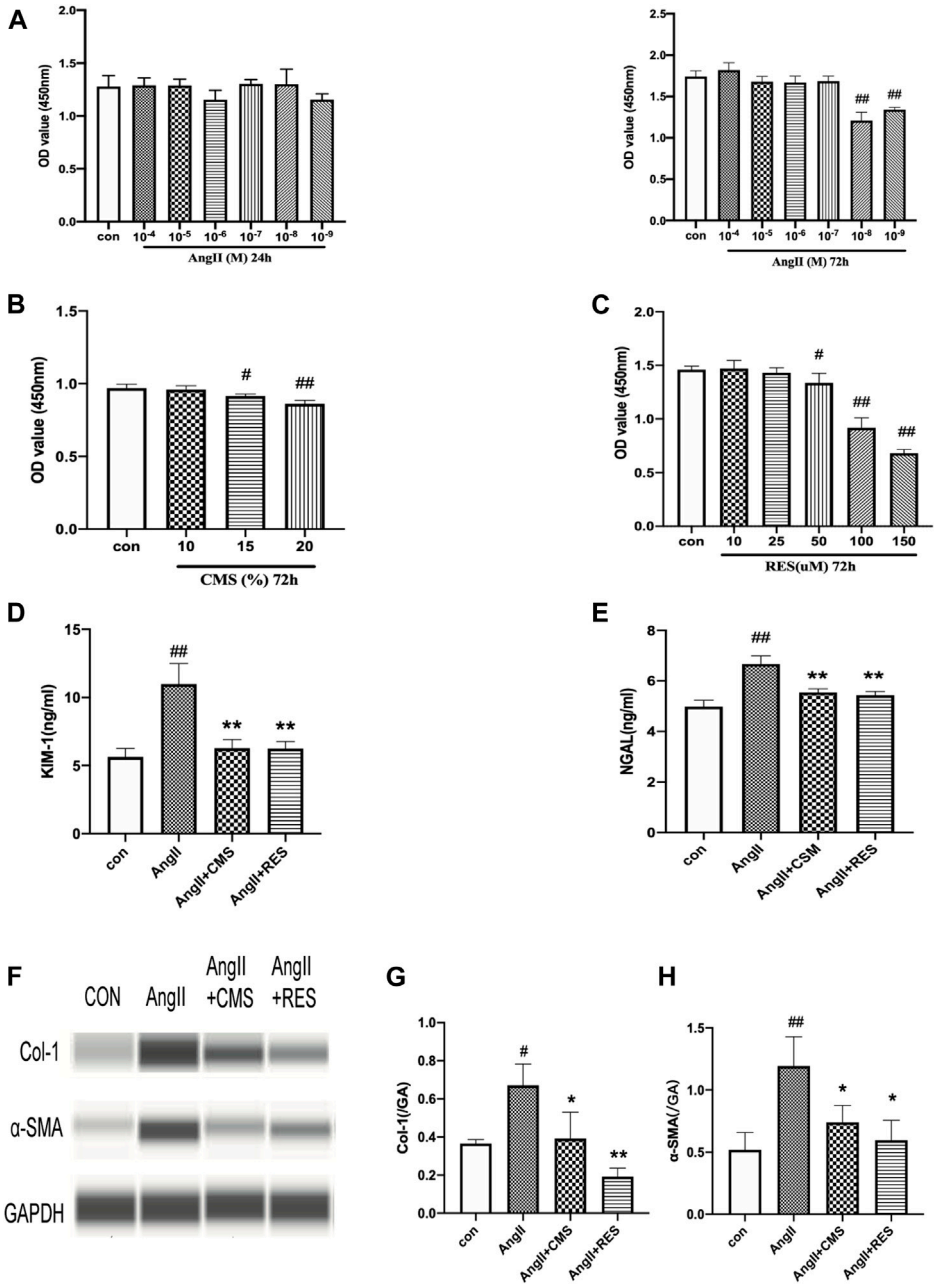

FIGURE 2 | CMS attenuated AngII-associated injury and inhibited ECM accumulation in rat renal tubular epithelial cells. **(A)** NRK-52E cells were exposed to various concentrations of AngII for 24 and 72 h. **(B)** Effects of CMS on viability for 72 h. **(C)** Effects of RES on NRK-52E cell viability for 72 h. **(D,E)** Effect of CMS on NRK-52E cell injury. The level of cell injury was examined by KIM-1 and NGAL ELISA kits. **(F)** Effect of CMS on the expression of Col-1 and α-SMA. **(G,H)** The relative intensities of fibrosis-related protein in cells were calculated after normalization against GAPDH. Data are expressed as the mean ± SD of three separate experiments. $^{\#}p < 0.05$, $^{\#\#}p < 0.01$ compared with control cells. $^{*}p < 0.05$, $^{**}p < 0.01$, compared with the model group.

treatment, while no reversed effect was achieved due to the RAP treatment (**Figure 4D**). In addition, the NRK-52E cells treated with *C. cicadae* as well as RAP suppressed the antifibrotic effect of *C. cicadae*. These results indicated that *C. cicadae* ameliorated hypertension-induced renal fibrosis by suppressing autophagic induction, reducing autophagy vesicle formation, and suppressing autophagy stress.

C. cicadae Increased SIRT1/FOXO3a Expression and Decreased Oxidative Stress in Hypertensive Renal Damage

To assess clinical relevance, we determined SIRT1/FOXO3a expression levels in human renal biopsy samples obtained from normotensive health controls as well as patients with HN. The result of the immunohistochemistry showed that

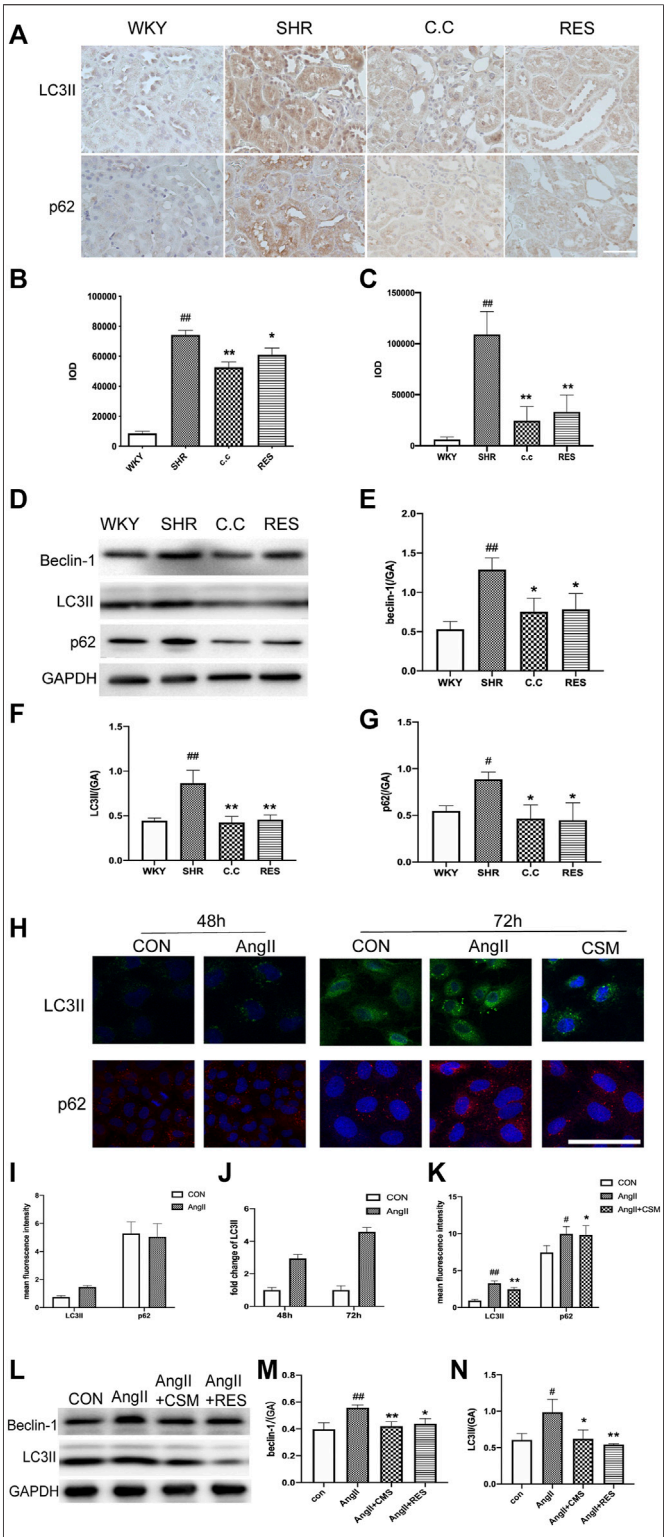

FIGURE 3 | *C. cicadae* and RES regulated autophagic stress in hypertensive kidney damage. **(A)** IHC staining result (×400) of LC3II and p62 in paraffin sections. Bar = 50 μm. **(B,C)** Statistical results of IHC staining of LC3II and p62, respectively. The value of mean optical density (IOD) obtained by IPP software. **(D)** Expression of beclin-1, LC3II, and p62. The results of evaluation are shown in **(E–G)**. $^{\#}p < 0.05$, $^{\#\#}p < 0.01$: compared with controls. (*Continued*)

FIGURE 3 | $^{*}p < 0.05$, $^{**}p < 0.01$: relative to the model group. N.S. No significance. **(H)** Immunofluorescence images show the levels of LC3II (green channel) and the levels of p62 (red channel) for 48 and 72 h. Bar = 20 μm. **(I–K)** Statistical results of immunofluorescence staining of LC3II and p62. The value of IOD obtained by IPP software. **(L)** Expression of beclin-1 and LC3II. The results of evaluation are shown in **(M)** and **(N)**. $^{\#}p < 0.05$, $^{\#\#}p < 0.01$: compared with controls, respectively. $^{*}p < 0.05$, $^{**}p < 0.01$: relative to the model group, respectively.

higher levels of SIRT1 and FOXO3a existed in healthy subjects, while significant downregulation was seen in the HN patients (**Figure 5A**). Furthermore, there was a positive correlation between SIRT1 and FOXO3a. Thus, SIRT1/FOXO3a might play an important role in HN.

Then, the SIRT1 and FOXO3a expression was determined using capillary electrophoresis immunoquantification in the SHRs and NRK-52E cells. We found that the SIRT1 and FOXO3a expression was low in all of the model groups, while *C. cicadae* upregulated the SIRT1 and FOXO3a levels in hypertensive renal damage (**Figures 5B,C**). Similar results were obtained using *in vitro* immunofluorescence, in which *C. cicadae* induced an increase in the fluorescence intensity of SIRT1 in NRK-52E cells compared with the AngII group (**Figures 5D,F**). However, the immunofluorescence images showed that no significant change existed in the FOXO3a expression (**Figures 5E,G**). This might have been related to the nuclear translocation of FOXO3a (**Supplementary Figure 1A**). MDA and SOD regulate the production of ROS and are related to oxidative stress intimately. The trend of the MDA in the SHRs and AngII-treated NRK-52E cells was significantly stimulated compared to the control, while it was suppressed by *C. cicadae* (**Figures 5H,J**). In contrast, *C. cicadae* restored the activity of SOD in hypertensive renal damage (**Figures 5I,K**).

C. cicadae Might Contribute to Renal Fibrosis and Injury via SIRT1/FOXO3a/ROS-Mediated Autophagy

Previous research revealed that *C. cicadae* induced fibrosis and apoptosis in SHRs by inhibiting the SIRT1/p53 pathway. Based on the fact that SIRT1/FOXO3a signaling also plays a major role in autophagy regulation, we investigated whether this pathway is associated with renal fibrosis and hypertension-induced autophagic stress both *in vivo* and *in vitro*. RES, a natural activator of SIRT1 that releases oxidative stress, has been reported in many studies. Consistent with our previous study, we found that RES increased the SIRT1 expression *in vivo* and *in vitro*. In addition, RES treatment upregulated FOXO3a while SIRT1 was activated. These results indicated that AngII suppressed the expression of SIRT1 and FOXO3a on the renal tubular epithelial cells, and the *C. cicadae* treatment reversed the downregulation equal to the RES (**Figures 5A–C**). Similar results were obtained by *in vitro* immunofluorescence, wherein RES or *C. cicadae* application increased the fluorescence intensity of SIRT1 in NRK-52E cells compared with the AngII group (**Figures 5D,F**). The immunofluorescence images showed an upward tendency,

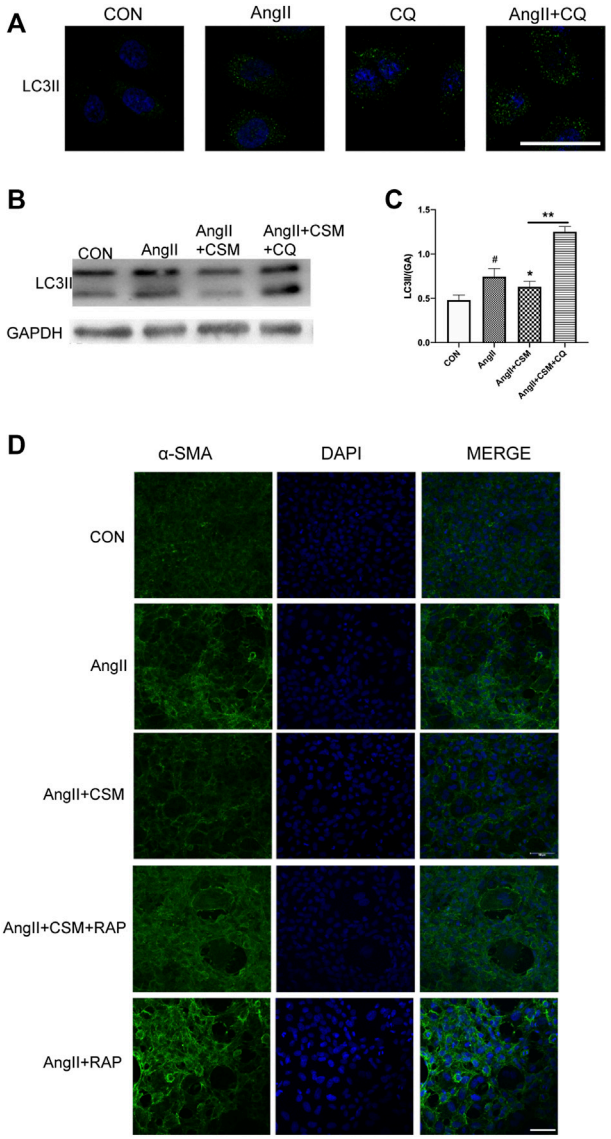

FIGURE 4 | CMS attenuated fibrosis via regulating autophagic stress *in vitro*. **(A)** NRK-52E cells were treated with AngII for 72 h, in the presence or absence of CQ (10 μM). **(B)** CMS regulated autophagic stress. LC3II protein expression was assessed by western blotting. **(C)** Statistical results of LC3II. **(D)** Immunofluorescence images show the levels of α-SMA (green channel) for 72 h. NRK-52E cells were exposed to AngII, with or without CMS and in the presence or absence of RAP (50 nM) for 72 h. The fluorescence intensity was detected with a laser confocal microscope, bar = 20 μm. $^{\#}p < 0.05$: relative to untreated cells. $^{*}p < 0.05$, $^{**}p < 0.01$: relative to the model group.

but no significant change existed in the FOXO3a expression compared with the AngII group ($p > 0.05$) (**Figures 5E,G**). Moreover, detection of the peroxidation levels indicated that RES also downregulated the oxidative stress levels (**Figures 5H–K**). The result indicated that the stimulated SIRT1 and suppressed peroxidation contributed to renal fibrosis and injury. The therapeutic effect of *C. cicadae* was realized through the SIRT1 pathway.

In the current study, the expression of the renal fibrosis-related protein was also evaluated. As shown in **Figure 1**, compared with *C. cicadae*, the RES treatment showed a downward regulation of α-SMA, Col-1, TGFβ1, and FN. Interestingly, western blot and immunostaining analyses revealed that RES and *C. cicadae* significantly disrupted autophagic induction, which is characterized by downregulated LC3II and beclin-1 expression (**Figure 3**) in hypertensive renal injury. Moreover, *C. cicadae* and RES exhibited downregulated levels of p62, indicating autophagic flux restoration (**Figure 3**). These results indicated that *C. cicadae* inhibited fibrosis processing by regulating autophagy in the NRK-52E cells or SHRs equal to RES. In addition, this stimulated SIRT1/FOXO3a and suppressed the oxidative stress levels that contributed to autophagic stress. Therefore, *C. cicadae* might enhance the antifibrotic effects in HN and regulate autophagy by regulating the SIRT1/FOXO3a/ROS signaling pathway.

DISCUSSION

Based on the current findings, our research revealed the antifibrotic and anti-injury effects of *C. cicadae* and its potential mechanisms. The new findings were as follows. (1) *C. cicadae* ameliorated renal injury and kidney fibrosis both *in vitro* and *in vivo*. (2) Autophagic stress existed in hypertensive renal damage. (3) *C. cicadae* suppressed the deposition of ECM markers by the inhibition of autophagic vesicles and the alleviation of autophagy stress. (4) *C. cicadae* regulated autophagy via the SIRT1 pathways, which might be achieved by regulating FOXO3a and oxidative stress. These results highlight a potential therapeutic strategy against hypertensive renal fibrosis and injury by natural medicine.

Hypertension is considered a major risk factor in the development of hypertensive renal injury. RAAS dysregulation contributes to the pathogenesis of cardiovascular and renal disorders. The majority of renal disorders result in renal fibrosis. Previous studies have demonstrated that the proliferation of epithelial and glomerular mesangial cells is stimulated by AngII and induces ECM deposition, which consequently causes additional renal damage (Grace et al., 2012; Ge et al., 2020; Liu et al., 2021). Here, the expression of various tubular injury markers, including KIM-1 and NGAL, was significantly upregulated in the AngII group relative to the control. In addition, AngII promoted ECM deposition, which contributes to fibrosis processing. SHRs provide an opportunity to study essential hypertension, as the natural progression of hypertension and organ damage in SHRs, including in the kidneys, is remarkably similar in humans. A previous study showed that SBP was higher in the SHR group than in the WKY, which was coupled with changes in BP and kidney function indicators (24-h urine albumin and ACR) (Huang X. et al., 2020). These results are supported by the current research that showed that the expression of TGFβ1, α-SMA, FN, and Col-1 was significantly elevated in the SHR group.

Autophagy is a cellular process involving bulk degradation of cytoplasmic components; in addition, its persistent activation is largely involved in renal damage (Bao et al., 2018). Renal fibrosis

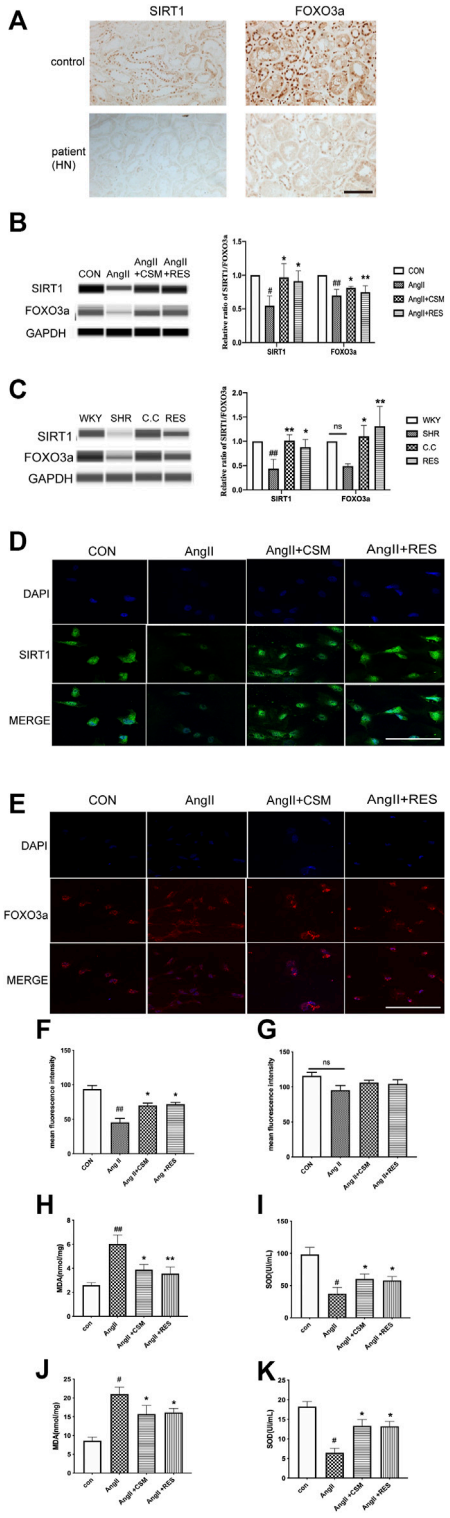

FIGURE 5 | Experimental validation of the SIRT1/FOXO3a/ROS signaling pathways *in vivo* and *in vitro*. **(A)** Downregulated SIRT1 and FOXO3a existed in HN patients (bar = 40 μm). **(B)** Capillary electrophoresis immunoquantification of SIRT1 and FOXO3a on NRK-52E cells in each group. **(C)** Capillary electrophoretic analysis of SIRT1 and FOXO3a expression in the rat renal cortex of various study groups. **(D,E)** CMS regulated SIRT1 (*Continued*)

FIGURE 5 | (green channel) and FOXO3a (red channel) signaling pathways on NRK-52E cells (bar = 20 μm). **(F,G)** Statistical results of immunofluorescence staining of SIRT1 and FOXO3a, respectively. Densitometry was conducted, and the ratio of SIRT1 or FOXO3a to GAPDH was expressed as fold changes relative to the control. **(H,I)** The content of intracellular MDA and SOD in different treatment rats. **(J,K)** The activity of MDA and SOD in different treatment cells. #$p < 0.05$, ##$p < 0.01$: relative to the control group. *$p < 0.05$, **$p < 0.01$: relative to the model group. N.S. No significance.

pertains to the common pathway associated with end-stage renal disease. Previous studies have demonstrated that autophagy in disease pathogenesis is complicated and related to both physiological and pathological regulation (Livingston et al., 2016; Wang et al., 2020). The present study observed a higher number of autophagosomes and autophagic stress existing in cells and rats, which was coupled with ECM deposition in interstitial hypertensive renal injury. However, *C. cicadae* treatment rescued the tubular epithelial cells from fibrosis processing and suppressed autophagic stress. Lysosomal-mediated diffusion systems are a key step of autophagy degradation, and a lysosomal inhibitor was used to examine the lysosomal function *in vitro*. The result suggested that the stability of lysosome was interrupted when exposed to AngII. Further elucidation demonstrated that lysosomal degradation also changed phase in this study. Hence, the activator of autophagy was used to investigate the potential mechanism. Here, we observed that *C. cicadae* downregulates the expression of LC3II and beclin-1 autophagosomal markers, which are two key factors that fuel the autophagic process, and it downregulates the expression of p62. In addition, both previous (Huang YS. et al., 2020) and current investigations revealed the inhibitory effect of *C. cicadae* on α-SMA expression, whereas RAP suppressed renoprotective activity. We considered mediated autophagy as a key point for therapeutic *C. cicadae* administration to inhibit ECM, thus blocking renal fibrosis.

FOXO3a regulates autophagy in various biological characteristics, including inflammation, apoptosis, oxidative stress, and aging (Liu et al., 2017; Fitzwalter and Thorburn, 2018; Galati et al., 2019; Ali et al., 2020; Xu et al., 2021). This activity is regulated by posttranslational modifications, including phosphorylation, acetylation, and ubiquitination (Daitoku et al., 2011). Various combinatorial drug treatments upregulate autophagy-related gene expression in rats via FOXO3a activation (Li et al., 2020; Zhu et al., 2020). Evidence has also indicated that FOXO3a participates in the regulation of lysosomal function (Lu et al., 2014; Carrino et al., 2019). SIRT1 activation also protects against hyperglycemia-induced renal tubular damage via the deacetylation of FOXO3a and the reduction of oxidative stress *in vivo* and *in vitro* (Wang et al., 2017). Natural compound (isoliquiritigenin and dioscin) treatment reduces kidney injury through the SIRT1-dependent mechanism (Song et al., 2019; Huang X. et al., 2020). Here, we observed that *C. cicadae* treatment upregulated SIRT1 and FOXO3a expression and relieved oxidative stress, which in turn regulated autophagy stress that was induced by hypertensive renal injury.

RES, a SIRT1 activator, increased the relative expression of beclin-1 and LC3II, while it decreased p62 expression compared with the untreated control group (Wang et al., 2018; Josifovska et al., 2020). The evidence also demonstrated that RES postponed the development of diabetes by inhibiting autophagy, which included improving cell apoptosis and cellular oxidative stress (Sha et al., 2021). Similar protective effects of RES, namely, reduction of autophagy and the restoration of SIRT1 and FOXO3a levels, were observed in the COPD animal model (Shi et al., 2012). The difference between these studies might be detected using different source cells or animal models. We determined that *C. cicadae* or RES downregulates p62 and disrupts relative expression of beclin-1 and LC3II, indicating that *C. cicadae* controls hypertension-induced autophagic stress by restoring SIRT1 levels in order to inhibit the development of renal fibrosis.

The SIRT1–FOXO3a axis plays a central role in autophagy. An earlier study reported that knocking down SIRT1 enhances cell viability under oxidative stress conditions, triggers nuclear translocation of FOXO3a, and drives FOXO3a acetylation (Han et al., 2016). Moreover, SIRT1 gene silencing disrupts both gAcrp-induced FOXO3a nuclear translocation and LC3II expression (Pun et al., 2015). Our observations are concordant with these viewpoints. For further assessment of the role of FOXO3a, immunofluorescence analysis revealed that the nuclear FOXO3a levels significantly increased compared with cytosolic FOXO3a expression due to its transport from the cytosol to the nucleus following *C. cicadae* treatment. In addition, AngII degraded SIRT1, which in turn increased nuclear translocation of FOXO3a (**Supplementary Figure 1A**), implying that acetylation of FOXO3a might be involved in AngII-induced fibrosis, and the effect of *C. cicadae* might be mediated by the SIRT1/FOXO3a/ROS-dependent pathway.

C. cicadae has been historically used in China for the treatment of CKD. Different biologically active chemical substances, including ergosterol peroxide (EP), N6-(2-hydroxyethyl) adenosine, cordycepic acid, polysaccharides, and effective nucleosides, have been reported (Li et al., 2018). The active components of *C. cicadae* were illustrated using the GC/MS analysis (**Supplementary Figure 2**). *C. cicadae* also had few sides effects, low toxicity, and no chemical substances (**Supplementary Figure 3**). Different from cordyceps (*C. sinensis*), *C. cicadae* belongs to the kidney meridian. It is cold in nature according to the theory of TCM, and it is often used to treat CKD without harming the performance of the kidney. TCM has the advantage of being multi-targeted. Recently, *C. cicadae* has been shown to possess a wide range of pharmacological activities in the kidney, which include renal interstitial fibrosis, anti-apoptosis, anti-inflammatory, antiaging, antioxidative stress, and immunoregulatory effects (Xie et al., 2019; Yang et al., 2020; Zhang X. et al., 2021; Chyau et al., 2021). In our study, *C. cicadae* displayed an advantage for reducing renal fibrosis compared with RES. *C. cicadae* inhibited renal fibrosis progression primarily by decreasing ECM deposition through SIRT1-mediated autophagy. The mechanisms may involve the regulation of FOXO3a and oxidative stress. This study provides novel insights into the correlation between TCM and HN.

CONCLUSION

This study demonstrated the effects of *C. cicadae* on the pathogenesis of HN and elucidated the underlying mechanisms that may be involved in the SIRT1/FOXO3a/ROS pathway. We revealed that *C. cicadae* upregulates SIRT1/FOXO3a expression, suppresses oxidative stress, decreases ECM accumulation, and controls autophagic stress, which in turn inhibits renal fibrosis and ameliorates hypertensive renal injury. Results of our study provide useful information for the treatment of hypertensive renal injury using TCM by regulating autophagy via the SIRT1 pathway.

DATA AVAILABILITY STATEMENT

The original contributions presented in the study are included in the article/**Supplementary Material**, further inquiries can be directed to the corresponding authors.

ETHICS STATEMENT

The studies involving human participants were reviewed and approved by the Affiliated Hospital of Guangdong Medical College. The patients/participants provided their written informed consent to participate in this study. The animal study was reviewed and approved by the Beijing University of Chinese Medicine.

AUTHOR CONTRIBUTIONS

YNL, WJL, and YZC contributed to the conception, design, and drafting of the manuscript. ZDF, QJ, and YZC performed the experiments and analyzed the data. YXW, JG, and PNZ helped optimize the drafting of the manuscript. QHZ helped screen the literature. The final version was approved for submission by all authors. YZC, ZDF, and QJ contributed equally to this work.

FUNDING

This study was supported by the National Natural Science Foundation of China (grant nos. 81373829).

SUPPLEMENTARY MATERIAL

The Supplementary Material for this article can be found online at: https://www.frontiersin.org/articles/10.3389/fphar.2021.801094/full#supplementary-material

Supplementary Figure 1 | (A) Immunofluorescence images show the expression of FOXO3a (green channel) for various times and the location of unclear and cytosolic FOXO3a following AngII treatment (bar = 20 μm).

Supplementary Figure 2 | Quality control of *C. cicadae* was evaluated by HPLC GC/MS analysis.

Supplementary Figure 3 | LC-MS/MS identification of no chemical substances added into *C. cicadae*.

REFERENCES

Aibara, Y., Nakashima, A., Kawano, K. I., Yusoff, F. M., Mizuki, F., Kishimoto, S., et al. (2020). Daily Low-Intensity Pulsed Ultrasound Ameliorates Renal Fibrosis and Inflammation in Experimental Hypertensive and Diabetic Nephropathy. *Hypertension* 76 (6), 1906–1914. doi:10.1161/HYPERTENSIONAHA.120.15237

Ali, T., Rahman, S. U., Hao, Q., Li, W., Liu, Z., Ali Shah, F., et al. (2020). Melatonin Prevents Neuroinflammation and Relieves Depression by Attenuating Autophagy Impairment through FOXO3a Regulation. *J. Pineal Res.* 69 (2), e12667. doi:10.1111/jpi.12667

Bao, J., Shi, Y., Tao, M., Liu, N., Zhuang, S., and Yuan, W. (2018). Pharmacological Inhibition of Autophagy by 3-MA Attenuates Hyperuricemic Nephropathy. *Clin. Sci. Lond.* 132 (21), 2299–2322. doi:10.1042/CS20180563

Carrino, M., Quotti Tubi, L., Fregnani, A., Canovas Nunes, S., Barilà, G., Trentin, L., et al. (2019). Prosurvival Autophagy Is Regulated by Protein Kinase CK1 Alpha in Multiple Myeloma. *Cell Death Discov* 5, 98. doi:10.1038/s41420-019-0179-1

Chen, J., Yu, Y., Li, S., Liu, Y., Zhou, S., Cao, S., et al. (2017). MicroRNA-30a Ameliorates Hepatic Fibrosis by Inhibiting Beclin1-Mediated Autophagy. *J. Cel Mol Med* 21 (12), 3679–3692. doi:10.1111/jcmm.13278

Chen, R. J., Lee, Y. H., Yeh, Y. L., Wang, Y. J., and Wang, B. J. (2016). The Roles of Autophagy and the Inflammasome during Environmental Stress-Triggered Skin Inflammation. *Int. J. Mol. Sci.* 17 (12), 2063. doi:10.3390/ijms17122063

Chen, Y., Zhao, W., Liu, C., Meng, W., Zhao, T., Bhattacharya, S. K., et al. (2019). Molecular and Cellular Effect of Angiotensin 1-7 on Hypertensive Kidney Disease. *Am. J. Hypertens.* 32 (5), 460–467. doi:10.1093/ajh/hpz009

Chyau, C. C., Wu, H. L., Peng, C. C., Huang, S. H., Chen, C. C., Chen, C. H., et al. (2021). Potential Protection Effect of ER Homeostasis of N6-(2-Hydroxyethyl) adenosine Isolated from Cordyceps Cicadae in Nonsteroidal Anti-inflammatory Drug-Stimulated Human Proximal Tubular Cells. *Int. J. Mol. Sci.* 22, 4–1577. doi:10.3390/ijms22041577

Cinque, L., Forrester, A., Bartolomeo, R., Svelto, M., Venditti, R., Montefusco, S., et al. (2015). FGF Signalling Regulates Bone Growth through Autophagy. *Nature* 528, 272–275. doi:10.1038/nature16063

da Silva Cristino Cordeiro, V., de Bem, G. F., da Costa, C. A., Santos, I. B., de Carvalho, L. C. R. M., Ognibene, D. T., et al. (2018). Euterpe Oleracea Mart. Seed Extract Protects against Renal Injury in Diabetic and Spontaneously Hypertensive Rats: Role of Inflammation and Oxidative Stress. *Eur. J. Nutr.* 57 (2), 817–832. doi:10.1007/s00394-016-1371-1

Daitoku, H., Sakamaki, J., and Fukamizu, A. (2011). Regulation of FoxO Transcription Factors by Acetylation and Protein-Protein Interactions. *Biochim. Biophys. Acta* 1813 (11), 1954–1960. doi:10.1016/j.bbamcr.2011.03.001

De Rechter, S., Decuypere, J. P., Ivanova, E., van den Heuvel, L. P., De Smedt, H., Levtchenko, E., et al. (2016). Autophagy in Renal Diseases. *Pediatr. Nephrol.* 31 (5), 737–752. doi:10.1007/s00467-015-3134-2

Deng, J. S., Jiang, W. P., Chen, C. C., Lee, L. Y., Li, P. Y., Huang, W. C., et al. (2020). Cordyceps Cicadae Mycelia Ameliorate Cisplatin-Induced Acute Kidney Injury by Suppressing the TLR4/NF-Kb/MAPK and Activating the HO-1/Nrf2 and Sirt-1/AMPK Pathways in Mice. *Oxid Med. Cel Longev* 2020, 7912763. doi:10.1155/2020/7912763

Eckhart, L., Tschachler, E., and Gruber, F. (2019). Autophagic Control of Skin Aging. *Front Cel Dev Biol* 7, 143. doi:10.3389/fcell.2019.00143

Fitzwalter, B. E., and Thorburn, A. (2018). FOXO3 Links Autophagy to Apoptosis. *Autophagy* 14 (8), 1467–1468. doi:10.1080/15548627.2018.1475819

François, H., Placier, S., Flamant, M., Tharaux, P. L., Chansel, D., Dussaule, J. C., et al. (2004). Prevention of Renal Vascular and Glomerular Fibrosis by Epidermal Growth Factor Receptor Inhibition. *FASEB J.* 18, 926–928. doi:10.1096/fj.03-0702fje

Galati, S., Boni, C., Gerra, M. C., Lazzaretti, M., and Buschini, A. (2019). Autophagy: A Player in Response to Oxidative Stress and DNA Damage. *Oxidative Med. Cell Longevity* 2019, 1–12. doi:10.1155/2019/5692958

Ge, Z., Chen, Y., Wang, B., Zhang, X., Yan, Y., Zhou, L., et al. (2020). MFGE8 Attenuates Ang-II-Induced Atrial Fibrosis and Vulnerability to Atrial Fibrillation through Inhibition of TGF-β1/Smad2/3 Pathway. *J. Mol. Cel Cardiol* 139, 164–175. doi:10.1016/j.yjmcc.2020.01.001

Grace, J. A., Herath, C. B., Mak, K. Y., Burrell, L. M., and Angus, P. W. (2012). Update on New Aspects of the Renin-Angiotensin System in Liver Disease: Clinical Implications and New Therapeutic Options. *Clin. Sci. (Lond)* 123 (4), 225–239. doi:10.1042/CS20120030

Guclu, A., Erdur, F. M., and Turkmen, K. (2016). The Emerging Role of Sirtuin 1 in Cellular Metabolism, Diabetes Mellitus, Diabetic Kidney Disease and Hypertension. *Exp. Clin. Endocrinol. Diabetes* 124, 131–139. doi:10.1055/s-0035-1565067

Guo, J., Zheng, H. J., Zhang, W., Lou, W., Xia, C., Han, X. T., et al. (2020). Accelerated Kidney Aging in Diabetes Mellitus. *Oxidative Med. Cell. longevity* 2020, 1–24. doi:10.1155/2020/1234059

Guzik, T. J., and Touyz, R. M. (2017). Oxidative Stress, Inflammation, and Vascular Aging in Hypertension. *Hypertension* 70 (4), 660–667. doi:10.1161/HYPERTENSIONAHA.117.07802

Han, C., Linser, P., Park, H. J., Kim, M. J., White, K., Vann, J. M., et al. (2016). Sirt1 Deficiency Protects Cochlear Cells and Delays the Early Onset of Age-Related Hearing Loss in C57BL/6 Mice. *Neurobiol. Aging* 43, 58–71. doi:10.1016/j.neurobiolaging.2016.03.023

Hao, C. M., and Haase, V. H. (2010). Sirtuins and Their Relevance to the Kidney. *J. Am. Soc. Nephrol.* 21 (10), 1620–1627. doi:10.1681/ASN.2010010046

Huang, S., You, S., Qian, J., Dai, C., Shen, S., Wang, J., et al. (2021). Myeloid Differentiation 2 Deficiency Attenuates AngII-Induced Arterial Vascular Oxidative Stress, Inflammation, and Remodeling. *Aging (Albany NY)* 13 (3), 4409–4427. doi:10.18632/aging.202402

Huang, X., Shi, Y., Chen, H., Le, R., Gong, X., Xu, K., et al. (2020a). Isoliquiritigenin Prevents Hyperglycemia-Induced Renal Injuries by Inhibiting Inflammation and Oxidative Stress via SIRT1-dependent Mechanism. *Cell Death Dis* 11, 1040. doi:10.1038/s41419-020-03260-9

Huang, Y. S., Wang, X., Feng, Z., Cui, H., Zhu, Z., Xia, C., et al. (2020b). Cordyceps Cicadae Prevents Renal Tubular Epithelial Cell Apoptosis by Regulating the SIRT1/p53 Pathway in Hypertensive Renal Injury. *Evid. Based Complement. Alternat Med.* 2020, 7202519. doi:10.1155/2020/7202519

Jiang, Y., Luo, W., Wang, B., Wang, X., Gong, P., and Xiong, Y. (2020). Resveratrol Promotes Osteogenesis via Activating SIRT1/FoxO1 Pathway in Osteoporosis Mice. *Life Sci.* 246, 117422. doi:10.1016/j.lfs.2020.117422

Josifovska, N., Albert, R., Nagymihály, R., Lytvynchuk, L., Moe, M. C., Kaarniranta, K., et al. (2020). Resveratrol as Inducer of Autophagy, Pro-survival, and Anti-inflammatory Stimuli in Cultured Human RPE Cells. *Int. J. Mol. Sci.* 21 (3)–813. doi:10.3390/ijms21030813

Kobayashi, Y., Furukawa-Hibi, Y., Chen, C., Horio, Y., Isobe, K., Ikeda, K., et al. (2005). Sirt1 Is Critical Regulator of Foxo-Mediated Transcription in Response to Oxidative Stress. *Int. J. Mol. Med.* 16, 237–243. doi:10.3892/ijmm.16.2.237

Lakhani, H. V., Zehra, M., Pillai, S. S., Puri, N., Shapiro, J. I., Abraham, N. G., et al. (2019). Beneficial Role of HO-1-SIRT1 Axis in Attenuating Angiotensin II-Induced Adipocyte Dysfunction. *Int. J. Mol. Sci.* 20 (13), 3205. doi:10.3390/ijms20133205

Li, J. R., Ou, Y. C., Wu, C. C., Wang, J. D., Lin, S. Y., Wang, Y. Y., et al. (2020). Endoplasmic Reticulum Stress and Autophagy Contributed to Cadmium Nephrotoxicity in HK-2 Cells and Sprague-Dawley Rats. *Food Chem. Toxicol.* 146, 111828. doi:10.1016/j.fct.2020.111828

Li, L., Zhang, T., Li, C., Xie, L., Li, N., Hou, T., et al. (2018). Potential Therapeutic Effects of Cordyceps Cicadae and Paecilomyces Cicadae on Adenine-Induced Chronic Renal Failure in Rats and Their Phytochemical Analysis. *Drug Des. Devel Ther.* 13, 103–117. doi:10.2147/DDDT.S180543

Li, Y., Song, B., Ruan, C., Xue, W., and Zhao, J. (2021). AdipoRon Attenuates Hypertension-Induced Epithelial-Mesenchymal Transition and Renal Fibrosis via Promoting Epithelial Autophagy. *J. Cardiovasc. Transl Res.* 14 (3), 538–545. doi:10.1007/s12265-020-10075-8

Lim, J., Lachenmayer, M. L., Wu, S., Liu, W., Kundu, M., Wang, R., et al. (2015). Proteotoxic Stress Induces Phosphorylation of p62/SQSTM1 by ULK1 to

Regulate Selective Autophagic Clearance of Protein Aggregates. *Plos Genet.* 11 (2), e1004987. doi:10.1371/journal.pgen.1004987

Lin, T. A., Wu, V. C., and Wang, C. Y. (2019). Autophagy in Chronic Kidney Diseases. *Cells* 8 (1), 61. doi:10.3390/cells8010061

Liu, J., Feng, Y., Li, N., Shao, Q. Y., Zhang, Q. Y., Sun, C., et al. (2021). Activation of the RAS Contributes to Peritoneal Fibrosis via Dysregulation of Low-Density Lipoprotein Receptor. *Am. J. Physiol. Ren. Physiol* 320 (3), F273–F284. doi:10.1152/ajprenal.00149.2020

Liu, N., Wang, L., Yang, T., Xiong, C., Xu, L., Shi, Y., et al. (2015). EGF Receptor Inhibition Alleviates Hyperuricemic Nephropathy. *J. Am. Soc. Nephrol.* 26, 2716–2729. doi:10.1681/ASN.2014080793

Liu, W., Wang, X., Liu, Z., Wang, Y., Yin, B., Yu, P., et al. (2017). SGK1 Inhibition Induces Autophagy-dependent Apoptosis via the mTOR-Foxo3a Pathway. *Br. J. Cancer* 117 (8), 1139–1153. doi:10.1038/bjc.2017.293

Liu, X., Cai, S., Zhang, C., Liu, Z., Luo, J., Xing, B., et al. (2018). Deacetylation of NAT10 by Sirt1 Promotes the Transition from rRNA Biogenesis to Autophagy upon Energy Stress. *Nucleic Acids Res.* 46 (18), 9601–9616. doi:10.1093/nar/gky777

Livingston, M. J., Ding, H. F., Huang, S., Hill, J. A., Yin, X. M., and Dong, Z. (2016). Persistent Activation of Autophagy in Kidney Tubular Cells Promotes Renal Interstitial Fibrosis during Unilateral Ureteral Obstruction. *Autophagy* 12 (6), 976–998. doi:10.1080/15548627.2016.1166317

Lu, Q., Ma, Z., Ding, Y., Bedarida, T., Chen, L., Xie, Z., et al. (2019). Circulating miR-103a-3p Contributes to Angiotensin II-Induced Renal Inflammation and Fibrosis via a SNRK/NF-κB/p65 Regulatory axis. *Nat. Commun.* 10 (1), 2145. doi:10.1038/s41467-019-10116-0

Lu, Z., Yang, H., Sutton, M. N., Yang, M., Clarke, C. H., Liao, W. S., et al. (2014). ARHI (DIRAS3) Induces Autophagy in Ovarian Cancer Cells by Downregulating the Epidermal Growth Factor Receptor, Inhibiting PI3K and Ras/MAP Signaling and Activating the FOXo3a-Mediated Induction of Rab7. *Cell Death Differ* 21 (8), 1275–1289. doi:10.1038/cdd.2014.48

Martinez-Arroyo, O., Ortega, A., Galera, M., Solaz, E., Martinez-Hervas, S., Redon, J., et al. (2020). Decreased Urinary Levels of SIRT1 as Non-invasive Biomarker of Early Renal Damage in Hypertension. *Int. J. Mol. Sci.* 21, 17–6390. doi:10.3390/ijms21176390

Mizushima, N., and Komatsu, M. (2011). Autophagy: Renovation of Cells and Tissues. *Cell* 147, 728–741. doi:10.1016/j.cell.2011.10.026

Ni, H. M., Du, K., You, M., and Ding, W. X. (2013). Critical Role of FoxO3a in Alcohol-Induced Autophagy and Hepatotoxicity. *Am. J. Pathol.* 183 (6), 1815–1825. doi:10.1016/j.ajpath.2013.08.011

Ornatowski, W., Lu, Q., Yegambaram, M., Garcia, A. E., Zemskov, E. A., Maltepe, E., et al. (2020). Complex Interplay between Autophagy and Oxidative Stress in the Development of Pulmonary Disease. *Redox Biol.* 36, 101679. doi:10.1016/j.redox.2020.101679

Park, J. H., Park, S. A., Lee, Y. J., Joo, N. R., Shin, J., and Oh, S. M. (2020). TOPK Inhibition Accelerates Oxidative Stress-induced G-ranulosa C-ell A-poptosis via the p53/SIRT1 axis. *Int. J. Mol. Med.* 46 (5), 1923–1937. doi:10.3892/ijmm.2020.4712

Pun, N. T., Subedi, A., Kim, M. J., and Park, P. H. (2015). Globular Adiponectin Causes Tolerance to LPS-Induced TNF-α Expression via Autophagy Induction in RAW 264.7 Macrophages: Involvement of SIRT1/FoxO3A Axis. *PloS one* 10 (5), e0124636. doi:10.1371/journal.pone.0124636

Qin, Y. D., Fang, F. M., Wang, R. B., Zhou, J. J., and Li, L. H. (2020). Differentiation between Wild and Artificial Cultivated Stephaniae Tetrandrae Radix Using Chromatographic and Flow-Injection Mass Spectrometric Fingerprints with the Aid of Principal Component Analysis. *Food Sci. Nutr.* 8, 4223–4231. doi:10.1002/fsn3.1717

Sha, W., Liu, M., Sun, D., Qiu, J., Xu, B., Chen, L., et al. (2021). Resveratrol Improves Gly-LDL-Induced Vascular Endothelial Cell Apoptosis, Inflammatory Factor Secretion and Oxidative Stress by Regulating miR-142-3p and Regulating SPRED2-Mediated Autophagy. *Aging (Albany NY)* 13 (5), 6878–6889. doi:10.18632/aging.202546

Shi, J., Yin, N., Xuan, L. L., Yao, C. S., Meng, A. M., and Hou, Q. (2012). Vam3, a Derivative of Resveratrol, Attenuates Cigarette Smoke-Induced Autophagy. *Acta Pharmacol. Sin* 33 (7), 888–896. doi:10.1038/aps.2012.73

Song, S., Chu, L., Liang, H., Chen, J., Liang, J., Huang, Z., et al. (2019). Protective Effects of Dioscin against Doxorubicin-Induced Hepatotoxicity via Regulation of Sirt1/FOXO1/NF-Kb Signal. *Front. Pharmacol.* 10, 1030. doi:10.3389/fphar.2019.01030

Sun, Y., Wink, M., Wang, P., Lu, H., Zhao, H., Liu, H., et al. (2017). Biological Characteristics, Bioactive Components and Antineoplastic Properties of Sporoderm-Broken Spores from Wild Cordyceps Cicadae. *Phytomedicine* 36, 217–228. doi:10.1016/j.phymed.2017.10.004

Tang, B. L. (2016). Sirt1 and the Mitochondria. *Mol. Cell* 39 (2), 87–95. doi:10.14348/molcells.2016.2318

Tao, M., Shi, Y., Tang, L., Wang, Y., Fang, L., Jiang, W., et al. (2019). Blockade of ERK1/2 by U0126 Alleviates Uric Acid-Induced EMT and Tubular Cell Injury in Rats with Hyperuricemic Nephropathy. *Am. J. Physiol. Ren. Physiol* 316, F660–F673. doi:10.1152/ajprenal.00480.2018

Wang, J., Li, J., Cao, N., Li, Z., Han, J., and Li, L. (2018). Resveratrol, an Activator of SIRT1, Induces Protective Autophagy in Non-small-cell Lung Cancer via Inhibiting Akt/mTOR and Activating P38-MAPK. *Onco Targets Ther.* 11, 7777–7786. doi:10.2147/OTT.S159095

Wang, X., Meng, L., Zhao, L., Wang, Z., Liu, H., Liu, G., et al. (2017). Resveratrol Ameliorates Hyperglycemia-Induced Renal Tubular Oxidative Stress Damage via Modulating the SIRT1/FOXO3a Pathway. *Diabetes Res. Clin. Pract.* 126, 172–181. doi:10.1016/j.diabres.2016.12.005

Wang, Y. J., Chen, Y. Y., Hsiao, C. M., Pan, M. H., Wang, B. J., Chen, Y. C., et al. (2020). Induction of Autophagy by Pterostilbene Contributes to the Prevention of Renal Fibrosis via Attenuating NLRP3 Inflammasome Activation and Epithelial-Mesenchymal Transition. *Front. Cel Dev Biol* 8, 436. doi:10.3389/fcell.2020.00436

Wu, F., Li, Z., Cai, M., Xi, Y., Xu, Z., Zhang, Z., et al. (2020). Aerobic Exercise Alleviates Oxidative Stress-Induced Apoptosis in Kidneys of Myocardial Infarction Mice by Inhibiting ALCAT1 and Activating FNDC5/Irisin Signaling Pathway. *Free Radic. Biol. Med.* 158, 171–180. doi:10.1016/j.freeradbiomed.2020.06.038

Xie, H., Li, X., Chen, Y., Lang, M., Shen, Z., and Shi, L. (2019). Ethanolic Extract of Cordyceps Cicadae Exerts Antitumor Effect on Human Gastric Cancer SGC-7901 Cells by Inducing Apoptosis, Cell Cycle Arrest and Endoplasmic Reticulum Stress. *J. Ethnopharmacol* 231, 230–240. doi:10.1016/j.jep.2018.11.028

Xu, D., Liu, L., Zhao, Y., Yang, L., Cheng, J., Hua, R., et al. (2020). Melatonin Protects Mouse Testes from Palmitic Acid-Induced Lipotoxicity by Attenuating Oxidative Stress and DNA Damage in a SIRT1-dependent Manner. *J. Pineal Res.* 69 (4), e12690. doi:10.1111/jpi.12690

Xu, S., Ma, Y., Chen, Y., and Pan, F. (2021). Role of Forkhead Box O3a Transcription Factor in Autoimmune Diseases. *Int. Immunopharmacol* 92, 107338. doi:10.1016/j.intimp.2020.107338

Yang, J., Dong, H., Wang, Y., Jiang, Y., Zhang, W., Lu, Y., et al. (2020). Cordyceps Cicadae Polysaccharides Ameliorated Renal Interstitial Fibrosis in Diabetic Nephropathy Rats by Repressing Inflammation and Modulating Gut Microbiota Dysbiosis. *Int. J. Biol. Macromol* 163, 442–456. doi:10.1016/j.ijbiomac.2020.06.153

Yoon, J. J., Lee, H. K., Kim, H. Y., Han, B. H., Lee, H. S., Lee, Y. J., et al. (2020). Sauchinone Protects Renal Mesangial Cell Dysfunction against Angiotensin II by Improving Renal Fibrosis and Inflammation. *Int. J. Mol. Sci.* 21 (19), 7003. doi:10.3390/ijms21197003

Zhang, J.-h., Li, J., Ye, Y., and Yu, W.-q. (2021a). rAAV9-mediated Supplementation of miR-29b Improve Angiotensin-II Induced Renal Fibrosis in Mice. *Mol. Med.* 27 (1), 89. doi:10.1186/s10020-021-00349-5

Zhang, M., Zhang, Q., Hu, Y., Xu, L., Jiang, Y., Zhang, C., et al. (2017). miR-181a Increases FoxO1 Acetylation and Promotes Granulosa Cell Apoptosis via SIRT1 Downregulation. *Cel Death Dis* 8 (10), e3088. doi:10.1038/cddis.2017.467

Zhang, S. F., Mao, X. J., Jiang, W. M., and Fang, Z. Y. (2020). Qian Yang Yu Yin Granule Protects against Hypertension-Induced Renal Injury by Epigenetic Mechanism Linked to Nicotinamide N-Methyltransferase (NNMT) Expression. *J. Ethnopharmacol* 255, 112738. doi:10.1016/j.jep.2020.112738

Zhang, X., Li, J., Yang, B., Leng, Q., Li, J., Wang, X., et al. (2021b). Alleviation of Liver Dysfunction, Oxidative Stress, and Inflammation Underlines the Protective Effects of Polysaccharides from Cordyceps Cicadae on High Sugar/High Fat Diet-Induced Metabolic Syndrome in Rats. *Chem. biodiversity* 18 (5), e2100065. doi:10.1002/cbdv.202100065

Zheng, H. J., Zhang, X., Guo, J., Zhang, W., Ai, S., Zhang, F., et al. (2020). Lysosomal Dysfunction-Induced Autophagic Stress in Diabetic Kidney Disease. *J. Cel Mol Med* 24 (15), 8276–8290. doi:10.1111/jcmm.15301

Zheng, R., Zhu, R., Li, X., Li, X., Shen, L., Chen, Y., et al. (2018). N6-(2-Hydroxyethyl) Adenosine from Cordyceps Cicadae Ameliorates Renal Interstitial Fibrosis and Prevents Inflammation via TGF-β1/Smad and NF-Kb Signaling Pathway. *Front. Physiol.* 9, 1229. doi:10.3389/fphys.2018.01229

Zhu, Y., Ding, A., Yang, D., Cui, T., Yang, H., Zhang, H., et al. (2020). CYP2J2-produced Epoxyeicosatrienoic Acids Attenuate Ischemia/reperfusion-Induced Acute Kidney Injury by Activating the SIRT1-FoxO3a Pathway. *Life Sci.* 246, 117327. doi:10.1016/j.lfs.2020.117327

Conflict of Interest: The authors declare that the research was conducted in the absence of any commercial or financial relationships that could be construed as a potential conflict of interest.

Publisher's Note: All claims expressed in this article are solely those of the authors and do not necessarily represent those of their affiliated organizations, or those of the publisher, the editors and the reviewers. Any product that may be evaluated in this article, or claim that may be made by its manufacturer, is not guaranteed or endorsed by the publisher.

frontiers in Pharmacology

ORIGINAL RESEARCH
published: 11 February 2022
doi: 10.3389/fphar.2022.819787

Atorvastatin Restores PPARα Inhibition of Lipid Metabolism Disorders by Downregulating miR-21 Expression to Improve Mitochondrial Function and Alleviate Diabetic Nephropathy Progression

Jiayi Xiang[1,2,3], *Huifang Zhang*[1,2,3], *Xingcheng Zhou*[1,2,3], *Dan Wang*[1,2,3], *Rongyu Chen*[1,2,3], *Wanlin Tan*[1,2], *Luqun Liang*[1,2,3], *Mingjun Shi*[1,2,3], *Fan Zhang*[1,2,3], *Ying Xiao*[1,2,3], *Yuxia Zhou*[1,2,3], *Yuanyuan Wang*[1,2,3]* *and Bing Guo*[1,2,3]*

[1]State Key Laboratory of Functions and Applications of Medicinal Plants, Guizhou Medical University, Guiyang, China, [2]Department of Pathophysiology, Guizhou Medical University, Guizhou, China, [3]International Scientific and Technological Cooperation Base of Pathogenesis and Drug Research on Common Major Diseases, Guizhou Medical University, Guizhou, China

OPEN ACCESS

Edited by:
Zhiyong Guo,
Second Military Medical University, China

Reviewed by:
Milton Prabu,
Annamalai University, India
Hong-Ping Guan,
Rezubio Pharmaceuticals Co. Ltd, China

***Correspondence:**
Yuanyuan Wang
Yuan.yuan.wang.@outlook.com
Bing Guo
Guobingbs@126.com

Specialty section:
This article was submitted to Renal Pharmacology, a section of the journal Frontiers in Pharmacology

Received: *22 November 2021*
Accepted: *05 January 2022*
Published: *11 February 2022*

Citation:
Xiang J, Zhang H, Zhou X, Wang D, Chen R, Tan W, Liang L, Shi M, Zhang F, Xiao Y, Zhou Y, Wang Y and Guo B (2022) Atorvastatin Restores PPARα Inhibition of Lipid Metabolism Disorders by Downregulating miR-21 Expression to Improve Mitochondrial Function and Alleviate Diabetic Nephropathy Progression. Front. Pharmacol. 13:819787. doi: 10.3389/fphar.2022.819787

Atorvastatin is a classical lipid-lowering drug. It has been reported to have renoprotective effects, such as reducing urinary protein excretion and extracellular matrix aggregation. The present study aimed to investigate the specific mechanism of action of Atorvastatin in type 1 diabetic mice (T1DM) in inhibiting renal tubular epithelial cell injury following treatment with high glucose and high fat. The anti-injury mechanism of Atorvastatin involved the inhibition of miR-21 expression and the upregulation of the transcription and expression of its downstream gene Peroxisome proliferator-activated receptors-α(PPARα). An increase in blood glucose and lipid levels was noted in the T1DM model, which was associated with renal fibrosis and inflammation. These changes were accompanied by increased miR-21 levels, downregulation of PPARα and Mfn1 expressions, and upregulation of Drp1 and IL6 expressions in renal tissues. These phenomena were reversed following the administration of Atorvastatin. miR-21 targeted PPARα by inhibiting its mRNA translation. Inhibition of miR-21 expression or Fenofibrate (PPARα agonist) administration prevented the decrease of PPARα in renal tubular epithelial cells under high glucose (HG) and high fat (Palmitic acid, PA) conditions, alleviating lipid metabolism disorders and reducing mitochondrial dynamics and inflammation. Consistent with the *in vivo* results, the *in vitro* findings also demonstrated that mRTECs administered with Atorvastatin in HG + PA increased PPARα expression and restored the normal expression of Mfn1 and Drp1, and effectively increasing the number of biologically active mitochondria and ATP content, reducing ROS production, and restoring

Abbreviations: DKD, Diabetic kidney disease; RTECs, Renal tubular epithelial cells; PPARα, Peroxisome proliferator-activated receptors-α; FN, Fibronectin; Mfn1, Mitofusin1; Drp1, dynamin-like protein 1; IL-6, Interleukin-6; STZ, Streptozocin; FA, Fatty acids; T1D, Type 1 diabetes; PAS, Periodic acid-Schiff; DMEM, Dulbecco's modified Eagle's medium; FBS, Fetal bovine serum; NG, Normal glucose; HG, High glucose; PA, Palmitic acid; α-SMA, α-smooth muscle actin; Col III, Collagen III.

mitochondrial membrane potential following Atorvastatin intervention. In addition, these effects were noted to the inhibition of FN expression and tubular cell inflammatory response; however, in the presence of miR-21mimics, the aforementioned effects of Atorvastatin were significantly diminished. Based on these observations, we conclude that Atorvastatin inhibits tubular epithelial cell injury in T1DM with concomitant induction of lipid metabolism disorders by a mechanism involving inhibition of miR-21 expression and consequent upregulation of PPARα expression. Moreover, Atorvastatin regulated lipid metabolism homeostasis and PPARα to restore mitochondrial function. The results emphasize the potential of Atorvastatin to exhibit lipid-regulating functions and non-lipid effects that balance mitochondrial dynamics.

Keywords: atorvastatin, miR-21, PPARα, fenofibrate, mitochondrial dynamics, diabetic kidney disease, lipid metabolism disorders

INTRODUCTION

In 2019, the International Diabetes Federation (IDF) predicted that the global prevalence of diabetes will be 9.3% (463 million people). This incidence is predicted to rise to 10.2% (578 million people) by 2030 and to 10.9% (700 million people) by 2045. As one of the most common microvascular complications of diabetes, diabetic nephropathy (DN) is a major cause of the end-stage renal disease (ESRD) (Saeedi et al., 2019). Diabetic kidney disease (DKD) has been a difficult clinical problem to treat, and intensive glycemic control can only reduce but not eradicate the progression of the disease. It has been found that patients with diabetes mellitus usually have abnormal glucose metabolism along with abnormal lipid metabolism. Dyslipidemia is a significant risk factor for the development of DN (Herman-Edelstein et al., 2014).

As a highly perfused organ, the renal tubules are the main site of transmembrane transport of substances in the kidney, and therefore abundant mitochondria are present in the tubular epithelial cells (Bhargava and Schnellmann, 2017). The participation of oxygen allows mitochondria to synthesize large amounts of ATP through oxidative phosphorylation to ensure the energy supply of the renal tubules. Mitochondrial dynamics is the process of determining the length, shape, and size of mitochondria. Mitochondria are dynamic organelles that adapt to cellular energy demands through morphological changes. Mitochondria regulate their morphology through fusion and fission, which is further regulated mainly by the balance between mitochondrial fission and fusion factors. These factors are essential for the repair of damaged mitochondrial components, allowing the exchange of materials between damaged and undamaged mitochondria through the fusion process, or the separation of damaged components through the fission process. This process maintains appropriate mitochondrial dynamics, which is essential for their normal function (Chen and Chan, 2004; Jheng et al., 2012). Mitochondria are also one of the main sources of the production of cellular ROS. Damaged mitochondria can substantially increase ROS production, leading to oxidative stress and tissue damage (Yu et al., 2006; Gerber and Rutter, 2017). Persistent mitochondrial dysfunction plays an important role in the progression of renal diseases, such as acute kidney injury (AKI) and diabetic nephropathy. It has been reported that hyperglycemia increases the production of NADH and FADH2 through the tricarboxylic acid cycle, while it promotes the mitochondrial electron transport chain (ETC), and releases ROS, which impairs and blocks the expression of proteins that affect mitochondrial function (Simon and Hertig, 2015; Coughlan and Sharma, 2016). This ultimately leads to the development of DKD. Therefore, improving mitochondrial dynamics and restoring their function has the potential to restore renal function.

Statins are a class of clinical hypolipidemic agents that reduce cholesterol biosynthesis by inhibiting the activity of 3-hydroxy-3-methyl-Glu-Daryl (HMG)-CoA reductase 6. This results in lowering lipid levels (Kogawa et al., 2019). A clinical study (Athyros et al., 2015) indicated that statin therapy reduced the rate of proteinuria and renal function loss. Recently, several studies have shown that statins can regulate the expression of miRNAs. For example, Atorvastatin treatment reduced the expression levels of miR-29b, miR-214, and miR-36-3p in human umbilical vascular endothelial cells after the establishment of an *in vitro* atherosclerotic cell model (Jia et al., 2019). Atorvastatin also downregulated miR-21 expression in a rat model of bile duct ligation (BDL)-induced liver fibrosis (Nozari et al., 2020). Furthermore, one study demonstrated that Atorvastatin protected the kidneys of diabetic rats by inhibiting the expression of inflammatory factors (Liao et al., 2016). Although accumulating evidence has demonstrated the potential benefit of statins in diabetic nephropathy, the exact mechanism has not been fully elucidated. In the present study, we investigated whether Atorvastatin was involved in delaying diabetic kidney fibrosis via inhibition of miR-21 expression.

Peroxisome proliferator-activated receptor-α (PPARα) is a ligand-dependent nuclear receptor that can be activated by exogenous compounds, such as fibrates, or by endogenous ligands, including fatty acids and prostaglandins. It is an important transcriptional regulator of genes involved in peroxisome and mitochondrial β-oxidation, FA transport, and hepatic gluconeogenesis, with important antioxidant, anti-inflammatory, and antiapoptotic roles (Xu et al., 2002). In addition, PPARα is involved in the activation of autophagy

and mitochondrial homeostasis in mice infected with *Mycobacterium avium* via nuclear-mitochondrial interactions (Kim et al., 2019). It has been reported in the literature that miR-21 was found to inhibit the expression of PPARα in both cardiac tissue (Chuppa et al., 2018) and Hela cells (Zhou et al., 2011). The predicted results were analyzed by the bioinformatics website Targetscan and indicated that the seed sequence of miR-21 (5′-AGCUUA-'3) was complementary to the 3′UTR sequence of human PPARα mRNA (5′-UAAGCU-3′). It remains unclear whether miR-21 acts on PPARα and affects lipid metabolism disorders and mitochondrial dynamics, which are involved in the course of DKD.

In the present study, we demonstrated that Atorvastatin could inhibit DKD fibrosis by inhibiting miR-21 expression. Moreover, it was able to restore the levels of PPARα, which is a key transcription factor that regulates lipid metabolism, and improve mitochondrial dynamics.

MATERIALS AND METHODS

Chemicals and Antibodies

The primary antibodies used against the proteins were as follows: Anti-actin (1:1,000), obtained from PumeiBiotechnology (Pumei, China); anti-fibronectin (1:1,000), anti-collagen-I (1:1,000), anti-α-smooth muscle actin (α-SMA, 1:1000), anti-interleukin 6 (IL-6,1:1000), anti-PPARα (1:1000 for Western blot, 1:100 for immunohistochemical staining), anti-CPT1a (1:1,000), anti-Mfn1 ((1:1,000 for Western blot, 1:100 for immunohistochemical staining) and anti-Drp1, which were obtained from ProteintechGroup (Proteintech, China);

Animal Models

The T1DM model was established in C57 black mouse (4–6weeks, 18–22 g,males) (Liaoning Changsheng Biotechnology Co. Ltd., Liaoning, China). The animals were randomly divided into the normal control (NC) group (n = 6) and the DM group (n = 12). The mice of the DM group were intraperitoneally injected with 55 mg/kg streptozotocin (STZ, Sigma); the mice in the NC group were injected with the same amount of pH 4.5 sterile citric acid-sodium citrate buffer (lysozyme) for five consecutive days. Fasting blood glucose levels in mice were assessed at 72 h following treatment, and values ≥16.7 mmol/l indicated that DM mice were successfully established. Following 5 weeks of feeding, the diabetic mice were randomized into the diabetic group (n = 6) and Ato group (DM + Ato) (n = 6). Atorvastatin was administered at 20 mg/(kgd) (Pfizer, China) to the Ato group for 4 weeks. The NC and DM groups were intragastrically administered with carboxymethyl cellulose for 4 weeks. The mouse kidneys were collected at the ninth week. Urine samples were obtained and measured in the 24-h period preceding euthanasia. All mice had fasted 6 h prior to sacrifice. Blood specimens were collected from the femoral artery and centrifuged for serum preparation. The samples were kept at −20°C for biochemical assessment. Both kidneys were removed, of which one was stored at −80°C (RNA and protein preparations) and the other used for fixation with 4% formalin and subsequent histological and immunohistochemical evaluations. All animal studies complied with the regulations and guidelines of Guizhou Medical University institutional animal care and followed the AAALAC and IACUC guidelines. The approval form for Animal Experimentation Ethics Group of Guizhou Medical University certificate number (No. 1602230).

Cell Culture and Transfection

Mouse renal tubular epithelial cells (mRTECs) were obtained from the Cell Bank of the Type Culture Collection, Shanghai Institute of Cell Biology, Chinese Academy of Sciences. The cells were maintained in Dulbecco's modified Eagle's medium (DMEM; Gibco, USA) supplemented with 10% fetal bovine serum (FBS; Gibco) and 5.5 mM glucose, in an incubator containing 5% CO_2 at 37°C.

Cell proliferation was performed in the presence of normal glucose levels (NG; 5.5 mM), high glucose levels (HG; 30 mM), palmitic acid (PA; 0.2 mM), and high glucose levels with palmitic acid (HG 30 mM + PA 0.2 mM), which were supplemented with 2% FBS. mRTECs were transiently transfected with Lipofectamine 3,000 (Invitrogen, USA) based on the manufacture's protocol. The relevant cell groups were treated with Atorvastatin (Ato; 10 μM; Pfizer, China) or Fenofibrate (a PPARα agonist; 25μM; APExBIO, USA). Si-PPARα was purchased from Longqian Biotech (China).

HK-2 cells were purchased from the American Type Culture Collection (ATCC®, Rockefeller, Maryland, USA) and cultured in Dulbecco's modified Eagle medium/nutrient mixture F-12 (DMEM/F-12, Gibco, Grand Island, NY, USA) containing 10% fetal bovine serum (FBS, Gibco, USA) with 5% CO2 at 37°C. The cells in the logarithmic phase were used for subsequent experiments using the Luciferase reporter assay.

Transfection of miR-21 Mimics or Inhibitor

miR-21 mimics, miR-21 inhibitor and their controls (Ribobio, China) were separately transfected into mRTECs and HK-2 cells. The procedure of transfection of miRNA mimics or inhibitors was performed as previously described.

Biochemical Assays

Blood and urine specimens of mice were sent to Guiyang Jinwei (China) for detection of glucose, cholesterol, urea nitrogen, triglyceride, creatinine and 24 h urine microalbumin (mg/24 h). The 24 h urine microalbumin (mg/24 h) was assessed as follows: Microalbumin (mg/ml) × urine volume (ml)/24 h. The total Superoxide Dismutase (T-SOD) assay kit and the Malondialdehyde (MDA) assay kit of the mice were obtained from Nanjing Jiancheng Bioengineering Institute (Njjcbio, China). The assay was performed as described by the manufacturer.

Histology and Immunohistochemical Staining

The paraffin sections of the kidney tissue samples were harvested. The resulting sections underwent staining with Hematoxylin-eosin (Solarbio, China), periodic acid-Schiff (Solarbio, China)

TABLE 1 | Primers used in qRT-PCR.

Gene	Sequence
PPARα-mouse	Forward: 5′-AAAAGAATCCCCAGCTTATCCA-3′
	Reverse: 5′-TTGGTGACTTCCCCTAGGTATA-3′
GAPDH-mouse	Forward: 5′-GAACGGGAAGCTCACTGG-3′
	Reverse: 5′-GCCTGCTTCACCACCTTCT-3′
ACOX1-mouse	Forward: 5′-GGCTTTGGTGGATGCCTTTG-3′
	Reverse: 5′-GGACTTCTTGCCCACTCAA-3′
CPT1a-mouse	Forward: 5′-CGGCAGACCTATTTTGCACG-3′
	Reverse: 5′-TAGATGCCTCAGGGTCCTCC-3′

and sirius red staining (BestBio, China) reagents according to corresponding recommended protocols. Diaminobenzidine (DAB) color developing kit (ZSGB-BIO, Beijing, China) and hematoxylin were used for immunohistochemical staining. The areas of positive staining were quantified by ImageJ in six random fields (200×) per sample, with three individuals assessed in each group.

Western Blot Analysis

The kidney tissue and cell samples were lysed with RIPA buffer (R0020; Solarbio, China) and total protein amounts were determined with the BCA kit (PC0020; Solarbio). Following addition of the corresponding loading buffer (P1040 or P1019; Solarbio), the mixture was incubated for 10 min in boiling water. Equal amounts of total protein were resolved by SDS-PAGE and electro-transferred onto PVDF compound membranes (Millipore, USA) treated with methanol. Following blocking with 5% nonfat milk for 1 h at room temperature, the membranes were incubated with a primary antibody overnight at 4°C, and subsequently with horseradish peroxidase-conjugated secondary antibody for 1 h at room temperature. Finally, the ECL solution was added, and a Bio-Rad gel imaging system (Bio-Rad, USA) was employed for analysis.

Real Time-Quantitative PCR

Total RNA was purified from kidneys and cells with TRIzol reagent (Invitrogen, USA) as described by the manufacturer. The Bulge-Loop™ miRNA qRT-PCR primer kit (Ribobio, China) was used to assess miR-21 expression levels. In addition, qPCR was carried out with SuperReal PreMix (SYBR Green) (Tiangen, China) and iQ SYBR Green SuperMix (Bio-Rad). The gene expression levels were normalized to those of GADPH or U6. The Bulge-Loop™ RT primer and qPCR primers specific for miR-21 and U6 genes were designed and synthesized by RiboBio (RiboBio, China). The $2-\Delta\Delta Ct$ method was employed for quantification. The sequences of the other primers used are described in **Table 1**.

The PPARα-promoter luciferase reporter was constructed by Longqian Biotech (China). Actively proliferating HK-2 cells were trypsinized and seeded in plates at a suitable density for routine culture. Following 24 h of incubation, transfection was carried out with Lipofectamine 3,000 (Invitrogen) as directed by the manufacturer for 48 h. This was followed by cell lysis and sample analysis with a Dual-Luciferase Reporter Assay System (E1960; Promega, USA). Renilla and Firefly luciferase activities were measured, and the ratio of Renilla luciferase activity to that of Firefly luciferase was derived. Triplicate experiments were independently repeated 3 times.

Measurement of ATP Levels, ROS Production, Mitochondrial Membrane Potential, and Active Mitochondria

ATP was measured using an ATP Assay kit (Beyotime Biotechnology, China) as determined by the manufacturer's instructions. The luminescence produced was measured with a luminometer counter (perkin-elmer, Waltham, MA and United States), and the concentration of ATP was calculated using an ATP standard curve.

Mitochondrial membrane and intracellular ROS were measured using the relevant assay kit (MedChemExpress,USA) as determined by the manufacturer's instructions. Flow cytometry was performed on the NovoCyte Flow Cytometer (3,130; ACEA, China) and the data were analyzed by FlowJo software (Treestar, Ashland, OR, USA).

The active mitochondria in the primary cardiomyocytes were labeled with MitoTracker Red CMXRos probe (Beyotime Biotechnology, China) and imaged using a confocal laser-scanning microscope (Olympus + Confocal Microscope).

Statistical Analysis

The assays were performed at least 3 times independently, and the animal experiments exhibited six samples per group. The data are indicative of mean ± standard deviation (SD). The unpaired Student t-test and the one-way analysis of variance (ANOVA) were carried out for group pair and multiple group comparisons, respectively. Spearman (nonparametric) correlation analysis was performed to evaluate the association of PPARα expression with miR-21. SPSS 22 was used for data analysis. $p < 0.05$ was considered to indicate statistical significant differences.

RESULTS

Atorvastatin Improves Renal Fibrosis and Restores Renal Function in Diabetic Mice

Diabetic mice indicated a significant increase in blood glucose levels and were characterized by a significant increase in renal function-related parameters (urea nitrogen, creatinine, and microalbuminuria) compared with age-matched non-diabetic control mice. The mice treated with Atorvastatin [20 mg/(kg-d)] for 4 weeks indicated no significant change in blood glucose levels (**Figure 1A**), whereas a significant decrease was noted in urea nitrogen and creatinine levels, as well as in the incidence of microalbuminuria (**Figures 1B–D**). H&E, PAS, and Sirius red staining indicated lymphocyte infiltration, thylakoid zone expansion, glomerular hypertrophy, tubular vacuole formation, and periglomerular fibrosis. In the Atorvastatin group, the lymphocyte infiltration was reduced, the thylakoid expansion fraction was decreased, and the fibrosis was significantly reduced (**Figures 1E–J**). The levels of fibronectin, collagen-I, α-SMA, and IL-6 were increased in the kidneys of DM mice compared with those of the control group. In contrast to these findings, the

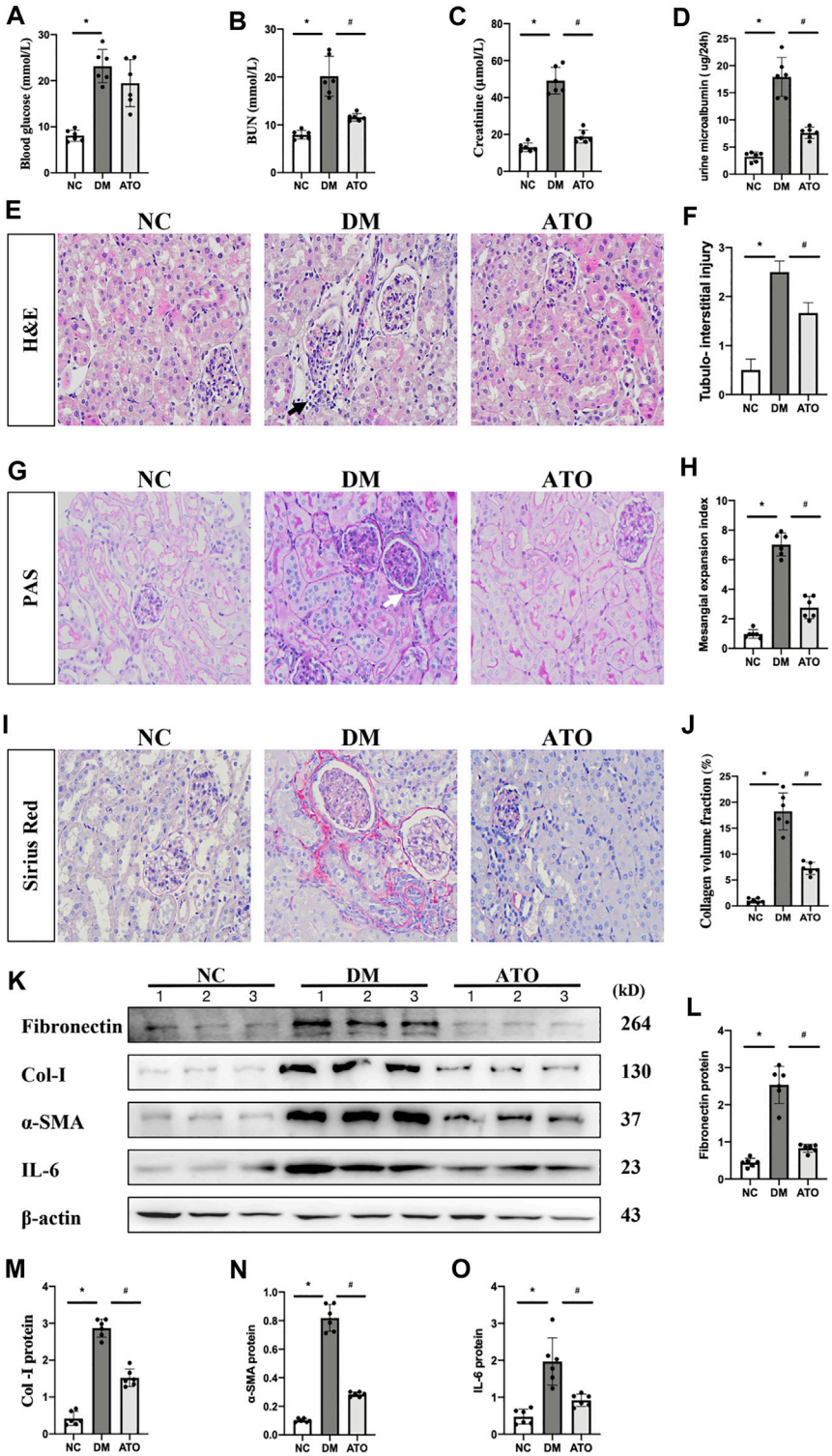

FIGURE 1 | Atorvastatin improves renal fibrosis and restores renal function in diabetic mice. Effects of Atorvastatin on blood glucose, renal function, and fibrotic lesions in diabetic mice. **(A)** The blood glucose levels in the DM group were significantly higher than those in the control group, while no statistically significant difference was noted in the Atorvastatin group. The renal urea nitrogen **(B)**, serum creatinine **(C)**, and 24-h total urine microalbumin **(D)** levels were measured. H&E staining **(E)** was performed to observe the renal pathological changes in mice and to assess the tubular injury index **(F)**. PAS staining **(G)** was performed to assess the thylakoid expansion index **(H)**. Sirius red staining **(I)**, collagen deposition fraction **(J)**. Black arrows indicate the site of lymphocyte infiltration; white arrows indicate the glomerular basement membrane. Immunoblotting bands **(K)** and quantitative data **(L–O)** of FN, PPARα, Mfn1, Drp1, and IL-6 in each group of mice. All images are magnified ×200. NC: normal diet-fed rats; DM: type 1 diabetic mice; ATO: type 1 diabetic mice treated with Atorvastatin. All data are presented as mean ± SD from three independent experiments. n = 6; *$p < 0.05$ vs. NC group. #$p < 0.05$, compared with the DM group.

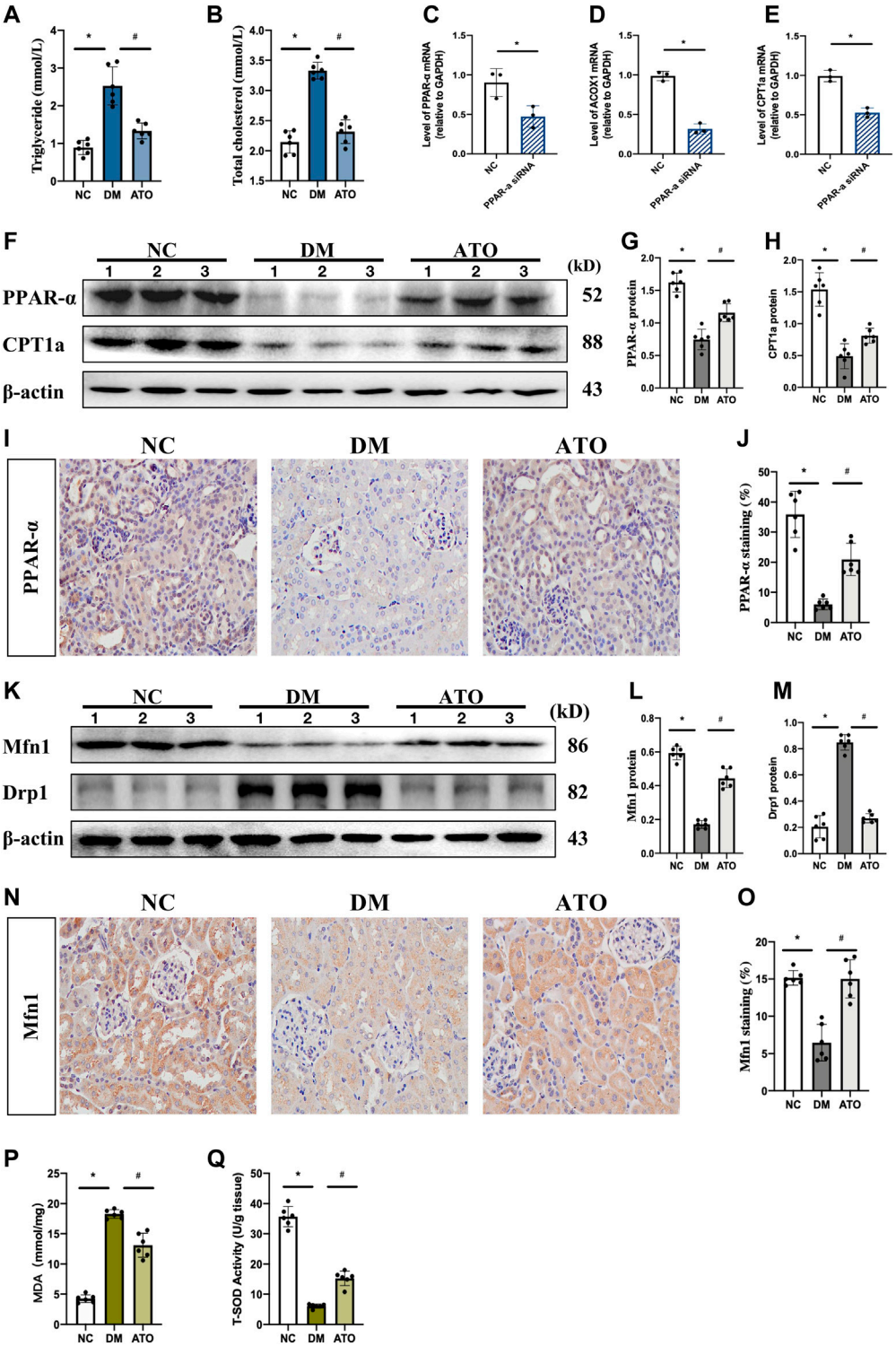

FIGURE 2 | Atorvastatin restores PPARα expression and improves lipid metabolism and mitochondrial dysfunction in diabetic mice. Atorvastatin improves renal fibrosis and restores renal function in diabetic mice. The effects of Atorvastatin in blood. The experiments aimed to detect the changes in lipid metabolism and mitochondria-related indicators in each group. **(A, B)** Quantification of triglycerides **(A)** and total cholesterol **(B)** in three groups of kidney tissues. **(C–E)** Transfection of si-PPARα and its control sequence into mRTECs cells. qPCR was performed to detect the expression levels of PPARα **(C)**, and its downstream target genes ACOX1 **(D)** and CPT1a **(E)**. **(F–G)** Immunoblot analysis of PPARα, CPT1a in the three groups of kidney tissues, presenting quantitative data **(G, H)**. **(I–J)** Immunohistochemical staining **(I)**, and quantitative analysis **(J)** of PPARα. **(K–M)**. Immunoblotting for the detection of Mfn1 and Drp1 expression **(K)** and quantitative

(*Continued*)

FIGURE 2 | analysis of the results **(L, M)**. **(N–O)** Immunohistochemical staining **(N)**, and quantitative analysis **(O)** of Mfn1. **(P, Q)** Detection of malondialdehyde (MDA) content **(P)** and total superoxide dismutase (T-SOD) content **(Q)** in the three groups of kidney tissues. The *in vivo* experiments included the following groups: NC: normal diet-fed rats; DM: type 1 diabetic mice; ATO: type 1 diabetic mice treated with Atorvastatin. All data are indicative of mean ± SD from three independent experiments. n = 6; $*p < 0.05$ vs NC group. $\#p < 0.05$, compared with the DM group.

expression levels of the aforementioned proteins were decreased in the Atorvastatin group (**Figures 1K–O**).

Atorvastatin Restores PPARα Expression and Improves Lipid Metabolism and Mitochondrial Dysfunction in Diabetic Mice

The data indicated that plasma triglycerides and total cholesterol levels were significantly increased in DM mice, while the levels of these markers were significantly decreased in the ATO group. The kidney is a metabolically active tissue that uses fatty acids (FA) as a major energy source, PPARα, a key transcription factor of the fatty acid oxidation (FAO) pathway, can ameliorate the development of renal fibrosis (Wang, 2010; Su et al., 2020). The data indicated that the mRNA levels of carnitine palmitoyltransferase 1a (CPT1a) and acyl-coenzyme A oxidase 1 (ACOX1), which are genes related to lipid metabolism and play an important role in FA synthesis and TG accumulation, were significantly reduced following *in vitro* knockdown of PPARα expression (**Figures 2C–E**). *In vivo* experiments indicated that the levels of PPARα and CPT1a proteins were significantly reduced in the kidneys of DM mice. IHC further confirmed the decrease in PPARα levels, which was mainly expressed in the nucleus of renal tubular epithelial cells. Its expression was restored following administration of Atorvastatin (**Figures 2I,J**). These data combined with the results of the biochemical indices demonstrated that DM mice had developed lipid metabolism disorders, and that Atorvastatin could effectively improve these lipid metabolism disorders caused by insulin deficiency.

Mfn1 promotes mitochondrial fusion and maintains ATP production, while Drp1 mediates mitochondrial separation (Galvan et al., 2017). Both of the proteins are regulated by PPARα (Zolezzi et al., 2013). In the DM group, Mfn1 expression was decreased and Drp1 was increased. Following administration of Atorvastatin, the expression levels of Mfn1 were increased and those of Drp1 were decreased (**Figures 2K–M**). IHC results further indicated that Mfn1 expression in each group was mainly located in the cytoplasm of renal tubular epithelial cells (**Figures 2N,O**). These findings suggested that Atorvastatin could balance mitochondrial dynamics. The changes in mitochondrial dynamic can directly affect mitochondrial function, while ROS and total antioxidant capacity can reflect mitochondrial function to a certain extent. The levels of malondialdehyde (MDA) and total superoxide dismutase (T-SOD) represent the degree of lipid peroxidation and the antioxidant capacity of the cell under free radical attack, respectively. An increase in MDA levels and a decrease in antioxidant capacity was noted in the kidney tissues of DM mice (**Figures 2P,Q**), while MDA levels were decreased and the antioxidant capacity was increased in the ATO group. It was suggested that Atorvastatin could improve mitochondrial function and reduce the production of ROS and its peroxidative effects.

PPARα is a Downstream Target Gene of miR-21, and Their Expression Levels are Negatively Correlated With the Progression of DKD

Bioinformatic analysis predicted that the seed sequence of miR-21 was complementary to the 3′ UTR sequence of PPARα mRNA (**Figure 3C**). In our previous study, it was shown that miR-21 expression was significantly increased in the DKD process and promoted fibrotic lesions in the renal tubular interstitium (Liu et al., 2019). In the present study, we detected a significant decrease in the protein (**Figure 2F**) and mRNA expression levels (**Figure 3B**) of PPARα. These changes were accompanied by a significant upregulation of miR-21 (**Figure 3A**) in the kidney tissues of DM mice, while Atorvastatin intervention significantly upregulated the protein and mRNA expression of PPARα and downregulated its miR-21 expression. The experiments further verified that PPARα was the target gene of miR-21 by the dual-luciferase reporter assay, and the results indicated that miR-21 could regulate PPARα mRNA levels. When the cells were transfected with wild-type vector WT-PPARα in HK-2 cells, the luciferase activity in the miR-21 group was significantly lower than that in the miR-NC group. However, when the cells were transfected with mutant vector MUT-PPARα, the luciferase activity in the miR-21 group was not statistically significant compared with that of the miR-NC group (**Figure 3D**). In addition, transfection of miR-21 mimics into HK-2 cells resulted in a significant decrease in PPARα protein levels (**Figures 3E,F**). Correlation analysis indicated that miR-21 expression demonstrated a negative correlation with PPARα protein expression (**Figure 3G**). This is consistent with the findings noted in human liver and diabetic eye disease mice [32], indicating that PPARα is a target gene of miR-21.

The miR-21 Inhibitor and Fenofibrate, an Exogenous Ligand of PPARα, Inhibit High-Glucose, High-Fat, and High-Glucose High-Fat-Mediated Renal Tubular Epithelial Cell Injury

mRTEC cells were cultured with high glucose (HG) medium to assess the effects of the DM-induced high glucose environment on renal tubular cells. RTEC cells were cultured with high concentrations of palmitate (PA) to investigate the effects of DM-induced high fat environment on renal tubular cells. The cells were treated with transfected miR-21 inhibitor and the PPARα-specific agonist Fenofibrate, respectively. The results indicated that the protein levels of FN, IL-6, and Drp1 were increased in the cells cultured under HG and PA conditions, while the protein levels of PPARα and Mfn1 were decreased compared with those of the control group. However, following inhibition of miR-21 expression, the expression levels of FN, IL-6,

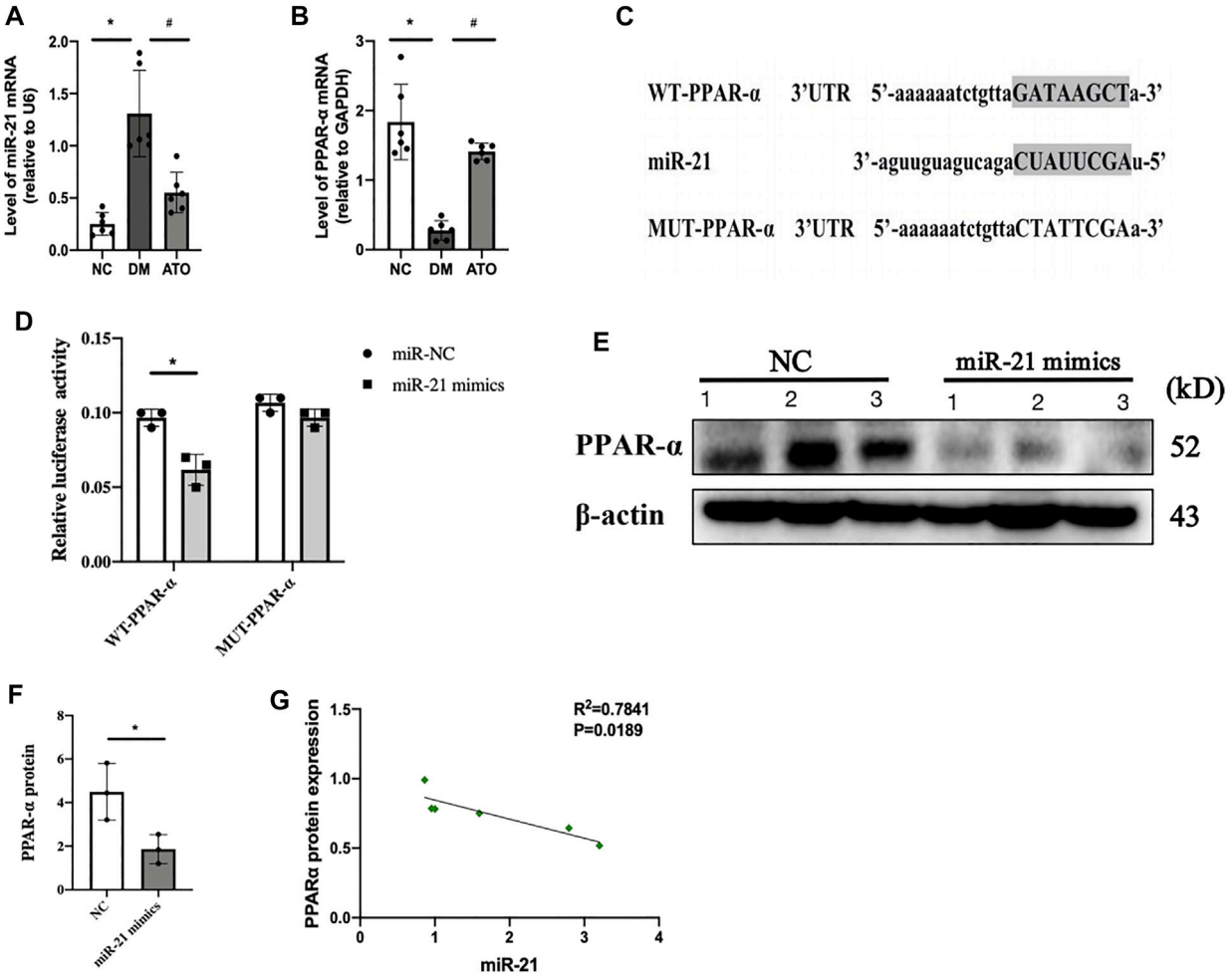

FIGURE 3 | miR-21 directly targets and inhibits PPARα expression. The effects of Atorvastatin on specific blood parameters. The experiments aimed to detect the changes in lipid metabolism and mitochondria-related indicators in each group. miR-21 directly targets and inhibits PPARα expression. **(A, B)** The expression levels of miR-21 **(A)** and PPARα mRNA **(B)** were detected in the kidney tissues of mice in each group. n = 6; *$p < 0.05$ vs NC group. #$p < 0.05$, compared with the DM group. **(C)** Predicted binding sequences and mutation sites between miR-21 and PPARα 3′UTR seed sites. **(D)** Cotransfection of HK-2 cells with 50 nM miR-21 mimic or NC mimic and 100 ng of WT or MUT plasmid containing PPARα 3′UTR and 5 ng of Renilla plasmid. The dual-luciferase reporter assay was used to detect luciferase activity of WT and MUT plasmids. The data represent mean ± SEM, n = 3, *$p < 0.05$. (E. F) The expression levels of PPARα were detected by western blot analysis 24 h following transfection with miR-22 or NC mimics **(E)**. ImageJ optical density analysis of protein levels **(F)**. **(G)** Correlation analysis between miR-21 expression and PPARα protein expression. All data represent mean ± SD from three independent experiments. n = 3; *$p < 0.05$ vs NC group. #$p < 0.05$, compared with the DM group.

and Drp1 proteins were decreased in cells cultured in the presence of either HG or PA, while the expression levels of PPARα and Mfn1 were increased (**Figures 4A– B**). Fenofibrate, which is a ligand of PPARα, is often used clinically as a PPARα-specific agonist. This compound exhibited similar effects to those of miR-21 inhibitors under different conditions of HG, PA, and HG + PA (**Figures 4C–E**). These findings suggest that both high-glucose or high-fat environments cause downregulation of PPARα expression, impair mitochondrial function, and promote the expression of inflammatory factors and fibronectin to mediate renal tubular injury. In contrast to these findings, miR-21 inhibitor and Fenofibrate both upregulated PPARα expression, which in turn restored the expression levels of proteins affecting mitochondrial function and reversed the inflammatory response and fibrosis progression in renal tubular epithelial cells induced by hyperglycemia and hyperlipidemia. These results suggested that miR-21 may contribute to high glucose or high fat-induced renal tubular epithelial cell injury by downregulating PPARα expression leading to impaired mitochondrial function and lipid metabolism disorders.

Atorvastatin Restores PPARα Expression by Inhibiting miR-21 Expression and Improves Mitochondrial Function Impairment in Renal Tubular Epithelial Cells Induced by High Glucose and High Fat

Subsequent experiments were performed to clarify whether Atorvastatin restores the transcription and protein expression

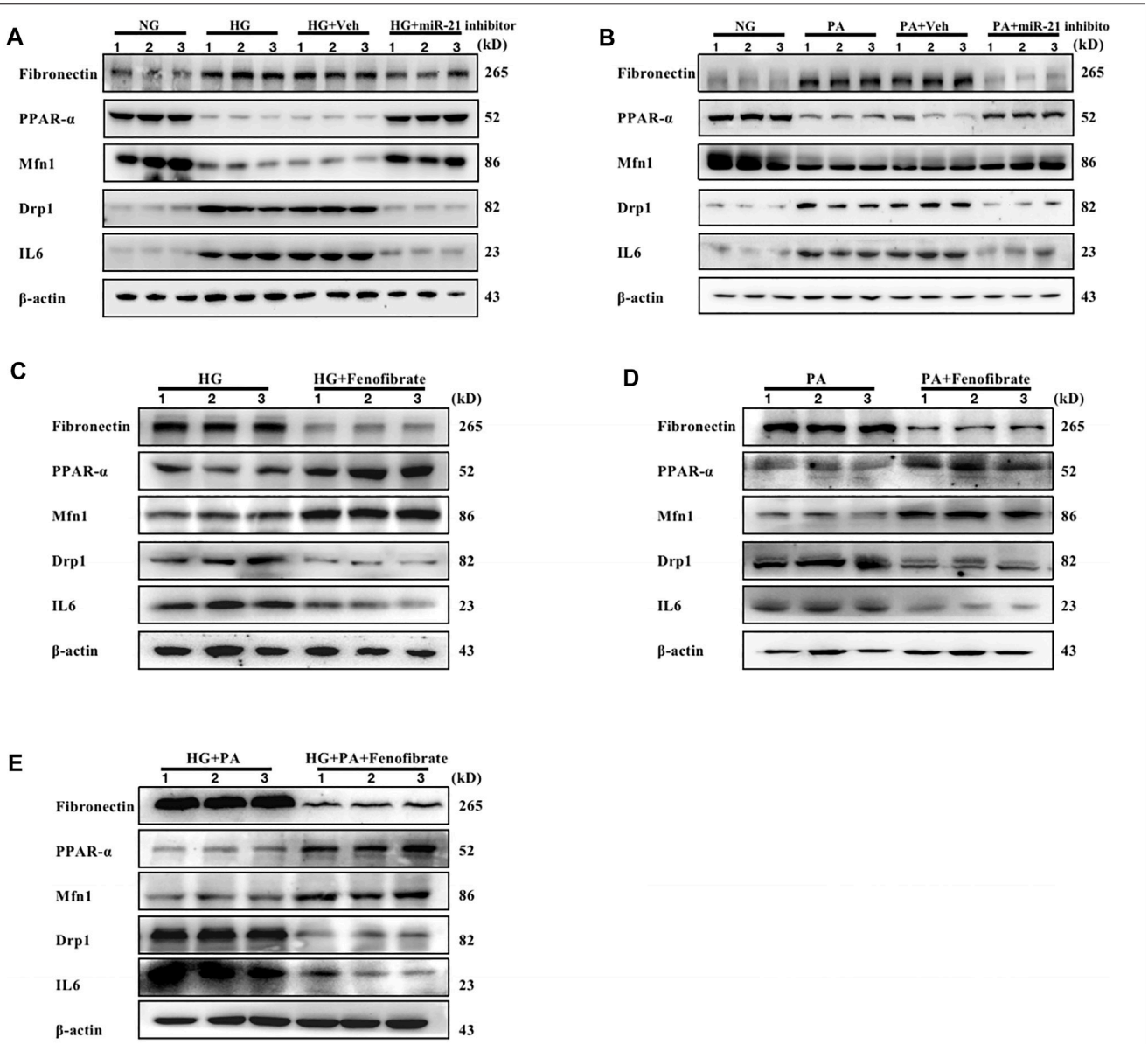

FIGURE 4 | Both miR-21 inhibitors and Fenofibrate slow down renal tubular injury caused by high glucose or high fat. mRTEC cells were incubated with NG (5.5 mM) and HG (25 mM) medium, respectively, and transfected with miR-21 inhibitor and its control agent as (HG + Veh group, HG + miR-21 inhibitor group) in HG-treated cells for 48 h. **(A)** Immunoblotting bands corresponding to FN, PPARα, Mfn1, Drp1, and IL-6 expressions in RTEC cells of each group. mRTEC cells were treated with palmitic acid solvent. 95% anhydrous ethanol (0.02 ml) was added in the NC group and palmitic acid PA (0.2 mM) in the PA group (PA-treated). RTEC cells were transfected with miR-21 inhibitor and its control agent (PA + Veh group, PA + miR-21 inhibitor group) following 48 h of incubation. Subsequently, the samples were analyzed. **(B)** Immunoblotting bands corresponding to FN, PPARα, Mfn1, Drp1, and IL-6 expressions in RTEC cells of each group. **(C–E)** The expression levels of FN, PPARα, Mfn1, Drp1, and IL-6 in RTEC cells treated with HG, PA, and HG + PA, respectively, and subsequently incubated with Fenofibrate (0.05 mM) for 48 h. The expression levels of FN, PPARα, Mfn1, Drp1, and IL-6 proteins were analyzed under HG (F), PA (G), and HG + PA(H) conditions, respectively. All data are indicative of mean ± SD from three independent experiments. n = 3.

of PPARα, which is a key factor in lipid metabolism. It was hypothesized that Atorvastatin could downregulate miR-21 expression, thereby improving mitochondrial function and inhibiting the damage to renal tubular epithelial cells caused by high glucose and high fat. In order to confirm this hypothesis, we transfected miR-21 mimics into RTEC cells following treatment of the cells with high glucose and high fat in the presence of Atorvastatin. The expression levels of PPARα were evaluated, in combination with mitochondrial kinetics and function, and the induction of the inflammatory response was assessed. The high glucose and high-fat environment led to a decrease in PPARα levels, a decrease in the protein expression levels of Mfn1, which is an important protein in mitochondrial dynamics, and an increase in Drp1 levels, which were

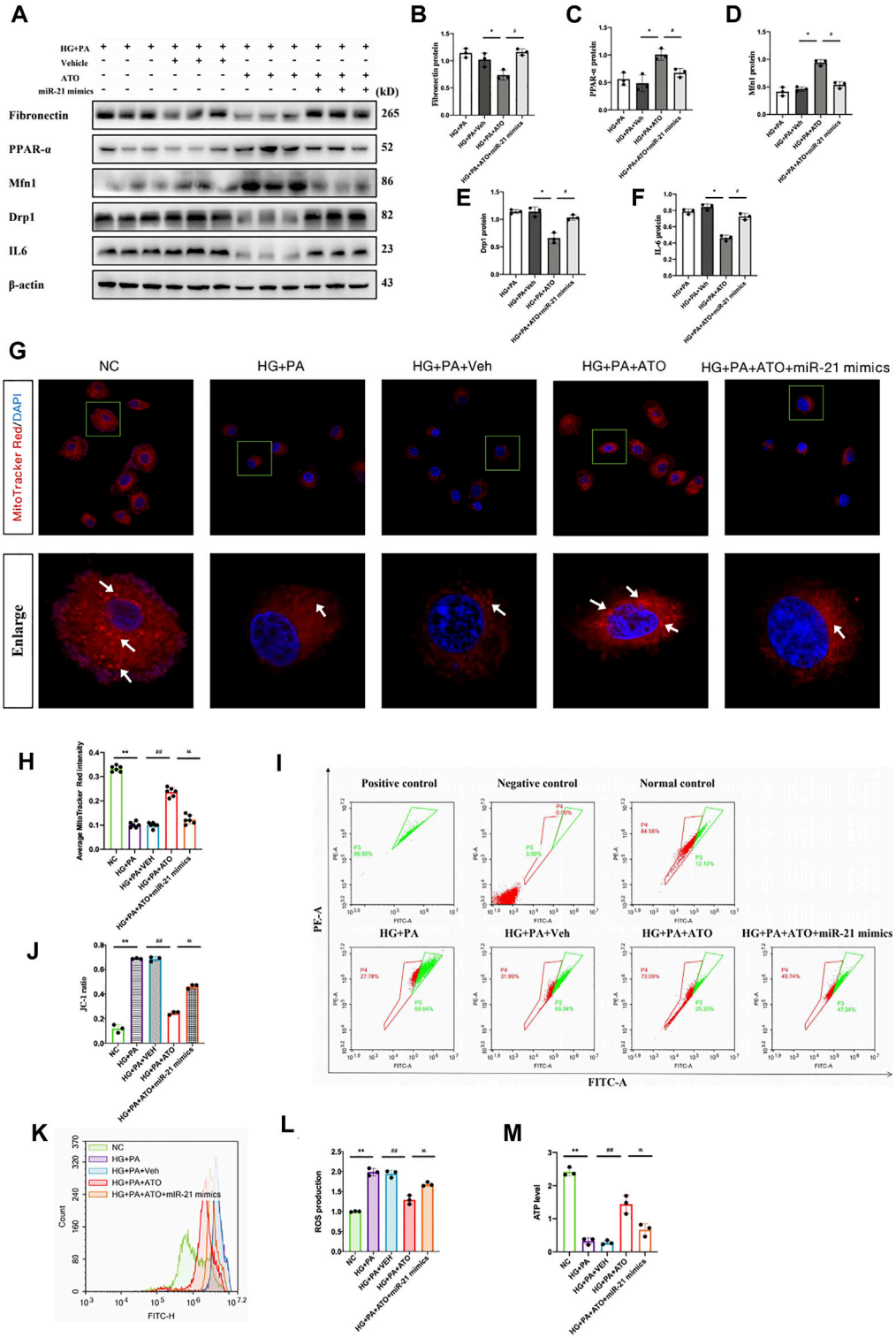

FIGURE 5 | Atorvastatin restores PPARα expression by inhibiting miR-21 expression and improves mitochondrial function impairment in renal tubular epithelial cells induced by high glucose and high fat. The mRTEC cells were cultured with NG and HG + PA medium, and Atorvastatin and its solvent DMSO were added to the HG + PA-treated cells as the treatment group and treatment control group, respectively. The cells were also transfected with miR-21 mimics and treated with HG + PA + ATO. (A-F)They were subsequently cultured for 48 h. Immunoblot bands **(A)** and quantitative data **(B–F)** of FN, PPARα, Mfn1, Drp1, and IL-6 in each cell group. **(G)**

(*Continued*)

FIGURE 5 | Representative confocal microscope images of mitochondrial morphology stained by MitoTracker Red. Original magnification ×600. **(H)** Quantification of mitochondrial number per cell. White arrows represent high fluorescence intensity. **(I–J)** Flow cytometry analysis of mitochondrial membrane potential changes in each group of cells **(I)**, quantitative data **(J)**. **(K–L)** Flow cytometry analysis of ROS production **(K)**, quantitative data **(L)** for each group of cells. **(M)** Assessment of the ATP content in the cells of each group. All data are mean ± SD from three independent experiments. n = 3; $^{*}p < 0.05$ vs NC group. $\#p < 0.05$, compared with the HG + PA group. $p < 0.05$, compared with the HG + PA + ATO group; $^{**}p < 0.01$ vs NC group. $\#\#p < 0.01$, compared with the HG + PA group. $p < 0.01$, compared with the HG + PA + ATO group.

accompanied by fibrotic damage and inflammatory response (**Figure 5A**); it also led to reduced the number of biologically active mitochondria and ATP content, mitochondrial depolarization, and a significant increase in ROS production (**Figures 5H–M**). In contrast to these observations, Atorvastatin caused an upregulation in the protein expression levels of PPARα and Mfn1, a reduction in the expression levels of Drp1, FN, and IL6, and in the levels of ROS and led to restoration of the ATP content, mitochondrial activity, and polarization response. Following transfection of the cells with miR-21 mimics and treatment of Atorvastatin, the aforementioned effects of this compound were significantly inhibited. This suggested that miR-21 significantly inhibited the restoration of PPARα expression by Atorvastatin, improved HG- and PA-induced mitochondrial dysfunction, and reversed the inflammatory response and fibrosis progression effects in renal tubular epithelial cells cultured under hyperglycemic and hyperlipidemic conditions. Therefore, it is suggested that Atorvastatin exhibits a protective effect on mitochondrial dysfunction in renal tubular epithelial cells treated with high glucose and lipids by inhibiting miR-21 expression and restoring PPARα expression.

DISCUSSION

The kidneys require large amounts of mitochondria to remove waste products from the blood and to regulate fluid and electrolyte balance. Following mitochondrial dysfunction, a reduction in the ATP production is noted, in combination with altered cell function and structure, and loss of kidney function. These changes eventually lead to the progression of the chronic kidney disease (CKD). Restoring mitochondrial function may subsequently reverse cellular damage and restore renal function. In recent years, studies on mitochondrial dysfunction in diabetic nephropathy have focused on hyperglycemia-induced ATP depletion, which triggers changes in mitochondrial morphology. However, type 1 diabetes mellitus (T1DM) can also lead to dyslipidemia and proteinuria (Vergès, 2020). Therefore, in type 1 diabetes, the disorders in glucose metabolism caused by islet damage are the only factors responsible for the progression of the disease. Specific conditions, such as alterations in lipid transport, lipid storage, and membrane lipids can affect mitochondrial function (Ducasa et al., 2019). For example, the accumulation of FA in acute kidney injury and diabetic nephropathy leads to decreased β-oxidation in mitochondria and increased formation of intracellular lipid droplets, which inhibit ATP production (Bhargava and Schnellmann, 2017)and exacerbate kidney damage. Therefore, improving mitochondrial function plays a major role in combating acute and chronic injury.

Statins, also known as hydroxymethylglutaryl coenzyme A (HMG-CoA) reductase inhibitors, demonstrate a competitive mechanism to inhibit endogenous HMG-CoA reductase, lowering cholesterol and triglyceride and exerting a lipid-regulating effect (Xu and Wu, 2020). Atorvastatin, is a highly effective statin lipid-lowering drug that has been widely used in clinical practice. The current research on Atorvastatin is mainly focused on its cardiovascular protective effects, in addition to its significant lipid-lowering efficacy. It has been reported that statins can exert renoprotective effects, such as anti-inflammatory and antifibrotic effects through the activation of various pathways (Pose et al., 2019). However, the renoprotective mechanism of Atorvastatin in diabetic nephropathy, which is caused via hypolipidemic effects has not been previously clarified. In the present study, the data indicated that T1DM mice exhibited significant disorders in glucolipid metabolism, whereas their kidney morphology exhibited apparent pathological changes, such as widening of the thylakoid zone, collagen deposition, and lymphocyte infiltration. The expression levels of the fibrosis-related proteins fenonectin, collagen-I, a-SMA, and inflammatory factor IL-6 were significantly increased in the kidney tissues of DM mice. The triglyceride and total cholesterol levels were reduced in the ATO group of mice following administration of Atorvastatin in DM mice. Although the blood glucose levels of DM mice did not change significantly following drug administration, the expression levels of fibrotic proteins and inflammatory factors were significantly reduced. Moreover, the renal function was restored. Their pathological morphology was significantly improved and the area of collagen deposition was reduced. Our results clearly indicated that Atorvastatin was effective in slowing down the progression of T1DM mice, which prompted us to investigate the mechanism by which inhibition of lipid metabolism disorder can alleviate the progression of DKD.

Recently, the role of the impaired fatty acid oxidation (FAO) pathway in the development of renal interstitial fibrosis has been reported in the literature (Kang et al., 2015). It has been shown that renal tubular epithelial cells were heavily dependent on FAO, which was their main energy source. Moreover, diminished FAO was associated with intracellular lipid accumulation. PPARα is a key transcription factor of FAO and it is involved in oxidative metabolism noted in the majority of the tissues, since it activates numerous genes involved in the following pathways: Carnitine palmitoyltransferase 1 a (CPT1a), acyl-coenzyme A oxidase 1 (ACOX1), acyl-coenzyme A dehydrogenase (ADH), and mitochondrial thioesterase 1 (MTE1) (Grabacka et al., 2013). Our results also validated that downregulation of PPARα

expression suppressed the expression levels of CPT1a with ACOX1. Increasing evidence supports a link between PPARα and the incidence of metabolic diseases including diabetes, obesity, dyslipidemia and fatty liver. Therefore, the role of PPARα in the development of renal diseases has recently been extensively studied (Wang, 2010), such as in mouse kidney tissues with hyperlipidemia (Chung et al., 2018)and renal stone disease (Su et al., 2020). Low expression of PPARα leads to lipid accumulation in renal tubular cells, which causes lipotoxicity and can manifest as mitochondrial dysfunction associated with increased reactive oxygen species production and decreased ATP production, apoptosis, and elevated inflammatory cytokine dysfunction (Jao et al., 2019). Therefore, we examined the changes in PPARα transcription and protein expression in mouse kidney tissues. In addition, we examined the role of the FAO-rate-limiting enzyme CPT1, whose protein levels were downregulated in DM mice compared with those of the control mice. These changes also reduced PPARα transcripts and protein expression levels. Following administration of Atorvastatin, PPARα and CPT1 expression were significantly increased. Recent studies have highlighted the importance of mitochondrial fusion and fission in cell function and animal physiology (Detmer and Chan, 2007). For example, fibroblasts lacking Mfn1 completely did not indicate mitochondrial fusion and exhibited severe cellular defects, including poor growth and heterogeneity of mitochondrial membrane potential (Chen et al., 2005). In contrast to these findings, downregulation of Drp1 expression reversed palmitate-induced mitochondrial damage and ROS production in skeletal muscle cells (Jheng et al., 2012). It has also been reported that the PPARα agonist (WY 14.643) was able to protect neurons by regulating mitochondrial fusion and fission in the brain of a transgenic mouse model of Alzheimer's disease (Zolezzi et al., 2013). Therefore, balanced mitochondrial dynamics are essential to maintain mitochondrial function and energy production. In the present study, we examined the expression levels of these two important proteins, Mfn1 and Drp1, which directly affected mitochondrial function. The expression levels of Mfn1 were decreased and those of Drp1 were increased in DM mice, whereas the expression levels of both of these proteins were reversed following administration of Atorvastatin. This implies that Atorvastatin exhibits antilipidemic effects that directly or indirectly balance mitochondrial dynamics and protect its function, in addition to its regulatory effects on lipid metabolism disorders.

MicroRNAs (miRNAs) are single-stranded, non-coding small RNA molecules that negatively regulate gene expression by binding to the 3′ untranslated region (UTR) of the target mRNA. This in turn regulates a variety of biological and pathological processes (Filipowicz et al., 2008). The results of the bioinformatics analysis suggested that miR-21 exhibited specific binding sites for PPARα. We observed elevated miR-21 expression and decreased PPARα expression in T1DM mice. Increased miR-21 expression significantly decreased PPARα protein levels. The luciferase reporter gene assay confirmed that PPARα was a downstream target gene of miR-21, which was consistent with the findings of Su B in a mouse model of renal stones with renal calcium oxalate deposition (Su et al., 2020). To simulate the damaging effects of high glucose and high-fat environments on renal tubular epithelial cells *in vivo*, renal tubular epithelial cells were treated with high glucose and palmitate, a saturated fatty acid commonly used as a diabetic stressor. The results indicated induction of oxidative stress leading to cellular dysfunction and apoptosis in various cell types (Cacicedo et al., 2005; Staiger et al., 2006). Moreover, it was shown that high sugar and palmitate levels contributed to decreased PPARα expression, whereas inhibition of miR-21 expression increased PPARα expression and protected mitochondrial dynamics leading to reduction of fibrosis and the inflammatory response.

Fenofibrate is a specific agonist of PPARα and is used clinically to reduce lipid levels in patients with dyslipidemia and cardiovascular disease (McKeage et al., 2011). Fenofibrate was administered to mRTECs subjected to high glucose, high fat, and high glucose combined with high fat conditions, respectively. The data indicated similar effects with those of the miR-21 inhibitors. These results described for the first time the relationship between the PPARα agonist Fenofibrate and mitochondrial dynamics and confirmed that by regulating PPARα expression, which is the key factor of lipid metabolism, mitochondrial dynamics and the corresponding protein expressions are affected. Concomitantly, the inflammatory response and fibrous deposition were inhibited, exerting a protective effect against DKD.

To further explore the association and role of Atorvastatin, the expression levels of miR-21, PPARα, and the mitochondrial function were assessed in DKD. Following administration of Atorvastatin in RTECS treated under high fat and high glucose conditions, the cells were transfected with miR-21 mimics. We found that administration of Atorvastatin significantly reduced the effects of high glucose conditions, whereas the combination with high fat conditions increased PPARα expression and altered the expression levels of two important proteins involved in mitochondrial dynamics. Specifically, Mfn1 levels were increased and Drp1 levels were decreased. Following transfection of the cells with miR-21 mimics and Atorvastatin administration, the protective effect of this drug was significantly inhibited and mitochondrial function was again impaired. This further confirmed our previous hypothesis that Atorvastatin improves mitochondrial function by downregulating miR-21-mediated-inhibition of lipid metabolism disorders to alleviate the progression of diabetic nephropathy.

In conclusion, Atorvastatin plays a protective role in the pathogenesis of DKD by promoting the expression of PPARα, a key transcription factor regulating lipid metabolism. In addition, it improved mitochondrial function and inflammatory response to counteract renal tubulointerstitial fibrosis. The specific mechanism involved the ability of Atorvastatin to promote PPARα transcription and expression by downregulation miR-21 expression, while restoring mitochondrial function to maintain the structure and function of renal tubular epithelial cells.

DATA AVAILABILITY STATEMENT

The original contributions presented in the study are included in the article/**Supplementary Materials**, further inquiries can be directed to the corresponding authors.

ETHICS STATEMENT

The animal study was reviewed and approved by Institutional Animal Ethics Committee of Guizhou Medical University, Guiyang, China.

AUTHOR CONTRIBUTIONS

XJ completed the majority of experiments, performed the statistical analysis and wrote the manuscript; ZH, ZX conducted some parts of experiments; CR, LU, WD, TW, XY, ZF, ZY and SM gave the guide of experiment methods; WY and GB conceived this study.

FUNDING

This work was supported by the National Natural Science Foundation of China (U1812403 and 82060141), Regional Common Diseases and Adult Stem Cell Transformation Research and Innovation Platform of Guizhou Provincial Department of Science and Technology, Grant/Award Number (2019) 4008.

SUPPLEMENTARY MATERIAL

The Supplementary Material for this article can be found online at: https://www.frontiersin.org/articles/10.3389/fphar.2022.819787/full#supplementary-material

REFERENCES

Athyros, V. G., Katsiki, N., Karagiannis, A., and Mikhailidis, D. P. (2015). Statins Can Improve Proteinuria and Glomerular Filtration Rate Loss in Chronic Kidney Disease Patients, Further Reducing Cardiovascular Risk. Fact or Fiction. *Expert Opin. Pharmacother.* 16 (10), 1449–1461. doi:10.1517/14656566.2015.1053464

Bhargava, P., and Schnellmann, R. G. (2017). Mitochondrial Energetics in the Kidney. *Nat. Rev. Nephrol.* 13 (10), 629–646. doi:10.1038/nrneph.2017.107

Cacicedo, J. M., Benjachareowong, S., Chou, E., Ruderman, N. B., and Ido, Y. (2005). Palmitate-induced Apoptosis in Cultured Bovine Retinal Pericytes: Roles of NAD(P)H Oxidase, Oxidant Stress, and Ceramide. *Diabetes* 54, 1838–1845. doi:10.2337/diabetes.54.6.1838

Chen, H., and Chan, D. C. (2004). Mitochondrial Dynamics in Mammals. *Curr. Top. Dev. Biol.* 59, 119–144. doi:10.1016/S0070-2153(04)59005-1

Chen, H., Chomyn, A., and Chan, D. C. (2005). Disruption of Fusion Results in Mitochondrial Heterogeneity and Dysfunction. *J. Biol. Chem.* 280 (28), 28026185–28026192. doi:10.1074/jbc.M503062200

Chung, K. W., Lee, E. K., Lee, M. K., Oh, G. T., Yu, B. P., and Chung, H. Y. (2018). Impairment of PPARα and the Fatty Acid Oxidation Pathway Aggravates Renal Fibrosis during Aging. *J. Am. Soc. Nephrol.* 29 (4), 1223–1237. doi:10.1681/ASN.2017070802

Chuppa, S., Liang, M., Liu, P., Liu, Y., Casati, M. C., Cowley, A. W., et al. (2018). MicroRNA-21 Regulates Peroxisome Proliferator-Activated Receptor Alpha, a Molecular Mechanism of Cardiac Pathology in Cardiorenal Syndrome Type 4. *Kidney Int.* 93 (2), 375–389. doi:10.1016/j.kint.2017.05.014

Coughlan, M. T., and Sharma, K. (2016). Challenging the Dogma of Mitochondrial Reactive Oxygen Species Overproduction in Diabetic Kidney Disease. *Kidney Int.* 90 (2), 272–279. doi:10.1016/j.kint.2016.02.043

Detmer, S. A., and Chan, D. C. (2007). Functions and Dysfunctions of Mitochondrial Dynamics. *Nat. Rev. Mol. Cel Biol.* 8 (11), 870–879. doi:10.1038/nrm2275

Ducasa, G. M., Mitrofanova, A., and Fornoni, A. (2019). Crosstalk between Lipids and Mitochondria in Diabetic Kidney Disease. *Curr. Diab. Rep.* 2119 (12), 144. doi:10.1007/s11892-019-1263-x

Filipowicz, W., Bhattacharyya, S. N., and Sonenberg, N. (2008). Mechanisms of post-transcriptional Regulation by microRNAs: Are the Answers in Sight. *Nat. Rev. Genet.* 9 (2), 102–114. doi:10.1038/nrg2290

Galvan, D. L., Green, N. H., and Danesh, F. R. (2017). The Hallmarks of Mitochondrial Dysfunction in Chronic Kidney Disease. *Kidney Int.* 92 (5), 1051–1057. doi:10.1016/j.kint.2017.05.034

Gerber, P. A., and Rutter, G. A. (2017). The Role of Oxidative Stress and Hypoxia in Pancreatic Beta-Cell Dysfunction in Diabetes Mellitus. *Antioxid. Redox Signal.* 126 (10), 501–518. doi:10.1089/ars.2016.6755

Grabacka, M., Pierzchalska, M., and Reiss, K. (2013). Peroxisome Proliferator Activated Receptor α Ligands as Anticancer Drugs Targeting Mitochondrial Metabolism. *Curr. Pharm. Biotechnol.* 14 (3), 342–356. doi:10.2174/1389201011314030009

Herman-Edelstein, M., Scherzer, P., Tobar, A., Levi, M., and Gafter, U. (2014). Altered Renal Lipid Metabolism and Renal Lipid Accumulation in Human Diabetic Nephropathy. *J. Lipid Res.* 55 (3), 561–572. doi:10.1194/jlr.P040501

Jao, T. M., Nangaku, M., Wu, C. H., Sugahara, M., Saito, H., Maekawa, H., et al. (2019). ATF6α Downregulation of PPARα Promotes Lipotoxicity-Induced Tubulointerstitial Fibrosis. *Kidney Int.* 95 (3), 577–589. doi:10.1016/j.kint.2018.09.023

Jheng, H. F., Tsai, P. J., Guo, S. M., Kuo, L. H., Chang, C. S., Su, I. J., et al. (2012). Mitochondrial Fission Contributes to Mitochondrial Dysfunction and Insulin Resistance in Skeletal Muscle. *Mol. Cel Biol.* 32 (2), 309–319. doi:10.1128/MCB.05603-11

Jia, Z., An, L., Lu, Y., Xu, C., Wang, S., Wang, J., et al. (2019). Oxidized Low Density Lipoprotein-Induced Atherogenic Response of Human Umbilical Vascular Endothelial Cells (HUVECs) Was Protected by Atorvastatin by Regulating miR-26a-5p/Phosphatase and Tensin Homolog (PTEN). *Med. Sci. Monit.* 25 (25), 9836–9843. doi:10.12659/MSM.918405

Kang, H. M., Ahn, S. H., Choi, P., Ko, Y. A., Han, S. H., Chinga, F., et al. (2015). Defective Fatty Acid Oxidation in Renal Tubular Epithelial Cells Has a Key Role in Kidney Fibrosis Development. *Nat. Med.* 21 (1), 37–46. doi:10.1038/nm.3762

Kim, T. S., Jin, Y. B., Kim, Y. S., Kim, S., Kim, J. K., Lee, H. M., et al. (2019). SIRT3 Promotes Antimycobacterial Defenses by Coordinating Mitochondrial and Autophagic Functions. *Autophagy* 15 (8), 1356–1375. doi:10.1080/15548627.2019.1582743

Kogawa, A. C., Pires, A. E. D. T., and Salgado, H. R. N. (2019). Atorvastatin: A Review of Analytical Methods for Pharmaceutical Quality Control and Monitoring. *J. AOAC Int.* 102 (3), 801–809. doi:10.5740/jaoacint.18-0200

Liao, D., Liu, Y. Q., Xiong, L. Y., and Zhang, L. (2016). Renoprotective Effect of Atorvastatin on STZ-Diabetic Rats through Inhibiting Inflammatory Factors Expression in Diabetic Rat. *Eur. Rev. Med. Pharmacol. Sci.* 20 (9), 1888–1893.

Liu, L., Wang, Y., Yan, R., Liang, L., Zhou, X., Liu, H., et al. (2019). BMP-7 Inhibits Renal Fibrosis in Diabetic Nephropathy via miR-21 Downregulation. *Life Sci.* 238, 116957. doi:10.1016/j.lfs.2019.116957

McKeage, K., and Keating, G. M. (2011). Fenofibrate: a Review of its Use in Dyslipidaemia. *Drugs* 71 (14), 1917–1946. doi:10.2165/11208090-000000000-00000

Nozari, E., Moradi, A., and Samadi, M. (2020). Effect of Atorvastatin, Curcumin, and Quercetin on miR-21 and miR-122 and Their Correlation with TGFβ1 Expression in Experimental Liver Fibrosis. *Life Sci.* 259, 259118293. doi:10.1016/j.lfs.2020.118293

Pose, E., Trebicka, J., Mookerjee, R. P., Angeli, P., and Ginès, P. (2019). Statins: Old Drugs as New Therapy for Liver Diseases. *J. Hepatol.* 70 (1), 194–202. doi:10.1016/j.jhep.2018.07.019

Saeedi, P., Petersohn, I., Salpea, P., Malanda, B., Karuranga, S., Unwin, N., et al. (2019). Global and Regional Diabetes Prevalence Estimates for 2019 and Projections for 2030 and 2045: Results from the International Diabetes Federation Diabetes Atlas, 9th Edition. *Diabetes Res. Clin. Pract.* 157, 107843. doi:10.1016/j.diabres.2019.107843

Simon, N., and Hertig, A. (2015). Alteration of Fatty Acid Oxidation in Tubular Epithelial Cells: From Acute Kidney Injury to Renal Fibrogenesis. *Front. Med. (Lausanne)* 2 (2), 52. doi:10.3389/fmed.2015.00052

Staiger, K., Staiger, H., Weigert, C., Haas, C., Häring, H. U., and Kellerer, M. (2006). Saturated, but Not Unsaturated, Fatty Acids Induce Apoptosis of Human Coronary Artery Endothelial Cells via Nuclear Factor-kappaB Activation. *Diabetes* 55, 3121–3126. doi:10.2337/db06-0188

Su, B., Han, H., Ji, C., Hu, W., Yao, J., Yang, J., et al. (2020). MiR-21 Promotes Calcium Oxalate-Induced Renal Tubular Cell Injury by Targeting PPARA. *Am. J. Physiol. Ren. Physiol.* 319 (2), F202–F214. doi:10.1152/ajprenal.00132.2020

Vergès, B. (2020). Dyslipidemia in Type 1 Diabetes: AMaskedDanger. *Trends Endocrinol. Metab.* 31 (6), 422–434. doi:10.1016/j.tem.2020.01.015

Wang, Y. X. (2010). PPARs: Diverse Regulators in Energy Metabolism and Metabolic Diseases. *Cell Res.* 20, 124–137. doi:10.1038/cr.2010.13

Xu, Y., and Wu, Y. (2020). Atorvastatin Associated with Gamma Glutamyl Transpeptidase Elevation in a Hyperlipidemia Patient: A Case Report and Literature Review. *Medicine (Baltimore)* 99 (40), e22572. doi:10.1097/MD.0000000000022572

Xu, J., Xiao, G., Trujillo, C., Chang, V., Blanco, L., Joseph, S. B., et al. (2002). Peroxisome Proliferator-Activated Receptor Alpha (PPARalpha) Influences Substrate Utilization for Hepatic Glucose Production. *J. Biol. Chem.* 277, 50237–50244. doi:10.1074/jbc.M201208200

Yu, T., Robotham, J. L., and Yoon, Y. (2006). Increased Production of Reactive Oxygen Species in Hyperglycemic Conditions Requires Dynamic Change of Mitochondrial Morphology. *Proc. Natl. Acad. Sci. U S A.* 21103 (8), 2653–2658. doi:10.1073/pnas.0511154103

Zhou, J., Wang, K. C., Wu, W., Subramaniam, S., Shyy, J. Y., Chiu, J. J., et al. (2011). MicroRNA-21 Targets Peroxisome Proliferators-Activated Receptor-Alpha in an Autoregulatory Loop to Modulate Flow-Induced Endothelial Inflammation. *Proc. Natl. Acad. Sci. U S A.* 108 (25), 10355–10360. doi:10.1073/pnas.1107052108

Zolezzi, J. M., Silva-Alvarez, C., Ordenes, D., Godoy, J. A., Carvajal, F. J., Santos, M. J., et al. (2013). Peroxisome Proliferator-Activated Receptor (PPAR) γ and PPARα Agonists Modulate Mitochondrial Fusion-Fission Dynamics: Relevance to Reactive Oxygen Species (ROS)-related Neurodegenerative Disorders. *PLoS One* 138 (5), e64019. doi:10.1371/journal.pone.0064019

Conflict of Interest: The authors declare that the research was conducted in the absence of any commercial or financial relationships that could be construed as a potential conflict of interest.

Publisher's Note: All claims expressed in this article are solely those of the authors and do not necessarily represent those of their affiliated organizations, or those of the publisher, the editors and the reviewers. Any product that may be evaluated in this article, or claim that may be made by its manufacturer, is not guaranteed or endorsed by the publisher.

frontiers in Pharmacology

ORIGINAL RESEARCH
published: 25 February 2022
doi: 10.3389/fphar.2021.788977

Roxadustat (FG-4592) Facilitates Recovery From Renal Damage by Ameliorating Mitochondrial Dysfunction Induced by Folic Acid

Xue Li[1,2†], Bo Jiang[3†], Yu Zou[1], Jie Zhang[1], Yuan-Yuan Fu[1] and Xiao-Yue Zhai[1,4]*

[1]Department of Histology and Embryology, Basic Medical College, China Medical University, Shenyang, China, [2]Department of Nephrology, Shengjing Hospital of China Medical University, Shenyang, China, [3]Department of Vascular Surgery, First Hospital of China Medical University, Shenyang, China, [4]Institute of Nephropathology, China Medical University, Shenyang, China

OPEN ACCESS

Edited by:
Zhiyong Guo,
Second Military Medical University, China

Reviewed by:
Sandra Rayego-Mateos,
Health Research Institute Foundation Jimenez Diaz (IIS-FJD), Spain
Subhadeep Roy,
Indian Institute of Technology Delhi, India

***Correspondence:**
Xiao-Yue Zhai
xyzhai@cmu.edu.cn

[†]*These authors share first authorship*

Specialty section:
This article was submitted to Renal Pharmacology, a section of the journal Frontiers in Pharmacology

Received: *04 October 2021*
Accepted: *14 December 2021*
Published: *25 February 2022*

Citation:
Li X, Jiang B, Zou Y, Zhang J, Fu Y-Y and Zhai X-Y (2022) Roxadustat (FG-4592) Facilitates Recovery From Renal Damage by Ameliorating Mitochondrial Dysfunction Induced by Folic Acid. Front. Pharmacol. 12:788977. doi: 10.3389/fphar.2021.788977

Incomplete recovery from acute kidney injury induced by folic acid is a major risk factor for progression to chronic kidney disease. Mitochondrial dysfunction has been considered a crucial contributor to maladaptive repair in acute kidney injury. Treatment with FG-4592, an inhibitor of hypoxia inducible factor prolyl-hydroxylase, is emerging as a new approach to attenuate renal damage; however, the underlying mechanism has not been fully elucidated. The current research demonstrated the protective effect of FG-4592 against renal dysfunction and histopathological damage on the 7th day after FA administration. FG-4592 accelerated tubular repair by promoting tubular cell regeneration, as indicated by increased proliferation of cell nuclear antigen-positive tubular cells, and facilitated structural integrity, as reflected by up-regulation of the epithelial inter-cellular tight junction molecule occludin-1 and the adherens junction molecule E-cadherin. Furthermore, FG-4592 ameliorated tubular functional recovery by restoring the function-related proteins aquaporin1, aquaporin2, and sodium chloride cotransporter. Specifically, FG-4592 pretreatment inhibited hypoxia inducible factor-1α activation on the 7th day after folic acid injection, which ameliorated ultrastructural abnormalities, promoted ATP production, and attenuated excessive reactive oxygen species production both in renal tissue and mitochondria. This was mainly mediated by balancing of mitochondrial dynamics, as indicated by down-regulation of mitochondrial fission 1 and dynamin-related protein 1 as well as up-regulation of mitofusin 1 and optic atrophy 1. Moreover, FG-4592 pretreatment attenuated renal tubular epithelial cell death, kidney inflammation, and subsequent interstitial fibrosis. In vitro, TNF-α-induced HK-2 cells injury could be ameliorated by FG-4592 pretreatment. In summary, our findings support the protective effect of FG-4592 against folic acid-induced mitochondrial dysfunction; therefore, FG-4592 treatment can be used as a useful strategy to facilitate tubular repair and mitigate acute kidney injury progression.

Keywords: FG-4592, HIF-1α, repair, mitochondria dysfunction, FA-induced renal damage

INTRODUCTION

Acute kidney injury (AKI), characterized by renal dysfunction, is involved in failure to maintain important physiological parameters such as volume and electrolyte balance (Kellum et al., 2017). AKI is associated with increased rates of mortality and morbidity (Chan et al., 2020). Ischemia and toxicity are common causes of AKI, which are the major contributors to chronic kidney disease (CKD) and are closely associated with aberrant repair (Humphreys et al., 2016). This relationship highlights how renal recovery from AKI may determine long-term outcomes; however, no effective interventions are currently available to alter the natural course (Bao et al., 2018). Therefore, it is essential to explore the possible mechanisms and seek novel therapeutic options involving maximization of kidney repair to ameliorate AKI prognosis (Lin and Hsu 2020). The regenerative capacity of tubules is limited; in comparison, tubular cells have more regenerative capacity after injury, although the mechanisms are unknown (Soofi et al., 2020). Moreover, maladaptive repair could lead to CKD, which is closely related to cell death and continuous inflammation, eventually leading to increased extracellular matrix accumulation (Gibbs et al., 2018).

Folic acid (FA)-induced AKI is mainly caused by tubular crystal formation and oxidative stress, which leads to epithelial necrosis and inflammation (Gupta et al., 2012). This further exacerbates persistent tissue hypoxia, and the tissue usually cannot fully recover; the condition may easily progress to CKD. Thus, FA-induced AKI model is becoming a valuable tool to explore the mechanisms of maladaptive repair of AKI (Basile et al., 2012; Aparicio-Trejo et al., 2019). In addition, AKI can trigger the degradation of cell-cell tight junction (TJ) and adherens junction (AJ) proteins, including the major transmembrane proteins E-cadherin and zonular occludin-1 (ZO-1). Furthermore, the potential of tubular cells to regenerate is pivotal for reestablishment of tubule integrity (Zhou et al., 2012; Jiang et al., 2016a). Moreover, structural integrity is indispensable for restoration of tubular barrier function, especially the regulation of body fluid volume. Aquaporins (AQPs), which are water channel proteins, are expressed in different segments of the tubule that maintain the normal urine concentration and volume (He and Yang 2019). Moreover, the kidneys play an important role in regulating the balance of electrolytes. For example, sodium chloride cotransporter (NCC), which plays an essential role in ion transport, is mostly expressed in the distal convoluted tubule and drives water reabsorption through active sodium transport (Gamba 2012).

Furthermore, tubular recovery from AKI is associated with a high metabolic demand to perform intense reabsorption processes. Mitochondria are the central energy sources in tubular epithelial cells, and mitochondrial dysfunction has been identified as a critical contributor to abnormal kidney repair (Cheng et al., 2020). Moreover, mitochondria are dynamic organelles that undergo constant fusion and fission, which are balanced to maintain mitochondrial homeostasis under physiological conditions. Excessive mitochondrial fission results in mitochondrial fragmentation, which is found in different models of AKI (Sun et al., 2019). Mitochondrial dysfunction could further impair ATP production and enhance the release of oxides that induce iron-dependent cell death (Battaglia et al., 2020). Moreover, ferroptosis has been reported to be the major cause in FA-induce renal damage, which could be a driver of other pathways of cell death (Diego, Martin-Sanchez et al., 2016; Li et al., 2020). While specific expression of GPX4 can play an important role in anti-oxidative stress, and further inhibit cell ferroptosis (Reichert et al., 2020).

Mitochondrial dysfunction has been found to be the main pathogenic factor in FA-induced renal damage. Restoring the generation of functional mitochondria is essential for cell survival and measures that ameliorate mitochondrial dynamics that could accelerate endogenous regeneration processes, further facilitating recovery from AKI (Reichert et al., 2020). Mitochondrial fusion, primarily driven by mitochondrial fusion proteins such as optic atrophy type 1 (Opa1) on the inner mitochondrial membrane (IMM) and mitofusin 1 (Mfn1) and mitofusin 2 (Mfn2) on the outer mitochondrial membrane (OMM), has been demonstrated to be able to protect against renal damage (Zhan et al., 2013). Mitochondrial fission is mainly regulated by dynamin-related protein 1 (Drp1), a dynamin-related GTPase, which is regulated by anchor protein fission protein 1 (Fis1) (Zhan et al., 2013). Studies have shown that both Opa1 and Mfn2 can maintain the stability of mitochondrial cristae and promote mitochondrial fusion. However, persistent upregulation of Drp1 contributes to mitochondrial fragmentation, which has been found to occur in FA-induced AKI (Aparicio-Trejo et al., 2019). Hypoxia inducible factor-1α (HIF-1α), the transcriptional regulator that responds to hypoxia, has been reported to negatively modulate mitochondrial dynamics by promoting the expression of Drp1 (Chen et al., 2019). In addition, HIF-1α has been reported to inhibit the expression of Mfn2, which directly or indirectly influences mitochondrial function (Martin et al., 2014; Dabrowska et al., 2015).

FG-4592, an inhibitor of prolyl-4-hydroxylases (PHDs), can stabilize the level of HIF-1α through inhibition of PHDs under physiological conditions (Wu et al., 2016). Pretreatment with FG-4592 has been reported to protect against AKI through antiapoptotic effects (Yang et al., 2018). Additionally, in our previous study, FG-4592 pretreatment exerted potential protective effects against FA-induced tubular injury at the acute phase through anti-ferroptosis with up-regulation of HIF-1α, but a decreased level of HIF-1α mRNA was observed, which was probably related to negative feedback (Li et al., 2020). To date, the effect of FG-4952 on FA-induced tubular damage at the repair phase has not been well studied, and the underlying mechanism is still unknown. It has been reported that kidney recovery occurs from the 6th day after FA overdose injection. In this regard, we speculate that the protein level of HIF-1α is down-regulated with time because of the short half-life of the protein and the inhibition of HIF-1α mRNA expression with FG-4592 pretreatment, which may ameliorate mitochondrial dysfunction induced by FA injection. These findings are important because suppressing mitochondrial fission and promoting mitochondrial fusion are promising therapeutic approaches to restore the

balance between fission and fusion, which is an attractive strategy for tubular repair and amelioration of AKI prognosis.

MATERIALS AND METHODS

Animals

The protocols were abided by the NIH Policy on Animal Care and Use, and complied with the ethics committee of the China Medical University on Laboratory Animals (protocol no. 2011037). Six- to eight-week-old C57BL/6 male mice were obtained from China Medical University and housed in a specific pathogen-free facility. They were allocated to four groups (six mice for each group): (1) Control group, the mice were intraperitoneally administrated with 0.5 ml of 300 mM $NaHCO_3$; (2) Folic acid (FA) group, the mice were intraperitoneally injected with one dose of FA (250 mg/kg) diluted in 300 mM $NaHCO_3$; (3) FG-4592 group, the mice were intraperitoneally injected with FG-4592 (10 mg/kg) diluted in DMSO and then PBS to 1 mg/ml; (4) FA + FG-4592 group, the mice were injected with one dose of FG-4592 2 days before FA injection. At day 7 after FA injection, tissue and blood samples were obtained for further test.

Cell Culture and Treatment

Human proximal tubule epithelial cells (HK-2 cells), purchased from American Type Culture Collection, were cultured in DMEM/F-12 medium supplemented with 10% bovine serum albumin, 100 μg/ml streptomycin, and 100 U/ml penicillin (Invitrogen, Carlsbad CA, United States). Cells were grown to the confluence of 50% and stimulated with TNF-α (50 ng/ml) for 24 h in the presence or not of FG-4592 pretreatment for 24 h.

Reagents and Antibodies

Rabbit anti-Mfn1 (14739s), rabbit anti-Opa1 (67589s), rabbit anti-Fis1 (86668s), rabbit anti-Drp1 (8570s), rabbit anti-IL-1β (12703s), rabbit anti-CD3 (26582s), rabbit anti-Myeloperoxidase (MPO^+) (14569T), rabbit anti-F4/80 (30325s), and rabbit anti-collagen I (72026T) antibodies were taken from CST; mouse anti-β-actin (ab8226), rabbit anti-HIF-1α (ab216842), mouse anti-PCNA (ab29), rabbit anti-E-cadherin (ab76319), rabbit anti-NCC (ab203674), rabbit anti-α-SMA (ab5694), mouse anti-vimentin (ab92547), rabbit anti-GPX-4 (ab125066), and rabbit anti-fibronectin (Fn) (ab2413) antibodies were obtained from Abcam; rabbit anti-TNF-α (7B8A11) antibody was purchased from Proteintech; rabbit anti-ZO-1 (PA524716), rabbit anti-AQP1 (101AP), and rabbit anti-AQP2 (201AP) antibodies were obtained from Invitrogen; anti-IL-33 (AF3626) antibody was acquired from R&D Systems. FG-4592 was obtained from Selleck and FA was acquired from Dalian Meilun Biotechnology Co. of China.

Cell Counting Kit-8 Assay

Cell viability was assayed with the CCK-8 kit (Beyotime, China, C0038). In brief, HK-2 cells were treated with FG-4592 (5–80 μM) for 24 h, or HK-2 cells were treated with TNF-α (50 ng/ml; abs00847, absin, China) for 24 h with and without 24 h pretreatment with FG-4592 (20 μM), then 10 μl CCK-8 solution was added to incubate for 2 h. The absorbance was measured at 450 nm.

Assays for Renal Function and ROS

In brief, blood was collected from the retro-orbital vein of the mice and serum was acquired by centrifugation at 600 X g for 10 min. BUN was assessed with a BUN test kit (C013-2) and Creatinine was assessed with the Creatinine determination kit (C011-2) from Jiancheng, China, by enzymatic colorimetric methods according to the manufacturer's instructions. Then the levels of ROS in kidneys were assessed by DCFH-D test kit according to the manufacturer's instructions (Beyotime, China, S0033) (Shen et al., 2020).

Tissue ATP Levels

ATP levels were measured using the ATP test kit (Beyotime, China, S0026). Renal tissue was lysed in the lysis solution, then centrifuged at 16,000g for 5 min. Then the ATP levels were assessed by mixing the equal volume of the supernatant and luciferase reagent, and the chemiluminescence was measured.

Histology

Kidney samples were fixed in 4% paraformaldehyde overnight, dehydrated in an ethanol gradient, cleared in xylene, and embedded in paraffin. Then 3-μm slides were used for hematoxylin and eosin (H&E) staining (Shen et al., 2021), periodic acid-schiff (PAS) staining (Chen et al., 2018), and Masson's trichrome staining (Fan et al., 2017) to evaluate histopathologic injury. At last, the slides were viewed using Nikon 90i microscope. The H&E sections were used to access degrees of tubular damage from 10 fields in each kidney slide (Brooks et al., 2009).

Immunofluorescence Staining

The slides were prepared according to the routine procedure, and IF staining was performed as described previously (Li et al., 2020). Kidney samples were antigen retrieved in 10 mM sodium citrate buffer, washed with PBS, and blocked with goat serum. Then, they are incultured with primary monoclonal antibody anti-CD3 (1: 200), anti-MPO^+ (1:200), and anti-collagen I (1:200) antibodies overnight. Subsequently, the slides were incubated with TRITC-conjugated or FITC-conjugated secondary antibodies.

Immunohistochemical Staining

The sections were performed in accordance with the previous protocals (Li et al., 2020). Briefly, kidney slides were incubated in antigen retrieval buffers, boiled with high power, and then rinsed in PBS, followed by incubation with 3% H_2O_2 and goat serum. They were stained with anti-PCNA (1:200), anti-E-cadherin (1: 200), anti-ZO-1 (1:200), anti-AQP1 (1:250), anti-AQP2 (1:250), anti-NCC (1:250), anti-F4/80 (1:250), anti-TNF-α (1:250), anti-IL-1β (1:250), and anti-fibronectin (1:200) antibodies. Next day, they were washed and incubated with biotinylated goat anti-mouse/rabbit IgG for 1 h. The reaction results were visualized with DAB (1809270031, MXB-BIO, Fuzhou, China) and the slides were counterstained with hematoxylin.

MitoSOX Fluorescence

Freshly kidneys were cut and 10-μm-thick slides were obtained to incubate in PBS containing 10 μM MitoSOX Red reagent (Invitrogen, M36008) for 40 min. Then the sections were rinsed in PBS and mounted onto microscope slides.

Electron Microscopy

Renal cortex was fixed with 2.5% glutaraldehyde in 150 mM cacodylate solution, post-fixed with 1% osmium tetroxide. Subsequent ultrathin sections (50–80 nm) were contrasted by uranyl acetate and lead citrate, and observed with electron microscope (Hitachi H-7650, Japan).

Western Blot

Kidney sample were lysed with the lysis buffer and protein concentration was measured with BCA Protein Assay Kit (Beyotime). Samples were separated by 10% SDS-PAGE, transferred to PVDF membranes and then blocked in 5% milk for 1 h. The primary antibodies were detected, including anti-HIF-1α (1:500), anti-E-cadherin (1:1,000), anti-ZO-1 (1:1,000), anti-AQP1 (1:1,000), anti-AQP2 (1:1,000), anti-Mfn1 (1:1,000), anti-Opa1(1:1,000), anti-Fis1 (1:1,000), anti-Drp1 (1:1,000), anti-TNF-α (1:1,500), anti-IL-1β (1:1,500), anti-vimentin (1:1,000), anti-α-SMA (1:1,000), and anti-β-actin (1:3,000) antibodies. Then the blots were incubated with the corresponding secondary antibodies (1:10,000, Dako).

Quantitative Real-Time PCR

RNA extraction and real-time PCR were performed in accordance with the previous procedure (Zhang et al., 2017). In brief, RNA from kidneys was isolated using Trizol reagent (Vazyme) according to manufacturer' skit, and then the RNA was reverse-transcribed to cDNA following the PrimeScript RT reagent kit. At last, amplification of RT-PCR was following the protocols with a SYBR Green Mix (Vazyme) (Li et al., 2020). The primers were as follows:

HIF-1α forward: 5′-TCATCGGAAACTCCAAAGCCA-3′and reverse:
5′-GGCTGGGAAAAGTTAGGAGTG-3′; collagen I forward:
5′-GGCGGTGCACAGTCAGACCAT -3′ and reverse:
5′-CCAGTTGGTAATGCCATGT-3′; Fn forward:
5′-ATGTGGACCCCTCCTGATAGT -3′ and reverse:
5′-GCCCAGTGATTTCAGCAAAGG-3 ′; TNF-α forward:
5′-CCCTCACACTCAGATCATCTTCT-3′ and reverse:
5′-GCTACGACGTGGGCTACAG-3'; IL-6 forward:
5′-GAGGATACCACTCCCAACAGACC-3′and reverse:
5′-AAGTGCATCATCGTTGTTCATACA-3'; α-SMA forward:
5′-CTTCGCTGGTGATGATGCTC-3′and reverse:
5′-GTTGGTGATGATGCCGTGTT-3'; β-actin forward:
5′-GGCTGTATTCCCCTCCATCG-3′ and reverse:
5′-CCAGTTGGTAATGCCATGT-3′;

The relative mRNA levels were analyzed using the $2^{-\Delta\Delta Ct}$ method.

Statistical Analysis

The values presented were expressed as means ± standard deviations. Statistical comparisons were determined by one-way ANOVA test using SPSS software v.21.0, followed by the Bonferroni test. Values of $p < 0.05$ were considered statistically significant.

RESULTS

FG-4592 Pretreatment Ameliorated FA-Induced Kidney Injury and Facilitated Tubular Recovery

We conducted pathological staining to confirm whether FG-4592 pretreatment could alleviate kidney injury induced by FA overdose injection and promote tubular recovery on the 7th day. Histopathological examination of HE (**Figure 1A**) and PAS (**Figure 1B**) staining showed that FA induced severe lesions in the tubules with obvious maladaptive repair, including tubular dilation, tubular epithelial cell edema or loss, and inflammatory cell infiltration into the interstitium. In contrast, FG-4592 pretreatment dramatically alleviated the lesions and facilitated recovery, as indicated by an improved tubular structure and decreased tubular injury score (**Figure 1C**). Consistent with the histological changes, the FA group showed deteriorated renal function, as indicated by increased levels of BUN (**Figure 1D**) and creatinine (**Figure 1E**), but the levels were decreased with FG-4592 pretreatment.

FG-4592 Pretreatment Promoted Structural Regeneration of Tubules on the 7th Day After FA Injection

Regeneration of tubular epithelial cells can accelerate kidney repair after AKI (Jiang et al., 2015). To substantiate the regenerative effect, we examined tubular cell repopulation by staining for PCNA. As shown in **Figure 2A**, IHC analysis indicated that the number of PCNA-positive tubular cells was slightly increased on the 7th day in FA-injected mice compared with mice without FA administration; in contrast, the mice with FG-4592 pretreatment exhibited greater increases in the numbers of PCNA-positive tubular cells. Consistent with the results of IHC, Western blot analysis (**Figures 2B,C**) demonstrated that the level of PCNA was up-regulated after FA insult, and this up-regulation was further promoted with FG-4592 pretreatment, suggesting that FG-4592 pretreatment can facilitate tubular cell proliferation.

In addition, recovery of the integrity of epithelial cell-cell junctions is essential for renal tubule repair. IHC analysis (**Figure 3A**) showed that E-cadherin, an adherens junction molecule, was highly expressed at the basolateral junction sites between neighboring cells in normal tubules. In comparison, the expression of E-cadherin was significantly reduced on the 7th day after FA injection but was restored with FG-4592 pretreatment. In addition, ZO-1 (a marker of tight junctions) was normally localized at the apical and basolateral junction sites between neighboring cells in the tubules but was significantly down-regulated after FA injection; however, its expression was partly restored with FG-4592 pretreatment. As described for IHC, these changes were further confirmed through Western blot analysis, and significantly decreased expression of E-cadherin and ZO-1

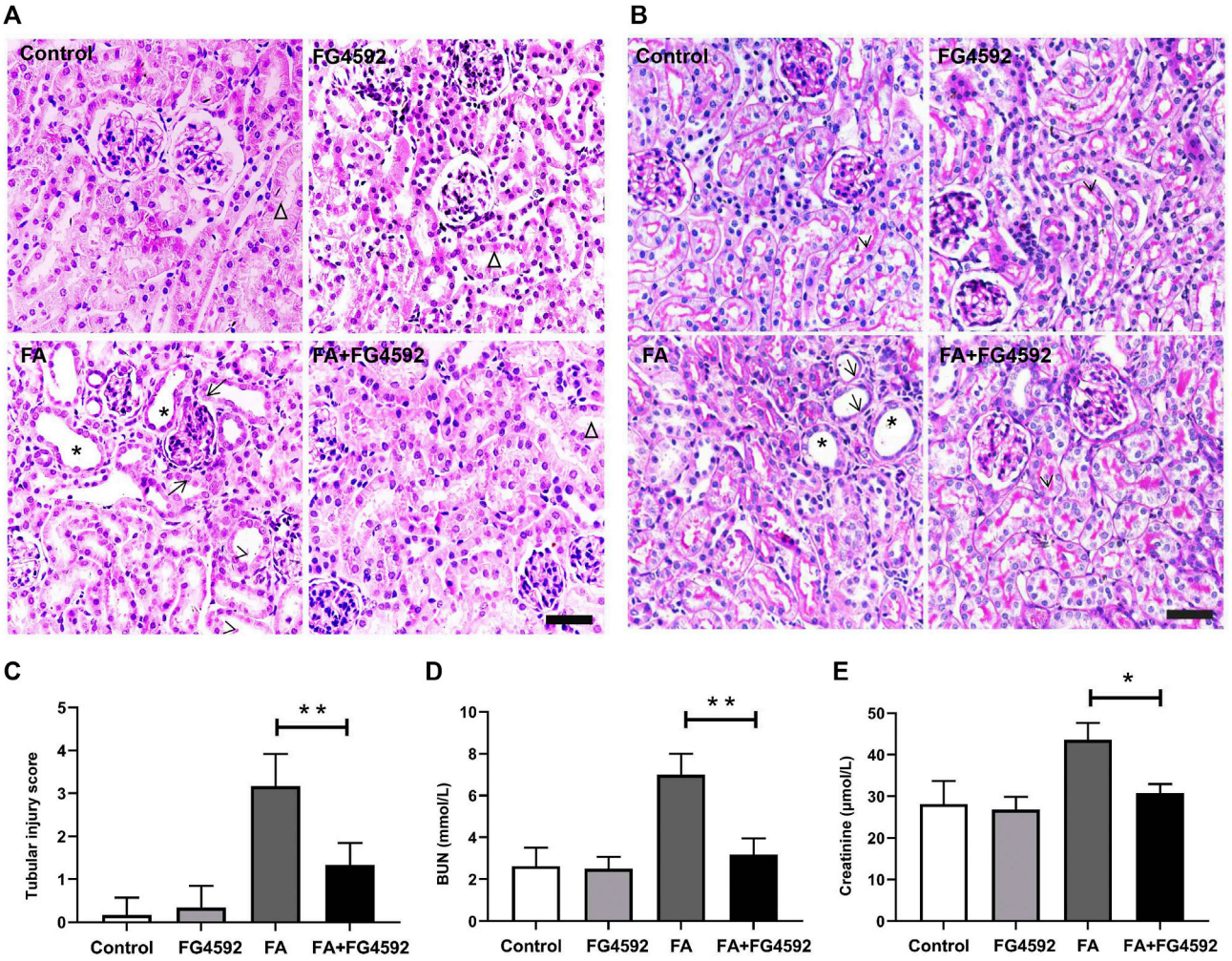

FIGURE 1 | FG-4592 pretreatment ameliorated FA-induced renal damage and facilitated tubular recovery. **(A)** Renal histological assessment by HE staining. The asterisks indicate dilated tubules, the arrows indicate swollen epithelial cells, the arrowheads indicate tubules with cellular debris, the triangles indicate the normal tubule. **(B)** Renal histological assessment by PAS staining. The asterisks indicate tubular ectasia, the arrows indicate loss of tubular cells, and the arrowheads indicate the brush border. **(C)** Tissue injury scores relying on HE staining. **(D)** Serum BUN. **(E)** Serum creatinine. The data are expressed as the mean ± SE. Scale = 50 μm, $^{*}p < 0.05$, $^{**}p < 0.01$.

was found in FA-injured kidneys, whereas FG-4592 pretreatment reversed these effects, as depicted in **Figures 3B–D**.

FG-4592 Pretreatment Facilitated Functional Recovery of Tubules on the 7th Day After FA Injection

The recovery of epithelial structural integrity plays a fundamental role in the restoration of tubular functions, such as absorption of fluid and solutes (Wang et al., 2008). We further detected functional recovery in different tubular segments with FG-4592 pretreatment on the 7th day after FA injection. IHC analysis (**Figure 4A**) demonstrated that AQP1 was widely expressed in the normal proximal tubules but down-regulated with dilation of the tubules after FA injection. However, FG-4592 pretreatment caused AQP1 to be re-expressed. Moreover, NCC, one of the essential sodium transporters, was highly expressed in normal distal tubules, but FA administration caused down-regulation of NCC. NCC expression was restored with FG-4592 pretreatment. Moreover, the level of AQP2 in the collecting ducts was significantly reduced after FA injection, while it was partially restored with FG-4592 pretreatment. Consistently, Western blot analysis indicated that compared with that in the FA group, the expression of AQP1 and AQP2 in the FA + FG-4592 group was significantly higher, as shown in **Figures 4B–D**.

FG-4592 Pretreatment Alleviated Ferroptosis and Inflammation, and Further Inhibited Interstitial Fibrosis on the 7th Day After FA Injection

Ferroptosis was evidenced to be the major cause in FA-induced AKI, which has been reported to be a driver of other pathways of cell death (Martin-Sanchez et al., 2017) To better evaluate the effect

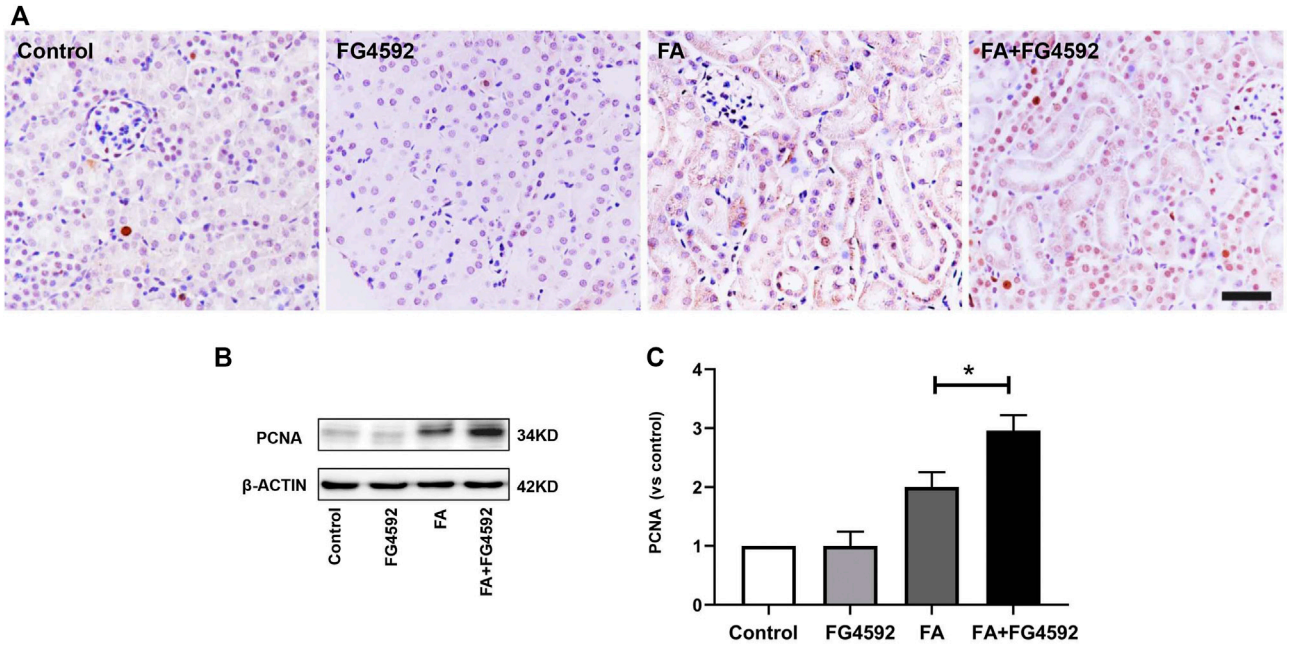

FIGURE 2 | FG-4592 pretreatment promoted tubular cell proliferation in FA-induced renal damage. **(A)** Renal micrographs by IHC for PCNA. **(B)** Western blot analysis of PCNA in kidney lysates. **(C)** Relative abundance of PCNA. The data are expressed as the mean ± SE. Scale = 50 μm, $^{*}p < 0.05$, $^{**}p < 0.01$.

of FG-4592 on the ferroptosis, the expressions of IL-33 and GPX4 were assessed by Western blot analysis. As depicted in **Figures 5A–C**, FA induced up-regulation of cleaved IL-33, while this effect could be partly inhibited with FG-4592 pretreatment. In addition, we observed that FG-4592 pretreatment was able to prevent the down-regulation of GPX4. Then we further explore whether FG-4592 pretreatment could inhibit inflammatory responses during the repair phase in FA-induced AKI. As described in **Figures 5D–F**, Western blot analysis indicated that FA induced up-regulation of the inflammatory cytokines TNF-α and IL-1β, which could be inhibited by FG-4592 pretreatment. Also, IHC analysis showed that TNF-α- and IL-1β-positive tubular cells were rarely expressed in non-FA-injected kidneys, but an abundance of these cells were observed after FA injection. However, these effects were prevented with FG-4592 pretreatment (**Figure 5G**). Furthermore, we assessed the levels of inflammatory cells, including macrophages, lymphocytes, and neutrophils on the 7th day after FA insult. As depicted in **Figure 5G**, few F4/80-positive cells were detectable in the kidneys of control or FG-4592-treated mice in kidney specimens by IHC staining. In contrast, following folic acid injury, abundant F4/80-positive cells were found in the renal interstitium, while pretreatment with FG-4592 markedly reduced the number of F4/80 + macrophages in the FA-injured kidneys. Consistently, FA-injured kidneys exhibited significant infiltrations of lymphocytes and neutrophils, as indicated by up-regulation of CD3- and MPO-positive cells, compared to that in the kidneys of control or FG-4592-treated mice, as shown by IF staining in **Figure 5H**, the numbers of these positive inflammatory cells in the kidneys were reduced by FG-4592 pretreatment, denoting anti-inflammatory activity. Furthermore, maladaptive repair after AKI aggravates inflammation, which may further drive CKD progression (Jiang et al., 2016a). To investigate the impact of FG-4592 pretreatment on interstitial fibrosis, Masson staining was performed. The results (**Figure 6A**) showed that FA injection induced severe tubular atrophy and collagen deposition in the interstitial space at Day 7 after FA injection, while FG-4592 pretreatment ameliorated these alterations. Moreover, we assessed some matrix proteins, such as collagen I and fibronectin. As depicted in **Figures 6B,C**, increased accumulation of fibronectin (Fn) and collagen I in the renal tubulointerstitium was observed in FA-injected mice at Day 7. The morphologic findings were further confirmed by RT-PCR, which showed that the gene levels of fibronectin and collagen I were upregulated after FA injection and were reduced by FG-4592 pretreatment (**Figures 6D,E**). In accordance with this findings, increased protein expression of α-SMA and vimentin in FA-injected kidneys was observed by Western blot analysis, while this effect was remarkably abrogated by FG-4592 pretreatment, indicating less epithelial-to-mesenchymal transition (EMT) and better recovery, as noted in **Figures 6F–H**.

FG-4592 Pretreatment Suppressed the Activation of HIF-1α and Ameliorated Mitochondrial Dysfunction on the 7th Day After FA Injection

To determine the role of FG-4592 pretreatment in the alterations in HIF-1α on the 7th day after FA administration, the protein and gene expression levels of HIF-1α were evaluated. Western blot analysis (**Figures 7A,B**) showed that the level of HIF-1α was increased after FA injection, whereas this increase was inhibited with FG-4592 pretreatment. A similar pattern was observed in the

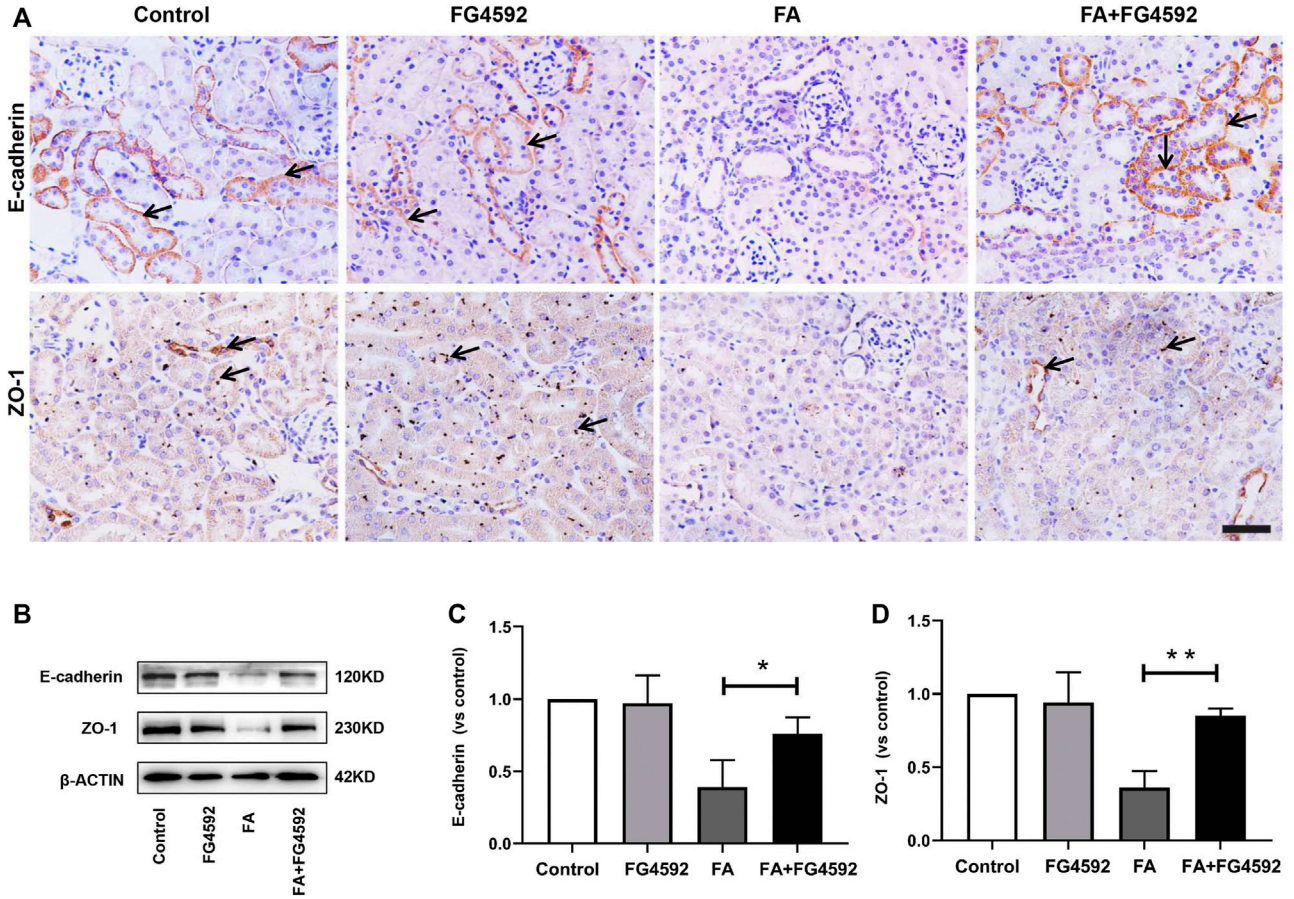

FIGURE 3 | FG-4592 pretreatment promoted the restoration of tubular structural integrity in FA-induced renal damage. **(A)** Renal micrographs of IHC for E-cadherin and ZO-1. **(B)** Western blot analysis of E-cadherin and ZO-1. **(C)** Relative abundance of E-cadherin. **(D)** Relative abundance of ZO-1. The data are expressed as the mean ± SE. Scale = 50 μm, $^{*}p < 0.05$, $^{**}p < 0.01$.

RT-PCR results (**Figure 7C**), in which FG-4592 pretreatment suppressed the up-regulation of HIF-1α mRNA levels induced by FA administration.

Furthermore, hypoxia-induced HIF-1α activation has been reported to be related to mitochondrial fragmentation (Zhang et al., 2018), which is one of the major factors that causes kidney injury and subsequent incomplete repair (Chung et al., 2019). Next, we assessed the ultrastructure of mitochondria (**Figure 7D**) and found that a large number of long filamentous mitochondria were present at the basolateral side in normal proximal tubular cells, while mitochondria in the perinuclear position showed cross-sectioning and appeared fragmented. In contrast, mitochondria were destroyed to a great extent and completely fragmented into swollen and short mitochondria with effacement of cristae after FA injection; moreover, this phenotype was accompanied by remarkably decreased ATP levels. While FG-4592 pretreatment could alleviate these alterations and promote ATP production, as shown in **Figure 7E**. In addition, mitochondrial dysfunction was characterized by excessive ROS production, which could be inhibited by FG-4592 pretreatment (**Figure 7F**). Moreover, the dynamic imbalance of mitochondria could induce increased level of mitochondrial ROS, which was further confirmed by analysis of the fluorescence intensity of MitoSOX, as shown in **Figure 7G**.

Moreover, we evaluated the effect of FG-4592 pretreatment on mitochondrial dynamics, which are mainly regulated by mitochondrial fusion and fission proteins. Western blot analysis showed increased expression of mitochondrial fission proteins (Fis1 and Drp1) (**Figures 8A–C**) and reduced expression of mitochondrial fusion proteins (Opa1 and Mfn1) (**Figures 8D–F**) after FA injection, indicating a shift in mitochondrial dynamics toward the fission process. On the other hand, FG-4592 pretreatment improved all these alterations, supporting the idea that FG-4592 pretreatment promoted the transition from mitochondrial fission to fusion. The dynamic alterations in mitochondrial activity indicated that mitochondrial damage induced by FA could be partially attenuated by FG-4592 pretreatment.

FG-4592 Pretreatment Alleviated HK-2 Cells Injury Induced by TNF-α

We evaluated the impact of FG-4592 on cell viability in the HK-2 cells at concentrations of 5–80 μM by CCK-8 assay. As shown in

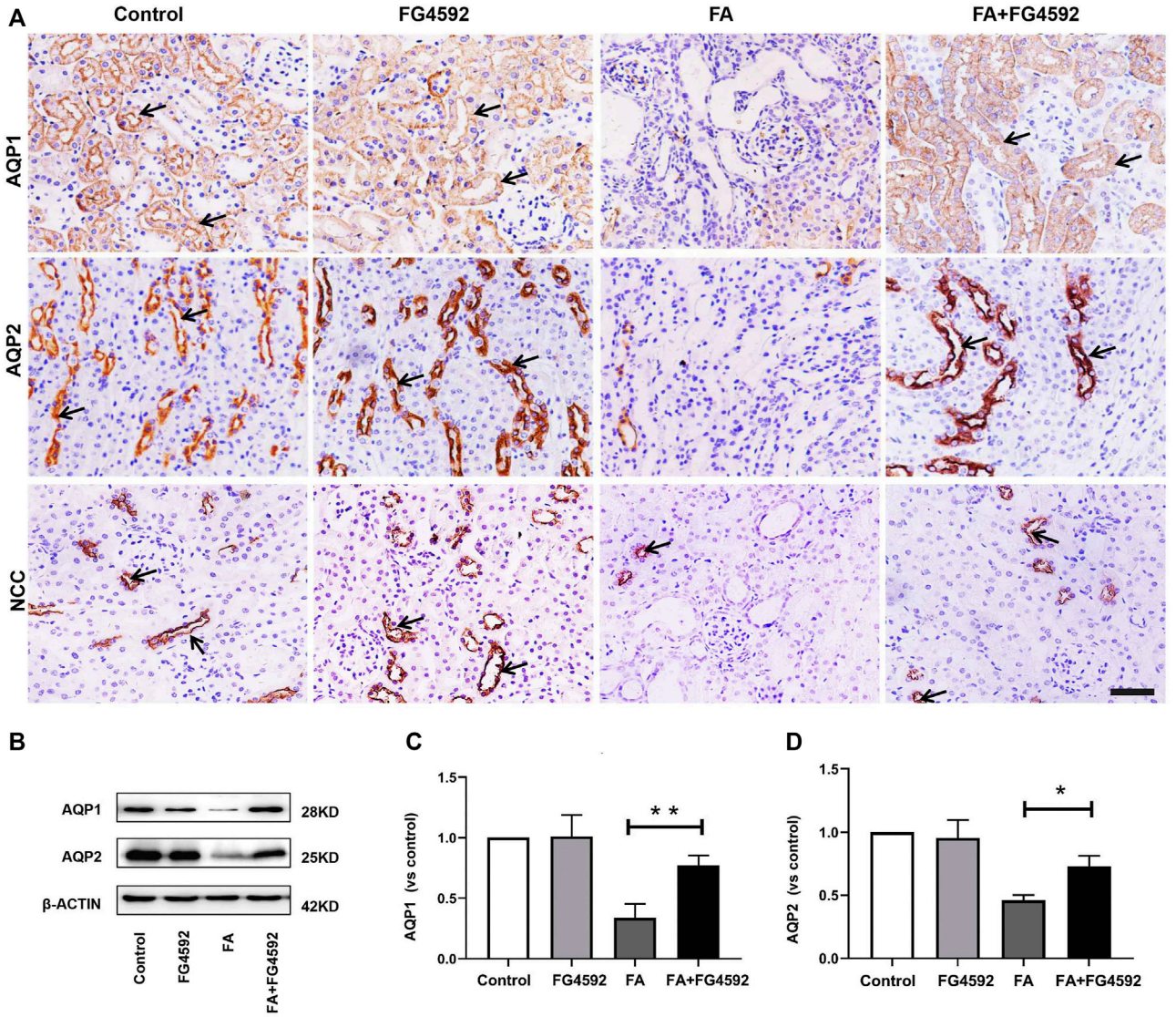

FIGURE 4 | FG-4592 pretreatment promoted tubular functional recovery in FA-induced renal damage. **(A)** Renal micrographs of IHC for AQP1, AQP2, and NCC. **(B)** Western blot analysis of AQP1 and AQP2. **(C)** Relative abundance of AQP1. **(D)** Relative abundance of AQP2. The data are expressed as the mean ± SE. Scale = 50 μm, $^{*}p < 0.05$, $^{**}p < 0.01$.

Figure 9A, FG-4592 had no cellular toxicity at concentrations of 5–20 μM, while FG-4592 at concentrations of 40 and 80 μM decreased cell viability. Moreover, we explored the effect of FG-4592 treatment on TNF-α-treated HK-2 cells and found that FG-4592 pretreatment could attenuate the reduced cell viability induced by TNF-α (**Figure 9B**). In addition, we measured the level of inflammation and found that FG-4592 at concentrations of 20 μM could down-regulate the gene levels of the inflammatory cytokines TNF-α and IL-6 induced by TNF-α (**Figures 9C,D**). In addition, we accessed the impact of FG-4592 on the expression of E-cadherin in HK-2 cells with or without FG-4592 pretreatment. As shown in **Figures 9E,F**, the Western blot results showed that E-cadherin was highly expressed in normal HK-2 cells but that the expression was significantly reduced after TNF-α stimulation, while the levels of E-cadherin were restored with FG-4592 pretreatment. Moreover, pretreatment with FG-4592 could markedly reduce the increased gene of α-SMA caused by TNF-α (**Figure 9G**, **Supplementary Figure S1**).

DISCUSSION

Mitochondrial dysfunction is a central factor to maladaptive repair after AKI (Stallons et al., 2014), and promoting the balance of mitochondrial dynamics is closely associated with the recovery of tubular cells that undergo sublethal injury (Wills et al., 2012). Thus, drugs that can ameliorate mitochondrial dysfunction may accelerate the recovery of

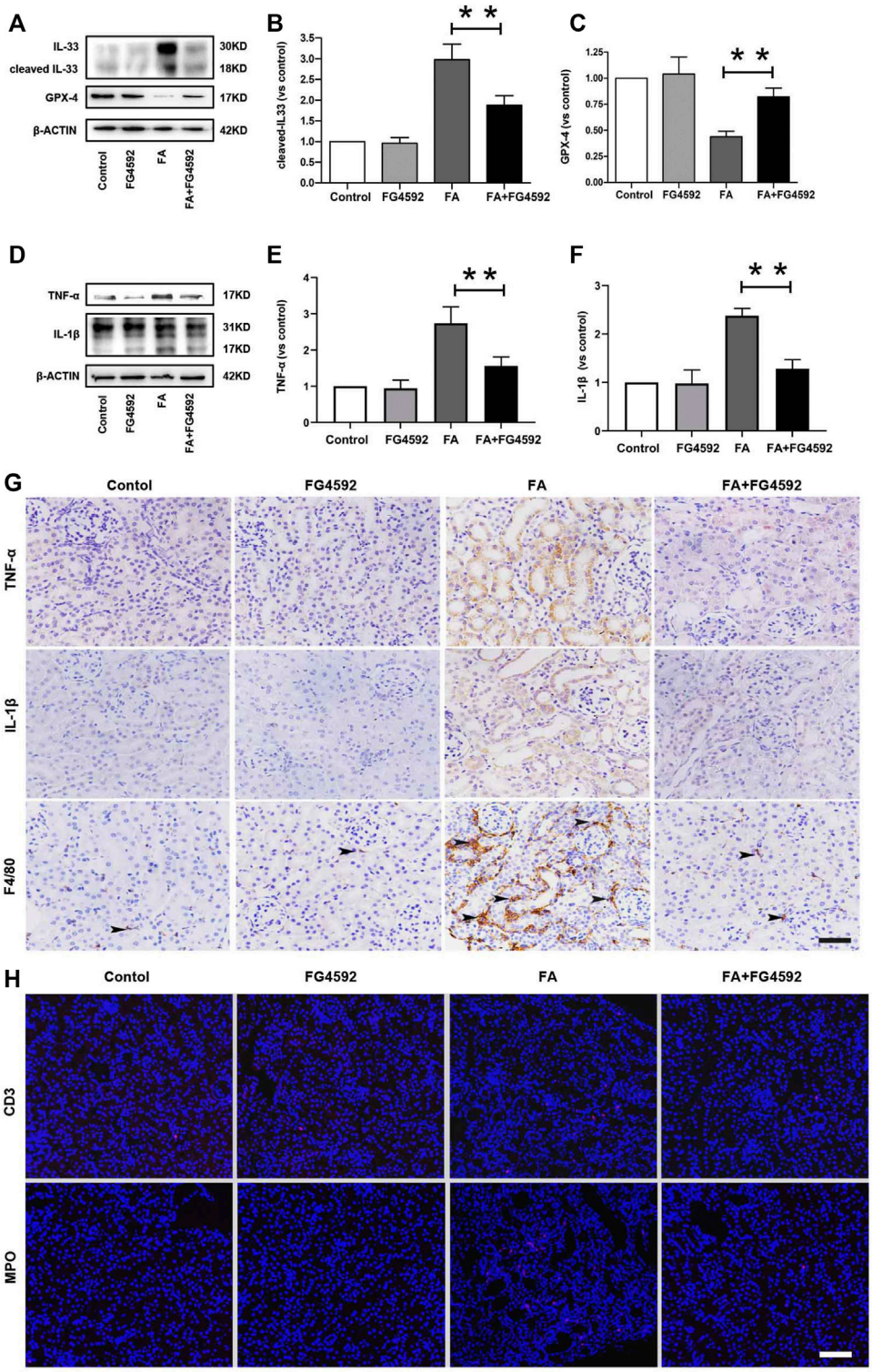

FIGURE 5 | FG-4592 pretreatment alleviated ferroptosis and inflammation on the 7th day after FA injection. **(A)** Western blot analysis of IL-33 and GPX-4. **(B)** Relative abundance of cleaved-IL-33. **(C)** Relative abundance of GPX-4. **(D)** Western blot analysis of TNF-α and IL-1β. **(E)** Relative abundance of TNF-α. **(F)** Relative abundance of IL-1β. **(G)** Renal micrographs of IHC for TNF-α, IL-1β and F4/80-positive macrophages. **(H)** Renal micrographs of IF for CD3-positive lymphocytes and MPO-positive neutrophils. The data are expressed as the mean ± SE. Scale = 50 μm, $^{*}p < 0.05$, $^{**}p < 0.01$.

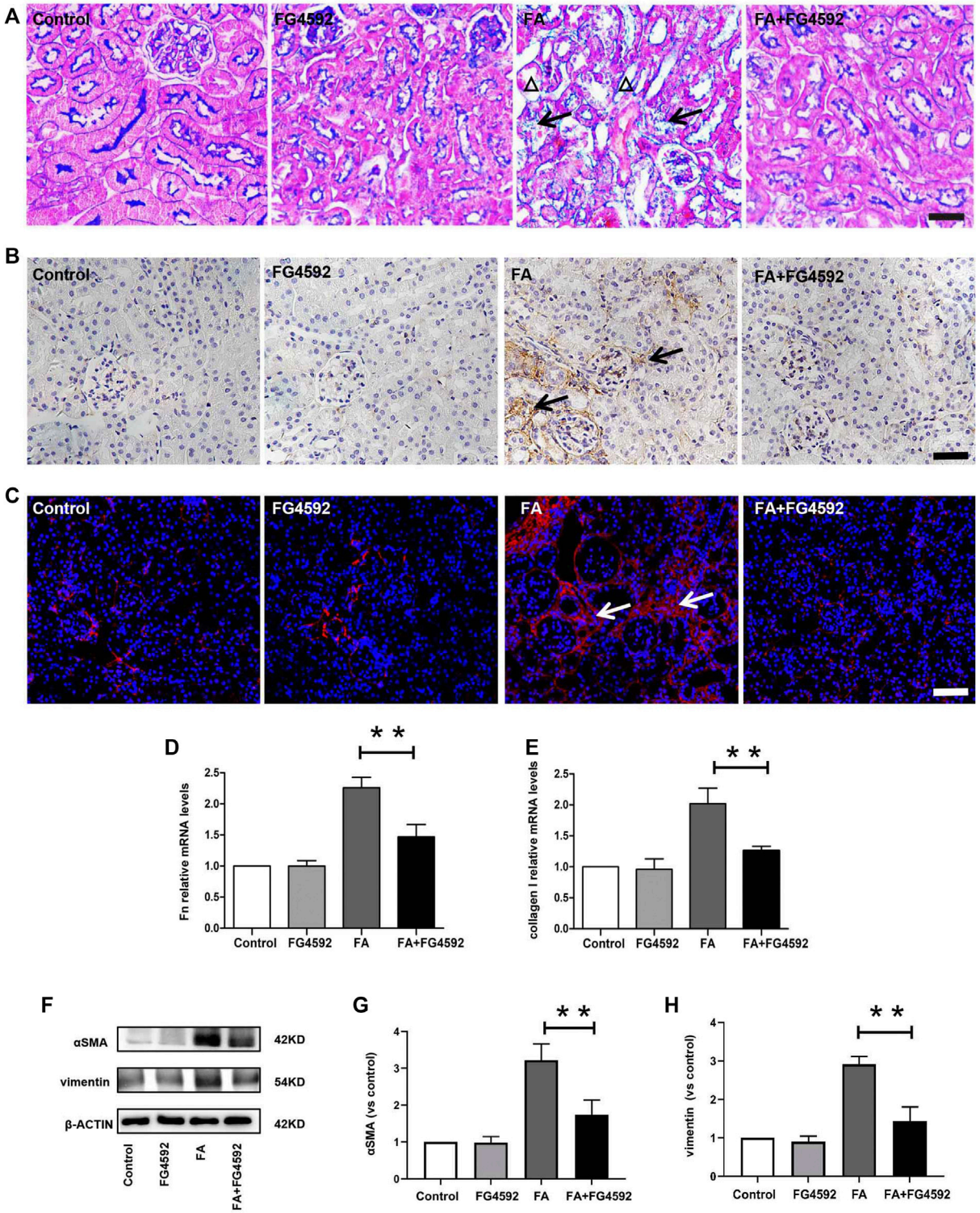

FIGURE 6 | FG-4592 pretreatment inhibited renal fibrosis on the 7th day after FA injection. **(A)** Renal histological assessment by Masson trichrome staining. The triangles indicate the tubular atrophy and the arrows indicate collagen deposition. **(B)** Renal micrographs of IHC for Fibronectin. **(C)** Renal micrographs of IF for collagen I. **(D)** Relative mRNA level of Fibronectin. **(E)** Relative mRNA level of collagen I. **(F)** Western blot analysis of α-SMA and vimentin. **(G)** Relative abundance of α-SMA. **(H)** Relative abundance of vimentin. The data are expressed as the mean ± SE. Scale = 50 μm, $^{*}p < 0.05$, $^{**}p < 0.01$.

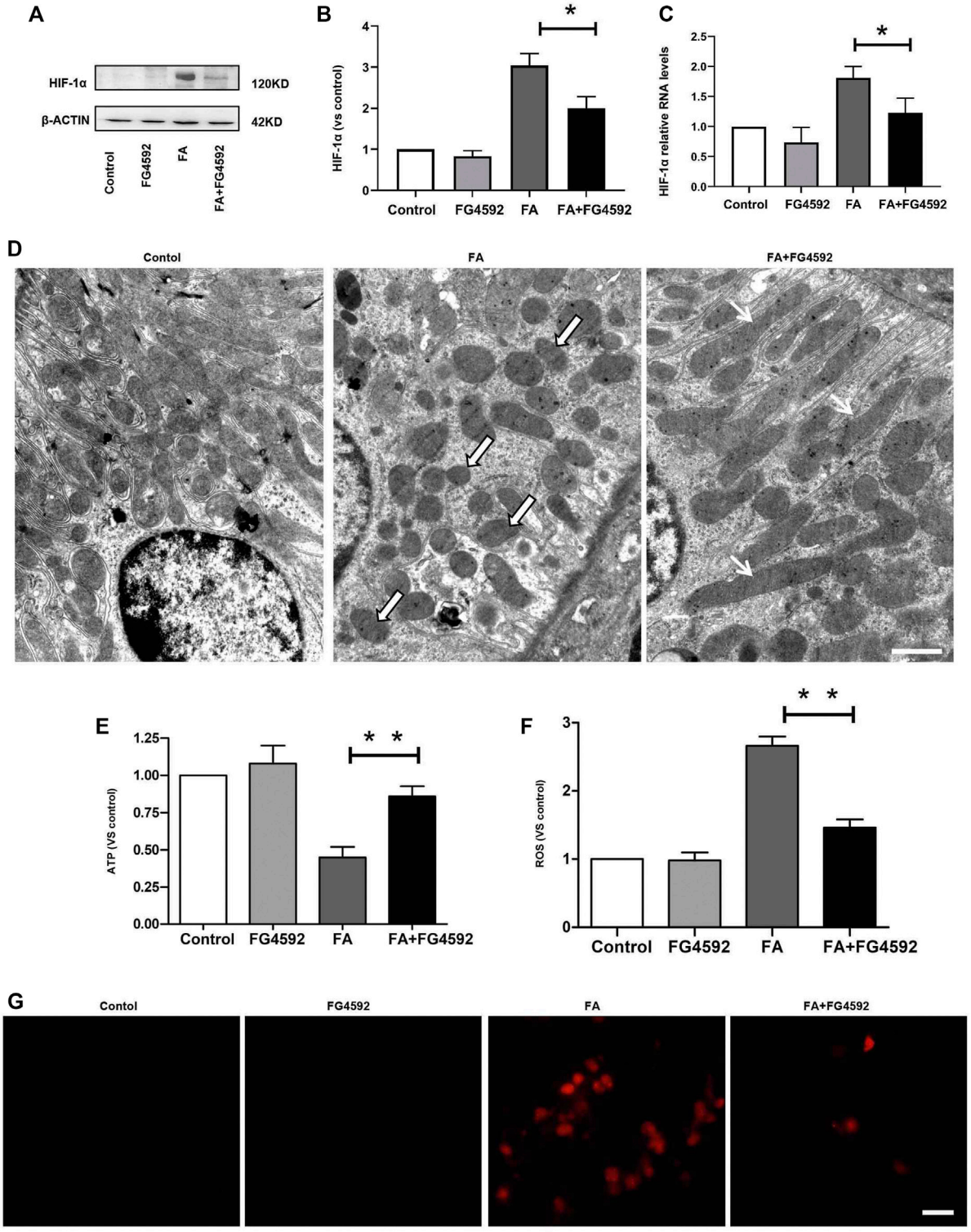

FIGURE 7 | FG-4592 pretreatment suppressed HIF-1α activation and restored the alterations in mitochondrial morphology and function induced by FA injection. **(A)** Western blot analysis of HIF-1α. **(B)** Relative abundance of HIF-1α. **(C)** Relative mRNA level of HIF-1α. **(D)** Representative transmission electron microscopy for mitochondrial morphology at 20,000× magnification, Scale = 1 μm. Black and White Arrows indicate mitochondrial fragmentation; Black Arrows indicate elongated (>2 μm) mitochondria.). **(E)** ATP level in the kidney. **(F)** The level of ROS in the kidney. **(G)** Mitochondrial superoxide was detected by MitoSOX Red fluorogenic dye. The data are expressed as the mean ± SE. Scale = 50 μm, $^{*}p < 0.05$, $^{**}p < 0.01$.

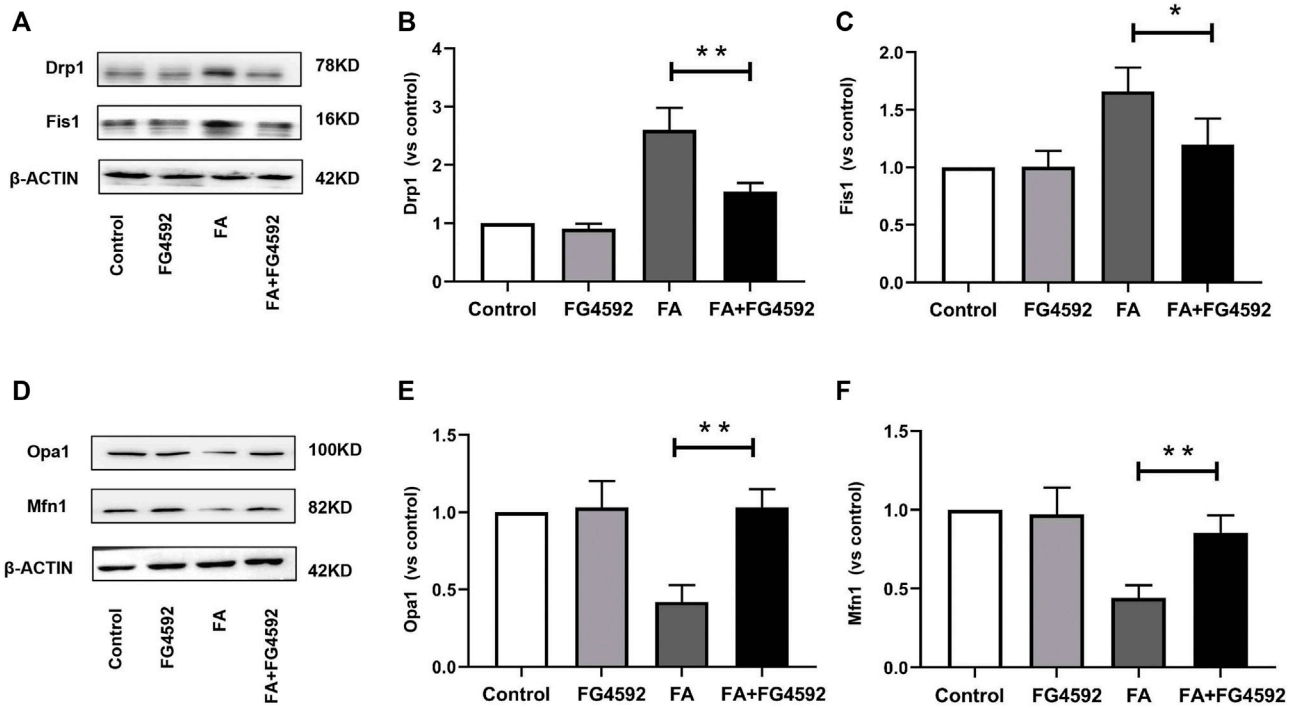

FIGURE 8 | FG-4592 pretreatment attenuated FA-induced imbalance of mitochondrial dynamics. **(A)** Western blot analysis of Drp1 and Fis1. **(B)** Relative abundance of Drp1. **(C)** Relative abundance of Fis1. **(D)** Western blot analysis of Opa1 and Mfn1. **(E)** Relative abundance of Opa1. **(F)** Relative abundance of Mfn1. The data are expressed as the mean ± SE. Scale = 50 μm, $^{*}p < 0.05$, $^{**}p < 0.01$.

renal tubules in AKI. Hypoxia and mitochondrial dynamics have been reported to be closely connected, while continuous hypoxia can induce the activation of HIF-1α, which negatively regulates mitochondrial function (LaGory et al., 2015; Jun et al., 2017).

FG-4592, a kind of prolyl hydroxylase inhibitor, has been used as a pretreatment to attenuate AKI through anti-oxidative stress in our previous study by increasing the levels of HIF-1α at the acute phase (Li et al., 2020); however, inhibition of HIF-1α mRNA was observed (data not shown) at the same time, which may be related to negative feedback. Here, we investigated the role of FG-4592 pretreatment in HIF-1α activity and renal damage in the repair phase. Tubular repair caused by FA overdose injection has been reported to commence from the 6th day, and maladaptive recovery occurs due to severe damage (Stallons et al., 2014). In view of this, we performed HE and PAS staining and observed the partial restoration of normal kidney architecture on the 7th day after FA administration, which was characterized by repopulation of some of the tubular epithelial cells. FG-4592 pretreatment facilitated recovery and alleviated tubular damage induced by FA. Furthermore, in contrast to the increases in HIF-1α protein levels observed on the 2nd day in FA-injected kidneys with FG-4592 pretreatment, inhibition of HIF-1α protein expression was observed on the 7th day. This was in line with the suppression of HIF-1α mRNA levels, indicating that the protein expression of HIF-1α is time-dependent with FG-4592 pretreatment and that the role of this protein may differ in different phases of AKI. In this regard, we speculate that FG-4592 pretreatment may be a powerful strategy to prevent the activation of HIF-1α induced by constant hypoxia during the recovery phase of AKI, thereby promoting tubular repair and improving its prognosis. Our study supports previous findings that suppression of HIF-1α activation induced by consistent hypoxia can alleviate tubular damage (Takiyama et al., 2011).

In addition, adaptive tubular repair is an important process to delay AKI progression, and tubular cell regeneration is a key event (Basile et al., 2016). It has been reported that fully differentiated tubular cells have equal chances of proliferation after injury (Humphreys et al., 2016; Soofi et al., 2020). In our study, increased cell proliferation was observed in the FG-4592-treated mice, indicating the stimulation of tubular repair. Furthermore, tubular cell proliferation drives restoration of tubular epithelial integrity, which is critical to the repair of AKI (Nony and Schnellmann 2003). E-cadherin, a major component of cell-cell AJs, plays an important role in tubular integrity and polarity (Gao et al., 2018). It has been demonstrated that the E-cadherin levels in tubular cells are significantly reduced in response to cisplatin, but tubular damage can be alleviated with restoration of E-cadherin expression (Ni et al., 2019). Another study has demonstrated that decreased expression of E-cadherin is part of the phenotype of epithelial-to-mesenchymal transition and is closely associated with renal fibrosis (Fragiadaki and Mason 2011). Moreover, the assembly of AJs is associated with that of TJs, and destruction of E-cadherin-mediated AJs also delays TJ assembly (Capaldo and Macara 2007). ZO-1, the critical TJ protein, is essential for tubular barrier formation.

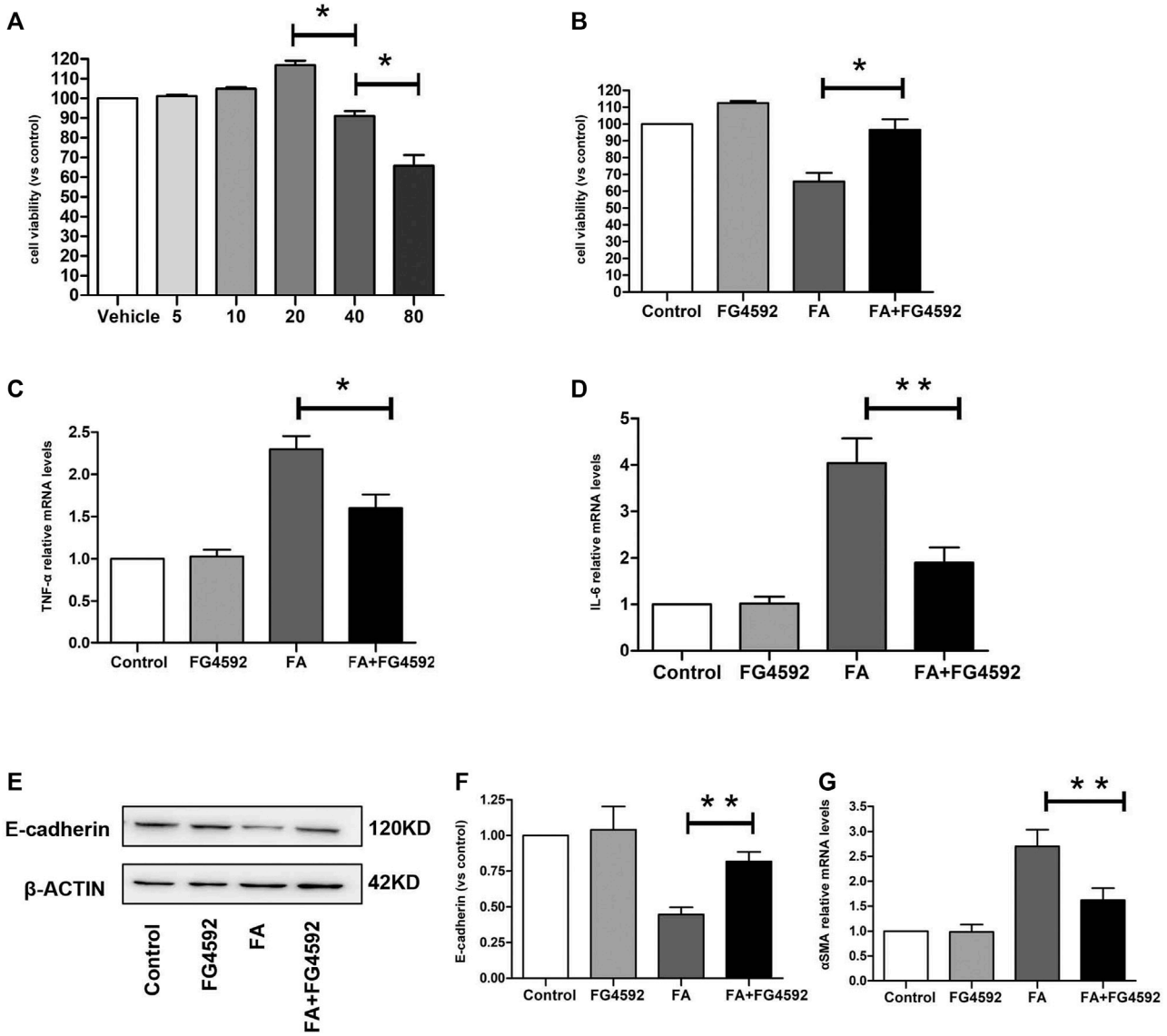

FIGURE 9 | Effect of FG-4592 pretreatment on HK-2 cell induced by TNF-α. **(A)** CCK8 assay of the viability in HK-2 cells treated with FG-4592. **(B)** CCK8 assay of the viability in HK-2 cells treated by TNF-α with or without FG-4592 pretreatment. **(C)** Relative mRNA level of TNF-α. **(D)** Relative mRNA level of IL-6. **(E)** Western blot analysis of E-cadherin. **(F)** Relative abundance of E-cadherin. **(G)** Relative mRNA level of α-SMA. The data are expressed as the mean ± SE. $^{*}p < 0.05$, $^{**}p < 0.01$.

Eadon and colleagues observed decreased expression of ZO-1 in LPS-mediated AKI (Eadon et al., 2012). Our findings are consistent with these observations that FA injury induces disruption of tubular AJs and TJs, as reflected by down-regulation of E-cadherin and ZO-1 levels. However, FG-4592 pretreatment retained the expression of these molecules in tubular cells, indicating the ability to maintain the structural integrity of tubular cells. Along with the protective effects shown *in vivo*, FG-4592 pretreatment could also protect renal tubular cells against TNF-α induced down-regulation of E-cadherin *in vitro*.

Moreover, restoration of the tubular epithelial barrier is indispensable for maintaining tubular function and is mainly involved in reabsorption capacity and ion transport, which contribute to body fluid volume regulation and electrolyte handling (Pozzi and Zent 2010; Fattah and Vallon 2018). AQPs, especially AQP1 and AQP2, account for the regulation of water transport and urinary concentration (Agre et al., 2002). Previous studies have shown that AQP1, which is widely expressed in the proximal tubules as well as descending thin limbs, is downregulated by I/R injury, which contributes to urinary concentration defects (Ma et al., 1998). Moreover, endotoxemia can induce more severe tubular injury in AQP1-null mice than in wild-type mice, which is characterized by polyuria (Hua et al., 2019). In contrast, AQP1 overexpression can alleviate aristolochic acid-induced nephropathy (Anger et al.,

2020). In addition, it has been reported that AQP1 levels in the proximal tubule together with AQP2 levels in the collecting duct are decreased in I/R-induced kidney injury, which results in impaired urinary osmolality (Kwon et al., 1998; Kortenoeven and Fenton 2014). Down-regulation of the sodium cotransporter, NCC, is also associated with dysfunction of sodium excretion and impaired urinary concentration ability in AKI (Bae et al., 2008; Yang et al., 2013). Furthermore, restoration of urinary concentration capacity may inhibit the transition from AKI to CKD (Asvapromtada et al., 2018). Our observations are in line with these reports. Specifically, we found that FA injury decreased the expression of AQP1, NCC, and AQP2 but that the expression of these molecules was restored with FG-4592 pretreatment, facilitating tubular functional recovery.

In addition, AKI is often accompanied by tubular epithelial necrosis, which could further inhibit the repair of injured kidneys. While ferroptosis was reported to act as an important mechanism that contributes to FA-induced acute renal damage, the protective effect of FA-induced AKI might be achieved by inhibiting ferroptosis (Hu et al., 2019). Similarly, we observed that FG-4592 pretreatment reversed the elevation in IL-33 and decrease in GPX4 induced by FA injection, suggesting that anti-ferroptosis may be the main pathway involved in the protection against FA-induced AKI. Moreover, maladaptive repair of tubules can further activate proinflammatory and profibrotic effects (Jiang et al., 2016b). Disruption of E-cadherin has been shown to promote inflammation in cisplatin-induced tubular injury (Gao et al., 2018). Restoration of AQP1 has been reported alleviate inflammation in LPS-induced renal damage (Li et al., 2019). Consistently, our discoveries indicate that FG-4592 pretreatment can reduce the recruitment of numerous macrophages, lymphocytes, and neutrophils, as well as the release of the inflammatory factors TNF-α and IL-1β induced by FA insult, thereby reducing renal damage of function and structure. Although we did not differentiate the subtypes of macrophages, a previous study has indicated that the majority of macrophages that infiltrate the interstitium on the 7th day after FA injection are M1 macrophages, which exhibit proinflammatory activities (Jiang et al., 2016b). In consistency, we observed that inflammatory factors were increased by stimulating HK-2 cells with TNF-α, while FG-4592 pretreatment could attenuate these alterations. Meanwhile, FG-4592 pretreatment could reduce α-SMA level, indicating the amelioration of EMT *in vitro*. What is more, down-regulation of HIF-1α along with mitochondrial stress modulation strategy was demonstrated to curtail inflammation in mammary gland chemoprevention (Roy et al., 2017).

Mitochondria are the main energy sources in tubular cells, but mitochondrial dysfunction can lead to maladaptive progression of AKI and further accelerate fibrosis development (Yu and Bonventre 2020). It has been reported that mitochondrial fragmentation is significantly increased in tubular epithelial cells treated with cisplatin or glycerol (Brooks et al., 2009). Moreover, maladaptive repair from FA-induced AKI is recognized as a complex multifactorial process in which mitochondrial impairments play important roles (Sun et al., 2019). Through subcellular structure analysis, we found that mitochondrial fragmentation or mitochondrial shrinkage induced by FA injection increased under hypoxia, leading to a reduction in intracellular ATP, while FG-4592 pretreatment improved the situation. Moreover, mitochondrial damage not only contributes to decreases in ATP levels but also results in excessive production of ROS, which adversely affects cell survival and recovery (Apostolova and Victor 2015). Consistently, a marked elevation in mitochondrial ROS after FA injection was observed in our study, and this elevation was attenuated by FG-4592 pretreatment. In addition, up-regulation of HIF-1α level was found to be closely associated with dysfunction of mitochondria, which can induce mammary gland carcinoma progression (Singh et al., 2021b). Polyl hydroxylase (PHD-2) activation was considered as a novel strategy to control HIF-1α to modulate mitochondrial stress in mammary gland pathophysiology of ER + subtype (Singh et al., 2021a). Meanwhile, down-regulation of HIF-1α/fatty acid synthase co-axis was shown to combat tumor growth in mammary gland carcinoma by activating PHD-2 (Gautam et al., 2018) (Manral et al., 2016).

Furthermore, inactivation of HIF-1α induced by consistent hypoxia can ameliorate mitochondrial dysfunction and alleviate tubular damage (Takiyama et al., 2011). During AKI, mitochondria experience dynamic imbalance, which depletes cellular ATP and further induces the loss of tight junctions and adherens junctions (Molitoris 2004). The balance of mitochondrial fusion and fission is important for appropriate mitochondrial morphology and function to meet the energy needs of tubular cells and restore ATP production. Targeted treatment with drugs that ameliorate mitochondrial function by inhibiting the expression of Drp1 and restoring the expression of Mfn2 have been reported to ameliorate AKI (Ishimoto and Inagi 2016). Drp1, a GTPase, regulates mitochondrial fission processes, but its upregulation is detrimental because it enhances mitochondrial fragmentation (Tang et al., 2013). Perry et al. showed that suppression of Drp1 expression in proximal tubular cells accelerated recovery, therefore attenuating fibrosis following renal IR (Perry et al., 2018). Consistent with these mechanisms, we found that FA induced mitochondrial fragmentation through increased expression of fission proteins (Drp1 and Fis1) and decreased expression of fusion proteins (Opa1 and Mfn1). In contrast, FG-4592 pretreatment recovered the balance of mitochondrial dynamics by reversing these changes, therefore promoting mitochondrial elongation. Moreover, mitochondrial hyperfission is critical for promoting cellular necrosis, which is characterized by a reduced number of mitochondrial cristae and the change of mitochondrial membrane potential, resulting in cell volume shrinkage (Spurlock et al., 2020). Specifically, GPX4 is partially located in the intermembrane spaces of mitochondria to maintain mitochondrial membrane potential, which can counteract ferroptotic cell death. GPX4-ablated cells contain swollen mitochondria with disappearance of cristae and a lamellar architecture (Baseler et al., 2013).

In summary, our findings indicate that mitochondrial dysfunction may be pathogenic in the maladaptive repair of FA-induced AKI. Moreover, we show the beneficial effects of FG-4592 pretreatment against renal damage associated with FA overdose injection. FG-4592 decreases tubular structural and functional injury, inhibits tubular ferroptosis and inflammation, and specifically accelerates recovery from tubular injury. As a result of these actions, FG-4592 pretreatment decreases interstitial fibrosis. Finally, we identified facilitation of the homeostasis of mitochondrial dynamics as a key pathway involved in the protective effects of FG-4592 pretreatment. FG-4592 improves the balance of mitochondrial dynamics by inhibiting mitochondrial fission and promoting mitochondrial fusion. The mechanism underlying this phenomenon involves downregulation of the primary mediator proteins of mitochondrial fission (Drp1 and Fis1) and upregulation of fusion proteins (Opa1 and Mfn1). Overall, the major consequence of FG-4592-mediated balancing of mitochondrial dynamics is recovery of functional mitochondria; therefore, FG-4592 is a potential therapeutic agent for nephrotoxic AKI.

DATA AVAILABILITY STATEMENT

The original contributions presented in the study are included in the article/**Supplementary Material**, further inquiries can be directed to the corresponding author.

ETHICS STATEMENT

The animal study was reviewed and approved by this study was approved by the Ethics Committee of the China Medical University Institutional Animal Care and Use Committee (protocol no. 2011037).

AUTHOR CONTRIBUTIONS

XL wrote the manuscript. X-YZ conceived and designed the experiments. YZ analyzed the data. Y-YF did the statistics. All authors contributed to the article and approved the submitted version.

FUNDING

The work was financially supported by the National Natural Science Foundation of China (contract no. 31371219 and 31971115).

SUPPLEMENTARY MATERIAL

The Supplementary Material for this article can be found online at: https://www.frontiersin.org/articles/10.3389/fphar.2021.788977/full#supplementary-material

REFERENCES

Agre, P., King, L. S., Yasui, M., Guggino, W. B., Ottersen, O. P., Fujiyoshi, Y., et al. (2002). Aquaporin Water Channels-Ffrom Atomic Structure to Clinical Medicine. *J. Physiol.* 542 (Pt 1), 3–16. doi:10.1113/jphysiol.2002.020818

Anger, E. E., Yu, F., and Li, J. (2020). Aristolochic Acid-Induced Nephrotoxicity: Molecular Mechanisms and Potential Protective Approaches. *Int. J. Mol. Sci.* 21 (3), 1157. doi:10.3390/ijms21031157

Aparicio-Trejo, O. E., Reyes-Fermín, L. M., Briones-Herrera, A., Tapia, E., León-Contreras, J. C., Hernández-Pando, R., et al. (2019). Protective Effects of N-Acetyl-Cysteine in Mitochondria Bioenergetics, Oxidative Stress, Dynamics and S-Glutathionylation Alterations in Acute Kidney Damage Induced by Folic Acid. *Free Radic. Biol. Med.* 130, 379–396. doi:10.1016/j.freeradbiomed.2018.11.005

Apostolova, N., and Victor, V. M. (2015). Molecular Strategies for Targeting Antioxidants to Mitochondria: Therapeutic Implications. *Antioxid. Redox Signal.* 22 (8), 686–729. doi:10.1089/ars.2014.5952

Asvapromtada, S., Sonoda, H., Kinouchi, M., Oshikawa, S., Takahashi, S., Hoshino, Y., et al. (2018). Characterization of Urinary Exosomal Release of Aquaporin-1 and -2 after Renal Ischemia-Reperfusion in Rats. *Am. J. Physiol. Ren. Physiol* 314 (4), F584–F601. doi:10.1152/ajprenal.00184.2017

Bae, E. H., Lee, K. S., Lee, J., Ma, S. K., Kim, N. H., Choi, K. C., et al. (2008). Effects of Alpha-Lipoic Acid on Ischemia-Reperfusion-Induced Renal Dysfunction in Rats. *Am. J. Physiol. Ren. Physiol* 294 (1), F272–F280. doi:10.1152/ajprenal.00352.2007

Bao, Y. W., Yuan, Y., Chen, J. H., and Lin, W. Q. (2018). Kidney Disease Models: Tools to Identify Mechanisms and Potential Therapeutic Targets. *Zool Res.* 39 (2), 72–86. doi:10.24272/j.issn.2095-8137.2017.055

Baseler, W. A., Dabkowski, E. R., Jagannathan, R., Thapa, D., Nichols, C. E., Shepherd, D. L., et al. (2013). Reversal of Mitochondrial Proteomic Loss in Type 1 Diabetic Heart with Overexpression of Phospholipid Hydroperoxide Glutathione Peroxidase. *Am. J. Physiol. Regul. Integr. Comp. Physiol.* 304 (7), R553–R565. doi:10.1152/ajpregu.00249.2012

Basile, D. P., Anderson, M. D., and Sutton, T. A. (2012). Pathophysiology of Acute Kidney Injury. *Compr. Physiol.* 2 (2), 1303–1353. doi:10.1002/cphy.c110041

Basile, D. P., Bonventre, J. V., Mehta, R., Nangaku, M., Unwin, R., Rosner, M. H., et al. (2016). Progression after AKI: Understanding Maladaptive Repair Processes to Predict and Identify Therapeutic Treatments. *J. Am. Soc. Nephrol.* 27 (3), 687–697. doi:10.1681/ASN.2015030309

Battaglia, A. M., Chirillo, R., Aversa, I., Sacco, A., Costanzo, F., and Biamonte, F. (2020). Ferroptosis and Cancer: Mitochondria Meet the "Iron Maiden" Cell Death. *Cells* 9 (6), 1505. doi:10.3390/cells9061505

Brooks, C., Wei, Q., Cho, S. G., and Dong, Z. (2009). Regulation of Mitochondrial Dynamics in Acute Kidney Injury in Cell Culture and Rodent Models. *J. Clin. Invest.* 119 (5), 1275–1285. doi:10.1172/JCI37829

Capaldo, C. T., and Macara, I. G. (2007). Depletion of E-Cadherin Disrupts Establishment but Not Maintenance of Cell Junctions in Madin-Darby Canine Kidney Epithelial Cells. *Mol. Biol. Cel* 18 (1), 189–200. doi:10.1091/mbc.e06-05-0471

Chan, L., Chaudhary, K., Saha, A., Chauhan, K., Vaid, A., Zhao, S., et al. (2020). AKI in Hospitalized Patients with COVID-19. *J. Am. Soc. Nephrol.* 32, 151–160. doi:10.1681/asn.2020050615

Chen, C., Tang, Q., Zhang, Y., Yu, M., Jing, W., and Tian, W. (2018). Physioxia: a More Effective Approach for Culturing Human Adipose-Derived Stem Cells for Cell Transplantation. *Stem Cel Res Ther* 9 (1), 148. doi:10.1186/s13287-018-0891-4

Chen, X., Yao, J. M., Fang, X., Zhang, C., Yang, Y. S., Hu, C. P., et al. (2019). Hypoxia Promotes Pulmonary Vascular Remodeling via HIF-1α to Regulate Mitochondrial Dynamics. *J. Geriatr. Cardiol.* 16 (12), 855–871. doi:10.11909/j.issn.1671-5411.2019.12.003

Cheng, Q. Q., Wan, Y. W., Yang, W. M., Tian, M. H., Wang, Y. C., He, H. Y., et al. (2020). Gastrodin Protects H9c2 Cardiomyocytes against Oxidative Injury by Ameliorating Imbalanced Mitochondrial Dynamics and Mitochondrial

Dysfunction. *Acta Pharmacol. Sin* 41 (10), 1314–1327. doi:10.1038/s41401-020-0382-x

Chung, K. W., Dhillon, P., Huang, S., Sheng, X., Shrestha, R., Qiu, C., et al. (2019). Mitochondrial Damage and Activation of the STING Pathway Lead to Renal Inflammation and Fibrosis. *Cell Metab* 30 (4), 784–e5. doi:10.1016/j.cmet.2019.08.003

Dabrowska, A., Venero, J. L., Iwasawa, R., Hankir, M. K., Rahman, S., Boobis, A., et al. (2015). Erratum: PGC-1α Controls Mitochondrial Biogenesis and Dynamics in lead-induced Neurotoxicity. *Aging (Albany NY)* 7 (9), 1023–1647. doi:10.18632/aging.100837

Eadon, M. T., Hack, B. K., Xu, C., Ko, B., Toback, F. G., and Cunningham, P. N. (2012). Endotoxemia Alters Tight junction Gene and Protein Expression in the Kidney. *Am. J. Physiol. Ren. Physiol* 303 (6), F821–F830. doi:10.1152/ajprenal.00023.2012

Fan, Y., Xiao, W., Lee, K., Salem, F., Wen, J., He, L., et al. (2017). Inhibition of Reticulon-1a-Mediated Endoplasmic Reticulum Stress in Early AKI Attenuates Renal Fibrosis Development. *J. Am. Soc. Nephrol.* 28 (7), 2007–2021. doi:10.1681/ASN.2016091001

Fattah, H., and Vallon, V. (2018). Tubular Recovery after Acute Kidney Injury. *Nephron* 140 (2), 140–143. doi:10.1159/000490007

Fragiadaki, M., and Mason, R. M. (2011). Epithelial-mesenchymal Transition in Renal Fibrosis - Evidence for and against. *Int. J. Exp. Pathol.* 92 (3), 143–150. doi:10.1111/j.1365-2613.2011.00775.x

Gamba, G. (2012). Regulation of the Renal Na+-Cl- Cotransporter by Phosphorylation and Ubiquitylation. *Am. J. Physiol. Ren. Physiol* 303 (12), F1573–F1583. doi:10.1152/ajprenal.00508.2012

Gao, L., Liu, M. M., Zang, H. M., Ma, Q. Y., Yang, Q., Jiang, L., et al. (2018). Restoration of E-Cadherin by PPBICA Protects against Cisplatin-Induced Acute Kidney Injury by Attenuating Inflammation and Programmed Cell Death. *Lab. Invest.* 98 (7), 911–923. doi:10.1038/s41374-018-0052-5

Gautam, S., Rawat, A. K., Sammi, S. R., Roy, S., Singh, M., Devi, U., et al. (2018). DuCLOX-2/5 Inhibition Attenuates Inflammatory Response and Induces Mitochondrial Apoptosis for Mammary Gland Chemoprevention. *Front. Pharmacol.* 9, 314. doi:10.3389/fphar.2018.00314

Gibbs, W. S., Collier, J. B., Morris, M., Beeson, C. C., Megyesi, J., and Schnellmann, R. G. (2018). 5-HT1F Receptor Regulates Mitochondrial Homeostasis and its Loss Potentiates Acute Kidney Injury and Impairs Renal Recovery. *Am. J. Physiol. Ren. Physiol* 315 (4), F1119–F1128. doi:10.1152/ajprenal.00077.2018

Gupta, A., Puri, V., Sharma, R., and Puri, S. (2012). Folic Acid Induces Acute Renal Failure (ARF) by Enhancing Renal Prooxidant State. *Exp. Toxicol. Pathol.* 64 (3), 225–232. doi:10.1016/j.etp.2010.08.010

He, J., and Yang, B. (2019). Aquaporins in Renal Diseases. *Int. J. Mol. Sci.* 20 (2), 366. doi:10.3390/ijms20020366

Hu, Z., Zhang, H., Yang, S. K., Wu, X., He, D., Cao, K., et al. (2019). Emerging Role of Ferroptosis in Acute Kidney Injury. *Oxid Med. Cel Longev* 2019, 8010614. doi:10.1155/2019/8010614

Hua, Y., Ying, X., Qian, Y., Liu, H., Lan, Y., Xie, A., et al. (2019). Physiological and Pathological Impact of AQP1 Knockout in Mice. *Biosci. Rep.* 39 (5), BSR20182303. doi:10.1042/BSR20182303

Humphreys, B. D., Cantaluppi, V., Portilla, D., Singbartl, K., Yang, L., Rosner, M. H., et al. (2016). Acute Dialysis Quality InitiativeTargeting Endogenous Repair Pathways after AKI. *Jasn* 27 (4), 990–998. doi:10.1681/asn.2015030286

Ishimoto, Y., and Inagi, R. (2016). Mitochondria: a Therapeutic Target in Acute Kidney Injury. *Nephrol. Dial. Transpl.* 31 (7), 1062–1069. doi:10.1093/ndt/gfv317

Jiang, C., Shao, Q., Jin, B., Gong, R., Zhang, M., and Xu, B. (2015). Tanshinone IIA Attenuates Renal Fibrosis after Acute Kidney Injury in a Mouse Model through Inhibition of Fibrocytes Recruitment. *Biomed. Res. Int.* 2015, 867140. doi:10.1155/2015/867140

Jiang, C., Zhu, W., Shao, Q., Yan, X., Jin, B., Zhang, M., et al. (2016a). Tanshinone IIA Protects against Folic Acid-Induced Acute Kidney Injury. *Am. J. Chin. Med.* 44 (4), 737–753. doi:10.1142/S0192415X16500403

Jiang, C., Zhu, W., Yan, X., Shao, Q., Xu, B., Zhang, M., et al. (2016b). Rescue Therapy with Tanshinone IIA Hinders Transition of Acute Kidney Injury to Chronic Kidney Disease via Targeting GSK3β. *Sci. Rep.* 6, 36698. doi:10.1038/srep36698

Jun, J. C., Devera, R., Unnikrishnan, D., Shin, M. K., Bevans-Fonti, S., Yao, Q., et al. (2017). Adipose HIF-1α Causes Obesity by Suppressing Brown Adipose Tissue Thermogenesis. *J. Mol. Med. (Berl)* 95 (3), 287–297. doi:10.1007/s00109-016-1480-6

Kellum, J. A., Sileanu, F. E., Bihorac, A., Hoste, E. A., and Chawla, L. S. (2017). Recovery after Acute Kidney Injury. *Am. J. Respir. Crit. Care Med.* 195 (6), 784–791. doi:10.1164/rccm.201604-0799OC

Kortenoeven, M. L., and Fenton, R. A. (2014). Renal Aquaporins and Water Balance Disorders. *Biochim. Biophys. Acta* 1840 (5), 1533–1549. doi:10.1016/j.bbagen.2013.12.002

Kwon, T. H., Frøkiaer, J., Knepper, M. A., and Nielsen, S. (1998). Reduced AQP1, -2, and -3 Levels in Kidneys of Rats with CRF Induced by Surgical Reduction in Renal Mass. *Am. J. Physiol.* 275 (5), F724–F741. doi:10.1152/ajprenal.1998.275.5.F724

LaGory, E. L., Wu, C., Taniguchi, C. M., Ding, C. C., Chi, J. T., von Eyben, R., et al. (2015). Suppression of PGC-1α Is Critical for Reprogramming Oxidative Metabolism in Renal Cell Carcinoma. *Cell Rep* 12 (1), 116–127. doi:10.1016/j.celrep.2015.06.006

Li, B., Liu, C., Tang, K., Dong, X., Xue, L., Su, G., et al. (2019). Aquaporin-1 Attenuates Macrophage-Mediated Inflammatory Responses by Inhibiting P38 Mitogen-Activated Protein Kinase Activation in Lipopolysaccharide-Induced Acute Kidney Injury. *Inflamm. Res.* 68 (12), 1035–1047. doi:10.1007/s00011-019-01285-1

Li, X., Zou, Y., Xing, J., Fu, Y. Y., Wang, K. Y., Wan, P. Z., et al. (2020). Pretreatment with Roxadustat (FG-4592) Attenuates Folic Acid-Induced Kidney Injury through Antiferroptosis via Akt/GSK-3β/Nrf2 Pathway. *Oxid Med. Cel Longev* 2020, 6286984. doi:10.1155/2020/6286984

Lin, T. Y., and Hsu, Y. H. (2020). IL-20 in Acute Kidney Injury: Role in Pathogenesis and Potential as a Therapeutic Target. *Int. J. Mol. Sci.* 21 (3), 1009. doi:10.3390/ijms21031009

Ma, T., Yang, B., Gillespie, A., Carlson, E. J., Epstein, C. J., and Verkman, A. S. (1998). Severely Impaired Urinary Concentrating Ability in Transgenic Mice Lacking Aquaporin-1 Water Channels. *J. Biol. Chem.* 273 (8), 4296–4299. doi:10.1074/jbc.273.8.4296

Manral, C., Roy, S., Singh, M., Gautam, S., Yadav, R. K., Rawat, J. K., et al. (2016). Effect of β-sitosterol against Methyl Nitrosourea-Induced Mammary Gland Carcinoma in Albino Rats. *BMC Complement. Altern. Med.* 16, 260. doi:10.1186/s12906-016-1243-5

Martin, O. J., Lai, L., Soundarapandian, M. M., Leone, T. C., Zorzano, A., Keller, M. P., et al. (2014). A Role for Peroxisome Proliferator-Activated Receptor γ Coactivator-1 in the Control of Mitochondrial Dynamics during Postnatal Cardiac Growth. *Circ. Res.* 114 (4), 626–636. doi:10.1161/CIRCRESAHA.114.302562

Martin-Sanchez, D., Ruiz-Andres, O., Poveda, J., Carrasco, S., Cannata-Ortiz, P., Sanchez-Niño, M. D., et al. (2017). Ferroptosis, but Not Necroptosis, Is Important in Nephrotoxic Folic Acid-Induced AKI. *J. Am. Soc. Nephrol.* 28 (1), 218–229. doi:10.1681/ASN.2015121376

Molitoris, B. A. (2004). Actin Cytoskeleton in Ischemic Acute Renal Failure. *Kidney Int.* 66 (2), 871–883. doi:10.1111/j.1523-1755.2004.00818.x

Ni, J., Hou, X., Wang, X., Shi, Y., Xu, L., Zheng, X., et al. (2019). 3-deazaneplanocin A Protects against Cisplatin-Induced Renal Tubular Cell Apoptosis and Acute Kidney Injury by Restoration of E-Cadherin Expression. *Cell Death Dis* 10 (5), 355. doi:10.1038/s41419-019-1589-y

Nony, P. A., and Schnellmann, R. G. (2003). Mechanisms of Renal Cell Repair and Regeneration after Acute Renal Failure. *J. Pharmacol. Exp. Ther.* 304 (3), 905–912. doi:10.1124/jpet.102.035022

Perry, H. M., Huang, L., Wilson, R. J., Bajwa, A., Sesaki, H., Yan, Z., et al. (2018). Dynamin-Related Protein 1 Deficiency Promotes Recovery from AKI. *J. Am. Soc. Nephrol.* 29 (1), 194–206. doi:10.1681/ASN.2017060659

Pozzi, A., and Zent, R. (2010). ZO-1 and ZONAB Interact to Regulate Proximal Tubular Cell Differentiation. *J. Am. Soc. Nephrol.* 21 (3), 388–390. doi:10.1681/ASN.2010010061

Reichert, C. O., de Freitas, F. A., Sampaio-Silva, J., Rokita-Rosa, L., Barros, P. L., Levy, D., et al. (2020). Ferroptosis Mechanisms Involved in Neurodegenerative Diseases. *Int. J. Mol. Sci.* 21 (22), 8765. doi:10.3390/ijms21228765

Roy, S., Rawat, A. K., Sammi, S. R., Devi, U., Singh, M., Gautam, S., et al. (2017). Alpha-linolenic Acid Stabilizes HIF-1 α and Downregulates FASN to Promote Mitochondrial Apoptosis for Mammary Gland Chemoprevention. *Oncotarget* 8 (41), 70049–70071. doi:10.18632/oncotarget.19551

Shen, S., Yan, Z., Wu, J., Liu, X., Guan, G., Zou, C., et al. (2020). Characterization of ROS Metabolic Equilibrium Reclassifies Pan-Cancer Samples and Guides Pathway Targeting Therapy. *Front. Oncol.* 10, 581197. doi:10.3389/fonc.2020.581197

Shen, W. C., Chou, Y. H., Shi, L. S., Chen, Z. W., Tu, H. J., Lin, X. Y., et al. (2021). AST-120 Improves Cardiac Dysfunction in Acute Kidney Injury Mice via Suppression of Apoptosis and Proinflammatory NF-Kb/icam-1 Signaling. *J. Inflamm. Res.* 14, 505–518. doi:10.2147/JIR.S283378

Singh, L., Roy, S., Kumar, A., Rastogi, S., Kumar, D., Ansari, M. N., et al. (2021a). Repurposing Combination Therapy of Voacamine with Vincristine for Downregulation of Hypoxia-Inducible Factor-1α/Fatty Acid Synthase Co-axis and Prolyl Hydroxylase-2 Activation in ER+ Mammary Neoplasia. *Front Cel Dev Biol* 9, 736910. doi:10.3389/fcell.2021.736910

Singh, L., Singh, M., Rastogi, S., Choudhary, A., Kumar, D., Raj, R., et al. (2021b). Effect of Voacamine upon Inhibition of Hypoxia Induced Fatty Acid Synthesis in a Rat Model of Methyln-Nitrosourea Induced Mammary Gland Carcinoma. *BMC Mol. Cel Biol* 22 (1), 33. doi:10.1186/s12860-021-00371-9

Soofi, A., Kutschat, A. P., Azam, M., Laszczyk, A. M., and Dressler, G. R. (2020). Regeneration after Acute Kidney Injury Requires PTIP-Mediated Epigenetic Modifications. *JCI Insight* 5 (3), e130204. doi:10.1172/jci.insight.130204

Spurlock, B., Tullet, J., Hartman, J. L., and Mitra, K. (2020). Interplay of Mitochondrial Fission-Fusion with Cell Cycle Regulation: Possible Impacts on Stem Cell and Organismal Aging. *Exp. Gerontol.* 135, 110919. doi:10.1016/j.exger.2020.110919

Stallons, L. J., Whitaker, R. M., and Schnellmann, R. G. (2014). Suppressed Mitochondrial Biogenesis in Folic Acid-Induced Acute Kidney Injury and Early Fibrosis. *Toxicol. Lett.* 224 (3), 326–332. doi:10.1016/j.toxlet.2013.11.014

Sun, J., Zhang, J., Tian, J., Virzì, G. M., Digvijay, K., Cueto, L., et al. (2019). Mitochondria in Sepsis-Induced AKI. *J. Am. Soc. Nephrol.* 30 (7), 1151–1161. doi:10.1681/ASN.2018111126

Takiyama, Y., Harumi, T., Watanabe, J., Fujita, Y., Honjo, J., Shimizu, N., et al. (2011). Tubular Injury in a Rat Model of Type 2 Diabetes Is Prevented by Metformin: a Possible Role of HIF-1α Expression and Oxygen Metabolism. *Diabetes* 60 (3), 981–992. doi:10.2337/db10-0655

Tang, W. X., Wu, W. H., Qiu, H. Y., Bo, H., and Huang, S. M. (2013). Amelioration of Rhabdomyolysis-Induced Renal Mitochondrial Injury and Apoptosis through Suppression of Drp-1 Translocation. *J. Nephrol.* 26 (6), 1073–1082. doi:10.5301/jn.5000268

Wang, W., Li, C., Summer, S. N., Falk, S., Wang, W., Ljubanovic, D., et al. (2008). Role of AQP1 in Endotoxemia-Induced Acute Kidney Injury. *Am. J. Physiol. Ren. Physiol* 294 (6), F1473–F1480. doi:10.1152/ajprenal.00036.2008

Wills, L. P., Trager, R. E., Beeson, G. C., Lindsey, C. C., Peterson, Y. K., Beeson, C. C., et al. (2012). The β2-adrenoceptor Agonist Formoterol Stimulates Mitochondrial Biogenesis. *J. Pharmacol. Exp. Ther.* 342 (1), 106–118. doi:10.1124/jpet.112.191528

Wu, K., Zhou, K., Wang, Y., Zhou, Y., Tian, N., Wu, Y., et al. (2016). Stabilization of HIF-1α by FG-4592 Promotes Functional Recovery and Neural protection in Experimental Spinal Cord Injury. *Brain Res.* 1632, 19–26. doi:10.1016/j.brainres.2015.12.017

Yang, S. S., Fang, Y. W., Tseng, M. H., Chu, P. Y., Yu, I. S., Wu, H. C., et al. (2013). Phosphorylation Regulates NCC Stability and Transporter Activity *In Vivo*. *J. Am. Soc. Nephrol.* 24 (10), 1587–1597. doi:10.1681/ASN.2012070742

Yang, Y., Yu, X., Zhang, Y., Ding, G., Zhu, C., Huang, S., et al. (2018). Hypoxia-inducible Factor Prolyl Hydroxylase Inhibitor Roxadustat (FG-4592) Protects against Cisplatin-Induced Acute Kidney Injury. *Clin. Sci. (Lond)* 132 (7), 825–838. doi:10.1042/CS20171625

Yu, S. M., and Bonventre, J. V. (2020). Acute Kidney Injury and Maladaptive Tubular Repair Leading to Renal Fibrosis. *Curr. Opin. Nephrol. Hypertens.* 29 (3), 310–318. doi:10.1097/MNH.0000000000000605

Zhan, M., Brooks, C., Liu, F., Sun, L., and Dong, Z. (2013). Mitochondrial Dynamics: Regulatory Mechanisms and Emerging Role in Renal Pathophysiology. *Kidney Int.* 83 (4), 568–581. doi:10.1038/ki.2012.441

Zhang, D., Liu, Y., Tang, Y., Wang, X., Li, Z., Li, R., et al. (2018). Increased Mitochondrial Fission Is Critical for Hypoxia-Induced Pancreatic Beta Cell Death. *PLoS One* 13 (5), e0197266. doi:10.1371/journal.pone.0197266

Zhang, T., Zhang, X., Han, K., Zhang, G., Wang, J., Xie, K., et al. (2017). Analysis of Long Noncoding RNA and mRNA Using RNA Sequencing during the Differentiation of Intramuscular Preadipocytes in Chicken. PLoS One 12 (2), e0172389. doi:10.1371/journal.pone.0172389

Zhou, D., Li, Y., Lin, L., Zhou, L., Igarashi, P., and Liu, Y. (2012). Tubule-specific Ablation of Endogenous β-catenin Aggravates Acute Kidney Injury in Mice. *Kidney Int.* 82 (5), 537–547. doi:10.1038/ki.2012.173

Conflict of Interest: The authors declare that the research was conducted in the absence of any commercial or financial relationships that could be construed as a potential conflict of interest.

Publisher's Note: All claims expressed in this article are solely those of the authors and do not necessarily represent those of their affiliated organizations, or those of the publisher, the editors, and the reviewers. Any product that may be evaluated in this article, or claim that may be made by its manufacturer, is not guaranteed or endorsed by the publisher.

frontiers in Pharmacology

REVIEW
published: 04 March 2022
doi: 10.3389/fphar.2022.800810

Natural Products Against Renal Fibrosis *via* Modulation of SUMOylation

Peng Liu[1†], *Jing Zhang*[2†], *Yun Wang*[1†], *Chen Wang*[1], *Xinping Qiu*[1] *and Dan-Qian Chen*[3*]

[1]*Shunyi Hospital, Beijing Hospital of Traditional Chinese Medicine, Beijing, China,* [2]*Institute of Plant Resources, Yunnan University, Kunming, China,* [3]*Department of Emergency, China-Japan Friendship Hospital, Beijing, China*

Renal fibrosis is the common and final pathological process of kidney diseases. As a dynamic and reversible post-translational modification, SUMOylation and deSUMOylation of transcriptional factors and key mediators significantly affect the development of renal fibrosis. Recent advances suggest that SUMOylation functions as the promising intervening target against renal fibrosis, and natural products prevent renal fibrosis *via* modulating SUMOylation. Here, we introduce the mechanism of SUMOylation in renal fibrosis and therapeutic effects of natural products. This process starts by summarizing the key mediators and enzymes during SUMOylation and deSUMOylation and its regulation role in transcriptional factors and key mediators in renal fibrosis, then linking the mechanism findings of SUMOylation and natural products to develop novel therapeutic candidates for treating renal fibrosis, and concludes by commenting on promising therapeutic targets and candidate natural products in renal fibrosis via modulating SUMOylation, which highlights modulating SUMOylation as a promising strategy for natural products against renal fibrosis.

Keywords: renal fibrosis, sumoylation, SUMO-specific protease, natural products, NF-κB

OPEN ACCESS

Edited by:
Manish Kumar Gupta,
University of Central Florida,
United States

Reviewed by:
Yong Li,
Shanghai Jiao Tong University, China
Tzer-Bin Lin,
Taipei Medical University, Taiwan

***Correspondence:**
Dan-Qian Chen
chendanqian2013@163.com

†These authors have contributed equally to this work

Specialty section:
This article was submitted to Renal Pharmacology, a section of the journal Frontiers in Pharmacology

Received: *24 October 2021*
Accepted: *08 February 2022*
Published: *04 March 2022*

Citation:
Liu P, Zhang J, Wang Y, Wang C, Qiu X and Chen D-Q (2022) Natural Products Against Renal Fibrosis via Modulation of SUMOylation. Front. Pharmacol. 13:800810. doi: 10.3389/fphar.2022.800810

1 INTRODUCTION

Epigenetic modification is dynamic and responses to environmental influences, including chromatin remodeling proteins and histone post-translational modifications (PTM). SUMOylation is a PTM process. SUMOylation shares similar reaction scheme and enzyme classes, but the conjugation involves in small ubiquitin-like modifiers (SUMOs) rather than ubiquitin. Emerging evidences support SUMOylation as a promising therapeutic target for renal fibrosis through modulating transcription factor and key mediator. NR5A2 is a key mediator on the transcriptional regulation of the calreticulin gene, and its SUMOylation exacerbates renal fibrosis in the unilateral ureteric obstruction model (Arvaniti et al., 2016). In addition, SUMOylation of Samd4 by SUMO2/3 activates TGF-β/Smad signaling and then upregulates the expression of fibronectin in high glucose induced renal mesangial cells (Zhou et al., 2014). Here, we introduce the mechanism of SUMOylation in renal fibrosis and therapeutic effects of natural products. This process starts by summarizing the key mediators and enzymes during SUMOylation and deSUMOylation and its regulation role in transcriptional factors and key mediators in renal fibrosis, then linking the mechanism findings of SUMOylation and natural products to develop novel therapeutic candidates for treating renal fibrosis, and concludes by commenting on promising therapeutic targets and candidate natural products in renal fibrosis via modulating SUMOylation.

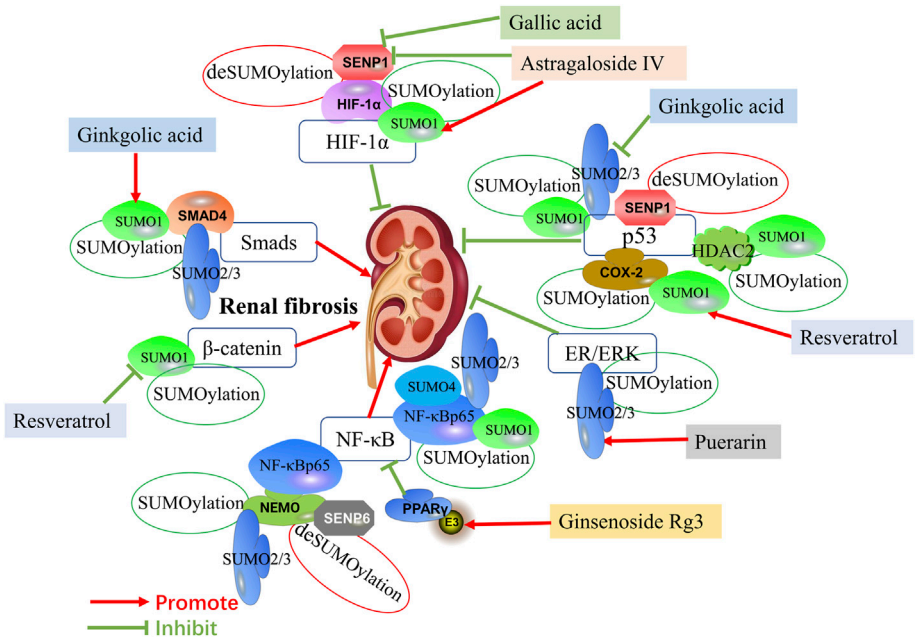

FIGURE 1 | Mechanisms of SUMOylation and deSUMOylation by transcription factors in renal fibrosis and therapeutic targets of natural products against renal fibrosis *via* SUMOylation. Mechanisms of SUMOylation and deSUMOylation by transcription factors in renal fibrosis are including TGF-β/Smad signaling, HIF-1α signaling, p53 pathway, ER/ERK pathway, NF-κB signaling, and β-catenin pathway. Smad4 is SUMOylated by SUMO1 and SUMO2/3. HIF-1α is SUMOylated by SUMO1. P53 is SUMOylated by SUMO1 and SUMO2/3, and also is upregulate by HDAC2 and COX-2 SUMOylated by SUMO1. ER/ERK is SUMOylated by SUMO2/3. NF-κBp65 is SUMOylated by SUMO1, SUMO2/3 and SUMO4, and also is upregulate by NEMO SUMOylated by SUMO2/3. PPARγ activated by SUMO ligase E3 could inhibit NF-κB signaling. β-catenin is SUMOylated by SUMO1. SNEP1 deSUMOylates HIF-1α and p53. Additionally, SNEP6 deSUMOylates NEMO. Ginkgolic acid promotes the expression of Smad4 by upregulating SUMO1, while inhibits the expression of p53 by downregulating SUMO2/3. Astragaloside IV promotes the expression of HIF-1α by upregulating SUMO1 and downregulating SENP1. Gallic acid also promotes the expression of HIF-1α by downregulating SENP1. Resveratrol induces SUMOylated COX-2 by SUMO1, thus enhancing the expression of p53. In addition, Resveratrol inhibits the expression of β-catenin by downregulating SUMO1. Puerarin activates ER/ERK pathway by upregulating SUMO2/3. Ginsenoside Rg3 inhibits NF-κB by upregulating PPARγ via activating E3.

2 SUMOYLATION

2.1 SUMO Proteins

SUMO proteins are small acidic proteins with distant homology to ubiquitin. At primary amino acid sequence, they are 10–20% identical to ubiquitin. On a structural level, and their relatedness is much more pronounced. As shown in **Figure 1**, ubiquitin and SUMO share the classical ubiquitin superfold. Characteristic for all members of the SUMO family and absent from ubiquitin or other ubiquitin-related proteins, is the N-terminal flexible extension of 10–30 amino acids. The function of this extension remains however currently unknown.

As a type of PTMs, SUMOylation are widely existed in eukaryotes. SUMOs modification mediates the protein–protein interactions of target substrates, and affects their enzymatic function, subcellular localization, and stability (Kukkula et al., 2021). SUMO proteins covalently bind to their target proteins at lysine (k) residues. To date, five SUMO proteins (SUMO1–5) have been found in human genome harbors genes (Enserink, 2015). Due to the sequence of SUMO2 and SUMO3 is very similar, they are commonly known as SUMO2/3 (Saitoh and Hinchey, 2000). Although SUMO2/3 and SUMO1 share 50% sequence homology, significant differences have been shown in function and location. Interestingly, SUMO1 knockout mice are survivable because SUMO2/3 can compensate for most functions of SUMO1 (Zhang et al., 2008; Wang et al., 2014a). SUMO1 and SUMO2/3 are common, while SUMO4 is only expressed in few organs, such as spleen and kidney (Du et al., 2021). SUMO4 is associated with the pathogenesis of type I diabetes mellitus. SUMO5 is first discovered in promyelocytic leukemia, which mediates the growth and disruption of promyelocytic leukemia nuclear bodies (Liang et al., 2016). However, whether SUMO5 is expressed at the protein level remains controversial.

2.2 SUMOylation and deSUMOylation Process

The SUMOylation starts from precursor synthesis, hydrolytic activation to covalent binding to the substrate protein that relies on the synergistic effect of three enzymes: E1 (SUMO-activating enzyme); E2 (SUMO- transferring enzyme); and E3 (SUMO ligase) (Yeh, 2009). First, SUMOs are activated by E1, and the C-terminal glycine is connected to the cysteine residue of E1 through a thiolipid bond. Thus, its group is adenylated to provide ATP energy and completes the activation of SUMOs. Then, SUMOs are transferred to the cysteine residues of E2, which can directly recognize the substrate, and finally couple SUMO to the lysine of the substrate protein through an isopeptide bond

TABLE 1 | The SUMOylation of transcription factors and key mediators in renal fibrosis.

Model	SUMO proteins or enzymes	Target genes	References
Modulating transcription factors			
High glucose induced renal mesangial cells	SUMO2/3	Smad4	Zhou et al. (2014)
Senp1(–/–) mice	SENP1	HIF-1α	Xu et al. (2010)
Co-culture models of glomerular endothelial cells with podocytes	SENP1	HIF-1α	Wang et al. (2015)
Puromycin aminonucleoside-induced podocyte	SENP1	p53	Wang et al. (2014)
Renal mesangial cells	SUMO1	p53	Wu et al. (2021)
Rat kidney proximal tubular cells	SUMO2/3	p53	Guo et al. (2015)
HEK 293T, HCT- 116 $p53^{-/-}$ and all RKO cells	SUMO1	p53	Wagner et al. (2015)
High glucose stimulated rat glomerular mesangial cells	SUMO1 and SUMO2/3	NF-κB p65	Huang et al. (2013)
High glucose stimulated rat glomerular mesangial cells	E3	NF-κB p65	Huang et al. (2017)
Lipopolysaccharide (LPS)-induced human renal proximal tubular cells	E3	PPARγ	Lu et al. (2013)
diabetic GK rats	SUMO4	NF-κB p65	Chen et al. (2014)
C57BL/6 mice, HEK293T, MEF and RAW264.7 cells	SUMO2/3	NEMO/IKKγ	Liu et al. (2013)
C57BL/6 mice, HEK293T, MEF and RAW264.7 cells	SENP6	NEMO	Liu et al. (2013)
Modulating key mediators			
C57/Bl6 mice and podocytes HEK-293T	SUMO1 and SUMO2/3	Nephrin	Tossidou et al. (2014)
Podocytes	SUMO1 and SUMO2/3	CIN85	Tossidou et al. (2012)
HEK293 and HeLa cells	SENP3	Drp1	Guo et al. (2017)
COS-7 fibroblasts	SENP2	OAT3	Wang and You, (2019)
COS-7 fibroblasts	SUMO2/3	OAT3	Wang et al. (2019)

residues. There are three main types of E3: activated STAT protein inhibits protein inhibitor of activated STAT (PIAS) family members, Pc2 and Ran BP2. It can enhance the efficiency and specificity of E2 transferring SUMOs to substrate proteins (K et al., 2021).

As a highly regulated and reversible process, SUMOylation is regulated by a series of proteases (Wilkinson and Henley, 2010). As one of the key proteases, SUMO-specific proteases (SENPs) contain seven types (SENP1–3 and SENP5–8). SENP1/2 prefers SUMO1–3 as the substrate (Wilkinson and Henley, 2010), while SENP3/5 and SENP6/7 have broad specificity for SUMO2/3 (Mukhopadhyay and Dasso, 2007), and SENP8 does not act on SUMO protein (Kunz et al., 2018). Under the action of SENPs, SUMOs are cleaved from the substrate protein, and the SUMOs precursor is processed into mature SUMOs re-enter the new SUMO cycle.

The abnormal SUMOylation usually leads to disorders of function of target proteins, and causes the damage of important physiological processes (Bertke et al., 2019). The balance of SUMOylation and deSUMOylation is crucial for embryonic development, since knockout of SENP1, SENP2, or SENP3 leads to embryonic lethality in mice (Chiu et al., 2008; Lao et al., 2018).

3 SUMOYLATION IN RENAL FIBROSIS

SUMOs involve in many cellular processes including DNA damage repair, protein stability regulation, cell cycle progression and regulation of signal transduction (Eifler and Vertegaal, 2015; Zeng et al., 2020). Consequently, abnormal SUMO modification can also results in many diseases such as cancers, diabetes, liver diseases, and kidney diseases (Bettermann et al., 2012; Li et al., 2019; Yang et al., 2019; Xie et al., 2020; Zeng et al., 2020). Especially, SUMOylation is activated by some factors, such as hypoxia, metabolic stress, oxidation, genotoxicity, and osmosis (Sun et al., 2018; Appelman et al., 2021; Ma et al., 2021).

Notably, recent studies indicate that SUMOylation functions as a critical role in maintaining renal fibrosis process. As the final pathological process of kidney diseases, renal fibrosis is caused by a decrease in matrix degradation, inflammatory cell infiltration, dysregulation of cell-matrix interaction, and the accumulation of extracellular matrix (ECM) proteins, which mainly involves fibronectin, various collagen and laminin. Although many researches have described the pathogenesis of renal fibrosis, few studies have investigated the role and mechanism of protein SUMOylation during renal fibrosis. Under certain pathological conditions, the signal pathway regulated by SUMOylation is associated with the pathophysiological changes of renal fibrosis. The regulation of renal fibrosis processes involves multiple signaling pathways, therefore we will elaborate on the SUMOylation of transcriptional factors and key mediators in renal fibrosis (**Table 1**). The molecular mechanisms involved in SUMOs and renal fibrosis are present in **Figure 1** and **Figure 2**.

3.1 The SUMOylation of Transcription Factors in Renal Fibrosis

3.1.1 Smads

TGF-β/Smad signaling pathways play a critical role in renal fibrosis through Smad and non-Smad pathways (Meng et al., 2015; Frangogiannis, 2020). Sumoylation of type I TGF-β receptor increases its ligand recruitment ability by

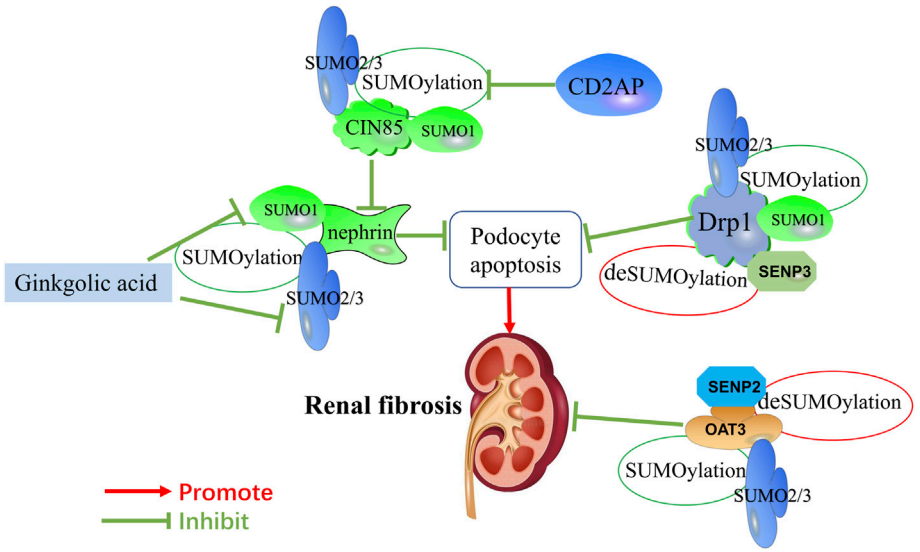

FIGURE 2 | Mechanisms of SUMOylation and deSUMOylation by key mediators in renal fibrosis and therapeutic targets of natural products against renal fibrosis via SUMOylation. Mechanisms of SUMOylation and deSUMOylation by key mediators in renal fibrosis are including podocyte apoptosis, and OAT3-mediated transfer channels. As one of component of the slit diaphragm, nephrin is SUMOylated by SUMO1 and SUMO2/3. CD2AP promotes the expression of nephrin by inhibiting the SUMOylation of CIN85. Drp1 is SUMOylated by SUMO1 and SUMO2/3. OAT3 is SUMOylated by SUMO2/3. SNEP3 deSUMOylates Drp1, and SNEP2 deSUMOylates OAT3. Ginkgolic acid inhibits the expression of nephrin by downregulating SUMO1 and SUMO2/3.

phosphorylation of Smad3 (Kang et al., 2008). Smad3 is involved in TGF-β-mediated signaling pathway. E3 ligase PIASy suppresses TGF-β signaling through SUMOylating Smad3 and Smad4 (Imoto et al., 2008; Lee et al., 2014). SUMOylated Smad4 increases the activation of TGF-β1/Smad signaling (Lee et al., 2003; Long et al., 2004; Wang Z. et al., 2018). In high glucose induced renal mesangial cells, SUMOylation of Samd4 by SUMO2/3 activates TGF-β/Smad signaling and then upregulates the expression of fibronectin (Zhou et al., 2014). In addition, some studies reveal that SUMO1 also enhances Smad4 SUMOylation (Ohshima and Shimotohno, 2003; Wang Z. et al., 2018; Liu et al., 2020). Ski and SnoN can inhibit TGF-β pathway through blocking its interaction with Smads. Arkadia (a RING domain E3 ubiquitin ligase) mediates noncovalent interaction with poly-SUMO2, and activates TGF-β/Smad signaling via degradation of Ski and SnoN (Erker et al., 2013). Taken together, targeting SUMOylation of TGF-β/Smad signaling might function as a promising therapeutic approach against renal fibrosis.

3.1.2 HIF-1α Pathways

Decreased oxygen significantly affects gene expression, metabolic changes and regeneration processes, including angiogenesis and stimulation of stem cell proliferation, differentiation, and migration (Hadanny and Efrati, 2020). Glomerular damage leads to a decrease in oxygen supply, and recent studies have emphasized the key role of hypoxia in the development of renal fibrosis (Bessho et al., 2019; Ishiuchi et al., 2020; Wakashima et al., 2020). The expression of SUMO proteins is increased under conditions of hypoxia *in vivo* and *in vitro* (Comerford et al., 2003; Shao et al., 2004).

The expression of hypoxia-inducible factor-1α (HIF-1α) in kidney is upregulated under conditions of hypoxia (Bessho et al., 2019). Meanwhile, the upregulation of HIF-1α expression can improve the viability and angiogenesis of bone marrow mesenchymal stem cells (Luo et al., 2019). Evidences show that vascular endothelial growth factor A (VEGFA) promotes the survival of bone marrow mesenchymal stem cells and angiogenesis, while HIF-1α can upregulate the expression of VEGFA (Utispan and Koontongkaew, 2021; Wang B. et al., 2021). Hypoxia enhances the SUMOylation of HIF-1α by SUMO1 and SUMO2/3 (Carbia-Nagashima et al., 2007); whereas SENP1 could deconjugate SUMOylated HIF-1α and reduce HIF-1α degradation during hypoxia (Cheng et al., 2007). SENP1 enhances HIF-1α deSUMOylation and increases VEGF production in endothelial cells following exposure to hypoxia (Xu et al., 2010; Cui et al., 2017). In SENP1(−/−) mice, the vascular endothelial cells in embryonic renal glomeruli and the VEGF production were significantly reduced (Xu et al., 2010). In co-culture models of glomerular endothelial cells with podocytes, the expression of SENP1 in podocytes increases under conditions of hypoxia, which induces endothelial cells survival via deSUMOylation of HIF-1α signaling (Wang et al., 2015). Therefore, SUMOylation of HIF-1α has the potential to be clinically developed as an antifibrotic target.

3.1.3 p53 Pathways

Podocyte apoptosis is a main cause of the decrease in the number of podocytes, which can lead to proteinuria, glomerulosclerosis and renal fibrosis. Recent studies found that the p53 protein participates in the pathogenesis of podocyte apoptosis (Choy

et al., 2021; Liang et al., 2021; Yang et al., 2021). As a tumor suppressor, p53 could safeguard the genome and prevent malignant transformation by halting the cell cycle and promoting apoptosis (Jiang et al., 2021; Thoms and Stark, 2021). p53 is increased under stimulation, and then upregulates the expression of pro-apoptotic genes (Eliaš and Macnamara, 2021). SUMOylated p53 could bind to the anti-apoptotic factor Bax and Bcl-2, and lead to apoptosis (Nowakowski et al., 2021). SENP1 deficiency significantly increases podocyte apoptosis by increasing expression of the p53 target pro-apoptotic genes (Noxa, PUMA and BAX) and aggravating accumulation of SUMOylated p53 protein in puromycin aminonucleoside-induced podocyte injury (Wang et al., 2014b). Mesangial cell proliferation is a core pathological feature of many kidney diseases. In renal mesangial cells, Krüppel-like factor 15 (KLF15) targeted SUMO1 to inhibit cell proliferation via enhancing the stability of p53 (Wu et al., 2021). However, ginkgolic acid (a pharmacological inhibitor of SUMOylation) suppresses p53 SUMOylation by SUMO2/3 and enhances apoptosis in rat kidney proximal tubular cells (Guo et al., 2015). SUMOylation of histone deacetylase 2 (HDAC2) by SUMO1 reduced DNA damage-induced apoptosis via deacetylation of p53 (Wagner et al., 2015).

3.1.4 NF-κB Signaling

As a nuclear transcription factor, nuclear factor κB (NF-κB) regulates the accumulation and release of cytokines and adhesion molecules by leukocytes (Wenzl et al., 2021). During the resting state, NF-κB binds to the inhibitor of κB (IκB) in the cytoplasm (Lee et al., 2021). SUMOylation of NF-κB plays a core role in the regulation of renal inflammation and fibrosis (Al Za'abi et al., 2021; You et al., 2021). With the modification by SUMO2/3, IκBα is separated from NF-κB, and enhance the activation of NF-κB (Chang and Abe, 2016). In high glucose stimulated rat glomerular mesangial cells, IκBα SUMOylation reduces the expression of monocyte chemotactic protein 1 (MCP-1), and ameliorates cellular inflammatory response through inhibiting NF-κB signaling (Huang et al., 2013). As one of E3 ligases, PIAS promotes SUMOylation of NF-κB via enhancing the expression of SUMO1 and SUMO2/3, and leads to the release of MCP-1 and IL-6 from glomerular mesangial cells (Huang et al., 2017).

The utilization of renal energy is partially determined by peroxisome proliferator activated receptors (PPARs) mediated fatty acid oxidation (Aranda-Rivera et al., 2021). PPARγ plays a key role in physiological and pathological processes of renal fibrosis. The reduction of PPARγ SUMOylation suppresses the activation of anti-apoptotic and anti-inflammatory cytokines through inhibiting the NF-κB activity (Xie et al., 2018; Zhao et al., 2021b). In lipopolysaccharide (LPS)-induced human renal proximal tubular cells, rosiglitazone (an agonist of PPARγ) decreases chemokines expression via inhibiting NF-κB activation by activating PPARγ SUMOylation (Lu et al., 2013). SUMO4 also plays a key role in regulating NF-κB signaling in glomerular cells (Chen et al., 2014). SUMOylation NEMO/IKKγ (NF-κB essential modifier) by SUMO2/3 enhanced the activity of NF-κB pathway, whereas SENP6 reverses this process by catalyzing the deSUMOylation of NEMO (Liu et al., 2013). These results indicate that the regulation of NF-κB SUMOylation has become a potential therapeutic strategy for renal fibrosis.

3.2 The SUMOylation of Key Mediators in Renal Fibrosis

3.2.1 Podocyte Apoptosis Pathway

Podocyte injury is the basic pathological feature of many kidney diseases, including decreased expression of the fissure membrane components and ultrastructural changes. Recently, SUMOylation has also been implicated in podocyte injury. As one of components of the slit diaphragm, nephrin is a target protein for SUMOylation by SUMO1 and SUMO2/3 (Tossidou et al., 2014). In podocytes, SUMOylation plays a key role in the tight orchestration of nephrin turnover at the slit diaphragm. The SUMOylation inhibitor ginkgolic acid decreases PI3K/AKT signaling and reduces membrane expression of nephrin (Tossidou et al., 2014). Besides nephrin, CD2-associated protein (CD2AP) also plays a crucial role in slit diaphragm (Chung et al., 2020; Basgen et al., 2021). Due to high sequence and structural similarities with CD2AP, Cbl-interacting protein of 85 kDa (CIN85) is a binding partner of nephrin and then increases endocytosis of nephrin (Tossidou et al., 2010). CD2AP reduces the binding of CIN85 to nephrin via CIN85 SUMOylation (Tossidou et al., 2012).

Mitochondrial dysfunction caused excessive mitochondrial fission, and then promoted podocyte apoptosis through the overproduction of reactive oxygen species (Su et al., 2021; Zhu et al., 2021). Moreover, mitochondrial dysfunction in damaged podocytes causes the development of marked glomerulosclerosis and albuminuria (Zhou et al., 2019). SUMOylation of dynamin-related protein (Drp) 1 activates mitochondrial autophagy and inhibits ROS production *via* regulating mitochondrial morphology and division (Din et al., 2013). SUMO1 SUMOylates Drp1, and then prevents the mitochondrial translocation (Jin et al., 2021). On the other hand, SENP2 deSUMOylates Drp1 by removing SUMO1, whereas SENP3 and SENP5 removes SUMO2/3 from deSUMOylation of Drp1 (Fu et al., 2014; Shimizu et al., 2016). DeSUMOylation of Drp1 by SENP3 promotes cell death by enhancing Drp1 partitioning to the mitochondrial outer membrane and improving cytochrome c release and apoptosis (Guo et al., 2017).

3.2.2 OAT3-Mediated Transfer Channels

Organic anion transporter 3 (OAT3) is an important transporter that located in the basolateral membrane of proximal renal tubules. OAT3 plays vital parts in removing a variety of drugs from the kidney, so as to avoid their possibly toxic side effects in the body (Fu et al., 2021). Activated OAT3 attenuates renal lipid accumulation and alleviates renal injury associated with renal inflammation and fibrosis in high-fat diet-induced obese rats (Pengrattanachot et al., 2020). In COS-7 fibroblasts, the downregulation of Senp2 results in an increased OAT3 SUMOylation via enhancing OAT3 expression and transport

TABLE 2 | Natural products and therapeutic targets against renal fibrosis via SUMOylation.

Compounds	Resource	SUMO proteins or enzymes	Therapeutic target	References
Modulating transcription factors				
Ginkgolic acid	Ginkgo	SUMO2/3	p53	Guo et al. (2015)
		SUMO1	Smad4	Liu et al. (2020)
Astragaloside IV	*Astragalus membranaceus*	SUMO1	HIF-1α	Wang et al. (2021)
		SENP1	—	Liu et al. (2021)
		SUMO1	—	Wang et al. (2021a)
Resveratrol	Vitis L., Veratrum L., *Arachis*, Polygonum	SUMO1	β-catenin	Wang et al. (2020)
		SUMO1	COX-2	Cheng et al. (2018); Lin et al. (2011)
Puerarin	Radix Puerariae	SUMO2	ER/ERK	Zhao et al. (2021)
Gallic acid	gallnut, sumac, tea leaves, and oak bark	SENP1	HIF-1α	Taghvaei et al. (2021)
Ginsenoside Rg3	Panax ginseng	E3	NF-κB	Zou et al. (2018)
Modulating key mediators				
Ginkgolic acid	Ginkgo	SUMO1 and SUMO2/3	nephrin	Tossidou et al. (2014)

activity (Wang and You, 2019). In addition, protein kinase A (PKA) accelerates the OAT3 SUMOylation by SUMO2/3 (Wang et al., 2019).

4 NATURAL PRODUCTS AGAINST RENAL FIBROSIS VIA REGULATING SUMOYLATION

4.1 Natural Products Against Renal Fibrosis via Regulating the SUMOylation of Transcription Factors

Numerous natural products have been widely applied to the treatment of fibrosis via inhibition of SUMOylation (**Table 2**). However, few studies have investigated the role and mechanism of natural products against renal fibrosis *via* modulating SUMOylation. Recent studies reveal that ginkgolic acid, a natural product from ginkgo, could regulate the SUMOylation of p53 to attenuate renal fibrosis (Tossidou et al., 2014; Guo et al., 2015).

Astragaloside IV, isolated from *Astragalus membranaceus*, plays a key role in antioxidant, antifibrosis, antitumor and anti-diabetic effects (Zhang et al., 2020). Astragaloside IV improves angiogenesis in adverse hypoxic conditions through stabilizing the presence of HIF-1α protein via enhancing SUMO1 expression (Wang B. et al., 2021).

Additionally, natural products also play protective effects via SUMOylation in extrarenal tissue. Wnt/β-catenin signaling pathway plays a key role in promoting fibrosis (Li. S. S. et al., 2021). Resveratrol, a natural active antioxidant, alleviates inflammatory response and fibrosis by modulating SUMO1 through Wnt/β-catenin pathway in dextran sodium sulfate-induced inflammatory bowel disease mice (Wang et al., 2020). Resveratrol also induces SUMOylated cyclooxygenase (COX)-2 by SUMO1, thus enhancing the expression of pro-apoptotic genes via activating p53 in human prostate cancer LNCaP cells and human ovarian carcinoma (OVCAR-3) cells (Lin et al., 2011; Cheng et al., 2018). In heart failure mice, astragaloside IV reduces the levels of reactive oxygen species (ROS), and improves cardiac function by inhibiting the overexpression of SENP1 (Liu et al., 2021). Meanwhile, astragaloside IV promotes the proliferation and migration of vascular endothelial cells and antagonizes the adverse microenvironment of hypoxia and high glucose by enhancing SUMO1 expression in human umbilical vein endothelial cells (Wang B. S. et al., 2021). In cardiomyocytes, puerarin attenuates cellular inflammatory response and fibrosis through activating ER/ERK pathway by increasing the expression of SUMO2 (Zhao et al., 2021a). In oral squamous cell carcinoma cells, ginkgolic acid suppresses tumorigenicity and tumor progression through inhibition of the enhancement of SUMOylation of Smad4 (Liu et al., 2020). Ginsenoside Rg3, extracted from Panax ginseng, inhibits NF-κB signaling through increasing the phosphorylation of RanBP2 (E3 SUMO-protein ligase) in breast cancer cells (Zou et al., 2018).

Numerous studies have demonstrated that SENP1 could bind to HIF-1α for deSUMOylation (Bai et al., 2021; Taghvaei et al., 2021). Gallic acid plays an essential role in antioxidant, anti-inflammatory, antimutagenic and anticancer through reducing deSUMOylation via inhibiting SENP1 expression (Taghvaei et al., 2021). Natural products against renal fibrosis via regulating the SUMOylation of transcription factors are present in **Figure 1**.

4.2 Natural Products Against Renal Fibrosis via Regulating the SUMOylation of Key Mediators

Ginkgolic acid, extracted from Ginkgo biloba leaves and seed coat, have beneficial effects including anti-inflammatory (Li et al., 2018), antitumor (Zhao Q. et al., 2021), and anti-bacterial effects (Bhutta et al., 2021). Unfortunately, ginkgolic acid could aggravate kidney damage by enhancing apoptosis and downregulating the expression of nephrin. Ginkgolic acid enhances apoptosis through suppressing SUMOylation by SUMO2/3 and sensitizes renal tubular cells to apoptosis during cisplatin treatment of rat kidney proximal tubular cells (Guo et al., 2015). Additionally, ginkgolic acid reduces membrane expression of nephrin via suppressing SUMOylation by SUMO1 and SUMO2/3, leading to a significant proteinuria in mice (Tossidou et al., 2014). Natural products against renal fibrosis

via regulating the SUMOylation of key mediators are present in **Figure 2**.

5 DISCUSSION AND CONCLUSION

In summary, the present study provides a systemic review of the role of SUMOylation in renal fibrosis, and the therapeutic effects of natural products through modulating transcription factors and key mediators. The pathological processes of renal fibrosis are regulated by complex signal pathways and factors, thus leading to a series of stress responses. The imbalance of protein SUMOylation is involved signal pathways and factors in renal fibrosis. SUMOylation significantly affects renal fibrosis through modulating transcription factors and key mediators, including Smads, HIF-1α, p53, NF-κB, podocyte apoptosis pathway, OAT3-mediated transfer channels, and Wnt/β-catenin pathway.

However, the effective treatment via SUMOylation remains a formidable challenge. The lack of effective treatment for renal fibrosis indicates that a deep understanding of the molecular mechanisms contributing to renal fibrosis remain urgent. Fortunately, researches of natural products in modulating SUMOylation have been carried out recently, which probably reveals the role of SUMOylation in the progression of renal fibrosis soon, including astragaloside IV, resveratrol, puerarin, gallic acid, and ginsenoside Rg3.

Additionally, the techniques that help to high-throughput screening of effective natural products targeting SUMOylation also facilitate to discover the candidate drug for treating renal fibrosis *via* modulating SUMOylation. It is worth noting that natural products mentioned above still needs more attention since the lack of underlying mechanism are far not enough for a candidate drug clinically. The detailed and in-depth basic research are urgent to investigate the underlying mechanisms of natural products against renal fibrosis, and the finding in reveal novel signaling pathways and treatment targets are necessary.

AUTHOR CONTRIBUTIONS

PL, JZ, YW, CW, XQ, and D-QC mainly drafted the work critical for important intellectual content. PL and D-QC participated in the funding acquisition. All authors read and approved the final manuscript. PL, JZ, and YW contributed equally to this work.

FUNDING

This work was supported by supported by Research Projects of the National Natural Science Foundation of China (Nos 81904174, 82104511), China Postdoctoral Science Foundation (No. 2021M693579).

REFERENCES

Al Za'abi, M., Ali, H., and Ali, B. H. (2021). Effect of Flaxseed on Systemic Inflammation and Oxidative Stress in Diabetic Rats with or without Chronic Kidney Disease. *PLoS One* 16 (10), e0258800. doi:10.1371/journal.pone.0258800

Appelman, M. D., van der Veen, S. W., and van Mil, S. W. C. (2021). Post-translational Modifications of FXR; Implications for Cholestasis and Obesity-Related Disorders. *Front. Endocrinol. (Lausanne)* 12, 729828. doi:10.3389/fendo.2021.729828

Aranda-Rivera, A. K., Cruz-Gregorio, A., Aparicio-Trejo, O. E., and Pedraza-Chaverri, J. (2021). Mitochondrial Redox Signaling and Oxidative Stress in Kidney Diseases. *Biomolecules* 11 (8), 1144. doi:10.3390/biom11081144

Arvaniti, E., Vakrakou, A., Kaltezioti, V., Stergiopoulos, A., Prakoura, N., Politis, P. K., et al. (2016). Nuclear Receptor NR5A2 Is Involved in the Calreticulin Gene Regulation during Renal Fibrosis. *Biochim. Biophys. Acta* 1862 (9), 1774–1785. doi:10.1016/j.bbadis.2016.06.013

Bai, Y. T., Xiao, F. J., Wang, H., Ge, R. L., and Wang, L. S. (2021). Hypoxia Protects H9c2 Cells against Ferroptosis through SENP1-Mediated Protein DeSUMOylation. *Int. J. Med. Sci.* 18 (7), 1618–1627. doi:10.7150/ijms.50804

Basgen, J. M., Wong, J. S., Ray, J., Nicholas, S. B., and Campbell, K. N. (2021). Podocyte Foot Process Effacement Precedes Albuminuria and Glomerular Hypertrophy in CD2-Associated Protein Deficient Mice. *Front. Med. (Lausanne)* 8, 745319. doi:10.3389/fmed.2021.745319

Bertke, M. M., Dubiak, K. M., Cronin, L., Zeng, E., and Huber, P. W. (2019). A Deficiency in SUMOylation Activity Disrupts Multiple Pathways Leading to Neural Tube and Heart Defects in Xenopus Embryos. *BMC Genomics* 20 (1), 386. doi:10.1186/s12864-019-5773-3

Bessho, R., Takiyama, Y., Takiyama, T., Kitsunai, H., Takeda, Y., Sakagami, H., et al. (2019). Hypoxia-inducible Factor-1α Is the Therapeutic Target of the SGLT2 Inhibitor for Diabetic Nephropathy. *Sci. Rep.* 9 (1), 14754. doi:10.1038/s41598-019-51343-1

Bettermann, K., Benesch, M., Weis, S., and Haybaeck, J. (2012). SUMOylation in Carcinogenesis. *Cancer Lett.* 316 (2), 113–125. doi:10.1016/j.canlet.2011.10.036

Bhutta, M., Shechter, O., Gallo, E., Martin, S., Jones, E., Doncel, G., et al. (2021). Ginkgolic Acid Inhibits Herpes Simplex Virus Type 1 Skin Infection and Prevents Zosteriform Spread in Mice. *Viruses* 13 (1), 86. doi:10.3390/v13010086

Carbia-Nagashima, A., Gerez, J., Perez-Castro, C., Paez-Pereda, M., Silberstein, S., Stalla, G. K., et al. (2007). RSUME, a Small RWD-Containing Protein, Enhances SUMO Conjugation and Stabilizes HIF-1alpha during Hypoxia. *Cell* 131 (2), 309–323. doi:10.1016/j.cell.2007.07.044

Chang, E., and Abe, J. I. (2016). Kinase-SUMO Networks in Diabetes-Mediated Cardiovascular Disease. *Metabolism* 65 (5), 623–633. doi:10.1016/j.metabol.2016.01.007

Chen, S., Yang, T., Liu, F., Li, H., Guo, Y., Yang, H., et al. (2014). Inflammatory Factor-specific Sumoylation Regulates NF-Kb Signalling in Glomerular Cells from Diabetic Rats. *Inflamm. Res.* 63 (1), 23–31. doi:10.1007/s00011-013-0675-3

Cheng, J., Kang, X., Zhang, S., and Yeh, E. T. (2007). SUMO-specific Protease 1 Is Essential for Stabilization of HIF1alpha during Hypoxia. *Cell* 131 (3), 584–595. doi:10.1016/j.cell.2007.08.045

Cheng, T. M., Chin, Y. T., Ho, Y., Chen, Y. R., Yang, Y. N., Yang, Y. C., et al. (2018). Resveratrol Induces Sumoylated COX-2-dependent Anti-proliferation in Human Prostate Cancer LNCaP Cells. *Food Chem. Toxicol.* 112, 67–75. doi:10.1016/j.fct.2017.12.011

Chiu, S. Y., Asai, N., Costantini, F., and Hsu, W. (2008). SUMO-specific Protease 2 Is Essential for Modulating P53-Mdm2 in Development of Trophoblast Stem Cell Niches and Lineages. *Plos Biol.* 6 (12), e310. doi:10.1371/journal.pbio.0060310

Choy, J., Kan, Y., Cifelli, S., Johnson, J., Chen, M., Shiao, L. L., et al. (2021). High-Throughput Screening to Identify Small Molecules that Selectively Inhibit APOL1 Protein Level in Podocytes. *SLAS Discov.* 26 (9), 1225–1237. doi:10.1177/24725552211026245

Chung, J. J., Goldstein, L., Chen, Y. J., Lee, J., Webster, J. D., Roose-Girma, M., et al. (2020). Single-Cell Transcriptome Profiling of the Kidney Glomerulus

Identifies Key Cell Types and Reactions to Injury. *J. Am. Soc. Nephrol.* 31 (10), 2341–2354. doi:10.1681/ASN.2020020220

Comerford, K. M., Leonard, M. O., Karhausen, J., Carey, R., Colgan, S. P., and Taylor, C. T. (2003). Small Ubiquitin-Related Modifier-1 Modification Mediates Resolution of CREB-dependent Responses to Hypoxia. *Proc. Natl. Acad. Sci. U S A.* 100 (3), 986–991. doi:10.1073/pnas.0337412100

Cui, C. P., Wong, C. C., Kai, A. K., Ho, D. W., Lau, E. Y., Tsui, Y. M., et al. (2017). SENP1 Promotes Hypoxia-Induced Cancer Stemness by HIF-1α deSUMOylation and SENP1/HIF-1α Positive Feedback Loop. *Gut* 66 (12), 2149–2159. doi:10.1136/gutjnl-2016-313264

Din, S., Mason, M., Völkers, M., Johnson, B., Cottage, C. T., Wang, Z., et al. (2013). Pim-1 Preserves Mitochondrial Morphology by Inhibiting Dynamin-Related Protein 1 Translocation. *Proc. Natl. Acad. Sci. U S A.* 110 (15), 5969–5974. doi:10.1073/pnas.1213294110

Du, C., Chen, X., Su, Q., Lu, W., Wang, Q., Yuan, H., et al. (2021). The Function of SUMOylation and its Critical Roles in Cardiovascular Diseases and Potential Clinical Implications. *Int. J. Mol. Sci.* 22 (19), 10618. doi:10.3390/ijms221910618

Eifler, K., and Vertegaal, A. C. O. (2015). SUMOylation-Mediated Regulation of Cell Cycle Progression and Cancer. *Trends Biochem. Sci.* 40 (12), 779–793. doi:10.1016/j.tibs.2015.09.006

Eliaš, J., and Macnamara, C. K. (2021). Mathematical Modelling of P53 Signalling during DNA Damage Response: A Survey. *Int. J. Mol. Sci.* 22 (19), 10590. doi:10.3390/ijms221910590

Enserink, J. M. (2015). Sumo and the Cellular Stress Response. *Cell Div* 10, 4. doi:10.1186/s13008-015-0010-1

Erker, Y., Neyret-Kahn, H., Seeler, J. S., Dejean, A., Atfi, A., and Levy, L. (2013). Arkadia, a Novel SUMO-Targeted Ubiquitin Ligase Involved in PML Degradation. *Mol. Cell. Biol.* 33 (11), 2163–2177. doi:10.1128/MCB.01019-12

Frangogiannis, N. (2020). Transforming Growth Factor-β in Tissue Fibrosis. *J. Exp. Med.* 217 (3), e20190103. doi:10.1084/jem.20190103

Fu, J., Yu, H. M., Chiu, S. Y., Mirando, A. J., Maruyama, E. O., Cheng, J. G., et al. (2014). Disruption of SUMO-specific Protease 2 Induces Mitochondria Mediated Neurodegeneration. *Plos Genet.* 10 (10), e1004579. doi:10.1371/journal.pgen.1004579

Fu, R., Wang, X. N., Guo, C. H., Li, Y., Ding, C. Y., Li, Y. J., et al. (2021). Wuzhi Capsule Increased Systemic Exposure to Methotrexate by Inhibiting the Expression of OAT1/3 and P-Gp. *Ann. Transl Med.* 9 (10), 845. doi:10.21037/atm-21-1303

Guo, C., Wei, Q., Su, Y., and Dong, Z. (2015). SUMOylation Occurs in Acute Kidney Injury and Plays a Cytoprotective Role. *Biochim. Biophys. Acta* 1852 (3), 482–489. doi:10.1016/j.bbadis.2014.12.013

Guo, C., Wilkinson, K. A., Evans, A. J., Rubin, P. P., and Henley, J. M. (2017). SENP3-mediated deSUMOylation of Drp1 Facilitates Interaction with Mff to Promote Cell Death. *Sci. Rep.* 7, 43811. doi:10.1038/srep43811

Hadanny, A., and Efrati, S. (2020). The Hyperoxic-Hypoxic Paradox. *Biomolecules* 10 (6), 958. doi:10.3390/biom10060958

Huang, W., Liang, Y., Dong, J., Zhou, L., Gao, C., Jiang, C., et al. (2017). SUMO E3 Ligase PIASy Mediates High Glucose-Induced Activation of NF-Kb Inflammatory Signaling in Rat Mesangial Cells. *Mediators Inflamm.* 2017, 1685194. doi:10.1155/2017/1685194

Huang, W., Xu, L., Zhou, X., Gao, C., Yang, M., Chen, G., et al. (2013). High Glucose Induces Activation of NF-Kb Inflammatory Signaling through IκBα Sumoylation in Rat Mesangial Cells. *Biochem. Biophys. Res. Commun.* 438 (3), 568–574. doi:10.1016/j.bbrc.2013.07.065

Imoto, S., Ohbayashi, N., Ikeda, O., Kamitani, S., Muromoto, R., Sekine, Y., et al. (2008). Sumoylation of Smad3 Stimulates its Nuclear export during PIASy-Mediated Suppression of TGF-Beta Signaling. *Biochem. Biophys. Res. Commun.* 370 (2), 359–365. doi:10.1016/j.bbrc.2008.03.116

Ishiuchi, N., Nakashima, A., Doi, S., Yoshida, K., Maeda, S., Kanai, R., et al. (2020). Hypoxia-preconditioned Mesenchymal Stem Cells Prevent Renal Fibrosis and Inflammation in Ischemia-Reperfusion Rats. *Stem Cell Res. Ther.* 11 (1), 130. doi:10.1186/s13287-020-01642-6

Jiang, W. W., Zhang, Z. Z., He, P. P., Jiang, L. P., Chen, J. Z., Zhang, X. T., et al. (2021). Emerging Roles of Growth Differentiation Factor-15 in Brain Disorders (Review). *Exp. Ther. Med.* 22 (5), 1270. doi:10.3892/etm.2021.10705

Jin, J. Y., Wei, X. X., Zhi, X. L., Wang, X. H., and Meng, D. (2021). Drp1-dependent Mitochondrial Fission in Cardiovascular Disease. *Acta Pharmacol. Sin.* 42 (5), 655–664. doi:10.1038/s41401-020-00518-y

K, S. T., Joshi, G., Arya, P., Mahajan, V., Chaturvedi, A., and Mishra, R. K. (2021). SUMO and SUMOylation Pathway at the Forefront of Host Immune Response. *Front Cell Dev Biol* 9, 681057. doi:10.3389/fcell.2021.681057

Kang, J. S., Saunier, E. F., Akhurst, R. J., and Derynck, R. (2008). The Type I TGF-Beta Receptor Is Covalently Modified and Regulated by Sumoylation. *Nat. Cell Biol.* 10 (6), 654–664. doi:10.1038/ncb1728

Kukkula, A., Ojala, V. K., Mendez, L. M., Sistonen, L., Elenius, K., and Sundvall, M. (2021). Therapeutic Potential of Targeting the SUMO Pathway in Cancer. *Cancers (Basel)* 13 (17), 4402. doi:10.3390/cancers13174402

Kunz, K., Piller, T., and Müller, S. (2018). SUMO-specific Proteases and Isopeptidases of the SENP Family at a Glance. *J. Cell Sci.* 131 (6), jcs211904. doi:10.1242/jcs.211904

Lao, Y., Yang, K., Wang, Z., Sun, X., Zou, Q., Yu, X., et al. (2018). DeSUMOylation of MKK7 Kinase by the SUMO2/3 Protease SENP3 Potentiates Lipopolysaccharide-Induced Inflammatory Signaling in Macrophages. *J. Biol. Chem.* 293 (11), 3965–3980. doi:10.1074/jbc.M117.816769

Lee, E. J., Kim, H. J., Choi, M. S., and Chang, J. E. (2021). Crosstalk between Autophagy and Inflammatory Processes in Cancer. *Life (Basel)* 11 (9), 903. doi:10.3390/life11090903

Lee, P. S., Chang, C., Liu, D., and Derynck, R. (2003). Sumoylation of Smad4, the Common Smad Mediator of Transforming Growth Factor-Beta Family Signaling. *J. Biol. Chem.* 278 (30), 27853–27863. doi:10.1074/jbc.M301755200

Lee, S. H., Kim, P. H., Oh, S. M., Park, J. H., Yoo, Y. C., Lee, J., et al. (2014). SUMO Proteins Are Not Involved in TGF-B1-Induced, Smad3/4-Mediated Germline α Transcription, but PIASy Suppresses it in CH12F3-2A B Cells. *Immune Netw.* 14 (6), 321–327. doi:10.4110/in.2014.14.6.321

Li, J., Li, A., Li, M., Liu, Y., Zhao, W., and Gao, D. (2018). Ginkgolic Acid Exerts an Anti-inflammatory Effect in Human Umbilical Vein Endothelial Cells Induced by Ox-LDL. *Pharmazie* 73 (7), 408–412. doi:10.1681/ph.2018.8397

Li, O., Ma, Q., Li, F., Cai, G. Y., Chen, X. M., and Hong, Q. (2019). Progress of Small Ubiquitin-Related Modifiers in Kidney Diseases. *Chin. Med. J. (Engl)* 132 (4), 466–473. doi:10.1097/CM9.0000000000000094

Li, S. S., Sun, Q., Hua, M. R., Suo, P., Chen, J. R., Yu, X. Y., et al. (2021). Targeting the Wnt/β-Catenin Signaling Pathway as a Potential Therapeutic Strategy in Renal Tubulointerstitial Fibrosis. *Front. Pharmacol.* 12, 719880. doi:10.3389/fphar.2021.719880

Liang, Y., Liu, H., Zhu, J., Song, N., Lu, Z., Fang, Y., et al. (2021). Inhibition of p53/miR-34a/SIRT1 axis Ameliorates Podocyte Injury in Diabetic Nephropathy. *Biochem. Biophys. Res. Commun.* 559, 48–55. doi:10.1016/j.bbrc.2021.04.025

Liang, Y. C., Lee, C. C., Yao, Y. L., Lai, C. C., Schmitz, M. L., and Yang, W. M. (2016). SUMO5, a Novel Poly-SUMO Isoform, Regulates PML Nuclear Bodies. *Sci. Rep.* 6, 26509. doi:10.1038/srep26509

Lin, C., Crawford, D. R., Lin, S., Hwang, J., Sebuyira, A., Meng, R., et al. (2011). Inducible COX-2-dependent Apoptosis in Human Ovarian Cancer Cells. *Carcinogenesis* 32 (1), 19–26. doi:10.1093/carcin/bgq212

Liu, J., Li, Y., Bian, X., Xue, N., Yu, J., Dai, S., et al. (2021). Astragaloside IV Alleviates Heart Failure by Regulating SUMO-specific Protease 1. *Exp. Ther. Med.* 22 (4), 1076. doi:10.3892/etm.2021.10510

Liu, K., Wang, X., Li, D., Xu, D., Li, D., Lv, Z., et al. (2020). Ginkgolic Acid, a SUMO-1 Inhibitor, Inhibits the Progression of Oral Squamous Cell Carcinoma by Alleviating SUMOylation of SMAD4. *Mol. Ther. Oncolytics* 16, 86–99. doi:10.1016/j.omto.2019.12.005

Liu, X., Chen, W., Wang, Q., Li, L., and Wang, C. (2013). Negative Regulation of TLR Inflammatory Signaling by the SUMO-Deconjugating Enzyme SENP6. *Plos Pathog.* 9 (6), e1003480. doi:10.1371/journal.ppat.1003480

Long, J., Wang, G., He, D., and Liu, F. (2004). Repression of Smad4 Transcriptional Activity by SUMO Modification. *Biochem. J.* 379 (Pt 1), 23–29. doi:10.1042/BJ20031867

Lu, Y., Zhou, Q., Shi, Y., Liu, J., Zhong, F., Hao, X., et al. (2013). SUMOylation of PPARγ by Rosiglitazone Prevents LPS-Induced NCoR Degradation Mediating Down Regulation of Chemokines Expression in Renal Proximal Tubular Cells. *PLoS One* 8 (11), e79815. doi:10.1371/journal.pone.0079815

Luo, Z., Wu, F., Xue, E., Huang, L., Yan, P., Pan, X., et al. (2019). Hypoxia Preconditioning Promotes Bone Marrow Mesenchymal Stem Cells Survival by

Inducing HIF-1α in Injured Neuronal Cells Derived Exosomes Culture System. *Cell Death Dis* 10 (2), 134. doi:10.1038/s41419-019-1410-y

Ma, Y., North, B. J., and Shu, J. (2021). Regulation of Topoisomerase II Stability and Activity by Ubiquitination and SUMOylation: Clinical Implications for Cancer Chemotherapy. *Mol. Biol. Rep.* 48 (9), 6589–6601. doi:10.1007/s11033-021-06665-7

Meng, X. M., Tang, P. M., Li, J., and Lan, H. Y. (2015). TGF-β/Smad Signaling in Renal Fibrosis. *Front. Physiol.* 6, 82. doi:10.3389/fphys.2015.00082

Mukhopadhyay, D., and Dasso, M. (2007). Modification in Reverse: the SUMO Proteases. *Trends Biochem. Sci.* 32 (6), 286–295. doi:10.1016/j.tibs.2007.05.002

Nowakowski, P., Markiewicz-Żukowska, R., Bielecka, J., Mielcarek, K., Grabia, M., and Socha, K. (2021). Treasures from the forest: Evaluation of Mushroom Extracts as Anti-cancer Agents. *Biomed. Pharmacother.* 143, 112106. doi:10.1016/j.biopha.2021.112106

Ohshima, T., and Shimotohno, K. (2003). Transforming Growth Factor-Beta-Mediated Signaling via the P38 MAP Kinase Pathway Activates Smad-dependent Transcription through SUMO-1 Modification of Smad4. *J. Biol. Chem.* 278 (51), 50833–50842. doi:10.1074/jbc.M307533200

Pengrattanachot, N., Cherngwelling, R., Jaikumkao, K., Pongchaidecha, A., Thongnak, L., Swe, M. T., et al. (2020). Atorvastatin Attenuates Obese-Induced Kidney Injury and Impaired Renal Organic Anion Transporter 3 Function through Inhibition of Oxidative Stress and Inflammation. *Biochim. Biophys. Acta Mol. Basis Dis.* 1866 (6), 165741. doi:10.1016/j.bbadis.2020.165741

Saitoh, H., and Hinchey, J. (2000). Functional Heterogeneity of Small Ubiquitin-Related Protein Modifiers SUMO-1 versus SUMO-2/3. *J. Biol. Chem.* 275 (9), 6252–6258. doi:10.1074/jbc.275.9.6252

Sapir, A. (2020). Not So Slim Anymore-Evidence for the Role of SUMO in the Regulation of Lipid Metabolism. *Biomolecules* 10 (8), 1154–6258. doi:10.3390/biom10081154

Shao, R., Zhang, F. P., Tian, F., Anders Friberg, P., Wang, X., Sjöland, H., et al. (2004). Increase of SUMO-1 Expression in Response to Hypoxia: Direct Interaction with HIF-1alpha in Adult Mouse Brain and Heart *In Vivo*. *FEBS Lett.* 569 (1-3), 293–300. doi:10.1016/j.febslet.2004.05.079

Shimizu, Y., Lambert, J. P., Nicholson, C. K., Kim, J. J., Wolfson, D. W., Cho, H. C., et al. (2016). DJ-1 Protects the Heart against Ischemia-Reperfusion Injury by Regulating Mitochondrial Fission. *J. Mol. Cell. Cardiol.* 97, 56–66. doi:10.1016/j.yjmcc.2016.04.008

Su, J., Gao, C., Xie, L., Fan, Y., Shen, Y., Huang, Q., et al. (2021). Astragaloside II Ameliorated Podocyte Injury and Mitochondrial Dysfunction in Streptozotocin-Induced Diabetic Rats. *Front. Pharmacol.* 12, 638422. doi:10.3389/fphar.2021.638422

Sun, Q., Qing, W., Qi, R., Zou, M., Gong, L., Liu, Y., et al. (2018). Inhibition of Sumoylation Alleviates Oxidative Stress-Induced Retinal Pigment Epithelial Cell Senescence and Represses Proinflammatory Gene Expression. *Curr. Mol. Med.* 18 (9), 575–583. doi:10.2174/1566524019666190107154250

Taghvaei, S., Sabouni, F., Minuchehr, Z., and Taghvaei, A. (2021). Identification of Novel Anti-cancer Agents, Applying In Silico Method for SENP1 Protease Inhibition. *J. Biomol. Struct. Dyn.* 3, 1–15. doi:10.1080/07391102.2021.1880480

Thoms, H. C., and Stark, L. A. (2021). The NF-Kb Nucleolar Stress Response Pathway. *Biomedicines* 9 (9), 1082. doi:10.3390/biomedicines9091082

Tossidou, I., Himmelseher, E., Teng, B., Haller, H., and Schiffer, M. (2014). SUMOylation Determines Turnover and Localization of Nephrin at the Plasma Membrane. *Kidney Int.* 86 (6), 1161–1173. doi:10.1038/ki.2014.198

Tossidou, I., Niedenthal, R., Klaus, M., Teng, B., Worthmann, K., King, B. L., et al. (2012). CD2AP Regulates SUMOylation of CIN85 in Podocytes. *Mol. Cell. Biol.* 32 (6), 1068–1079. doi:10.1128/MCB.06106-11

Tossidou, I., Teng, B., Drobot, L., Meyer-Schwesinger, C., Worthmann, K., Haller, H., et al. (2010). CIN85/RukL Is a Novel Binding Partner of Nephrin and Podocin and Mediates Slit Diaphragm Turnover in Podocytes. *J. Biol. Chem.* 285 (33), 25285–25295. doi:10.1074/jbc.M109.087239

Utispan, K., and Koontongkaew, S. (2021). Mucin 1 Regulates the Hypoxia Response in Head and Neck Cancer Cells. *J. Pharmacol. Sci.* 147 (4), 331–339. doi:10.1016/j.jphs.2021.08.007

Wagner, T., Kiweler, N., Wolff, K., Knauer, S. K., Brandl, A., Hemmerich, P., et al. (2015). Sumoylation of HDAC2 Promotes NF-κb-dependent Gene Expression. *Oncotarget* 6 (9), 7123–7135. doi:10.18632/oncotarget.3344

Wakashima, T., Tanaka, T., Fukui, K., Komoda, Y., Shinozaki, Y., Kobayashi, H., et al. (2020). JTZ-951, an HIF Prolyl Hydroxylase Inhibitor, Suppresses Renal Interstitial Fibroblast Transformation and Expression of Fibrosis-Related Factors. *Am. J. Physiol. Ren. Physiol* 318 (1), F14–F24. doi:10.1152/ajprenal.00323.2019

Wang, B., Zhang, C., Ma, X., Yu, T., Liu, X., Hu, C., et al. (2021). Astragaloside IV Improves Angiogenesis under Hypoxic Conditions by Enhancing Hypoxia-inducible F-actor-1α SUMOylation. *Mol. Med. Rep.* 23 (4), 244. doi:10.3892/mmr.2021.11883

Wang, H., and You, G. (2019). The SUMO-specific Protease Senp2 Regulates SUMOylation, Expression and Function of Human Organic Anion Transporter 3. *Biochim. Biophys. Acta Biomembr* 1861 (7), 1293–1301. doi:10.1016/j.bbamem.2019.04.007

Wang, H., Zhang, J., and You, G. (2019). Activation of Protein Kinase A Stimulates SUMOylation, Expression, and Transport Activity of Organic Anion Transporter 3. *AAPS J.* 21 (2), 30. doi:10.1208/s12248-019-0303-4

Wang, J., Zhang, Z., Fang, A., Wu, K., Chen, X., Wang, G., et al. (2020). Resveratrol Attenuates Inflammatory Bowel Disease in Mice by Regulating SUMO1. *Biol. Pharm. Bull.* 43 (3), 450–457. doi:10.1248/bpb.b19-00786

Wang, L., Wansleeben, C., Zhao, S., Miao, P., Paschen, W., and Yang, W. (2014a). SUMO2 Is Essential while SUMO3 Is Dispensable for Mouse Embryonic Development. *EMBO Rep.* 15 (8), 878–885. doi:10.15252/embr.201438534

Wang, L., Zhang, T., Fang, M., Shen, N., Wang, D., Teng, J., et al. (2015). Podocytes Protect Glomerular Endothelial Cells from Hypoxic Injury via deSUMOylation of HIF-1α Signaling. *Int. J. Biochem. Cell Biol* 58, 17–27. doi:10.1016/j.biocel.2014.10.030

Wang, L., Zhu, J., Fang, M., Zhang, T., Xie, H., Wang, N., et al. (2014b). Inhibition of P53 deSUMOylation Exacerbates Puromycin Aminonucleoside-Induced Apoptosis in Podocytes. *Int. J. Mol. Sci.* 15 (11), 21314–21330. doi:10.3390/ijms151121314

Wang, Z., Wang, K., Wang, R., and Liu, X. (2018). SUMOylation Regulates TGF-β1/Smad4 Signalling In-Resistant Glioma Cells. *Anticancer Drugs* 29 (2), 136–144. doi:10.1097/CAD.0000000000000578

Wang, B. S., Ma, X. F., Zhang, C. Y., Li, Y. X., Liu, X. Z., and Hu, C. Q. (2021). Astragaloside IV Improves Angiogenesis and Promotes Wound Healing in Diabetic Rats via the Activation of the SUMOylation Pathway. *Biomed. Environ. Sci.* 34 (2), 124–129. doi:10.3967/bes2021.018

Wang, Z., Jiang, L., Wang, J., Chai, Z., and Xiong, W. (2021). Morphine Promotes Angiogenesis by Activating PI3K/Akt/HIF-1α Pathway and Upregulating VEGF in Hepatocellular Carcinoma. *J. Gastrointest. Oncol.* 12 (4), 1761–1772. doi:10.21037/jgo-20-394

Wenzl, F. A., Ambrosini, S., Mohammed, S. A., Kraler, S., Lüscher, T. F., Costantino, S., et al. (2021). Inflammation in Metabolic Cardiomyopathy. *Front. Cardiovasc. Med.* 8, 742178. doi:10.3389/fcvm.2021.742178

Wilkinson, K. A., and Henley, J. M. (2010). Mechanisms, Regulation and Consequences of Protein SUMOylation. *Biochem. J.* 428 (2), 133–145. doi:10.1042/BJ20100158

Wu, L., Li, O., Zhu, F., Wang, X., Chen, P., Cai, G., et al. (2021). Krüppel-like Factor 15 Suppresses Renal Glomerular Mesangial Cell Proliferation via Enhancing P53 SUMO1 Conjugation. *J. Cell. Mol. Med.* 25 (12), 5691–5706. doi:10.1111/jcmm.16583

Xie, B., Liu, X., Yang, J., Cheng, J., Gu, J., and Xue, S. (2018). PIAS1 Protects against Myocardial Ischemia-Reperfusion Injury by Stimulating PPARγ SUMOylation. *BMC Cell Biol* 19 (1), 24. doi:10.1186/s12860-018-0176-x

Xie, M., Yu, J., Ge, S., Huang, J., and Fan, X. (2020). SUMOylation Homeostasis in Tumorigenesis. *Cancer Lett.* 469, 301–309. doi:10.1016/j.canlet.2019.11.004

Xu, Y., Zuo, Y., Zhang, H., Kang, X., Yue, F., Yi, Z., et al. (2010). Induction of SENP1 in Endothelial Cells Contributes to Hypoxia-Driven VEGF Expression and Angiogenesis. *J. Biol. Chem.* 285 (47), 36682–36688. doi:10.1074/jbc.M110.164236

Yang, L., Li, D. X., Cao, B. Q., Liu, S. J., Xu, D. H., Zhu, X. Y., et al. (2021). Exercise Training Ameliorates Early Diabetic Kidney Injury by Regulating the H 2 S/SIRT1/p53 Pathway. *FASEB j.* 35 (9), e21823. doi:10.1096/fj.202100219R

Yang, Z., Zhang, Y., and Sun, S. (2019). Deciphering the SUMO Code in the Kidney. *J. Cell. Mol. Med.* 23 (2), 711–719. doi:10.1111/jcmm.14021

Yeh, E. T. (2009). SUMOylation and De-SUMOylation: Wrestling with Life's Processes. *J. Biol. Chem.* 284 (13), 8223–8227. doi:10.1074/jbc.R800050200

You, Y. K., Wu, W. F., Huang, X. R., Li, H. D., Ren, Y. P., Zeng, J. C., et al. (2021). Deletion of Smad3 Protects against C-Reactive Protein-Induced Renal Fibrosis and Inflammation in Obstructive Nephropathy. *Int. J. Biol. Sci.* 17 (14), 3911–3922. doi:10.7150/ijbs.62929

Zeng, M., Liu, W., Hu, Y., and Fu, N. (2020). Sumoylation in Liver Disease. *Clin. Chim. Acta* 510, 347–353. doi:10.1016/j.cca.2020.07.044

Zhang, F. P., Mikkonen, L., Toppari, J., Palvimo, J. J., Thesleff, I., and Jänne, O. A. (2008). Sumo-1 Function Is Dispensable in normal Mouse Development. *Mol. Cell. Biol.* 28 (17), 5381–5390. doi:10.1128/MCB.00651-08

Zhang, J., Wu, C., Gao, L., Du, G., and Qin, X. (2020). Astragaloside IV Derived from Astragalus Membranaceus: A Research Review on the Pharmacological Effects. *Adv. Pharmacol.* 87, 89–112. doi:10.1016/bs.apha.2019.08.002

Zhao, Q., Zhang, K., Li, Z., Zhang, H., Fu, F., Fu, J., et al. (2021). High Migration and Invasion Ability of PGCCs and Their Daughter Cells Associated with the Nuclear Localization of S100A10 Modified by SUMOylation. *Front. Cell Dev Biol* 9, 696871. doi:10.3389/fcell.2021.696871

Zhao, W., Zhang, X., and Rong, J. (2021a). SUMOylation as a Therapeutic Target for Myocardial Infarction. *Front. Cardiovasc. Med.* 8, 701583. doi:10.3389/fcvm.2021.701583

Zhao, W., Zhao, J., Zhang, X., Fan, N., and Rong, J. (2021b). Upregulation of Small Ubiquitin-like Modifier 2 and Protein SUMOylation as a Cardioprotective Mechanism against Myocardial Ischemia-Reperfusion Injury. *Front. Pharmacol.* 12, 731980. doi:10.3389/fphar.2021.731980

Zhou, D., Zhou, M., Wang, Z., Fu, Y., Jia, M., Wang, X., et al. (2019). PGRN Acts as a Novel Regulator of Mitochondrial Homeostasis by Facilitating Mitophagy and Mitochondrial Biogenesis to Prevent Podocyte Injury in Diabetic Nephropathy. *Cell Death Dis* 10 (7), 524. doi:10.1038/s41419-019-1754-3

Zhou, X., Gao, C., Huang, W., Yang, M., Chen, G., Jiang, L., et al. (2014). High Glucose Induces Sumoylation of Smad4 via SUMO2/3 in Mesangial Cells. *Biomed. Res. Int.* 2014, 782625. doi:10.1155/2014/782625

Zhu, Z., Liang, W., Chen, Z., Hu, J., Feng, J., Cao, Y., et al. (2021). Mitoquinone Protects Podocytes from Angiotensin II-Induced Mitochondrial Dysfunction and Injury via the Keap1-Nrf2 Signaling Pathway. *Oxid. Med. Cell. Longev.* 2021, 1394486. doi:10.1155/2021/1394486

Zou, M., Wang, J., Gao, J., Han, H., and Fang, Y. (2018). Phosphoproteomic Analysis of the Antitumor Effects of Ginsenoside Rg3 in Human Breast Cancer Cells. *Oncol. Lett.* 15 (3), 2889–2898. doi:10.3892/ol.2017.7654

Conflict of Interest: The authors declare that the research was conducted in the absence of any commercial or financial relationships that could be construed as a potential conflict of interest.

Publisher's Note: All claims expressed in this article are solely those of the authors and do not necessarily represent those of their affiliated organizations, or those of the publisher, the editors, and the reviewers. Any product that may be evaluated in this article, or claim that may be made by its manufacturer, is not guaranteed or endorsed by the publisher.

frontiers in Pharmacology

ORIGINAL RESEARCH
published: 18 March 2022
doi: 10.3389/fphar.2022.790937

Fucoidan Alleviates Renal Fibrosis in Diabetic Kidney Disease *via* Inhibition of NLRP3 Inflammasome-Mediated Podocyte Pyroptosis

Mei-Zi Wang[1,2,3†], Jie Wang[1,2†], Dong-Wei Cao[4†], Yue Tu[5], Bu-Hui Liu[1], Can-Can Yuan[1], Huan Li[1], Qi-Jun Fang[1,2], Jia-Xin Chen[1], Yan Fu[1], Bing-Ying Wan[1], Zi-Yue Wan[6], Yi-Gang Wan[3‡] and Guo-Wen Wu[7*‡]*

[1]Department of Traditional Chinese Medicine, Nanjing Drum Tower Hospital Clinical College of Nanjing University of Chinese Medicine, Nanjing, China, [2]Institute of Chinese Medicine, Nanjing University, Nanjing, China, [3]Department of Traditional Chinese Medicine, Nanjing Drum Tower Hospital, The Affiliated Hospital of Nanjing University Medical School, Nanjing, China, [4]Department of Nephrology, Nanjing Drum Tower Hospital, The Affiliated Hospital of Nanjing University Medical School, Nanjing, China, [5]Department of Traditional Chinese Medicine Health Preservation, Acupuncture, Moxibustion and Massage College, Health Preservation and Rehabilitation College, Nanjing University of Chinese Medicine, Nanjing, China, [6]Graduate School of Social Sciences, Faculty of Social Sciences, Hitotsubashi University, Tokyo, Japan, [7]Jilin Province Huinan Chonglong Bio-Pharmacy Co., Ltd., Huinan, China

OPEN ACCESS

Edited by:
Dan-Qian Chen,
Northwest University, China

Reviewed by:
Guangbi Li,
Virginia Commonwealth University, United States
Xiangsheng Zhang,
Capital Medical University, China

***Correspondence:**
Yi-Gang Wan
wyg68918@sina.com
Guo-Wen Wu
jl-wgw@163.com

[†]These authors have contributed equally to this work and share first authorship

[‡]These authors have contributed equally to this work and share senior authorship

Specialty section:
This article was submitted to Renal Pharmacology, a section of the journal Frontiers in Pharmacology

Received: 07 October 2021
Accepted: 08 February 2022
Published: 18 March 2022

Citation:
Wang M-Z, Wang J, Cao D-W, Tu Y, Liu B-H, Yuan C-C, Li H, Fang Q-J, Chen J-X, Fu Y, Wan B-Y, Wan Z-Y, Wan Y-G and Wu G-W (2022) Fucoidan Alleviates Renal Fibrosis in Diabetic Kidney Disease via Inhibition of NLRP3 Inflammasome-Mediated Podocyte Pyroptosis. Front. Pharmacol. 13:790937. doi: 10.3389/fphar.2022.790937

Background: Fucoidan (FPS) has been widely used to treat renal fibrosis (RF) in patients with diabetic kidney disease (DKD); however, the precise therapeutic mechanisms remain unclear. Recently, research focusing on inflammation-derived podocyte pyroptosis in DKD has attracted increasing attention. This phenomenon is mediated by the activation of the nucleotide-binding oligomerization domain (Nod)-like receptor family pyrin domain-containing 3 (NLRP3) inflammasome, leading to RF during DKD progression. Therefore, we designed a series of experiments to investigate the ameliorative effects of FPS on RF in DKD and the mechanisms that are responsible for its effect on NLRP3 inflammasome-mediated podocyte pyroptosis in the diabetic kidney.

Methods: The modified DKD rat models were subjected to uninephrectomy, intraperitoneal injection of streptozotocin, and a high-fat diet. Following induction of renal injury, the animals received either FPS, rapamycin (RAP), or a vehicle for 4 weeks. For *in vitro* research, we exposed murine podocytes to high glucose and MCC950, an NLRP3 inflammasome inhibitor, with or without FPS or RAP. Changes in the parameters related to RF and inflammatory podocyte injury were analyzed *in vivo*. Changes in podocyte pyroptosis, NLRP3 inflammasome activation, and activation of the adenosine monophosphate-activated protein kinase (AMPK)/mammalian target of rapamycin complex 1 (mTORC1)/NLRP3 signaling axis involved in these changes were analyzed *in vivo* and *in vitro*.

Results: FPS and RAP ameliorated RF and inflammatory podocyte injury in the DKD model rats. Moreover, FPS and RAP attenuated podocyte pyroptosis, inhibited NLRP3 inflammasome activation, and regulated the AMPK/mTORC1/NLRP3 signaling axis *in vivo* and *in vitro*. Notably, our data showed that the regulative effects of FPS, both *in vivo* and *in vitro*, on the key signaling molecules, such as p-AMPK and p-raptor, in the AMPK/

mTORC1/NLRP3 signaling axis were superior to those of RAP, but similar to those of metformin, an AMPK agonist, *in vitro*.

Conclusion: We confirmed that FPS, similar to RAP, can alleviate RF in DKD by inhibiting NLRP3 inflammasome-mediated podocyte pyroptosis via regulation of the AMPK/mTORC1/NLRP3 signaling axis in the diabetic kidney. Our findings provide an in-depth understanding of the pathogenesis of RF, which will aid in identifying precise targets that can be used for DKD treatment.

Keywords: fucoidan, diabetic kidney disease, renal fibrosis, podocyte pyroptosis, NLRP3 inflammasome

INTRODUCTION

An increasing body of evidence in both clinical and experimental animal models has shown that inflammation is an important contributor to renal fibrosis (RF) in the progression of diabetic kidney disease (DKD) (Cooper and Warren, 2019). Inflammatory podocyte injury is the key pathogenic factor that triggers and sustains RF, which is closely associated with renal dysfunction and renal failure (Dai et al., 2017). Therefore, precision therapies that protect against podocyte inflammation are considered to have great significance in treatment of RF in DKD. Inflammation-derived podocyte pyroptosis is a newly discovered cell death pathway that plays a critical role in podocyte injury in DKD (Lin et al., 2020). Pyroptosis is mediated by the nucleotide-binding oligomerization domain (Nod)-like receptor family pyrin domain-containing 3 (NLRP3) inflammasome activation, caspase activation, cell membrane pore formation characterized by gasdermin D (GSDMD), and release of interleukin (IL)-1β and IL-18. NLRP3 inflammasome activation plays a central role in pyroptosis (He et al., 2015; Shi et al., 2015; Liu et al., 2016). It has been demonstrated that podocytes, as a group of renal residential cells, express all the necessary components of NLRP3 inflammasome, which is activated and contributes to inflammatory damage induced by high glucose (HG) (Xiong et al., 2020). In addition, Birnbaum et al. (2018) report a combination of sodium-dependent glucose transporters-2 inhibitor and dipeptidyl peptidase-4 (DPP-4) inhibitors can delay DKD progression, and that their therapeutic actions are closely related to the inhibition of NLRP3 inflammasome activation. Therefore, it is possible to alleviate inflammatory podocyte injury in glomeruli of kidneys affected by DKD by targeting NLRP3 inflammasome activation.

NLRP3 inflammasome can be activated by diverse stimuli and involves multiple signaling pathways, including the reactive oxygen species/thioredoxin-interacting protein, nuclear factor (NF)-κB, nuclear factor erythroid-related factor 2, long non-coding RNA, and mitogen-activated protein kinases (Paik et al., 2021). In addition, some studies demonstrated the NLRP3 inflammasome's crucial role in pyroptosis initiation and pro-inflammatory cytokine production in DKD (Xiong et al., 2021). For instance, NLRP3 deficiency in diabetic mice significantly blocks Caspases-1 mediated IL-1β secretion and protects against renal injury *in vivo* (Yu et al., 2020). A strong upregulation of pyroptosis-related proteins, including NLRP3 and Caspase-1, in diabetic tissue has been observed (Lin et al., 2020). Additional research showed that many signaling mechanisms of NLRP3 inflammasome activation are involved in diabetic complications. Zhang et al. (2017) found that autophagy can downregulate NLRP3 inflammasome via mammalian target of rapamycin (mTOR) signaling. Accordingly, Yang et al. (2019) reported that NLRP3 inflammasome can be inhibited by metformin and rapamycin (RAP, an mTOR inhibitor) by targeting the adenosine monophosphate-activated protein kinase (AMPK)/mTOR complex 1 (mTORC1)-dependent effects in diabetic cardiomyopathy. Thus, we suggest that regulating the AMPK/mTORC1-related signaling axis is of great importance in the inhibition of NLRP3 inflammasome activation.

Fucoidan (FPS) is a class of fucose-rich sulfated carbohydrates found in brown marine algae and echinoderms, and it was recently identified in *Laminaria japonica*, a traditional Chinese herbal medicine (van Weelden et al., 2019). Previous studies have indicated that FPS has an attractive array of bioactivities and potential applications, including anti-inflammation and anti-cancer activities as well as the inhibition of the immune response and of pathogens (Fitton et al., 2015). Over the last few years, research into FPS has continued to gained pace and suggests potential therapeutic or beneficial roles in DKD (Wang et al., 2019). Chen et al. (2015) reported that low molecular weight FPS ameliorates DKD by inhibiting epithelial-mesenchymal transition (EMT) and RF. Despite this, the pharmacological mechanistic link between anti-RF actions and protection against podocyte inflammation correlated with diabetic kidney remains poorly understood.

In this study, we used a modified DKD rat model and murine podocytes to assess the ameliorative effects of FPS on RF and inflammatory podocyte injury *in vivo* and *in vitro* and to clarify the anti-RF mechanisms of FPS via targeting NLRP3 inflammasome-mediated podocyte pyroptosis in the diabetic kidney. These results may provide a precise therapeutic strategy for RF in patients with DKD.

MATERIALS AND METHODS

Animals, Drug, and Reagents

All experiments were performed using male Sprague-Dawley rats weighing 200–220 g, purchased from the Experimental Animal Centre of Nanjing University (Nanjing, China) (License No: SCXK [Shanghai] 2012-0006). All rats were housed (six rats/

cage) at 22 ± 3°C and 50 ± 10% humidity using a 12 h light/dark cycle, fed a specific pathogen-free grade standard rat chow (catalogue number 1010008) from Xietong Pharmaceutical Bio-engineering Co., Ltd. (Nanjing, China), and provided tap water ad libitum in the Experimental Animal Centre of Nanjing Drum Tower Hospital, the Affiliated Hospital of Nanjing University Medical School. The animal ethics committee of Nanjing University Medical School approved the surgical procedures and protocols. FPS ($C_6H_{10}O_7S$, CAS: 9072-19-9) was obtained from Jilin Province Huinan Chonglong Bio-Pharmacy Co., Ltd. (Huinan, China), and dissolved in 10% dimethyl sulfoxide at a concentration of 1 g/L. RAP and lipopolysaccharide (LPS) were purchased from Gene Operations (Shanghai, China). Novolin N was obtained from Novo Nordisk Company (Tianjin, China). STZ was purchased from Sigma-Aldrich (St. Louis, MO, United States). The total protein extraction kit and bicinchoninic acid protein assay kit were provided by Key-Gentec (Nanjing, China). Antibodies against fibronectin (FN), collagen type I (collagen I), transforming growth factor-β1 (TGF-β1), Smad2/3, IL-6, toll-like receptor 4 (TLR4), phosphorylated AMPK (p-AMPK), raptor, phosphorylated raptor (p-raptor), mTORC1, phosphorylated mTORC1 (p-mTORC1), CD2-associated protein (CD2AP), and glyceraldehydes-3-phosphate dehydrogenase (GAPDH) were obtained from Cell Signalling Technology (Danvers, MA, United States). Antibodies against nephrin, podocin, neph1(KIRREL), NLRP3, C-terminal caspase recruitment domain (ASC), pro IL-18, pro IL-1β, IL-1β, IL-18, and β-actin were obtained from Abcam (Cambridge, United Kingdom). Antibodies against Caspase-1, pro-Caspase-1, and cleaved-Caspase-1 were obtained from Absin (Shanghai, China). Antibodies against GSDMD and GSDMD-N were obtained from Proteintech (Wuhan, China).

Animal Experimental Design

Twenty-six rats were divided into four groups using a random number table, with five, seven, seven, and seven rats in the sham-operated group, the DKD model group, the FPS-treated group, and the RAP-treated group, respectively. In particular, the left kidney was exposed during surgery for the rats in the sham-operated group. The rats were then given distilled water and a standard diet for 18 weeks. In contrast, the rats in the other three groups were given a 40% high-fat diet containing 19.8% fat, 22.3% crude protein, and 44.6% carbohydrates, for 4 weeks. The rats in these three groups were then subjected to left nephrectomy and received two intraperitoneal injections (3 days apart) of STZ at a dosage of 35 mg/kg. This process lasted for 10 weeks, finally establishing a modified rat model of DKD, as described in detail in our previous studies (Mao et al., 2015; Wu et al., 2017; Wu et al., 2018; Han et al., 2019). Once the DKD rat models had been established, we used gastric gavage to administer appropriate daily treatments: FPS was administered to rats in the FPS-treated group (abbreviated as the FPS group), while the rats of the sham-operated group, the DKD model group, and the RAP-treated group (abbreviated as the Sham, the Vehicle, and the RAP groups) were treated with 2 ml of distilled water (vehicle) or RAP, respectively. After 4 weeks of treatment with the different interventions, all rats were anesthetized and sacrificed by cardiac puncture. Blood, urine, liver, and kidneys were collected for the detection of various indicators. The *in vivo* experimental process is shown in **Supplementary Figure S1**. In the clinic, 600 mg/day of FPS is normally used to treat a 60 kg patient with CKD. Based on the standard animal conversion formula, the effective amount of FPS in a rat weighing 200 g was determined to be 120 mg/kg/day. The RAP dose used in this experiment (1 mg/kg/day) was used previously by Wu et al. (2018). Two rats died in the Vehicle, FPS, and RAP groups, respectively, due to severe diabetes and its associated complications during the experiment. Therefore, at the end of the experiment, only five rats were included in each group.

Biochemical Parameters

Body weight (BW) and blood glucose (BG) were tested before modeling and every 2 weeks thereafter. The left kidneys of rats in the experimental groups were removed and weighed after cardiac puncture. After 4 weeks of drug intervention, the rats were anesthetized, and blood samples (5 ml) were drawn from the heart. A range of biochemical parameters were tested, including serum alanine transaminase (ALT), serum aspartate transaminase (AST), serum creatinine (Scr), and blood urea nitrogen (BUN) levels. Prior to sacrifice, we collected urinary samples from the four groups and used these samples to detect 24 h urinary albumin (UAlb) levels. Chromatometry was used to determine these parameters, as previously described (Liu et al., 2019).

Foot Process Form and Glomerular Basement Membrane Thickness

Tissue samples from renal cortex for electron microscopy (EM) assessment were fixed in 2.5% glutaraldehyde in 0.1 mol/L phosphate buffer (PB) for several days at 4°C. After washing in PB and post-fixing in 1% osmium tetroxide (OsO_4) for 2 h, the fixed material was dehydrated through an ethanol propylene oxide series and embedded in Araldite M. Ultrathin sections were prepared and stained with uranyl acetate and lead citrate, and foot process form and GBM thickness were observed and photographed under a JEM-1011 transmission electron microscope (JEOL, Tokyo, Japan). Five glomeruli were randomly selected from each section. According to the method described by Haas (2009), GBM thickness was directly measured and calculated using Image-Pro Plus (IPP) 6.0 software (Media Cybernetic). The results were confirmed by a professional pathologist.

Immunohistochemistry and Histological Assay

Kidney samples were fixed in 4% paraformaldehyde and embedded in paraffin. Sections of 3 μm thickness were cut perpendicularly to the long axis of the kidney for immunohistochemistry (IHC) and morphometric analyses. For IHC analysis, the paraffin-embedded kidney sections were deparaffinized in xylene, hydrated in graded alcohol and water, and subsequently placed in 3% hydrogen peroxide (H_2O_2) to eliminate endogenous peroxidase activity. Then, the sections were blocked with normal goat serum, followed by incubation with anti-podocin, anti-CD2AP, anti-FN, anti-collagen I, anti-NLRP3, anti-ASC, and anti-Caspase-1

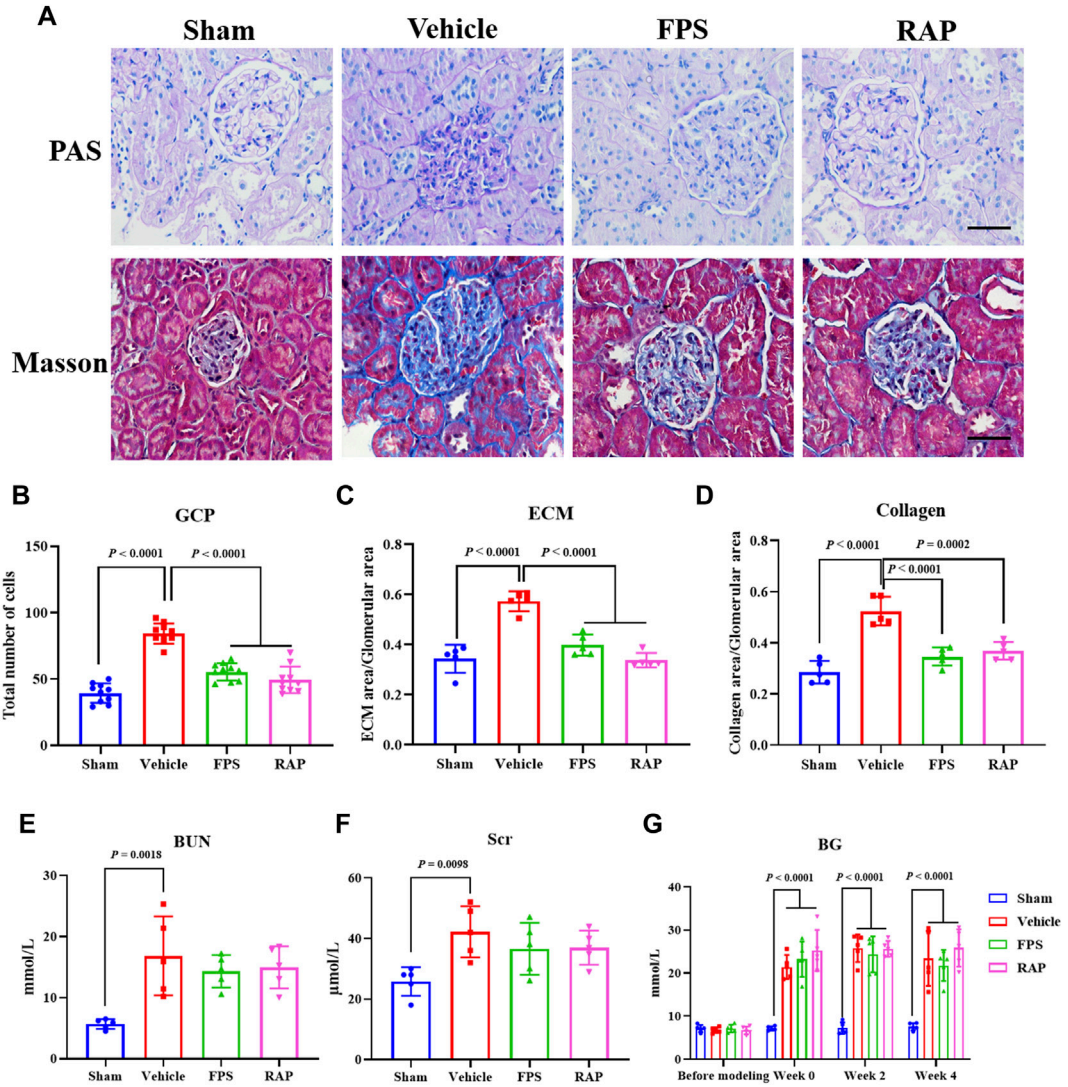

FIGURE 1 | Effects of FPS and RAP on GS and renal function *in vivo*. **(A)** The staining of PAS and Masson stains in the diabetic kidneys (×400). Scale bar = 50 μm. **(B)** The number of GCP. **(C)** The rate of ECM area/glomerular area. **(D)** The rate of collagen area/glomerular area. **(E,F)** The levels of Scr and BUN. **(G)** The dynamic changes in BG after drug intervention during 4 weeks. The data are expressed as the mean ± SD.

antibodies overnight at 4°C, and then with goat anti-rabbit IgG for 30 min at 37°C. The sections were stained with diaminobenzidine, counterstained with hematoxylin, dehydrated with gradient ethanol, purified with xylene, and fixed with neutral balsam. The proportion (%) of positively stained glomerular area across five fields of view was analyzed using IPP. For histological analysis, the sections were stained with periodic acid-Schiff (PAS) staining, Masson's trichrome staining, and hematoxylin-eosin (H&E) staining. The kidney and liver sections were examined using light microscopy (LM). Five sections (PAS staining) from each group were randomly selected to calculate glomerular cell population (GCP) per glomerulus by IPP. Analogously, five sections (Masson staining) from each group were randomly selected to calculate the area of extracellular matrix (ECM) and the area of collagen per glomerulus by IPP. Liver sections were stained with H&E. These results were confirmed by a professional pathologist.

Immunofluorescence *in Vivo* Assay

Paraffin-embedded kidney sections were used to assess the co-localization of zonula occludens-1 (ZO-1) and GSDMD-N. First, the sections were subjected to microwave-based antigen retrieval using ethylene diamine tetraacetic acid antigen retrieval solution (pH 8.0), followed by tyramide signal amplification (TSA). Briefly, the following steps were performed: 1) incubation of sections with anti-GSDMD-N (1:200; Abcam; EPR20829-408) at 4°C overnight, 2) incubation with horseradish peroxidase (HRP) (1:500; Servicebio)-conjugated secondary antibody for 50 min at room temperature, 3) reaction with CY3-TSA (Servicebio, China) for 10 min in the dark, 4) removal of nonspecific binding antibodies by microwave treatment, 5) incubation with anti-

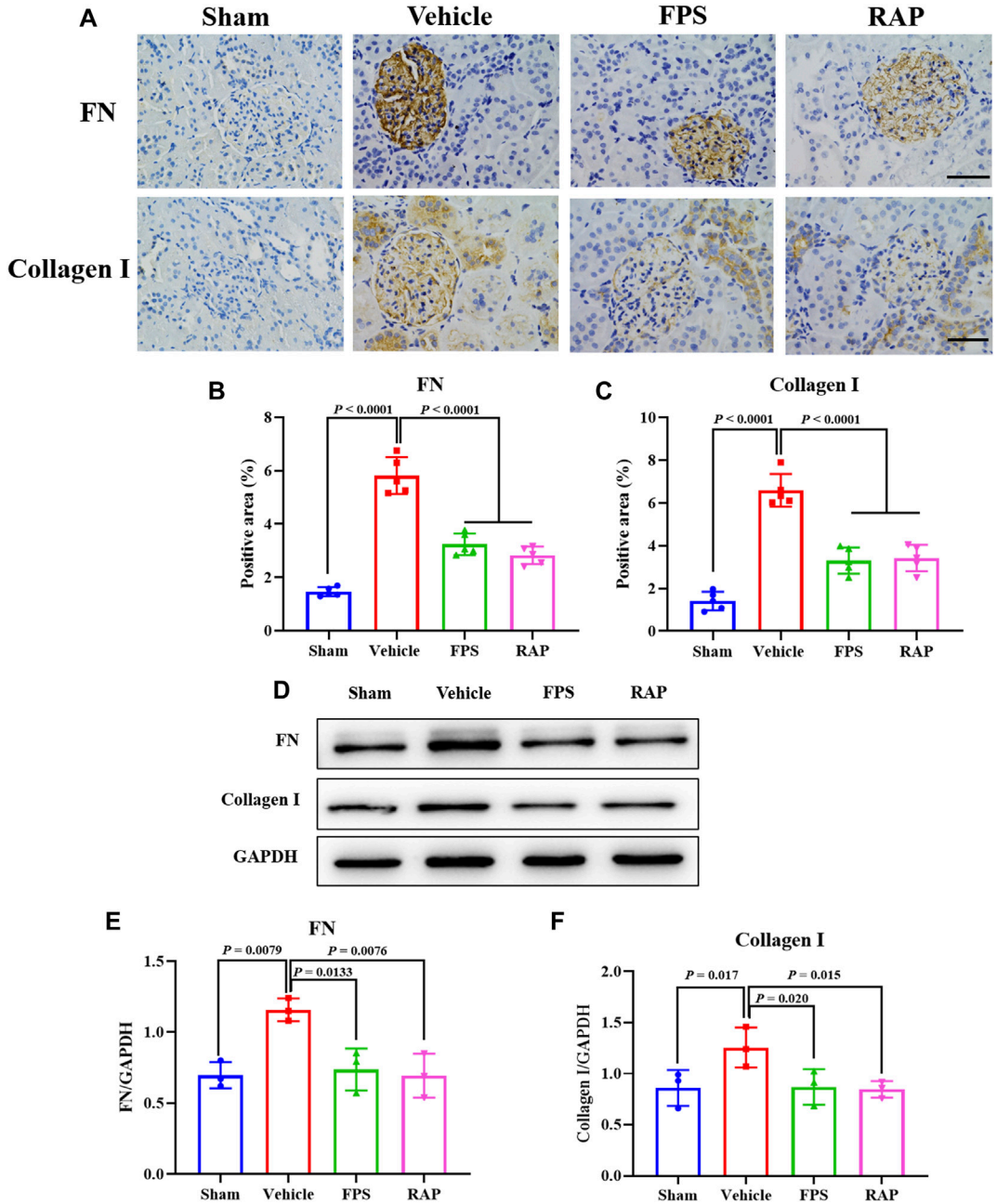

FIGURE 2 | Effects of FPS and RAP on the expression levels of FN and collagen I *in vivo*. **(A)** The immunostaining of FN and collagen I in glomeruli (×400). Scale bar = 50 μm. **(B,C)** The positive area of FN and collagen I in glomeruli. **(D)** The WB analysis of FN and collagen I in the diabetic kidneys. **(E,F)** The rate of FN and collagen I to GAPDH, respectively. The data are expressed as the mean ± SD.

ZO-1 (1:200; Servicebio) at 4°C overnight, 6) incubation with HRP (1:500; Servicebio)-conjugated secondary antibody for 50 min in the dark, 7) reaction with fluorescein isothiocyanate-TSA (Servicebio; China) for 10 min in the dark, and 8) staining with diamidine phenyl indole solution for 10 min. The images were captured by fluorescence microscopy using excitation wavelengths of 330–380 nm (blue), 510–560 nm (red) and 515–555 nm (green). The proportion (%) of positively stained glomerular area across three fields of view was analyzed using IPP. The results were confirmed by a professional pathologist.

Western Blotting *in Vivo* Analysis

Western blotting (WB) analysis was performed as previously described (Wang et al., 2021). The protein expression levels of FN, collagen I, TGF-β1, Smad2/3, podocin, CD2AP, nephrin,

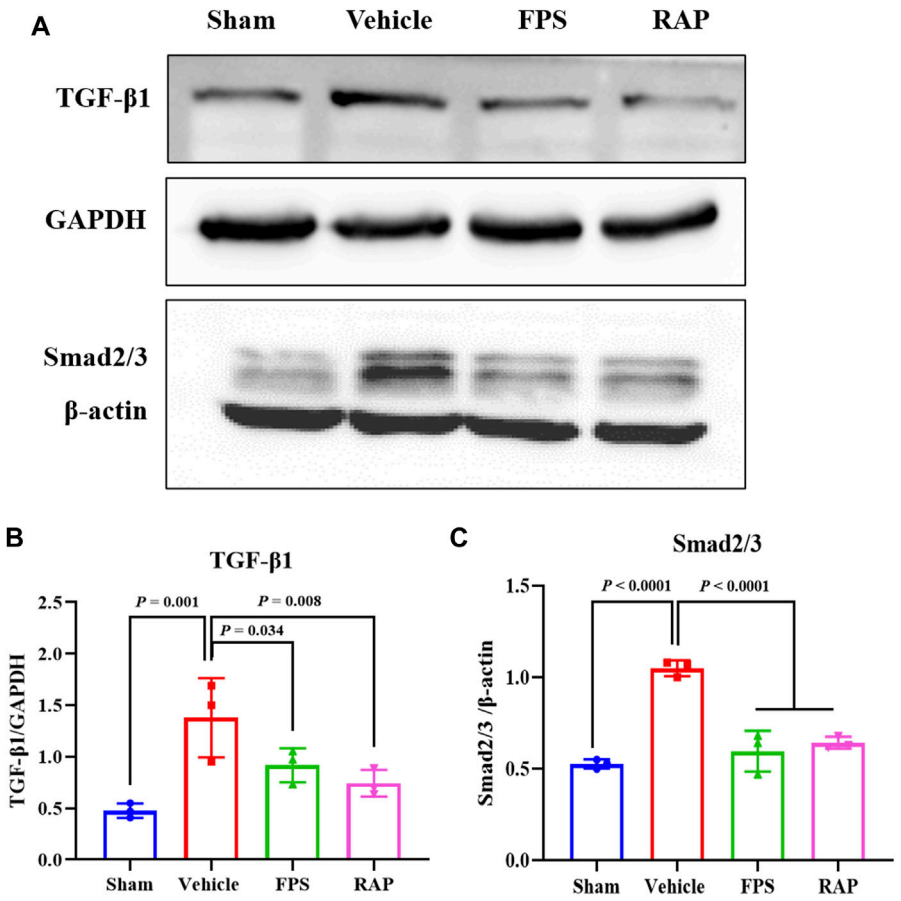

FIGURE 3 | Effects of FPS and RAP on the TGF-β1/Smad2/3 pathway *in vivo*. **(A)** The WB analysis of TGF-β1 and Smad2/3 l in the diabetic kidneys. **(B,C)** The rate of TGF-β1 and Smad2/3 to GAPDH or β-actin, respectively. The data are expressed as the mean ± SD.

neph1, IL-6, TLR4, GSDMD, GSDMD-N, NLRP3, ASC, pro-Caspase-1, cleaved-Caspase-1, p-AMPK, p-raptor, raptor, p-mTORC1, mTORC1, GAPDH, and β-actin were examined, respectively. WB analysis was then performed on kidney samples from each group. We used the protocol described in our previous publications (Tu et al., 2020; Liu et al., 2021b).

Cell Culture Treatment

An immortalized mouse podocyte cell-5 line (MPC-5 cells) was kindly provided by Dr. Jian Yao (University of Yamanashi, Chuo, Japan) and cultured as described previously (Liu et al., 2021b). In brief, MPC-5 cells were cultured at a permissive temperature (33°C) in 5% carbon dioxide (CO_2) in Dulbecco's modified Eagle's medium (DMEM) containing 10% fetal bovine serum (FBS; Gibco, Grand Island, NY, United States) and recombinant interferon (IFN)-γ (10 U/ml, Cambridge, United Kingdom). Following passage, MPC-5 cells were cultured at 37°C in 5% CO_2 for 14 days in DMEM without IFN-γ to induce differentiation. The cells were then exposed to HG (30 mmol/L D-glucose) and MCC950 (10 μmol/L, an NLRP3 inhibitor), with or without FPS, at a dose of 20 μg/ml or RAP at a dose of 20 nmol/L for 24 h. For this experiment, the doses of FPS, RAP, and MCC950 were described by Liu et al. (2021a), Wu et al. (2018), and Liu et al. (2021b), respectively.

Cell Viability Assessment

The viability of MPC-5 cells was assessed using the cell counting kit (CCK-8) (Beyotime, Shanghai, China). The cells were seeded into 96-well plates, with three replicate wells for each group, at a density of 1×10^4 cells per well, in 100 μl medium. After the cells were incubated for the indicated time period, 10 μl of CCK-8 solution was added to each well, followed by incubation for 2 h. The optical density was determined at an absorbance of 450 nm, and cell viability was calculated.

Immunofluorescence *in Vitro* Assay

First differentiated podocytes grown on glass coverslips were fixed with paraformaldehyde (4% in PBS) and permeabilised with Triton ×-100 (0.25%). Then the cells were incubated with primary antibody directed against GSDMD-N (1:200) at

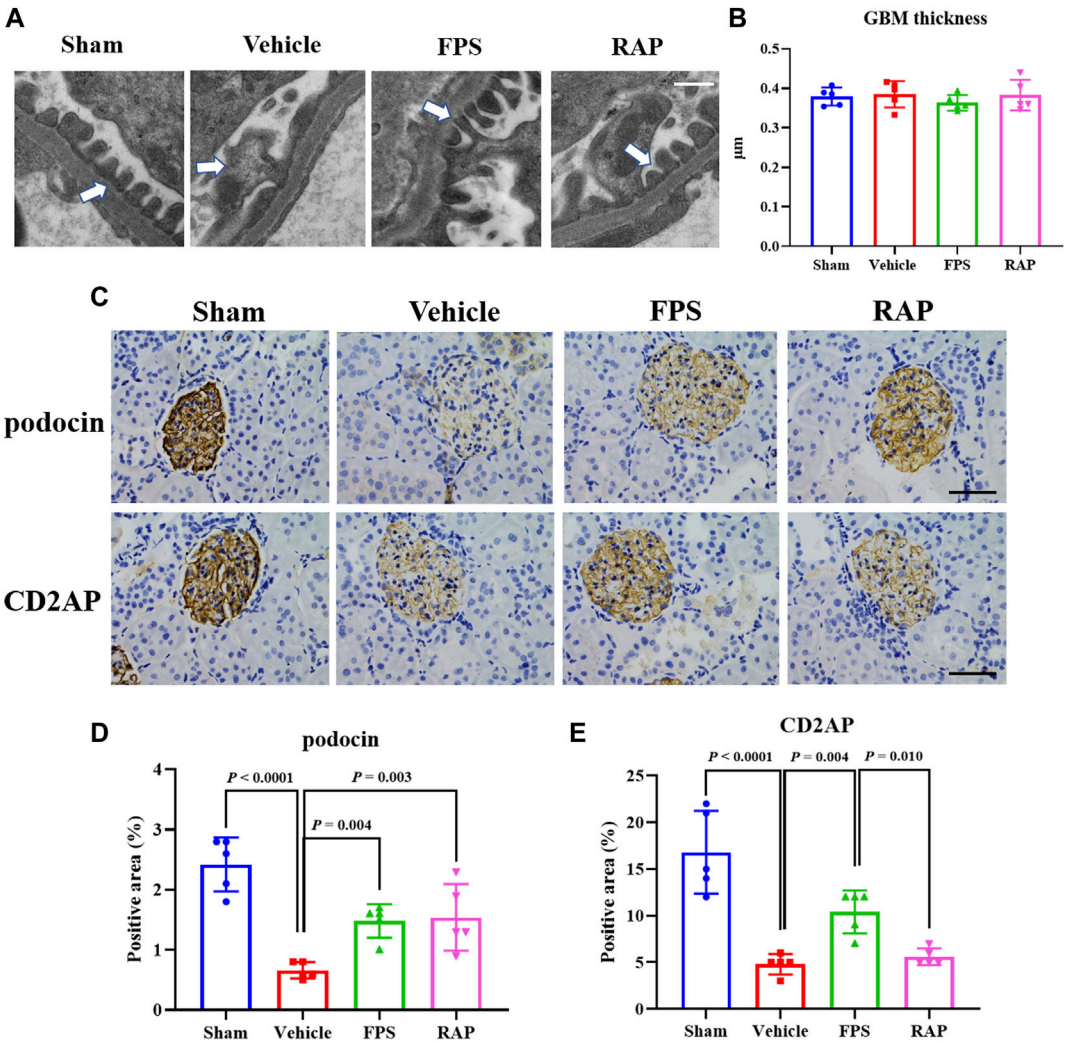

FIGURE 4 | Effects of FPS and RAP on foot process form, GBM thickness, and the expression characteristics of podocin and CD2AP *in vivo*. **(A)** The ultra-microstructure of foot process form and GBM (×11,500). Scale bar = 500 nm. **(B)** The GBM thickness. **(C)** The immunostaining of podocyte and CD2AP in glomeruli (×400). Scale bar = 50 μm. **(D,E)** The positive area of podocin and CD2AP in glomeruli. The data are expressed as the mean ± SD.

4°C overnight. Next, the coverslips were incubated with Alexa Fluor 488 goat anti-rabbit IgG (1:200) as a secondary antibody for 1 h at room temperature. Finally, the coverslips were mounted with Fluoroshield™ and 4′,6-diamidine-2′-phenylindole dihydrochloride (DAPI; F6057, Sigma-Aldrich, blue fluorescent dye) for 10 min in the dark. The images were acquired using an epifluorescence inverted microscope (IX81, Olympus, Tokyo, Japan) equipped with a cell imaging software (Soft Imaging System GmbH, Munster, Germany). The results were confirmed by a professional pathologist.

WB *In Vitro* Analysis

MPC-5 cells were treated with appropriate treatments for 24 h. Following treatment, the cell lysates were separated by gel electrophoresis and blotted with antibodies against GSDMD, GSDMD-N, NLRP3, ASC, pro-Caspase-1, cleaved-Caspase-1, pro IL-18, IL-18, pro IL-1β, IL-1β, p-AMPK, p-raptor, raptor, p-mTORC1, mTORC1, GAPDH and β-actin, respectively. HRP-conjugated anti-rabbit IgG antibody was used as the secondary antibody. WB analysis was then performed on the samples of cells from each group. We used the protocol described in our previous publications (Tu et al., 2020; Liu et al., 2021b).

Statistical Analysis

The WB assessment was repeated at least three independent times, and the individual data were subjected to densitometric analysis. The data are expressed as the mean ± standard deviation (SD). Statistical analysis was performed by one-way analysis of variance (ANOVA) on normally distributed data, with least significant difference (LSD) post-hoc test, or non-parametric Kruskal–Wallis test if not. A p-value < 0.05 or <0.01 indicated a statistically significant difference.

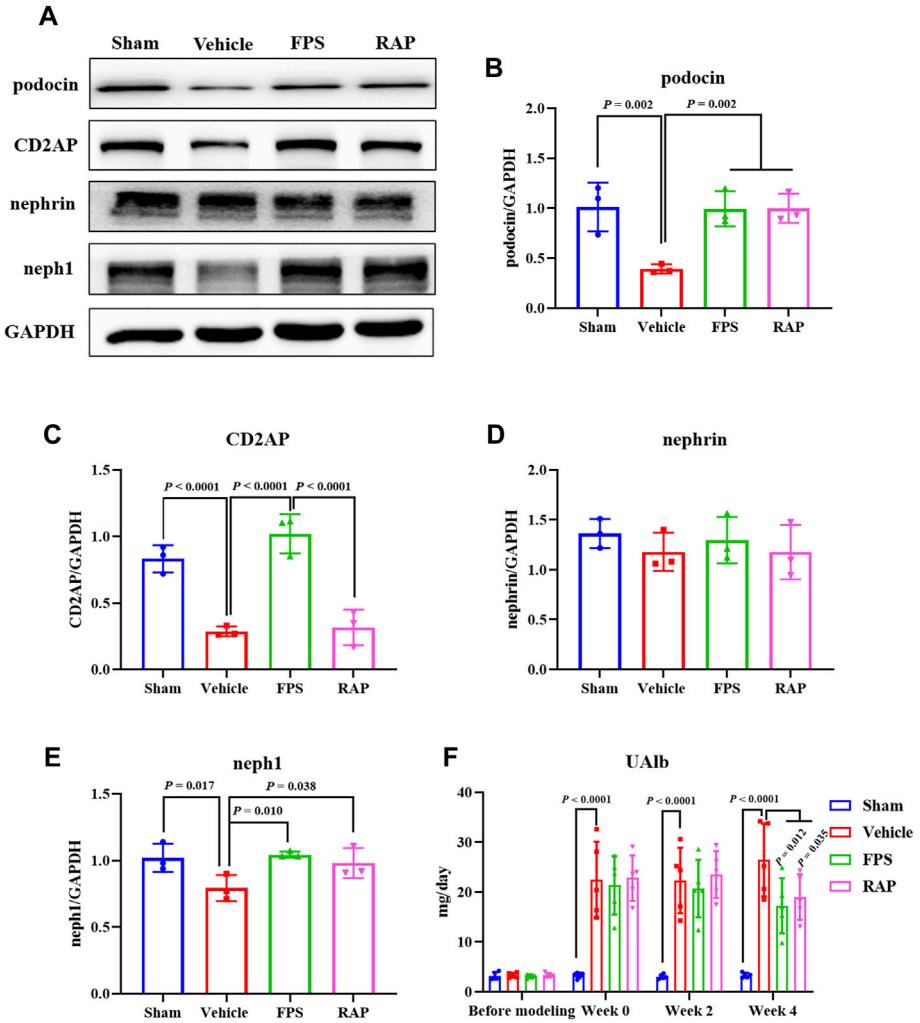

FIGURE 5 | Effects of FPS and RAP on the expression levels of podocin, CD2AP, nephrin, and neph1 *in vivo*, as well as UAlb in the DKD model rats. **(A)** The WB analysis of podocin, CD2AP, nephrin, and neph1 in the diabetic kidneys. **(B–E)** The rate of podocin, CD2AP, neph1, and nephrin to GAPDH, respectively. **(F)** The dynamic change of UAlb after drug intervention during 4 weeks. The data are expressed as the mean ± SD.

RESULTS

FPS and RAP Ameliorate Renal Fibrosis *In Vivo*

As is widely known, the pathomorphological changes of RF in DKD are mainly characterized by glomerular sclerosis (GS) (Alicic et al., 2017). Thus, we first studied the effects of FPS and RAP on GS in these DKD model rats. In **Figure 1A**, we found that, compared with the Sham group rats, after modeling, the obvious pathological changes in the Vehicle group rats, including glomerular mild hypertrophy, capillary loop area reduction, glomerular cell proliferation, ECM expansion, and collagen deposition were detected. After treatment with FPS or RAP, the degree of pathological changes in GS in these DKD model rats, including GCP, and the rates of ECM and collagen area to glomerular area were improved significantly when compared to the Vehicle group rats (**Figures 1B–D**). In addition, after treatment with FPS or RAP, the decreasing tendency of BUN and Scr in the FPS and RAP group rats was also observed at different degrees when compared to the Vehicle group rats (**Figures 1E,F**). Here, notably, in **Figure 1G**, we found that FPS and RAP did not affect hyperglycemia in these modified DKD model rats.

We then examined the effects of FPS and RAP on the expression levels of FN and collagen I as the markers of RF in the kidneys of these DKD model rats by PAS staining and WB analysis. In **Figures 2A,D**, we found that, compared with the Sham group rats, after modeling, the altered immunostaining extent of FN and collagen I in glomeruli and the higher protein expression levels of FN and collagen I in the kidneys of these DKD model rats were detected, respectively, and significantly improved in the FPS and RAP group rats after treatment with FPS or RAP when compared to the Vehicle group rats (**Figures 2B,C,E,F**).

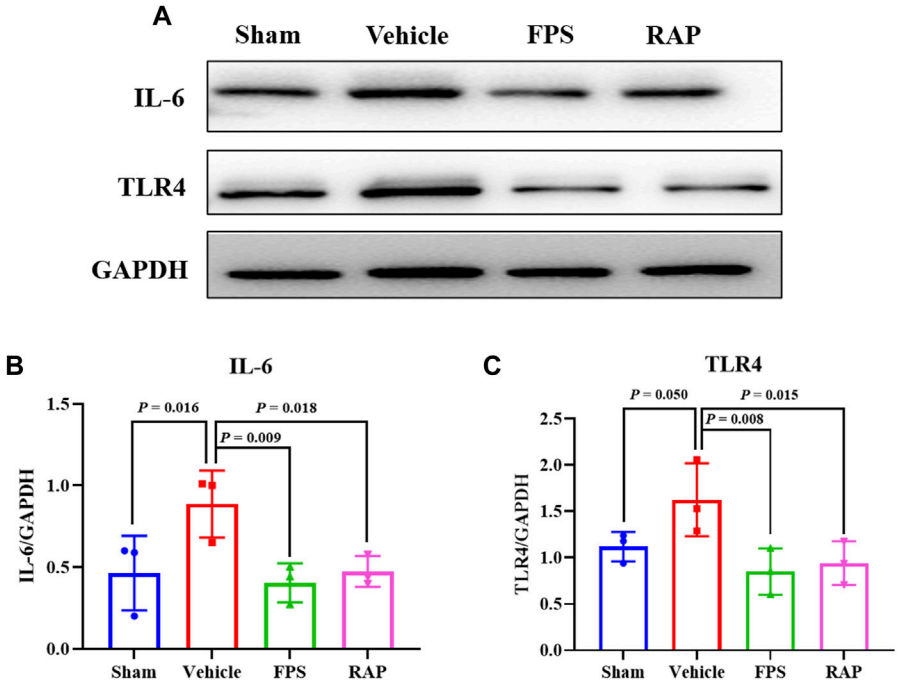

FIGURE 6 | Effects of FPS and RAP on the expression levels of IL-6 and TLR4 *in vivo*. **(A)** The WB analysis of IL-6 and TLR4 in the diabetic kidneys. **(B,C)** The rate of IL-6 and TLR4 to GAPDH, respectively. The data are expressed as the mean ± SD.

Further, using WB analysis, we investigated the effects of FPS and RAP on the TGF-β1/Smad2/3 pathway as a given signaling mechanism inducing RF in the kidneys of these DKD model rats. In **Figure 3A**, after modeling, the increased protein expression levels of TGF-β1 and Smad2/3 in the kidneys of these DKD model rats were appeared, respectively, and significantly decreased in the FPS and RAP group rats when compared to the Vehicle group rats (**Figures 3B,C**).

In brief, the above results showed that FPS and RAP significantly ameliorated RF in the DKD model rats.

FPS and RAP Alleviate Inflammatory Podocyte Injury *In Vivo*

During the progression of DKD, inflammatory podocyte injury is an important mechanism by which hyperglycemia contributes to GS (Alicic et al., 2017). We first investigated the effects of FPS and RAP on foot process form and GBM thickness by EM in these DKD model rats. In **Figure 4A**, we found that, compared with the Sham group rats, widened, shortened, and fused foot processes were clearly evident in the Vehicle group rats. After treatment with FPS or RAP, foot process effacement in these DKD model rats was significantly improved in the FPS and RAP group rats when compared to the Vehicle group rats. However, no significant difference in GBM thickness was detected among the four groups (**Figure 4B**).

We then examined the effects of FPS and RAP on the expression levels of the injurious and inflammatory markers in podocytes, including podocin, CD2AP, nephrin, and neph1, as well as IL-6 and TLR4 in glomeruli and in the kidneys of these DKD model rats by IHC staining and WB analysis. In **Figures 4C**, **5A**, **6A**, we found that, compared with the Sham group rats, after modeling, the changed immunostaining extent of podocin and CD2AP in glomeruli, and the altered protein expression levels of podocin, CD2AP, neph1, IL-6, and TLR4 in the kidneys of these DKD model rats were detected, respectively, and significantly improved in the FPS and RAP group rats after treatment with FPS or RAP when compared to the Vehicle group rats. Notably, the expression characteristic of CD2AP in glomeruli and the protein expression level of CD2AP in the kidneys of the FPS group rats were better than those of the RAP group rats (**Figures 4E**, **5C**). However, no significant difference in the protein expression level of nephrin was found among the four groups (**Figure 5D**). In addition, after treatment with FPS or RAP for 4 weeks, the increased level of UAlb in these DKD model rats was significantly decreased in the FPS and RAP group rats when compared to the Vehicle group rats (**Figure 5F**).

Taken together, the above results showed that FPS and RAP could significantly reduce inflammatory podocyte injury in the DKD model rats.

FPS and RAP Attenuate Podocyte Pyroptosis *In Vivo* and *In Vitro*

GSDMD is a universal substrate for inflammatory caspases that play a specific role in inflammatory caspase-initiated pyroptosis (Humphries et al., 2020). As a downstream effector of multiple inflammasomes, GSDMD is hydrolyzed by activated inflammatory

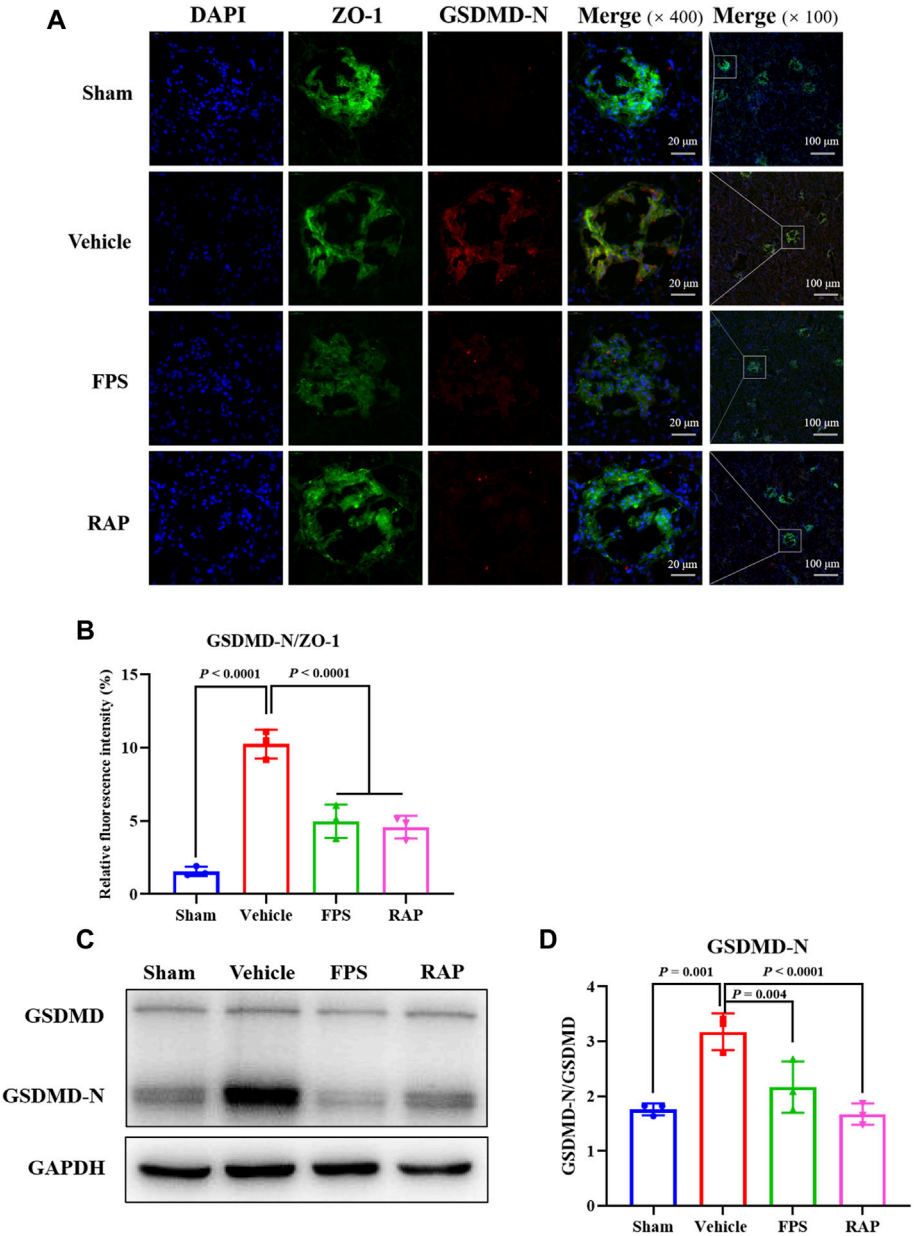

FIGURE 7 | Effects of FPS and RAP on podocyte pyroptosis *in vivo*. **(A)** The immunofluorescent co-localization of ZO-1 and GSDMD-N in glomeruli. Nuclei counterstained with DAPI. Scale bar = 20 and 100 μm. **(B)** The relative fluorescence intensity of GSDMD-N/ZO-1. **(C)** The WB analysis of GSDMD and GSDMD-N in the diabetic kidneys. **(D)** The rate of GSDMD-N to GSDMD. The data are expressed as the mean ± SD.

caspases, and the released N-terminus of GSDMD (GSDMD-N) translocates to the cell membrane (Xie et al., 2019; Zhu et al., 2020). On the other hand, ZO-1 is a specific scaffolding marker of podocytes (Rincon-Choles et al., 2006). Therefore, we used immunofluorescence co-localization and semi-quantitative analysis to observe whether pyroptosis could occur in podocytes treated with FPS and RAP in glomeruli. In **Figure 7A**, GSDMD-N mainly co-localized with ZO-1 in glomeruli, indicating that pyroptosis occurred in podocytes. Compared with the Sham group rats, the relative fluorescence intensity of GSDMD-N in podocytes in the Vehicle group rats was significantly stronger. After treatment with FPS or RAP, the increased fluorescence intensity of GSDMD-N in glomeruli of these DKD model rats was significantly decreased in the FPS and RAP group rats, respectively (**Figure 7B**). On the contrary, the fluorescence intensity of ZO-1 at the same position in glomeruli of the Vehicle, FPS, and RAP group rats appeared the inverse changes, respectively. Accordingly, as shown in **Figure 7C**, we also found that, after treatment with FPS or RAP, the increased protein expression level of GSDMD-N in the kidneys of these DKD model rats was significantly decreased in the FPS and RAP group rats compared to the Vehicle group rats

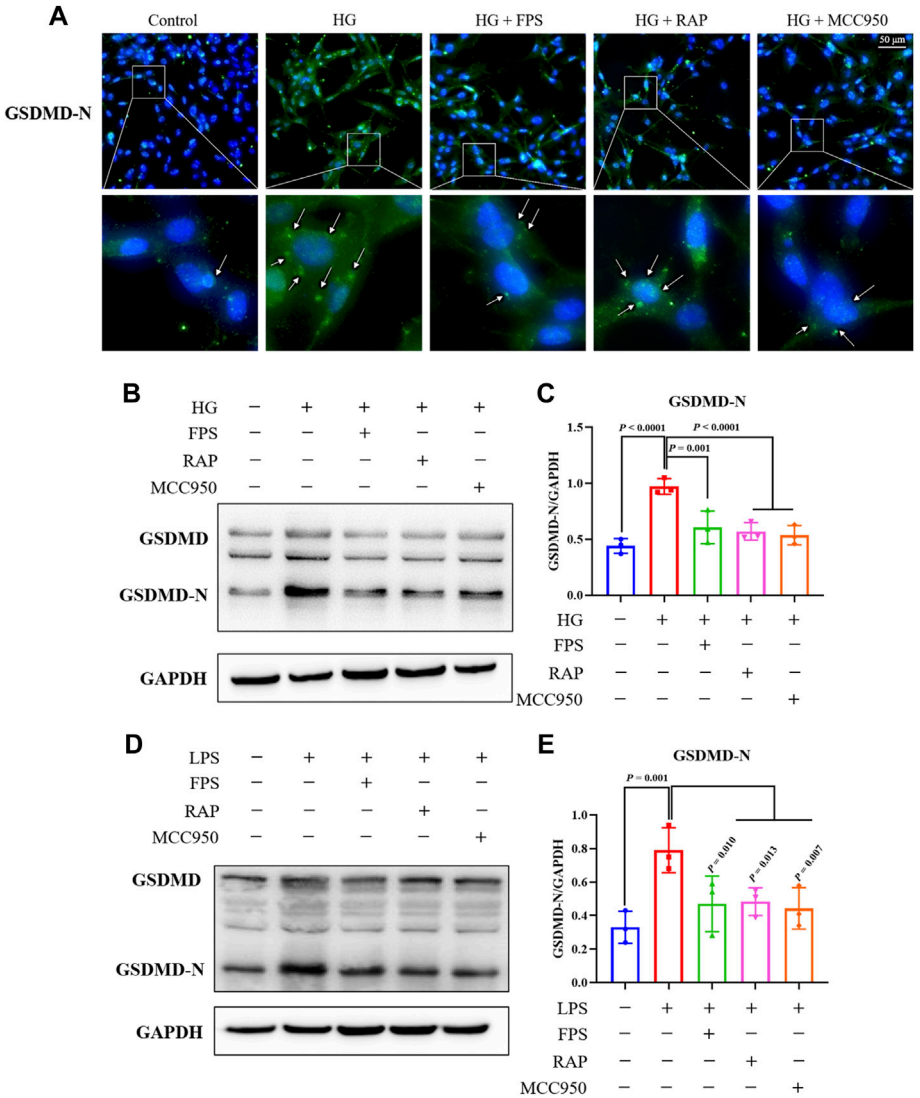

FIGURE 8 | Effects of FPS and RAP on podocyte pyroptosis *in vitro*. **(A)** Immunofluorescent labeling with GSDMD-N. Nuclei counterstained with DAPI. In the locally enlarged lower panel, the arrow shows that GSDMD-N relocated to the cell membrane (×400). Scale bar = 50 μm. **(B)** The WB analysis of GSDMD and GSDMD-N in MPC-5 cells exposed to HG with or without FPS or RAP for 24 h; **(C)** The rate of GSDMD-N to GSDMD. **(D)** The WB analysis of GSDMD and GSDMD-N in MPC-5 cells exposed to LPS with or without FPS or RAP or MCC950 for 24 h; **(E)** The rate of GSDMD-N to GSDMD. The data are expressed as the mean ± SD.

(**Figure 7D**). Here, there was no significant changes in the protein expression level of GSDMD in the kidneys among the four groups.

To investigate whether FPS or RAP could reduce podocyte pyroptosis *in vitro*, we examined immunofluorescence staining of GSDMD-N and the protein expression levels of GSDMD and GSDMD-N in podocytes exposed to HG with or without FPS or RAP for 24 h. Prior to the formal cellular experiments, we determined the cytotoxicity of FPS or RAP on podocytes using a CCK-8 kit. As shown in **Supplementary Figure S2**, we found that the cellular viability of podocytes was significantly reduced when treated with higher concentrations of FPS (25 μg/ml) and RAP (25 nmol/L) when compared to a 20 μg/ml dose of FPS and a 20 nmol/L dose of RAP. According to these results, we selected the safe and effective doses for both FPS (20 μg/ml) and RAP (20 nmol/L). **Figure 8A** shows that GSDMD-N staining positive podocytes were tagged with the most powerful fluorescence at the cell membrane of the HG-treated alone group when compared to the other groups including the HG + FPS-treated group, the HG + RAP-treated group, and the HG + MCC950 (an NLRP3 inhibitor)-treated group. In addition, the protein expression level of GSDMD-N was significantly higher in the podocytes exposed to HG than in the control cells (**Figure 8B**). FPS or RAP treatment significantly ameliorated these changes in the podocytes exposed to HG compared to HG treatment alone. Moreover, we also found an improvement in the protein expression level of GSDMD-N in the podocytes exposed to HG

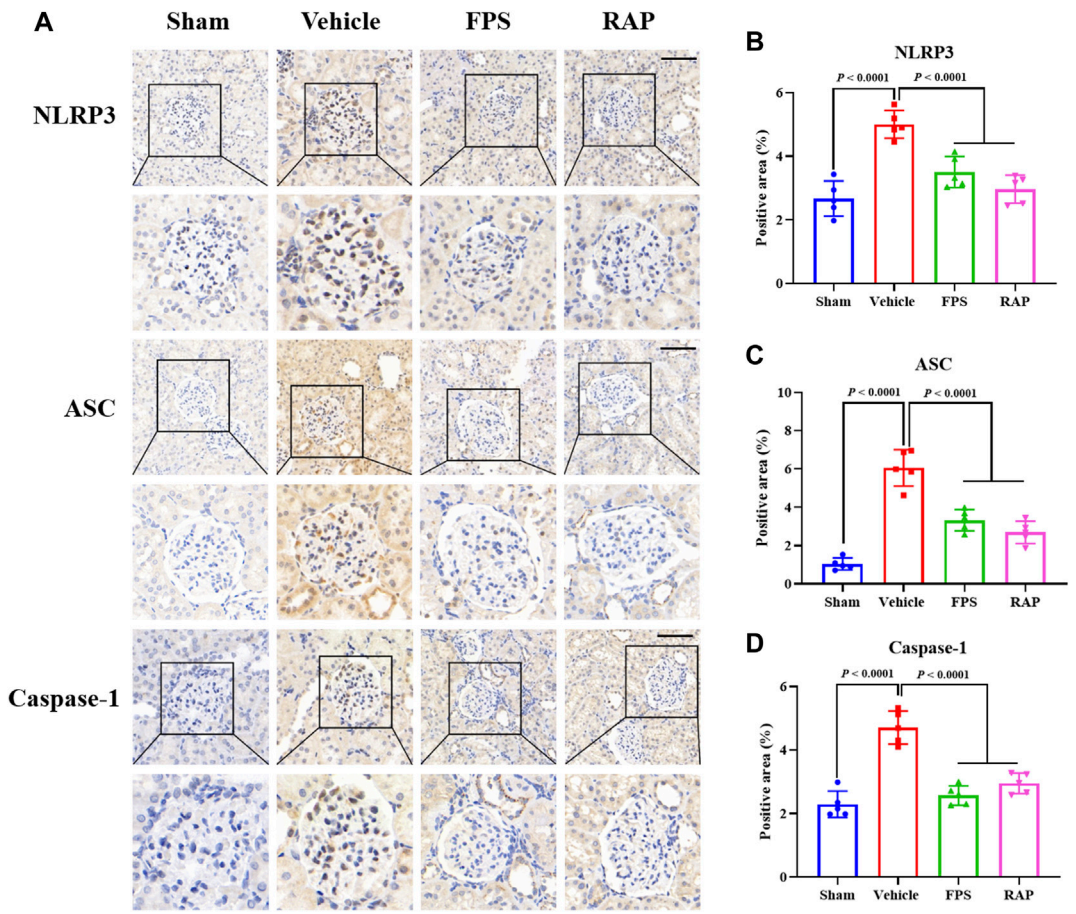

FIGURE 9 | Effects of FPS and RAP on the expression characteristic of NLRP3 inflammasome *in vivo*. **(A)** The immunostaining of NLRP3, ASC, and Caspase-1 in glomeruli (×400). Scale bar = 50 μm. **(B–D)** The positive area of NLRP3, ASC, and Caspase-1, respectively. The data are expressed as the mean ± SD.

and MCC950 when compared to those treated with HG alone (**Figure 8C**). Here, the inhibitory effects of FPS and MCC950 on the protein expression levels of GSDMD-N in podocytes were very similar. Further, to confirm the effects *in vitro* of FPS or RAP on podocyte pyroptosis under a state of inflammation, we also tested the protein expression levels of GSDMD and GSDMD-N in the podocytes exposed to LPS, an inflammatory inducer, with or without FPS or RAP for 24 h. Interestingly, when compared with the podocytes exposed to HG, we got similar results (**Figures 8D,E**).

In short, the above results showed that FPS and RAP could significantly attenuate podocyte pyroptosis *in vivo* and *in vitro*.

FPS and RAP Inhibit NLRP3 Inflammasome Activation *In Vivo* and *In Vitro*

NLRP3 inflammasome activation is an important factor that acts upstream of pyroptosis (Xiong et al., 2020). Thus, we evaluated the expression of NLRP3, ASC, and Caspase-1 as the markers of NLRP3 inflammasome activation in glomeruli and in the kidneys of these DKD model rats by IHC staining and WB analysis. In **Figure 9A**, IHC staining showed that, after treatment with FPS or RAP, the immunostaining of NLRP3, ASC, and Caspase-1 in glomeruli in these DKD model rats were significantly decreased in the FPS and RAP group rats when compared to the Vehicle group rats (**Figures 9B–D**). In addition, in **Figure 10A**, WB analysis showed that changes in the protein expression levels of NLRP3, ASC, and Caspase-1 in the kidneys of the Vehicle, FPS, and RAP group rats were consistent with the above-mentioned results of IHC staining (**Figures 10B–D**).

To confirm whether FPS or RAP could inhibit NLRP3 inflammasome activation *in vitro*, we tested the protein expression levels of NLRP3, ASC, Caspase-1, IL-18, and IL-1β in the podocytes exposed to HG with or without FPS or RAP for 24 h, compared to MCC950. **Figures 11A**, **12A** show that, compared with the control cells, the podocytes exposed to HG exhibited significantly higher protein expression levels of NLRP3, ASC, cleaved-Caspase-1, IL-18, and IL-1β. After treatment with FPS or RAP, the podocytes exposed to HG showed a significant reduction in the protein expression levels of NLRP3, ASC, cleaved-Caspase-1, IL-18, and IL-1β

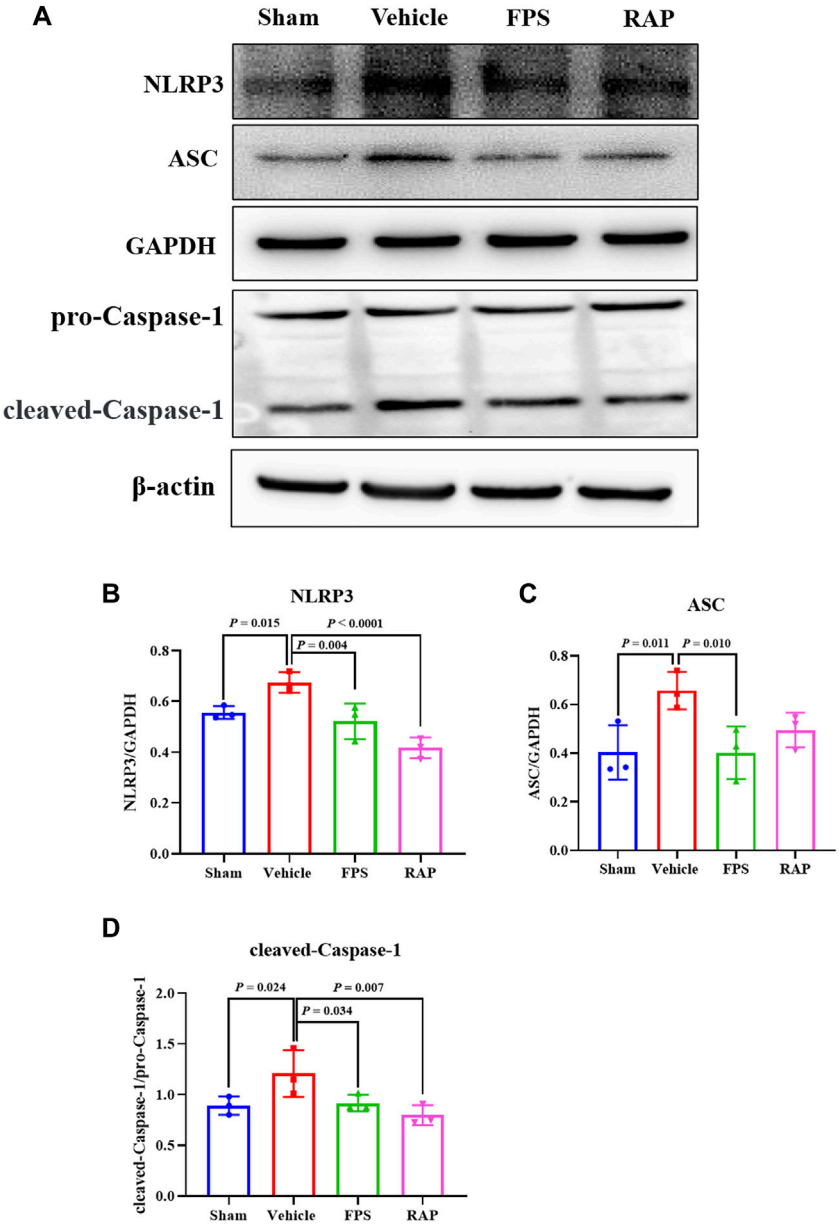

FIGURE 10 | Effects of FPS and RAP on the activation of NLRP3 inflammasome *in vivo*. **(A)** The WB analysis of NLRP3, ASC, pro-Caspase-1, and cleaved-Caspase-1 in the diabetic kidneys. **(B–D)** The rate of NLRP3, ASC, and cleaved-Caspase-1 to GAPDH or pro-Caspase-1, respectively. The data are expressed as the mean ± SD.

when compared to HG treatment alone. In addition, we found a decrease in NLRP3, ASC, cleaved-Caspase-1, IL-18, and IL-1β protein expression levels in the podocytes exposed to HG and MCC950. Here, the inhibitory effects of FPS on NLRP3 inflammasome activation in the podocytes exposed to HG were similar to those in the podocytes treated with MCC950 and HG (**Figures 11B–D**, **12B–C**). Notably, there was no significant changes in the protein expression levels of pro-Caspase-1, pro IL-1β, and pro IL-18 *in vivo* and *in vitro* under the same treatment.

Overall, the above results showed that FPS and RAP could significantly inhibit NLRP3 inflammasome activation *in vivo* and *in vitro*.

FPS and RAP Regulate the AMPK/mTORC1/NLRP3 Signaling Axis *In Vivo* and *In Vitro*

The AMPK/mTORC1/NLRP3 signaling axis is an important regulatory mechanism in NLRP3 inflammasome activation (Bullón et al., 2016; Qiu et al., 2016). Thus, we used WB

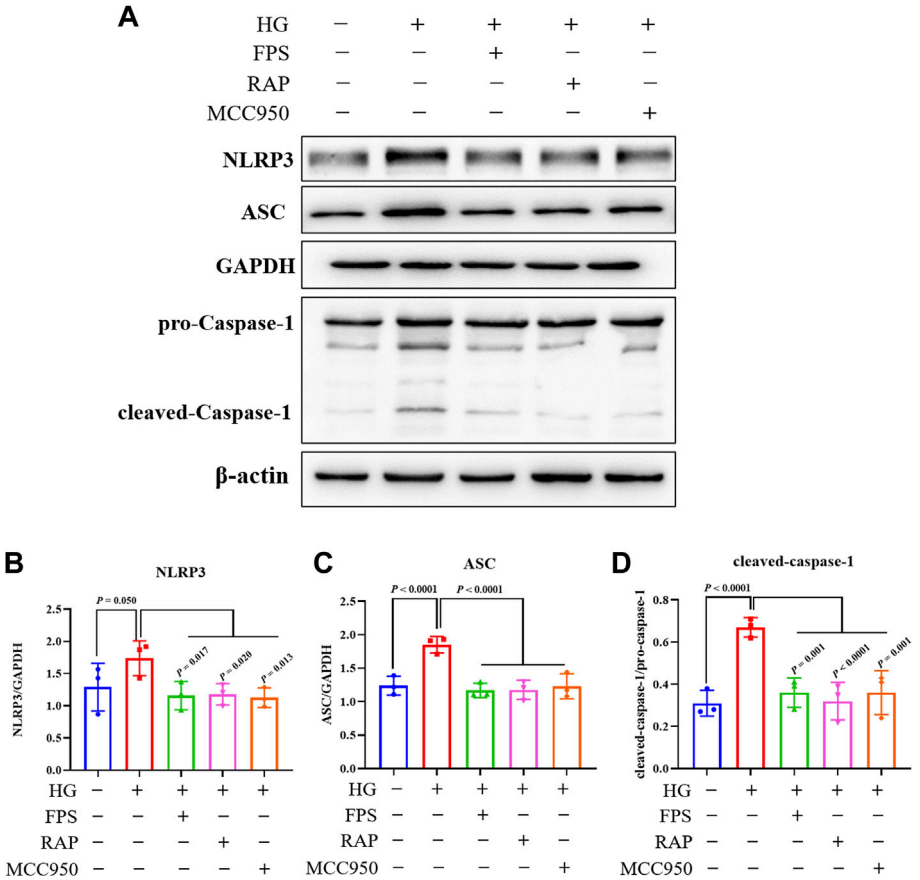

FIGURE 11 | Effects of FPS and RAP on the activation of NLRP3 inflammasome *in vitro*. **(A)** The WB analysis of NLRP3, ASC, pro-Caspase-1, and cleaved-Caspase-1 in MPC-5 cells exposed to HG with or without FPS or RAP or MCC950 for 24 h. **(B–D)** The rate of NLRP3, ASC, and cleaved Caspase-1 to GAPDH or pro-Caspase-1, respectively. The data are expressed as the mean ± SD.

analysis to investigate the protein expression levels of the key signaling molecules of the AMPK/mTORC1/NLRP3 signaling axis in the kidneys of these DKD model rats. **Figure 13A** shows that the protein expression levels of p-AMPK, p-raptor, p-mTORC1, and NLRP3 in the kidneys of the Vehicle group rats were significantly different from those in the Sham group rats. After treatment with FPS or RAP, changes in the protein expression levels of the above-mentioned key signaling molecules in the kidneys of these DKD model rats were significantly improved in the FPS or RAP group rats when compared to the Vehicle group rats (**Figures 13B–E**). Notably, the regulative effects of FPS on the protein expression levels of p-AMPK and p-raptor in the kidneys of the FPS group rats were better than those of the RAP group rats (**Figures 13B,C**).

To determine whether FPS or RAP could regulate the AMPK/mTORC1/NLRP3 signaling axis *in vitro*, we tested the protein expression levels of the key signaling molecules in the AMPK/mTORC1/NLRP3 signaling axis in the podocytes exposed to HG with or without FPS or RAP for 24 h, compared to metformin (an AMPK agonist). **Figure 14A** shows that the protein expression levels of p-AMPK, p-raptor, p-mTORC1, and NLRP3 in the podocytes exposed to HG were significantly different from those in the control cells. In comparison with HG treatment alone, the protein expression levels of p-AMPK, p-raptor, p-mTORC1, and NLRP3 in the podocytes exposed to FPS or RAP were all significantly reversed. In addition, we also found an increase in p-AMPK protein expression level and a decrease in p-raptor, p-mTORC1, and NLRP3 protein expression levels in the podocytes exposed to HG and metformin. Here, notably, the regulative effects of FPS on the protein expression levels of p-AMPK and p-raptor in the podocytes exposed to HG were better than those treated with HG and RAP, and similar to those treated with HG and metformin (**Figures 14B,C**).

In a nutshell, the above results showed that FPS and RAP could significantly regulate the AMPK/mTORC1/NLRP3 signaling axis *in vivo* and *in vitro*.

DISCUSSION

In the progression of DKD, RF is one of the main underlying causes of end-stage kidney disease. Podocyte injury is involved in

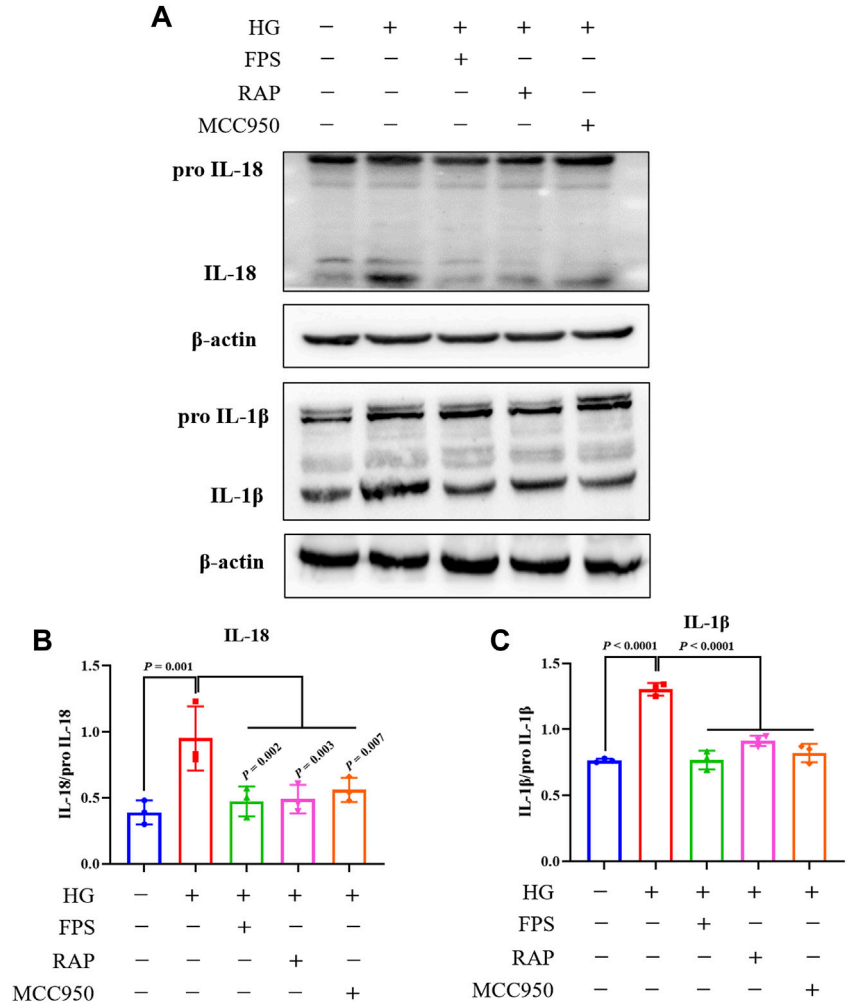

FIGURE 12 | Effects of FPS and RAP on the expression levels of IL-18 and IL-1β *in vitro*. **(A)** The WB analysis of pro IL-18, pro IL-18, pro IL-1β, and IL-1β in MPC-5 cells exposed to HG with or without FPS or RAP or MCC950 for 24 h **(B,C)** The rate of IL-18 and IL-1β to pro IL-18 or pro IL-1β, respectively. The data are expressed as the mean ± SD.

almost all pathological changes in diabetes mellitus (DM)-related glomerular diseases, namely GS (Alicic et al., 2017; Lu et al., 2019). A series of pathological changes in podocyte injury in DKD such as podocyte hypertrophy, EMT, detachment, apoptosis, and autophagy has been conformed, respectively (Zhang et al., 2020). In recent years, emerging evidence has shown that podocyte pyroptosis plays a significant role in the pathological mechanisms of inflammation-derived podocyte injury (Lin et al., 2020). Therefore, in this study, we first attempted to establish a modified DKD rat model accompanied by GS and inflammatory podocyte injury. Our results showed that these modified DKD model rats not only exhibited stable hyperglycemia and abnormal levels of UAlb, Scr, and BUN, but also had typical GS characteristics and podocyte injurious features, especially widened, shortened, and fused foot processes. Furthermore, significant changes in the expression of podocyte injurious markers, such as podocin, CD2AP, nephrin, and nephr1, as well as inflammatory markers, including IL-6 and TLR4, in the kidneys of the DKD model rats were detected. Therefore, we considered that these modified rat models of DKD induced by uninephrectomy, STZ intraperitoneal injection, and a high-fat diet should be helpful in understanding the mechanisms underlying inflammatory podocyte injury-related RF and to identify novel therapeutic targets for RF in DKD.

Previous studies have shown that FPS, as a natural anti-inflammatory phytomedicine, protects the kidney from dysfunction and fibrogenesis by inhibiting the TGF-β pathway and has the potential to slow down the progression of STZ-induced DKD (Chen et al., 2015). Accordingly, in this study, using the modified DKD model rats, we found that FPS and RAP not only reduced glomerular cell proliferation and ECM deposition, but also improved the expression levels of podocin, CD2AP, nephrin, nephr1, IL-6, and TLR4 in diabetic kidneys. In addition, FPS and RAP could inhibit the TGF-β1/Smad2/3 signaling pathway in the kidneys of the DKD model rats. Thus, we concluded that FPS, similar

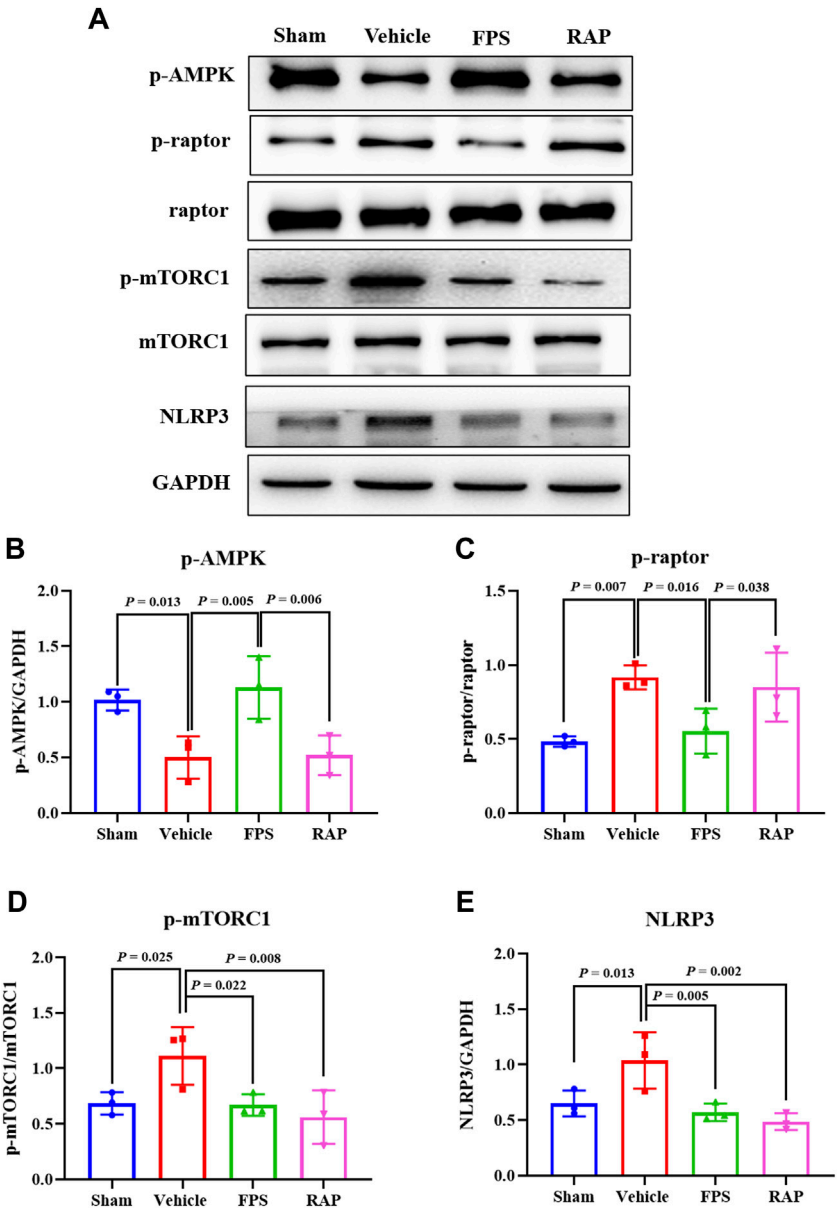

FIGURE 13 | Effects of FPS and RAP on the AMPK/mTORC1/NLRP3 signaling axis *in vivo*. **(A)** The WB analysis of the key signaling molecules in the AMPK/mTORC1/NLRP3 signaling axis in the diabetic kidneys. **(B–E)** The rate of p-AMPK, p-raptor, p-mTORC1, and NLRP3 to GAPDH or raptor or mTORC1, respectively. The data are expressed as the mean ± SD.

to RAP, can alleviate RF and inflammatory podocyte damage *in vivo*, which are the main injurious characteristics of the kidneys in DKD.

Pyroptosis is a newly discovered type of programmed cell death. The essence of pyroptosis is the activation of NLRP3 inflammasome, which mediates GSDMD and rapidly causes cell membrane rupture and cell content release, leading to an inflammatory response (Galluzzi et al., 2012; Galluzzi et al., 2018). In the pyroptosis pathway, GSDMD is cleaved by inflammatory caspases at an aspartate site within the linking loop, thereby generating the GSDMD-C terminal and the active group GSDMD-N terminal (Xie et al., 2019; Zhu et al., 2020). In the progression of DKD, GSDMD-N acts as a perforating protein, forming pores in proper renal cells, gradually triggering cell death, releasing pro-inflammatory factors, such as IL-1β and IL-18, and aggravating RF, including GS and renal tubulointerstitial fibrosis (Gu et al., 2019). In this study, we first examined a range of pyroptosis markers and inflammasome component proteins in diabetic kidneys to investigate whether pyroptosis could occur in podocytes treated with FPS and RAP *in vivo*. Immunofluorescence co-localization and semi-quantitative analysis showed that, after

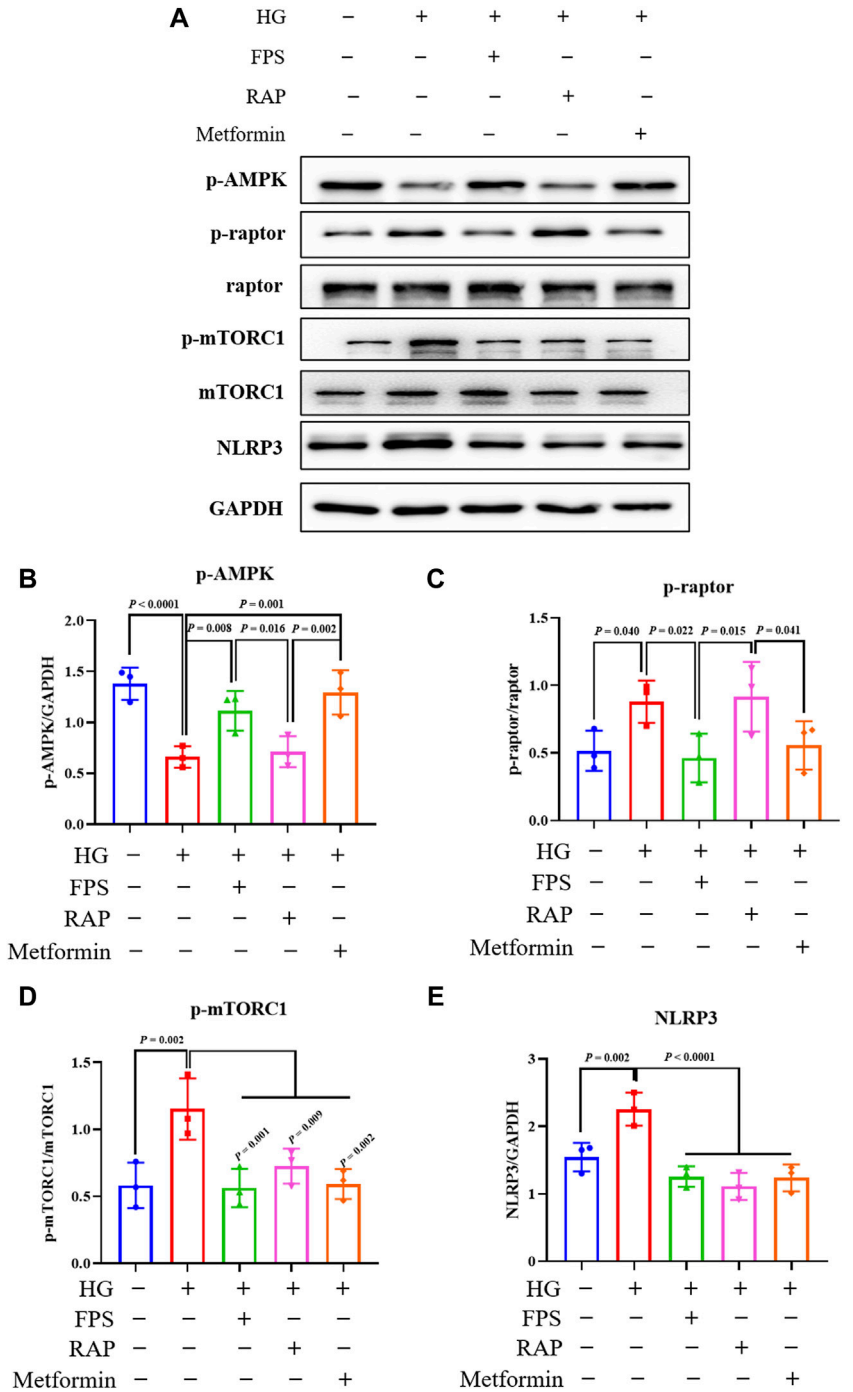

FIGURE 14 | Effects of FPS and RAP on the AMPK/mTORC1/NLRP3 signaling axis *in vitro*. **(A)** The WB analysis of the key signaling molecules in the AMPK/mTORC1/NLRP3 signaling axis in MPC-5 cells exposed to HG with or without FPS or RAP or metformin for 24 h **(B–E)** The rate of p-AMPK, p-raptor, p-mTORC1, and NLRP3 to GAPDH or raptor or mTORC1, respectively. The data are expressed as the mean ± SD.

treatment with FPS or RAP, the relative fluorescence intensity of GSDMD-N in glomeruli and the increased protein expression level of GSDMD-N in the kidneys of the DKD model rats were significantly decreased. Furthermore, in the *in vitro* study, we also found that FPS or RAP treatment significantly reduced the number of GSDMD-N staining positive podocytes and ameliorated the higher protein expression level of GSDMD-N in podocytes exposed to HG, and that the inhibitory effects of FPS and MCC950 (an NLRP3 inflammasome inhibitor) on GSDMD-N *in vitro* were very similar. Therefore, we considered that

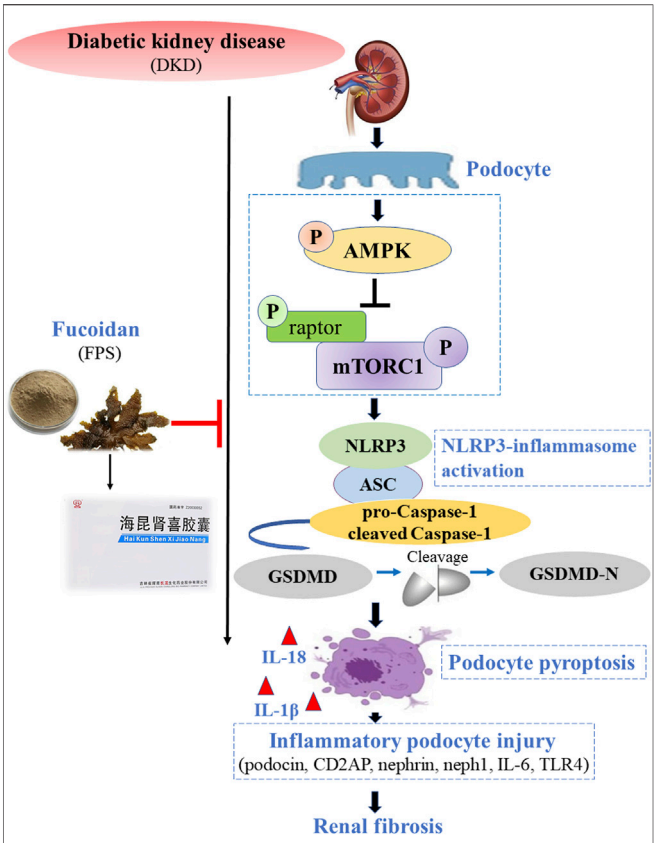

FIGURE 15 | Overview of the effects of FPS on RF in DKD via inhibition of NLRP3 inflammasome-mediated podocyte pyroptosis.

podocyte pyroptosis occurs in glomeruli of the modified DKD rat model, and FPS, similar to RAP, can impart anti-podocyte pyroptosis effects *in vivo* and *in vitro*.

It is well known that a variety of exogenous stimuli can promote NLRP3 inflammasome activation. Two canonical steps were considered to occur. First, microbial molecules or endogenous factors promote the expression of NLRP3, pro IL-1β, and pro IL-18 via the NF-κB signaling pathway (Bauernfeind et al., 2009). Second, these stimuli induce oligomerization and activation of NLRP3 and recruitment of the adapter protein ASC and pro-Caspase-1, the latter of which undergoes autoproteolytic cleavage into Caspase-1 to activate pro IL-1β and pro IL-18 to produce the active cytokines (Martinon et al., 2002; Lamkanfi and Dixit, 2014; Man and Kanneganti, 2015). It has been reported that NLRP3 inflammasome not only mediates inflammatory response but is also related to pyroptosis in RF during DKD progression (Zhang and Wang, 2020). In this study, IHC staining and WB analysis showed that the increased immunostaining of NLRP3, ASC, and Caspase-1 in glomeruli and the higher protein expression levels of NLRP3, ASC, and cleaved-Caspase-1 in the kidneys of the DKD model rats were significantly decreased after treatment with FPS or RAP. Likewise, in the *in vitro* study, we also found that, after treatment with FPS or RAP, the podocytes exposed to HG showed a significant reduction in the protein expression levels of NLRP3, ASC, cleased-Caspase-1, IL-18, and IL-1β. In addition, the inhibitory effects of FPS on NLRP3 inflammasome activation in the podocytes exposed to HG were similar to those in the podocytes treated with MCC950 and HG. Hence, we concluded that NLRP3 inflammasome in the diabetic kidneys of the modified DKD rat model is activated, and FPS, similar to RAP, can inhibit NLRP3 inflammasome activation *in vivo* and *in vitro*.

Previous research has shown that mTOR is widely distributed in renal cortex and medulla of patients with DKD, in which mTORC1 activation plays a key regulatory role in podocyte injury (Lu et al., 2011). In addition, AMPK, an important metabolic stress protein kinase, can be activated by stimulation of numerous hormones, adipokines, and cytokines in DKD (Sanders et al., 2007). Under HG conditions, the phosphorylation level of AMPK decreases and its activation is inhibited. Upstream AMPK inhibits mTORC1 activation and induces autophagy through phosphorus acidification of raptor-related regulatory proteins (Kim et al., 2011). Ding et al. (2010) reported that resveratrol, an AMPK activator, reduces podocyte injury by restoring AMPK activation in STZ-induced diabetic rats. Jin et al. (2017) also reported that berberine reduces HG-induced podocyte damage by enhancing AMPK activation. In this study, our *in vivo* and *in vitro* data clearly indicated that the protein expression levels of p-AMPK, p-raptor, p-mTORC1, and NLRP3 in the kidneys of the DKD model rats and in the cultured podocytes exposed to HG both revealed significant changes. After treatment with FPS or RAP, changes in the protein expression levels of the above-mentioned key signaling molecules *in vivo* and *in vitro* were significantly improved. More importantly, we found that the regulative effects of FPS on p-AMPK and p-raptor *in vivo* and *in vitro* were better than those of RAP. Consequently, we concluded that FPS, in contrast to RAP, can regulate the AMPK/mTORC1/NLRP3 signaling axis *in vivo* and *in vitro*.

Finally, it is important to discuss certain additional points. First, FPS as a natural anti-inflammatory phytomedicine alleviated RF in DKD without affecting hyperglycemia. Second, to exclude the side effects of FPS on the liver, we observed the histological characteristics of liver tissue and biochemical indices of liver function in the DKD model rats after treatment with FPS for 4 weeks. As shown in **Supplementary Figure S3**, we did not find that FPS has any obvious side effects on the liver. Third, it is important to identify the specific targets of FPS that possess the ability to attenuate podocyte pyroptosis. Although FPS was shown to inhibit NLRP3 inflammasome activation and regulate the AMPK/mTORC1/NLRP3 signaling axis *in vivo* and *in vitro*, we were unable to identify the specific molecules involved in the pyroptosis pathway in this study. Future studies should be devoted to the *in vitro* experiments, further clarifying the precise targets of treating podocyte pyroptosis in DKD.

CONCLUSION

In this study, we confirmed that FPS can alleviate RF in DKD in a manner similar to RAP by inhibiting NLRP3 inflammasome-

mediated podocyte pyroptosis via regulation of the AMPK/mTORC1/NLRP3 signaling axis in the diabetic kidney (**Figure 15**). Our findings provide an in-depth understanding of the pathogenesis of RF, which will aid in identifying precise targets that can be used for DKD treatment.

DATA AVAILABILITY STATEMENT

The original contributions presented in the study are included in the article/**Supplementary Material**, further inquiries can be directed to the corresponding authors.

ETHICS STATEMENT

The animal study was reviewed and approved by The animal ethics committee of Nanjing University Medical School.

AUTHOR CONTRIBUTIONS

Y-GW and G-WW conceived and designed this research. M-ZW, D-WC, JW, HL, B-HL, YT, C-CY, Q-JF, J-XC, YF, and B-YW performed the experiments. M-ZW and JW performed the supplementary experiments. M-ZW, D-WC, JW, and Z-YW analyzed and interpreted the data. M-ZW, D-WC, and JW prepared the figures. M-ZW, D-WC, and JW drafted the manuscript. Y-GW and G-WW edited and revised the manuscript. M-ZW, JW, D-WC, and Y-GW approved the final version of the manuscript and all authors approved the final edited version.

FUNDING

This research was supported by the National Natural Science Foundation of China (Grant numbers: 81573903 and 82174472), the Fundamental Research Funds for the Central Universities (Grant number: 021414380518), the Natural Science Foundation of Jiangsu Province (Grant number: BK20211298), the Natural Science Foundation of Jiangsu Province for Young Scholars (Grant number: BK20161046), Jiangsu Provincinal Scientific Research Innovation Fund for post-secondary graduate students (Grant number: KYCX21_1699, KYCX21_1712, KYCX20_1546, SJCX21_0672), and the Nanjing Famous TCM Doctor's Studio Programme (Grant number: No).

ACKNOWLEDGMENTS

The authors thank Professor Jian Yao (Division of Molecular Signaling, Department of Advanced Biomedical Research, Interdisciplinary Graduate School of Medicine and Engineering, University of Yamanashi, Yamanashi, Japan) and Dr. Wei Hu (Department of Pharmacy, Nanjing Drum Tower Hospital, The Affiliated Hospital of Nanjing University Medical School, Nanjing, China) for their helpful discussions and technical assistance.

SUPPLEMENTARY MATERIAL

The Supplementary Material for this article can be found online at: https://www.frontiersin.org/articles/10.3389/fphar.2022.790937/full#supplementary-material

REFERENCES

Alicic, R. Z., Rooney, M. T., and Tuttle, K. R. (2017). Diabetic Kidney Disease: Challenges, Progress, and Possibilities. *Clin. J. Am. Soc. Nephrol.* 12, 2032–2045. doi:10.2215/CJN.11491116

Bauernfeind, F. G., Horvath, G., Stutz, A., Alnemri, E. S., MacDonald, K., Speert, D., et al. (2009). Cutting Edge: NF-kappaB Activating Pattern Recognition and Cytokine Receptors License NLRP3 Inflammasome Activation by Regulating NLRP3 Expression. *J. Immunol.* 183, 787–791. doi:10.4049/jimmunol.0901363

Birnbaum, Y., Bajaj, M., Yang, H. C., and Ye, Y. (2018). Combined SGLT2 and DPP4 Inhibition Reduces the Activation of the Nlrp3/ASC Inflammasome and Attenuates the Development of Diabetic Nephropathy in Mice with Type 2 Diabetes. *Cardiovasc. Drugs Ther.* 32, 135–145. doi:10.1007/s10557-018-6778-x

Bullón, P., Alcocer-Gómez, E., Carrión, A. M., Marín-Aguilar, F., Garrido-Maraver, J., Román-Malo, L., et al. (2016). AMPK Phosphorylation Modulates Pain by Activation of NLRP3 Inflammasome. *Antioxid. Redox Signal.* 24, 157–170. doi:10.1089/ars.2014.6120

Chen, J., Cui, W., Zhang, Q., Jia, Y., Sun, Y., Weng, L., et al. (2015). Low Molecular Weight Fucoidan Ameliorates Diabetic Nephropathy Via Inhibiting Epithelial-Mesenchymal Transition and Fibrotic Processes. *Am. J. Transl. Res.* 7, 1553–1563.

Cooper, M., and Warren, A. M. (2019). A Promising Outlook for Diabetic Kidney Disease. *Nat. Rev. Nephrol.* 15, 68–70. doi:10.1038/s41581-018-0092-5

Dai, H., Liu, Q., and Liu, B. (2017). Research Progress on Mechanism of Podocyte Depletion in Diabetic Nephropathy. *J. Diabetes Res.* 2017, 2615286. doi:10.1155/2017/2615286

Ding, D. F., You, N., Wu, X. M., Xu, J. R., Hu, A. P., Ye, X. L., et al. (2010). Resveratrol Attenuates Renal Hypertrophy in Early-Stage Diabetes by Activating AMPK. *Am. J. Nephrol.* 31, 363–374. doi:10.1159/000300388

Fitton, J. H., Stringer, D. N., and Karpiniec, S. S. (2015). Therapies from Fucoidan: An Update. *Mar. Drugs* 13, 5920–5946. doi:10.3390/md13095920

Galluzzi, L., Vitale, I., Aaronson, S. A., Abrams, J. M., Adam, D., Agostinis, P., et al. (2018). Molecular Mechanisms of Cell Death: Recommendations of the Nomenclature Committee on Cell Death 2018. *Cell Death Differ* 25, 486–541. doi:10.1038/s41418-017-0012-4

Galluzzi, L., Vitale, I., Abrams, J. M., Alnemri, E. S., Baehrecke, E. H., Blagosklonny, M. V., et al. (2012). Molecular Definitions of Cell Death Subroutines: Recommendations of the Nomenclature Committee on Cell Death 2012. *Cell Death Differ* 19, 107–120. doi:10.1038/cdd.2011.96

Gu, J., Huang, W., Zhang, W., Zhao, T., Gao, C., Gan, W., et al. (2019). Sodium Butyrate Alleviates High-Glucose-Induced Renal Glomerular Endothelial Cells Damage via Inhibiting Pyroptosis. *Int. Immunopharmacol.* 75, 105832. doi:10.1016/j.intimp.2019.105832

Haas, M. (2009). Alport Syndrome and Thin Glomerular Basement Membrane Nephropathy: a Practical Approach to Diagnosis. *Arch. Pathol. Lab. Med.* 133, 224–232. doi:10.1043/1543-2165-133.2.224

Han, W., Ma, Q., Liu, Y., Wu, W., Tu, Y., Huang, L., et al. (2019). Huangkui Capsule Alleviates Renal Tubular Epithelial-Mesenchymal Transition in Diabetic Nephropathy via Inhibiting NLRP3 Inflammasome Activation and TLR4/NF-Kb Signaling. *Phytomedicine* 57, 203–214. doi:10.1016/j.phymed.2018.12.021

He, W. T., Wan, H., Hu, L., Chen, P., Wang, X., Huang, Z., et al. (2015). Gasdermin D Is an Executor of Pyroptosis and Required for Interleukin-1β Secretion. *Cell Res* 25, 1285–1298. doi:10.1038/cr.2015.139

Humphries, F., Shmuel-Galia, L., Ketelut-Carneiro, N., Li, S., Wang, B., Nemmara, V. V., et al. (2020). Succination Inactivates Gasdermin D and Blocks Pyroptosis. *Science* 369, 1633–1637. doi:10.1126/science.abb9818

Jin, Y., Liu, S., Ma, Q., Xiao, D., and Chen, L. (2017). Berberine Enhances the AMPK Activation and Autophagy and Mitigates High Glucose-Induced Apoptosis of Mouse Podocytes. *Eur. J. Pharmacol.* 794, 106–114. doi:10.1016/j.ejphar.2016.11.037

Kim, J., Kundu, M., Viollet, B., and Guan, K. L. (2011). AMPK and mTOR Regulate Autophagy through Direct Phosphorylation of Ulk1. *Nat. Cell Biol.* 13, 132–141. doi:10.1038/ncb2152

Lamkanfi, M., and Dixit, V. M. (2014). Mechanisms and Functions of Inflammasomes. *Cell* 157, 1013–1022. doi:10.1016/j.cell.2014.04.007

Lin, J., Cheng, A., Cheng, K., Deng, Q., Zhang, S., Lan, Z., et al. (2020). New Insights into the Mechanisms of Pyroptosis and Implications for Diabetic Kidney Disease. *Int. J. Mol. Sci.* 21, 7057. doi:10.3390/ijms21197057

Liu, B. H., Chong, F. L., Yuan, C. C., Liu, Y. L., Yang, H. M., Wang, W. W., et al. (2021a). Fucoidan Ameliorates Renal Injury-Related Calcium-Phosphorus Metabolic Disorder and Bone Abnormality in the CKD-MBD Model Rats by Targeting FGF23-Klotho Signaling Axis. *Front. Pharmacol.* 11, 586725. doi:10.3389/fphar.2020.586725

Liu, B. H., Tu, Y., Ni, G. X., Yan, J., Yue, L., Li, Z. L., et al. (2021b). Total Flavones of Abelmoschus Manihot Ameliorates Podocyte Pyroptosis and Injury in High Glucose Conditions by Targeting METTL3-dependent m6A Modification-Mediated NLRP3-Inflammasome Activation and PTEN/PI3K/Akt Signaling. *Front. Pharmacol.* 12, 667644. doi:10.3389/fphar.2021.667644

Liu, X., Zhang, Z., Ruan, J., Pan, Y., Magupalli, V. G., Wu, H., et al. (2016). Inflammasome-activated Gasdermin D Causes Pyroptosis by Forming Membrane Pores. *Nature* 535, 153–158. doi:10.1038/nature18629

Liu, Y., Shi, G., Yee, H., Wang, W., Han, W., Liu, B., et al. (2019). Shenkang Injection, a Modern Preparation of Chinese Patent Medicine, Diminishes Tubulointerstitial Fibrosis in Obstructive Nephropathy via Targeting Pericyte-Myofibroblast Transition. *Am. J. Transl. Res.* 11, 1980–1996. PMID: 31105812.

Lu, C. C., Wang, G. H., Lu, J., Chen, P. P., Zhang, Y., Hu, Z. B., et al. (2019). Role of Podocyte Injury in Glomerulosclerosis. *Adv. Exp. Med. Biol.* 1165, 195–232. doi:10.1007/978-981-13-8871-2_10

Lu, M. K., Gong, X. G., and Guan, K. L. (2011). mTOR in Podocyte Function: Is Rapamycin Good for Diabetic Nephropathy? *Cell Cycle* 10, 3415–3416. doi:10.4161/cc.10.20.17686

Man, S. M., and Kanneganti, T. D. (2015). Regulation of Inflammasome Activation. *Immunol. Rev.* 265, 6–21. doi:10.1111/imr.12296

Mao, Z. M., Shen, S. M., Wan, Y. G., Sun, W., Chen, H. L., Huang, M. M., et al. (2015). Huangkui Capsule Attenuates Renal Fibrosis in Diabetic Nephropathy Rats through Regulating Oxidative Stress and p38MAPK/Akt Pathways, Compared to α-lipoic Acid. *J. Ethnopharmacol.* 173, 256–265. doi:10.1016/j.jep.2015.07.036

Martinon, F., Burns, K., and Tschopp, J. (2002). The Inflammasome: a Molecular Platform Triggering Activation of Inflammatory Caspases and Processing of proIL-Beta. *Mol. Cell* 10, 417–426. doi:10.1016/s1097-2765(02)00599-3

Paik, S., Kim, J. K., Silwal, P., Sasakawa, C., and Jo, E. K. (2021). An Update on the Regulatory Mechanisms of NLRP3 Inflammasome Activation. *Cell Mol. Immunol.* 18, 1141–1160. doi:10.1038/s41423-021-00670-3

Qiu, J., Wang, M., Zhang, J., Cai, Q., Lu, D., Li, Y., et al. (2016). The Neuroprotection of Sinomenine against Ischemic Stroke in Mice by Suppressing NLRP3 Inflammasome via AMPK Signaling. *Int. Immunopharmacol.* 40, 492–500. doi:10.1016/j.intimp.2016.09.024

Rincon-Choles, H., Vasylyeva, T. L., Pergola, P. E., Bhandari, B., Bhandari, K., Zhang, J. H., et al. (2006). ZO-1 Expression and Phosphorylation in Diabetic Nephropathy. *Diabetes* 55, 894–900. doi:10.2337/diabetes.55.04.06.db05-0355

Sanders, M. J., Grondin, P. O., Hegarty, B. D., Snowden, M. A., and Carling, D. (2007). Investigating the Mechanism for AMP Activation of the AMP-Activated Protein Kinase cascade. *Biochem. J.* 403, 139–148. doi:10.1042/BJ20061520

Shi, J., Zhao, Y., Wang, K., Shi, X., Wang, Y., Huang, H., et al. (2015). Cleavage of GSDMD by Inflammatory Caspases Determines Pyroptotic Cell Death. *Nature* 526, 660–665. doi:10.1038/nature15514

Tu, Y., Fang, Q. J., Sun, W., Liu, B. H., Liu, Y. L., Wu, W., et al. (2020). Total Flavones of Abelmoschus Manihot Remodels Gut Microbiota and Inhibits Microinflammation in Chronic Renal Failure Progression by Targeting Autophagy-Mediated Macrophage Polarization. *Front. Pharmacol.* 11, 566611. doi:10.3389/fphar.2020.566611

van Weelden, G., Bobiński, M., Okła, K., van Weelden, W. J., Romano, A., and Pijnenborg, J. M. A. (2019). Fucoidan Structure and Activity in Relation to Anti-cancer Mechanisms. *Mar. Drugs* 17, 32. doi:10.3390/md17010032

Wang, J., Geng, L., Yue, Y., and Zhang, Q. (2019). Use of Fucoidan to Treat Renal Diseases: A Review of 15 Years of Clinic Studies. *Prog. Mol. Biol. Transl. Sci.* 163, 95–111. doi:10.1016/bs.pmbts.2019.03.011

Wang, W. W., Liu, Y. L., Wang, M. Z., Li, H., Liu, B. H., Tu, Y., et al. (2021). Inhibition of Renal Tubular Epithelial Mesenchymal Transition and Endoplasmic Reticulum Stress-Induced Apoptosis with Shenkang Injection Attenuates Diabetic Tubulopathy. *Front. Pharmacol.* 12, 662706. doi:10.3389/fphar.2021.662706

Wu, W., Hu, W., Han, W. B., Liu, Y. L., Tu, Y., Yang, H. M., et al. (2018). Inhibition of Akt/mTOR/p70S6K Signaling Activity with Huangkui Capsule Alleviates the Early Glomerular Pathological Changes in Diabetic Nephropathy. *Front. Pharmacol.* 9, 443. doi:10.3389/fphar.2018.00443

Wu, W., Yang, J. J., Yang, H. M., Huang, M. M., Fang, Q. J., Shi, G., et al. (2017). Multi-glycoside of Tripterygium Wilfordii Hook. F. Attenuates Glomerulosclerosis in a Rat Model of Diabetic Nephropathy by Exerting Anti-microinflammatory Effects without Affecting Hyperglycemia. *Int. J. Mol. Med.* 40, 721–730. doi:10.3892/ijmm.2017.3068

Xie, C., Wu, W., Tang, A., Luo, N., and Tan, Y. (2019). lncRNA GAS5/miR-452-5p Reduces Oxidative Stress and Pyroptosis of High-Glucose-Stimulated Renal Tubular Cells. *Diabetes Metab. Syndr. Obes.* 12, 2609–2617. doi:10.2147/DMSO.S228654

Xiong, W., Meng, X. F., and Zhang, C. (2020). Inflammasome Activation in Podocytes: a New Mechanism of Glomerular Diseases. *Inflamm. Res.* 69, 731–743. doi:10.1007/s00011-020-01354-w

Xiong, W., Meng, X. F., and Zhang, C. (2021). NLRP3 Inflammasome in Metabolic-Associated Kidney Diseases: An Update. *Front. Immunol.* 12, 714340. doi:10.3389/fimmu.2021.714340

Yang, F., Qin, Y., Wang, Y., Meng, S., Xian, H., Che, H., et al. (2019). Metformin Inhibits the NLRP3 Inflammasome via AMPK/mTOR-dependent Effects in Diabetic Cardiomyopathy. *Int. J. Biol. Sci.* 15, 1010–1019. doi:10.7150/ijbs.29680

Yu, Z. W., Zhang, J., Li, X., Wang, Y., Fu, Y. H., and Gao, X. Y. (2020). A New Research Hot Spot: The Role of NLRP3 Inflammasome Activation, a Key Step in Pyroptosis, in Diabetes and Diabetic Complications. *Life Sci.* 240, 117138. doi:10.1016/j.lfs.2019.117138

Zhang, H., and Wang, Z. (2020). Effect and Regulation of the NLRP3 Inflammasome during Renal Fibrosis. *Front Cell Dev Biol* 7, 379. doi:10.3389/fcell.2019.00379

Zhang, L., Wen, Z., Han, L., Zheng, Y., Wei, Y., Wang, X., et al. (2020). Research Progress on the Pathological Mechanisms of Podocytes in Diabetic Nephropathy. *J. Diabetes Res.* 2020, 7504798. doi:10.1155/2020/7504798

Zhang, Q., Sun, J., Wang, Y., He, W., Wang, L., Zheng, Y., et al. (2017). Antimycobacterial and Anti-inflammatory Mechanisms of Baicalin via Induced Autophagy in Macrophages Infected with *Mycobacterium tuberculosis*. *Front. Microbiol.* 8, 2142. doi:10.3389/fmicb.2017.02142

Zhu, B., Cheng, X., Jiang, Y., Cheng, M., Chen, L., Bao, J., et al. (2020). Silencing of KCNQ1OT1 Decreases Oxidative Stress and Pyroptosis of Renal Tubular Epithelial Cells. *Diabetes Metab. Syndr. Obes.* 13, 365–375. doi:10.2147/DMSO.S225791

Conflict of Interest: G-WW was employed by the company Jilin Province Huinan Chonglong Bio Pharmacy Co., Ltd.

The remaining authors declare that the research was conducted in the absence of any commercial or financial relationships that could be construed as a potential conflict of interest.

GLOSSARY

ALT alanine transaminase

AMPK adenosine monophosphate-activated protein kinase

ASC C-terminal caspase recruitment domain

AST aspartate transaminase

BG blood glucose

BUN blood urea nitrogen

BW body weight

collagen I collagen type I

DKD diabetic kidney disease

ECM extracelluar matrix

FN fibronectin

FPS Fucoidan

GBM glomerular basement membrane

GCP glomerular celluar population

GS glomerular sclerosis

GSDMD gasdermin D

GSDMD-N Nterminus of GSDMD

GAPDH glyceraldehyde-3-phosphate dehydrogenase

HG high glucose

HRP horse radish peroxidase

IHC immunohistochemistry

IL interleukin

IPP Image-Pro Plus

LPS lipopolysaccharide

mTOR mammalian target of rapamycin

mTORC1 mTOR complex 1

NLRP3 nucleotide-binding oligomerization domain (Nod)-like receptor family pyrin domain-containing 3

p-AMPK phosphorylated AMPK

PAS Periodic acid-Schiff

p-mTOR phosphorylated mTOR

p-raptor phosphorylated raptor

RAP Rapamycin

RF renal fibrosis

Scr serum creatinine

STZ Streptozotocin

TGF-β1 transforming growth factor-β1

TSA tyramide signal amplification

UAlb 24 h urinary albumin

WB Western blotting

frontiers in Pharmacology

ORIGINAL RESEARCH
published: 21 March 2022
doi: 10.3389/fphar.2022.794139

Potential Therapeutic Targets of Rehmannia Formulations on Diabetic Nephropathy: A Comparative Network Pharmacology Analysis

Kam Wa Chan†, Kam Yan Yu, Wai Han Yiu, Rui Xue, Sarah Wing-yan Lok, Hongyu Li, Yixin Zou, Jinyuan Ma, Kar Neng Lai and Sydney Chi-wai Tang†*

Department of Medicine, The University of Hong Kong, Hong Kong SAR, China

OPEN ACCESS

Edited by:
Dan-Qian Chen,
Northwest University, China

Reviewed by:
Nicolas Roberto Robles,
University of Salamanca, Spain
Shao-Yu Yang,
National Taiwan University Hospital, Taiwan

****Correspondence:***
Sydney Chi-wai Tang
scwtang@hku.hk

†ORCID:
Kam Wa Chan
orcid.org/0000-0002-3175-1574
Sydney Chi-wai Tang
orcid.org/0000-0002-6862-1941

Specialty section:
This article was submitted to Renal Pharmacology, a section of the journal Frontiers in Pharmacology

Received: *01 November 2021*
Accepted: *10 February 2022*
Published: *21 March 2022*

Citation:
Chan KW, Yu KY, Yiu WH, Xue R, Lok SW-y, Li H, Zou Y, Ma J, Lai KN and Tang SC-w (2022) Potential Therapeutic Targets of Rehmannia Formulations on Diabetic Nephropathy: A Comparative Network Pharmacology Analysis. Front. Pharmacol. 13:794139. doi: 10.3389/fphar.2022.794139

Background: Previous retrospective cohorts showed that Rehmannia-6 (R-6, Liu-wei-di-huang-wan) formulations were associated with significant kidney function preservation and mortality reduction among chronic kidney disease patients with diabetes. This study aimed to investigate the potential mechanism of action of common R-6 variations in a clinical protocol for diabetic nephropathy (DN) from a system pharmacology approach.

Study Design and Methods: Disease-related genes were retrieved from GeneCards and OMIM by searching "Diabetic Nephropathy" and "Macroalbuminuria". Variations of R-6 were identified from a published existing clinical practice guideline developed from expert consensus and pilot clinical service program. The chemical compound IDs of each herb were retrieved from TCM-Mesh and PubChem. Drug targets were subsequently revealed via PharmaMapper and UniProtKB. The disease gene interactions were assessed through STRING, and disease–drug protein–protein interaction network was integrated and visualized by Cytoscape. Clusters of disease–drug protein–protein interaction were constructed by Molecular Complex Detection (MCODE) extension. Functional annotation of clusters was analyzed by DAVID and KEGG pathway enrichment. Differences among variations of R-6 were compared. Binding was verified by molecular docking with AutoDock.

Results: Three hundred fifty-eight genes related to DN were identified, forming 11 clusters which corresponded to complement and coagulation cascades and signaling pathways of adipocytokine, TNF, HIF-1, and AMPK. Five variations of R-6 were analyzed. Common putative targets of the R-6 variations on DN included ACE, APOE, CCL2, CRP, EDN1, FN1, HGF, ICAM1, IL10, IL1B, IL6, INS, LEP, MMP9, PTGS2, SERPINE1, and TNF, which are related to regulation of nitric oxide biosynthesis, lipid storage, cellular response to lipopolysaccharide, inflammatory response, NF-kappa B transcription factor activity, smooth muscle cell proliferation, blood pressure, cellular response to interleukin-1, angiogenesis, cell proliferation, peptidyl-tyrosine phosphorylation, and protein kinase B signaling. TNF was identified as the seed for the most significant cluster of all R-6 variations. Targets specific to each formulation were identified. The key chemical compounds of R-6 have good binding ability to the putative protein targets.

Conclusion: The mechanism of action of R-6 on DN is mostly related to the TNF signaling pathway as a core mechanism, involving amelioration of angiogenesis, fibrosis, inflammation, disease susceptibility, and oxidative stress. The putative targets identified could be validated through clinical trials.

Keywords: integrative medicine, traditional Chinese medicine, diabetic nephropathy, chronic kidney disease, Rehmannia, mechanism, network pharmacology, TNF

INTRODUCTION

In 2021, 10.5% of the world population were diabetic, with a rising trend (Sun et al., 2021). Of the diabetic patients, 25%–40% develop nephropathy from long-standing diabetes, characterized by glomerular basement membrane thickening, foot process effacement, mesangial expansion, glomerulosclerosis, interstitial fibrosis, and the formation of Kimmelstiel-Wilson nodules (Alsaad and Herzenberg, 2007; Alicic et al., 2017). The pathogenesis of diabetic nephropathy (DN) is multifactorial (Tang and Yiu, 2020) involving the complement cascade (Flyvbjerg, 2017; Yiu et al., 2018), metabolic (Forbes et al., 2003; Goh and Cooper, 2008), immunity (Lin et al., 2012; Pichler et al., 2017; Tang and Yiu, 2020), inflammatory, (Navarro-González et al., 2011; Pichler et al., 2017), oxidative stress (Kashihara et al., 2010; Li et al., 2014a; Sagoo and Gnudi, 2018), coagulation (Madhusudhan et al., 2016; Oe et al., 2016), and hemodynamic (Jerums et al., 2010; Premaratne et al., 2015; Alicic et al., 2017; Tonneijck et al., 2017) pathways, ending with renal fibrosis.

Diabetic kidney disease (DKD) is conventionally diagnosed by the presence of albuminuria, reduced kidney function, and clinical history excluding other etiologies (Alicic et al., 2017; Heerspink et al., 2019). Macroalbuminuria signifies established nephropathy and increases the specificity of DKD diagnosis (Furuichi et al., 2018; Persson and Rossing, 2018). The conventional renin–angiotensin–aldosterone system (RAAS) blockade offers limited effect in reducing end-stage kidney failure and mortality (Hsu et al., 2014; Palmer et al., 2015; Chan and Tang, 2018; Nistor et al., 2018). More regimens targeting other mechanisms are needed. DKD leads the cause of end-stage kidney failure in most regions among other types of chronic kidney disease (CKD). Kidney replacement therapy (dialysis or transplantation) is required once end stage is reached, and the accessibility is often limited (Thomas et al., 2016; Tang et al., 2020; Tang and Yiu, 2020).

Previous registry studies showed that individualized Chinese medicine (CM) treatment was associated with slower decline of kidney function and reduced risk of end-stage kidney failure and mortality among patients with CKD and diabetes (Hsieh et al., 2014; Lin et al., 2015; Huang et al., 2018; Chan et al., 2022). CM formulations are prescribed based on symptom-based diagnosis (Chan et al., 2020a; Chan et al., 2020b; Chan et al., 2021a; Chan et al., 2021b; Chan et al., 2021c; Shu et al., 2021), which predicts renal function decline independent of blood pressure, blood glucose, lipids, and urine albumin control (Chan et al., 2021b). The CM used in these cohorts mostly contained a classical CM formulation, namely, Rehmannia-6 complex (R-6, Liu-wei-di-huang-wan) with variations according to the symptom-based diagnosis. R-6 contains *Rehmanniae Radix* (Di-huang) (Yokozawa et al., 2004), *Corni Fructus* (Shan-zhu-yu) (Gao et al., 2021), *Dioscoreae Rhizoma* (Shan-yao) (Luo, 2008), *Poria* (Fu-ling) (Sun, 2014), *Moutan Cortex* (Mu-dan-pi) (Wang et al., 2017b), and *Alismatis Rhizoma* (Ze-xie) (Zhang et al., 2017a). According to classical CM theory, R-6 replenishes the *kidney* and clears the waste including fluid retention.

Unlike single herbal extracts or synthesized chemical compounds, CM formulations are complex, containing multiple chemicals, and therefore exerts systemic effects through orchestrated pathways in real-world practice (Zhang et al., 2019). Traditional *in vivo* and *in vitro* studies focusing on specific mechanisms may have limitations for the assessment of interaction between CM formulations and disease with multifactorial pathophysiology (Li et al., 2014b; Zhang et al., 2019). Network pharmacology offers a whole-system approach to delineate the possible mechanisms underpinning observed clinical effect based on existing *in vivo* and *in vitro* evidence (Hopkins, 2008; Zhang et al., 2019). This systematic and systemic approach could identify the mechanisms and target proteins of each formulation for subsequent validation in clinical trials.

A protocol with five variations of R-6 was formulated based on previous expert consensus and a pilot service program and is undergoing clinical trial (Chan et al., 2016). R-6 was modified based on the phenotypes of patients according to the traditional CM theory. There are limited system pharmacology data regarding the putative mechanism of these R-6 variations on DN. This study aims to investigate the potential mechanism of the therapeutic action of common R-6 variations for DN. We retrieved the genes and potential targets of DN, the chemical compounds of CMs, and the corresponding targets of R-6 through data mining. A drug–disease network was then constructed with pathway analysis to delineate the interaction between R-6 and DN. Through comparing the pathways expected to act on by different R-6 variations, we identified the putative targets of R-6 on DN and the potential differences among different variations.

MATERIALS AND METHODS

Genes and Potential Targets Related to DN

The computational workflow is summarized in **Figure 1**. First, disease-related genes were retrieved from GeneCards (https://www.genecards.org/) (Stelzer et al., 2016) and the Online Mendelian Inheritance in Man (OMIM) (https://www.omim.org/) (Hamosh et al., 2000). GeneCards, operated by The Weizmann Institute of Science and LifeMap Sciences, provides richly annotated disease genetics integrated from over 150 web sources. OMIM provides genotypic and phenotypic information

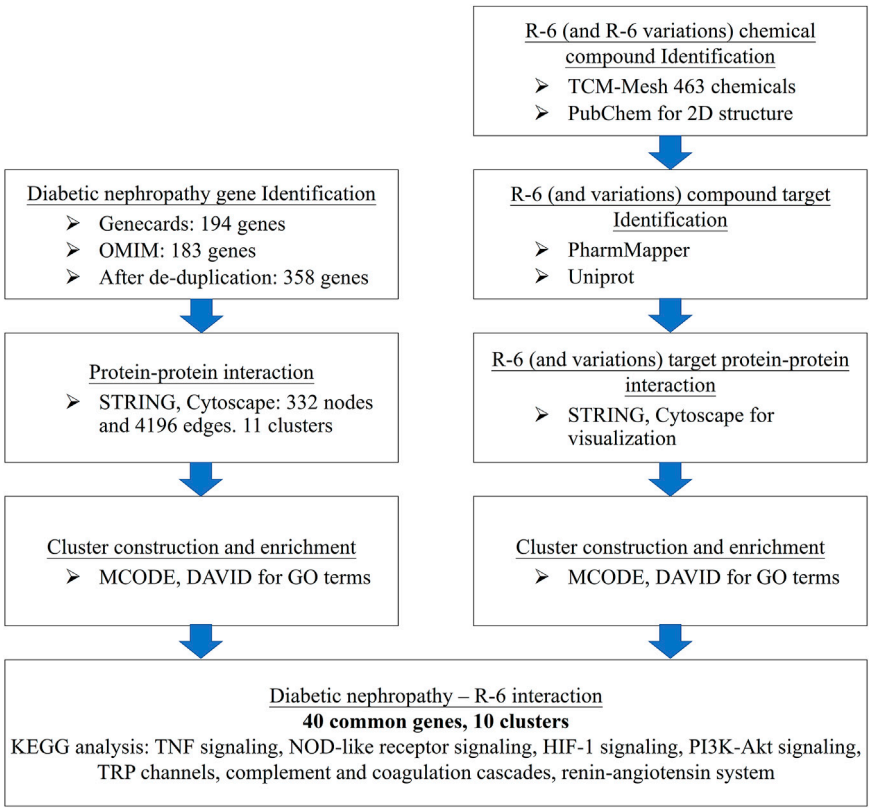

FIGURE 1 | Computational workflow of disease–drug network analysis. Disease-related genes were retrieved from GeneCards and OMIM. The chemical compound IDs of each herb were retrieved from TCM-Mesh and PubChem. Drug targets were revealed via PharmaMapper and UniProtKB. The disease gene interactions were assessed through STRING, and the disease–drug protein–protein interaction network was integrated and visualized by Cytoscape. Functional annotation of clusters was analyzed by DAVID and KEGG pathway enrichment.

on molecular contributions in human genetic disorders. We searched the databases with keywords "Diabetic Nephropathy" and "Macroalbuminuria" as macroalbuminuria signifies the development of nephropathy and increases the specificity of DN (Tang and Yiu, 2020) and is commonly included as a recruitment criterion of diabetic kidney disease-related clinical trials (Heerspink et al., 2019; Perkovic et al., 2019). The genetic datasets from GeneCards and OMIM were integrated for a more comprehensive analysis (**Supplementary Table S1**).

Compounds of R-6 and Their Potential Targets

The variations of R-6 were identified from an existing clinical practice guideline developed based on expert consensus in mainland China (Zhang, 2010; Chan, 2018), which is undergoing a randomized clinical trial for evaluation in Hong Kong (Chan et al., 2016; Chan et al., 2019). The clinical guideline is compatible with the prescription pattern of previously reported big-data studies from Taiwan (Hsieh et al., 2014; Lin et al., 2015; Huang et al., 2018; Guo et al., 2021b) and a pilot service program in Hong Kong (Chan, 2018; Chan et al., 2022).

TCM-Mesh (http://mesh.tcm.microbioinformatics.org/) (Zhang et al., 2019; Zhang et al., 2017b), with data on chemicals, genes, and disease association of more than 6,000 herbs, was used to collect the compound IDs of chemicals in each herb. A total of 463 chemicals were identified including flavonoids, phenolic acids, and alkaloids (**Supplementary Table S2**). Compound IDs were identified by PubChem (https://pubchem.ncbi.nlm.nih.gov/) (Kim et al., 2019), a freely accessible chemistry database maintained by the National Institutes of Health (NIH), where we acquired the 2D structures of each chemical in sdf format files. sdf format files were then imported into an open web server, PharmaMapper (http://www.lilab-ecust.cn/pharmmapper/) (Wang et al., 2017a), to identify human drug targets of chemicals. UniProtKB (https://www.uniprot.org/) (The UniProt Consortium, 2019), a central hub that integrates the functional annotations of proteins, was applied to convert the unstandardized protein naming into the official symbol by selecting "Homo sapiens".

Disease–Drug Network Construction

Both the integrated disease and drug targets were imported into the Search Tool for the Retrieval of Interacting Genes/Proteins (STRING) (https://string-db.org/, version 11.0) (Szklarczyk et al., 2019) to assess and visualize the protein–protein interactions between disease and drug mechanisms at the molecular level to identify potential targets of R-6 on DN. The returned interaction data were expressed with a network visualization software, namely,

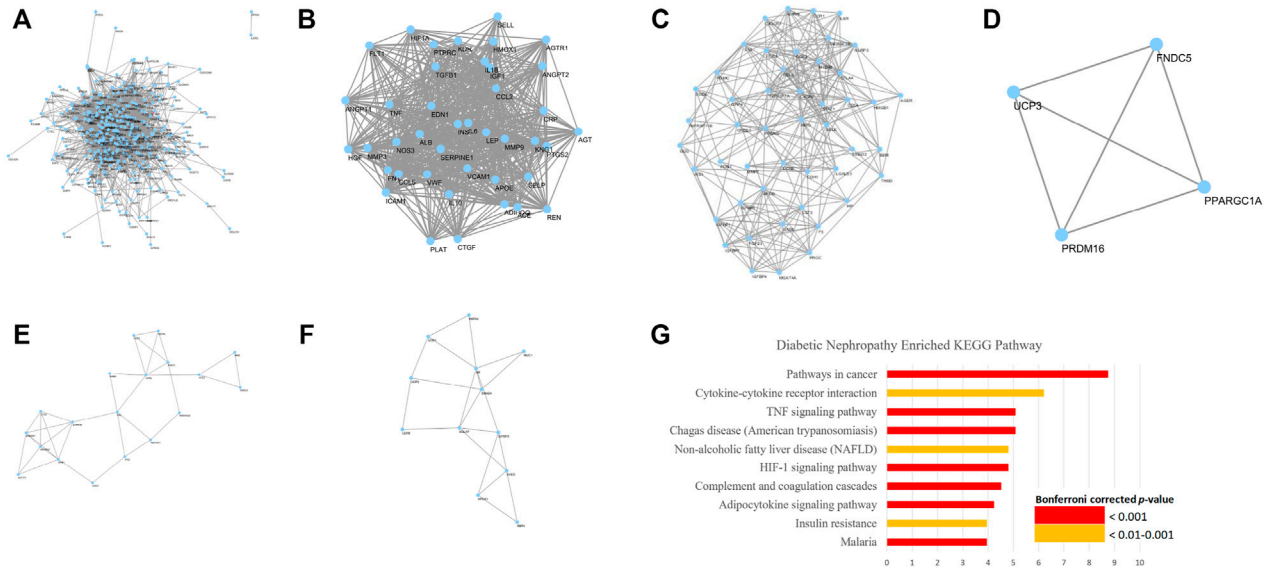

FIGURE 2 | Network and representative clusters of DN. Key pathogenesis of DN includes the complement and coagulation cascades, adipocytokine signaling pathway, TNF signaling pathway, HIF-1 signaling pathway, and AMPK signaling pathway. **(A)** A total of 9,621 pairs of genes were identified from GeneCards and OMIM. **(B–F)** Major Cluster of Genes Related to Diabetic Nephropathy and **(G)** KEGG enrichment analysis on the DN pathogenesis

Cytoscape (http://cytoscape.org/, version 3.7.2) (Shannon et al., 2003), to integrate the complex network of molecular interactions. To explore relevant clusters with extensive protein interactions, we used the Molecular Complex Detection (MCODE), a plug-in of Cytoscape, to identify clusters (densely interconnected regions) in the network. Each cluster represents an independent network of biological mechanisms. The disease, drug, and disease–drug protein–protein interaction networks and clusters were constructed for DN, R-6, and variations of R-6.

Gene Ontology and Pathway Enrichment Analysis

Each cluster returned by MCODE was imported into the Database for Annotation, Visualization and Integrated Discovery (DAVID) (https://david.ncifcrf.gov/summary.jsp, version 6.8) (Huang et al., 2009), a web server which integrates the functional annotations of a large set of genes with reference to disease association, biological pathways from various databases for a more profound understanding of disease pathogenesis, and identification of potential targets for treatment. All functional annotation data were corrected by the Bonferroni method to minimize type 1 error arising from multiple comparisons. All targets of DN and R-6 variations and the top cluster of the disease–gene interaction were further analyzed and compared by the Kyoto Encyclopedia of Genes and Genomes (KEGG) pathway enrichment.

Validation by Molecular Docking

The chemical structure of key compounds of the CMs of R-6 was extracted from PubChem as mol2 files and processed in pdbqt format in AutoDockTools 1.5.6 for binding analysis. The crystal structures of the putative gene/protein targets obtained from the network and pathway analyses were extracted from the RCSB Protein Data Bank (https://www.rcsb.org/). Water molecules and inactive ligands were removed before the proteins were hydrogenated and charged (Guo et al., 2021a). A blind docking strategy was used to screen through each protein for all possible binding sites with a grid size of 126 × 126× 126 points. Free energy of binding (in kcal/mol) were obtained from AutoDock Vina as the indicator of the binding likelihood (Lee et al., 2012; Cournia et al., 2017; Heinzelmann and Gilson, 2021). Negative values of free energy indicate possible binding in simulation. More negative scoring indicates stronger binding affinity.

RESULTS

DN

A total of 358 DN-related genes were obtained from GeneCards and OMIM (**Figure 2A**). The network contains 332 nodes and 4,196 edges. Eleven clusters (**Figures 2B–F**) were identified from the analysis by MCODE. Gene ontology analysis showed that these genes corresponded to 71 ontology terms. The top 20 most significant terms included the response to hypoxia (GO: 0001666), inflammatory response (GO: 0006954), glucose homeostasis (GO: 0042593), response to drug (GO: 0042493), positive regulation of angiogenesis (GO: 0045766), regulation of blood pressure (GO: 0008217), leukocyte migration (GO: 0050900), positive regulation of smooth muscle cell proliferation (GO: 0048661), response to activity (GO: 0014823), positive regulation of cytosolic calcium ion concentration (GO: 0007204), acute-phase response (GO: 0006953), platelet degranulation (GO: 0002576), positive regulation of gene expression (GO: 0010628), positive

TABLE 1 | Variations of R-6.

R-6	Formulation 1	Formulation 2	Formulation 3	Formulation 4	Formulation 5
Rehmanniae Radix (Di-huang)	*Rehmanniae Radix* (Di-huang)	*Rehmanniae Radix* (Di-huang)	*Rehmanniae Radix* (Di-huang)	*Rehmanniae Radix* (Di-huang)	*Rehmanniae Radix* (Di-huang)
Dioscoreae Rhizoma (Shan-yao)	*Dioscoreae Rhizoma* (Shan-yao)	*Dioscoreae Rhizoma* (Shan-yao)	*Dioscoreae Rhizoma* (Shan-yao)	*Dioscoreae Rhizoma* (Shan-yao)	*Dioscoreae Rhizoma* (Shan-yao)
Corni Fructus (Shan-zhu-yu)	*Corni Fructus* (Shan-zhu-yu)	*Corni Fructus* (Shan-zhu-yu)	*Corni Fructus* (Shan-zhu-yu)	*Corni Fructus* (Shan-zhu-yu)	*Corni Fructus* (Shan-zhu-yu)
Moutan Cortex (Mu-dan-pi)	*Moutan Cortex* (Mu-dan-pi)	*Moutan Cortex* (Mu-dan-pi)	*Moutan Cortex* (Mu-dan-pi)	*Moutan Cortex* (Mu-dan-pi)	*Moutan Cortex* (Mu-dan-pi)
Poria (Fu-ling)	*Poria* (Fu-ling)	*Poria* (Fu-ling)	*Poria* (Fu-ling)	*Poria* (Fu-ling)	*Poria* (Fu-ling)
Alismatis Rhizoma (Ze-xie)	*Alismatis Rhizoma* (Ze-xie)	*Alismatis Rhizoma* (Ze-xie)	*Ginseng Radix et Rhizoma* (Ren-shen)	*Alismatis Rhizoma* (Ze-xie)	*Alismatis Rhizoma* (Ze-xie)
	Aucklandiae Radix (Mu-xiang)	*Chaenomelis Fructus* (Mu-gua)	*Astragali Radix* (Huang-qi)	*Ligustri Lucidi Fructus* (Nv-zhen-zi)	*Cinnamomi Ramulus* (Gui-zhi)
	Amomi Fructus (Sha-ren)	*Aucklandiae Radix* (Mu-xiang)	*Zingiberis Rhizoma Recens* (Sheng-jiang)	*Eclipta prostrata* (Mo-Han-Lian)	*Aconiti Lateralis Radix Praeparata* (Fu-zi)
	Citri Reticulatae Pericarpium (Chen pi)	*Arecae Semen* (Bing-lang)	*Jujubae Fructus* (Da-zao)		*Ligustri Lucidi Fructus* (Nv-zhen-zi)
	Ginseng Radix et Rhizoma (Ren-shen)	*Aconiti Lateralis Radix Praeparata* (Fu-zi)			
	Pinelliae Rhizoma (Ban-xia)	*Zingiberis Rhizoma* (Gan-jiang)			
	Atractylodis Macrocephalae Rhizoma (Bai-zhu)	*Glycyrrhizae Radix et Rhizoma* (Gan-cao)			
	Glycyrrhizae Radix et Rhizoma (Gan-cao)	*Zingiberis Rhizoma Recens* (Sheng-jiang)			
		Jujubae Fructus (Da-zao)			
		Tsaoko Fructus (Cao-guo)			

Rehmannia-6 complex (R-6, Liu-wei-di-huang-wan) was the most used Chinese medicine formulation in the cohorts showing beneficial effect on diabetic kidney disease. Variations of R-6 were identified from a published existing clinical practice guideline developed from expert consensus and pilot clinical service program, which is undergoing a randomized clinical trial for evaluation.

regulation of nitric oxide biosynthetic process (GO: 0045429), aging (GO: 0007568), response to glucocorticoid (GO: 0051384), positive regulation of transcription from RNA polymerase II promoter (GO: 0045944), cellular response to lipopolysaccharide (GO: 0071222), negative regulation of apoptotic process (GO: 0043066), and response to mechanical stimulus (GO: 0009612) (**Supplementary Datasheet S3**).

Further KEGG pathway analysis showed that the DN-related pathways were closely related to the complement and coagulation cascades, adipocytokine signaling pathway, TNF signaling pathway, HIF-1 signaling pathway, and AMPK signaling pathway, which share similar mechanisms with insulin resistance, rheumatoid arthritis, non-alcoholic fatty liver disease, and various infectious diseases and cancers (**Figure 2G**; **Supplementary Datasheet S4**).

Putative Targets of R-6

R-6 is a formulation containing *Rehmanniae Radix*, *Corni Fructus*, *Dioscoreae Rhizoma*, *Poria*, *Moutan Cortex*, and *Alismatis Rhizoma* (**Table 1**) and contains 64 identifiable chemical compounds (**Supplementary Table S2**) (out of the 463 chemicals from all R-6 variations). Four hundred forty-nine potential gene targets of R-6 were identified (**Figure 3A**). The top 20 most significant terms included steroid hormone-mediated signaling pathway (GO: 0043401), peptidyl-tyrosine autophosphorylation (GO: 0038083), transcription initiation from RNA polymerase II promoter (GO: 0006367), negative regulation of apoptotic process (GO: 0043066), proteolysis (GO: 0006508), protein autophosphorylation (GO: 0046777), extracellular matrix disassembly (GO: 0022617), peptidyl-tyrosine phosphorylation (GO: 0018108), response to hypoxia (GO: 0001666), oxidation-reduction process (GO: 0055114), response to drug (GO: 0042493), positive regulation of phosphatidylinositol 3-kinase signaling (GO: 0014068), protein phosphorylation (GO: 0006468), cellular response to insulin stimulus (GO: 0032869), glutathione metabolic process (GO: 0006749), phosphatidylinositol-mediated signaling (GO: 0048015), collagen catabolic process (GO: 0030574), response to estrogen (GO: 0043627), leukocyte migration (GO: 0050900), and purine-containing compound salvage (GO: 0043101) (**Supplementary Data S5**).

KEGG pathway analysis showed that the R-6-related pathways involve complement and coagulation cascades, VEGF signaling pathway, HIF-1 signaling pathway, T-cell and B-cell receptor signaling pathway, Fc epsilon RI signaling pathway, PI3K-Akt signaling pathway, MAPK signaling pathway, Ras signaling pathway, ErbB signaling pathway, FoxO signaling pathway, PPAR signaling pathway, sphingolipid signaling pathway, Rap1 signaling pathway, neurotrophin signaling pathway, prolactin, estrogen and thyroid hormone signaling pathway, metabolic pathways, insulin signaling pathway, and purine metabolism, sharing similar mechanisms with various infectious diseases and cancers (**Supplementary Data S6**).

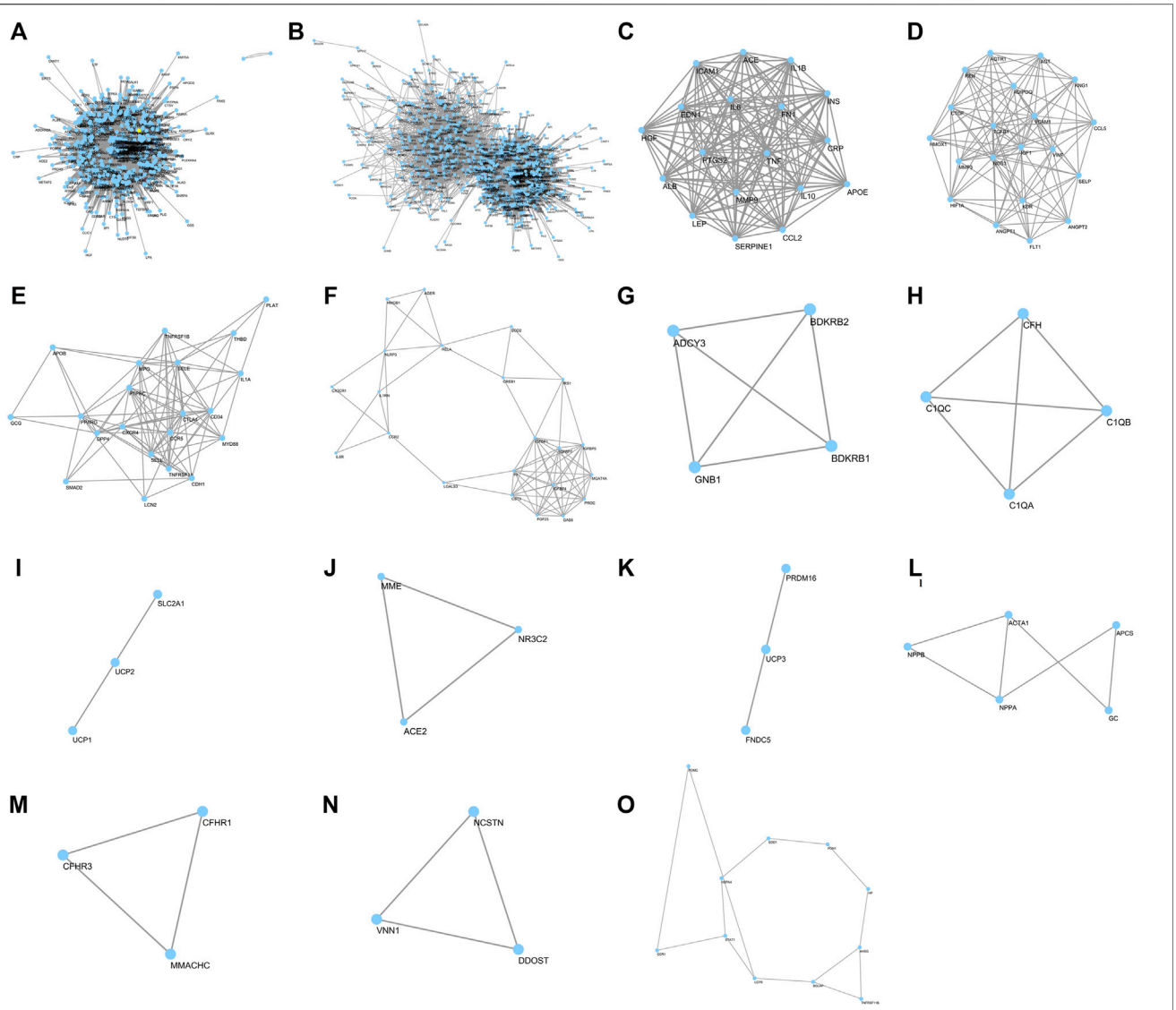

FIGURE 3 | Network of R-6 putative targets and clusters of DN–R-6 interaction network. Forty DN-related genes were overlapped with and R-6; **(A)** 449 potential gene targets of R-6; **(B)** putative targets of R-6 on diabetic DN; **(C–O)** Major clusters of putative targets of R-6 on DN

TABLE 2 | List of common proteins between diabetic nephropathy and R-6 variations.

	Common target proteins
Between DN and R-6	ACADM, ACE, AKR1B1, ALB, AR, DPP4, F7, GC, HMOX1, HSD11B1, IGF1, KDR, LCK, LCN2, MME, MMP3, MMP7, MMP9, NR3C2, PPARG, RBP4, REN, SHBG, SOD2, SORD, VDR, APCS, CCL5, HGF, LGALS3, NOS3, PADI4, PARP1, REG1A, SELE, SELP, STAT1, PLAT, ACE2, and CRP
Between DN and R-6 variations	ACE, APOE, CCL2, CRP, EDN1, FN1, HGF, ICAM1, IL10, IL1B, IL6, INS, LEP, MMP9, PTGS2, SERPINE1, and TNF[a]

[a]*TNF was identified as the seed for the most significant cluster of all variations of R-6.*

Putative Targets of R-6 on DN

Forty DN-related genes were overlapped with R-6 (**Figure 3B–O**; **Table 2**). Gene ontology analysis on the most significant cluster showed that the putative targets of R-6 on DN are strongly related to 44 ontology terms in 10 clusters, which included positive regulation of nitric oxide biosynthetic process (GO: 0045429), negative regulation of lipid storage (GO: 0010888), cellular response to

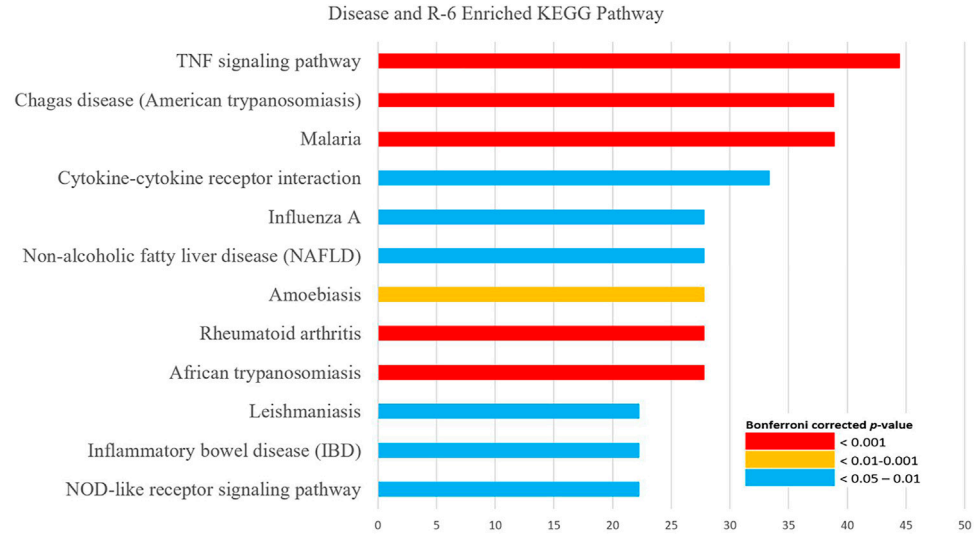

FIGURE 4 | KEGG pathway enrichment analysis of the interaction between DN and R-6. KEGG pathway analysis showed that the putative targets of R-6 on diabetic nephropathy are related to the TNF signaling pathway, NOD-like receptor signaling pathway, HIF-1 signaling pathway, PI3K-Akt signaling pathway, inflammatory mediator regulation of TRP channels, complement and coagulation cascades, and renin–angiotensin system.

lipopolysaccharide (GO: 0071222), inflammatory response (GO: 0006954), positive regulation of NF-kappa B transcription factor activity (GO: 0051092), positive regulation of smooth muscle cell proliferation (GO: 0048661), regulation of blood pressure (GO: 0008217), response to glucocorticoid (GO: 0051384), cellular response to interleukin-1 (GO: 0071347), angiogenesis (GO: 0001525), and negative regulation of blood coagulation (GO: 0030195) in cluster 1; positive regulation of phosphatidylinositol 3-kinase signaling (GO: 0014068), angiogenesis (GO: 0001525), positive regulation of cellular protein metabolic process (GO: 0032270), response to hypoxia (GO: 0001666), positive regulation of peptidyl-tyrosine phosphorylation (GO: 0050731), platelet degranulation (GO: 0002576), renin–angiotensin regulation of aldosterone production (GO: 0002018), positive regulation of ERK1 and ERK2 cascade (GO: 0070374), positive regulation of cell migration (GO: 0030335), regulation of blood pressure (GO: 0008217), and response to glucose (GO: 0009749) in cluster 2; inflammatory response (GO: 0006954), leukocyte migration (GO: 0050900), and response to lipopolysaccharide (GO: 0032496) in cluster 3; positive regulation of dendritic cell differentiation (GO: 2001200) and inflammatory response (GO: 0006954) in cluster 4; positive regulation of cytosolic calcium ion concentration (GO: 0007204) in cluster 5; complement activation (GO: 0006956), innate immune response (GO: 0045087), and proteolysis (GO: 0006508) in cluster 6; mitochondrial transport (GO: 0006839) in cluster 7; angiotensin maturation (GO: 0002003) in cluster 8; positive regulation of brown fat cell differentiation (GO: 0090336) in cluster 9; and response to hydrogen peroxide (GO: 0042542) in cluster 13 (**Supplementary Data S7**).

KEGG pathway analysis showed that the possible mechanisms of R-6 on DN are related to the TNF signaling pathway, NOD-like receptor signaling pathway, HIF-1 signaling pathway, PI3K-Akt signaling pathway, inflammatory mediator regulation of TRP channels, complement and coagulation cascades, and renin–angiotensin system, which share similar mechanisms with non-alcoholic fatty liver disease, inflammatory bowel disease, rheumatoid arthritis, and various types of infectious diseases and cancers (**Figure 4**; **Supplementary Data S8**).

Comparative Analysis on the Putative Targets of R-6 Variations on DN

Five variations of R-6 were identified from an existing clinical practice guideline and were analyzed (**Table 1**). The common putative targets of the R-6 variations on DN included ACE, APOE, CCL2, CRP, EDN1, FN1, HGF, ICAM1, IL10, IL1B, IL6, INS, LEP, MMP9, PTGS2, SERPINE1, and TNF. TNF was identified as the seed for the most significant cluster of all R-6 variations. These common targets were related to the TNF signaling pathway, NOD-like receptor signaling pathway, HIF-1 signaling pathway, PI3K-Akt signaling pathway, inflammatory mediator regulation of TRP channels, complement and coagulation cascades, and renin–angiotensin system, which share similar mechanisms with rheumatoid arthritis, systemic lupus erythematosus, non-alcoholic fatty liver disease, inflammatory bowel disease, and various types of infectious diseases and cancers.

Formulation 1, 3, and 4 had 9, 10, and 7 clusters with significant interactions with DN, respectively. These clusters involved positive regulation of the nitric oxide biosynthetic process (GO: 0045429), negative regulation of lipid storage (GO: 0010888), cellular response to lipopolysaccharide (GO:

TABLE 3 | Binding affinity of key chemical compounds of R-6 to putative targets.

Drug	Key chemical constituents	TNFR1	TNF	SERPINE1	MMP9	INS	IL6	IL10	ICAM1	HGF	FN1	EDN1	APOE	IL1B	CCL2	LEP
Alismatis Rhizoma	alisol a	−4.73	−2.85	−5.93	−4.51	−5.04	−5.75	−6.2	−3.77	−5.21	−5.24	−5.87	−3.35	−6.12	−3.98	−5.26
	alisol b	−5.26	−4.44	−4.65	−5.93	−6.01	−7.05	−6.77	−3.82	−5.89	−6.02	−5.13	−3.42	−6.97	−4.55	−7.71
	alisol c	−6.28	−3.22	−7.97	−3.29	−7.61	−7.1	−6.29	−3.61	−6.04	−4.78	−5.62	−2.89	−7.47	−5.4	−6.37
Corni Fructus	3,6-digalloylglucose	1.98	2.44	2.13	2.57	-2.51	-0.83	4.77	0.05	0.52	0.54	1.69	2.28	2.73	1.51	−2.34
	7,8-dehydropenstemoside	−1.99	−0.56	−1.12	−2.32	−1.68	−2.18	−1.6	−0.14	−2.07	−1.42	−3.73	0.06	−1.65	−1.89	−4.69
	7-*O*-methyl morroniside	−2.93	−2.63	−1.89	−3.87	−3.67	−4.05	−2.15	−1.28	−3.33	−3.81	−4.08	−2.01	−1.95	−2.05	−4.02
Dioscoreae Rhizoma	campesterol	−6.47	-4.04	−5.85	−5.76	−6.48	−6.84	−6.03	−5.32	−6.53	−2.01	−6.05	−4.29	−5.74	−5.08	−6.19
	deltoside	−4.3	−2.97	−4.5	−4.79	−4.58	−5.28	−3.83	−3.07	−3.76	−4.41	−5.23	−3.97	−3.8	−3.53	−5.15
	dioscin	−1.25	1.07	−1.29	−4.37	−3.74	-4.03	−4.27	−1.49	−4.73	−2.89	−3.95	4.47	−1.71	−2.25	−3.53
Moutan Cortex	benzoylpaeoniflorin	−2.84	−0.6	−1.2	−0.39	−5.41	−3.45	0.36	0.29	−2.62	−2.16	−1.47	1.37	0.59	−1.76	−3.85
	paeoniflorin	−1.12	−0.08	−3.63	−0.94	−4.06	−4.53	−1.63	−0.82	−2.52	−4.01	−3.76	−0.79	−4.7	−2.39	−2.83
	suffruticoside a	−0.86	0.15	−2.79	−2.4	−3.67	−3.46	−0.34	−0.87	−2.01	−2.7	−3.13	−0.24	−0.31	−0.55	−2.32
Poria	20-hexadecanoylingenol	1.65	−1.12	−0.78	−1.77	−3.68	−1.41	−3.41	1.59	−5.72	−1.98	−3.53	1.49	−3.98	−1.63	−3.75
	adenine	−3.08	−2.46	−4.23	−3.14	−3.8	−4.46	−3.65	−2.61	−3.47	−4.34	−4.92	−3.75	−4.23	−3.16	−4.49
	beta-amyrin acetate	−6.9	−6.22	−6.89	−5.76	−7.77	−7.42	−8.49	−6.29	−7.71	−6.91	−6.95	−6.5	−8.34	−7.34	−8.44
	p-hydroxybenzyl alcohol	−3.51	−3.12	−3.38	−4.4	−3.84	−3.66	−3.01	−3.16	−3.62	−3.39	−3.45	−2.16	−3.73	−3.15	−4.09
Rehmanniae Radix	acteoside	5.97	5.97	0.24	1.65	0.22	−0.9	−1.53	5.96	1.94	3.07	0.57	5.97	0.37	3.89	0.64
	catalpol	0.04	−0.25	−2.49	−1.89	−1.18	−2.77	−1.28	−0.79	−2.74	−1.62	−1.92	−0.25	−3.1	−1.91	−1.99

Free energy of binding (in Kcal/mol) were obtained from AutoDock Vina as the indicator of the binding likelihood. Negative values of free energy indicate possible binding in simulation. More negative scoring indicates stronger binding affinity. ACE, CRP, PTGS, and TNF receptor 2 were not assessable due to the large crystal structure.

0071222), and inflammatory response (GO: 0006954) and positive regulation of NF-kappa B transcription factor activity (GO: 0051092) in cluster 1; positive regulation of phosphatidylinositol 3-kinase signaling (GO: 0014068), angiogenesis (GO: 0001525), positive regulation of cellular protein metabolic process (GO: 0032270), response to hypoxia (GO: 0001666), positive regulation of peptidyl-tyrosine phosphorylation (GO: 0050731), platelet degranulation (GO: 0002576), and renin–angiotensin regulation of aldosterone production (GO: 0002018) in cluster 2; and inflammatory response (GO: 0006954) and leukocyte migration (GO: 0050900) in cluster 3, which was highly similar to R-6. Both formulations 1 and 4 also had a cluster with significant interaction on complement activation (GO: 0006956).

There were six clusters with a significant function between formulation 2 and DN. The major cluster of interaction involved regulation of blood pressure (GO: 0008217), positive regulation of ERK1 and ERK2 cascade (GO: 0070374), positive regulation of cell proliferation (GO: 0008284), positive regulation of cell migration (GO: 0030335), positive regulation of T-cell proliferation (GO: 0042102), negative regulation of the endothelial cell apoptotic process (GO: 2000352), cellular response to interleukin-1 (GO: 0071347), negative regulation of the extrinsic apoptotic signaling pathway via death domain receptors (GO: 1902042), positive regulation of MAPK cascade (GO: 0043410), positive regulation of protein kinase B signaling (GO: 0051897), aging (GO: 0007568), cellular response to tumor necrosis factor (GO: 0071356), and extracellular matrix organization (GO: 0030198) in addition to that of R-6 and DN alone.

Formulation 5 formed eight clusters with significant interactions with DN. The two clusters with the most significant interactions included positive regulation of phosphatidylinositol 3-kinase signaling (GO: 0014068), angiogenesis (GO: 0001525), positive regulation of cellular protein metabolic process (GO: 0032270), response to hypoxia (GO: 0001666), positive regulation of peptidyl-tyrosine phosphorylation (GO: 0050731), platelet degranulation (GO: 0002576), and renin–angiotensin regulation of aldosterone production (GO: 0002018) in cluster 2; inflammatory response (GO: 0006954) and leukocyte migration (GO: 0050900) in cluster 3; and complement activation (GO: 0006956) in cluster 6 (**Supplementary Data S9**).

KEGG analysis showed that formulations 1, 3, and 5 involved the TNF signaling pathway, NOD-like receptor signaling pathway, non-alcoholic fatty liver disease, and inflammatory bowel disease, and formulations 2 and 4 involved inflammatory mediator regulation of TRP channels in addition to the shared pathways (**Supplementary Data S10**).

Validation of Binding

From the molecular docking, the key chemical constituents from R-6 have good binding affinity to APOE, CCL2, EDN1, FN1, HGF, ICAM1, IL10, IL1B, IL6, INS, LEP, MMP9, PTGS2, SERPINE1, TNF, and TNF receptor 1, which supported the mechanistic involvement of these related pathways in the R-6's effect on DN. ACE, CRP, PTGS, and TNF receptor 2 were not assessable due to the large crystal structure (**Table 3**).

DISCUSSION

DN, R-6, and the Interaction From a Whole-System Perspective

Eleven clusters of pathophysiology were identified from DN. From a systemic perspective, the complement and coagulation cascades, adipocytokine signaling pathway, TNF signaling pathway, HIF-1 signaling pathway, and AMPK signaling pathway were the key pathways mediating the pathogenesis of DN based on the current evidence from *in vivo* and *in vitro* studies. These pathways are also shared by insulin resistance, rheumatoid arthritis, non-alcoholic fatty liver disease, and various types of infectious diseases and cancers, indicating a possibility in repurposing established therapeutics of these diseases for the DN management.

R-6's mechanistic action involves modulation of complement, coagulation, angiogenesis (VEGF), oxidative stress (HIF-1), innate and adaptive immunity (T cell, B cell receptor and Fc epsilon RI), cell proliferation and survival (PI3K-Akt, MAPK, Ras, ErbB, neurotrophin, and FoxO), cell adhesion (Rap1 and MAPK), and hormonal (prolactin, estrogen, and thyroid) and metabolism (PPAR, sphingolipid, insulin, and purine) pathways.

From the network inferences, R-6 likely acts on DN via the TNF, NOD-like receptor, HIF-1 and PI3K-Akt signaling pathway, complement and coagulation cascades, and renin–angiotensin system. These share similar mechanisms with non-alcoholic fatty liver disease, inflammatory bowel disease, and rheumatoid arthritis, which could support the use of R-6 in these conditions.

From the *in silico* binding affinity assessment, alisol (*Alismatis Rhizoma*), 7-o-methyl morroniside (*Corni Fructus*), campesterol (*Dioscoreae Rhizoma*), paeoniflorin (*Moutan Cortex*), beta-amyrin acetate (*Poria*), and catalpol (*Rehmanniae Radix*) have the highest likelihood of interacting with the proteins involved in these pathways.

TNF Signaling as the Key Mechanism of R-6's Action on DN

From KEGG enrichment analysis, the TNF signaling pathway was demonstrated as the key signaling involved in the action of R-6 on DN with the highest number of involved pathways. TNF signaling activates multiple pathways (e.g., NF-κB, JNK, MAPK, and PI3K-Akt) via receptors including TNF receptor type I (TNFR1) and TNF receptor type II (TNFR2), leading to apoptosis, necroptosis, inflammatory response, and vascular response. The TNF signaling pathway has been suggested as a therapeutic target for general CKD (Al-Lamki and Mayadas, 2015; Breyer and Susztak, 2016), autoimmune diseases, and cancers (Shaikh et al., 2018; Steeland et al., 2018). Elevated sera TNFR1 and TNFR2 were associated with reduced total filtration surface per glomerulus, podocyte number per glomerulus, filtration slit frequency, fenestrated endothelium,

and increased glomerular basement membrane width, foot process width, mesangial fractional volume, and global glomerular sclerosis in diabetic patients with early nephropathy (Pavkov et al., 2016). Previous longitudinal cohorts also demonstrated that higher baseline serum TNFR1 and TNFR2 levels increased the risk of end-stage kidney disease among type 2 diabetes patients (Niewczas et al., 2012; Pavkov et al., 2015).

TNF-α suppression by inhibitor or antibody alleviated albuminuria, macrophage infiltration, and glomerular and tubular injury in STZ-induced diabetic rats and *Ins2*^{Akita} mice (Awad et al., 2015; Cheng et al., 2021). Nevertheless, clinical pan-TNF intervention leads to concerns of the off-target effect (e.g., fever, hypotension, tuberculosis, and malignancy) as the TNF signaling pathway is a master regulator of innate immunity (Steeland et al., 2018), and TNFR1 is expressed widely in most cell types. Unlike TNFR1, which is pro-inflammatory and apoptotic, TNFR2 is more restricted to endothelial, immune, neuronal, and tumor cells and associated with immunomodulatory and anti-inflammatory effects (Steeland et al., 2018; Murakoshi et al., 2020). Targeted TNFR2 inhibition that modulates the TNF signaling homeostasis could alleviate the off-target effect in TNF signaling pathway intervention (Shaikh et al., 2018; Steeland et al., 2018; Murakoshi et al., 2020). The clinical efficacy, specificity to TNFR2, and the associated adverse events of R-6 on DN requires further clinical studies.

Differences Between R-6—DN Interaction Among R-6 Variations

From the comparative analysis of the interaction between R-6 variations and DN, formulations 1, 3, and 5 involved the NOD-like receptor signaling pathway, and formulations 2 and 4 involved regulation of TRP channels on top of the common targeting mechanisms, respectively. Similar to and synergistic with the toll-like receptor, NOD-like receptors are highly conserved pattern recognition receptors that mediate innate immunity through the activation of NF-κB, MAPK, inflammasome, and the production of pro-inflammatory cytokines and chemokines (Geddes et al., 2009). Polymorphisms of TLR and NLR were also associated with dyslipidemia, higher glucose level (Geddes et al., 2009; Gomes Torres et al., 2019), and insulin resistance (Zhou et al., 2017). NLRP3 has been shown to induce epithelial–mesenchymal transition of the tubular epithelial cells via TGF-beta (Wang et al., 2013). A previous study showed that NOD2 was upregulated in diabetic patient biopsies, and NOD2 knockout alleviated the hyperglycemia-induced nephrin expression reduction in diabetic mice (Du et al., 2013).

TRP channels are extensively expressed in the kidney and pancreas that modulate the transporting and signaling mechanisms underpinning glomerular filtration, reabsorption, and secretion of water and solutes in the kidney, and insulin secretion in the pancreas (Tomilin et al., 2016). TRP channels have six subfamilies, namely, TRPC, TRPV, TRPM, TRPP, TRPA, TRPML, and TRPN (Tomilin et al., 2016). TRP channels respond to mechanical stimuli and mediate vascular remodeling in various disease models (Smani et al., 2015; Kanthakumar and Adebiyi, 2021). Under a diabetic environment, the TRPC6 expression increases via the renin–angiotensin system and ATP signaling, leading to calcium influx and subsequent damage of the podocyte structure and detachment (Roshanravan and Dryer, 2014; Sonneveld et al., 2014; Wang et al., 2020). A late clinical trial TRACTION-2 using GFB-887, a podocyte targeted small molecule TRPC5 inhibitor, to treat diabetic kidney disease was designed based on previous *in vitro* and *in vivo* studies showing a protective effect of TRPC5 inhibition via the Rac1 signaling pathway (Walsh et al., 2021). Goshajinkigan, a Japanese herbal formulation similar to R-6, was shown to suppress the oxaliplatin-induced increase of TRPA1 and TRPM8 mRNA expression in dorsal root ganglia (Mizuno et al., 2014). Nevertheless, the involvement of the NOD-like receptor pathway and TRP channels was revealed through network inferences. Current research on the direct effect of R-6 on these two mechanisms in diabetes is limited.

Strengths and Limitations

A network pharmacological approach was used to delineate the systemic interaction between DN and R-6 with multifactorial pathophysiology and multiple chemical constituents. The whole-system effect of R-6 specific to DN was revealed for further clinical validation. Nevertheless, we limited the analysis to DN with macroalbuminuria for a more specific DN diagnosis (Persson and Rossing, 2018), and we did not perform HPLC or UPLC analysis on the chemical constituents of the formulations as the CMs involved are well studied and available in the existing databases. Network pharmacology analysis focuses on protein–protein interaction. The direction of effect (e.g., positive, negative, or cyclic effect) and the associated epigenetic regulations require further investigations.

Besides, we did not perform *in vivo* or *in vitro* validation as (1) the study medication involves multiple drugs and chemicals, (2) network pharmacology analysis is already a systematic integration of all existing *in vivo* and *in vitro* data (Hopkins, 2008), and (3) further validation data from a single study with experimental models are unlikely to add much evidence to the result from network analysis. We used *in silico* docking analysis as a validation from the chemistry perspective. Free energy was used to estimate the strength of bonding for better estimating the binding affinity instead of using root-mean-square deviation from geometric assessment (Cournia et al., 2017; Mobley and Gilson, 2017). Subsequent validation from clinical samples screening the biomarkers of key mechanisms would serve better to evaluate the whole-system effect and the relative involvement of different mechanisms of the formulations in real clinical settings (Chan et al., 2021c).

CONCLUSION

The complement and coagulation cascades, adipocytokine signaling pathway, TNF signaling pathway, HIF-1 signaling

pathway, and AMPK signaling pathway orchestrated the pathogenesis of DN from a systemic perspective. The therapeutic effect of R-6 on DN likely involves the TNF, NOD-like receptor, HIF-1, and PI3K-Akt signaling pathways; the complement and coagulation cascades; and the renin–angiotensin system. The analysis of R-6 and the comparative analysis of R-6 variations converged to suggest that the TNF signaling pathway is the key mechanism involved in the action of R-6 on DN among patients with DN presenting with different clinical phenotypes. Variations of R-6 used in clinical protocols may also involve the NOD-like receptor signaling pathway and TRP channels on top of the common mechanisms from indirect inferences. These putative targets could be validated through further trials with clinical samples.

DATA AVAILABILITY STATEMENT

The original contributions presented in the study are included in the article/**Supplementary Material**, further inquiries can be directed to the corresponding author.

AUTHOR CONTRIBUTIONS

KC and ST conceived the study. KY and KC collected the data and performed the pathway analysis. KC, WY, RX, SW-YL, HY, YZ, JM, and KL interpreted the pathway-related pathophysiology. KC, KY, and ST drafted the manuscript. All authors involved in the interpretation of data and manuscript revision.

FUNDING

This project was made possible in part through the support of Health and Medical Research Fund (Ref: 12133341, 14151731), and the philanthropic donations from Mrs. Louise Mon (Perennial International Ltd.), Ting Lai Ling, Chan Wing Kwan, Patrick, and Sa Sa Making Life Beautiful Charity Fund. In addition, ST was supported by the HKU Outstanding Researcher Award, Croucher Senior Medical Research Fellowship Award, and the Yu endowed professorship at HKU. The funding organizations had no role in the design and conduct of the study; collection, management, analysis, and interpretation of the data; preparation, review, or approval of the manuscript; and decision to submit the manuscript for publication.

SUPPLEMENTARY MATERIAL

The Supplementary Material for this article can be found online at: https://www.frontiersin.org/articles/10.3389/fphar.2022.794139/full#supplementary-material

REFERENCES

Al-Lamki, R. S., and Mayadas, T. N. (2015). TNF Receptors: Signaling Pathways and Contribution to Renal Dysfunction. *Kidney Int.* 87 (2), 281–296. doi:10.1038/ki.2014.285

Alicic, R. Z., Rooney, M. T., and Tuttle, K. R. (2017). Diabetic Kidney Disease: Challenges, Progress, and Possibilities. *Clin. J. Am. Soc. Nephrol.* 12 (12), 2032–2045. doi:10.2215/CJN.11491116

Alsaad, K. O., and Herzenberg, A. M. (2007). Distinguishing Diabetic Nephropathy from Other Causes of Glomerulosclerosis: an Update. *J. Clin. Pathol.* 60 (1), 18–26. doi:10.1136/jcp.2005.035592

Awad, A. S., You, H., Gao, T., Cooper, T. K., Nedospasov, S. A., Vacher, J., et al. (2015). Macrophage-derived Tumor Necrosis Factor-α Mediates Diabetic Renal Injury. *Kidney Int.* 88 (4), 722–733. doi:10.1038/ki.2015.162

Breyer, M. D., and Susztak, K. (2016). The Next Generation of Therapeutics for Chronic Kidney Disease. *Nat. Rev. Drug Discov.* 15 (8), 568–588. doi:10.1038/nrd.2016.67

Chan, G. C. W., and Tang, S. C. W. (2018). Proteinuria Reaffirmed as a Risk Modifier in Diabetic Chronic Kidney Disease. *Nephrol. Dial. Transpl.* 33 (11), 1873–1874. doi:10.1093/ndt/gfy208

Chan, K. (2018). *Integrative Management for Diabetic Kidney Disease – Patients' and Clinicians' Perspectives, Clinical Effectiveness and Possible Mechanisms [PhD Thesis]*. Hong Kong: The University of Hong Kong.

Chan, K. W., Chow, T. Y., Yu, K. Y., Feng, Y., Lao, L., Bian, Z., et al. (2022). Effectiveness of Integrative Chinese-Western Medicine for Chronic Kidney Disease and Diabetes: A Retrospective Cohort Study. *Am. J. Chin. Med.* 2022, 1–18. doi:10.1142/s0192415x2250015x

Chan, K. W., Ip, T. P., Kwong, A. S., Lui, S. L., Chan, G. C., Cowling, B. J., et al. (2016). Semi-individualised Chinese Medicine Treatment as an Adjuvant Management for Diabetic Nephropathy: a Pilot Add-On, Randomised, Controlled, Multicentre, Open-Label Pragmatic Clinical Trial. *BMJ Open* 6 (8), e010741. doi:10.1136/bmjopen-2015-010741

Chan, K. W., Kwong, A. S. K., Tsui, P. N., Cheung, S. C. Y., Chan, G. C. W., Choi, W. F., et al. (2021a). Efficacy, Safety and Response Predictors of Adjuvant astragalus for Diabetic Kidney Disease (READY): Study Protocol of an Add-On, Assessor-Blind, Parallel, Pragmatic Randomised Controlled Trial. *BMJ Open* 11 (1), e042686. doi:10.1136/bmjopen-2020-042686

Chan, K. W., Wong, V. T., and Tang, S. C. W. (2020a). COVID-19: An Update on the Epidemiological, Clinical, Preventive and Therapeutic Evidence and Guidelines of Integrative Chinese-western Medicine for the Management of 2019 Novel Coronavirus Disease. *Am. J. Chin. Med.* 48 (3), 737–762. doi:10.1142/S0192415X20500378

Chan, K. W., Lee, P. W., Leung, C. P. S., Chan, G. C. W., Yiu, W. H., Cheung, H. M., et al. (2020b). Patients' and clinicians' Expectations on Integrative Medicine Services for Diabetes: A Focus Group Study. *BMC Complement. Med. Ther.* 20 (1), 205. doi:10.1186/s12906-020-02994-5

Chan, K. W., Chow, T. Y., Yu, K. Y., Xu, Y., Zhang, N. L., Wong, V. T., et al. (2021b). SYmptom-Based STratification of DiabEtes Mellitus by Renal Function Decline (SYSTEM): A Retrospective Cohort Study and Modeling Assessment. *Front. Med.* 8, e682090. doi:10.3389/fmed.2021.682090

Chan, K. W., Kwong, A. S. K., Chan, G. C. W., Leung, C. P. S., Yiu, W. H., Lui, S. L., et al. (2019). Semi-individualised Chinese Medicine Treatment for Diabetic Kidney Disease - from Users' Perspectives to SCHEMATIC Trial Interim Result and Potential Mechanisms. *Adv. Integr. Med.* 6, S12. doi:10.1016/j.aimed.2019.03.033

Chan, K. W., Lee, P. W., Leung, C. P.-s., Law, Y. K., Gao, L., Chan, G. C.-w., et al. (2021c). PRAgmatic Clinical Trial Design of Integrative MediCinE (PRACTICE): A Focus Group Series and Systematic Review on Trials of Diabetes and Kidney Disease. *Front. Med.* 8, 668913. doi:10.3389/fmed.2021.668913

Cheng, D., Liang, R., Huang, B., Hou, J., Yin, J., Zhao, T., et al. (2021). Tumor Necrosis Factor-α Blockade Ameliorates Diabetic Nephropathy in Rats. *Clin. Kidney J.* 14 (1), 301–308. doi:10.1093/ckj/sfz137

Cournia, Z., Allen, B., and Sherman, W. (2017). Relative Binding Free Energy Calculations in Drug Discovery: Recent Advances and Practical Considerations. *J. Chem. Inf. Model.* 57 (12), 2911–2937. doi:10.1021/acs.jcim.7b00564

Du, P., Fan, B., Han, H., Zhen, J., Shang, J., Wang, X., et al. (2013). NOD2 Promotes Renal Injury by Exacerbating Inflammation and Podocyte Insulin Resistance in Diabetic Nephropathy. *Kidney Int.* 84 (2), 265–276. doi:10.1038/ki.2013.113

Flyvbjerg, A. (2017). The Role of the Complement System in Diabetic Nephropathy. *Nat. Rev. Nephrol.* 13 (5), 311–318. doi:10.1038/nrneph.2017.31

Forbes, J. M., Cooper, M. E., Oldfield, M. D., and Thomas, M. C. (2003). Role of Advanced Glycation End Products in Diabetic Nephropathy. *J. Am. Soc. Nephrol.* 14 (8 Suppl. 3), S254–S258. doi:10.1097/01.asn.0000077413.41276.17

Furuichi, K., Shimizu, M., Okada, H., Narita, I., and Wada, T. (2018). Clinico-pathological Features of Kidney Disease in Diabetic Cases. *Clin. Exp. Nephrol.* 22 (10), 1046–1051. doi:10.1007/s10157-018-1556-4

Gao, X., Liu, Y., An, Z., and Ni, J. (2021). Active Components and Pharmacological Effects of Cornus Officinalis: Literature Review. *Front. Pharmacol.* 12 (513), e633447. doi:10.3389/fphar.2021.633447

Geddes, K., Magalhães, J. G., and Girardin, S. E. (2009). Unleashing the Therapeutic Potential of NOD-like Receptors. *Nat. Rev. Drug Discov.* 8 (6), 465–479. doi:10.1038/nrd2783

Goh, S. Y., and Cooper, M. E. (2008). Clinical Review: The Role of Advanced Glycation End Products in Progression and Complications of Diabetes. *J. Clin. Endocrinol. Metab.* 93 (4), 1143–1152. doi:10.1210/jc.2007-1817

Gomes Torres, A. C. M. B., Leite, N., Tureck, L. V., de Souza, R. L. R., Titski, A. C. K., Milano-Gai, G. E., et al. (2019). Association between Toll-like Receptors (TLR) and NOD-like Receptor (NLR) Polymorphisms and Lipid and Glucose Metabolism. *Gene* 685, 211–221. doi:10.1016/j.gene.2018.11.065

Guo, C., Kang, X., Cao, F., Yang, J., Xu, Y., Liu, X., et al. (2021a). Network Pharmacology and Molecular Docking on the Molecular Mechanism of Luo-hua-zi-zhu (LHZZ) Granule in the Prevention and Treatment of Bowel Precancerous Lesions. *Front. Pharmacol.* 12 (144). doi:10.3389/fphar.2021.629021

Guo, J. C., Pan, H. C., Yeh, B. Y., Lu, Y. C., Chen, J. L., Yang, C. W., et al. (2021b). Associations between Using Chinese Herbal Medicine and Long-Term Outcome Among Pre-dialysis Diabetic Nephropathy Patients: A Retrospective Population-Based Cohort Study. *Front. Pharmacol.* 12, 616522. doi:10.3389/fphar.2021.616522

Hamosh, A., Scott, A. F., Amberger, J., Valle, D., and McKusick, V. A. (2000). Online Mendelian Inheritance in Man (OMIM). *Hum. Mutat.* 15 (1), 57–61. doi:10.1002/(SICI)1098-1004(200001)15:1<57::AID-HUMU12>3.0.CO;2-G

Heerspink, H. J. L., Parving, H. H., Andress, D. L., Bakris, G., Correa-Rotter, R., Hou, F. F., et al. (2019). Atrasentan and Renal Events in Patients with Type 2 Diabetes and Chronic Kidney Disease (SONAR): a Double-Blind, Randomised, Placebo-Controlled Trial. *Lancet* 393 (10184), 1937–1947. doi:10.1016/S0140-6736(19)30772-X

Heinzelmann, G., and Gilson, M. K. (2021). Automation of Absolute Protein-Ligand Binding Free Energy Calculations for Docking Refinement and Compound Evaluation. *Sci. Rep.* 11 (1), 1116. doi:10.1038/s41598-020-80769-1

Hopkins, A. L. (2008). Network Pharmacology: the Next Paradigm in Drug Discovery. *Nat. Chem. Biol.* 4 (11), 682–690. doi:10.1038/nchembio.118

Hsieh, C. F., Huang, S. L., Chen, C. L., Chen, W. T., Chang, H. C., and Yang, C. C. (2014). Non-aristolochic Acid Prescribed Chinese Herbal Medicines and the Risk of Mortality in Patients with Chronic Kidney Disease: Results from a Population-Based Follow-Up Study. *BMJ Open* 4 (2), e004033–004033. doi:10.1136/bmjopen-2013-004033

Hsu, T. W., Liu, J. S., Hung, S. C., Kuo, K. L., Chang, Y. K., Chen, Y. C., et al. (2014). Renoprotective Effect of Renin-Angiotensin-Aldosterone System Blockade in Patients with Predialysis Advanced Chronic Kidney Disease, Hypertension, and Anemia. *JAMA Intern. Med.* 174 (3), 347–354. doi:10.1001/jamainternmed.2013.12700

Huang, da. W., Sherman, B. T., and Lempicki, R. A. (2009). Systematic and Integrative Analysis of Large Gene Lists Using DAVID Bioinformatics Resources. *Nat. Protoc.* 4 (1), 44–57. doi:10.1038/nprot.2008.211

Huang, K. C., Su, Y. C., Sun, M. F., and Huang, S. T. (2018). Chinese Herbal Medicine Improves the Long-Term Survival Rate of Patients with Chronic Kidney Disease in Taiwan: a Nationwide Retrospective Population-Based Cohort Study. *Front. Pharmacol.* 9, 1117. doi:10.3389/fphar.2018.01117

Jerums, G., Premaratne, E., Panagiotopoulos, S., and MacIsaac, R. J. (2010). The Clinical Significance of Hyperfiltration in Diabetes. *Diabetologia* 53 (10), 2093–2104. doi:10.1007/s00125-010-1794-9

Kanthakumar, P., and Adebiyi, A. (2021). Renal Vascular TRP Channels. *Curr. Res. Physiol.* 4, 17–23. doi:10.1016/j.crphys.2021.02.001

Kashihara, N., Haruna, Y., Kondeti, V. K., and Kanwar, Y. S. (2010). Oxidative Stress in Diabetic Nephropathy. *Curr. Med. Chem.* 17 (34), 4256–4269. doi:10.2174/092986710793348581

Kim, S., Chen, J., Cheng, T., Gindulyte, A., He, J., He, S., et al. (2019). PubChem 2019 Update: Improved Access to Chemical Data. *Nucleic Acids Res.* 47 (D1), D1102–d9. doi:10.1093/nar/gky1033

Lee, H. S., Jo, S., Lim, H. S., and Im, W. (2012). Application of Binding Free Energy Calculations to Prediction of Binding Modes and Affinities of MDM2 and MDMX Inhibitors. *J. Chem. Inf. Model.* 52 (7), 1821–1832. doi:10.1021/ci3000997

Li, R. X., Yiu, W. H., Wu, H. J., Wong, D. W., Chan, L. Y., Lin, M., et al. (2014). BMP7 Reduces Inflammation and Oxidative Stress in Diabetic Tubulopathy. *Clin. Sci.* 9, 9. doi:10.1042/cs20140401

Li, S., Fan, T. P., Jia, W., Lu, A., and Zhang, W. (2014). Network Pharmacology in Traditional Chinese Medicine. *Evid. Based Complement. Alternat Med.* 2014, 138460. doi:10.1155/2014/138460

Lin, M., Yiu, W. H., Wu, H. J., Chan, L. Y., Leung, J. C., Au, W. S., et al. (2012). Toll-like Receptor 4 Promotes Tubular Inflammation in Diabetic Nephropathy. *J. Am. Soc. Nephrol.* 23 (1), 86–102. doi:10.1681/ASN.2010111210

Lin, M. Y., Chiu, Y. W., Chang, J. S., Lin, H. L., Lee, C. T., Chiu, G. F., et al. (2015). Association of Prescribed Chinese Herbal Medicine Use with Risk of End-Stage Renal Disease in Patients with Chronic Kidney Disease. *Kidney Int.* 88 (10), 1365–1373. doi:10.1038/ki.2015.226

Luo, D. (2008). Identification of Structure and Antioxidant Activity of a Fraction of Polysaccharide Purified from Dioscorea Nipponica Makino. *Carbohydr. Polym.* 71 (4), 544–549. doi:10.1016/j.carbpol.2007.06.023

Madhusudhan, T., Kerlin, B. A., and Isermann, B. (2016). The Emerging Role of Coagulation Proteases in Kidney Disease. *Nat. Rev. Nephrol.* 12 (2), 94–109. doi:10.1038/nrneph.2015.177

Mizuno, K., Kono, T., Suzuki, Y., Miyagi, C., Omiya, Y., Miyano, K., et al. (2014). Goshajinkigan, a Traditional Japanese Medicine, Prevents Oxaliplatin-Induced Acute Peripheral Neuropathy by Suppressing Functional Alteration of TRP Channels in Rat. *J. Pharmacol. Sci.* 125 (1), 91–98. doi:10.1254/jphs.13244fp

Mobley, D. L., and Gilson, M. K. (2017). Predicting Binding Free Energies: Frontiers and Benchmarks. *Annu. Rev. Biophys.* 46, 531–558. doi:10.1146/annurev-biophys-070816-033654

Murakoshi, M., Gohda, T., and Suzuki, Y. (2020). Circulating Tumor Necrosis Factor Receptors: a Potential Biomarker for the Progression of Diabetic Kidney Disease. *Ijms* 21 (6), 1957. doi:10.3390/ijms21061957

Navarro-González, J. F., Mora-Fernández, C., Muros de Fuentes, M., and García-Pérez, J. (2011). Inflammatory Molecules and Pathways in the Pathogenesis of Diabetic Nephropathy. *Nat. Rev. Nephrol.* 7 (6), 327–340. doi:10.1038/nrneph.2011.51

Niewczas, M. A., Gohda, T., Skupien, J., Smiles, A. M., Walker, W. H., Rosetti, F., et al. (2012). Circulating TNF Receptors 1 and 2 Predict ESRD in Type 2 Diabetes. *J. Am. Soc. Nephrol.* 23 (3), 507–515. doi:10.1681/ASN.2011060627

Nistor, I., De Sutter, J., Drechsler, C., Goldsmith, D., Soler, M. J., Tomson, C., et al. (2018). Effect of Renin-Angiotensin-Aldosterone System Blockade in Adults with Diabetes Mellitus and Advanced Chronic Kidney Disease Not on Dialysis: a Systematic Review and Meta-Analysis. *Nephrol. Dial. Transpl.* 33 (1), 12–22. doi:10.1093/ndt/gfx072

Oe, Y., Hayashi, S., Fushima, T., Sato, E., Kisu, K., Sato, H., et al. (2016). Coagulation Factor Xa and Protease-Activated Receptor 2 as Novel Therapeutic Targets for Diabetic Nephropathy. *Arterioscler Thromb. Vasc. Biol.* 36 (8), 1525–1533. doi:10.1161/ATVBAHA.116.307883

Palmer, S. C., Mavridis, D., Navarese, E., Craig, J. C., Tonelli, M., Salanti, G., et al. (2015). Comparative Efficacy and Safety of Blood Pressure-Lowering Agents in Adults with Diabetes and Kidney Disease: a Network Meta-Analysis. *Lancet* 385 (9982), 2047–2056. doi:10.1016/S0140-6736(14)62459-4

Pavkov, M. E., Nelson, R. G., Knowler, W. C., Cheng, Y., Krolewski, A. S., and Niewczas, M. A. (2015). Elevation of Circulating TNF Receptors 1 and 2 Increases the Risk of End-Stage Renal Disease in American Indians with Type 2 Diabetes. *Kidney Int.* 87 (4), 812–819. doi:10.1038/ki.2014.330

Pavkov, M. E., Weil, E. J., Fufaa, G. D., Nelson, R. G., Lemley, K. V., Knowler, W. C., et al. (2016). Tumor Necrosis Factor Receptors 1 and 2 Are Associated with Early Glomerular Lesions in Type 2 Diabetes. *Kidney Int.* 89 (1), 226–234. doi:10.1038/ki.2015.278

Perkovic, V., Jardine, M. J., Neal, B., Bompoint, S., Heerspink, H. J. L., Charytan, D. M., et al. (2019). Canagliflozin and Renal Outcomes in Type 2 Diabetes and Nephropathy. *N. Engl. J. Med.* 380 (24), 2295–2306. doi:10.1056/NEJMoa1811744

Persson, F., and Rossing, P. (2018). Diagnosis of Diabetic Kidney Disease: State of the Art and Future Perspective. *Kidney Int. Suppl.* 8 (1), 2–7. doi:10.1016/j.kisu.2017.10.003

Pichler, R., Afkarian, M., Dieter, B. P., and Tuttle, K. R. (2017). Immunity and Inflammation in Diabetic Kidney Disease: Translating Mechanisms to Biomarkers and Treatment Targets. *Am. J. Physiol. Ren. Physiol* 312 (4), F716–f31. doi:10.1152/ajprenal.00314.2016

Premaratne, E., Verma, S., Ekinci, E. I., Theverkalam, G., Jerums, G., and MacIsaac, R. J. (2015). The Impact of Hyperfiltration on the Diabetic Kidney. *Diabetes Metab.* 41 (1), 5–17. doi:10.1016/j.diabet.2014.10.003

Roshanravan, H., and Dryer, S. E. (2014). ATP Acting through P2Y Receptors Causes Activation of Podocyte TRPC6 Channels: Role of Podocin and Reactive Oxygen Species. *Am. J. Physiol. Ren. Physiol* 306 (9), F1088–F1097. doi:10.1152/ajprenal.00661.2013

Sagoo, M. K., and Gnudi, L. (2018). Diabetic Nephropathy: Is There a Role for Oxidative Stress? *Free Radic. Biol. Med.* 116, 50–63. doi:10.1016/j.freeradbiomed.2017.12.040

Shaikh, F., He, J., Bhadra, P., Chen, X., and Siu, S. W. I. (2018). TNF Receptor Type II as an Emerging Drug Target for the Treatment of Cancer, Autoimmune Diseases, and Graft-Versus-Host Disease: Current Perspectives and *In Silico* Search for Small Molecule Binders. *Front. Immunol.* 9 (1382), 1382. doi:10.3389/fimmu.2018.01382

Shannon, P., Markiel, A., Ozier, O., Baliga, N. S., Wang, J. T., Ramage, D., et al. (2003). Cytoscape: a Software Environment for Integrated Models of Biomolecular Interaction Networks. *Genome Res.* 13 (11), 2498–2504. doi:10.1101/gr.1239303

Shu, Z., Chang, K., Zhou, Y., Peng, C., Li, X., Cai, W., et al. (2021). Add-On Semi-individualized Chinese Medicine for Coronavirus Disease 2019 (ACCORD): a Retrospective Cohort Study of Hospital Registries. *Am. J. Chin. Med.* 49 (3), 1–33. doi:10.1142/s0192415x21500257

Smani, T., Shapovalov, G., Skryma, R., Prevarskaya, N., and Rosado, J. A. (2015). Functional and Physiopathological Implications of TRP Channels. *Biochim. Biophys. Acta* 1853 (8), 1772–1782. doi:10.1016/j.bbamcr.2015.04.016

Sonneveld, R., van der Vlag, J., Baltissen, M. P., Verkaart, S. A., Wetzels, J. F., Berden, J. H., et al. (2014). Glucose Specifically Regulates TRPC6 Expression in the Podocyte in an AngII-dependent Manner. *Am. J. Pathol.* 184 (6), 1715–1726. doi:10.1016/j.ajpath.2014.02.008

Steeland, S., Libert, C., and Vandenbroucke, R. E. (2018). A New Venue of TNF Targeting. *Int. J. Mol. Sci.* 19 (5), 1442. doi:10.3390/ijms19051442

Stelzer, G., Rosen, N., Plaschkes, I., Zimmerman, S., Twik, M., Fishilevich, S., et al. (2016). The GeneCards Suite: from Gene Data Mining to Disease Genome Sequence Analyses. *Curr. Protoc. Bioinformatics* 54, 1. doi:10.1002/cpbi.5

Sun, H., Saeedi, P., Karuranga, S., Pinkepank, M., Ogurtsova, K., Duncan, B. B., et al. (2021). IDF Diabetes Atlas: Global, Regional and Country-Level Diabetes Prevalence Estimates for 2021 and Projections for 2045. *Diabetes Res. Clin. Pract.* 183, 109119. doi:10.1016/j.diabres.2021.109119

Sun, Y. (2014). Biological Activities and Potential Health Benefits of Polysaccharides from Poria Cocos and Their Derivatives. *Int. J. Biol. Macromol* 68, 131–134. doi:10.1016/j.ijbiomac.2014.04.010

Szklarczyk, D., Gable, A. L., Lyon, D., Junge, A., Wyder, S., Huerta-Cepas, J., et al. (2019). STRING V11: Protein-Protein Association Networks with Increased Coverage, Supporting Functional Discovery in Genome-wide Experimental Datasets. *Nucleic Acids Res.* 47 (D1), D607–d13. doi:10.1093/nar/gky1131

Tang, S. C. W., and Yiu, W. H. (2020). Innate Immunity in Diabetic Kidney Disease. *Nat. Rev. Nephrol.* 16 (4), 206–222. doi:10.1038/s41581-019-0234-4

Tang, S. C. W., Yu, X., Chen, H. C., Kashihara, N., Park, H. C., Liew, A., et al. (2020). Dialysis Care and Dialysis Funding in Asia. *Am. J. Kidney Dis.* 75 (5), 772–781. doi:10.1053/j.ajkd.2019.08.005

Thomas, M. C., Cooper, M. E., and Zimmet, P. (2016). Changing Epidemiology of Type 2 Diabetes Mellitus and Associated Chronic Kidney Disease. *Nat. Rev. Nephrol.* 12 (2), 73–81. doi:10.1038/nrneph.2015.173

Tomilin, V., Mamenko, M., Zaika, O., and Pochynyuk, O. (2016). Role of Renal TRP Channels in Physiology and Pathology. *Semin. Immunopathol* 38 (3), 371–383. doi:10.1007/s00281-015-0527-z

Tonneijck, L., Muskiet, M. H., Smits, M. M., van Bommel, E. J., Heerspink, H. J., van Raalte, D. H., et al. (2017). Glomerular Hyperfiltration in Diabetes: Mechanisms, Clinical Significance, and Treatment. *J. Am. Soc. Nephrol.* 28 (4), 1023–1039. doi:10.1681/ASN.2016060666

The UniProt Consortium (2019). UniProt: a Worldwide Hub of Protein Knowledge. *Nucleic Acids Res.* 47 (D1), D506–d15. doi:10.1093/nar/gky1049

Walsh, L., Reilly, J. F., Cornwall, C., Gaich, G. A., Gipson, D. S., Heerspink, H. J. L., et al. (2021). Safety and Efficacy of GFB-887, a TRPC5 Channel Inhibitor, in Patients with Focal Segmental Glomerulosclerosis, Treatment-Resistant Minimal Change Disease, or Diabetic Nephropathy: TRACTION-2 Trial Design. *Kidney Int. Rep.* 6 (10), 2575–2584. doi:10.1016/j.ekir.2021.07.006

Wang, Q., Tian, X., Wang, Y., Wang, Y., Li, J., Zhao, T., et al. (2020). Role of Transient Receptor Potential Canonical Channel 6 (TRPC6) in Diabetic Kidney Disease by Regulating Podocyte Actin Cytoskeleton Rearrangement. *J. Diabetes Res.* 2020, 6897390. doi:10.1155/2020/6897390

Wang, W., Wang, X., Chun, J., Vilaysane, A., Clark, S., French, G., et al. (2013). Inflammasome-independent NLRP3 Augments TGF-β Signaling in Kidney Epithelium. *J. Immunol.* 190 (3), 1239–1249. doi:10.4049/jimmunol.1201959

Wang, X., Shen, Y., Wang, S., Li, S., Zhang, W., Liu, X., et al. (2017a). PharmMapper 2017 Update: a Web Server for Potential Drug Target Identification with a Comprehensive Target Pharmacophore Database. *Nucleic Acids Res.* 45 (W1), W356–w60. doi:10.1093/nar/gkx374

Wang, Z., He, C., Peng, Y., Chen, F., and Xiao, P. (2017b). Origins, Phytochemistry, Pharmacology, Analytical Methods and Safety of Cortex Moutan (*Paeonia Suffruticosa* Andrew): a Systematic Review. *Molecules* 22 (6), 946. doi:10.3390/molecules22060946

Yiu, W. H., Li, R. X., Wong, D. W. L., Wu, H. J., Chan, K. W., Chan, L. Y. Y., et al. (2018). Complement C5a Inhibition Moderates Lipid Metabolism and Reduces Tubulointerstitial Fibrosis in Diabetic Nephropathy. *Nephrol. Dial. Transpl.* 33 (8), 1323–1332. doi:10.1093/ndt/gfx336

Yokozawa, T., Kim, H. Y., and Yamabe, N. (2004). Amelioration of Diabetic Nephropathy by Dried Rehmanniae Radix (Di Huang) Extract. *Am. J. Chin. Med.* 32 (6), 829–839. doi:10.1142/S0192415X04002442

Zhang, L. (2010). *The Optimization Study of Clinical Pathway Formulation Based on Chronic Renal Failure Diagnosis Scheme [MD Thesis]*. Guangzhou: Guangzhou University of Chinese Medicine.

Zhang, L. L., Xu, W., Xu, Y. L., Chen, X., Huang, M., and Lu, J. J. (2017). Therapeutic Potential of *Rhizoma Alismatis*: a Review on Ethnomedicinal Application, Phytochemistry, Pharmacology, and Toxicology. *Ann. N. Y Acad. Sci.* 1401 (1), 90–101. doi:10.1111/nyas.13381

Zhang, R., Zhu, X., Bai, H., and Ning, K. (2019). Network Pharmacology Databases for Traditional Chinese Medicine: Review and Assessment. *Front. Pharmacol.* 10, 123. doi:10.3389/fphar.2019.00123

Zhang, R. Z., Yu, S. J., Bai, H., and Ning, K. (2017). TCM-mesh: The Database and Analytical System for Network Pharmacology Analysis for TCM Preparations. *Sci. Rep.* 7 (1), 2821. doi:10.1038/s41598-017-03039-7

Zhou, H., Feng, L., Xu, F., Sun, Y., Ma, Y., Zhang, X., et al. (2017). Berberine Inhibits Palmitate-Induced NLRP3 Inflammasome Activation by Triggering Autophagy in Macrophages: a New Mechanism Linking Berberine to Insulin Resistance Improvement. *Biomed. Pharmacother.* 89, 864–874. doi:10.1016/j.biopha.2017.03.003

Conflict of Interest: The authors declare that the research was conducted in the absence of any commercial or financial relationships that could be construed as a potential conflict of interest.

Publisher's Note: All claims expressed in this article are solely those of the authors and do not necessarily represent those of their affiliated organizations, or those of the publisher, the editors and the reviewers. Any product that may be evaluated in this article, or claim that may be made by its manufacturer, is not guaranteed or endorsed by the publisher.

GLOSSARY

ACE Angiotensin-converting enzyme
AMPK Adenosine monophosphate-activated protein kinase
APOE Apolipoprotein E
CCL2 chemokine (C-C motif) ligand 2
CKD Chronic kidney disease
CM Chinese medicine
CRP C-reactive protein
DAVID Database for Annotation, Visualization and Integrated Discovery
DKD Diabetic kidney disease
DN Diabetic nephropathy
EDN1 Endothelin 1
ErbB Erythroblastic leukemia viral oncogene homolog
ERK1/2 Extracellular signal-regulated protein kinase 1/2
Fc epsilon RI Fc epsilon receptor I
RI Fc epsilon receptor I
FN1 Fibronectin 1
FoxO Forkhead Box O
HGF Hepatocyte growth factor
HIF Hypoxia-inducible factor
HPLC High-performance liquid chromatography
ICAM1 Intercellular adhesion molecule 1
IL10 interleukin 10
IL1B Interleukin 1 beta
IL6 Interleukin 6
INS Insulin
Ins2Akita Heterozygous Akita spontaneous mutation
JNK c-Jun N-terminal kinase
KEGG Kyoto Encyclopedia of Genes and Genomes
LEP Leptin
MAPK Mitogen-activated protein kinase
MCODE Molecular complex detection
MMP9 Matrix metallopeptidase 9
NF-kappa B Nuclear factor-kappa B
NLR NOD-like receptor
NLRP3 NOD-like receptor protein 3
OMIM Online Mendelian Inheritance in Man
PI3K Phosphoinositide 3-kinases
AKT Protein kinase B
PPAR Peroxisome proliferator-activated receptor
PTGS2 Prostaglandin-endoperoxide synthase 2
R-6 Rehmannia-6
Rap1 Ras-related protein 1
Ras Rat sarcoma
RCSB Research Collaboratory for Structural Bioinformatics
SERPINE1 Serpin family E member 1
STRING Search Tool for the Retrieval of Interacting Genes/Proteins
STZ Streptozotocin
TLR Toll-like receptor
TNF Tumor necrosis factor
TNFR1/2 Tumor necrosis factor receptor 1 or 2
TRP Transient receptor potential
TRPA Transient receptor potential ankyrin
TRPC Transient receptor potential canonical
TRPM Transient receptor potential melastatin
TRPML Transient receptor potential mucolipin
TRPN Transient receptor potential no mechanoreceptor potential C
TRPP Transient receptor potential polycystin
TRPV Transient receptor potential vanilloi
UPLC Ultra performance liquid chromatography

frontiers | Frontiers in Pharmacology

REVIEW
published: 20 April 2022
doi: 10.3389/fphar.2022.805281

Fatty Acid β-Oxidation in Kidney Diseases: Perspectives on Pathophysiological Mechanisms and Therapeutic Opportunities

Zhumei Gao[1] *and Xiangmei Chen*[1,2]*

[1]Department of Nephrology, The Second Hospital of Jilin University, Jilin, China, [2]Department of Nephrology, The First Medical Center, Chinese PLA General Hospital, Beijing, China

The kidney is a highly metabolic organ and requires a large amount of ATP to maintain its filtration-reabsorption function, and mitochondrial fatty acid β-oxidation serves as the main source of energy to meet its functional needs. Reduced and inefficient fatty acid β-oxidation is thought to be a major mechanism contributing to kidney diseases, including acute kidney injury, chronic kidney disease and diabetic nephropathy. PPARα, AMPK, sirtuins, HIF-1, and TGF-β/SMAD3 activation have all been shown to play key roles in the regulation of fatty acid β-oxidation in kidney diseases, and restoration of fatty acid β-oxidation by modulation of these molecules can ameliorate the development of such diseases. Here, we disentangle the lipid metabolism regulation properties and potential mechanisms of mesenchymal stem cells and their extracellular vesicles, and emphasize the role of mesenchymal stem cells on lipid metabolism. This review aims to highlight the important role of fatty acid β-oxidation in the progression of kidney diseases, and to explore the fatty acid β-oxidation effects and therapeutic potential of mesenchymal stem cells for kidney diseases.

Keywords: acute kidney injury, chronic kidney disease, diabetic nephropathy, fatty acid β-oxidation, mesenchymal stem cell therapy

OPEN ACCESS

Edited by:
Dan-Qian Chen,
Northwest University, China

Reviewed by:
Gang Cao,
Zhejiang Chinese Medical University, China
Xiaoxin Wang,
Georgetown University Medical Center, United States
Qingqing Wei,
Augusta University, United States

***Correspondence:**
Xiangmei Chen
xmchen301@126.com

Specialty section:
This article was submitted to Renal Pharmacology, a section of the journal Frontiers in Pharmacology

Received: *30 October 2021*
Accepted: *31 March 2022*
Published: *20 April 2022*

Citation:
Gao Z and Chen X (2022) Fatty Acid β-Oxidation in Kidney Diseases: Perspectives on Pathophysiological Mechanisms and Therapeutic Opportunities. Front. Pharmacol. 13:805281. doi: 10.3389/fphar.2022.805281

1 INTRODUCTION

Over the last 20 years, approximately 850 million people have been suffering from some form of kidney disease (Bharati and Jha, 2022). Many kidney diseases eventually progress to end-stage renal disease (ESRD) due to the lack of specific treatment drugs. To date, renal replacement therapy is the only effective treatment for ESRD, which imposes a very large economic burden on the health system and individuals. Therefore, there is an urgent need to find potential novel therapeutic targets and develop sustainable and effective strategies to prevent ESRD.

Abbreviations: ACC, acetyl-CoA carboxylase; AKI, acute kidney injury; AMPK, adenosine monophosphate-activated protein kinase; CKD, chronic kidney disease; CPT1A, Carnitine palmitoyl transferase 1A; DN, diabetic nephropathy; ECHA, enoyl-CoA hydratase; ESRD, end-stage renal disease; EVs, extracellular vesicles; FAs, fatty acids; FABPs, FA-binding proteins; FAO, fatty acid β-oxidation; FATPs, FA-transport proteins; LCAD, long-chain acyl-CoA dehydrogenase; L-FABP, Liver-FABP; LKB1, Liver kinase B1; MCAD, medium chain acyl-CoA dehydrogenase; MSCs, mesenchymal stem cells; PGC-1α, peroxisome proliferator-activated receptor γ coactivator 1α; PPARα, peroxisome proliferators-activated receptor α; SIRT3, sirtuin 3; SIRT5, sirtuin 5; TEC, tubular epithelial cell; UCP, uncoupling protein.

The kidney requires a tremendous amount of energy to maintain a stable internal environment of the body. Approximately 70% of the glomerular filtrate and its solutes are reabsorbed in the proximal tubules, so tubular epithelial cells (TECs) are mitochondrially enriched and primarily relying on fatty acid β-oxidation (FAO) as their energy source to meet their functional needs (-). Fatty acids are converted into products, such as acetyl-CoA, to generate energy through fatty acid uptake, activation, transportation to the matrix, and FAO processes in the body. Dysregulation of lipid uptake and FAO mediated lipid deposition are thought to contribute to kidney diseases, including acute kidney injury (AKI), chronic kidney disease (CKD), and diabetic nephropathy (DN) (Li et al., 2020a; Rong et al., 2021; Li et al., 2022). An impaired FAO is thought to be a major mechanism underlying kidney injury.

Carnitine palmitoyl transferase 1A (CPT1A) is a rate-limiting enzyme in the FAO pathway. A recent study showed that CPT1A overexpression in kidney tubules significantly reduced renal fibrosis and protected against kidney function deterioration by restoring FAO function, preventing mitochondrial dysfunction, TEC differentiation, and increasing cellular oxidative capacity in 3 CKD animal models (Miguel et al., 2021a). This discoveries have expanded the understanding of the relationship between FAO and kidney injury.

Several reports have demonstrated that mesenchymal stem cells (MSCs) and their constituents, extracellular vesicles (EVs), are a novel therapeutic target for kidney diseases (Yea et al., 2021; Li et al., 2021a; Peng et al., 2022). Recently, it has been demonstrated that MSCs and MSC-EVs can regulate the lipid metabolism by increasing the expression of FAO-related genes and reducing fatty acid uptake (CD36) in metabolic diseases (Li et al., 2019a; El-Derany and AbdelHamid, 2021). However, the underlying mechanisms involving MSCs and FAO in kidney diseases remain poorly understood. Therefore, in this review, we focus on an in-depth discussion of the mechanisms and regulation of FAO in kidney diseases. In addition, we explore the effects of MSCs on FAO disorder, thereby aiding the application of MSCs in kidney diseases.

2 FATTY ACIDS UPTAKE IN KIDNEY DISEASES

Fatty acids (FAs) are the preferred substrate for proximal tubule ATP generation (Nieth and Schollmeyer.1966). In plasma, water-insoluble free FA are solubilized by complexing with albumin and transported to specific parts of the body for utilization. Although free FAs can enter the cytoplasm by passive diffusion, most of long-chain fatty acids (LCFAs) are taken up by transporters in proximal tubules. The cluster of differentiation-36 (CD36), FA-binding proteins (FABPs) and FA-transport proteins (FATPs) families are the most common and frequently studied FAs transporters in the kidney (Storch and McDermott.2009; Khan et al., 2018).

2.1 Cluster of Differentiation-36

CD36, also known as fatty acid translocase, is a scavenger receptor capable of binding many ligands, and is responsible for cellular uptake of long-chain fatty acids (Coburn et al., 2000). Human CD36 overexpression in the proximal tubules is associated with aggravation or progression of AKI after folic acid treatment (Jung et al., 2018). An increased expression of CD36 and CD36-mediated lipid deposition was also observed in the kidney of CKD and DN (Okamura et al., 2007).

CD36 is an important receptor for macrophages to recognize and phagocytize apoptotic cells and oxidized lipids. The severity of renal fibrosis in macrophage CD36-deficient mice was significantly lower than that in wild mice. This difference was associated with the attenuation of oxidative and proinflammatory pathways that promote fibrogenesis in CKD (Okamura et al., 2009; Pennathur et al., 2015).

Renal CD36 is also highly expressed in TECs (Susztak et al., 2005). An high glucose stimulated CD36-dependent Wnt/β-catenin activation in TECs is related to advanced oxidation protein product-induced lipid accumulation, which is thought to contribute to renal fibrosis (Li et al., 2019b). In addition, an elevated CD36 expression in TECs promotes mtROS production, apoptosis, epithelial-mesenchymal transition, and inflammatory responses, which in turn promote DN progression (Susztak et al., 2005; Hou et al., 2015; Hou et al., 2021). Interestingly, Susztak et al. generated a mouse model with kidney-specific overexpression of CD36 and found that FA accumulation was already evident in 8-week-old CD36-transgenic animals, while markers of fibrosis increased by 20 weeks of age (Kang et al., 2015). Thus, CD36 plays an important roles in kidney diseases, but an increased expression of CD36-induced lipid accumulation is not a major contributor to renal fibrosis. Moreover, the ubiquitous expression and cell-specific effects of CD36 must be considered when development of novel peptides that target CD36.

2.2 FA-Binding Proteins and FA-Transport Proteins 2

FABPs bind long-chain FAs with high affinity and play a central role in coordinating lipid transport and metabolism (Storch and McDermott, 2009), which comprises at least nine homologous proteins with similar tertiary structures and specific tissue distribution patterns (Li et al., 2020b). Liver-FABP (L-FABP) is expressed in the proximal tubules of both the normal and diseased human kidney (Maatman et al., 1991; Kamijo-Ikemori et al., 2011), which facilitates the excretion of lipid peroxidation products from TECs, promotes FAO and then attenuates tubulointerstitial damage to achieve renoprotection (Xu et al., 2015). Numerous studies have demonstrated that L-FABP is a promising biomarker for several kidney diseases, and it has also been shown that upregulation of renal L-FABP can protect renal function in human L-FABP transgenic mice after cisplatin treatment (Negishi et al., 2008; Manabe et al., 2012).

Adipose-FABP (also known as FABP4) has been reported to be significantly elevated in many AKI models, and inhibition of FABP4 can attenuate endoplasmic reticulum stress,

mitochondrial dysfunction, inflammation, and apoptosis and restore kidney function (Huang et al., 2018; Tan et al., 2019; Li et al., 2021b). Inhibition of FABP4 can also enhance FAO and rebalance abnormal lipid metabolism in TECs and attenuate the progression of kidney fibrosis (Chen et al., 2021).

FATP2, which is encoded by *Slc27a2* and is localized most prominently on the proximal tubule apical membrane, is another protein that is implicated in the uptake of lipids in the kidney (Khan et al., 2018). It has been proven that FATP2 promotes renal interstitial fibrosis by inhibiting FAO in TECs, and inhibition of FATP2 could improve kidney function and alleviate fibrotic responses in a UUO kidney and DN (Khan et al., 2020; Chen et al., 2020).

In summary, the transport of FAs in the kidney exhibits unique characteristics in specific cells. In particular, FABP members exhibit unique functions in different tissues and microenvironments. Further understanding as to how the transport of FAs are specifically regulated in different cells will provide novel insights into the transport actions of FAs and facilitate their applications in kidney diseases.

3 FATTY ACIDS β-OXIDATION IN KIDNEY DISEASES

FAs are activated to acyl-CoA before entering the mitochondria for complete β-oxidation. CPT1 is present in the outer membrane of mitochondria, catalyzes the synthesis of acyl carnitine from long chain fatty acyl CoA and carnitine. Then, under the action of carnitine-acylcarnitine translocase, the acyl carnitine enters the mitochondrial matrix and is transformed into acyl-CoA under the action of carnitine acyl transferase II in the inner membrane of mitochondria.

FA β-oxidation is the core process of FA catabolism and depends on the concerted action of both peroxisomes and mitochondria (Fransen et al., 2017). Peroxisomes and mitochondria contain different enzymes for β-oxidation, which preferentially oxidize short- and medium-chain FAs, whereas peroxisomes metabolize very long-chain FAs (Vasko.2016). These very-long-chain FAs are transported to the peroxisome matrix through ATP-binding protein ABCD1-3, which shortens the FA chain after several rounds of peroxisomal β-oxidation, and are then transferred into mitochondria for complete FAO (Lodhi and Semenkovich.2014; He et al., 2021). Acyl-CoA undergoes a β-oxidation reaction to form acetyl-CoA, which is completely oxidized by the tricarboxylic acid cycle.

3.1 Regulation of Fatty Acid β-Oxidation

3.1.1 Peroxisome Proliferators-Activated Receptor α

Peroxisome proliferators-activated receptor α (PPARα) activation induces FAO and is most prominently expressed in the adult kidney (Braissant et al., 1996; Montaigne et al., 2021). The assembled complex containing PPRE/PPARα/RXRα/ligands/coactivators controls the expression of the genes involved in FAO (Libby et al., 2021).

Regulation of PPARα activity factors, including PPARα gene expression and protein translation, ligand specificity and availability, cofactor recruitment, corepressors or coactivators, and posttranslational modification, is an effective strategy to prevent and treat lipid disorders in kidney diseases (Bougarne et al., 2018). Blanquart demonstrated that synthetic PPARα ligands such as Wy14643, GW7647, or fibrates can increase the stability of PPARα, thereby regulating the transcription of PPARα target genes (Blanquart et al., 2002). In addition, PPARα ligands fibrates can also directly activate PPARα to induce the expression of fatty acid metabolism-related genes (Staels et al., 1998). Peroxisome proliferator-activated receptor γ coactivator 1α (PGC-1α) is a important coactivator of PPARa, and regulates FAO by increasing the activity of PPARα in the proximal tubule epithelial cells (Vega et al., 2000; Portilla et al., 2002).

3.1.2 Adenosine Monophosphate-Activated Protein Kinase

Adenosine monophosphate-activated protein kinase (AMPK) is a master regulator of metabolism, which restores energy balance during metabolic stress both at the cellular and physiological levels (Garcia and Shaw.2017). Liver kinase B1 (LKB1) is the upstream kinase of AMPK, causing an increased Thr172 phosphorylation and AMPK activation under energy stress conditions (Lin and HardiE, 2018). Malonyl-CoA is a potent inhibitor of CPT1, activated LKB1/AMPK inhibits the conversion of acetyl-CoA to malonyl-CoA by phosphorylating acetyl-CoA carboxylase 1 (ACC1) and ACC2, which in turn promotes FAO (Jeon et al., 2012). Moreover, AMPK initiates many important gene regulatory functions in skeletal muscles by directly phosphorylating PGC-1α protein at threonine-177 and serine-538 (Jager et al., 2007).

3.1.3 TGF-β/SMAD3

TGF-β is an important upstream modulator of fatty acid metabolism (Kang et al., 2015). TGF-β-driven SMAD3-dependent manner inhibit the expression of PGC-1α and downstream lipid deposition (Yadav et al., 2011). Moreover, TGF-β/SMAD3 signaling pathways reduce PPARα target gene expression and lower the rates of FAO in cultured myocytes by suppressing PPARα activity (Sekiguchi et al., 2007).

3.1.4 Sirtuins

Sirtuins are a family of NAD^+-dependent deacylases that exhibit a broad range of cellular functions. SIRT3 is localized in the mitochondrial matrix, where it promotes fatty acid oxidation in the liver and heart by deacetylating enzymes, such as long-chain acyl-CoA dehydrogenase (LCAD) (Hirschey et al., 2010). Unlike SIRT3, SIRT5 is also present in peroxisomes. It was observed that SIRT5 promotes the efficiency of mitochondrial FAO by increasing the activity of enoyl-CoA hydratase (ECHA) in the heart (Sadhukhan et al., 2016). However, in contrast to mitochondria, SIRT5 suppresses peroxisomal FAO by inhibiting ACOX1 activity *in vitro* and in rodent liver (Chen et al., 2018).

3.1.5 Hypoxia-Inducible Factor 1

Hypoxia-inducible factor 1(HIF1) is a key transcription factor regulating lipid metabolism and mediating inhibition of PPARα expression during hypoxia (Narravula and Colgan.2001). CPT1A

is a direct target gene of HIF and is repressed by HIF1 and HIF2, thereby reducing fatty acid transport into the mitochondria, and forcing fatty acids to lipid droplets for storage (Du et al., 2017).

3.2 Defective Fatty Acid β-Oxidation in Kidney Diseases

3.2.1 Acute Kidney Injury

Reduction of FAO-related metabolic enzymes (CPT1 and medium chain–specific acyl-CoA dehydrogenase) and increased intrarenal lipid accumulation in proximal tubule cells were observed during ischemia reperfusion- and cisplatin-induced AKI (Portilla et al., 2000; Portilla et al., 2002; Tran et al., 2016). It is suggested that nucleocytoplasmic shuttling of PPARα is involved in lipid disorders in AKI. PPARα is a dynamic shuttling between the cytosol and the nucleus under physiological conditions and active PPARα is mainly located in the nucleus (Bougarne et al., 2018). The mitochondrial matrix protein cyclophilin D in mitochondria binds to PPARα and sequestration lead to inhibition of its nuclear translocation and transcription of PPARα-regulated FAO genes during cisplatin-induced AKI (Jang et al., 2020). Sirtuins also play an important role in FAO regulation in AKI. In addition to regulating FAO by modulating PPARα expression, SIRT3 further regulates FAO by deacetylating the LBK1 and activating the AMPK signaling pathway in cisplatin-induced AKI (Li et al., 2020a). In contrast to SIRT3, loss-of-function of SIRT5 was renoprotective in AKI. SIRT5 regulates the balance between mitochondrial and peroxisomal FAO in proximal tubular epithelial cells, and SIRT5 deficiency appears to be protective by increasing peroxisomal FAO to protect against injury in ischemia-induced or cisplatin-induced AKI (Chiba et al., 2019).

3.2.2 Chronic Kidney Disease

Genome-wide unbiased transcriptomic analysis revealed that FAO-related key metabolic enzymes and FAO transcriptional regulator factors were markedly decreased in CKD (Kang et al., 2015). In ischemia reperfusion-induced CKD, activated transcription factor of the unfolded protein response ATF6α inhibited PPARα expression, resulting in the downregulation of FA β-oxidation and mitochondrial dysfunction, and consequent lipid deposition and apoptosis induction, which eventually accelerated profibrogenic phenotypes (Jao et al., 2019). TGF-β1-induced and SMAD3-mediated repression of PGC1-α also play a critical role in the regulation of FAO in TECs (Kang et al., 2015). Moreover, LKB1 and AMPK are further important controllers of FAO in TECs. It was observed that deletion of LKB1 in renal tubular epithelial cells downregulated the transcript levels of rate-limiting enzymes in the β-oxidation pathway via the AMPK signaling pathway, and an impaired LKB1 led to CKD (Han et al., 2016). HIF-1α directly regulates the expression of PPARα and CPT1α. In CKD, an upregulated mitochondrial uncoupling protein 2 (UCP2) protein increased HIF-1α stabilization, which in turn stimulated lipid deposition and extracellular matrix accumulation and promoted fibrosis (Ke et al., 2020).

Several microRNAs have been shown to be involved in the pathophysiology of renal fibrosis. Recently, a study employing an microRNA array-based strategy indicated that both miR-150 and miR-495 are upregulated in UUO-induced fibrotic kidneys, and that microRNAs are capable of reducing the expression of CPT1A, PGC1-α, and TFAM mitochondrial function-related genes, leading to renal epithelial cell dedifferentiation and a TGF-β1-induced fibrosis phenotype (Miguel et al., 2021b). Notably, miR-21, which has been extensively studied in renal fibrosis, is highly expressed in kidney fibrosis (Chau et al., 2012). Indeed, miR-21 efficiently decreases PPARα expression, impairs FAO, and aggravates renal fibrosis development during aging (Chau et al., 2012; Chung et al., 2018).

3.2.3 Diabetic Nephropathy

Studies have also revealed that mouse models with DN display a lower expression of key enzymes and regulators of FAO, and a higher intracellular lipid deposition than controls (Lee et al., 2020). Advanced glycation end products (AGEs) are thought to be involved in this pathogenesis, which induced a decrease in CPT2 expression that led to mitochondrial FAO damage and, eventually, renal fibrosis and DN (Lee et al., 2020).

3.3 Targeting Fatty Acid Oxidation in Kidney Diseases

Defective FAO is closely linked to the pathogenesis and progression of kidney diseases. Hence, relieving lipid accumulation could be an effective strategy to suppress the progression of kidney diseases.

Some studies have shown that restoration of PPARα activity and/or expression is a potential treatment strategy for preventing the progression of kidney diseases. PPARα agonists are the most treatable option targeting defective FAO. In cisplatin-induced AKI, PPARα ligand Wy-14643 (WY) prevented cisplatin-induced reduction of mRNA levels and the enzyme activity of mitochondrial medium chain acyl-CoA dehydrogenase (MCAD), and rescued MCAD-mediated FAO to ameliorated acute tubular necrosis (Li et al., 2004). PPARα agonists also had a very excellent effect in the CKD model. For example, treatment with fenofibrate restored FAO-related enzyme expression, improved renal function, and reduced kidney injury and fibrosis in a folic acid- and UUO-induced kidney fibrosis model (Kang et al., 2015). Similar results were observed after treatment with BAY PP1, a new PPARα agonist, in UUO and 5/6 nephrectomy models of renal fibrosis (Boor et al., 2011). Moreover, PPARα/β activator MHY2013 can significantly increase the expression of FAO-associated genes and prevent renal fibrosis during aging (Chung et al., 2020).

Activation of AMPK is another effective way to restore FAO. LKB1-deficient cells treated with an AMPK agonist (A769662) restored the levels of CPT1, CPT2, and ACOX1 in FAO and reduced apoptosis and dedifferentiation (Han et al., 2016). Moreover, it has been reported that metformin could reduce renal fibrosis by activation of energy-sensing kinase AMPK, thereby increasing phosphorylation of ACC and altering fatty acid metabolism (Lee et al., 2018). Uncoupling protein (UCP-1) located in the inner

TABLE 1 | Intervene fatty acid β-oxidation in AKI.

Model	Treatment	Regulatory factor	Effect on kidney injury	Reference
Cisplatin	Genetic or pharmacological inhibition of cyclophilin D	PPARα activity↑ Fatty acid oxidation↑ Lipid accumulation↓	Mitochondrial function↑ Apoptotic↓ Inflammation↓ Cell cycle G2/M arrest↓	Jang et al. (2020)
Cisplatin	SIRT3 agonist	LKB1-AMPK pathway↑ Fatty acid oxidation↑ Lipid accumulation↓	Mitochondrial function↑ Renal function↑ Necrosis↓	Li et al. (2020b)
Cisplatin/Ischemic AKI	SIRT5-deficient mice	Peroxisomal fatty acid oxidation↑	Tubular injury↓ Oxidative stress↓ Renal function↑	Chiba et al. (2019)
Cisplatin	UCP1 agonist	AMPK/ULK1 pathway↑ Lipid accumulation↓	Apoptotic↓ Inflammation↓ Autophagy↑	Xiong et al. (2021)
Cisplatin	PPARα ligand	PPARα activity↑ Fatty acid oxidation↑ Pyruvate dehydrogenase kinase-4 (PDK4)↑	Apoptotic↓ Inflammation↓ Necrosis	Li et al. (2004)

mitochondrial membrane inhibits the progression of acute renal injury by promoting the AMPK/ULK1/autophagy pathway (Xiong et al., 2021).

Indeed, the delivery of microRNA mimics or inhibitors has been proposed as a promising therapeutic strategy to prevent the development of renal fibrosis (Petrillo et al., 2017). For example, treatment with miR-9-5p was shown to reverse the downregulation of the expression of PPARα and PGC1A and FAO-related enzymes in a mouse model of UUO, further protecting against renal fibrosis (Fierro-Fernandez et al., 2020). In addition, miR-21 inhibition was shown to prevent CKD, which may be related to the enhancement of PPARα/RXR activity and improved mitochondrial function (Gomez et al., 2015). The details of intervention in fatty acid β-oxidation in AKI and CKD are summarized in **Tables 1**, **2**.

4 FATTY ACID β-OXIDATION AND STEM CELL-BASED THERAPY

MSCs are pluripotent stem cells with the ability of self-renewal and multidirectional differentiation that have been isolated

TABLE 2 | Intervene fatty acid β-oxidation in CKD.

Model	Treatment	Regulatory factor	Effect on kidney injury	Reference
Folic acid	Overexpression of PGC1-α; Fenofibrate (PPARα agonist); Etoxomir (inhibitor CPT)	PGC1-α, CPT, PPARα Fatty acid oxidation↑	Fibrosis↓ Apoptosis↓ Renal function↑ Tabular injury↓	Kang et al. (2015)
UUO; 5/6 nephreetomized rats	BAY PPI (PPAR-α against)	PPAR-α↑ TGF-β1 expression↓	Fibrosis↓ Renal function↑ Interstital cell proliferation↓	Boor et al. (2011)
Tubule epithclial Lkb1 deletion mice	Fenofibrate A769662 (A MPK against)	PPARα↑ AMPK↑	Fibrosis↓ Apoptosis↓ Dedifferentiation↓	Han et al. (2016)
Unilateral ischemia-reperfusion injury	Atf6α-/- mice fenofibrate	PPARα↑ Lipid accumulation↓	Apoptosis↓ Fibrosis↓	Jao et al. (2019)
UUO	Mir-9-5p	PGC-1α↑ Fatty acid metabolism↓	Fibrosis↓ Mitochondrial function↑ apoptosis↓ Inflammation↓	Fierro-fermandez et al. (2020)
Alport nephropathy	Anti-microRNA-21	PPARα/RXR activity↑ PGC-1α↑ Fatty acid metabolism	Fibrosis↓ Mitochondrial function↑ Oxidative stress↓ Inflammation↓	Gomez et al. (2015)
Ischemia-representation injury; Folic acid nephropathy (FAN); Aristolochic acid nephropathy (AAN)	UCP2-deficient mice; Genetic inhibition of HIF-1α	PPARα↑ CPT1A↑ Lipid accumulation↓	ECM accumulation↓ Mitochondrial function↑	Ke et al. (2020)
UUO; FAN; Adenine-induced nephrotoxicity	CPC1A-knockin mice	Fatty acid metabolism↑	Fibrosis Mitochondrial function↑ Apoptosis↓ Inflammation↓ Cell cycle arrest↓	Miguel et al. (2021a)

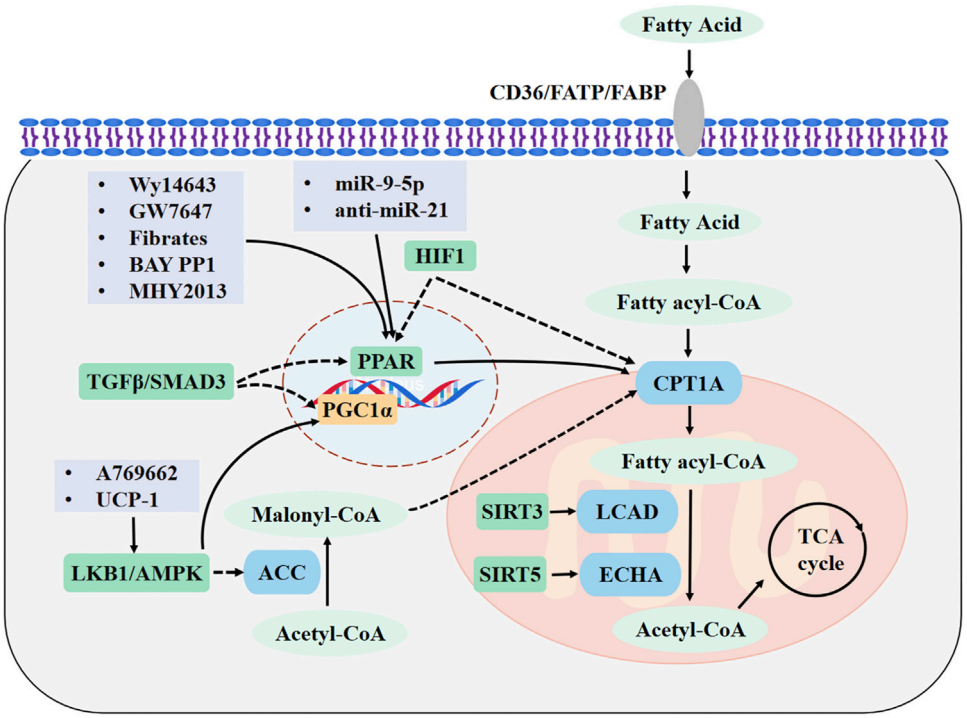

FIGURE 1 | Major FAO pathways involved in kidney diseases and drug targets. Fatty acids (FAs) enter the cytoplasm through CD36, FABPs, or FATPs. In the cytosol, FAs are activated to fatty acyl-CoA and transported into the mitochondrial matrix through CPT1A. The acyl-CoA undergoes a β-oxidation reaction to form acetyl-CoA, which is completely oxidized by the tricarboxylic acid cycle. FAO is promoted by upregulating CPT1A and PPAR signaling. Drugs are highlighted in light purple boxes. Enzymes are shown in blue and metabolites are shown in light green. Regulatory molecules are shown in green boxes. FAO, fatty acid β-oxidation; CPT1A, carnitine palmitoyl transferase 1A; FABP, FA-binding protein; FATPs, FA-transport protein; PPAR, peroxisome proliferators-activated receptor; PGC-1α, peroxisome proliferator-activated receptor γ coactivator 1α; AMPK, adenosine monophosphate-activated protein kinase; LKB1, Liver kinase B1; ACC, acetyl-CoA carboxylase; LCAD, long-chain acyl-CoA dehydrogenase; ECHA, enoyl-CoA hydratase; SIRT3, sirtuin 3; SIRT5, sirtuin 5.

from various biological tissues (Naji et al., 2019; Zhou et al., 2021).

The regulation of lipid metabolism by MSCs and/or their EVs is well explored in cancer and metabolic diseases. Increasing evidence suggests that MSCs improve the stemness and drug-resistance of cancer cells through regulating CPT1 expression and FAO, which is mediated by the miR-3619-5p/AMPK/PGC1α/CEBPB axis in gastric cancer (Wu et al., 2020; Han et al., 2021). In a non-alcoholic steatohepatitis animal model, treatment with bone marrow-derived MSCs and their EVs significantly improved liver steatosis and ballooning in rats (El-Derany and AbdelHamid. 2021). Further mechanistic studies have shown that MSC-EVs could reduce the expression of fatty acid uptake and the synthesis genes CD36, SREB1, SREB2 and ACC, upregulate the gene expression levels of PPARα and the FAO metabolic enzyme CPT1, and increase mitophagy genes (Parkin, PINK1, ULK1, BNIP3L, ATG5, ATG7, ATG12) to improve nonalcoholic steatohepatitis (El-Derany and AbdelHamid. 2021). Moreover, MSCs and EVs can modulate lipid metabolism by activating the AMPK signaling pathway. For example, in diet-induced obesity mice, AD-MSCs treatment inhibited ACC1 activity by increasing the expression and phosphorylation of AMPK, which in turn promoted FAO and regulated lipid metabolism disorders (Liu et al., 2016). Furthermore, human amniotic MSC-EVs significantly inhibited high-fat diet-induced obesity by inhibiting lipid synthesis, activating AMPK and increasing UCP1/PPARα/PGC1α-regulated lipid consumption (Tan et al., 2021).

It is worth noting that different tissue-derived MSCs can confer different therapeutic efficacy in ameliorating lipid metabolic disorders in diabetic animals (Ma et al., 2021). Umbilical cord Wharton's jelly (UC-MSCs) showed the strongest efficacy in reducing serum low-density lipoprotein cholesterol (LDL-C) levels, but AD-MSCs showed an very weak effect on LDL-C and substantially reduced lipid deposition in the liver (Ma et al., 2021). Moreover, lipid metabolic disturbance in diet-induced obesity mice was significantly alleviated after AD-MSC treatment but not in the UC-MSC treated group (Liu et al., 2016).

Unfortunately, few experimental studies have identified the impact of MSCs on lipid metabolism in kidney diseases. In a rat renal ischemia reperfusion model (right nephrectomy was performed and left renal ischemia lasted for 45 min) with, MSCs injection 7 days before surgery, after 48 h reperfusion, it was observed that MSCs administration induced the activation of the PPARα pathway and decreased the availability of free FAs,

which in turn prevented lipid peroxidation and attenuated renal I/R damage (Erpicum et al., 2017). Given the importance of mitochondrial function in FAO and kidney diseases (Forbes and Thorburn, 2018; Chung et al., 2019; Jiang et al., 2020), we summarize the function and mechanism of MSCs in mitochondrial homeostasis in kidney diseases below.

MSCs play a protective role in mitochondria for renal repair mainly through the following mechanisms: 1) transfer of mitochondria to damaged proximal tubular epithelial cells (Konari et al., 2019); 2) regulation of mitochondrial biogenesis by enhancing PGC1-α expression, NAD + biosynthesis, and SIRT3 activity (Perico et al., 2017); 3) inhibition of mitochondria-mediated apoptosis and mitophagy (in hexavalent chromium-injured kidney) (Yin et al., 2019); and 4) activation of mitophagy (in sepsis- and cisplatin-induced AKI) (Wang et al., 2017; Guo et al., 2021). Recent studies have indicated that MSC-EVs also have a protective effect on mitochondrial damage caused by AKI, which protects TECs against injury by reducing mitochondrial fragmentation, normalizing mitochondrial membrane potential, and reversing mitochondrial DNA deletion and oxidative phosphorylation defects (Cao et al., 2020; Zhao et al., 2021).

In conclusion, MSCs and MSC-EVs can promote FAO and regulate lipid metabolism disorders, and can also effectively improve mitochondrial dysfunction in kidney diseases. However, relatively few studies have identified the impact of MSCs on lipid metabolism in kidney diseases. Future research in this area will help deepen our understanding of the metabolic regulation mechanism of MSCs therapy for kidney diseases and help discover more potential therapeutic targets.

5 SUMMARY AND FUTURE PERSPECTIVES

In this review, we have summarized the most recent findings on the pathophysiological mechanisms of FAO in kidney diseases. The evidences demonstrates that FAO is damaged in AKI, CKD and DN, and that recovery of FAO can effectively protect against kidney dysfunction. The HIF-1, TGF-β/SMAD3, and LBK1/AMPK signaling pathways can directly or indirectly affect the expression of key FAO metabolic enzymes. In addition, PPARα, sirtuins, and microRNAs are involved in the regulation of FAO. Thus, direct regulation of the key metabolic enzymes of FAO, such as CPT1A, or increasing the activity of their regulatory factors can significantly restore FAO and promote the recovery of kidney function. The major FAO pathways involved in kidney diseases and drug targets are shown in **Figure 1**.

One of the most important issues in kidney diseases is that each nephron segment has distinct physiological characteristics, consistent with different enzyme activities, protein abundances, and substrate utilizations (Tian and Liang, 2021). Moreover, in the context of kidney diseases, disruption of the local microenvironment promptly initiates changes in cellular metabolism and phenotypic changes (Basso et al., 2021; Dumas et al., 2021). Therefore, it is very important to elaborate the dynamic changes in the cellular metabolism of different nephron segments in the process of disease development. Furthermore, AKI can have different etiologies that are conditioned by different pathophysiological mechanisms (Ronco et al., 2019). Different disease models may have different metabolic characteristics. It has been reported that metabolic alterations precede changes in serum creatinine in cisplatin-induced nephrotoxicity (Portilla et al., 2006), but whether changes in metabolites can represent a potential marker for early diagnosis and progression of kidney diseases needs to be explored further.

Moreover, emerging experimental evidence suggests that the protective effect of MSCs and MSC-EVs on kidney diseases is partly attributed to their ability to regulate energy metabolism. However, few studies have explored the relationship between MSCs and FA metabolism. Hence, additional experimental studies are warranted to deepen our understanding of the energy metabolism mechanisms of MSC therapy and to discover additional potential therapeutic targets for AKI and CKD.

AUTHOR CONTRIBUTIONS

ZG conceived and wrote the manuscript, XC revised the manuscript. Both authors approved the manuscript for publication.

FUNDING

This work was supported by the National Natural Science Foundation of China (82030025).

REFERENCES

Basso, P. J., Andrade-Oliveira, V., and Câmara, N. O. S. (2021). Targeting Immune Cell Metabolism in Kidney Diseases. *Nat. Rev. Nephrol.* 17, 465–480. doi:10.1038/s41581-021-00413-7

Bharati, J., and Jha, V. (2022). Global Kidney Health Atlas: a Spotlight on the Asia-Pacific Sector. *Kidney Res. Clin. Pract.* 41, 22–30. doi:10.23876/j.krcp.21.236

Blanquart, C., Barbier, O., Fruchart, J. C., Staels, B., and Glineur, C. (2002). Peroxisome Proliferator-Activated Receptor Alpha (PPARalpha) Turnover by the Ubiquitin-Proteasome System Controls the Ligand-Induced Expression Level of its Target Genes. *J. Biol. Chem.* 277, 37254–37259. doi:10.1074/jbc.M110598200

Boor, P., Celec, P., Martin, I. V., Villa, L., Hodosy, J., Klenovicsová, K., et al. (2011). The Peroxisome Proliferator-Activated Receptor-α Agonist, BAY PP1, Attenuates Renal Fibrosis in Rats. *Kidney Int.* 80, 1182–1197. doi:10.1038/ki.2011.254

Bougarne, N., Weyers, B., Desmet, S. J., Deckers, J., Ray, D. W., Staels, B., et al. (2018). Molecular Actions of PPARα in Lipid Metabolism and Inflammation. *Endocr. Rev.* 39, 760–802. doi:10.1210/er.2018-00064

Braissant, O., Foufelle, F., Scotto, C., Dauça, M., and Wahli, W. (1996). Differential Expression of Peroxisome Proliferator-Activated Receptors (PPARs): Tissue Distribution of PPAR-Alpha, -beta, and -gamma in the Adult Rat. *Endocrinology* 137, 354–366. doi:10.1210/endo.137.1.8536636

Cao, H., Cheng, Y., Gao, H., Zhuang, J., Zhang, W., Bian, Q., et al. (2020). *In Vivo* Tracking of Mesenchymal Stem Cell-Derived Extracellular Vesicles Improving Mitochondrial Function in Renal Ischemia-Reperfusion Injury. *ACS Nano* 14, 4014–4026. doi:10.1021/acsnano.9b08207

Chau, B. N., Xin, C., Hartner, J., Ren, S., Castano, A. P., Linn, G., et al. (2012). MicroRNA-21 Promotes Fibrosis of the Kidney by Silencing Metabolic Pathways. *Sci. Transl Med.* 4, 121ra18. doi:10.1126/scitranslmed.3003205

Chen, X. F., Tian, M. X., Sun, R. Q., Zhang, M. L., Zhou, L. S., Jin, L., et al. (2018). SIRT5 Inhibits Peroxisomal ACOX1 to Prevent Oxidative Damage and Is Downregulated in Liver Cancer. *EMBO Rep.* 19. e45124. doi:10.15252/embr.201745124

Chen, Y., Dai, Y., Song, K., Huang, Y., Zhang, L., Zhang, C., et al. (2021). Preemptive Pharmacological Inhibition of Fatty Acid-Binding Protein 4 Attenuates Kidney Fibrosis by Reprogramming Tubular Lipid Metabolism. *Cell Death Dis* 12, 572. doi:10.1038/s41419-021-03850-1

Chen, Y., Yan, Q., Lv, M., Song, K., Dai, Y., Huang, Y., et al. (2020). Involvement of FATP2-Mediated Tubular Lipid Metabolic Reprogramming in Renal Fibrogenesis. *Cel Death Dis* 11, 994. doi:10.1038/s41419-020-03199-x

Chiba, T., Peasley, K. D., Cargill, K. R., Maringer, K. V., Bharathi, S. S., Mukherjee, E., et al. (2019). Sirtuin 5 Regulates Proximal Tubule Fatty Acid Oxidation to Protect against AKI. *J. Am. Soc. Nephrol.* 30, 2384–2398. doi:10.1681/ASN.2019020163

Chung, K. W., Dhillon, P., Huang, S., Sheng, X., Shrestha, R., Qiu, C., et al. (2019). Mitochondrial Damage and Activation of the STING Pathway Lead to Renal Inflammation and Fibrosis. *Cell Metab* 30, 784–e5. doi:10.1016/j.cmet.2019.08.003

Chung, K. W., Ha, S., Kim, S. M., Kim, D. H., An, H. J., Lee, E. K., et al. (2020). Pparα/β Activation Alleviates Age-Associated Renal Fibrosis in Sprague Dawley Rats. *J. Gerontol. A. Biol. Sci. Med. Sci.* 75, 452–458. doi:10.1093/gerona/glz083

Chung, K. W., Lee, E. K., Lee, M. K., Oh, G. T., Yu, B. P., and Chung, H. Y. (2018). Impairment of PPARα and the Fatty Acid Oxidation Pathway Aggravates Renal Fibrosis during Aging. *J. Am. Soc. Nephrol.* 29, 1223–1237. doi:10.1681/ASN.2017070802

Coburn, C. T., Knapp, F. F., Jr., Febbraio, M., Beets, A. L., Silverstein, R. L., and Abumrad, N. A. (2000). Defective Uptake and Utilization of Long Chain Fatty Acids in Muscle and Adipose Tissues of CD36 Knockout Mice. *J. Biol. Chem.* 275, 32523–32529. doi:10.1074/jbc.M003826200

Du, W., Zhang, L., Brett-Morris, A., Aguila, B., Kerner, J., Hoppel, C. L., et al. (2017). HIF Drives Lipid Deposition and Cancer in ccRCC via Repression of Fatty Acid Metabolism. *Nat. Commun.* 8, 1769. doi:10.1038/s41467-017-01965-8

Dumas, S. J., Meta, E., Borri, M., Luo, Y., Li, X., Rabelink, T. J., et al. (2021). Phenotypic Diversity and Metabolic Specialization of Renal Endothelial Cells. *Nat. Rev. Nephrol.* 17, 441–464. doi:10.1038/s41581-021-00411-9

El-Derany, M. O., and AbdelHamid, S. G. (2021). Upregulation of miR-96-5p by Bone Marrow Mesenchymal Stem Cells and Their Exosomes Alleviate Non-alcoholic Steatohepatitis: Emphasis on Caspase-2 Signaling Inhibition. *Biochem. Pharmacol.* 190, 114624. doi:10.1016/j.bcp.2021.114624

Erpicum, P., Rowart, P., Poma, L., Krzesinski, J. M., Detry, O., and Jouret, F. (2017). Administration of Mesenchymal Stromal Cells before Renal Ischemia/reperfusion Attenuates Kidney Injury and May Modulate Renal Lipid Metabolism in Rats. *Sci. Rep.* 7, 8687. doi:10.1038/s41598-017-08726-z

Fierro-Fernández, M., Miguel, V., Márquez-Expósito, L., Nuevo-Tapioles, C., Herrero, J. I., Blanco-Ruiz, E., et al. (2020). MiR-9-5p Protects from Kidney Fibrosis by Metabolic Reprogramming. *FASEB J.* 34, 410–431. doi:10.1096/fj.201901599RR

Forbes, J. M., and Thorburn, D. R. (2018). Mitochondrial Dysfunction in Diabetic Kidney Disease. *Nat. Rev. Nephrol.* 14, 291–312. doi:10.1038/nrneph.2018.9

Fransen, M., Lismont, C., and Walton, P. (2017). The Peroxisome-Mitochondria Connection: How and Why? *Int. J. Mol. Sci.* 18. 1126. doi:10.3390/ijms18061126

Garcia, D., and Shaw, R. J. (2017). AMPK: Mechanisms of Cellular Energy Sensing and Restoration of Metabolic Balance. *Mol. Cel* 66, 789–800. doi:10.1016/j.molcel.2017.05.032

Gomez, I. G., MacKenna, D. A., Johnson, B. G., Kaimal, V., Roach, A. M., Ren, S., et al. (2015). Anti-microRNA-21 Oligonucleotides Prevent Alport Nephropathy Progression by Stimulating Metabolic Pathways. *J. Clin. Invest.* 125, 141–156. doi:10.1172/JCI75852

Guo, J., Wang, R., and Liu, D. (2021). Bone Marrow-Derived Mesenchymal Stem Cells Ameliorate Sepsis-Induced Acute Kidney Injury by Promoting Mitophagy of Renal Tubular Epithelial Cells via the SIRT1/Parkin Axis. *Front. Endocrinol. (Lausanne)* 12, 639165. doi:10.3389/fendo.2021.639165

Han, J., Qu, H., Han, M., Ding, Y., Xie, M., Hu, J., et al. (2021). MSC-induced lncRNA AGAP2-AS1 Promotes Stemness and Trastuzumab Resistance through Regulating CPT1 Expression and Fatty Acid Oxidation in Breast Cancer. *Oncogene* 40, 833–847. doi:10.1038/s41388-020-01574-8

Han, S. H., Malaga-Dieguez, L., Chinga, F., Kang, H. M., Tao, J., Reidy, K., et al. (2016). Deletion of Lkb1 in Renal Tubular Epithelial Cells Leads to CKD by Altering Metabolism. *J. Am. Soc. Nephrol.* 27, 439–453. doi:10.1681/ASN.2014121181

He, A., Dean, J. M., and Lodhi, I. J. (2021). Peroxisomes as Cellular Adaptors to Metabolic and Environmental Stress. *Trends Cel Biol.* 31, 656–670. doi:10.1016/j.tcb.2021.02.005

Hirschey, M. D., Shimazu, T., Goetzman, E., Jing, E., Schwer, B., Lombard, D. B., et al. (2010). SIRT3 Regulates Mitochondrial Fatty-Acid Oxidation by Reversible Enzyme Deacetylation. *Nature* 464, 121–125. doi:10.1038/nature08778

Hou, Y., Wang, Q., Han, B., Chen, Y., Qiao, X., and Wang, L. (2021). CD36 Promotes NLRP3 Inflammasome Activation via the mtROS Pathway in Renal Tubular Epithelial Cells of Diabetic Kidneys. *Cel Death Dis* 12, 523. doi:10.1038/s41419-021-03813-6

Hou, Y., Wu, M., Wei, J., Ren, Y., Du, C., Wu, H., et al. (2015). CD36 Is Involved in High Glucose-Induced Epithelial to Mesenchymal Transition in Renal Tubular Epithelial Cells. *Biochem. Biophys. Res. Commun.* 468, 281–286. doi:10.1016/j.bbrc.2015.10.112

Huang, R., Shi, M., Guo, F., Feng, Y., Feng, Y., Liu, J., et al. (2018). Pharmacological Inhibition of Fatty Acid-Binding Protein 4 (FABP4) Protects against Rhabdomyolysis-Induced Acute Kidney Injury. *Front. Pharmacol.* 9, 917. doi:10.3389/fphar.2018.00917

Jäger, S., Handschin, C., St-Pierre, J., and Spiegelman, B. M. (2007). AMP-activated Protein Kinase (AMPK) Action in Skeletal Muscle via Direct Phosphorylation of PGC-1alpha. *Proc. Natl. Acad. Sci. U S A.* 104, 12017–12022. doi:10.1073/pnas.0705070104

Jang, H. S., Noh, M. R., Jung, E. M., Kim, W. Y., Southekal, S., Guda, C., et al. (2020). Proximal Tubule Cyclophilin D Regulates Fatty Acid Oxidation in Cisplatin-Induced Acute Kidney Injury. *Kidney Int.* 97, 327–339. doi:10.1016/j.kint.2019.08.019

Jao, T. M., Nangaku, M., Wu, C. H., Sugahara, M., Saito, H., Maekawa, H., et al. (2019). ATF6α Downregulation of PPARα Promotes Lipotoxicity-Induced Tubulointerstitial Fibrosis. *Kidney Int.* 95, 577–589. doi:10.1016/j.kint.2018.09.023

Jeon, S. M., Chandel, N. S., and Hay, N. (2012). AMPK Regulates NADPH Homeostasis to Promote Tumour Cell Survival during Energy Stress. *Nature* 485, 661–665. doi:10.1038/nature11066

Jiang, M., Bai, M., Lei, J., Xie, Y., Xu, S., Jia, Z., et al. (2020). Mitochondrial Dysfunction and the AKI to CKD Transition. *Am. J. Physiol. Ren. Physiol* 319, F1105–F1116. doi:10.1152/ajprenal.00285.2020

Jung, J. H., Choi, J. E., Song, J. H., and Ahn, S. H. (2018). Human CD36 Overexpression in Renal Tubules Accelerates the Progression of Renal Diseases in a Mouse Model of Folic Acid-Induced Acute Kidney Injury. *Kidney Res. Clin. Pract.* 37, 30–40. doi:10.23876/j.krcp.2018.37.1.30

Kamijo-Ikemori, A., Sugaya, T., Matsui, K., Yokoyama, T., and Kimura, K. (2011). Roles of Human Liver Type Fatty Acid Binding Protein in Kidney Disease Clarified Using hL-FABP Chromosomal Transgenic Mice. *Nephrology (Carlton)* 16, 539–544. doi:10.1111/j.1440-1797.2011.01469.x

Kang, H. M., Ahn, S. H., Choi, P., Ko, Y. A., Han, S. H., Chinga, F., et al. (2015). Defective Fatty Acid Oxidation in Renal Tubular Epithelial Cells Has a Key Role in Kidney Fibrosis Development. *Nat. Med.* 21, 37–46. doi:10.1038/nm.3762

Ke, Q., Yuan, Q., Qin, N., Shi, C., Luo, J., Fang, Y., et al. (2020). UCP2-induced Hypoxia Promotes Lipid Accumulation and Tubulointerstitial Fibrosis during Ischemic Kidney Injury. *Cel Death Dis* 11, 26. doi:10.1038/s41419-019-2219-4

Khan, S., Cabral, P. D., Schilling, W. P., Schmidt, Z. W., Uddin, A. N., Gingras, A., et al. (2018). Kidney Proximal Tubule Lipoapoptosis Is Regulated by Fatty Acid Transporter-2 (FATP2). *J. Am. Soc. Nephrol.* 29, 81–91. doi:10.1681/ASN.2017030314

Khan, S., Gaivin, R., Abramovich, C., Boylan, M., Calles, J., and Schelling, J. R. (2020). Fatty Acid Transport Protein-2 Regulates Glycemic Control and Diabetic Kidney Disease Progression. *JCI Insight* 5. e136845. doi:10.1172/jci.insight.136845

Konari, N., Nagaishi, K., Kikuchi, S., and Fujimiya, M. (2019). Mitochondria Transfer from Mesenchymal Stem Cells Structurally and Functionally Repairs Renal Proximal Tubular Epithelial Cells in Diabetic Nephropathy *In Vivo*. *Sci. Rep.* 9, 5184. doi:10.1038/s41598-019-40163-y

Lee, J., Hyon, J. Y., Min, J. Y., Huh, Y. H., Kim, H. J., Lee, H., et al. (2020). Mitochondrial Carnitine Palmitoyltransferase 2 Is Involved in Nε-(carboxymethyl)-Lysine-Mediated Diabetic Nephropathy. *Pharmacol. Res.* 152, 104600. doi:10.1016/j.phrs.2019.104600

Lee, M., Katerelos, M., Gleich, K., Galic, S., Kemp, B. E., Mount, P. F., et al. (2018). Phosphorylation of Acetyl-CoA Carboxylase by AMPK Reduces Renal Fibrosis and Is Essential for the Anti-fibrotic Effect of Metformin. *J. Am. Soc. Nephrol.* 29, 2326–2336. doi:10.1681/ASN.2018010050

Li, B., Cheng, Y., Yu, S., Zang, L., Yin, Y., Liu, J., et al. (2019a). Human Umbilical Cord-Derived Mesenchymal Stem Cell Therapy Ameliorates Nonalcoholic Fatty Liver Disease in Obese Type 2 Diabetic Mice. *Stem Cell Int* 2019, 8628027. doi:10.1155/2019/8628027

Li, B., Hao, J., Zeng, J., and Sauter, E. R. (2020a). SnapShot: FABP Functions. *Cell* 182, 1066–e1. doi:10.1016/j.cell.2020.07.027

Li, J., Yang, Y., Li, Q., Wei, S., Zhou, Y., Yu, W., et al. (2022). STAT6 Contributes to Renal Fibrosis by Modulating PPARα-Mediated Tubular Fatty Acid Oxidation. *Cel Death Dis* 13, 66. doi:10.1038/s41419-022-04515-3

Li, J. K., Yang, C., Su, Y., Luo, J. C., Luo, M. H., Huang, D. L., et al. (2021a). Mesenchymal Stem Cell-Derived Extracellular Vesicles: A Potential Therapeutic Strategy for Acute Kidney Injury. *Front. Immunol.* 12, 684496. doi:10.3389/fimmu.2021.684496

Li, L., Tao, S., Guo, F., Liu, J., Huang, R., Tan, Z., et al. (2021b). Genetic and Pharmacological Inhibition of Fatty Acid-Binding Protein 4 Alleviated Inflammation and Early Fibrosis after Toxin Induced Kidney Injury. *Int. Immunopharmacol* 96, 107760. doi:10.1016/j.intimp.2021.107760

Li, M., Li, C. M., Ye, Z. C., Huang, J., Li, Y., Lai, W., et al. (2020b). Sirt3 Modulates Fatty Acid Oxidation and Attenuates Cisplatin-Induced AKI in Mice. *J. Cel Mol Med* 24, 5109–5121. doi:10.1111/jcmm.15148

Li, S., Wu, P., Yarlagadda, P., Vadjunec, N. M., Proia, A. D., Harris, R. A., et al. (2004). PPAR Alpha Ligand Protects during Cisplatin-Induced Acute Renal Failure by Preventing Inhibition of Renal FAO and PDC Activity. *Am. J. Physiol. Ren. Physiol* 286, F572–F580. doi:10.1152/ajprenal.00190.2003

Li, X., Zhang, T., Geng, J., Wu, Z., Xu, L., Liu, J., et al. (2019b). Advanced Oxidation Protein Products Promote Lipotoxicity and Tubulointerstitial Fibrosis via CD36/β-Catenin Pathway in Diabetic Nephropathy. *Antioxid. Redox Signal.* 31, 521–538. doi:10.1089/ars.2018.7634

Libby, A. E., Jones, B., Lopez-Santiago, I., Rowland, E., and Levi, M. (2021). Nuclear Receptors in the Kidney during Health and Disease. *Mol. Aspects Med.* 78, 100935. doi:10.1016/j.mam.2020.100935

Lin, S. C., and Hardie, D. G. (2018). AMPK: Sensing Glucose as Well as Cellular Energy Status. *Cel Metab* 27, 299–313. doi:10.1016/j.cmet.2017.10.009

Liu, G. Y., Liu, J., Wang, Y. L., Liu, Y., Shao, Y., Han, Y., et al. (2016). Adipose-Derived Mesenchymal Stem Cells Ameliorate Lipid Metabolic Disturbance in Mice. *Stem Cell Transl Med* 5, 1162–1170. doi:10.5966/sctm.2015-0239

Lodhi, I. J., and Semenkovich, C. F. (2014). Peroxisomes: a Nexus for Lipid Metabolism and Cellular Signaling. *Cel Metab* 19, 380–392. doi:10.1016/j.cmet.2014.01.002

Ma, Y., Wang, L., Yang, S., Liu, D., Zeng, Y., Lin, L., et al. (2021). The Tissue Origin of Human Mesenchymal Stem Cells Dictates Their Therapeutic Efficacy on Glucose and Lipid Metabolic Disorders in Type II Diabetic Mice. *Stem Cel Res Ther* 12, 385. doi:10.1186/s13287-021-02463-x

Maatman, R. G., Van Kuppevelt, T. H., and Veerkamp, J. H. (1991). Two Types of Fatty Acid-Binding Protein in Human Kidney. Isolation, Characterization and Localization. *Biochem. J.* 273 (Pt 3), 759–766. doi:10.1042/bj2730759

Manabe, K., Kamihata, H., Motohiro, M., Senoo, T., Yoshida, S., and Iwasaka, T. (2012). Urinary Liver-type Fatty Acid-Binding Protein Level as a Predictive Biomarker of Contrast-Induced Acute Kidney Injury. *Eur. J. Clin. Invest.* 42, 557–563. doi:10.1111/j.1365-2362.2011.02620.x

Miguel, V., Ramos, R., García-Bermejo, L., Rodríguez-Puyol, D., and Lamas, S. (2021a). The Program of Renal Fibrogenesis Is Controlled by microRNAs Regulating Oxidative Metabolism. *Redox Biol.* 40, 101851. doi:10.1016/j.redox.2020.101851

Miguel, V., Tituaña, J., Herrero, J. I., Herrero, L., Serra, D., Cuevas, P., et al. (2021b). Renal Tubule Cpt1a Overexpression Protects from Kidney Fibrosis by Restoring Mitochondrial Homeostasis. *J. Clin. Invest.* 131. e140695. doi:10.1172/JCI140695

Montaigne, D., Butruille, L., and Staels, B. (2021). PPAR Control of Metabolism and Cardiovascular Functions. *Nat. Rev. Cardiol.* 18, 809–823. doi:10.1038/s41569-021-00569-6

Naji, A., Eitoku, M., Favier, B., Deschaseaux, F., Rouas-Freiss, N., and Suganuma, N. (2019). Biological Functions of Mesenchymal Stem Cells and Clinical Implications. *Cell Mol Life Sci* 76, 3323–3348. doi:10.1007/s00018-019-03125-1

Narravula, S., and Colgan, S. P. (2001). Hypoxia-inducible Factor 1-mediated Inhibition of Peroxisome Proliferator-Activated Receptor Alpha Expression during Hypoxia. *J. Immunol.* 166, 7543–7548. doi:10.4049/jimmunol.166.12.7543

Negishi, K., Noiri, E., Maeda, R., Portilla, D., Sugaya, T., and Fujita, T. (2008). Renal L-type Fatty Acid-Binding Protein Mediates the Bezafibrate Reduction of Cisplatin-Induced Acute Kidney Injury. *Kidney Int.* 73, 1374–1384. doi:10.1038/ki.2008.106

Nieth, H., and Schollmeyer, P. (1966). Substrate-utilization of the Human Kidney. *Nature* 209, 1244–1245. doi:10.1038/2091244a0

Okamura, D. M., López-Guisa, J. M., Koelsch, K., Collins, S., and Eddy, A. A. (2007). Atherogenic Scavenger Receptor Modulation in the Tubulointerstitium in Response to Chronic Renal Injury. *Am. J. Physiol. Ren. Physiol* 293, F575–F585. doi:10.1152/ajprenal.00063.2007

Okamura, D. M., Pennathur, S., Pasichnyk, K., López-Guisa, J. M., Collins, S., Febbraio, M., et al. (2009). CD36 Regulates Oxidative Stress and Inflammation in Hypercholesterolemic CKD. *J. Am. Soc. Nephrol.* 20, 495–505. doi:10.1681/ASN.2008010009

Peng, L., Chen, Y., Shi, S., and Wen, H. (2022). Stem Cell-Derived and Circulating Exosomal microRNAs as New Potential Tools for Diabetic Nephropathy Management. *Stem Cel Res Ther* 13, 25. doi:10.1186/s13287-021-02696-w

Pennathur, S., Pasichnyk, K., Bahrami, N. M., Zeng, L., Febbraio, M., Yamaguchi, I., et al. (2015). The Macrophage Phagocytic Receptor CD36 Promotes Fibrogenic Pathways on Removal of Apoptotic Cells during Chronic Kidney Injury. *Am. J. Pathol.* 185, 2232–2245. doi:10.1016/j.ajpath.2015.04.016

Perico, L., Morigi, M., Rota, C., Breno, M., Mele, C., Noris, M., et al. (2017). Human Mesenchymal Stromal Cells Transplanted into Mice Stimulate Renal Tubular Cells and Enhance Mitochondrial Function. *Nat. Commun.* 8, 983. doi:10.1038/s41467-017-00937-2

Petrillo, F., Iervolino, A., Zacchia, M., Simeoni, A., Masella, C., Capolongo, G., et al. (2017). MicroRNAs in Renal Diseases: A Potential Novel Therapeutic Target. *Kidney Dis. (Basel)* 3, 111–119. doi:10.1159/000481730

Portilla, D., Dai, G., McClure, T., Bates, L., Kurten, R., Megyesi, J., et al. (2002). Alterations of PPARalpha and its Coactivator PGC-1 in Cisplatin-Induced Acute Renal Failure. *Kidney Int.* 62, 1208–1218. doi:10.1111/j.1523-1755.2002.kid553.x

Portilla, D., Dai, G., Peters, J. M., Gonzalez, F. J., Crew, M. D., and Proia, A. D. (2000). Etomoxir-induced PPARalpha-Modulated Enzymes Protect during Acute Renal Failure. *Am. J. Physiol. Ren. Physiol* 278, F667–F675. doi:10.1152/ajprenal.2000.278.4.F667

Portilla, D., Li, S., Nagothu, K. K., Megyesi, J., Kaissling, B., Schnackenberg, L., et al. (2006). Metabolomic Study of Cisplatin-Induced Nephrotoxicity. *Kidney Int.* 69, 2194–2204. doi:10.1038/sj.ki.5000433

Ronco, C., Bellomo, R., and Kellum, J. A. (2019). Acute Kidney Injury. *Lancet* 394, 1949–1964. doi:10.1016/S0140-6736(19)32563-2

Rong, Q., Han, B., Li, Y., Yin, H., Li, J., and Hou, Y. (2021). Berberine Reduces Lipid Accumulation by Promoting Fatty Acid Oxidation in Renal Tubular Epithelial Cells of the Diabetic Kidney. *Front. Pharmacol.* 12, 729384. doi:10.3389/fphar.2021.729384

Sadhukhan, S., Liu, X., Ryu, D., Nelson, O. D., Stupinski, J. A., Li, Z., et al. (2016). Metabolomics-assisted Proteomics Identifies Succinylation and SIRT5 as Important Regulators of Cardiac Function. *Proc. Natl. Acad. Sci. U S A.* 113, 4320–4325. doi:10.1073/pnas.1519858113

Sekiguchi, K., Tian, Q., Ishiyama, M., Burchfield, J., Gao, F., Mann, D. L., et al. (2007). Inhibition of PPAR-Alpha Activity in Mice with Cardiac-Restricted Expression of Tumor Necrosis Factor: Potential Role of TGF-beta/Smad3. *Am. J. Physiol. Heart Circ. Physiol.* 292, H1443–H1451. doi:10.1152/ajpheart.01056.2006

Staels, B., Dallongeville, J., Auwerx, J., Schoonjans, K., Leitersdorf, E., and Fruchart, J. C. (1998). Mechanism of Action of Fibrates on Lipid and Lipoprotein Metabolism. *Circulation* 98, 2088–2093. doi:10.1161/01.cir.98.19.2088

Storch, J., and McDermott, L. (2009). Structural and Functional Analysis of Fatty Acid-Binding Proteins. *J. Lipid Res.* 50 (Suppl. l), S126–S131. doi:10.1194/jlr.R800084-JLR200

Susztak, K., Ciccone, E., McCue, P., Sharma, K., and Böttinger, E. P. (2005). Multiple Metabolic Hits Converge on CD36 as Novel Mediator of Tubular Epithelial Apoptosis in Diabetic Nephropathy. *Plos Med.* 2, e45. doi:10.1371/journal.pmed.0020045

Tan, H. L., Guan, X. H., Hu, M., Wu, J., Li, R. Z., Wang, L. F., et al. (2021). Human Amniotic Mesenchymal Stem Cells-Conditioned Medium Protects Mice from High-Fat Diet-Induced Obesity. *Stem Cel Res Ther* 12, 364. doi:10.1186/s13287-021-02437-z

Tan, Z., Guo, F., Huang, Z., Xia, Z., Liu, J., Tao, S., et al. (2019). Pharmacological and Genetic Inhibition of Fatty Acid-Binding Protein 4 Alleviated Cisplatin-Induced Acute Kidney Injury. *J. Cel Mol Med* 23, 6260–6270. doi:10.1111/jcmm.14512

Tian, Z., and Liang, M. (2021). Renal Metabolism and Hypertension. *Nat. Commun.* 12, 963. doi:10.1038/s41467-021-21301-5

Tran, M. T., Zsengeller, Z. K., Berg, A. H., Khankin, E. V., Bhasin, M. K., Kim, W., et al. (2016). PGC1α Drives NAD Biosynthesis Linking Oxidative Metabolism to Renal protection. *Nature* 531, 528–532. doi:10.1038/nature17184

Vasko, R. (2016). Peroxisomes and Kidney Injury. *Antioxid. Redox Signal.* 25, 217–231. doi:10.1089/ars.2016.6666

Vega, R. B., Huss, J. M., and Kelly, D. P. (2000). The Coactivator PGC-1 Cooperates with Peroxisome Proliferator-Activated Receptor Alpha in Transcriptional Control of Nuclear Genes Encoding Mitochondrial Fatty Acid Oxidation Enzymes. *Mol. Cel Biol* 20, 1868–1876. doi:10.1128/mcb.20.5.1868-1876.2000

Wang, B., Jia, H., Zhang, B., Wang, J., Ji, C., Zhu, X., et al. (2017). Pre-incubation with hucMSC-Exosomes Prevents Cisplatin-Induced Nephrotoxicity by Activating Autophagy. *Stem Cel Res Ther* 8, 75. doi:10.1186/s13287-016-0463-4

Wu, H., Liu, B., Chen, Z., Li, G., and Zhang, Z. (2020). MSC-induced lncRNA HCP5 Drove Fatty Acid Oxidation through miR-3619-5p/AMPK/PGC1α/CEBPB axis to Promote Stemness and Chemo-Resistance of Gastric Cancer. *Cel Death Dis* 11, 233. doi:10.1038/s41419-020-2426-z

Xiong, W., Xiong, Z., Song, A., Lei, C., Ye, C., and Zhang, C. (2021). Relieving Lipid Accumulation through UCP1 Suppresses the Progression of Acute Kidney Injury by Promoting the AMPK/ULK1/autophagy Pathway. *Theranostics* 11, 4637–4654. doi:10.7150/thno.56082

Xu, Y., Xie, Y., Shao, X., Ni, Z., and Mou, S. (2015). L-FABP: A Novel Biomarker of Kidney Disease. *Clin. Chim. Acta* 445, 85–90. doi:10.1016/j.cca.2015.03.017

Yadav, H., Quijano, C., Kamaraju, A. K., Gavrilova, O., Malek, R., Chen, W., et al. (2011). Protection from Obesity and Diabetes by Blockade of TGF-β/Smad3 Signaling. *Cel Metab* 14, 67–79. doi:10.1016/j.cmet.2011.04.013

Yea, J. H., Yoon, Y. M., Lee, J. H., Yun, C. W., and Lee, S. H. (2021). Exosomes Isolated from Melatonin-Stimulated Mesenchymal Stem Cells Improve Kidney Function by Regulating Inflammation and Fibrosis in a Chronic Kidney Disease Mouse Model. *J. Tissue Eng.* 12, 20417314211059624. doi:10.1177/20417314211059624

Yin, F., Yan, J., Zhao, Y., Guo, K. J., Zhang, Z. L., Li, A. P., et al. (2019). Bone Marrow Mesenchymal Stem Cells Repair Cr (VI)- Injured Kidney by Regulating Mitochondria-Mediated Apoptosis and Mitophagy Mediated via the MAPK Signaling Pathway. *Ecotoxicol Environ. Saf.* 176, 234–241. doi:10.1016/j.ecoenv.2019.03.093

Zhao, M., Liu, S., Wang, C., Wang, Y., Wan, M., Liu, F., et al. (2021). Mesenchymal Stem Cell-Derived Extracellular Vesicles Attenuate Mitochondrial Damage and Inflammation by Stabilizing Mitochondrial DNA. *ACS Nano* 15, 1519–1538. doi:10.1021/acsnano.0c08947

Zhou, T., Yuan, Z., Weng, J., Pei, D., Du, X., He, C., et al. (2021). Challenges and Advances in Clinical Applications of Mesenchymal Stromal Cells. *J. Hematol. Oncol.* 14, 24. doi:10.1186/s13045-021-01037-x

Conflict of Interest: The authors declare that the research was conducted in the absence of any commercial or financial relationships that could be construed as a potential conflict of interest.

frontiers | Frontiers in Pharmacology

ORIGINAL RESEARCH
published: 21 April 2022
doi: 10.3389/fphar.2022.820130

The Ameliorative Effect of Mahuang Fuzi and Shenzhuo Decoction on Membranous Nephropathy of Rodent Model is Associated With Autophagy and Wnt/β-Catenin Pathway

Yu Gao[1,2†], Haoran Dai[3†], Na Zhang[1,2], Hanxue Jiang[1], Zihan Zhang[1,4], Zhendong Feng[5], Zhaocheng Dong[1,4], Wenbin Liu[1,4], Fei Liu[1,4], Xuan Dong[1,2], Qihan Zhao[1,4], Xiaoshan Zhou[1,4], Jieli Du[1,4], Naiqian Zhang[1,4], Hongliang Rui[1,6] and Baoli Liu[1]**

[1]Beijing Hospital of Traditional Chinese Medicine, Capital Medical University, Beijing, China, [2]School of Traditional Chinese Medicine, Capital Medical University, Beijing, China, [3]Shunyi Branch, Beijing Hospital of Traditional Chinese Medicine, Beijing, China, [4]School of Life Sciences, Beijing University of Chinese Medicine, Beijing, China, [5]Pinggu Hospital, Beijing Hospital of Traditional Chinese Medicine, Beijing, China, [6]Beijing Institute of Chinese Medicine, Beijing, China

The increased incidence of membranous nephropathy (MN) has made it the most common pathological type of primary nephrotic syndrome in adults in China. According to the theory of Traditional Chinese Medicine (TCM), Mahuang Fuzi (Chinese ephedra and Radix Aconiti Lateralis Preparata) and Shenzhuo Decoction (MFSD) could be used to treat such diseases. We treated patients of MN with MFSD, and observed comparable efficacy to glucocorticoid and/or immunosuppressants. In this study, we observed the therapeutic effect of MFSD on the rat model of passive Heymann nephritis (PHN), a classical MN model. Our results showed that MFSD treatment significantly reduced urinary protein level and podocyte injury in PHN rats, and correspondingly improved renal pathology, with the improvement effect on MN comparable to that of Cyclosporine A (CsA) alone. To explore the potential therapeutical mechanism of MFSD, the main chemical components of MFSD were determined by High-performance liquid chromatography-mass spectrometry (HPLC-MS). There were about 30 active components of MFSD. Next, based on network pharmacology methods, we screened related targets of MSFD on MN, which provided a preliminary understanding of the MFSD bioactive compounds. The clustering analysis showed that its active site might be in the autophagy-related protein and Wnt/β-catenin pathway, which was related to podocyte injury. Finally, we observed an improvement in renal autophagy and a down-regulation of the Wnt/β-catenin pathway after MSFD treatment in a PHN rat model. According to this study, autophagy and Wnt/β-catenin pathway may be potential targets for MFSD in the treatment of MN.

Keywords: mahuang fuzi and shenzhuo decoction, podocyte injury, autophagy, wnt/β-catenin, membranous nephropathy

OPEN ACCESS

Edited by:
Zhiyong Guo,
Second Military Medical University, China

Reviewed by:
Bin Yang,
University of Leicester, United Kingdom
Yuhua Ma,
Kunshan Traditional Chinese Medicine Hospital, China

***Correspondence:**
Baoli Liu
liubaoli@bjzhongyi.com
Hongliang Rui
ruihongliang@bjzhongyi.com

†These authors have contributed equally to this work

Specialty section:
This article was submitted to Renal Pharmacology, a section of the journal Frontiers in Pharmacology

Received: *22 November 2021*
Accepted: *17 March 2022*
Published: *21 April 2022*

Citation:
Gao Y, Dai H, Zhang N, Jiang H, Zhang Z, Feng Z, Dong Z, Liu W, Liu F, Dong X, Zhao Q, Zhou X, Du J, Zhang N, Rui H and Liu B (2022) The Ameliorative Effect of Mahuang Fuzi and Shenzhuo Decoction on Membranous Nephropathy of Rodent Model is Associated With Autophagy and Wnt/β-Catenin Pathway. Front. Pharmacol. 13:820130. doi: 10.3389/fphar.2022.820130

INTRODUCTION

Membranous nephropathy (MN) is an immune-mediated glomerular disease whose pathological characteristics are the immune deposits under the glomerular capillary epithelium and thereby the diffuse thickening of the basement membrane. It is a major cause of non-diabetic nephrotic syndrome (Liu et al., 2019). In China, the incidence of MN has been increasing year by year, and the detection rate of MN in elderly patients over 60 years old with nephrotic syndrome was 67. 3% (Xu et al., 2016; Xiong et al., 2020). At present, the common background medications for MN are glucocorticoids, cyclophosphamide, calcineurin inhibitors (CNIs), and rituximab. However, high recurrence rate and low complete remission rate still exist, and the side effects such as infection caused by immunosuppression need to be overcome (von Mering et al., 2003; Qiu et al., 2017). The herbs can effectively improve membranous nephropathy (Ahmed et al., 2007; Liu et al., 2019; Tian et al., 2019) *via* this multi-target treatment of membranous nephropathy. Herein, it is possible to treat MN by repairing the function of podocytes (Feng et al., 2020).

Network pharmacology is a developing paradigm that uses multi-disciplinary technologies such as system biology, multi-directional pharmacology, computational biology, and network analysis to expose the fundamental molecular targets and pharmacodynamics methods of TCM in a systematic manner (Hopkins, 2008; Li and Zhang, 2013). Using multiple technologies, such as Omics technology, high-throughput screening, network visualization, or network analysis, the multi-level association between "drug-compound-target pathway-disease" was established using this approach. Understanding the molecular foundation of disease, predicting the pharmacological mechanism, and identifying herbal substances with high efficacy and minimal toxicity were all provided as inspirations.

Mahuang Fuzi and Shenzhuo Decoction (MFSD), as a classic prescription in Treatise on Febrile Diseases used clinically for 1800 years, consists of 6 kinds of Chinese herbs, namely ephedra, aconite, dried ginger, poria cotta, atractylodes, and licorice. These ingredients have been reported in the literature for kidney disease treatment (Tan et al., 2014; Liu et al., 2019; Dai et al., 2020). MFSD activates podocyte autophagy by inhibiting activation of the Wnt/β-catenin signaling pathway and alleviates hyperglycemia-induced podocyte injury (Dai et al., 2020). According to the TCM theory, MFSD can treat MN through warming yang and resolving exterior methods. No study has been conducted on the treatment of membranous nephropathy with MFSD. However, in our previous clinical trials, the efficacy of MFSD in the treatment of membranous nephropathy has been observed, but the mechanism is still unclear (Dong et al., 2021).

The Wnt/β-catenin pathway influences different nephritic-related diseases, renal fibrosis, acute renal failure, and ischemic injury (Kawakami et al., 2013). Activation of the Wnt/β-catenin pathway has been found in the glomeruli of both FSGS and diabetic nephropathy patients, damaging podocytes and leading to proteinuria formation (Dai et al., 2009; Kato et al., 2011). Activation of the Wnt/β-catenin pathway and inhibition of autophagy could also be observed in high-glycemic podocytes (Dai et al., 2020). Insufficient autophagy of podocytes can be observed in podocyte disease (Liu et al., 2017; Jin et al., 2018; Li et al., 2021). According to previous studies, C5b-9 blocks the lysosome-dependent autophagy pathway, leading to podocyte injury (Liu et al., 2017). It can be seen that podocyte autophagy is down-regulated in MN. Autophagy is also regulated by various mechanisms, including the Wnt/β-catenin pathway (Petherick et al., 2013; Kühn et al., 2015; Zhou et al., 2019; Yun et al., 2020). In our previous studies, changes in the Wnt/β-catenin pathway and autophagy in podocytes incubated with C5b-9 were observed, but it was unclear whether MFSD could improve MN through the Wnt/β-catenin pathway and regulate autophagy.

In this study, passive Heymann nephritis (PHN) model was used to observe the therapeutic effect of MFSD on MN rodent model, and a deliberate strategy integrating network pharmacology and pharmacodynamics methods was employed to investigate the potential target of MFSD for the MN treatment.

MATERIALS AND METHODS

Animals and Model Establishment

Sprague-Dawley (SD) rats in special pathogen-free (SPF) levels were fed adaptively for 3 days before animal experiments. Beijing Huafukang Biotechnology Co., Ltd. provided the rats (No. SCXK Jing 2016–0,002) and housed them at the Beijing Institute of Chinese medicine. All experiments were conducted following the internationally recognized standard guidelines for using animals and were reviewed and approved by the Experimental Animal Welfare Ethics Committee of the Beijing Institute of Chinese Medicine (Ethics No. 2019060103). Thirty-two male SD rats weighing between 150 and 180 g were raised under standard environmental conditions (21 ± 2°C, 55 ± 5% humidity, 12 h/12 h light/dark cycle in SPF condition) and offered with free water and standard laboratory diet.

Eight rats in the normal group were injected intravenously with normal saline 0.5 ml/100g, while the rest were intravenously injected with anti-Fx1A Serum (Probetex, Beijing, China) 0.5 ml/100 g once. After 1 week, the 24 h urine proteinuria was detected, proving the success of the model. Then, the successful model rats were further randomly divided into three groups: model group, MFSD group, and Cyclosporine A (CsA, Huadong Medicine Co., Ltd., Hangzhou, China) group. All treatment groups were treated for 12 weeks by giving medicine by gavage every day. The dose of MFSD was 1 ml/100 g/d, and CsA of 25 mg/kg/d. Since CsA was the main therapeutic regimen for MN (Floege et al., 2019), we chose CsA as the positive control drug. The dose was selected according to the equivalent human dose in clinical use. The normal and model groups received the same volume of distilled water.

Urine and Serum Collection and Biochemical Analysis

After the final treatment, the 24-h urine was collected in a metabolic cage, and the urine protein was quantified by the

Laboratory Department of Beijing Hospital of Traditional Chinese Medicine, Capital Medical University. Rats were anesthetized with 1% sodium pentobarbital before obtaining their blood from the abdominal aorta. After centrifugation, the serum was stored at -80°C until analysis, and the serum biochemical indexes (ALB, CHO, TG, BUN, Cr, ALT, AST) were measured with Hitachi 7,600 automatic biochemical analyzer.

Histological Analysis of Renal Tissues

The kidney tissues were fixed with 4% paraformaldehyde. After 24 h, the tissue was embedded in paraffin, cut into 4 μm thick sections, and stained with hematoxylin and eosin (HE), periodic acid-silver methenamine (PASM), and Masson according to standard protocols.

In order to evaluate the severity of tubulointerstitial injury, semi-quantitative renal tubule-interstitium score were used as described (Li et al., 2012). Briefly, the tubular atrophy, interstitial inflammation, and fibrosis area were evaluated in 10 fields on each HE stained renal section under a microscope with ×100 magnification. The score was graded from 0 to 3 points (0 points, normal tubulointerstitial; 1 point, lesion area <25% of the section; 2 points, lesion area in 25–50% of the section; and 3 points, lesion area >50% of the section). The mean value was referred to as the tubulointerstitial lesion index.

Immunohistochemical Assay

Kidney tissues were fixed with 4% paraformaldehyde, embedded in paraffin, and cut into 3 mum-thick sections. For antigen retrieval, the sections were placed in 10 mm sodium citrate buffer (pH 6. 0) and heated to near boiling (95–98°C) in a water bath for 20 min (or an oven), followed by 20 min cooling at room temperature. The antigen was repaired with sodium citrate and then immersed in 3% H_2O_2 for 15 min to remove endogenous catalase.

Afterward, the sections were added to goat serum blocking solution at room temperature for 30 min and then incubated with rabbit anti-GSK-3β (#27C10, CST, United States) overnight at 4°C. Next the sections were incubated with an HRP-labeled secondary antibody (#SP-00223, Bioss, Beijing). Finally, DAB was added and stained with hematoxylin. All sections were taken under a light microscope with a 400× (Zeiss Axio Imager, Germany). Brown color would be considered as positive staining.

Immunofluorescence Assays

Kidney tissues were fixed with 4% paraformaldehyde, embedded in paraffin, and cut into 3 mum-thick sections. After dewaxing and hydration, sodium citrate buffer was added before heating in a water bath and cooling to room temperature. The sections were incubated with rabbit anti-LC3A/B (#12741, CST, United States), rabbit anti-p62 (#16177, CST, United States), rabbit anti-β-catenin (#8480, CST, United States) or rabbit anti-nephrin (#ab216341, Abcam, UK) respectively at 4°C overnight. Afterward, the sections were added with Alexa Fluor 488 (Thermo Fisher Scientific, United States) or Alexa Fluor 594 (Thermo Fisher Scientific, United States) and incubated for 2 h, and stained with DAPI (Sigma, United States). All the sections were observed *via* a confocal microscope (LSM 800, ZEISS, Germany). Three independent researchers scored at least 10 fluorescent stains in each group. The positive expression aera in glomerulus was calculated using Image-Pro Plus (Version 6.0, Media Cybernetics, United States).

Western Blotting

The protein samples were then boiled with a ×5 sample buffer and electrophoresed on a 10% or 12% polyacrylamide gel, then transfer to PVDF membranes. The PVDF membranes were blocked in 5% skim milk for 2 h and incubated overnight at 4°C with rabbit anti-LC3A/B (#12741, CST, United States), rabbit anti-p62 (#16177, CST, United States), rabbit anti-β-catenin (#8480, CST, United States) or rabbit anti-GAPDH (#2118, CST, United States) at 4°C, respectively. The membranes were then washed three times for 10 min in PBS with 0.1% Tween-20 and incubated with anti-rabbit secondary antibody in blocking buffer at room temperature for 1 h. Finally, the membranes were scanned with the Odyssey infrared imaging system (LI-COR Biosciences, NE, United States). All protein bands were analyzed by ImageJ software (Version 1.53, Bethesda, United States).

Preparation of MFSD and Ultra-Performance Liquid Chromatography/Mass Spectrometry Assay

The ingredients of MFSD were purchased from Guangdong Yifang Pharmaceutical Co., ltd., Foushan, China. Each herb was adjusted to the therapeutic dose of the rat based on the conversion coefficient of the clinical dose of the herb. MFSD was dissolved in water and then stored at 4°C. The contents of MFSD are shown in **Table 1**.

Identification of Active Compounds and Related Targets in MFSD

To determine the chemical ingredients of the six herbs in MFSD, we searched the Traditional Chinese Medicine Systems Pharmacology Database (TCMSP, http://old.tcmsp-e.com/tcmsp.php). The absorption, distribution, metabolism, and excretion (OAME) system in this study includes predicting oral bioavailability (OB) and drug-likeness (DL). Meanwhile, compounds were retained only if OB ≥ 30% and DL ≥ 0. 18 to satisfy the criteria suggested by the TCMSP database (Ru et al., 2014). By analyzing the ingredients and target interactions obtained from TCMSP Database, the integrative efficacy of the ingredients in MFSD was determined.

Prediction of the Therapeutic Targets Acting on MN

MN targets were found in the GeneCards database (https://www.genecards.org/), which contains detailed information on all annotated and predicted human genes.

TABLE 1 | The composition of MFSD.

TCM	Latin Name	Part Used	Lot. Number	Dry Weight (g) of Daily Clinic Dose
Ma Huang	*Ephedra sinica* Stapf	stem	7051972	20
Fu Zi	*Aconitum carmichaelii* Debx	lateral radix	6120142	20
Gan Jiang	*Zingiber officinale* Rose	rhizome	7090862	30
Fu Ling	*Poria cocos (Schw.)* Wolf	Sclerotium	7010742	30
Bai Zhu	*Atractylodes macrocephala* Koidz	rhizome	6126142	10
Gan Cao	*Glycyrrhizae uralensis* Fisch	rhizome	7021762	10

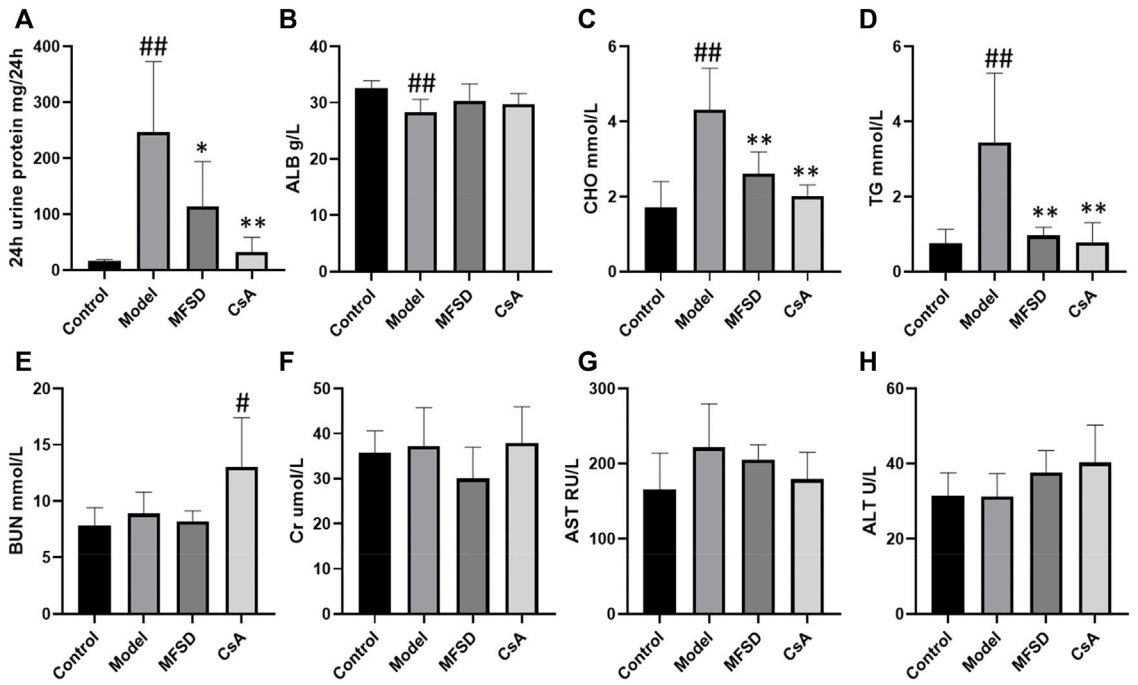

FIGURE 1 | The effect of MFSD on the urine protein and serum biochemical indicators in PHN rats**. (A)** The contents of 24 h urine protein excretion in the last week ($n = 8$) **(B)** The levels of ALB in serum ($n = 8$) **(C, D)** The levels of TC and TG in serum ($n = 8$) **(E, F)** The levels of BUN and Cr in serum ($n = 8$) **(G,H)** The levels of ALT and AST in serum ($n = 8$). Data were expressed as mean ± SD. $^{\#}p < 0.05$ and $^{\#\#}p < 0.01$ *vs*. control group, $^{*}p < 0.05$ and $^{**}p < 0.01$ *vs*. model group.

Network Construction and Analysis

Interactions between proteins of putative targets of active drugs in MFSD and known therapeutic targets for MN were integrated with putative MFSD target-known therapeutic targets of the MN network to build putative MFSD target-known therapeutic targets of the MN network. It can be used to show the connections between the suspected targets in MFSD and recognized treatment targets. Cytoscape software was used to visualize the graphical interactions in this network (version 3. 6. 0, Boston, MA, United States).

Protein-Protein Interaction Data

These data of protein-protein interaction (PPI) are from STRING (http://stringdb. org/, version 10), a database of known and forecasted protein-protein interactions (von et al. , 2003) with the species limited to "*Homo sapiens*" and the confidence score >0. 7. Each node represents a protein, and each edge represents an interaction. More edges mean more importance of the node.

Gene Ontology and KEGG Enrichment Analysis for Targets

In order to validate whether potential targets are related to MN, we examined the gene ontology (GO) involving biological process (BP), molecular function (MF), and cellular component (CC). An enrichment analysis according to Tokyo Encyclopedia of Genes and Genomes (KEGG) was conducted to predict the potential signaling pathway of MFSD in MN. The GO and KEGG enrichment analysis was performed using the functional annotation tool of DAVID Bioinformatics Resources 6.7 (https://davidd.ncifcrf.gov/)

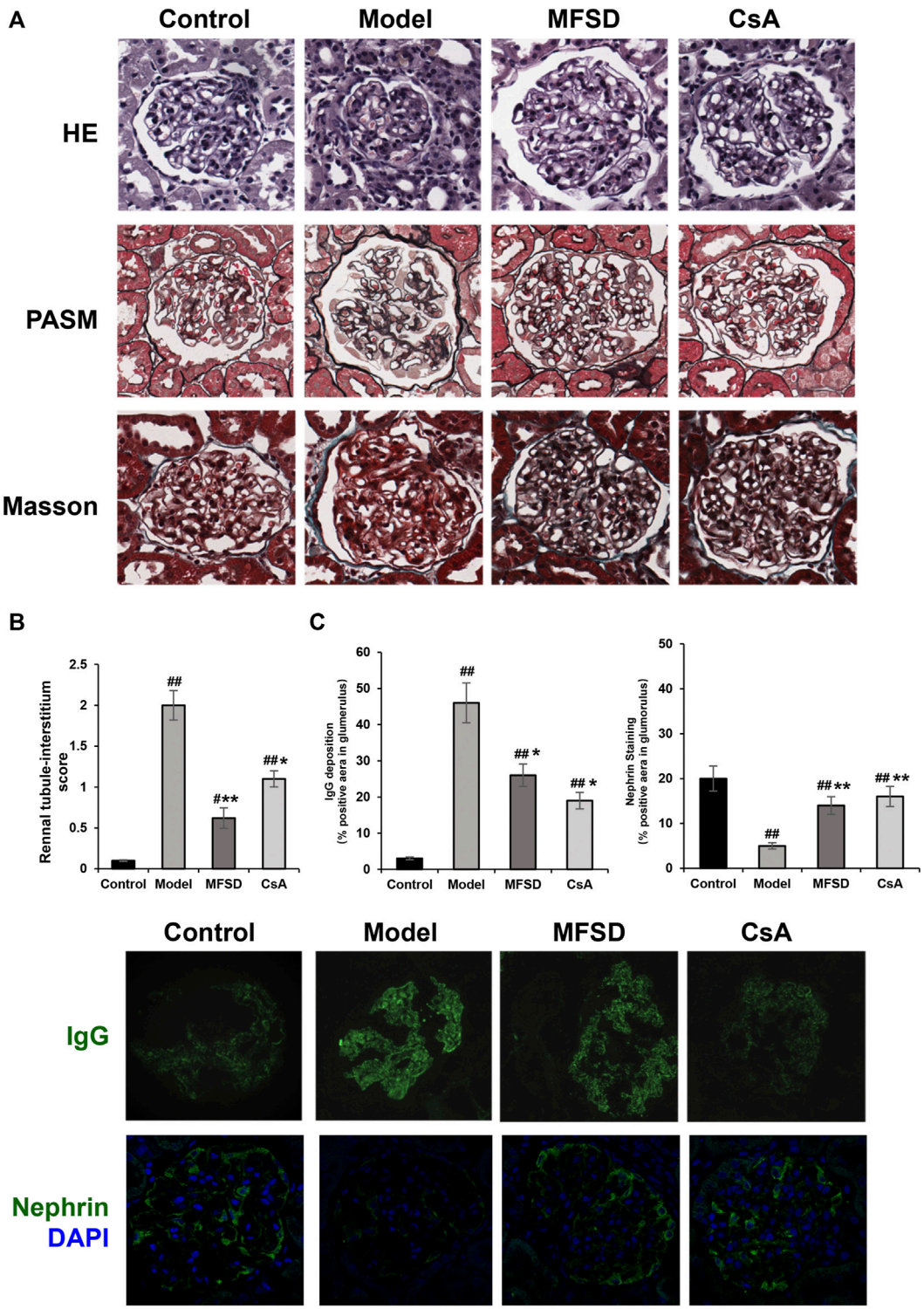

FIGURE 2 | MFSD ameliorated glomerular pathomorphological and podocyte injuries in PHN rats**. (A)** Representative renal pathological staining images of different groups. Top, the images of renal tissues by HE staining were obtained under a light microscope (×400 magnification) (scale bar = 20 μm), Middle and bottom, images of renal tissues by PASM staining and Masson staining were obtained under a light microscope (×400 magnification) (scale bar = 20 μm) **(B)** Histogram is the statistical results of renal tubule-interstitium score of different groups; **(C)** Representative images of IgG and nephrin were observed under a confocal microscope at ×400 magnification (scale bar = 20 μm).

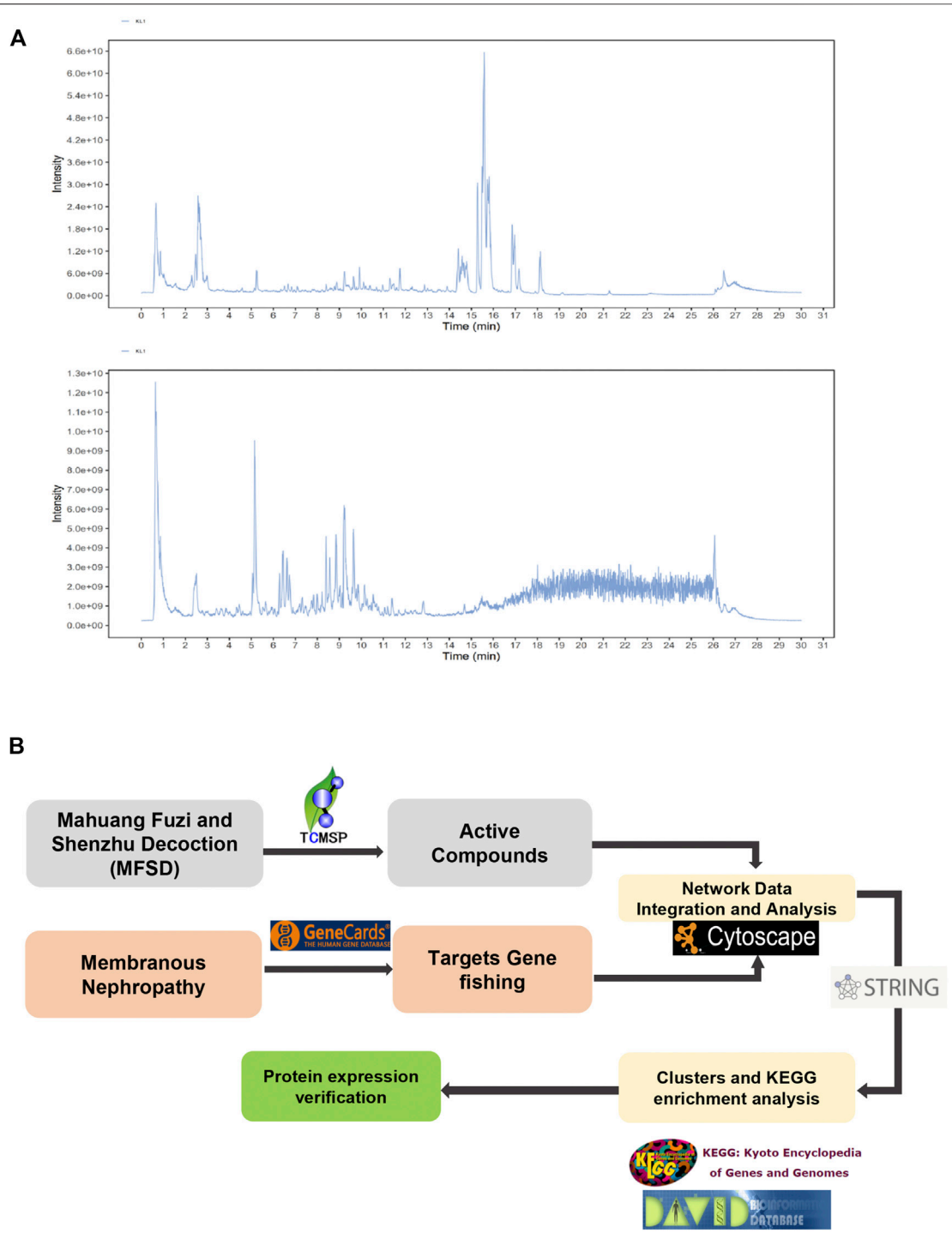

FIGURE 3 | Analysis of the target of MFSD based on network pharmacology **(A)** UPLC-MS Assay of the concentration of MFSD. **(B)** Schematic flow chart of network pharmacology analysis of target of MFSD.

(Huang et al., 2009). With Benjamini–Hochberg method to control the false discovery rate (FDR) for multiple hypothesis tests, the adjusted p-value < 0. 05 was used as the significance cutoff.

Statistical Analysis

Data were presented as mean ± SEM. One-way analysis of variance was adopted to analyze the statistics *via* a two-sided t-test (two groups) or one-way analysis of variance

TABLE 2 | Compounds in MFSD with oral bioavailability (OB) larger than 30% and drug-likeness (DL) larger than 0.18, which combined with the results of ultra-performance liquid chromatography-mass spectrometry (UPLC-MS).

Comp	Molecule name	OB(%)	DL
1	Herbacetin	36.07	0.27
2	kaempferol	41.88	0.24
3	delphinidin	40.63	0.28
4	quercetin	46.43	0.28
5	Supraene	33.55	0.42
6	naringenin	59.29	0.21
7	Pectolinarigenin	41.17	0.3
8	(+)-Leucocyanidin	37.61	0.27
9	Deoxyandrographolide	56.3	0.31
10	isotalatizidine	50.82	0.73
11	kaempferol	41.88	0.24
12	Isolicoflavonol	45.17	0.42
13	quercetin	46.43	0.28
14	Calycosin	47.75	0.24
15	Medicarpin	49.22	0.34
16	isorhamnetin	49.6	0.31
17	Glabrone	52.51	0.5
18	Glabridin	53.25	0.47
19	naringenin	59.29	0.21
20	liquiritin	65.69	0.74
21	formononetin	69.67	0.21
22	Licochalcone B	76.76	0.19
23	Poricoic acid A	30.61	0.76
24	pachymic acid	33.63	0.81
25	α-Amyrin	39.51	0.76
26	8β-ethoxy atractylenolide III	35.95	0.21

(ANOVA) followed by Bonferroni's multiple comparison test (>2 groups). $p < 0.05$ was considered statistically significant.

RESULTS

MFSD can Reduce 24 hUTP, CHO, and TG in PHN Rats

To evaluate the efficacy of MFSD in PHN rats, we examined the 24 h urinary protein excretion (24 hUTP), albumin (ALB), total cholesterol (CHO), triglycerides (TG), creatinine (Cr), blood urea nitrogen (BUN), alanine aminotransferase (ALT), and aspartate aminotransferase (AST). As shown in **Figures 1A,C,D** compared with the control group, 24-h urinary protein, CHO, TG significantly increased in PHN rats ($p < 0.01$). Meanwhile, MFSD reduced 24 hUTP after treatment compared with the model group ($p < 0.05$), and CsA reduced the proteinuria excretion ($p < 0.01$). In addition, MFSD and CsA significantly reduced serum levels of CHO and TG ($p < 0.01$). Although there was no statistical significance in ALB between the groups, it can be seen from **Figure1B** that ALB in the model group was lower than that in the normal group, while MFSD and CsA could improve levels of ALB. At the same time, the BUN, Cr, ALT, AST of the MFSD group were not significantly abnormal compared with the control group, reflecting that MFSD has no obvious hepatotoxicity and renal toxicity in rats (**Figures 1E–H**).

MFSD Ameliorates Glomerular Pathomophology and Podocyte Injury in PHN Rats

As shown in **Figure 2A**, the morphological changes of different groups of kidneys were indicated *via* the optical microscope. Diffusion thickening of the basement membrane was observed in the model group. PASM staining showed the formation of "spike process,", vacuoles and granular degeneration of renal tubular epithelial cells, flattening, exfoliation, and regeneration of epithelial cells, while HE staining showed inflammatory cell infiltration in the renal interstitium (**Figure 2B**).

In the CsA group, the basement membrane was diffusely thickened, forming the "nailing process". Renal tubules and interstitial changes were similar to those in the model group. In addition, the appearance of segmental sclerosis in the glomeruli could be noted. MFSD group showed "spike" like changes. We found through renal tubule-interstitium score analysis that the changes in renal tubules and interstitium of MFSD group were reduced compared with the model ($p < 0.01$) and CsA groups (**Figure 2A**). IgG was expressed in the glomeruli in the model group, while IgG expression in the MFSD and CsA groups was comparatively lower ($p < 0.05$). It can be referred that MFSD and CsA have therapeutic effects on PHN rats, reducing renal injury and immune injury (**Figure 2C**).

In addition, immunofluorescence showed that the expression of nephrin in glomerulus of model group was significantly down-regulated ($p < 0.01$), while MFSD or CSA treatment could improve the expression of the down-regulated nephrin in glomerulus ($p < 0.01$) (**Figure 2C**). This result suggests that similar to CsA, MFSD can improve the damage of glomerular podocytes.

Herbal Compounds in MFSD

Figure 3A shows a typical chromatogram. According to the TCMSP database, 945 compounds were retrieved, including 363 species of Mahuang, 65 species of Fuzi, 148 species of Ganjiang, 55 species of Baizhu, 34 species of Fuling, and 280 species of Gancao. According to the criteria of OB ≥ 30% and DL ≥ 0.18, 106 chemical ingredients were screened out, among which 23 species of Mahuang, 21 species of Fuzi, 5 species of Ganjiang, 7 species of Baizhu, 15 species of Fuling, and 92 species of Gancao. After taking out the duplicated parts, combined with the results of UPLC-MS assay, 103 chemical constituents were accepted. Finally, 26 chemical ingredients were screened out for further target prediction analysis. (**Figure 3B** and **Table 2**).

Identification of MFSD-Related Targets

As a result, GenesCard produced 3,427 distinct targets associated with MN, including almost all the targets related to MN that have already been identified or are currently being investigated. Potential targets of MFSD include genes associated with MN progression or treatment. 66 of the 3,427 MN-related genes were closely associated with MFSD. **Figure 4A** shows the number of overlaps between MFSD-related genes and MN-related genes.

86 nodes and 346 edges (**Figures 4B,C**) were included in a global view of the compound-target–pathway (C-T-P) network,

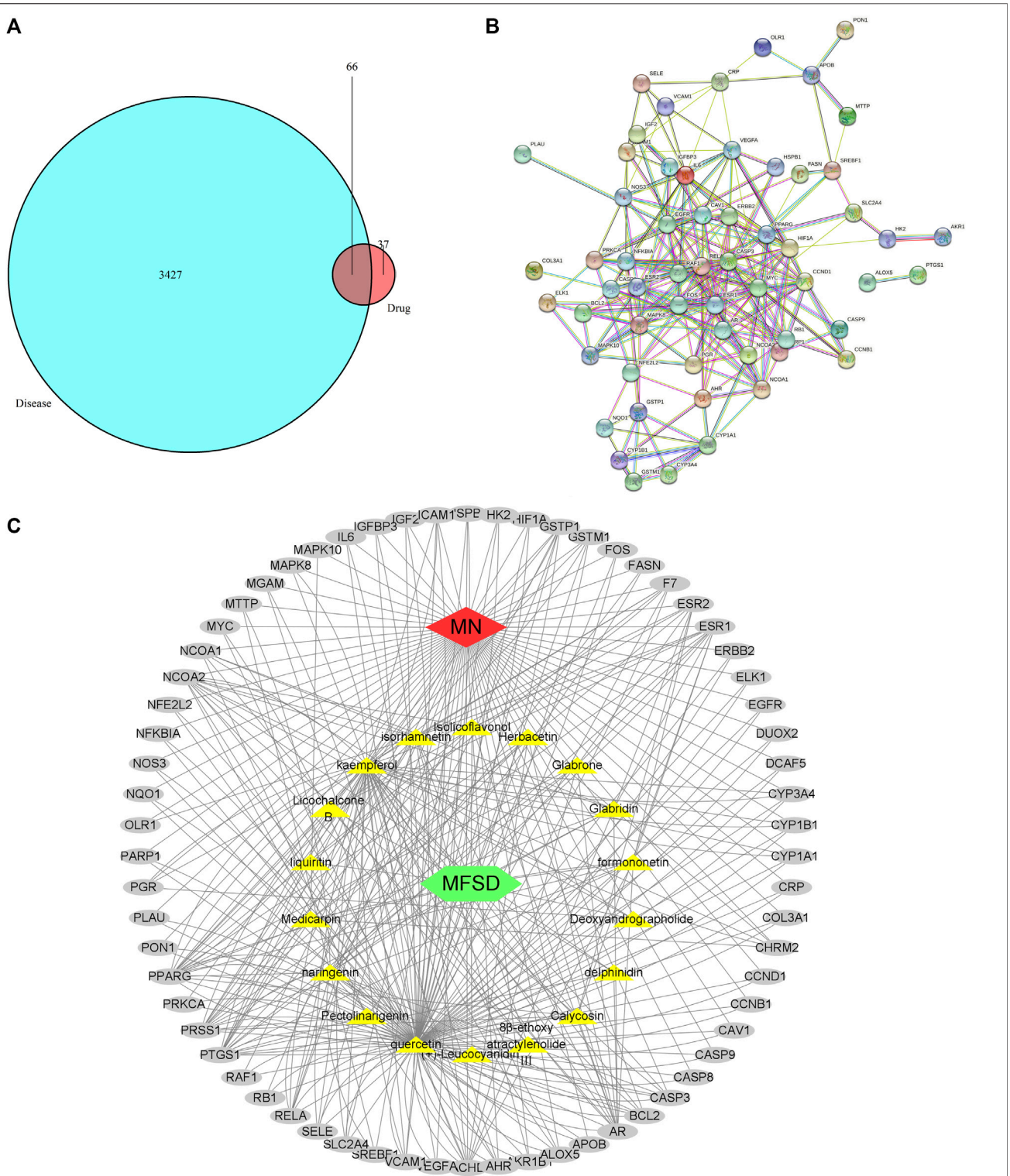

FIGURE 4 | Active compound of MFSD target MN and protein–protein interaction (PPI) network analysis **(A)** Venn diagram of drug-disease targets. The cyan circle represents 3,427 known therapeutic targets for the treatment of MN. The red circle represents 103 known drug targets of MFSD. In total, 66 shared targets were shown between MFSD and MN. **(B)** The PPI analysis of 66 overlapping targets of MFSD and MN. The nodes get larger with an increasing degree. Edges: PPI between shared targets and their interactive partners **(C)** Potential Compound-Targets-Pathway (pC-T-P) network of MFSD in the treatment of MN. There were 6 kinds of herbs, 18 compounds, 66 predicted targets. The yellow hexagon represents 6 kinds of herbs in MFSD, while the grey circle represents potential targets. (For interpretation of the references to color in this figure legend, please refer to the Web version of this article.)

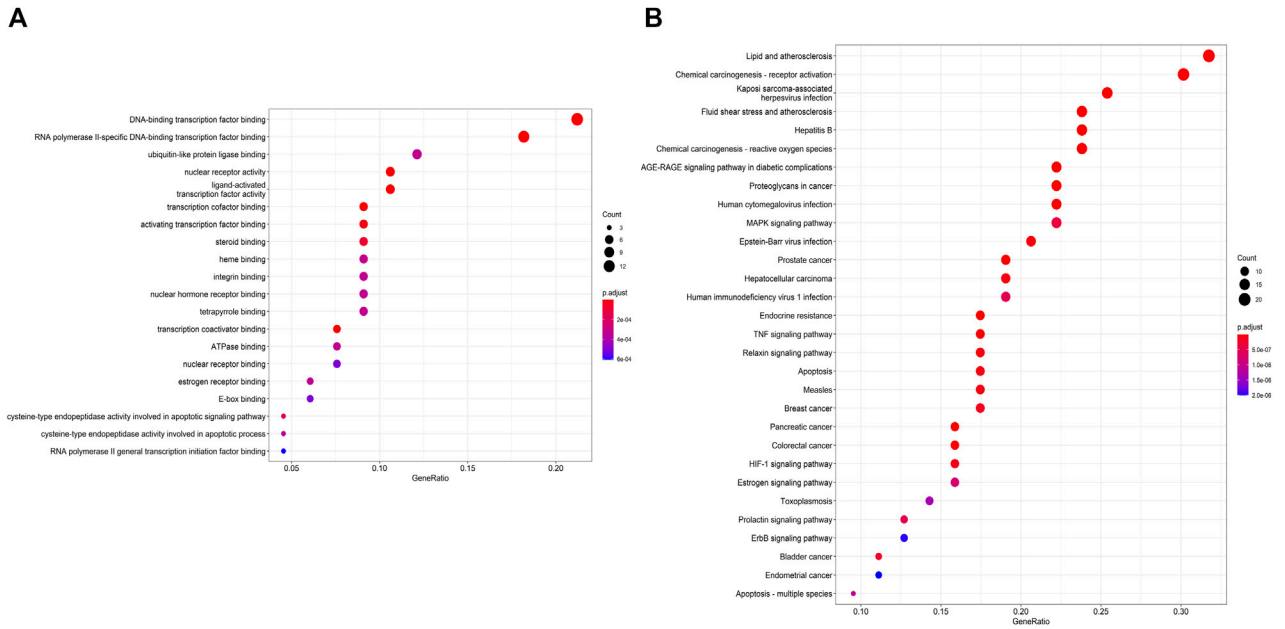

FIGURE 5 | Gene Ontology (GO) enrichment and KEGG pathways analysis for drug-disease targets **(A)** The top 20 significant GO enrichment analyses. The red circle represents the gene count of each biological process. **(B)** The top 30 significant KEGG pathways. (For interpretation of the references to color in this figure legend, please refer to the Web version of this article.)

clarifying the specifics of the MFSD mechanism. As this network demonstrates, MFSD components and their targets are intricately linked. These findings suggested that MFSD interacted with MN in a multi-target, multi-pathway, and overall integrative manner.

Enrichment Analysis and Construction of the Regulatory Network

The above-mentioned possible MFSD target genes were then imported into KEGG pathway enrichment to investigate potential signaling pathways for MFSD in the treatment of MN. **Figure 5** shows the top 30 possible signaling pathways. The MAPK signaling pathway (hsa04010), apoptosis (hsa04210), autophagy—animal (hsa04140), Wnt signaling pathway (hsa04310) were discovered to be involved in apoptosis, inflammation, immunity, or oxidative stress biological processes in MN.

MFSD Adjusted Podocyte Autophagy in PHN Rats

Studies have shown that autophagy is down-regulated in MN (Liu et al., 2017; Jin et al., 2018; Yang et al., 2021). In order to clarify the autophagy in MN, it needs to be explored whether the pathogenesis of PHN involves changes in autophagy and whether the therapeutic effect of MFSD is related to this change. We analyzed the expressions of p62 and LC3B in kidney tissue by immunofluorescence staining (**Figure 6A**) and Western blot methods (**Figure 6B**). As shown in **Figure 6B**, compared with the control group, the expressions of LC3-II and p62 in the model group were higher than that in the control group ($p < 0.01$), whereas the expressions of LC3-II ($p < 0.01$) and p62 ($p < 0.05$) were reduced in the MFSD group, respectively. These data indicated that the treatment of PHN rats by MFSD was at least partially achieved by regulating autophagy.

MFSD Inhibits the Wnt/β-Catenin Pathway in PHN Rats

More studies have shown that the Wnt/β-catenin pathway is critical in CKD pathogenesis. According to cancer-related research, the Wnt/β-catenin pathway is related to autophagy, but the relationship in membranous nephropathy remains unclear. As shown in **Figure 7A**, immunofluorescence and immunohistochemical staining showed that the model group has a higher expression of β-catenin and GSK-3β compared with the control group ($p < 0.01$). In addition, in the MFSD group, both protein levels of β-catenin and GSK-3β were decreased compared with model group ($p < 0.01$). However, there was only β-catenin in CsA treatment group, but no significant decrease in GSK-3β (**Figure 7B**). Our results indicate that MFSD may improve podocyte injury by inhibiting Wnt/β-catenin pathway.

DISCUSSION

Idiopathic membranous nephropathy is a common cause of adult nephrotic syndrome (Ponticelli and Glassock, 2014). In clinical practice, about 70% of patients present with nephrotic syndrome, and 30% of patients can spontaneously relieve, but patients with

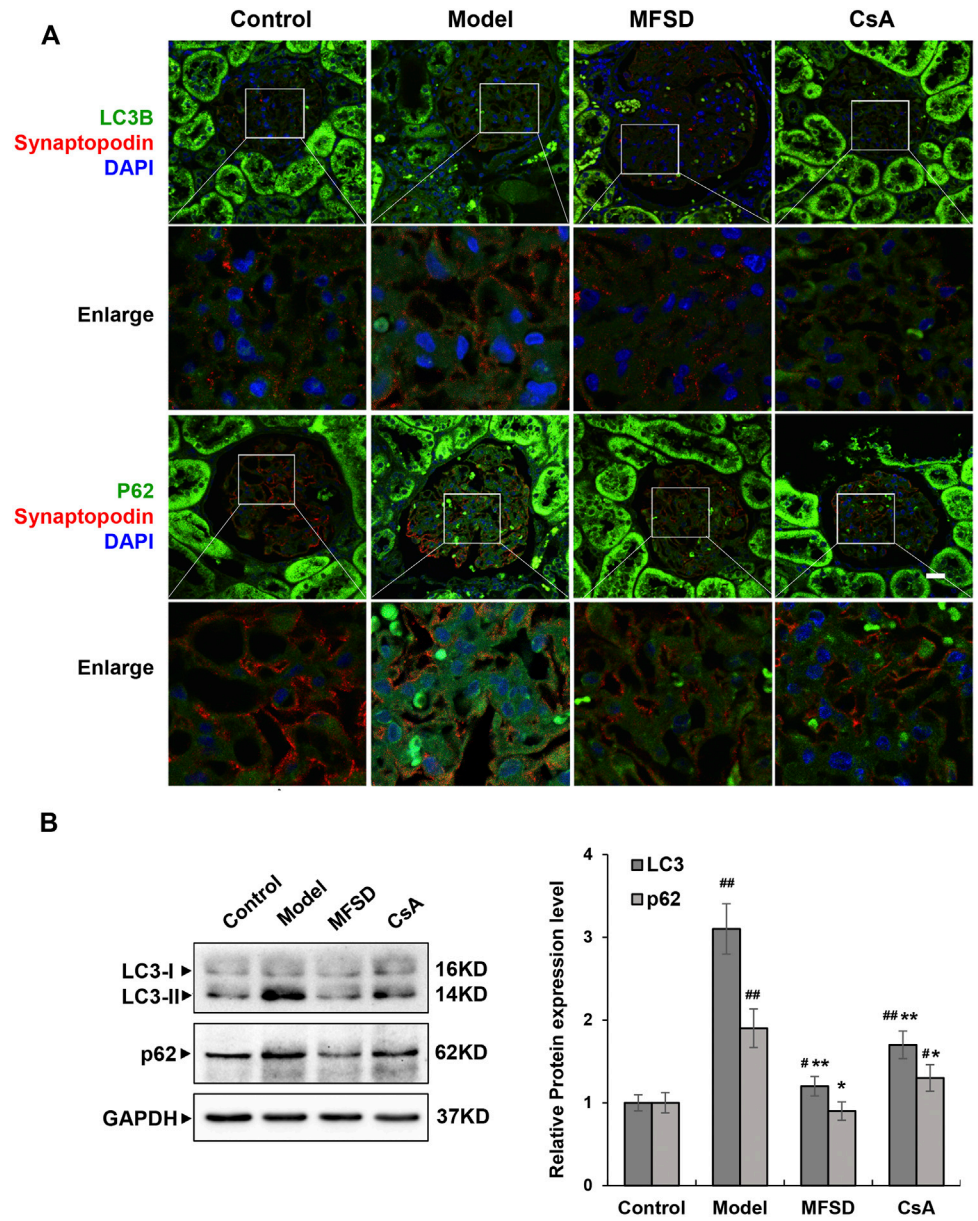

FIGURE 6 | MFSD adjusted podocyte autophagy in PHN rats **(A)** Immunofluorescent analysis of LC3B-positive puncta (green) and p62-positive puncta (green) accumulated in podocytes of PHN. The podocytes in glomeruli were identified by immunofluorescent double-labeling with synaptopodin (red), a podocyte foot process-specific protein. The nuclei were stained with DAPI (blue). Images were obtained using a confocal microscope. **(B)** The relative protein expression levels of renal LC3I/II and p62 of PHN rats were analyzed by western blot assay. The relative protein expression level was expressed as the target protein/GAPDH ratio. Values are represented as mean ± SD. $^{\#}p < 0.05$ and $^{\#\#}p < 0.01$ *vs*. control group, $^{*}p < 0.05$ and $^{**}p < 0.01$ *vs*. model group.

large proteinuria will develop into end-stage renal disease (Polanco et al., 2010; Moroni et al., 2017). The current medications for the MN treatment are mainly cyclosporine, cyclophosphamide, and rituximab, but serious side effects still exist (van den Brand et al., 2017; Zhang et al., 2018).

MFSD is a common clinical prescription to treat kidney disease. It is mainly composed of ephedra, aconite, licorice, dried ginger, poria, and fried atractylodes, and its main components have been identified as effective. Moreover, traditional Chinese medicine prescriptions other than a single ingredient have effectively treated various diseases for hundreds of years. Our team has found that MFSD is effective in treating MN through clinical applications, but the specific mechanism is still unknown. The classic animal model of MN is intravenously injected with anti-Fx1A Serum named Passive Heymann Nephritis (Heymann et al., 1959). Therefore, in our study, a PHN rat model induced by Fx1A injection was performed to evaluate the effect of MFSD on MN.

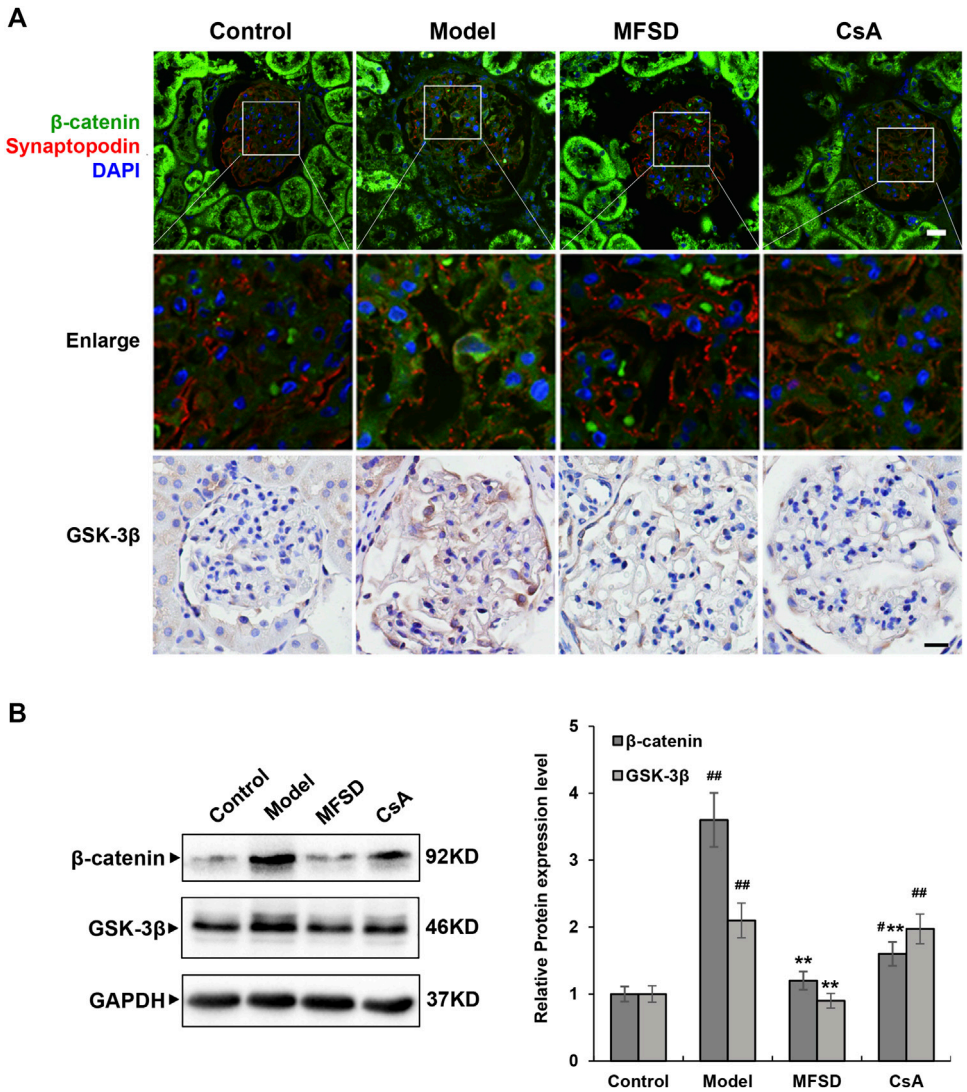

FIGURE 7 | MFSD inhibits the Wnt/β-catenin pathway in PHN rats **(A)** Immunofluorescent staining of β-catenin-positive puncta (green) accumulated in podocytes of PHN. The podocytes in glomeruli were identified by immunofluorescent double-labeling with synaptopodin (red), a podocyte foot process-specific protein. The nuclei were stained with DAPI (blue). Immunohistochemical staining of GSK-3βwas conducted using a confocal microscope. Images were collected under a light microscope at ×400 magnification (scale bar = 20 μm). **(B)** The relative protein expression levels of renal β-catenin and GSK-3β of PHN rats were analyzed by western blot assay. The relative protein expression level was expressed as the target protein/GAPDH ratio. Values are represented as mean ± SD. $^{\#}p < 0.05$ and $^{\#\#}p < 0.01$ *vs*. control group, $^{**}p < 0.01$ *vs*. model group.

The "one-drug and one target" mode is not appropriate to develop TCM's action mechanism because it is characterized by a multi-component, multi-target, and multi-pathway synergistic action mode. Network pharmacology is a new approach that combines system biology, multi-directional pharmacology, and computational biology to investigate the interaction between medications and diseases from a broad perspective. It is particularly well suited to elucidating the complicated interaction between medications, targets, pathways, and illnesses. In this study, a global perspective of the prospective chemical target pathway network was established using network pharmacology to investigate the molecular mechanism and potential targets of MFSD in MN treatment.

The active components related to MFSD were obtained from TCMSP. Through the enrichment of biological pathways in the Mendelian genetic and KEGG database, the protein targets in MFSD were screened. In addition to active components and target genes, several meaningful signal pathways include apoptosis, autophagy, the TNF, MAPK, and Wnt/β-catenin pathways. Abundant biological functions and literature studies suggest that these pathways are mainly related to oxidative stress, apoptosis, inflammation, and immune response involved in the progression of MN,

providing a preliminary understanding and stimulating the interest in further research.

After preliminarily determining the role of the multidimensional regulatory network in MN treatment, MFSD was verified in the PHN rat model. PHN rats treated with MFSD can significantly reduce proteinuria, slightly increase serum albumin without obvious liver and kidney function abnormalities. Therefore, it can be concluded that MFSD has a potential therapeutic effect on MN.

There are 19 different secreted proteins in Wnts. The Wnt/β-catenin signal cascade plays an important role in organogenesis, tissue homeostasis, and human diseases (MacDonald et al., 2009; Clevers and Nussw, 2012). Wnt/β-catenin signaling pathway-related proteins are expressed in the kidney, especially in tubular epithelial cells, fibroblasts, and macrophages (Schunk et al., 2021). Evidence has been accumulated that the Wnt/β-catenin signaling pathway is closely related to kidney disease, and relevant research is mostly about inflammation and fibrosis (Tan et al., 2014; Edeling et al., 2016). Regarding the Wnt/β-catenin signaling pathway and the occurrence of proteinuria, it is found that β-catenin can inhibit the expression of nephrin, leading to the destruction of the glomerular slit diaphragm and the formation of proteinuria (Dai et al., 2009). MN manifests as podocyte damage in the kidney, but the mechanism of protective action of MFSD in MN is unknown. In our study, PHN rats were observed to activate the Wnt/β-catenin signaling pathway compared with the control group. Interestingly, we discovered that in the model group, β-catenin levels increased considerably, indicating aberrant Wnt/β-catenin signaling. The expression of these Wnt/β-catenin signaling-related proteins was considerably reduced in the MFSD groups, showing that MFSD prevented the Wnt/β-catenin signaling pathway from becoming overactive.

However, it is not sufficient to explain the remission of proteinuria in MN patients with MFSD, and further research is needed to rule out the entire mechanism. Although it was documented that autophagy could be inhibited in MN, our experimental results showed that the expression levels of autophagy-related proteins p62 and LC3B increased in the model group but decreased in the MFSD group, which meant that autophagy was inhibited in the MFSD group.

Autophagy, being highly conservative, is a common living phenomenon in eukaryotic cell organisms. It is a programmed cell death mechanism alongside apoptosis and necrosis. Autophagy plays an extremely important role in cell waste removal, structural reconstruction, organelle renewal, and growth and development (Levine and Kroemer, 2008; Kroemer et al., 2010). Some intracellular contents degrade under physiological and pathological conditions (Kroemer, 2015; Gatica et al., 2018; Wong et al., 2018). Podocytes are cells that maintain high levels of autophagy (Bork et al., 2020). At the same time, abnormal autophagy exists in chronic kidney disease (Liu et al., 2017; Jin et al., 2018; Zhou et al., 2019; Li et al., 2021; Yang et al., 2021). Studies in membranous nephropathy have shown that autophagy is down-regulated in membranous nephropathy (Liu et al., 2017; Yang et al., 2021), but the mechanism leading to its down-regulation is not yet clear. Our experimental results show that autophagy protein expression in the PHN rat model group tends to increase, which is statistically significant.

To clarify the situation of autophagy in MN, our team believes that the mechanism of inhibiting/activating autophagy is related to the Wnt pathway. The main regulator of autophagy is the mTOR pathway (Ravikumar et al., 2004; Kim et al., 2011). Some studies have also shown the complex relationship between autophagy and the Wnt/β-catenin pathway (Petherick et al., 2013; Kühn et al., 2015; Yun et al., 2020; Zhou et al., 2021). Autophagy and Wnt/β-catenin pathway-related proteins are highly expressed in cancer cells (Zhou et al., 2019), and the Wnt/β-catenin pathway is a negative regulator of p62 (Petherick et al., 2013). However, there is no research on this pathway in MN.

Meanwhile, our research discovered that inhibiting the Wnt/-catenin signaling pathway lowered autophagy in complement-treated podocytes in cellular experiments (Dong et al., 2021). Our study showed that in MN, the expression of the Wnt/β-catenin pathway and autophagy in podocytes were up-regulated, while the expression of Wnt/β-catenin and autophagy were down-regulated after the application of MFSD. This study confirmed the connection between the Wnt/β-catenin signal and autophagy in MN, also proving that MFSD could treat MN through this pathway.

MFSD is a traditional Chinese medicine compound that treats membranous nephropathy through multiple targets, and one of the mechanisms may be to inhibit the Wnt/β-catenin signaling pathway and autophagy. The main therapeutic ingredient of MFSD may be ephedrine, ephedra polysaccharide, or other effective ingredients, which our team will further explore. At the same time, we will also explore more targets for MFSD to treat MN.

DATA AVAILABILITY STATEMENT

The original contributions presented in the study are included in the article/Supplementary Material, further inquiries can be directed to the corresponding authors.

ETHICS STATEMENT

All experiments were conducted following the internationally recognized standard guidelines for using animals and were reviewed and approved by the Experimental Animal Welfare Ethics Committee of the Beijing Institute of Chinese Medicine (Ethics No. 2019060103).

AUTHOR CONTRIBUTIONS

BL and HR were responsible for conception of the study. BL, YG, HD, FL, XZ, and XD were responsible for the feeding the experimental rats and the detection of related indicators. HD, HJ, NZ, and ZF were responsible for data analysis and interpretation. YG

and ZZ participated in the drafting of the manuscript. BL, ZF, WL, and QZ were responsible for conception of the study and responsible for critical revision of important content, and undertook part of the data analysis and interpretation work. BL and HR are responsible for approving the final version to be published. All authors read and approved this manuscript.

FUNDING

This work was supported by grants from the National Natural Science Foundation of China (No. 81973793 to BL, 82004269 to HD), the National Key Research and Development Project of China (No. 2019YFC1709402 to BL), Capital's Funds for Health Improvement and Research (No. 2020-2-2234 to BL), and Research and Cultivation Program of Beijing Municipal Hospital Management Center (No. PZ2019016 to HD).

ACKNOWLEDGMENTS

The authors sincerely acknowledge the support of Dr. Xiao-hong Cheng, Dr. Jia-rong Mao and Dr. Ling Mao for the kidney sections were then stained with H&E, Masson, PASM and Immunofluorescence of IgG for pathological evaluation during this work.

REFERENCES

Ahmed, M. S., Hou, S. H., Battaglia, M. C., Picken, M. M., and Leehey, D. J. (2007). Treatment of Idiopathic Membranous Nephropathy with the Herb Astragalus Membranaceus. *Am. J. Kidney Dis.* 50 (6), 1028–1032. doi:10.1053/j.ajkd.2007.07.032

Bork, T., Liang, W., Yamahara, K., Lee, P., Tian, Z., Liu, S., et al. (2020). Podocytes Maintain High Basal Levels of Autophagy Independent of Mtor Signaling. *Autophagy* 16 (11), 1932–1948. doi:10.1080/15548627.2019.1705007

Clevers, H., and Nusse, R. (2012). Wnt/β-catenin Signaling and Disease. *Cell* 149 (6), 1192–1205. doi:10.1016/j.cell.2012.05.012

Dai, C., Stolz, D. B., Kiss, L. P., Monga, S. P., Holzman, L. B., and Liu, Y. (2009). Wnt/beta-catenin Signaling Promotes Podocyte Dysfunction and Albuminuria. *J. Am. Soc. Nephrol.* 20 (9), 1997–2008. doi:10.1681/ASN.2009010019

Dai, H., Liu, F., Qiu, X., Liu, W., Dong, Z., Jia, Y., et al. (2020). Alleviation by Mahuang Fuzi and Shenzhuo Decoction in High Glucose-Induced Podocyte Injury by Inhibiting the Activation of Wnt/β-Catenin Signaling Pathway, Resulting in Activation of Podocyte Autophagy. *Evid. Based Complement. Alternat Med.* 2020, 7809427. doi:10.1155/2020/7809427

Dong, Z., Dai, H., Gao, Y., Jiang, H., Liu, M., Liu, F., et al. (2021). Effect of Mahuang Fuzi and Shenzhuo Decoction on Idiopathic Membranous Nephropathy: A Multicenter, Nonrandomized, Single-Arm Clinical Trial. *Front. Pharmacol.* 12, 724744. doi:10.3389/fphar.2021.724744

Edeling, M., Ragi, G., Huang, S., Pavenstädt, H., and Susztak, K. (2016). Developmental Signalling Pathways in Renal Fibrosis: the Roles of Notch, Wnt and Hedgehog. *Nat. Rev. Nephrol.* 12 (7), 426–439. doi:10.1038/nrneph.2016.54

Feng, Z., Liu, W., Jiang, H. X., Dai, H., Gao, C., Dong, Z., et al. (2020). How Does Herbal Medicine Treat Idiopathic Membranous Nephropathy? *Front. Pharmacol.* 11, 994. doi:10.3389/fphar.2020.00994

Floege, J., Barbour, S. J., Cattran, D. C., Hogan, J. J., Nachman, P. H., Tang, S. C. W., et al. (2019). Management and Treatment of Glomerular Diseases (Part 1): Conclusions from a Kidney Disease: Improving Global Outcomes (KDIGO) Controversies Conference. *Kidney Int.* 95 (2), 268–280. doi:10.1016/j.kint.2018.10.018

Gatica, D., Lahiri, V., and Klionsky, D. J. (2018). Cargo Recognition and Degradation by Selective Autophagy. *Nat. Cel Biol* 20 (3), 233–242. doi:10.1038/s41556-018-0037-z

Heymann, W., Hackel, D. B., Harwood, S., Wilson, S. G., and Hunter, J. L. (1959). Production of Nephrotic Syndrome in Rats by Freund's Adjuvants and Rat Kidney Suspensions. *Proc. Soc. Exp. Biol. Med.* 100 (4), 660–664. doi:10.3181/00379727-100-24736

Hopkins, A. L. (2008). Network Pharmacology: the Next Paradigm in Drug Discovery. *Nat. Chem. Biol.* 4 (11), 682–690. doi:10.1038/nchembio.118

Huang, da. W., Sherman, B. T., and Lempicki, R. A. (2009). Systematic and Integrative Analysis of Large Gene Lists Using DAVID Bioinformatics Resources. *Nat. Protoc.* 4 (1), 44–57. doi:10.1038/nprot.2008.211

Jin, J., Hu, K., Ye, M., Wu, D., and He, Q. (2018). Rapamycin Reduces Podocyte Apoptosis and Is Involved in Autophagy and mTOR/P70S6K/4EBP1 Signaling. *Cell Physiol Biochem* 48 (2), 765–772. doi:10.1159/000491905

Kato, H., Gruenwald, A., Suh, J. H., Miner, J. H., Barisoni-Thomas, L., Taketo, M. M., et al. (2011). Wnt/β-catenin Pathway in Podocytes Integrates Cell Adhesion, Differentiation, and Survival. *J. Biol. Chem.* 286 (29), 26003–26015. doi:10.1074/jbc.M111.223164

Kawakami, T., Ren, S., and Duffield, J. S. (2013). Wnt Signalling in Kidney Diseases: Dual Roles in Renal Injury and Repair. *J. Pathol.* 229 (2), 221–231. doi:10.1002/path.4121

Kim, J., Kundu, M., Viollet, B., and Guan, K. L. (2011). AMPK and mTOR Regulate Autophagy through Direct Phosphorylation of Ulk1. *Nat. Cel Biol* 13 (2), 132–141. doi:10.1038/ncb2152

Kroemer, G. (2015). Autophagy: a Druggable Process that Is Deregulated in Aging and Human Disease. *J. Clin. Invest.* 125 (1), 1–4. doi:10.1172/JCI78652

Kroemer, G., Mariño, G., and Levine, B. (2010). Autophagy and the Integrated Stress Response. *Mol. Cel* 40 (2), 280–293. doi:10.1016/j.molcel.2010.09.023

Kühn, K., Cott, C., Bohler, S., Aigal, S., Zheng, S., Villringer, S., et al. (2015). The Interplay of Autophagy and β-Catenin Signaling Regulates Differentiation in Acute Myeloid Leukemia. *Cell Death Discov* 1, 15031. doi:10.1038/cddiscovery.2015.31

Levine, B., and Kroemer, G. (2008). Autophagy in the Pathogenesis of Disease. *Cell* 132 (1), 27–42. doi:10.1016/j.cell.2007.12.018

Li, P., Ma, L. L., Xie, R. J., Xie, Y. S., Wei, R. B., Yin, M., et al. (2012). Treatment of 5/6 Nephrectomy Rats with Sulodexide: a Novel Therapy for Chronic Renal Failure. *Acta Pharmacol. Sin* 33 (5), 644–651. doi:10.1038/aps.2012.2

Li, S., and Zhang, B. (2013). Traditional Chinese Medicine Network Pharmacology: Theory, Methodology and Application. *Chin. J. Nat. Med.* 11 (2), 110–120. doi:10.1016/S1875-5364(13)60037-0

Li, Y., Pan, Y., Cao, S., Sasaki, K., Wang, Y., Niu, A., et al. (2021). Podocyte EGFR Inhibits Autophagy through Upregulation of Rubicon in Type 2 Diabetic Nephropathy. *Diabetes* 70 (2), 562–576. doi:10.2337/db20-0660

Liu, W., Gao, C., Dai, H., Zheng, Y., Dong, Z., Gao, Y., et al. (2019). Immunological Pathogenesis of Membranous Nephropathy: Focus on PLA2R1 and its Role. *Front. Immunol.* 10, 1809. doi:10.3389/fimmu.2019.01809

Liu, W. J., Li, Z. H., Chen, X. C., Zhao, X. L., Zhong, Z., Yang, C., et al. (2017). Blockage of the Lysosome-dependent Autophagic Pathway Contributes to Complement Membrane Attack Complex-Induced Podocyte Injury in Idiopathic Membranous Nephropathy. *Sci. Rep.* 7 (1), 8643. doi:10.1038/s41598-017-07889-z

MacDonald, B. T., Tamai, K., and He, X. (2009). Wnt/beta-catenin Signaling: Components, Mechanisms, and Diseases. *Dev. Cel* 17 (1), 9–26. doi:10.1016/j.devcel.2009.06.016

Moroni, G., Depetri, F., Del Vecchio, L., Gallelli, B., Raffiotta, F., Giglio, E., et al. (2017). Low-dose Rituximab Is Poorly Effective in Patients with Primary Membranous Nephropathy. *Nephrol. Dial. Transpl.* 32 (10), 1691–1696. doi:10.1093/ndt/gfw251

Petherick, K. J., Williams, A. C., Lane, J. D., Ordóñez-Morán, P., Huelsken, J., Collard, T. J., et al. (2013). Autolysosomal β-catenin Degradation Regulates Wnt-Autophagy-P62 Crosstalk. *EMBO J.* 32 (13), 1903–1916. doi:10.1038/emboj.2013.123

Polanco, N., Gutiérrez, E., Covarsí, A., Ariza, F., Carreño, A., Vigil, A., et al. (2010). Spontaneous Remission of Nephrotic Syndrome in Idiopathic Membranous Nephropathy. *J. Am. Soc. Nephrol.* 21 (4), 697–704. doi:10.1681/ASN.2009080861

Ponticelli, C., and Glassock, R. J. (2014). Glomerular Diseases: Membranous Nephropathy-Aa Modern View. *Clin. J. Am. Soc. Nephrol.* 9 (3), 609–616. doi:10.2215/CJN.04160413

Qiu, T. T., Zhang, C., Zhao, H. W., and Zhou, J. W. (2017). Calcineurin Inhibitors versus Cyclophosphamide for Idiopathic Membranous Nephropathy: A Systematic Review and Meta-Analysis of 21 Clinical Trials. *Autoimmun. Rev.* 16 (2), 136–145. doi:10.1016/j.autrev.2016.12.005

Ravikumar, B., Vacher, C., Berger, Z., Davies, J. E., Luo, S., Oroz, L. G., et al. (2004). Inhibition of mTOR Induces Autophagy and Reduces Toxicity of Polyglutamine Expansions in Fly and Mouse Models of Huntington Disease. *Nat. Genet.* 36 (6), 585–595. doi:10.1038/ng1362

Ru, J., Li, P., Wang, J., Zhou, W., Li, B., Huang, C., et al. (2014). TCMSP: a Database of Systems Pharmacology for Drug Discovery from Herbal Medicines. *J. Cheminform* 6, 13. doi:10.1186/1758-2946-6-13

Schunk, S. J., Floege, J., Fliser, D., and Speer, T. (2021). WNT-β-catenin Signalling - a Versatile Player in Kidney Injury and Repair. *Nat. Rev. Nephrol.* 17 (3), 172–184. doi:10.1038/s41581-020-00343-w

Tan, R. J., Zhou, D., Zhou, L., and Liu, Y. (2014). Wnt/β-catenin Signaling and Kidney Fibrosis. *Kidney Int. Suppl. (2011)* 4 (1), 84–90. doi:10.1038/kisup.2014.16

Tian, R., Wang, L., Chen, A., Huang, L., Liang, X., Wang, R., et al. (2019). Sanqi Oral Solution Ameliorates Renal Damage and Restores Podocyte Injury in Experimental Membranous Nephropathy via Suppression of NFκB. *Biomed. Pharmacother.* 115, 108904. doi:10.1016/j.biopha.2019.108904

van den Brand, J. A. J. G., Ruggenenti, P., Chianca, A., Hofstra, J. M., Perna, A., Ruggiero, B., et al. (2017). Safety of Rituximab Compared with Steroids and Cyclophosphamide for Idiopathic Membranous Nephropathy. *J. Am. Soc. Nephrol.* 28 (9), 2729–2737. doi:10.1681/ASN.2016091022

von Mering, C., Huynen, M., Jaeggi, D., Schmidt, S., Bork, P., and Snel, B. (2003). STRING: a Database of Predicted Functional Associations between Proteins. *Nucleic Acids Res.* 31 (1), 258–261. doi:10.1093/nar/gkg034

Wong, D. W. L., Yiu, W. H., Chan, K. W., Li, Y., Li, B., Lok, S. W. Y., et al. (2018). Activated Renal Tubular Wnt/β-Catenin Signaling triggers Renal Inflammation During overload Proteinuria. *Kidney Int.* 93 (6), 1367–1383. doi:10.1016/j.kint.2017.12.017

Xiong, M., Wang, L., Liu, X., Yue, S., Dong, J., Li, Y., et al. (2020). Kidney Biopsies in Elderly Chinese Patients: A Nationwide Survey. *Am. J. Kidney Dis.* 76 (2), 295–297. doi:10.1053/j.ajkd.2020.02.438

Xu, X., Wang, G., Chen, N., Lu, T., Nie, S., Xu, G., et al. (2016). Long-Term Exposure to Air Pollution and Increased Risk of Membranous Nephropathy in China. *J. Am. Soc. Nephrol.* 27 (12), 3739–3746. doi:10.1681/ASN.2016010093

Yang, L., Wu, Y., Lin, S., Dai, B., Chen, H., Tao, X., et al. (2021). sPLA2-IB and PLA2R Mediate Insufficient Autophagy and Contribute to Podocyte Injury in Idiopathic Membranous Nephropathy by Activation of the p38MAPK/mTOR/ULK1 Ser757 Signaling Pathway. *FASEB j.* 35 (2), e21170. doi:10.1096/fj.202001143R

Yun, E. J., Kim, S., Hsieh, J. T., and Baek, S. T. (2020). Wnt/β-catenin Signaling Pathway Induces Autophagy-Mediated Temozolomide-Resistance in Human Glioblastoma. *Cell Death Dis* 11 (9), 771. doi:10.1038/s41419-020-02988-8

Zhang, J., Bian, L., Ma, F. Z., Jia, Y., and Lin, P. (2018). Efficacy and Safety of Rituximab Therapy for Membranous Nephropathy: a Meta-Analysis. *Eur. Rev. Med. Pharmacol. Sci.* 22 (32), 8021–8029. doi:10.26355/eurrev_201811_16431

Zhou, C., Liang, Y., Zhou, L., Yan, Y., Liu, N., Zhang, R., et al. (2021). TSPAN1 Promotes Autophagy Flux and Mediates Cooperation between WNT-CTNNB1 Signaling and Autophagy via the MIR454-Fam83a-TSPAN1 axis in Pancreatic Cancer. *Autophagy* 17 (10), 3175–3195. doi:10.1080/15548627.2020.1826689

Zhou, X. J., Klionsky, D. J., and Zhang, H. (2019). Podocytes and Autophagy: a Potential Therapeutic Target in Lupus Nephritis. *Autophagy* 15 (5), 908–912. doi:10.1080/15548627.2019.1580512

Conflict of Interest: The authors declare that the research was conducted in the absence of any commercial or financial relationships that could be construed as a potential conflict of interest.

Publisher's Note: All claims expressed in this article are solely those of the authors and do not necessarily represent those of their affiliated organizations, or those of the publisher, the editors and the reviewers. Any product that may be evaluated in this article, or claim that may be made by its manufacturer, is not guaranteed or endorsed by the publisher.

Advantages of publishing in Frontiers

OPEN ACCESS
Articles are free to read for greatest visibility and readership

FAST PUBLICATION
Around 90 days from submission to decision

HIGH QUALITY PEER-REVIEW
Rigorous, collaborative, and constructive peer-review

TRANSPARENT PEER-REVIEW
Editors and reviewers acknowledged by name on published articles

Frontiers
Avenue du Tribunal-Fédéral 34
1005 Lausanne | Switzerland

Visit us: www.frontiersin.org
Contact us: frontiersin.org/about/contact

REPRODUCIBILITY OF RESEARCH
Support open data and methods to enhance research reproducibility

DIGITAL PUBLISHING
Articles designed for optimal readership across devices

FOLLOW US
@frontiersin

IMPACT METRICS
Advanced article metrics track visibility across digital media

EXTENSIVE PROMOTION
Marketing and promotion of impactful research

LOOP RESEARCH NETWORK
Our network increases your article's readership